

Nanojoule Adsorption Calorimetry

Design, Construction, Novel Evaluation

Approach, Software Development,

Characterization, and Exemplary Measurements

D i s s e r t a t i o n

Volume 1

zur Erlangung des
Doktorgrades der Naturwissenschaften
(Dr. rer. nat.)

dem Fachbereich Chemie
der Philipps-Universität Marburg

vorgelegt von

Hans-Jörg Drescher

Diplom Chemiker Universität

aus Erlangen

Marburg an der Lahn
2016

Der praktische Teil der vorliegenden Arbeit wurde unter Leitung von Herrn Prof. Dr. J. Michael Gottfried in der Zeit von August 2008 bis Dezember 2011 im Department Chemie und Pharmazie der Friedrich-Alexander-Universität Erlangen-Nürnberg und in der Zeit von Januar 2012 bis Juli 2014 am Fachbereich Chemie der Philipps-Universität Marburg angefertigt.

Vom Fachbereich Chemie der Philipps-Universität Marburg mit der Hochschulkennziffer 1180 als Dissertation am 13.06.2016 angenommen.

Tag der Disputation: 19.07.2016

Erstgutachter: Prof. Dr. J. Michael Gottfried

Zweitgutachter: Prof. Dr. Andreas Seubert

Selbständigkeitserklärung

gemäß § 10, Absatz 1 der Promotionsordnung der Mathematisch-Naturwissenschaftlichen Fachbereiche und des Medizinischen Fachbereichs für seine mathematisch-naturwissenschaftlichen Fächer der Philipps-Universität Marburg vom 15.07.2009.

Ich erkläre, dass eine Promotion noch an keiner anderen Hochschule als der Philipps-Universität Marburg, Fachbereich Chemie, von mir versucht wurde und versichere, dass ich meine vorgelegte Dissertation

Nanojoule Adsorption Calorimetry

*Design, Construction, Novel Evaluation Approach, Software Development,
Characterization, and Exemplary Measurements*

selbst und ohne fremde Hilfe verfasst, nicht andere als die in ihr angegebenen Quellen oder Hilfsmittel benutzt, alle vollständig oder sinngemäß übernommenen Zitate als solche gekennzeichnet sowie die Dissertation in der vorliegenden oder einer ähnlichen Form noch bei keiner anderen in- oder ausländischen Hochschule anlässlich eines Promotionsgesuches oder zu anderen Prüfungszwecken eingereicht habe.

Hans-Jörg Drescher

Abstract

The interaction of single molecules with surfaces as well as the interaction between surfaces, *i.e.*, interfaces, are often of great interest and thus a vast field of applied sciences arises therefrom. Most ultra high vacuum based surface science techniques are only able to deliver information about an already formed interface. The desire for knowledge of the energetics describing the processes during the formation of such a contact layer motivates the usage of nanojoule adsorption calorimetry.

This work presents the construction of the experimental setup necessary to study the coverage dependent heat of adsorption. The setup is optimized for investigations involving the adsorption of metal atoms on organic thin films and of large organic molecules on surfaces of single crystalline metals. The software developed for this work and used for data treatment is also covered by this thesis. In this respect, the user interface as well as the program code processing the data are both well discussed. The characterization of the components involved in calorimetric experiments is presented in detail later in this work. Finally, selected experiments involving the adsorption of magnesium, zinc, copper, and calcium on the pristine and cleaned detector surface as well as on 3,4,9,10-perylene-tetracarboxylic dianhydride, tetraphenylporphyrin, α -sexithiophene, and poly(3-hexylthiophene) are exemplarily discussed.

This paper is completed by design drawings of the constructed elements for this work, the source code of the data treatment program developed for this work, an overview of the investigated systems, and the parameters used to operate the scientific equipment.

Considering all individual aspects presented in this dissertation conjoined, the scientific framework necessary to study coverage dependent heats of adsorption precisely is established.

Kurzzusammenfassung

Da sowohl die Wechselwirkung von einzelnen Molekülen mit Oberflächen als auch die Wechselwirkung zwischen Oberflächen, also Grenzschichten, oft von großem Interesse sind, eröffnet sich daraus ein weites Feld von angewandten Wissenschaften. Die meisten Methoden zur Untersuchung von Oberflächen unter Ultrahochvakuumbedingungen können lediglich Informationen über bereits gebildete Grenzschichten liefern. Das Streben nach Erkenntnissen über die Energetik, welche den Bildungsprozess einer solchen Kontaktfläche beschreibt, motiviert die Verwendung der Nanojoule-Adsorptions-Kalorimetrie als Methode.

Die vorliegende Arbeit stellt die Konstruktion des experimentellen Aufbaus vor, der notwendig ist, um bedeckungsabhängige Adsorptionswärmen zu bestimmen. Diese Anlage ist für die Erforschung von Systemen optimiert, bei denen Metallatome auf organischen Dünnschichten, beziehungsweise große organische Moleküle auf Einkristalloberflächen adsorbiert werden. Die für die Datenauswertung dieser Arbeit entwickelten Computerprogramme werden erläutert. Im Zuge dessen erfolgt auch eine ausführliche Erörterung sowohl der Benutzeroberfläche als auch des eigentlichen Programms. Im Folgenden wird die Charakterisierung aller in ein Kalorimetrie-Experiment involvierten Komponenten eingehend dargelegt. Zum Abschluss sind einige ausgewählte Experimente exemplarisch diskutiert. Diese Beispiele umfassen die Adsorption von Magnesium, Zink, Kupfer und Calcium auf der ursprünglichen und gesäuberten Detektoroberfläche, sowie auf Dünnschichten aus 3,4,9,10-Perylentetracarbonsäuredianhydrid, Tetraphenylporphyrin, α -Sexithiophen und Poly(3-Hexylthiophen).

Vervollständigt wird diese Abhandlung sowohl durch technische Zeichnungen der für diese Arbeit konstruierten Bauteile, den für diese Arbeit entwickelten Quelltext des Auswertungsprogramms, als auch durch eine Übersicht über die untersuchten Systeme und die Betriebsparameter für die Laborausrüstung.

Aus der zusammenfassenden Betrachtung der einzelnen in dieser Dissertation präsentierten Aspekte, lässt sich feststellen, dass alle aus wissenschaftlicher Sicht notwendigen Rahmenbedingungen geschaffen wurden, um bedeckungsabhängige Adsorptionswärmen präzise bestimmen zu können.

Contents

Selbständigkeitserklärung	iii
Abstract	v
Kurzzusammenfassung	vii
Contents	ix
Abbreviations	xix
1 Introduction	1
1.1 Enthalpy of Adsorption	3
1.1.1 Deduction from Desorption Kinetics	3
1.1.2 Derivation from Adsorption-Desorption Equilibria	5
1.1.3 Direct Measurement by Adsorption Calorimetry	5
1.2 Theoretical Background	7
1.3 Involved Principles	10
1.3.1 Beam Source	10
1.3.2 Infrared Radiation	10
1.3.3 Pyroelectric Detector	11
1.3.4 Detector Calibration	13
1.3.5 Pulsing	14
1.3.6 Deposition Rate Measurement	14
1.3.7 Sticking Measurement	15
2 Experimental Setup	17
2.1 Sample Holder	20
2.2 Detector Stage	23
2.3 Molecular Beam	30
2.3.1 Main Evaporator	30
2.3.2 Optics Stage	35
2.3.3 Beam Chopper	39

2.3.4	Inline Valve	44
2.3.5	Parts in the Main Chamber	46
2.3.6	Beam Housing	49
2.3.7	Assembled Beam	52
2.4	Ancillaries Stage	55
2.4.1	Hot Plate	56
2.4.2	Quartz Crystal Microbalance	57
2.4.3	Mirror	58
2.4.4	Infrared Transparent Window	59
2.4.5	Assembled Ancillaries	60
2.5	Main Chamber Additions	63
2.5.1	Mass Spectrometer	63
2.5.2	Optical Meters	65
2.5.3	Fiber Positioner	69
2.5.4	Miscellaneous Additions	72
2.6	Load Lock	76
2.7	Sample Handling	82
2.8	Glove Box	85
2.9	Assembled System	87
2.10	Synopsis of the Experimental Setup	91
3	Data Evaluation	93
3.1	User Interface	94
3.1.1	Menu	94
3.1.2	Main Panel	101
3.1.3	Interactive Windows	101
3.2	Loading Data	104
3.3	Data Filtering	106
3.3.1	High Pass Filter	106
3.3.2	Line Notch Filter	108
3.3.3	Extra Notch Filter	109
3.3.4	Nyquist Cut Off Filter	109
3.3.5	Effects on the Calorimetry Data	110
3.4	Quartz Crystal Microbalance Measurements	113
3.4.1	Sample Coating	113
3.4.2	Calorimetry Deposition Rate Measurement	114

3.5	Measured References	117
3.5.1	Deconvolution	120
3.5.2	Clean Sample	121
3.5.3	Coated Sample	121
3.5.4	Laser Reference	122
3.5.5	Transmission of Infrared Transparent Window	124
3.5.6	Radiation Contribution	124
3.5.7	Zero Sticking	125
3.6	Statistics	126
3.7	Automatic Outlier Removal	128
3.8	Calorimetry Measurement	132
3.8.1	Heat Measurement	132
3.8.2	Sticking Measurement	134
3.8.3	Enthalpy Calculation	136
3.9	Fitted Trends	138
3.10	Deconvolution of Measurements	143
3.11	Averaging Experiments	146
3.12	Lazy Operations	148
3.13	Comparison to Previous Approach	149
3.14	Status Display	154
3.15	Synopsis of the Data Evaluation	155
4	Software	157
4.1	File Formats	158
4.1.1	Deposition Files	158
4.1.2	Calorimetry Files	160
4.1.3	Auxiliary Files	161
4.1.4	Logging Files	162
4.2	NAC Program Package	163
4.2.1	Definitions	164
4.2.2	Initialization	166
4.2.3	Graphical User Interface	178
4.2.4	Data Processing	186
4.2.5	Fitting Functions	194
4.2.6	File Input/Output	199
4.2.7	Controls Handling	202
4.2.8	Statistics Functions	208

4.2.9	Experiment Averaging Functions	210
4.2.10	Miscellaneous	213
4.2.11	Extensions to the Status Package	215
4.2.12	Version History	215
4.2.13	Known Issues	215
4.3	Error Handling Package	216
4.3.1	Definitions	216
4.3.2	Initialization	217
4.3.3	Error Handling	217
4.3.4	Graphical User Interface	218
4.3.5	Version History	218
4.3.6	Known Issues	218
4.4	Status Report Package	219
4.4.1	Definitions	219
4.4.2	File Input/Output	220
4.4.3	User Interface	220
4.4.4	Tools	221
4.4.5	Version History	221
4.4.6	Known Issues	221
4.5	Synopsis of the Software Packages	222
5	Characterizing Experiments	223
5.1	External Reflectivity Measurement	224
5.2	Sputtering	228
5.3	Partially Loaded Quartz Crystal Microbalance	233
5.4	Sample Preparation in the Load Lock	238
5.4.1	Evaporator	238
5.4.2	Effects of Coating	239
5.4.3	Thermal Degrading During Deposition	241
5.4.4	Tooling of the Quartz Crystal Microbalance in the Load Lock	242
5.5	Additional Instrumentation	245
5.5.1	Digital Acquisition Card	245
5.5.2	Laser Stability	245
5.5.3	Amplifier	247
5.6	Molecular Beam	249
5.6.1	Main Evaporator	249
5.6.2	Inline Valve	252

5.6.3	Chopper	253
5.6.4	Deflector Plates	257
5.6.5	Evaporator Radiation in Reference Measurements	258
5.7	Mass Spectrometer	260
5.7.1	Intensity Estimation	260
5.7.2	Mass Spectrometer Settings	261
5.7.3	Mass Spectrometer Peak Shape <i>vs.</i> Pulse Length	263
5.8	Ancillaries Stage	268
5.8.1	Infrared Transparent Window	268
5.8.2	Quartz Crystal Microbalance	275
5.8.3	Mirror	277
5.8.4	Hot Plate	279
5.9	Pyroelectric Detector	293
5.9.1	Linearity Regarding Input Power	293
5.9.2	Linearity Regarding Active Area	294
5.9.3	External Heat Treatment of β -Polyvinylidene Fluoride	297
5.9.4	Temperature Influence on Detector Sensitivity	299
5.9.5	Detailed Detector Composition	301
5.9.6	Thermal Insulation of the Detector Stage	304
5.9.7	Deconvolution Test	305
5.10	Statistical Considerations	308
5.11	Synopsis of the Characterization Experiments	312
6	Investigated Systems	315
6.1	Choice of Materials	317
6.1.1	Magnesium	318
6.1.2	Calcium	319
6.1.3	Copper	320
6.1.4	Zinc	321
6.1.5	Lead	321
6.1.6	Unaltered Detector Material	321
6.1.7	Sputter Cleaned Detector Material	322
6.1.8	3,4,9,10-Perylene-Tetracarboxylic Dianhydride	322
6.1.9	Poly(3-Hexylthiophene)	323
6.1.10	Sexithiophene	324
6.1.11	Tetraphenyl Porphyrin	325
6.2	Reaction Thicknesses	326

6.3	Measurement Procedure	329
6.4	Adsorption of Magnesium	333
6.4.1	Experiment	333
6.4.2	Results	333
6.4.3	Discussion	336
6.5	Adsorption of Calcium	339
6.5.1	Experiment	339
6.5.2	Results	340
6.5.3	Discussion	355
6.6	Adsorption of Copper	363
6.6.1	Experiment	363
6.6.2	Results	363
6.6.3	Discussion	365
6.7	Adsorption of Zinc	367
6.7.1	Experiment	367
6.7.2	Results	367
6.7.3	Discussion	370
6.8	Gigantic Signal Effect	373
6.9	Inverted Signal Effect	378
6.10	Synopsis of the Results from the Investigated Systems	383
7	Summary and Outlook	387
8	Zusammenfassung und Ausblick	395
	Acknowledgment	403
	Danksagung	404
	<i>Curriculum Vitae</i>	405
	List of Figures	407
	List of Tables	417
	Bibliography	419

Contents	441
A Operating Parameters	450
A.1 Magnesium	451
A.2 Calcium	451
A.3 Copper	452
A.4 Zinc	452
A.5 Perylenetetracarboxylic Dianhydride	453
A.6 Phthalocyanine	453
A.7 Sexithiophene	454
A.8 5,10,15,20-Tetraphenyl-Porphyrin	454
B Design Drawings	455
B.1 Molecular Beam	455
B.1.1 Main Evaporator	456
B.1.2 Internal Valve	465
B.1.3 Optics Stage	473
B.1.4 Beam Chopper	483
B.1.5 Nozzle in Main Chamber	490
B.1.6 Beam Housing	495
B.2 Main Chamber	511
B.2.1 Sample Holder	512
B.2.2 Sample Carrier	520
B.2.3 Detector	525
B.2.4 Sample Heater	550
B.2.5 Mass Spectrometer Mount	561
B.2.6 Ancillaries Stage	568
B.2.7 Main Chamber Additions	589
B.2.8 Optical Meters	606
B.2.9 Fiber Positioner	623
B.3 Load Lock	638
B.3.1 Mount for Load Lock	639
B.3.2 Load Lock Housing	647
B.3.3 Sample Storage	654
B.3.4 Transfer Rod Support	662
B.4 Miscellaneous	668
B.4.1 Glove Box	669

B.4.2	Evaporator for Synchrotron Applications	673
B.4.3	Mounting Stand	682
B.4.4	Threefold Evaporator	690
B.4.5	Battery Box	701
C	Program Codes	703
C.1	NAC Package	704
C.1.1	Definitions	704
C.1.2	Initialization	706
C.1.3	Graphical User Interface	710
C.1.4	Data Processing	740
C.1.5	Fitting Functions	770
C.1.6	Input/Output	775
C.1.7	Controls Handling	793
C.1.8	Statistics Functions	813
C.1.9	Experiment Averaging Functions	819
C.1.10	Miscellaneous	827
C.1.11	Extensions to the Status Package	837
C.1.12	Version History	837
C.2	Error Handling Package	841
C.2.1	Definitions	841
C.2.2	Initialization	841
C.2.3	Error Handling	841
C.2.4	Graphical User Interface	844
C.2.5	Version History	844
C.3	Machine Status Package	846
C.3.1	Definitions	846
C.3.2	File Input/Output	846
C.3.3	User Interface	849
C.3.4	Tools	852
C.3.5	Version History	853
D	Overview of the Investigated Systems	855
D.1	Magnesium Adsorbed on Pristine Detector	856
D.2	Magnesium Adsorbed on Sputter Cleaned Detector	858
D.3	Magnesium Adsorbed on PTCDA	860
D.4	Calcium Adsorbed on Sputter Cleaned Detector	862

D.5	Calcium Adsorbed on Tetraphenyl Porphyrin	864
D.6	Calcium Adsorbed on PTCDA	866
D.7	Calcium Adsorbed on PTCDA at Low Temperature	869
D.8	Calcium Adsorbed on Sexithiophene	871
D.9	Calcium Adsorbed on Sexithiophene at Low Temperature	875
D.10	Zinc Adsorbed on Sputter Cleaned Detector	877
D.11	Zinc Adsorbed on PTCDA	879
D.12	Zinc Adsorbed on PTCDA at Low Temperature	881
E	Supplementary Information	883
E.1	Previous Data Evaluation Approach	883
E.2	Filtering	889
E.2.1	Laser Reference Measurement	890
E.2.2	Radiation Reference Measurement	895
E.2.3	Calorimetry Measurement	900
	List of Figures	905
	List of Tables	915
	Bibliography	917

Abbreviations

Symbols¹

\cdot	Scalar product	
\times	Vector product	
\approx	Approximately	
\equiv	Identical	
(hkl)	Crystal plane	
(hkl)	Crystal plane (hexagonal)	
$[hkl]$	Crystal axis	
$[hkl]$	Crystal axis (hexagonal)	
$[\dots; \dots]$	Closed interval	
$]\dots; \dots[$	Open interval	
β	Beta phase	
∂	Partial differential	
d	Total differential	
Δ	Transition operator	$1/\text{mol}$
δ	Difference	
	Variation	
∞	Infinity	
\int	Integral	
Σ	Sum	
$^{-1}$	Inverse	
'	Alternative	
\rightarrow	Vector	
\sim	Substitute	
\ominus	Standard	
\propto	Proportional	
\approx	Approximately	
\equiv	Identical	
\emptyset	Diameter	

¹ Given together with the context dependent units.

®	Registered trademark
™	Trademark

Constants²

ϵ_0	Vacuum permittivity	$8.854187817 \cdot 10^{-12} \text{ F/m}$
π	Pi	3.14159265358979
σ	Stefan-Boltzmann constant	$5.670373 \cdot 10^{-8} \text{ W/m}^2 \cdot \text{K}^4$
c	Speed of light	$2.99792 \cdot 10^8 \text{ m/s}$
e	Euler's number	2.71828182845905
h	Planck constant	$6.62607 \cdot 10^{-34} \text{ J}\cdot\text{s}$
		$4.13567 \cdot 10^{-15} \text{ eV}\cdot\text{s}$
k_B	Boltzmann constant	$1.38065 \cdot 10^{-23} \text{ J/K}$
N_A	Avogadro constant	$6.02214085774 \cdot 10^{23} \text{ 1/mol}$
R	Gas constant	$8.3144621 \text{ J/K}\cdot\text{mol}$

Functions

arcsin	Arc sine
arctan	Arc tangent
cos	Cosine
[...]	Floor function
exp	Exponential function
ln	Natural logarithm
log	Logarithm
tan	Tangent

Variables³

α	Absorbed fraction		
	Expansion coefficient	$1/\text{K}$	
	Ratio		
β	Unit cell angle	°	rad
	Heating rate	K/s	
	Unit cell angle	°	rad
γ	Unit cell angle	°	rad

² Including units and the used accuracy.

³ Given together with the context dependent units. “d.l.”, *i.e.*, dimensionless, is omitted where possible.

ϵ	Emissivity		
ε	Permittivity	F/m	
ζ	Material		
θ	Coverage	d.l.	ML
ϑ	Angle	°	rad
	Temperature	K	
Θ	Debye temperature	K	
λ	Wavelength	m	
μ	Mean value		
ν	Frequency	Hz	
	Frequency factor	1/s	
ξ	Variable		
Ξ	Data set		
ρ	Reaction equivalent	ML	
	Reflected fraction		
ϱ	Density	g/cm ³	
σ	Monolayer density	1/m ²	1/m ² ·ML
	Period	s	
	Standard deviation		
τ	Decay constant	s	
	Period	s	
	Transmitted fraction		
ϕ	Phase	s	
Φ	Distribution function		
	Work function		
ω	Mass fraction		
Ω	Data set		
a	Coefficient		
	Unit cell edge length	m	
A	Amplitude		
	Area	m ²	
b	Coefficient		
	Unit cell edge length	m	
B	Spectral radiance	W/m ² ·m	
c	Molar heat capacity	J/K·mol	
	Unit cell edge length	m	

C	Electric capacity	F		
	Heat capacity	J/K		
d	Diameter	m		
	Distance	m		
	Thickness	m		
D	Dose	mol		
\mathcal{D}	Desorption reference data set			
E	Energy	J	eV	
	Young's modulus	Pa		
f	Frequency	Hz		
	Function			
h	Molar enthalpy	J/mol		
H	Enthalpy	J		
\mathcal{H}	Heat measurement data set			
I	Current	A		
	Intensity	W/m ²		
\mathcal{I}	Ideal deconvolution data set			
j	Impingement rate	1/m ² ·s		
J	Deposition rate	m/s	ML/s	1/s
K	Bulk modulus	Pa		
	Correction term	J/mol		
\mathcal{L}	Laser reference data set			
m	Mass	kg		
M	Molar Mass	g/mol		
m/z	Mass to charge ratio			
n	Amount of substance	mol		
	Desorption order			
	Number of reactive centers			
N	Amount			
	Frequency constant	Hz · m		
p	Pressure	Pa		
	Probability			
	Purity			
	Pyroelectric coefficient	C/K·m ²		
P	Polarization	C/m ²		
	Power	W		

q	Molar heat Quartile	J/mol
Q	Electrical charge Heat	C J
r	Desorption rate Radius Ratio	$1/\text{s}$ m
R	Electrical resistance Relative response	Ω
\mathcal{R}	Radiation reference data set	
s	Specific heat capacity per volume	$\text{J/m}^3\cdot\text{K}$
S	Sensitivity	
\mathcal{S}	Sticking measurement data set	
t	Duration Temperature alias Time Tooling factor	s K s
T	Temperature	K
u	Molar internal energy	J/mol
U	Internal energy Voltage	J/mol V
V	Potential Volume	m^3
w	Limit	
\mathbf{w}	Coefficient set	
\mathbf{wc}	Coefficient set	
\mathbf{wx}	Set of x -values	
\mathbf{wy}	Set of y -values	
x	Time in IGOR PRO functions Variable	
y	Variable	
z	Particle partition function Position Variable	m
Z	Acoustic impedance Molecules per unit cell	$\text{kg/m}^2\cdot\text{s}$

Indices

↓	Adsorbed	fit	Fitted
↕	Reflected	found	Found
+	Ionized	h	Heat
0	Basis	\mathcal{H}	Heat
	Ground state	in	Inner
2	Binary		Input
ζ	Material	ion	Ion
g	Gas phase	kin	Kinetic
s	Solid phase	L	Load
a	After	\mathcal{L}	Laser reference
<i>a</i>	Stoichiometric index	LL	Load lock
abs	Absorbed	low	Low
ads	Adsorption	Me	Metal
Ads	Adsorbate	ML	Monolayer
Al	Aluminum	Ni	Nickel
amp	Amplitude	ofs	Offset
avg	Averaged	out	Outer
<i>b</i>	Stoichiometric index	Ox	Oxide
b	Before	p	Isobar
BaF ₂	Barium fluoride	pristine	Pristine
c	Critical	P	Parity
cal	Calorimetry	PVDF	β -polyvinylidene fluoride
clean	Clean sample	Q	Quartz
coat	Coated sample	r	Relative
cr	Crucible	ref	Reference
\mathcal{D}	Desorption reference	refl	Reflected
dep	Deposition	rel	Relative
det	Detector	\mathcal{R}	Radiation reference
e	End	s	Start
eff	Effective	\mathcal{S}	Sticking
el	Electric	sam	Sample
evap	Evaporator	st	Isosteric
<i>f</i>	Frequency	stroke	Stroke
f	Formation	sub	Sublimation
F	Film	Substr	Substrate

tot	Total	v	Isochor
T	Isotherm	win	Window
up	Up	wire	Wire
v	Isochor		

Methods

AES	Auger electron spectroscopy
AFM	Atomic force microscopy
HREELS	High resolution electron energy loss spectroscopy
LEED	Low energy electron diffraction
LEIS	Low energy ion scattering spectroscopy
NAC	Nanojoule adsorption calorimetry
NEXAFS	Near edge X-ray absorption fine structure
PES	Photoemission spectroscopy
PID	Proportional/Integral/Differential
PVD	Physical vapor deposition
SIMS	Secondary ion mass spectrometry
TDS	Thermal desorption spectroscopy
TEM	Transmission electron microscopy
TPD	Temperature programmed desorption
UPS	Ultraviolet photoelectron spectroscopy
XPS	X-ray photoelectron spectroscopy

Materials

2HTPP	5,10,15,20-Tetraphenyl-21 <i>H</i> ,23 <i>H</i> -porphine Tetraphenyl porphyrin
2HPc	Phthalocyanine
Al	Aluminum
Ar	Argon
BaF ₂	Barium fluoride
C	Carbon
CO	Carbon monoxide
Cu	Copper
LT	Lithium tantalate
MgO	Magnesium oxide
Ni	Nickel
NO	Nitric oxide

O	Oxygen
OFHC-Cu	Oxygen-free high thermal conductivity copper
Po	Polonium
Pt	Platinum
PTCDA	Perylenetetracarboxylic dianhydride
PTFE	Polytetrafluoroethylene
PVDF	Polyvinylidene fluoride

Instruments

QCM	Quartz crystal microbalance
QMS	Quadrupole mass spectrometer
SEM	Secondary electron multiplier

Miscellaneous

" "	Empty string
AF	Width across flats, <i>i.e.</i> , wrench size
AM	<i>Ante meridiem</i>
Amp	Amplitude
ANSI	American National Standards Institute
Avg	Average
BNC	Bayonet Neill-Concelman
CAS	Chemical Abstracts Service
CCP	Cubic close-packed
CF	ConFlat™
CR	Carriage return
cw	Continuous wave
DC	Direct current
DD	Day
Dep.	Deposition
<i>e.g.</i>	<i>exempli gratia</i>
<i>etc.</i>	<i>et cetera</i>
FCC	Face-centered cubic
GUI	Graphical user interface
HCP	Hexagonal close-packed
HF	High frequency
<i>i.e.</i>	<i>id est</i>

<i>Inf</i>	Infinity
LF	Line feed
MM	Month
<i>NaN</i>	Not a number
NIST	National Institute of Standards and Technology
PDF	Portable document format
PID	Proportional-Integral-Derivative
<i>p.m.</i>	<i>Post meridiem</i>
PM	<i>Post meridiem</i>
Rad	Radiation
RS	Recommended standard
SI	<i>Système international</i>
<i>sic</i>	<i>Sic erat scriptum</i>
TAB	Tabulator
UHV	Ultra high vacuum
USB	Universal serial bus
VCR	Variable compression ratio
wc	Coefficient wave
wx	Input wave
wy	Return wave
YY	Year 20YY
YYYY	Year

Non SI-Units

%	Percent
a.u.	Arbitrary units
d.l.	Dimensionless
h	Hours
in	Inch
L	Liter
min	Minute
ML	Monolayer
pnts	Points
Torr	Torr
u	Unified atomic mass unit

1 Introduction

The interaction of single molecules with surfaces as well as the interaction between surfaces, *i.e.*, interfaces, is often of great interest in various ways. Besides the straight academic approach to quantify and to aim for a gain in knowledge, a vast field of applied sciences is arising from surfaces and interfaces.

In heterogeneous catalysis, the catalyst and the reactants reside in different phases where the latter ones are either liquid or gaseous and in most cases the catalyst forms a solid phase^[1]. In these cases, one or both reactants adsorb on the solid catalyst and form reactive surface species. In order to improve catalysts in a directed way it is necessary to get knowledge of the active sites, *e.g.*, adatoms, steps, kinks, *etc.* and of how strong the reactants are bound to these sites.

Myriads of publications cover the characterization of surfaces with and without adsorbed molecules utilizing a tremendous amount of different surface science techniques. However, most of these techniques are not providing *direct* insight into the involved energetics. Even though adsorption calorimetry is a rather exotic method, it is the only one capable of measuring adsorption enthalpies directly. It has been applied to study gas and metal adsorption on various polycrystalline substrates^[2–8]¹, on single crystals^[12–48], supported nano particles^[49–52], and on polymer surfaces^[53–61].

Interfaces also play a tremendous role in electronics, *e.g.*, *p/n*-junctions in diodes and transistors. These interfaces determine the electrical behavior of the device. Semiconducting polymers established a new branch of *organic electronic devices*. Organic field effect transistors (“OFET”) and organic solar cells (“OPV”) are of industrial interest. Mostly known, and already sold as consumer products, are organic light emitting diodes (“OLED”) in cellular phones, televisions, computer displays, *etc.*^[62–65]. All these systems include contacts between the semiconducting organic phase(s) and electrodes consisting of either of indium-tin-oxide (“ITO”) or metallic layers. Some properties of the devices can be tuned by choice of the electrode materials^[66] due to material dependent work functions, reactivities, *etc.* This situation illustrates the desire to investigate regular interfaces (metal atoms on organic substrates) as well as inter-organic (organic molecules on polymer substrates) or inverted (molecules on organic substrates) systems.

¹ Also see references in [9–11].

While such interfaces are already well studied by spectroscopic and imaging techniques, *e.g.*, *photoelectron spectroscopy*^[67–79] (UPS/XPS), *near edge X-ray absorption fine structure*^[67,80,81] (NEXAFS), *high resolution electron energy loss spectroscopy*^[67,82–84] (HREELS), *secondary ion mass spectrometry*^[67] (SIMS), *transmission electron microscopy*^[67] (TEM), *atomic force microscopy*^[67] (AFM), *Raman spectroscopy*^[85], *etc.*, the energetics of the interface and its formation have only been studied for a few systems^[53–61] so far.

Motivated by the demand on investigation on further interface systems comprising a metal and an organic component and inspired by the work^[86,87] of C. T. CAMPBELL, it was decided to build a new calorimeter. The here presented calorimeter is devoted to investigations involving adsorption of metal atoms on organic thin films and adsorption of vaporable organic molecules on metallic surfaces. Hence, it provides a way to study the commutative properties of the complementary formation of the junction. Metal atoms deposited on polymers are known to diffuse into the organic layer^[57,60,69,71] forming a diffuse *interphase*. In contrast, metals atoms in a crystal are not very likely to segregate into organic adsorbate layers^[88] and hence form an abrupt *interface*.

This work includes the construction of the experimental setup², the software used for data evaluation³, a broad spectrum of experiments characterizing the experimental setup⁴, and a selection of results from conducted experiments⁵. Hence, the scope of this work is limited to the projects involving the construction of the nanojoule adsorption calorimeter and excludes the work on other projects^[88–91].

This introduction covers the general aspects concerning nanojoule adsorption calorimetry. Due to the multifarious aspects of the characterizing experiments, individual background information is given with each topic in Chapters 5 and 6 together with suggested improvements and further possible verifications.

A synopsis at the end of each chapter, each corresponding to the main aspects of this work, provides a local summary of the achieved goals, results, and suggestions.

2 See Chapter 2 and Appendix B.

3 See Chapters 3 and 4 as well as Appendix C.

4 See Chapter 5 and Appendix A.

5 See Chapter 6 and Appendix D.

1.1 Enthalpy of Adsorption

Considering typical thermodynamical quantities involved in the interaction of gases with solid surfaces, the most important are the heat capacity of the adsorbed phase, the entropy of adsorption^[92–95], and, most relevant to this work, the *heat of adsorption* Q_{ads} . The latter is often, and also in this work, used synonymously with the idiom *enthalpy of adsorption* $\Delta_{\text{ads}}H$. To be precise, they describe the same process, but from different points of view and thus have the same absolute value. The absolute sign is given by the fact that adsorption processes are exothermic and, according to the usual convention, the enthalpy is negative in this case.

In general, the heat of adsorption is given by the difference^[9] between an initial, *i.e.*, before adsorption, and final, *i.e.*, after adsorption, state of a system comprising adsorbent, *i.e.*, a surface, and an adsorptive, *e.g.*, a vapor. A considerable number of effects contribute to the heat. Examples^[9] include the energy of the surface bond, change of the degrees of freedom of the adsorptive, interaction between the adsorbed molecules, surface relaxation or rearrangement, and perturbation of the electronic structure of the adsorbate including dissociation. The latter two may be used to distinguish between physisorption and chemisorption, which is altering electronic structures. Since the degree of electronic interaction and thus the bond strength might be affected by the exact geometry of the adsorption position, *e.g.*, on-top, bridging, and hollow site adsorption^[96,97], composite results are possible even for simple gases, *e.g.*, CO and NO, on optimal defined surfaces, *e.g.*, Pt(111). The exact contribution of each binding position to the total released heat usually is a function of the coverage of the adsorptive on the surface.

Since many aspects contribute to the heat of adsorption, it is a versatile tool to study a wide variety of surface processes. As a drawback, a straight interpretation solely from this single quantity is rarely possible and combination with other techniques is often desirable^[9].

Heats of adsorption are obtainable in essentially three ways, which are described in the following with an emphasis on adsorption calorimetry.

1.1.1 Deduction from Desorption Kinetics

A very well established method, introduced by I. LANGMUIR^[98], to determine desorption energies is *thermal desorption spectroscopy* (TDS), which is also known as *temperature programmed desorption* (TPD). Under certain assumptions the desired energy of adsorption E_{ads} can be deduced from the corresponding quantity of the reverse process, the desorption activation energy E_{des} . This implies that adsorption

and desorption share the same reaction pathway. Another requirement on this model demands a negligible activation barrier for the adsorption process.

The generic approach to determine the desorption activation energy involves the Polanyi-Wigner equation

$$\begin{aligned} r(\theta, T) &= -\frac{d\theta(T)}{dt} \\ &= -\frac{d\theta(T)}{dT} \frac{dT}{dt} \\ &= \frac{\nu_n(\theta)}{\beta} \cdot (\theta(T))^n \cdot \exp\left(-\frac{E_{\text{des}}}{RT}\right) \end{aligned} \quad (1.1)$$

using a measurable quantity, *e.g.*, partial or total pressure⁶, which can be related⁷ to the corresponding desorption rate r . The desorption rate is equivalent to the decrease in coverage θ , *i.e.*, the number of adsorbed molecules, by time t and to the Arrhenius term comprising a frequency factor ν_n , the coverage, desorption order n , and temperature T . Correlation between temperature and time is established by a constant heating rate β .

In general, the desorption order and the frequency factor are unknown and the latter often depends on the coverage. This unsatisfactory situation led to several different approaches^[100–102] to reduce the influence of these variables. Worth mentioning are the *Redhead Analysis*^[99], the *Leading Edge Analysis*^[103], and the *Complete Analysis*^[104].

All methods involving desorption kinetics rely on truly reversible adsorption processes in the temperature range where desorption occurs. Thus, these techniques reach the end of their scope for systems comprising dissociation, cluster formation, subsurface diffusion, or reaction with the substrate or co-adsorbates. Detailed derivations are given elsewhere^[105,106].

It should be noted that the quantities obtained from the different measurement methods are not directly comparable^[12]. Depending on the method and on the components of the investigated system, interaction between the individual adsorbed molecules or pressure-volume work has to be accounted for.

⁶ Depending on the investigated system and experimental setup.

⁷ Proportional to the pressure in case of high pumping speed and proportional to the derivative of pressure in case of vanishing pumping speed^[99].

1.1.2 Derivation from Adsorption-Desorption Equilibria

The temperature T dependence of the equilibrium pressure p to establish a constant coverage θ on a surface is related to the isosteric heat of adsorption q_{st} via the Clausius-Clapeyron-equation

$$q_{st} = -R \left(\frac{d \ln(p)}{d^{1/T}} \right)_{\theta} . \quad (1.2)$$

This relation assumes a true equilibrium state of the investigated system with no alteration of the adsorptive and substrate during the adsorption process. Hence, its application to systems comprising chemisorbed species should be regarded with suspicion^[107–109]. Detailed derivations are given elsewhere^[105,106].

1.1.3 Direct Measurement by Adsorption Calorimetry

Adsorption calorimetry overcomes the requirement of the adsorption process' reversibility which is limiting the other two mentioned indirect methods. Many interesting adsorbate systems comprise large organic molecules, as adsorbent or adsorptive, which rather decompose than desorb upon increase of temperature or are unable to establish an adsorption/desorption equilibrium. In contrast, a direct heat measurement, as in adsorption calorimetry, is also applicable in these cases and is even able to probe metastable states, cluster growth, co-adsorption and displacement processes, reactions in the adlayer, and irreversible decomposition upon adsorption^[9]. As an extra benefit, compared to the indirect methods, this method does not rely on a temperature dependence. This enables the independent investigation of adsorption processes at different temperatures. Hence, the adjustable temperature parameter might be used to target specific adsorbed species in case of reaction of the adsorptive with the surface^[32] or to study kinetics.

A historical overview of the development of adsorption calorimetry in surface science is covered by several reviews. The substrates discussed there include

- metal wires^[9,10,110] pioneered by J. K. ROBERTS using thermistors,
- metal ribbons^[9,110] pioneered by P. KISLIUK using thermistors,
- evaporated metallic thin films^[9,10,110] pioneered by O. BEECK using thermistors,
- single crystal discs^[9,10] pioneered by R. J. MASEL using thermistors,
- polycrystalline samples^[9,10,110] pioneered by S. ČERNÝ using pyroelectric crystals,

- single crystal films^[9–11,110,111] pioneered by D. A. KING using infrared emission,
- organic thin films^[110,111] pioneered by C. T. CAMPBELL using pyroelectric polymers, and
- supported clusters^[110,112] pioneered by S. SCHAUERMANN using pyroelectric polymers.

Different approaches including

- micromechanics^[9,10,110] pioneered by R. R. SCHLITTLER,
- interferometry on thin crystals^[111] pioneered by C. PUNCKT,
- solvent based electrochemistry^[110] pioneered by R. SCHUSTER using pyroelectric polymers, and
- a scanning technique^[113] pioneered by K. EDINGER using electron beam fabricated thermal probes

are also reported. Especially the work of Campbell's group led to great progress in the recent past^[111] and motivated the investigation of metalation reactions of organic thin film applied on pyroelectric detectors in this work.

Other calorimeters based on pyroelectric detectors and their improvements are described elsewhere^[55,86,87,114–122].

1.2 Theoretical Background

The following considerations regarding the involved thermodynamics are necessary to understand the values obtained from a calorimetric experiment^[110]. The calorimeter used in this work comprises a pulsed molecular⁸ beam impinging on a prepared surface. Ultra high vacuum conditions are necessary to prevent contamination of the sample and to provide sufficiently long mean free paths to avoid interaction of the dosed material with the residual gas. Each of the generated pulses striking the sample generates heat causing an increase of the sample's temperature which is measured. Simultaneously, the fraction of molecules adsorbing on the sample, subsequently called *sticking probability*, is recorded. This, together with knowledge of the absolute number of molecules in a pulse, allows the determination of the adsorbed amount of substance.

Since the conditions in a vacuum system can be considered to be isochore, the measured, calorimetric heat q_{cal} is equivalent to the change in internal energy of the sample ΔU_{sam} . The sample experiences two components contained in ΔU_{sam} . One arises from molecules adsorbed on the sample ΔU_{\downarrow} and the other from molecules reflected from the sample after energy exchange ΔU_{\uparrow} . Hence, the adsorbed heat can be written as

$$q_{\text{cal}} = \Delta U_{\text{sam}} = \Delta U_{\downarrow} + \Delta U_{\uparrow} . \quad (1.3)$$

Each of the two changes of inner energy can be evaluated further, starting with the fraction of adsorbed molecules which comprises three terms. The major component is the actual adsorption energy ΔU_{ads} . This is the change of the internal energy for the system formed by the gas phase and the surface under the assumption that the gas phase exhibits the same temperature as the sample T_{sam} . The second one covers the difference^[123] between a *flux* and a volume of a pulse from the beam leaving the source, *i.e.*, evaporator, at a temperature T_{evap} and amounts to $1/2RT_{\text{evap}}$. The third correction deals with the change in inner energy caused by the temperature of the gas pulse from evaporator temperature to sample temperature. Altogether, ΔU_{\downarrow} can be expressed by

$$\Delta U_{\downarrow} = \Delta \left(-U_{\text{ads}} + n_{\text{ads}} \left(\frac{1}{2}R \cdot T_{\text{evap}} - \int_{T_{\text{evap}}}^{T_{\text{sam}}} c_v^{\text{g}} dT \right) \right) \quad (1.4)$$

with the amount, given in moles, of adsorbed substance n_{ads} and the molar isochore heat capacity of the gas phase c_v^{g} .

⁸ Gas phase atoms are considered as molecules in this work.

The last, *i.e.*, integral, term in Equation (1.4) models the correction regarding the temperature change of the gas phase. An analogue correction needs to be taken into account correlated to the fraction of dosed molecules recoiled from the sample. Under the assumption that all reflected molecules leave the surface with sample temperature, *i.e.*, that complete thermalization occurs, $\Delta U_{\downarrow\uparrow}$ can be expressed as

$$\Delta U_{\downarrow\uparrow} = \Delta \left(-n_{\text{refl}} \int_{T_{\text{evap}}}^{T_{\text{sam}}} c_v + \frac{1}{2}R \, dT \right) \quad (1.5)$$

with n_{refl} denoting the amount of substance of reflected molecules. Again, the additional term $\frac{1}{2}R$ takes into account that a flux of molecules carries more inner energy than a corresponding stationary volume of gas^[123].

The adsorption enthalpy, $\Delta_{\text{ads}}H$, at sample temperature T_{sam} consists of the adsorption energy ΔU_{ads} and the volume work which would result – under isobaric conditions – from the compression of the gas phase into the solid adsorbed phase. Due to the low pressures involved, the gas phase is assumed to exhibit ideal behavior. Furthermore, the volume of the solid phase is considered to be negligible compared to the volume of the gas phase. Hence, the enthalpy is given by

$$\Delta_{\text{ads}}H = \Delta (U_{\text{ads}} - n_{\text{ads}} \cdot R \cdot T_{\text{sam}}) \quad (1.6)$$

and allows for comparison with tabulated thermodynamic standard quantities, such as the heat of sublimation, after referencing to standard temperature.

By combination of Equations (1.4), (1.5), and (1.6) and division by the amount of substance adsorbed on the sample one obtains the relation for the molar heat of adsorption

$$-\Delta_{\text{ads}}H = \frac{1}{n_{\text{ads}}} (Q_{\text{cal}} - K_{\text{ads}} - K_{\text{refl}}) \quad (1.7)$$

which is, as mentioned above, the negative of the molar adsorption enthalpy $-\Delta_{\text{ads}}H$ and thus always positive. The temperature dependent corrections

$$K_{\text{ads}} = n_{\text{ads}} \left(\int_{T_{\text{sam}}}^{T_{\text{evap}}} c_v^g \, dT + \frac{1}{2}R \cdot T_{\text{evap}} - R \cdot T_{\text{sam}} \right) \quad (1.8)$$

and

$$K_{\text{refl}} = n_{\text{refl}} \int_{T_{\text{sam}}}^{T_{\text{evap}}} c_v^g + \frac{1}{2}R \, dT \quad (1.9)$$

are gathered by components related to adsorbed (K_{ads}) and reflected (K_{refl}) molecules.

The discussion above implied small, *i.e.*, infinitesimal, coverage changes rendering $-\Delta_{\text{ads}}H$ the differential heat of adsorption. This work gets along exclusively with differential heats. A discussion about integral heats, useful for comparison with many computational methods, can be found elsewhere^[32,110,124].

Considering the nature of the investigated systems in this work, the previously usage of “heat of adsorption” needs to be extended from formation of an adsorbate to reaction of adsorptive with adsorbent. The latter shares the regular heat of adsorption and a possible *heat of reaction*. The major difference lies in the situation of final states. While the previous adsorbate formation implies a defined final state, *e.g.*, one carbon monoxide molecule binding with its carbon atom to one platinum atom embedded in a (111) surface in a linear geometry, the final state is intrinsically much less precise in case of heats of reaction, *e.g.*, reaction of calcium atoms with a polythiophene film. However, it is still necessary that the formed system relaxes sufficiently fast enough, *i.e.*, ideally within the sample time of one acquired data point, into the final state or a sufficiently long-lived intermediate, *i.e.*, metastable, state.

Due to the vague nature of the product structure, complementary surface characterizing methods become more important and higher requirements on computational models are necessary in order to obtain a complete picture of the involved processes.

The sample’s surface is usually covered by a polycrystalline film of the dosed metal in this work towards the end of an experiment. This establishes the rather well defined situation in which the metal vapor resublimates on its bulk material. Here, the obtained adsorption enthalpy equals the sublimation enthalpy at sample temperature and provides a sensitive internal reference.

1.3 Involved Principles

This experimental setup collects the benefits from several other calorimeters built by the groups of D. A. KING^[115,116], S. ČERNÝ^[117,118], C. T. CAMPBELL^[86,87,119]^[121,125], S. SCHAUERMANN^[122], and R. SCHÄFER^[126]. Subsequently, only the common instruments, differences, and improvements are pointed out, since a discussion of the individual calorimeter types can be found elsewhere^[9–11,105,106,110–112]. Technical details about the setup built and used in this work are given in Chapter 2.

1.3.1 Beam Source

The present calorimeter is optimized for studies concerning metal adsorption on organic thin films. A vertical arrangement of the evaporator is used in order to handle liquid metals and high filling levels. The system is designed to accept a commercial electron beam evaporator^[87,120] as well as a self made Knudsen cell evaporator^[86,119]. This construction feature distinguishes the presented work from most^[87] other calorimeters, which typically comprise horizontal beam arrangements^[86,115–119,126,127]. In case of dosed gases or high vapor pressure liquids, *e.g.*, cyclohexane, a horizontal alignment is preferable, since it has no distinct drawback and benefits from reduced spatial constraints.

The presented setup is capable of evaporating metals with high and medium vapor pressures as well as larger organic molecules. Special interest arises from the possibility of investigating *inverted* systems, *i.e.*, adsorption of typical substrate molecules on predeposited layers of reactive metals, or the formation of layered system comprising two different organic substances.

1.3.2 Infrared Radiation

Operation of the evaporators cause emission of infrared radiation⁹, due to the elevated temperatures. This radiation is absorbed by the sample and thus contributes to the recorded calorimetry signal. In order to separate the contributions two methods are reported. The first involves a rotating mass filter, letting only atoms pass and blocking photons^[120]. The standard method uses an infrared transparent material to block the particles completely, while a known or measured fraction of the radiation^[86,87] is transmitted.

⁹ Although visible light can contribute to the thermal radiation at high crucible temperatures, this work uses the term infrared radiation.

This setup uses the approach involving a transparent window. Further background on the influence of infrared radiation is presented in Section 5.8.1

1.3.3 Pyroelectric Detector

The system uses a detector based on a pyroelectric polymer brought in contact with the backside^[86,87,119,121,122,125,126] of thin sheet samples, *e.g.*, thin single crystals, or organic thin films produced on polycrystalline thin carrier materials, *e.g.*, oxidized aluminum foil. Another approach implemented in this setup and employed in this work uses molecular or polymer organic thin films fabricated directly on pyroelectric detector materials. Common materials are lithium tantalate^[115–118] and β -polyvinylidene fluoride^[53,56–61]. The latter one is used in this work mainly due to its lower cost and higher mechanical resilience.

The pyroelectric effect describes the reaction of a permanently electrically polarized material to temperature changes. A permanent, macroscopic polarization implies several requirements on the material. In the first place, the unit cell of the underlying crystal structure must be able to exhibit a dipole moment. This excludes all centrosymmetric crystal classes. Second, the polarization in the unit cell needs to occur spontaneously, which is the case in the polar crystal classes^[128]. Finally, a long range ordering of the individual dipoles is mandatory to achieve a macroscopic effect. Due to microscopic effects, *e.g.*, atomic vibrations in the unit cell, and macroscopic effects, *e.g.*, phase changes, the polarization is a function of temperature. The dependency of the macroscopic polarization \vec{P} on the temperature T defines the temperature dependent pyroelectric coefficient p , which can be expressed¹⁰ as

$$p_T = \left. \frac{d\vec{P}}{dT} \right|_T . \quad (1.10)$$

Since the observed temperature changes within one experiment are very small, the pyroelectric coefficient can be assumed to be locally constant. However, pronounced changes are possible in case of experiments carried out at different temperatures¹¹.

A detailed discussion of the pyroelectric effect in general^[128–130], its applications for detector polymers^[114,131], and specific properties of β -polyvinylidene fluoride^[132,133] can be found elsewhere.

Permanent polarization is defined as the vector field that expresses the density of

¹⁰ Since the direction of the polarization remains unchanged, the coefficient is commonly reported as a scalar.

¹¹ An increase by a factor of 2.5 has been found in this work by cooling β -polyvinylidene fluoride from ambient temperature to 80 K.

permanent dipole moments in a dielectric material. A dipole moment is given by the product of the displacement vector of two complementary charges and their absolute value. Implying a direction of the polarization perpendicular to the metalized surfaces of the detector, collection of these quantities identifies the polarization as charge per electrode area^[128].

Heat, either due to adsorption of molecules or absorption of electromagnetic radiation, deposited on the sample leads to an increased temperature of the sample and, due to the thermal contact, also of the detector. The value of the temperature change ΔT is related to the deposited heat Q_h and the absolute heat capacity C_h of the sample/detector assembly by

$$\Delta T = \frac{Q_h}{C_h} . \quad (1.11)$$

Equation (1.11) readily illustrates the necessity of small heat capacities for the sample and the detector as the temperature difference is the measured quantity and the deposited heat is fixed. As the used materials cannot be altered and the lateral extensions are irrelevant, *i.e.*, the heat is equally distributed over the whole *active area*, a sensitivity gain can only be achieved by a reduction of the sample thickness. However, a certain mechanical stability, and thus minimum thickness of both components, is required to establish the thermal contact between the detector and the sample. Deposition of thin films directly onto the detector polymer avoids the heat capacity of the sample sheet and thus leads to an increased temperature change upon an identical heat input. This is one aspect motivating the use of deposited thin films in this work.

With the assumption of a homogeneous polarization throughout the detector^[114], a change of the average temperature in the detector induces a charge Q_{el} on the electrodes with area A of the detector by

$$\frac{\delta Q_{el}}{A} = \delta P = p_T \cdot \delta T . \quad (1.12)$$

Since the geometry of the detector is constant, the generated charge is proportional to the temperature change δT .

The electrodes and the dielectric detector material, with the dielectric constant ε , form a parallel plate capacitor with electrical capacity $C_{el} = \varepsilon A/d$. Separation of the charge Q_{el} on the plates at a distance d leads to a voltage U_{el} given by

$$U_{el} = \frac{Q_{el}}{C_{el}} = d \cdot \frac{Q_{el}}{\varepsilon \cdot A} \quad (1.13)$$

which is proportional to the electric charge. Combination of Equations (1.11), (1.12), and (1.13) results in

$$U_{\text{el}} = d \cdot \frac{Q_{\text{el}}}{\varepsilon \cdot A} = d \cdot p_T \cdot \delta T = \frac{d \cdot p_T}{C_h} \cdot Q_h \quad (1.14)$$

and proves proportionality of the measurable voltage output U of the detector to the heat deposited in the detector Q_h .

The temperature changes are tiny. This leads to minimal voltage responses of the detector which are difficult to measure and require extreme input impedance amplifiers. As can be seen from this discussion, *i.e.*, by the usage of *changes*, this detector cannot be operated in continuous mode and hence requires a pulsed input.

At this point, it should be mentioned that the pyroelectric effect is always associated with the piezoelectric effect^[128] but not *vice versa*. The latter effect is describing the electrical response of a material to mechanical stress. A detailed discussion on the piezoelectric effect, even for the here used detector material, is given elsewhere^[130,134]. Summarizing, the piezoelectric effect causes an electric signal upon mechanical stress which cannot be separated from the desired pyroelectric signal. Hence, great care must be taken to avoid mechanical stress in the sensor. While vibrations can be damped by the experimental setup, mechanical strain due to processes on the detector surface itself can not be avoided. Thus, an additional signal component is expected in case of pressing, bending, or stretching^[135] of the detector.

1.3.4 Detector Calibration

The influences of all constants, geometries, and material properties involved in the setup are bypassed by the usage of calibration measurements.

The defined wavelength of a laser as light source facilitates a precise power measurement and thus an energy determination. Typically, red lasers, either helium-neon-gas laser^[86,87,116,121,122,125] (632.8 nm) or lasing semiconductors^[117,118] (670 nm), are reported in literature for this purpose. Since the reflectivity of many metals^[136–138] is very high at these wavelengths (> 0.9), the relative errors of the corresponding absorption become rather large¹². In order to circumvent this challenge, this work uses a semiconductor based laser with purple light (405 nm). Generally, the reflectivity at this wavelength is smaller for a wide range of materials. This renders a higher accuracy of the detector calibration possible.

¹² An absolute error of 0.01 at a reflectivity of 0.95 becomes a relative error of 20% in the corresponding absorption.

1.3.5 Pulsing

All systems rely on a pulsed heat input and thus on a pulsed molecular beam. Various methods have been utilized to interrupt the molecular flow including rotating discs operated from air side^[86,119] and vacuum side^[87], air side operated slides^[115,116,118], vacuum side operated blades^[127] (also used in this work), and even piezoelectric plunger valves^[126]. The mechanism used for pulsing the adsorptive is also employed to generate a defined heat input. Identical spatial and temporal properties are obtained by guiding laser light along the molecular beam path. The use of a stepper motor driven chopper blade enables this setup to control the pulse repetition rate and pulse duration independently.

1.3.6 Deposition Rate Measurement

The total amount of substance leaving the beam, which would impinge on the sample, is measured with commercial quartz crystal micro balance^[86,87,119], since stagnation gauges^[115,116,122,126] are not applicable for condensing matter. The provided layer thickness on the oscillator crystal is derived from the resonance frequency by the viscoelastic extension^[139,140] to the Sauerbrey theory of loaded crystal oscillators^[141]

$$d_F = \frac{\varrho_Q}{\varrho_F} \cdot \frac{N_Q}{f} \cdot \frac{Z_F}{\pi Z_Q} \cdot \arctan \left(\frac{Z_Q}{Z_F} \cdot \tan \left(\pi \frac{f_0 - f}{f_0} \right) \right) \quad (1.15)$$

using the densities of quartz ϱ_Q and the film ϱ_F , the frequency constant of quartz N_Q , corresponding to the orientation of the *cut* of the crystal, and the nominal center frequency f_0 of the unloaded oscillator circuit. In case of identical acoustic impedances of the film Z_F and of quartz Z_Q , Equation (1.15) is reduced to the *period measurement* equation

$$d_F = \frac{\varrho_Q}{\varrho_F} \cdot \frac{N_Q}{f} \cdot \frac{f_0 - f}{f_0} = \frac{\varrho_Q}{\varrho_F} \cdot N_Q \cdot (\tau - \tau_0) , \quad (1.16)$$

which is typically used in case of an unknown acoustic impedance¹³, providing a linear relation of the film thickness and the change of oscillation periods $\tau_0 - \tau$. In these cases, a good agreement^[139] is still given, if the frequency shift amounts to less than 15 %, which corresponds to 900 kHz for the used *AT*-cut 6 MHz crystals in this work. The associated crystal frequency of 5.1 MHz is coincidentally used by the controlling unit to detect the *end of life* load of the crystal^[142]. Equations (1.15)

¹³ Alternatively, the acoustic impedance of the film is set to the same value as for quartz, resulting in the same equation.

and (1.16) imply a decrease of the resonance frequency, if material is deposited onto the sensor crystal.

The reported high accuracies^[139,140,143] apply to studies involving a homogeneous deposition on the whole “front” surface of the oscillator crystal or, at least, a covered area, which fully overlaps the back-electrode^[141]. As the experimental setup involves a beam diameter smaller than this critical dimension, its influence is not negligible^[143,144]. Since this limitation is only present in rare cases¹⁴, there is not much literature present covering this issue^[141,143–145].

Summarizing, the area of deposition *concentric* to the back electrode influences the sensitivity of the instrument and a correction from an empirically sigmoid fit of the data given in Reference [141] needs to be applied. Additionally, an off-center deposition causes additional sensitivity losses^[141,144,145] and should be avoided.

1.3.7 Sticking Measurement

Knowledge of the actual deposited amount of substance is vital to compute two properties together with the known dosage per pulse. On the one hand, the amount of adsorbed and reflected molecules is necessary to calculate the heat of adsorption, as discussed in Section 1.2. On the other hand, the adsorbed fraction of the dosed molecules is essential for calculating the coverage of the dosed species on the sample for every pulse.

A well established method to determine coverage dependent sticking probabilities is described^[146] by D. A. KING and H. G. WELLS. It uses a sensor without direct view to the sample and the beam source. The sticking factor is derived from the different pressure readings obtained with and without sample in the beam path. This method utilizes the integrating and inert properties of the vacuum chamber to eliminate a possible angular dependency of the scattered species.

Since this established method is not applicable for metal vapors as they are effectively pumped away by the walls of the vacuum system. Hence, a modified approach^[86] was introduced by C. T. CAMPBELL and is adopted for other calorimeters^[87,119,122] including the one presented in this work. A mass spectrometer is placed at 35° from the surface normal which is collinear with the incident beam.

The use of this specific geometry is motivated since it is known that the angular distribution of molecules desorbing from a surface can vary widely from desorbate to desorbate and for different substrates^[147]. However, these distributions can be approximated by summation over (fractional) powers of cosines^[123], typically with

¹⁴ In general, the experimental conditions can be adjusted to provide full-area deposition.

one or two dominant summands^[147]. Variation of the detection angle allows for a minimization of the influence of the usually unknown exponents and results in this so-called *magic angle*^[147]. The desorption characteristics depend on the properties of the surface, which is altered during this kind of experiment. The adsorption on the sample changes the surface composition from pure substrate to, at sufficiently high coverages, entirely adsorbate. It should be mentioned in this context, that neither of the relevant surfaces, the organic thin film constituting the sample nor the hot plate for the reference measurement, are atomically flat. In the ideal picture, elastically scattered species^[123] would be reflected back into the molecular beam. Thus, they are unable to reach the mass spectrometer and hence cannot be detected. Surfaces with a finite roughness exhibit surfaces with a ranged random orientation. This leads to a superposition of many geometries and could even lead to a contribution of elastically scattered molecules to the signal. As the discussed processes might lead to an unpredictable variation of sensitivity, a reduced dependency on the desorption characteristics is highly desirable.

2 Experimental Setup

The major goal of this work is to design, realize, and test all the components of an ultra high vacuum apparatus for measuring heats of adsorption on single crystals and on organic thin films. Additionally, IGOR PRO procedure packages for data treatment and status monitoring had to be developed.

The tasks and handling of the individual components are described in this chapter. Parts and assemblies in the figures are labeled with capital letters in Gothic print¹. Subordinated components, such as parts within an already labeled parent assembly, are addressed with lower case characters as index. If applicable, the index uses the same letter as in the figure describing the more detailed view.

The setup presented in Figure 2.1 places emphasis on the adsorption of metals with relatively high vapor pressures on organic thin films.

The focus can be adjusted to study the adsorption of organic molecules on single crystals by minor changes. Details therefore are given in the descriptions of the relevant features of this machine.

In contradiction to the initial design^[106], only a minimum configuration was realized with one beam/calorimeter section and no surface characterizing devices in this work. New constructed components, *i.e.*, all the presented devices in this work, had to align with the previously constructed parts^[105,106], *i.e.*, the main chamber and the supporting frame, and the existing equipment, *i.e.*, a mass spectrometer, pumps, *etc.*

The system comprises the main chamber, the molecular beam, and the load lock. The main chamber is used for the calorimetry related measurements and sample preparation, especially sample cleaning. The molecular beam provides the adsorbent and the load lock serves for introduction and storage of samples as well as for sample preparation by physical vapor deposition (PVD). In future, the system might be extended by a manipulator stage in the main chamber to improve the possibilities for sample preparation. Desirable are also surface characterizing techniques, *e.g.*, Auger electron spectroscopy (AES), photoemission spectroscopy (PES/XPS), low energy electron diffraction (LEED), low energy ion scattering spectroscopy (LEIS),

¹ Due to the strong resemblance of some letters to another, E, J, O, Q, S, and V are omitted in the labeling sequence.

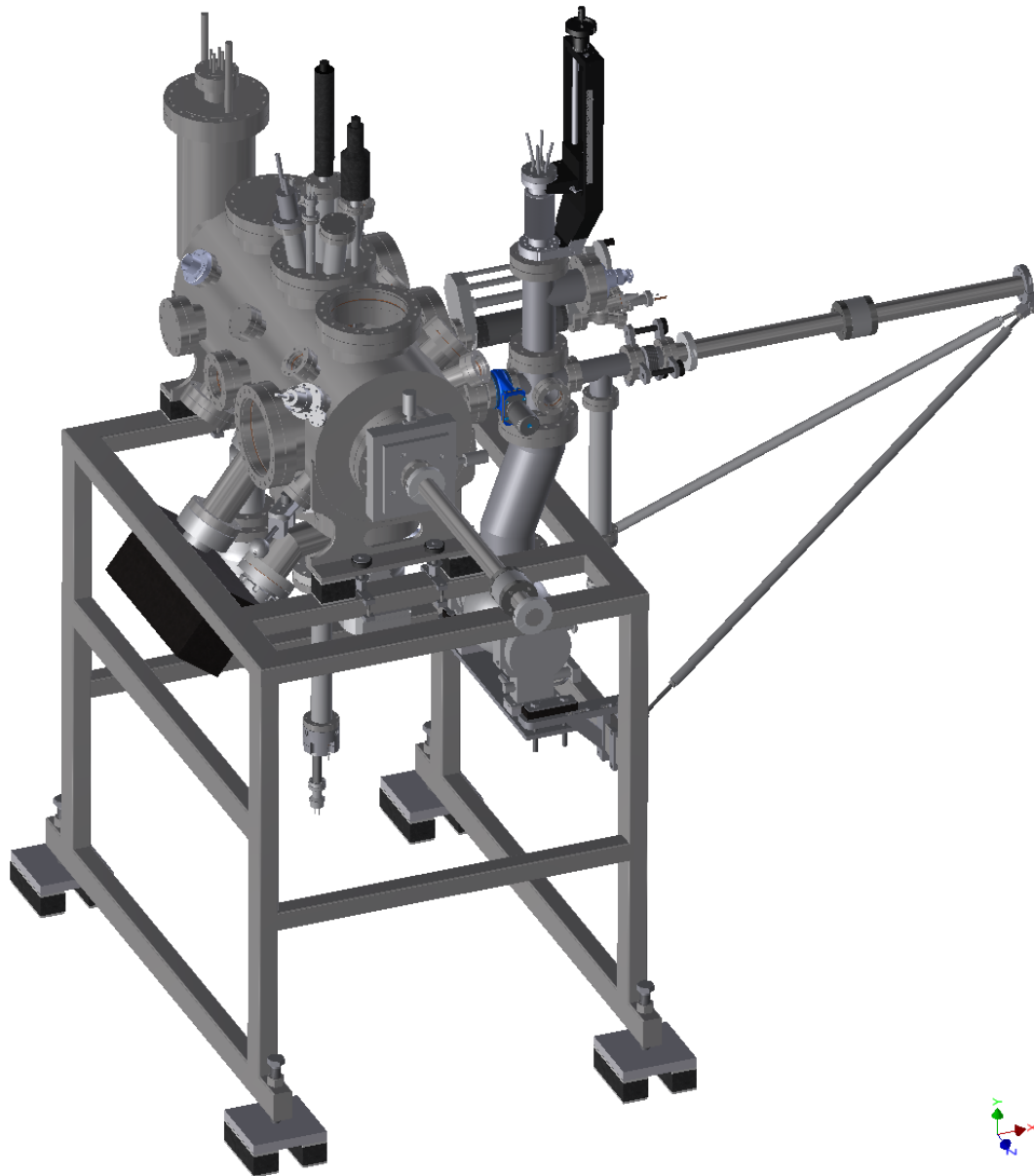


Figure 2.1: Assembly of the NAC System — The design of the assembled Nanojoule Adsorption Calorimeter system is illustrated as a computer generated image. The individual features are labeled in Figures 2.64 and 2.65. Details are discussed below.

etc., and imaging techniques such as atomic force microscopy (AFM).

Sources of supply and mounting instructions are usually given in the captions of the exploded views. Manufacturing and modifications on purchased parts has mainly been performed by the in-house mechanical workshops of the universities in Erlangen and Marburg. Some more complex parts, *e.g.*, the molecular beam housing shown in Figure 2.30, have been produced by the central mechanical workshop of

the university in Erlangen.

The standard material for machined parts is stainless steel 1.4301 which is commonly used in ultra high vacuum systems. Cooling lines and pieces that are supposed to be chemically cleaned, *e.g.*, orifices with magnesium residues being cleaned in diluted nitric acid, are usually made from the more corrosion resistant stainless steel types 1.4541 or 1.4571. Components requiring high thermal conductivity are made from copper or aluminum. If mechanical strength is required at the same time, copper beryllium bronze is used. Electrically isolating parts are usually made from Macor[®], *i.e.*, a machinable glass ceramic. Heating wires and their hookups are made from tantalum, which is preferred over the commonly used tungsten since it is easier to spot-weld and does not become brittle upon heating.

Power lines are usually made from loud speaker twin cables² and 4 mm-banana-plugs. Data connections are mainly established *via* RS-232 standard cables. Data acquisition is carried out by a dedicated measurement card³ controlled by a LABVIEW-application⁴. Two analogue channels record the analogue output from the controller of the mass spectrometer and the amplified detector signal. The connection between the devices is established by coaxial cables and thus referenced to ground. In order to increase the signal quality of the calorimetry channel this link should be altered to a differential design.

Standard screws to tighten CF connections are omitted in the figures to improve clarity. *Top, left, etc.* refers to a laboratory coordinate system whereas *north, east, etc.* refers to directions in the figures. Coverages are given in monolayers (ML) and/or meters. Deposition rates are stated in deposited meters per second or monolayers per second (^{ML/s}) and are proportional to the corresponding fluxes since the relevant deposition regions have constant area.

Here, one monolayer is defined as a closed packed layer of atoms in a specified plane. The typically used plane is the closest packed plane for the most stable phase at room temperature, *i.e.*, the (111) plane for metals with cubic and the (0001) plane for metals with hexagonal crystal structure, *e.g.*, copper and magnesium, respectively. Both structures with their primitive spatial and corresponding planar unit cells are shown in the description of the used materials in Figures 6.1 and 6.2.

Unfortunately, all devices are attached to the NAC machine and were not available for taking pictures.

2 '607012' $2 \times 2.50 \text{ mm}^2$ from Conrad Electronic SE.

3 'PCI-6221 (37pin)' from National Instruments Germany GmbH.

4 Programmed by H. ZHOU.

2.1 Sample Holder

Two versions of sample holders can be used in the current setup. The first one was originally intended to be used with thin single crystals analogue to other calorimeters^[121]. It consists of a solid copper body holding the single crystal, which is spot-welded between two thin tantalum sheets, as shown in Figure 2.2. Its usage can be extended to, *e.g.*, organic, thin films created by physical vapor deposition on polycrystalline metal sheets. In this case all parts of the sample holder are made from aluminum. The thickness of the sample material should not exceed 100 μm and the samples should have a minimum diameter of 10 mm. Single crystals with these dimensions are commercially available⁵. The use of transparent substrates is not possible since they are incompatible with the calibration process, see Section 3.5.4.

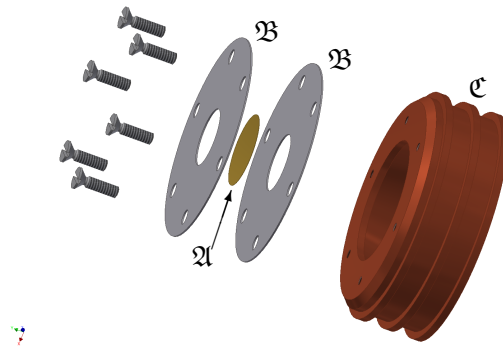


Figure 2.2: Assembly of the Sample Holder for Crystals — A single crystal (α) or other thin sheet material is spot-welded between two tantalum^a sheets (β) and fastened on the copper sample holder (ϵ).

a ‘ASTM B708’ 0.2 mm from STS Metalle GmbH.

Separation of the detector ribbon from the sheet material samples allows the use of standard preparation techniques, especially annealing and thermal cleaning. Due to the loss of polarization of the involved detector materials at approximately 400 K for β -polyvinylidene fluoride^[148] and at approximately 930 K for lithium tantalate^[149], a permanent bonding of the sample to the detector is often not desirable.

As a substrate for thin films, prepared by physical vapor deposition, discs with 12 mm diameter punched from 30 μm laboratory aluminum foil⁶ seem to be promising. They are readily available, cheap, and rather smooth. Additionally, they are as pure as other standard materials (min. 99%), passivated by a thin but closed layer of aluminum oxide, and rigid enough not to wrinkle. If desired, it is possible to clean the

5 MaTecK GmbH.

6 ‘2596.1’ from Carl Roth GmbH + Co. KG.

aluminum disks by sputtering⁷ to remove a small carbon containing contamination, see Figure 5.4.

The second version is built up from an aluminum body and contact pieces isolated by Macor[®] and Kapton[®] parts. Poled and metalized β -polyvinylidene fluoride punched as 12 mm disks from sheet material are clamped between an aluminum cover and the inner contact piece as depicted in Figure 2.3. Since the detector polymer is poled, it exhibits a positive and a negative side. Hence, mounting it upside down results in a signal with constant opposite polarity. Since the data treatment process is independent of the absolute polarity, see Chapter 3, this polarity change does not affect the experiment.

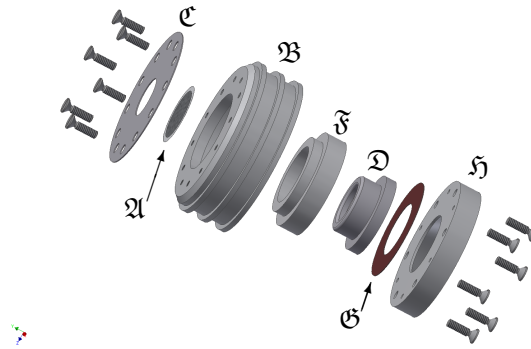


Figure 2.3: Assembly of the Sample Holder for Thin Films — The β -polyvinylidene fluoride^a detector disc (A) is held on the body (B) by a thin aluminum disc (C) from the front. It is contacted by an aluminum piece from the backside (D), isolated by pieces of Macor^{®b} (E) and Kapton^{®c} (F). This stack is held in place by another aluminum piece (H).

a ‘28um/w 400CU/150NI’ from Measurement Specialties.

b ‘158-3102’ from RS Components GmbH.

c ‘500HN’ 125 μm from Katco Ltd. – Lohmann Technologies UK Ltd.

Sputtering, as described for the above mentioned thin sheet samples, is also possible for this kind of sample in order to enhance the thin film quality. Removing the outer perimeter of the detector discs by chemical etching⁸ – as recommended for single crystal samples^[121] – to prevent electrical short circuits between the two metal layers is not necessary.

Since the detector is included in the sample assembly, it is as transferable as a regular sample. Hence, it is possible to protect the pyroelectric material from the thermal load, and thus from degradation, during bake-out routines by relocation in the load lock. It might be worth to consider a transferable detector head for thin

⁷ $E_{\text{kin}} = 3 \text{ keV}$, $p = 1 \cdot 10^{-4} \text{ Pa}$, $t = 10 \text{ min}$.

⁸ Etched for 10 min. in 0.2 mol/L nitric acid at ambient temperature; rinsed with deionized water.

sheet samples as well, see Figure 2.6, in order to avoid accidental degradation during the conditioning of the vacuum system. It would also reduce the downtime of the experiment in case of failure of the detector ribbon.

The body pieces of both sample holders, and among them the sheet sample or the front side of the thin film sample, are on ground potential while being transferred or during calorimetric measurements. A floating acceptance for samples – on which sputter currents *etc.* could be measured – was planned on a manipulator stage but not realized yet. The conical inner face, in combination with the corresponding detector head, provides a self aligning approach mechanism. This property is necessary to establish a reproducible detector/crystal contact which is indispensable for a precise measurement.

Design drawings with dimensions and materials for both types of sample holders can be found in Appendix B.2.1.

2.2 Detector Stage

The detector assembly is mounted on a custom made 150CF flange, which is equipped with four 16CF and five 40CF flanges, see Figure 2.4. The thermal reservoir, see Figure 2.5, is mounted on the vacuum side of the base flange. Threaded steel rods hold the fixed copper piece with the fluid connectors and provide thermal insulation. Two additional pieces made from copper allow adjustment of the sample position in three spatial directions. The assembly is designed to be operated between a lower⁹ limit of 80 K and an upper¹⁰ limit of 370 K. Desired temperatures between these limits can be established by an external thermostat.

Copper braids attached to the thermal reservoir also provide temperature alignment for the detector head, see Figures 2.6 and 2.7, as well as the sample heater, see Figure 2.8. The use of copper for all pieces near the sample provides a uniform temperature which can be monitored by two thermocouples, one on the sample reception and one on the detector head. The massive copper construction provides a passive way to stabilize the temperature of the calorimeter.

Another benefit from the possibility of the temperature adjustment results in an increased maximal bake-out temperature of the system equipped with the detector for thin sheet samples. An upper limit is given by the degradation temperature of the used pyroelectric material, *e.g.*, 370 K in case of β -polyvinylidene fluoride. Cooling of the reservoir to 350 K in combination with a cap, which is inserted in sample position protecting the otherwise exposed ribbon, should render typical system conditioning temperatures of 450 K for the remaining parts possible.

In order to minimize piezoelectric noise from the detector a wobble free contact between the sample acceptance, the sample, and the detector head is essential. This is ensured by a spring suspended mount for the detector head, see Figure 2.9. Three guided springs separate the part attached to the linear shift from the mounting stage for the detector head to allow for small angular movement. The large wire diameter of the springs results in a high spring stiffness enabling the transmission of large forces onto the sample and its acceptance. This improves mechanical stability as well as thermal conduction in this arrangement. It also enhances the reproducibility of the positioning of the detector head to the sample.

Each of the two sample holder variants has a designated detector head. The assembly used with single crystals or thin sheet material is shown in Figure 2.6. The design is analogue to the design presented in [121]. Etched ribbons¹¹ made

⁹ Cooled with liquid nitrogen.

¹⁰ Heated with water or silicone oil.

¹¹ Dimensions are given in Appendix B.2.3.

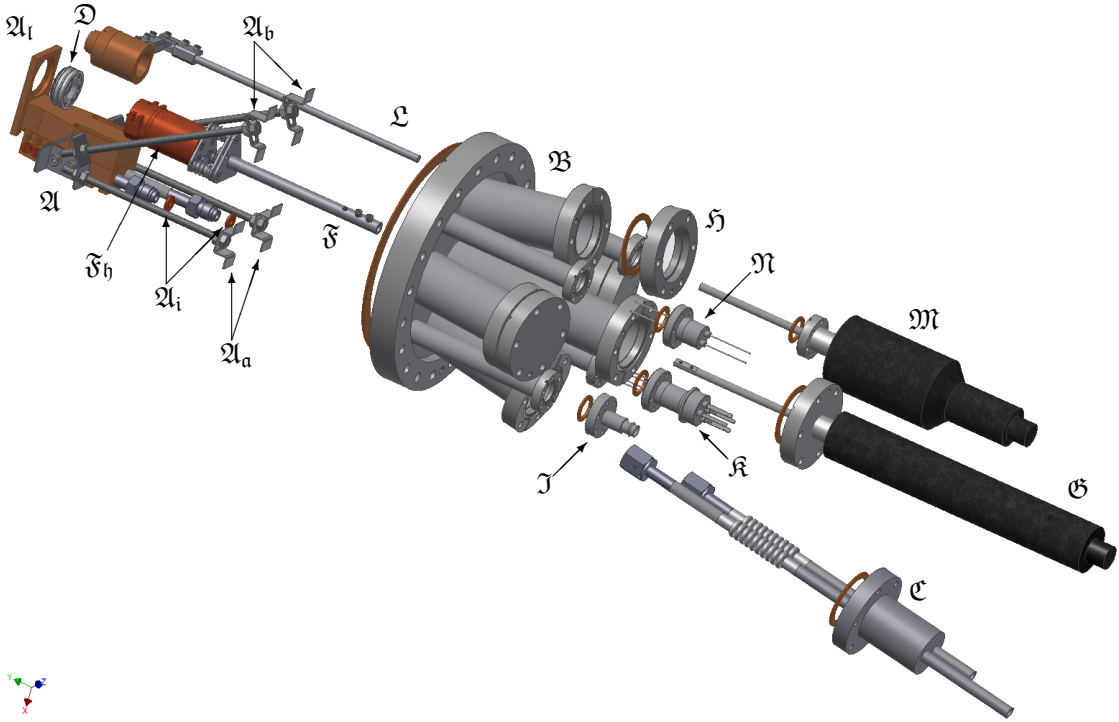


Figure 2.4: Assembly of the Detector Stage — The fixtures (\mathcal{A}_a , \mathcal{A}_b) of the thermal reservoir (\mathcal{A} , Figure 2.5) is welded to the vacuum side of the base flange (\mathcal{B}) and connected with custom copper gaskets (\mathcal{A}_i) to fluid feedthroughs on a 40CF flange (\mathcal{C}) for an external heating/cooling system (not shown). The sample holder (\mathcal{D} , Figures 2.2 or 2.3) is inserted into the sled on the reservoir (\mathcal{G}). The detector mount (\mathcal{F} , Figure 2.9) with its actuator^a and detector head (\mathcal{F}_h , Figures 2.6 and 2.7) are fixed on the central 40CF flange. A 40CF window (\mathcal{H}) is mounted opposite to the thermostat feedthrough (\mathcal{C}). The other 40CF flanges are sealed by blind flanges. A BNC^b (\mathcal{J}) and a twin Type K thermocouple feedthrough^c (\mathcal{K}) are mounted close to the thermostat feedthrough (\mathcal{C}). The remaining 16CF flanges carry the heater assembly (\mathcal{L} , Figure 2.8) with its actuator^d (\mathcal{J}) and its power feedthrough^e (\mathcal{M}).

a ‘BLM-275-4’ from MDC Vacuum Products, LLC.

b ‘A0237-2-CF’ from MPF Products, Inc. *via* tectra GmbH.

c ‘A0407-2-CF’ from MPF Products, Inc. *via* tectra GmbH.

d ‘BRLM-133’ from MDC Vacuum Products, LLC.

e Similar to ‘A0261-3-CF’ from MPF Products, Inc.

from oriented, poled, and metalized β -polyvinylidene fluoride are stacked together with Kapton[®] and copper pieces as shown in Figure 2.6. Additional Kapton[®] bits are added at the sides to isolate the inner contacts from the grounded body pieces. Upon assembly, it is important to pay attention to the correct polarity of the ribbons, *i.e.*, which side is facing the crystal, and proper flush alignment of the arcs. This stack is inserted in the main body part and tightened with a screw matching the

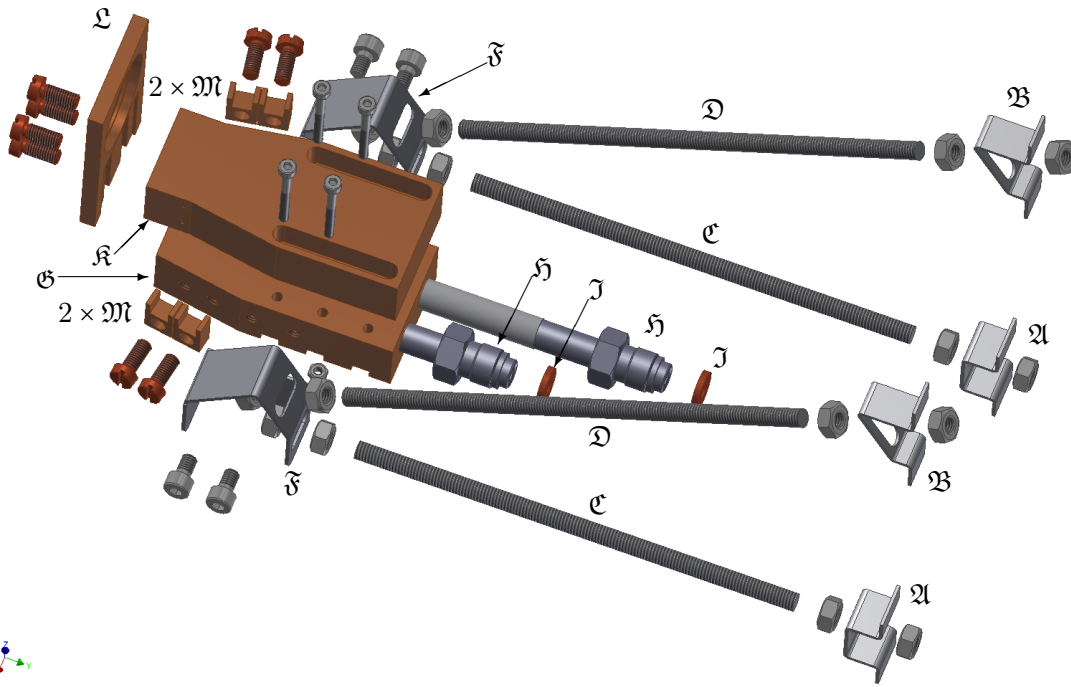


Figure 2.5: Assembly of the Thermal Reservoir — A custom made base flange (not shown, see Figure 2.4) with welded fixtures (A, B) holds the thermal reservoir (copper) with four threaded rods (C, D) on laterally adjustable shackles (F). The reservoir consists of a base part (G) equipped with VCR^{®a} connections (H) used with custom made copper gaskets (I) and an adjustable sled (K) carrying the moveable sample reception (L). The steady part also carries copper braids (M, only connector blocks shown) used to temperate the calorimeter head (not shown, see Figures 2.6 and 2.7). Joints with a desired high thermal conductivity are equipped with copper screws.

a '6LV-4-HVCR-1-6TB7' from HPS Handels GmbH.

ribbons with the sample. For maximal signal intensity the contact area should be maximized. This can be achieved by a small deformation of the ribbons as shown in Figure 2.10.

The head piece for thin films acts only as a contact, as shown in Figure 2.7. The spring loaded inner pin presses on the inner conductor piece of the thin film sample holder. Due to the adaptive behavior of this connection, it is also able to compensate thermal expansions and maintain a stable connection even upon temperature changes. These inner pieces are isolated from the grounded body by Macor[®] parts.

This variant eliminates the thermal resistance between the thin substrate material and the detector material leading to an increased sensitivity. A further increase is devoted to the reduction of total heat capacity, since the thin sheet material is absent. The overall simpler design and the expected higher sensitivity led to the

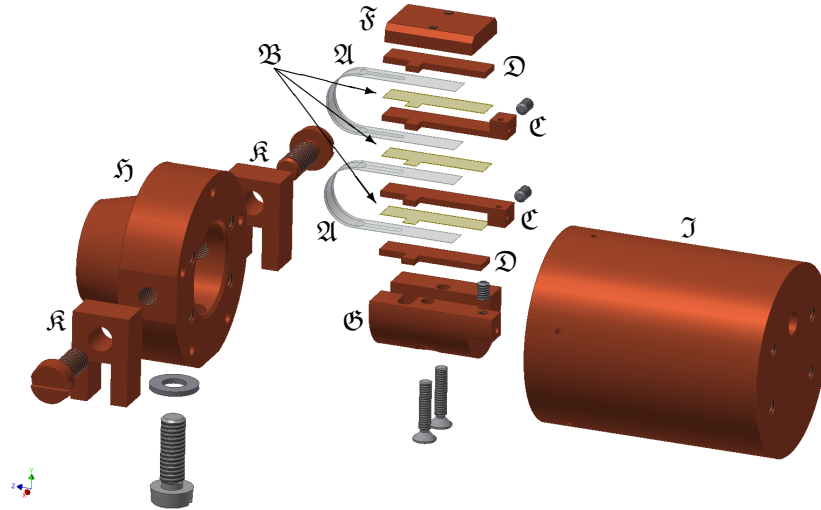


Figure 2.6: Assembly of the Detector for Crystal Samples — Two etched β -polyvinylidene fluoride^a ribbons (\mathcal{A} , silver) are stacked together with Kapton^{®b} isolation pieces (\mathcal{B} , yellow) to a temporary tripolar setup. The outer coating remains on ground whereas the other surfaces are in contact with two pickup electrodes (\mathcal{C}) connected to a coaxial cable^c. Electrical contact to the air side amplifier (not shown) is established by a BNC-feedthrough^d (not shown). The detector stack is completed by two copper plates (\mathcal{D}) and held together by two copper half shells (\mathcal{F} , \mathcal{G}) inserted into the housing part (\mathcal{H}). A copper cap (\mathcal{I}) added to the mounting assembly (Figure 2.9) provides electrical shielding as well as an increased heat capacity. Optional copper braids (\mathcal{I} , only connector blocks shown) provide thermal contact to the thermal reservoir. Isolation material on the sides of the stack is not shown for clarity.

a ‘FV301890/1’ from Goodfellow GmbH – discontinued.

b ‘500HN’ 125 μm from Katco Ltd. – Lohmann Technologies UK Ltd.

c ‘KAPWC1X025’ from LewVac Components Ltd.

d ‘A0237-2-CF’ from MPF Products, Inc. *via* tectra GmbH.

decision to install this detector head version for the presented work.

Both built detector heads are equipped with mounting options for copper braids allowing temperature alignment with the reservoir. Electrical shielding is provided by a copper cap on the backside of both assemblies. Their massive design also provides additional heat capacity which helps to maintain the temperature while the head is disconnected from the sample, *e.g.*, for sputtering.

The detector stage is also equipped with a sample heater as depicted in Figure 2.8. The filament is approaching the sample, which is mounted in a sheet material holder, from the backside without touching it. The copper housing can be cooled using copper braids attached to the thermal reservoir. It is designated to remove adsorbates like carbon monoxide on single crystal samples by short but intense

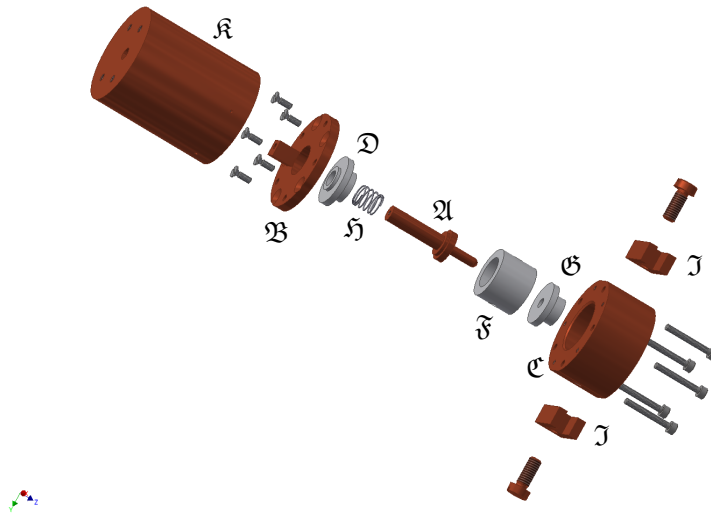


Figure 2.7: Assembly of the Detector for Polymer Samples — A copper pin (\mathfrak{A}) is isolated from the grounded housing (\mathfrak{B} , \mathfrak{C}) by three Macor^{®a} pieces (\mathfrak{D} to \mathfrak{F}). A spring (\mathfrak{H}) presses the pin on the back contact of the sample holder (not shown) establishing a stable contact. The temperature of this setup is aligned to the temperature of the reservoir by attached copper braids (\mathfrak{J} , only connector blocks shown). A copper cap (\mathfrak{K}) added to the mounting assembly (Figure 2.9) provides electrical shielding as well as an increased heat capacity.

a '158-3102' from RS Components GmbH.



Figure 2.8: Assembled Heater for Crystal Samples — Assembled heater for crystal samples as designed by O. LYTKEN with a linear/rotational motion feedthrough^a and a light bulb^b filament for sample heating.

a 'BRLM-133' from MDC Vacuum Products, LLC.

b 'Osram HLX 64655 EHJ 24V 250W' from HANS RAUM GmbH.

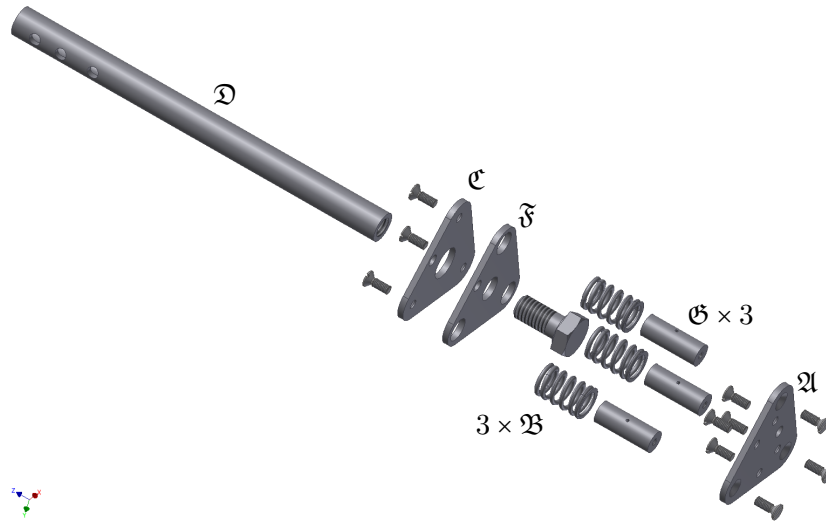


Figure 2.9: Assembly of the Spring Suspended Detector Mount — To ensure planar, wobble-free contact of the sample holder (not shown, see Figures 2.2 and 2.3) and the detector head (not shown, see Figures 2.6 and 2.7), the mounting plate (A) is suspended by three guided springs (B) countered by a plate (E) sliding over the connection rod (D). This allows for compensating small angular misalignment in combination with transmission of large forces induced by the pressing plate (F) sliding along the guidance pieces (G). This assembly is completed by a linear shift^a (not shown) connecting the spring stage to the base flange (not shown, see Figure 2.4).

a ‘BLM-275-4’ from MDC Vacuum Products, LLC.

heating also known as “flashing”. The goal is to keep the sample holder as cool as possible while heating the crystal above the desorption temperature of the adsorbate. This heater setup is designed for radiative heating. It can be extended to electron bombardment heating if a floating filament power supply is used.

The amplifier, used to convert the charge on the detector polymer into the acquired voltage, is plugged directly onto the BNC feedthrough on the flange. This minimizes unwanted electrical capacity in the detector circuit. An additional capacity would cause a decrease of the signal along with an increase in the time constant of the amplifier requiring a smaller pulse repetition rate and thus a longer experiment time. The direct mounting also reduces the risk of triboelectric noise in the system. In order to avoid thermal drift, the amplifier should be separated by StyrofoamTM, or a similar material, from the feedthrough used to stabilize the temperature of the thermal reservoir.

Design drawings with dimensions and materials for the detector stage can be found in Appendix B.2.3.

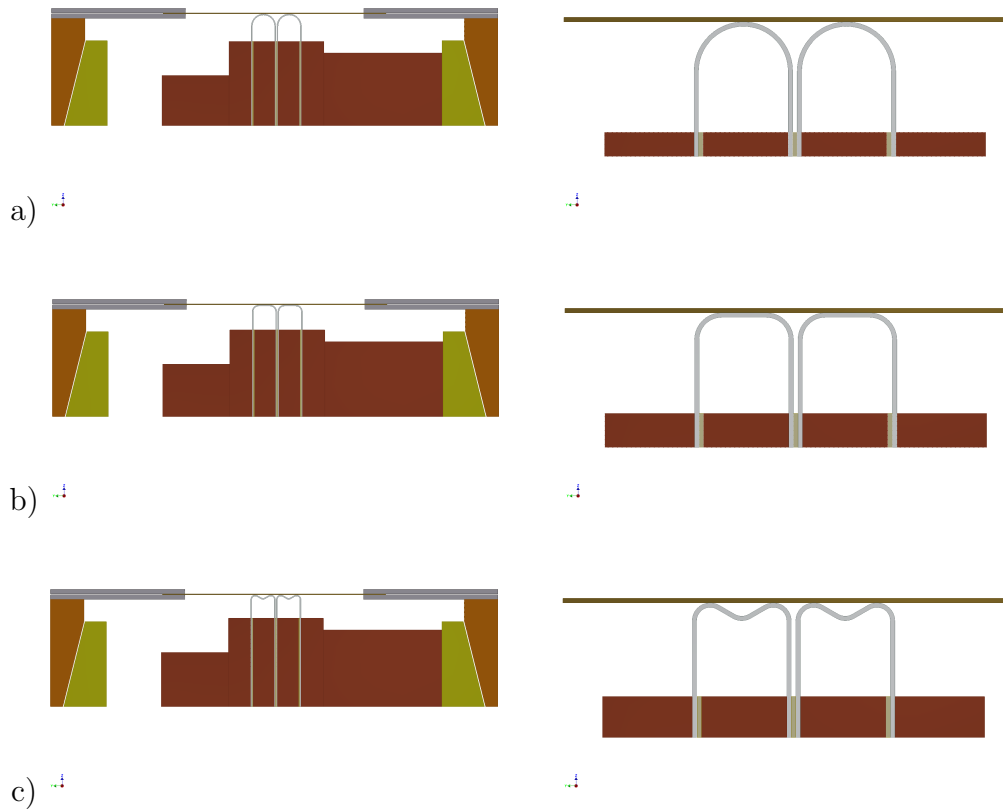


Figure 2.10: Sample/Ribbon Contact Cases — A detailed view of the possible sample/ribbon contacts is given for thin sheet specimen. The sample is sandwiched between its mounting sheets (gray) on the sample holder (orange). The position of the outer head piece (yellow) to the sample is fixed. The alignment of the ribbon can be adjusted by moving the inner detector stack (copper) of the detector head (Figure 2.6). a) Insufficient pressing – the contact area is too small. b) Good alignment – the ribbon adapts to the sample. c) Excessive pressing – the ribbon curls back.

2.3 Molecular Beam

The molecular beam, as shown in Figure 2.11, comprises the main evaporator as an adsorbate source, a beam chopper to pulse the source, an optics stage to reflect the calibration laser onto the sample, an inline valve to separate the compartments, and two pumping stages. This source was designed to be capable of evaporating molecular substances, *e.g.*, perylenetetracarboxylic dianhydride (PTCDA), and metals, *e.g.*, calcium, with suitable vapor pressures. Although metals usually evaporate as atoms and only metals have been used as adsorbates in this work, this paper refers to the source as *molecular beam*. Since organic molecules decompose at elevated temperatures their reachable vapor pressure is limited. In order to provide a sufficiently high flux the beam housing has a very compact design to minimize the distance between the sample and the evaporator. In this context, the constraints of the already manufactured main chamber as well as the requirement of separable compartments have to be taken into account.

As an alternative evaporation source the beam housing is able to accept an electron beam evaporator¹² for substances with lower vapor pressures, *e.g.*, copper. The benefit of accessing these materials is paid by a much shorter run-time per crucible filling. Due to the required high fluxes, severe deposition of the material in the evaporator is inevitable. This led to a failure of the filament after a few experiments by means of copper deposition on the running filament. The use of this source has been successfully tested but comprehensive service is *often* necessary.

2.3.1 Main Evaporator

The base flange of the Knudsen-cell type main evaporator exhibits several special features, as shown in Figure 2.12.

To provide an individual mount of the evaporator and its heat shield, see Figure 2.13, it contains clearances for the mounting screws of the heat shield. It provides an off center 16CF port for mounting thermocouple feedthroughs. A reception for the crucible is located on the 40CF side. Its hexagonal shape allows easy tightening of the crucible mount with standard wrenches. Apart two welded power feedthroughs, this piece is machined from the solid. Two nuts, each together with an aluminum ring, form compression fittings grasping the crucible.

Several versions of crucibles are possible, depending on the requirements of the evaporant, *e.g.*, reactivity, wetting behavior, evaporation temperatures, *etc.* In order

¹² ‘EFM-4’ from FOCUS GmbH *via* Omicron NanoTechnology GmbH.

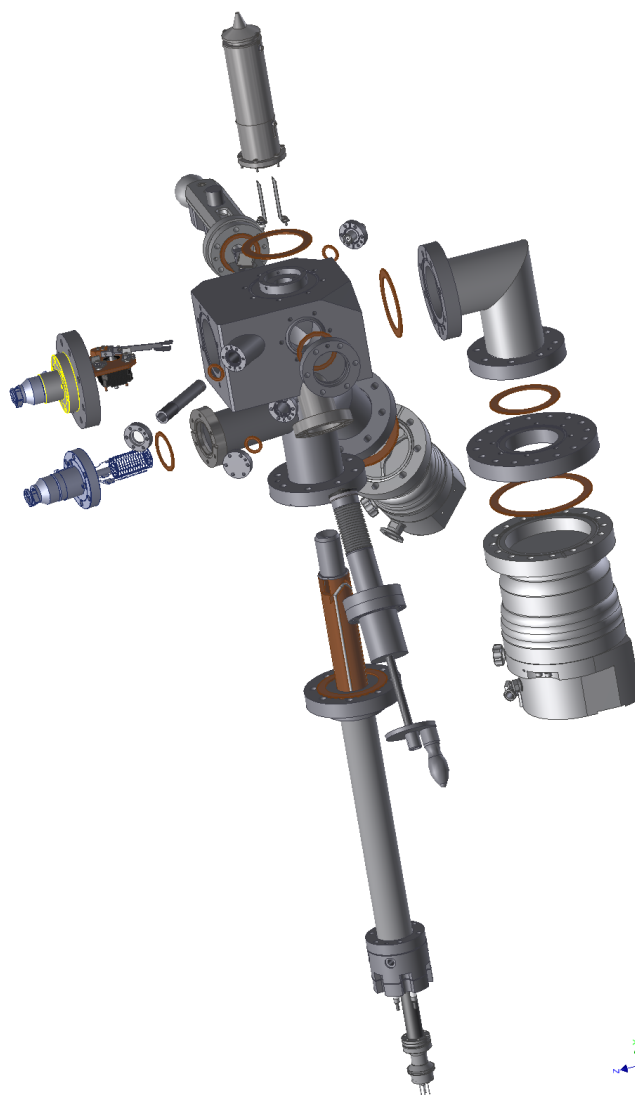


Figure 2.11: Assembly of the Molecular Beam — Detailed mounting instructions, recommended to assemble the molecular beam, are given in Figures 2.31, 2.32 and 2.33.

to stabilize the temperature of the crucible, one main and one backup thermocouple are attached to the crucible. If necessary, *e.g.*, if spitting of the evaporant occurs, see Section 5.6, the evaporant can be topped with a plug made from stainless steel wool or quartz glass fiber.

Upon evaporation of material, a layer of residues, *i.e.*, carbon or oxides, builds up on top of the evaporant and might exhibit a different infrared emission than the initial material. Since the top material is facing the sample, changes in its emission behavior have a direct influence on the measurement and should be avoided. The plug on top of the evaporant provides a changeless surface and minimizes changes in the infrared emission characteristics of the evaporator.

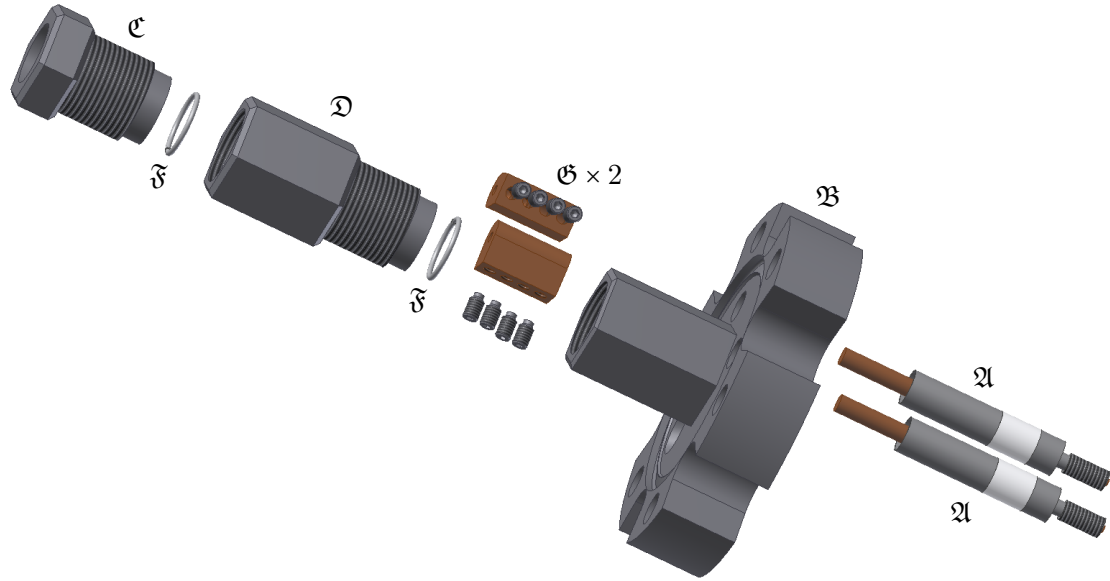


Figure 2.12: Assembly of the Main Evaporator’s Base Flange — Two ceramic isolated electrical feedthroughs (A) are welded into a custom made 40CF flange (B) with a hexagonal extension. The crucible (not shown, see Figure 2.13) is held by two compression fitting connections. Nuts (C, D) mold the ferrules (F), which are made from pure aluminum wire^a, against the crucible and keep it safe in place. The copper barrel G connectors join the feedthroughs with the tantalum posts (Figure 2.14) of the heater for the crucible.

a $\varnothing 1$ mm from Drahtwerk ELISENTAL W. Erdmann GmbH & Co.

If insulating materials, such as fused silica (quartz glass), are used, the thermocouples are not grounded and might exhibit dangerous voltages from the heating wire. In this case, special protection for the user and the laboratory equipment has to be installed. In early versions of the steel crucibles, the thermocouples were glued and not spot-welded. The used glue turned out to become slightly conductive at elevated temperatures (850 K), causing an additional potential on the thermocouples (≈ 20 V) with enough current to cause malfunctions of the temperature read out. A worsening of this behavior is expected with non-conductive (quartz) crucibles with glued¹³ thermocouples and heating wire in combination with an unavailable ground potential.

This work uses a steel crucible with two spot-welded Type K thermocouples.

13 ‘Ceramabond 835’ from KAGER Industrieprodukte GmbH.

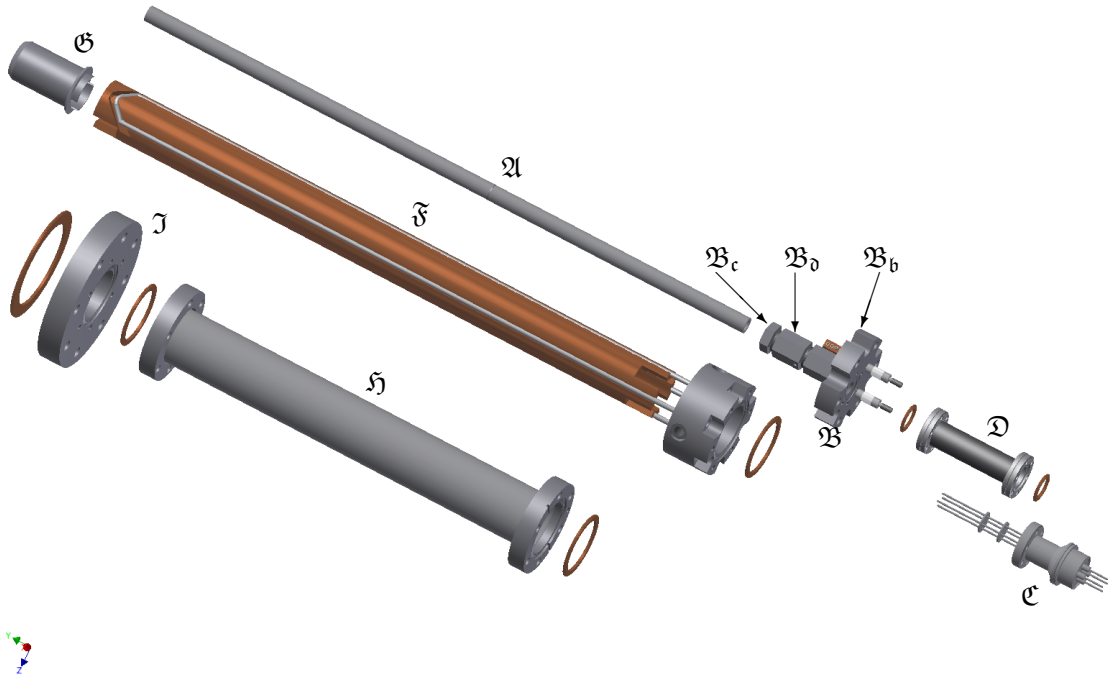


Figure 2.13: Assembly of the Main Evaporator — The crucible made from stainless steel or quartz (\mathfrak{A}) is inserted into the base flange (\mathfrak{B}) and tightened with the compression fittings (\mathfrak{B}_b , \mathfrak{B}_d , \mathfrak{B}_c). A thermocouple feedthrough Type K^a (\mathfrak{C}) with a 5 inch 16CF extension tube (\mathfrak{D}) is also mounted on the base flange. After establishing the power and thermocouple connections the water cooled shield (\mathfrak{F}) is carefully slid over the crucible. The cap (\mathfrak{G}), used to retain most of the evaporated material, completes the evaporator. The 40CF tube (\mathfrak{E}) substitutes a setup intended to be used with air sensitive evaporants (Figure 2.63). A standard 40CF/63CF adapter (\mathfrak{J}) completes the assembly.

a ‘A0423-1-CF’ from MPF Products, Inc. *via* tectra GmbH.

The heating wire is isolated from the crucible by a layer of suitable ceramic glue¹⁴. An 0.5 mm thick layer is applied on the crucible. After drying of the glue, the tantalum heating wire is folded into a U-shape and wound around the crucible, as shown in Figure 2.14. It must not touch the metallic center of the crucibles and the thermocouples. Polytetrafluoroethylene tape¹⁵ for plumbing is used to temporarily retain the wire on the crucible. The fixed wire is covered with the same glue as before and after drying the tape is removed. The open areas are treated the same way. After curing¹⁶, the crucible can be inserted in the base flange and the electrical connections can be established.

14 ‘Ceramabond 671’ from KAGER Industrieprodukte GmbH.

15 ‘Gewindedichtband 12 mm x 0.1 mm’ from OBI GmbH & Co. Deutschland KG.

16 At ambient temperature for 24 hours.

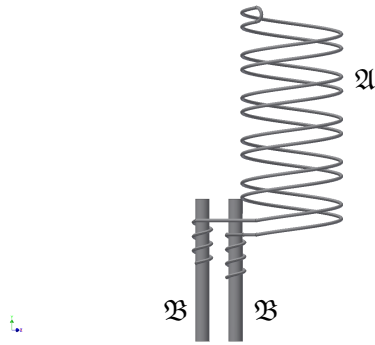


Figure 2.14: Schematic of the Heating Wire — Tantalum wire^a (A) with a length of approximately 8 m is folded in a U-shape and wound around the isolated crucible in form of a double helix starting at its top. The open ends are wound around two tantalum posts^b (B) and spot-welded at several positions. The pitch should be around 4 mm and the distance between two strands 2 mm. The wire should be wound slightly denser at the top. This image uses an increased pitch to emphasize on the double helix structure.

a $\varnothing 0.5$ mm from Haines & Maassen Metallhandelsgesellschaft mbH.

b $\varnothing 2.0$ mm from Haines & Maassen Metallhandelsgesellschaft mbH.

The crucible with the base flange is inserted in a cooling shield made from solid copper to reduce degassing, thermal load on the housing, and emission of infrared radiation into the middle stage of the molecular beam. A cap on top of the shield retains most of the evaporated material. This is desirable since the collected material cannot reach the sample for geometric reasons and would otherwise soil the inside of the molecular beam housing. As a benefit, it provides an option to recover expensive material. The design can be extended to a variant in which refilling of the crucible and cleaning of the cap can be performed in an inert gas environment, see Section 2.8. In addition, the cap serves as an orifice for differential pumping.

Typically, the crucible is driven by four power supplies¹⁷ hooked up in series and synchronized by a PID regulation software¹⁸. This setup provides currents up to 10 A and voltages up to 80 V. Communication with the host computer equipped with a USB-RS485 converter¹⁹ is established with the built-in RS-485 interfaces of the power supplies. Temperature feedback for the regulation software is provided by an eight channel USB converter²⁰. This allows for a constant temperature of the evaporator within the measurement accuracy of ± 0.1 K. The evaporator has been successfully tested for temperatures between 300 K and 960 K. In this temperature

17 ‘PeakTech 1890’ from ConeleK Electronic.

18 LABVIEW application by H. ZHOU.

19 ‘USB-Nano-485’ from NienTech.

20 ‘TC-08’ from Pico Technology Limited *via* Conrad Electronic SE.

range, suitable deposition rates between 0.1 ML/s and 1 ML/s could be achieved for magnesium, calcium, and lead²¹.

Upon first heating, the glue degases severely. Subsequent heating only shows significant degassing for a new maximum temperature. In order to minimize re-adsorption of water on the crucible, it should be refilled while it is still warm ($\approx 370 \text{ K}$), taking appropriate safety measures.

Design drawings with dimensions and materials for the main evaporator can be found in Appendix B.1.1.

2.3.2 Optics Stage

The diode based laser²², which is used for detector calibration, is equipped with a fiber docking station²³. The emitted light is guided in the optical fiber to an exit collimator which can be adjusted towards the molecular beam, see Section 2.5.3. It enters the vacuum system through a small window and is defocused by a lens to the same extent as the molecular beam spreads. The focal point should have the same distance to the sample as the top of the evaporator, taking the reflection by the mirror, see Figure 2.16, into account. The lens holder, as shown in Figure 2.15, acts as an adjustment screw in the housing of the molecular beam. In order to maximize the transmission at small wavelengths, quartz is used for all parts the laser passes through.

A mirror, which is mounted on a guided wobble stick, as shown in Figures 2.16 and 2.17, is used to reflect the defocused laser upwards through the chopper stage, see Section 2.3.3 and the nozzle in the main chamber, see Section 2.3.5, onto the sample, see Section 2.1. Adjustment of the reflection angle is done by bending the sheet metal of the mirror holder. It should be mentioned, that a medium alignment is sufficient here. The final position of the laser spot is adjusted outside the vacuum chamber by the fiber positioner, see Section 2.5.3.

This stage also carries a replaceable orifice protecting the inline valve in the molecular beam from unwanted deposition. Since the opening of the orifice gets closed up during operation of the evaporator, regular cleaning is necessary.

21 One monolayer (ML) corresponds to a hexagonal closed packed layer of the adsorbed material's atoms.

22 'iBeam-405-S-3V5' from TOPTICA Photonics AG.

23 'FiberDock' from TOPTICA Photonics AG

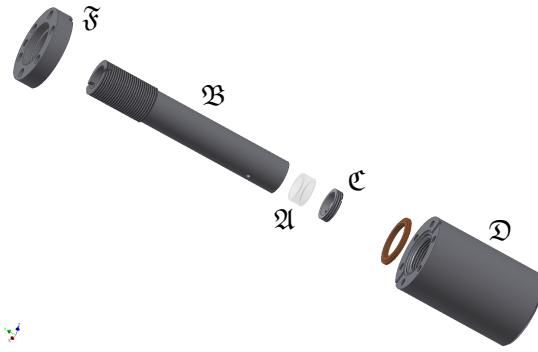


Figure 2.15: Assembly of the Lens Holder — A quartz lens^a (A) is inserted into the holding tube (B). The lens is held by a small threaded retainer ring (C). The tube itself is screwed into the beam housing (D, partially shown) allowing to adjust the position of the focal point. The 16CF flange opening is sealed by a quartz 16CF window^b (F).

- a ‘G340164000’ f:-50 from Qioptiq Photonics GmbH & Co. KG.
 b ‘VPZL-133Q’ from Kurt J. Lesker Company.

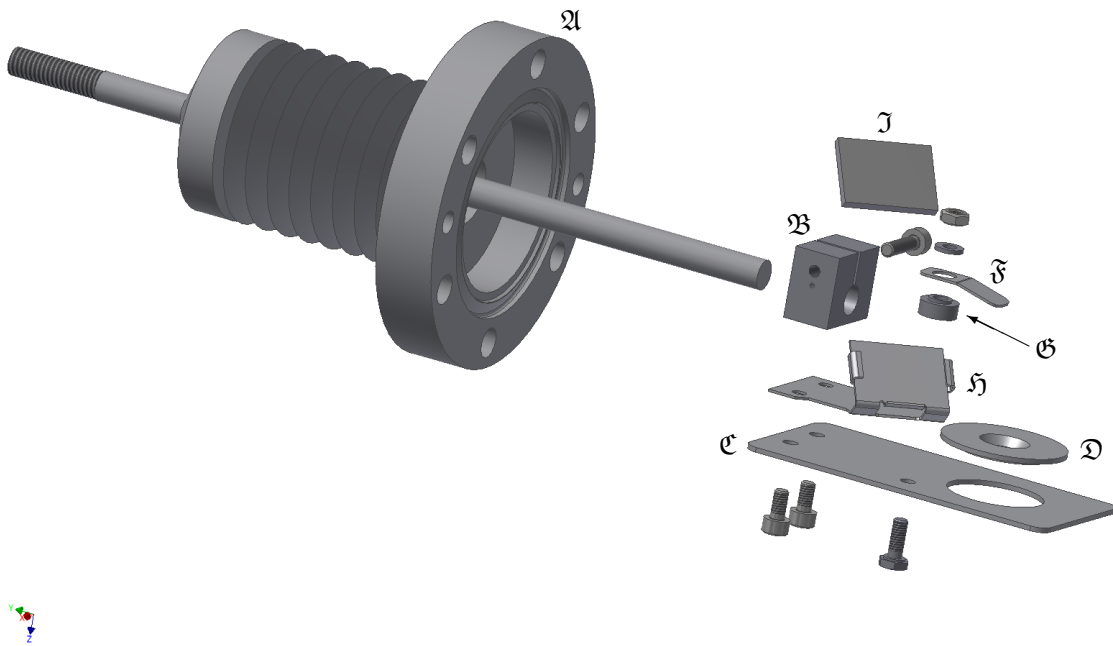


Figure 2.16: Mirror/Orifice Assembly Vacuum Side — A modified wobble stick^a (A) is equipped with a clamped mounting base (B). This piece carries a holder (C) for an exchangeable orifice (D) held by a small latch (F) with a distance piece (G) as well as a pod (H) made from sheet metal for a mirror^b (I).

- a ‘WS-275’ from MDC Vacuum Products, LLC.
 b ‘G340057000’ from Qioptiq Photonics GmbH & Co. KG.

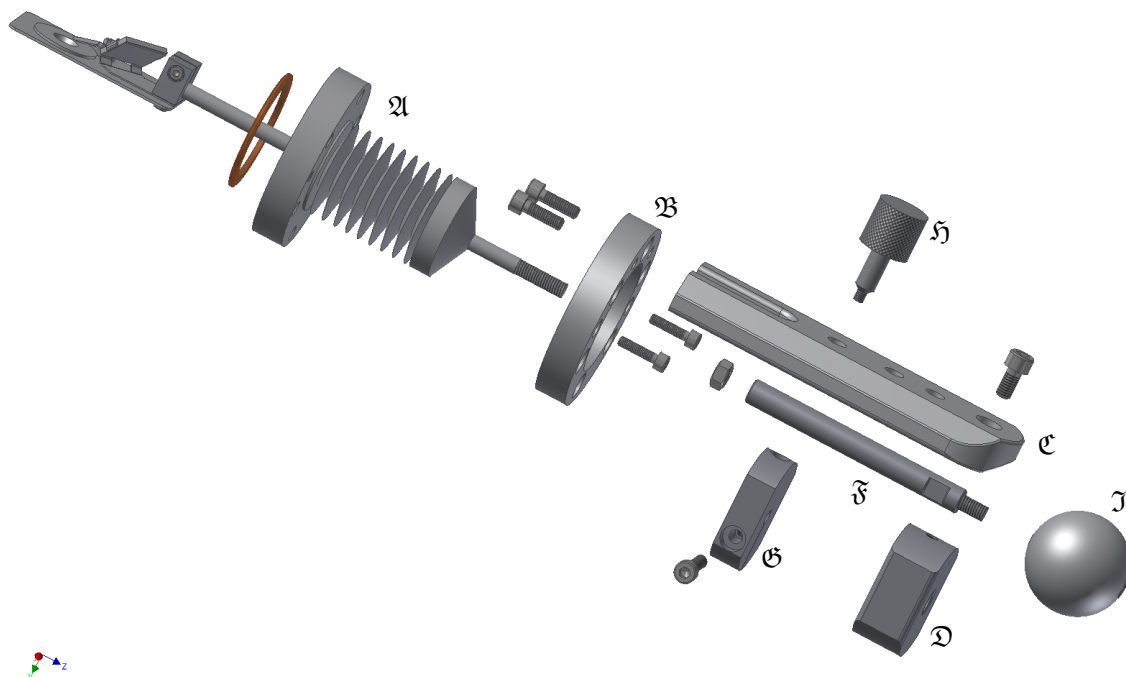


Figure 2.17: Mirror/Orifice Assembly Air Side — The modified wobble stick with its attachments from Figure 2.16 (A) carries a base plate (B) holding a track (C). The screws (not shown) to tighten the 40CF connection are accessible without removing the track. It is equipped with a guidance piece (D) holding the extension rod (E) of the wobble stick. The track has three distinct resting positions: laser, molecular beam and valve operation. The wobble stick is held by a clamp (G) which can be easily fixed in these positions with a knurled screw (H). A knob (F) at the end of the extension rod provides user friendly handling.

The air side of the assembly limits the flexibility of the wobble stick to an in/out motion. The moveable part can be locked by a knurled screw in three well defined positions used in the different measurements²⁴:

- The position closest to the chamber places the mirror in the path of the molecular beam. The mounting sheet metal blocks the evaporated substance and most of the infrared radiation emitted from the evaporator. The mirror can reflect the laser towards the sample. This position is used for the laser involved measurements, *i.e.*, the clean sample, the coated sample, and the detector calibration. It is also the recommended position during temperature stabilization of the main evaporator since it prevents unnecessary deposition on devices further up in the beam.

²⁴ Detailed instructions are presented in Section 6.3.

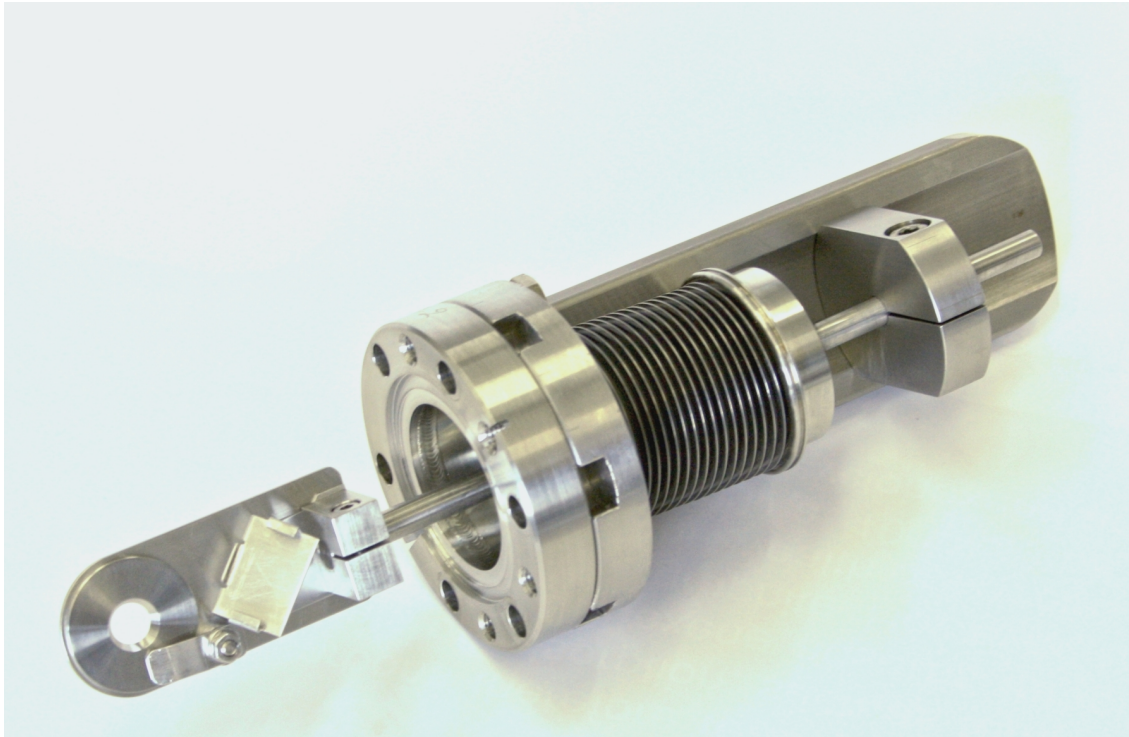


Figure 2.18: Assembled Mirror/Orifice Stage — A photograph of the preliminary assembly of the mirror/orifice stage as described in Figure 2.17 is shown. The actuation part has been altered afterwards.

- The middle position aligns the orifice above the exit of the evaporator, clearing the path between the evaporator and the sample. This position is used for all measurements not using the laser.
- The third, out-most position retracts the vacuum side assembly enough to let the inline valve pass by. This position should be verified before the valve is operated since maloperation will cause severe damage.

The assembled device is shown in Figure 2.18. Design drawings with dimensions and materials for the optics stage can be found in Appendix B.1.3.

2.3.3 Beam Chopper

The detector material only responds to temperature changes and thus cannot measure continuous input. Hence, the molecular beam from the main evaporator as well as the laser beam need to be converted into pulses. This task is performed by the chopper stage shown in Figure 2.19. Its main part is a ultra high vacuum compatible stepper motor operated by a programmable controller.

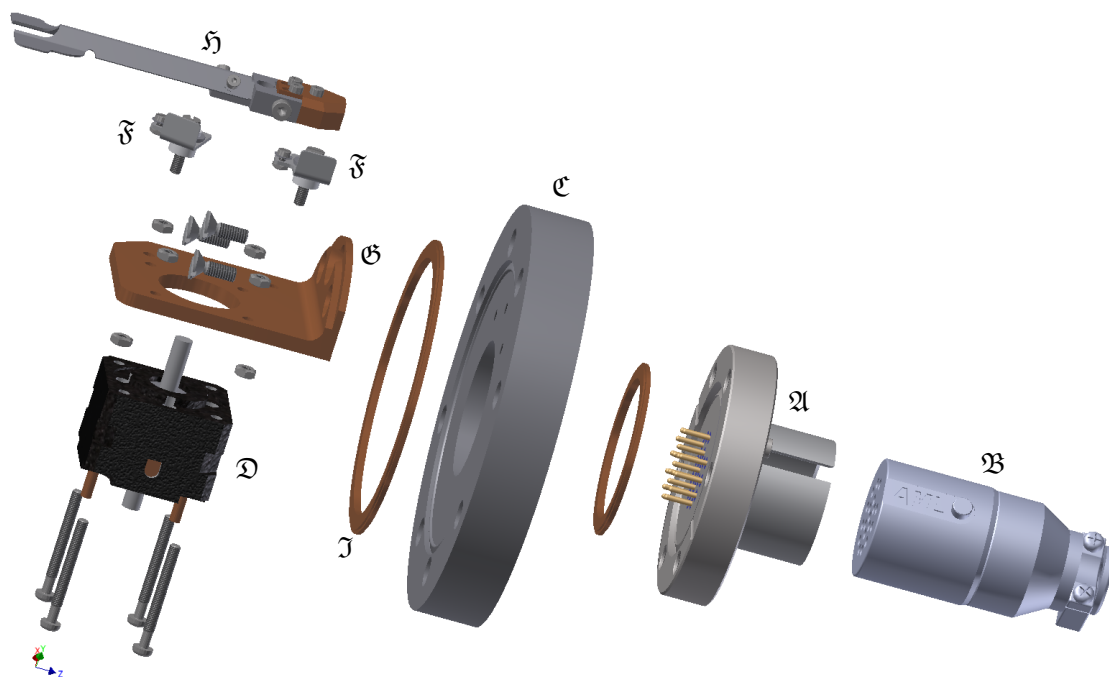


Figure 2.19: Assembly of the Chopper — A standard multi pin feedthrough^a (A) with the matching air-side connector (B) is fastened to a modified zero length 63CF/40CF adapter (C). The stepper motor^b (D) driven by a programmable controller^c (not shown) is mounted together with two end switches (F, Figure 2.20) onto a copper strap (E) attached to the adapter flange (C). The shutter blade (H, Figure 2.21) is clamped on the axle of the motor (D). A wide bore copper gasket (G) is necessary to mount this assembly.

a ‘MLF18F’ from Arun Microelectronics Ltd. *via* tectra GmbH.

b ‘C14.1’ from Arun Microelectronics Ltd. *via* tectra GmbH – discontinued.

c ‘SMD2’ from Arun Microelectronics Ltd. *via* tectra GmbH.

The measurement software²⁵ converts the pulse parameters to a program for the controller. The software only triggers the start of the stored program. Thus, the timing is done by a dedicated system and synchronized every measurement cycle. The setup also includes end-of-travel switches, see Figure 2.20, and a fork-like metal

²⁵ LABVIEW application programmed by H. ZHOU.

sheet, see Figure 2.21, blocking the beam in the two outer positions and allowing the beam to pass in the center position, as shown in Figure 2.22. A counterweight on the chopper blade is used to reduce vibrations arising from an unbalance. The remaining vibrations from torque of inertia cannot be observed in the detector signal. This design enables usage of a long chopper blade in order to realize fast switching of the beam.

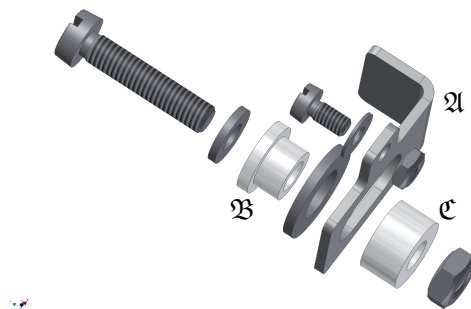


Figure 2.20: Assembly of the End Switches — The hookup wire (not shown) is fixed with the small screw to the actual contact (A). This steel part is insulated by alumina splint bushes^a (B, C) and attached to the motor holder (not shown, see Figure 2.19) by the larger screw. The switch is triggered if the grounded shutter blade (not shown, see Figure 2.21) contacts switch plate and pulls the sensing output of the stepper motor controller (not shown) to low potential.

^a ‘BGB-M3’ from tectra GmbH.

In order to allow clearance for the built-in valve, the chopper blade can be moved into a niche in the housing. Operation of the valve is permitted only if the chopper blade is in this parking position. Otherwise severe damage might occur!

This three stage operation offers the advantage of free choice of the open and close durations at a constant switching speed. The two impenetrable positions are indispensable since a homogenous deposition of the adsorbate is required. Settings for a two stage movement (“there and back again”^[150]) would lead to a coverage gradient on the sample since one end of the sample is exposed twice the switching time longer than the other end. This gradient²⁶ would also depend on the exposure time per pulse rendering a precise measurement impossible. As a drawback the three stage setup generates two subsets of pulses: pulses with clockwise moving chopper and pulses with counter-clockwise moving chopper. Since they appear always in pairs, and thus are strictly alternating, one measurement cycle is called a *pulse pair* and due to the continuous numbering in a measurement these two subsets are called

²⁶ Up to 15%.

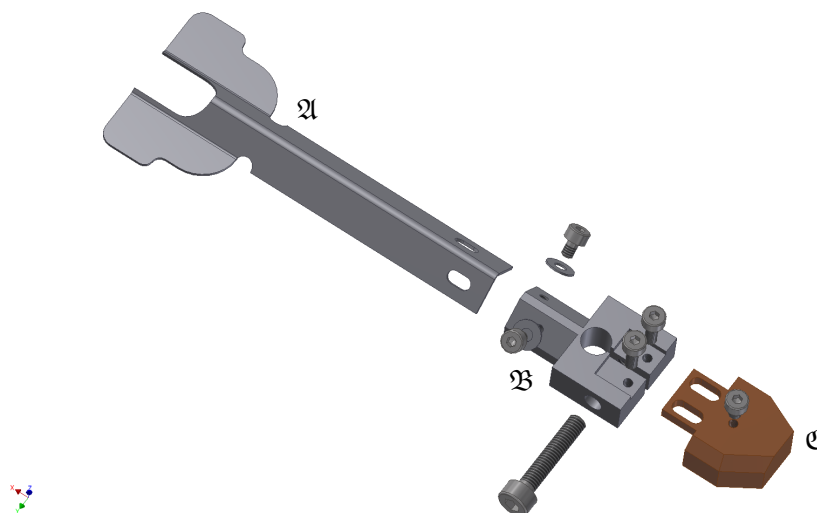


Figure 2.21: Assembly of the Chopper Blade — The chopper blade consists of a bent steel sheet (\mathfrak{A}) screwed (welded in an older version) to the hub (\mathfrak{B}). A copper counterweight (\mathfrak{C}) is also mounted to the hub (\mathfrak{B}) to shift the center of mass on the motor's axle and thus minimize vibrations. The assembly is clamped by the slitted hub (\mathfrak{B}) onto the axle of the stepper motor (not shown, Figure 2.19).

odd and *even*. Since data also includes the delay around the pulse, a set of data corresponding to a pulse from the beam source is labeled a *frame*.

If the setup is arranged symmetrically about the center of the beam, odd and even frames should be identical since the detector has area integrating properties and cannot distinguish between the rotational directions of the stepper motor. This assumption holds well for the laser and the molecules from the beam source which are not reflected by the walls of the beam housing. This situation is in compliance with the assumption that ray optics apply. The infrared radiation from the evaporator is reflected many times on the walls and thus forms a diffuse background radiation field. Changing the position of the chopper blade influences the intensity distribution in the field and thus the output of the infrared radiation onto the sample. This leads to a different infrared radiation input into the sample in the two closed positions and hereby breaking the symmetry assumption.

Due to these asymmetry issues, the chopper position and delays should be aligned to the mass spectrometer signal and neither to the laser pulse position nor to the radiation signal. A mismatch of the delays obtained by a laser based measurement and a zero sticking measurement indicate poor adjustment of the laser fiber output.

Design drawings with dimensions and materials for the chopper stage can be found in Appendix B.1.4.

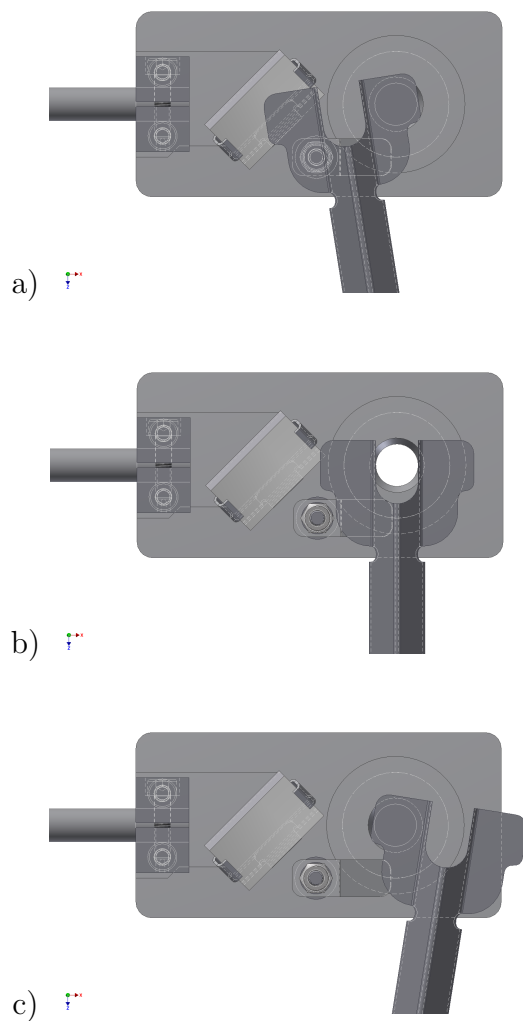


Figure 2.22: Positions of the Chopper Blade — a) The molecular beam is blocked with the chopper blade in default position. b) The chopper blade clears the path of the beam. c) The molecular beam is blocked with the chopper blade in the second position. A measurement cycle consists of the sequence $a \rightarrow b \rightarrow c \rightarrow b \rightarrow a$.

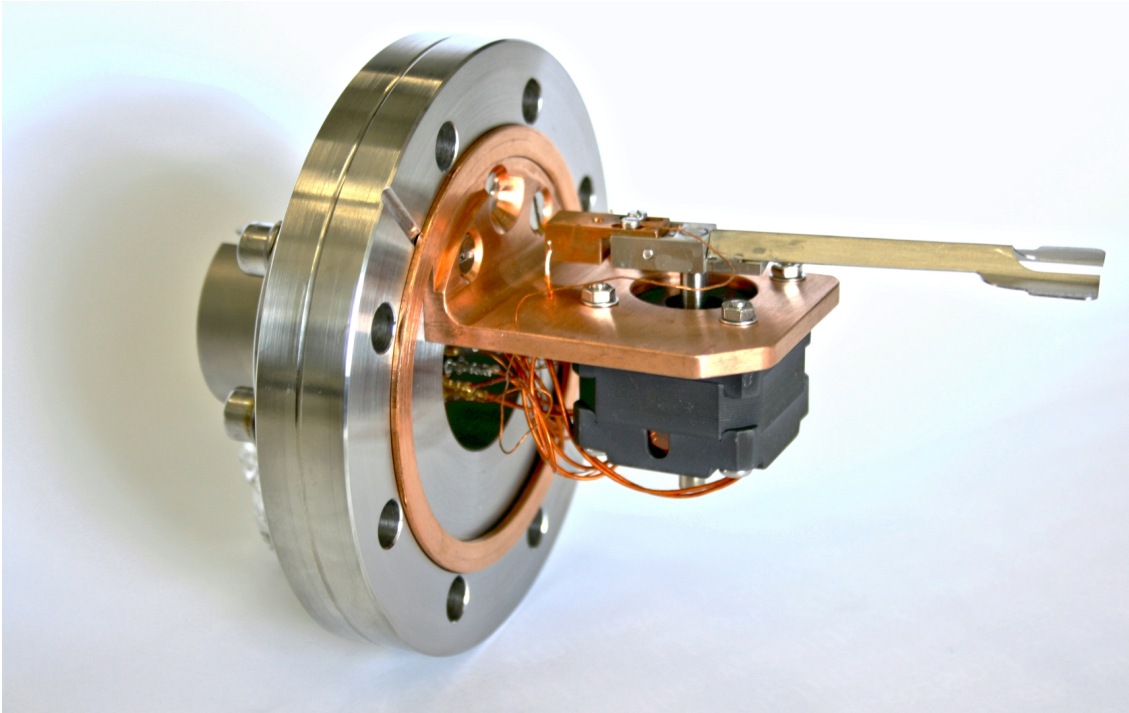


Figure 2.23: Assembled Chopper — A photograph of the assembled chopper is shown as described in Figure 2.19. The end switches have been added later.

2.3.4 Inline Valve

In order to separate the main chamber from the compartment of the molecular beam, a valve, see Figure 2.24, is built into the housing of the molecular beam. Since the

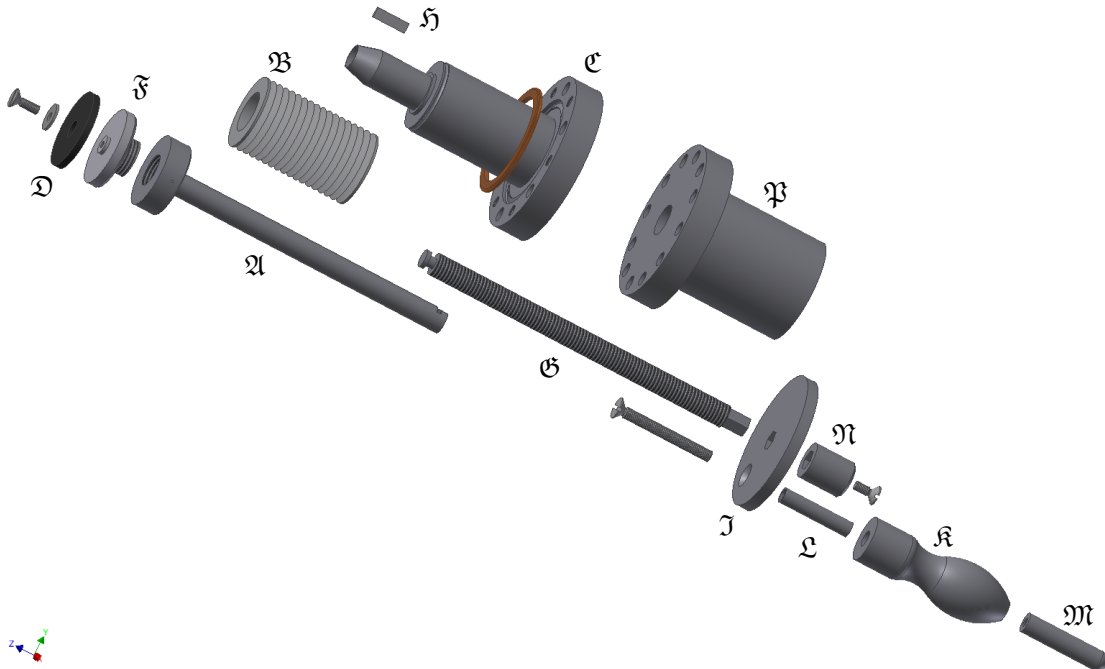


Figure 2.24: Assembly of the Molecular Beam Valve — The bonnet of the valve comprises a moveable seat (A) for different gaskets, an edge welded bellow^a (B) and a base flange (C). This figure shows the currently used option with a Viton[®] gasket (D) on an adapter plug (E). A conical end stop guides the bellow on the base flange (C) and prevents it from excessive compression. The linear actuator (A) is driven by a threaded rod (G) latched into its air side in order to transfer pushing and pulling forces. This shaft (A) is guided by a parallel key (H) to prevent torque on the bellow. The spindle (G) is turned by a hand wheel (I) equipped with a handle (K) and the corresponding spacer pieces (L, M). Defined torque can be applied by a nut (N) mounted to the hand wheel (I). The thread in the holder (P), which is mounted on the bonnet flange (C), converts the rotation to linear motion. The seat of the valve is implemented in the housing (not shown, see Figure 2.29) of the molecular beam.

a Custom made from Huntington Mechanical Laboratories Inc.:
 $\varnothing_{\text{in}} = 3/4 \text{ in.}$, $\varnothing_{\text{out}} = 1.5 \text{ in.}$, stroke = 3 in.

part of the beam outside the main chamber should be as compact as possible, the use of a standard component has been out of question. The seat of the valve is machined out of the solid in the beam housing. The long stroke bonnet, as shown in Figure 2.24, allows the valve to fully clear the beam path and the instruments

attached to the beam housing. The Viton[®]-gasket allows for independent bake-out of the molecular beam after refilling the evaporator. After contact of the rubber gasket with the seat of the valve, which is easily perceptible by an increase of the torque necessary to operate the valve, a quarter turn seals the connection. If desired, the position can be locked with a counter nut.

Figure 2.25 shows the assembled valve. Design drawings with dimensions and materials for the valve stage can be found in Appendix B.1.2.



Figure 2.25: Assembled Valve — A photograph of the preliminary assembly of the valve as described in Figure 2.24 is shown. The mount of the flat gasket has been altered later.

2.3.5 Parts in the Main Chamber

If the molecular beam is equipped with the electron beam evaporator, the emitted atomic beam includes ions due to interaction of the evaporated material and the accelerated electrons. Since ions would cause discharge energy in addition to the investigated reaction energies, their presence is undesirable. A convenient way to remove these slow ions is to apply an electric field perpendicular to the direction of the beam. This is realized by the deflector plates shown in Figure 2.26 which act as a parallel plate capacitor charged by an external power source. If ions are present in the beam, they will cause a current through the capacitor. Although the measurement of tiny pulsed currents is difficult, the ion current could be used to monitor the flux of the evaporator.

Figure 2.27 shows the deflector plates mounted on the beam housing, see Section 2.3.6.

The nozzle of the molecular beam, see Figure 2.28, extends into the main chamber to prevent unwanted deposition. It also serves as a support for the ancillaries stage, see Section 2.4. Its exchangeable center piece provides options for additional devices in the molecular beam, such as a mirror based infrared pass-filter. Its top piece defines the diameter of the laser and molecular beams and acts as an orifice for differential pumping.

Design drawings with dimensions and materials for the nozzle stage can be found in Appendix B.1.5.

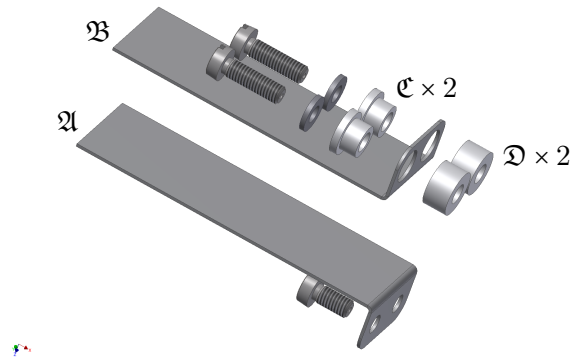


Figure 2.26: Assembly of the Deflector Plates — Two plates (A, B) form a parallel plate capacitor perpendicular to the molecular beam. Ions formed during the evaporation process experience a lateral force and are thus removed from the beam. In order to apply the necessary voltage, one of the plates (B) is isolated by alumina splint bushes^a (C, D). The assembly is mounted on the beam housing (not shown, see Figure 2.29) with vented screws.

^a 'BGB-M3' from tectra GmbH.

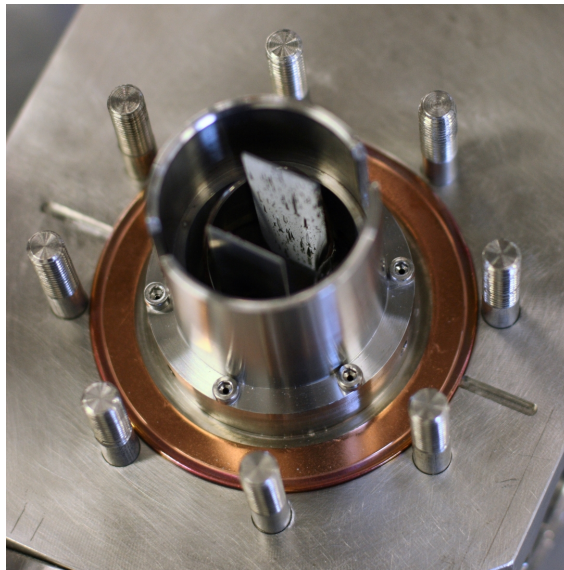


Figure 2.27: Assembled Deflector Plates — The assembly from Figure 2.26 after intense evaporation of Magnesium without stainless steel wool in the crucible. Worth mentioning are the particles on the plates and the shadows cast by them. After application of the wool no larger grains could be observed. The base mount of the nozzle is also visible.

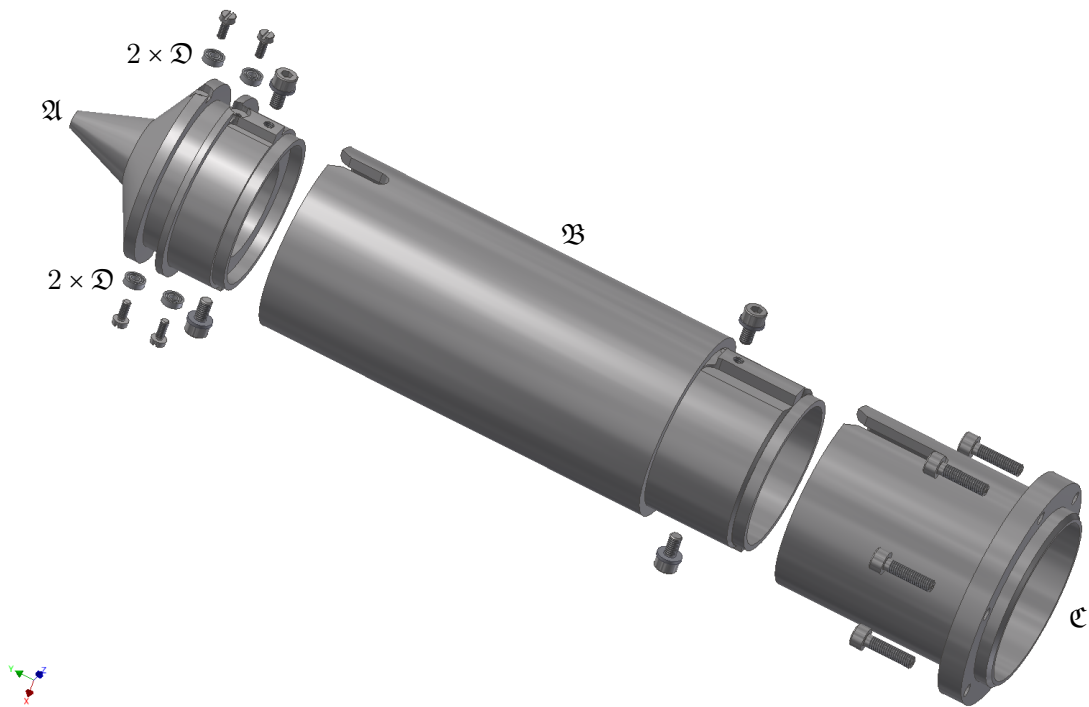


Figure 2.28: Assembly of the Nozzle — The nozzle (A) is mounted on an extension tube (B) which can be replaced by other instruments, *e.g.*, a mirror arrangement to separate molecules and radiation from the evaporator. The extender is attached to a base piece (C) held by six vented screws on the beam housing (not shown, see Figure 2.29). The nozzle carries four ball bearings^a (D) to guide the movement of the ancillaries stage (not shown, see Figure 2.39).

a '682-offen' from Kugellager Express GmbH.

2.3.6 Beam Housing

Due to several requirements on the molecular beam, its housing, see Figure 2.29, masters several technical challenges. On the one hand, it should be as compact as possible in order to preserve as much flux as possible, on the other hand, it has to contain differential pumping, the optics for the laser, ion removal, and the beam chopper.

Its lower part accepts the evaporator, see Figure 2.3.1, and forms a first pumping

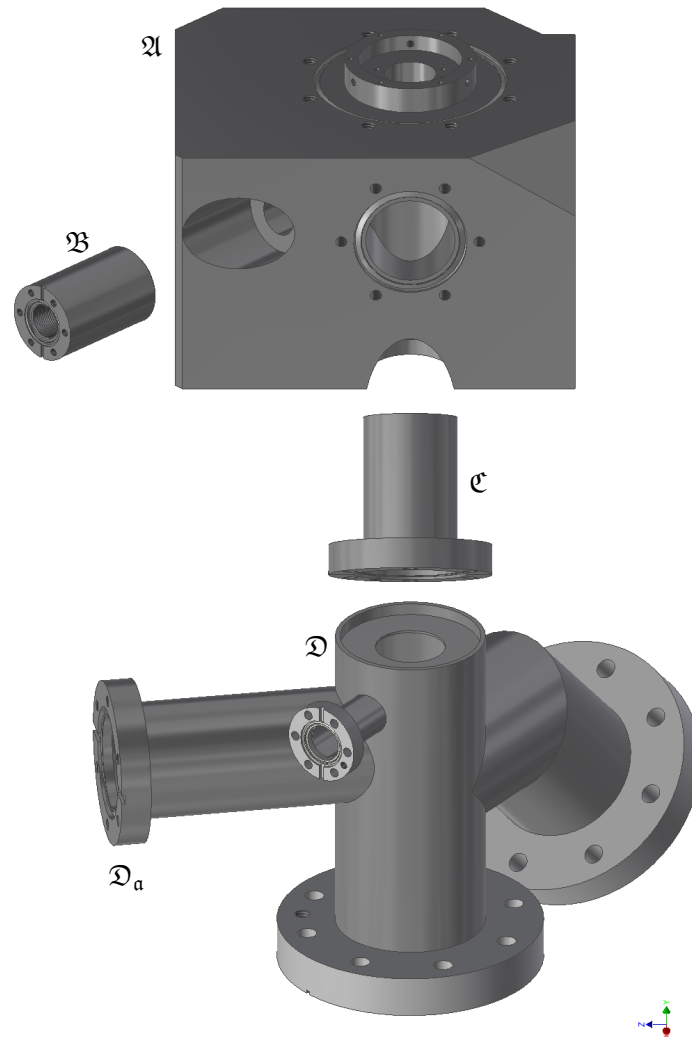


Figure 2.29: Assembly of the Beam Housing — Several pieces are welded into the block shaped main part (\mathfrak{A}) of the molecular beam. The laser port (\mathfrak{B}) is located left, the valve port (\mathfrak{C}) sticks out to the front and the tube part (\mathfrak{D}) of the beam is attached from below. The tapped 40CF flange (\mathfrak{D}_a) is modified to fit a $\varnothing 50$ mm tube. Otherwise, standard components are used.

stage. It provides a tapped 40CF port with a $\varnothing 50$ mm tube for a nude ion gauge²⁷. The lower section is welded to the main part of the beam housing machined from the solid. The main part incorporates the seat for the inline valve, see Section 2.3.4, together with a CF port for the other half of the valve. The reception for the lens holder, see Section 2.3.2, is welded into the main piece as well. Mounting options for the deflector plates and the nozzle are machined inside the CF feature on top of the cuboid main piece and are protruding into the main chamber. The 16CF port used to wire the deflector plates also connects to the volume above the valve. The block is completed by ports for a window, the optics stage, see Section 2.3.2, and pumping. Design drawings with dimensions and materials for the beam housing can be found in Appendix B.1.6.

Figure 2.30 shows the welded main part of the beam housing.

²⁷ This temporary cost effective solution (due to a shared controller) should be replaced by a more suitable cold cathode gauge.

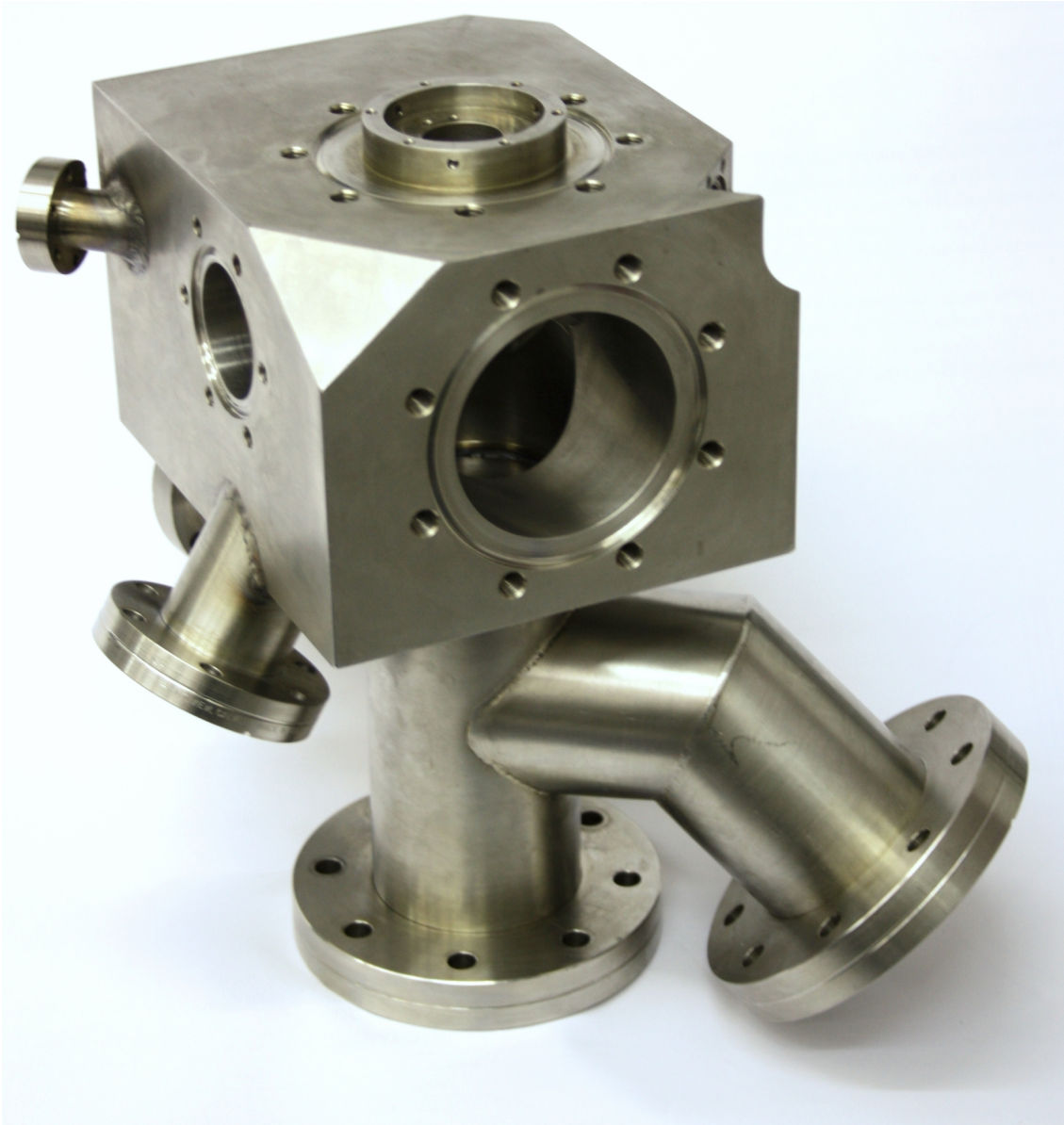


Figure 2.30: Welded Beam Housing — A photograph of the welded beam housing as described in Figure 2.29 is shown here. This version uses the first revision of the laser port.

2.3.7 Assembled Beam

Figures 2.31, 2.32, and 2.33 show the positions of the previously discussed individual devices attached to the beam housing, see Section 2.3.6. The molecular beam is

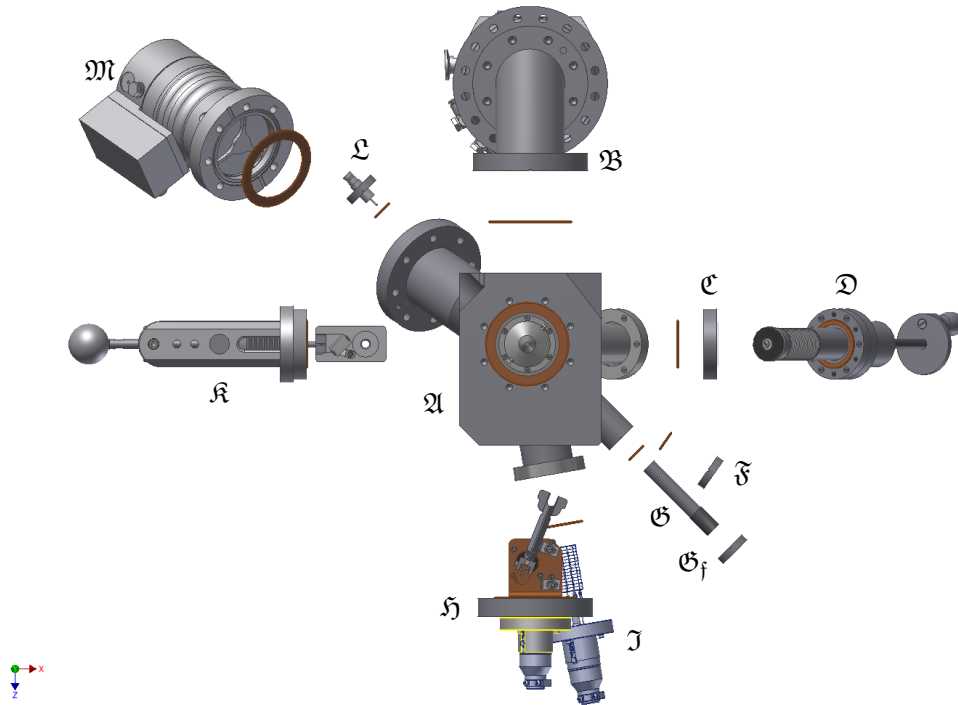


Figure 2.31: Assembly of the Molecular Beam (Top View) — North of the main part (**A**, Figure 2.29) a knee (**B**) is mounted in order to substitute a 80 L/s turbo molecular pump^a by a 300 L/s turbo molecular pump^b, see Figure 2.33 for details. East of the block shaped part (**A**) a window (**C**) is mounted directly onto it. The built-in valve (**D**, Figure 2.24) is attached to the CF-nipple. A 16CF blind flange (**F**) and the lens holder (**G**, Figure 2.15) together with its 16CF window (**G_f**) are mounted from the south east, see Figure 2.32 for details. The south faced flange carries the beam chopper (**H**, Figure 2.19). The other nipple in this direction accepts a Bayard-Alpert gauge head^c (**J**), see Figure 2.33 for details. The mirror/orifice assembly (**K**, Figure 2.17) is tightened onto the west opening of the block (**A**). The small recess northwest in the main part (**A**) holds the feedthrough (**L**) for the deflector plates (not shown). The nipple in the same direction holds a 80 L/s turbo molecular pump^d (**M**).

a ‘HiPace[®] 80’ from Pfeiffer Vacuum GmbH.

b ‘TMU260’ from Pfeiffer Vacuum GmbH.

c ‘AIG17G’ from Arun Microelectronics Ltd. *via* tectra GmbH.

d ‘TPU071P’ from Pfeiffer Vacuum GmbH.

equipped with two turbo molecular pumps, several windows, and a Bayard-Alpert gauge head. It further carries the optics stage, see Section 2.3.2, the chopper stage, see Section 2.3.3, and the parts reaching into the main chamber, *i.e.*, the deflector

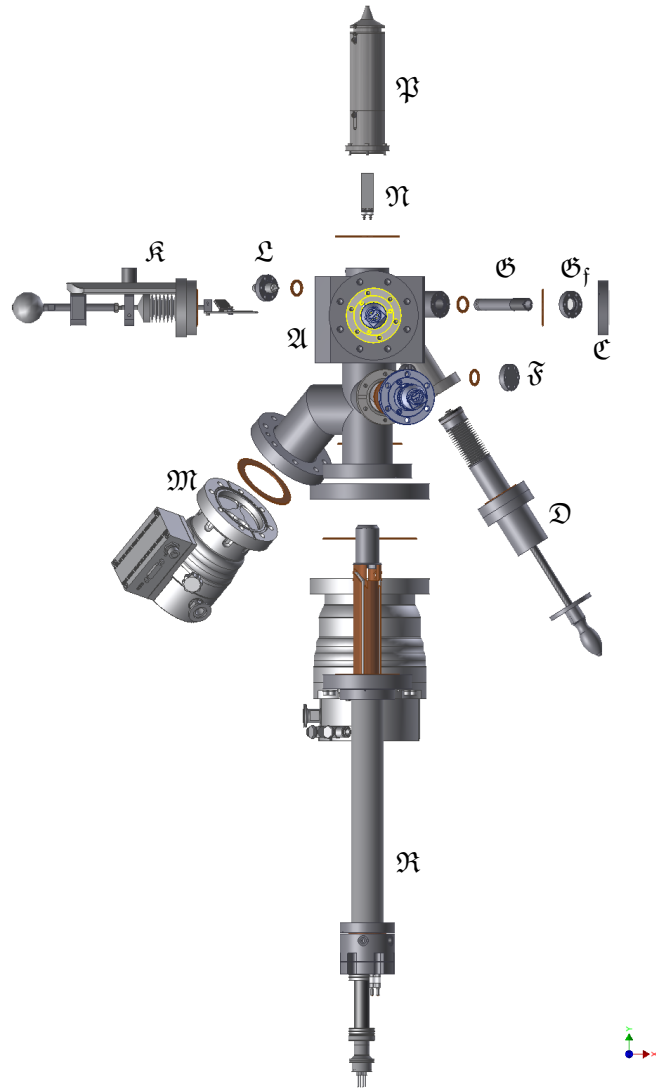


Figure 2.32: Assembly of the Molecular Beam (Front View) — The northern part of the block (A, Figure 2.29) carries the deflector plates (C, Figure 2.26) as well as the nozzle (B, Figure 2.28) and is attached to the main chamber (not shown). Located on the east, there are the laser port (D) with its window (E), the 40CF window (F), the 16CF blind flange (G), and the built-in valve (H) mentioned in Figure 2.31. The south 63CF flange of the beam housing (A) accepts the main evaporator (L, Figure 2.13). On the west side, there are the feedthrough (I) for the deflector plates (C), the mirror/orifice assembly (J, Figure 2.17) and a 80 L/s turbo molecular pump^a (K) shown.

^a ‘TPU071P’ from Pfeiffer Vacuum GmbH.

plates and the nozzle, see Section 2.3.5. The molecular beam is completed by the built-in valve, see Section 2.3.4, and the main evaporator.

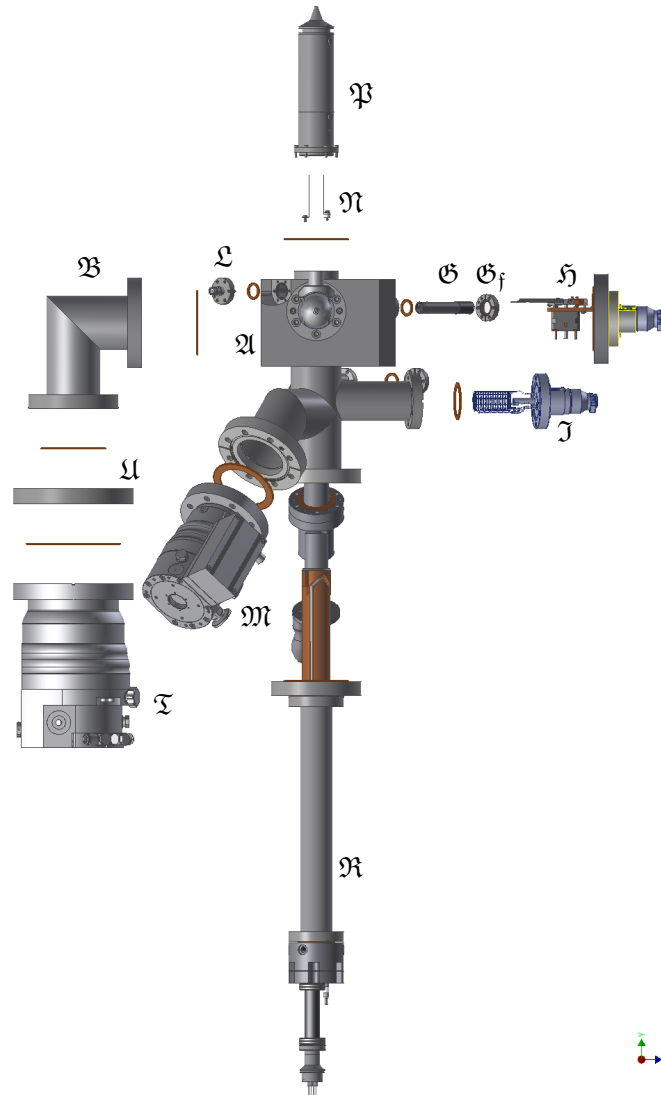


Figure 2.33: Assembly of the Molecular Beam (Left View) — The northern part of the block (A, Figure 2.29) carries the deflector plates (N, Figure 2.26) as well as the nozzle (P, Figure 2.28) and is attached to the main chamber (not shown). The beam chopper assembly (H, Figure 2.19) and the laser port (G, Figure 2.15) with its window (G_f) are mounted onto the CF ports at the east side of the main part (A). The Bayard-Alpert gauge^a (J) is mounted on the flanged tube facing east as well. The south 63CF flange of the beam housing (A) accepts the main evaporator (R, Figure 2.13). The west port holds the knee (B) referenced in Figure 2.31. A turbo molecular pump^b (T) is mounted to it *via* a standard 63CF/40CF adapter flange (U). Furthermore, the feedthrough (L) for the deflector plates (N) and a 80 L/s turbo molecular pump^c (M) are mounted on this side.

a ‘AIG17G’ from Arun Microelectronics Ltd. *via* tectra GmbH.

b ‘TMU260’ from Pfeiffer Vacuum GmbH.

c ‘TPU071P’ from Pfeiffer Vacuum GmbH.

2.4 Ancillaries Stage

In addition to the actual caloric measurement, several ancillary, *i.e.*, calibration, measurements have to be performed. The here presented stage, see Figure 2.34, provides utilities to measure a zero sticking reference with a heated plate, the deposition rate of the molecular beam with a quartz crystal microbalance (QCM), and the infrared radiation from the evaporator through a window. In addition, the stage provides a mirror to reflect the laser beam out of the chamber and can be retracted to a position in which it does not interfere with the calorimetric measurement.

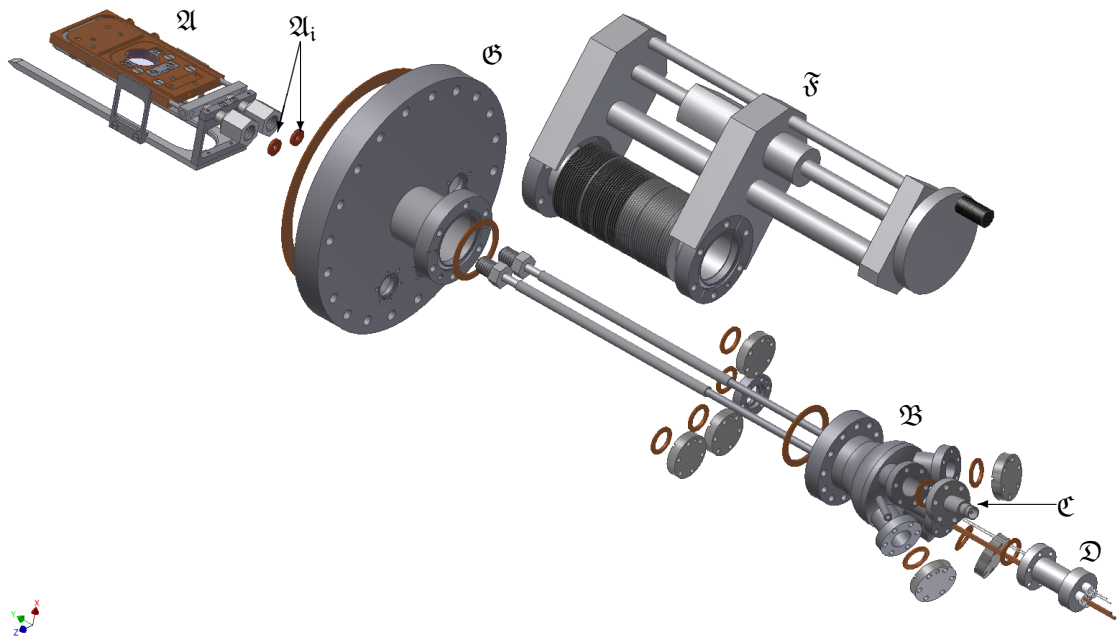


Figure 2.34: Assembly of the Ancillaries Flange — The ancillaries setup (A), see Figure 2.39 for details, is attached to the cooling lines of a cluster flange^a (B). VCR[®] connections are sealed by custom copper gaskets (A_i). A BNC feedthrough^b (C) provides a high frequency connection to the quartz crystal microbalance. The hot plate is powered by a combination feedthrough^c (D). A linear shift^d (F) mounted on the base flange (G), carries the cluster flange (B) and allows the individual sections of the ancillaries setup (A) to be moved into their operating positions in front of the sample (not shown). The vacant openings are currently sealed by 16CF blind flanges.

a ‘CLFW40-16/5’ from VAb Vakuum-Anlagenbau GmbH.

b ‘A0237-2-CF’ from MPF Products, Inc. *via* tectra GmbH.

c ‘A0443-1-CF’ from MPF Products, Inc. *via* tectra GmbH.

d ‘LSM38-150-H-ES’ from Kurt J. Lesker Company.

The solid copper body carrying these minor devices also comprises a cooling line and an option to upgrade it with a heating element. Cooling is possible by using compressed dry air, water, or liquid nitrogen. The first two options are used to stabilize the temperature of the assembly during operation of the hot plate. This is necessary to avoid a thermal frequency drift of the QCM's oscillator crystal. The latter option is useful if substances are to be deposited on the QCM crystal that do not exhibit unity sticking at ambient temperature, *e.g.*, magnesium.

The heating option should provide the possibility to desorb substances from the infrared transparent window and the QCM crystal in this stage. The target temperature of 550 K is not high enough to desorb metal layers, see Table 5.7, but sufficient to desorb large organic molecules like tetraphenyl porphyrin, see Table 5.3.

Design drawings with dimensions and materials for the ancillaries stage and its components can be found in Appendix B.2.6.

2.4.1 Hot Plate

In order to obtain a reference for the sticking measurement, a hot surface is used. It is heated to a higher temperature than the main evaporator to ensure complete desorption of the dosed molecules from the beam source. Up to this point two surfaces have been used. One comprises tantalum sheet material with a thickness of 0.2 mm modified with two constrictions for increased resistivity, as shown in Figure 2.35. As a variant, a straight tantalum stripe with a thickness of 0.1 mm has been used. The second version uses a sapphire plate²⁸ wrapped in 0.1 mm tantalum foil, leaving the polished surface exposed. Both types were tested for temperatures up to 1600 K. Since a Type K thermocouple is used, the operation temperature should not exceed the mentioned value to avoid degrading or melting of the sensor. In both versions, resistive heating through the tantalum sheet is employed. The current is provided by a manually controlled external high current power supply²⁹. Due to the high currents used for heating, the electrical connections and cables³⁰ require special attention.

Since the hot plate is not at the same position as the sample, the obtained value might be affected by the different geometries towards the mass spectrometer. Another issue is the different velocity of molecules being reflected from the hot plate which might lead to a different sensitivity of the mass spectrometer. Section 5.8.4 gives further information about these obstacles.

28 '66 40T350' from KORTH KRISTALLE GMBH.

29 'Voltcraft HPS-11560' from Conrad Electronic SE.

30 '606071' 2 × 6.00 mm² from Conrad Electronic SE.

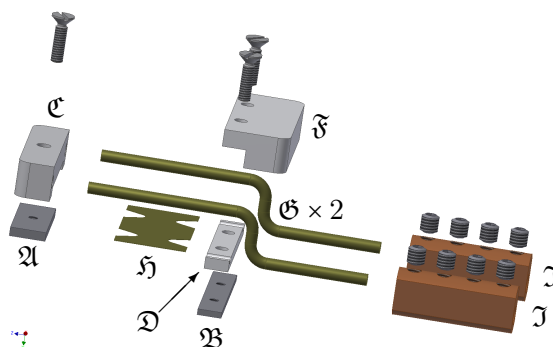


Figure 2.35: Assembly of the Hot Plate — Three screws and two threaded plates (A, B) clamp three isolation pieces (C, D, E) machined from Macor^{®a} onto the main part (not shown). The isolation holds two tantalum electrodes^b (G) with a spot-welded tantalum sheet^c (F) in this version. Four barrel connectors (H, only two shown) and copper wire^d (not shown) isolated with glass fiber sleeves^e (not shown) establish the electrical connection to a power/thermocouple feedthrough^f (not shown). A thermocouple^g is spot-welded to the hot plate (J) and connected to two terminals (not shown, see Figure 2.39). Kapton[®] isolated thermocouple wire^h (not shown) is used to reach the feedthrough from the terminals.

a ‘158-3180’ from RS Components GmbH.

b 99.9% Ø2 mm from Haines & Maassen Metallhandelsgesellschaft mbH.

c 99.9% 0.2 mm from Haines & Maassen Metallhandelsgesellschaft mbH.

d 4 mm².

e ‘PIF2409 NA005’ from Alpha Wire *via* Premier Farnell plc.

f ‘A0443-1-CF’ from MPF Products, Inc. *via* tectra GmbH.

g ‘THD’ Ø0.13 mm from Therma Thermofühler GmbH.

h ‘KFD-30-KK-IEC’ from Therma Thermofühler GmbH.

2.4.2 Quartz Crystal Microbalance

The deposition rate of the molecular beam is measured by a quartz crystal microbalance arrangement included in the joint copper piece, as shown in Figure 2.36. Due to the geometry of the experiment the diameter of the molecular beam is smaller than the back electrode. This leads to a situation in which the balance is used outside it’s specifications where the whole front of the oscillator crystal is coated. As a consequence, it is necessary to correct the influence of this partial loading.

It is highly recommended to verify that all dosed molecules stick to the oscillator crystal. This can be done by monitoring the intensity of a characteristic mass to charge ratio with the mass spectrometer, *e.g.*, $m/z = 40$ for calcium³¹. The deposition rate measurement should be started when the baseline with closed shutter matches the intensity while dosing on the crystal. Further information about the quartz

³¹ Usually the units are implicitly omitted; the correct formula would be $\{m/z\} = 40$.

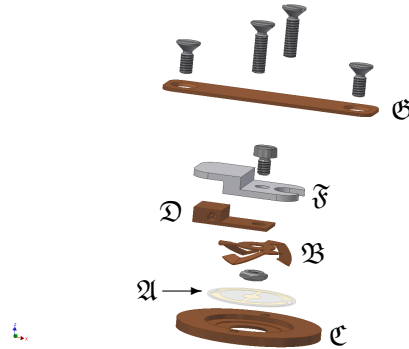


Figure 2.36: Assembly of the QCM Section — The oscillator crystal (A) is sandwiched by a copper beryllium spring (B) and a copper beryllium lid (C) fastened from the other side of the main part (not shown). The spring is mounted on a contact (D) and isolated by a Macor^{®a} piece (F) from the main part. A coaxial cable^b (not shown) connects the spring with a BNC-feedthrough^c (not shown). A copper plate (G) closes the mounting opening on the main part.

a ‘158-3180’ from RS Components GmbH.

b ‘KAPWC1X025’ from LewVac Components Ltd.

c ‘A0237-2-CF’ from MPF Products, Inc. *via* tectra GmbH.

crystal microbalance measurement is given in Section 5.8.2.

2.4.3 Mirror

A mirror is included in the copper main piece with a small retainer, as shown in Figure 2.37.

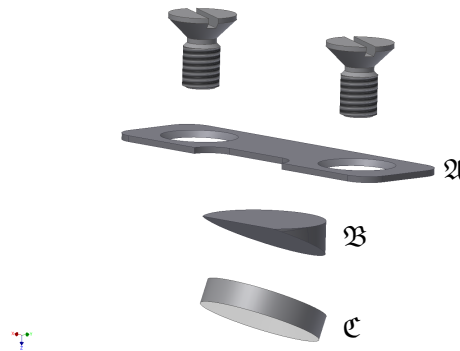


Figure 2.37: Assembly of the Mirror Section — A steel plate (A) presses on a steel adapter (B) to hold the mirror^a (C) in the designated pouch of the main part (not shown).

a ‘G340333400’ Ø10 mm x 2 mm with silver coating ‘RAGV’ from Qioptiq Photonics GmbH & Co. KG.

This provides a possibility to reflect the laser back out of the chamber. This is

necessary since standard detectors for the measurement of the laser intensity are not available for a vacuum environment. The measured laser power outside of the chamber has to be corrected by the reflectivity of the mirror and the transmission of the window on the chamber. Comparison between theoretical and experimental values are given in Section 5.8.3.

While the NAC machine is operated, high attention should be paid to avoid contamination of the mirror!

2.4.4 Infrared Transparent Window

During a calorimetric measurement, the sample is exposed to the wanted molecules and the unwanted infrared radiation, both originating from the main evaporator. Either leads to an increase in temperature of the β -polyvinylidene fluoride detector polymer. Hence, the measured signal comprises the heats released by adsorption (molecules) and absorption (radiation). An infrared transmissive window, shown with its holder in Figure 2.38, blocks all molecules and renders a quantification of the radiation component possible.

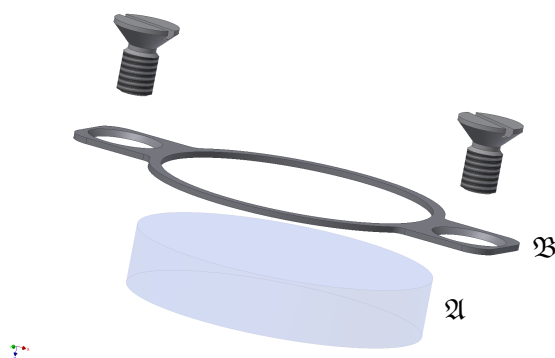


Figure 2.38: Assembly of the Infrared Transparent Window Section — A barium fluoride window^a (A) is pressed with a springy steel rim (B) onto the main part (not shown).

a '25 40 007' \varnothing 25 mm x 5 mm from KORTH KRISTALLE GMBH.

An alternate approach would involve a velocity selector blocking photons and letting atoms pass^[120]. Due to the delicate setup, this option was not chosen at this time.

If the amount of radiation in the far infrared, where the used barium fluoride becomes opaque, is no longer negligible, it is possible to replace the window with a mirror setup in the nozzle part of the molecular beam, see Section 2.3.5. Since the

employed materials did not exhibit the aforementioned behavior, this setup was not tested.

During an experiment, molecules are deposited on this window and its transparency will change along its run-time. This leads to the requirement of a transparency measurement for each experiment which is carried out with the laser, resulting in a transparency valid for the wavelength of the laser. This method relies on the assumption that the window and the deposition on the window have a constant absorption over a very broad spectral range. A closer inspection of these properties is presented in Section 5.8.1. In this setup, the obtained value is used as an initial value for the data treatment described in Section 3 and as an indicator whether the deposited layer becomes too thick and is affecting the transmitted radiation by an intolerable extent. In order to extend the necessary service interval, a rather large window is mounted where several spots can be used.

2.4.5 Assembled Ancillaries

The positions of the devices on the copper main piece are displayed in Figure 2.39 and the assembled ancillaries stage is shown in Figure 2.40. Table 2.1 provides the set positions on the linear shift for the individual measurements.

Table 2.1: Positions for Ancillary Measurements — Recommended positions for operation of the individual ancillary devices.

Device	Position ^a		
	Minimum	Exact	Maximum
Open	62		70
Hot Plate		100	
Window	138		148
Mirror		159.5	
QCM		178.5	

a. In terms of the scale on the ruler attached to the linear shift.

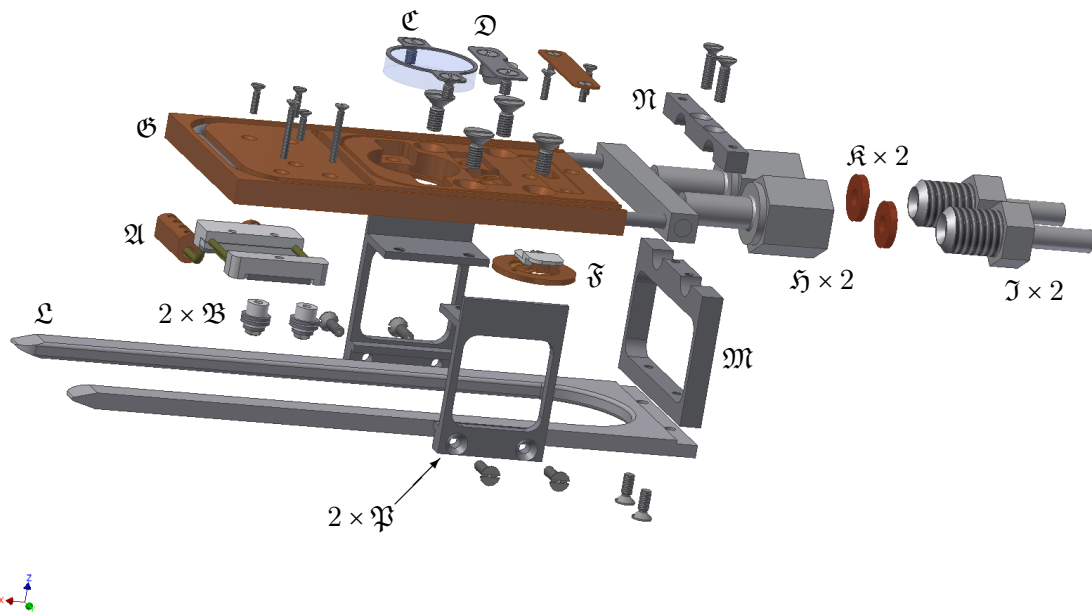


Figure 2.39: Assembly of the Ancillary Instruments — All the instruments – the hot plate (\mathfrak{A} , Figure 2.35) with its thermocouple terminals (\mathfrak{B}), the infrared radiation transparent window (\mathfrak{C} , Figure 2.38), the mirror (\mathfrak{D} , Figure 2.37, and the quartz crystal microbalance (\mathfrak{F} , Figure 2.36) – are mounted on the main part (\mathfrak{G}). It is held by the cooling tubes (not shown) connected by two VCR[®]-connections (\mathfrak{H} , \mathfrak{J}) equipped with custom copper gaskets (\mathfrak{K}). The cluster is supported on the nozzle (not shown, see Figure 2.28) in the main chamber (not shown) by an aluminum sled (\mathfrak{L}) clamped (\mathfrak{M} , \mathfrak{N}) to the cooling lines. Further stability is added by two spacers (\mathfrak{P}).

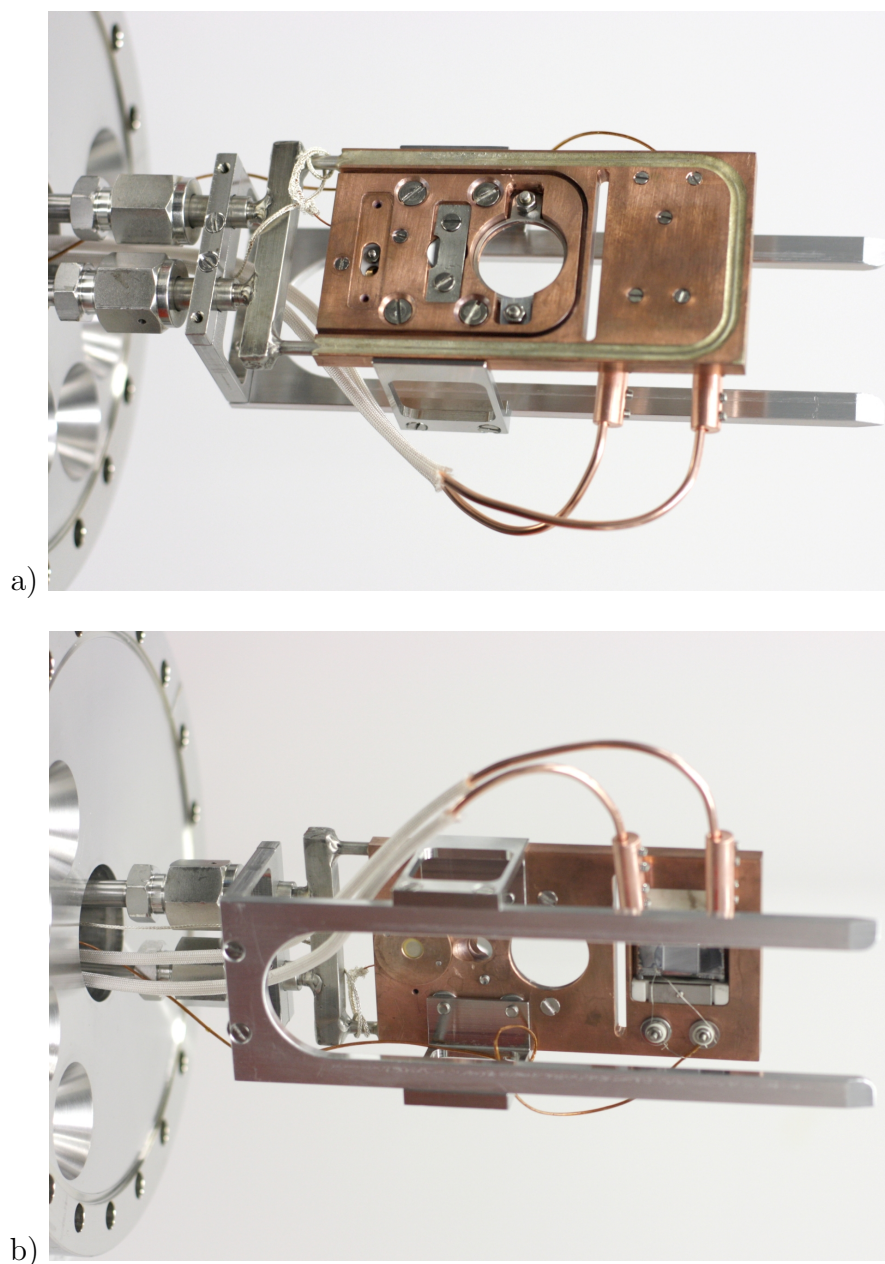


Figure 2.40: Assembled Ancillaries Stage — Photographs of the assembled ancillaries stage as described in Figure 2.39 show the of sample facing (a) and beam facing (b) side. The lid covering the quartz crystal microbalance is removed. This version carries a sapphire plate^a one sided wrapped into a tantalum foil^b with a Type K thermocouple^c as an alternative hot plate option.

a '66 40T350' 10 mm x 10 mm x 2 mm from KORTH KRISTALLE GMBH.

b 99.9% 0.1 mm from Haines & Maassen Metallhandelsgesellschaft mbH.

c 'THD' \varnothing 0.13 mm from Therma Thermofühler GmbH.

2.5 Main Chamber Additions

Several minor assemblies attached directly to the main chamber or to the frame the chamber is resting on are collected in this section.

2.5.1 Mass Spectrometer

The mass spectrometer³² is mounted on a CF nipple equipped with two BNC feedthroughs and four wire meshes, as shown in Figure 2.42. External electrical potentials can be applied on two of these meshes in order to prevent electrons emitted from the mass spectrometer reaching the sample and ions from the sample stage reaching the mass spectrometer. Electrons might cause an alteration of the sample in case of organic thin film^[58]. Ions from the sample stage might contribute to the intensity of the mass spectrometer signal in an unknown way and are thus unwanted.

Electrons accelerated in the ion source of the mass spectrometer can escape from it with a kinetic energy matching the set ionization energy, *i.e.*, typically 70 eV. Electrons traveling towards the sample feel the gradient between the grounded first grid and the second grid at maximal negative potential. If their kinetic energy is smaller than the barrier, they are repelled and cannot reach the sample. The same argument holds for ions from the sample stage with a kinetic energy of about $k_B \cdot 1000 \text{ K} \approx 0.1 \text{ eV}$. Figure 2.41 illustrates the used potential. Initially, all grids are

³² ‘HAL IV’ from Hiden Analytical.

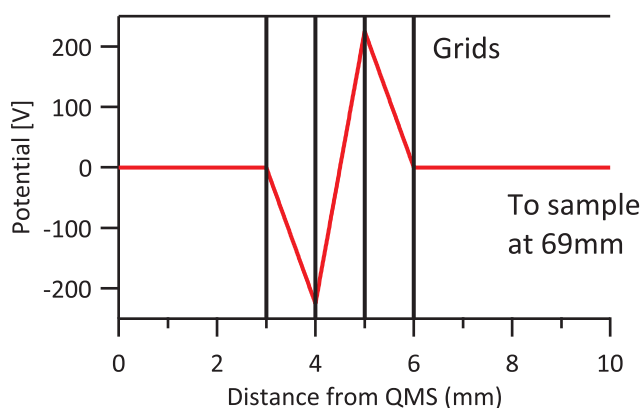


Figure 2.41: Electrical Potential Between Mass Spectrometer and Sample — The first and last grid are on ground potential providing electrical shielding. The inner grids are set to, *e.g.*, 225 V. The mesh closer to the mass spectrometer is at negative potential to repel stray electrons, the other one at positive potential to repel positive ions resulting in a pass filter for neutral species.

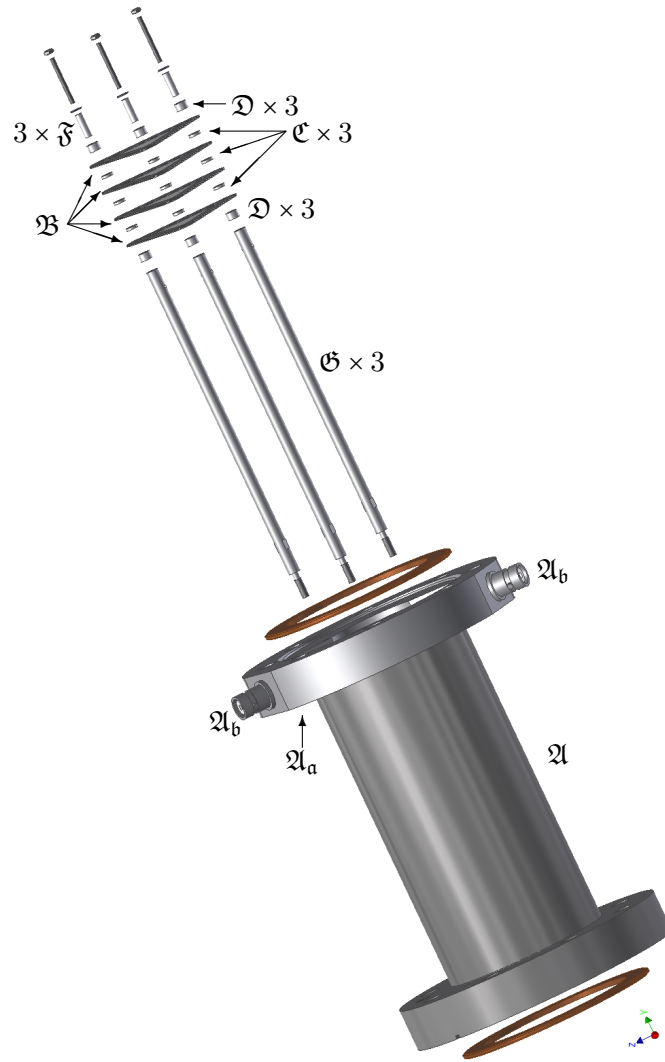


Figure 2.42: Assembly of the Mass Spectrometer Mount — The mass spectrometer^a is mounted on an extension nipple (\mathfrak{A}) equipped with a filter for charged particles. Nickel mesh^b is spot-welded between two stainless steel frames (\mathfrak{B}). Four of these sandwiches are, insulated from each other by alumina rings^c (\mathfrak{C} , \mathfrak{D}) and from the mounting screw by alumina tubes^d (\mathfrak{F}), assembled on top of three distance rods (\mathfrak{G}). The latter are screwed into the base flange (\mathfrak{A}_a), comprising two welded BNC feedthroughs^e (\mathfrak{A}_b), of the extension tube (\mathfrak{A}). The grid-side is mounted on the main chamber (not shown) and the mass spectrometer is attached to the vacant 63CF flange.

- a 'HAL IV' from Hiden Analytical.
- b Similar to 'NI008711' from Goodfellow GmbH.
- c Similar to 'C 799 5.0 x 3.0' from Morgan Advanced Materials Haldenwanger GmbH *via* Buntenkötter Technische Keramik GmbH.
- d Similar to 'C 799 3.0 x 2.0' from Morgan Advanced Materials Haldenwanger GmbH *via* Buntenkötter Technische Keramik GmbH.
- e 'A0058-2-W' from MPF Products, Inc. *via* tectra GmbH.

floating. The first and last grid are typically connected to ground potential to avoid unwanted electrical fields in the main chamber while the inner grids are energized. Only neutral species or charged particles with a kinetic energy of more than 225 eV can pass this electrostatic filter.

The used voltages are provided by an in-house made battery-box containing 90 batteries³³ in a serial arrangement. The ground reference is set in the middle of this setup and taps are wired to BNC sockets every five batteries providing -225 V to $+225\text{ V}$ DC in steps of 45 V .

Design drawings with dimensions and materials for the mass spectrometer stage can be found in Appendices Appendix B.2.7 and B.4.5.

2.5.2 Optical Meters

The laser beam exiting the fiber-out is collimated and the laser diode is able to deliver high powers. Hence, the laser system is potentially hazardous. In addition to the common laser safety precautions, the laser should generally be operated at low powers. Due to the short wavelength of 405 nm , light on the operators' skin should be avoided^[151].

Four instruments need a CF port facing the sample. The main chamber provides only three such ports while two of them are occupied by the molecular beam and the mass spectrometer. The remaining port is closed by a CF window and equipped with a quick coupling adapter, as shown in Figure 2.43, for a pyrometer and a photometer. If neither is mounted, the port provides visual access to inspect the sample.

Since adjustment is done in each of the adapter pieces for the two optical meters and the mounting of these pieces is reproducible, they can be exchanged without any further adjustment.

Upon cleaning thin sheet samples by flash desorption utilizing the sample heater, see Figure 2.8, it is necessary to monitor the sample temperature in order to prevent damage to the sample, *e.g.*, melting. Since no thermocouples can be attached directly to the samples, an optical method to measure the sample temperature is suggested for this setup. A pyrometer can be mounted on an adapter piece, see Figure 2.44, fitting into the quick coupling from Figure 2.43. It can be slid in from one side and locked in place by two knurled screws. Alignment of the pyrometer could be done by adjusting the force on the rubber spacers.

One aspect of measuring temperatures through windows, *e.g.*, on a vacuum chamber, should be mentioned in this context. Most pyrometers are so-called

³³ '6LR61' – "9 V Block" from ALDI Einkauf GmbH & Co. OHG.

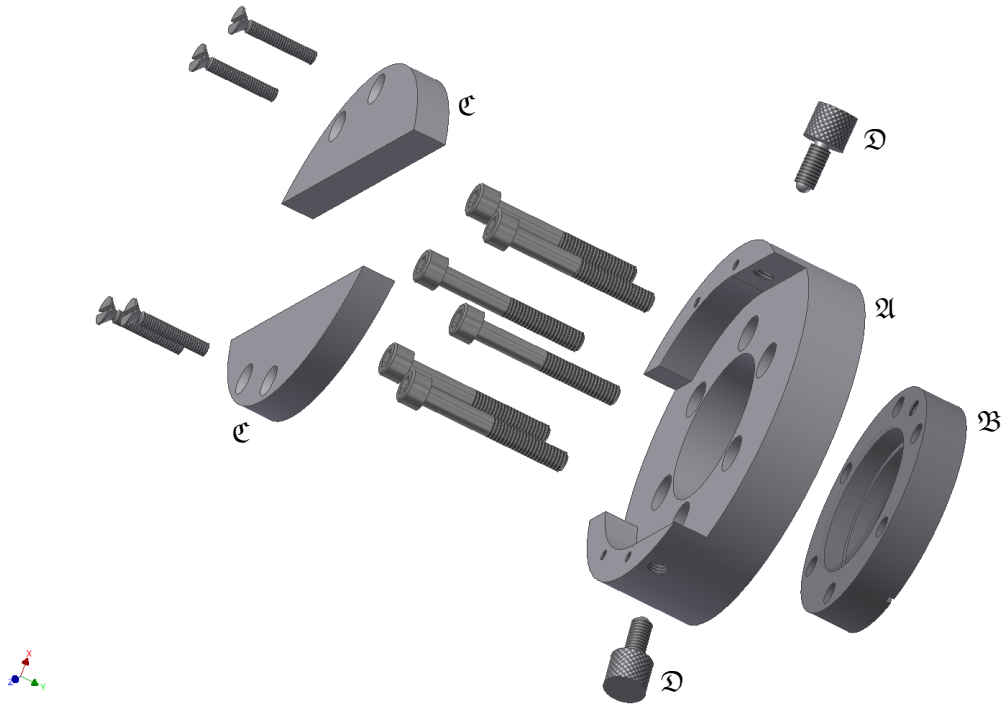


Figure 2.43: Assembly of the Seat for Optical Meters — The base (A) is mounted together with a 40CF window (B) on the main chamber (not shown). Two half shells (C) hold the mounts (not shown) for the pyrometer (Figure 2.44) and the photometer (Figure 2.45). The pyrometer is fixed with two knurled screws (D) whereas controlled lateral movement is possible for the photometer attached from the backside of the assembly.

brightness pyrometers measuring the emitted infrared radiation in a certain range, typically $2.0\ \mu\text{m}$ to $2.8\ \mu\text{m}$ ^[152]. Together with the emissivity of the surface as input parameter, a surface temperature is calculated. Unfortunately, the common window materials, *i.e.*, Kodial and quartz glass, show strong absorption in this range^[153]. As a result the calculated temperature is smaller than the real temperature. If this kind of pyrometer is used, it is essential to calibrate it against a thermocouple with the used window. The situation can be improved upon usage of sapphire windows exhibiting a lower and less changing absorption but calibration is still necessary. Furthermore, the measured temperature is calculated from the average infrared intensity emitted from the area seen by the pyrometer. This will result in additional inaccuracies for this setup, since the samples are small compared to the view area and cannot be heated uniformly due to the mechanically necessary holder.

As an alternative, ratio pyrometers can be used which operate at two different wavelengths and calculate the temperature from the ratio of the corresponding intensities. If the window acts as a gray filter, *i.e.*, the absorption is the same at

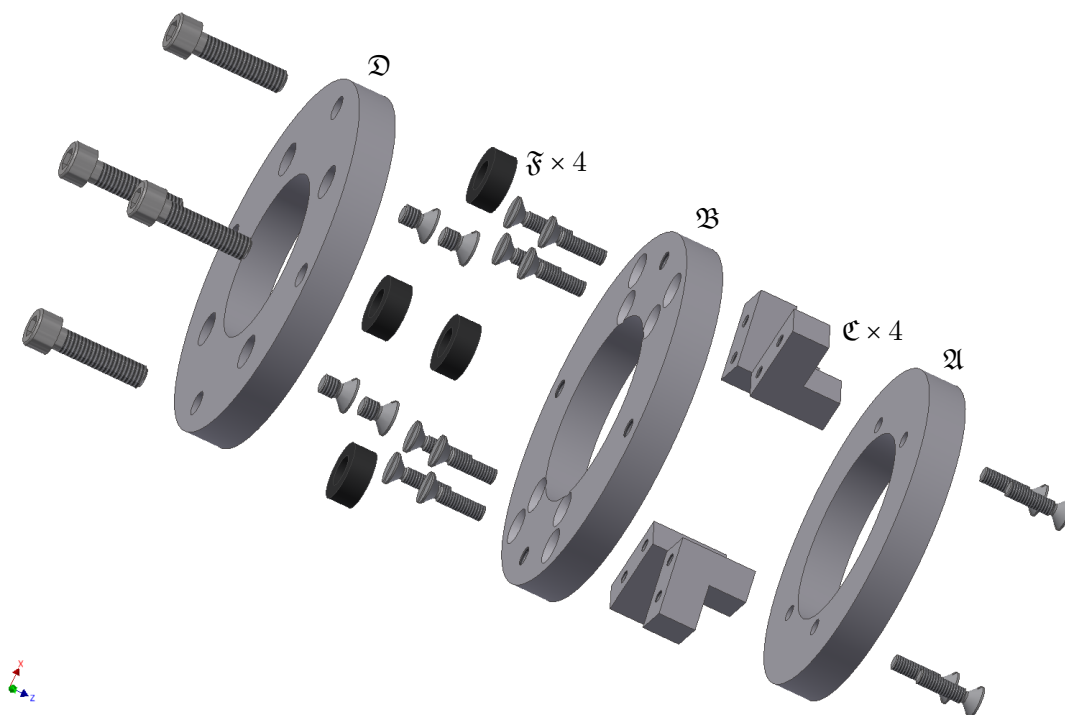


Figure 2.44: Assembly of the Pyrometer Mount — The base ring (A) in the south west slides into the seat from Figure 2.43 and is held by the three mentioned screws. The middle ring (B), mounted on distance pieces (C) to the base part (A), carries the mounting ring (D) for the pyrometer (not shown) and provides two angular degrees of freedom using four rubber spacers (F, black), in order to aim precisely at the sample (not shown). This setup is optimized for a brightness pyrometer^a which was already available in Erlangen. Since the measurement is performed through a glass window and the emissivity of the sample is unknown, the use of a ratio pyrometer^b would be recommended.

a ‘IMPAC IP 140’ from LumaSense Technologies Inc.

b *E.g.*, ‘ISR 6 Advance’ from LumaSense Technologies Inc.

both wavelengths like in sapphire, it will provide an accurate temperature.

A vital parameter for a calorimetry experiment is the power of the laser on the sample. As this value cannot be measured in the vacuum chamber, the laser is reflected out of the chamber, see Section 2.4.3, and measured through a window. With knowledge of the reflectivity of the mirror and the transmission of the window, the input power on the sample can be calculated by an outside measurement. The detector of the photometer is mounted in an adapter piece, see Figure 2.45, fitting into the quick coupling from Figure 2.43. It is locked in place by one screw and can be reproducibly inserted and removed.

The position of the detector on the adapter can be adjusted by two independent jackscrews.

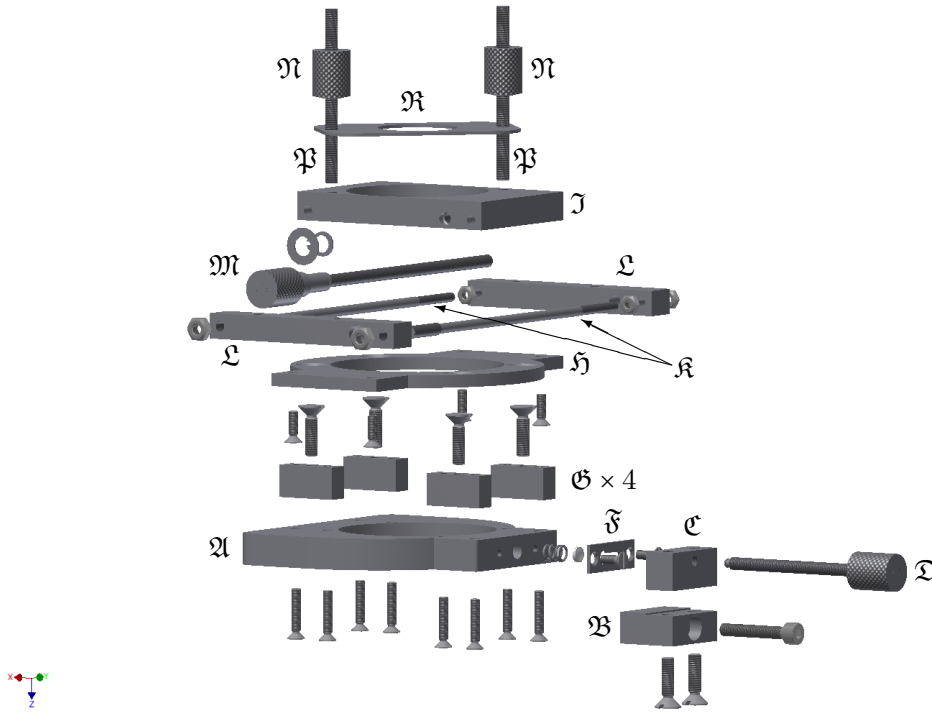


Figure 2.45: Assembly of the Photometer Mount — The socle plate (A, south) is mounted to the base plate (not shown) from Figure 2.43 by two small steel blocks (B, C). A spring loaded long screw (D), trapped by a plate (E), through one of the blocks allows defined lateral movement in one dimension of the remaining setup in this seat. Four spacers (G) and a secondary base plate (H) carry another moving component (I). This piece moves, guided by two rods (K) which are held by two bars (J) mounted to secondary base plate (H), on a threaded rod (M) perpendicular to the first degree of freedom. It also holds the detector^a (not shown), with two knurled nuts (N) on threaded rods (O) and a steel plate (P).

a '918D-SL-OD1' (not shown), operated by a '842-PE' powermeter from Newport Spectra-Physics GmbH.

Design drawings with dimensions and materials for the optical meters stage can be found in Appendix B.1.3.

2.5.3 Fiber Positioner

The laser used for detector calibration is spread and reflected onto the sample in the molecular beam, see Section 2.3.2. In order to align the center of the defocused laser beam, the output of the laser fiber can be adjusted in four degrees of freedom. The used device is shown in Figures 2.46 and 2.47.

A drawback of this design is the dependency of vertical position and tilt angle. On the one hand, the adjustment could be simplified with two independent adjustment options. On the other hand, alignment is not necessary very often and usually can be done within half an hour by an experienced user. Hence, a redesign was considered to be unnecessary.

In order to adjust the mounted laser output, the laser power should first be limited to 1 μ W and checked with the powermeter. The pan angle should be set to zero and the laser should be centered on the window. The screws for vertical positioning should be inserted to the same extend. The optics stage, see Section 2.3.2, and the ancillaries stage, see Section 2.4, are each set to their mirror position. The inside of the molecular beam should be dark. If it is lit up blue, the laser is hitting the housing of the beam. The screws for vertical adjustment should be altered until the laser is only hitting the mirror in the molecular beam. With removed detector in the optical meters assembly, see Section 2.5.2, the laser should be visible on a white piece of paper after it is reflected out of the chamber. Since it is attenuated by a factor of approximately 25, it is less dangerous now.

Fine adjustment is done by maximizing the reading of the power meter with the detector mounted in its adapter. All four adjustment screws may be used. Typically, the tilt and vertical position require most tuning. The adjustment of the individual degrees of freedom can be summarized as follows.

Horizontal position: This position along the chamber can be adjusted by the guided sled running on the spindle.

Pan angle: The horizontal angle can be aligned by panning the moveable frame (blue in the figures).

Vertical position: This position can be adjusted by identical rotation of the two screws on the sled.

Tilt angle: The vertical angle can be aligned by a small rotation of one of the two screws on the sled.

Design drawings with dimensions and materials for the fiber positioner can be found in Appendix B.2.9.

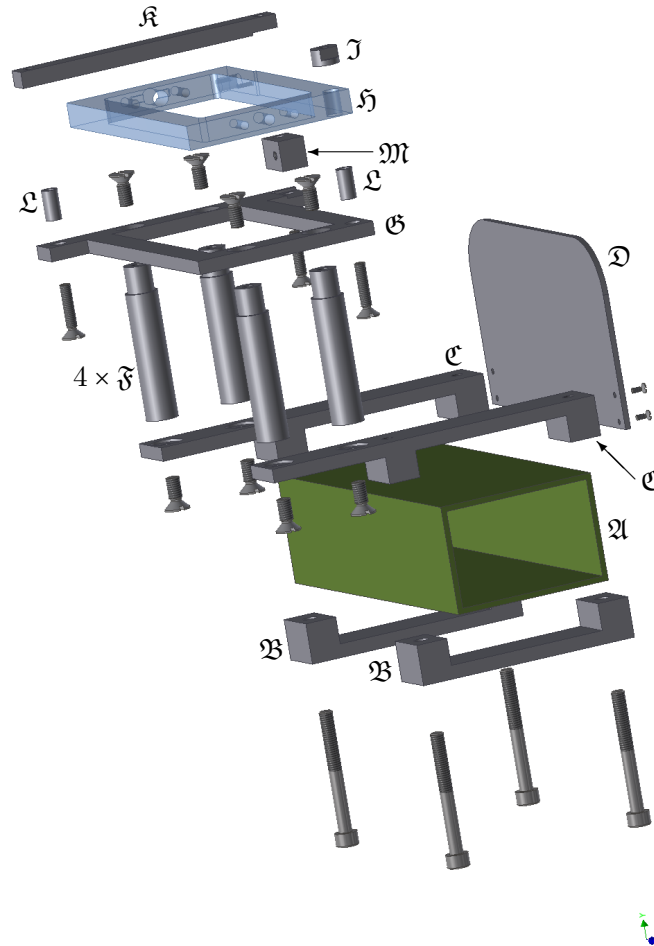


Figure 2.46: Fixed Part of the Fiber Positioner — The fixture is clamped to the frame (A, green) by four half shells (B, C). Two of them (C) carry a plate (D) to protect the optical fiber (not shown) and four distance pieces (F). A base plate (E) holds a frame (H, blue – also see Figure 2.47) which is able to pan. It is held in place by a nut (J), a bar (K), and three spacers (L, M).

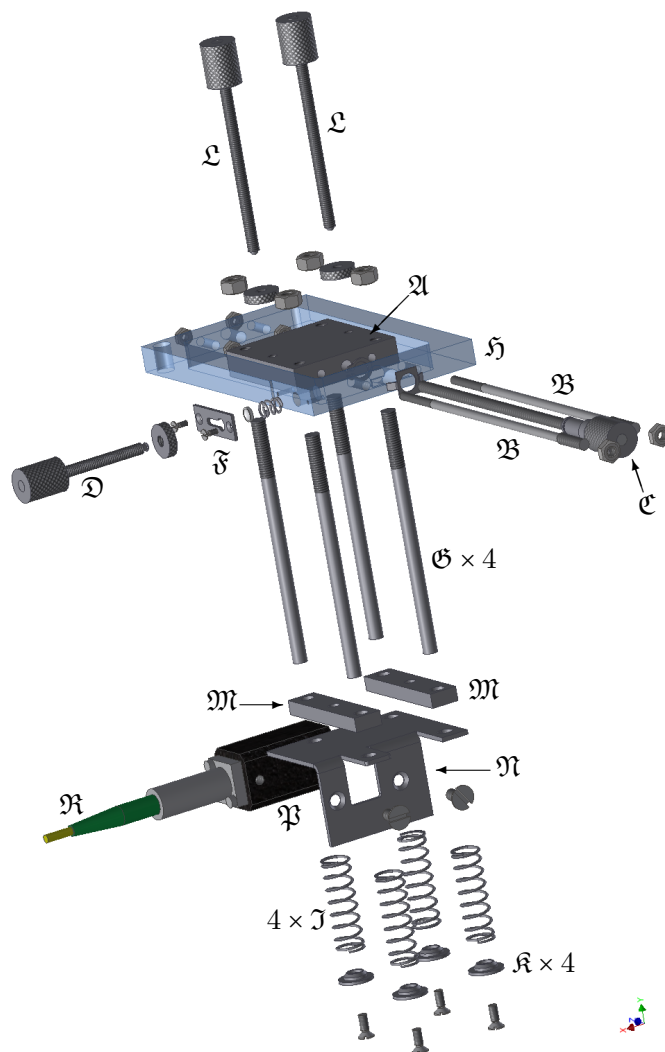


Figure 2.47: Moveable Part of the Fiber Positioner — The frame (S, blue) from Figure 2.46 comprises a sled (A) guided by two rods (B) providing lateral movement along the long axis of the main chamber (not shown). It is actuated by a spindle (C). Panning is possible with the short spring loaded knurled screw (D) trapped by a plate (F). Four steering rods (G) are attached to the sled (A) together with four springs (J) and their retainers (K). Vertical adjustment as well as tilting is provided by interaction of the four springs (J) and two knurled screws (L) pressing on the balancing bars (M) on the holder (N) for the fiber-out^a (P, black) connected to the optical fiber^b (R, green/yellow).

a 'FiberOut' from TOPTICA Photonics AG.

b '#OK-000634' from TOPTICA Photonics AG.

2.5.4 Miscellaneous Additions

The tool shown in Figure 2.48 is designed to lift the chamber off its steel/rubber vibration dampers. The chamber's height can be set by the turning of the nut with an extra long 19 mm wrench. Upon lifting or lowering the chamber, the nuts should be rotated in an alternating pattern to avoid a skew position of the chamber.

If the machine needs to be moved from one laboratory to another, *e.g.*, from Erlangen to Marburg, the main chamber can be fixed on the frame by four clamps as shown in Figure 2.49 to form a stable shipping unit. Upon the necessity to transport the machine with a pallet truck along the long axis, *e.g.*, through a narrow door, the frame can be equipped with three trusses, as shown in Figure 2.50.

Cooling water for various purposes, *e.g.*, cooling turbo molecular pumps, evaporators, *etc.*, is provided by a commercial distribution center. It is mounted on the frame by the clamp setup shown in Figure 2.51. The flow can be adjusted by partially opening the attached ball valves. Due to the many taps, all devices can be operated on their own cooling line. This simplifies work on the cooling system but requires a higher inlet pressure. Valves for low conductance loops, *e.g.*, the main evaporator, should be fully opened and the other loops, *e.g.*, turbo molecular pumps, should be regulated.

The setup shown in Figure 2.52 provides a possibility to safely attach “Minicans” to the frame of the machine. The clamp is permanently mounted. The can itself is held by a hose clamp.

Design drawings with dimensions and materials for the miscellaneous additions can be found in Appendix B.2.7.

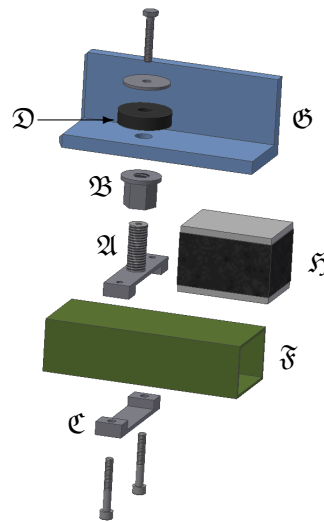


Figure 2.48: Assembly to Lift the Main Chamber — The main chamber (not shown) can be lifted on a screw welded to a half shell (A) for bake-out with the large nut (B). A counter shell (C) secures this part, while a screw into this part from top prevents unwanted lateral movement of the chamber. A piece of rubber^a (D, black disc) provides vibrational isolation from the brackets (A, C) clamping on the frame (F, green). During measurements the nut (B) is not touching the truss (G, blue) of the main chamber. Instead, it is resting on metal rubber rails^b (H, black block). Four sets of this assembly are needed for the setup.

a 'Waschmaschinenunterlage' from HORNBACH-Baumarkt-AG.

b 'Gummi-Metall-Schiene 50 mm x 50 mm, Metallauflage 5 mm, 70°Shore' from Erwin Telle GmbH.

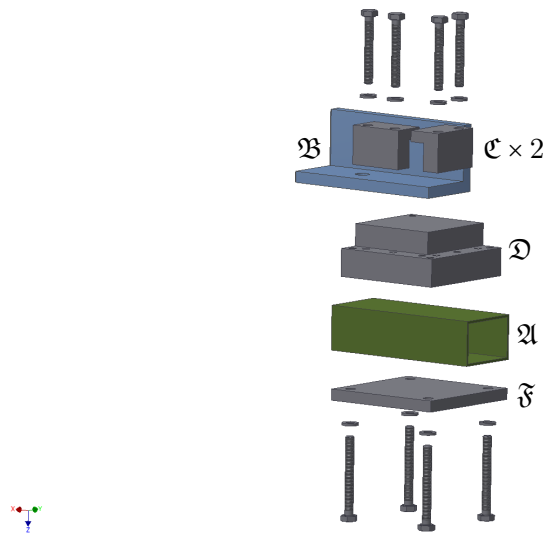


Figure 2.49: Upper Assembly for Moving the NAC Machine — In order to establish a secure mount between the main chamber (not shown) and the frame (A, green), the truss (B, blue) of the chamber can be fastened by two brackets (C) on the massive spacer piece (D). Four of these assemblies are clamped to each corner of the frame with a counter plate (F).

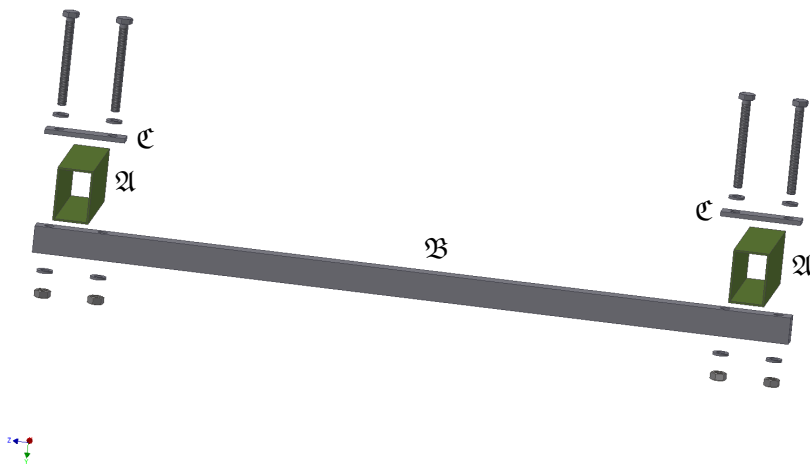


Figure 2.50: Lower Assembly for Moving the NAC Machine — If a pallet truck is used to move the machine along its long axis, the frame (A, green) can be equipped with trusses (B) clamped by counter plates (C). Up to three sets of the assembly can be used for transportation.

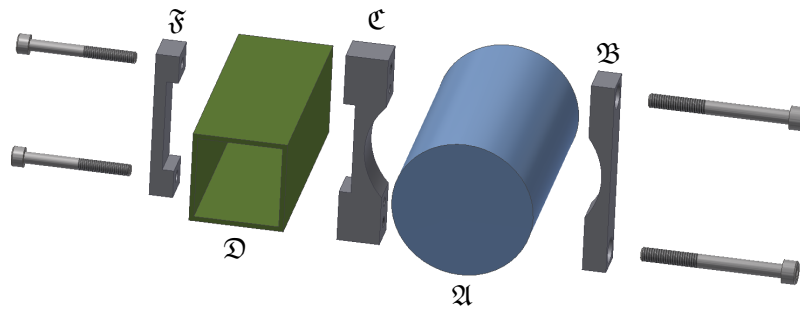


Figure 2.51: Assembly of the Water Distribution Mount — Cooling water distribution centers^a (A, blue) are clamped with a shaped bar (B) to a two sided bracket (C) which itself is attached to a support strut of the frame (D, green) by another clamp (F).

a '120910HPSP' from HPS Handels GmbH.

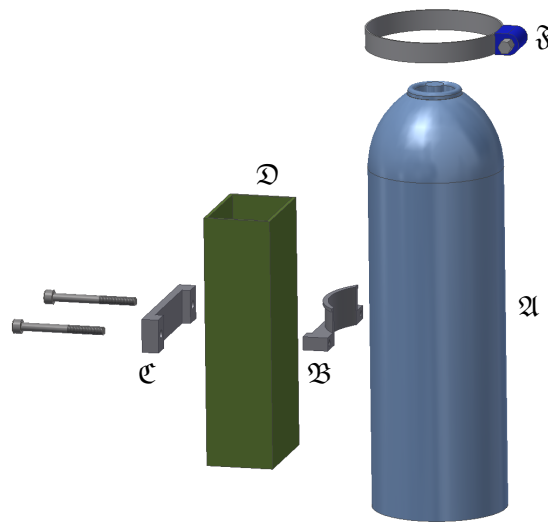


Figure 2.52: Assembly to Hold Minicans — Minicans^a (A, blue) can be added to the setup by a pair of fasteners (B, C) clamped to the frame (D, green). The can itself is held by a large hose clamp^b (F).

a 'HiQ[®] MINICAN' from Linde Aktiengesellschaft.

b 'ABA 3223 77 95' from Theo Förch GmbH & Co.KG.

2.6 Load Lock

The load lock depicted in Figure 2.53 provides in vacuum storage for up to ten samples and a simple facility to create (organic) thin films on the samples by physical vapor deposition as well as degassing of spin coated samples. Since the load lock is rather large, it exerts a large torque on the main chamber and on its mounting flange. Thus it is necessary to support the assembly as shown in Figure 2.54.

This task is done by two tools. On the one hand, the transfer rod is supported by two struts, as shown in Figure 2.55. In addition, the included turnbuckles provide, in combination with the port aligner, adjustment of the sample transfer.

On the other hand, the turbo molecular pump of the load lock is resting on an adjustable console mounted on the frame, as shown in Figure 2.56. The pump is suspended by rubber pieces for vibrational isolation.

Design drawings with dimensions and materials for the load lock can be found in Appendix B.3.

Thin layers of, *e.g.*, organic, material can be deposited on the samples by physical vapor deposition with an evaporator, shown in Figure 2.57, in the load lock. It provides coarse thickness control by an included quartz crystal microbalance. The quartz crucible has been successfully tested for temperatures up to 570 K in combination with metalized and poled β -polyvinylidene fluoride as substrate. At even higher crucible temperatures, the detector polymer might get heated by the infrared radiation to a point where it loses its polarization and thus its suitability as detector.

Since the sensor crystal lacks a cooling option, thermal frequency shifts are inevitable in this setup. Two possible methods can circumvent this drawback. On the one hand, the sample can be moved in – and later taken out off – the coating position after a stable deposition rate reading has been established. Due to the geometry of the available components, deposition occurs on the transfer rod in this case. On the other hand, the sample can be placed in deposition position before the heating is turned on. A correct *final* thickness reading is given in this case by the time the sensor reading is stabilized after switching off the heating power. This method avoids unwanted deposition but suffers from a variable – but well reproducible – deposition rate. In other words, it exhibits an intrinsic deposition rate profile.

Design drawings with dimensions and materials for the evaporator in the load lock can be found in Appendix B.4.4. The shutter port is used for a BNC feedthrough and the copper shroud is replaced by a holder for a QCM crystal.

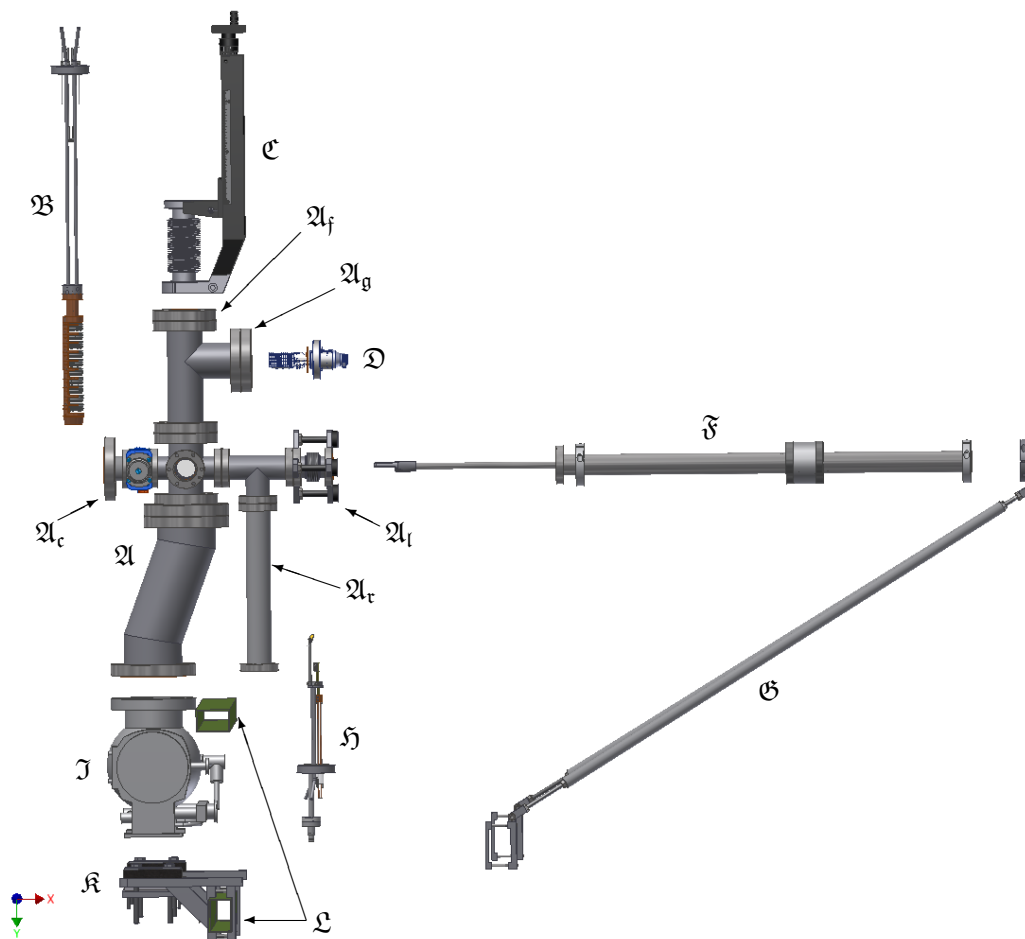


Figure 2.53: Assembly of the Load Lock — The northern port of the housing of the load lock (\mathcal{A} , Figure 2.54), accepts the sample storage (\mathcal{B} , Figure 2.58) mounted on a linear shift^a (\mathcal{C}) on a tapped adapter flange^b (\mathcal{A}_f). A similar adapter flange (\mathcal{A}_g) is equipped with a Bayard-Alpert gauge head^c (\mathcal{D}). A magnetically coupled transfer rod^d equipped with a sample reception (\mathcal{F} , Figure 2.60) is mounted to the port aligner (\mathcal{A}_l) and positioned by its support (\mathcal{G} , Figure 2.55). An evaporator (\mathcal{H} , Figure 2.57) is attached to the extension tube (\mathcal{A}_t). The turbo molecular pump^e (\mathcal{J}) is located at the southern end of the assembly resting on its support console (\mathcal{K} , Figure 2.56). The whole setup is connected to the main chamber (not shown) *via* the remaining CF adapter nipple (\mathcal{A}_c) on the west. Both supporting assemblies (\mathcal{G} , \mathcal{K}) are mounted to the frame (\mathcal{L} , green).

a ‘LD40-200’ with stepper motor actuation from VAb Vakuum-Anlagenbau GmbH.

b ‘RF450X275MT’ from Kurt J. Lesker Company.

c ‘AIG17G’ from Arun Microelectronics Ltd. *via* tectra GmbH.

d ‘VF-1695-24’ from Huntington Mechanical Laboratories Inc. *via* tectra GmbH.

e ‘TPU330’ from Pfeiffer Vacuum GmbH.

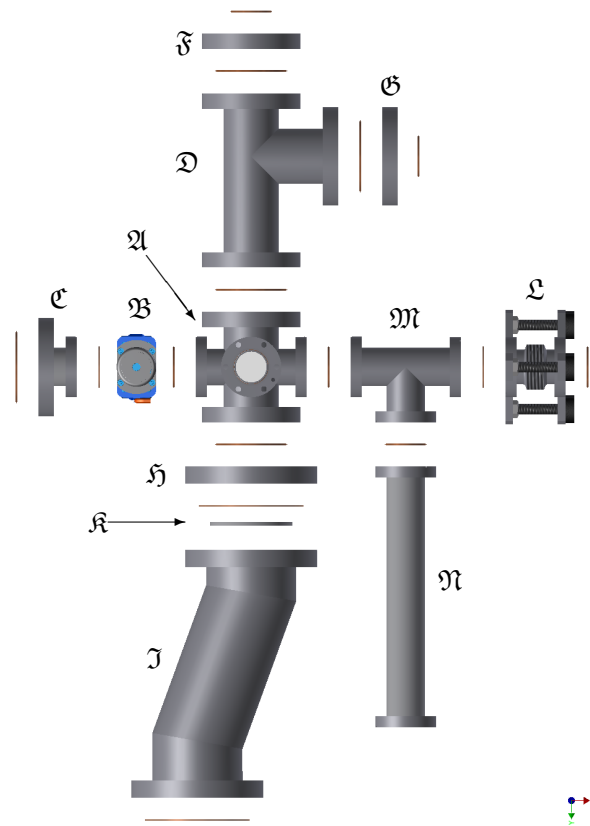


Figure 2.54: Assembly of the Load Lock Housing — The central position of the load lock is occupied by a modified six-way 40CF/63CF cross^a (A). The load lock is attached to the main chamber (not shown) with its west port by a gate valve^b (B) and an adapter nipple (C). The north facing flange carries a large asymmetric tee (D) and two adapter flanges (F, G). Another adapter flange^c (H) and a custom off-center nipple (J) on the south flange connect to the turbo molecular pump^d (not shown) from Figure 2.56. It is equipped with a heavy duty protective grid (K). A magnetically coupled transfer rod^e (not shown) is mounted on a port aligner (L) and a tee piece^f (M) fitted with the evaporator (not shown) from Figure 2.57 on a distance tube (N). 40CF windows^g seal the front and back ports of the center cross. All 40CF gaskets on the horizontal path need an inner diameter of 40 mm.

a Modified ‘RK 63/40CF’ from VAb Vakuum-Anlagenbau GmbH.

b ‘315370A’ from VAT Vacuumvalves AG.

c ‘RF600X450M’ from Kurt J. Lesker Company.

d ‘TPU330’ from Pfeiffer Balzers - now Pfeiffer Vacuum GmbH.

e ‘VF-1695-24’ from Huntington Mechanical Laboratories Inc. *via* tectra GmbH.

f ‘TCF40’ from VAb Vakuum-Anlagenbau GmbH.

g ‘VPZL-275’ from Kurt J. Lesker Company.

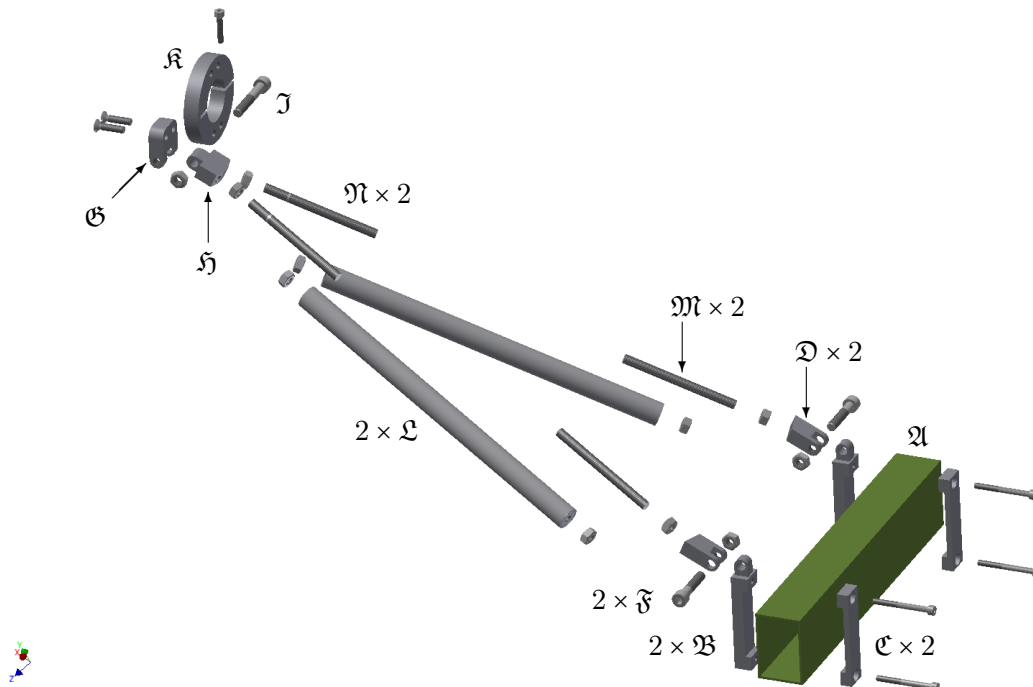


Figure 2.55: Assembly to Support Transfer Rods — The assembly is fastened on the frame (\mathfrak{A} , green) by two different half shells (\mathfrak{B} , \mathfrak{C}). The upper part of the first one (\mathfrak{B}) exhibits the middle section of a three knuckle mortise hinge. The other half of the hinge (\mathfrak{D}) provides a mounting option for the movable parts. The threadless part of a screw^a (\mathfrak{F}) serves as pin completing the joint. A similar hinge comprising a stationary (\mathfrak{G}) and a movable (\mathfrak{H}) as well as a center pin^a (\mathfrak{J}) is attached to a clamp ring (\mathfrak{K}) holding the transfer rod (not shown). The position of the transfer rod can be adjusted by inverted turnbuckles. A right handed and a left handed thread are machined into each of the distance tubes (\mathfrak{L}). Matching threaded rods, either all right handed (\mathfrak{M}) or with a partial left handed thread (\mathfrak{N}) are mounted in the hinges. The distance between them can be adjusted by rotation of the distance part (\mathfrak{L}).

a 'DIN EN ISO 4762 M8x40'.

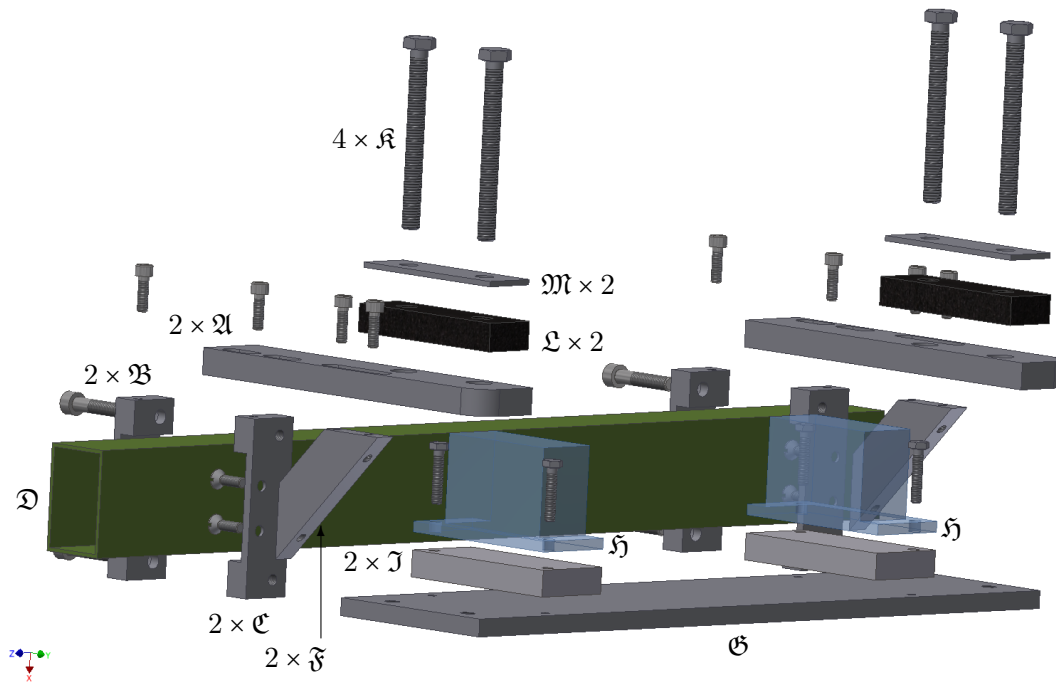


Figure 2.56: Assembly to Support the Load Lock — Two proximaly adjustable struts (A) are mounted on half shells (B, C) clamped on the frame (D, green). To support higher off-axis loads stiffeners (F) are added on one clamp type (C). The resting plate (G) for the turbo molecular pump^a (H, partially shown, blue) with its two spacer plates (J) is hanging on four screws (K) which are vibrationally isolated from the frame (D) by rubber^b pieces (L, black) and load distributing plates (M).

- a 'TPU330' from Pfeiffer Balzers - now Pfeiffer Vacuum GmbH.
 b 'Waschmaschinenunterlage' from HORNBACH-Baumarkt-AG.

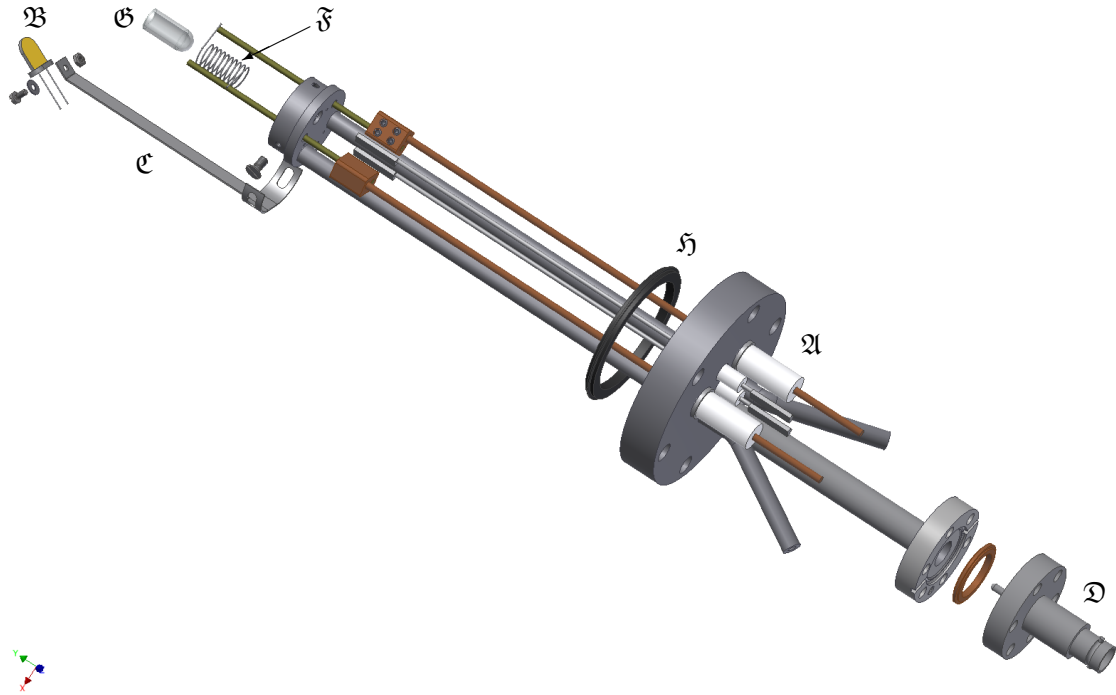


Figure 2.57: Assembly of the Load Lock Evaporator — One of the sources (A) of the three fold evaporator^a is modified by a quartz crystal microbalance option instead of a shutter and cooled orifice. The quartz crystal^b (B, gold) is held by sheet metal (C) and connected to a BNC feedthrough^c (D) by a coaxial cable^d (not shown). Tungsten wire^e (F) holds a homemade quartz crucible (G). Due to frequent refilling this evaporator is mounted with a rubber gasket^f (H, black).

a Designed by O. LYTKE.

b Excised from ‘6.000MHZ HC49 30/50/40/18PF/ATF’ from Euroquartz Ltd *via* Conrad Electronic SE.

c ‘A0237-2-CF’ from MPF Products, Inc. *via* tectra GmbH.

d ‘KAPWC1X025’ from LewVac Components Ltd.

e $\varnothing 0.5$ mm from Haines & Maassen Metallhandelsgesellschaft mbH.

f ‘402DFL040-S2’ from Pfeiffer Vacuum GmbH.

2.7 Sample Handling

The setup holds up to ten samples available in the storage device in the load lock, as shown in Figure 2.58. The upper groove of a sample holder is inserted in one of the ridges of the storage assembly.

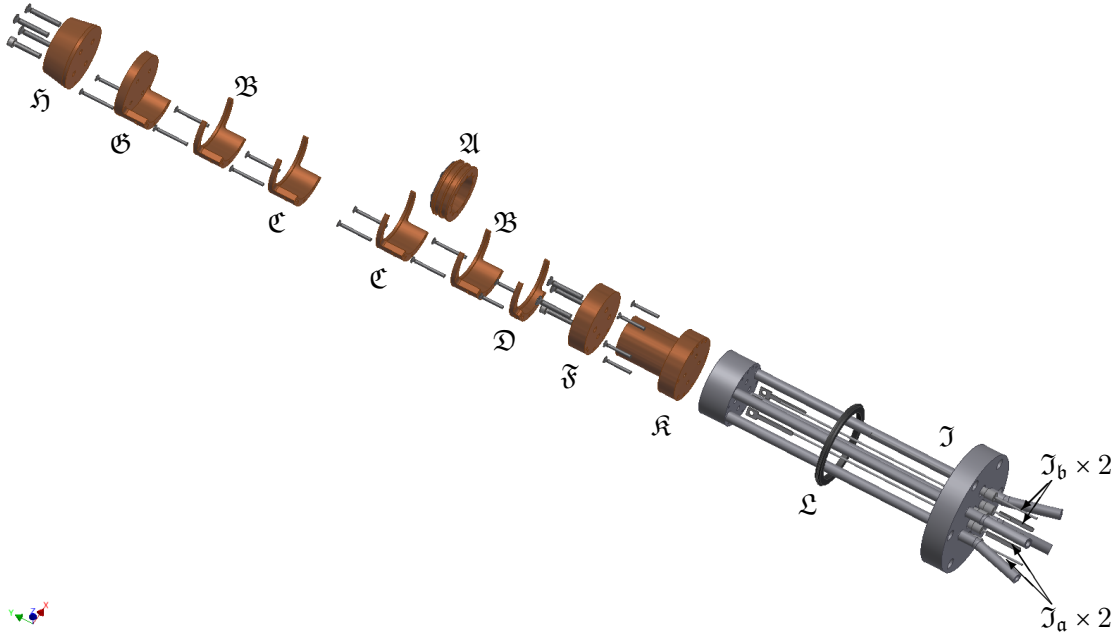


Figure 2.58: Assembly of the Sample Storage System — Ten samples (A, one shown) can be inserted into nine stacked holding pieces (B, C, only two shown each) and an initial, shorter holder (D). The top (F) and the, by a spacer (E) separated, bottom piece (G) have Type K thermocouples^a attached. The latter are wired to two Type K thermocouple feedthroughs^b (K_a, K_b) welded into the base flange (I, length of cooling lines reduced for clarity). The end piece (H) near the mounting flange (I) has an attached heater (K) which is counter cooled. Since this assembly is removed quite often, it is sealed by a reusable 40CF rubber gasket^c (J, black) which is also used to align the sample holders to the transfer system.

a ‘KFD-30-KK-IEC’ from Therma Thermofühler GmbH.

b ‘A0636-1-W’ from MPF Products, Inc. *via* tectra GmbH

c ‘402DFL040-S2’ from Pfeiffer Vacuum GmbH.

In order to remove a sample from the storage, the sample reception from Figure 2.59 is slid onto the lower groove in the sample holder shown in Figures 2.2 and 2.3. The storage is lowered by 1 mm to release the upper ridge of the sample holder and lock the middle ridge into the sample reception, see Figure 2.62 b. After returning the sample storage to its top position, the sample can be transferred into the main

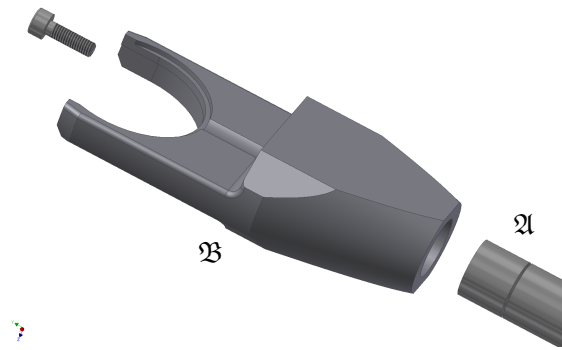


Figure 2.59: Assembly of the Load Lock Sample Transfer System — A magnetically coupled transfer rod^a (A, partially shown) carries the sample reception (B). The sample is held in place by a small jut, see Figure 2.62.

a 'VF-1695-24' from Huntington Mechanical Laboratories Inc. *via* tectra GmbH.

chamber or placed above the evaporator shown in Figure 2.57 in order to deposit a thin film on it.

A similar mechanism is used to hand over the sample holder into the sample reception, shown in Figure 2.60, in the main chamber. As shown in Figure 2.61, the reception is slid over the upper groove until the pin secures the sample holder. Lifting the part attached to the main chamber by 1 mm releases the sample holder from the other transfer unit.

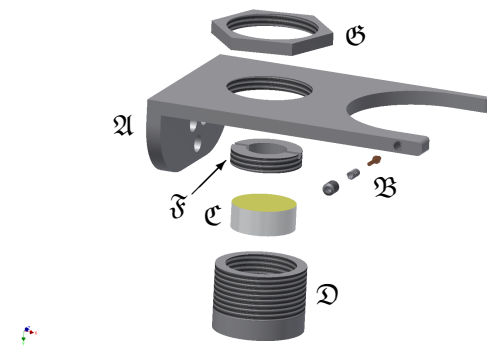


Figure 2.60: Assembly of the Main Chamber Sample Transfer — A magnetically coupled transfer rod^a (not shown) mounted on an *xy*-stage (not shown) carries the sample bracket (A). The sample (not shown) is secured in its reception by a small spring loaded copper pin (B). The sample carrier (A) also offers the option to mount a mirror^b (C) in the main chamber. It is secured in its positioner (D) by a small retainer ring. The position can be fixed by a small counter nut (E).

a 'VF-1695-18' from Huntington Mechanical Laboratories Inc. *via* tectra GmbH.

b 'G340704000' from Qioptiq Photonics GmbH & Co. KG.

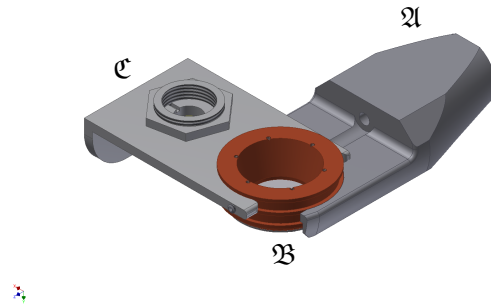


Figure 2.61: Sample Handover — The load lock's sample carrier (A) holds the sample (B) in its pouch while the main chamber's sample carrier (C) is clicked onto the sample holder (B, copper).

The sample in the transfer unit can be transferred into measurement position by lowering the holder into the designated pouch of the thermal reservoir, see Figure 2.5. After establishing the connection to the detector head, the transfer part can be retracted to release the sample.

Transfer to the storage system is performed by the same steps in reverse order. The individual retaining mechanism and positions are shown in Section 2.62.

Since the sample is grounded in the main chamber's transfer system it is possible to sputter it. Unfortunately, it is impossible with this setup to measure the ion current onto the sample. A manipulator for sample preparation in the main chamber with an electrically floating sample acceptance is planned but not realized at this time.

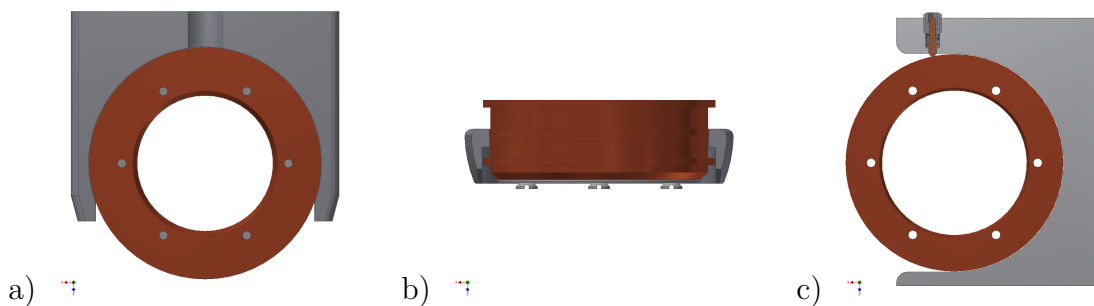


Figure 2.62: Sample Retaining Mechanisms — a) and b) Load lock: The sample holder (copper) is inserted into a notch in the load lock's sample carrier (gray) and held by small juts. c) Main chamber: The sample holder (copper) is slid into the grooves of the carrier (gray) and secured by a spring loaded copper pin.

2.8 Glove Box

An available glove box has been modified as shown in Figure 2.63. It provides an inert gas environment for handling evaporants that are sensitive to water or oxygen. Besides storage and purification of evaporants, refilling the main evaporator and recovery of material from the main evaporator's cap are the main purposes of this setup.

The main evaporator mounted on a linear shift and equipped with a gate valve can be attached to the bottom flange of the glove box, as shown in Figure 2.63. The interjacent dead volume can be evacuated and flushed with inert gas. After clearing both gate valves, the top part of the evaporator can be moved into the accessible volume of the glove box.

A refilled evaporator can be attached back to the vented beam with the closed valve. In order to maintain the protection of the sensitive evaporant, the volume of the beam above the valve attached to the evaporator assembly, see Figure 2.13, is pumped to roughing vacuum before an opening of the gate valve. This step needs to be executed carefully since an abrupt opening of the valve might lead to an ejection of material from the crucible. After complete opening of the valve and insertion of the evaporator, the turbo molecular pumps can be started.

This setup extends the scope of investigate-able materials into the very interesting region of delicate, *i.e.*, more reactive materials. Examples would include organic materials sensitive to air like pentacene or the reactive alkaline metals. Among these susceptible materials are several source materials used in organic electronics^[154].

Design drawings with dimensions and materials for the glove box additions can be found in Appendix B.4.1.

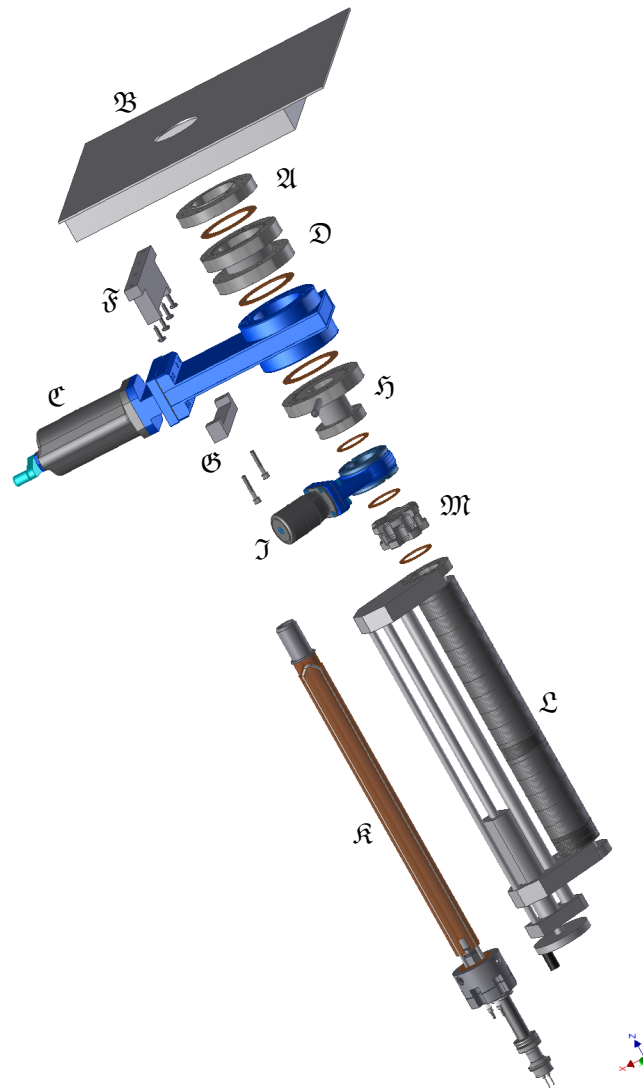


Figure 2.63: Assembly of the Glove Box Connection — A modified 63CF flange (\mathfrak{A}) is welded to the floor (\mathfrak{B} , partially shown) of the glove box. The sealing of the glove box is preserved by a 63CF gate valve^a (\mathfrak{C}) mounted on a short 63CF coupler (\mathfrak{D}). The valve is also fixed to the frame of the glove box by two half shells (\mathfrak{F} , \mathfrak{G}). A 63CF/40CF reducing nipple (\mathfrak{H}) provides connection to a gate valve^b (\mathfrak{I}) and to the nitrogen/vacuum system (not shown) of the glove box. The main evaporator (\mathfrak{K} , Figure 2.13) is attached to a linear shift^c (\mathfrak{L}) via a short coupling 40CF adapter^d (\mathfrak{M}).

-
- a ‘10836-CE01’ from VAT Vacuumvalves AG.
 b ‘01032-CE01’ from VAT Vacuumvalves AG.
 c ‘LSM38-350-H-ES’ from Kurt J. Lesker Company.
 d ‘MCF275-ClsCplr-C2-1400’ from Kimball Physics Inc.

2.9 Assembled System

Figures 2.64 and 2.65 illustrate the attachment positions of the individual devices on the main chamber. The load lock provides introduction of new samples, in vacuum sample storage, simple sample preparation, and sample transfer. Equipment for assisting measurements is provided by the ancillaries stage and the mass spectrometer. The molecular beam source delivers the pulsed adsorptive and the detector stage performs the main measurement. A sputter gun offers sample cleaning and an ionization gauge offers pressure measurement. The vacuum is maintained by a titanium sublimation pump and a turbo molecular pump. CF blind flanges and CF windows to provide visual feedback upon sample manipulation finalize the setup.

Since the transmitted light through the windows is detectable in the calorimetry signal, all unused windows should be covered with aluminum foil during the measurements.

Figure 2.66 gives an impression of the fully assembled NAC system when it was moved to Marburg. Several changes have been applied to improve safety, experimental scope, and convenience.

Roughing vacuum is provided by three rotary vane pumps³⁴ for the three independent sections of the system. The largest pump is connected to the main chamber since it has to handle the elevated gas load during sputtering. Each vacuum line is equipped with a pneumatic valve closing in case of a power failure. A line power distribution center provides a common ground potential for the equipment and also prevents unattended start up of the system after a power loss.

³⁴ 'DUO 3 M', 'DUO 2.5' from Pfeiffer Vacuum GmbH, 'RV5' from Edwards Germany GmbH.

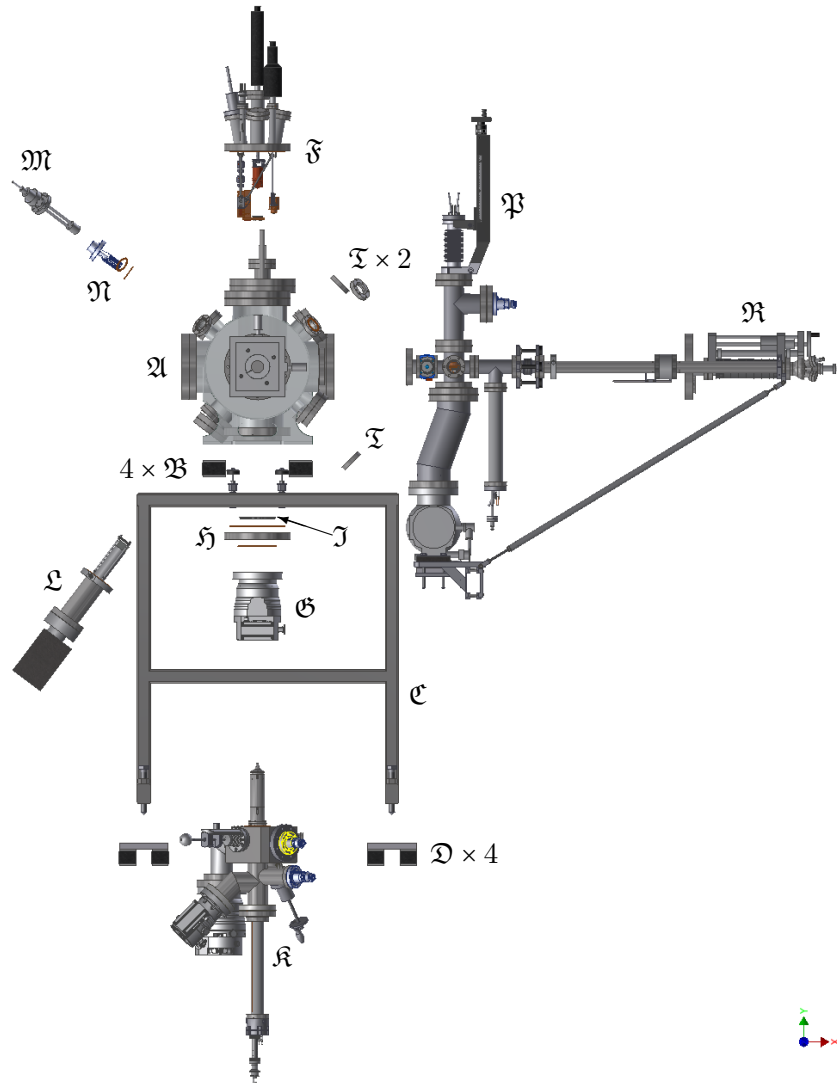


Figure 2.64: Assembly of the NAC system (Front View) — The main chamber (A) rests on rubber spacers^a (B) on the frame (C) which is vibrationally isolated from the floor (not shown) by its feet^a (D). The detector unit (F, Figure 2.4) is mounted from the north side to the main chamber (A). A turbo molecular pump^b (G) on an adapter (H) holding a heavy duty protection grid (I) and the molecular beam source (K, Figure 2.11) are attached from the south. The mass spectrometer^c (L, Figure 2.42), a sputter gun^d (M), and a Bayard-Alpert gauge head^e (N) are mounted on the west side. The east facing side of the chamber (A) is equipped with the load lock (P, Figure 2.53) and the ancillaries stage (R, Figure 2.34). Several blind flanges and CF windows complete the setup.

- a ‘Gummi-Metall-Schiene 50 mm x 50 mm, Metallauflage 5 mm, 70°Shore’ from Erwin Telle GmbH.
- b ‘TMU262’ from Pfeiffer Vacuum GmbH.
- c ‘HAL IV’ from Hiden Analytical.
- d ‘IQE11/35’ from SPECS Surface Nano Analysis GmbH.
- e ‘AIG17G’ operated by an ‘NGC2’ from Arun Microelectronics Ltd. *via* tectra GmbH.

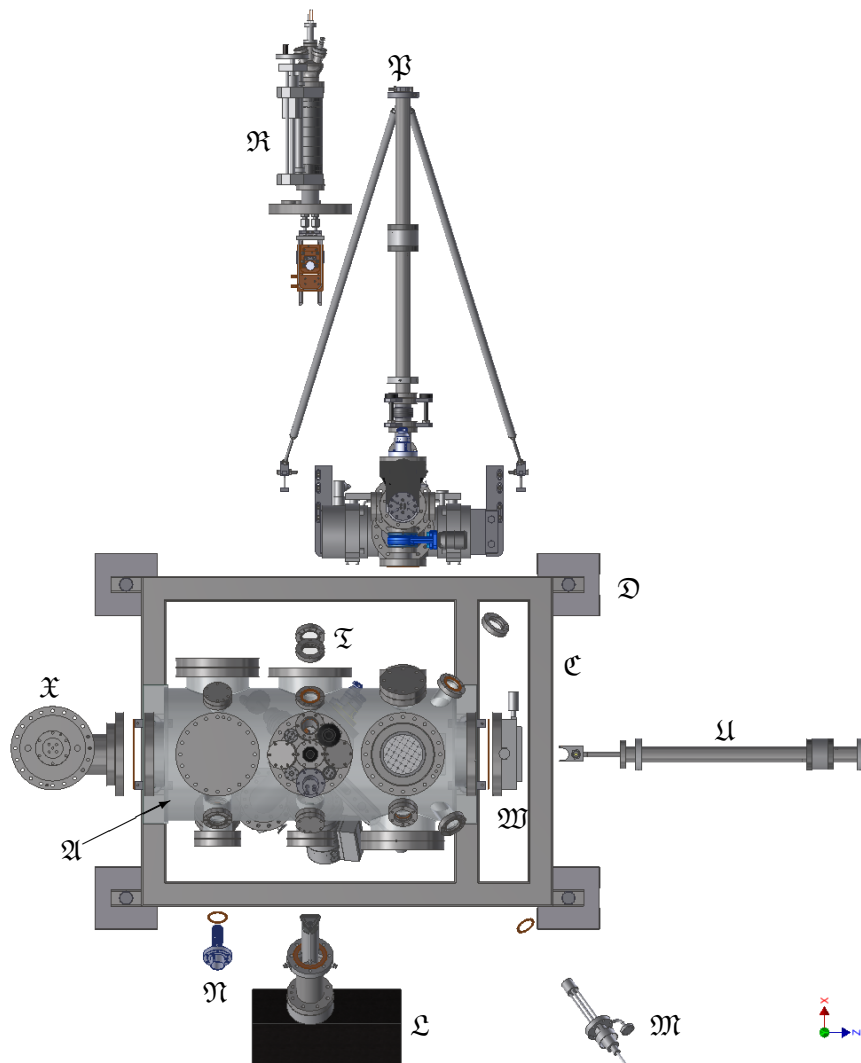


Figure 2.65: Assembly of the NAC system (Top View) — The ancillaries stage (R, Figure 2.34) combined with a 40CF window^a (T) on the port directly below the stage, and the load lock (B, Figure 2.53) are mounted from the north onto the main chamber (A) on the frame (C) placed on the feet (D). A magnetically coupled transfer rod^b equipped with the main chamber sample carrier (U, Figure 2.60) is mounted on an xy -adjustment table (W). Sample cleaning is provided by a sputter gun^c (M). An ion gauge^d N and the mass spectrometer^e (L, Figure 2.42) are located on the south side. Getter pumping is provided by a TSP (X) mounted on the west side.

a 'VPZL-275' from Kurt J. Lesker Company.

b 'VF-1695-18' from Huntington Mechanical Laboratories Inc. *via* tectra GmbH.

c 'IQE11/35' from SPECS Surface Nano Analysis GmbH.

d 'AIG17G' operated by an 'NGC2' from Arun Microelectronics Ltd. *via* tectra GmbH.

e 'HAL IV' from Hiden Analytical.

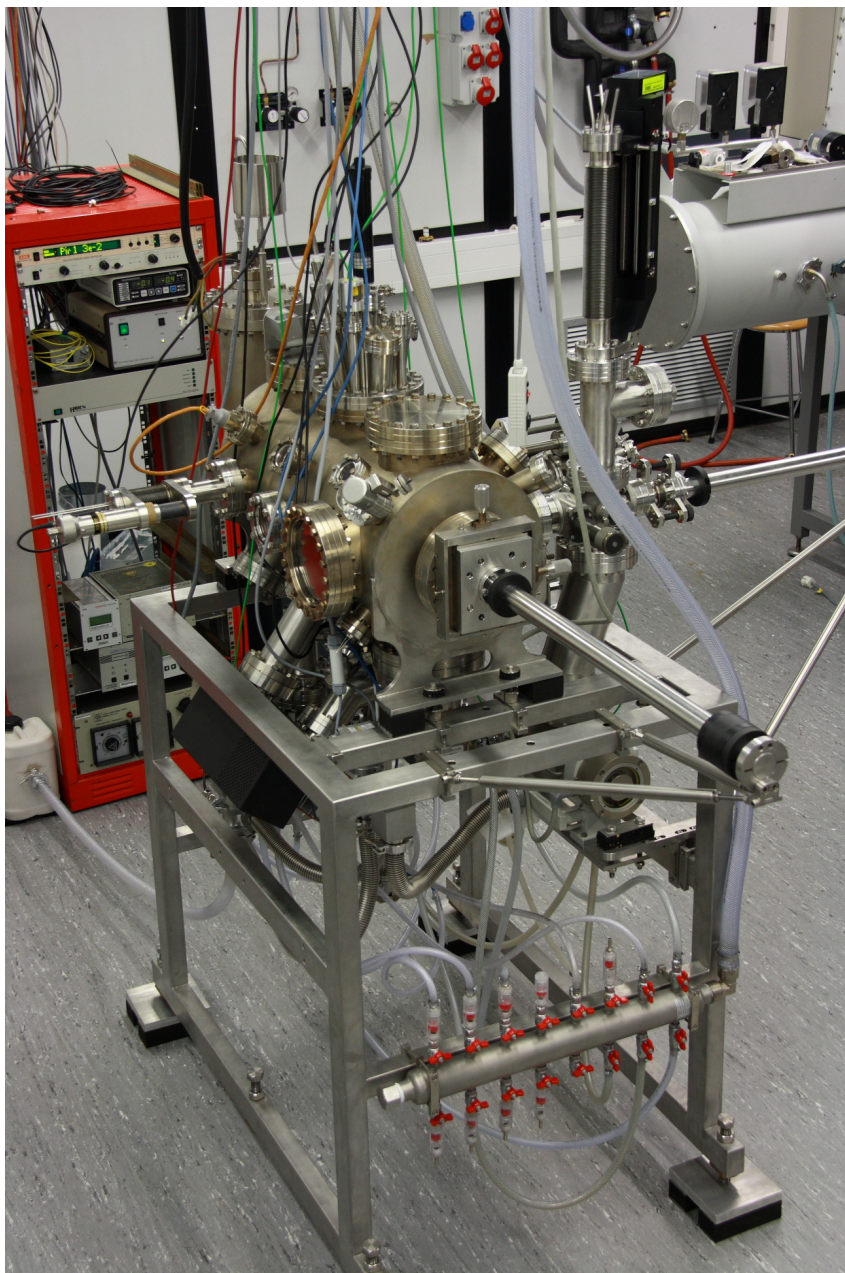


Figure 2.66: The Nanojoule Adsorption Calorimeter — A photograph of the Nanojoule Adsorption Calorimeter as presented in Figure 2.1 is shown here. The electronics for operation of the system are accommodated in the red rack in the left background. The glove box can be discerned by its main load lock in the right background.

2.10 Synopsis of the Experimental Setup

All parts designed for the calorimetry experiments have been manufactured by the mechanical workshops in Erlangen and Marburg. Subsequently, the vacuum system has been assembled and tested. The performance of the individual components is evaluated in Chapter 5.

Two compatible kinds of sample holders allow the investigation of adsorption on thin films and single crystals. The temperature of the sample reception is adjustable allowing for temperature dependent measurement series.

The molecular beam compartment is able to accept different evaporators and to create a pulsed molecular beam. It is also capable of guiding a laser beam to the sample. The included valve provides refilling of the evaporators without venting of the main chamber. The standard evaporator provides constant and high deposition rates with long runtimes.

The ancillaries stage combines several devices utilized to perform several reference measurements. The hot plate provides a reference for the mass spectrometer channel, the quartz crystal microbalance is able to measure the deposition rate from the beam source, the mirror renders an air-side measurement of the laser power possible, and the infrared transparent window separates molecules and radiation from the evaporator.

Several instruments, *e.g.*, a mass spectrometer and a sputter gun, are attached to the main chamber with special adapters. Air based instruments, *e.g.*, power meters, use adjustable mounts to be aligned to the sample.

The load lock is capable of storing different kinds of samples in high vacuum and transfer them to preparation and measurement positions. Additionally, it is possible to deposit organic thin films in this separate compartment.

Preparations for the handling of air sensitive materials in a glove box have been taken.

In summary, one of the central aspects of this work has been successfully completed and was extensively used to obtain the results presented in Chapters 5 and 6.

3 Data Evaluation

Together with a typical data treatment routine several specific properties of the IGOR PRO *Nanojoule Adsorption Calorimetry* program package are presented here. Along the program description the effects of individual actions are investigated. The utilized functions are illustrated in Chapter 4 whereas the source code can be found in Appendix C.1.

The presented program follows the philosophy of using averaged data sets as references instead of individual values. This approach was originally motivated from the fact that the rising part of a pulse is not strictly linear, *e.g.*, in Figure 3.3. The symmetry breaking into distinct odd and even frames in the radiation measurement made this strategy necessary on the one hand. On the other hand, it lead to the possibility to separate radiation and reaction heat directly from the measurement reducing the influence of the transmission measurement as a source of error.

The experiment used as example suffered from some beat in the raw signal, see Figure 3.7, of unknown or origin leading to an increased scatter in the results. Nevertheless, it was chosen since it provides insight into the compensation mechanisms.

Coverages are given in monolayers (ML) and/or meters. Deposition rates are stated in deposited meters per second or monolayers per second (ML/s) and are proportional to the corresponding fluxes since the relevant deposition regions have constant area.

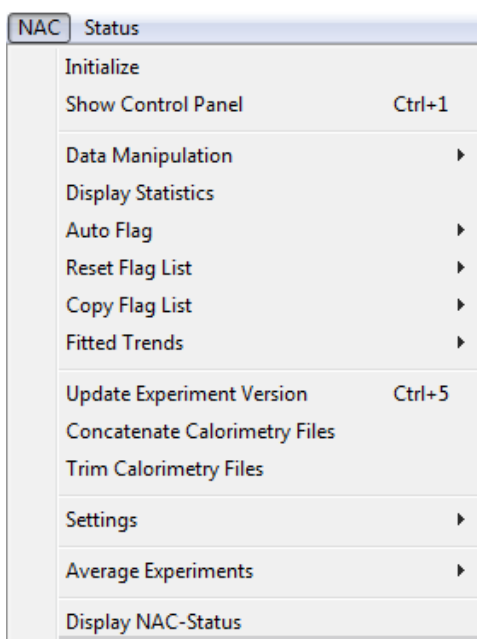
Here, one monolayer is defined as a closed packed layer of the deposited atoms in a specified plane. The typically used plane is the closest packed plane for the most stable phase at room temperature, *i.e.*, the (111) plane for metals with cubic and the (0001) plane for metals with hexagonal crystal structure, *e.g.*, copper and magnesium, respectively. Both structures with their primitive spatial and corresponding planar unit cells are shown in the description of the used materials in Figures 6.1 and 6.2.

3.1 User Interface

This section explains the individual features of the user interface. The most used functions use buttons in the main panel, see Section 3.1.2, or are accessible *via* hot keys. The hot keys and the less common functions are organized in the menu structure, see Section 3.1.1.

3.1.1 Menu

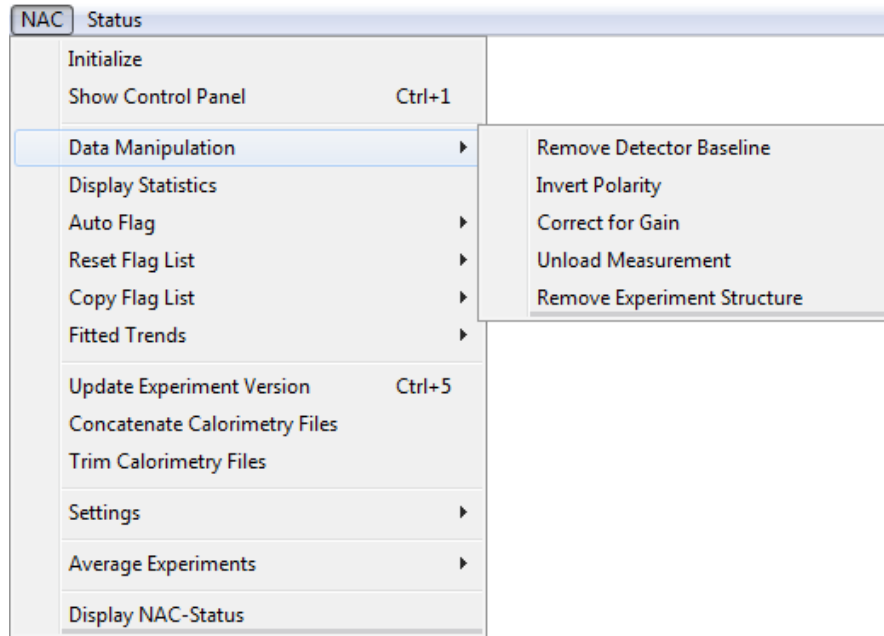
This section explains the functions accessible through the menu system of the data evaluation software.



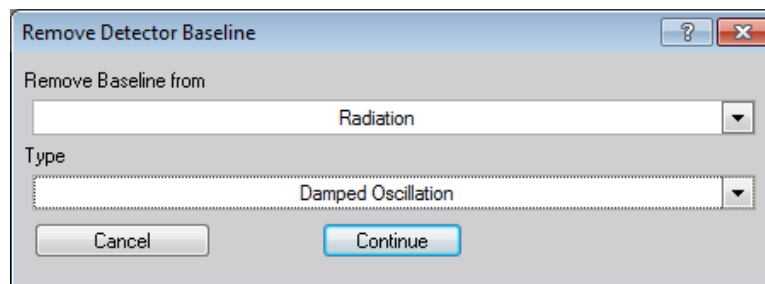
Initialize creates the data structure used by the software package and initiates the display of the control panel. Loaded data will be overwritten.

Show Control Panel displays the main window. The assigned default hot key is **Ctrl+1**. For detailed information see Section 3.1.2.

Data Manipulation contains methods of manipulating the raw data.

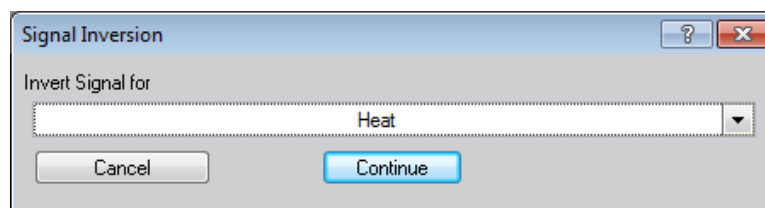


Remove Detector Baseline provides a manual way to remove a selectable baseline from the detector data set.



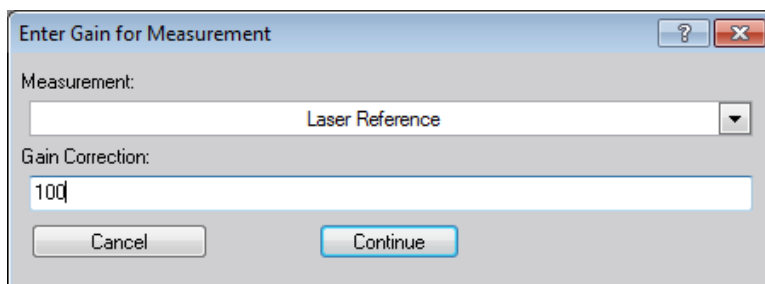
Only loaded data sets are provided. The selection of functions used to remove a base line can be extended in the program code, see Section 4.2.10.

Invert Polarity allows to multiply a selectable detector signal by -1 .



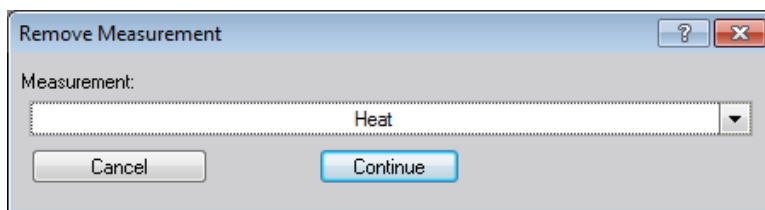
The data treatment is independent of the polarity of the sample as long as it is consistent in the individual measurements. This option is indented to produce publishable graphics rather than for data treatment.

Correct for Gain is a feature to use old data files recorded with a second amplifier.



The data stored in **Detector** is divided by the number given for **Gain** in the selected experiment. It is obsolete for newer data files recorded without the second amplifier. The data set needs to be processed again manually.

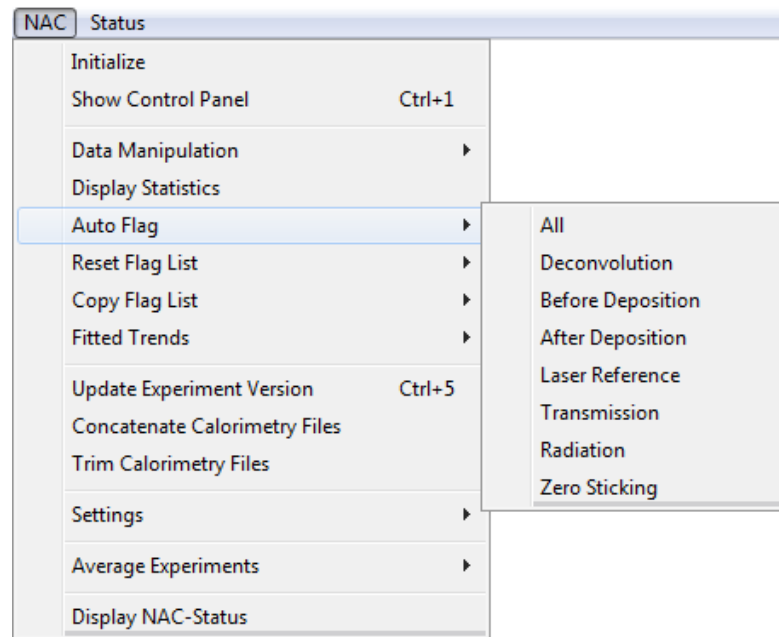
Unload Measurement prompts the user to select a loaded experiment and resets the corresponding objects. The calorimetry data, *i.e.*, the heat and sticking measurements, are removed together.



Remove Experiment Structure deletes the entire NAC data folder after confirmation by the user. Due to the internal dependencies, a manual removal of the whole data folder, *e.g.*, by the *Data Browser*, is not possible.

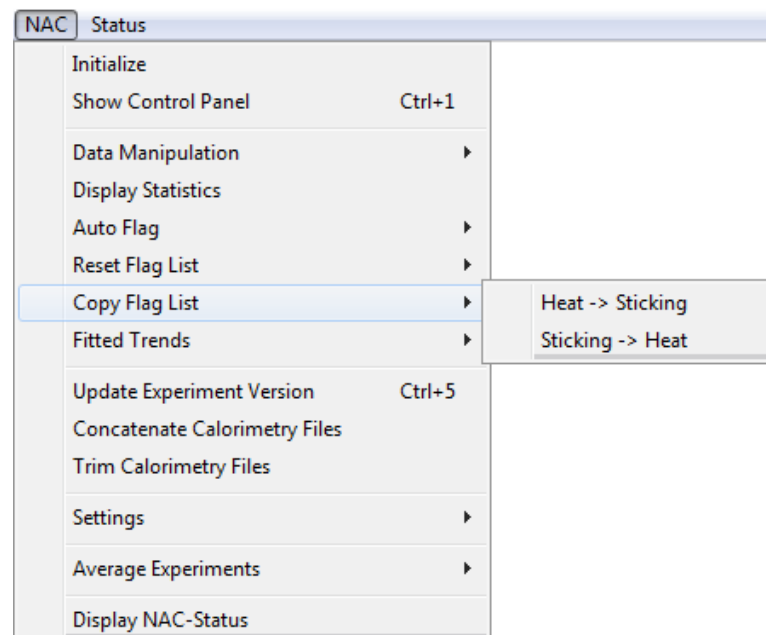
Display Statistics presents the result of the statistical analysis of the already analyzed data in form of box plots, see Section 3.6.

Auto Flag automatically marks outlier frames in All or the selected data set, see Section 3.7.

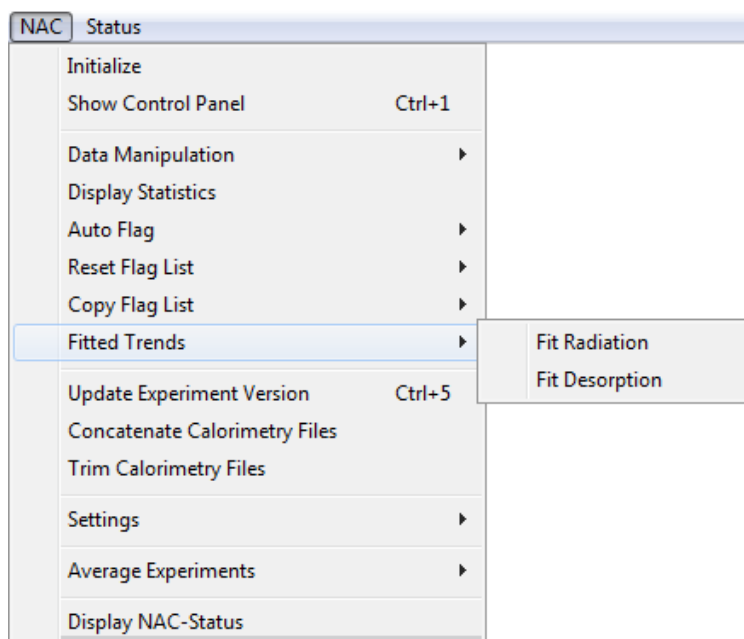


Marked frames will be subsequently ignored by the data processing procedures. Individual as well as all measurements can be treated with this operation. It is also included in the Lazy Process routine in case the Auto Flag option is enabled.

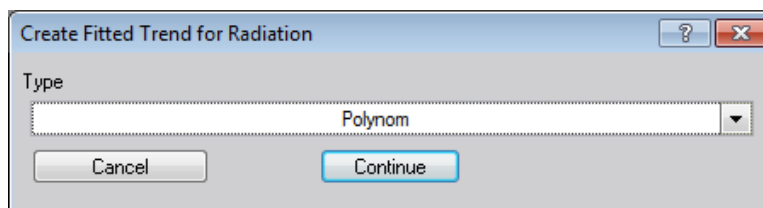
Copy Flag List conveniently synchronizes the excluded frames in the heat and sticking probability measurements and *vice versa*.



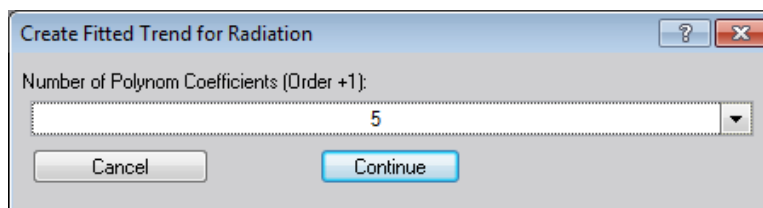
Fitted Trends provides a method to reduce fitting artifacts by overriding fit parameters in an additional iteration of the data treatment, see Section 3.9.



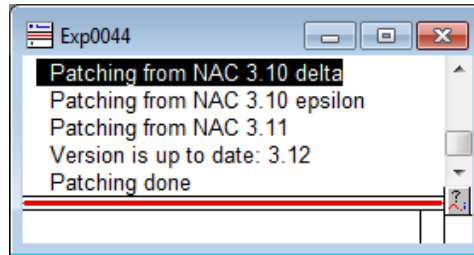
The original data is displayed and the user is prompted to select a function describing the trend or to load an average from an experiment file.



Subsequently, further parameters are inquired if applicable.



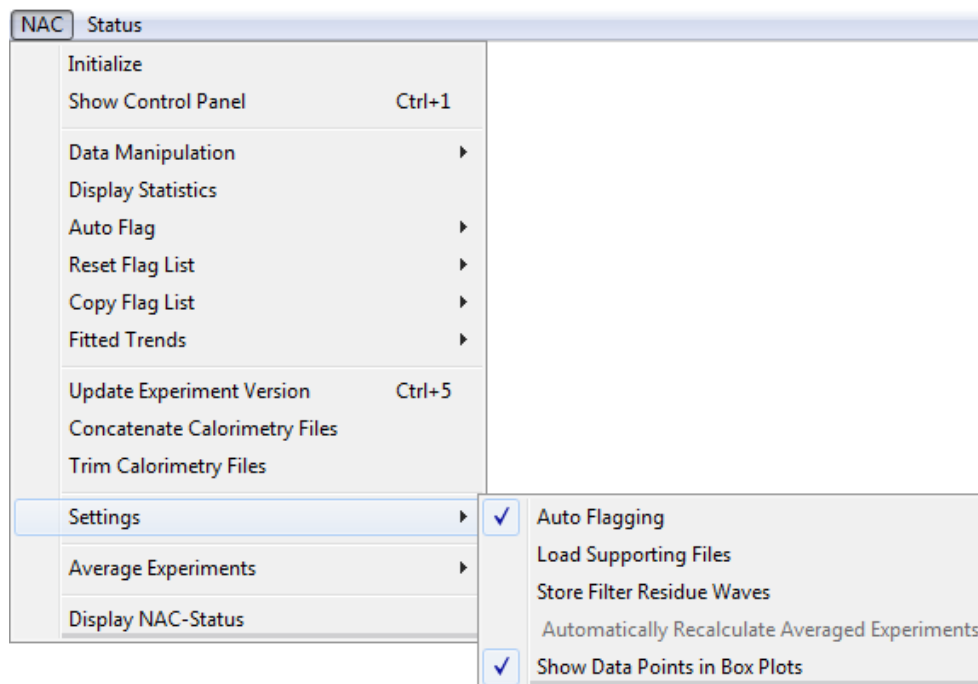
Update Experiment Version adjusts the data structure of old experiment files to the newest software version if possible. Notes about the patching process are printed in the *Command Window*. The assigned default hot key is **Ctrl+5**.



Concatenate Calorimetry Files combines two calorimetry files including the check relevant parameters. This feature is not necessary for standard experiments. Since it is still *alpha* state it might give unexpected results or errors.

Trim Calorimetry Files extracts a subset from a calorimetry file including the check relevant parameters. This feature is not necessary for standard experiments. Since it is still *alpha* state it might give unexpected results or errors.

Settings provides adjustment of the general behavior of the program.



Auto Flagging set to enabled alters the **Lazy Process** routine. With this option it automatically masks outlier frames and performs an additional

process cycle before the heat and sticking probability measurements are processed. It is enabled by default.

Load Supporting Files switches from loading the default experiment data files to the supplementary files usually used for characterization and testing if this option is enabled. It is disabled by default.

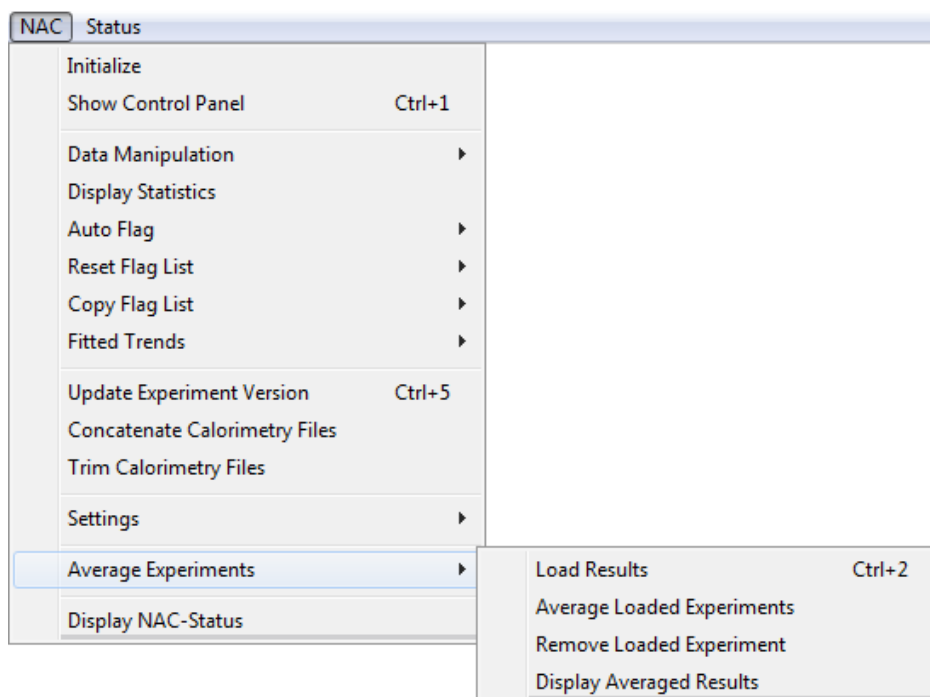
Store Filter Residue Waves keeps the residue from the Fourier filtering in the load function if enabled. This option provides a way to inspect the details of the baseline removed by the filtering. Since it is not necessary for data treatment and consumes a rather large amount of memory it is disabled by default.

Automatically Recalculate Averaged Experiments

defines if newly added experiments are automatically included in the calculation of the averaged sticking probability, coverage and enthalpy. Since the calculation becomes slow for many large data sets it is disabled by default.

Show Data Points in Box Plots defines whether individual data points are displayed in the statistics windows or not.

Average Experiments comprises the controls of the subsystem utilized to average individual experiments with the same parameters.



Load Results loads the relevant data from a calorimetry experiment file. The assigned default hot key is **Ctrl+2**.

Average Loaded Experiments averages the data in the loaded calorimetry experiments.

Remove Loaded Experiment deletes the data from a previously loaded calorimetry experiment.

Display Averaged Results creates the graphs related to the averaged data.

Display NAC-Status extends the **Status Package** and provides a tailored display of the status of the NAC machine.

3.1.2 Main Panel

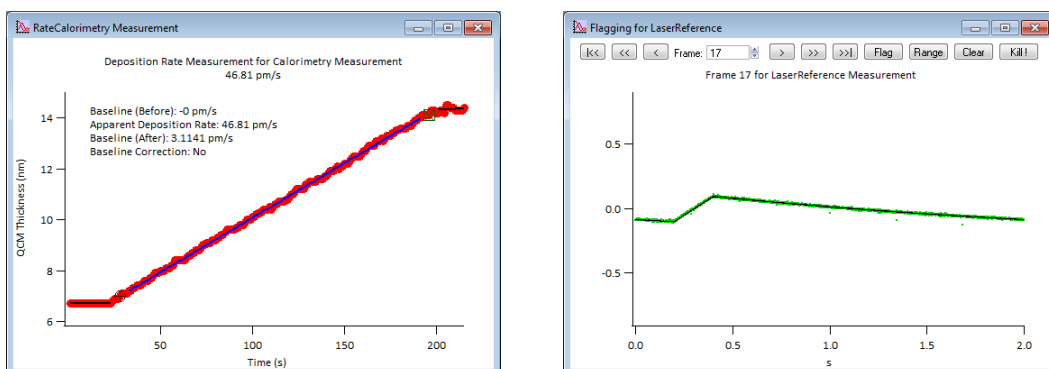
The data evaluation main panel is divided into three sections, as shown in Figure 3.1.

The upper part displays the machine and experiment parameters which also might be calculated from the evaluated data. The middle section contains the control buttons to process or display the data as well as information specific to the individual experiments. The lower set comprises options and constrains used in the evaluation process. Since the labeling used in Figure 3.1 is self-explaining, *e.g.*, the **Show** button shows the file header, a detailed description is omitted here.

The quantities related to the variables are explained in Section 4.2.2 together with their standard values if applicable.

3.1.3 Interactive Windows

Some graphs accept user input by placing cursors or by pressing buttons. Buttons are used to navigate through the data set and set a flag to ex- or include frames from the data treatment.



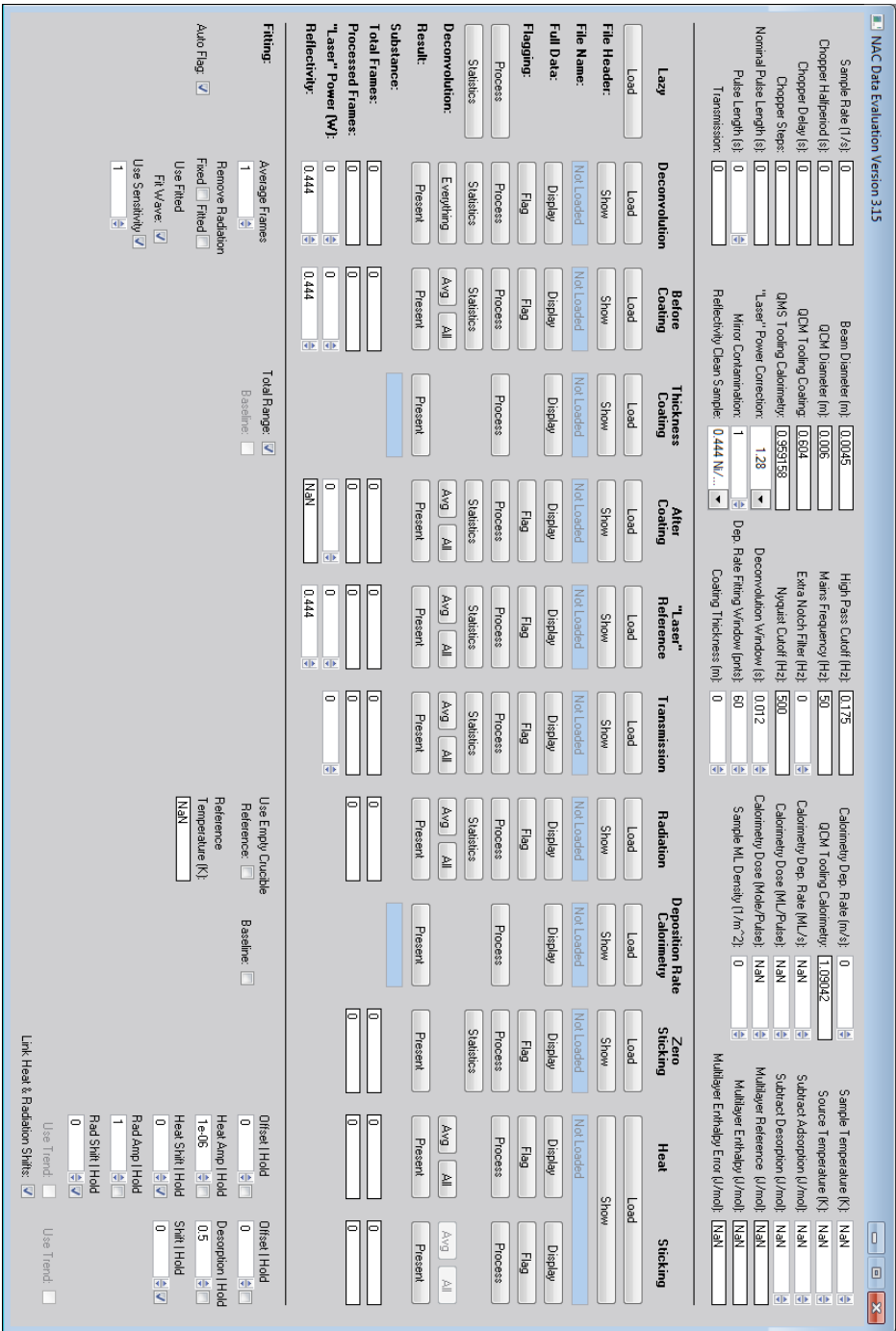
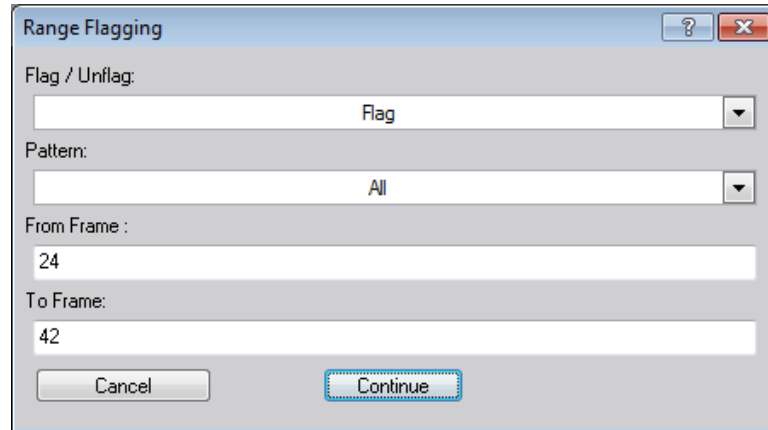
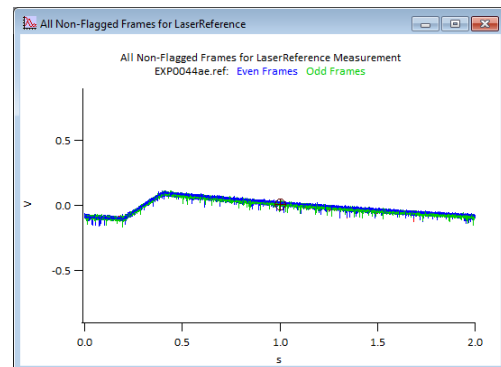
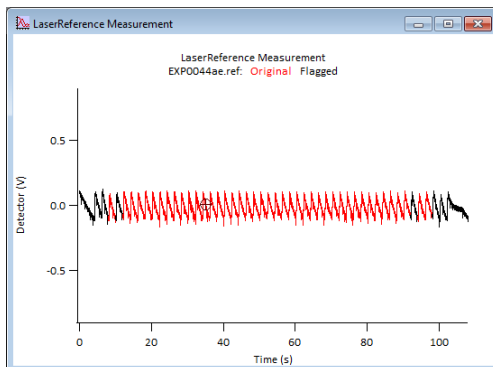


Figure 3.1: Main Panel of the NAC Data Evaluation Program — The upper part displays the machine and experiment parameters which also might be calculated from the evaluated data. The middle section contains the control buttons to process or display the data. The lower set comprises options and constraints used in the evaluation process.

As an example, the **Range** button also allows to set the marker for all frames with a specified sub pattern in a given range while the **Clear** button resets all marked frames. The **Kill** button sets a frame to zero in case a severely disturbed frame leads to a malfunction of the automatic range adjustment.



Cursor pairs are generally used to define ranges used to calculate averages. Single cursors are utilized to indicate or select the currently displayed frame of a measurement.

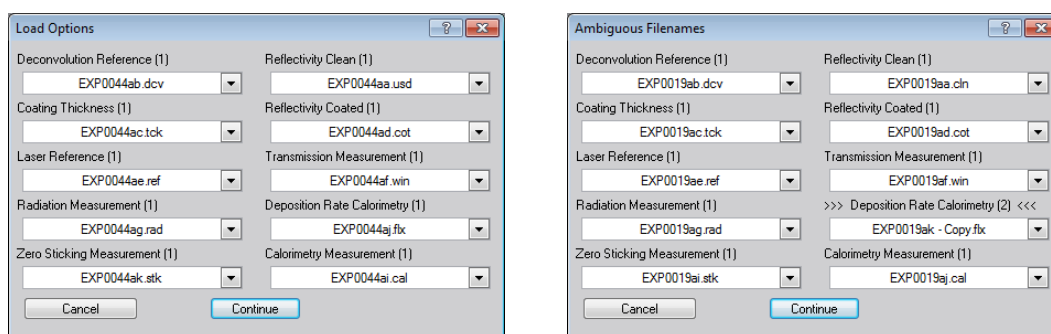


The individual actions are presented, together with the corresponding data treatment, later in this chapter.

3.2 Loading Data

Calorimetry related data is imported into IGOR PRO *via* the Load buttons on the main panel. The software package determines the kind of measurement from the pressed button and suggests the appropriate files by specific filters for the standard file open dialogue. Since the heat and sticking measurements are recorded simultaneously they are also loaded together.

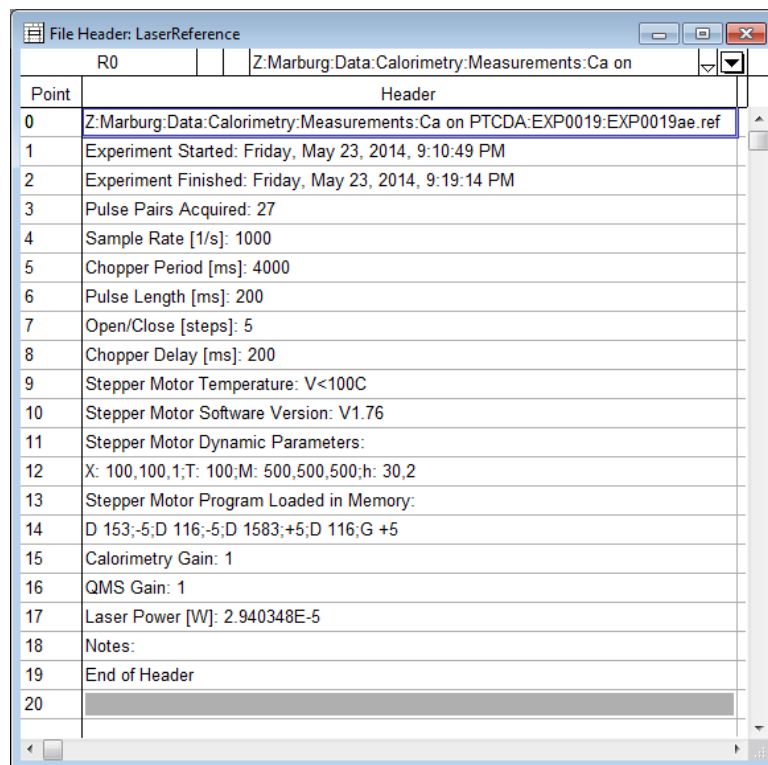
If the data has been saved with the standardized file extensions, see Section 4.1, all data of one experiment can be loaded with the “Lazy Load” button. A dialogue is displayed to select which measurement files should be loaded. Additionally, the Load button lights up red in case two or more files qualify to be loaded for the same measurement and the corresponding file is slightly highlighted.



During the import process the files are checked for integrity and whether the experimental parameters are compatible. Upon the first loaded file these parameters are assigned to the experiment file, see Section 4.2.2. In case the record corresponding to the stepper motor status can be found in the auxiliary file, the frame pairs with an unsuccessful motor program, *i.e.*, a return value differing from "Y", are marked as unqualified for data treatment. This includes the pairs used to document the base line at the beginning and at the end of the measurement.

Thickness measurements are displayed automatically after loading. Calorimetric measurement files are loaded, filtered, and resampled according to the set parameters.

The file headers of the loaded files can be displayed with the Show button for inspections of the measurement details and the stored technical notes.



Point	Header
0	Z:\Marburg\Data:Calorimetry:Measurements:Ca on PTCDA:EXP0019:EXP0019ae.ref
1	Experiment Started: Friday, May 23, 2014, 9:10:49 PM
2	Experiment Finished: Friday, May 23, 2014, 9:19:14 PM
3	Pulse Pairs Acquired: 27
4	Sample Rate [1/s]: 1000
5	Chopper Period [ms]: 4000
6	Pulse Length [ms]: 200
7	Open/Close [steps]: 5
8	Chopper Delay [ms]: 200
9	Stepper Motor Temperature: V<100C
10	Stepper Motor Software Version: V1.76
11	Stepper Motor Dynamic Parameters:
12	X: 100,100,1;T: 100;M: 500,500,500;h: 30,2
13	Stepper Motor Program Loaded in Memory:
14	D 153;-5;D 116;-5;D 1583;+5;D 116;G +5
15	Calorimetry Gain: 1
16	QMS Gain: 1
17	Laser Power [W]: 2.940348E-5
18	Notes:
19	End of Header
20	

3.3 Data Filtering

The filtering process during the load routine of the calorimetric measurement files comprises four components. Three of those can be disabled by setting the corresponding frequency to zero in the **Machine** parameters section.

A filter needs to fulfill two requirements. On the one hand, the wanted signal component should not be perturbed and, on the other hand, the unwanted signal component needs to be removed as well as possible.

Three of the four parameters used for filtering are rarely about to be changed and are only displayed on the main panel. They can only be changed by a variable assignment or *via* the *data browser*. The frequency for the **Extra Notch Filter** can be changed on the panel. Setting its value to zero disables the filter.

High Pass Cutoff (Hz):	<input type="text" value="0.175"/>
Mains Frequency (Hz):	<input type="text" value="50"/>
Extra Notch Filter (Hz):	<input type="text" value="0"/>
Nyquist Cutoff (Hz):	<input type="text" value="500"/>

3.3.1 High Pass Filter

This feature was implemented to remove the ring-on artifact of the signal amplifier on the calorimetry channel as shown by the black trace in Figure 3.2. The radiation reference measurement was chosen as a probe for the performance of the filtering routine since it implies a periodicity twice of the laser reference measurement, *i.e.*, two frames and one frame, respectively. Hence, it contains relevant contribution at lower frequencies than the laser measurements.

Figure 3.2 illustrates the effects of different filter transition frequencies on the whole filtered data. A too low setting (blue), *i.e.*, 0.02 Hz, results in artifacts due to an incomplete removal of the base line. An intermediate setting of 0.1 Hz flattens the signal while it preserves the signal shape. At too high settings (red), *i.e.*, 0.5 Hz, the signal shape and amplitude are altered to an extend which is intolerable.

Figure 3.3 illustrates the effects of different filter transition frequencies on the averaged data for a radiation reference measurement. At low settings (blue and green), *i.e.*, below 0.2 Hz, almost no change in the shape is caused while at higher settings (red), *i.e.*, 0.5 Hz, the signal shape is seriously affected.

Since the base line artifact shown in Figure 3.2 is rather a damped oscillation and not a decay, *i.e.*, it exhibits a zero crossing, it does not originate solely from the load resistor in the amplifier and the capacity of the measurement setup, see Section

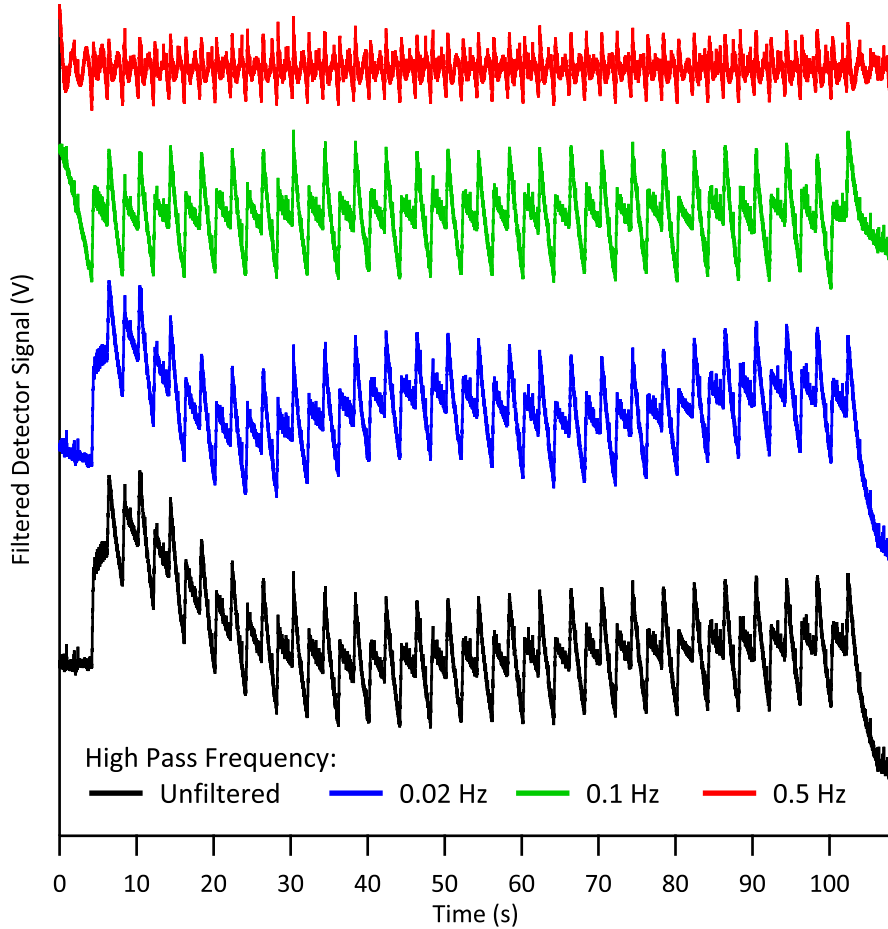


Figure 3.2: Filtered Radiation Reference Measurement — A radiation reference measurement is displayed together with the results for several filter settings. The unfiltered data (black) exhibits an unwanted slow oscillation. The filtered data set corresponding to a transition frequency of 0.02 Hz (blue) suffers from incomplete removal of the baseline, the data set corresponding to 0.1 Hz (green) matches the ring on at the beginning and shows no contribution of the pulses. An increase of the filter frequency to 0.5 Hz (red) leads to a pronounced contribution of the pulses and thus to a severe distortion of the signal. Data is vertically offset for better comparison.

5.5.3. The voltage $U(t)$ of damped oscillation at the time t is given by

$$U(t) = U_{\text{ofs}} + U_{\text{amp}} \cdot \exp\left(-\frac{t}{\tau}\right) \cdot \cos\left(\frac{t}{\sigma} - \varphi\right) \quad (3.1)$$

with a constant offset U_{ofs} voltage, an amplitude U_{amp} , a time constant for the decay τ , a periodicity of the oscillation σ , and a phase φ .

This pattern is more pronounced in the relaxation regime of a deconvolution reference measurement, as shown in Figure 3.4. The experimentally measured time

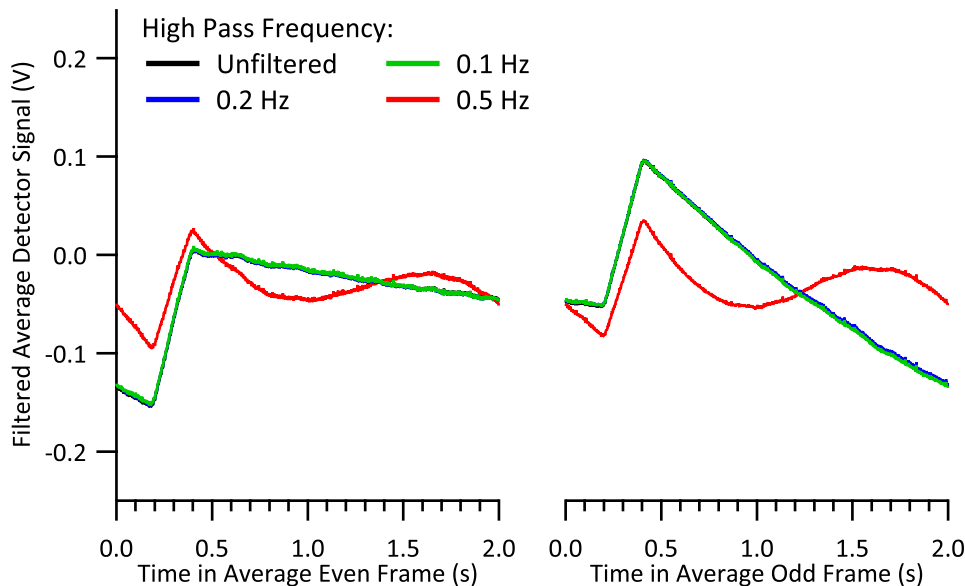


Figure 3.3: Average Frames of a Filtered Radiation Reference Measurement — The average of twelve frame pairs of a radiation reference measurement is displayed for several filter settings. The unfiltered (black) and filtered waves with a transition frequency of 0.1 Hz (green) and of 0.2 Hz (blue) are almost identical. An increase in the filter frequency to 0.5 Hz (red) leads to a severe distortion of the signal.

constant for the decay τ in this case is 5.9 s corresponding to a frequency of 0.17 Hz. The periodicity amounts to 69 s. These results suggest a pass frequency of 0.175 Hz for the high pass filter. A comparison to the theoretical time constant is made in Section 5.5.3.

Effects of a variety of filtering settings and more examples of removed base lines are given in Appendix E.2. The data in the mass spectrometer channel is not processed by the high pass filter.

3.3.2 Line Notch Filter

This filter with a fixed band width of 1 Hz is used to remove noise picked up from the power lines, *e.g.*, due to ground loops. Since the measurement equipment was extensively optimized, the signal quality is hardly affected by this frequency anymore. Nevertheless, this feature is kept in case of technical difficulties with the laboratory equipment. The effect of the filter is similar to the illustration given in Figure 3.5. Both channels are affected by this filter.

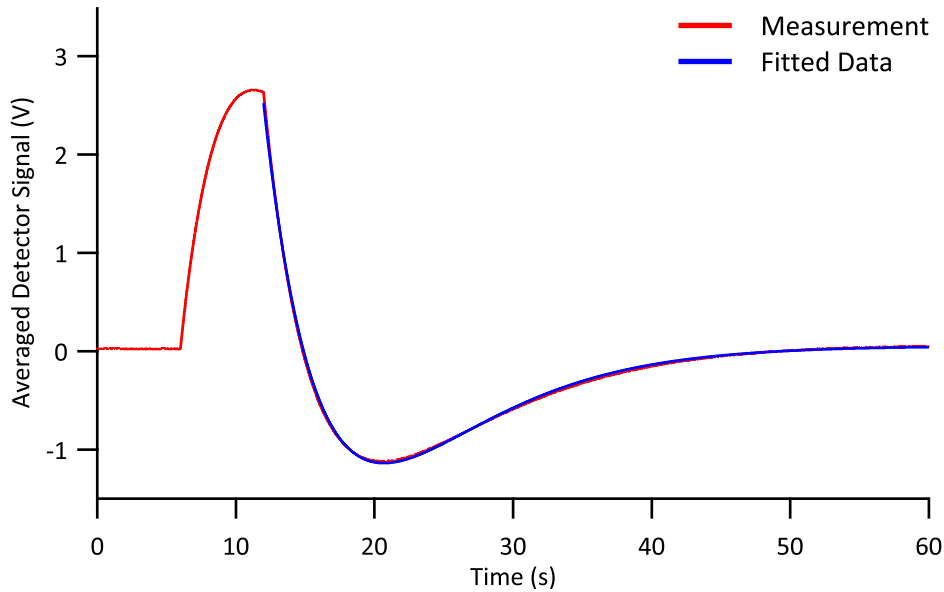


Figure 3.4: Time Constant of the Measurement Setup — An excerpt of the average of pulses from a deconvolution reference measurement is approximated by the function of a damped oscillation.

3.3.3 Extra Notch Filter

It was discovered that some measurements were affected by noise of an unclear origin with a frequency around 94 Hz of small band width. It is most likely not the second harmonic of the line frequency since it is not located at exactly 100 Hz. In contrast the third harmonic at precisely 150 Hz can be observed in the data.

The effect of the filter is illustrated in Figure 3.5. Both channels are affected by this filter.

3.3.4 Nyquist Cut Off Filter

This frequency defines the highest processable frequency in the data. Contributions of higher frequencies in oversampled data are discarded in the filtering process. The data points are deleted from the Fourier transformed data set and not set to zero. On the one hand, this leads to a desired intrinsic resampling of the data to twice the Nyquist frequency aliased by the `ProcessRate`. On the other hand, it implies an amplitude change which is corrected analytically after the inverse Fourier transformation^[155]. In case of oversampled raw data this approach prevents unnecessary excessive memory consumption.

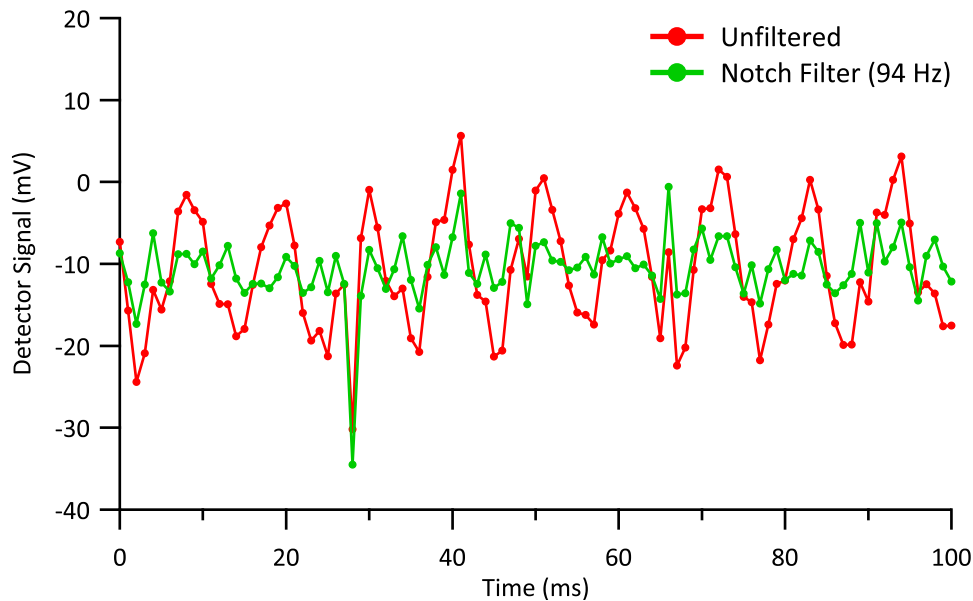


Figure 3.5: Effect of the Additional Notch Filter — An excerpt of a single frame of a radiation measurement shown with (green) and without (red) applied filtering illustrates the effect of the additional notch filter. Lines between data points added for enhanced clarity.

3.3.5 Effects on the Calorimetry Data

As shown before, the signal shape and amplitude are preserved in case of reference measurements. In case of the heat measurement it is essential that the filtering process has no unwanted influence on the result of the experiment.

The results of a calorimetry experiment treated with and without filtering are compared in Figure 3.6. The artifacts due to ring on effect at the beginning of the data, *i.e.*, the large amplitude oscillation due to the changing base line, are completely removed. The major center part of the experiment benefits from the filtering since the scatter is reduced and the general trend of the data is preserved. The final pulses suffer from the filtering procedure. Since they usually carry the same information as the few tens pulses before, they can be neglected without severe consequences and are marked as excluded from processing in the load routine by default. In order to improve the quality of the fit waves and minimize filtering artifacts on these references the first and last pair containing a pulse are also excluded from the data processing.

Some measurements suffer from a beat in the signal of still unknown origin. A nearby explanation would be that it is caused by the filtering process. However, this can be ruled out since the beat is also visible during data acquisition and in

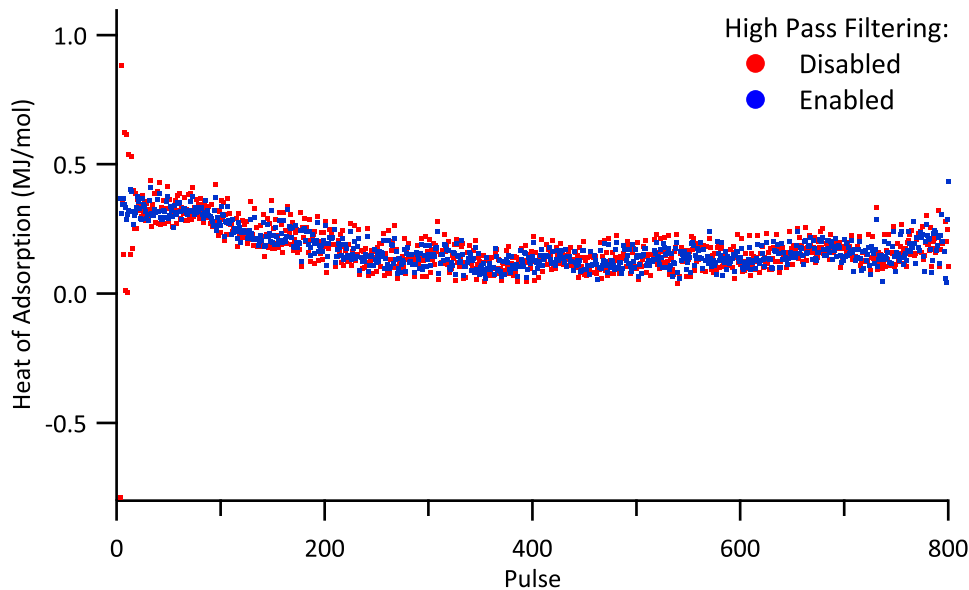


Figure 3.6: Effect of the Filtering on the Data — The results of a calorimetry experiment treated with (blue) and without (red) filtering are opposed. The artifacts due to ring on effect at the beginning of the data are completely removed. The major center part of the experiment benefits from the filtering since only the scatter is reduced. The irrelevant final pulses suffer from the filtering procedure.

the unfiltered raw data, as shown in Figure 3.7. Furthermore, some measurements on the same sample show this behavior and some do not. A probable source might be mechanical vibrations of the setup. The turbo molecular pumps utilized in the setup could cause such a pattern by one pump keeping its rotational speed while another pump oscillates around its set motor frequency. Additional explanations would include noise from the ventilation system or a movement of the building due to external forces, *e.g.*, wind. Due to the unfortunate location in the spectrum and its large bandwidth it cannot be removed by Fourier filtering.

The filtering process improves the quality of the data and only causes negligible side effects.

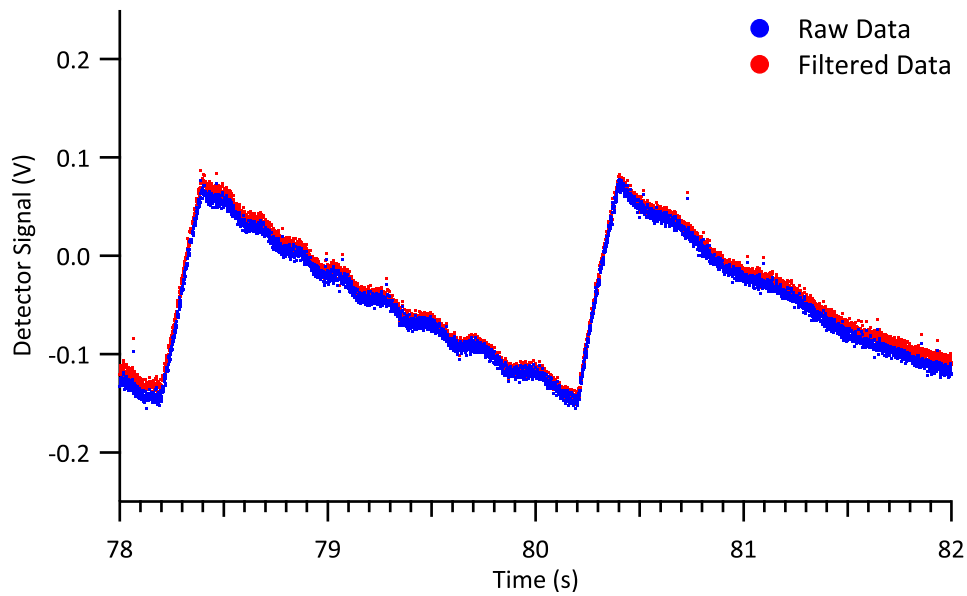


Figure 3.7: Filtering and Beat in Signal — Raw (blue) and filtered (red) data of a transmission measurement contain a contribution of a signal with a frequency oscillating between 1 Hz and 10 Hz with a relevant amplitude. Since this symptom is present in both data sets it is not an artifact arising from the filter process.

3.4 Quartz Crystal Microbalance Measurements

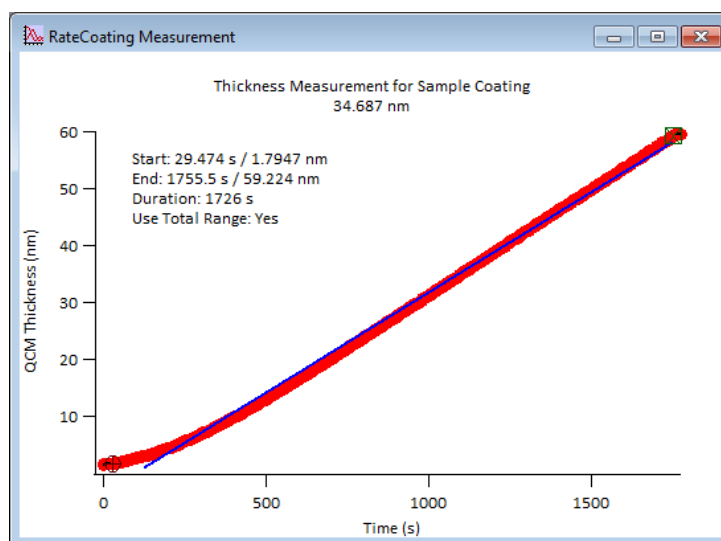
The measurements carried out by the quartz crystal microbalances are automatically displayed when loaded and can be recreated or brought to the front by the **Display** buttons on the main panel, see Figure 3.1. The displayed thickness (red dots) is the one read by the controller and thus not corrected by the tooling factors.

Two cursors provide a way to select the range used for the actual deposition if necessary. A linear approximation of the thickness change is indicated between the cursors (blue line). The regions before the left and after the right cursor are used to calculate base lines (black lines). If desired, they can be used to correct the deposited thickness or the deposition rate in case the sensor experienced drifting.



3.4.1 Sample Coating

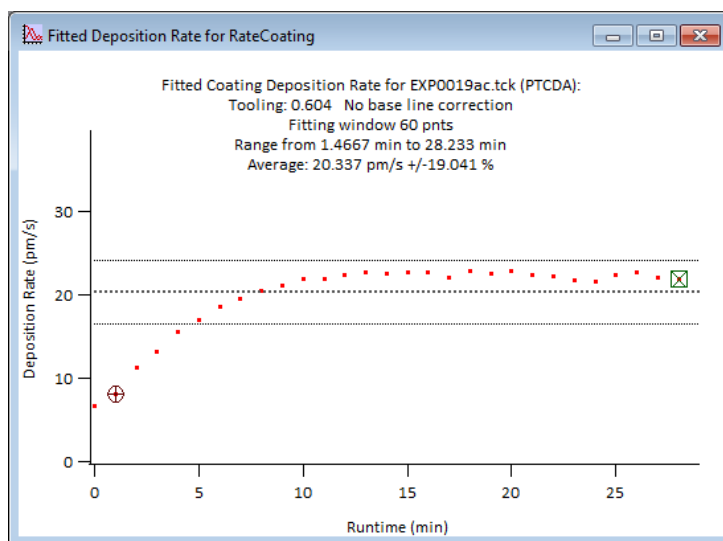
In order to be able to verify the deposition conditions during the substrate coating process the thickness deposited on the sensor crystal in the load lock, see Figure 2.57, is recorded and evaluated by the software.



With standard settings the thickness is calculated from the difference in thickness at the cursor positions. It is also possible to calculate the layer thickness from the deposition rate, corrected by the base lines if applicable, and the deposition time. The calculated layer thickness in the graph title contains all selected corrections.

The obtained substrate thickness is stored and used later as experiment descriptor. It is also imported by the experiment averaging sub system.

In case of a constant deposition rate becoming necessary to obtain a specific substrate structure the recorded data can be linearized piecewise. The window used can be chosen by Dep. Rate Fitting Window given in data points.

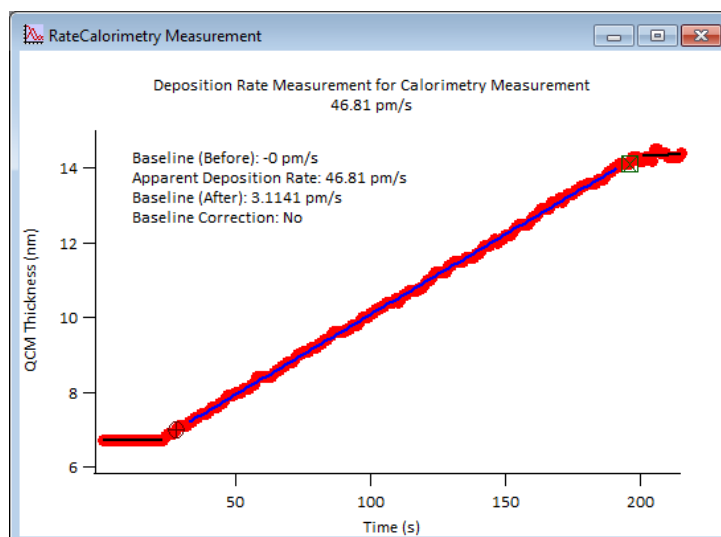


The resulting deposition rate is returned in m/s and is thus independent of the spacing of the data points. The displayed average and error ranges are calculated from the data between the cursors.

Typical parameters used for deposition of several substances are given in Appendix A. The layer thicknesses ranged from a few nanometers to about one micrometer. The substrate molecules have usually been deposited on a sputtered detector disc, see Section 5.2.

3.4.2 Calorimetry Deposition Rate Measurement

One of the main parameters used in the calculation of the heat of adsorption is the amount of atoms dosed on the sample. This quantity is derived from the pulse length and the continuous deposition rate measured with the quartz crystal microbalance in the ancillaries stage, see Section 2.4.2.



With standard settings the deposition rate is calculated from the slope of the thickness change with respect to time between the cursor positions. If desired, it can be corrected by the averaged base lines. The displayed rates are already corrected by the tooling factors, see Sections 5.3 and 5.8.2.

Unreasonable data points, *e.g.*, due to small frequency jumps, need to be removed manually by replacing their respective values by *NaN*. Various parameters are automatically calculated from the Calorimetry Deposition Rate J given in m/s .

Calorimetry Dep. Rate (m/s):	4.68104e-11
QCM Tooling Calorimetry:	1.09042
Calorimetry Dep. Rate (ML/s):	0.14772
Calorimetry Dose (ML/Pulse):	0.029544
Calorimetry Dose (Mole/Pulse):	5.76977e-12
Sample ML Density ($1/\text{m}^2$):	7.39477e+18

The calorimetry deposition rate J_{ML} in ML/s is calculated from the deposition rate J given in m/s by

$$J_{\text{ML}} = \frac{J \cdot \varrho \cdot 10^3 \cdot N_{\text{A}}}{M \cdot 10^{-3} \cdot \sigma} \quad (3.2)$$

using the density ϱ , the molar mass M , and the monolayer density σ provided in the file header of the data file. This quantity as well as the dose per pulse D_{ML} in monolayers

$$D_{\text{ML}} = J_{\text{ML}} \cdot t \quad (3.3)$$

for a pulse with the duration t are only used as illustrative aliases.

The molar dose per pulse, which is the relevant property for the calculation of the heat of adsorption, is calculated by

$$D_{\text{cal}} = \frac{J \cdot t \cdot \varrho \cdot 10^3 \cdot A}{M \cdot 10^{-3}} \quad (3.4)$$

$$= 10^6 \cdot \frac{J \cdot t \cdot \rho \cdot \left(\frac{1}{2}d\right)^2 \cdot \pi}{M} \quad (3.5)$$

with the area $A = \left(\frac{1}{2}d\right)^2 \pi$ of the beam calculated from its diameter d .

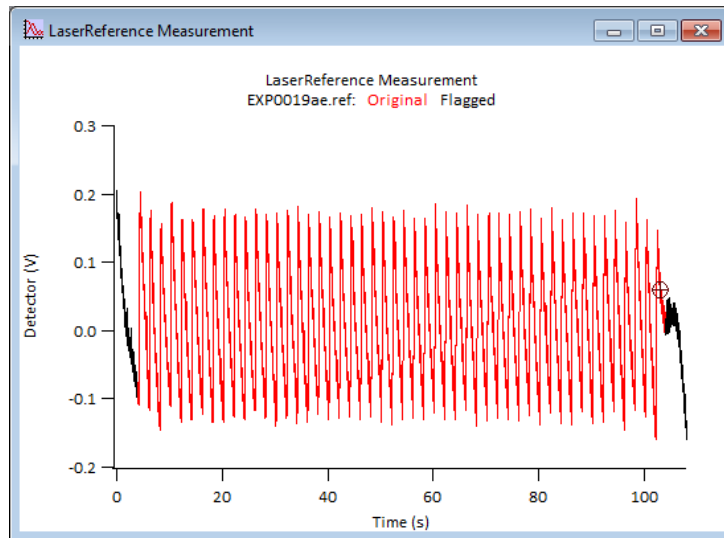
Typical values for a deposition rate used in a calorimetric experiment range from 0.05 ML/s to 1 ML/s. The LABVIEW control program¹ provides a rough estimate of the deposition rate during its measurements used to adjust the deposition rate for the experiment.

¹ Programmed by H. ZHOU.

3.5 Measured References

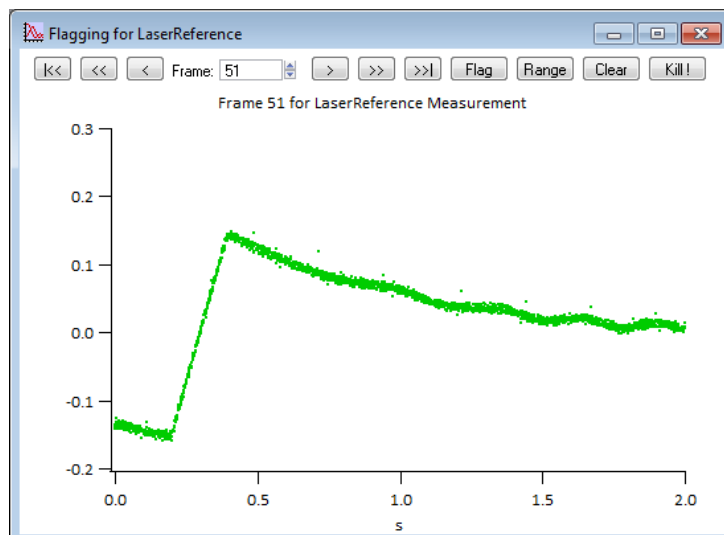
The processing procedure of the loaded reference measurements is mostly identical. The common part is discussed using a laser reference measurement as example, since all radiation, *e.g.*, laser or infrared, based measurements give a similar signal shape.

The entire data set can be visualized with the **Display** button.

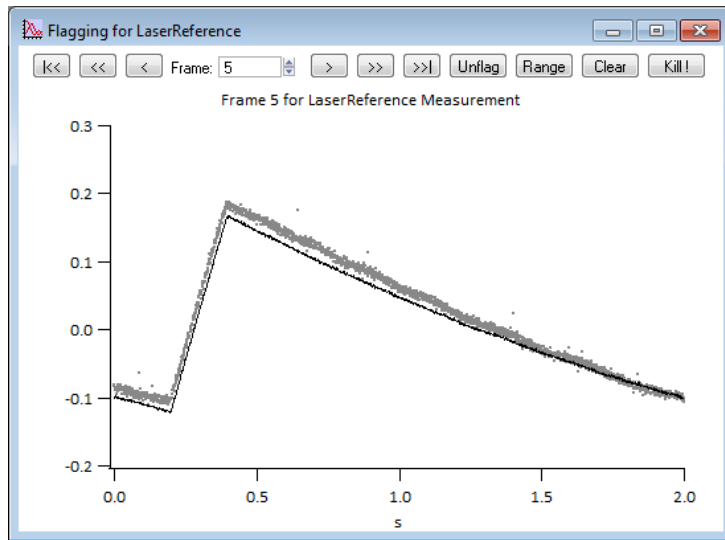


The frames with standing motor, *i.e.*, the first and last frame pair used to document the base line, are marked as unqualified by the loading routine, see Section 3.2.

Frames suffering from distortion, *e.g.*, a measurement artifact arising from a slammed door, can be identified and masked in the windows displayed by pressing the **Flag** button on the main panel.

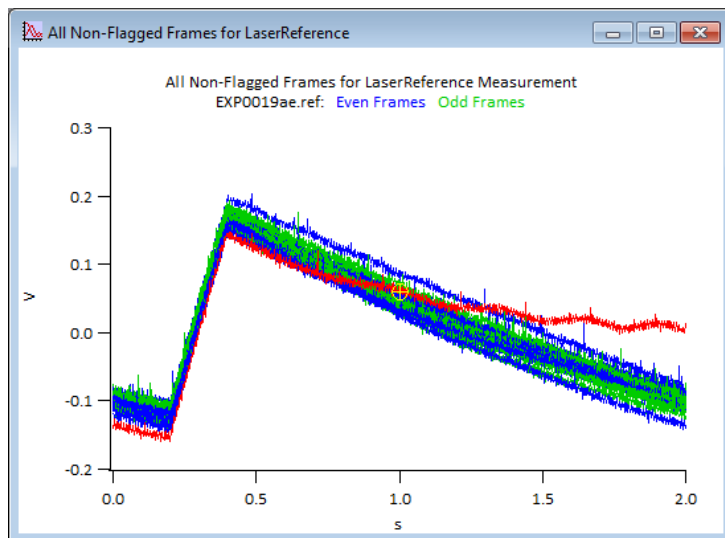


The displayed frame is colored in blue for frames with even parity, colored in green for frames with odd parity, and colored in gray for frames omitted from further processing.

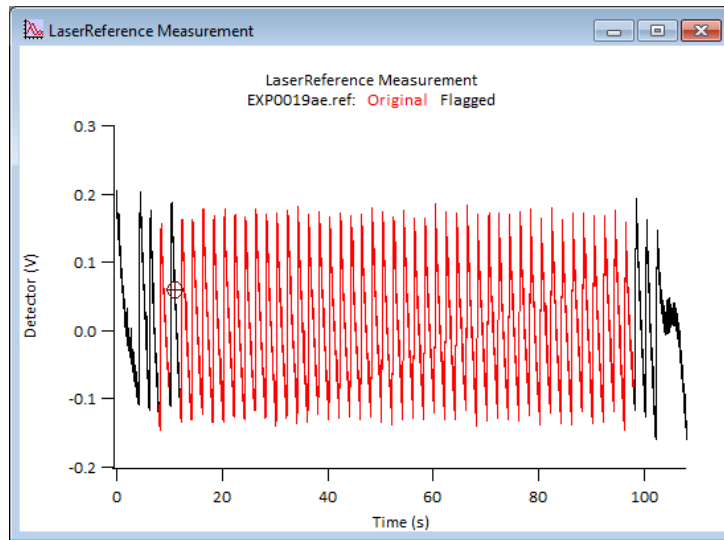


In case the corresponding average has been calculated, it is added to the individual frame as a black trace as a reference for the eye.

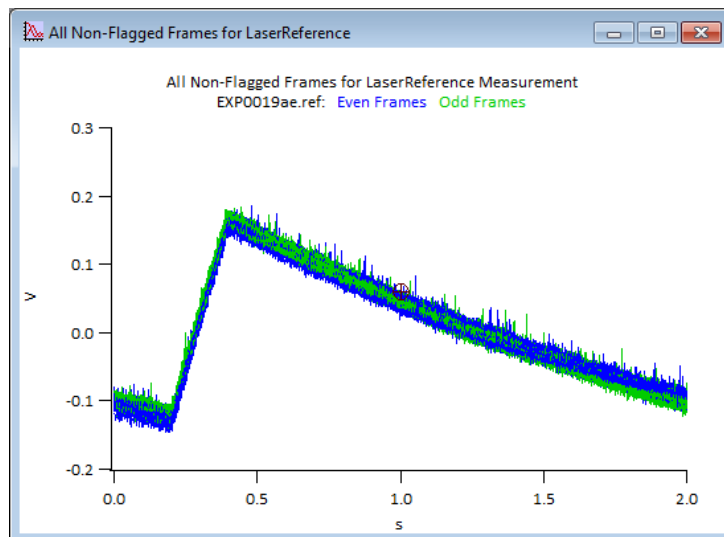
In addition to the linear representation of the data the frames are also displayed piled on top of another.



The current frame can be selected by the navigation objects in the window for an individual frame or by cursors in the windows for the whole data set. The selected frame is highlighted red and by a cursor in the stacked view.



Since the first and last frame pair with started motor can suffer slightly from filtering artifacts they are also masked by default. Manually excluded frames or frames masked by the **Auto Flag** feature are displayed black in the full experiment and set invisible in the view of piled frames.

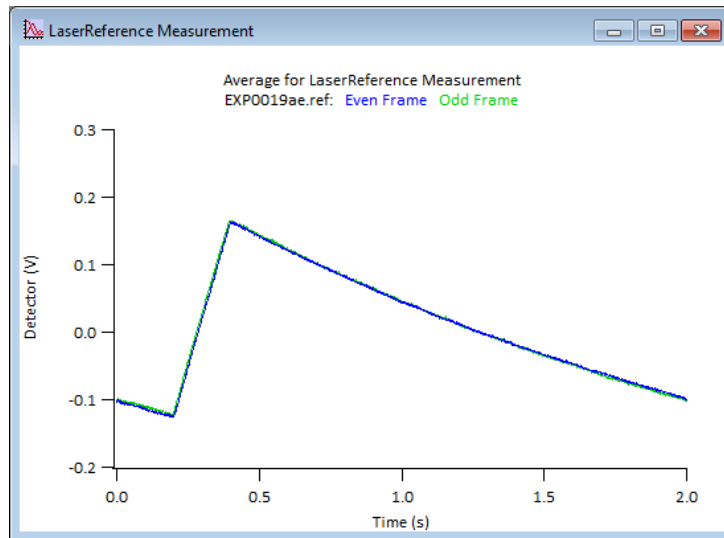


The number of total amount of frames and frames used to calculate the fitting waves is indicated on the main panel.

Total Frames:	54
Processed Frames:	44

After the removal of outlier frames the data evaluation is continued by usage of the `Process` button. Depending on the previously treated measurements different actions are carried out according to the type of measurement. Details are given in the corresponding sections later in this chapter and in Section 4.2.4.

In any case the averages of the qualified frames are calculated for both parities and displayed.



The `Laser Power` and the calculated respectively default or a custom `Reflectivity` are used to calculate the normalized fit waves if applicable.

"Laser" Power (W):	<input type="text" value="3.08283e-05"/>	<input type="text" value="2.92571e-05"/>	<input type="text" value="3.01924e-05"/>
Reflectivity:	<input type="text" value="0.436"/>	<input type="text" value="0.436"/>	<input type="text" value="0.326652"/>

The fit waves, exemplarily shown in Figure 3.8, are created in the `:Experiment:` data folder and are not displayed. In order to enable a temporal shifting of the pulses the fit waves comprise the second half of the normalized average with complementary parity, the actual fit wave in the center, and the first half of the normalized average with complementary parity in that order.

3.5.1 Deconvolution

The normalized fit wave is generated. It differs from the other measurements in several aspects. The position of the switch-on is derived from the data and the start time is set to zero. The duration is set to about three times the length of a regular frame and aligned symmetrically to zero, as shown in Figure 3.9. In addition, a noise free fit wave is generated, see Section 4.2.5, which reduces the noise in the deconvoluted data sets significantly.

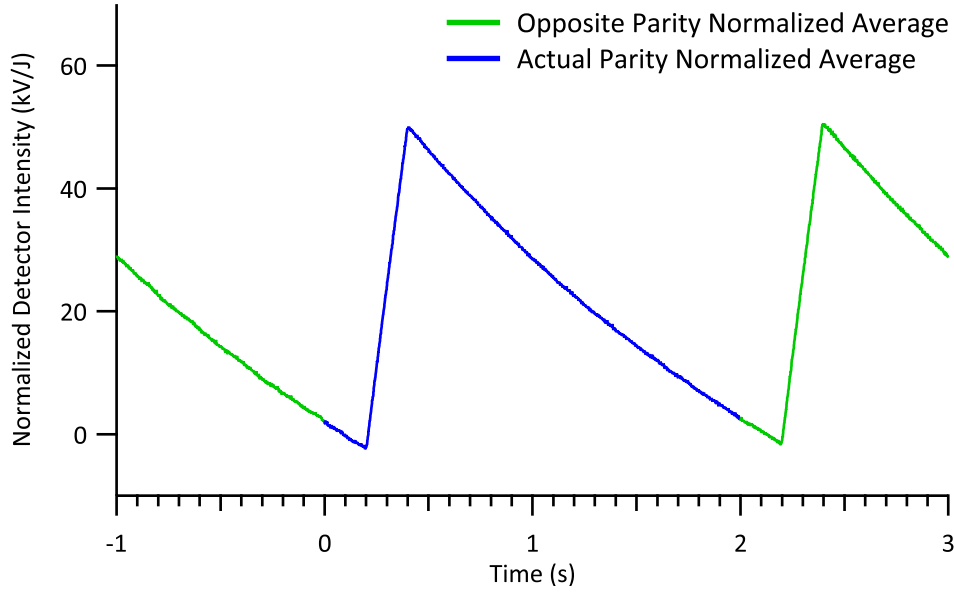


Figure 3.8: Constitution of Fit Waves — The fit waves comprise the second half of the normalized average with complementary parity (green), the actual fit wave in the center (blue), and the first half of the normalized average with complementary parity in that order. This provides a logical continuation capable of handling temporal offsets.

3.5.2 Clean Sample

The normalized reference wave is generated and in case the measurement of a coated sample has been processed its reflectivity R_{coat} is calculated, see Section 3.5.3.

3.5.3 Coated Sample

The normalized reference wave is generated and, in case the measurement of a clean sample has been processed, the reflectivity of the coated sample is calculated from the amplitude ratio r of the normalized averaged peaks, and the reflectivity of the clean sample R_{clean} by means of

$$R_{\text{coat}} = 1 - r \cdot (1 - R_{\text{clean}}) . \quad (3.6)$$

The basic assumption is that the sensitivity of the detector remains unaltered and the changed signal intensity is entirely caused by the different reflectivities, see Section 5.4.2.

If the laser reference measurement has been processed the temperature induced sensitivity change is determined, see Section 3.5.4.

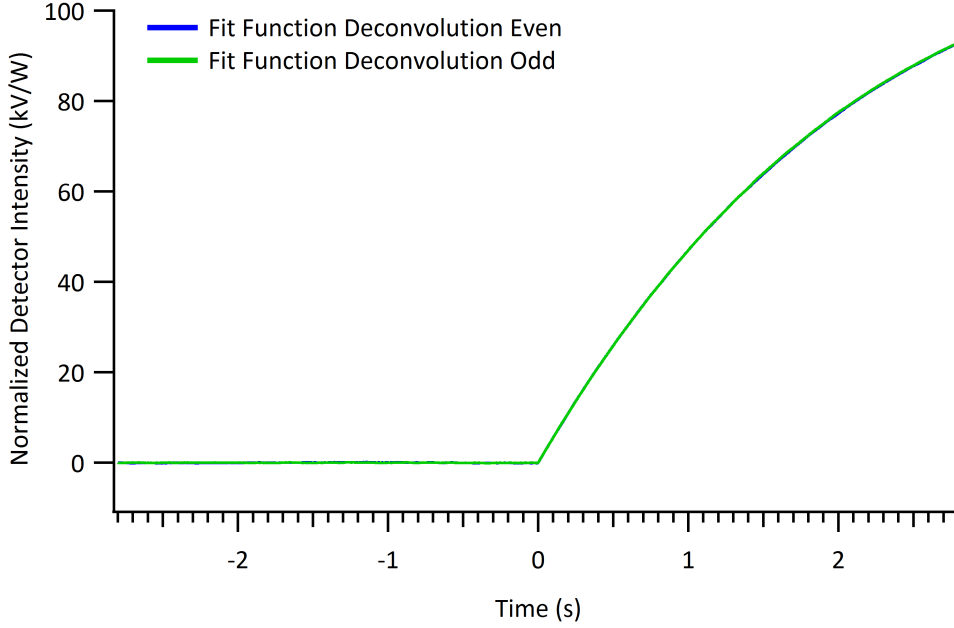


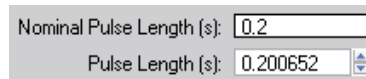
Figure 3.9: Constitution of Fit Waves for Deconvolution — The fit waves contain 1.4 nominal frame lengths for calorimetric experiments before and after the chopper opens. This represents the system response to a Heaviside function.

3.5.4 Laser Reference

In a first step the pulse length is detected from the laser reference measurement. Linear approximations before $y_b = a_b + b_b \cdot t$ and after $y_a = a_a + b_a \cdot t$ the nominal positions of the pulse are calculated excluding the close vicinity of the nominal peak start position, as shown in Figure 3.10. The position of the start t_s and end t_e is defined as the times both corresponding lines intersect

$$\begin{aligned}
 y_{b,\{s,e\}} &= y_{a,\{s,e\}} \\
 a_{b,\{s,e\}} + b_{b,\{s,e\}} \cdot t_{\{s,e\}} &= a_{a,\{s,e\}} + b_{a,\{s,e\}} \cdot t_{\{s,e\}} \\
 t_{\{s,e\}} &= \frac{a_{a,\{s,e\}} - a_{b,\{s,e\}}}{b_{b,\{s,e\}} - b_{a,\{s,e\}}}
 \end{aligned} \tag{3.7}$$

and their difference yields the pulse length $\delta t = t_e - t_s$.



Subsequently, the normalized fit wave is generated. If the coated sample measurement has been processed the temperature induced sensitivity change is determined which can be used for the reconstruction of the energy input if the deconvolution

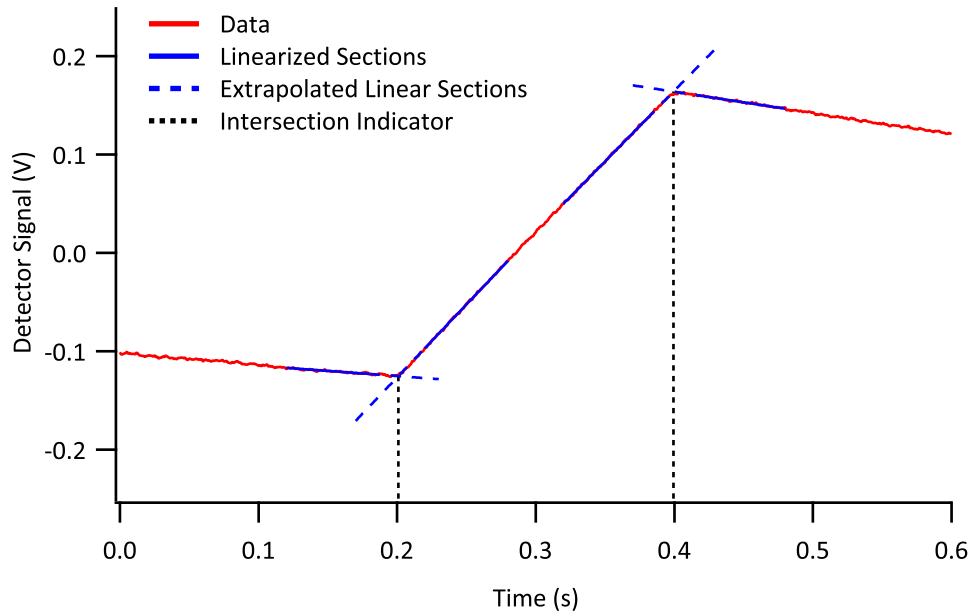


Figure 3.10: Pulse Length Determination — The detector signal (red dots) from a laser reference measurement is linearized (blue solid lines) before and after the start and the end of the nominal peak position. The close vicinity is excluded to avoid artifacts from a shifted pulse. The pulse length is calculated from the start and end points (dotted black lines) obtained from the intersections of the extrapolated line pairs (blue dashed lines).

reference was measured at a different temperature than the measurement to be processed.



The sensitivity is identical to the ratio of the normalized averaged peaks and very close to unity for experiments carried out at ambient temperature. The sensitivity rises for experiments conducted at approximately 100 K up to around 2.5 and is expected to drop in case of elevated temperatures below unity, which is the value for isothermal measurements. This emphasizes the necessity for a well defined and stable temperature of the detector polymer for all measurements. This is especially critical for measurements after the coating process, since the sample experiences heating from the evaporator. In case the transmission measurement is processed the transmission of the window is calculated, see Section 3.5.5.

3.5.5 Transmission of Infrared Transparent Window

The normalized reference wave is generated and the transmission is calculated. The numerical value of the transmission of the infrared transparent window is identical to the ratio of the normalized averaged peaks of the transmission and the laser reference measurements. Its reciprocal value is provided as initial value to the fitting routine for the heat measurement.



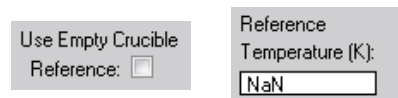
Since the related measurements are conducted with the laser the obtained value is valid only for the wavelength of the laser. The infrared radiation is not monochromatic and is not containing the wavelength used to obtain the transmission. Hence, this measurement only provides an approximation of the infrared transmission, see Section 5.8.1. Nevertheless, it is able to give an estimate of the defilement of the window.

3.5.6 Radiation Contribution

The fit wave used for the radiation component is not normalized, instead the inverse transmission coefficient is used as an initial value for the data processing.

The different shapes of the laser based signals and the radiation signal enable a decomposition of the heat signal into these two components. The relevant part for this procedure is not the peak but the evolution of the signal after the pulse, as shown in Figure 3.11.

Reference measurements performed using an empty crucible to calculate the contribution of the thermal radiation, see Section 5.8.1, substitute this data set. The calculated amplitude is set as a parameter for the treatment of the heat measurement, see Section 3.8.1.



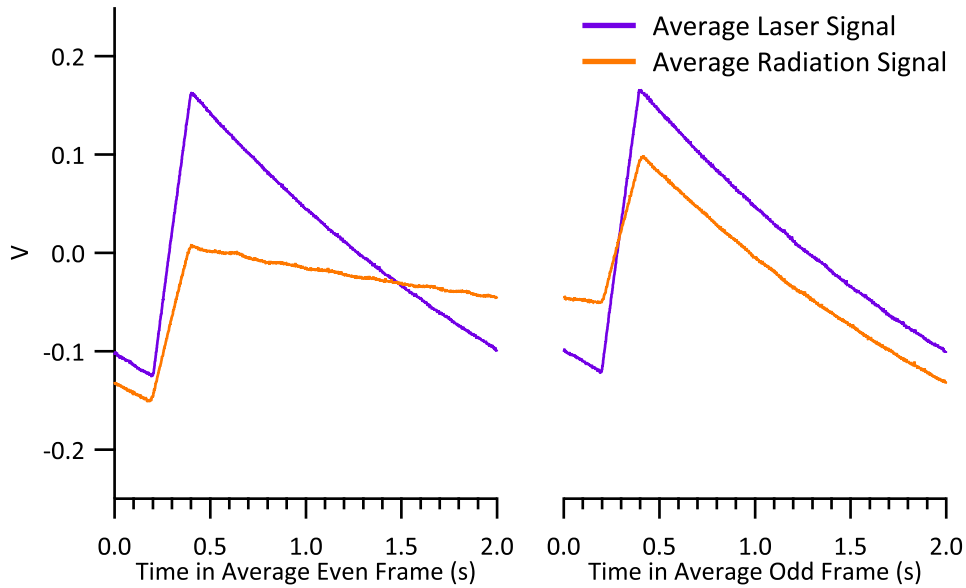
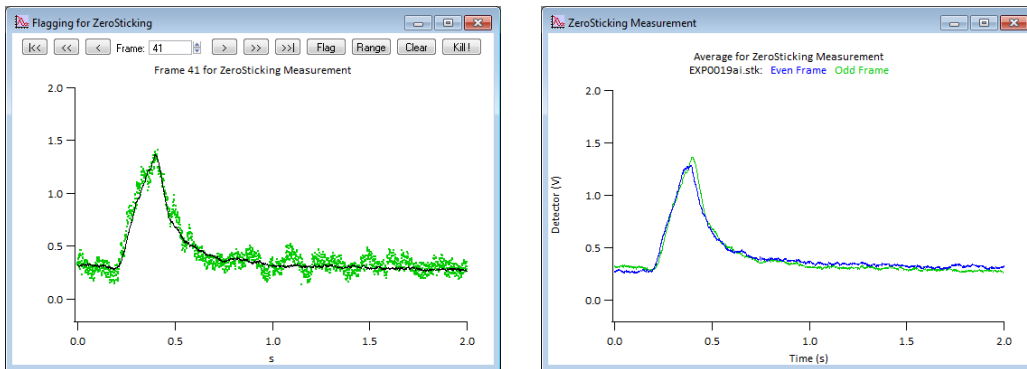


Figure 3.11: Comparison of Laser Based and Radiation Signal — The discrepancy in signal shape of the laser based (purple) and radiation (orange) signal provides a deconvolution of the heat signal. While the rise during the pulse is similar for both kinds, the subsequent decay of the radiation signal differs in a characteristic way.

3.5.7 Zero Sticking

The fit wave for the sticking measurement is generated and normalized by the provided coefficient.

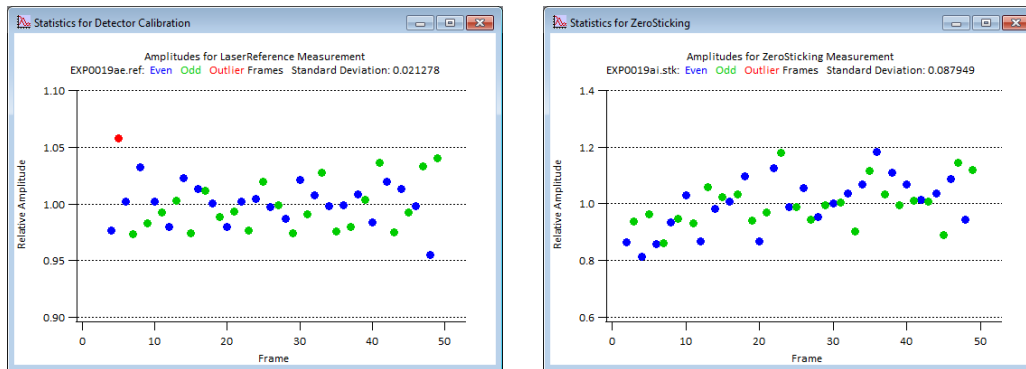


The signal from the mass spectrometer usually contains a high level of noise and an unstable baseline. Thus, a simple integration of the signal to obtain a total intensity is not advised. As a consequence of the unexpected shape of the mass spectrometer signal, *i.e.*, non-rectangular, see Section 5.8.4, it is questionable if an integrative analysis is still providing a proportional result.

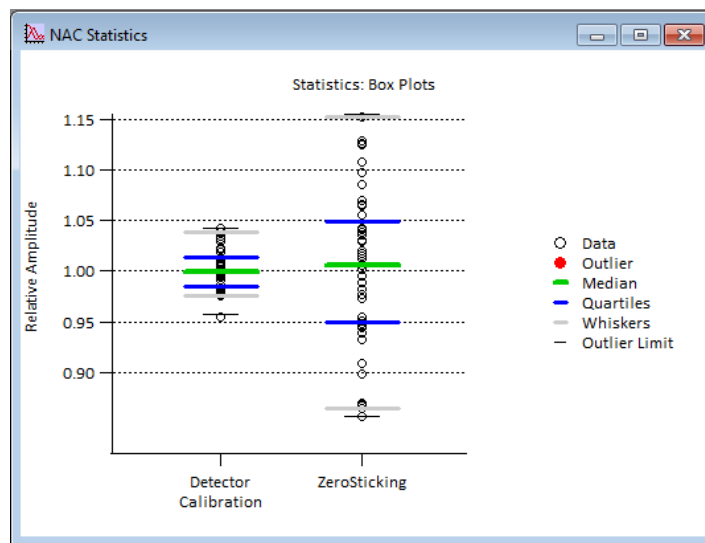
3.6 Statistics

A simple statistical analysis on the loaded reference measurements can be conducted for all measurements or a selected one. The amplitudes of the qualified frames are obtained in relation to the averaged data of the measurement, see Section 4.2.8.

The result is displayed in two ways. One plots the calculated amplitudes against the pulse number and is suitable to detect an unwanted long term change of the corresponding data.



Unfortunately, this representation tends to fool the eye about the scatter of the data. A better way to visualize this dispersion is a *box plot*.



The main components for each measurement comprise the *median* (green line) and the upper and lower *quartile* (blue lines). Assuming a monotonically increasing order of the regarded amplitudes, the median is defined as the value of the data point at half the counting span of the data set. The upper and lower quartile are defined in an analogue way at $1/4$ and $3/4$ of the span count, respectively. These

quantities are robust regarding pronounced outliers in contrast to other common statistical values, *e.g.*, the average of a data set.

Attributes for a “good” data set consist of a median close to the average, *i.e.*, unity since relative amplitudes are regarded, and a small distance of the quartiles to the median. Furthermore, outlier data points (solid circles) should be absent. The limits for outliers (black lines) are explained in Section 3.7. The *whiskers* (gray lines) are defined as the data points with the largest difference to the median within the limits for outliers. The actual data points (open circles) are added to the graph to provide a visual tool to identify clustering of data points and can be suppressed if not desired, see Section 3.1.1.

This representation is not relying of an underlying statistical distribution and is not affected by bin sizes influencing the appearances of histograms. Since it is very robust to the data structure and quite compact, it is ideal to compare the quality of the individual reference measurements.

3.7 Automatic Outlier Removal

Selected frames can be excluded automatically from the creation of the applicable fit functions for a given measurement, if desired.

A data point is classified as outlier if its amplitude A exceeds the lower w_{low} or upper w_{up} whisker limit

$$A \leq w_{\text{low}} \quad \vee \quad A \geq w_{\text{up}} . \quad (3.8)$$

These limits are defined as the corresponding quartile, *i.e.*, q_{low} or q_{up} , expanded by one and a half times the distance between these quartiles

$$w_{\text{low}} = q_{\text{low}} + 1.5 \cdot |q_{\text{up}} - q_{\text{low}}| \quad A > \mu \quad (3.9)$$

$$w_{\text{up}} = q_{\text{up}} + 1.5 \cdot |q_{\text{up}} - q_{\text{low}}| \quad A > \mu . \quad (3.10)$$

To motivate this criterion the probability of a falsely rejected data point should be discussed. A standard normal distribution of the data points, see Section 5.10, with the distribution function Φ

$$\Phi(z) = \frac{1}{\sqrt{2\pi}} \int_{-\infty}^z \exp\left(-\frac{x^2}{2}\right) dx \quad (3.11)$$

and its inverse Φ^{-1} is assumed. The probability p to find a data point in the interval $[\mu - z\sigma; \mu + z\sigma]$ around the center μ and a standard deviation σ of the data set is given by

$$\begin{aligned} p &= \frac{1}{\sqrt{2\pi}} \int_{-z}^z \exp\left(-\frac{x^2}{2}\right) dx \\ &= 2 \cdot \frac{1}{\sqrt{2\pi}} \int_0^z \exp\left(-\frac{x^2}{2}\right) dx \\ &= 2 \cdot \frac{1}{\sqrt{2\pi}} \int_{-\infty}^z \exp\left(-\frac{x^2}{2}\right) dx - 2 \cdot \frac{1}{\sqrt{2\pi}} \int_{-\infty}^0 \exp\left(-\frac{x^2}{2}\right) dx \\ &= 2\Phi(z) - 2\Phi(0) \\ &= 2\Phi(z) - 1 \end{aligned} \quad (3.12)$$

utilizing the symmetry and normalization of Φ . Rearrangement yields

$$z(p) = \Phi^{-1}\left(\frac{p+1}{2}\right) \quad p \in [0; 1] \quad (3.13)$$

providing a method to obtain the interval's limits for a given probability from tabulated values for Φ^{-1} . With the assumption that the lower and upper quartile are symmetrical to the median located at $\mu = 1$ and cover 50% of the data set, *i.e.*, $p = 0.5$, calculation results in a statistical significance of 0.67449σ . Thus the inter quartile distance computes to $2 \cdot 0.67449\sigma = 1.34898\sigma$ and the outlier limit to $0.67449\sigma + 1.5 \cdot 1.3490\sigma \approx 2.36\sigma$. This can be converted back to a probability of $p = 0.993$ that a data point is located inside the limits. This corresponds to a probability of 0.7% for a falsely rejected data point, *i.e.*, one in 143 frames.

It should be reminded that this is an exemplary calculation with the assumption of a standard normal distribution. The criterion of the box is of similar strength, independent of the nature of the distribution.

A high number of outlier frames likely indicates a faulty measurement setup. According to the statistical consideration, two outlier frames are to be expected for the measured amount of three hundred frames in the presented example and six frames are found, as shown in Figure 3.12. It should be reminded that the presented example is imperfect and that it was chosen in order to demonstrate the effects of the correction mechanisms.

After removal of outliers the averages, fit waves, and statistics need to be recalculated. Since the limits for outliers change upon exclusion of frames, it is possible that new frames are ranked as outliers, as shown in Figure 3.13. The program package allows automatic removal of outlier frames only in the first iteration. It is advised to inspect the second generation outlier frames manually by the selection procedure, see Section 3.5. However, persisting outlier frames are typically not present in successful measurements and their presence indicates a disturbed experiment.

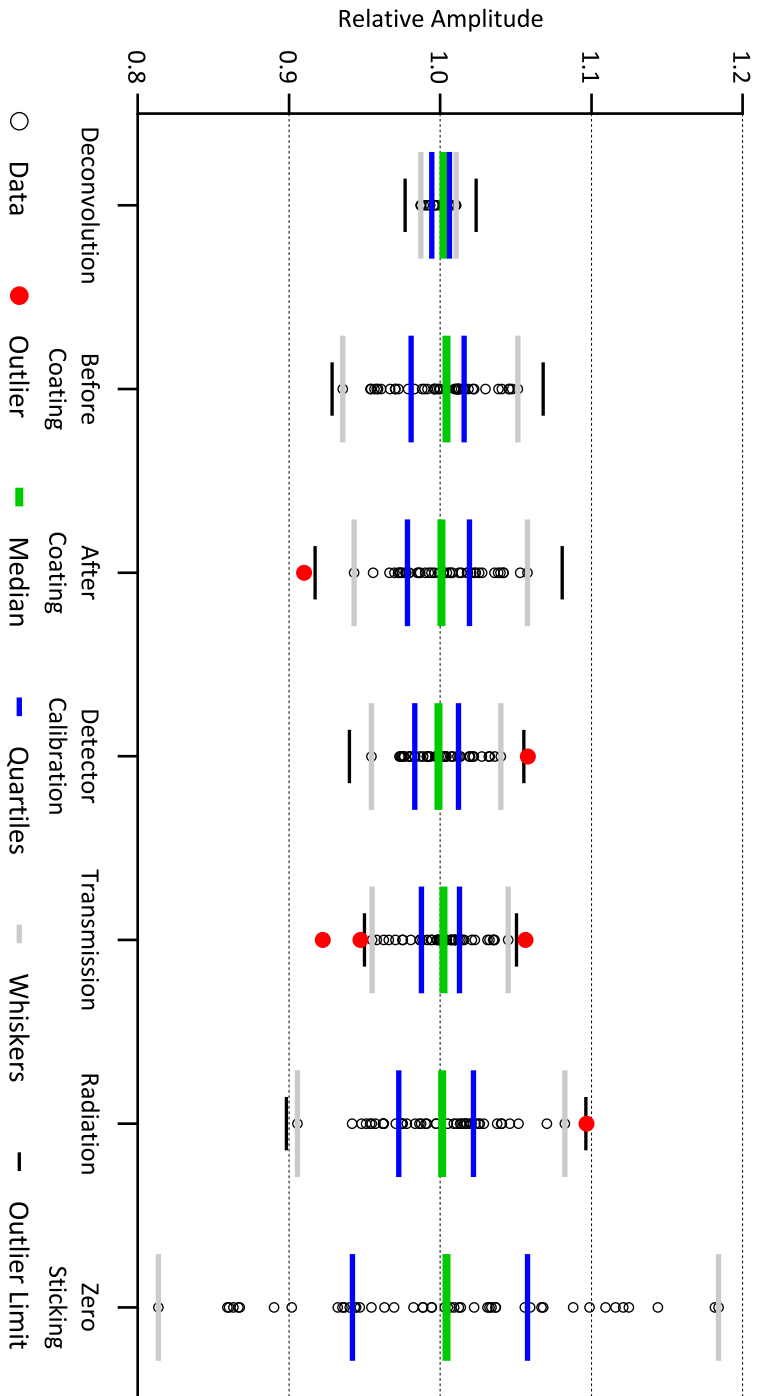


Figure 3.12: Statistical Comparison of the References — The graphical representation of all reference measurements for a calorimetry experiment is given as a box plot before automatic removal of outliers. The relative quality of the experiments is readily visible and reveals the zero sticking measurement as least certain. The medians lie close to the average, *i.e.*, unity, and the lower and upper quartiles are symmetrical to the median. The high number of outliers indicates issues with the experimental setup.

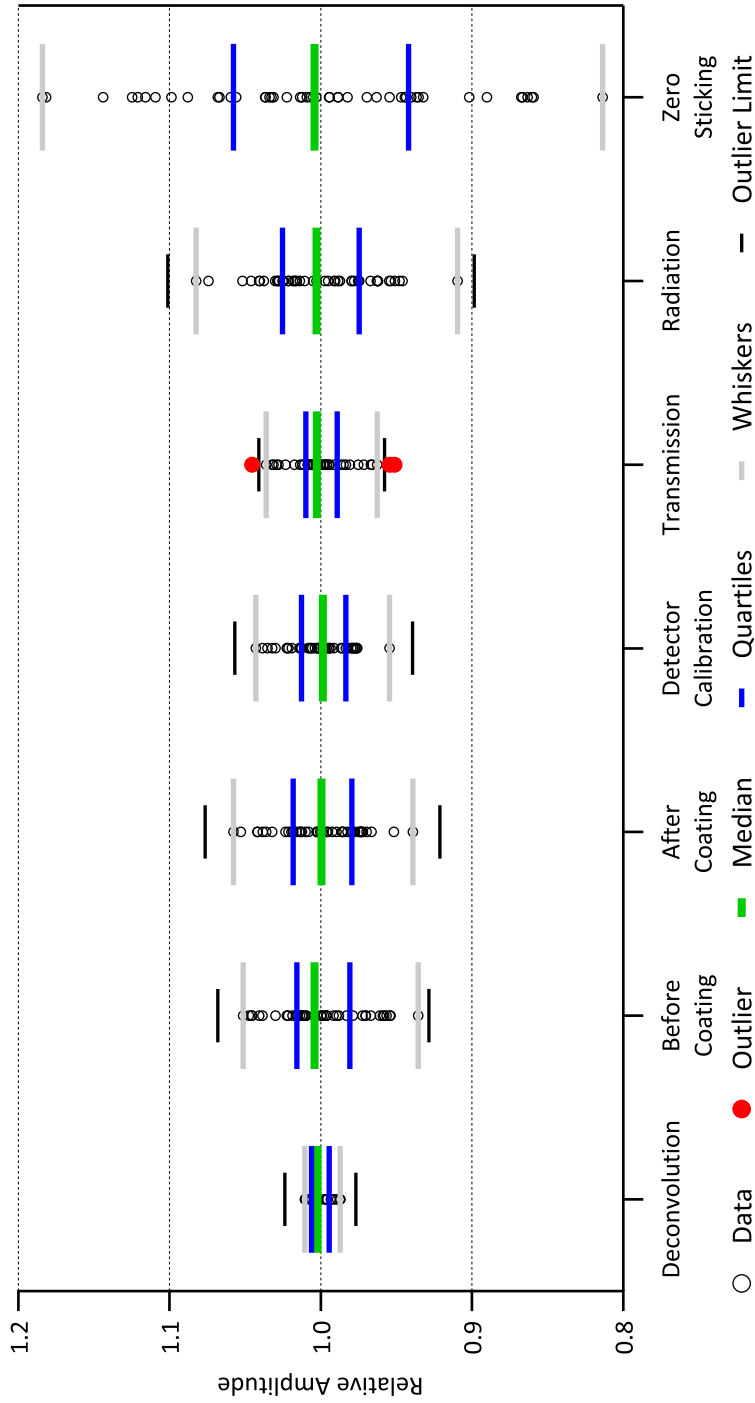


Figure 3.13: Statistical Comparison of the References — The graphical representation of all reference measurements for a calorimetry experiment is given as a box plot after automatic removal of outliers. The relative quality of the experiments is readily visible and reveals the zero sticking measurement as least certain. The medians lie close to the average, *i.e.*, unity, and the lower and upper quartiles are symmetrical to the median. The outliers in the transmission measurement arise from altered limits for outlier detection.

3.8 Calorimetry Measurement

In a first step, the parity dependent averages of the qualified frames are calculated. There is no automatic outlier detection for these measurements since changes in intensity are expected. However, frames resulting in a fit error during the evaluation are removed from the results.

3.8.1 Heat Measurement

The data points in a frame $\mathcal{H}_n(t)$ of a heat measurement are fitted with a function comprising an offset A_0 and a linear combination of the normalized laser reference $\mathcal{L}_P(t)$ shifted by $t_{0,\mathcal{L}}$ with an amplitude $A_{\mathcal{L}}$ and the average response to radiation $\mathcal{R}_P(t)$ shifted by $t_{0,\mathcal{R}}$ with an amplitude $A_{\mathcal{R}}$

$$\mathcal{H}_n(t) = A_0 + A_{\mathcal{L}}(n) \cdot \mathcal{L}_P(t - t_{0,\mathcal{L}}) + A_{\mathcal{R}}(n) \cdot \mathcal{R}_P(t - t_{0,\mathcal{R}}) \quad (3.14)$$

separating the radiative part from the reaction heat as illustrated in Figure 3.14. The parity P is determined by the frame number n . The initial coefficients are adjustable by the user in the lower part of the control panel. Typical values are preset in the program with exception of the radiation coefficient which is unity by default and replaced by the inverse of the calculated transmission of the window, see Section 3.5.5.

The image shows a control panel with the following settings:

- Offset | Hold: 0
- Heat Amp | Hold: 1e-06
- Heat Shift | Hold: 0
- Rad Amp | Hold: 1
- Rad Shift | Hold: 0
- Use Trend:
- Link Heat & Radiation Shifts:

It also provides options to hold a coefficient at the given value or to force the use of a trend for the radiative contribution, *i.e.*, a “smoothing” replacement function, see Section 3.9. If the value is held at the value of the inverse transmission coefficient, the procedure acts like a constant, parity sensitive removal of the radiative contribution to the signal.

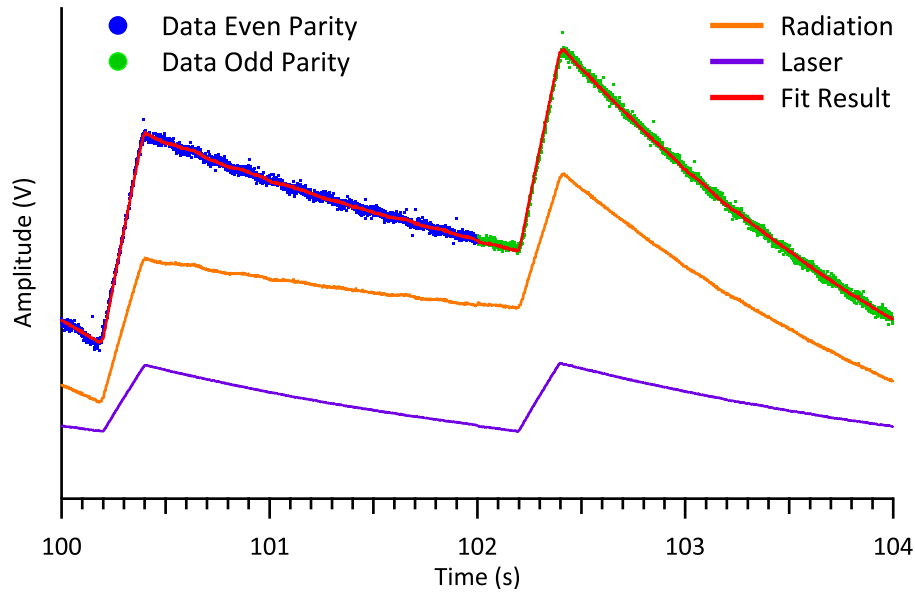
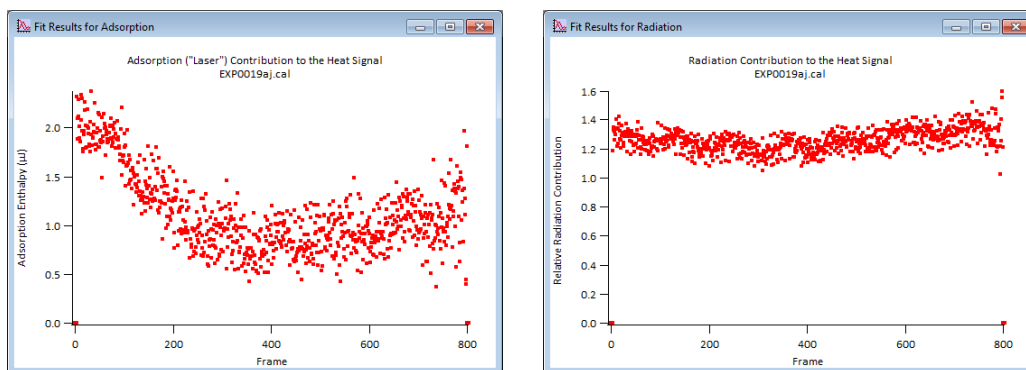


Figure 3.14: Fit Contributions Heat Measurement — Two consecutive data sets (blue and green dots) are fitted (black) with a linear combination of a laser like (purple) and radiation like (orange) component. For enhanced clarity the constituents are vertically offset.

Offset Hold	0	Offset Hold	0
Heat Amp Hold	1e-06	Desorption Hold	0.5
Heat Shift Hold	0	Shift Hold	0
Rad Amp Hold	1.36538		
Rad Shift Hold	0		
Use Trend:	<input type="checkbox"/>	Use Trend:	<input type="checkbox"/>
Link Heat & Radiation Shifts:		<input checked="" type="checkbox"/>	

Alternatively to the hold option, the shift parameters can be constrained to be identical, *i.e.*, both contributions are shifted by the same amount. If both shifts are linked and one parameter is hold, the other one is set to the value of the first one. In case both hold options are enabled, this feature has no effect. Upon unequal initial values describing the shifts and enabled linking, the both shift parameters are set to their average value.

The results for every frame are displayed.



The resulting amplitudes related to the laser-like component directly contain the energy deposited on the sample due to the normalization process. In contrast, the amplitude of the radiative contribution is purely relative and might be used to detect a coverage dependent absorption change for infrared radiation of the sample. Upon application of a radiation measurement performed using an empty crucible and omitting the window, see Section 5.8.1, the coefficient corresponding to the radiation contribution needs to be constrained to the correction factor automatically derived from the sample and source temperatures during the reference and heat measurements, see Section 5.8.1.

Typically, the shift parameters are pinned to zero and are intended to catch a glitch of the position of the chopper motor.

3.8.2 Sticking Measurement

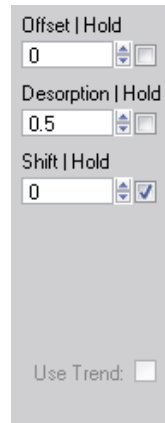
The data points in a frame $\mathcal{S}(t)$ of a sticking measurement are fitted with a function comprising an offset A_0 and the normalized zero sticking, *i.e.*, desorption, reference \mathcal{D} shifted by $t_{0,\mathcal{D}}$ with an amplitude $A_{\mathcal{D}}$

$$\mathcal{S}_n(t) = A_0 + A_{\mathcal{D}}(n) \cdot \mathcal{D}_P(t - t_{0,\mathcal{D}}) \quad (3.15)$$

quantifying the fraction of molecules not sticking, *i.e.*, recoiled molecules or molecules desorbing from a weakly bound precursor state after a certain residence time, see Figure 5.8.4. The parity P is determined by the frame number n .

Due to the noisy and unstable base line of the mass spectrometer, as shown in Sections 3.5.7 and 3.6, a fitting mechanism is utilized rather than an integration based method.

The initial fit coefficients are adjustable by the user in the lower part of the control panel. Typical values are preset in the program



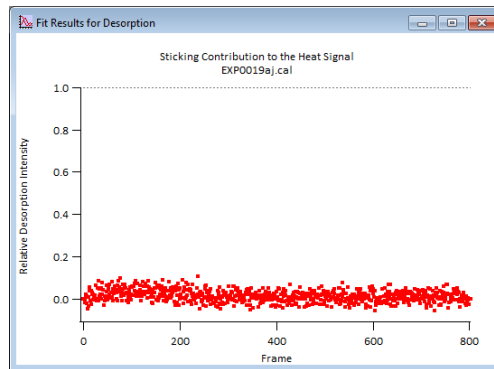
Offset | Hold
0

Desorption | Hold
0.5

Shift | Hold
0

Use Trend:

with no further derived values. It also provides options to hold a coefficient at the given value or to force the use of a trend, *i.e.*, a “smoothing” replacement function, see Section 3.9, for the desorption in the dependent calculations in order to reduce scatter.



The results of the desorption measurement should be located in the interval $[0;1]$ where the boundaries are equivalent to no molecule leaving the surface and all molecules leaving the surface, respectively. If a running average exceeds this range significantly, it is an indicator for an incorrect measurement or correction factor.

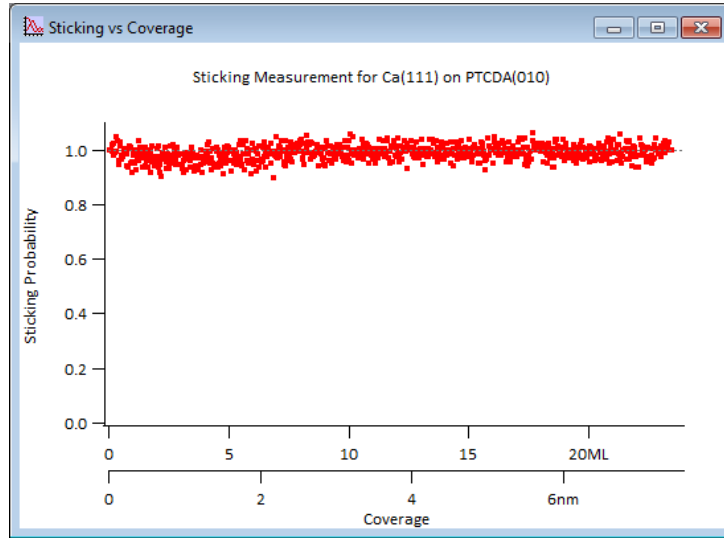
In case the deposition rate for the calorimetry experiment is determined, the coverage $\theta(n)$ for a certain pulse number n on the sample is computed. The calculation uses the dose per pulse D_{ML} in monolayers and the sticking probabilities $A_{\mathcal{S}}(n)$ as a function of the pulse number n

$$A_{\mathcal{S}}(n) = 1 - A_{\mathcal{D}}(n) \quad (3.16)$$

computed from the corresponding desorption amplitudes $A_{\mathcal{D}}(n)$. The result

$$\theta(n) = \sum_{i=0}^n D_{\text{ML}} \cdot A_{\mathcal{S}}(i) \quad (3.17)$$

is used to map the heat of adsorption and sticking coefficients to a coverage, see Section 3.8.3. For enhanced clarity the coverage axis is doubled and provides this property in monolayers and meters.



3.8.3 Enthalpy Calculation

Upon treatment of either the heat or sticking measurement, the calculation of molar enthalpies is executed in case all relevant information is provided. The thermodynamical corrections, see Section 1.1, are automatically calculated from the sample's and source's temperatures and the heat capacity of the dosed substance.

Sample Temperature (K):	309.77
Source Temperature (K):	848.441
Subtract Adsorption (J/mol):	17227.4
Subtract Desorption (J/mol):	18515.1

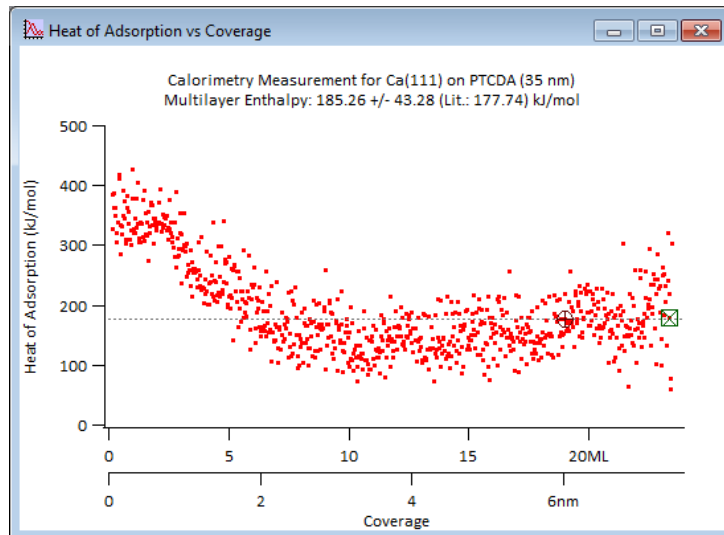
The uncorrected heat of adsorption $A_{\mathcal{H}}$ of each individual pulse n is calculated from the fitting coefficient $A_{\mathcal{S}}$ for a laser like input, the fitting coefficient $A_{\mathcal{D}}$ for the desorption, and the molar dose per pulse D_{mol} by

$$\Delta A_{\mathcal{H}}(n) = \frac{A_{\mathcal{S}}(n)}{(1 - A_{\mathcal{D}}(n)) \cdot D_{\text{mol}}} . \quad (3.18)$$

This preliminary enthalpy is rectified by the mentioned corrections. Finally, combination of Equations Equation (3.17) and Equation (3.18) yields the heat of adsorption

as a function of coverage $\Delta_{\text{ads}}H(\theta)$. However, both values are internally still indexed by the frame number and appear as (θ, H) -pairs in this context. A conversion to a true dependence of the heat on the coverage is performed by the experiment averaging features, see Section 3.11.

This main result of the experiment is displayed together with the average value between two user adjustable cursors and the heat of re-sublimation as a reference. For enhanced clarity the coverage axis is doubled and provides this property in monolayers and meters.



The mentioned average is also documented in the main panel

Multilayer Reference (J/mol):	177494
Multilayer Enthalpy (J/mol):	153014
Multilayer Enthalpy Error (J/mol):	19325.6

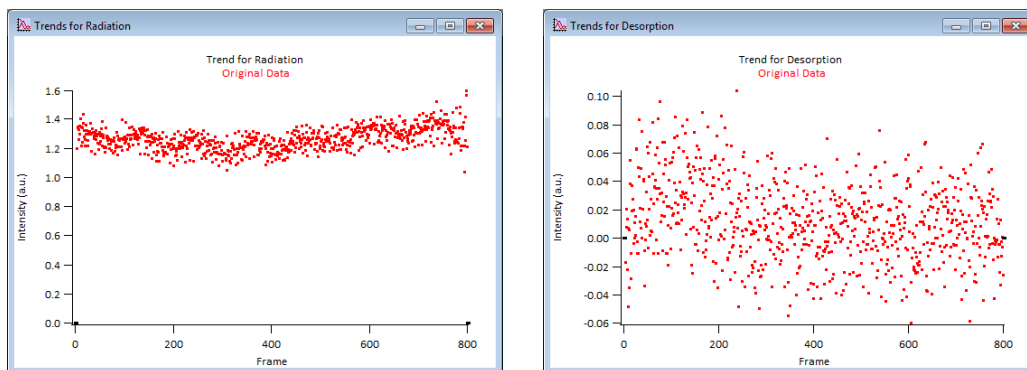
together with the standard deviation and the calculated reference enthalpy.

3.9 Fitted Trends

It is unlikely that the contribution of the infrared radiation to the measured signal changes rapidly in a random direction. A slow smooth change is expectable in case of an organic substrate layer overgrown by a dense metal film which involves a change of the absorption coefficient relevant for the radiative power input. The same argument holds for the desorption/sticking measurement. Long term changes are to be expected since the pristine surface might exhibit a different sticking coefficient than the built up reacted inter-layer and subsequent metallic cover layer.

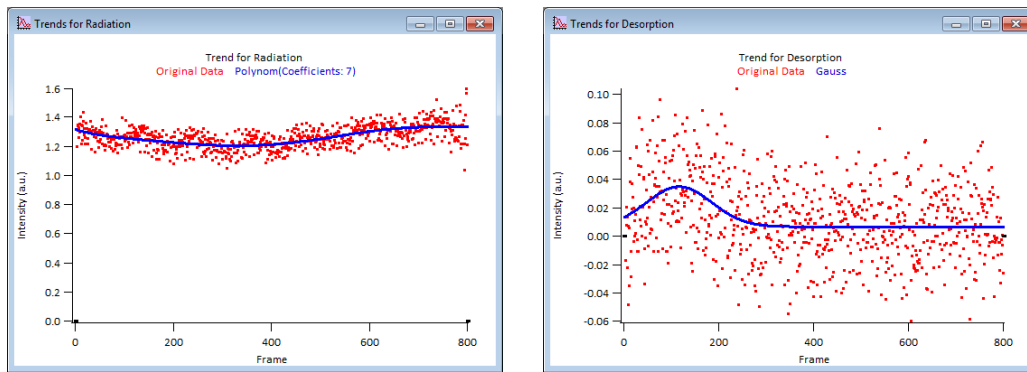
Hence, the jitter in these results originates from noise in the data and, therefrom, influences the fitting routine. Two approaches are feasible to increase the quality of the calculated data. One way is to repeat the experiment with identical conditions and to average the results. This option is presented in Section 3.11. The other way uses the assumption that the changes can be approximated by a function or by partial averages, *i.e.*, data *smoothing*. The data set resulting from this feature called from the menu is denoted here as fitted trend.

The original data is displayed and the user is prompted to select an approximation method, see Section 3.1.1.



The exact function and parameters depend on the actual data but typically the radiation component is well approximated with polynomials, *e.g.*, of order six or a sigmoid function, while the desorption usually follows a sigmoid, Gauss, or Lorentz function. Since there is no reliable theory about the behavior, the user's experience is challenged to find a function and parameters that match the measured data.

After selection of the method and parameters the trend is calculated and displayed with the original data and the user input.



The process can be repeated as often as desired. Especially for low amplitude sticking measurements it can be tedious to find a satisfying set of properties. It should be mentioned that frames removed from the data treatment are displayed black in the graph and are ignored in the actual fitting routine. Nevertheless, the fit results in this area are displayed as well, since they may be used in case the frames are included again.

The use of the trends in the fitting procedure is enabled automatically in case that a trend was created.

Offset Hold	Offset Hold
0	0
Heat Amp Hold	Desorption Hold
1e-06	0.5
Heat Shift Hold	Shift Hold
0	0
Rad Amp Hold	
1.3653	
Rad Shift Hold	
0	
Use Trend: <input checked="" type="checkbox"/>	Use Trend: <input checked="" type="checkbox"/>
Link Heat & Radiation Shifts: <input type="checkbox"/>	

It is possible to create an individual trend, *e.g.*, as results from a user defined function, by overwriting values in `root:NAC:Heat:fit_Radiation` and `root:NAC:Heat:fit_Desorption`. These data sets should be initialized by an iteration of the regular trend creation process.

Reprocessing of the heat and sticking measurements apply the created trends to the data evaluation and provide an improved result, as shown in Figure 3.15. The main requirements of such a procedure are fulfilled. On the one hand, the local amplitude and evolution of the data is unchanged while, on the other hand, the scatter is reduced.

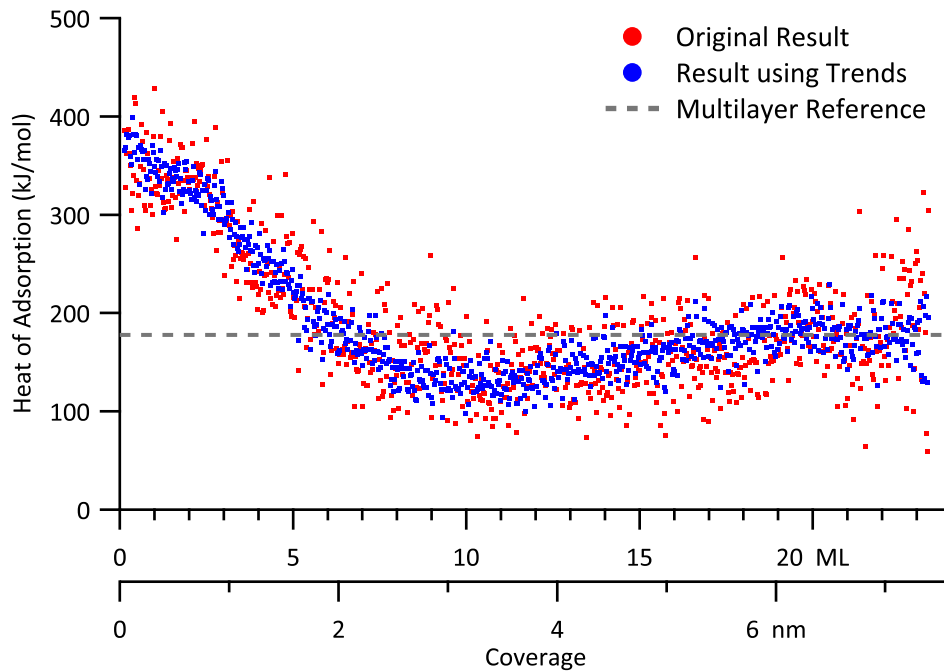


Figure 3.15: Effect of Fitted Trends: Noise — The same data set evaluated without (red dots) and with (blue dots) trends used as fit coefficients in the evaluation. The amplitude and shape of the data remain unchanged while the scatter is reduced. The calculated re-sublimation enthalpy is added as a reference for the expected results for deposition on multilayers. The coverage axis is duplicated to provide measures in monolayers and meters.

This feature also eliminates artifacts in the fitting routine manifesting as overestimation of the radiative contribution for strictly even frames and underestimating the contribution for strictly odd frames.

This behavior is only observed at changing enthalpy, *i.e.*, changes in the amplitude of the signal, as shown in Figure 3.16.

The initial values in the fit routine are reset to the same values for all frames. Hence, it is unlikely that this artifact is caused by a fault in the fitting routine and thus probably induced by the amplifier readjusting its baseline during the measurement.

It should be mentioned that the given options are not necessarily physically meaningful. Depending on the growth behavior of the adsorbed species a linear or sigmoid change in the reflectivity can be expected in simple cases, *e.g.*, in case of Frank-van der Merwe respectively Volmer-Weber growth. However, in more complex cases, *e.g.*, cluster growth in combination with surface reaction, the use of the entirely empirical shape matching approach is indicated.

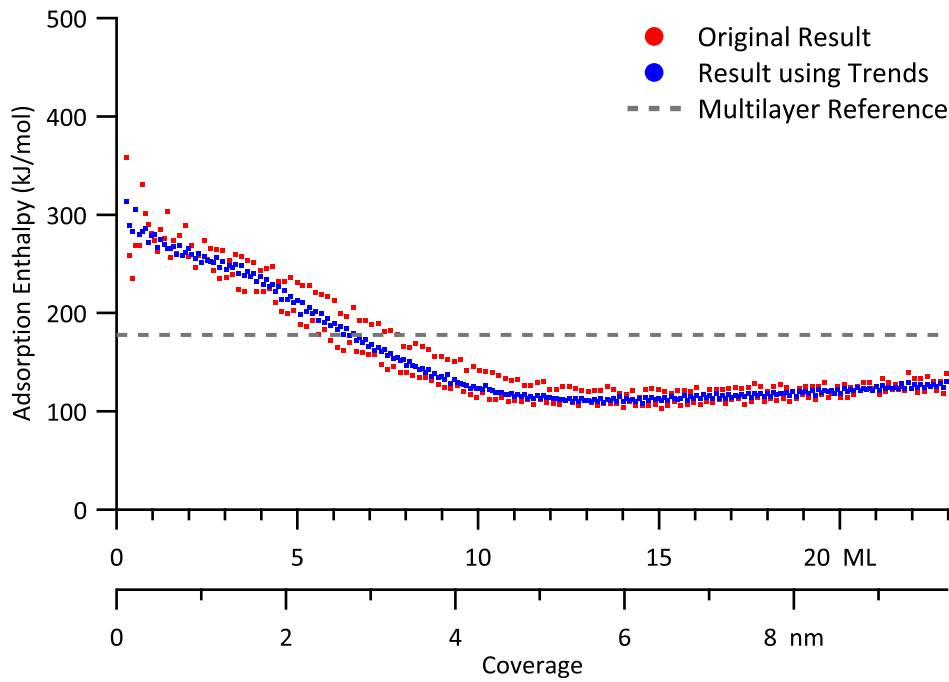
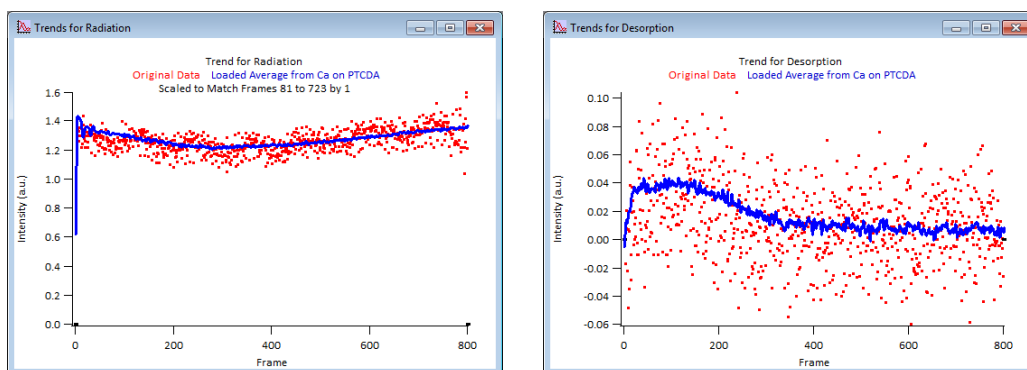
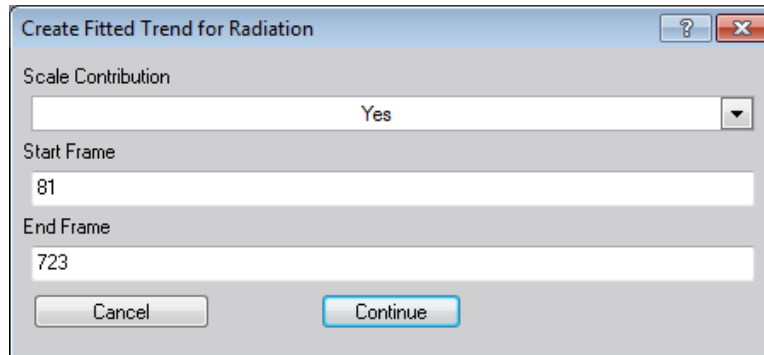


Figure 3.16: Effect of Fitted Trends: Balancing — The same data set evaluated without (red dots) and with (blue dots) trends used as fit coefficients in the evaluation. The twinning of the amplitudes is removed while the general data structure is preserved. The calculated re-sublimation enthalpy is added as a reference for the expected results for deposition on multilayers.

Additionally, it is possible to replace the local radiation or sticking contribution with an average contribution obtained from several experiments, see Section 3.11. This option requires a set of trustworthy experiments used to calculate a valid average. Hence, data sets exhibiting uncommon trends need to be excluded in the averaging procedure.



If the radiation contribution is approximated, it is possible to scale the loaded average to match a selectable range of the local data. This step is usually necessary, since the absolute contribution depends on the transmission of the infrared transparent window, see Section 2.4.4.

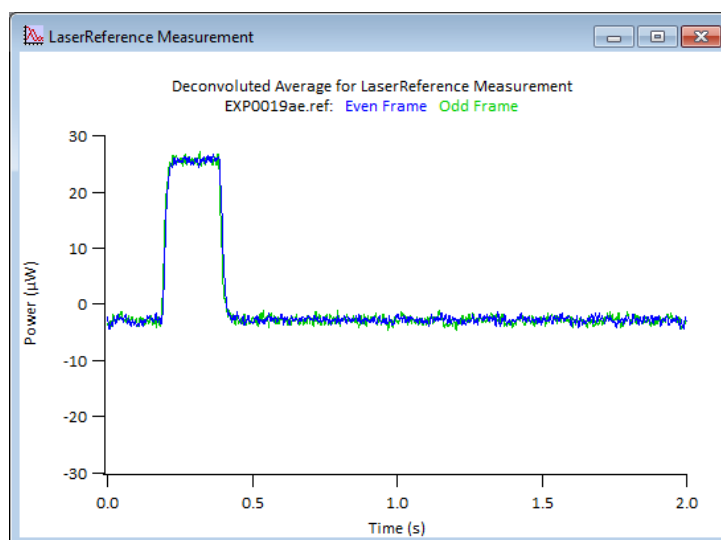


3.10 Deconvolution of Measurements

Several cases might require a deeper analysis of the measured data. A profane situation is to discover reasons for an unexpected peak shape, *i.e.*, fault diagnostics. More elaborate questions could address reactions which are of medium speed, *i.e.*, exhibit kinetic time constants comparable to the temporal resolution of the setup, *e.g.*, approximately between 0.01 s and 0.1 s. It might even be possible to obtain activation barriers for these reactions if the observed time constants are determined as a function of temperature.

The response of the detector/amplifier to a scaled Heaviside input is obtained in the deconvolution reference measurement, *i.e.*, it contains the response to a “sudden” turning-on of a constant input power. The program uses this information together with a small window from the data of the frame to extrapolate the signal later in the frame. The prediction is removed from the set, the window is shifted by one step to a later time, and the prediction is carried out again. This cycle is repeated until the end of the frame is reached, see Section 4.2.4. Integration yields the power input as a function of time.

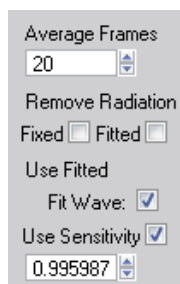
The deconvolution routine can be carried out in two different ways. One performs the analysis only on the averaged frames of a measurement and is initiated by the corresponding Avg button.



The other possibility also includes a detailed treatment of the data set started with the All button.



If the individual frames of a data set are about to be performed, it is possible to create parity preserving averages of subsets in the data set according to the **Average Frames** setting. In case of a heat measurement to be processed, it is possible to remove the radiative contribution, if favored. In this case two possibilities can be selected. The first one removes a constant radiation given in the initial fit parameter section. The other one derives the removed amount from the result of the fitting procedure.



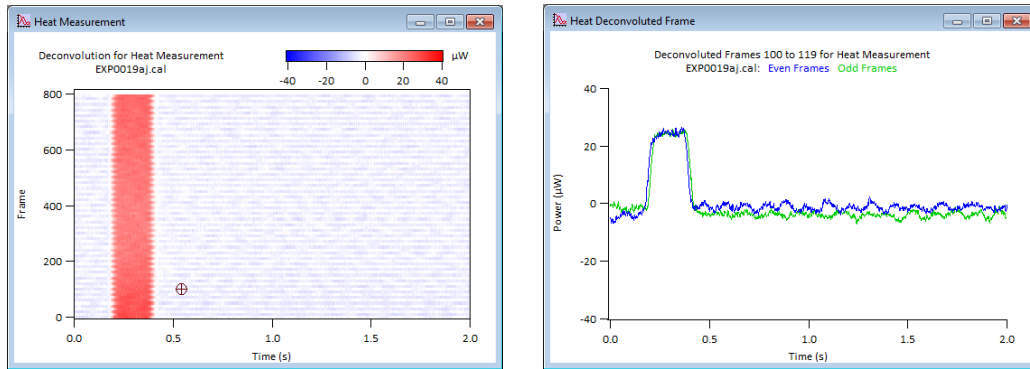
In case of excellent signal quality, it is possible to perform the deconvolution with the measured data. Nevertheless, it is advised to perform this action with the noise free fit function derived from the measured data since it improves the quality of the deconvoluted data significantly, as shown in Figure 3.17.

If the quality of the deconvolution reference is insufficient, an attempt to perform the procedure with the real data is futile, while the variant with the fitted system response still might lead to good results.

Due to the fact that the deconvolution measurement is time consuming, it was usually carried out only at room temperature. Since the sensitivity of the detector changes with temperature, see Section 5.9.4, it is at least necessary to apply a linear correction. The strength of this effect is derived from the after coating reference and laser reference measurements, see Section 3.5.4. This feature is enabled by default and is sufficient for qualitative and semi-quantitative experiments.

For high accuracy data deconvolution of measurements recorded with the sample at non-ambient temperature the deconvolution measurement should be performed at the same temperature as the calorimetric measurement. In that specific case the sensitivity correction needs to be turned off.

After the deconvolution of the measurement is accomplished the color coded input power is displayed as function of time and frame. A cursor in the image provides a way to select a frame pair in the measurement whose power is plotted as a function of time. Metaphorically speaking a cut parallel to the time axis perpendicular to the paper plane is made and the color is converted back to an intensity.



It should be mentioned that this procedure actually requires an absolute input signal to return absolute values. However, the used amplifier incorporates an automatic offset compensation which is removing exactly this information. Hence, only relative quantities are accessible here. This also leads to a constant background in the deconvolution result of opposite polarity compared to the pulse.

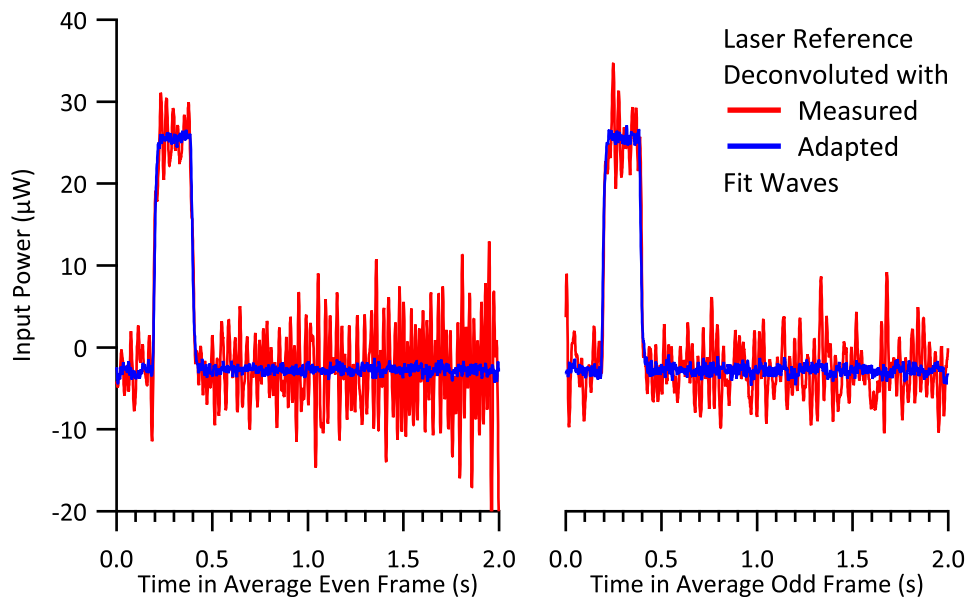
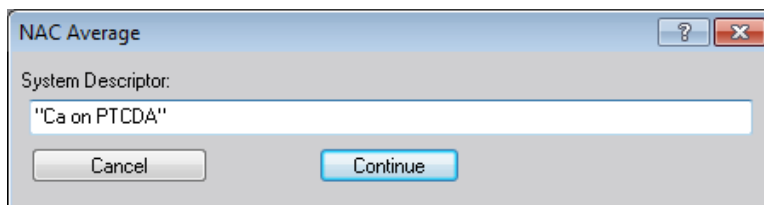


Figure 3.17: Influence of Noise in the Deconvolution Reference — The same averages frames of a laser reference measurement were deconvoluted with the measured fit wave (red) and with the adapted noise free fit wave (blue). The process was carried out for both parities separately. Both frames, with the boundary at 2s, suffer from an increased noise. The algorithm is close to its converging limit in case of the first frame recognizable by the increasing amplitude of the noise.

3.11 Averaging Experiments

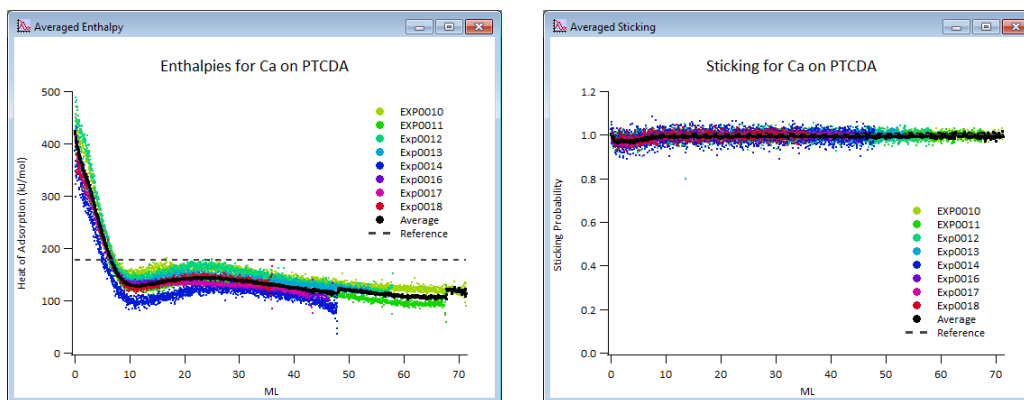
This part is somehow different from the other parts of the program package. It is designed to operate independently from the aforementioned functions. The user interaction is entirely handled by the menu, see Section 3.1.1.

Upon initialization, carried out automatically upon the first function call, the user is prompted for an identifier for the set of experiments.

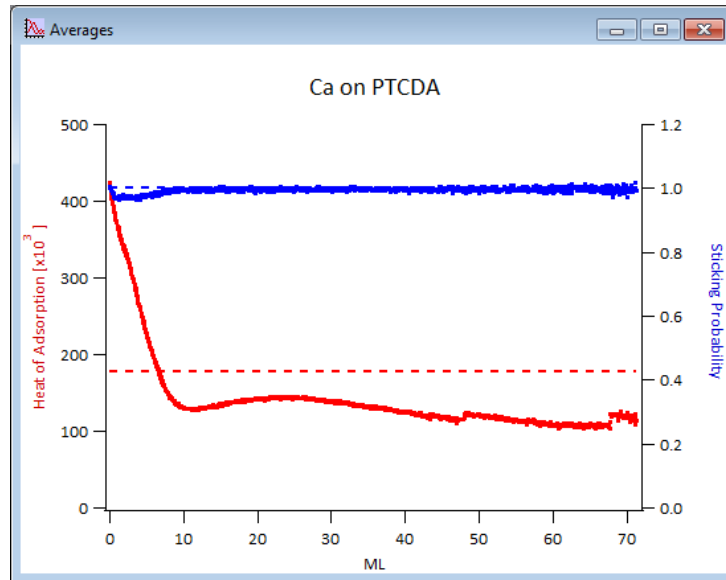


Since this is a string variable, the quotes are essential. The next steps imply loading of the related experiments.

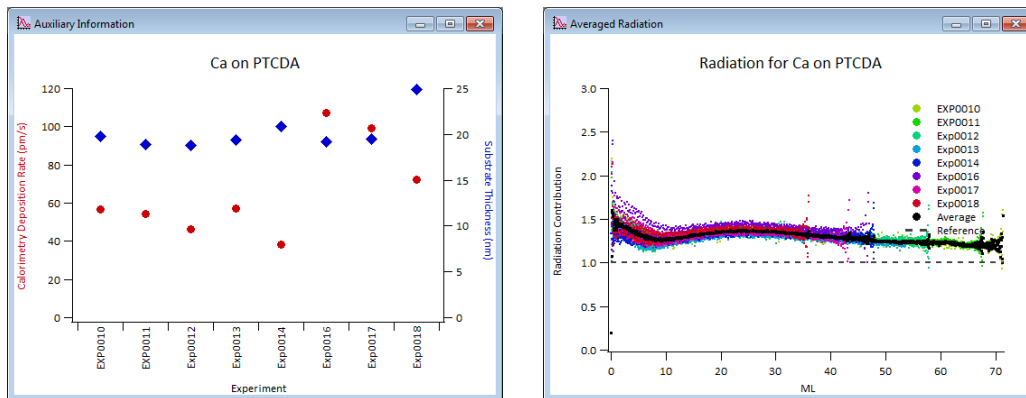
At the beginning of the averaging process an integrity check of the data and a compatibility check of the loaded experiments are performed. Details on the settings and processing can be found in Section 4.2.9. Afterwards, the sticking and enthalpy results of the individual experiments are displayed, providing an option to identify and remove experiments with improper results.



The averaged sticking probabilities and averaged enthalpies are presented in one graph. Abrupt changes in the traces typically originate from a diverging experiment with a smaller coverage range, *i.e.*, a non matching result is suddenly not contributing any more.



Error ranges are not included since the individual errors of the imported experiments can be adjusted by the user by choice of cursor positions, see Section 3.8.3. Auxiliary parameters on the averaged experiments are also visualized as well as the radiation contribution.



In case the automatic processing is enabled, the data is averaged and displayed after each load action. Due to the non-linear relationship of the frame number and the coverage, an analytical determination of the error margins is not possible.

3.12 Lazy Operations

Experienced users can benefit from the routines labeled **Lazy**. Since all related features are based on the standard routines, the data is processed the same way.



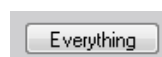
One feature is the automated loading algorithm. In case the file extensions are used properly, the procedure determines which file contains which measurement and loads all files at once.

The processing routine initially processes all deposition rate and reference measurements. If the automatic outliers removal is enabled, the deconvolution of the averaged data is omitted.



In a second step, the corresponding statistics are calculated and the automatic outlier removal is performed for all reference measurements, if desired, see Section 3.7. In this case the reference measurements are processed again, including the statistical analysis to adapt the calculated data to the changed situation concerning the excluded frames. In case of loading a deconvolution reference, the energy input into the calorimetry detector is reconstructed for the averaged frames and displayed, see Section 3.10.

In all cases the statistics are displayed, see Section 3.6, and the heat and sticking measurements are processed, see Section 3.8. If desired, all measurements can be processed by the **Everything** deconvolution routine, see Section 3.10.



Depending on the size of the data sets, the specific settings, and the computer's performance this operation might take several hours.

3.13 Comparison to Previous Approach

As mentioned above, the presented data evaluation procedure follows a different philosophy than other groups^[32]. As a matter of course, both approaches need to be compared. Since identical data is treated with both methods, the experimental conditions are irrelevant here². This chapter has presented the novel method in detail. In the following, the previous method is briefly described.

The former approach utilizes only the initial slope of the signal after the pulse has started. Normalization by means of laser power, pulse length, and sample absorption yields a *sensitivity value* correlating the signal amplitude to the deposited heat. Furthermore, a constant thermal radiation contribution is assumed^[56]. This constitute of the signal is measured through the infrared transparent window, see Section 2.4.4, corrected by the window's transmission, quantified *via* the sensitivity value, and subtracted from the calorimetry result as a number. It should be pointed out that the transmission measurement is performed at non-infrared, *i.e.*, visible, wavelengths³. Thus the measured transmission is potentially differing from the true infrared transmission, see Section 5.8.1, and an incorrect amount of thermal heat might be assumed for the correction. Furthermore, the absorption properties of the sample for thermal radiation must remain constant during deposition of the adsorbate. Regarding the different properties of metals and organic compounds, the assumption of an unchanged infrared absorption is questionable.

The sticking probability is obtained from the integrated mass spectrometer signals considering constant offsets^[56]. This approach requires a low noise signal from the instrument.

As it has been shown in Section 3.5.7 and will be shown in Section 5.7 in detail, the signal from the mass spectrometer is far from noise free in this setup. This observation is echoed in the results from an exemplary sticking measurement, illustrated in Figure 3.18.

The novel approach yields a significantly reduced scatter compared to the traditional one. Furthermore, the general shape is reproduced while the differing amplitude can be attributed to the *unusual* peak shape, see Section 5.7. Hence, the novel data evaluation method should be preferred for analyzing the mass spectrometer data.

Figure 3.19 opposes the results of an exemplary calorimetry experiment processed with the former as well as the novel data evaluation approach. The scatter is

² The sticking data is taken from 'Exp0052' in Figure D.19 and the heat data is taken from 'Exp0026LT' in Figure D.30.

³ At 405 nm in this work and at 633 nm elsewhere^[56].

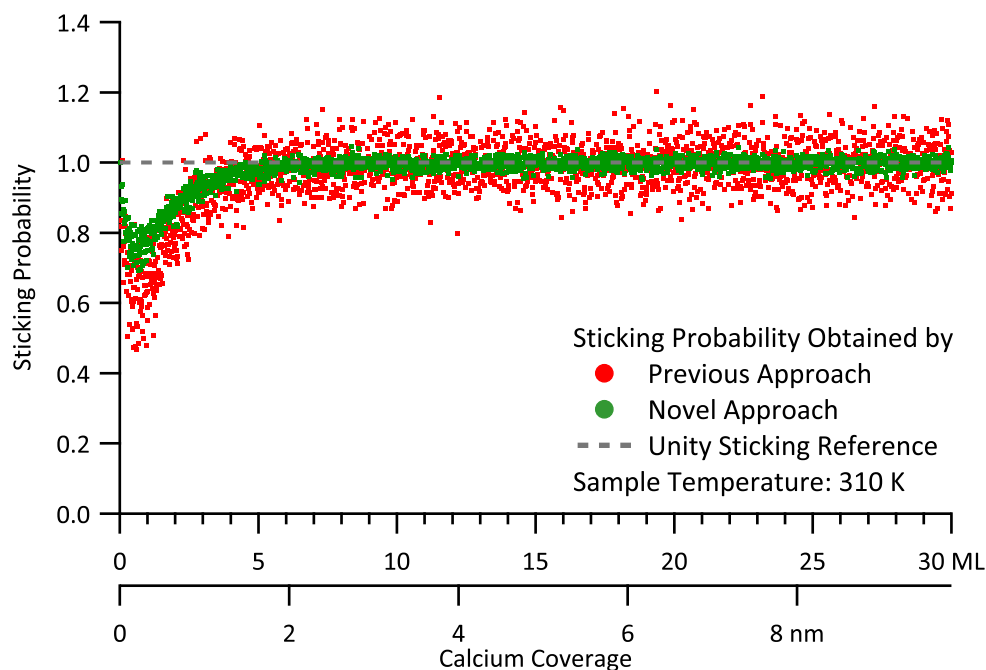


Figure 3.18: Comparison of the Novel and Previous Data Evaluation Approach: Sticking — The results of a sticking measurement for the adsorption of calcium on 300 nm tetraphenyl porphyrin at ambient temperature are given as a function of coverage utilizing the previous (red dots) and novel (green) data evaluation approach. The scatter is significantly reduced utilizing the novel approach.

similar with slight advantages towards the traditional method. This might arise from a combination of effects. The discussed experiment was measured at cryogenic temperatures. The coolant, *i.e.*, liquid nitrogen, causes mechanical vibrations in the detector unit which are picked up by the sensor. As the relevant data range is much smaller⁴ in case of the previous approach, it is less affected by this noise and thus produces less scatter. An improvement of the cooling method, such as blowing cold gas through the thermal reservoir (see Section 2.2) instead of sucking liquid nitrogen into it, could reduce the scatter in the resulting data.

In addition, the absolute heats of adsorption obtained by the previous and novel approaches differ in the entire studied range. Comparison of the heats of adsorption at high metal coverages with the negative heat of sublimation yields excellent agreement in case of the novel approach, see Section 6.5.3. This outcome practically disqualifies the traditional evaluation method.

Close inspection of the results from the novel and the previous method reveals

⁴ By a factor of 20.

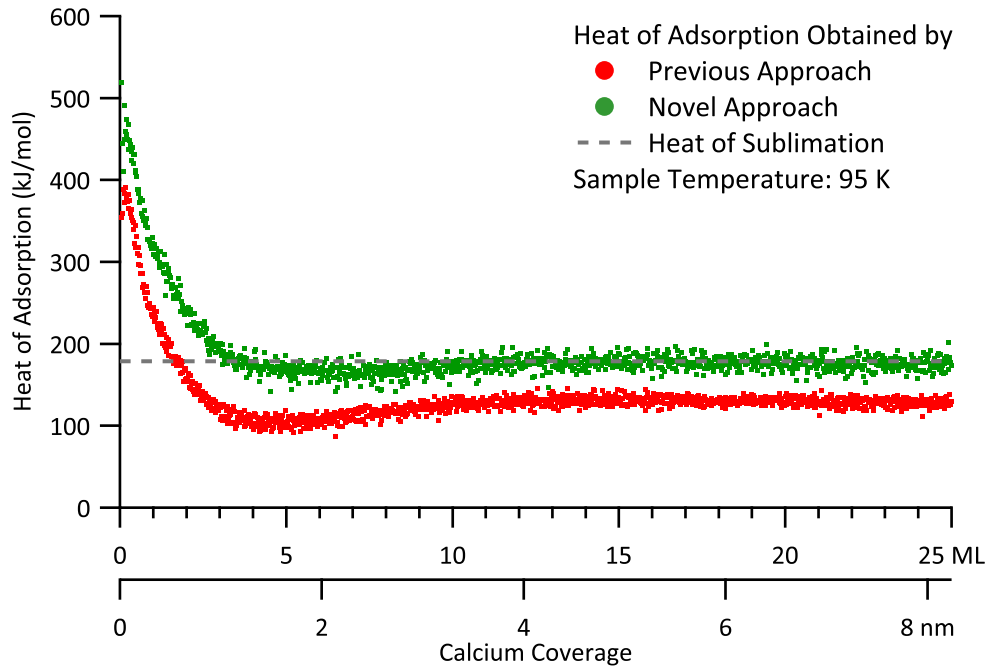


Figure 3.19: Comparison of the Novel and Previous Data Evaluation Approach: Calculated Heat — The results of a calorimetric measurement for the adsorption of calcium on 20 nm PTCDA^a at cryogenic temperature are given as a function of coverage utilizing the previous (red dots) and novel (green) data evaluation approach. The reference enthalpy is matched only in case of the novel approach.

a Perylenetetracarboxylic dianhydride.

that their difference is not only a constant offset but includes some internal structure at calcium coverages between 4 ML and 8 ML. In this range, the data corresponding to the traditional approach exhibits a minimum while the results from the novel approach lack this feature. Such minima can be explained by the Kelvin-effect^[156] and are reported for adsorption of metals on organic substrates^[55,60,61] as well as on inorganic substrates^[16–22,27,33,34,42]. However, this effect takes place at lower metal coverages and is less pronounced in case of organic substrates.

Another possible explanation of the observed minimum might arise from a changing reflectivity, and thus absorption, of the specimen for infrared radiation. Since the layer thicknesses of the substrate and the adsorbed metal (a few ten nanometers) are small compared to the wavelengths of infrared radiation (one to ten micrometers), a systematic prediction utilizing bulk material properties is not possible. However, a change in color of the sample's area exposed to the metal vapor is often visible with the bare eye. This motivates the assumption of a changing infrared absorption.

Figure 3.20 opposes the relative radiation contribution obtained by the novel

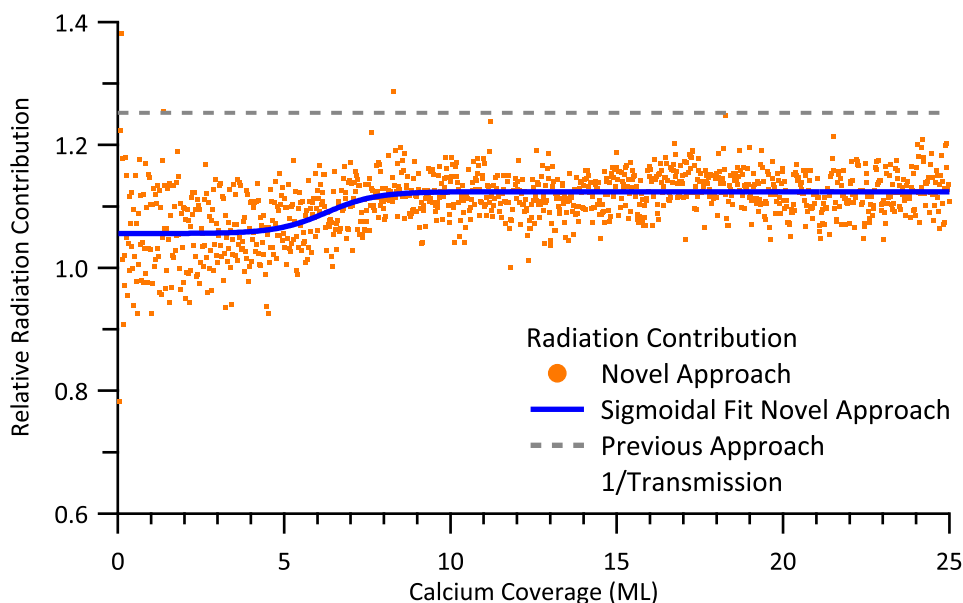


Figure 3.20: Comparison of the Novel and Previous Data Evaluation Approach: Radiation Contribution — The resulting radiation contribution of a calorimetric measurement for the adsorption of calcium on 20 nm PTCDA^a at cryogenic temperature is given as a function of coverage utilizing the previous (gray dashed line) and novel (orange dots) data evaluation approach and a sigmoidal fit of the latter (blue solid line). The novel method results in a lower amount of radiation and is able to detect a change in radiation absorption between 4 ML and 8 ML.

a Perylenetetracarboxylic dianhydride.

evaluation approach to the theoretical value derived from the transmission measurement and used in the previous method. The latter overestimates the radiation contribution in the entire studied range. Using a sigmoidal approximation of the relative radiation contribution obtained by the novel approach, a transition between two surfaces with different infrared reflectivity is directly visible.

Since a smaller radiation contribution implies a larger reaction heat, it is evident that the abovementioned minimum is less pronounced in case of the novel data evaluation approach. Since the novel data evaluation approach only uses the transmission of the window as a starting value⁵ and not as an input parameter, it depends on one – even non constant, and thus error prone – input parameter less.

A tuning of the transmission of the window in order to match the enthalpy of adsorption to the heat of sublimation is possible but requires the sacrifice of the internal standard. Furthermore, this rescue effort requires a stable and perturbation free enthalpy of adsorption for a larger range of higher coverages. Several examples

⁵ A possible documentation of the soiling of the window is also possible.

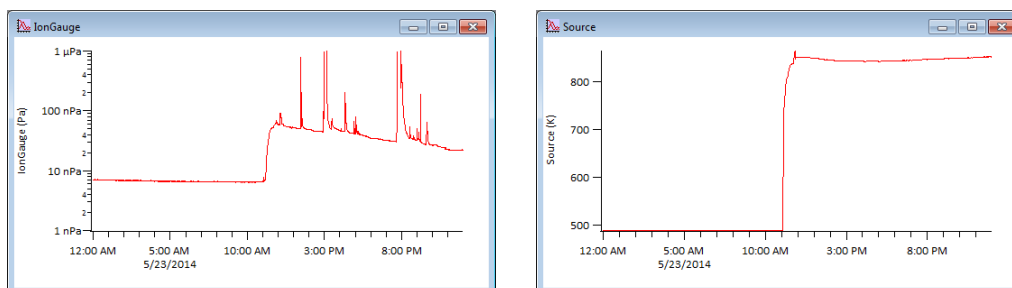
in this work show that this is not necessarily the case, see Sections 6.8 and 6.9. In addition, the change in reflectivity cannot be compensated this way. This would require a different setup involving an online reflectivity monitoring^[87] which is not possible with the present experimental setup.

Altogether, the novel data evaluation approach exceeds the capabilities of the previous method and is able to achieve correct results.

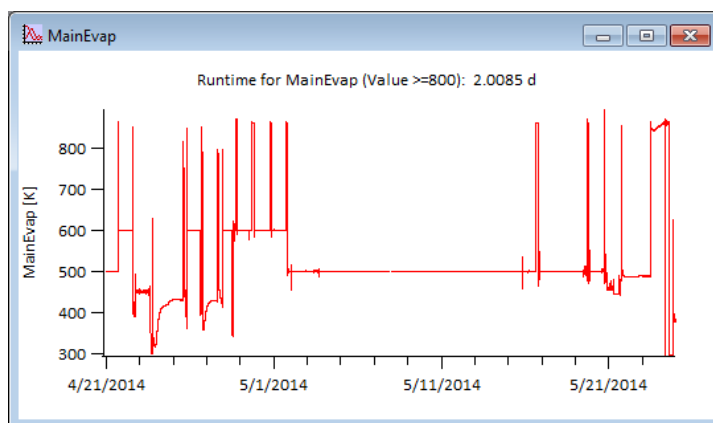
Examples of the individual steps using the previous data evaluation approach can be found in Appendix E.1.

3.14 Status Display

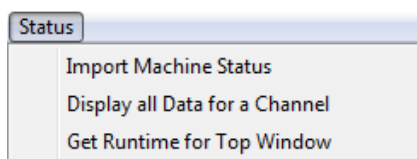
If logging information of the machine is loaded, a standardized display is possible with the Display NAC-Status feature using default labels.



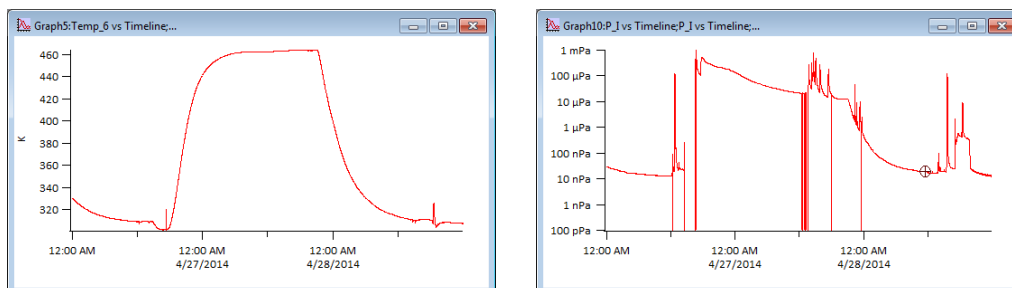
This feature is useful for troubleshooting or to obtain evaporator runtimes from comparison with a user supplied threshold value for a given channel.



Since the runtime determination is also applicable to other experimental setups, it is not located in the NAC menu but in the Status menu.



It is also helpful for documentation of bake-out processes of the system.



Details to the status package are given in Section 4.4.

3.15 Synopsis of the Data Evaluation

The usage of the data treatment program based on IGOR PRO is explained in this chapter along with the evaluation of an exemplary experiment.

Interaction with the menu, the contents and actions of the main panel, and of several user interactive windows has been explained. The load operation and the effects of different filters upon data import have been discussed. Data from the quartz crystal microbalances for sample coating and deposition rate measurements is mostly automatically processed. The processing of the various reference measurements and the derivation of related parameters is explained in detail.

A part of the program package dedicated to statistical analysis also provides an automatic removal of outliers. The fundamental criterion to identify those unreliable data points is motivated.

Treatment of the calorimetric data, comprising heat and sticking measurements, as a function of the reference experiments is illustrated. Further improvement of the scatter in the result is possible by the use of fitted trends.

The reconstruction of the power input into the detector is provided by the deconvolution part of the program package.

Averaging of compatible experiments, together with display of the most important parameters, is included in order to improve the quality of the final results.

Comparison with the previous data evaluation approach used in other groups reveals that the here presented novel approach is superior, since it requires one input parameter less and is able to detect changing infrared absorption of the sample without a dedicated measurement.

Finally, the package is rounded-up by explanation of convenience functions concerning automated data treatment and display of status information related to the experimental setup.

4 Software

This chapter describes the used file formats and presents a global view on the developed IGOR PRO packages. The entire program codes can be found in Appendix C. The packages require IGOR PRO Version 6.3 and are ready¹ for IGOR PRO Version 7. It is recommended to disable the “Debug On Error” feature^[155] since some conditions cause, despite properly handling, a run time error and since it increases computation speed.

The definition *measurements* refers to a single data acquisition run, *e.g.*, a laser reference measurement. The term *experiment* corresponds to a complete set of measurements necessary to compute the coverage dependent heat of adsorption. A set of data points related to a single dose from the beam is called a *frame*. Here, one monolayer is defined as a closed packed layer of the dosed atoms in a specified plane. The typically used plane is the closest packed plane for the most stable phase at room temperature, *i.e.*, the (111) plane for metals with cubic and the (0001) plane for metals with hexagonal crystal structure, *e.g.*, copper and magnesium, respectively. Both structures with their primitive spatial and corresponding planar unit cells are shown in the description of the used materials in Figures 6.1 and 6.2.

This chapter focuses on the explanatory part of the program packages. Examples of the displayed windows and further illustration is given in Chapter 3. Special characters are printed in SMALL CAPITALS and keywords in `typewriter` font. In the PDF version of this document `function names` are bidirectionally linked to the actual program code. One way links to descriptions of lower level functions are printed `without serifs`.

Mandatory parameters are given in parentheses after the function name and optional parameters are enclosed in additional square brackets.

¹ Although it is successfully tested with version 7.00B02, the performance is reduced.

4.1 File Formats

In general there are four types of data files used in a calorimetry project. All types are text based with ANSI encoding and are readily readable for humans. Columns are separated by TAB-characters and ended by a CR LF sequence. The calorimetry and the deposition measurement files contain a file header with general information about the measurement and a column designator including units. The status logging files only contain the latter. In addition to the calorimetry files, auxiliary files are created. These files contain status information relevant for calorimetry measurements with a lower temporal resolution. The measured data is usually single precision floating point. To cover this accuracy the usual amount of seven digits per value is written to the file. None of the data file types contains a specific end-of-file sequence.

For a convenient processing the files for one experiment should start with a fixed string, *e.g.*, 'Exp0042', followed by an incremental part like 'aa', and end with a measurement specific file extension. Except the latter, this is automatically carried out by the LABVIEW programs which are operating the NAC machine and collecting the raw data.

4.1.1 Deposition Files

This file type stores information on the thickness measurements, as parts of the calorimetry experiment. The two main purposes are the deposition rate measurement for calorimetry in the main chamber and the determination of the deposited thickness for sample preparation in the load lock.

- .**flx** This file type contains a deposition rate measurement.
- .**tck** This file type contains a thickness measurement.
- .**qcm** This file type contains a quartz crystal microbalance measurement (QCM) which is not directly related to a calorimetry experiment.

The file header consists of time stamps for **Start** and **End** of the data acquisition. It is followed by a designator for the used **Substance**. For further processing the full name or chemical symbol for elements should be used, *e.g.*, Calcium or Ca. This is especially recommended in the case of deposition rate measurements since this string is used to automatically calculate heat capacities. For organic substances abbreviations are usually used, *e.g.*, '2HTPP' for '5,10,15,20-Tetraphenyl-21*H*,23*H*-porphyrin'. The substance identifier is followed by the Miller index for the exposed lattice plane in parentheses. It also contains information of the assumed surface

structure. ‘Ca(100)’ designates a square pattern of Calcium atoms whereas ‘Ca(111)’ corresponds to a hexagonal arrangement. The **Molar Mass** is given in g/mol . The **ML Atom Density** denotes the number of surface atoms per square meter in the structure given by the Miller index. **ML Thickness** gives the distance in nm between two equivalent lattice planes corresponding to specified growth direction. This value is not used in the calorimetry program but is recalculated from monolayer density, molar mass, and density.

The next section in the header lists several settings of the QCM-controller. The **Density**, given in g/cm^3 and **Z Value**, *i.e.*, the acoustic impedance, given in $10^5 \frac{\text{g}}{\text{s}\cdot\text{cm}^2}$. The **Tooling** factor of the controller is ignored in the program and must be set to unity. The file header is completed by the **Number of Data Points** recorded in the file for integrity checking and a **Notes** section for free text remarks.

In the newest file version, units are also included in the designators in square brackets, *e.g.*, ‘**Molar Mass [g/mol]:**’.

The data section starts with the column label including units. The first column must be labeled **Time**. This keyword ends the notes section and starts the data section. Since the acquisition is software timed, the data points are not necessarily equally spaced. Hence, it is mandatory to record a time stamp. The **Rate** is too small to be used in the calorimetry setup but is recorded for compatibility to other applications. The column **Thickness** contains the thickness as read from the controller including its error correction mechanisms. Corrected errors, *e.g.*, adhered particles on the probe crystal, can be identified by abrupt changes in the **Crystal Frequency**. The temperature of the in the calorimetry software selected thermocouple is stored in the **Temp**-column. The **Pressure** will contain the reading of the pressure gauge in the molecular beam or in the load lock. Since these are not installed at the time of this thesis it usually reads the pressure in the main chamber.

The IGOR PRO software uses the **Time** and **Thickness** columns to calculate the deposition rate for the calorimetry experiment. To be able to distinguish between an unstable deposition rate – which is proportional to the corresponding flux – and a not complete adsorption on the probe crystal in deposition rate measurements, the analogue output of the mass spectrometer (QMS) is also recorded.

4.1.2 Calorimetry Files

This file type stores the signal from the calorimetry probe and the analogue output of the mass spectrometer. All calorimetry files have an identical inner structure. For simplified usage several file extensions are used.

- .dcv This file type contains a laser measurement with deconvolution parameters.
- .cln This file type contains a laser measurement on a clean sample.
- .usd This file type contains a laser measurement on a clean sample whose backside has been used before.
- .cot This file type contains laser measurement on a coated sample.
- .ref This file type contains a laser reference measurement.
- .win This file type contains a laser measurement with the infrared transparent window in front of the sample.
- .rad This file type contains a radiation measurement with the infrared transparent window in front of the sample.
- .cal This file type contains a calorimetry measurement.
- .stk This file type contains a mass spectrometer based measurement, which is not directly related to a calorimetry experiment.
- .las This file type contains a laser measurement, which is not directly related to a calorimetry experiment.

The file header consists of time stamps for **Start** and **End** of the data acquisition. It is followed by the number of acquired pulse pairs used for integrity checking. It differs from the value set in the LABVIEW program by +2. This is due to the fact that the LABVIEW program is using a net pulse counter and the IGOR PRO software is using an absolute counter. The latter includes the baseline pulse pair at the beginning and at the end of the measurement.

The following section contains the set parameters of the experiment. The **Sample Rate** is used to calculate the spacing of the data points. The **Chopper Period** contains the time for a full chopper cycle, *i.e.*, a pulse pair. Hence, the duration of a single frame is half the chopper period and the amount of frames is twice the number of pulse pairs. The dosing time per frame is set by the **Pulse Length** and the temporal position in the frame is given by **Chopper Delay**. The paragraph is completed by status information of the stepper motor controller actuating the chopper and the program used in the controller.

The **Calorimetry Gain** and **QMS Gain** settings are currently ignored and should be set to unity. The **Laser Power** reads the measured power of the laser after being reflected out of the main chamber. In the newest file version, the additional

entry `Laser Set Level` contains the power set to the laser diode and `Reflectivity` provides an interface to import the reflectivity used as the one of a clean sample.

The file header is completed by a user `Notes` section.

In past versions the units were given in parentheses and time values in ‘ms’. The latest file version uses square brackets and SI units without prefix.

The data section contains the column headers, in the newest version with units. The column header is only used for detection of the end of the notes section and the begin of the data part. The column header as well as the data must be in the format `Calorimetry TAB MassSpec...` to ensure correct processing. The notes section must not contain such a text fragment. The IGOR PRO software loads the first two columns expecting the calorimetry data in the first one and the data from the mass spectrometer in the second one.

4.1.3 Auxiliary Files

For each calorimetry measurement file an auxiliary file is created. Each file contains experiment related data with a temporal resolution of a pulse pair.

`.aux` This file type contains additional information to calorimetry files.

The file header is identical with the file header of the measurement file. The column header must start with `Time` to end the notes section. The auxiliary files should contain the `Sample` and `Source` temperature as well as the `Motor_FB`, *i.e.*, motor feed back. The temperatures are used to calculate correction terms. The motor response ‘Y’ is used to detect valid frames in the measurement. It also contains ‘MnS’, *i.e.*, motor not started, at the beginning and end of a measurement, or an error code from the stepper motor controller.

Besides the first column there is no specific order or maximal amount of columns. The names in the header should comply with the IGOR PRO naming syntax². Duplicate identifiers should be avoided.

The import function uses the units given in square brackets. One special case is the unit `TXT` denoting a text column. Other special cases are millibar (`mBar`) and torr (`Torr`) which are converted to Pascals (`Pa`). Degrees Centigrade `C` and Fahrenheit `F` are converted to Kelvin (`K`). These temperature units must lack the degree character, *i.e.*, ‘°’, since it is not compliant with the used standard. Additional legal unit symbols for temperatures are `degC` and `degF`, respectively.

² 31 characters, no blanks, no numeral as first character, ‘_’ is always allowed.

4.1.4 Logging Files

The `StatusLogging` package uses this type to track the long term status of the NAC machine. This feature may also be used for other instruments. Typical applications for this feature are pressure and temperature logging during bake-out of the system or tracking of malfunctions.

`.log` This file type contains additional information on the machine status.

Every day a new file is created and stored in the file name. Three formats for the date are valid, *i.e.*, `DDMMYY`, `YYYYMMDD` and `YYYY-MM-DD`. `DD` denotes the day in two digit notation, *e.g.*, '04'. `MM` and `YY` denote month and year in the same way³. `YYYY` contains the year in four digit representation.

This file type contains no file header. The column header is identical to the one in auxiliary files. Units are also treated like in auxiliary files.

³ `YY` uses the year 2000 as offset.

4.2 NAC Program Package

The basic ideas used in the data treatment process are presented in this chapter. The entire program codes can be found in Appendix C.1. In order to increase the calculation speed for some operations the option for a dynamic base data folder was discarded in the development process of this package.

For syntax and general programming techniques in IGOR PRO the software manual^[155] should be consulted. All public names start with the prefix `NAC_` to avoid interference with other loaded extensions to IGOR PRO. Private, *i.e.*, `Static` functions are only accessible by this software package and are thus lacking a prefix. This readily illustrates the scope of a given function. Since almost all features of the software package are accessible either from the control panel or the menu bar it is neither recommended nor necessary to call functions from the `Command Window`.

All data related to an individual calorimetric experiment is stored in the data folder `root:NAC`. In order to maintain clear arrangement the data is subdivided into common folders containing machine parameters, *e.g.*, the `BeamDiameter`, program settings, *e.g.*, window sizes, experiment parameters, *e.g.*, the `NominalPulseLength`, and data for the enthalpy calculation, *e.g.*, thermodynamical corrections. Additionally, a folder for each measurement holds the specific data, *e.g.*, the `Detector` signal. These folders contain subfolders for the statistical analysis of the experiment and for auxiliary data recorded along the measurement.

Data related to a family of experiments, *e.g.*, calcium adsorbed on a thin layer of perylenetetracarboxylic dianhydride (PTCDA) at ambient temperature, is located in `root:NAC_Average`. The settings are stored in a separate subfolder from the experimental data. The data related to a specific experiment is placed in a subfolder given the name of the underlying IGOR PRO experiment file.

Errors are usually `cleared` upon new user actions. Some functions, only called by top level functions, still lack a detailed integrity check and since errors are usually already caught by the overlying functions their implementation is still pending.

4.2.1 Definitions

Compiler settings, version requirements, pointers to physical data folders, and error messages are defined.

Compiler Settings

The package requires an IGOR PRO version of 6.2 or higher and uses global access method, *i.e.*, all variables, strings, and waves have to be accessed explicitly. It also provides the definition for the menu operating the package.

Constants

Several constant expressions are used in the program package. The string constant `NAC_DataPathStr` points to a default folder containing the calorimetry data and is used when the package is initialized. Since IGOR PRO uses the backslash character as an escape character the path should be given in Macintosh notation with only colons as separators. The current revision of the software is stored in `NAC_Version`.

The constants for the error codes are labeled with plain text and are self explaining. They are partitioned into a group of serious errors that need user interaction and well handled errors which might also occur during normal processing of the data. By default only the first group of errors is reported by the `Error Handling Package` but this behavior can be changed for debugging in the settings in that package, see Section 4.3.

Menu

The menu bar provides less often used features of the package and some control options.

`Initialize` creates the data structure used by the software package. If an experiment is already loaded it will be overwritten in case no user windows have been created.

`Show Control Panel` displays the main window providing access to the most frequently used features and parameters. The assigned default hot key is `Ctrl+1` and might be changed here.

`Data Manipulation` contains methods to manipulate the raw data.

`Remove Detector Baseline` provides a manual way to **remove** a selectable baseline from the detector data set in case the filtering algorithm in the `load` function fails.

Invert Polarity allows to multiply a selectable detector signal by -1 . The data treatment is independent of the polarity of the sample as long as it is consistent in the individual measurements. This option is indented to produce publishable graphics rather than for data treatment.

Correct for Gain is a feature to use old data files recorded with a second amplifier instead of utilizing⁴ the range setting of the measurement setup. It is obsolete for newer data files.

Unload Measurement removes a loaded measurement from the experiment.

Display Statistics shows the result of the statistical analysis of the already analyzed data in form of box plots.

Auto Flag automatically marks outlier frames in all or the selected data set. Marked frames will be subsequently ignored by the data processing procedures. Individual as well as all measurements can be treated with this operation. It is also included in the **Lazy Process** routine for all meas, if the **Auto Flag** option is enabled.

Reset Flag List resets the flag list to the same state as after loading in all or the selected data set.

Copy Flag List conveniently synchronizes the excluded frames in the heat and sticking probability measurements and *vice versa*.

Fitted Trends provides a method to reduce fitting artifacts by overriding fit parameters in the next iteration.

Update Experiment Version adjusts the data structure of old experiment files to the newest software version. Experiment files with a version older than 3.7 cannot be updated.

Concatenate Calorimetry Files combines two calorimetry files including the check relevant parameters.

Trim Calorimetry Files extracts a subset from a calorimetry file including the check relevant parameters.

Settings provides adjustment of the general behavior of the program.

Auto Flagging set to enabled alters the behavior of the **Lazy Process** routine. With this option it automatically masks outlier frames and performs an additional process cycle before the heat and sticking probability measurements are processed. It is enabled by default.

⁴ See LABVIEW control program by H. ZHOU.

Load Supporting Files switches from loading the default experiment data files to the supplementary files usually used for characterization and testing if this option is enabled. It is disabled by default.

Store Filter Residue Waves keeps the residue from the Fourier filtering in the load function if enabled. This option provides a way to inspect the details of the baseline removed by the filtering. Since it is not necessary for data treatment and consumes a rather large amount of memory it is disabled by default.

Automatically Recalculate Averaged Experiments defines if newly added experiments are automatically included in the calculation of the averaged sticking probability, coverage and enthalpy. Since the calculation becomes slow for many large data sets it is disabled by default.

Show Data Points in Box Plots defines if regular data points are displayed in the statistical box plot.

Average Experiments comprises the controls of the subsystem utilized to average individual experiments with the same parameters.

Load Results loads the relevant data from a calorimetry experiment file. The assigned default hot key is **Ctrl+2** and might be changed here.

Average Loaded Experiments averages the data in the loaded calorimetry experiments.

Remove Loaded Experiment deletes the data from a previously loaded calorimetry experiment.

Display Averaged Results creates the graphs related to the averaged data.

Display NAC-Status extends the **Status Package** and provides a tailored display of the status of the NAC machine.

4.2.2 Initialization

This part contains the initialization routines for the package. Old data is deleted, the data structure is created, the machine specific parameters are set to their standard values, and the control panel is displayed.

NAC_Initialize()

This function (re-)initializes the NAC program package. It sets the default location of the stored data and initializes the Error packages.

If the software was already initialized the standard windows are closed and the dependencies are lifted in order to be able to delete the data folder containing all data corresponding to the calorimetry application. If this fails an error is reported.

Subsequently, the data structure, dependencies, and the control panels⁵ are created.

Variables()

This function initializes all variables and waves used in the program arranged by the parent data folder. Relevant standard values are given in parentheses and are used without the given unit.

:GUI: This data folder contains all variables concerning the graphical user interface.

`WWidth(400), WHeight(300), MarginTop(45)`

are dimensions used to display data windows.

`ReEntryFlagWin(0), ReEntryCursor(0), ReEntryPosProc(0)`

prevent a reentry of *WinHook* functions.

`ProgressValue` is used to indicate the progress for batch fitting procedures.

`PositiveRange, NegativeRange` is used to synchronize signal axis ranges for calorimetry graphs.

`PositiveRangeSticking, NegativeRangeSticking`

is used to synchronize signal axis ranges for mass spectrometer graphs.

`RangeDeconvolution` is used to synchronize power axis ranges for deconvolution graphs.

`LoadSupportFiles(0)` defines if standard experiment files of supplementary files are suggested.

`StoreFilteredWaves(0)` defines if residual waves from filtering are stored in the experiment.

`ShowBoxPlotData(1)` defines if regular data points are shown in box plots.

`PositiveName(""), NegativeName("")`

holds the name of the calorimetry measurement which is defining the range settings.

⁵ Additional panels are intended to be used in future versions capable of handling data acquisition and machine control.

`PositiveNameSticking("")`, `NegativeNameSticking("")`

holds the name of the sticking probability measurement which is defining the range settings.

`NameRangeDeconvolution` holds the name of the deconvoluted measurement which is defining the range settings.

`StatsLabelPos` provides positions for the labels in the statistics plot.

`StatsLabels` provides labels for the labels in the statistics plot.

:Machine: This data folder contains all variables concerning the parameters related to the experimental setup. Important standard values are given with the property.

`LaserPowerCorrectionList` stores the possible values used to correct the laser power measured outside the chamber to obtain the laser power on the sample, see Section 5.8.3. It provides a convenient way to adjust this parameter to older experiments. Entries must be separated by semicolons.

`ReflectivityCleanList` stores reflectivities of frequently used clean samples, see Section 5.1. In case of a labeled entry the numeric value has to be followed by a blank and the describing text, *e.g.*, "0.444 Ni/PVDF;". Each entry must be followed by a semicolon.

`LaserPowerCorrection()` provides the value used in the program to correct the laser power measured. The standard value is the first entry of `LaserPowerCorrectionList`.

`ReflectivityClean()` contains an average value of the reflectivity of a pristine sample measured outside the vacuum chamber, see Section 5.1. It is passed on to uninitialized reflectivities. The standard value is the first entry of `ReflectivityCleanList`.

`BeamDiameter(0.0045 m)` contains the diameter of the beam defining orifice, see Section B.1.5.

`QCMDiameter(0.006 m)` provides the diameter of the back electrode of the used QCM oscillator crystal.

`QCMToolingCalorimetry(1.09042)`

provides the value used to correct the deposition rate measured with the quartz crystal microbalance in the ancillaries stage to obtain the artifact free value, see Section 5.8.2.

`QCMToolingCoating(0.604)` provides the value used to estimate the thickness of the substrate layer prepared in the load lock, see Section 5.4.4.

`QMSToolingCalorimetry(0.959158)`

provides the value used to correct the intensity of the reference mass spectrometer signal measured with the hot plate in the ancillaries stage, see Section 5.8.4.

`RateFittingWindow(60 pnts)` defines the interval in data points used to calculate the temporal evolution of the deposition rate in a deposition measurement. Smaller numbers give higher temporal resolution on expense of higher noise.

`DeconvolutionWindow(0.012 s)` defines the time window the deconvolution routine is allowed to see to predict the posterior signal shape. Smaller numbers give higher temporal resolution at expense of higher noise.

`PulseLengthDetectionWindow(0.1 s)`

provides a parameter used in pulse length detection, see Section 3.5.4.

`HighpassFrequency(0.175 Hz)` defines the low pass cut off frequency for data filtering used to remove the transient oscillation at the beginning of the data, see Section 3.3.

`LineNotchFrequency(50 Hz)` defines the center frequency of a 1 Hz wide notch filter used to remove picked up power line noise.

`SecondNotchFrequency(0 Hz)` defines the center frequency of a 2 Hz wide additional notch filter used to remove setup specific noise.

`NyquistFrequency(500 Hz)` defines the low pass cut off frequency for data filtering and is used to down sample data acquired with a higher rate.

`ProcessRate` defines the spacing of the data points of the calorimetry data independent from the sample rate during acquisition and is twice the `NyquistFrequency`.

`TrimTrendRange(5)` defines the number of frames at the beginning and at the end of a data set which are ignored during the creation of a trend, see Section 3.9.

:Enthalpies: This data folder contains and accepts the metadata, *e.g.*, fit waves and results, of the calorimetry experiment.

`MultiLayerPosLow(NaN)`, `MultiLayerPosHigh(NaN)`

store the cursor positions used for the interval to calculate the average adsorption enthalpy.

`MultiLayerEnthalpy` stores the calculated average adsorption enthalpy in joules per mole considering the interval set by the cursors.

MultiLayerEnthalpyError stores the calculated standard deviation of the adsorption enthalpy in joules per mole considering the interval set by the cursors.

SubtractAdsorbed(*NaN*), **SubtractDesorbed(*NaN*)**

store the automatically computed thermodynamical corrections in joules per mole.

MultiLayerReference stores the calculated sublimation enthalpy at the sample temperature as internal reference value in joules per mole.

ThicknessRange is used to create the secondary axis in meters for the properties plotted versus a coverage in addition to the axis in monolayers.

StickingLimit(1) provides a guide to the eye for an upper limit of the sticking probability.

Coverage contains the coverage in monolayers determined from the calorimetry deposition rate and sticking probability measurements as a function of pulse number.

Enthalpy contains the final result of a calorimetry experiment as a function of pulse number.

Sticking contains the sticking probability as a function of pulse number.

Thickness contains the coverage converted to meters.

:Experiment: This data folder contains the global parameters of an individual calorimetry experiment.

ProjectVersion(NAC_Version) stores the version information of the software package upon initialization.

ExperimentName contains an identifier of the experiment.

SampleRate stores the sample rate in hertz used to acquire the data.

DataPointsPerFrame stores number of data points in a frame of the acquired data.

OpenCloseSteps stores the number of steps used by the stepper motor of the chopper.

ChopperPeriod, **ChopperDelay**, **NominalPulseLength**

contain parameters in seconds used to define the pulse shape to generate the pulses.

PulseLength represents the determined experimental pulse length in seconds, see Section 3.5.4.

`LengthDetectFailed` indicates that the automatic algorithm to detect the experimental pulse length has failed and the nominal pulse length is used instead.

`TemperatureSample(NaN)`, `TemperatureSource(NaN)`

contain the average temperatures of the sample and of the source from a heat measurement.

`AutoFlag`, `AutoFlagged` indicate if outlier frames are and have been automatically detected.

`UseFittedRadiation(0)`, `UseFittedDesorption(0)`

determine if the trends approximating the evolution of the fit coefficient are used, see Section 3.9.

`MirrorContamination(1)` provides a temporary, multiplicative correction factor in case of a contamination of the mirror in the ancillaries stage.

`SwitchDeadTime(0 s)` is implemented to mask the range in a frame disturbed if a resettable amplifier is implemented in the setup. This parameter is intended for future use only.

`UseEmptyCrucibleReference(0)` defines whether a reference obtained from an empty evaporator crucible is to be used to calculate the radiation contribution, see Section 5.8.1.

`EmptyCrucibleTemperature(NaN)` stores the crucible temperature of the radiation reference obtained from an empty evaporator.

:CalorimetryMeasurements: Each of these data folders contains the variables related to calorimetric measurements, see Section 4.1.2. It also contains a data folder for auxiliary data. Measurement specific variables are described later.

`Header("Not Loaded")` contains the file header of a loaded data file line by line.

`FileName("Not Loaded")` contains the file name of a loaded data file.

`Loaded(0)` indicates if a data file is loaded for this type of measurement.

`DisplayRaw`, `DisplayFit` store data used to display individual frames of raw and processed data.

`FlagList` stores information if frames are marked for exclusion in further data processing.

`NumberOfFrames`, `EffectiveFrames`

store the total amount of recorded frames and the amount of frames qualifying for data treatment.

`CurrentFrame(0)` provides the number of the currently displayed frame.

`BrowseDeconvolutionIndex(0)` provides the number of the currently displayed deconvoluted frame.

`:Statistics:` This data folder contains the statistical analysis of a data set corresponding to a reference measurement, see Section 3.6.

`Amplitude` contains the amplitude of a frame with respect to the average of the measurement.

`Position` contains a position index for box plots.

`Medians(NaN)` contain the median of the amplitudes.

`Quartiles(NaN)` contain the upper and lower quartiles of the amplitudes.

`Whiskers(NaN)` contain the value of the smallest respectively largest amplitude within the whisker limits.

`WhiskerLimits(NaN)` contains the whisker limits.

`AutoFlagged(0)` indicates if automatic frame selection has been performed.

`StdDev(NaN)` contains the standard deviation of the amplitudes.

`ChiSq` reports a relative measure for the quality of the fit to the corresponding frame. Negative values encode the, actually positive, error code arising from a fit error.

`Outlier` contains the amplitudes of a frame in case it exceeds the whisker limits and `NaN` otherwise.

`:RateMeasurements:` Each of these data folders contain the variables related to thickness measurements, see Section 4.1.1. It also contains a data folder for auxiliary data.

`Header("Not Loaded")` contains the file header of a loaded data file line by line.

`FileName("Not Loaded")` contains the file name of a loaded data file.

`Loaded(0)` indicates if a data file is loaded for this type of measurement.

`Substance("")` contains the identifier of the deposited substance including a designator for the assumed growth direction.

`SubstanceName("")` contains the plain text name of the deposited substance.

`FittedRateAvg`, `FittedRateErrorPos`, `FittedRateErrorNeg` contain the averaged deposition rate and the corresponding error bands in meters per second.

`BaselineTo`, `BaselineFrom` define the range for deposition.

`UseBaseline` switches base line correction on or off.

`DepositionRate(0)` provides the measured deposition rate including base line correction if applicable in meters per second.

`BaselineBefore(0)`, `ApparentRate(0)`, `BaselineAfter(0)`
store the results of the linear regressions of the three sections in the thickness measurements in meters per second.

`TotalThickness(0)`, `ThicknessMonoLayers(0)`
contain the complete thickness including corrections if applicable in meters and monolayers.

`Duration(0)` provides the duration of a deposition in seconds.

`Density` provides the density of the deposited substance in grams per cubic centimeter.

`MolarMass` provides the molar mass of the deposited substance in grams per mole.

`MonolayerDensity` provides the monolayer density of the deposited substance in atoms per square meter.

`FittedFrom(NaN)`, `FittedTo(NaN)` define the range applying to the statistical analysis on the processed deposition rate.

`FittedAvg(NaN)`, `FittedSDev(NaN)` contain the average and standard deviation of the processed deposition rate.

:Deconvolution: This section describes variables unique to the deconvolution measurement in addition to the above mentioned variables and waves. Since frame and pulse parameters are different in this measurement additional variables are stored in this folder.

`Reflectivity` contains the reflectivity of the sample during the deconvolution measurement.

`LaserPower` contains the laser power used in the deconvolution measurement.

`SampleRate` stores the sample rate in hertz used to acquire the data.

`DataPointsPerFrame` stores number of data points in a frame of the acquired data.

`OpenCloseSteps` stores the number of steps used by the stepper motor of the chopper.

`ChopperPeriod`, `ChopperDelay`, `NominalPulseLength`
contain parameters in seconds used to define the pulse shape to generate the pulses.

`PulseLength` is synchronized with the nominal pulse length.

`AverageFrames(1)` determines the amount of frames of the same parity to be averaged during a deconvolution of the whole data set. This option is intended to improve the noise level or to save time in case of a preliminary data treatment.

`RemoveFixedRadiation`, `RemoveFittedRadiation`

define the handling of the radiation component if a heat measurement is deconvoluted, see Section 3.10.

`UseFittedFitWave(1)` defines whether a noise free function fitted to measured data or the actual data should be used for deconvolution.

`Sensitivity(1)` contains a value for the relative sensitivity change upon a temperature change of the detector.

`UseSensitivity(1)` defines if the calculated sensitivity value is used. It should be switched to zero if the deconvolution measurement is performed at the same detector temperature as during the heat measurement, see Section 5.9.4.

`SwitchDeadTime(0 s)` is implemented to mask the perturbed range of a frame in case a resettable amplifier is implemented in the setup. This parameter is intended for future use only.

`:BeforeCoating`: This section describes variables unique to the before deposition measurement.

`Reflectivity` contains the reflectivity of the pristine sample.

`LaserPower` contains the laser power used in the measurement.

`:AfterCoating`: This section describes variables unique to the after deposition measurement.

`Reflectivity(NaN)` contains the calculated reflectivity of the coated sample.

`LaserPower` contains the laser power used in the measurement.

`:LaserReference`: This section describes variables unique to the laser reference measurement.

`Reflectivity` contains the reflectivity of the sample.

`LaserPower` contains the laser power used in the measurement.

`:Transmission`: This section describes variables unique to the transmission reference measurement.

`Reflectivity` contains the reflectivity of the sample.

`LaserPower` contains the laser power used in the measurement.

:Heat: This section describes variables and waves unique to the heat measurement.

`InitOffset(0)`, `InitAdsorption(1e-6)`, `InitRadiation(1)`

provide initial coefficients for the fitting procedure for the offset, adsorption, *i.e.*, laser like, and radiation contribution.

`InitAdsorptionShift(0)`, `InitRadiationShift(0)`

provide initial coefficients for shifts in the pulse position for the adsorption, *i.e.*, laser like, and radiation contribution.

`HoldOffset(0)`, `HoldAdsorption(0)`, `HoldRadiation(0)`

define if the initial coefficients should be held at their given values, *e.g.*, if a constant radiation contribution is assumed.

`HoldAdsorptionShift(1)`, `HoldRadiationShift(1)`

define if the pulse position for the adsorption, *i.e.*, laser like, and radiation contribution is allowed to change or held at the given value.

`LinkShifts(1)` defines whether the shifts of the radiation and heat contributions to the fit result experience identical shifts or are independent.

`Offset` contains the contribution of the offset to the corresponding frame obtained by fitting.

`Adsorption` contains the contribution of the adsorption to the corresponding frame obtained by fitting in joules.

`Radiation` contains the amount of the radiation to the corresponding frame obtained by fitting relative to the averaged radiation measurement.

`ShiftAds`, `ShiftRad` report the time shifts of the pulse components to the corresponding frame and are obtained by fitting.

`ChiSq` reports a relative measure for the quality of the fit to the corresponding frame. Negative values encode the, actually positive, error code arising from a fit error.

`fit_Radiation` contains a fitted evolution of the radiation component which might be used to reduce scatter, see Section 3.9.

`orig_Radiation` contains a copy of the original radiation contribution in case trends are used in the fitting routine.

:Sticking: This section describes variables and waves unique to the sticking probability measurement.

`InitOffset(0)`, `InitDesorption(0.5)`

provide initial coefficients for the fitting procedure for the offset and sticking contribution.

`InitShift(0)` provides an initial coefficient for the shifts in the pulse position for the sticking contribution.

`HoldOffset(0)`, `HoldDesorption(0)`, `HoldShift(1)`

define if the initial coefficients should be held at their given values.

`Offset` contains the contribution of the offset to the corresponding frame obtained by fitting.

`Desorption` contains the amplitude of the mass spectrometer signal which is proportional to the not-adsorbed, *i.e.*, desorbed, molecules.

`Shift` reports the time shift of the pulse components to the corresponding frame and are obtained by fitting.

`ChiSq` reports a relative measure for the quality of the fit to the corresponding frame. Negative values encode the, actually positive, error code arising from a fit error.

`fit_Desorption` contains a fitted evolution of the desorption component which might be used to reduce scatter, see Section 3.9.

`orig_Desorption` contains a copy of the original desorption contribution in case trends are used in the fitting routine.

`StickingLimit(1)` provides a guide to the eye for an upper limit of the sticking probability.

:RateCoating: This section describes variables unique to the coating measurement.

`UseTotalRange(1)` defines, whether the beginning and end thickness in a data set should be used to calculate the deposited thickness, or the range between the set cursors.

:RateCalorimetry: This section describes variables unique to the calorimetry deposition rate measurement.

`DosePerPulse(0)`, `MoleDosePerPulse(0)`

provide the amount of the dosed substance in monolayers per pulse and moles⁶ per pulse, respectively.

`RateMonoLayer(0)` provide the deposition rate of the dosed substance in monolayers per second.

Finally, the scaling of the waves is set and the calculation of the auxiliary Debye integral is initiated.

⁶ The unit, not the members of the *Talpidae* family.

Dependencies()

Several values are automatically calculated using the IGOR PRO feature of dependent objects^[155] which are updated whenever an object in the dependency relation is modified.

`:Machine:ProcessRate` is a machine parameter defined as twice the Nyquist cutoff frequency.

`:BeforeDeposition:Reflectivity` contains the machine parameter for the reflectivity of a clean sample.

`:Deconvolution:Reflectivity` contains the machine parameter for the reflectivity of a clean sample.

`:Deconvolution:PulseLength` is linked to the nominal pulse length of the deconvolution measurement.

`:RateCalorimetry:DepositionRate` contains the deposition rate of a calorimetry experiment in meters per second and is corrected by the baselines if applicable.

`:RateCalorimetry:RateMonoLayer` contains the deposition rate of a calorimetry experiment in monolayers per signal and is calculated from the deposition rate in meters per second, the density of the substance, molar mass of the substance, and the insinuated monolayer density used for illustration.

`:RateCalorimetry:DosePerPulse` contains the dose in monolayers per pulse calculated from the deposition rate in monolayer per second and the pulse length used for illustration.

`:RateCalorimetry:MoleDosePerPulse` contains the dose in moles per pulse calculated from the deposition rate in meters per second, the pulse length, the density of the substance, molar mass of the substance, and the diameter of the beam. This is one relevant quantity for the enthalpy calculation.

`:RateCoating:Duration` represents the duration of coating the sample in seconds defined by the positions of the corresponding cursors.

`:RateCoating:DepositionRate` contains the deposition rate of a coating procedure in meters per second and is corrected by the baselines, if applicable.

`:RateCoating:TotalThickness` contains the thickness of the deposited substrate according to the set calculation method and is corrected for geometrical aspects.

- `:Enthalpies:SubtractAdsorbed` represents the thermodynamical correction for adsorbed molecules.
- `:Enthalpies:SubtractDesorbed` represents the thermodynamical correction for repelled molecules.
- `:Enthalpies:MultiLayerEnthalpy` contains the average enthalpy in the range given by cursors, usually set at high coverages.
- `:Enthalpies:MultiLayerReferenceError` contains the standard deviation of the multilayer enthalpy value in the range given by cursors.
- `:Enthalpies:MultiLayerReference` contains the theoretical enthalpy value the dosed substance deposited on itself and can be used as an internal standard to the experiment.
- `:Enthalpies:Thickness` contains the conversion of the coverage in monolayers into meters.
- `:Calorimetry Measurement:EffectiveFrames` contain the amount of qualified frames for each calorimetric measurement and is calculated from the marking `FlagList`.

CreateDebyeIntegral()

An auxiliary wave used in the calculation for heat capacities from Debye temperatures is prepared in this function to speed up calculations in other parts of the software. This method is used in case of absent tabulated heat capacities and the employed relation corresponds to the third Debye function.

KillDependencies()

Since IGOR PRO does not allow to kill waves which are a part of a dependency these dependencies need to be lifted. This task is executed in this function.

4.2.3 Graphical User Interface

This section gathers all functions related to the user interface including input, output, and graphing. Most functions carrying the string “Display” in their name check if the window corresponding to the measurement already exists. In that case the function brings the window to the front, update axes, and gets terminated. The

descriptions in these sections assume that the applying window has not been created yet.

NAC_RemoveNAC()

In case the package is initialized, the user is prompted whether the data inside the NAC data folder should be deleted. Upon confirmation, the related windows are closed, the dependencies are revoked, and the data folder is removed.

NAC_Unload()

After determination of the loaded measurement files, a user prompt is displayed to select the measurement about to be removed. Subsequently, the data structure of the chosen measurement is reset.

NAC_CorrectGain()

After determination of the loaded measurement files a user prompt to select the measurement and to enter the used gain is displayed. Upon validation the `Detector` data of the selected measurement is divided by the provided gain.

NAC_MenuAutoFlag()

This string function returns the text displayed as the `Auto Flag` menu item. It adds a preceding format character, if the package is not initialized to disable the menu item, or if the function is activated to signalize whether the auto flagging feature is enabled.

NAC_MenuLoadSupport()

This string function returns the text displayed as the `Load Supporting Files` menu item. It adds a preceding format character, if the package is not initialized to disable the menu item, or if the function is activated to signalize whether default files or supporting files are displayed in the file open dialogue.

NAC_MenuStoreFiltered()

This string function returns the text displayed as the `Store Filter Residue Waves` menu item. It adds a preceding format character, if the package is not initialized to disable the menu item, or if the function is activated to signalize whether the residual waves from filtering are calculated and stored.

NAC_MenuAutoUpdateAverages()

This string function returns the text displayed as the **Automatically Recalculate Averaged Experiments** menu item. It adds a preceding format character, if the package is not initialized to disable the menu item, or if the function is activated to indicate whether added experimental results are processed automatically by the averaging subsystem.

NAC_MenuShowBoxPlotData()

This string function returns the text displayed as the **Show Data Points in Box Plots** menu item. It adds a preceding format character, if the package is not initialized to disable the menu item, or if the function is activated to indicate whether regular data points are displayed in the statistical box plot.

SetDeconvolutionGraphRanges(Name, Type)

In order to be able to visually compare the results of the deconvolution the power axis, *i.e.*, ordinate, is synchronized to the same range in all deconvolution windows, *i.e.*, with a name ending by **Deconv**, **BrowseDeconv**, and **AvgDeconv**, by this function.

After checking, if the function is applicable to the measurement given by **Name**, the relevant trace determined by **Type** is assigned. From this data temporary rounded boundaries are calculated symmetric to zero. If the measurement was defining before or the new ranges are larger than the old limits, the ranges are updated. Finally, the ordinates or color scales are set to the new ranges in all corresponding windows.

SetGraphRanges(Name, ProcessWave)

In order to be able to visually compare the intensity of the measured data, the signal axis, *i.e.*, ordinate, is synchronized to the same range in all windows related to measured data, *i.e.*, with a name ending by **Full**, **Flag**, **Frames**, and **Avg**, by this function. Windows for calorimetry data and mass spectrometer data are treated in two individual subsets.

After checking, if the function is applicable to the measurement given by **Name**, the relevant trace determined by **ProcessWave** or by default the **Detector** signal is assigned. From this data temporary rounded boundaries are calculated for positive and negative values. If the measurement was defining or if the absolute value of a new range is larger than the absolute value of the corresponding old limit, the ranges are updated. Finally, the ordinates are set to the new ranges in all applicable windows.

DisplayTrend(Name, ShowTrend)

As a possible way of reducing the scatter in the ultimately calculated heat of adsorption data the contributions of the sticking probability measurement and the portion of infrared radiation in the heat signal can each be substituted by a trend line, see Section 3.9. This function displays the original data and, if requested by **ShowTrend**, the corresponding substitute.

During a check, if the function is applicable to the measurement given by **Name**, the waves for original and approximated data are assigned. The two data sets are displayed, the traces are colored and the axes labeled. The trace for the trend is shown according to **ShowTrend** in both cases.

DisplayFittedRate(Name)

This function displays the **piecewise fitted** thickness change of data from the quartz crystal microbalance for visual inspection of the evolution of the deposition rate.

First, it is checked whether the function is applicable to the measurement given by **Name**. The fitted deposition rate and an indicator for an average are displayed and colored. The average is calculated between two cursors added at the same positions used to mark the end and beginning of the base line sections in a calorimetry deposition rate measurement. Finally, the text box with detailed information and the traces for the average with error intervals are **created** and an **action function** responding to changes of the cursors' positions is installed.

DisplayVsCoverage(Name)

The intention of this function is to display the sticking probability or the measured heat against the coverage of the adsorbed material. Additionally, it provides two cursors defining a range used to calculate an average heat in the latter case.

Initially, it is checked whether the function is applicable to the measurement given by **Name**. The result related to the kind of data is displayed together with a trace for unity, *i.e.*, total, sticking or for the averaged heat. Subsequently, the traces are colored and the ordinate is labeled. In case of the measured sticking a text box with details is displayed. In case of the measured heat, an action function responding to changes in cursors' positions is installed. This function creates and updates a text box with details. Further on, the cursors defining the range to average the heat are added. Finally, the coverage ranges are **synchronized**, an additional axis displaying the thickness in meters rather than monolayers is added, and the abscissas are labeled.

SetRangesCoverage(Name)

This function provides a mechanism to adjust the axis ranges for the results of the sticking probability and heat calculation displayed versus the coverage of the adsorbed material.

If the window corresponding to the data set specified by **Name** exists, the ranges of the ordinates are calculated and set.

DisplayVsPulse(Name)

The intention of this function is to display the sticking probability or the components of the measured heat, *i.e.*, the radiation and adsorption related part, as a function of the running number of the acquired frame which is proportional to the dose.

During a test, if the measurement given by **Name** is applicable, the individual axis labels and derived measurements, *i.e.*, **Adsorption** and **Radiation** respectively **Desorption**, are assigned. If no data was processed, the function quits. Subsequently, the results are displayed, colored, information text is added, and the axes are labeled. In case of the **Desorption** intensity an indication for the theoretical maximum, *i.e.*, one, is added and the ordinate is adjusted to the range of the data.

DisplayNonFlagged(Name)

This function displays all acquired frames of a measurement specified by **Name** on top of each other to identify and select disturbed frames.

After checking, if the measurement is applicable and loaded, experimental parameters are assigned and the window is created. Subsequently, all measured frames are added, colored according to their parity, and hidden if removed from data processing. An action function responding to the also added cursor is installed providing a convenient way to select disturbed frames by visual inspection. A text box with information rounds up this feature.

CheckButtons(Name, WName)

After a test, if the window given by **WName** is valid, the navigation buttons are enabled or disabled according to the position of the currently displayed frame in the data set specified by **Name**. The appearance of the button, used to mark frames as excluded from processing, is also controlled by this function.

DisplayFlagWindow(Name)

This function displays the currently selected frame for a measurement specified by **Name** together with the average frame correlated with the measurement or the result of the fitting routine. This provides a method to identify deviations of the calculation to the measurement and to decide whether the specific frame is used for a (re-)calculation.

At the beginning, the function tests whether the data related to the measurement given by **Name** is loaded. Fixed display waves for raw and fitted respectively averaged data are displayed together with buttons to navigate through the data set. The data corresponding to the currently displayed frame are assigned to these display waves when the windows get updated.

UpdateFlagWin(Name)

The window, related to the frame selection procedure for a measurement specified by **Name**, is updated by this function including reassignment of data, coloring, and updating of informational text boxes.

This function prevents infinite loops due to invoking itself, if it has already been called, by a forced exit. The raw data corresponding to the current frame of the measurement and the corresponding averages, if already calculated, are assigned to their display waves for the reference measurements. In case of the sticking and heat measurements the result of the corresponding fit is displayed instead of the average, if it has been calculated. In case data is not available, the display wave is transparent. Subsequently, the navigation buttons are updated. Coloring of the traces also extends to the displays of the full data, *i.e.*, stacked and linear, if they are already displayed.

KillWins(Name)

All windows related to the measurement given by **Name** are closed.

DisplayAverage(Name)

The averages for both parities of the qualified frames of a measurement stated by **Name** are displayed by this function in case the averages have previously been calculated. The traces are colored, the axes are labeled, and an information text box is added.

DisplayDeconvolutedAverage(Name)

The deconvolutions of the averages for both parities of the qualified frames of a measurement stated by **Name** are displayed by this function if they have previously been calculated. The traces are colored, the axes are labeled and their ranges **adjusted**, and an information text box is added.

DisplayDeconvolution(Name)

The deconvolution of a measurement stated by **Name** is displayed by this function as a color coded image if the deconvolution was performed before. The image is color coded. A color map is added and labeled together with the other axes. All ranges are **adjusted** and an information text box is added. A cursor controlling an action function is installed in order to select an individual deconvolution which is displayed in a separate window.

DisplayDeconvolutedFrame(Name)

The deconvolution of a frame pair or the average pair of several frames in a measurement stated by **Name** is displayed by this function in case the deconvolution has previously been calculated. Two display traces are colored, the axes are labeled, their ranges **adjusted**, and an information text box is **added**. The actual data is assigned to the display waves by an action function.

DisplayMeasurement(Name)

All frames of a measurement given by **Name** are displayed in a linear way. A cursor provides a way to select an individual frame for closer inspection. Frames excluded from further data processing are color coded.

If the data is loaded, a window is created and all individual frames are appended to it with an x -offset calculated from the running frame number. The axes are labeled, their ranges **set**, and an information text box is added. An installed **action** function allows the cursor to select the **CurrentFrame**.

DisplayRateFile(Name)

The thickness as a function of exposure time recorded during a deposition rate measurement is displayed, in case it was loaded, together with three traces for linear regressions. Two of those represent the base line before and after the exposure. The slope of the third, *i.e.*, middle, one corresponds to the apparent rate during the deposition. The traces are colored, the axes are labeled, and two cursors are

added separating the deposition region from the base lines. Changes of the cursors' positions trigger an installed **action function** calculating the linear regressions. A text box with details completes the window.

DoRateTextBoxes(Name)

If applicable, this feature updates the text boxes displayed together with a deposition rate measurement specified by **Name** containing detailed information.

UpdateFittedRate(Name)

If applicable, this feature recalculates the statistics of the piecewise fitted deposition rate measurement specified by **Name** and updates the values for the average, the error intervals, and the text box containing detailed information.

DoHeatTextBox()

If applicable, this feature updates the text box displayed together with the results of a heat measurement containing detailed information.

DoDeconvolutionTextBox(Name)

If applicable, this feature updates the text box displayed together with the results of the deconvolution of a measurement specified by **Name** containing detailed information.

NAC_ShowControlPanel()

This function brings the control panel to the front if the package is loaded or otherwise starts the **initialization** process.

NAC_Panels()

This feature gathers all functions initializing control panels. Since currently there is only the panel used for **data treatment**, this operation is preparatory for later package versions capable of controlling the experimental setup or of data acquisition.

NAC_DataPanel()

This function builds the data treatment control panel comprising the most frequent parameters and operations. Details of the usage are given in Chapter 3. The corresponding action functions derive the name of the measurement from the name given to the control.

The first segment contains commands creating controls to display the most important variables and parameters of the whole calorimetric experiment. Variables can be altered directly in this panel, parameters are only displayed and have to be modified *via* the *data browser*, the *command line*, or, for a permanent change, in the program code.

The second segment consists of commands creating the horizontal headings denoting the single measurements in an experiment arranged by columns. It also contains the vertically arranged captions labeling the elements in a row. The command buttons in this section apply to all experiments and spare the user gratuitous repetition of actions, *e.g.*, upon load of an experiment clicking the **Load** button and selecting one file from one listed file for all eleven measurements.

The third segment comprises the creation of data manipulation controls for each measurement. It is compressed by a loop structure covering all measurement types.

The same pattern is used in the fourth segment to generate the labels and display controls for variables and parameters, which are different in every measurement.

The fifth segment finally adds a progress bar, measurement specific control options, and variable displays to the panel.

4.2.4 Data Processing

This section covers all function related to the actual data processing, *i.e.*, the calculation of the desired properties, and forms the core of this package.

NAC_AutoFlagAll()

This feature calls the **AutoFlag** feature for all loaded experiments, **updates** the related windows, and sets a flag that it has been run.

Coverage2Thickness()

This tool converts a coverage θ_{ML} given in monolayers to a thickness d in meters according to the physical properties, *i.e.*, density ρ in g/cm^3 , molar mass M in g/mol , and monolayer density σ_{ML} in $1/\text{m}^2\cdot\text{ML}$ of the deposited material as

$$d = \frac{\theta_{\text{ML}} \cdot M \cdot \sigma_{\text{ML}}}{\rho \cdot N_{\text{A}}} . \quad (4.1)$$

ProcessProc(Name [, NoDecon])

This is the core function of the whole package. Depending on the type of measurement it invokes several lower level functions treating the data and provides a convenient way to process the data specified by **Name**. It also ensures that no steps are omitted and all steps are processed in the correct order. For intermediate calculation the deconvolution step can be skipped by setting of **NoDecon**.

Although the program code follows the lineup of the necessary actions, the description is sorted by measurement types to increase clarity.

In a first common step, it is tested whether the measurement is applicable and if the correlated fit waves have been generated. In case of calorimetric measurements, the **average** of the qualified frames is calculated.

Deconvolution measurements also **create** normalized fit waves.

Before Deposition measurements also **create** normalized fit waves and the **calculation** of the reflectivity of the coated sample is attempted.

Coating thickness measurements are **converted** to the differential deposition rate, displayed, and the information window is **updated**.

After Deposition measurements also **create** normalized fit waves and attempt the **calculations** of the reflectivity of the coated sample as well as of the temperature induced sensitivity change.

Laser Reference measurements also **obtain** the actual pulse length, **create** normalized fit waves, and attempt the **calculation** of the temperature induced sensitivity change.

Transmission Reference measurements also **calculate** the transmission of the infrared transparent window.

Radiation Reference measurements also **create** normalized fit waves.

Deposition Rate Reference measurements are **converted** to the differential deposition rate, displayed, and the information window is **updated**. The calorimetry deposition rate is recalculated automatically upon changes of the cursors' positions.

Zero Sticking Reference measurements also **create** normalized fit waves.

Heat Measurements also **perform** the evaluation process of the data, **calculate** the actual enthalpies, and **display** the result against the frame number. In addition, the results are also **displayed** as a function of coverage and the information is **updated** in case the coverage has been calculated.

Sticking Measurements also perform the evaluation process of the data including a recalculation of the coverage and **display** the result against the frame number. In addition, the results are also **displayed** as a function of coverage and the information is **updated** in case the coverage has been calculated.

For the calorimetric measurements⁷ the input is **reconstructed** for the averaged frames, if desired. Finally, the averaged frames are **displayed**, the axis ranges are **updated**, and the frame selection windows are **synchronized**.

DeconvoluteFrame(Data, Index, Result, Parity)

This function performs the reconstruction of a single data set in **Data** specified by **Index** with a given **Parity** which is stored in **Result**.

The data is fitted by the appropriate fit function in a small window at the start. Based on the obtained local amplitude the impact on the whole data set is calculated and subtracted from the data. The position of the window is moved by one **Step** and the procedure is repeated until the end of the data set is reached. The received differential power input is integrated and stored in the wave accepting the result.

DeconvolutionProcAverage(Name)

This function reconstructs the power input into the detector from the temporal evolution of the detector signal for the averaged frames of a measurement specified by **Name**. In order to remove boundary artifacts, the processed data is extended in a similar way used in the **normalization** of the fit waves.

In case the measurement is applicable, the average waves are **generated**, if necessary. In case the averages of a heat measurement are deconvoluted, the radiation is subtracted, if desired. According to the program setting the data is corrected by the temperature dependent detector sensitivity. Subsequently, the actual **deconvolution** is carried out. Finally, the resulting waves are trimmed, scaled, and the axis ranges related to deconvoluted measurements are **updated**.

DeconvolutionProc(Name)

This function reconstructs the power input into the detector from the temporal evolution of the detector signal for the individual frames or averaged subsets of a measurement specified by **Name**. In order to remove boundary artifacts, the processed data is extended in a similar way to the **normalization** of the fit waves.

⁷ Mass spectrometer measurements are not supported yet.

At the beginning, it is checked if measurement is applicable and the necessary waves are present. In case a heat measurement is deconvoluted, the radiation is subtracted, if desired. According to the program settings, the data is corrected by the temperature dependent detector sensitivity. During the preparation routine, which averages the subsets, if applicable, the radiative part is removed in the specified way if desired. Subsequently, the actual **deconvolution** is carried out for all entries of the prepared data. Finally, the resulting waves are trimmed, scaled, and the axis ranges related to deconvoluted measurements are **updated**.

CalcQCMRate(Name)

This function provides a tool to review the evolution of the rate during a deposition measurement given by **Name**. The thickness data is split in fractions given by **RateFitWindow**, the slope is calculated, and the scaling is adjusted.

NAC_CorrAdsorbed(Material, Sample, Source)

This function returns the thermodynamical correction for the adsorbed fraction of a given **Material** as a function of the **Sample** and **Source** temperatures, see Section 1.2.

NAC_CorrDesorbed(Material, Sample, Source)

This function returns the thermodynamical correction for the thermalized desorbing fraction of a given **Material** as a function of the **Sample** and **Source** temperatures, see Section 1.2.

CvGas(Material, Temperature)

This function returns the specific heat capacity at constant volume of a given *gas phase* **Material** at the specified **Temperature** T. The calculation uses the **Shomate equation** for heat capacities c with published^[157] or adapted coefficients. As all used adsorptives are mono-atomic, the value corresponding to an ideal gas of $c_v = 3/2 R$ at constant molar volume v is used. Since the reported coefficients are reported for c_p at constant pressure p , the result is corrected by the gas constant R

$$c_v = c_p - R \quad (4.2)$$

assuming ideal behavior of the gas phase.

An extension of this function towards calculation of the heat capacity c_v by other methods, *e.g.*, *via* the partition function z , using measured or calculated

spectroscopic data of the corresponding molecule, is possible with low efforts. In this case the relationship is given by

$$\begin{aligned}
 c_v &= \left(\frac{\partial u}{\partial T} \right)_V \\
 &= \frac{\partial}{\partial T} \left(R \cdot T^2 \frac{\partial \ln z}{\partial T} \right)_V \\
 &= \frac{R}{T^2} \left(\frac{\partial^2 \ln z}{\partial (1/T)^2} \right)_V
 \end{aligned} \tag{4.3}$$

with u denoting the molar inner energy and $_V$ a constant volume. Details about statistical thermodynamics and the individual contributions to the partition functions can be found in textbooks^[158,159] addressing physical chemistry.

CpCondensed(Material, Temperature[, Phase])

This function returns the specific heat capacity at constant pressure of a given *condensed phase* **Material** at the specified **Temperature**. A **Phase**, *e.g.*, **beta** for calcium, can be optionally be specified in case it differs from the standard phase, *e.g.*, **alpha** for calcium. The calculation uses either the **Shomate** equation for heat capacities with published^[157] or adapted coefficients. In case coefficients for the temperature of interest are not available, the heat capacity can be calculated according to Debye theory^[160]. The specific isochore heat capacity c_v at a temperature T is given by

$$c_v = 9R \left(\frac{T}{\Theta} \right)^3 \int_0^{\Theta/T} \frac{x^4 \cdot e^x}{(e^x - 1)^2} dx, \tag{4.4}$$

utilizing the material specific^[54] Debye temperature Θ together with the assumption that $c_p \approx c_v$. Correction towards the expansion of the volume V of the material with the volumetric thermal expansion coefficient α and bulk modulus K according to

$$C_p = C_V + V \cdot T \cdot \alpha^2 \cdot K \tag{4.5}$$

have not applied in this version yet, since the differences are small and due to a lack of reliable temperature dependent tabulated values. The Debye model exhibits its highest accuracy at low temperatures. This is beneficial, since parameters used in the Shomate approximation are usually not reported for “low” temperatures, *i.e.*, smaller than 273 K.

At the current state results from Debye theory are linearly scaled to match the data from the Shomate approximation manually.

NAC_RefEnthalpy(Material, Temperature)

This function returns the heat of sublimation $\Delta_{\text{sub}}H$ for a given **Material** at a given **Temperature** T . It is calculated from the tabulated sublimation enthalpy $\Delta_{\text{sub}}^{\ominus}H$ at standard temperature T^{\ominus} , the temperature dependent **solid phase** heat capacity at constant pressure $c_p^s(T)$, and the **gas phase** heat capacity $c_v^g(T)$ at constant volume according to

$$\Delta_{\text{sub}}H = \Delta_{\text{sub}}^{\ominus}H + \int_{T^{\ominus}}^T c_p^s(\vartheta) d\vartheta - \int_{T^{\ominus}}^T R + c_v^g(\vartheta) d\vartheta . \quad (4.6)$$

CalcHeat()

This function performs the calculation of the deposited enthalpy from the adsorption contribution of the heat measurement, the sticking probability measurement, the molar dose per pulse, and the thermodynamical corrections, see Section 1.2. It also adjusts the **ranges** for graphs plotted versus coverage.

CalcCoverage()

This function calculates the coverage as a function of pulse number from dose per pulse and the sticking probability. According to the settings either the measured data or the calculated trend is used. It also adjusts the **ranges** for graphs plotted versus coverage.

FitHeat()

After initialization of all related objects, according to the parameters in the experimental settings, all frames are fitted with the fit function of the matching parity, *i.e.*, for **even** or **odd** frames. The resulting fit parameters are stored in the correlated waves, see Section 4.2.2. Troublesome frames, *i.e.*, cases of a not converging fit, are automatically masked as not qualified and the error is stored in **ChiSq** with negative sign. Finally, the coverage as a function of frame number is calculated.

FitDesorption()

After initialization of all related objects, according to the parameters in the experimental settings, all frames are fitted with the fit function of the matching parity, *i.e.*, for **even** or **odd** frames. The resulting fit parameters are stored in the correlated waves, see Section 4.2.2. Troublesome frames, *i.e.*, cases of a not converging fit, are automatically masked as not qualified.

Averaging(Name)

This function calculates the average of the qualified frames in the measurement given by `Name` sorted by parity.

NormalizeFitWave(Name)

This function constitutes the waves used in the fitting processes.

If the measurement type, defined by `Name`, is applicable and the corresponding averages are calculated, the fit waves are created for both parities. In order to provide a time shift of the fit waves against the data to be processed, the fit waves have twice the length of a frame. The center of the fit wave is occupied by the average of the corresponding parity and the surrounding areas are continued with the opposite parity, see Section 3.5.

In case of the `Reflectivity` and `Sensitivity` fit waves, the data is normalized to the laser power.

In case of the `LaserReference` fit waves, the data is normalized to the laser power, its correction factor, a possible mirror contamination, the absorption, and the pulse length.

In case of the `Sticking` probability fit waves, the data is corrected by multiplication with the mass spectrometer correction factor.

In case of the `Radiation` fit waves, the data remains unchanged.

In case of the `Deconvolution` fit waves, the data is normalized to the laser power, its correction factor, a possible mirror contamination, the absorption, and the pulse length. Additionally, the position of the switching point is shifted to the nominal peak position.

Except for the `Deconvolution` fit waves, an offset calculated from the part before the pulse is subtracted.

GetRatio(Type)

This function returns the ratio of the detector response of two reference measurements defined by `Type`.

In case all necessary objects are initialized, the average frames of the experiments are normalized to the input laser power. The data set corresponding to the first measurement Ξ is assigned to the fit function and is adapted to the second data set by Ω

$$\Omega_P = A_0 + A_\Omega \cdot \Xi_P . \quad (4.7)$$

While the vertical offset A_0 is discarded, the amplitude A_Ω yields the relative intensity corresponding to the parity P . The average of the obtained amplitudes is returned.

GetPulseLength()

This function attempts to determine the true pulse length from the laser reference measurement, see Section 3.5.4. In case this is not possible, the nominal pulse length is used instead.

The start and end positions of the pulse are determined for both parities by calculation of the intersections of linear approximations of the detector signal before and after the nominal positions.

GetRadiationContribution(Name)

This function checks whether the measurement given by **Name** is applicable and if the temperatures for the sample and the source are loaded for the radiation reference as well as the heat measurement data sets. If the sample temperatures in both data sets, and thus the corresponding detector sensitivities, are similar, the correction factor is returned according to Equation (5.31).

FitQCMRate(Name)

This function calculates the baselines and the apparent deposition rate of a thickness measurement given by **Name** according to the adjustable cursor positions corrected by the corresponding correction factor. The heat and sticking probability calculations are repeated and the information in the heat measurement window is updated.

CalcQCMTooling(Name)

This function returns the correction factor used for a measurement type given by **Name**. In addition, it can report correction factors derived from other sources^[141,161] adjusted to the experimental setup, also specified by **Name**.

NAC_CreateTrend(Name)

This function creates the trends of the radiation and sticking probability measurements which can be used to reduce scatter in an individual experiment, see Section 3.9.

If the measurement, defined by **Name**, is applicable, the appropriate waves are assigned and if the measurement has been successfully processed before, the original result is displayed. Subsequently, the user is prompted to select a method to calculate the trend and, if applicable, for parameters specific to the used method.

After calculation of the trend, its corresponding trace is made visible in the graph and the experiment is adjusted to use the trend instead of the measured data.

4.2.5 Fitting Functions

Most functions use the extended syntax where a coefficient wave **wc**, a result wave **wy**, and a dependence wave **wx** are provided for the fit function as parameters. It has the advantage that all data points in the result wave are calculated at once and that the function is not called for every data point. This results in a significant decrease of computation time. In order to increase this effect, all contributing waves in the fit functions are hard linked instead of dynamically assigned on the cheap expense of a larger number of functions.

Usually, the coefficient wave contains a vertical offset **wc[0]**, an amplitude **wc[1]**, and an optional temporal offset **wc[2]**. It is used to calculate a wave of fitted data **wy** from a normalized reference wave Ξ according to

$$\mathbf{wy} = \mathbf{wc}[0] + \mathbf{wc}[1] \cdot \Xi(x) \quad (4.8)$$

$$\mathbf{wy} = \mathbf{wc}[0] + \mathbf{wc}[1] \cdot \Xi(x - \mathbf{wc}[2]) \quad (4.9)$$

as a function of time x inside a frame. The deconvolution function only use an amplitude coefficient **wc[0]**

$$\mathbf{wy} = \mathbf{wc}[0] \cdot \Xi(x) . \quad (4.10)$$

CpShomate(w, T)

This function is used to approximate the numerical coefficients **A** to **E** stored in the coefficients wave **w** of the Shoemate-equation^[157] which is used to describe the temperature dependency T provided in Kelvin of the specific heat capacity at constant pressure c_p given in $\frac{\text{J}}{\text{mol}\cdot\text{K}}$.

$$c_p = \mathbf{w}[0] + \mathbf{w}[1] \cdot t + \mathbf{w}[2] \cdot t^2 + \mathbf{w}[3] \cdot t^3 + \frac{\mathbf{w}[4]}{t^2} \quad (4.11)$$

with $t = T/1000$ as an alias. It can also be used to calculate the heat capacity at a given temperature if the coefficients are known.

HShomate(w, T)

This function is used to approximate the numerical coefficients **A** to **H** stored in the coefficients wave **w** of the Shoemate-equation^[157] from tabulated data. The dependency on temperature T of the enthalpy of formation $\Delta_f H$ is described by

$$\Delta_f H = \left(w[0] \cdot t + \frac{w[1]}{2} \cdot t^2 + \frac{w[2]}{3} \cdot t^3 + \frac{w[3]}{4} \cdot t^4 - \frac{w[4]}{t} + w[5] - w[6] \right) \cdot 1000 \quad (4.12)$$

with $t = T/1000$ as an alias. If used for fitting either **G** or **H** has to be constrained to zero. Yet, these coefficients are kept for compatibility in case this function is used to compute enthalpies of formation. The calculation of reference enthalpies from known coefficients uses the same coefficients to calculate heat capacities.

DeconvolutionFunction(w, t)

This function is used to generate an artificial noise-free fit function $\mathcal{J}(t)$ for the deconvolution process which is based on measured data. It comprises a constant initial value A_0 before the detector is exposed at the time t_0 and an exponential part, related to the charging of the intrinsic capacitor of the detector setup, with a maximal amplitude $A_{\mathcal{J}}$ and a time constant τ as follows

$$\mathcal{J}(t) = \begin{cases} A_0 & t \leq t_0 \\ A_0 + A_{\mathcal{J}} \cdot (1 - e^{-(t-t_0)\tau}) & t > t_0 \end{cases} \quad (4.13)$$

using the internal time scaling t of the wave.

DampedOscillation(wc, wy, wx)

This function was used to remove a base line corresponding to a damped oscillation from the detector signal in order to minimize the influence of the initial transient as follows

$$f(x) = wc[0] + wc[1] \cdot \exp(-wc[2] \cdot t) \cdot \cos(wc[3] \cdot t - wc[4]) \quad (4.14)$$

with an offset $wc[0]$, an amplitude $wc[1]$, a decay constant $wc[2]$, an oscillation frequency $wc[3]$, and a phase $wc[4]$ as a function of time t . It was replaced by Fourier filtering, which exhibits better performance.

DeconvolutionFuncEven(wc, wy, wx)

This function returns the normalized fit wave for deconvolution with even parity according to Equation (4.10).

DeconvolutionFuncOdd(wc,wy,wx)

This function returns the normalized fit wave for deconvolution with odd parity according to Equation (4.10).

DeconvolutionFuncEvenFitted(wc,wy,wx)

This function returns the artificial, noise-free, normalized fit wave for deconvolution with even parity according to Equation (4.10).

DeconvolutionFuncOddFitted(wc,wy,wx)

This function returns the artificial, noise-free, normalized fit wave for deconvolution with odd parity according to Equation (4.10).

CalorimetryEven(wc,wy,wx)

This function returns the fitted wave wy for a heat measurement with even parity. It comprises an offset $wc[0]$ and a linear combination of the normalized laser reference \mathcal{L}_E shifted by $wc[2]$ with an amplitude $wc[1]$ and the average response to radiation \mathcal{R}_E shifted by $wc[4]$ with an amplitude $wc[3]$ according to

$$wy = wc[0] + wc[1] \cdot \mathcal{L}_E(x - wc[2]) + wc[3] \cdot \mathcal{R}_E(x - wc[4]) \quad (4.15)$$

as a function of time x inside a frame.

CalorimetryOdd(wc,wy,wx)

This function returns the fitted wave wy for a heat measurement with odd parity. It comprises an offset $wc[0]$ and a linear combination of the normalized laser reference \mathcal{L}_O shifted by $wc[2]$ with an amplitude $wc[1]$ and the average response to radiation \mathcal{R}_O shifted by $wc[4]$ with an amplitude $wc[3]$ according to

$$wy = wc[0] + wc[1] \cdot \mathcal{L}_O(x - wc[2]) + wc[3] \cdot \mathcal{R}_O(x - wc[4]) \quad (4.16)$$

as a function of time x inside a frame.

RatioEven(wc,wy,wx)

This is fit function using the data provided in the `FitRatio` wave with even parity according to Equation (4.8).

RatioOdd(wc,wy,wx)

This is fit function using the data provided in the FitRatio wave with odd parity according to Equation (4.8).

LaserReferenceEven(wc,wy,wx)

This is a standard fit function using the normalized laser reference with even parity according to Equation (4.9).

LaserReferenceOdd(wc,wy,wx)

This is a standard fit function using the normalized laser reference with odd parity according to Equation (4.9).

StickingEven(wc,wy,wx)

This is a standard fit function using the sticking probability reference with even parity according to Equation (4.9).

StickingOdd(wc,wy,wx)

This is a standard fit function using the sticking probability reference with odd parity according to Equation (4.9).

StatLaserReferenceEven(wc,wy,wx)

This is a standard fit function using the average laser reference with even parity according to Equation (4.8).

StatLaserReferenceOdd(wc,wy,wx)

This is a standard fit function using the average laser reference with odd parity according to Equation (4.8).

StatTransmissionEven(wc,wy,wx)

This is a standard fit function using the average transmission reference with even parity according to Equation (4.8).

StatTransmissionOdd(wc,wy,wx)

This is a standard fit function using the average transmission reference with odd parity according to Equation (4.8).

StatBeforeCoatingEven(wc,wy,wx)

This is a standard fit function using the average before coating reference with even parity according to Equation (4.8).

StatBeforeCoatingOdd(wc,wy,wx)

This is a standard fit function using the average before coating reference with odd parity according to Equation (4.8).

StatAfterCoatingEven(wc,wy,wx)

This is a standard fit function using the average after coating reference with even parity according to Equation (4.8).

StatAfterCoatingOdd(wc,wy,wx)

This is a standard fit function using the average after coating reference with odd parity according to Equation (4.8).

StatDeconvolutionEven(wc,wy,wx)

This is a standard fit function using the average deconvolution reference with even parity according to Equation (4.8).

StatDeconvolutionOdd(wc,wy,wx)

This is a standard fit function using the average deconvolution reference with odd parity according to Equation (4.8).

StatRadiationEven(wc,wy,wx)

This is a standard fit function using the radiation reference with even parity according to Equation (4.8).

StatRadiationOdd(wc,wy,wx)

This is a standard fit function using the radiation reference with odd parity according to Equation (4.8).

StatZeroStickingEven(wc,wy,wx)

This is a standard fit function using the sticking probability reference with even parity according to Equation (4.8).

StatZeroStickingOdd(wc,wy,wx)

This is a standard fit function using the sticking probability reference with odd parity according to Equation (4.8).

4.2.6 File Input/Output

This section comprises the functions used to import data for a measured calorimetry experiment.

LoadCalFile(Name, FileNameOpen)

This function imports the data related to the calorimetric measurements and sets the corresponding variables for the data treatment.

Depending on the type of measurement, defined by **Name**, and the global setting, whether supporting files are to be loaded, the standard files types are assigned. In case the data file specified by **FileName** exists, it is opened or a file open dialogue is displayed. Subsequently, the header of the opened file is parsed for parameters which are temporarily stored. Values of outdated keywords are converted during this process to maintain compatibility to older data files. In case the experimental parameters of the data file are consistent with the settings of the IGOR PRO experiment file, which are set by the first loaded data file, the actual data is loaded and tested for integrity. In case the reflectivity of an individual sample is stored in the data file, its value is assigned to the corresponding measurement.

If the **Load Supporting File** option is enabled, only a warning message is generated and the load procedure is continued. Upon a positive evaluation the temporarily stored data is transferred to the related experiment variables and waves.

Subsequently, related objects for the loaded measurement are adjusted to the new data set and reinitialized, if needed. This includes the closing of all windows and discarding of fit waves in relation with this measurement type.

In a second step, the permanently, *i.e.*, not used for data file manipulation, loaded data is filtered, see Section 3.3, according to the set parameters, if desired.

Thereupon, the additions data with a temporal resolution of a frame pair is loaded in case a matching auxiliary file is found.

If the loaded data corresponds to a heat measurement, the average temperatures of the **Sample** and **Source**, *i.e.*, the main evaporator, are calculated in case the data set contains the relevant data streams. If information about the motor state can be found in the data set, all frames are marked as excluded, in case the motor was not responding a positive feed back. For reference measurements, the first and last

qualified pair are also marked, since they are likely to be affected by the measurement setup and the filtering process.

LoadRateFile(Name, FileName)

This file imports the data related to the deposition measurements and sets the corresponding variables for the data treatment.

Depending on the type of measurement, defined by **Name**, and the global setting, whether supporting files are to be loaded, the standard files types are assigned. In case the data file specified by **FileName** exists, it is opened or a file open dialogue is displayed. Subsequently, the header of the opened file is parsed for parameters which are temporarily stored. The actual load of the data is performed by the routine designed to **load** auxiliary files.

If the loaded data contains the relevant waves, the data structure is rearranged and the stored parameters are transferred to the related experiment variables. Further on, the suggestions for the positions of the transition from base line data to deposition data and *vice versa* are calculated. Finally, the file folder is set as a new default location to open measurement files and the loaded data is **displayed**.

LoadAuxFile(Name, FileName, [Delta])

This function loads a data file specified by **FileName** containing auxiliary information, see Section 4.1.3, related to a calorimetric measurement given by **Name**. Since the function is also utilized to **load** deposition thickness measurements, it accepts a switch to adjust the unit and spacing **Delta** of the data.

If an absolute complete file name including a path is provided this file is opened. Otherwise, the file name for auxiliary data is derived from the measurement file name and opened. The file is skipped to the end of the file header which is ignored⁸. Subsequently, the information of the file header is parsed and wave names are assigned. The extracted units are stored for a following processing. After the actual load operations the units and data are converted to standard SI units if applicable, *e.g.*, torr to pascal. Finally, the data is loaded and the wave scales are set.

LoadTrend(Name, FileName)

This function prompts the user to select an experiment file containing averaged calorimetry data, see Section 3.11. It loads the average specified by **Name** and stores the name of the experiment in **FileName** accessible for the calling function.

⁸ The functions used to load calorimetry or thickness measurement files interpret the identical corresponding file headers.

Subsequently, the trend wave is filled with the loaded data considering the conversions of monolayers to frames of the specific experiment.

Since the coverage is depending on the sticking probabilities and the radiation is loaded as a function thereof, it is recommended to load the averaged radiation contribution after the averaged sticking coefficients.

NAC_ConCat()

This function loads two data files, concatenates them, adjusts the parameters in the file header, and stores the data in a new file. This function is rarely used and still *alpha* state. Hence, error management and routines to check the data integrity are not fully implemented.

First, a temporary data structure to hold data of two measurement files, together with the general experimental settings, is created. Upon a successful load of the first file, the user can select a second file which is also loaded. In a next step, the file header for the new files is created from the two original headers along adjustment of the experimental parameters and is saved together with the combined calorimetric data.

Subsequently, the related auxiliary files are **loaded**. The already created header is again saved together with the combined auxiliary data.

NAC_Trim()

This function loads a data file, extracts a subset, adjusts the parameters in the file header, and stores the data in a new file. This function is rarely used and still *alpha* state. Hence, error management and routines to check the data integrity are not fully implemented.

First, a temporary data structure to hold data of a measurement file, together with the general experimental settings, is created. Upon a successful load, the file header for the new files is created from the original header along adjustment of the experimental parameters and is saved together with the selected subset of calorimetric data.

Subsequently, the related auxiliary file is **loaded**. The already created header is again saved together with the corresponding subset of auxiliary data.

4.2.7 Controls Handling

This section gathers the function reacting to user action such as moving a cursor or pressing a button. The first kind receives a *data structure* from the IGOR PRO main instance, see the manual^[155] for details, and, by convention, the cursor labeled A is kept left of cursor B. The other functions used as *button controls* are passed the name of the calling control. Buttons are disabled at the beginning of the function to prevent a call of the functions while they are running, **errors** are cleared, and, if applicable, the corresponding measurement is derived from the control's name. At the end of the code the buttons are enabled again.

NAC_LaserPowerCorrectionPopUp(ctrlName, popNum, popStr)

This function synchronizes the displayed Laser Power Correction string with the corresponding variable.

NAC_ReflectivityCleanPopUp(ctrlName, popNum, popStr)

This function synchronizes the displayed Reflectivity Clean Sample string with the corresponding variable.

NAC_WinHookDeconvolution(Data)

This function reacts to the **EventCode** associated with a moved cursor. Since it also sets cursor positions, it is capable of calling itself in an infinite loop and must be terminated in case the event was caused by itself. The type of the measurement is derived from the associated window name and, after a check if the type is applicable, the number of the selected frame is deduced from the *y*-position of the cursor. In case the window for the deconvolution of the individual frames corresponding to the measurement is not available, it is **displayed** and the display waves are filled with the data belonging to the selection. Finally, the text box with detailed information is updated.

NAC_WinHookRate(Data)

This function reacts to the **EventCode** associated with a moved cursor. Since it also sets cursor positions, it is capable of calling itself in an infinite loop and must be terminated in case the event was caused by itself. The kind of the measurement is derived from the associated window name and, after a check if the kind is applicable, the thickness change by time is **linearized** and the result is **displayed** in the

corresponding text boxes. Due to the dependency relations the derived quantities are updated automatically.

NAC_WinHookFittedRate(Data)

This function reacts to the `EventCode` associated with a moved cursor. Since it also sets cursor positions, it is capable of calling itself in an infinite loop and must be terminated in case the event was caused by itself. The kind of the measurement is derived from the associated window name and, after a check if the kind is applicable, ranges to calculate an average deposition rate are set and the corresponding objects are updated.

NAC_WinHookCal(Data)

This function reacts to the `EventCode` associated with a moved cursor. Since it also sets cursor positions, it is capable of calling itself in an infinite loop and must be terminated in case the event was caused by itself. The kind of the measurement is derived from the associated window name and, after a check if the kind is applicable, the `Type` of corresponding window is determined.

In case of a window showing the whole data set, *i.e.*, `Type=0`, the pulse number set to `CurrentFrame` is derived from the name of the selected trace, the cursor is placed in the middle of that trace, and the windows corresponding to the measurement are updated.

In case of a window showing the qualified frames, *i.e.*, `Type=1`, the pulse number set to `CurrentFrame` is derived from the name of the selected trace and the windows corresponding to the measurement are updated.

In case of the window showing the finally calculated enthalpy, *i.e.*, `Type=2`, the positions of the cursors are checked and assigned to the limits for the calculation of the `MultiLayerEnthalpy`, which is carried out automatically. Finally, the text box containing detailed information is updated.

NAC_ToggleAutoFlagging()

This is the action function of the `Auto Flag` menu item and inverts the corresponding variable.

NAC_ToggleLoadSupport()

This is the action function of the `Load Supporting Files` menu item and inverts the corresponding variable.

NAC_ToggleStoreFiltered()

This is the action function of the `Store Filter Residue Waves` menu item and inverts the corresponding variable.

NAC_ToggleAutoUpdateAverages()

This is the action function of the `Automatically Recalculate Averaged Experiments` menu item and inverts the corresponding variable.

NAC_ToggleShowBoxPlotData()

This is the action function of the `Show Data Points in Box Plots` menu item and inverts the corresponding variable. In case the statistics window containing the box plots is already displayed, its appearance is adjusted to the set value.

NAC_ResetFlagList(ExpName)

This function resets the state of the `FlagList` to a similar state as after loading the measurement file. If applicable, the window showing the full data and frame selection windows are `recreated`, respectively `updated`.

NAC_LoadLazyButton(CtrlName)

This function inquires a file folder by a *FileOpen* dialogue displaying all files associated with calorimetry measurements. It scans the selected folder for applicable files by file extensions. Subsequently, the found files per measurement are sorted in lists and an option not to load a file is added. A user dialogue gathers information which or if files should be loaded. The associated button is dyed red in case of several matching files. Thereupon, the selected files are loaded by the standard routines for calorimetry and thickness files. Finally, the selected folder is set as a default location to load other measurement files.

NAC_StatisticsLazyButton(CtrlName)

This function initiates the calculation of the statistics for all reference measurements and displays the results.

NAC_ProcessLazyButton(CtrlName)

The deconvolution, before deposition, after deposition, laser, transmission, radiation, and zero sticking probability reference measurements are `processed` with the standard routine. If the `Auto Flag` feature is disabled, the deconvolution of the average frames

is included. Otherwise, the calculation is inhibited, the statistics are **calculated**, the outliers are **marked** for all measurements, and the mentioned measurements are processed again. In any case, the statistics are calculated (again) for all measurements and **displayed**. Subsequently, the sticking probability and heat measurements are processed.

NAC_DeconvoluteFullButton(CtrlName)

Since this function triggers a sequence with long computation time, a warning message is displayed and upon confirmation the **deconvolution** of all measurements is started by the **Everything** button. After one measurement is finished, the **power map** and the window for individual frames are displayed.

NAC_KillFrameProc(CtrlName)

In case of a severely disturbed current frame, *e.g.*, with an intense spike messing up the automatic axis range **synchronization**, it can be set to constant zero and marked to be ignored by this function by the **Kill** button. Finally, the windows correlated to the measurement are updated and the axis ranges are **recalculated**.

NAC_FlagProc(CtrlName)

This function displays the whole data set and the window for included frames, toggles the status if the frame is used, updates the coloring for the currently displayed pulse as well as the related windows by pressing the **Flag/Unflag** button.

NAC_ClearProc(CtrlName)

This function sets all frames of a measurement to be included and updates the coloring as well as the related windows by pressing the **Clear** button.

NAC_RangeProc(CtrlName)

This function sets all frames in a range for a given pattern to be in- or excluded from the data treatment by pressing the **Range** button. The information is acquired by a user input dialogue. If the provided data, is valid the windows for the **whole data set** and for **included frames** are displayed, the masking information is applied to the measurement, the **statuses** of the control buttons, and the **windows** related to the measurement are updated.

NAC_NavProc(CtrlName)

This function is called by the six navigation buttons and thus a double function call is prevented by a variable. According to the pressed button, encoded in its name, the `CurrentFrame` variable of the corresponding measurement is modified and the related windows are updated. The '|<' button jumps to the first frame of the measurement, the '<<' button jumps two frames back, the '<' button jumps one frame back, the '>' button jumps one frame ahead, the '>>' button jumps two frames ahead, and the '>|' button jumps to the end of the measurement.

NAC_CurrentFrameProc(CtrlName)

This function, called by the numerical input to select a frame, sets the `CurrentFrame` variable to the provided value and updates all related windows.

NAC_UseEmptyCrucibleProc(CtrlName)

This function defines whether a radiation reference from an empty crucible, see Section 5.8.1, is used in the evaluation of the heat measurement or not and invokes the calculation of the corresponding coefficient.

NAC_UseBaselineProc(CtrlName)

This function updates the information text box for thickness measurements according to whether the deposition rate is corrected by the base lines or not.

NAC_UseTotalRangeProc(CtrlName)

This function updates the information text box for a coating thickness measurement according to whether the thickness between the cursors is used or from the beginning of the measurement to its end.

NAC_DCRproc(CtrlName)

This feature synchronizes the check boxes as to whether the radiative part should be excluded from a deconvolution of a heat measurement as from the fitting, as a fixed amount, or not at all.

NAC_ReCalcHeat(CtrlName)

This function initiates a recalculation of the final enthalpy upon changes of the thermodynamic corrections.

NAC_HeaderButton(CtrlName)

If a measurement is loaded, this function displays the header of the corresponding measurement file as a table by pressing a **Show** button.

NAC_LoadButton(CtrlName)

Depending on the type of measurement, this function initiates the loading procedure of a calorimetry or thickness measurement file by pressing a **Load** button.

NAC_DisplayFullButton(CtrlName)

Depending on the type of measurement, this function displays the **whole data set** of a calorimetry measurement or of a **thickness** measurement by pressing a **Display** button.

NAC_DisplayFlagButton(CtrlName)

This function displays the windows for the **whole data set**, the **current frame**, and the **qualified frames** for data treatment and **adjusts** the axes ranges by pressing a **Flag** button.

NAC_ProcessButton(CtrlName)

This function initiates the **data processing** for the correlated measurement by pressing a measurement related **Process** button.

NAC_StatisticsButton(CtrlName)

This function initiates the **calculation** and the **display** of the statistics for the correlated measurement by pressing a measurement related **Statistics** button.

NAC_DeconvoluteAverageButton(CtrlName)

This function **deconvolutes** and **displays** the result for the correlated measurement by pressing an **Avg** button.

NAC_DeconvoluteAllButton(CtrlName)

This function **deconvolutes** all included frames related to a measurement by pressing an **All** button. Subsequently, the **power map** and the window for **individual frames** are displayed.

NAC_ResultButton(CtrlName)

The outcomes of the calculation for the individual measurements are displayed by pressing a **Present** button. Depending on the measurement different actions are executed.

In cases of thickness measurements the **fitted deposition rate** window is displayed.

In case of the deconvolution measurement the **averaged** frames are displayed.

In cases of a before deposition, an after deposition, a laser, a transmission, a radiation, or a zero sticking probability reference measurement the windows for **averaged** frames, the **deconvolution** of the average frames, the **power map**, and for the **deconvoluted individual frames** are displayed.

In cases of the sticking probability or heat measurements, the same windows as for the above mentioned reference measurements are displayed. In addition, the obtained results are displayed as a function of **frame number** and **coverage**. Finally, the **trend** used to reduce scatter in the processing is displayed.

NAC_CopyFlagList(From, To)

This function invoked by the **Copy Flag List** submenu entries synchronizes the flag lists of the heat and sticking probability measurements in the desired direction.

4.2.8 Statistics Functions

This section contains functions and tools related to the statistical analysis of the reference measurements.

NAC_GetAllStatistics()

This function invokes the **statistical analysis** of all applicable measurements.

NAC_GetStatistics(Name)

This function evaluates the relative amplitudes in a calorimetric reference measurement and calculates statistical values.

If the experiment is applicable, loaded, the average of the qualified frames has been calculated, and not all frames are excluded, the relative amplitudes of the individual frames with respect to the average are calculated. Not qualified, *e.g.*, already masked or in case of an unsuccessful fit, frames are assigned with *NaN*.

NAC_DisplayStatistics(ExpNames)

This function displays the results of the statistical analysis of processed measurements as box plots.

The function examines the measurements given by **ExpNames**, with the alias **All** for all applicable measurements, for results of the statistical analysis. In case that measurements have already been processed the existing display window is closed and recreated, since the layout of the window depends on the obtained number of measurements.

The amplitudes of the enumerated experiments are displayed versus a constant display index, vernacular “on top of each other”, the median, quartiles, whiskers, and the whisker limits are added to the graph and colored. In case the display of regular data points is unwanted, the corresponding traces are hidden. The axes are labeled and adjusted. Finally, a legend is added.

NAC_AutoFlag(Name)

If the measurement type provided by **Name** is applicable, the statistical analysis on this measurement has been performed, and this is the first run of this procedure for the specified measurement, all frames corresponding to amplitudes outside the *whisker limit*, see Section 3.7 are marked as not qualified, and the amplitude is set to *NaN*. These reference levels are defined as the corresponding quartile plus or minus the one and a half fold distance between the lower and upper quartile.

Quantile(Input, Level)

This function removes invalid entries, *i.e.*, *Inf* and *NaN* from the **Input** wave, and sorts the remaining values in ascending order. If the quantile provided in **Level** is negative, the smallest value in the data is returned and if it exceeds unity, the maximal value is returned. For a regular level the average value of the two data points closest to the relative position in the sorted data set corresponding to level is returned.

Particular values for level are 0.5 which calculates the *median* and 0.25 or 0.75 corresponding to the lower respectively upper *quartile*.

GetWhisker(Input, Threshold)

This function extracts the value farthest away from the center of the data set provided by **Input** within the boundary of **Threshold**.

4.2.9 Experiment Averaging Functions

This section contains the sub package used to average several treated calorimetry experiments with similar experimental parameters, see Section 3.11. It is independent of the other functionalities of the main package, but can be activated at the same time.

Results_Initialize()

This feature uses its own data folder structure located in `root:NAC_Average` initialized by this function if necessary.

:Experiments: This data folder contains results of added experiments organized by another level of data folders.

:Experiment Name: These data folders contain the actual data related to added experiments and are created upon loading an experiment.

DosePerPulse contains the dose from a single pulse in monolayers.

SubstrateThickness contains the thickness of the predeposited substrate in meters.

DepositionRate contains the deposition rate during the calorimetric measurement in meters per second.

Enthalpy contains the calculated adsorption enthalpy in joules per mole as a function of pulse number.

Sticking contains the original sticking probability as a function of pulse number.

Radiation contains the original radiation contribution as a function of pulse number.

Coverage contains the coverage in monolayers as a function of pulse number.

MultiLayerReference contains the calculated sublimation enthalpy at the sample temperature as internal reference value in joules per mole.

MultiLayerEnthalpy stores the measured multilayer enthalpy.

MultiLayerEnthalpyError stores the standard deviation of the multilayer enthalpy.

AveragedEnthalpy contains the result of the averaging procedure for the enthalpies with a resolution given by **BinSize**.

AveragedSticking contains the result of the averaging procedure for the sticking probability measurement with a resolution given by **BinSize**. This development can be imported to individual experiments as a trend *via* the **Fitted Trends→Loaded Average** function.

AveragedRadiation contains the result of the averaging procedure for the obtained radiation contribution with a resolution given by **BinSize**. This development can be imported to individual experiments as a trend *via* the **Fitted Trends**→**Loaded Average** function.

DepositionRates contains the individual deposition rates of the loaded experiments. **Thicknesses** contains the individual substrate thicknesses of the loaded experiments.

MultiLayerEnthalpies contains the individual multilayer enthalpies of the loaded experiments.

MultiLayerEnthalpyErrors contains the standard deviation of the multilayer enthalpies of the loaded experiments.

Experiments contains the name tag of the individual experiments derived from the file name of the loaded experiment.

StickingLimit(1) provides a guide to the eye for an upper limit for the sticking probability.

EnthalpyLimit stores the average sublimation enthalpy at the sample temperature as a guide to the eye in joules per mole and its coverage range is synchronized with the **MultiLayerReference** wave.

RadiationLimit(1) provides a guide to the eye for a lower limit of the radiation contribution.

ReferenceEnthalpy provides the calculated multilayer reference enthalpy.

System contains a string describing the global experiment, *e.g.*, **Calcium on PTCDA**⁹.

Settings This data folder contains the parameters used for the averaging features.

BinSize(0.05) defines the resolution used in the averaging process.

WWidth(400), **WHeight(300)**, **MarginTop(45)** are dimensions used to display graphs of averaged measurements.

Processed(0) indicates if the data has been processed since the last added or removed experiment.

AutoRecalculate(1) sets if an automatic calculation of the averages should be performed upon adding or removal of an experiment.

AutoDisplay(1) defines if displays for the results are automatically recreated after calculation of the averages. This option must be altered manually.

Finally, the user is prompted for a descriptor of the global experiment.

9 Perylenetetracarboxylic dianhydride.

NAC_Results_Load()

If needed, this function initializes the sub package prior to prompt the user for an experiment file to load data from and to store it in a temporary data folder. The imported data is then copied to the final data folder. The enthalpy of adsorption and coverages are taken from the **Enthalpies** data folder. The sticking and radiation coefficients are imported from the original results in order to prevent an unintentional recursive calculation. If desired, a calculation of the averages is initiated.

NAC_Results_Average()

This function calculates the average of the loaded experiments considering a fixed increment in coverage. Since the coverage a frame is attributed to depends on the history of the coverage itself¹⁰, a simple relation between coverages and frames is not in existence and thus would require a sophisticated algorithm.

If needed, this function initializes the sub package and enumerates the loaded experiments. Subsequently, the integrity of all loaded data sets is verified, the highest occurring coverage is determined, and the compatibility of the experiments is checked by comparing the reference enthalpies.

Auxiliary waves are created in accordance with the so far obtained parameters. Marked frames in the original experiment located at the beginning or at the end are removed from the data. The information if frames had been marked can be deduced from two properties. Either if the sticking probability is exactly one and the enthalpy is exactly zero, or the enthalpy contains a non-finite number.

The sticking, radiation, and enthalpy values as functions of the coverage are interpolated and summarized while the number of contributing experiments is tracked. Subsequently, the average is calculated and the data is down-sampled to the desired resolution.

This simple method ignores the fact that the coverage is dependent on the sticking probabilities which are a function of coverage themselves. A linear connection between the frame number and the coverage is not existent and depends on the average of the individual experiments. A sophisticated, formally correct, algorithm was programmed but suffered from numerical instabilities resulting in a squeezed coverage axis and is deferred therefore.

If desired the results are automatically **displayed**.

Since the multilayer enthalpy and its error depend on the placement of cursors by the user, they are somewhat arbitrary. An automatic calculation of the uncertainties

¹⁰ The sticking probability as a function of coverage contains itself in the calculation of the coverage which derives from sticking probability and dose.

is therefore not implemented yet. Nevertheless, the individual values are gathered for manual treatment.

NAC_Results_Remove()

This function removes an experiment from the loaded experiments.

If necessary, this function initializes the sub package, enumerates the loaded experiments, and prompts the user for an experiment to be removed. After removal of traces related to the selected experiment in the result windows, the data folder corresponding to the experiment is deleted.

NAC_Results_Display()

This function presents the results of the experiment averaging procedure.

If necessary, this function initializes the sub package, enumerates the loaded experiments, and verifies if the calculated averages are up to date. Subsequently, the integrity of all loaded data sets is verified and the highest occurring coverage is determined.

The windows for the individual sticking probability, the radiation contribution, and enthalpy data are closed and recreated. The corresponding traces of all loaded experiments are added to the graphs together with the related reference and average traces and are color coded. The graphs are finalized with by a dynamical legend.

Furthermore, the graph displaying the averaged enthalpies and averaged sticking probability is recreated, and the references and averages are added and color coded.

Finally, a graph displaying the calorimetry deposition rate and the substrate thickness for every experiment is created and labeled.

4.2.10 Miscellaneous

This section gathers functions and tools which are not directly related to the other sections in this program package.

GetPrefix(str)

This function is used to extract the prefix of an SI unit, *e.g.*, 10^{-3} for millisecond (ms) from a given string **str**. Since there are exceptions¹¹ and it only affects old data files – new files use SI base units – the function uses an easy to extend, but sloppy comparison algorithm.

¹¹ There is no “mkg”.

SauerbreyThickness(F0, F, Z, D)

Calculates the thickness of a deposited layer on an oscillator crystal according to the “z-matching” method from the base frequency F0, the measured frequency F, the acoustic impedance Z of the deposited material, and the density D of the deposited material according to Equation (1.15).

HSL2RGB(Hue, Sat, Lum, Ch)

This function converts a color defined by Hue, saturation Sat, and luminescence Lum to the corresponding value in the red, green, or blue channel Ch.

This function might get relocated to a tools collection in later versions.

GetSubstanceName(Substance)

This string function returns a plain text substance name for registered identifiers, *e.g.*, ‘Magnesium’ for ‘Mg(0001)’, without the orientation statement. Not registered ones are returned with the orientation statement removed, *e.g.*, ‘Po(100)’ yields ‘Po’.

NAC_UpdateVersion()

This function changes the data structure of old experiments to be compatible with the most recent code version. This work describes the latest version of the package.

NAC_Invert()

This function provides a convenient way to change the polarity of a loaded **Detector** signal for a measurement, a set of related measurements, or the whole experiment as requested from the user.

NAC_RemoveBaseline()

This function provides a selectable method to remove a baseline from the whole data set for a selectable measurement in case the included filter algorithm fails.

ZeroOffset(GraphName, [StartX, EndX])

This preliminary command line tool provides a shortcut to set an individual vertical *offset* to all traces in the graph specified by GraphName in a way that the average between StartX and EndX is zero. If GraphName is an empty string, the function uses the top graph. The parameters StartX and EndX are optional. Their default values are negative infinity and positive infinity, respectively.

This function might get relocated to a tools collection in later versions.

4.2.11 Extensions to the Status Package

NAC_DisplayStatus()

This function displays all channels recorded for the calorimetry machine with plain text labels for all loaded data sets and modifies the graphs according to the content.

4.2.12 Version History

A brief version history which describes the changes of the program code.

4.2.13 Known Issues

- Deconvolution of sticking measurements is not implemented yet.
- Recalculation of the average fitted deposition rate with a changed fitting window results in wrong displayed information.
- Checks if measurement types are applicable are not completely implemented for low level functions.
- Material constants are read from file. Maybe they should be stored in the program or a local data base.
- Dependent waves are not updated upon inversion of the detector data. Manual reprocessing is necessary.
- The averaging routine uses the individual coverages instead of a globally recalculated coverage.
- Integrity check for auxiliary files is not fully implemented.
- The usage of radiation references using and empty evaporator has not been tested in an actual experiment yet.

4.3 Error Handling Package

This package provides a simple error management system. Error codes are converted to plain text messages, collected in a list, and displayed in a dedicated window. The window is shown only in case of errors and minimized otherwise. The package distinguishes between critical errors, well-handled errors, and common exceptions. The level of displayed and concealed errors can be adjusted.

4.3.1 Definitions

Compiler settings, version requirements, pointers to physical data folders, and error messages are defined in this part.

Compiler Settings

The package requires an IGOR PRO version of 6.2 or higher and uses global access method, *i.e.*, all variables, strings, and waves have to be accessed explicitly.

Data Paths

The data structure of the error handling packages is located in the folder provided by `ErrorDataFolder`.

Standard Error Codes

The package provides several standard errors, *e.g.*, a `UserAbort`, and an indication for a successful function call, *i.e.*, `NoError`.

Constants

The amount of reported errors is defined by the constant `Error_TalkLevel`:

- 0, 1 Disables error messages.
- 2, 3 Displays only serious errors.
- 4, 5 Displays serious and well-handled errors.
- 8, 9 Displays even exceptions and is recommended only for debugging.

If the least significant bit is set, *i.e.*, odd values are given, extended information, *e.g.*, function names, is included in the message.

4.3.2 Initialization

This part contains the initialization routine of the package.

Error_Init()

This function initializes the **Error** program package. It sets up the data structure for the package, **creates** the message window, and initializes the error list.

4.3.3 Error Handling

This part contains the main functions of the package.

Error_Clear()

This function resets the error list to the entry “**No Error**” and hides the message window.

Error_Add(Msg)

This function either overwrites the “**No Error**” entry with the error message provided by **Msg** or adds another line to the list.

Error_Message(ErrorCode, FunctionName, ProcedureName, Argument)

This function initializes the package, if necessary, and checks whether the **ErrorCode** is potentially a valid number. Otherwise it replaces the error message with a corresponding information. If desired, it extends the name of the calling routine (**ProcedureName**) by the name of the called function (**FunctionName**) and a user provided **Argument**.

Subsequently, it decodes the numerical constants of the errors into plain text, **adds** the result to the error list and returns the error code in order to give the calling program the possibility to react to the error in a proper way.

New error messages must be added manually as constants in the host program as well as in the decoding structure.

4.3.4 Graphical User Interface

This part contains the functions related to user interaction.

Error_Panel()

This function creates the window displaying the error messages. The error list is updated automatically.

4.3.5 Version History

A brief version history which describes the changes of the program code.

4.3.6 Known Issues

- Addition of dynamic user errors is not supported yet.
- This package is still *beta* state.

4.4 Status Report Package

This software package provides a convenient method to load and display different recorded properties related to the experimental setup. It also comprises a few tools to extract useful information. Typical applications are the determination of evaporator runtimes as well as temperature and pressure history of bake-outs.

Errors are usually cleared upon new user actions.

4.4.1 Definitions

Compiler settings, version requirements, pointers to physical data folders, and error messages are defined in this part.

Compiler Settings

The package requires an IGOR PRO version of 6.2 or higher and uses global access method, *i.e.*, all variables, strings, and waves have to be accessed explicitly.

Data Paths

The data structure of the status report packages is located in the folder provided by `Status_DataFolderStr`.

Constants

The standard location for status logging files is given by `Status_DataPathStr` and the version information is provided in `Status_Version`.

Error Codes

The constants for the error codes are labeled with plain text and are self explaining.

Menu

The menu bar provides often used features of the package.

`Import Machine Status` initiates the `import` of a machine status file.

`Display all Data for a Channel` initiates the `display` of prompted channel.

`Get Runtime for Top Window` initiates the calculation and display of the time, the channel in the top window resides above a prompted threshold value. Multiple added data sets are not recognized and are all included in the calculation.

4.4.2 Menu

This section covers the routines used to import status logging files. For the data format see Section 4.1.4.

Status_Import()

This function initializes the data folder in case it is not yet created, prompts a file open dialogue, and initiates the loading routine for every selected file.

Status_Load(FileName)

This function handles the actual data import for recorded machine information.

It initializes the data folder in case it is not yet created, opens the file given by `FileName`, and generates a standardized name from the date for the child data folder about to contain the dynamic data structure from the logging file. In case the child data folder already exists, it is prompted whether the data should be over written.

Subsequently, the information of the file header is analyzed and wave names assigned. The extracted units are stored for a following processing. After the actual load operations, the units and data are converted to standard SI units, if applicable, *e.g.*, torr to pascal. Finally, the data is loaded and the wave scales are set.

4.4.3 User Interface

Status_GetRuntimeMenu()

This function prompts the user for a threshold level, above which the properties displayed in the top windows are considered “on”, and initiates the actual calculation of the runtime.

Status_AddRuntimeText(Runtime, Threshold, [WindowName])

This function converts a `Runtime` from seconds to a more convenient unit, if applicable, and adds a text box with the runtime, the used `Threshold` level to the top window or a window specified by `WindowName`.

Status_DisplayChannel([Channel, ChannelName])

If no `Channel` is provided, this function gathers the available loaded channels and prompts the user to select one. In case no `ChannelName` is provided to label the window, the user is prompted to provide a name. `Align` defines whether the left (default) or right y -axis should be used for the trace. Finally, the function starts the actual display routine.

Status_Display(DateStr, ChannelStr, [Right, New, WindowName])

If necessary, this function generates a default date string from the provided `DateStr`, checks if the data in `ChannelStr` is available, and displays the trace. The left axis is used unless otherwise specified by `Right`. A separate window is only generated in case the parameter `New` is set or no graph window exists in the IGOR PRO experiment file. Data is appended to the top window unless otherwise stated by `WindowName`.

Finally, the data is displayed, colored, and the axes are labeled.

Status_DisplayAll(ChannelStr, [WindowName, Right])

This function examines all status data folders if data matching the channel given in `ChannelStr` is loaded. If at least one data set is found, the optional parameters are initialized and a sub function is invoked to display the data.

4.4.4 Tools

This section collects the tools related to the status package.

Status_GetRuntime(Threshold, [WindowName, ChannelName])

This function enumerates the traces in the top or specified by `WindowName` graph window and therein the traces matching `ChannelName`, if given. It further determines the intervals where the value of the channel exceeds the given `Threshold` and returns the summed up time in seconds.

Status_ListChannelNames()

This string function examines all child data folders in the status parent data folder for named channels, avoids duplicates, and returns all available channel names.

4.4.5 Version History

A brief version history which describes the changes of the program code.

4.4.6 Known Issues

- This package is still *beta* state.

4.5 Synopsis of the Software Packages

File formats produced by the experiment controlling computer in the laboratory for the different measurement types have been reviewed and requirements of the importing programs have been pointed out.

The individual components of the data evaluation package and the two auxiliary packages, covering machine status and error handling, have been discussed. This included descriptions of the employed data structure comprising data folders, waves, and numerical as well as string variables. A brief description of the purpose of every function is given. More complex functions are described with a higher level of detail.

Individual data folders provide a clearly structured arrangement of these three packages. This concept is consequently applied within the program packages.

Functions of the calorimetry package are divided into groups according to their usage, *e.g.*, user interface or fitting functions. Calculations relevant to the experimental results are presented as formulae along the description of the functions.

The error handling package is still beta state and is not able to use dynamically generated errors. However, since the source code can be altered, individual error codes and messages from additional packages can be easily inserted.

Status reports keep track of a dynamic range of indicators, such as pressures, temperatures, *etc.*, rendering a *post mortem* analysis possible in case of a failure. The most frequently used functions are provided on the menu bar.

The here described program packages have extensively been used to compute the results presented in Chapters 5 and 6.

5 Characterizing Experiments

To ensure correct results in the main, calorimetric, experiments it is obligatory to characterize each contributing measurement. A detailed examination of the behavior of each component provides benchmark results for comparison to normal experiments. It also procures guide values and suitable range settings to operate the machine or to expect as results from the experimental setup. Furthermore, these additional experiments allow to determine weak points in the design. They also serve as guidelines for troubleshooting in case the equipment is not performing as anticipated.

This chapter also includes theoretical considerations only applicable to the specific characterizing experiments. Focus lies on properties affecting the calorimetric experiments and determination of possible improvements.

Coverages are given in monolayers (ML) and/or meters. Deposition rates are stated in deposited meters per second or monolayers per second (ML/s) and are proportional to the corresponding fluxes since the relevant deposition regions have constant area.

Here, one monolayer is defined as a closed packed layer of the deposited atoms in a specified plane. The typically used plane is the closest packed plane for the most stable phase at room temperature, *i.e.*, the (111) plane for metals with cubic and the (0001) plane for metals with hexagonal crystal structure, *e.g.*, copper and magnesium, respectively. Both structures with their primitive spatial and corresponding planar unit cells are shown in the description of the used materials in Figures 6.1 and 6.2.

Error bars and error ranges correspond to the standard deviations or propagated standard deviations where applicable. The pulse length, where appropriate, has been set to 200 ms, unless otherwise stated.

5.1 External Reflectivity Measurement

The absorption α of a pristine sample, *i.e.*, mounted on a sample holder with no further treatment, such as sputtering, is the fundamental reference quantity of the whole calorimetry experiment. Light of a wavelength λ impinging on a surface can experience three different processes. The total intensity is partitioned into a transmitted τ , reflected ρ , and absorbed α fraction according to

$$1 = \alpha(\lambda) + \rho(\lambda) + \tau(\lambda) . \quad (5.1)$$

Since it is difficult to measure the adsorption directly, the corresponding reflectivity and transmission are measured and the absorption is calculated. In case of the used metalized detector material¹ the transmissive contribution can be neglected, since the transmission^[162,163] through the in sum 100 nm thick metal layers is smaller than 0.1 % at the used wavelength of 405 nm. Hence, Equation (5.1) is reduced to

$$\alpha(\lambda) = 1 - \rho(\lambda) \quad (5.2)$$

and used in this way in the data treatment software, see Section 3.5.

As only the integral reflectivity is relevant to the calculation of the absorption, the angular dependency of the reflection arising from, *e.g.*, the specular and diffuse reflection is irrelevant. This motivates for the usage of an integrating sphere. The collimated incident laser beam is reflected by the sample or a standard. The reflected light, specular and diffuse, is reflected inside the sphere several times before it is able to reach the attached detector. Direct light from the sample towards the detector is blocked by an included baffle, as depicted in Figure 5.1.

If the transmission τ can be neglected, the measured powers for the sample P_{sam} and the reference P_{ref} are given by

$$P_{\text{sam}} = \rho_{\text{sam}} \cdot P_0 \quad \text{and} \quad P_{\text{ref}} = \rho_{\text{ref}} \cdot P_0 \quad (5.3)$$

at a constant input power P_0 as a function of the reflectivities of the sample ρ_{sam} and the reference ρ_{ref} . Combination and rearrangement yield

$$\rho_{\text{sam}} = \frac{P_{\text{sam}}}{P_{\text{ref}}} \cdot \rho_{\text{ref}} \Big|_{P_0} \quad (5.4)$$

as an expression for the reflectivity of the sample.

¹ ‘28um/w 400CU/150NI’ from Measurement Specialties.

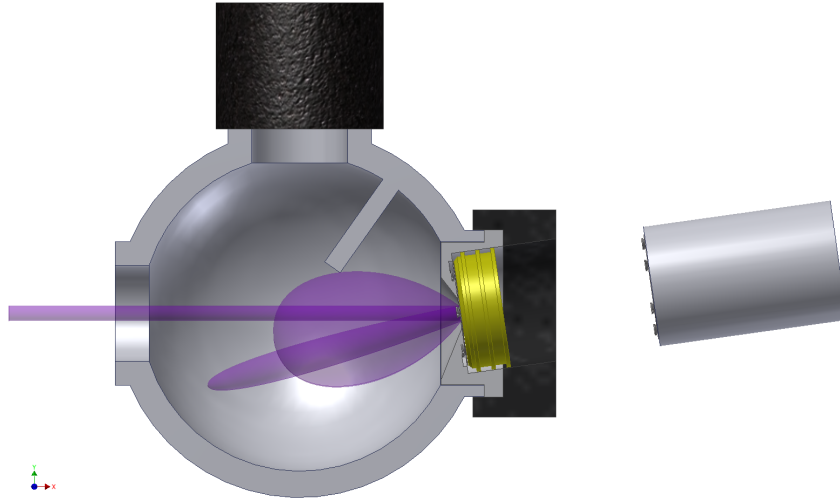


Figure 5.1: Geometry for the External Reflectivity Measurement — The laser (purple) enters the integrating sphere^a from the west port and strikes the sample in its holder (yellow) mounted on the east port at eight degrees. The reflected light comprises a specular (narrow lobe) and a diffuse (wide lobe) part. Direct light from the sample to the detector (black) on the north port is blocked by an internal baffle in the northeast section in the sphere. The sample can be replaced with a reference made from a piece of polytetrafluoroethylene equipped with a sample retaining plate simulating the sample holder.

a ‘819C-SL-3.3-CAL’ equipped with a ‘918D-UV-OD3’ detector operated with an ‘842-PE’ energy meter from Newport Spectra-Physics GmbH.

48 metalized β -polyvinylidene fluoride discs alternating with the polytetrafluoroethylene reference were measured on three occasions in the setup, described by Figure 5.1, using the 405 nm laser from the calorimetry setup. The samples have undergone an annealing procedure for various combinations of temperatures and durations of up to 100 °C for up to 72 h. A temperature of 125 °C leads to macroscopic changes of the samples. Hence, these specimens are excluded from further considerations. Due to the fact that the samples were not entirely flat, the reading from the powermeter was maximized by rotation of the sample in the sample reception.

With a reflectivity of the compact polytetrafluoroethylene sample^[164] of $\rho_{\text{ref}} = 0.948$ the reflectivity of the samples computed to $\rho_{\text{sam}} = 0.444 \pm 0.019$, as shown in Figure 5.2. This value is significantly lower than the theoretical value^[165] of $\rho_{\text{Ni}} = 0.49062$.

This difference might arise from a “contaminated” surface or different losses related to the ports in the integrating sphere for the sample and the reference. Nevertheless, the measurement appears reproducible although the samples experienced a different

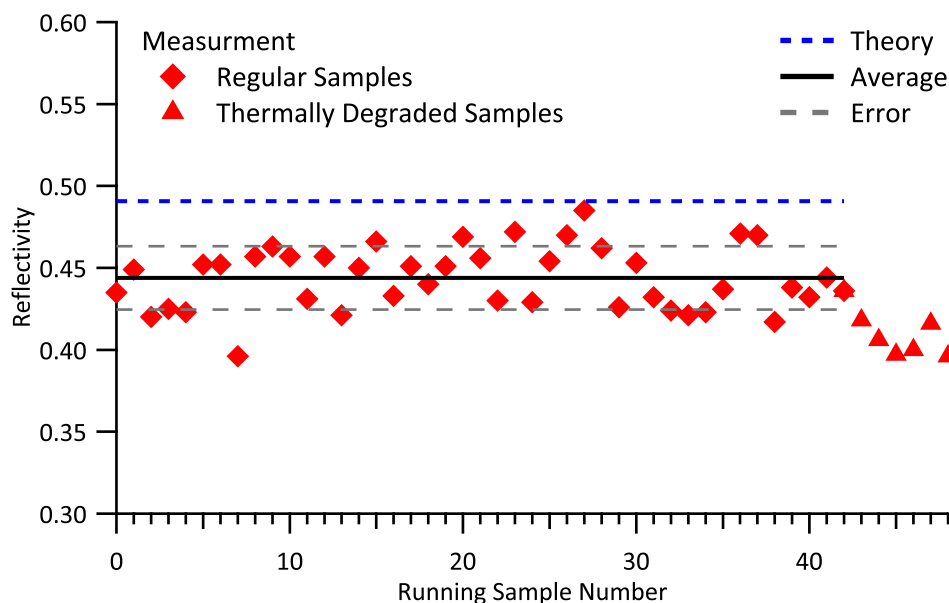


Figure 5.2: Reflectivity Measurement — The reflectivities of 48 samples (diamonds) with different thermal treating are averaged (black solid line) and opposed to the theoretical value (blue dashed line). The latter is significantly higher since it is located outside the error range (gray dashed lines). The last six samples visually suffered from the thermal treatment and are excluded from the average.

thermal treatment.

The β -polyvinylidene fluoride film is metalized with 40 nm of copper and 15 nm of nickel on both sides resulting in a theoretical combined transmission^[162,163] of $3.8 \cdot 10^{-4}$. Since this value is smaller than the scatter of the data, it is considered to be negligible.

Although a separate measurement of the specular and the diffuse component of the reflected light is basically possible, it has not been performed. Optical inspection of the reflected light revealed reflection characteristics dominated by the diffuse part. This motivated the use of a diffuse reflecting reference like polytetrafluoroethylene. A specular reflecting reference like a gold foil might be more stable but the experiment might suffer from different losses of light out of the ports.

In order to improve the reliability of the measurements, this measurement should be repeated with a diffuse reference with a reflectivity around 0.5 to be closer to the measured value and to avoid influences from a calibration point far away from the measured value. In addition a second reference should be measured serving as a control test.

Since the detector discs are not perfectly flat, the direction of the diffuse lobe, see

Figure 5.1, is not well defined. The opening for the laser input should be narrowed by a SpectralonTM plug with a small hole. The best solution would be a fiber coupled port attached to the integrating sphere. These arrangements will minimize the fraction of light reflected out of the port after hitting the sample, and thus increase the accuracy of this measurement.

If a possible transmission of the metalized film is observed, the reflectivity of the sample connector piece in the sample holder has to be taken into account. It reflects transmitted light back to the backside of the sample, where it is partially absorbed and partially reflected back onto the connector piece and so on. Since the aluminum contact piece is highly reflective^[136] at the used wavelength, *i.e.*, $\rho_{Al} = 0.923$, most of the light is absorbed by the metal coating of the detector disc. This effect keeps the error rather small, since the transmitted light is not completely lost but absorbed in a second attempt.

Cleaning the samples by ion bombardment and a subsequent comparison of the detector response to laser pulses of three tested samples suggest an increase of the reflectivity by approximately 5% upon this cleaning procedure. This supports the assumption of a contamination layer on the nickel surface reducing the *ex situ* measured reflectivity. If desired, this effect might be studied in a systematic way employing better references.

5.2 Sputtering

Early deposition experiments with magnesium on oscillator crystals of the quartz crystal microbalance (QCM) and metalized β -polyvinylidene fluoride foils exhibited unexpected behavior. The sticking coefficient, *i.e.*, the probability that a dosed atom will stay on the surface, was almost zero for a pristine sample and increased slowly with dosage. Metals usually adsorb very well at room temperature on various metallic surfaces^[18,24], moderate to high on oxides^[20,22,27], and exhibit a varying behavior on polymers ranging from barely to very well^[55–58,61]. Concerning the passivation of nickel by nickel oxide^[166], this low sticking probability could be reasonable for the β -polyvinylidene fluoride detector foils, but due to the absence of such an oxide layer on gold, it should not occur in this case.

As a consequence of intended but not installed surface characterizing techniques, an unconventional attempt to characterize the contamination layer has been executed. Removal of material on the QCM crystal results in an increase in resonance frequency, as discussed in Section 1.3.6. At constant operation conditions, sputtering effectuates a constant sputter rate, *i.e.*, ablation of material per time. The absolute rate depends on ion energy, ion current density on the sample, which is correlated to the pressure of the gas used, and the properties of the material which is removed – especially the mass in relation to the sputtering species and binding forces to the layer. A similar mass provides good momentum transfer and small binding energies result in high cleavage probabilities^[167]. Both aspects lead to high sputter rates. Hence, a change in the sputter rate indicates a change in the material’s properties and thus a change of the removed material.

A commercial QCM crystal has been treated the same way as the β -polyvinylidene fluoride detector discs, *i.e.*, washed with 2-propanol², mounted in a sample holder, introduced in the load lock, and kept in vacuum for degassing for 24 h, before being transferred into the main chamber. The crystal has been sputtered with argon ions of a kinetic energy of 3 keV at an argon background pressure of $1 \cdot 10^{-4}$ Pa. Every 60 s the crystal has been moved out of the sputter position to the detector stage in order to establish an electrical connection and to measure the resonance frequency with a standard QCM controller³.

The effect of sputtering on the change of the oscillator frequency $\delta f = f - f_0$ from its initial frequency f_0 is shown in Figure 5.3. As expected, the resonance frequency f increases since δf is always non-negative. The frequency increase between the

2 ‘7343.1’ HPLC grade from Carl Roth GmbH + Co. KG.

3 ‘IL150’ from Intellemetrics Global Limited *via* tectra GmbH.

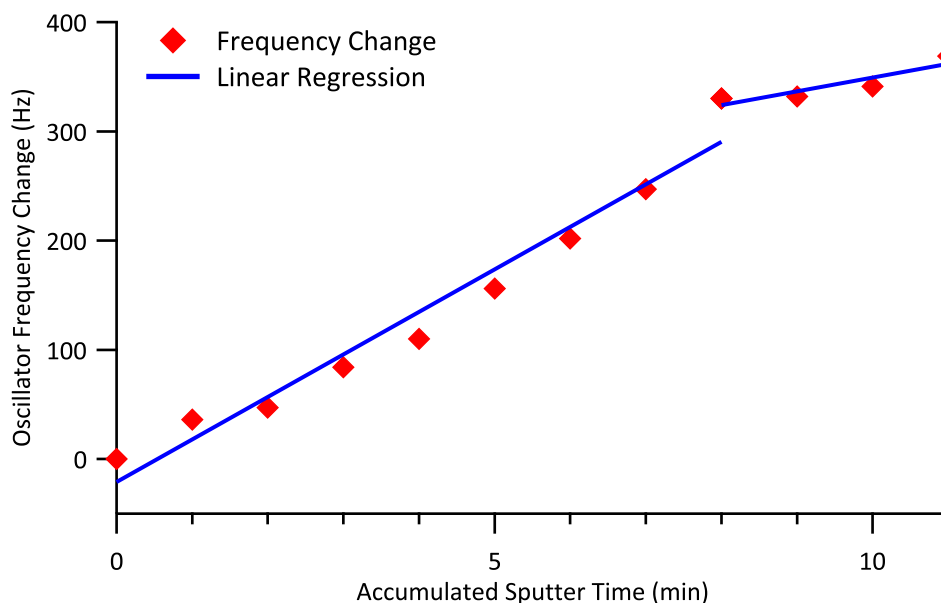


Figure 5.3: Sputtering of a QCM Crystal — The change in oscillating frequency (diamonds) is plotted versus accumulated sputter^a time at constant conditions. There is a distinct change in the sputter efficiency around 8 min indicated by smaller differences in frequency. Here, the soft contamination layer is removed and the clean gold coating of the QCM crystal is exposed. Linear regressions (lines) emphasize the different increments.

a $E_{\text{kin}} = 3 \text{ keV}$, $I_{\text{em}} = 10 \text{ mA}$, $p = 1 \cdot 10^{-4} \text{ Pa}$.

measurements is approximately constant at the beginning followed by an abrupt change after a total sputter time of 480 s. The blue lines correspond to an averaged sputter rate before and after 480 s.

The clearly visible change of the averaged sputter rates in Figure 5.3 indicate a distinct change of the removed material. Since the rate decreases, the material is harder to remove at the end of the experiment which is well in agreement that the gold surface is reached.

An aluminum sample⁴ prepared in a similar way shows species containing carbon and oxygen as contamination in an X-ray photoelectron spectrum, see Figure 5.4. While the carbon component is obvious, the oxygen component is derived from the fact that the increase of the O 1s signal after sputtering does not correspond to the reduced damping of the Al 1s peak and cannot arise solely from the oxide passivation layer^[166] on the aluminum foil.

This leads to the conclusion that the contamination consists of non-volatile polyglycols, which are a typical contamination in 2-propanol, or other oxygen

4 '2596.1' from Carl Roth GmbH + Co. KG.

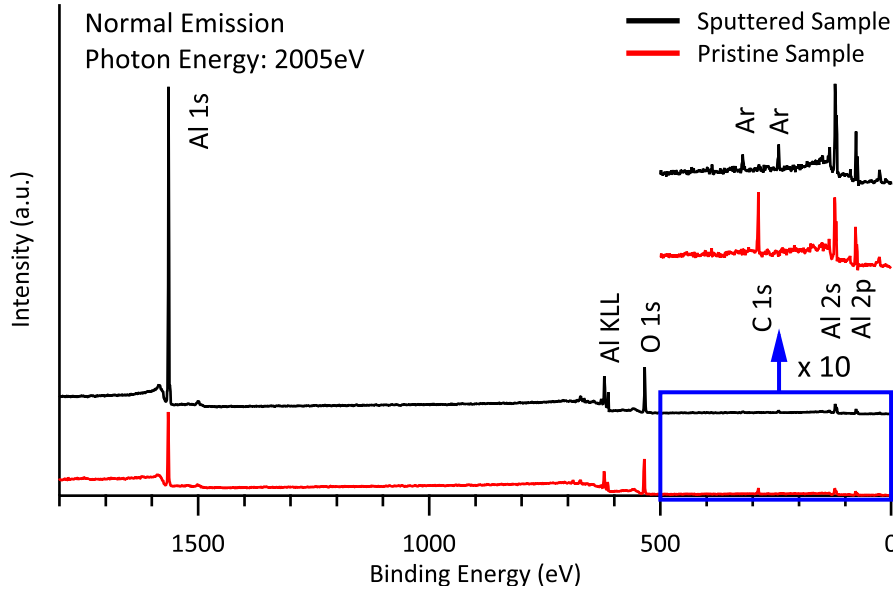


Figure 5.4: Photoemission Spectra of Aluminum Foils — According to the designated peaks, a minor carbon contamination can be seen in the pristine aluminum foil cleaned with 2-propanol. Short sputtering^a removes most of this surface impurity while the oxide layer stays intact. Data is vertically offset for better comparison.

a $E_{\text{kin}} = 1 \text{ keV}$, $I_{\text{em}} = 10 \text{ mA}$, $p = 5 \cdot 10^{-5} \text{ Pa}$, $t = 10 \text{ min}$.

containing polymers from the cleaning solvent. Fragments of hydrocarbons have a similar mass as argon atoms⁵ and feature smaller bond energies^[167] than gold atoms embedded in a surface. This agrees with the more efficient sputtering of the contamination. Since multilayers of water desorb below 230 K from gold films^[168] water cannot be the main component of the soiling.

Ion etching, *i.e.*, sputtering with reactive gases like oxygen or fluorine, of the samples is not supported with the current setup, since the sputter gun is intended to be operated with noble gases only.

Implying a density of $\rho = 1$ for the contamination⁶ one can, according to Equation (1.15), calculate its Sauerbrey-thickness. The observed frequency change of 324 Hz corresponds in this case to a thickness of approximately 60 nm.

A coarse calculation⁷ of the thickness of the contamination layer from damping of the Al 1s peak intensity yields 3 nm. Identical calculation using the O 1s peaks

5 $m_{\text{Ar}} = 40 \text{ u}$, $m_{\text{Au}} = 197 \text{ u}$, $m_{(\text{CH}_2)_3} = 42 \text{ u}$.

6 Poly(propylene glycol)^[169] as example for a polyglycol.

7 Using the peak maximum to background difference and the inelastic mean free path of electrons in polyethylene^[170] as a function of kinetic energy.

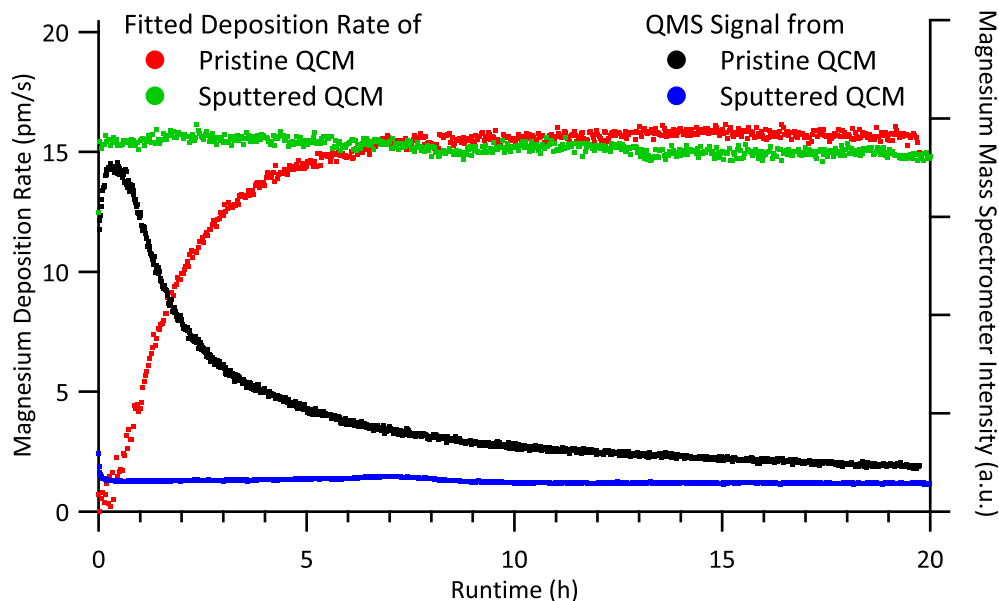


Figure 5.5: Magnesium Deposition on QCM Crystals — On a sputtered^a QCM crystal^b the deposition rate (green) is constant and the mass spectrometer is not detecting magnesium ($m/z = 24$ – blue) typical for the adsorption of a metal on a metal. In contrast, the pristine crystal rejects most of the dosed magnesium resulting in a reduced initial reading while the mass spectrometer signal (black) exhibits a pronounced maximum. The evaporated amount of magnesium corresponds to a final layer thickness of $1.1 \mu\text{m}$ (*sic*) in both cases assuming complete adsorption.

a $E_{\text{kin}} = 1 \text{ keV}$, $I_{\text{em}} = 10 \text{ mA}$, $p = 5 \cdot 10^{-5} \text{ Pa}$, $t = 10 \text{ min}$.

b ‘SN66BG’ from Intellectrics Global Limited *via* tectra GmbH.

results in a thickness of 10 nm . Again, this points out the presence of oxygen in the contamination layer. The contradiction to the quartz crystal microbalance measurement indicates a non-uniform cover layer assuming a similar purity of the used solvent. As this layer has been removed for most of the experiments more detailed discussion is not productive.

The effect of the sputtering on the sticking behavior is demonstrated in Figure 5.5. Magnesium was continuously dosed on a pristine QCM-crystals followed up by a sputtered crystal at ambient temperature. Except for the sputtering⁸ both crystals were treated the same way as mentioned above.

The sputtered crystal shows a constant deposition rate and a constant low intensity in the mass spectrometer signal for magnesium. In contrast, the pristine crystal exhibits a pronounced induction period until the deposition rate reaches a plateau.

⁸ Argon: 10^{-4} Pa , Ion Energy 3 keV , 10 minutes.

As the observed deposition rate increases, the intensity of the mass spectrometer signal for magnesium decreases in a correlated way. Since the flux is almost zero at the beginning, nearly all magnesium atoms are rebound from the contamination layer on the crystal.

These results led to the additional step of a sputtering for ten minutes in the standard sample preparation procedure mentioned in Section 6.3 for effectively removing the contamination layer.

5.3 Partially Loaded Quartz Crystal Microbalance

As mentioned in Section 1.3.6, the accuracy of the reading of a QCM relies on the size of the deposition area. In the ideal case the covered area should be larger than the size of the smaller electrode which is usually the back electrode. Since the diameter of the molecular beam is smaller than the diameter of the back electrode of the used crystals, one has to correct for this geometric factor.

The deposited mass m_{dep} is given by its density ρ and volume V

$$m_{\text{dep}} = \rho V = \rho \cdot \pi \cdot r^2 \cdot d \quad (5.5)$$

where the volume is calculated from the thickness d indicated by the QCM controller and the effective deposition diameter of $2r$, which is in this case the beam diameter. Since the source has a finite area, the deposition is not entirely homogeneous like for a plane source. Some material near the perimeter is spread outside of the nominal beam area. Since exactly the amount of material missing inside the nominal area is deposited outside, the total amount is unchanged and this calculation can be performed with the nominal diameter.

As a consequence of the inhomogeneous deposition, the diameter entering the theoretical correction needs to be examined more closely. The profile of the deposited layer is reminiscent of a bellmouthed disc. The innermost part contains a layer of constant thickness with a smaller diameter than the nominal beam diameter surrounded by a transition region with an approximately sigmoidal thickness profile. As discussed in Section 1.3.6, the resonance frequency is determined by the resonator feedback loop with the highest quality factor. Since it is obvious that a homogeneous disc will create a “better” shear mode resonator than the surrounding toroid, the oscillation frequency is determined by the central area with uniform coating and the resonance frequencies from the penumbra region are not excited. This leads to the conclusion that the inner diameter is relevant for the calculation of the correction factor.

A source of error in this experiment is reaction of the deposited material with the residual gas in the vacuum chamber which typically comprises hydrogen, water, and carbon monoxide. Although the pressure of the main chamber is in the 10^{-8} Pa range during operation of the molecular beam, the pressure on the sample might be higher if the beam source is degassing. Together with the long deposition periods of approximately a day contamination is possible.

The dominant contamination is most likely the formation of oxides in case of the investigated reactive metals, *e.g.*, magnesium. Hydroxides may be formed as intermediates but are likely to dehydrogenate to the corresponding oxide^[171] or further oxidize the deposited metal.

In case of a partially oxidized sample with the deposited mass m_{dep} the total mass m of the metal, regardless of its chemical state, is given by

$$m = p \cdot m_{\text{dep}} + (1 - p) \cdot \omega \cdot m_{\text{dep}} \quad (5.6)$$

with the mass fraction ω of a metal in its oxide Me_aO_b , and a mixing coefficient describing the purity $p \in [0, 1]$. Together with the mass fraction ω , which is defined by the ratio of the molar masses of the metal M_{Me} and of its oxide M_{Ox}

$$\omega = \frac{a \cdot M_{\text{Me}}}{M_{\text{Ox}}} \quad (5.7)$$

weighted with the indices, *i.e.*, a and b , of the chemical empirical formula Equation (5.6) can thus be rewritten as

$$\begin{aligned} m &= p \cdot m_{\text{dep}} + \frac{a \cdot M_{\text{Me}}}{M_{\text{Ox}}} \cdot (1 - p) m_{\text{dep}} \\ &= m_{\text{dep}} \left(p + \frac{a \cdot M_{\text{Me}}}{M_{\text{Ox}}} \cdot (1 - p) \right) . \end{aligned} \quad (5.8)$$

Since ω lies in the open interval $]0, 1[$, a contamination of the deposited material will result in a metal content smaller than indicated by the QCM controller and thus in

$$\frac{m}{m_{\text{dep}}} = p + \frac{a \cdot M_{\text{Me}}}{M_{\text{Ox}}} \cdot (1 - p) < 1 . \quad (5.9)$$

Further complications might arise from a temperature dependent frequency constant N_f of the crystal. This dependence arises from the correlation of the frequency constant to the density ρ and Young's modulus E of oscillator material by

$$N_f = \frac{1}{2} \sqrt{\frac{E}{\rho}} . \quad (5.10)$$

The density and the elastic module are both temperature dependent. However, this influence seems to be small as quartz crystal microbalances are used at cryogenic temperatures without this specific correction in similar experimental setups^[23] providing correct values^[23,32,37,38,41,45,47].

In order to verify the theoretical correction^[141] factors regarding the partial

Table 5.1: Thick Layer Deposition Parameters — The parameters used for the deposition of thick layers on QCM crystals are listed here. Unless otherwise stated the temperature of the QCM crystal has been set 307 K. Sputtering has been executed with 10^{-4} Pa argon with an ion energy of 3 keV for 10 minutes.

Substance	Experiment	Crucible Temperature	Sputtered
Magnesium	A ^a	800 K	no
Magnesium	B	800 K	yes
Magnesium	C	800 K	yes
Magnesium	D	820 K	yes
Zinc	E	670 K	yes
Zinc	F ^b	670 K	yes

a Uneven deposition.

b QCM cooled to 95 K.

loading, macroscopic amounts were deposited on commercial oscillator crystals and the deposited portion was externally quantified by the service division of the analytical chemistry department. Since the used methods, *e.g.*, ICP-AES or ICP-AAS, are element specific, an oxidation or contamination of the specimens after extraction from the vacuum system is uncritical as long as the contamination is free of the probed element.

This experiment is also capable of detecting the usage of a wrong crystal type, *i.e.*, a *BT cut* instead of a *AT cut* crystal, which are both commonly available. The frequency constant of the oscillator crystals with *BT cut* is one and a half times larger than for *AT cut* crystals^[141]. Hence, confusion of these two crystal types would result in a systematic error of the same magnitude.

Several QCM crystals⁹ have been mounted in the polymer sample holder and placed in sample position. Thick layers of magnesium have been deposited on one pristine and two sputtered oscillator crystals from the molecular beam source. The same experiment has been performed with thick layers of zinc on two sputtered crystals of which one has been cooled with liquid nitrogen, as listed in Table 5.1.

Table 5.2 summarizes the deposited masses calculated from thickness and found masses together with their experimental ratios. Furthermore, the average ratio is opposed to the expected ratios according to the model presented in Section 1.3.6. Four of the six experiments give similar results with an average of 110 % which is in agreement with the predicted value of 109 % assuming an electrode diameter

⁹ ‘SN66BG’ from Intellectrics Global Limited *via* tectra GmbH.

Table 5.2: Thick Layer Deposition Results — From thickness calculated masses are opposed to masses found by quantitative chemical analysis. The averaged ratios are compared to theoretical values according to the model presented in Section 1.3.6.

Substance	Experiment	Measured Thickness	Mass		$\frac{m_{\text{found}}}{m_{\text{dep}}}$
			Deposited	Found	
Magnesium	A ^a	1.000 μm	27.62 μg	27.64 μg	99.9 %
Magnesium	B	1.500 μm	41.46 μg	45.29 μg	109 %
Magnesium	C	1.500 μm	41.46 μg	45.01 μg	109 %
Magnesium	D	1.000 μm	27.64 μg	30.35 μg	110 %
Zinc	E ^a	2.103 μm	238.8 μg	223 μg	93.4 %
Zinc	F ^b	1.897 μm	215.4 μg	240 μg	111 %
Experimental Average:					110 %
Expectation ^[141] :					109 %

a Excluded from average.

b Thickness corrected by $-0.103 \mu\text{m}$ caused by changing temperature.

of 6 mm and a diameter of the oscillating area – with homogeneous thickness – of 4.37 mm for a QCM crystal placed in the sample position. The latter diameter is obtained from the geometry of the experimental setup.

A possible explanation of the slight excess could arise from a deposition which was not concentric with the electrodes since a lateral offset leads to an additional, yet small sensitivity loss of the oscillator crystal^[141,145]. The excess also indicates that no major contamination of the deposited material occurred since this would lead to a reduced ratio.

While “Experiment A” suffered from visible inhomogeneous deposition and was not considered to give a reliable result, the deviation of “Experiment E” is surprising. The obtained ratio would correspond, according to Equation (5.9), to a contamination of the deposited zinc with approximately $1/3$ zinc oxide which seems unreasonable considering the good agreement of the other experiments.

A dependency of the measured thickness of the oscillator’s temperature seems unlikely, since the experiment carried out at low temperature, *i.e.*, “Experiment F”, agrees well with theory and literature^[119,172]. Typically the calorimetry deposition rate is determined with the oscillator crystal held at ambient temperature. Hence, this effect is irrelevant in this case. If the nature of the adsorptive requires cryogenic cooling of the quartz crystal, an influence of the temperature on the measured rate should be excluded explicitly.

Due to the good agreement of theory and experiment, the remaining source of error involving confusion of *AT cut* and *BT cut* oscillator crystals, can be excluded.

As mentioned in Section 1.3.6, the acoustic impedance plays only a minor role for lightly loaded crystals. A light loading of the crystals is considered to reveal a reduced frequency shift of up to 15 %. The crystals used throughout this work never exceeded a relative shift of more than 3 % and hence can be considered as sparsely loaded. This virtually excludes errors arising from a mismatch of the acoustic impedances.

The calculation of the mass on the QCM crystal from the deposited thickness corrected with the partial loading model in [141] matches the mass found by analytical chemistry and excludes major contamination. This result confirms the use of a quartz crystal microbalance to quantify the deposition rate and thus the flux of the molecular beam in the sample position.

A possibility to avoid the correction necessary due to the partial loading would involve the usage of custom made oscillator crystals with a back electrode smaller than the beam spot. However, it is unknown whether the present electronics are compatible and will give accurate readings.

5.4 Sample Preparation in the Load Lock

Although the main purpose of the load lock is sample storage and the transfer of samples into the vacuum system, it is also used for sample preparation. An evaporator provides deposition of organic thin films and an attached quartz crystal microbalance renders a rough estimate of the film thickness possible.

5.4.1 Evaporator

Various substances can be deposited by the evaporator installed on the load lock onto the samples. Table 5.3 lists the operation parameters for a deposition rate of approximately $10 \text{ nm}/\text{min}$. This rate easily allows to deposit thin and thick layers on reasonable time scales. The settings used in the QCM controller are given in appendix A.

Table 5.3: Load Lock Evaporator Parameters — Operation parameters for the quartz crystal microbalance equipped evaporator in the load lock are listed for the investigated substances using twelve turns of tungsten wire^a as heating filament. While the currents are accurate, temperatures given rely on the position of the filament and the heat conductance of the thermocouple/glue/crucible interface.

Substance	Temperature	Current
PTCDA ^{bc}	540 K	2.7 A
Phthalocyanine ^d	550 K	2.8 A
Sexithiophene ^{ef}	410 K	2.2 A
Tetraphenyl porphyrin ^g	550 K	2.8 A

a $\varnothing 0.5 \text{ mm}$ from Haines & Maassen Metallhandelsgesellschaft mbH.

b Perylenetetracarboxylic dianhydride.

c ‘P11255’ from Sigma-Aldrich Co. LLC.

d ‘253103’ from Sigma-Aldrich Co. LLC.

e ‘594687’ from Sigma-Aldrich Co. LLC.

f Evaporates yellow 4T impurity at 1.8 A corresponding to 370 K first.

g ‘PO890001’ from Porphyrin Systems GbR.

5.4.2 Effects of Coating

In case of the investigation of metals adsorbed on deposited thin films on the used β -polyvinylidene fluoride detector disc, see Section 2.2, the heat capacity of the sensor and thus its sensitivity is changed. According to the structure of the detector film the total heat capacity $C_{p,\text{det}}$ of the detector is given by the involved layers ζ as

$$C_{p,\text{det}} = \sum_{\zeta \in \text{Layers}} c_{p,\zeta} \cdot \varrho_{\zeta} \cdot V_{\zeta} . \quad (5.11)$$

with their specific heat capacities at constant pressure $c_{p,\zeta}$, densities ϱ_{ζ} , and volumes V_{ζ} . The structure of the stacked layers is given in Table 5.4 together with their thicknesses and heat capacities. Since the relevant area A of the detector remains constant, the volume can be calculated from the layer thickness d according to

$$V_{\zeta} = A \cdot d_{\zeta} \quad (5.12)$$

and Equation (5.11) can be rewritten as

$$\frac{C_{p,\text{det}}}{A} = \sum_{\zeta \in \text{Layers}} c_{p,\zeta} \cdot \varrho_{\zeta} \cdot d_{\zeta} . \quad (5.13)$$

The detector voltage response U_{el} is proportional to the temperature change δT in the detector polymer. The temperature change depends on the heat capacity C_p of the active area and the deposited heat Q_{h} as

$$U_{\text{el}} \propto \delta T \propto \frac{Q_{\text{h}}}{C_p} . \quad (5.14)$$

The relative detector response R as a function of deposition thickness d is thus given by

$$R(d) = \frac{U_{\text{el}}(d)}{U_{\text{el}}(\text{pristine})} = \frac{C_{p,\text{pristine}}}{C_p(d)} \quad (5.15)$$

assuming identical heat input characteristics. Exemplary values for the relative response are given in Table 5.5 using the sample structure given in Table 5.4.

The relative response is close to one and even for the “thick” layer, *i.e.*, 1 μm , it changes only by approximately 2%. Since a determination of the changed heat capacity is laborious and the estimated influence is small, its effect is not considered further in this work.

Table 5.4: Sample/Detector Structure — The table compares the structural composition of the pristine and the coated samples together with physical properties. The thickness d of the deposited substrate is variable.

Substance	Heat Capacity ^a	Density ^b	Thickness	
			Pristine	Coated
PTCDA ^{cd}	1 J/g·K	1.69 g/cm ³	—	d
Contamination ^e	1 J/g·K	0.9 g/cm ³	60 nm	—
Nickel	0.444 J/g·K	8.9 g/cm ³	15 nm	15 nm
Copper	0.385 J/g·K	8.96 g/cm ³	40 nm	40 nm
PVDF ^f	1.5 J/g·K	1.76 g/cm ³	28 μm	28 μm
Copper	0.385 J/g·K	8.96 g/cm ³	40 nm	40 nm
Nickel	0.444 J/g·K	8.9 g/cm ³	15 nm	15 nm
Contamination	1 J/g·K	1 g/cm ³	60 nm	60 nm

a See References [173–175].

b See References [176–178].

c Perylenetetracarboxylic dianhydride.

d Example. Other substances used to create the molecular thin films have similar properties, see Appendix A.

e See Section 5.2.

f β-Polyvinylidene fluoride.

Table 5.5: Relative Response of a Coated Detector — Exemplary values for the relative response obtained from Equation (5.15) with the structural information from Table 5.4. The minor increase for the thinnest layer results from the removal of the contamination layer.

Thickness	Relative Response
10 nm	1.0006
50 nm	0.9997
0.1 μm	0.9986
0.5 μm	0.9896
1 μm	0.9786

5.4.3 Thermal Degrading During Deposition

As poled β -polyvinylidene fluoride loses its pyroelectricity^[148], also see Section 5.9.3, upon exposition to elevated temperatures, a possible source of error arises from the thermal load on the detector polymer during deposition of organic thin films with the evaporator in the load lock.

If the temperature during deposition of the detector polymer stays below its critical temperature, no change in the detector output at constant pulse length and laser power is expected to occur, *i.e.*, the sensitivity of the detector is unchanged.

Several frame pairs, using laser light pulsed on a pristine detector disc mounted in a polymer sample holder, see Section 2.1, have been recorded. Subsequently, the subject has been exposed to the thermal radiation of an empty crucible operated at a typical evaporation temperature of 520 K for about 15 minutes simulating the usual sample preparation routine, see Section 6.3, but without any deposition on the detector. Finally, the detector response has been measured with identical parameters again.

Figure 5.6 give no indication of a change in the sensitivity after the thermal treatment. A detailed examination following the procedure for a transmission measurement, see Section 3.5.5, reveals a change of less than 0.5 % in the signal intensity. This result excludes an influence of the coating procedure on the performance of the detector.

However, the coating does affect the reflectivity and thus the response of the detector. It is recommended to repeat this experiment if higher evaporator temperatures are used.

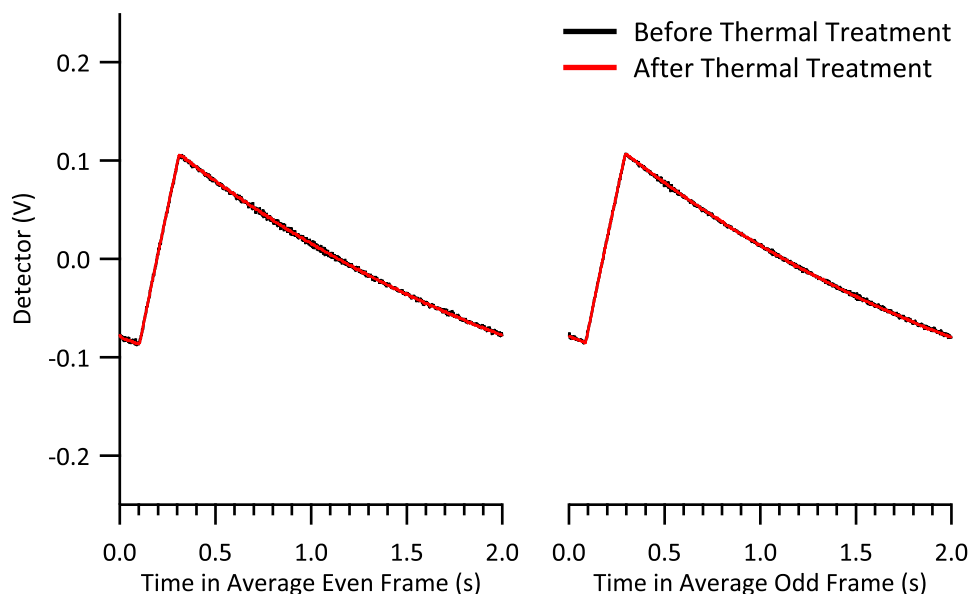


Figure 5.6: Detector Polymer Degradation upon Coating — The averages of the detector response to eleven pulse pairs on laser pulses before (black) and after a simulated deposition^a (red) in the load lock are opposed to each other. The absent difference in the amplitude at constant laser power indicates no degrading during coating of the detector discs.

^a Empty crucible, ≈ 15 min, 520 K.

5.4.4 Tooling of the Quartz Crystal Microbalance in the Load Lock

In order to produce organic thin films on the sputtered detector polymer, see Section 6.3, a simple evaporator is installed in the load lock, see Section 2.6. It is equipped with a simple quartz crystal microbalance to estimate the thickness of the deposited film. A precise measurement is considered not to be necessary as long as the deposited layer acts as bulk material.

As shown in Figure 5.7, the QCM crystal is far away from the sample. The crystal must not block the evaporant emitted towards the sample and also must not touch the housing which results in a geometry which is not advantageous. The positions suggest a non-homogeneous deposition on the sample. This leads to the situation where the calculation of the deposition rates in the positions of the oscillator crystal and the sample is futile since the response of the quartz crystal microbalance is not predictable in a way that honors the efforts compared to the needs of this setup.

Nevertheless, an entirely empirical approach is still reasonable, since it provides at least an estimate for the film thickness. The *tooling* factor t , *i.e.*, the quotient of

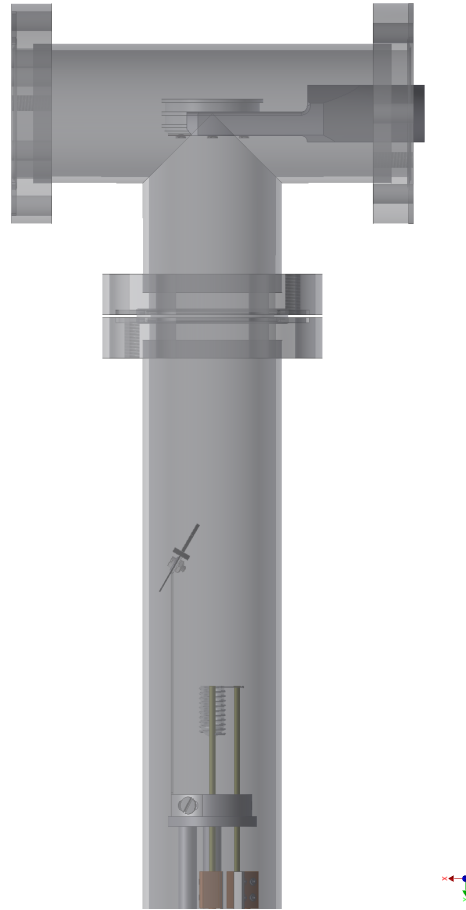


Figure 5.7: Schematic of the Load Lock Evaporator — The position of the crucible (bottom of the tube), the oscillator crystal (middle of the tube), and the sample (center of the tee-piece) in the load lock illustrates the need for an empirical approach to determine the thickness of the deposited layer on the sample.

the calculated deposition thicknesses on the crystal in the sample holder d_{sam} and on the evaporator d_{evap} ,

$$t_{\text{LL}} = \frac{d_{\text{sam}}}{d_{\text{evap}}} \quad (5.16)$$

provides a linear approximation if the deposition is carried out on a real sample since it rearranges to

$$d_{\text{sam}} = t_{\text{LL}} \cdot d_{\text{evap}} . \quad (5.17)$$

A commercial QCM crystal has been mounted in a polymer sample holder while a more cost efficient and readily mounted resonator crystal used in electronics, see Section 2.6, is attached to the evaporator. The evaporator was filled with perylenetetracarboxylic dianhydride (PTCDA) from former experiments and thus well degassed. The crystal on the evaporator has been monitored during the periods

Table 5.6: Tooling Factor of the Evaporator Quartz Crystal Microbalance in the Load Lock — Deposited thickness changes calculated from measured resonance frequencies of a QCM crystal in a sample holder δd_{sam} and mounted on the evaporator δd_{evap} are presented together with their ratios. The ratios' average represents the *tooling* factor t_{LL} used to calculate the thickness of a deposited layer on a β -polyvinylidene fluoride detector disc from the indicated thickness of the quartz crystal microbalance on the evaporator.

Thickness Change on QCM for		$\frac{\delta d_{\text{sam}}}{\delta d_{\text{evap}}}$
Sample	Evaporator	
38.9 nm	20.9 nm	0.535
99.5 nm	56.9 nm	0.572
100 nm	67.6 nm	0.673
97.9 nm	55.9 nm	0.571
96.2 nm	57.6 nm	0.598
103 nm	6.12 nm	0.597
Average:		0.60 ± 0.04

of simultaneous deposition. The frequency of the QCM crystal in the sample holder has been read the same way as in Section 5.3 before, after, and several times during deposition. The deposited thicknesses are calculated according to Equation (1.15) with a density of $\rho = 3.37 \cdot 10^3 \text{ kg}\cdot\text{m}^{-3}$ and the acoustic impedance of quartz $Z_{\text{q}} = 8.8 \cdot 10^6 \text{ kg}\cdot\text{m}^{-2}\cdot\text{s}^{-1}$ as a substitute for the unavailable value for PTCDA. Since the deposited layers only cause a small frequency shift, *i.e.*, less than 0.1 % of the usable range, the influence of the acoustic impedance can be neglected, as discussed in Section 1.3.6.

The relationship of the measured thicknesses on the two crystals is quantified in Table 5.6. The tooling factor evaluates to $t_{\text{LL}} = 0.60 \pm 0.04$ providing a sufficient estimate of the deposited thickness of the thin film.

5.5 Additional Instrumentation

This section gathers the characterization of the devices and instruments outside the vacuum system.

5.5.1 Digital Acquisition Card

Due to the fact that the most energies in this setup are calculated by power times duration it is advised to verify the time base of the measurement setup.

The 1 kHz output of an oscilloscope¹⁰ has been acquired with the standard measurement setup and positive flanks within one second were counted in the data.

Surprisingly, the expected amount of 1000 positive flanks was exceeded and found to be 1039. A cross check with a pulse counter in the electronic workshop resulted in 1040 events per second. Hence, the time base of the calorimetry measurement setup is correct and the time base of the oscilloscope should be adjusted.

The accuracy of the read voltage has been coarsely checked against a multimeter in all measurement ranges and no deviation could be found.

5.5.2 Laser Stability

All laser based measurements rely on the measured laser power and thus on its accuracy and the stability of the laser power output on a timescale of a calibration measurement.

The laser power was measured with two calibrated detectors, one was used direct¹¹, the other one¹² is attached to an integrating sphere¹³ on the same power meter¹⁴ giving exactly the same reading. A third uncalibrated power meter¹⁵ lend form another group showed a deviation of less than 1 %.

This results proves the accuracy of the reading of the power meter.

A typical calibration measurement, see Section 6.3, takes about five minutes which is the minimum requirement on the stability of the laser power.

The laser power was measured with the detector¹⁶ used for the calorimetric measurements and the data was recorded every second with the power meter¹⁷, for

¹⁰ 'HM 205' from HAMEG Instruments GmbH.

¹¹ '918D-SL-OD1' from Newport Spectra-Physics GmbH.

¹² '918D-UV-OD3' from Newport Spectra-Physics GmbH.

¹³ '819C-SL-3.3-CAL' from Newport Spectra-Physics GmbH.

¹⁴ '842-PE' from Newport Spectra-Physics GmbH.

¹⁵ 'Orion TH' from Ophir Optronics Solutions Ltd.

¹⁶ '918D-SL-OD1' from Newport Spectra-Physics GmbH.

¹⁷ '842-PE' from Newport Spectra-Physics GmbH.

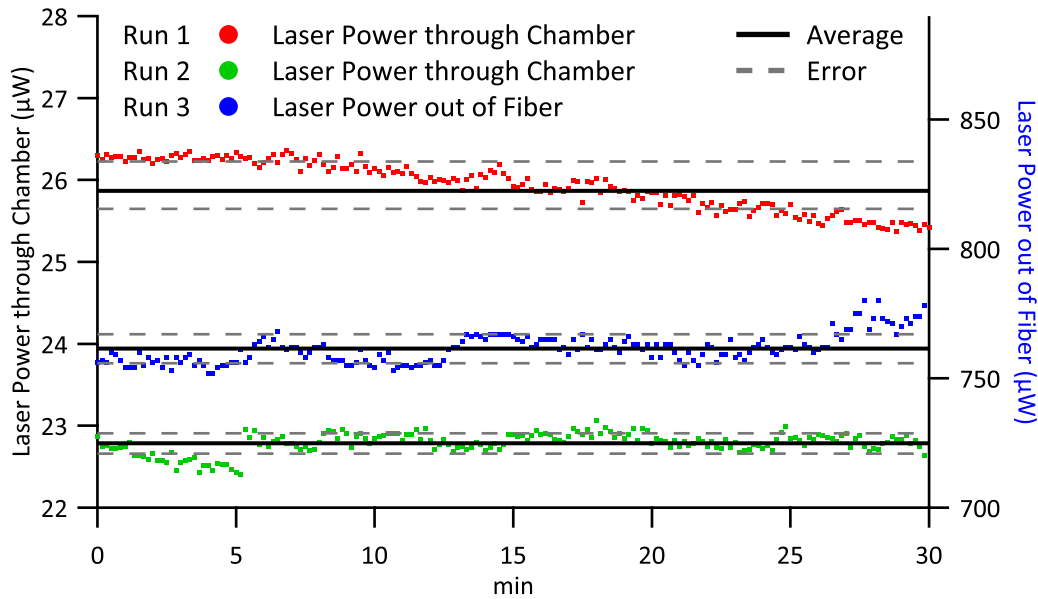


Figure 5.8: Stability of the Laser Diode — The power output of the laser diode^a measured with a calibrated power meter^b 30 minutes after startup (red, left axis), after three hours (green, left axis) through the chamber, as shown in Figure 5.29, and after four hours directly out of the fiber into the power detector (blue, right axis). While the stability is comparable to the stated^[151] 0.5% the first experiment has a much higher deviation. Additionally, the laser power dropped by approximately 15% within the first three hours. Since the fluctuations of the latter two experiments are similar, the transit of the laser beam through the chamber is not causing the scatter. The vertical axes cover the same relative range.

a 'iBeam405' from TOPTICA Photonics AG.

b '918D-SL-OD1' operated on '842-PE' both from Newport Spectra-Physics GmbH.

half an hour with the data stored in the meter and read out after the experiments. Two experiments used the configuration for the laser power measurement during a calorimetry experiment, see Figure 5.29, and the third one measured the output directly out of the fiber.

As illustrated in Figure 5.8 the intensity dropped during the first three hours in several steps with stable regions and appeared to be stable after this time. After this stabilization period, the laser reaches a stability level 0.6% comparable to the value stated in the manual^[151] of 0.5% over 30 minutes. This fulfills the requirement on the laser setup.

According to the manual, a stabilization period should not occur. Since this experiment indicates a looming problem with the laser diode and thus should be repeated regularly.

5.5.3 Amplifier

The amplifier is based on a monolithic ultra low input bias current instrumentation amplifier¹⁸ set to a gain of 100 and an input impedance of 5 G Ω . In the newest version under development, it is electrically isolated by a precision wide bandwidth isolation amplifier¹⁹ also serving as power supply for the instrumentation amplifier. In addition, it is configured to provide a selectable additional gain. The output is equipped with an active low pass filter set to 50 kHz. An automated offset correction forces the baseline to zero in less than 100 s.

The active material in the detector, see Section 1.3.3, changes its degree of polarization upon temperature changes and influences a compensating charge on the attached electrodes. The electrodes and the connecting wires form a capacitor with a total capacity of $C_{\text{tot}} = C_{\text{det}} + C_{\text{wire}}$ which is charged instantaneous upon heat input to the detector. This arrangement is discharged slowly by the load resistor R_L of the input amplifier. The time constant τ of the formed RC-circuit is given by $\tau = R_L \cdot C_{\text{tot}}$ and the voltage progression $U(t)$ is described by

$$U(t) = U(0) \cdot \exp\left(-\frac{t}{\tau}\right) \quad (5.18)$$

with the initial voltage $U(0)$ at the start of the discharge. It should be pointed out that Equation (5.18) is free of zero crossings and cannot describe the baseline discussed in Section 3.3.1.

Calculation with the experimental load resistance of $R_L = 5 \text{ G}\Omega$ and the total capacity of $C_{\text{tot}} = 0.9 \text{ nF}$, in which $C_{\text{det}} = 0.6 \text{ nF}$ and $C_{\text{wire}} = 0.3 \text{ nF}$ are gathered, yields a time constant of $\tau = 4.5 \text{ s}$.

The detector response has been measured at five different laser input powers. 50 frame pairs have been averaged in each measurement. The result is shown in Figure 5.9 illustrating the fast charging of the intrinsic capacitors during the pulse, *i.e.*, the positive linear parts in the figure, and the subsequent exponential decay. Evaluation of the latter regions results in a time constant of 0.44 s independent of the laser power and parity.

This value is in strong contrast to the theoretical value of 4.5 s. However, it agrees with the set time constant of 0.5 s of the secondary amplifier utilized at that time. This implies a change of the signal shape by the second amplifier. Since the calorimetric measurement and the reference measurements are affected in the same way, the perturbation should not affect the results. This assumption is supported by

¹⁸ ‘INA 116’.

¹⁹ ‘AD210’.

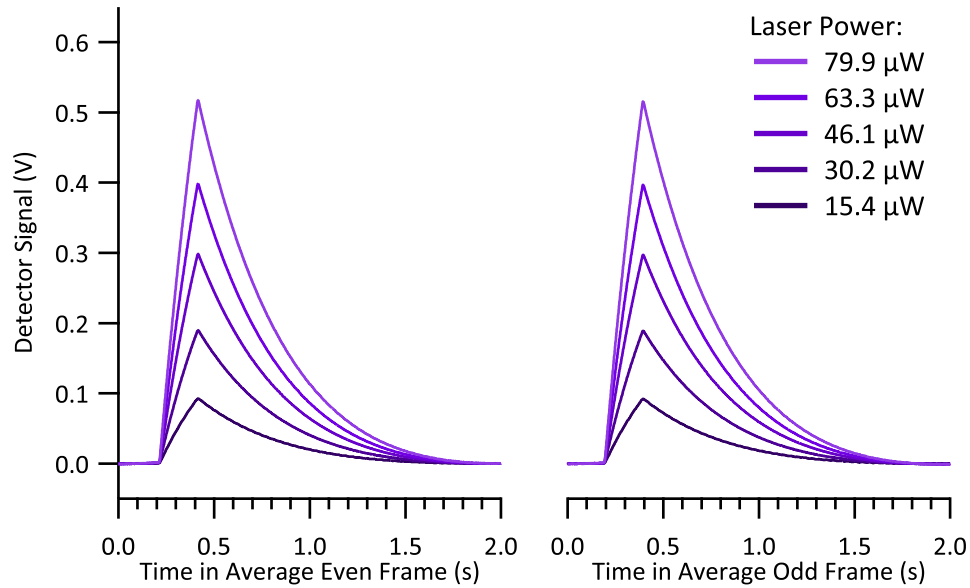


Figure 5.9: Voltage Response from the Detector — At each of five different laser powers 50 frame pairs were measured and averaged. While the slope of the positive flank is depending on the laser power and seems not to be limited, the subsequent exponential decay exhibits as a common time constant and is thus independent of the laser power. The data has been acquired utilizing a secondary amplifier.

the result of the linearity test, presented in Section 5.9.1.

After a reconfiguration of the measurement setup, it was possible to resign the second amplifier and acquire the raw signal without significant changes in the signal shape and quality.

It is advised to continue the development of the primary amplifier in order to obtain an optimal integration into the measurement equipment. This step should include a prevention of the oscillating baseline caused by the internal automatic offset correction mechanism. A possible approach could include a manually adjustable offset compensation.

5.6 Molecular Beam

The molecular beam is designed to deliver a high intensity, long term stable flux from a high volume Knudsen-cell in order to ensure a constant deposition rate. The source needs to be refillable while the vacuum in the main chamber is preserved. Furthermore, it has to provide a feature to convert the continuous flux into pulses of a user settable length. It also should contain an option to remove ions from the flux in case the utilized source is emitting ionized species.

5.6.1 Main Evaporator

Due to the construction-conditioned impossibility to measure the molecular flux during the reference and calorimetric measurements, the data evaluation relies on a constant flux from the source. Since the flux depends on the vapor pressure and thus it is correlated to the temperature of the crucible, a major requirement on the source is a well stabilized temperature.

The latter goal is achieved by use of a LABVIEW-based PID regulation of the power supplies with an accuracy of ± 0.1 K given by the accuracy of the temperature acquisition setup, as demonstrated in Figure 5.10. The graph also shows the excellent stability of the deposition rate with respect to time exhibiting a standard deviation of less than 2% within 27 hours. This is well sufficient for a calorimetric experiment running for about three hours.

Theory predicts a dependency of the flux on the filling level in the crucible and a detailed calculation of the evaporation characteristics of the evaporator can be found in [179]. In early experiments this behavior was foreshadowed but not fully verified. A major issue at this time was hauling of millimeter sized particles out off the evaporator onto the QCM oscillator crystal, as shown in Figure 5.11. Although the correction mechanisms of the QCM controller could handle a few particles on the crystal, operation time was reduced to about 60 minutes. This performance is already unacceptable by itself and also would render a meaningful calorimetric experiment impossible.

At this point a plug made from coarse stainless steel wool, as shown in Figure 5.12, has been installed in the crucible on top of the evaporant to avoid this misbehavior. The main purpose is to prevent emission of particles out of the crucible. Since it is obvious that this additional packing will reduce the conductance of the crucible above the evaporant, the flux is expected to be lessened. For all used materials it is possible to compensate the drop in deposition rate by a small increase of the crucible temperature.

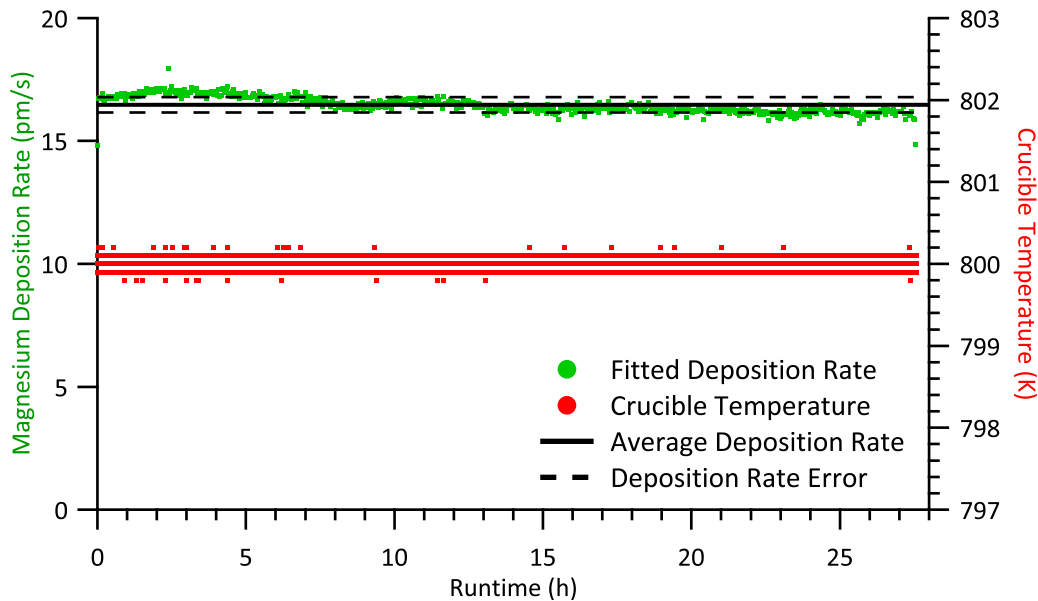


Figure 5.10: Deposition Rate and Temperature Stability — The thickness change during deposition of magnesium on a QCM crystal is converted to a deposition rate (green dots, left axis) by linear regression over 150 s intervals and exhibits an excellent stability, *i.e.*, less than 2% standard deviation from the average (dashed line), over a period of more than one day. The temperature of the crucible (solid line, right axis) is stabilized by a PID software^a and shows only fluctuations in the range of the temperature measurement uncertainty (± 0.1 K). The average deposition rate (black line, left axis) corresponds to 0.06 ML/s .

^a Programmed by H. ZHOU.

Furthermore, the plug acts as a throttling device maintaining a slightly higher pressure in the enclosed part of the crucible. This is supposed to lessen the dependency of the flux on the filling level of the crucible which is a highly desirable effect. Due to the frequent failures of the oscillator crystals without the stuffing, it was not possible to quantify this effect precisely.

A theoretical consideration of this situation is difficult and not productive since the influence of the steel wool is not well defined and can be compensated by an adjustment of the temperature of the crucible. Furthermore, the deposition rate is measured for every experiment and not calculated from the geometry and material properties.

In order to reduce maintenance, *i.e.*, refilling, of the source, it comprises a large crucible with a total volume of 13.8 cm^3 of which about 10 cm^3 can be filled with the evaporant. Table 5.7 lists some estimates for filling masses and runtimes. The given values only represent rough approximations since the masses fitting in the crucible

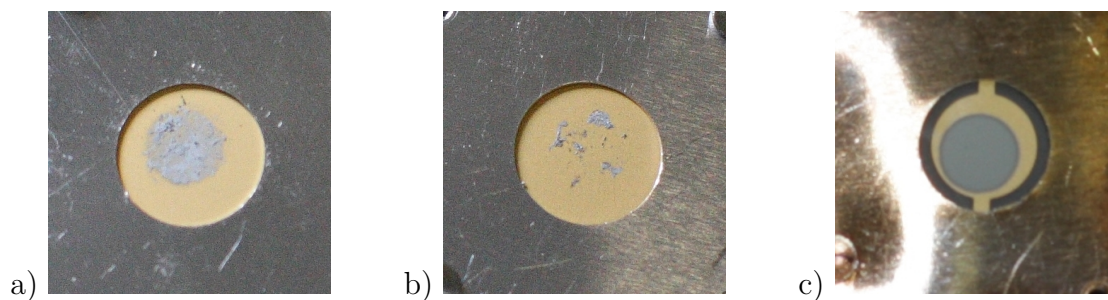


Figure 5.11: Photographs of “Spitted” Evaporant — Magnesium particles were “spitted” out of the evaporator and onto QCM crystals, causing them to fail. The visible golden area has a diameter of 8 mm. a) shows the deposition area and particles. b) only exhibits particles. c) demonstrates flawless deposition. In experiment c) the stainless steel wool has been applied and the QCM crystal is mounted upside down.

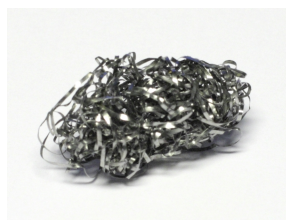


Figure 5.12: A photograph of the Steel Wool Plug — Steel wool^a with a diameter of 10 mm and a length of 20 mm is inserted in the crucible to prevent “spitting” of the evaporant and as a throttling device.

a ‘Topfreiniger 18/10’ from ALDI Einkauf GmbH & Co. OHG.

depend on grain size, shape, and packing behavior of the material. The runtime depends on the filled amount and the operation temperature which is expected to be varied along different experiments. Despite all these uncertainties, one can expect refilling of the evaporator about once per month which is in agreement with the latest usage of the beam source.

This evaporator version is used for magnesium, calcium, zinc, and lead in the form of flakes or pellets. For organic molecules the use of already present quartz crucibles in combination with a plug made from quartz fibers is recommended. A short evaluation concerning the usage of an electron beam evaporator²⁰ in the molecular beam, as mentioned in Section 2.3, is presented in Section 6.6.3 together with the discussion on experiments involving the deposition of copper.

²⁰ ‘EFM-4’ from FOCUS GmbH *via* Omicron NanoTechnology GmbH.

Table 5.7: Main Evaporator Fill Amounts — Masses of evaporants filling the main evaporator to the desired two thirds. Runtimes apply for a deposition rate of approximately 0.2 ML/s and are estimated over several operation conditions.

Substance	Filling	Runtime
Magnesium ^a	4.0 g	≈ 50 h
Calcium ^b	1.5 g	≈ 80 h
Zinc ^c	15 g	≈ 80 h
Lead ^{de}	20 g	> 20 h ^f
Copper ^{gh}	1.5 g	≈ 3 h

a ‘254118’ from Sigma-Aldrich Co. LLC.

b ‘327387’ from Sigma-Aldrich Co. LLC.

c ‘8780’ from Merck KGaA – discontinued.

d ‘p.a.’ from inorganic chemistry department.

e Without steel wool.

f Evaporator broken.

g ‘490DFL016-G-S5’ from Pfeiffer Vacuum GmbH.

h With a ‘C Mo M’ crucible in an ‘EFM-4’ electron beam evaporator from FOCUS GmbH *via* Omicron NanoTechnology GmbH.

5.6.2 Inline Valve

For routine maintenance of the molecular beam, *e.g.*, refilling of the main evaporator, it needs to be vented frequently. In order to preserve the vacuum in the main chamber, a valve is included, as mentioned in Section 2.3.4. Figure 5.13 visualizes the pressures in the main chamber measured with an ion gauge and the pressure in the fore-vacuum line measured with a Pirani gauge during a service vent of the molecular beam. The spike in the main chamber’s pressure at 2:00 *p.m.* indicates the closing of the valve and the step rise of the fore-line the actual venting. The pressure in the main chamber is maintained at 10 nPa during the five hour service meeting the requirements of an ultra high vacuum system. The spike in the fore-line pressure at 8:30 *p.m.* indicates degassing of the main evaporator while the slow rise of the pressure in the main chamber after 9:00 *p.m.* is attributed to degassing of the beam parts in the main chamber due to the bake-out after the venting procedure.

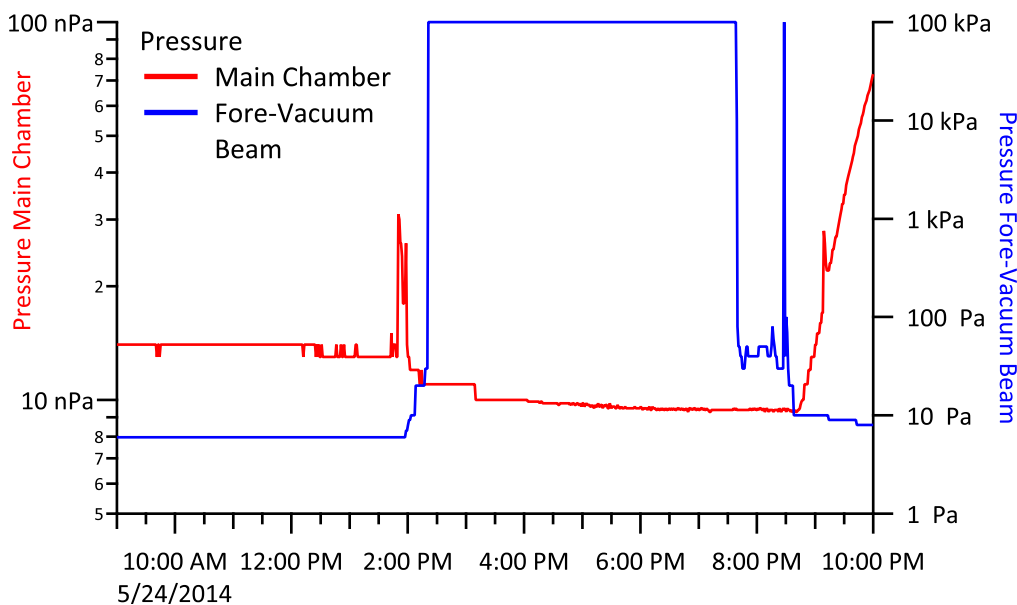


Figure 5.13: Performance of the Inline Valve — The pressure in the main chamber (red line) and the pressure of fore-vacuum line (blue line) of the molecular beam are shown for a service vent of the molecular beam. While the beam is at ambient pressure, the pressure in the main chamber is not affected. The subsequent increase arises from a bake-out of the beam.

5.6.3 Chopper

Considering a pulsed molecular beam there are three issues important to the mechanism converting the continuous output of the crucible into a periodic pattern.

The first aspect is the periodicity itself, *i.e.*, the position of the pulse in a frame. The controller of the chopper motor receives a start command from the controlling computer and starts the internal programmed routine containing a certain delay. An additional delay arises from the fact that the chopper does not open on the first step. If these delays are constant, it is possible to calculate a compensation and adjust the program to start the pulse at the desired time.

Second, the duration of a pulse is of major interest since it determines the amount of molecules in a pulse. While the exact length can be measured from the calibration measurements and also can be adjusted like the start delay, it would be fatal if the pulse length varies.

Third, the time from the closed to the open state and *vice versa* should be as small as possible to obtain the desired rectangular pulse shape.

Naturally, the chopper should be fully transmissive in the open state and completely blocking in the closed state.

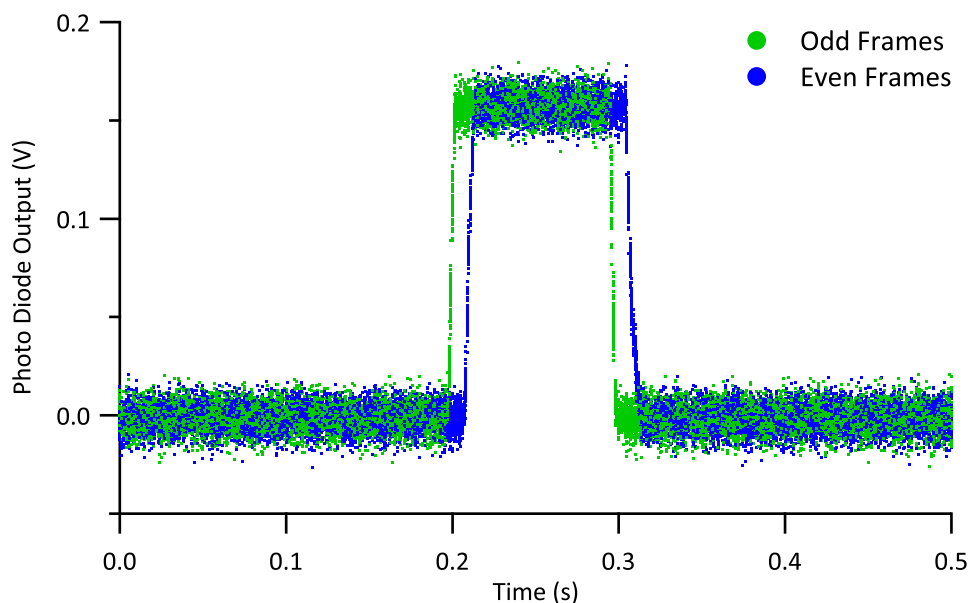


Figure 5.14: Performance of the Chopper: Photo Diode — 96 laser pulses measured with an external photo diode^a on a transimpedance amplifier for a power proportional output are displayed together. The pulse position and pulse length are constant for odd (green) and even (blue) pulses. The different position of the two subsets has been adjusted after this measurement. The fast switching is also clearly visible.

^a ‘PIN-10D’ from UDT Sensors, Inc. now OSI Optoelectronics.

Figure 5.14 demonstrates the reproducibility of the absolute position of the pulse in the frame. The position of the odd pulses is already adjusted to 200 ms. The position of the even pulses was adjusted after this measurement. The pulse length for both subsets is 97 ms measured at half intensity and was also adjusted to the desired 100 ms. The chopper opens and closes the beam within 3 ms. The shape matches the one obtained with the mass spectrometer in case of the line-of-sight measurement, see Figure 5.19 in Section 5.7.3.

In order to avoid systematic errors, this measurement should be repeated to ensure the accuracy of the chopper controller settings. As a misalignment of the laser path leads to a virtual shift in the peak position, it is advised to check the chopper position against a continuous mass spectrometer signal – see Sections 5.8.4, 6.3, and Appendix A – modulated by the chopper position. A baseline reference is given in case of a blocked molecular beam, *i.e.*, if the mirror/orifice stage is in reflection position, see Section 2.3.2. Full transmission is granted, if this stage is set to orifice position and the chopper is moved to the valve position. In normal operation, the chopper close positions should exhibit a mass spectrometer signal identical to the

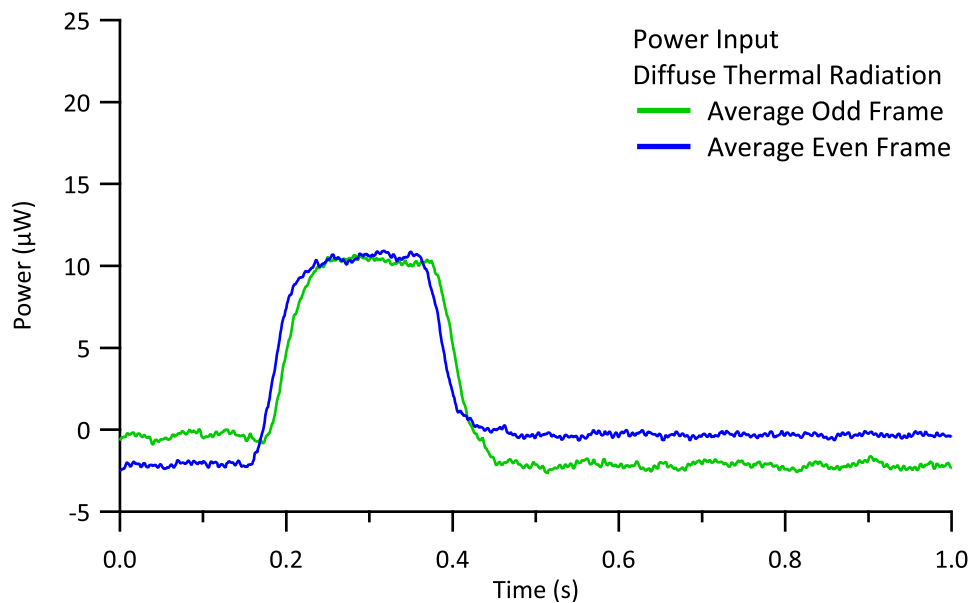


Figure 5.15: Performance of the Chopper: Deconvoluted, Diffuse Radiation — The power input of 44 averaged infrared radiation pulses measured through the barium fluoride window obtained by deconvolution is shown for even (green) and odd (blue) pulses. The direct radiation reaches the sample from 200 ms to 400 ms and causes a distinct peak. The base lines before and after the peaks are switched indicating a different power input during the off states.

baseline value. Analogue, the open position needs to show the same value as the full transmission reference.

Differing amplitudes indicate a misalignment of the chopper. In a second step, it should be verified that the pulse positions of laser pulses coincide with the positions of the mass spectrometer signal. These adjustments utilize the fact that the spread of molecules and laser light can be treated by geometrical optics. Implying correct adjustment, the chopper blade is blocking the beam or not.

In contrast to this behavior, the infrared radiation forms a diffuse background superimposing the direct infrared radiation from the evaporator. Figure 5.15 illustrates the power input on the detector by a deconvoluted radiation measurement, see Section 3.10. The direct radiation input between 200 ms and 400 ms causes a pronounced signal which is, in accordance to expectations, essentially rectangular. The base line level before and after the pulse changes in a way that the level before an even pulse becomes the level after an odd pulse and *vice versa*.

As shown in Figure 5.16, measurements with the laser have a common baseline. Since the setup is not changed, the difference arises solely from the chopper position. This leads to the conclusion that the diffuse radiative field is influenced in two

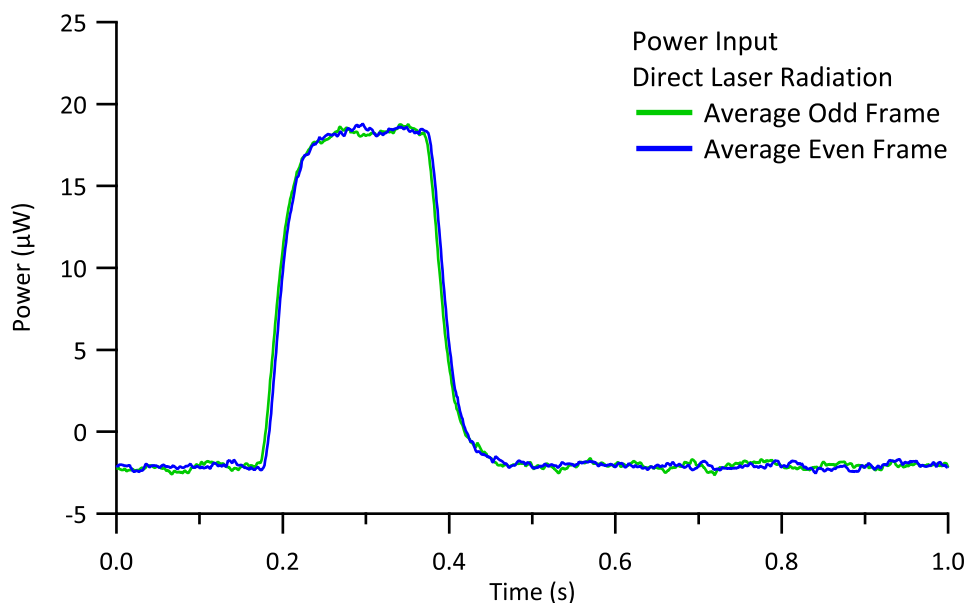


Figure 5.16: Performance of the Chopper: Deconvoluted, Direct Radiation — The power input of 46 averaged laser radiation pulses obtained by deconvolution is shown for even (green) and odd (blue) pulses. The laser radiation reaches the sample from 200 ms to 400 ms and causes a distinct peak. The base lines before and after the peaks are on the same level.

different ways for the two closed states. Furthermore, it implies a different yet respective “constant” input for the detector and thus an unequal peak shape for even and odd radiation pulses, as shown in Figure 5.23. Since the radiation participates in the calorimetry measurement, the peak shape of the calorimetry signal is also affected.

On first glance, this might appear as a vast drawback since it renders the data treatment more complicated. On second sight, it turned out to be beneficial since it allows to quantify the amount of radiation in a single calorimetric pulse from the peak shape even in case of changing infrared absorption of the sample, *e.g.*, an organic layer covered by a metal. Details on this procedure are given in Section 3.8.

Since the chopper has a default and a temporary close position, the thermal load of the evaporator is larger on the default position. This leads to a small temperature difference between the two legs of the chopper blade in case the used material is thin and exhibits a small thermal conductivity. Since the detector “sees” the chopper in the closed states it is also sensitive to the alternating radiation input from the two chopper legs. No influence is expected for calorimetric measurements at ambient temperature and has also not been observed. Experiments carried out at cryogenic sample temperature however might be sensitive to this effect manifesting

in a changing peak shape of a radiation measurement.

At the beginning the temperature gradient is established since one leg is heated by the evaporator and the other one is not. During the measurement the duty cycle for both legs is identical resulting in an identical heat input which leads to an adjustment of the temperatures. This implies an equal heat input in the closed states from the chopper²¹ and thus to a changed peak shape.

If this effect is observed, the chopper blade should be replaced by a copy made from aluminum in order to improve its thermal conductivity. This should lead to a more uniform temperature distribution prior to the start of the experiment.

5.6.4 Deflector Plates

The performance of the deflector plates has been tested with the standard main evaporator and the electron beam evaporator, as mentioned in Section 2.3.

The ratio α of ionized atoms to neutrals can be approximated by the Saha-Langmuir equation^[180]

$$\alpha = \frac{g_+}{g_0} \exp\left(\frac{e(\Phi - V_{\text{ion}})}{k_B \cdot T}\right). \quad (5.19)$$

The degeneracy of states for the ions is given by g_+ and for atoms by g_0 . The energy required to remove an electron from a neutral atom, *i.e.*, the ionization potential, is denoted by V_{ion} and Φ represents the electrostatic potential²² of the solid evaporant or the crucible, depending on which one is higher.

Table 5.8 lists the contribution of ions in the molecular beam and illustrates the absence of thermal ions for Magnesium and Zinc and a small contribution for calcium. However, if an electron beam evaporator is used the molecular beam may contain a larger contribution of ions due to electron collision ionization. In cases of the presence of ions their removal is possible with the deflector plates, see Section 2.3.5. The current resulting from the elimination of the ions can be chosen to monitor the amount of ions in a pulse. Together with the assumption of a constant generation rate it could be utilized to stabilize the flux of the source or to perform a relative *in situ* flux measurement. The current for the example with calcium from Table 5.8 computes to 0.7 pA which can still be measured with conventional methods.

Secondary, a dependency of the calorimetry signal on the plate voltage should have been investigated for the systems using copper as evaporant. Unfortunately, the used measurement device²³ was broken and no reliable data could be acquired.

²¹ But not from the radiative background field.

²² Multiplication by an elementary charge yields the work function.

²³ '6517' from Keithley Instruments Inc.

Table 5.8: Contribution of Ions to the Molecular Beam — The ionization probability according to Equation (5.19) is given for three substances and a stainless steel crucible with an approximate work function^a of 5 eV. Degeneracy is 2 for the ion and 1 for the ground state. The number of ions per pulse corresponds to a deposition rate of 0.1 ML/s and a pulse length of 200 ms.

Substance	Source Temperature	1 st Ionization Potential ^[182]	Ion Fraction α	Ions per Pulse	Ion Current
Magnesium	820 K	7.6 eV	$2 \cdot 10^{-16}$	$4 \cdot 10^{-4}$	$3 \cdot 10^{-22}$ A
Calcium	860 K	6.1 eV	$7 \cdot 10^{-7}$	$9 \cdot 10^{-5}$	$7 \cdot 10^{-13}$ A
Zinc	760 K	9.4 eV	$1 \cdot 10^{-29}$	$4 \cdot 10^{-17}$	$3 \cdot 10^{-35}$ A

a The work functions^[181] of the main alloy components iron, cobalt, and nickel are all close to 5 eV.

Since no ion contribution is expected for a thermal source, this is no drawback for the presented work.

This measurement should be repeated if an electron beam evaporator is used, since it is known for this kind of source to emit ions²⁴.

5.6.5 Evaporator Radiation in Reference Measurements

As Section 5.6.3 indicated and Section 5.8.1 will demonstrate, the infrared radiation from the evaporator causes a difference in the shape of the detector response in the radiation measurement. This rises the question if it also influences the laser reference measurements. Since the infrared radiation induces an asymmetry between odd and even pulses the laser based measurements could also carry this signature.

During radiation measurements the optics stage, see Section 2.3.2, the orifice is aligned with the axis of the molecular beam to let molecules pass while the holder of the mirror is blocking the direct path for radiation and molecules. The laser is reflected towards the sample interrupted by the chopper to form pulses. The crucible temperature has been varied between 500 K and 830 K and the measured 46 pulse pairs for each temperature have been averaged.

Figure 5.17 displays the acquired averages scaled to same intensity and offset. All traces exhibit the same shape leading to the conclusion that the laser based measurements are not influenced by the radiation from the main evaporator. Due to fluctuations in the laser power a quantitative analysis has not been possible.

²⁴ The ‘EFM-3i’ from FOCUS GmbH comes with an ion suppression feature.

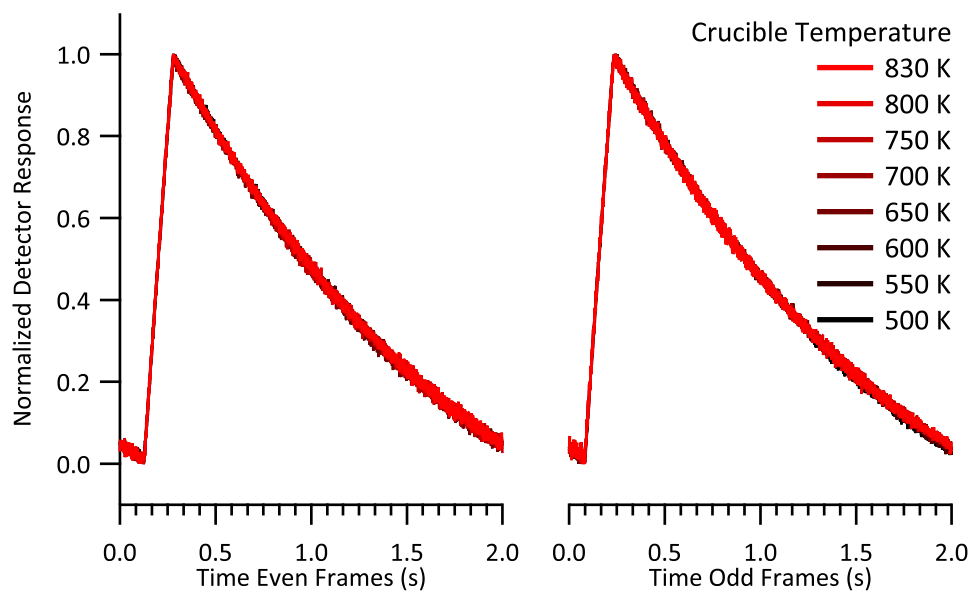


Figure 5.17: Crucible Radiation in Laser Measurement — A laser reference measurement, see Section 3.5.4, has been performed for several crucible temperatures. After normalization with respect to the absolute amplitudes, no influence of the infrared radiation on the averaged laser based data is detectable.

5.7 Mass Spectrometer

The molecular flux from the beam source is diffusely reflected by the hot plate and a fraction of the initial flux reaches the mass spectrometer. In order to estimate the necessary sensitivity the partial pressure of the evaporated species at the entrance of the mass spectrometer should be considered. Consequently, the influence of the settings of the mass spectrometer around the obtained estimate are investigated.

Additionally, effects of the chopper on the pulse shape are discussed. The influence of the hot plate on the mass spectrometer signal is discussed in detail in Section 5.8.4.

5.7.1 Intensity Estimation

Starting with the molar dose per pulse D_{mol} and the pulse length t the deposition rate on the hot plate J in Atoms/s is given by

$$J = \frac{D_{\text{mol}} \cdot N_{\text{A}}}{t} . \quad (5.20)$$

These molecules pass the half sphere around the hot plate with the radius r equivalent to the distance to the mass spectrometer with a surface area A of

$$A = \frac{1}{2} \cdot 4\pi \cdot r^2 \quad (5.21)$$

leading to the impingement rate j assuming a cosine distribution for the emission from the hot plate

$$j = \frac{J}{A} \cos(\vartheta) = \frac{J}{2\pi \cdot r^2} \cos(\vartheta) \quad (5.22)$$

with the angle ϑ to its surface normal. This includes the approximation of a small opening of the mass spectrometer compared to the size of the half sphere leading to a constant $\cos(\vartheta)$. The impingement rate is also defined by

$$j = \frac{p}{\sqrt{2\pi \cdot m \cdot k_{\text{B}} \cdot T}} \quad (5.23)$$

by the pressure p , the mass m of the molecule at the temperature T . Combination of Equations (5.20), (5.22) and (5.23) yields after rearrangement

$$p = \frac{D_{\text{mol}} \cdot \cos(\vartheta)}{2\pi \cdot r^2 \cdot t} \cdot \sqrt{2\pi \cdot m k_{\text{B}} \cdot T} \quad (5.24)$$

as an expression for the expected pressure during a pulse in the mass spectrometer.

With the geometry of the experimental setup of $r = 73$ mm, $\vartheta = 40^\circ$, and typical values for parameters for deposition of magnesium of $t = 0.2$ s, $D_{\text{mol}} = 1.5 \cdot 10^{-11} \frac{\text{mol}}{\text{pulse}}$, and a temperature of the magnesium atoms equal to the hot plate temperature of $T = 850$ K, the pressure computes to $p = 6 \cdot 10^{-8}$ Pa = $6 \cdot 10^{-10}$ mBar.

In order to treat the electron multiplier in the mass spectrometer gently and to maintain some reserve, it was operated at the beginning at medium voltages, *i.e.*, between 1000 V and 1500 V, compensated by a higher sensitivity level, *i.e.*, the “Range: 10^{-12} mBar” instead of the “Range: 10^{-10} mBar” setting, suggested by the calculation. In addition, the mass spectrometer suffered from some sensitivity loss due to its usage before it was attached to this machine. It should be mentioned that the mass spectrometer software gives a pressure read out but, since it is not calibrated and can be influenced by the multiplier voltage, its absolute value has no significance. Hence, this work internally uses volts for the mass spectrometer’s intensity and the data treatment software uses relative intensities, where possible.

5.7.2 Mass Spectrometer Settings

For early experiments the multiplier voltage was increased to a level where the 0 – 10 V analogue output of the mass spectrometer reached about 8 V to make use of the full measurement range of the data acquisition card. A detailed examination of the data revealed some “specialties”. The noise level during the on-state of the pulse was slightly lower than during the off-state and the peak shape seemed to change with intensity. Due to the rather poor noise level of the mass spectrometer’s signal in general, these subtle features remained hidden, until the replacement of the tantalum version of the hot plate by the sapphire version and the subsequent necessary recharacterization of this device.

Zinc has been dosed on the hot plate held at 900 K using a deposition rate of 0.1 ML/s . The signal of the mass spectrometer has been recorded altering the range setting of the mass spectrometer and the sample rate of the signal. The voltage of the secondary electron multiplier has been adjusted to the range setting.

The difference in the signal is illustrated in Figure 5.18 recorded at an increased sample rate of 10 kHz instead of the typical 1 kHz. While the envelopes and the reduced, *i.e.*, a piecewise average of ten data points, from the data set corresponding to the “Range: 10^{-12} mBar” setting match the peak shape of the data set corresponding to the “Range: 10^{-11} mBar” setting, the raw data differs significantly. The major component in this case is a high amplitude 1 kHz-sine while the actual measurement related information is modulated onto this signal as an offset. As demonstrated the

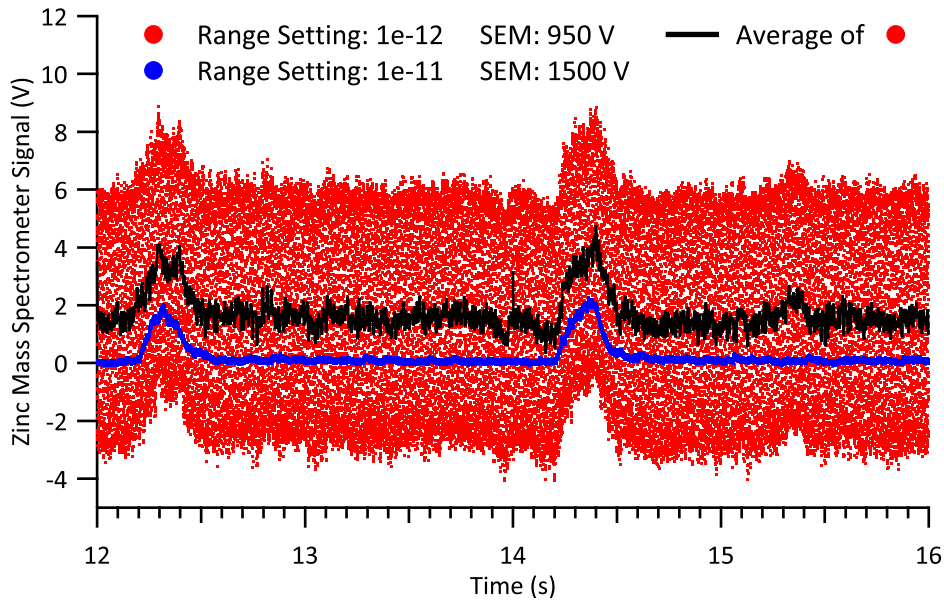


Figure 5.18: Influence of the Mass Spectrometer's Range Setting — Two pulse pairs of dosed zinc ($m/z = 64$) at unchanged experimental settings are recorded with 10 kHz with two range settings and adjusted electron multiplier settings of the mass spectrometer. The envelopes of the data set corresponding to the “Range: 10^{-12} mBar” setting (red) and its average over ten data points (black) match the data set measured with the “Range: 10^{-11} mBar” setting (blue). The former contains a vast contribution of a 1 kHz sine dominating the data and resulting in clipping of the signal at 10 V already for medium average intensities.

signal quality can be enhanced by oversampling, compare the red and black traces in Figure 5.18. However, this method fails if the envelope reaches the voltage limit of the analogue output or input circuit and gets limited by internal protection devices. In this case the averaged value is still in a safe appearing range but the linearity of the signal to the physical input is nullified and renders the measurement useless.

Since the measurement software included an unmonitored down sampling of the data this issue was not easy to discover. As consequences of this finding the display of the envelopes has been added and the measurement parameters are altered towards the “Range: 10^{-11} mBar” setting. At this setting the contribution of the 1 kHz component is small enough not to interfere with the sampling. If additional Nyquist-Shannon sampling noise is detectable, the measurement software can be configured to use over sampling in order to avoid this effect. Typical electron multiplier voltages extend from 1500 V to 1900 V.

5.7.3 Mass Spectrometer Peak Shape *vs.* Pulse Length

The chopper in the molecular beam opens and closes the beam path periodically allowing molecules to pass or not. Due to the finite switching times a trapezoidal signal profile is expected. A variation of the pulse length is expected to change only the width of the profile independent of operation settings and material.

Magnesium with a deposition rate of 0.3 ML/s has been dosed directly into the ion source of the mass spectrometer relocated to the position of the detector port and the intensity of the impinging magnesium has been recorded for 23 pulse pairs. In this case the mass spectrometer was set to “Range: 10^{-8} mBar ”. The pulse length has been varied between 100 ms and 300 ms in steps of 50 ms.

The operation voltage of the secondary electron multiplier in the mass spectrometer had been set to a level of maximal amplitude without clipping of the signal due to the 1 kHz component, mentioned in Section 5.7. The used mass spectrometer has a temporal resolution of about $\tau_0 = 5 \text{ ms}$ during software^[183] acquisition and about 1 ms for the analogue output.

As shown in Figure 5.19, the recorded peaks exhibit a trapezoidal shape with minor steps in the peak edges arising from the discrete movement of the chopper motor, similar to the measurement using laser and the photo diode, see Figure 5.14. A small variation of the total intensity is attributed to instabilities of the molecular flux, since, at the time of the measurements, several improvements had not been implemented yet.

The result matches the expectation and the observed temporal resolution exceeds the one stated in the manual.

In a similar experiment, calcium with a deposition rate of 0.3 ML/s has been dosed onto the hot plate held at 1180 K and the intensity of the desorbed calcium has been recorded for 23 pulse pairs. In this case the mass spectrometer was set to “Range: 10^{-11} mBar ”. The pulse length has been varied between 100 ms and 305 ms in steps of approximately 50 ms.

Again, the operation voltage of the secondary electron multiplier in the mass spectrometer has been set to a level of maximal amplitude without clipping of the signal, due to the 1 kHz component mentioned in Section 5.7.

The intensity of the obtained signal is not constant during the transmissive phase of the chopper, as illustrated in Figure 5.20. It exhibits an exponential increase early in the pulse and an exponential tail after the pulse. The initial phase of the signal exhibits a similar shape for all investigated pulse lengths. The subsequent evolution depends on the duration of the pulse. At long exposure times, the maximal

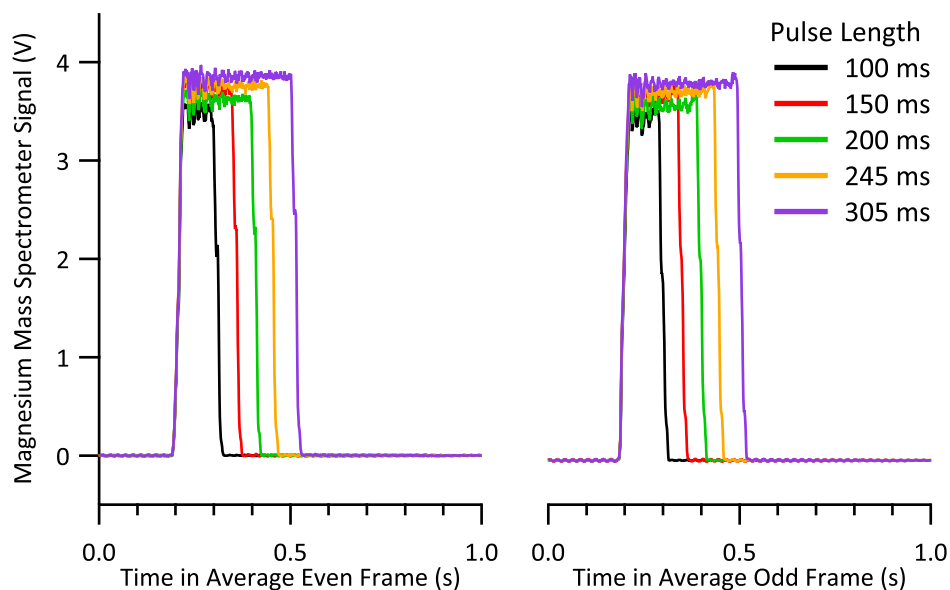


Figure 5.19: Influence of the Pulse Length on the Mass Spectrometer Signal: Direct Dosing — The averages of 23 frames recorded with five different pulse lengths of magnesium ($m/z = 24$) dosed directly into the mass spectrometer are opposed to each other. The trapezoidal peak shape is modulated with minor steps corresponding to the single motor steps. The differences in amplitude are attributed to instabilities of the molecular flux. A constant base line has been removed.

amplitude seems to approach a plateau.

The dependence of the signal shape on the pulse length is unexpected, especially considering the previous experiment. Two alterations of the experimental conditions come into consideration. On the one hand, the usage of the hot plate could influence the signal shape, *e.g.*, due to transient adsorption. On the other hand, it might be an artifact due to the change of the range setting in the mass spectrometer. This modification of the experimental conditions is inevitable as the direct flux into the mass spectrometer is significantly higher than the flux created by the diffuse reflection of the beam. Although the first possibility seems more likely, the changed signal shape is an artifact arising from the changed range setting. A detailed discussion about this effect is given in Section 5.8.4.

As a consequence of the altered signal shape, it is questionable whether the measurement results are proportional to the dosed amount of molecules which itself is proportional to the pulse length at constant deposition rate.

The data sets from the previous experiment have been corrected for the deposition rate of the molecular beam and individual constant offsets have been removed.

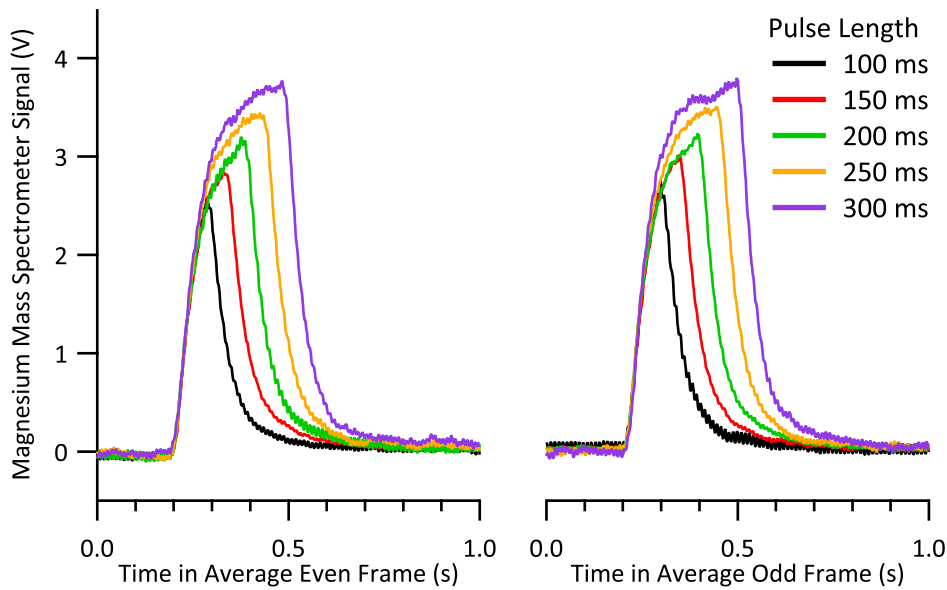


Figure 5.20: Influence of the Pulse Length on the Mass Spectrometer Signal: Indirect Dosing — The averages of 23 frames recorded with five different pulse lengths of calcium ($m/z = 40$) dosed on the hot sapphire plate are opposed to each other. The final output voltage is not reached for the short pulse lengths and a settling of the output is not completed at 300 ms. The difference in amplitude for the longer pulse length is attributed as an artifact arising from the increased base pressure. Individual constant base lines are removed.

The proportionality of pulse length and integrated mass spectrometer signal is demonstrated in Figure 5.21. As a finding of this measurement, it is concluded that the change in signal shape is not affecting the proportionality required for mass spectrometer measurements.

An investigation about the proportionality of the mass spectrometer signal to the molecular deposition rate is presented in Section 5.7.3.

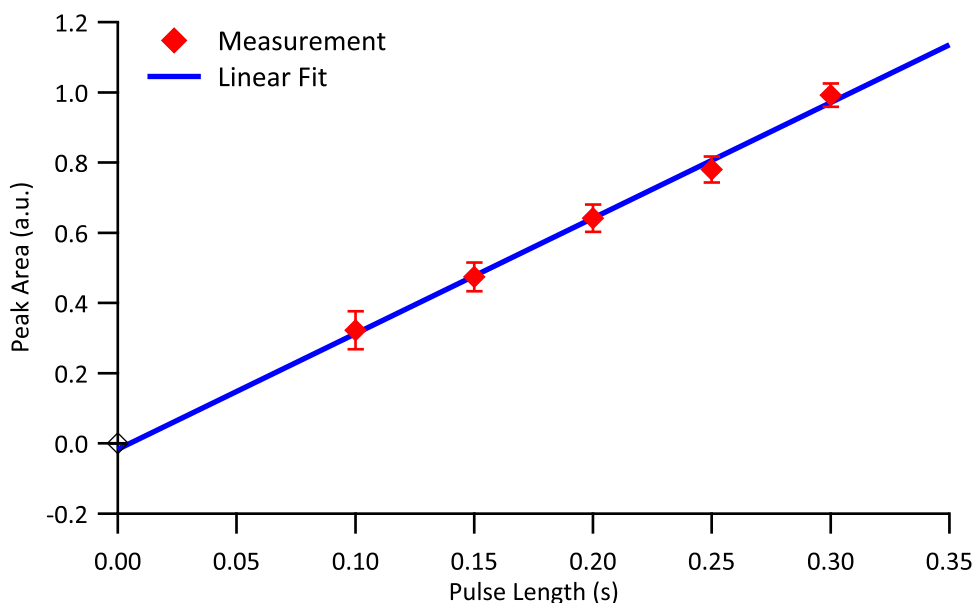


Figure 5.21: Integrated Mass Spectrometer Signal *vs.* Pulse Length — The missing intercept of the fit (line) for the offset corrected peak areas (diamonds) from Figure 5.20 indicates a proportional increase with the pulse length.

Linearity Regarding Deposition Rate

The determination of the sticking factor is relying on a response from the mass spectrometer which is proportional to the amount of the dosed species repelled from the sample. Since the geometry is fixed and the mass spectrometer is placed line-of-sight to the sample, the pressure at its location is certainly proportional to the fraction of the dosed molecules leaving the sample. Since mass spectrometers are widely used to measure partial pressures, it is assumed that the output is proportional to the pressure and thus the requirement is fulfilled. The commonly applied corrections regarding varying ionization probabilities of chemical species are irrelevant, since the temporal trend of one species is regarded in this setup.

The average intensity of the mass spectrometer from various zero sticking measurements with 25 frame pairs each of calcium as a function of the corresponding deposition rate is displayed in Figure 5.22. All presented measurements used a **SEM Voltage** of 1800 V. The data sets are analyzed similar to a sticking measurement with the set corresponding to the highest deposition rate chosen as reference.

A linear regression (solid blue line) of the obtained relative intensities does not include the origin. The forced proportional fit, *i.e.*, with a vanishing intercept, (dashed green line) is not representing the response of the mass spectrometer well. Although the temperature of the hot plate (color code) varied between 1150 K and

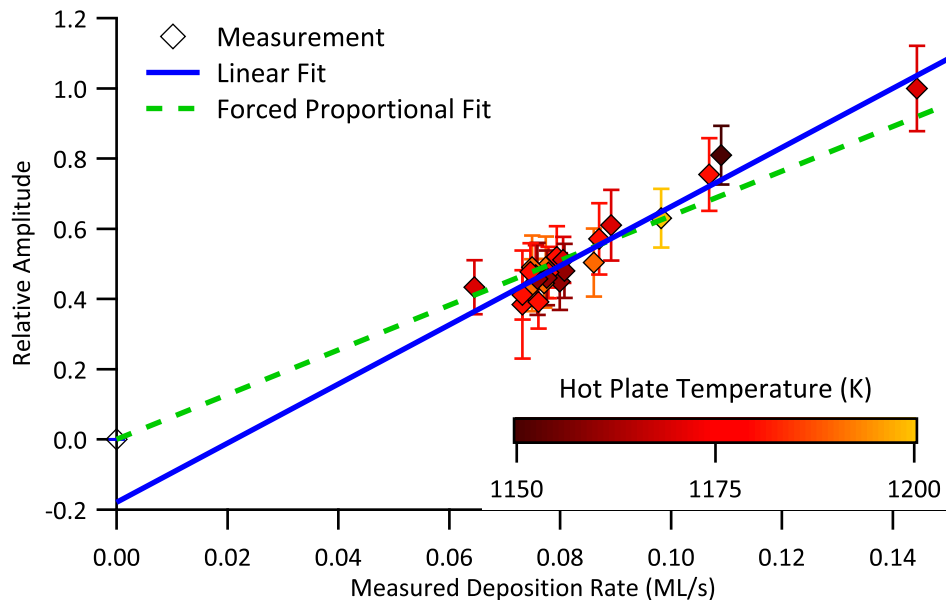


Figure 5.22: Mass Spectrometer Linearity Regarding Deposition Rate — The relative^a mass spectrometer response^b for calcium ($m/z = 40$ – diamonds) is plotted versus the measured and corrected deposition rate from the molecular beam source. In case of an assumed proportionality (dashed green line) the model seems to underestimate the relative intensity at higher deposition rates. A less restrictive linear approximation (solid blue line) is added for comparison. Since this is a meta analysis the temperature of the hot plate (color coded) varied but no distinct influence is observable. The error corresponding to the deposition rate is smaller than the data points.

a To the maximal observed intensity.

b SEM at 1800 V.

1190 K, no significant influence can be observed. The rather unflattering range of examined deposition rates is owed to the fact that no dedicated measurement could be performed so far.

Since the presented data suggests a hint towards a non-proportionality of the mass spectrometer, a dedicated experiment should be conducted²⁵. The temperature of the hot plate should be stabilized and the deposition rate varied over a wider range to obtain a more meaningful statement.

²⁵ A posterior experiment performed by H. ZHOU confirmed the here observed indication of a non-proportional response of the mass spectrometer.

5.8 Ancillaries Stage

Several ancillary, *i.e.*, referencing, measurements are necessary to calculate the heat of adsorption from the calorimetric measurement. The performance of the individual components is evaluated and compared to expected achievements. According to the general design concept to preserve the sample in the measurement position during the ancillary measurements, it might be necessary to correct for geometrical aspects in some of the measurements.

5.8.1 Infrared Transparent Window

Knudsen-type effusion cells, here, the main evaporator as described in Section 2.3.1, are operated at elevated temperatures and thus are emitting electromagnetic radiation. For an ideal emitting source this is black body radiation. The spectral radiance B at a certain wavelength λ of this radiation only depends on the temperature T of the body. Normalized to emitting surface area and solid angle, Planck's law includes the radiance normal to the surface in

$$B(\lambda, T) \, d\lambda = \frac{2h \cdot c^2}{\lambda^5} \frac{1}{\exp\left(\frac{h \cdot c}{\lambda \cdot k_B \cdot T}\right) - 1} \, d\lambda \quad (5.25)$$

as a function of wavelength. Accounting for the wavelength dependent emissivity $\epsilon(\lambda)$ of the emitting material one yields

$$B(\lambda, T, \epsilon) \, d\lambda = \epsilon(\lambda) \frac{2h \cdot c^2}{\lambda^5} \frac{1}{\exp\left(\frac{h \cdot c}{\lambda \cdot k_B \cdot T}\right) - 1} \, d\lambda . \quad (5.26)$$

Application of the gray body approximation, *i.e.*, a wavelength independent emissivity with $0 < \epsilon < 1$, and integration of the modified Planck equation, see Equation (5.26), by wavelength²⁶ leads to the Stefan-Boltzmann-law describing the emitted power of a convex body

$$\begin{aligned} P &= k' \cdot A \cdot \epsilon \frac{2\pi^5 \cdot k_B^4}{15c^2 \cdot h^3} \cdot T^4 \\ &= k' \cdot A \cdot \epsilon \cdot \sigma \cdot T^4 \end{aligned} \quad (5.27)$$

²⁶ Integration by emitting area, solid angle, and emission angle is also performed but, due to the fixed geometry, this ends up as a constant in the formula.

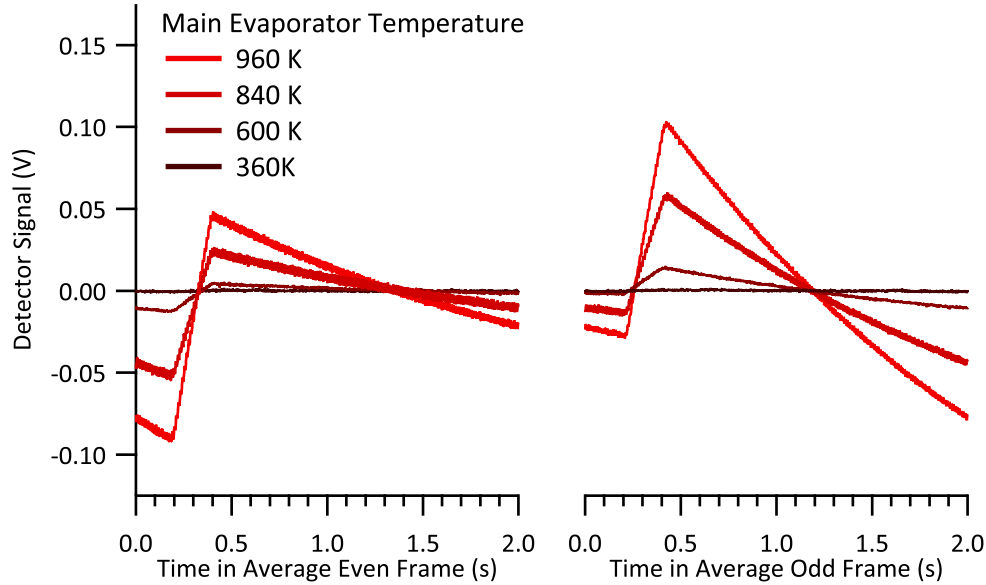


Figure 5.23: Temperature Dependence of Radiation — Averaged detector signals of pure radiation emitted from the main evaporator are shown for several operation temperatures of the crucible. The asymmetry of even (left) and odd (right) frames is clearly visible as well as the vanishing intensity for small temperatures.

with k' covering all geometric components specific to the fixed experimental setup, except the emitting area A . Natural constants are gathered in the Stefan-Boltzmann constant σ .

In order to characterize the transmission of the window in front of the sample, see Section 2.4.4, infrared radiation has been pulsed on pristine nickel coated β -polyvinylidene fluoride detector polymer held at 307 K. As source of radiation an empty crucible with a stainless steel wool plug, see Section 2.3.1 has been employed at temperatures between 360 K and 960 K. Since the sample is facing the plug's surface in both cases, a differing emissivity of the evaporant compared to the crucible can be neglected.

Every set for a window/temperature combination consists of 100 single pulses with the first and last pair omitted. This standard procedure for reference measurements reduces baseline artifacts. The remaining frames, with removed outliers, see Section 3.5, are averaged and processed. Examples for the averaged data is shown in Figure 5.23 for different temperatures of the crucible.

The data treatment follows the routine for the transmission measurement in a calorimetric experiment, see Section 3.5.5, with the unperturbed radiation as laser reference and the filtered radiation as transmission measurement. Thus, the obtained

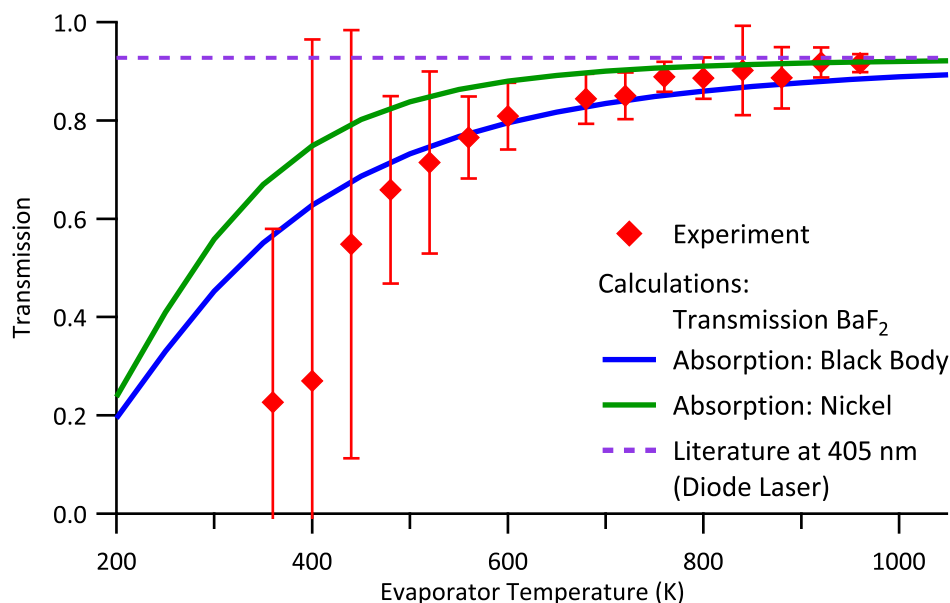


Figure 5.24: Transmission of the Barium Fluoride Window — The measured transmission (diamonds) of the barium fluoride window as a function of the molecular beam source is opposed to the theoretical values in a broad temperature range for an opaque nickel (green line) and a black body (blue line) surface. Relevant for this work are temperatures above 600 K. The experiment matches the theory well at these temperatures. The huge error bars at low temperature arise from vanishing signal intensity. For comparison to the laser based measurement the transmission of the window at 405 nm (dotted purple line) is added.

transmission is the ratio of the averaged signal intensity with the window in the beam path to the averaged intensity without the window. Figure 5.24 displays the results of the measurement for a wide temperature range.

Measured Window Transmission

Three effects need to be considered to obtain an estimate for the theoretical transmission of the barium fluoride window for a certain evaporator temperature. On the one hand, the radiation from the crucible has a temperature dependent emission spectrum. Second, the transmission $\tau_{\text{BaF}_2}(\lambda)$ of barium fluoride is a function of the wavelength, as shown in Figure 5.25, which results in a wavelength specific attenuation. Finally, the absorption $\alpha_{\text{Ni}}(\lambda)$ of the nickel surface which is also wavelength dependent needs to be included.

In the experimental case the total transmission T is given as the ratio of the unfiltered I_0 and filtered I_{win} signal intensities absorbed by the detector. The signal

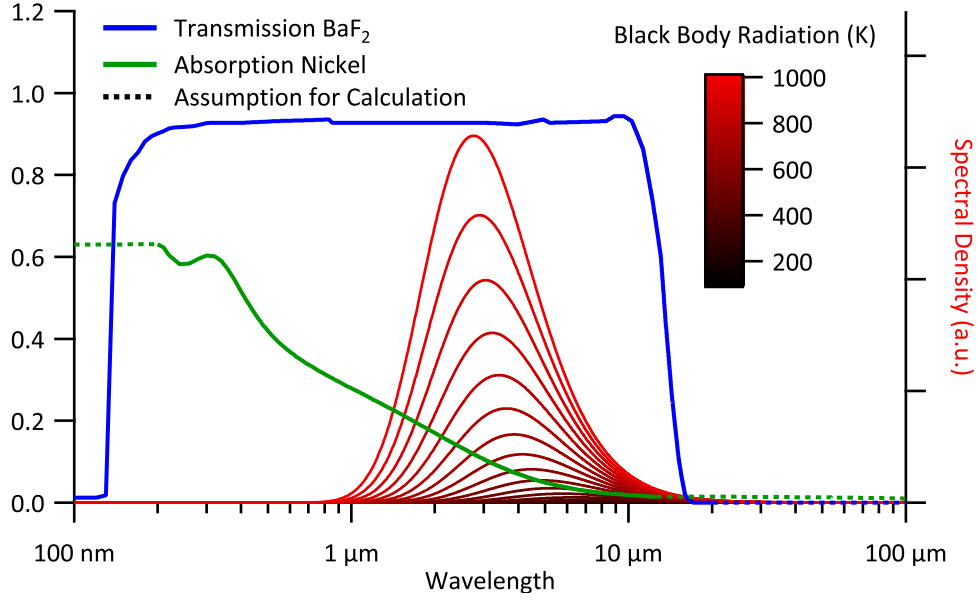


Figure 5.25: Wavelength Dependent Parameters — The tabulated coefficients for transmission of barium fluoride^[184] (blue line, left axis) and absorption of nickel^[165] (green line, left axis) as a function of wavelength are opposed to calculated black body spectra (black to red lines, right axis). The majority of the emitted radiation lies in the highly transmissive spectral region of barium fluoride. The absorption coefficient for the nickel surface is rather small for the wavelengths of the emitted radiation. Together this suggests only a minor dependency of the measured radiation contribution on the source's temperature in case of elevated temperatures.

intensities are proportional to the power irradiated onto the sample assuming a constant pulse length. Utilizing the radiance B as in Planck's law, see Equation (5.25), in combination with a gray-body approximation, *i.e.*, a constant emissivity $\epsilon_{\text{cr}} < 1$, for the crucible the transmission can be written as

$$\begin{aligned}
 T &= \frac{I_{\text{win}}}{I_0} = \frac{\int B_{\text{win}}(\lambda, T) d\lambda}{\int B_0(\lambda, T) d\lambda} \\
 &= \frac{\int \alpha_{\text{Ni}}(\lambda) \tau_{\text{BaF}_2}(\lambda) \epsilon_{\text{cr}} \frac{2hc^2}{\lambda^5} \frac{1}{e^{\frac{hc}{\lambda k_B T}} - 1} d\lambda}{\int \alpha_{\text{Ni}}(\lambda) \epsilon_{\text{cr}} \frac{2h \cdot c^2}{\lambda^5} \frac{1}{\exp\left(\frac{h \cdot c}{\lambda \cdot k_B \cdot T}\right) - 1} d\lambda}
 \end{aligned}$$

$$\begin{aligned}
& \int \alpha_{\text{Ni}}(\lambda) \tau_{\text{BaF}_2}(\lambda) \frac{1}{\lambda^5} \frac{1}{\exp\left(\frac{hc}{\lambda k_B T}\right) - 1} d\lambda \\
&= \frac{\int \alpha_{\text{Ni}}(\lambda) \frac{1}{\lambda^5} \frac{1}{\exp\left(\frac{h \cdot c}{\lambda \cdot k_B \cdot T}\right) - 1} d\lambda}{\int \alpha_{\text{Ni}}(\lambda) \frac{1}{\lambda^5} \frac{1}{\exp\left(\frac{h \cdot c}{\lambda \cdot k_B \cdot T}\right) - 1} d\lambda} . \quad (5.28)
\end{aligned}$$

Numerical integration is necessary at this point since the weight functions for transmission^[184] $\tau_{\text{BaF}_2}(\lambda)$ and for absorption^[165] $\alpha_{\text{Ni}}(\lambda) = 1 - \rho_{\text{Ni}}(\lambda)$ are not given in an analytical form. Figure 5.24 superimposes the spectrum of the emitted radiation with the used weight functions. The nickel layer is assumed to be opaque in this calculation.

The obtained total transmission of the window matches the theoretical values for elevated temperatures on the nickel surface (green line in Figure 5.25). The blue line represents a black coating, *i.e.*, $\alpha(\lambda) \equiv 1$, of the detector. This approximation is appropriate for thick layers of organic dyes deposited on the detector.

At the lower end of the measured temperature range almost no signal from infrared radiation is observable, as demonstrated in Figure 5.24, leading to the huge error bars in this range. Despite the error bars still covering the calculated values, it seems that the transmission drops faster than expected. A possible explanation for this discrepancy is the increasing transmission through the nickel coating at high wavelengths^[163] which is not included in the model. In order to cover this effect, the copper interlayer, the absorption of β -polyvinylidene fluoride, the similar layered back side, and wavelength dependent interference phenomena would have to be considered, highly exceeding the scope of this work.

Comparison with the transmission for the light of the laser diode used in the setup, see Section 2.3.2, reveals a similar transmission only for elevated evaporator temperatures. Since the standard data processing routine does not rely on the exact value of the transmission, it is only necessary for treatment with fixed used transmission, see Section 3.8. It should be mentioned that this consideration is done for a clean window and the invertible soiling due to the measurement process complicates the situation.

Total Measured Intensity

In addition to the total transmission, the dependency of the total infrared radiation intensity on the evaporator temperature is investigated.

The net power P on the detector comprises the power adsorbed by the detector from the crucible P_{cr} and the power emitted from the detector P_{det} into the crucible.

Both quantities have to be multiplied by a view factor F to cover geometrical aspects, and an exchange factor E to handle emissivities.

$$\begin{aligned} P &= P_{\text{cr}} - P_{\text{det}} \\ &= \sigma E F T_{\text{cr}}^4 - \sigma E F T_{\text{det}}^4 . \end{aligned} \quad (5.29)$$

Considering the signal intensity I for a detector at the temperature T_{det} for a given crucible temperature T_{cr} compared to the intensity I_{ref} at a reference temperature T_{ref} for the crucible as well at temperature T_{det} , one obtains

$$\begin{aligned} \frac{I}{I_{\text{ref}}} &\propto \frac{P}{P_{\text{ref}}} = \frac{P_{\text{cr}} - P_{\text{det}}}{P_{\text{ref}} - P_{\text{det}}} = \\ &= \frac{\sigma E F \cdot T_{\text{cr}}^4 - \sigma E F \cdot T_{\text{det}}^4}{\sigma E F \cdot T_{\text{ref}}^4 - \sigma E F \cdot T_{\text{det}}^4} \\ &= \frac{T_{\text{cr}}^4 - T_{\text{det}}^4}{T_{\text{ref}}^4 - T_{\text{det}}^4} . \end{aligned} \quad (5.30)$$

using the proportionality of the detector signal to the input power as well as the constancy of the geometry and emissivities. Rearranging and collection of constants into k yields

$$I = I_{\text{ref}} \cdot \frac{T_{\text{cr}}^4 - T_{\text{det}}^4}{T_{\text{ref}}^4 - T_{\text{det}}^4} = k \cdot (T_{\text{cr}}^4 - T_{\text{det}}^4) \quad (5.31)$$

as the correlation between crucible temperature and relative detector signal.

Figure 5.26 shows the excellent agreement of the measurements with the values calculated from theory. This result could provide a novel methodology to treat the radiative contribution in the calorimetry signal. It should be mentioned here, that the sensitivity of the detector depends on its temperature, see Section 5.9.4. Hence, the temperatures of the detector during the reference measurement and the calorimetry measurement need to match each other.

The current procedure uses a measurement of the radiation for the *filled* evaporator through a window removing the molecules and attenuating the infrared signal by an uncertain amount. The attenuation can be estimated with the transmission measurement, see Section 3.5.5, but it relies on a gray, *i.e.*, wavelength independent, absorption of the window and the adsorbate on the window. For the metallic adsorbates used in this work this assumption is valid but most likely it will not hold for organic molecules, *e.g.*, PTCDA which is red.

The altered procedure would use the calculated intensity at the evaporation temperature in the experiment in combination with a radiation measurement of an *empty* crucible at elevated temperatures. This has the advantages of a filter free setup

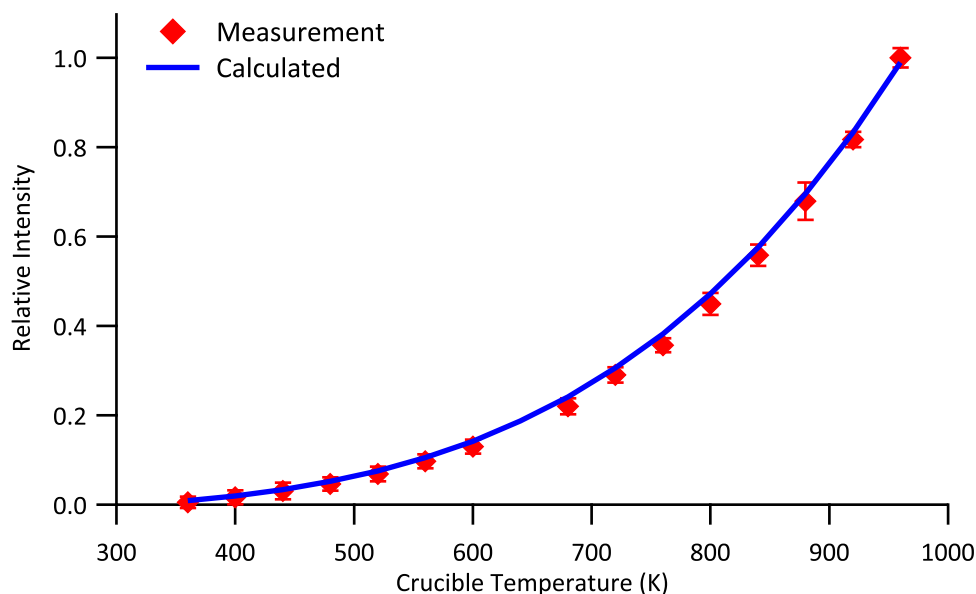


Figure 5.26: Temperature Dependent Relative Infrared Emission — The measured relative intensity (diamonds) as a function of the temperature of the molecular beam source and the corresponding calculated intensity (line) according to Equation (5.31) with $T_{\text{ref}} = 960$ K and $T_{\text{det}} = 307$ K match superbly in a broad temperature range.

and an enhanced signal quality. The elimination of the filter provides unperturbed infrared radiation which is highly desirable for low evaporation temperatures since emission takes place in the far infrared where most materials become opaque. Since there is no contamination of the filter, it is possible to increase the signal quality by averaging additional pulses. Another possibility to increase signal quality is to perform the radiation measurement at slightly higher temperature and to scale it down according to Equation (5.31). This increases the detector output signal and thus reduces reading noise from the data acquisition equipment. The error of the spectral change due to Wien's displacement, *i.e.*, the wavelength dependency of the emission maximum from the temperature of the emitter, might be smaller than the effects from a (soiled) filter.

A scaling of the radiation signal is only possible if the shape of the signal is preserved upon changes of the crucible temperature. Figure 5.27 shows two examples of the measured signal for radiation from the crucible at 480 K and 960 K located at the ends of the considered temperature range. The signal intensity for 960 K is about twenty times higher than for 480 K. The curve for the lower temperature exhibits a much higher noise level and small artifacts at 1.5 s and 3.5 s of unknown origin. Besides the artifacts and the perturbation therefrom, the shape of the signal

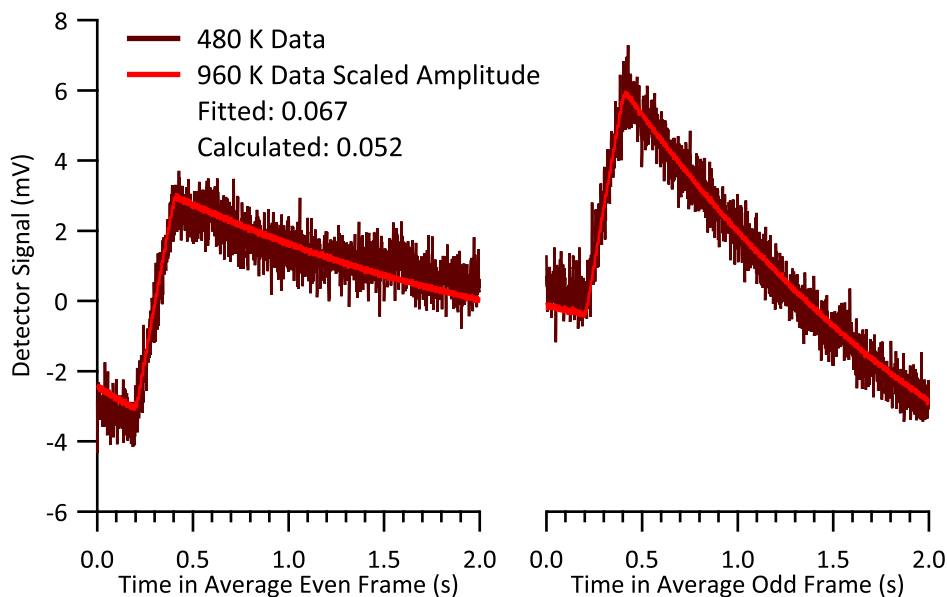


Figure 5.27: Infrared Radiation Compared for two Temperatures — The shape of the averaged detector signal at 480 K is opposed to the signal at 960 K. The latter is scaled to match the amplitude of the first signal. The signal shape is well preserved and the calculated value matches the scaling coefficient within its limit of error.

remains unaltered.

This method to handle the radiative component might be useful if large organic molecules are to be evaporated. Since the material of the crucible might need to be changed to quartz in these cases, this experiment needs to be repeated with the modified setup.

5.8.2 Quartz Crystal Microbalance

As discussed in Sections 1.3.6 and 5.3, the sensitivity of the quartz crystal microbalance is a function of the area of constant film thickness. Since the quartz crystal microbalance is about 10 mm in front of the sample, the molecular beam is less spread than on the sample plane. This circumstance influences the sensitivity of the quartz crystal microbalance and thus the measured thickness changes. Hence, it needs to be elaborated in order to provide a quantitative correction factor.

From the geometry of the experimental setup the relevant diameters for the sensitivity correction calculate to $d_{\text{sam}} = 4.37$ mm for the quartz crystal microbalance in the sample position and $d_{\text{anc}} = 4.46$ mm for the quartz crystal microbalance utilized in the ancillary deposition rate measurement. Since the flux itself is unchanged, a

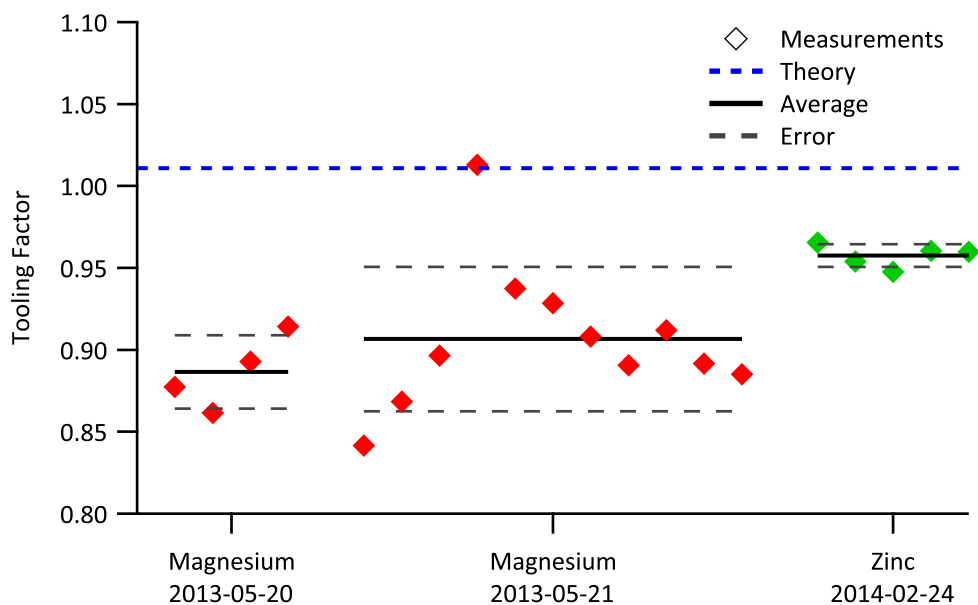


Figure 5.28: Ratio of Deposition Rate in Sample and Ancillary Position — The deposition rate ratios (diamonds) of a QCM sensor placed in sample position, see Section 2.2, and the one in the ancillary stage, see Section 2.4.2, were measured twice for magnesium and once for zinc. Despite the feasible error ranges (black dashed lines), all averages (black solid lines) exhibit a pronounced deviation from the theoretical value (blue dashed line) for all experiments.

difference in thickness change per time, *i.e.*, rate, can be attributed to the altered sensitivity. The ratio of the deposition rates should match the ratio of the correction factors k_{sam} and k_{anc} .

The ratio of the derived correction factors^[141] predict a ratio of $k_{\text{sam}}/k_{\text{anc}} = 1.011$. Three measurement series, two with magnesium and one with zinc as deposited materials, are summarized and opposed to the theoretical value in Figure 5.28.

Although the measurements within a series seem to be reproducible, they differ between the measurement sets and significantly from the theoretical value. Since the sample position was adjusted between the sets, it is appropriate to attribute the varying ratio to a sensitivity change related to a changing lateral offset^[145]. Visual inspection of the deposited layer on the crystals confirmed that the beam was not hitting the center of the sensor. It is advised to repeat this experiment with improved alignment.

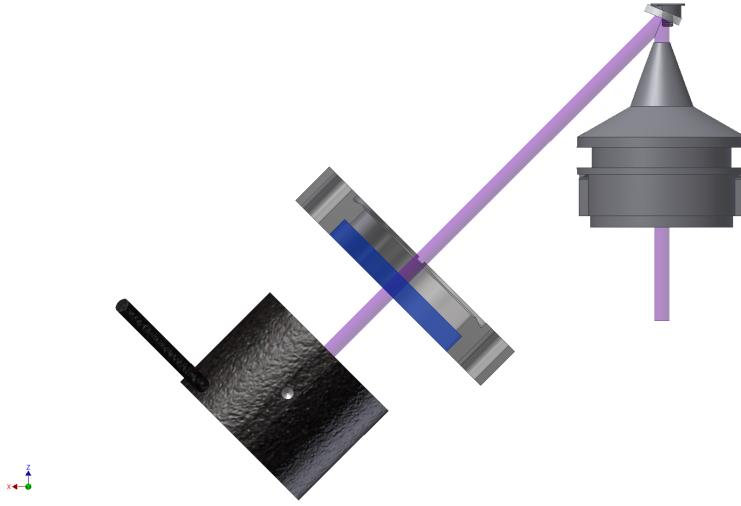


Figure 5.29: Schematic of the Laser Path — The laser beam (purple) leaves the nozzle on top of the beam (south, see Section 2.3.5) is reflected by the mirror in the ancillaries stage (north, see Section 2.4.3) and leaves the chamber through a window (blue) before it reaches the detector of the powermeter (black). The laser light experiences losses due to the reflection on the mirror and attenuation due to the passage through the window. The distances are not to scale and the spread of the laser beam is omitted for clarity.

5.8.3 Mirror

Since the power on the sample P_{sam} of the laser cannot be measured in the vacuum chamber, it is reflected out of the chamber as described in Section 2.4.3 and illustrated in Figure 5.29. The laser loses intensity due to the reflection ρ on the mirror in the rail and is further attenuated by the transmission τ of the window.

The power on the sample can thus be calculated from the power at the detector position P_{det} by

$$P_{\text{sam}} = \frac{1}{\rho \cdot \tau} \cdot P_{\text{det}} \quad (5.32)$$

leading to a correction factor k_{laser} defined either as the inverse of the product of transmission and reflection or the ratio of laser power in sample position to the power in detector position

$$k_{\text{laser}} = \frac{P_{\text{sam}}}{P_{\text{det}}} \quad k'_{\text{laser}} = \frac{1}{\rho \cdot \tau} \cdot \quad (5.33)$$

The laser power inside the chamber is measured with the detector flange, see Figure 2.4, removed from the main chamber and the power detector manually held in sample position, and read from the power meter in both cases. Without contamination of

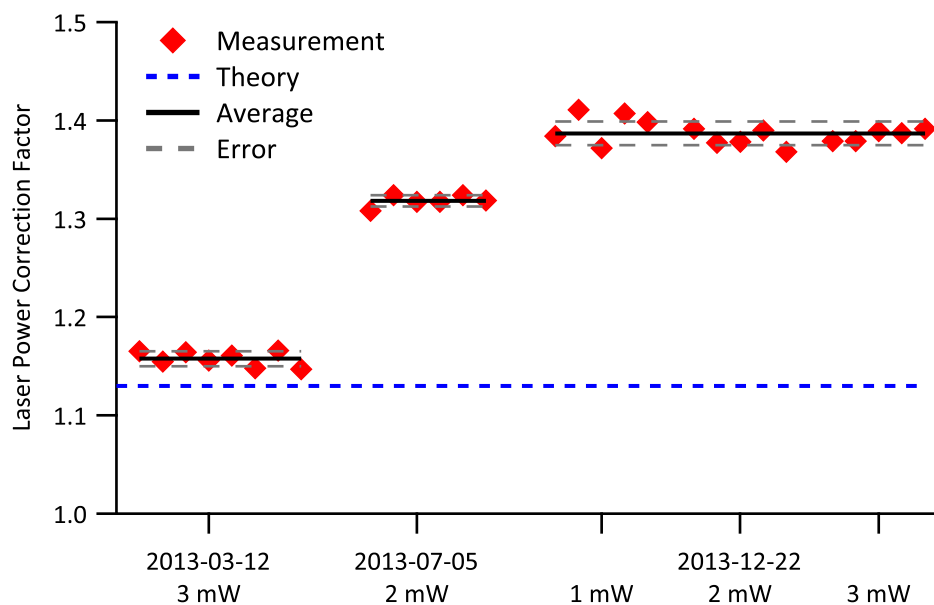


Figure 5.30: Laser Power Correction Factor — The laser power correction factor (diamonds) measured on three different occasions is compared to the theoretical value (blue dashed line). The first set of measurements in March agrees well with theory. A large increase indicates severe contamination before the second set measured in July and another contamination ahead of the measurement in December. The correction factor k_{laser} increased from 1.16 to 1.39. The nominal output power of the laser is given together with the measurement date.

the mirror and the window the two constants should be identical.

At the wavelength of the laser^[151] of 405 nm the transmission of the used Kodial glass window^[153] is tabulated as $\tau = 0.925$ and the reflectivity of the mirror^[185] by $\rho = 0.953$. This leads to a theoretical correction factor of $k'_{\text{laser}} = 1.13$.

The measurements conducted in March with a nominal laser power of 3 mW, corresponding to 45 μW at the sample position, yield an average correction factor $k_{\text{laser}} = 1.16$. This is well in agreement with the theoretical value of $k'_{\text{laser}} = 1.13$, as shown in Figure 5.30. The data set acquired in December differs from the theoretical value due to a mirror contamination with magnesium. The power correction factor has been measured with three nominal laser powers of 1 mW, 2 mW, and 3 mW, resulting in a power at the sample position of approximately 15 μW , 30 μW , and 45 μW , respectively, and computes to $k_{\text{laser}} = 1.39$.

This illustrates well the importance to avoid deposition on the mirror and great care should be exercised! It also demonstrated the necessity for a periodic inspection of the power correction factor in case of unnoticed soiling of the mirror.

5.8.4 Hot Plate

The hot plate serves as a reference for the maximal mass spectrometer intensity. It is heated to a temperature well above the temperature of the main evaporator in order to prevent adsorption of dosed material on itself. Since every dosed molecule is desorbing again after hitting the plate, its use as reference is obvious. Due to the experimental limitation that this reference cannot be measured in the same position as the sample, as for the quartz crystal microbalance in Section 5.8.2, the reference needs to be corrected to geometrical aspects. Another correction might arise from the fact that the sample and the hot plate have an immense temperature difference resulting in a different sensitivity of the mass spectrometer.

Spatial Correction

Analogue to Section 5.8.2 the sensitivity of the mass spectrometer's signal is a function of the distance to the sample and the angle the sample appears at. Since the hot plate is about 8 mm in front of the sample the angle and the distance to the entrance of the mass spectrometer is changed. Due to the construction limitations of the setup, it is impossible to measure the desorption characteristics of the hot plate as a function of emission angle. In addition, the inner setup of the ionization volume in the mass spectrometer is unknown. Its dimensions are likely at a similar range as the considered ones, rendering a detailed simulation of the correction factor impossible.

Since the measurement is carried out in only two positions, it is possible to measure a factor collecting corrections from the angular change and the distance change.

For geometrical reasons the differential flux $d^2\Phi$ through a surface element dA_2 tilted by an angle β to the emission direction of a surface element dA_1 at an angle α to the normal of dA_1 with a center distance of d is given by

$$d^2\Phi = \Phi_0 \frac{dA_1 \cos \alpha \cdot dA_2 \cos \beta}{d^2} \quad (5.34)$$

in an analogue way to the photometric law. Considering the limited knowledge of the quantities related to the mass spectrometer, *i.e.*, dA_2 , the integral over dA_2 is approximated by $A_2 = A_{\text{qms}}$ representing the opening into the mass spectrometer. Since the maximal β amounts to 3.7° its cosine can be approximated by 1. This leads to

$$\Phi = \Phi_0 \frac{A_1 \cos \alpha \cdot A_{\text{qms}}}{d^2} \quad (5.35)$$

describing the flux in the mass spectrometer as a function of distance and orientation.

Since a well adjusted mass spectrometer has a proportional response I to the flux one can rewrite Equation (5.35) as

$$I = I_0 \frac{A_1 \cos \alpha \cdot A_{\text{qms}}}{d^2}. \quad (5.36)$$

Upon the assumption that the spread of the molecular beam is partially compensated by an increased desorption area and the exact characteristics are not known, the integration by dA_1 can also be approximated by $A_1 = A_{\text{sam}} \approx A_{\text{plate}}$ which is identical to the nominal beam cross section. Regarding the ratio between the intensities of the desorbing molecules from the hot plate I_{plate} and sample I_{sam} one obtains

$$\begin{aligned} \frac{I_{\text{sam}}}{I_{\text{plate}}} &= \frac{I_0 \frac{A_{\text{sam}} \cos(\alpha_{\text{sam}}) \cdot A_{\text{qms}}}{d_{\text{sam}}^2}}{I_0 \frac{A_{\text{plate}} \cos(\alpha_{\text{plate}}) \cdot A_{\text{qms}}}{d_{\text{plate}}^2}} \\ &= \frac{\cos(\alpha_{\text{sam}}) d_{\text{plate}}^2}{d_{\text{sam}}^2 \cos(\alpha_{\text{plate}})} \end{aligned} \quad (5.37)$$

with α_{plate} and α_{sam} corresponding to the angle the spectrometer appears at from the hot plate and the sample position, respectively.

Several attempts to measure the correction factor have been made. The biggest challenge is to find matching conditions for the plate in sample position. While the hot plate is equipped with a thermocouple, integrated heating, and insulation to provide a constant and homogeneous temperature, the substitute in the sample position is lacking all these features.

For one part of the experiments a tantalum sheet²⁷ and for the other part a sapphire plate²⁸ were subsequently mounted in a sample holder for single crystals, see Figure 2.2. The assembly has been placed in the sample position and the sandwiched part has been heated with a filament from its back side, see Figure 2.8. The hot plate in the ancillaries stage, see Figure 2.35, has been operated as usual.

The nominal values obtained from the construction are $d_{\text{sam}} = 77.7$ mm, $d_{\text{plate}} = 72.9$ mm, $\alpha_{\text{sam}} = 37.2^\circ$, and $\alpha_{\text{plate}} = 40.1^\circ$ computing to a theoretical intensity ratio of $I_{\text{sam}}/I_{\text{plate}} = 0.917$ for a plain tantalum sheet. For a 1 mm thick sapphire piece the nominal values obtained from the construction change to $d_{\text{plate}} = 70.7$ mm, and $\alpha_{\text{plate}} = 40.7^\circ$ resulting in a ratio of $I_{\text{sam}}/I_{\text{plate}} = 0.867$. This tiny change of the hot plate's position causes already a change of 6 % in the theoretical correction factor emphasizing on the necessity of a reliable experimental value together with a very

²⁷ 99.9% 0.2 mm from Haines & Maassen Metallhandelsgesellschaft mbH.

²⁸ '66 40T350' from KORTH KRISTALLE GMBH.

precise mounting.

Several attempts were made to match operation conditions, as shown in Figure 5.31. One example is matching the parameters for the desorption of previously deposited material films for both devices and increasing the heating power by approximately 20% to 110 W. Another way to obtain similar conditions involved optical matching²⁹ of the color of the glowing tantalum sheets resulting in 150 W for the filament and 1000 K for the hot plate. Furthermore, the calibration has been carried out for sapphire sheets at approximately 300 K since the evaporated magnesium showed a low sticking probability on this target even at this “low” temperature. The final attempt comprised a match of the maximal intensity leading to a filament power of 25 W and a plate temperature of 1000 K. The necessary low power of the filament could be attributed to staining of the sapphire plate with evaporated tungsten during the 150 W experiment leading to a much higher absorption of the radiation emitted from the filament and thus more efficient heating.

Since the initial experiments for the cold sapphire sheets, *i.e.*, $I_{\text{sam}}/I_{\text{plate}} = 0.940 \pm 0.026$ and the settings for maximized individual intensity, *i.e.*, $I_{\text{sam}}/I_{\text{plate}} = 0.960 \pm 0.015$, are compatible, one might assume this is a reasonable value, although it is in contradiction to the theoretical value of $I_{\text{sam}}/I_{\text{plate}} = 0.867$.

Additionally, it has been discovered after these experiments that the output of the mass spectrometer has been acting in an unexpected partial-linear mode, see Section 5.7, that most likely affected this calibration.

²⁹ Carried out with a digital single lens reflex camera (‘EOS 1000D’ from Canon Deutschland GmbH) utilizing fixed settings.

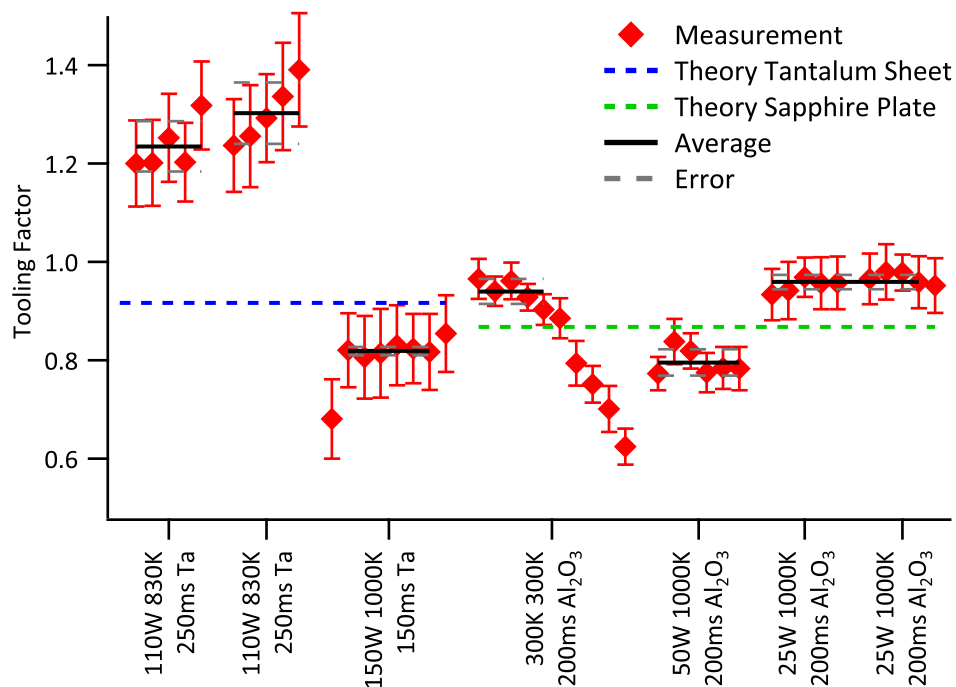


Figure 5.31: Sticking Reference Correction Factor — The determined correction factors (diamonds) together with their average (black lines) and uncertainties (gray dashed lines) for several operation parameters are compared to the theoretical value (blue dashed line). The axis labels give the heating power of the filament, the temperature of the hot plate, the pulse length, and the material of the hot plate. Although the experiment is well reproducible for one setting, the obtained results differ significantly from each other and from the theoretical value for different experimental conditions.

Temperature Influences

Since the crucible, the hot plate, and certainly the sample exhibit different temperatures T , the velocity of the molecules from the crucible differs from the velocities after desorption from the sample or hot plate, due to thermalization. The changed average velocity $v(T)$, *i.e.*, the root mean square, results in different residence times t in the ionization volume of the mass spectrometer. This region can be approximated with a cylinder of the effective length l . Hence, the residence time can be expressed according to

$$t(T) = \frac{l}{v(T)} = \frac{l}{\sqrt{\frac{3RT}{M}}} \quad (5.38)$$

with the molar mass M of the molecule. This leads to a temperature dependency of the relative intensity as given by

$$\frac{t(T)}{t(T_{\text{ref}})} = \frac{\frac{l}{\sqrt{\frac{3RT}{M}}}}{\frac{l}{\sqrt{\frac{3RT_{\text{ref}}}{M}}}} = \sqrt{\frac{T_{\text{ref}}}{T}}, \quad (5.39)$$

if the residence time in the mass spectrometer is the intensity limiting factor.

The hot tantalum plate has been positioned in front of the sample and heated with 27 A to approximately 1020 K. After stabilization of the temperature the current was reduced in steps of 1 A and 15 pulse pairs of dosed magnesium were recorded at each setting.

The data set corresponding to 26 A is used as reference and the measurements are evaluated analogue to a sticking measurement, see Section 3.8, with an altered mass spectrometer signal correction factor of unity as well as an additional calculation of an average and the standard deviation.

Figure 5.32 displays the obtained results and illustrates a range for the operation temperature of the hot plate within the plateau region. The increase in intensity predicted by Equation (5.39) can only be guessed at the highest temperatures. In the temperature range between 850 K and 950 K the intensity of the mass spectrometer is independent of the temperature of the hot plate and thus is suitable to be used in the zero sticking reference measurement. A possible explanation for the unpredicted behavior lies in the assumption of an ionization probability of less than unity in the mass spectrometer. If all incoming molecules are ionized, their residence time in the ionization zone becomes irrelevant.

Similar experiments have been conducted for other evaporants and the resulting temperature ranges, together with the corresponding heating currents therefor, are summarized in Table 5.9. Surprisingly, copper did not desorb from the heated sapphire sheet at all but it desorbed willingly from the cold barium fluoride window. This effect probably arises from the contamination of the solvent used for cleaning, see Section 5.2.

This experiment should be carried out for every new substance.

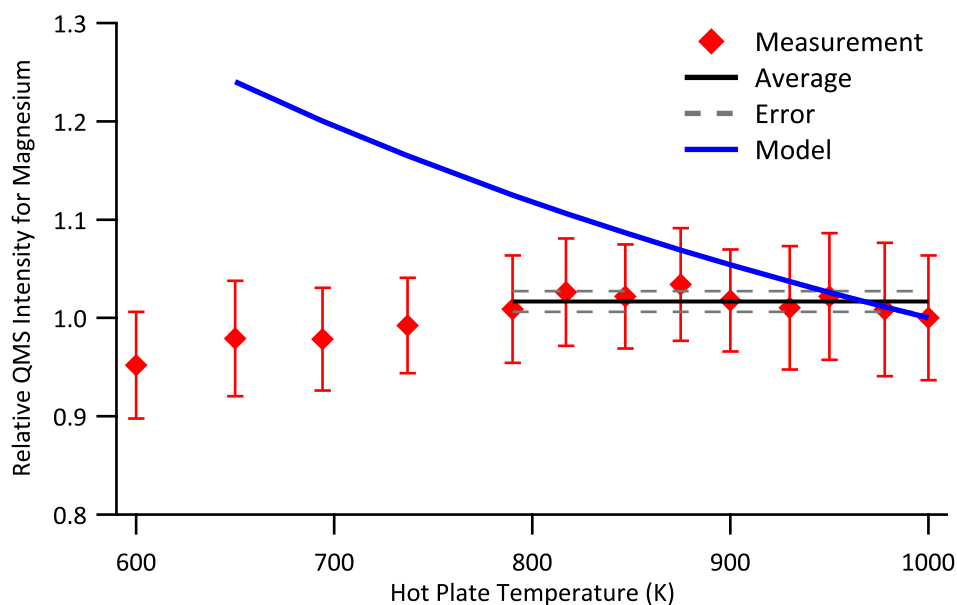


Figure 5.32: Relative Mass Spectrometer Intensity *vs.* Hot Plate Temperature — The intensity of the mass spectrometer signal is measured for 15 pulse pairs of magnesium on the hot tantalum plate and the average (diamonds) is displayed as a function of the temperature of the hot plate. The theoretical behavior in case the residence time of the molecules in the ionization zone limits the signal intensity is superimposed (blue line) together with the plateau range of constant intensity (black line) usable for the zero sticking reference measurement.

Table 5.9: Operation Parameters of the Hot Plate — Operation temperature ranges for the materials used in this work are presented for the plateau region suitable for zero sticking measurements. The given currents are guidelines for the sapphire plate^a wrapped in tantalum foil^b.

Substance	Hot Plate Temperature	Heating Current
Magnesium	850 K to 950 K	≈ 20 A to ≈ 24 A
Calcium	1100 K to 1200 K	≈ 33 A to ≈ 35 A
Copper	No QMS intensity	
Zinc	700 K to 800 K	≈ 14 A to ≈ 19 A
Maximum ^c	1640 K	52 A

a '66 40T350' from KORTH KRISTALLE GMBH.

b 99.9% 0.1 mm from Haines & Maassen Metallhandelsgesellschaft mbH.

c For use with a Type K thermocouple.

Mass Spectrometer Peak Shape *vs.* Hot Plate Temperature

Molecules dosed on the hot plate desorb again at sufficient temperature. This situation resembles the experiments used to deduce enthalpies of adsorption from desorption kinetics, see Section 1.1.1. The desorption rate r_{des} can be expressed as a rate law of n^{th} order:

$$r_{\text{des}} = -\frac{d\Theta(t)}{dt} = k_n \Theta^n(t) \quad (5.40)$$

with the coverage $\Theta(t)$ at the time t . A common *ansatz* for the rate constant is the use of the Arrhenius equation

$$k_n = \nu_n \exp\left(-\frac{\Delta E_{\text{des}}^{\text{PW}}}{RT}\right) \quad (5.41)$$

with a frequency factor ν_n , the temperature T , and the activation energy of desorption $E_{\text{des}}^{\text{PW}}$. Combination of Equation (5.40) and (5.41) results in the Polanyi-Wigner equation, here in a different notation,

$$r_{\text{des}} = -\frac{d\Theta(t)}{dt} = \nu_n \exp\left(-\frac{\Delta E_{\text{des}}^{\text{PW}}}{RT}\right) \cdot (\Theta(t))^n. \quad (5.42)$$

Since all experiments were using metal atoms, first order characteristics, *i.e.*, $n = 1$, can be assumed. Separation of variables yields

$$\frac{d\Theta}{\Theta} = -\nu \exp\left(-\frac{\Delta E_{\text{des}}^{\text{PW}}}{RT}\right) dt \quad (5.43)$$

and integration leads to

$$\ln(\Theta(t)) = -\nu \exp\left(-\frac{\Delta E_{\text{des}}^{\text{PW}}}{RT}\right) \cdot t \quad (5.44)$$

which can be rewritten as

$$\Theta(t) = \exp\left(-\nu \exp\left(-\frac{\Delta E_{\text{des}}^{\text{PW}}}{RT}\right) \cdot t\right) \quad (5.45)$$

and inserted in Equation (5.42)

$$r_{\text{des}} = \nu \exp\left(-\frac{\Delta E_{\text{des}}^{\text{PW}}}{RT}\right) \exp\left(-\nu \exp\left(-\frac{\Delta E_{\text{des}}^{\text{PW}}}{RT}\right) \cdot t\right) \quad (5.46)$$

to describe the desorption rate as a function of time. Inspection of Equation (5.46), illustrated in Figure 5.33, reveals an exponential decrease of the desorption rate with

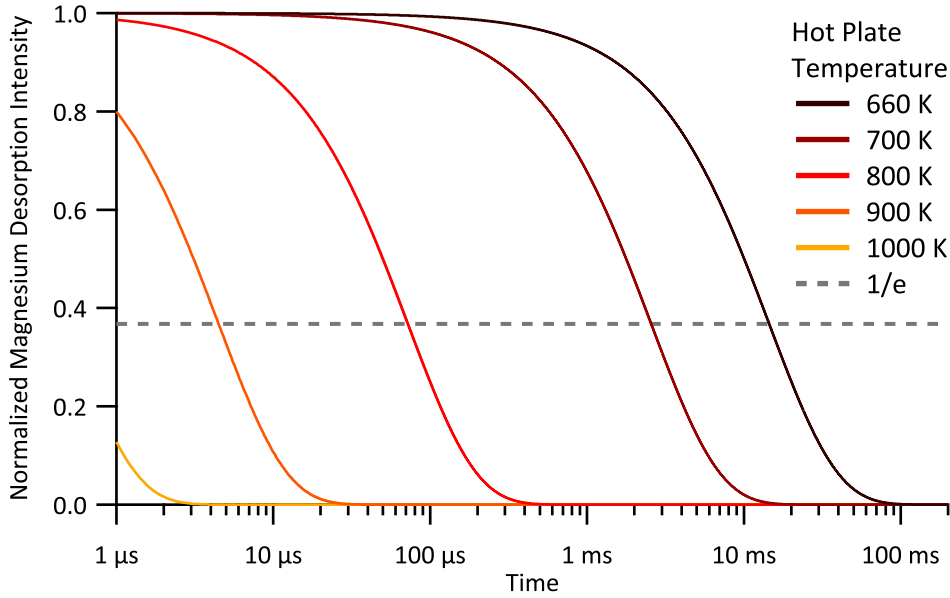


Figure 5.33: Temperature Dependency of Transient Adsorption — The normalized desorption rate calculated for magnesium atoms on a hot plate made from sapphire at four different temperatures exhibits an extreme temperature dependency. The condition for the transient adsorption lifetime calculation at the $1/e = 36.8\%$ level (dashed) is added as a guide to the eye. A visual estimation of the an upper limit for the residence time is also possible. The desorption activation energy and frequency prefactor for the calculation are taken from [186].

time and a super-exponential temperature dependency.

At the time where the ratio of the current desorption rate r and its initial value r_0 at $t_0 = 0$ equals $1/e$ it represents the residence time τ , *i.e.*, lifetime, of a metal atom on the surface. Together with Equation (5.46) one obtains

$$\begin{aligned} \frac{r_\tau}{r_0} &= \frac{\nu \exp\left(-\frac{\Delta E_{\text{des}}^{\text{PW}}}{RT}\right) \exp\left(-\nu \exp\left(-\frac{\Delta E_{\text{des}}^{\text{PW}}}{RT}\right) \cdot \tau\right)}{\nu \exp\left(-\frac{\Delta E_{\text{des}}^{\text{PW}}}{RT}\right) \exp\left(-\nu \exp\left(-\frac{\Delta E_{\text{des}}^{\text{PW}}}{RT}\right) \cdot t_0\right)} \\ \ln\left(\frac{1}{e} \frac{r_0}{r_0}\right) &= \ln\left(\frac{\exp\left(-\nu \exp\left(-\frac{\Delta E_{\text{des}}^{\text{PW}}}{RT}\right) \cdot \tau\right)}{\exp\left(-\nu \exp\left(-\frac{\Delta E_{\text{des}}^{\text{PW}}}{RT}\right) \cdot 0\right)}\right) \\ 1 &= \nu \exp\left(-\frac{\Delta E_{\text{des}}^{\text{PW}}}{RT}\right) \cdot \tau \end{aligned} \quad (5.47)$$

and thus

$$\tau = \frac{\exp\left(\frac{\Delta E_{\text{des}}^{\text{PW}}}{RT}\right)}{\nu} \quad (5.48)$$

for the residence time of an atom on the surface of the hot plate. In this setup an equilibrium coverage is established by continuous dosage of magnesium atoms and the pure desorption region is started by blocking the molecular beam source. Due to the principle of microscopical reversibility of adsorption and desorption in this situation the complementary transition results in an analogue behavior.

If the residence time is small compared to the lower limit of the temporal resolution of the measurement equipment τ_0 , *i.e.*, $\tau \ll \tau_0$, transient adsorption is obviously not observable.

Magnesium has been dosed onto a hot tantalum plate from the crucible, both held at 830 K, and the intensity of the desorbed magnesium has been recorded for 15 pulse pairs of 150 ms length. This measurement has been repeated for the settings “Range: 10^{-12} mBar”, “Range: 10^{-11} mBar”, and “Range: 10^{-10} mBar”. In a second step the mass spectrometer was relocated to the position of the detector port in order to be able to dose magnesium directly into the ion source of the mass spectrometer. In this case the mass spectrometer has been set to “Range: 10^{-8} mBar”. The operation voltage of the secondary electron multiplier in the mass spectrometer has been set to a level of maximal amplitude without clipping of the signal due to the 1 kHz component, mentioned in Section 5.7. The used mass spectrometer has a temporal resolution of about $\tau_0 = 5$ ms during software^[183] acquisition and about 1 ms for the analogue output.

The data set corresponding to the direct dosing (blue in Figure 5.34) resembles the rectangular pulse shape from the experiment with the photo diode, see Section 5.6.3. The data sets from the two measurements at high sensitivities (green and red) exhibit a pronounced exponential component which might indicate a transient adsorption. In contrast the data set corresponding to the low sensitivity setting (cyan) shows a similar shape as the pulses dosed directly. Since this signal severely suffers from the overlain 1 kHz component, the multiplier voltage can not be set to a high level. This results in a very noisy and weak signal which is unfortunately not utilizable for the calorimetry measurements.

According to Equation (5.48) the lifetime, *i.e.*, the inverse of the time constant of the exponential contribution to the peak shape, should exhibit a pronounced dependency on the temperature of the hot plate, as shown in Figure 5.35.

Magnesium has been dosed onto a hot stainless steel (1.4301) plate at various temperatures. In order to obtain an adsorption/desorption equilibrium on the hot plate the pulse length has been increased to 500 ms and 50 pulse pairs have been recorded for each temperature. The time window between 710 ms and 900 ms is

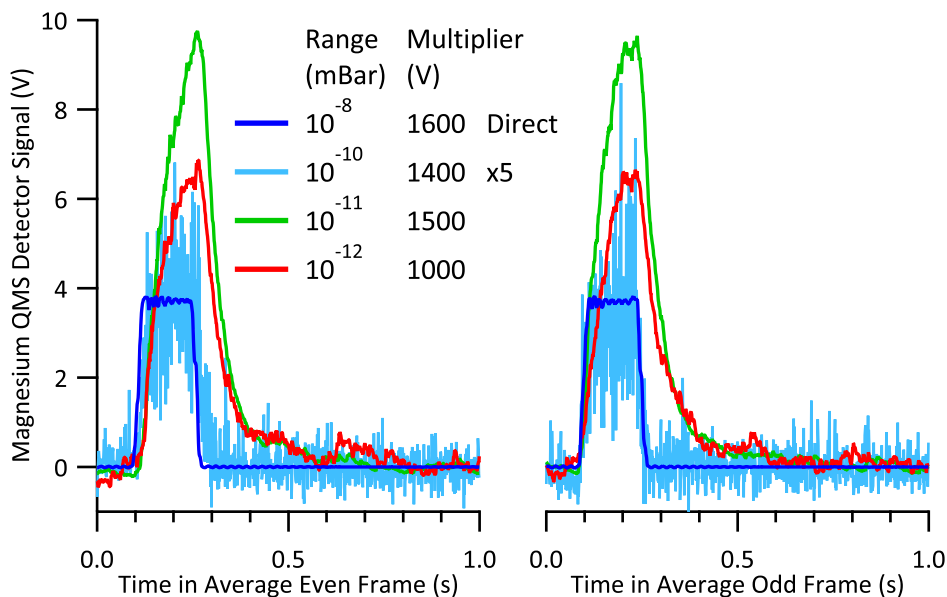


Figure 5.34: Mass Spectrometer Peak Shape at Different Range Settings — Approximately 15 pulse pairs of magnesium ($m/z = 24$) are dosed onto the hot plate held at 830 K (red, cyan, green) and recorded with the mass spectrometer at different settings, and subsequently averaged. For comparison the magnesium pulses are directly dosed into the mass spectrometer (blue). While the blue and cyan traces resemble the rectangular pulse shape from the experiment with the photo diode, see Section 5.6.3, the red and green traces exhibit a pronounced exponential contribution. Although this shape might be caused by transient adsorption, the experiment represented by the cyan curve reveals it as an artifact by the mass spectrometer.

fitted to an exponential function

$$y(x) = y_0 + A \exp\left(-\frac{x - x_0}{\tau}\right) \quad (5.49)$$

with the offset y_0 , amplitude A , an x -shift of x_0 and the lifetime τ . Detailed analysis of the rising and falling peak flanks resulted as expected in identical time constants for both cases.

The obtained lifetimes are displayed together with calculated values in Figure 5.36 utilizing a frequency factor of $\nu = 1.5 \cdot 10^{15} \text{ 1/s}$ and, due to missing experimental values, multiples of the enthalpy of sublimation (values are given in the graph) as approximation of the desorption activation energy. The first one is chosen in analogy to the value corresponding to desorption of magnesium from amorphous aluminum oxide^[186]. The latter approximation is motivated by values reported for the desorption of lead from molybdenum^[92]. The estimated lifetimes exceed the

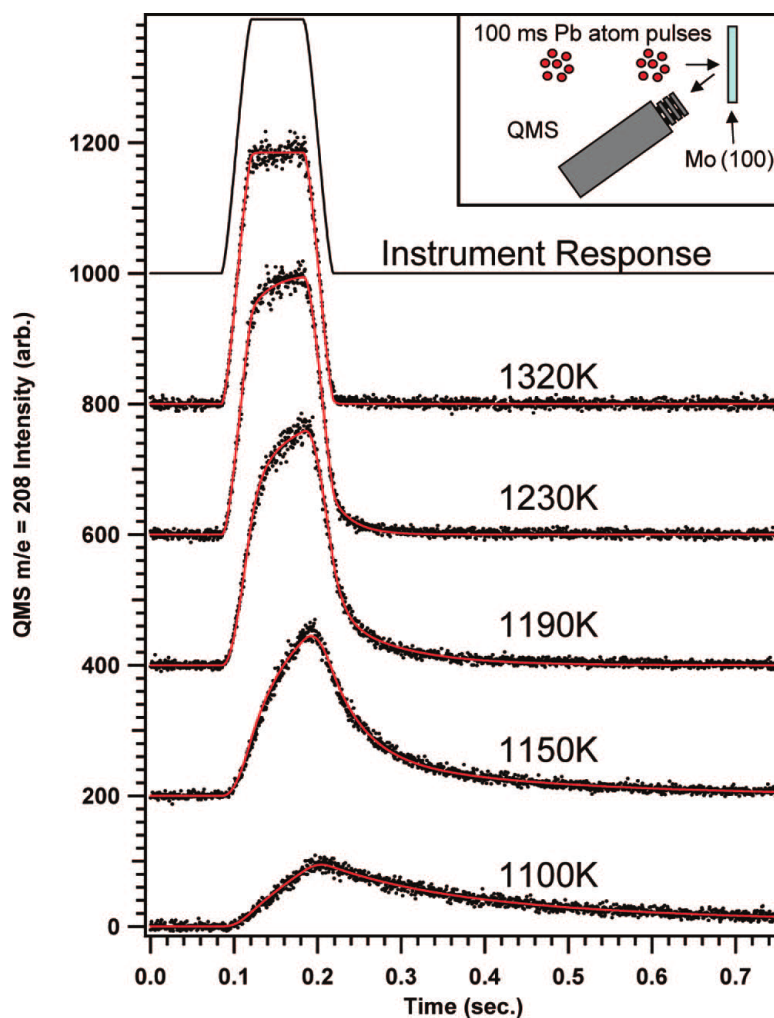


Figure 5.35: Example of Transient Adsorption: Lead on Molybdenum — “Observed lead QMS signal (at $m/z = 208$) as a function of time for 100 ms pulses at $1/2$ Hz onto a Mo(100) surface at various temperatures. The data points are averages of 25 measurements. The red line are fits to the data assuming desorption from two distinct and independent states.”^[92].

temporal resolution of the experimental setup of 1 ms at low temperature, as shown in Figure 5.36 and thus should be observable.

Figure 5.37 shows the dependency of the response of the mass spectrometer on the temperature of the hot plate together with a reference for direct dosage into the mass spectrometer with a pulse length of 200 ms. Due to the huge intensity difference of the molecular and the scattered molecular beam the sensitivity range of the mass spectrometer has been adjusted to “ 10^{-8} mBar” in the first case, and “ 10^{-11} mBar” in the latter. The mass spectrometer was placed line-of-sight to the opening of the crucible in the case of the direct dosage and as described above for the other measurements.

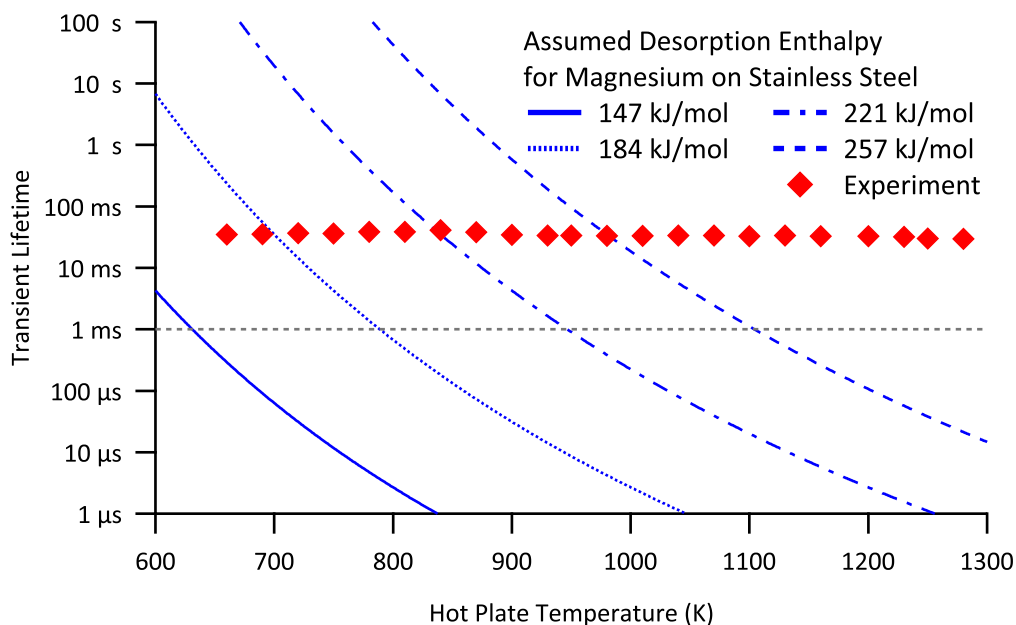


Figure 5.36: Calculated Transient Lifetimes — The transient adsorption lifetime is calculated as a function of substrate temperature for three different assumed enthalpies. This desorption activation enthalpy for magnesium from stainless steel is approximated with the single (solid blue line), 1.25-fold (dotted blue line), 1.5-fold (alternately dashed blue line), and 1.75-fold (equally dashed blue line) enthalpy of sublimation while the frequency factor is assumed as $\nu = 1.5 \cdot 10^{15} \text{ 1/s}$, similar to the case on an amorphous film of alumina^[186]. An observation would only be possible for lifetimes longer than 1 ms (dotted gray line) due to experimental limitations. Experimental obtained lifetimes (diamonds) show no temperature dependency.

The signal shapes of the direct instrument response and the scattered atomic beam in Figures 5.37 and 5.35 match at least for one intermediate temperature and hence suggest a transient adsorption of the magnesium atoms on the hot plate. Closer inspection reveals that the temperature dependency is barely visible in the experiments performed in this work. Although the literature example uses different materials, this comparison is reasonable since the signal shape of the experiment matches the trace labeled “1190 K”, presented in Figure 5.35, indicating a similar time constant at intermediate temperatures in both cases.

In contrast to theory and literature^[92], no temperature dependency can be observed. Additional data obtained for a wider range of plate temperatures, ranging from 300 K up to 900 K, yields the same observation. This data set suffered from artifacts during data acquisition, such as clipping and high noise levels, and should not be considered on its own. However, the expected pronounced dependency of the signal

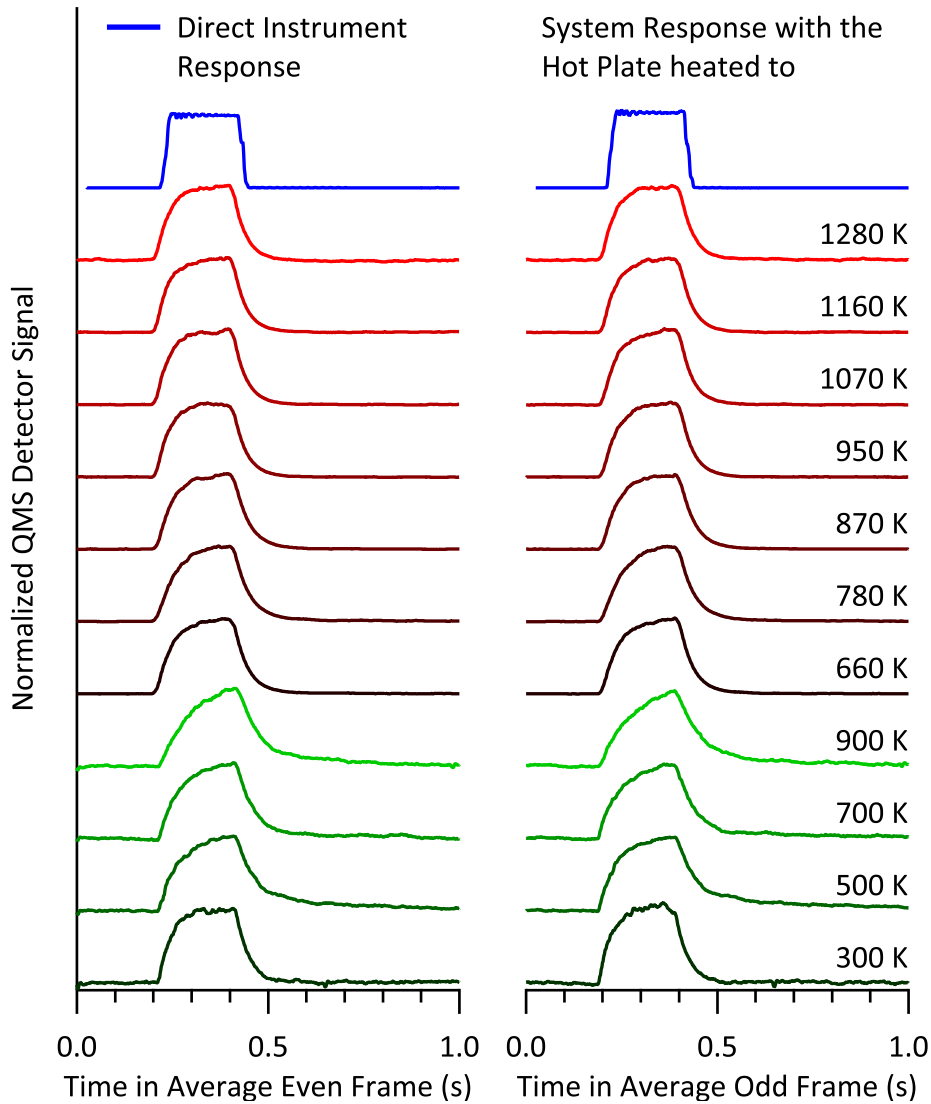


Figure 5.37: Peak Shape of the Mass Spectrometer Signal — The normalized mass spectrometer signal for magnesium ($m/z = 24$) of 50 averaged pulses as a function of time is displayed for recoiled atoms from a hot stainless steel (1.4301) plate held at several temperatures (Range: “ 10^{-11} mBar”, red and green lines) and direct dosage (Range: “ 10^{-8} mBar”, blue line) into the mass spectrometer. The signal shapes of the measurements utilizing the hot plate are similar at different temperatures but differ from the signal obtained by direct dosage. The data set with wider temperature range (green lines) suffered from artifacts, *e.g.*, clipping, during data acquisition.

shape on the temperature of the hot plate is clearly absent.

The marginal changes of the pulse shape exclude transient adsorption as the cause of the exponential part in the mass spectrometer signal. The trustworthy data set also provides a lower limit of approximately 40 ms for the lifetime from

which on direct observation of transient adsorption is possible. Utilizing a not yet implemented deconvolution procedure analogue to the procedure for data from the β -polyvinylidene fluoride detector, see Section 3.10, this limit might possibly be lowered by an order of magnitude.

A possible explanation for the change of the signal shape upon changes in the range settings of the mass spectrometer might be the connection of an additional RC -circuit in the electronics of the mass spectrometer since the (dis)charging curve of a capacitor is also represented by Equation (5.49). Furthermore, an upper limit of the desorption activation energy of 185 kJ/mol might be concluded from the experiment since the observed life time corresponding to the lowest temperature in the experiment should be affected otherwise.

The absence of transient adsorption is remarkable. Since the vapor pressure of magnesium at 300 K is negligible³⁰, no desorption from the plate should be observable. However, the signal intensity is only reduced by half in case of the measurement using a plate temperature of 300 K compared to the measurement performed at a plate temperature of 900 K. According to the tabulated values at these temperatures^[187], the ratio of the vapor pressures of magnesium, and thus of the corresponding signal intensities, should exceed ten orders of magnitude.

A possible explanation for the observed persisting signal intensity at low plate temperatures as well as for the absence of a temperature dependency of the signal shape as well as the signal intensity on the plate temperature might originate from elastic scattering of the impinging magnesium atoms, see Section 1.3.7. The elastic scattering is independent of temperature, since the velocity of the particle remains unchanged. One might argue, that elastic scattering should only occur perpendicular to the surface as a consequence of momentum conservation. However, the relevant surface is microscopically rough and not, as in previous studies^[123,147], atomically flat and scattering on *tilted* microscopic surface elements might contribute a significant amount to the observed signal intensity.

Verification of this proposed mechanism would require a reinvestigation of this experiment with a variation of the polar angle of the plate. In addition, well defined single crystal surfaces should be investigated as references. Unfortunately, these measurements are not possible since no suitable sample manipulation for this kind of experiment is included in the setup used in this work.

³⁰ Below the tabulated minimum of $< 10^{-11}$ Torr^[187].

5.9 Pyroelectric Detector

The heart of the measurement equipment are the β -polyvinylidene fluoride based detectors for either thin film samples or single crystal samples, see Section 2.2. Hence, thorough knowledge of their behavior under different circumstances is mandatory. The most important items are the verification of the linearity with respect to the power input, the influence of the operation temperature, and the effects of aging during system bake-outs.

This work only covers the characterization of the detector for thin film samples. It is advised to repeat the evaluation experiments for the thin sheet detector prior to its routine usage.

5.9.1 Linearity Regarding Input Power

The fundamental assumption on the used detector is a response I proportional to the input power P at constant pulse length t

$$I = k \cdot P|_t \quad (5.50)$$

with a constant k collecting all experimental and material parameters.

The laser power has varied between 0.4 μ W and 41.4 μ W while all other experimental parameters remained unchanged. 50 laser pulses fired onto one pristine sample have been recorded at each laser power while the first and last pair are omitted for the further treatment. The relative amplitudes and the scatter thereof are calculated along the transmission measurement with virtual laser powers of 1 W.

The proportionality of the detector response is well illustrated in Figure 5.38. The constant slope in combination with a negligible intercept confirms the most important requirement on the detector.

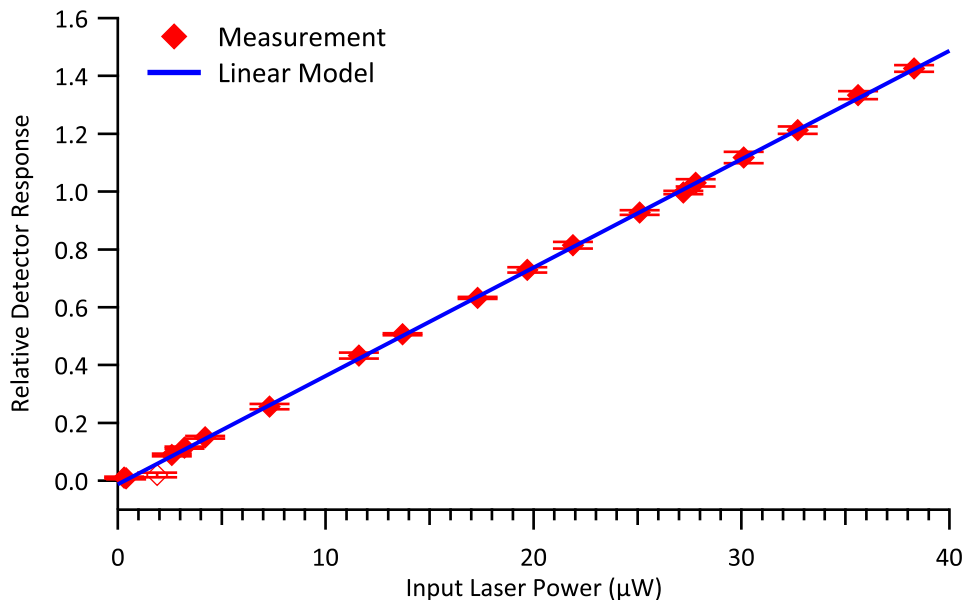


Figure 5.38: Detector Linearity Towards Input Power — The relative detector response (diamonds) is displayed against the measured input power of the laser reflected out of the chamber. The reference is calculated according to the standard procedure in Section 3.5.4. Each data point represents the average of 46 individual pulses. The outlier at $2\ \mu\text{W}$ most likely arises from a compromised measurement. The linear regression (blue line) exhibits only a marginal intercept.

5.9.2 Linearity Regarding Active Area

The general assumption of a homogeneous usage of the detector surface within the area accessible by the molecular beam motivates the investigation of a contrary example.

Depending on the nature of the detector two results are possible. It could be sensitive to the differential maximum input power, *i.e.*, power input per unit area, or proportional to the integrated input power.

An example of an analogous system would be a photo diode. The voltage output of the unloaded diode is independent of the illuminated area. This would result in an abrupt intensity drop when no power reaches the detector

$$I(z - z_0) = \begin{cases} I_0 & z \leq z_0 \\ 0 & z > z_0 \end{cases} \quad (5.51)$$

resulting in an on/off behavior of the detector. In contrast the current output of a loaded photo diode is proportional to the illuminated area. This leads to an intensity

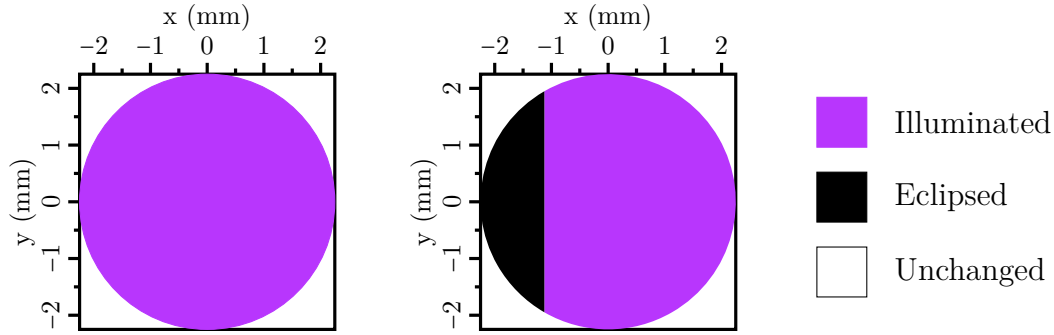


Figure 5.39: Illustration for Sample Occlusion — Illustration of the occluded part (black) of the potentially active area (purple) of the detector disk. The masked area is stepwise increased from small z -position values of the linear motion, corresponding to the negative end of the x -range, to a completed eclipse of the active area.

drop proportional to the eclipsed area which itself depends on the experimental setup.

As discussed in Section 1.3.3, the detector signal originates from a change in polarization upon a local temperature variation. Since polarization is defined as charge per area, a temperature change causes a charge on the surfaces of the detector leading to the signal.

Along the experiment the ancillary stage has been moved in between the nozzle and the sample in steps of 1 mm for each measurement. This caused an adjustable occlusion of the sample as illustrated in Figure 5.39.

The active area A_{eff} as a function of the z -movement of the ancillaries body piece is thus given by

$$A_{\text{eff}} = \begin{cases} A_0 & z \leq z_0 - \frac{1}{2}d \\ A(z) & z_0 - \frac{1}{2}d < z < z_0 + \frac{1}{2}d \\ 0 & z \geq z_0 + \frac{1}{2}d \end{cases} \quad (5.52)$$

with the total area $A_0 = \frac{d^2}{4}\pi$, the center position of the beam z_0 corresponding to $x = 0$ and $y = 0$ and the diameter d of the beam. The active area $A(z)$ in the transition region is given by

$$A(z) = 2 \cdot \int_{z-z_0}^{z_0+d/2} \sqrt{\left(\frac{d}{2}\right)^2 - \xi^2} d\xi \quad z \in \left[z_0 - \frac{d}{2}, z_0 + \frac{d}{2}\right] \quad (5.53)$$

representing the area between $y = 0$ and the perimeter of the positive half circle

while the factor 2 arises from symmetry. Integration^[188] yields

$$A(z) = 2 \cdot \left[\frac{1}{2} \left(\xi \sqrt{\left(\frac{d}{2}\right)^2 - \xi^2} + \left(\frac{d}{2}\right)^2 \arcsin\left(\frac{2\xi}{d}\right) \right) \right]_{\xi=z-z_0}^{\xi=z_0+\frac{d}{2}} \quad z \in \left[z_0 - \frac{d}{2}, z_0 + \frac{d}{2} \right] \quad (5.54)$$

which evaluates to

$$A(z) = \frac{\pi \cdot d^2}{8} - (z - z_0) \sqrt{\frac{d^2}{4} - (z - z_0)^2} - \frac{d^2}{4} \arcsin\left(\frac{2(z - z_0)}{d}\right) \quad z \in \left[z_0 - \frac{d}{2}, z_0 + \frac{d}{2} \right] . \quad (5.55)$$

Assuming a proportional relationship for the intensity I to the maximal intensity I_0 corresponding to the full area A_0 one obtains

$$I = I_0 \cdot \frac{A_{\text{eff}}}{A_0} \quad (5.56)$$

and for the relative signal intensity

$$\frac{I}{I_0} = \frac{A_{\text{eff}}}{A_0} \quad (5.57)$$

which alters Equation (5.52) to

$$\frac{I}{I_0} = \begin{cases} 1 & z \leq z_0 - \frac{1}{2}d \\ \frac{A_{\text{eff}}}{A_0} & z_0 - \frac{1}{2}d < z < z_0 + \frac{1}{2}d \\ 0 & z \geq z_0 + \frac{1}{2}d \end{cases} . \quad (5.58)$$

The laser has been pulsed on the sample and 50 pulses have been recorded for each measurement with a different z -position. The relative signal intensity is calculated along the procedure for a transmission measurement. As usual the first and last pulse pair are omitted from the data processing. Since the chopper suffered from timing faults individual pulse pairs with a wrong pulse delay are also excluded from this experiment.

Figure 5.40 opposes the measured data with the two presented models. The on/off state model, described in Equation (5.51), clearly does not match the measured data. On the other hand, the model predicting a proportional dependency from the irradiated area agrees very well with the measurement. Since there are only few data points in the transition region, the diameter of the beam is fixed to the nominal value of $d = 4.5$ mm. This result illustrates the integrating behavior of the detector.

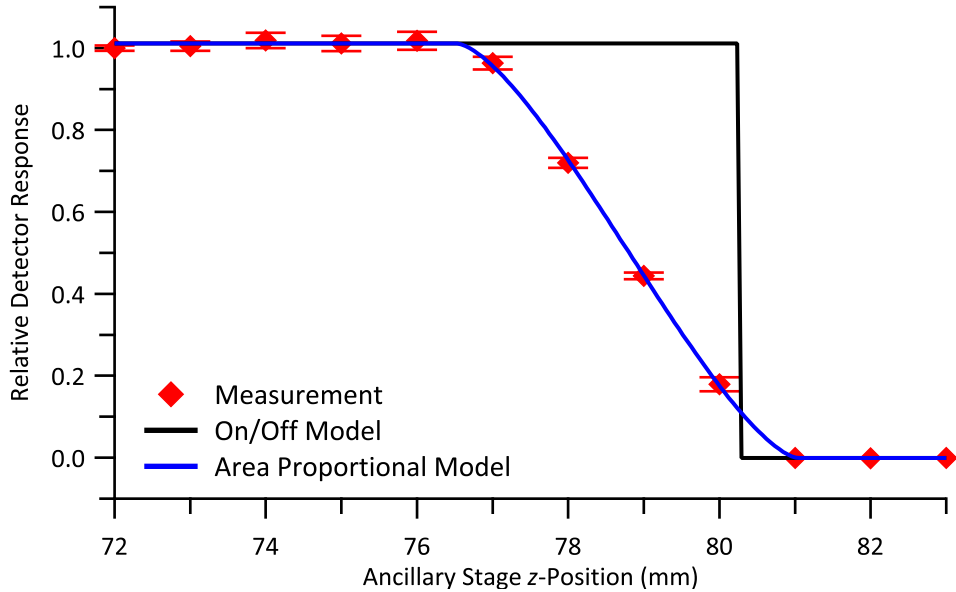


Figure 5.40: Detector Linearity Towards Active Area — The relative detector response (diamonds) measured as a function of the z -position of the ancillaries stage casting a shadow on the detector is compared to the two discussed models. The model implying a proportional relationship of the intensity to the irradiated area (blue line) is in excellent agreement^a with the measurement whereas the model considering a sharp transition (black line) clearly fails.

^a A fixed beam diameter of 4.5 mm as parameter is used.

If this measurement is carried out with higher z -resolution, it might be able to detect a clogging of the nozzle from deposited material without venting of the main chamber.

5.9.3 External Heat Treatment of β -Polyvinylidene Fluoride

Since the detector polymer for thin sheet sample, see Figure 2.3, remains in the main chamber it needs to withstand the thermal load during a bake-out of the main chamber. Hence, the knowledge of the degree of degradation of the detector upon thermal load is desirable. Protection of the detector is expected to be possible by limiting the bake-out temperature or by an adjustable counter cooling of the thermal reservoir, see Figure 2.5. Certainly the chamber should be heated as high as possible, depending on the installed components, to reduce the duration of this process.

The pyroelectric effect of β -polyvinylidene fluoride originates from oriented crystallites embedded in the amorphous phase. Quenching of this property at elevated temperatures is known^[189] and may arise from reorientation, phase change, or,

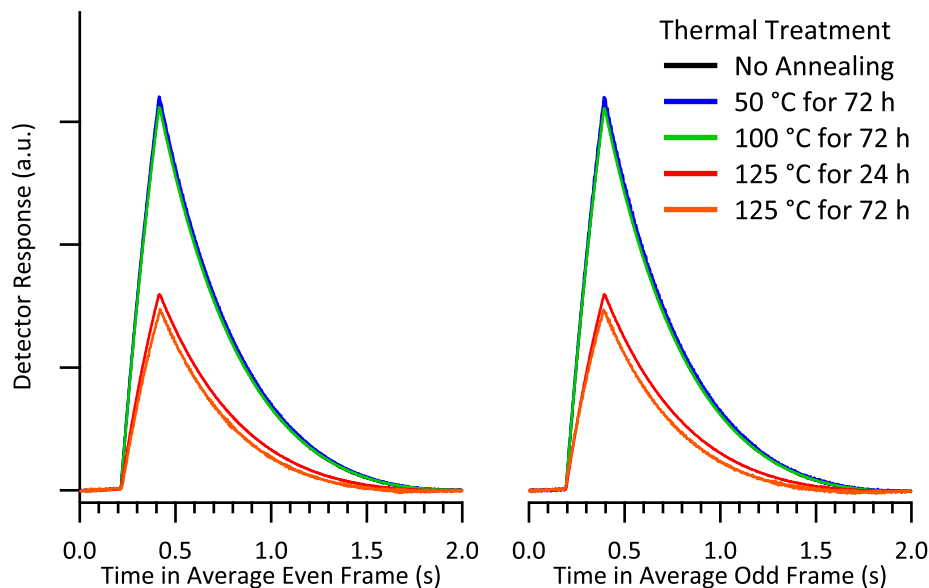


Figure 5.41: Annealing Effect on the Detector — The detector response of 96 pulses to 200 ms laser pulses has been acquired and averaged. The average normalized by the laser power is displayed for several temperature treatments. While temperatures up to 100 °C have no effect on the intensity, heating to 125 °C results in a loss by 50 % even after a short time. Heating to 150 °C (not shown) leads to a complete sensitivity loss after a short time.

ultimately, melting of the crystallites.

Along with the thermal also the temporal aspect for the specific used detector foils has been investigated. Annealing of several samples in air at temperatures of 50 °C, 100 °C, 125 °C and 150 °C for 12 h, 24 h, 48 h, and 72 h was executed before the usual introduction procedure in sample holders for polymer samples, see Figure 2.3.

For each parameter set 50 pulse pairs were recorded with the sample at ambient temperature, *i.e.*, 307 K, and evaluated analogue to a *transmission* measurement. The obtained average has been normalized to the laser power input.

The sensitivity, *i.e.*, the amplitude of the normalize average, remains unchanged for temperatures up to 100 °C and is independent of the annealing time, as shown in Figure 5.41. A further increase of the temperature to 125 °C results in a rapid sensitivity loss around 50 % which is not progressing with increased annealing time. This indicates the presence of at least two processes resulting in a sensitivity loss. A further investigation is beyond the scope of this work. A complete intensity loss is observed for the samples annealed at 150 °C for just 12 h.

The samples heated to the two highest temperatures exhibit macroscopic changes

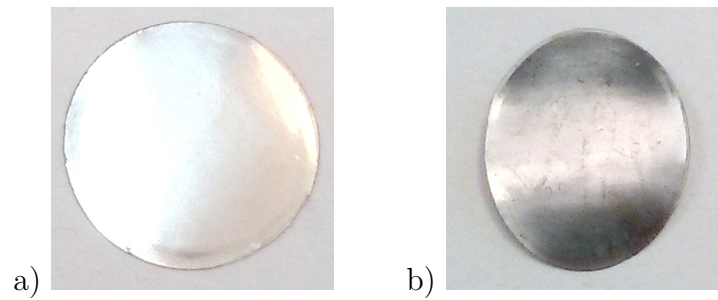


Figure 5.42: Thermal Treatment of Detector Polymer — Detector disks^a for thin film samples before (left) and after (right) a heat treatment at 125 °C for 12 h in air. Besides the darker surface a change in shape is observable indicating a reversal of the stretching used in the poling process. Photographs by H. ZHOU.

^a ‘28um/w 400CU/150NI’ from Measurement Specialties.

in shape and an altered surface finish from glossy to dull, as shown in Figure 5.42. This indicates a reversal of the stretching used in the poling process to align the crystallites in the matrix. Since this step in the processing is necessary to generate the poling, its turning back could explain the loss in permanent polarization and thus in sensitivity.

If the detector’s temperature is maintained below 100 °C, bake-out is possible. The common bake-out temperature of 150 °C is already too high. Individual cooling of the detector in the detector stage, see Section 2.4, might provide a way to protect the sensor while the rest of the chamber is at higher temperature.

The transferable sample holders for thin films, see Figure 2.3, are not affected by this limitation since they can be stored in the load lock during a thermal degassing of the main chamber.

5.9.4 Temperature Influence on Detector Sensitivity

The measurement can be performed at various sample temperatures, as mentioned in Section 2.2. This motivates an investigation of the dependency of the detector’s sensitivity with respect to its temperature during measurements. A naive approach would comprise no sensitivity change. However, the true nature is more complex and the sensitivity changes with operation temperature^[148].

This experiment and data evaluation has been carried out in an analogue way to the experiment in Section 5.9.3 with the sample not being at ambient temperature but cooled with liquid nitrogen to about 90 K.

Figure 5.43 clearly shows an influence of the detector’s temperature on its sensitivity. This lead to the necessity to perform the calibration measurements at the

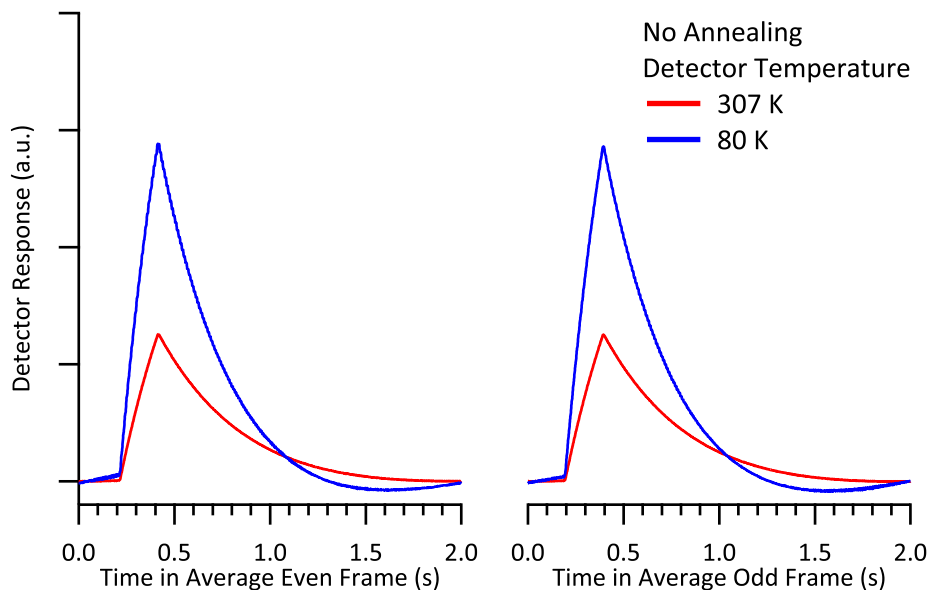


Figure 5.43: Temperature Dependency of the Detector Sensitivity — The detector response of 96 pulses to 200 ms laser pulses is acquired and averaged. The average normalized by the laser power is displayed for ambient and liquid nitrogen temperature of the same sensor during measurement. The lowered temperature results in a more than twofold increase of the detector response.

same temperature as the actual calorimetric measurement.

The change in signal shape arises from the used amplifiers. On the one hand, it could be an artifact from the time constant of the secondary amplifier, which was used at that time and removed later. On the other hand, it could originate from the offset compensation of the main amplifier. The latter option is less likely since this behavior is not observed in the linearity test conducted without the secondary amplifier, see Section 5.5.3. Temperature dependent material properties of the detector can be excluded since this artifact did not occur during the subsequent experiments conducted at low temperatures.

This insight led to an altered measurement routine for thin film systems, see Sections 3.5.3 and 3.5.4. Although the IGOR PRO program package, see Section 4.2, uses a correction derived from the sensitivities of the measurement of the coated sample and the laser reference measurement, it is recommended for precision data evaluation to record a deconvolution measurement at the temperature of the calorimetric measurement.

It is advisable to repeat this experiment for various temperatures between 90 K and 370 K in order to obtain a feel for signal levels at non-ambient temperatures.

5.9.5 Detailed Detector Composition

Alteration of the thin film detector discs, see Section 2.2, is possible in two ways. On the one hand, the thickness of the active β -polyvinylidene fluoride (PVDF) layer can be chosen different. This results in a different heat capacity and thus in a changed sensitivity. On the other hand, the conductive coating material on the polymer can be replaced. In general this leads to a changed reflectivity. Both effects are compensated by the laser reference measurement, see Section 3.5.4. This leads to the conclusion that the detailed composition of the detector unit is expected to be irrelevant for the obtained result, at least within certain boundaries, *e.g.*, a vanishing sensitivity due to excessive heat capacity.

Two complete calorimetry experiments with similar parameters but altered detector composition have been conducted and the results are presented in Figure 5.44. The standard nickel/copper coated detector with a polymer thickness of 28 μm yields similar results as the aluminum coated 9 μm thick pendant. Deviations in the absolute values can be attributed to uncertainties in the reflectivity of aluminum.

While the spectral reflectivity of pure aluminum, *e.g.*, 0.92 at 405 nm, is documented well^[136] less information is available for oxidized aluminum surfaces. An integral reflectivity of aluminum foil between 0.88 for the shiny side and 0.80 for the dull side is reported^[190]. Since the reflectivity is almost constant in the visible spectral range the same assumption is made for the surface covered by its natural oxide and a value of 0.89 is used. Although the absolute change in reflectivity is small, *i.e.*, 0.92 *vs.* 0.89, the corresponding absorption coefficients differ by 38 %, *i.e.*, 0.08 *vs.* 0.11. This illustrates the difficulties encountered with highly reflecting surfaces during the reference measurements where small changes in the input parameters can cause significant changes in the result.

Although the properties of the investigated detectors are rather different, the results are similar enough to exclude a pronounced dependency on the employed kind. This exclusion also demonstrates that the twin-layer metal coating, *i.e.*, copper and nickel, of the standard detector material is of no drawback compared to the single metal layer coated, *i.e.*, aluminum, material. Almost identical heats of adsorption are obtained at coverages below 10 ML for the different detectors. The facts, that the calibration chain³¹ involves different reflectivities and that the obtained heats are identical, attest the validity of the involved reflectivities, the measurement concept, and the corresponding parts of the data treatment procedure.

Closer examination of both experiments reveal an unexpected evolution of the

³¹ Response of pristine detector, sputtering, coating, response of coated detector, and the actual calibration.

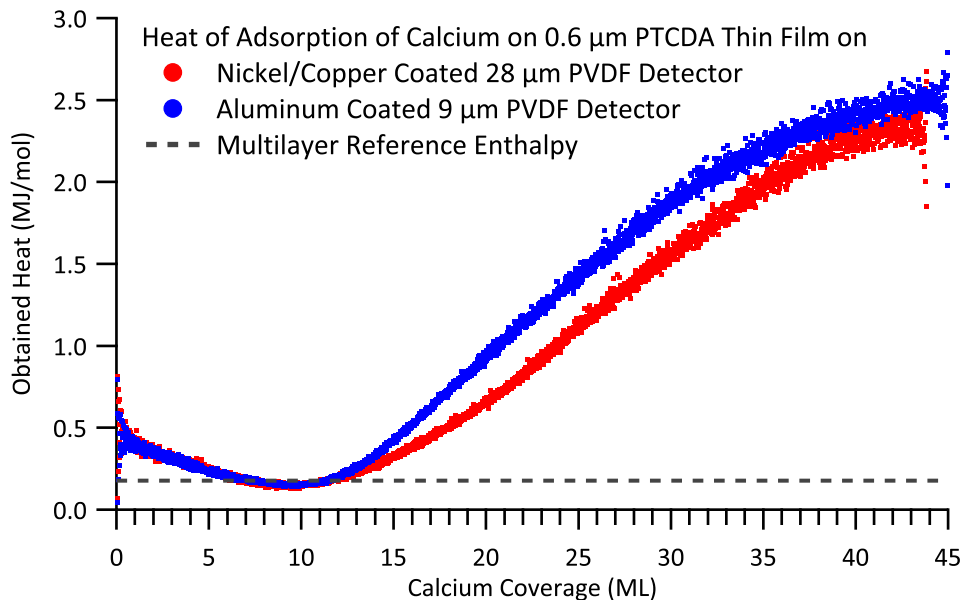


Figure 5.44: Influences of the Detector Structure — Two experiments with almost similar conditions, *e.g.*, deposition rate, substrate thickness, temperature, but different detector composition, are opposed. Both experiments exhibit the same unexpected behavior at high coverages. Instead of converging to the reference enthalpy (dashed line) the “measured heat” levels out at unreasonable high values. The slightly lower absolute value for the experiment with the aluminum coated 9 μm thick detector^a compared to the copper/nickle coated 28 μm detector^b (red dots) can be attributed to uncertainties of the assumed reflectivity of the aluminum layer.

^a ‘FV301890/1’ from Goodfellow GmbH – discontinued.

^b ‘28um/w 400CU/150NI’ from Measurement Specialties.

amplitudes. Instead of converging to reference enthalpy the “measured heat” levels out at unreasonable high values in both cases. A possible explanation for this artifact is discussed in Section 6.8.

Usage of lithium tantalate (LT), as an alternative detector material^[115–118] would provide a higher operation temperature limit of the detector and a higher flexural stiffness^[131]. Since the downstream amplifier is voltage sensitive, the relative detector sensitivity with respect to the detector material, *i.e.*, relative voltage increase across the capacitor formed by the detectors, is important to achieve high signal amplitudes. The output voltage U is given by the electrical capacity of the detector C_{el} and the generated electrical charge Q_{el} as

$$U = \frac{Q_{\text{el}}}{C_{\text{el}}} . \quad (5.59)$$

Table 5.10: Properties of Pyroelectric Materials — A selection of material properties^[131] with typical values at 20 °C relevant to this work.

Property		Unit	Lithium Tantalate	PVDF ^a
Pyroelectric Coefficient	p	$\frac{\text{C}}{\text{m}^2\text{K}}$	$1.8 \cdot 10^{-4}$	$0.3 \cdot 10^{-4}$
Relative Permittivity	ε_r		54	10
Heat Capacity per Volume	s	$\frac{\text{J}}{\text{m}^3\text{K}}$	$3.3 \cdot 10^6$	$2.4 \cdot 10^6$
Critical Temperature	T_c	K	890	390

a β -Polyvinylidene fluoride

As discussed in Section 1.3.3, the induced charge is given by

$$Q_{\text{el}} = p \cdot A \cdot \delta T \quad (5.60)$$

with the active area A and the pyroelectric coefficient p of the detector. The temperature change δT itself is obtained from the heat input Q_{h} and the specific heat capacity per volume of the used materials s

$$\delta T = \frac{Q_{\text{h}}}{s \cdot V} \quad (5.61)$$

and the active volume V of the detector. The electrical capacity C_{el} is derived from the area A and the distance d between the electrodes

$$C = \frac{A}{d \cdot \varepsilon_0 \cdot \varepsilon_r} \quad (5.62)$$

using the electric constant of vacuum, ε_0 , and the relative permittivity of the used materials ε_r . Altogether, one obtains

$$U = \frac{p \cdot Q_{\text{h}} \cdot d}{\varepsilon_0 \cdot \varepsilon_r \cdot s \cdot V} \quad (5.63)$$

for one material and thus

$$S_{\text{rel}} = \frac{U_{\text{PVDF}}}{U_{\text{LT}}} = \frac{p_{\text{PVDF}} \cdot \varepsilon_{\text{LT}} \cdot s_{\text{LT}}}{p_{\text{LT}} \cdot \varepsilon_{\text{PVDF}} \cdot s_{\text{PVDF}}} \quad (5.64)$$

as the relative sensitivity S_{rel} regarding voltage output to heat input at constant detector geometry.

Calculation utilizing the involved physical properties for β -polyvinylidene fluoride and lithium tantalate, see Table 5.10, reveals a theoretical relative sensitivity of 1.25 in favor of β -polyvinylidene fluoride. Considering the processability of both

materials one finds a lower thickness limit of 100 μm for lithium tantalate single crystals whereas the polymers used in this work feature thicknesses of approximately 10 μm and approximately 30 μm . As a result, the usage of lithium tantalate crystals mounted in the sample holders for thin films, see Section 2.1, would result in a reduction of the signal amplitude by approximately 90 %.

5.9.6 Thermal Insulation of the Detector Stage

An important property for low temperature experiments is the thermal insulation of the detector stage, see Section 2.2. Since heat exchange by convection is impossible in the vacuum environment, the cooled detector stage can be warmed by heat conductance through the mounting rods or by radiation. One source for the latter is the body of the main chamber and another source is the energized filament of the ion gauge. Since the base temperature of the detector stage is about 307 K at an ion gauge emission current of 5 mA, at 301 K at an emission current of 0.5 mA, while the room temperature amounts to 297 K the gauge's filament should cause a significant heat input to the cooled thermal reservoir.

The influence is characterized by a passive heat up of the detector stage, *i.e.*, cooling with liquid nitrogen has been stopped and the machine has been left on its own. Cooling of the detector stage has been achieved within 75 min by sucking liquid nitrogen out of a storage Dewar flask and through the thermal reservoir with membrane pumps^{32 33} equipped with an upstream thermal protection stage. The temperature has been recorded with the status logging software³⁴ and analyzed with the status logging package, see Section 4.4.

The final temperature of 89 K is not affected by the ion gauge at its low emission level. At high emission the limit is slightly lifted to 93 K. Figure 5.45 also illustrates a similar heating rate in all three cases since the traces do not exhibit pronounced differences. This leads to the conclusion that the radiative heating from the filament is negligible compared to other heat sources.

A further reduction of the heating rate might be achieved by a replacement of the mounting rod of the thermal reservoir, see Figure 2.5, by threaded tubes. This would result in a reduction in cross section and hence in total thermal conductivity. In case this modification is not providing the desired result, it might be necessary to install a cryo-shield around the detector stage.

32 'MZ 2C' from VACUUBRAND GMBH + CO KG.

33 'DIVAC 2.4' from Leybold AG - now Oerlikon Leybold Vacuum GmbH.

34 Programmed by H. ZHOU.

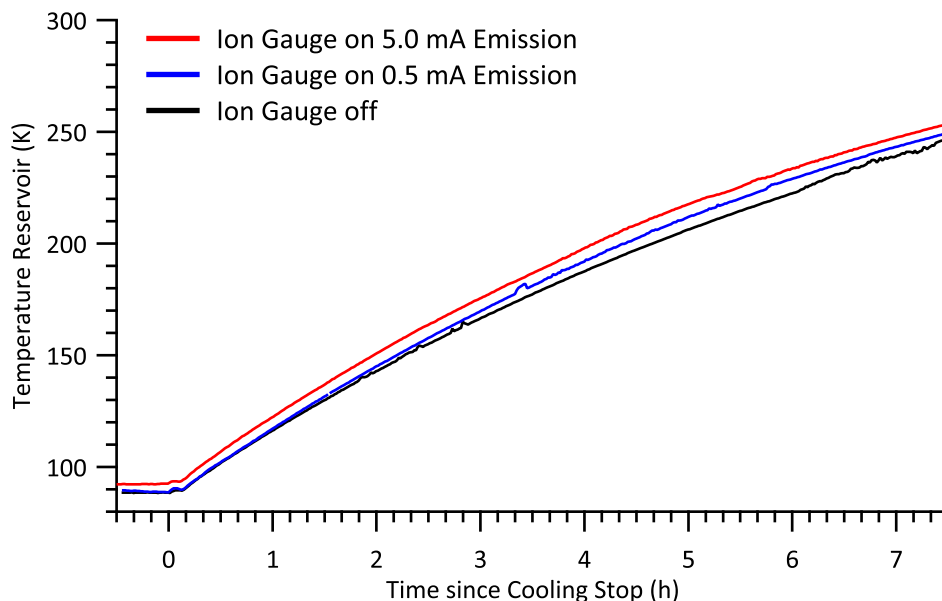


Figure 5.45: Thawing of the Thermal Reservoir — The temperature profile at the sample position of the thermal reservoir upon a passive heat up after low temperature experiments is presented for different ion gauge settings. Although the lower temperature limit is raised for high emission (red), the thaw rate is similar to the low emission setting (blue) and the switched off (black) ion gauge. Measured by H. ZHOU.

5.9.7 Deconvolution Test

While the heat of adsorption is deposited instantly on the detector’s surface, analogue to the heat from the laser pulse, reactions of the adsorbed atoms with the substrate might be slower. If the time constants of these reactions are in the range of milliseconds or longer, they will lead to an alteration of the peak shape and the “normal” data treatment routine from Section 3.8 is no longer appropriate. Instead, the power input as a function of time has to be considered as explained in Section 3.10.

Two properties, timing and amplitude, are relevant for this procedure and need to match a direct measurement.

In order to characterize this data evaluation routine, the amplified response of a metalized β -polyvinylidene fluoride detector disc mounted in a sample holder for thin films, see Figure 2.3, has been acquired³⁵ together with the voltage output from a photo diode³⁶ in *air*. The pulses have been generated by a remote controlled³⁷ red laser pointer³⁸ and distributed by a beam splitter made from a microscope

³⁵ ‘NI USB-6008’ from National Instruments Germany GmbH.

³⁶ ‘BPW 34’ from Conrad Electronic SE.

³⁷ Power switch bypassed by a ‘BC557’ transistor.

³⁸ ‘776265’ emitting at 654 nm from Conrad Electronic SE.

coverslip to the detector and the photo diode for synchronous data. The control of the laser pointer and data acquisition were carried out with a temporary setup³⁹ controlled by an IGOR PRO procedure. The reference data set used for deconvolution has been measured with the standard *purple* laser on a similar pristine sample in the *vacuum* chamber with the standard parameters, see Section 6.3, and processed by the standard procedure for a deconvolution measurement, see Section 3.5.1.

The power of the laser pointer after transition through the beam splitter has been measured before and after the experiment in continuous wave mode with an integrating sphere⁴⁰ equipped with a calibrated detector⁴¹. A measurement in pulsed mode has not been possible as the response time of the powermeter⁴² is too slow.

The in air measured sample data has been averaged manually, individual frames shifted in time from the average have been removed manually and the remaining frames have been averaged again for the detector signal and the diode voltage. The averaged detector signal has been processed analogue to a normal deconvolution, see Section 3.10.

Figure 5.46 illustrates the excellent agreement of the pulse lengths in the original and deconvoluted detector signal, and the diode response. The average power experienced by the detector disc amounts to 13.8 μW . The reflectivity of the disc has been measured as described in Section 5.1 at a wavelength of 654 nm and amounts to $\rho = 0.70$. This value is in good agreement with one value reported in literature^[191] but differs from another reported value^[192] of 0.65.

Since the deconvolution returns the absorbed power P_{abs} , the input power P_{in} can be calculated from the reflectivity $\rho(\lambda)$ by

$$P_{\text{in}} = \frac{P_{\text{abs}}}{1 - \rho(\lambda)} \quad (5.65)$$

and results in 46.0 μW , assuming the measured reflectivity is correct. Comparison with the measured power of the laser power of 46.3 μW reveals excellent agreement for this experiment. This compliance is striking since the measurement conditions are very different.

As this experiment successfully demonstrated the accuracy of the deconvolution and, since it uses *ex situ* and *in situ* measurement of the laser powers, it also confirms the reliability of the laser power measurement during calorimetric experiments.

In order to be able to obtain insight into reactions happening after adsorption

39 'NI USB-6008' from National Instruments Germany GmbH.

40 '819C-SL-3.3-CAL' from Newport Spectra-Physics GmbH.

41 '918D-UV-OD3' from Newport Spectra-Physics GmbH.

42 '842-PE' from Newport Spectra-Physics GmbH.

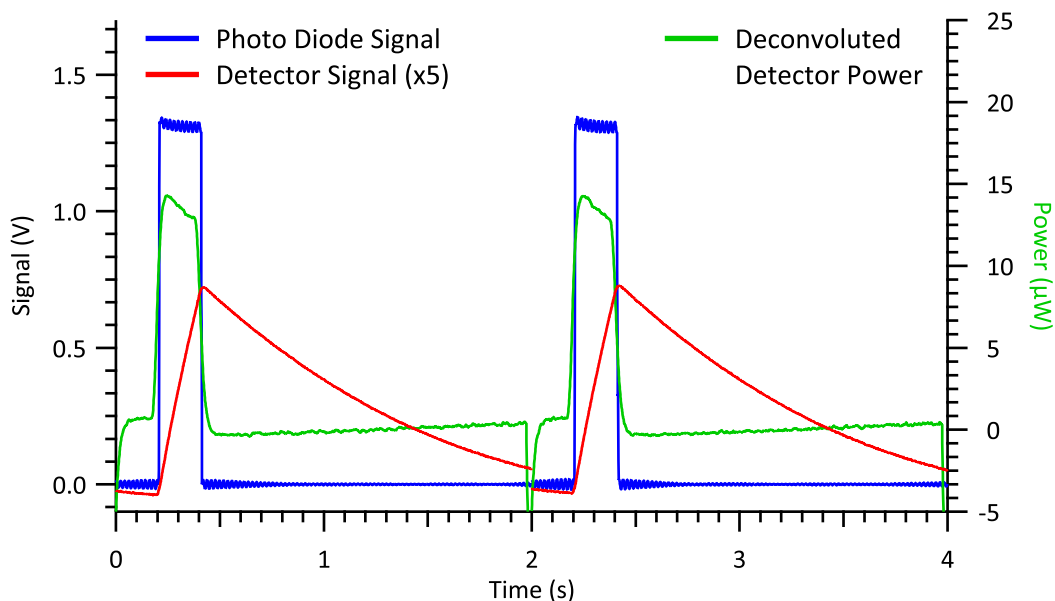


Figure 5.46: Round Robin Power Input Test — A data set obtained with the standard calorimetry setup was used to deconvolute (green) the average of 43 pulses from a hijacked^a red laser pointer^b. The data acquisition and the control of the laser were carried out with a temporary setup^c controlled by an IGOR PRO procedure. Parallel to the signal of the metalized β -polyvinylidene fluoride detector (red) the laser is recorded with a photo diode^d (blue) in voltage mode. The pulse length is well reproduced by the deconvolution. The decreasing power input clearly visible in the power is also present in the non-linear output of the photo diode. The discontinuity in the detector response originates from the measure equipment and causes the correlated dips in the deconvolution.

a Power switch bypassed by a ‘BC557’ transistor.

b ‘776265’ emitting at 654 nm from Conrad Electronic SE.

c ‘NI USB-6008’ from National Instruments Germany GmbH.

d ‘BPW 34’ from Conrad Electronic SE.

of a molecule on a thin film’s surface, this experiment should be repeated with better measurement equipment. Its focus should lie on a precise temporal control of the laser power and its measurement. While control of a laser pointer and data acquisition is already possible with the existing setup, the simultaneous power measurement needs to be improved. A possibility would be the use of a photo diode in combination with a transimpedance amplifier calibrated with continuous wave light against the available photometer⁴³. This setup would provide an output of the photo diode proportional to the input power.

43 ‘918D-UV-OD3’ attached to ‘819C-SL-3.3-CAL’ or ‘918D-SL-OD1’ operated by ‘842-PE’ all from Newport Spectra-Physics GmbH.

5.10 Statistical Considerations

The calibration of the detector relies on the reproducibility and stability of the laser based measurements. The calibration comprises several repetitions to measure the same property, *i.e.*, the response of the detector is measured to an energy input. Since the detector is linear, see Section 5.9.1, the input can be segregated. This situation suggests a normal, “Gaussian”, distribution of the obtained values.

During a reliability check of the stepper motor driving the beam chopper, see Section 2.3.3, the power of the laser during the measurement has been simultaneously recorded outside the vacuum system using a beam splitter made from a microscope coverslip. Since only one power meter was available, the absolute value of the recorded value has no significance. The relative values of the laser power and the detector response correlate, as shown in Figure 5.47.

The obtained $N = 360$ amplitudes have been normalized by the corresponding laser power and converted into a histogram. The number of bins has been chosen according to common practice^[193] to $\lceil 1 + \log_2(N) \rceil = 9$. The histogram agrees well with a normal distribution, as shown in Figure 5.48, and supports the assumption made in Section 3.7.

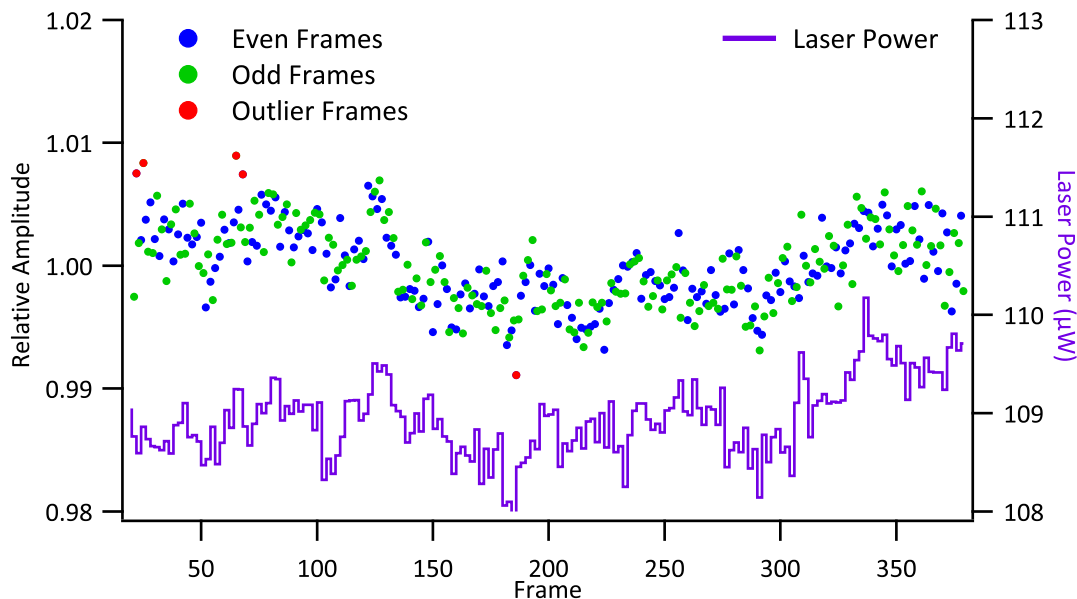


Figure 5.47: Relative Laser Reference Amplitudes — The relative amplitudes of an extended laser reference measurement (dots, left axis) are shown. The laser power (line, right axis) is acquired simultaneously using a simple beam splitter before entering the chamber. As expected the detector’s amplitudes follow the input power. The vertical axes span the same relative ranges.

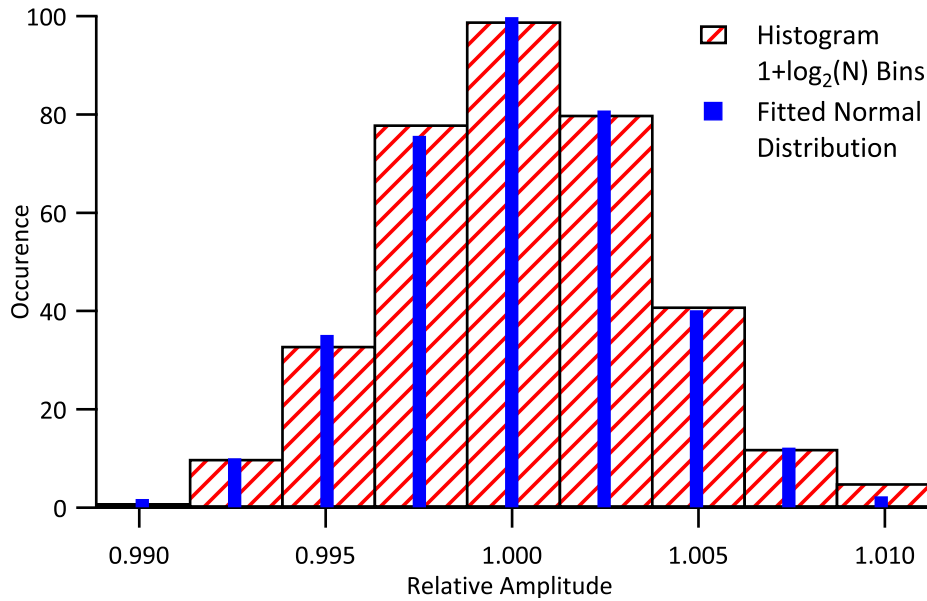


Figure 5.48: Histogram of Relative Laser Reference Amplitudes — A histogram containing the $N = 360$ pulses of the normalized amplitudes (red) from Figure 5.47 with a common bin size is superimposed with a fitted normal distribution (blue) with good agreement.

It should be emphasized that this sample is actually too small to proof this relationship since contaminated distributions can result in a very similar histogram. Additionally, a, legitimate, variation of the bin size can result in visually different histograms representing the same data.

The detector response is a function of the applied laser power, see Section 5.9.1. This rises the question whether the laser power has an influence on the parameters of the statistical distribution of the measured amplitudes. Since the utilized laser diode contains a power stabilizing mechanism^[151], no variation in the scatter of the amplitudes is expected.

Using the same detector disc, at each of five different nominal laser powers between 1 mW and 5 mW 100 frames have been recorded. The obtained data has been identically conditioned into box plots, see Section 3.6. The results are shown in Figure 5.49 suggesting a slightly lower stability only for the lowest power setting. Since the original focus of this measurement is a different topic, the higher scatter might also originate from external experimental conditions. The inter quartile range, *i.e.*, the range containing 50% of the data points, of 0.5% is well in agreement with the “cw-stability” stated in the manual^[151].

Subsequent to the short term time stability of the laser based measurements the demand to investigate the long term behavior is stimulated.

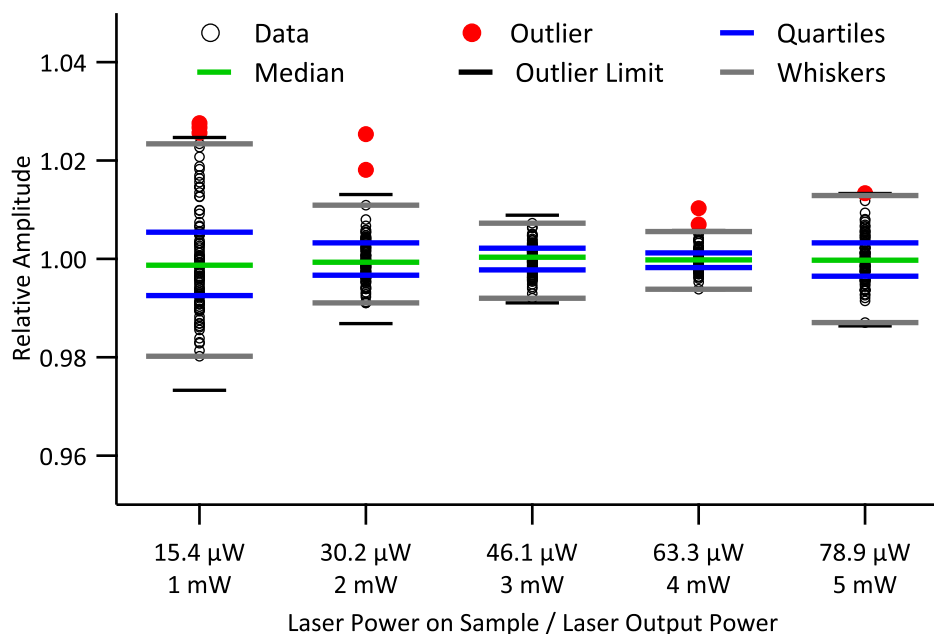


Figure 5.49: Scatter of the Laser Reference Amplitudes by Laser Power — The box plots, see Section 3.6, for five laser reference measurements with 100 frames each on the same sample with different laser power settings are shown. Except for the lowest setting with slightly higher scatter the laser power seems to have no influence. Outliers resulted from external interference.

Again, no significant influence is expected due to the power stabilizing mechanism^[151].

Figure 5.50 gathers box plots of several laser reference measurements over a period of about two years treated identically to obtain box plots. A significant degradation of the signal quality, *i.e.*, the inter quartile distance, can be observed between July 2013 and January 2014 which continued to worsen until February 2014 approaching a level of approximately 3%. Paradoxically, this period was dedicated to an optimization of the mass spectrometer with few usage of the laser.

Although the uncertainty seems to be stable enough to conduct further test measurements, a replacement of the laser diode should be considered prior to high precision measurements.

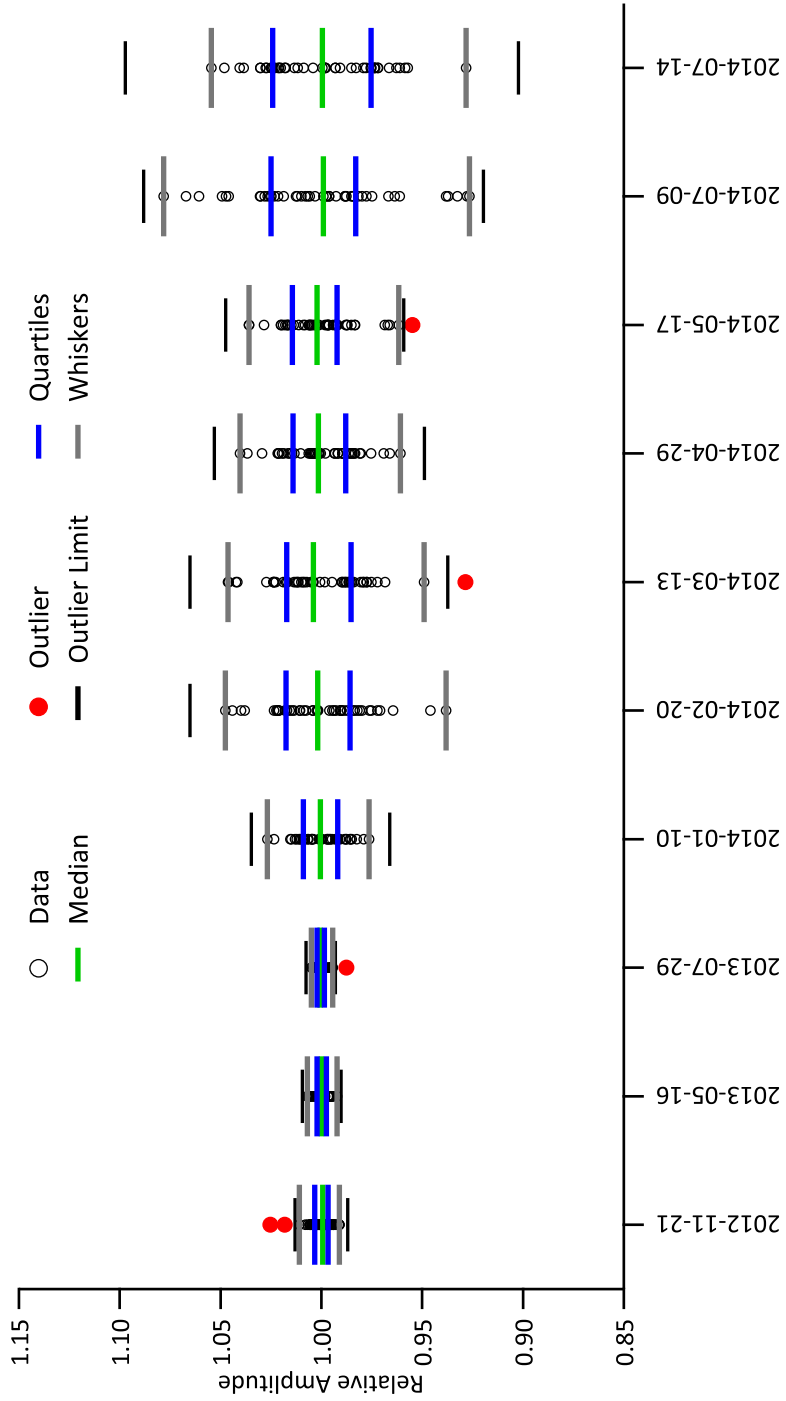


Figure 5.50: Scatter of the Laser Reference Amplitudes by Time — The box plots, see Section 3.6, for exemplary laser reference measurements with varying setting on different samples obtained during two years are shown. A degradation of the measurement quality is clearly visible, which is most likely related to a stability loss of the laser.

5.11 Synopsis of the Characterization Experiments

All individual measurements contributing to the actual calorimetric experiment have been characterized to ensure their reliability.

The reflectivity of the samples measured in an air based dedicated setup revealed a significantly lower value than reported in literature. This might originate from different specimen conditions or from a systematic error in the measurement setup and suggestions to improve the setup have been noted.

Sputter cleaning of samples was discovered to be essential to ensure a uniform deposition of substrate layers as well as during calorimetric experiments.

Influences of the partial loading, as a consequence of experimental requirements, were studied and the results counter-checked by a complementary method. The found values agreed with the experimental results corrected according to theory. A major contribution due to contamination was excluded.

The evaporator in the load lock was characterized by several means. One addressed the recommended evaporation temperatures of several organic substrate substances. Furthermore, an influence of the thermal load on the detector polymer during the deposition process was excluded for the presented materials. Finally, a conversion factor of the thickness read by the quartz crystal microbalance and the thickness of the organic layer on the sample was determined.

The specifications of the measurement card were successfully verified. The stability of the laser diode is lower than stated and a replacement or online monitoring of the laser power should be considered. The utilized amplifier is capable of measuring the pyroelectric signal. The automatic offset compensation affects the measurement and should be removed in an advanced version.

An extensive characterization of the pulsed molecular beam source was conducted. Evaporator temperatures, runtimes, and fill amounts have been obtained for several evaporants. The deposition rate was classified as stable and after installation of a choke, which also prevents macroscopic particles from being hauled out of the evaporator, as very stable. The intrinsic inline valve sustains ultra high vacuum conditions in the main chamber while the molecular beam source is vented. The chopper generates reproducible well defined pulses with adjustable temporal position. Ions from the resistively heated standard source are unlikely. However, the creation of ions is possible in case the electron beam evaporator is used. Measurement of the ion current was not possible and should be repeated. Laser based measurements are not influenced by the radiation from the evaporator as the carrier for the mirror in

the beam blocks infrared radiation effectively.

Several traps of the mass spectrometer have been identified and circumvented. Along this process, operation parameters for the mass spectrometer have been obtained and compared to theory.

All devices incorporated in the ancillaries stage were thoroughly characterized.

The infrared transparent window exhibits a comparable transmission factor for the used laser and the radiation from the evaporator only in case of high evaporation temperatures. The signal shape corresponding to radiation measurements is independent of the evaporator temperature. Together with the excellent agreement of the theoretical and the measured total intensity it renders a processing of the calorimetric data utilizing an optimized, independent radiation measurement possible. This is especially interesting in cases where usage of the window is not appropriate.

An attempt to measure the correlation of quartz crystal microbalances in sample position and in the ancillaries stage failed due to alignment problems and should be repeated. However, a major difference is not expected, since the theoretical correction can be applied successfully.

Degradation of the mirror located in the ancillaries stage and/or of the window used to couple the laser out of the vacuum system is observed and should be periodically verified.

The properties of the hot plate have been investigated with great efforts. The theoretical spatial correction differs from the observation. Yet, the theoretical value is very sensitive to positions which are not precisely obtainable. Instead of the improvised measurement setup used here, the experiment should be repeated with dedicated devices. An influence of the hot plate's temperature on the signal intensity could merely be guessed. As this experiment was only carried out for magnesium, it should be repeated for other adsorbates. The exponential decay of the mass spectrometer signal falsely indicated transient adsorption. A detailed theoretical investigation examines in which cases real transient adsorption can be observed. A meta analysis about the correlation of the peak intensity to the measured deposition rate indicated a non-proportional dependency. This result should be verified with a dedicated experiment.

Electrical responses of the pyroelectric detectors are proportional to the input power of the impinging laser and to the illuminated area. Annealing of the detector polymer to 370 K for three days resulted in no degradation of the sensitivity while exposure to 400 K lead to a rapid sensitivity loss. The dependency of the detector's sensitivity on the operation temperature has been demonstrated as well as the irrelevance of the detector thickness and plating material.

Considerable influence of the operation parameters of the ion gauge on the lower temperature of the sample has been discovered. However, the thawing time is not affected. Better thermal insulation is recommended.

A round robin test comparing the reconstructed power input with the directly measured input in air resulted in compatible values proving the correctness of the deconvolution algorithm. Additional significance arises from the facts that this experiment was carried out partially in vacuum and partially in air using different wavelength.

Finally, a glance upon the statistical contribution of the gathered data has been taken and the criterion to identify and automatically exclude faulty frames has been motivated.

Despite some hassle concerning the mass spectrometer whose response becomes irrelevant at high metal coverages, the characterization measurements predict accurate calorimetric results which involve several reference measurements.

6 Investigated Systems

The aim of this work is to build the experimental setup described in detail in Chapter 2, to develop the software for data treatment explained in Chapter 4, and to perform reference measurements. This chapter covers the latter topic and presents a tiny selection of conducted experiments. A compressed overview of experiments without obvious errors is given in Appendix D. As discussed in Section 2.2, the detector version for evaporated thin film on the metalized detector material was chosen due to the expected higher sensitivity.

The adsorption of metal atoms on different substrates is studied as a function of coverage by means of released energy and sticking probability.

Coverages are given in monolayers (ML) and/or meters. Deposition rates are stated in deposited meters per second or monolayers per second (ML/s) and are proportional to the corresponding fluxes since the relevant deposition regions have constant area.

Here, one monolayer is defined as a closed packed layer of the deposited atoms in a specified plane. The typically used plane is the closest packed plane for the most stable phase at room temperature, *i.e.*, the (111) plane for metals with cubic and the (0001) plane for metals with hexagonal crystal structure, *e.g.*, copper and magnesium, respectively. Both structures with their primitive spatial and corresponding planar unit cells are shown in the description of the used materials in Figures 6.1 and 6.2.

Detector discs made from 28 μm thick β -polyvinylidene fluoride metalized with 40 nm of copper topped by 15 nm of nickel have initially been cleaned by argon ion bombardment unless otherwise stated. For experiments involving an organic thin film substrate the substrate layers have been prepared on the cleaned discs by physical vapor deposition. The corresponding materials have been evaporated from quartz crucibles in the load lock, see Section 2.6, and the deposited thickness has been monitored simultaneously with a quartz crystal micro balance.

The individual parameters employed for calculations and operation of devices are listed in Appendix A and, unless otherwise stated, the sample has been at ambient temperature, *i.e.*, 310 K.

In general a multiple stage process can be assumed for adsorption measurements. The initial phase is dominated by the interaction of the dosed species with the

pristine substrate, *e.g.*, reaction with binding sites on the sample's surface or diffusion *into* the bulk material. Depending on the growth mode of the adsorbed material, transition phases, *e.g.*, diffusion *on* the surface and cluster growth are possible but not mandatory as also layer-by-layer growth is possible. During the final stage, after a sufficiently high coverage has been built up, the adsorbed species acts like bulk material.

As discussed in Section 1.2, the released heat in this case is identical to the negative heat of sublimation. As metals are deposited in this work the conducted experiments benefit from internal reference values. These enthalpies are well documented^[174] at standard temperature and can be precisely calculated at any given temperature. This turns the multilayer enthalpy into an ideal indicator for a successful experiment. It should be pointed out that this situation only applies to elements and simple inorganic compounds for which the heat capacities as a function of temperature, needed for the calculation, are well known. Potentially interesting organic molecules, *e.g.*, the chemicals used to form the thin films, exhibit a contrary record. While standard sublimation enthalpies can be found in literature or can be measured with moderate effort, there is a nearly total absence of temperature-dependent heat capacities and they need to be approximated by calculation, *e.g.*, using partition functions from statistical thermodynamics in combination with spectroscopic data.

The interest to deposit molecular substances rises from the possibility to study *inverted* systems in which the large organic molecules are deposited on the metallic substrate or layered systems formed by different organic substances, as mentioned in Section 1.3.

The presented experiments illustrate exemplarily which results and conclusions can be drawn from the obtained data. In advance to analysis and interpretation of the data sets, several runs using identical conditions should be averaged. This step is advised in order to improve the significance of the individual data points and to verify the reproducibility of the experiment. Since the focus of this work lies on the realization of the scientific framework for the experiment, the corresponding measurements could not be conducted during the assigned time in the laboratory. As a consequence, only individual cases of selected experiments are discussed in this chapter.

A complete overview of the investigated systems, presenting the full coverage ranges in the experiments, is given in Appendix D.

6.1 Choice of Materials

Materials used in this work, adsorptives (dosed matter) and adsorbents (substrates), are chosen primary by their hazard potentials, handling properties, availability, and price. Their scientific relevance, together with availability of results documented in literature, was only a secondary criterion as the focus of this work lies on the realization of the experimental environment and basic proof of concept measurements. Additionally, the scope of materials was intended to be limited to the adsorption of metals on reactive molecular substrates. Sublimating substances, *i.e.*, materials solid at evaporation temperature, are preferred due to the absence of the solid/liquid phase transition and their better evaporation characteristics, *e.g.*, higher vapor pressure stability due to the larger surface of a granular solid compared to a meniscus of a liquid in a crucible.

Candidates as adsorptives are given in Table 6.1. Criteria are temperatures for which certain vapor pressures are reached. As the system is degassed by heating, the vapor pressure during this bake-out procedure should not exceed 10^{-6} Pa, *i.e.*, approximately 10^{-8} Torr, which is equivalent to the statement that the temperature needed to reach this vapor pressure must be larger than 400 K. On the other hand, a reasonable vapor pressure needs to be established to form the atomic beam with high intensity within the operation range of the evaporator. The levels in this case were chosen to a temperature of less than 1100 K to provide a pressure of 10 Pa, *i.e.*, approximately 10^{-1} Torr.

Avoiding troublesome, *i.e.*, radioactive, toxic, *etc.*, materials, good adsorptives are strontium, lithium, calcium, magnesium, and zinc, of which the latter three were used in this work.

The choice of the organic substrates is somehow arbitrary. Previous work including the preparation of molecular organic thin films made from perylenetetracarboxylic dianhydride (PTCDA), tetraphenyl porphyrin, and phthalocyanine advise the use of these chemicals. The use of sexithiophene is motivated by preliminary work on one of its polymer derivatives, *i.e.*, poly(3-hexylthiophene). All compounds have been used as substrates.

In addition, the self-evident case without an organic layer, *i.e.*, the bare metalized detector material, is studied with and without cleaning by argon ion bombardment.

In this work materials were used as purchased. Vendors, purities, and evaporation parameters are listed in Appendix A. In this work, it is assumed that the thermodynamically most stable phases at ambient temperature are formed in the deposition process. Thus, all related properties, *e.g.*, monolayer densities, refer to these

Table 6.1: Properties of Selected Solid Elements — Solid elements are listed exhibiting a vapor pressure smaller than 10^{-8} Torr at 400 K and at least 10^{-1} Torr at 1100 K rendering them suitable for evaporation with the evaporator presented in Section 2.3.1. Commented elements should not be used.

Substance	Melting Point ^[187]	Temperature needed for a vapor pressure ^[187] of		Comments ^[166]
		10^{-8} Torr	10^{-1} Torr	
Antimony	903 K	552 K	885 K	Dimers and tetramers
Barium	983 K	545 K	984 K	Toxic
Bismuth	544 K	602 K	1050 K	Dimers and tetramers
Calcium	1123 K	555 K	962 K	
Europium	1099 K	556 K	981 K	Rare
Lithium	453 K	508 K	900 K	
Lead	600 K	615 K	1105 K	Toxic, liquid
Magnesium	923 K	458 K	782 K	
Radium	973 K	520 K	920 K	Radioactive
Strontium	1043 K	515 K	900 K	
Technetium	723 K	428 K	706 K	Radioactive, rare
Thallium	557 K	556 K	979 K	Toxic
Ytterbium	1097 K	520 K	920 K	Rare
Zinc	693 K	396 K	681 K	

phases. Especially for the organic substances, it is advised to implement additional purification steps prior to the physical vapor deposition or other coating processes. Nevertheless, the available purities of typically more than 95 % are sufficient for the presented exemplary measurements.

6.1.1 Magnesium

The use of magnesium is beneficial due to several aspects. It exhibits a rather high vapor pressure compared to other metals^[187] providing sufficient flux resulting in useful deposition rates for calorimetric experiments. Its passivating thin oxide layer^[166] permits storage and handling in air, and spares the use of inert gas or sealing liquid techniques reducing the experimental complexity. Despite its rather tame behavior in form of flakes, magnesium willingly undergoes various reactions if the oxide layer is removed^[166]. The affinity of magnesium to oxygen is remarkable and inspired the usage of PTCDA as one of the substrates. Finally, magnesium is commercially available, non-toxic, and economically efficient^[194].

The hexagonal structure of metallic magnesium is visualized in Figure 6.1 while

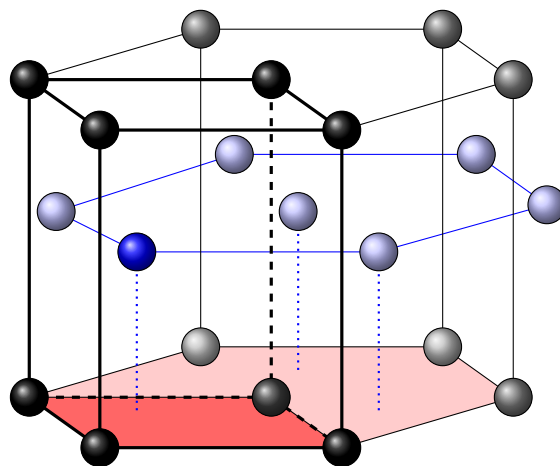


Figure 6.1: Crystal Structure of the Magnesium Type — The hexagonal structure (thin lines) of the magnesium type with its two sub-lattices (black and blue spheres) is shown together with the primitive unit cell (thick lines), the (0001) plane (light red) and the planar unit cell (red) within the (0001) plane used to derive the monolayer density. Magnesium and zinc crystallize in this structure.

the corresponding cell dimensions are listed in Appendix A.1.

6.1.2 Calcium

Calcium is non-toxic^[195] and exhibits a, compared to most other metals, slightly¹ lower vapor pressure^[187] than magnesium at a given temperature. However, the vapor pressure is still high enough to create a sufficient flux with the standard equipment. Although it must be stored in an inert gas atmosphere, it can be handled in air for short periods without self ignition^[166]. Oxidation of the surface during handling in air was ignored since the purchased material already showed a dull surface finish. In contrast, sublimation grade calcium sealed in argon filled glass ampules² exhibits a silver-like finish. Since calcium is slightly more reactive than magnesium^[166], a reaction with PTCDA seems also likely. Further on, the adsorption of calcium on various polymer substrates has already been studied by nanojoule adsorption calorimetry before. The organic films involve various reactive groups, like thiophene^[57,58,71,196], ester^[56,60,70], vinylene^[54,61,196], imide^[53], and cyano^[59] moieties. Additionally, studies on oxide surfaces are also reported^[27,29] investigating the adsorption energetics of calcium. The reactivity of calcium^[57,58,71,75,196] towards sulfur in the thiophene backbone in poly(3-hexylthiophene) inspired the usage of

¹ On a logarithmic scale. Compared to magnesium, the vapor pressure^[187] at 900 K of calcium is only a factor of 10^2 lower while the vapor pressure of gold is a factor of 10^{11} lower.

² ‘441872’ from Sigma-Aldrich Co. LLC.

sexithiophene, a molecular solid, in this work.

Metallic calcium crystallizes in the cubic face centered copper type, visualized in Figure 6.2. The corresponding cell dimensions are listed in Appendix A.2.

6.1.3 Copper

The main motivation to use copper as adsorptive was to test the applicability of the electron beam evaporator as an alternative source in the molecular beam, see Section 2.3. Besides the medium vapor pressure^[187], the low price, and high availability, the possibility to evaporate it from crucibles and convenient handling properties such as being nontoxic and air stable^[197], render it as the material of choice for this test. The presence of preliminary work on metalation reactions including copper^[88,198–200] and calorimetric measurements of copper adsorption on single crystals^[14,17,21,22] as well as polymer substrates^[53] support this decision even more.

The use of silver should also be possible with this setup. Although calorimetric data is available for the adsorption of silver on various substrates^[18,21,33,34,42], this substance was not tested since it is slightly more expensive than copper.

The cubic face centered structure of metallic copper is visualized in Figure 6.2 while the corresponding cell dimensions are listed in Appendix A.3.

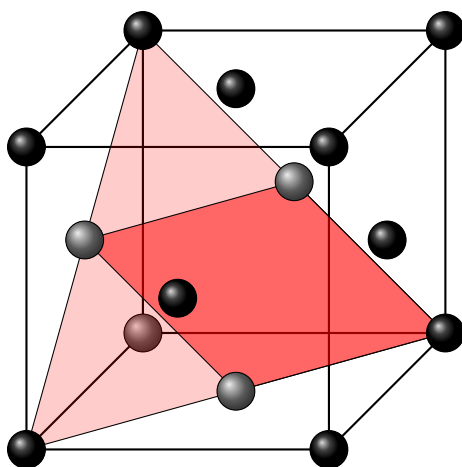


Figure 6.2: Crystal Structure of the Copper Type — The cubic face centered unit cell (thick lines) of the copper type is shown together with the (111) plane (light red) and the planar unit cell (red) within the (111) plane used to derive the monolayer density. Copper, calcium, and lead crystallize in this structure.

6.1.4 Zinc

The primary intention to use zinc as adsorptive was to test the applicability of the standard evaporator with an evaporant liquid at operation temperature. Besides the medium vapor pressure^[187], the low price, and high availability, its convenient handling properties such as being nontoxic and air stable^[201], render it the material of choice for this test. So far, no calorimetric measurements including the adsorption of zinc are published and also investigations utilizing other ultra high vacuum based methods are rare^[202]. This might be related to the rather high vapor pressure of zinc at comparable low temperatures resulting in distribution of this metal in the whole vacuum system and a possible contamination of attached instruments. Since most of the evaporated material is deposited in the cleanable molecular beam compartment, usage of zinc is still possible³.

Metallic zinc crystallizes in the hexagonal magnesium type, visualized in Figure 6.1. The corresponding cell dimensions are listed in Appendix A.4.

6.1.5 Lead

Lead as a heavy and rather nonreactive^[166] but yet harmful material^[203] was considered as a fitting material to calibrate the quartz crystals microbalance^[86,87,119] due to its low reactivity and high density. As consequence therefrom, impurities in the deposited material only have a minor stake in the calibration measurement, see Section 5.3. In addition, calorimetric data is available for the adsorption on single crystals^[15,19,20,24,34,55]. Unfortunately, the deposited lead reproducibly caused irreversible failure of the utilized oscillator crystals. Consequentially, the experiments involving lead have been aborted.

6.1.6 Unaltered Detector Material

The unaltered detector surface requires least handling and was thus chosen as one of the first investigated substrates. It is expected that adsorbed metals would at some point entirely cover a condoned contamination layer. In this case the contamination layer becomes “invisible” to the used technique. Hence, a correct heat of adsorption for multilayers is expected even for this poorly defined system. As a drawback, the heats of adsorption, before multilayers are built up, elude

³ Venting and chemical cleaning with diluted sulfuric acid followed by intensive rinsing with deionized water is recommended prior to any heating of the main chamber or the molecular beam.

interpretation. Furthermore, the reflectivity of this sample is known best, since samples are characterized in this state, see Section 5.1.

6.1.7 Sputter Cleaned Detector Material

Detectors cleaned by sputtering exhibit better defined surfaces. According to the data sheet the top layer consists of nickel which has been oxidized by storage in air. Since the sputtering time is adjusted to remove only the “soft” contamination layer, see Section 5.2, one can assume that the oxide layer is still present. The cleaning process slightly changes the reflectivity, but this alteration is taken into account by the software package, see Sections 3.5.2 and 3.5.3. Furthermore, no information is available about the influence of the sputtering process, *e.g.*, ion implantation, on the pyroelectrical properties of the detector polymer.

6.1.8 3,4,9,10-Perylene-Tetracarboxylic Dianhydride

PTCDA, *i.e.*, 3,4,9,10-perylene-tetracarboxylic dianhydride, shown in Figure 6.3, is commercially available in large quantities due to its use as colorant, where it is known as “Pigment Red 224”, and thus has an affordable price. PTCDA is non-toxic and tolerates ambient atmosphere^[204]. Its thermal stability renders preparation of smooth thin films^[85] possible using physical vapor deposition^[68,69,77]. Due to its outstanding dyeing capability, a rudimentary visual inspection of the film quality is possible, even for films with a thickness of a few nanometers.

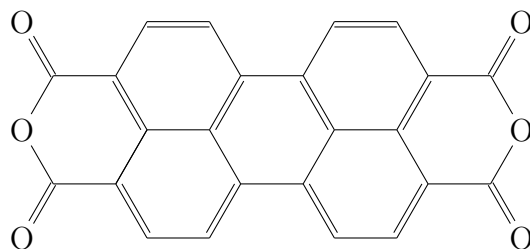


Figure 6.3: Chemical Structure of 3,4,9,10-Perylene-Tetracarboxylic Dianhydride — A perylene core has two anhydride groups attached which react with oxygenophilic metals. The formation of metal oxides or carboxylates are discussed as reaction products.

Its anhydride groups are known to react with a wide range of oxide forming metals^[68,69,77,85]. The known reactivity towards magnesium suggests also a strong interaction with the next heavier homologue, *i.e.*, calcium, also included in this work. Further interest arises from the usage of PTCDA as a low cost organic

semiconductor^[154,205,206]. The electronic properties of such devices depend on the metal organic interface and are thus tunable by the deposited material and deposition conditions^[207]. This rises interest for studies of these systems from an applied point of view.

6.1.9 Poly(3-Hexylthiophene)

Parallel to the terminal experiments including molecular substrates, attempts were made to start experiments involving spin-coated polymer substrates. Poly(3-hexylthiophene), shown in Figure 6.4, was chosen since this system has already been investigated by adsorption calorimetry^[57,58,71,196] and could serve as a reference system. Sample preparation was attempted in a similar way as described in [57] using an improvised spin coater. Besides, the polymer⁴ was dissolved in chloroform as it was purchased. The spin coating process did not reproduce the described results. The solution dried in a shorter period than the stated initial spinning time. Several coating attempts resulted in samples with visible non-uniform coating, *i.e.*, blotches and dewetted areas.

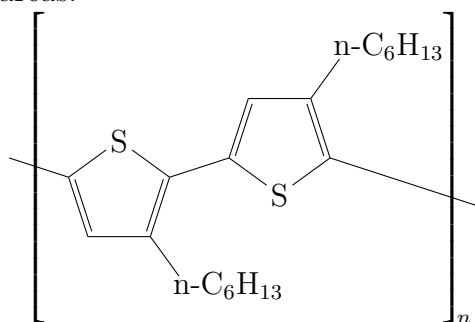


Figure 6.4: Chemical Structure of 2,5'-poly(3-Hexylthiophene) — This polythiophene is built from 2,5-concatenated thiophene monomers substituted in 3 position by a linear hexyl-chain. Reaction commences with the sulfur in the thiophene moieties presumably under formation of metal sulfides and cross-linking the carbon fragments.

Consequently, the sample preparation process needs to be improved. This would involve better substrate cleaning, *e.g.*, oxygen plasma etching, prior to the coating process. Furthermore, a dedicated spin coating setup would be beneficial. It should provide an inert gas atmosphere, which can be saturated with the used solvent during the distribution phase of the coating process. Unfortunately, this setup could not be realized within the given time.

Due to the poor surface condition and unreasonable results from sticking measurements, no experiments conducted on these samples are presented here. The *gigantic*

⁴ '594687' from Sigma-Aldrich Co. LLC.

signal effect, see Section 6.8, has not been observed on these samples so far.

6.1.10 Sexithiophene

Sexithiophene, shown in Figure 6.5, is a molecular oligothiophene and thus closely related to the backbone of other polythiophenes, *e.g.*, poly(3-hexylthiophene), with differences only in the number of repeat units and substituents. The reactivity of the monomer unit in the chain is expected to be comparable for both cases. The interaction of the reactive groups, *i.e.*, the sulfur atoms, with low work function metals, such as lithium, aluminum, sodium, and calcium, has been widely studied by calorimetry^[57,58,71,196] and other methods^[72–76].

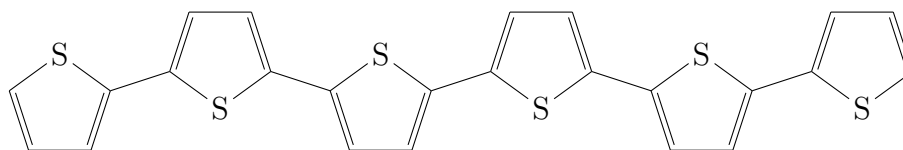


Figure 6.5: Chemical Structure of α -Sexithiophene — This oligothiophene is built from six 2,5-concatenated thiophene monomers. It occurs as a part of the backbone in poly(3-hexylthiophene) used in other publications. Reaction commences with the sulfur in the thiophene moieties presumably under formation of metal sulfides and cross-linking of the carbon fragments.

Further interest arises from the usage of sexithiophenes as organic semiconductors^[208–212]. The electronic properties of such devices depend on the metal organic interface and are thus tunable by the deposited material and deposition conditions. These possible modifications raise interest for studies of these systems from an applied point of view^[213–219].

6.1.11 Tetraphenyl Porphyrin

Tetraphenyl porphyrin, *i.e.*, 5,10,15,20-tetraphenyl-21*H*,23*H*-porphin – shown in Figure 6.6, is not toxic and air stable^[220]. In addition, experience has been gained to deposit thin films in previous work^[221,222] and metalation reactions with copper^[198–200] and zinc^[202] are known for tetraphenyl porphyrin. Furthermore, the metalation with copper is also known for the chemically related phthalocyanine^[88] exhibiting the same reactive site in the center of the molecule. However, calorimetric data investigating the adsorption of metals on porphyrin-like molecules is not known so far.

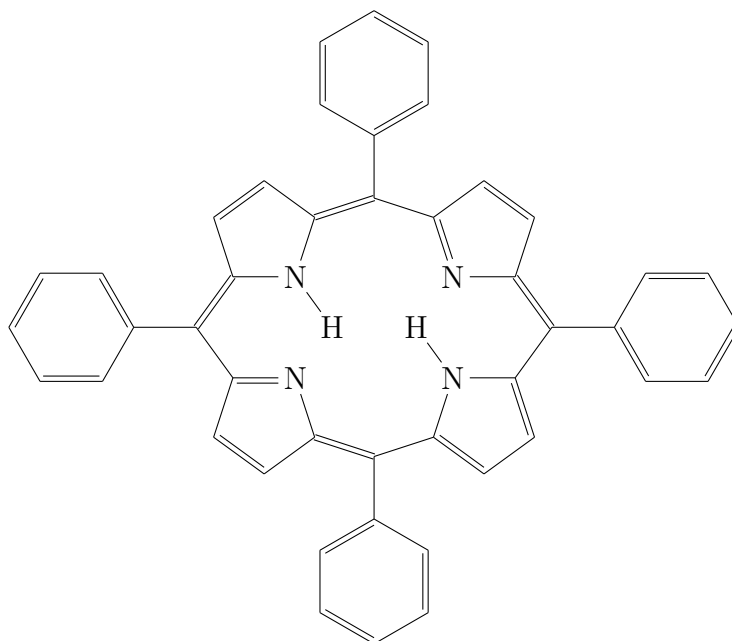


Figure 6.6: Chemical Structure of 5,10,15,20-Tetraphenyl-21*H*,23*H*-Porphin — The structure of the used four-fold phenyl substituted porphin is reacting in the center under oxidation of the metal atom about to be incorporated. This leads to formation of molecular hydrogen and the metalloporphyrin in which the metal is coordinated by the central four nitrogen atoms.

6.2 Reaction Thicknesses

As mentioned before, a major goal of this work is the investigation of developing interfaces. Besides the energetic point of view, it would be highly interesting to determine the thickness of the reaction zone between the unperturbed substrate and the adsorbate layer formed during the final stages of the measurement. However, in order to draw conclusions on the reaction thickness, nanojoule adsorption calorimetry requires additional information about the pristine surface structure. At the current state, the setup is not equipped with instruments to characterize surface morphologies.

Alternatively, the formed interphase could be studied after the calorimetry experiment by a complementary technique, *e.g.*, by X-ray photoemission spectroscopy utilizing angle variation or excitation energy alteration. Again, the current state of the setup does not contain instruments to perform these measurements.

Unfortunately, it has not been possible to perform all of these corresponding measurements yet.

In order to obtain at least a coarse approximation, one can consider the density of reaction centers in cubic reference volumes. The amount of reaction centers is given by the number of individual molecular reaction moieties n and the number of molecules per unit cell Z . The latter and the total volume V of the unit cell are listed as unit cell parameters, see Appendix A. This approximation allows to define a substitute area density of reaction centers $\tilde{\sigma}$ and an *ersatz* layer thickness \tilde{d} , as it has been reported analogously for polymer substrates^[56].

Using the geometrical properties of cubes, the thickness is given by

$$\tilde{d} = \sqrt[3]{\frac{V}{n \cdot Z}} \quad (6.1)$$

and the area density is given by

$$\tilde{\sigma} = \left(\sqrt[3]{\frac{n \cdot Z}{V}} \right)^2. \quad (6.2)$$

The volume V is given by the base vectors \vec{a} , \vec{b} , and \vec{c} or the lengths a , b , and d and the tilt angles α , β , and γ of the unit cell⁵ by

⁵ The unit cell can always be expressed as a parallelepiped^[188] and a certain basis therein.

$$\begin{aligned}
 V &= \vec{a} \cdot (\vec{b} \times \vec{c}) \\
 &= a \cdot b \cdot c \cdot \sqrt{1 + 2 \cdot \cos(\alpha) \cdot \cos(\beta) \cdot \cos(\gamma) - \cos^2(\alpha) - \cos^2(\beta) - \cos^2(\gamma)} . \quad (6.3)
 \end{aligned}$$

Table 6.2 lists the virtual values calculated by Equations 6.1 and 6.2 for the substrates used in this work.

Comparison of the substitute area density of the substrate $\tilde{\sigma}_{\text{Substr}}$ with the monolayer densities of the adsorbed species σ_{Ads} by

$$\rho_0 = \frac{\sigma_{\text{Ads}}}{\tilde{\sigma}_{\text{Substr}}} \quad (6.4)$$

yields the reaction equivalent ρ_0 describing the amount of adsorbate in monolayers to react with one *ersatz* layer of the substrate. Table 6.3 lists all possible combinations of adsorbates and substrates used in this work.

It should be pointed out again that this is an averaging and coarse approximation and will only provide an estimate. Due to its compensating nature, it will fail in case of highly ordered substrates, *e.g.*, molecules entirely lying flat on a substrate or entirely standing up straight. However, unordered and mixed phases should be approximated rather well since averaging is also needed in these cases to define a layer thickness.

Table 6.2: *Ersatz* Thicknesses and Area Densities — Virtual values used to approximate layer thicknesses and area densities for the used substrates are listed as calculated from Equations 6.1 and 6.2. Parameters for the unit cells are taken from literature and summarized in Appendix A.

Substance	Reaction Centers n	Virtual Area Density $\tilde{\sigma}$	Virtual Thickness \tilde{d}
PTCDA ^a [178,223]	2	$3 \cdot 10^{18} \text{ 1/m}^2$	0.6 nm
Phthalocyanine [224]	1	$1 \cdot 10^{18} \text{ 1/m}^2$	0.4 nm
Sexithiophene [225]	6	$5 \cdot 10^{18} \text{ 1/m}^2$	0.4 nm
Tetraphenyl porphyrin [226]	1	$1 \cdot 10^{18} \text{ 1/m}^2$	0.8 nm

a Perylenetetracarboxylic dianhydride

Table 6.3: Reaction Equivalents — Amounts of adsorbate given in monolayers necessary to react one *ersatz* layer of the substrate.

Substrate	Adsorbate			
	Magnesium	Calcium	Copper	Zinc
PTCDA ^a	0.3 ML	0.4 ML	0.2 ML	0.2 ML
Phthalocyanine	0.1 ML	0.2 ML	0.08 ML	0.09 ML
Sexithiophene	0.5 ML	0.7 ML	0.3 ML	0.3 ML
Tetraphenyl porphyrin	0.1 ML	0.2 ML	0.06 ML	0.07 ML

a Perylenetetracarboxylic dianhydride

6.3 Measurement Procedure

The sample-detector entities are assembled in air, see Section 2.2, and transferred into the load lock, see Section 2.6. After a degassing period of 36 h the samples can usually be introduced into the main chamber without increasing the base pressure of typically $8 \cdot 10^{-9}$ Pa above $2 \cdot 10^{-8}$ Pa. A typical experiment sequence is shown in Figure 6.7 and subsequently explained.

Due to the experimental situation, the reflectivity of the pristine sample needs to be measured outside the vacuum system in an analogue way as described in Section 5.1 or assumed to be constant.

As an initial reference, a measurement is performed on the unaltered sample, *i.e.*, the before coating measurement. The mirror in the molecular beam is moved to the position where it reflects the laser up towards the sample, see Section 2.3.2, to match the geometry of the molecular beam. The laser impinges on the sample and the response of the detector to the pulsed laser beam is recorded, see Sections 1.1.3 and 3.5.2. Subsequently, the power of the laser is measured, see Section 2.5.2. This step is necessary for all laser based measurements. It is recommended to read the laser power after the experiment since the moving of the ancillaries stage, see Section 2.4, causes a perturbation of the detector base line.

Typical parameters used for the measurements are listed in Table 6.4. Detailed information about the measurement procedure and the usage of the involved programs will be given in [227].

Since the reflectivity of the sample is known best at this time in the experimental sequence, it is recommended to conduct the deconvolution reference measurement at this point, see Section 3.5.1. If high accuracy in combination with a subsequent calorimetric measurement at non-ambient temperature is desired, the temperature of the sample should be adjusted and this step should be executed at the target temperature. In case of a supportive data deconvolution the program package provides an option to use a detector sensitivity correction, see Section 3.10.

Due to the external preparation steps, a minor contamination on the metal layer is present, see Section 5.2. Hence, the detector surface is cleaned by sputtering⁶ in the next step. This procedure is also applied to the systems containing a subsequent deposition process of an organic molecule on the now cleaned detector surface. The intermediate cleaning step appeared to be necessary since some specimens coated with an organic thin film exhibited inhomogeneities visible to the bare eye.

Information, *e.g.*, supply and purity, about the used chemicals are given in

⁶ Argon: 10^{-4} Pa, Ion Energy 3 keV, 10 minutes.

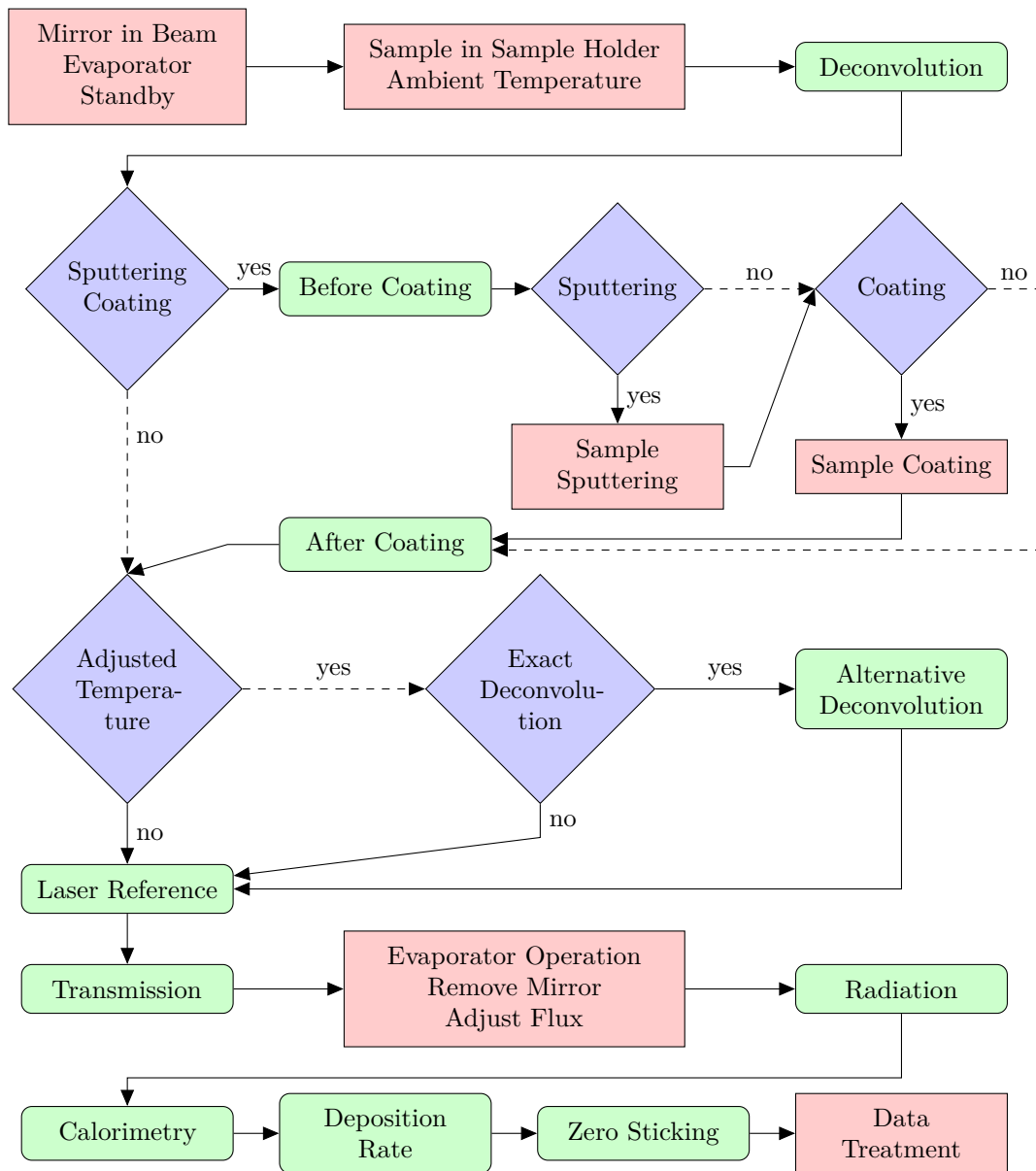


Figure 6.7: Work Flow of a Calorimetric Experiment — The sequence of typical experiments with user interactions (red), measurements (green), and typical decisions (blue) illustrates the standard (solid lines) and alternative (dashed lines) routes.

Table 6.4: Data Acquisition Parameters — Recommended data acquisition settings and experimental parameters are listed for different measurement types together with their dependencies.

Parameter	Regular	Deconvolution
	Measurement	
Pulse Delay	200 ms	3 s ^a
Pulse Length	200 ms ^b	3 s ^c
Chopper Period ^d	4 s ^e	120 s ^f
Laser Power ^g	≈ 20 μW	≈ 20 μW
Sample Rate	1 kHz	1 kHz
Range Calorimetry	±1 V	±5 V
Range Mass Spectrometer	±10 V	±10 V
Recorded Pulse Pairs	25	10

a Minimal one and a half times the chopper period of a regular measurement.

b Recommended range 100 ms to 300 ms.

c Minimal one and a half times the chopper period of a regular measurement.

d Time for a complete chopper cycle with two frames.

e Depends on the time for the signal to return to zero.

f Depends on the time for the signal to provide a flat baseline.

g Adjusted by `Laser Power Level` and measured after reflection out of the main chamber.

Appendix A together with the corresponding parameters for the instrumentation. Due to the absence of additional instrumentation the characterization of the prepared thin films by means of surface morphology, chemical composition, growth mode of the adsorbed species, *etc.* has not been possible.

The response of the detector to the laser, now with the prepared sample, is measured again, *i.e.*, the after coating measurement, to calculate the newly established reflectivity, see Section 3.5.3. This measurement has to be executed at the same temperature as the before coating measurement.

For all following measurements the temperature of the sample needs to be stabilized at the target temperature of the experiment.

The laser reference measurement provides the response of the detector to the laser input at the target temperature. At ambient temperature this experiment is identical to the after coating measurement. It is advised not to omit the apparently redundant after coating measurement since the temperature dependent sensitivity is calculated from these two data sets. A value differing from unity indicates a temperature difference in these two measurements and thus an incomplete temperature adjustment.

A similar measurement is performed with the infrared transparent window placed

in front of the sample. This transmission measurement is used to generate an initial value for the correction of the amount of thermal radiation from the evaporator, see Section 3.5.5. The effect of the different spectral ranges of the light used to measure the transmission and the actual attenuated radiation is discussed in Section 5.8.1.

To measure the reference for the radiation the evaporator is powered up from its stand-by⁷ to the evaporation temperature. The mirror in the beam is retracted and orifice is placed in operation position, see Section 2.5.2. After stabilization of the flux the infrared transparent window is moved to the same position as in the last mentioned measurement and the detector response to the radiative input can be acquired.

In order to minimize temperature fluctuations in the vacuum system the calorimetric measurement with the ancillaries stage moved most outward should be conducted at this point. The number of frame pairs being recorded depends on the deposition rate, pulse length, and sticking probability. Typical numbers range from 200 to more than 2000 frame pairs resulting in – depending on the employed deposition rate – around 1 to 100 dosed monolayer equivalents, corresponding for up to a few ten nanometers.

Next, the deposition rate of the material emitted from the evaporator is measured with the quartz crystal microbalance in the ancillaries stage, see Section 2.4.2. Due to the limited resolution of the corresponding controller, the thickness added during this measurement on the oscillator crystal should exceed 5 nm. Recording of the base lines before, in one chopper close position, and after, in the other chopper close position, the deposition measurement allows to identify and to compensate thermal drift. Another benefit arises from the possibility to detect a misadjustment of the chopper position manifesting in different slopes of the base lines. The deposition area is given by the experimental setup as $1.96 \cdot 10^{-6} \text{ m}^2$.

Subsequently, the zero sticking measurement is conducted. This position in the sequence reduces contamination due to a possible degassing of the hot plate and its surrounding as well as the influence of thermal drifts on the sample and the quartz crystal micro balance. The settings of the mass spectrometer need to be identical to the settings in the calorimetry experiment. The parameters for the mass spectrometer should have been obtained in an auxiliary experiment in advance to the actual calorimetry experiment with a similar deposition rate. The SEM voltage should be tuned to a value resulting in a clipping free output and an amplitude of approximately 5 V. Finally, the data was analyzed according to Chapter 3, typically employing fitted trends (polynomials of order 5 or 7) for the radiation contribution.

⁷ Typically $2/3$ of the operation temperature.

6.4 Adsorption of Magnesium

This section covers a selection of experiments in which magnesium has been adsorbed on various surfaces utilizing the calorimeter presented in Chapter 2 according to the procedure given in Section 6.3.

Experiments including magnesium formed the first investigated set due to the high vapor pressure and convenient handling of magnesium, see Section 6.1. As a drawback one might argue that adsorption of magnesium has not been studied by nanojoule adsorption calorimetry before and is less suitable as a proof of concept measurement. However, the magnesium/PTCDA interface has been studied before by other techniques, such as X-ray photoemission^[68,69] and Raman^[85] spectroscopy. These examples provide an illustration of results that could be expected.

6.4.1 Experiment: Adsorption of Magnesium

Magnesium evaporated from the molecular beam source has been converted into pulses and adsorbed on several substrates. Here, one monolayer is defined as $1.12 \cdot 10^{19} \text{ Atoms/m}^2$, corresponding to the basal plane of the hexagonal unit cell. Investigations using chromium and chromium oxide^[228] as substrates⁸ support the assumption that magnesium is growing along the [0001] direction, at least in the multilayer regime. The deposition rate has been adjusted to about 0.1 ML/s and the pulse length varied along the experiments between 0.15 s and 0.20 s resulting in doses of about $5 \cdot 10^{12}$ magnesium atoms per pulse which is equivalent to 8 picomole per pulse. The experiments have been conducted as described in Section 6.3 with the parameters mentioned there.

6.4.2 Results: Adsorption of Magnesium

Sticking Probabilities

Figure 6.8 presents the obtained coverage dependent sticking probabilities of magnesium on three different surfaces.

Magnesium on a raw, *i.e.*, as after introduction into the vacuum system, sample (pine) exhibits an initial sticking coefficient around 0.6 decreasing to 0.3 at 1.5 ML. With increasing coverage the sticking probability increases again to about 0.9 at 30 ML without an indication of saturation upon further deposition.

⁸ The calculated monolayer density in this work is incorrect.

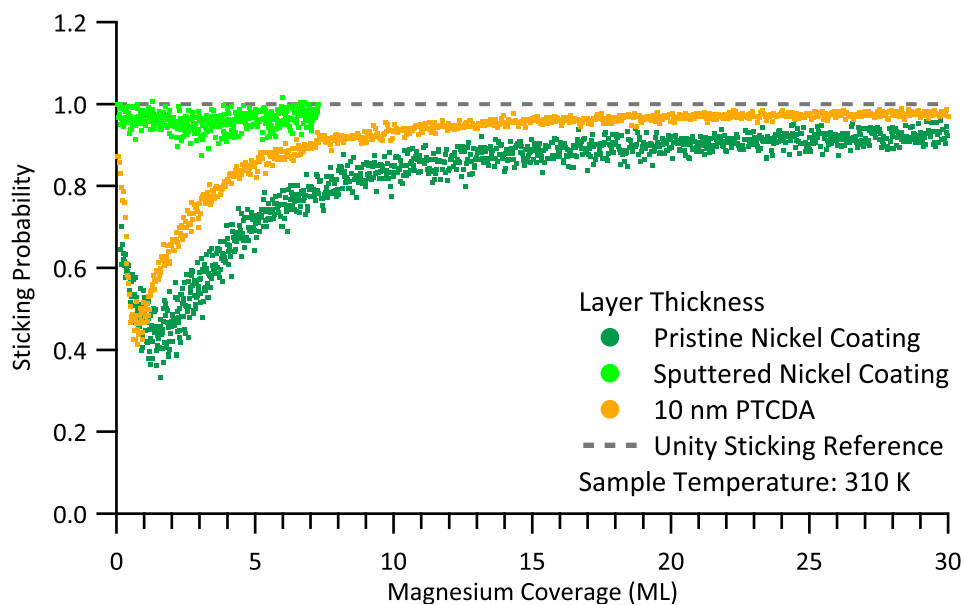


Figure 6.8: Adsorption of Magnesium: Sticking Probability — The sticking coefficients (dots) of magnesium adsorbed on different surfaces are plotted together with the unity sticking reference (dashed line) as a function of coverage. Each trace represents a single experiment. The pristine, *i.e.*, unaltered, detector surface (pine) exhibits a minimum of the sticking coefficient at low coverages which needs a large increase to recover and even at 30 ML unity sticking is not reached. The sticking coefficient of the freshly sputtered sample (green) is almost unity right from the start. A detector coated with 10 nm PTCDA (gold) shows a sharp minimum of the sticking probability at low coverages which slowly increases to the value of the sputtered sample.

In contrast to the unaltered specimen, a sample freshly cleaned by sputtering (green) exhibits almost unity sticking, *i.e.*, 0.98, from the first pulse on with a minor reduction to 0.95 between 2 ML and 4 ML.

The thin film of PTCDA (gold) prepared in the load lock, see Section 2.6, with a nominal thickness of 10 nm shows an initial sticking coefficient of about 0.9 which rapidly decreases to 0.4 at 0.9 ML. It slowly increases upon further dosage and reaches a similar magnitude as the sputter cleaned nickel surface.

Heats of Adsorption

Figures 6.9 and 6.10 compare the results of heat measurements for adsorption of magnesium on three different surfaces as a function of magnesium coverage.

The pristine, *i.e.*, unaltered, detector surface (pine) exhibits a heat of adsorption for the initial pulses of 385 kJ/mol for up to one monolayer. Subsequently, the released heat drops to approximately 105 kJ/mol for a coverage of 3 ML and rises again to 115 kJ/mol for higher coverages. The sputtered sample (green) shows the same initial value for the heat of adsorption but lacks the initial plateau region of the pristine sample. It undergoes a minimum at 3 ML reaching 75 kJ/mol and recovers around 6 ML at 90 kJ/mol . The specimen coated with PTCDA (gold) reveals a similar heat of adsorption of 380 kJ/mol for the first pulses as for the other two samples. It further contains a plateau region with a released heat of 270 kJ/mol between 0.6 ML and 1.2 ML and decreases monotonically to 110 kJ/mol at magnesium coverages of 6 ML and higher.

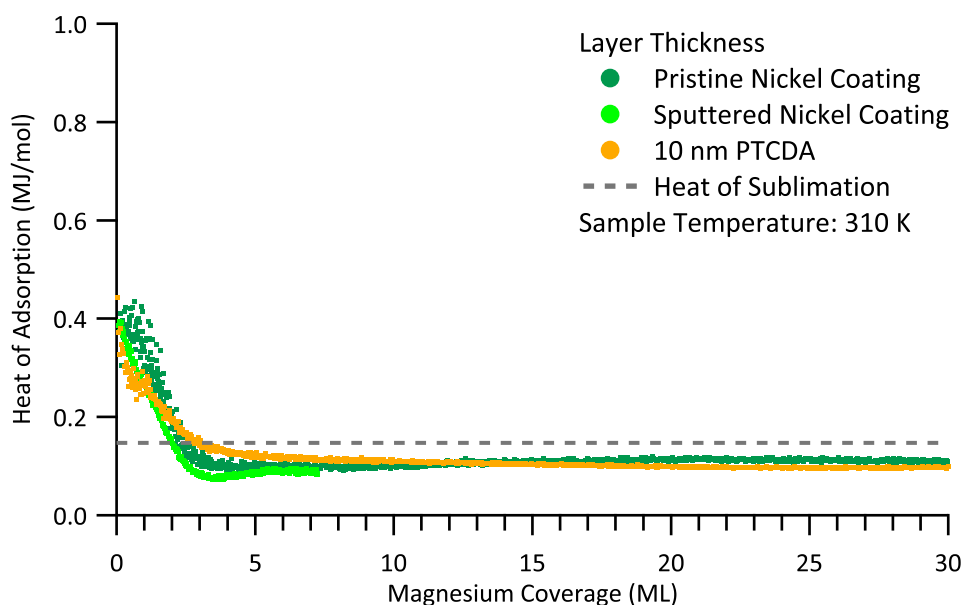


Figure 6.9: Adsorption of Magnesium: Heats of Adsorption — The derived heats of adsorption (dots) of magnesium dosed on different surfaces are plotted together with the calculated heat of sublimation reference (dashed line) as a function of coverage. Each trace represents a single experiment. The pristine, *i.e.*, unaltered, detector surface (pine), the freshly sputtered sample (green), and a detector coated with a thin layer of PTCDA (gold) exhibit the same global behavior. After a high initial released heat of adsorption it drops to a level below the sublimation enthalpy and remains at this level. Details for low coverages are given in Figure 6.10.

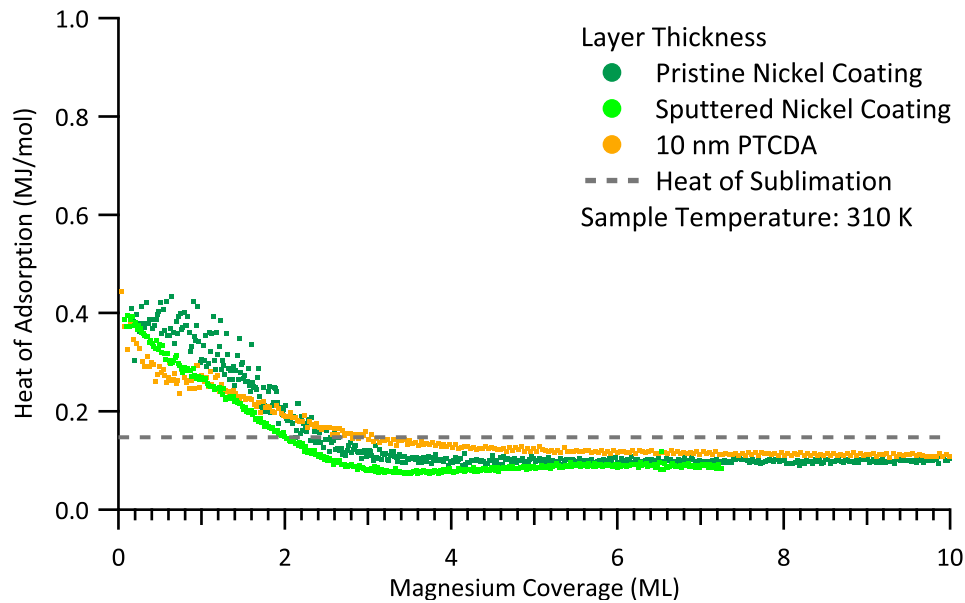


Figure 6.10: Adsorption of Magnesium: Heats of Adsorption at Low Coverages — The derived heats of adsorption (dots) of magnesium dosed on different surfaces are plotted together with the calculated heat of sublimation reference (dashed line) as a function of coverage. Each trace represents a single experiment. The heat of adsorption on the pristine detector surface (pine) exhibits an initial plateau. The result corresponding to the freshly sputtered sample (green) steadily decreases, reaches a minimum, and slightly rises again. The detector coated with 10 nm PTCDA (gold) exhibits a pronounced intermediate plateau.

6.4.3 Discussion: Adsorption of Magnesium

Results from the sticking measurements agree well with the observations made during characterization of the oscillator crystals for deposition rate measurements, see Section 5.2. The surface freshly cleaned by sputtering exhibits a very high sticking coefficient throughout the studied range. This behavior is generally expected if metals are dosed on metallic substrates^[15,17,18,24], especially on themselves.

Adsorption of magnesium on the unaltered detector results in a broad minimum of the sticking probability at low coverages. The constant released heat suggests a reaction of the first adsorbed monolayer of magnesium with the contamination layer, since a reaction with the nickel oxide layer results in a decreasing released heat. While the obtained heat is already reduced to a similar value as observed for multilayers, the sticking coefficient is still low. This suggests a modification of the surface during increasing adsorption of magnesium. A compound is formed from the dosed magnesium and the surface contamination which exhibits a low sticking probability and does not interact with magnesium. The absence of the minimum

in the heat of adsorption indicates a presence of larger clusters at a magnesium coverage of approximately 4 ML which already act like bulk material. These clues support a Volmer-Weber like growth mechanism in this case. At large coverages the heat of adsorption levels off below the heat of sublimation which is again the expected reference value. The result of a constant released heat beyond a magnesium coverage of 5 ML in combination with a variable sticking probability shows that the correction by the sticking coefficient is generally working.

The initially high heat of adsorption indicates a reaction or at least a very strong interaction with the cleaned detector surface. Its detailed nature cannot be specified further due to the lack of surface characterizing methods available in this setup. Possible reactions include the oxidation of water adsorbed after sputtering, reaction with defect sites created by the sputtering process, or a reduction of residual nickel oxide overlayer by the adsorbed magnesium. The latter type of reaction was reported for adsorption of magnesium on oxidized chromium^[228] while reaction with water is unlikely due to the low pressure in the system. Upon further dosage, the released heat is reduced and stabilizes at a coverage of 3 ML. The inflection point of the heat is located at approximately 1.2 ML, suggesting that roughly the first dosed monolayer of magnesium is reacting. A subsequent minimum in the calculated heat might originate from two possibilities. On the one hand, it might profanely arise from an artifact caused by the automatic base line offset removal in the employed amplifier, see Section 5.5.3, which is not entirely removed by the filtering process, see Section 3.3. Another model reported for other adsorbates^[15] implies a Stranski-Krastanov growth mode, *i.e.*, islands on an interlayer, which are higher in energy than the bulk material and thus release a reduced amount of heat. Larger scale errors induced by an incorrect zero sticking reference can be excluded in this experiment since its absolute finite amplitude becomes irrelevant as the corresponding coefficients are very close to zero. At higher coverages the obtained heat of adsorption does not match the heat of sublimation, which is the expected reference value, but remains reproducibly below this limit.

Upon adsorption of magnesium on a thin PTCDA layer, a strong decrease of the sticking probability suggests a pronounced change in the properties of the surface. Studies suggest a very strong interaction between PTCDA and the adsorbed magnesium^[68,69] including the cleavage of the C–O bonds in the anhydride groups resulting in the formation of magnesium oxide^[85]. This model is supported by the corresponding heats of adsorption which are very high at this coverage. The subsequent rapid diminishment of the observed heat and the fast increase in sticking probability argue in favor of a thin layer in which the dosed magnesium reacts with

the PTCDA and builds up a diffusion barrier. Using the inflection point located at a magnesium coverage of 1.4 ML in combination with the estimation from Section 6.2, one can conclude that about four layers of PTCDA react with the dosed metal. This is in agreement, within the scope of applied approximations, to results reporting a reaction thickness of approximately three layers determined by X-ray photoemission spectroscopy^[69].

This formed interface layer lessens the diffusion of dosed magnesium atoms to lower PTCDA layers and thus leads to growth of islands on the surface. Comparison with the sticking behavior of the cleaned sample reveals similar coefficients. It excludes a layer-by-layer growth on the reacted layer since the sticking probability should reach unity after the next monolayer of magnesium is adsorbed. Hence, a model in which magnesium clusters grow on a magnesium oxide layer covering the PTCDA substrate is applicable. This is also in accordance with X-ray photoemission spectroscopy investigations reported elsewhere^[69].

Due to the fact that the internal reference for the heat of adsorption is not matched for multilayers, the reported energies for the adsorption of magnesium on all mentioned substrates are questionable and thus not discussed on an absolute scale.

6.5 Adsorption of Calcium

This section presents a selection of experiments in which calcium has been adsorbed on various surfaces utilizing the calorimeter presented in Chapter 2 according to the procedure given in Section 6.3.

Experiments comprising calcium are motivated by the moderate handling efforts, the high vapor pressure, and preliminary work. The results for adsorption of calcium on various polymer substrates, *i.e.*, oxygen^[56,60,70] and sulfur^[57,58,71] containing similar moieties, inspired the use of PTCDA and sexithiophene as molecular substrates. The choice of tetraphenyl porphyrin as an additional substrate is based on the experience obtained from investigations by photo electron spectroscopy on metalation reactions with various metals forming double charged cations^[200,221,222,229]. However, no literature could be found addressing the metal/organic interface for PTCDA, sexithiophene, and tetraphenyl porphyrin exposed to calcium vapor. Due to the similar reactive groups in the corresponding substrates, *e.g.*, the thiophene units in sexithiophene and poly(3-hexylthiophene), comparable results can be expected.

6.5.1 Experiment: Adsorption of Calcium

Calcium evaporated from the molecular beam source has been converted into pulses and adsorbed on several substrates. One monolayer is defined as $7.40 \cdot 10^{18}$ Atoms/m² in this case, assuming growth in the [111] direction which is in agreement with other work^[56–61]. The deposition rate has been adjusted to 0.3 ML/s for the measurement using the sputtered detector and to about 0.08 ML/s for all other measurements. An identical pulse length of 0.20 s results in doses of about $9 \cdot 10^{12}$ calcium atoms per pulse which is equivalent to 15 picomole per pulse for the measurement on the sputtered detector and $2 \cdot 10^{12}$ calcium atoms per pulse which is equivalent to 4 picomole per pulse for the other experiments. The experiments have been conducted as described in Section 6.3 with the parameters mentioned there.

6.5.2 Results: Adsorption of Calcium

Sticking Probabilities

Figure 6.11 presents the obtained coverage dependent sticking probabilities of calcium on two different surfaces.

A sample freshly cleaned by sputtering (green) exhibits unity sticking from the first pulse on for calcium in the entire studied range. A contrary result is obtained in case calcium is adsorbed on a 310 nm thick layer of free base tetraphenyl porphyrin (purple). Here, the initial sticking coefficient of 0.9 is slightly lower and decreases to 0.75 at a calcium coverage 0.7 ML. It slowly increases upon further dosage and reaches unity at 6 ML and above.

Figure 6.12 shows the obtained coverage dependent sticking probabilities of calcium on vapor deposited PTCDA surfaces with thicknesses of 20 nm and about 660 nm. The specimen with the thinner layer (gold) exhibits unity sticking from the first pulse on for calcium adsorption in the entire studied range. The experiments involving the

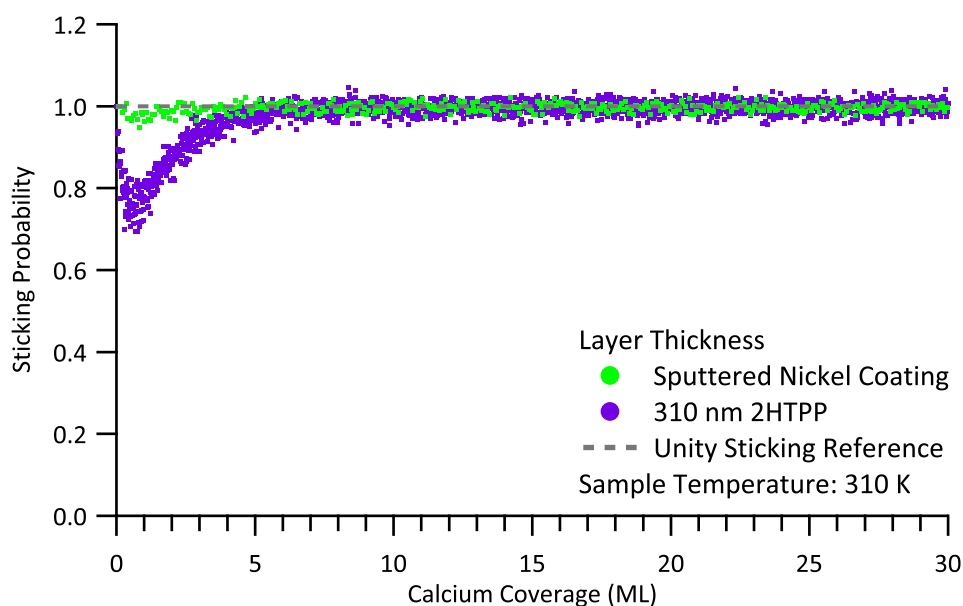


Figure 6.11: Adsorption of Calcium: Sticking Probabilities (Clean Detector, Tetraphenyl Porphyrin) — The sticking coefficients (dots) of calcium adsorbed on different surfaces are plotted together with the unity sticking reference (dashed line) as a function of coverage. Each trace represents a single experiment. The sticking coefficient of the freshly sputtered sample (green) is almost unity right from the start. A different behavior is shown upon adsorption on a thick layer of tetraphenyl porphyrin (2HTPP – purple). The initial sticking coefficient undergoes a minimum and finally reaches a constant high value similar to the other specimen, see Figures 6.12 and 6.14.

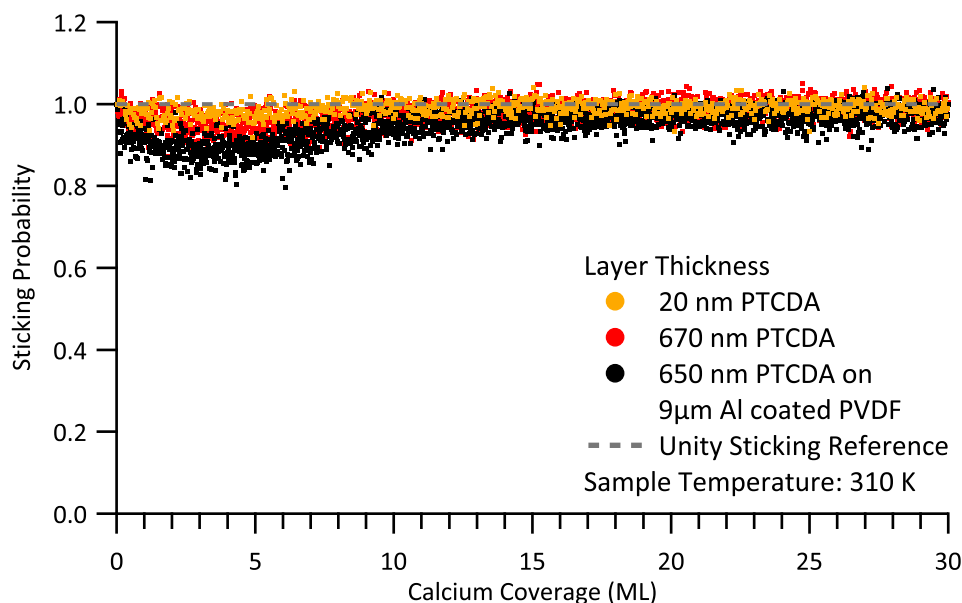


Figure 6.12: Adsorption of Calcium: Sticking Probabilities (PTCDA) — The sticking coefficients (dots) of calcium adsorbed on PTCDA surfaces with two different layer thicknesses are plotted together with the unity sticking reference (dashed line) as a function of coverage. Each trace represents a single experiment. The sticking coefficient of the detector coated with a thin layer of PTCDA (gold) is almost unity right from the start. Two different detectors each coated with a thick layer of PTCDA (red^a, black^b) show wide weak minima regarding the sticking probability between 2 ML and 6 ML returning to their initial value.

a Detector Material: '28um/w 400CU/150NI' from Measurement Specialties.

b Detector Material: 'FV301890/1' from Goodfellow GmbH – discontinued; not sputtered.

thicker layers each exhibit an initial sticking coefficient of 0.95 and undergo a broad shallow minimum between 1 ML and 9 ML dropping to 0.91 on the nickel coated (red) and to 0.89 for the aluminum coated unsputtered specimen (black). For higher coverages the sticking probability levels out at 0.98.

Figure 6.13 shows the obtained coverage dependent sticking probabilities of calcium on vapor deposited PTCDA surfaces with thicknesses of 20 nm (orange) and 620 nm (red) held at 80 K by liquid nitrogen cooling. Both specimens exhibit unity sticking probability in the entire studied range.

Figure 6.14 illustrates the obtained coverage dependent sticking probabilities of calcium on vapor deposited sexithiophene surfaces with thicknesses of 30 nm (cyan), 100 nm (azure), and 310 nm (blue). The specimen with the thin layer exhibits an initial sticking probability of 0.61, the one with the medium layer thickness a probability of 0.83, and the one with the thick layer a probability of 0.90. The

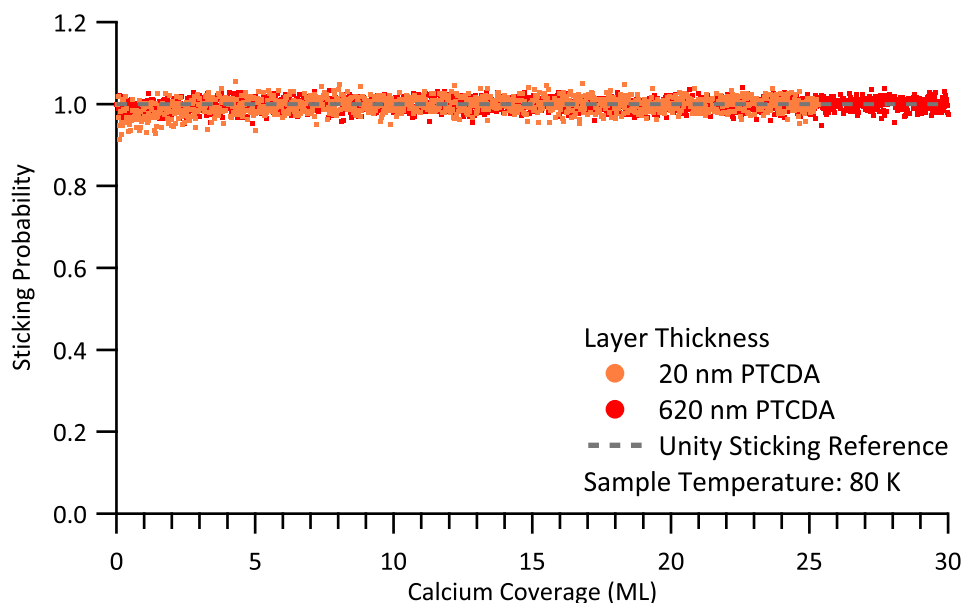


Figure 6.13: Low Temperature Adsorption of Calcium: Sticking Probabilities (PTCDA) — The sticking coefficients (dots) of calcium adsorbed at cryogenic temperatures on PTCDA surfaces with two different layer thicknesses are plotted together with the unity sticking reference (dashed line) as a function of coverage. Each trace represents a single experiment. The sticking coefficients of the detectors coated with a thin layer of PTCDA (orange) and with a thick layer of PTCDA (red) are both unity in the investigated range of calcium coverage.

sticking coefficient increases rapidly and reaches 0.95 at 3 ML. For higher calcium coverages it levels out at 0.98, which is identical to the final value obtained for the deposition of calcium on PTCDA, see Figure 6.12.

Figure 6.15 shows the obtained coverage dependent sticking probabilities of calcium on vapor deposited sexithiophene surfaces with thicknesses of 160 nm (azure) and 670 nm (blue) held at 80 K by liquid nitrogen cooling. Both specimens exhibit a high sticking probability of 0.95 for the initial pulses and level out at unity within 2.5 ML for the remaining studied range.

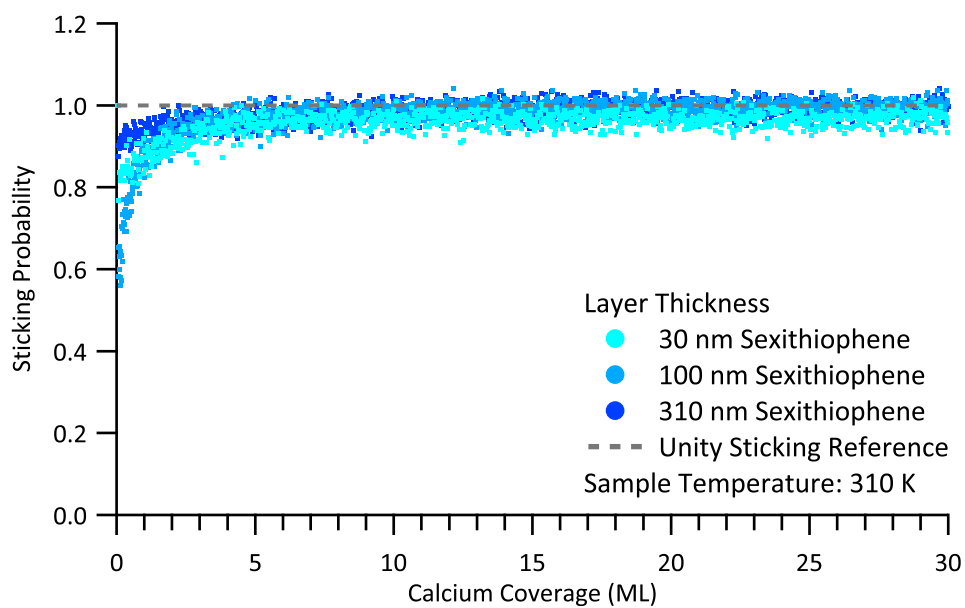


Figure 6.14: Adsorption of Calcium: Sticking Probabilities (Sexithiophene) — The sticking coefficients (dots) of calcium adsorbed on sexithiophene surfaces with different layer thicknesses are plotted together with the unity sticking reference (dashed line) as a function of coverage. Each trace represents a single experiment. The sticking probability on thin (cyan), medium (azure), and thick (blue) sexithiophene layers is moderate for the initial pulses and levels off within 2 ML slightly below unity independent of the layer thickness.

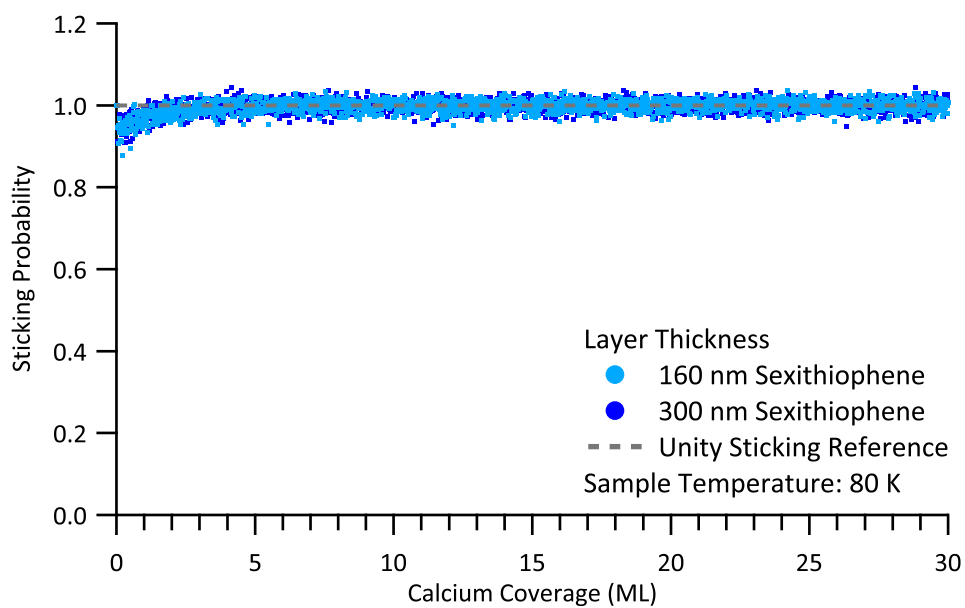


Figure 6.15: Low Temperature Adsorption of Calcium: Sticking Probabilities (Sexithiophene) — The sticking coefficients (dots) of calcium adsorbed at cryogenic temperatures on sexithiophene surfaces with different layer thicknesses are plotted together with the unity sticking reference (dashed line) as a function of coverage. Each trace represents a single experiment. The sticking probability on medium (azure) and thick (blue) sexithiophene layers is high even for the initial pulses and reaches unity within 2 ML independent of the layer thickness.

Heats of Adsorption

Figures 6.16 and 6.17 compare the results of heat measurements for adsorption of calcium on two different surfaces as a function of calcium coverage.

The detector surface cleaned by sputtering (green) exhibits a heat of adsorption for the initial pulses of 500 kJ/mol decreasing to a narrow plateau of 180 kJ/mol at a calcium coverage of 1.1 ML and reaches a minimum of 65 kJ/mol at 2.7 ML. Subsequently, the released heat increases again to approximately 85 kJ/mol for a coverage of 5 ML and further to 100 kJ/mol for coverages larger than 15 ML.

The specimen coated with 310 nm tetraphenyl porphyrin (purple) exhibits an initial heat of adsorption of 475 kJ/mol decreasing to a plateau value of 180 kJ/mol between 1 ML and 3 ML. Subsequently, the obtained value undergoes a shallow minimum around 4.5 ML dropping to 155 kJ/mol . At higher calcium coverages a pronounced maximum at 20 ML reaching 2 MJ/mol (*sic*) is noticed. This gigantic

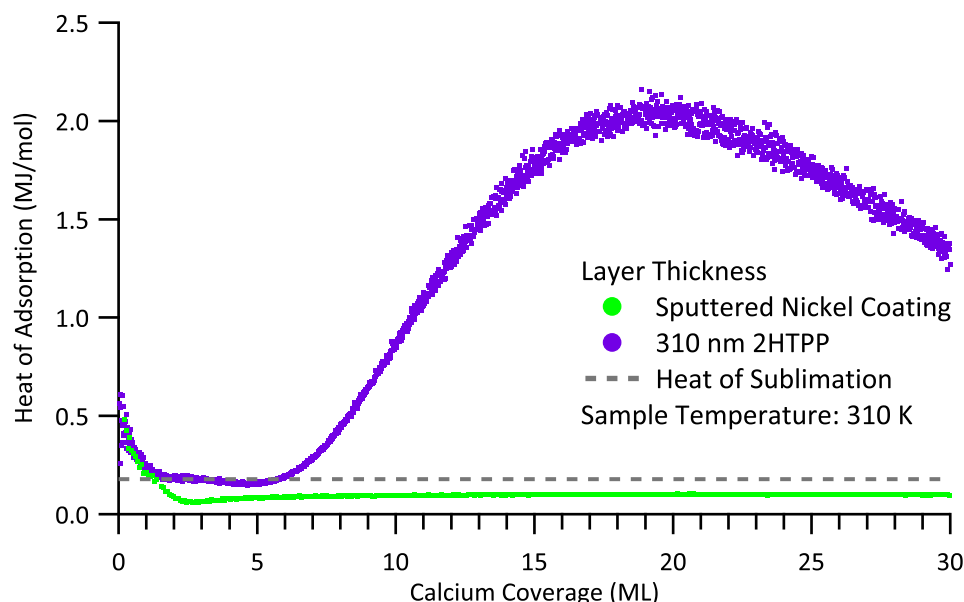


Figure 6.16: Adsorption of Calcium: Heats of Adsorption (Clean Detector, Tetraphenyl Porphyrin) — The derived heats of adsorption (dots) of calcium dosed on different surfaces are plotted together with the calculated heat of sublimation reference (dashed line) as a function of coverage. Each trace represents a single experiment. The freshly sputtered sample^a (green) and a detector coated with tetraphenyl porphyrin (2HTPP – purple) exhibit a high initial released heat of adsorption. It drops rapidly in case of the sputtered specimen and slowly in case of the coated specimen to levels stabilizing below the sublimation enthalpy. Details for low coverages are given in Figure 6.17.

^a Measured at a calcium deposition rate of 0.3 ML/s .

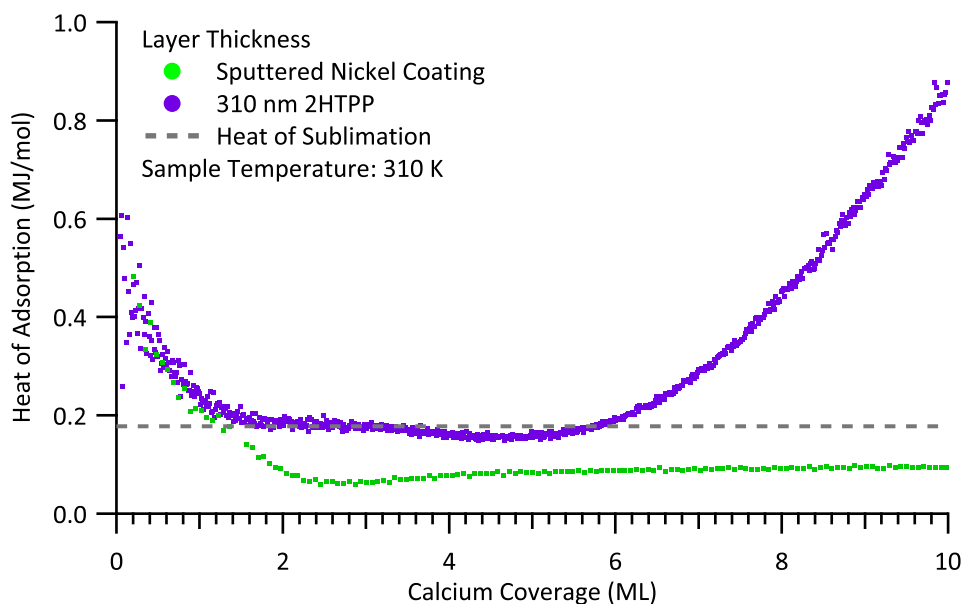


Figure 6.17: Adsorption of Calcium: Low Coverage Heats of Adsorption (Clean Detector, Tetraphenyl Porphyrin) — The derived heats of adsorption (dots) of calcium dosed on different surfaces are plotted together with the calculated heat of sublimation reference (dashed line) as a function of coverage. Each trace represents a single experiment. The heat of adsorption of calcium on the sputtered detector surface^a (green) exhibits a rapid drop during the initial pulses followed by a narrow plateau and a shallow minimum. The result corresponding to the sample coated tetraphenyl porphyrin (2HTPP – purple) exhibits a plateau at the sublimation enthalpy and subsequently exhibits a pronounced increase.

^a Measured at a calcium deposition rate of 0.3 ML/s .

increase independent of the detector material was also directly observable during the data acquisition and in the raw data.

Figures 6.18 and 6.19 illustrate the results of heat measurements for adsorption of calcium on two PTCDA layers of different thickness as a function of calcium coverage.

The detector coated with 20 nm of PTCDA (gold) exhibits a heat of adsorption for the initial pulses of 380 kJ/mol decreasing with two kinks at calcium coverages of 1 ML and 3 ML to 345 kJ/mol and 290 kJ/mol , respectively. Subsequently, the released heat undergoes a very broad and shallow minimum at 120 kJ/mol between 8 ML and 18 ML to level out again at 140 kJ/mol for higher calcium coverage.

The specimens coated with more than 650 nm of PTCDA on the two detector materials, see Section 5.9.5, exhibit a similar trend of the released heat as the sample with the thin coating. The initially released heat amounts to 500 kJ/mol in case of the

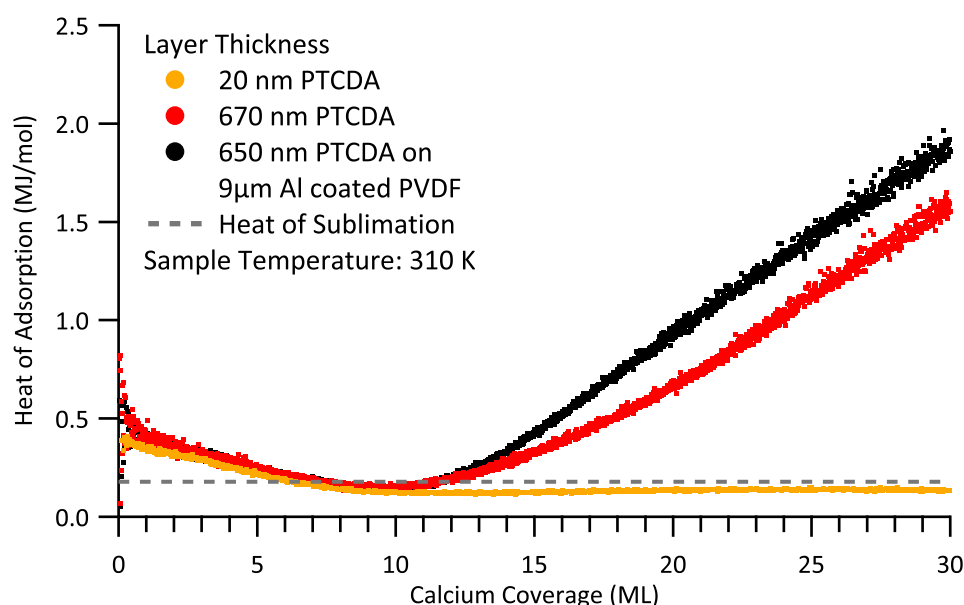


Figure 6.18: Adsorption of Calcium: Heats of Adsorption (PTCDA) — The derived heats of adsorption (dots) of calcium adsorbed on PTCDA surfaces with two different layer thicknesses and two detector materials are plotted together with the calculated heat of sublimation reference (dashed line) as a function of coverage. Each trace represents a single experiment. The detectors coated with a thin layer (gold) and coated with a thick layer of PTCDA (red^a, black^b) exhibit the similar behavior for small coverages. At high coverages the results differ dramatically as the value obtained for the thick layer samples increases immensely while remaining constant for the thin layer specimen. Details for low coverages are given in Figure 6.19.

a Detector Material: ‘28um/w 400CU/150NI’ from Measurement Specialties.

b Detector Material: ‘FV301890/1’ from Goodfellow GmbH – discontinued; not sputtered.

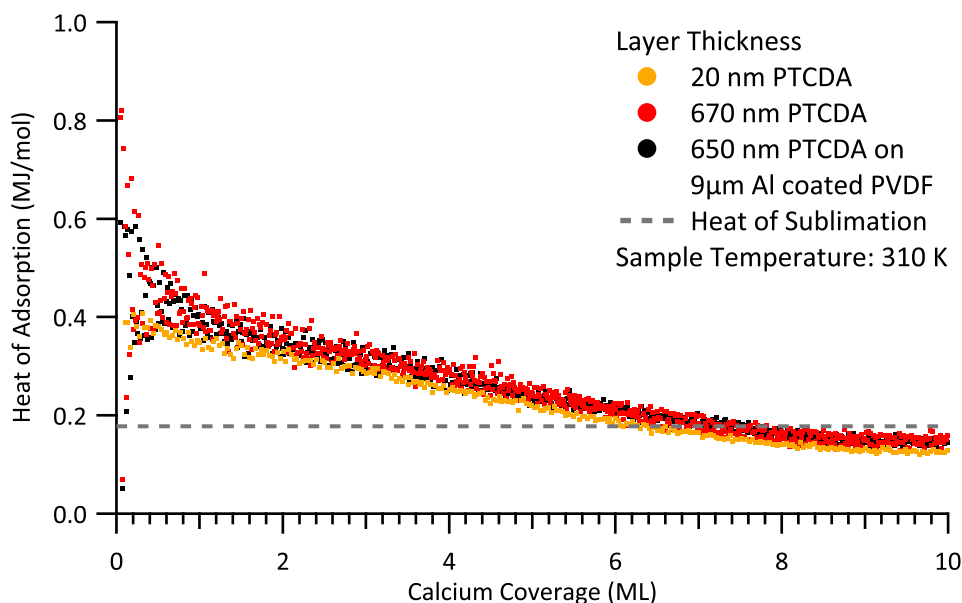


Figure 6.19: Adsorption of Calcium: Low Coverage Heats of Adsorption (PTCDA) — The derived heats of adsorption (dots) of calcium adsorbed on PTCDA surfaces with two different layer thicknesses and two detector materials are plotted together with the calculated heat of sublimation reference (dashed line) as a function of coverage. Each trace represents a single experiment. The heats of adsorption of calcium on the thin (gold) and thick (red^a, black^b) PTCDA layers are similar. The heat decreases continuously with two kinks at the same calcium coverage.

- a Detector Material: ‘28um/w 400CU/150NI’ from Measurement Specialties.
 b Detector Material: ‘FV301890/1’ from Goodfellow GmbH – discontinued; not sputtered.

regular detector material⁹ (red) and 460 kJ/mol for the alternate detector material¹⁰ (black). The first kink at a coverage of 1 ML exhibits similar adsorption enthalpies of approximately 395 kJ/mol in both cases. They share a second kink at a calcium coverage of 4 ML corresponding to a released heat of 280 kJ/mol. Subsequently, both obtained values undergo a minimum between 8 ML and 11 ML reaching 150 kJ/mol. At higher coverages the obtained results increase tremendously above 1 MJ/mol (*sic*) and continue to increase up to 2.5 MJ/mol (*sic*) at calcium coverages around 40 ML (not shown). This reproducible gigantic increase independent of the detector material, see Section D.6, is also directly observable during the data acquisition and in the raw data.

- 9 Nickel/copper coated 28 μm β-polyvinylidene fluoride: ‘28um/w 400CU/150NI’ from Measurement Specialties.
 10 Aluminum coated 9 μm β-polyvinylidene fluoride: ‘FV301890/1’ from Goodfellow GmbH – discontinued.

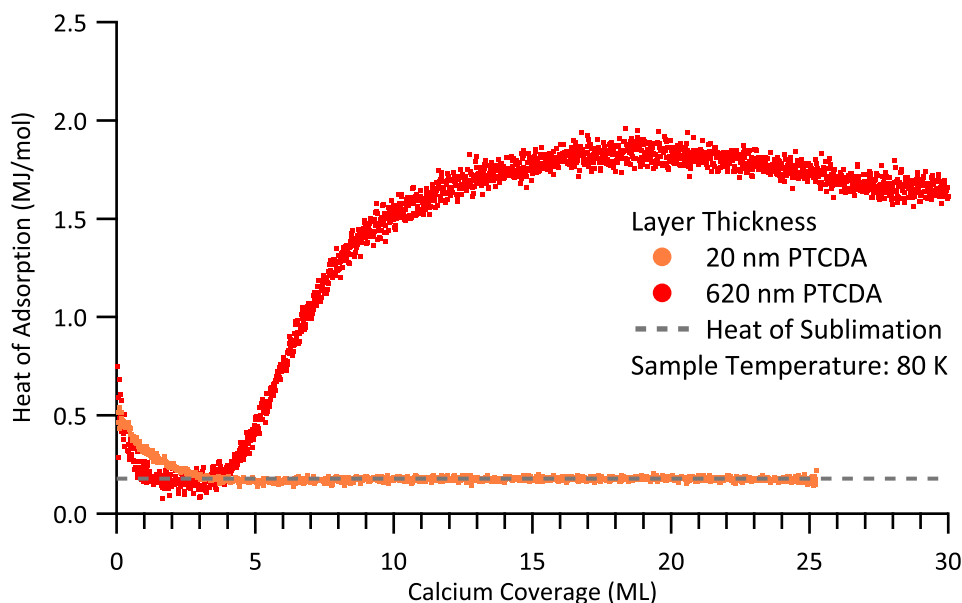


Figure 6.20: Low Temperature Adsorption of Calcium: Heats of Adsorption (PTCDA) — The derived heats of adsorption (dots) of calcium adsorbed at cryogenic temperatures on PTCDA surfaces with two different layer thicknesses are plotted together with the calculated heat of sublimation reference (dashed line) as a function of coverage. Each trace represents a single experiment. The detectors coated with a thin layer (orange) and coated with a thick layer of PTCDA (red) exhibit similar behavior. At medium coverages the obtained values, in contrast to the experiment at ambient temperature, see Figure 6.5.2, increase immensely for both specimens. Details for low coverages are given in Figure 6.21.

Figures 6.20 and 6.21 are illustrating the results of heat measurements for adsorption of calcium on two PTCDA layers of different thicknesses held at 80 K by liquid nitrogen cooling as a function of calcium coverage.

The detector coated with 20 nm of PTCDA (orange) exhibits a heat of adsorption for the initial pulses of 490 kJ/mol which is similar to the results obtained at room temperature. It decreases to a constant value of 175 kJ/mol for calcium coverage of 3 ML and more in the studied range.

The specimen coated with 620 nm PTCDA (red) shows an initial heat of adsorption of 510 kJ/mol , similar to the sample with a thin coating and the experiments carried out at ambient temperature, decreasing to 165 kJ/mol for calcium coverages between 1.2 ML and 3.5 ML. The obtained result increases to more than 1.5 MJ/mol (*sic*) for the specimen with thick coating at 9 ML and does not return below this value for the entire studied range. These reproducible huge increases, see Section D.7, are also directly observable during the data acquisition and in the raw data.

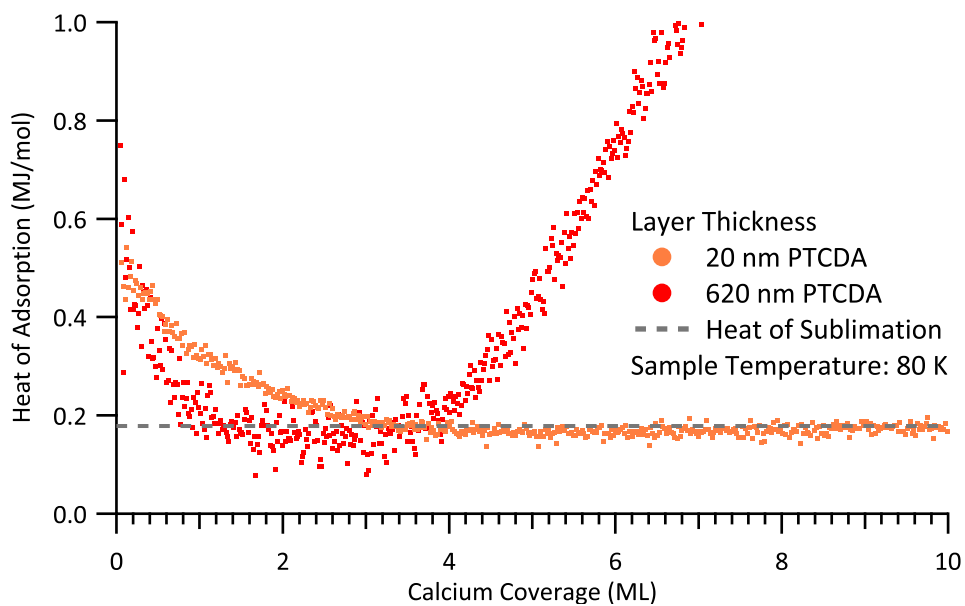


Figure 6.21: Low Temperature Adsorption of Calcium: Low Coverage Heats of Adsorption (PTCDA) — The derived heats of adsorption (dots) of calcium adsorbed on PTCDA surfaces with two different layer thicknesses are plotted together with the calculated heat of sublimation reference (dashed line) as a function of coverage. Each trace represents a single experiment. The heat of adsorption of calcium on the thin (orange) and thick (red) PTCDA layers increase during the initial pulses, reside at a plateau, and undergo minima at different calcium coverages before diverging at high coverages.

Figures 6.22 and 6.23 present the results of heat measurements for adsorption of Calcium on sexithiophene layers of different thickness as a function of calcium coverage.

The detector coated with 30 nm of sexithiophene (cyan) exhibits a heat of adsorption for the initial pulses of 500 kJ/mol rapidly decreasing within 1 ML to a plateau value of 310 kJ/mol which is identical to the initial released heat of the specimen with coatings of medium (100 nm – azure) and high (310 nm – blue) thickness. The obtained heat in case of the specimen with thin coating decreased sluggishly to 290 kJ/mol between calcium coverages of 16 ML and 30 ML. The other two samples experience a reduced released heat from 4 ML on reaching a minimum of 178 kJ/mol at 10 ML. Upon further dosage, the obtained value increases as in the case of deposition on PTCDA, see Figure 6.5.2. It seems to saturate at a calcium coverage of 40 ML (not shown) in both cases with derived heats of 440 kJ/mol for the detector

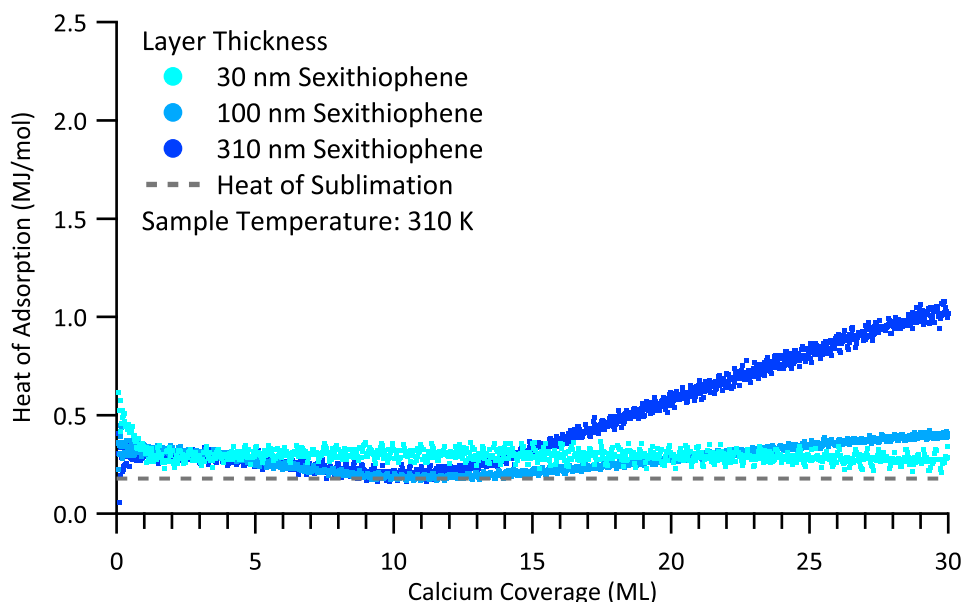


Figure 6.22: Adsorption of Calcium: Heats of Adsorption (Sexithiophene) — The derived heats of adsorption (dots) of calcium adsorbed on three sexithiophene surfaces with different layer thicknesses are plotted together with the calculated heat of sublimation reference (dashed line) as a function of coverage. Each trace represents a single experiment. The sample with a thin coating (cyan) exhibits an initially high heat of adsorption rapidly decreasing to an almost constant value, which is decreasing slightly for high calcium coverages ($> 10 \text{ ML}$). The released heats corresponding to the specimen with coatings of medium (azure) and high (blue) thickness undergo a minimum and exhibit a medium respectively strong increase of the obtained heat at high calcium coverages. Details for low coverages are given in Figure 6.23.

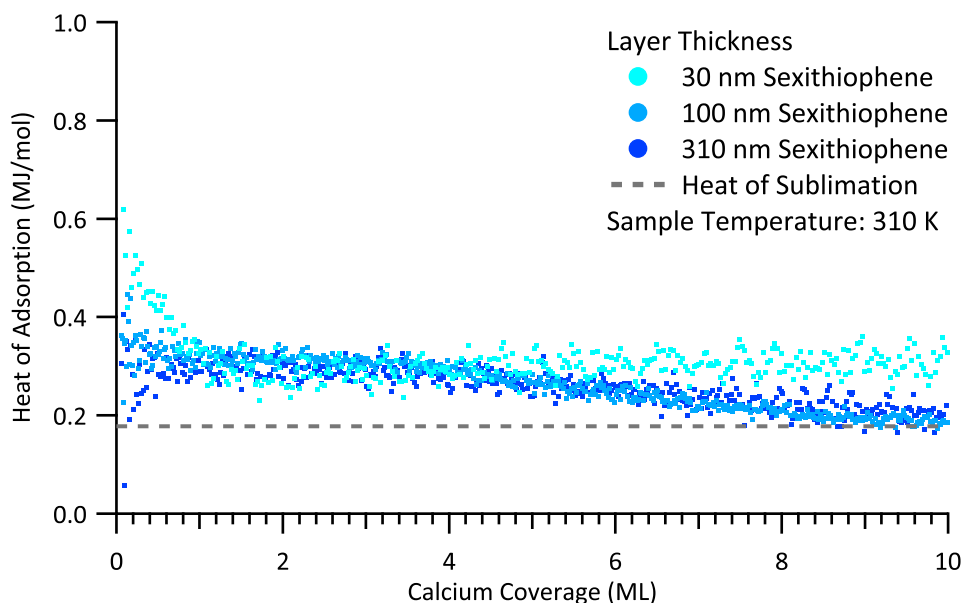


Figure 6.23: Adsorption of Calcium: Low Coverage Heats of Adsorption (Sexithiophene) — The derived heats of adsorption (dots) of calcium adsorbed on three sexithiophene surfaces with different layer thicknesses are plotted together with the calculated heat of sublimation reference (dashed line) as a function of coverage. Each trace represents a single experiment. The sample with a thin coating (cyan) exhibits an initially high heat of adsorption, rapidly decreasing to a constant value. The released heats corresponding to the specimen with coatings of medium (azure) and high (blue) thickness show similar released heats as the plateau value of the thin sample and decrease to the reference value.

with the coating of medium coating thickness and to 1.3 MJ/mol (*sic*) for the large coating thickness. This reproducible huge increase, see Section D.8, is also directly observable during the data acquisition and in the raw data.

Figures 6.24 and 6.25 present the results of heat measurements for adsorption of calcium on sexithiophene layers of different thicknesses held at 80 K by liquid nitrogen cooling as a function of calcium coverage.

The detector disc coated with a medium thick layer of 160 nm sexithiophene (azure) exhibits a constant heat of adsorption of 180 kJ/mol for calcium coverages of up to 2 ML. Upon further deposition, the released heat decreases to a minimum of 150 kJ/mol at 5 ML. Subsequently, the obtained value levels out at 340 kJ/mol for coverages of more than 30 ML.

The sample carrying the thick layer of 300 nm sexithiophene (blue) experiences a higher released heat of 290 kJ/mol for calcium coverages of up to 1.5 ML. As in the previous case, the released heat undergoes a minimum at 4 ML reaching 210 kJ/mol .

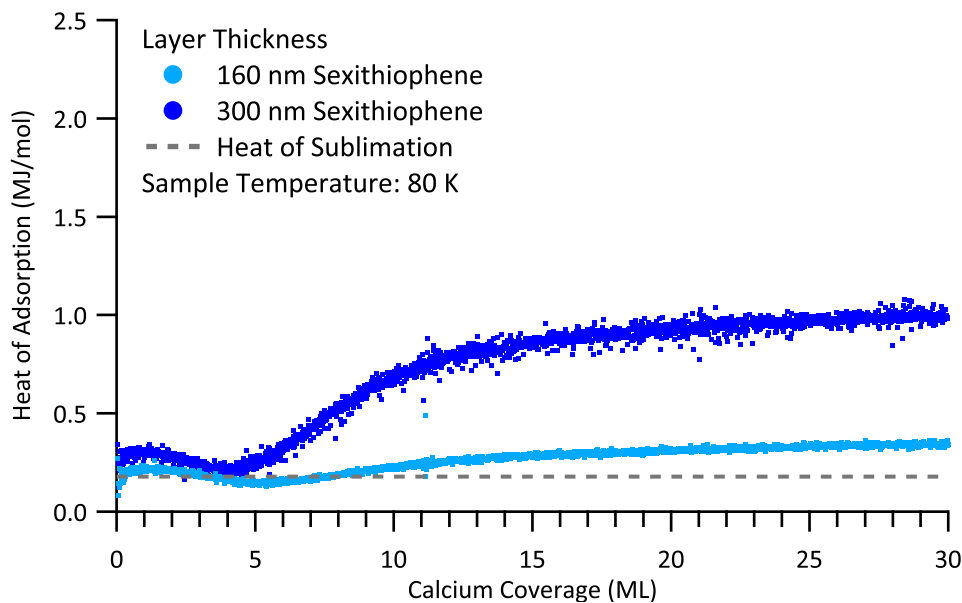


Figure 6.24: Low Temperature Adsorption of Calcium: Heats of Adsorption (Sexithiophene) — The derived heats of adsorption (dots) of calcium adsorbed at cryogenic temperatures on two sexithiophene surfaces with different layer thicknesses are plotted together with the calculated heat of sublimation reference (dashed line) as a function of coverage. Each trace represents a single experiment. Both samples exhibit an initially high heat of adsorption. The obtained heat of the sample with medium film thickness (azure) decreases to a constant value, even for high calcium coverages. The released heat corresponding to the specimen with a large coating thickness (blue) undergoes a minimum and exhibits a strong increase of the obtained heat at high calcium coverages. Details for low coverages are given in Figure 6.25.

Subsequently, it increases to 1 MJ/mol (*sic*) at 30 ML with a kink located at 12 ML and 0.8 MJ/mol (*sic*). This reproducible huge increase, see Section D.9, is also directly observable during the data acquisition and in the raw data.

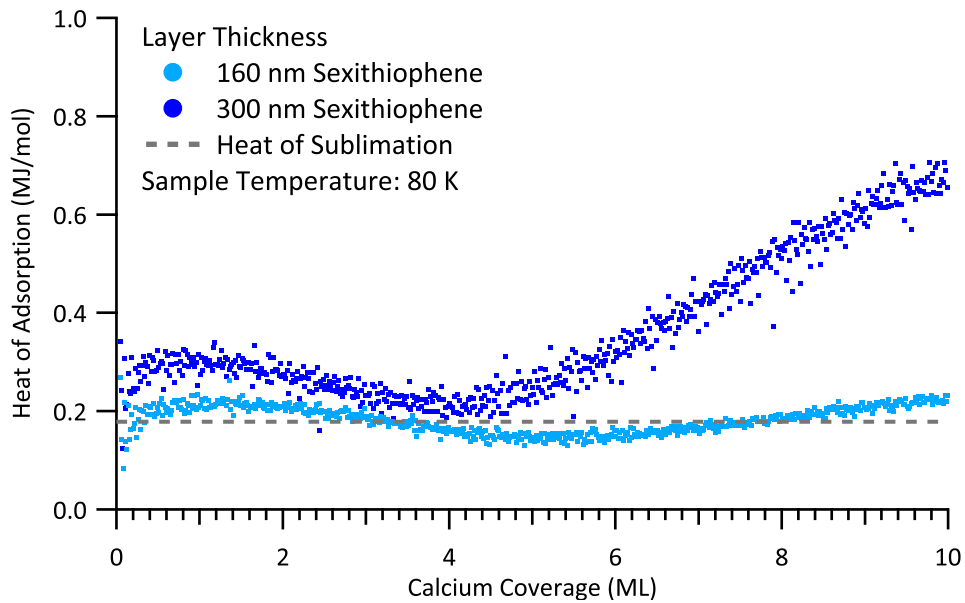


Figure 6.25: Low Temperature Adsorption of Calcium: Low Coverage Heats of Adsorption (Sexithiophene) — The derived heats of adsorption (dots) of calcium adsorbed on three sexithiophene surfaces with different layer thicknesses are plotted together with the calculated heat of sublimation reference (dashed line) as a function of coverage. Each trace represents a single experiment. The sample with a medium thickness (azure) coating exhibits an initially high heat of adsorption decreasing to a constant value. The released heats corresponding to the specimen with a coating of high thickness (blue) show a rapid decrease followed by a plateau region and an enormous increase of the obtained heat.

6.5.3 Discussion: Adsorption of Calcium

Considering the mass spectrometer data one has to keep in mind that the usage of calcium has a perfidious drawback. Its most abundant isotope (^{40}Ca) is isobaric to argon's most abundant isotope (^{40}Ar) and hence not distinguishable by the given instrumentation. The concentration of argon in air is high enough to affect the mass spectrometer measurement even in case of a small leakage. The software is able to ignore a constant low argon background but fails in case the partial pressure of argon is modulated by the chopper. Close inspection of the data presented here gave no indication of this effect.

Calcium exhibits a high to very high sticking probability on all investigated systems. This agrees well with results of adsorption of calcium on $\text{MgO}(100)$ ^[27] but it is in contrast to adsorption on polymer surfaces^[56–61]. Hence, larger scale errors induced by an incorrect zero sticking reference can be excluded as the absolute finite amplitudes become irrelevant since the corresponding coefficients in the measurement are very close to zero.

Adsorption of Calcium on Cleaned Detector

All dosed calcium atoms stick to the surface in the entire studied range which agrees well with the general expectation.

The released heat upon dosage of calcium on the sputter cleaned sample shows a similar trend as in the case of dosed magnesium on the same surface. The initially high heat of adsorption indicates a reaction or at least very strong interaction of calcium with the surface. Again, its exact nature cannot be specified further due to the lack of surface characterizing methods available in this setup. Possible reactions include the oxidation of water adsorbed after the sputtering process, reaction with defect sites created by the sputtering process, or a reduction of residual nickel oxide overlayer by the adsorbed calcium. The latter type of reaction was reported for magnesium adsorbed on chromium oxide on chrome^[228]. The higher reactivity of calcium compared to magnesium enables the occurrence of a similar reaction while reaction with water is unlikely due to the low pressure in the system.

Upon further dosage, the released heat is reduced and stabilizes at a coverage of 4 ML. A shoulder in the obtained heat is located at approximately 1 ML, suggesting that the first dosed monolayer of calcium is reacting. A subsequent minimum at a calcium coverage of 2 ML in the calculated heat might originate from two possibilities. On the one hand, it might profanely arise from an artifact caused by the automatic base line offset removal in the employed amplifier, see Section

5.5.3, which is not entirely removed by the filtering process, see Section 3.3. On the other hand, another model reported for adsorption of lead on molybdenum^[15] implies a Stranski-Krastanov growth mode, *i.e.*, islands on an interlayer, which are higher in energy than the bulk material and thus release a reduced amount of heat. At higher coverages the obtained heat of adsorption does not match the heat of sublimation, which is the expected reference value, but remains reproducibly below this limit. Hence, a discussion of absolute values is not reasonable. This result resembles experiments investigating the adsorption of magnesium on the same material and discourages a discussion of absolute values.

Adsorption of Calcium on Tetraphenyl Porphyrin

The sticking probability of the tetraphenyl porphyrin coated surface exhibits an adsorption behavior which is slightly differing from the other systems. After a small coverage range of high initial sticking probability, the probability undergoes a minimum, similar to the experiments involving magnesium, and subsequently increases to unity. The initially decreasing sticking factor might be attributed to a water contamination of the deposited organic layer. Reaction of calcium with water forms the corresponding oxide – and the hydroxide as an intermediate species – which might exhibit a lower sticking probability. However, the amount of reacting calcium implies unreasonable high amounts of water present in the top layer of the sample. Without complementary investigations, an assignment of this observation remains speculative.

The initially released high heat of adsorption might be related to a reaction in which calcium metalates the porphyrin core or at least to a very strong alternative interaction. This first reaction type is known for various metals^[230]. As the elevated released heat shows an inflection point at 0.8 ML, corresponding to the amount of reacted metal, exceeding the necessary amount for the first layer according to Section 6.2 of 0.2 ML, calcium atoms adsorbed on the surface are likely to diffuse deeper into the bulk material and to react there with the porphyrin. Since the released energy drops rather slowly and due to the stoichiometric excess, one can conclude that no effective barrier for diffusion is established. Similar behavior was found upon adsorption of calcium on polymer substrates and verified by X-ray photoemission spectroscopy^[57,58,71]. The here presented result remains speculative until further investigations probing the chemical state of the calcium or the nitrogen in the porphyrin and the reaction depth, *e.g.*, by X-ray photoemission spectroscopy, have been conducted. Comparison with Table 6.3 suggests a reaction depth of

approximately 4 layers.

For calcium coverages between 2 ML and 3 ML the obtained heat of adsorption matches the heat of sublimation¹¹, which is the expected reference value. The consecutive tremendous increase of the calculated “released heat” to chemically unreasonably high values is discussed in detail in Section 6.8.

Adsorption of Calcium on PTCDA

Calcium sticks very well on the prepared PTCDA substrates, independent of film thickness. Only the thick layer of PTCDA deposited on the pristine aluminum coated sample exhibits a slightly reduced sticking probability. This might originate from the omitted sputter process, agreeing with the visual observation of flaws in the vapor deposited films on other samples, see Section 5.2.

The released heats upon dosage of calcium on the samples coated with PTCDA show similar values at calcium coverages below 10 ML, independent of the substrate layer thickness. The initially elevated heat of adsorption indicates a reaction or at least very strong interaction of the calcium with the substrate. Again, its exact nature cannot be specified further due to the lack of surface characterizing methods available in this setup. Analogue to the adsorption of magnesium a reaction of calcium with the anhydride groups of PTCDA is proposed. The higher reactivity of calcium compared to magnesium^[166] supports the possibility of such a reaction. Adsorption of calcium on poly(methyl-methacrylate), a polymer containing methyl ester groups – which are chemically similar but usually less reactive – leads to the formation of calcium carboxylates^[56,60,70] under cleavage of the methyl group from the ester, demonstrating the reactivity of calcium towards the oxygen in ester groups. An exact stating of the reaction products is not possible with the given instrumentation. Possible outcomes would include calcium oxide clusters, the formation of carboxylates, or both.

Upon further dosage, the released heat is reduced and stabilizes at a coverage of 8 ML. A shoulder in the obtained heat is located at approximately 4 ML, suggesting a change in the reaction pathway. A formation of a diffusion barrier, which is present in the case of adsorbed magnesium, seems not likely since the released heat dropped much faster than in that case. In the present cases, reaction zones exhibit an estimated thickness of 10 layers according to Table 6.3 which is approximately a third of the *thin* substrate layer thickness. At higher coverages the obtained heat of adsorption does not match the heat of sublimation, which is the expected reference

¹¹ This result verifies that this setup is in principle able to fulfill its purpose and that the goal of this work is reached.

value, but remains reproducibly below this limit for the sample coated with a *thin* layer of PTCDA. This result resembles experiments investigating the adsorption of calcium on a cleaned detector surface and the experiments involving magnesium.

Surprisingly, the obtained heat rises beyond a calcium coverage of 10 ML to chemically unreasonable high values in the megajoule per mole (*sic*) regime which is reproducible in case of, amongst others, *thick* PTCDA substrate layers. However, this exorbitant increase is visible during data acquisition and in the raw data. Manual data evaluation assuming a constant radiation contribution retrieves even higher values. These two facts exclude the possibility that this effect is caused by the presented data treatment, see Chapters 3 and 4. Since the measurements have been carried out on two different detector materials (28 μm β -polyvinylidene fluoride with copper and nickel coating versus 9 μm β -polyvinylidene fluoride with aluminum coating) the reason for this behavior is not based on the detector material either. This tremendous increase is observable for two specimens with thick coating of which one was treated by argon ion bombardment and the other one was not. Hence, cleaning of the samples by sputtering also has no influence. However, additional experiments¹² suggest a dependency on film thickness. The origin of this effect is still unclear and also not reported in literature either. A detailed investigation dedicated to this behavior is given in Section 6.8.

Low Temperature Adsorption of Calcium on PTCDA

Reduction of the substrate temperature leads to an additional increase of the already very high sticking probability in accordance with experiments on similar, yet polymer, substrates^[59–61]. The probability turns out to be unity in the entire studied range.

Comparison with the data obtained at room temperature reveals similar initial heats of adsorption for both samples indicating an analogue reaction. However, the amplitude of the released heat decreases much faster in case of the cooled samples. This effect can be explained by a lower probability for a calcium atom to diffuse into the PTCDA layer, leading to reaction with the anhydride groups and thus a higher probability to form metallic clusters, analogue to the reported adsorption of calcium on poly(methyl-methacrylate)^[60]. Hence, the formation of calcium clusters is favored compared to the adsorption at ambient sample temperature. The results imply a smaller thickness of the reaction zone between the metallic cover layer and the unperturbed PTCDA substrate.

The inflection point of the released heat in the initial stage for the sample with

¹² Not shown here, see Appendix D.

the thick PTCDA coating at a calcium coverage of 0.5 ML suggests that this dosed amount is also reacting with the substrate. The corresponding point in case of the thinly coated sample is located at a calcium coverage of 1.2 ML. According to the considerations in Section 6.2 these correspond to one reacted layer in case of the sample with thin coating and to three layers in case of the sample with thick coating.

The larger reacting amount in case of the thinly coated sample might arise from a different surface morphology, especially the surface roughness leading to a larger surface area. A possible explanation for this difference might originate from the different deposition times during sample preparation. Due to the larger thickness in combination with similar fluxes, the coating takes longer. As a consequence, the temperature of the sample – heated by radiation of the evaporator – is likely to be higher at the end of the process for the thickly coated sample than in the case of the test subject with thin coating. Hence, this increased temperature can lead to an additional intrinsic tempering step of the film which is reducing surface defects and roughness. A direct investigation of the morphology was not possible at the experimental setup's stage of construction.

The initially released heat is similar to the heat measured at ambient temperature. This finding is in contrast to investigations on adsorption of calcium on poly(methylmethacrylate)^[60], reporting a strong decrease in the obtained heat upon reduction of the sample temperature. This fact might arise from a higher reactivity of the anhydride groups in PTCDA compared to ester groups of the polymer towards the dosed calcium atoms. Subsequently, the released heat drops to the bulk heat of sublimation¹³ validating the obtained values by matching the internal reference¹⁴.

The released heat in case of the sample with thin coating of 176 kJ/mol matches the heat of sublimation of calcium of 178 kJ/mol with a deviation of less than 1%. Furthermore, the obtained heat remains constant upon further dosage of calcium. This experiment depicts an ideal result. The absence of secondary effects, see Sections 6.8 and 6.9, at elevated coverage most likely arises on the one hand from increased mechanical strength of the detector due to cooling and on the other hand from a successful choice of the substrate layer's thickness.

Subsequently, the gigantic signal increase sets off at a calcium coverage of 4 ML in case of the sample carrying the thick PTCDA substrate similar to the samples with thick coating investigated at ambient temperature. A detailed investigation dedicated to this behavior is given in Section 6.8.

¹³ At least, the reference is reached intermediately in case of the sample with thick coating.

¹⁴ These results verify that this setup is in principle able to fulfill its purpose and that the goal of this work is reached.

Adsorption of Calcium on α -Sexithiophene

Calcium sticks well on the prepared sexithiophene films independent of film thickness. The higher sticking probability compared^[57,58] to a related polymer, *i.e.*, poly(3-hexylthiophene), probably arises from the absence of the hexyl side chains in this work. The surface in the cited work has a higher preference to expose the unreactive, nonpolar, aliphatic side chains to the vacuum than the polar thiophene units^[57]. This mechanism could be driven by sterical interaction or by minimization of the surface energy known for, *e.g.*, ionic liquids^[231,232] and polymers^[233]. As explained above, a situation in which the reactive center is covered by inert groups would lead to a decrease of the sticking probability. The difference in the low coverage regime between the small layer thickness and the larger layer thicknesses probably originates from an incomplete removal of the surface contamination, see Section 5.2, which might still influence the thin organic film. Since the shape of the obtained trace is similar for the thicker layers and deviates from the result corresponding to the thin layer, the minor difference is attributed to a compromised reference measurement. For higher coverages this error has no influence on the calculated heats as the belonging coefficient is zero.

Again, a competition of the adsorbed calcium between reaction and cluster formation is plausible while desorption is unlikely. As the sticking probability approaches unity at around 10 ML one can conclude that the surface is entirely covered in calcium at this point.

The released heat upon dosage of calcium on the samples coated with sexithiophene shows similar values at calcium coverages between 1 ML and 4 ML independent of the substrate layer thickness. The raised value regarding the thin layer sample could be explained by a reaction of the calcium with defects, a higher number of accessible reaction centers due to higher roughness, or coadsorbed water. Since the defects should also be present in the film with larger thickness, this explanation is less favorable. The initially high heat of adsorption indicates a reaction or at least very strong interaction of the calcium with the substrate. Again, its exact nature cannot be specified further due to the lack of surface characterizing methods available in this setup. Although this system has recently been studied by hard X-ray photoemission spectroscopy, results about the chemical states and the reaction depths therefrom were not available at the time this thesis has been written and likely will be presented in [227].

Analogue to the adsorption of calcium on poly(3-hexylthiophene)^[57,58], a reaction with the thiophene units under sulfur abstraction from the thiophene and formation

of calcium sulfide clusters is proposed. Due to the great chemical similarity of the substrates, it is assumed that a similar side reaction, *i.e.*, cross-linking – or in this case polymerization, occurs. From the inflection point of the released heat in case of the samples with medium and thick coatings which is located at a calcium coverage of 6 ML and the considerations from Section 6.2 the thickness of the reaction zone can be estimated to approximately 8 layers corresponding to 3.4 nm. The estimated thickness of the reaction zone is in accordance with results reported for adsorption of calcium on poly(3-hexylthiophene)^[57]. As in the case of adsorption of calcium on PTCDA at low temperature, the amount of reacting metal is larger for the thin substrate layer. Again, this effect can be attributed to the absence of the intrinsic tempering step during substrate deposition resulting in a larger surface roughness.

The lowered released heats at a coverage between 9 ML and 11 ML for the thicker layers match the observation of the sticking measurements that the dosed atoms form bulk-like, metallic calcium on the surface. The released heat, averaged from these two experiments, of 179 kJ/mol matches the heat of sublimation of calcium of 178 kJ/mol with a deviation of less than 0.5% in this case¹⁵. Although the obtained heat diverges again upon further dosage, see Section 6.8, the experimental result is considered to be correct as the internal reference in both cases is hit independently.

The heat measured during the plateau region at calcium coverages between 1 ML and 3 ML of 285 kJ/mol is significantly lower than the value of 405 kJ/mol reported^[57] for the polymer system. This discrepancy can be explained by considering the size of the formed calcium sulfide clusters. The smaller the clusters the higher the surface energy and thus less energy is released upon formation of a small particle than of a large particle. This is known as Kelvin effect^[156] and leads to the conclusion that the clusters in sexithiophene have a smaller size than the clusters formed in the poly(3-hexylthiophene) matrix. It implies either a higher nucleation rate in sexithiophene or a smaller mobility of the initially formed calcium sulfide monomers. Comparison with computational results^[57] suggests two to three monomers in the formed calcium sulfide particles in the organic matrix.

Low Temperature Adsorption of Calcium on Sexithiophene

By analogy with the experiments including PTCDA as substrate calcium sticks even better to the prepared sexithiophene films at low temperature, independent of film thickness. All impinging calcium atoms stay on the sample after a coverage of 2.5 ML is reached. This behavior indicates a faster formation of the metallic

¹⁵ These results verify that this setup is in principle able to fulfill its purpose and that the goal of this work is reached.

overlayer compared to the experiments at ambient temperature where a dense film grows at coverages larger than 10 ML.

The initially reduced released heat indicates the growth of small clusters due to the Kelvin effect^[156] in accordance with adsorption of copper and lead on MgO(111) reported elsewhere^[17,22]. The subsequent plateau region indicates an ongoing reaction of the dosed calcium with the substrate. In contrast to the experiments performed at ambient temperature and in agreement with the conclusions from the sticking measurement, the reacting amount of calcium is smaller at low temperature. This can be seen from the reduction of the released heat at a smaller calcium coverage. The position of corresponding inflection point at a coverage of approximately 3 ML suggests, in combination with the deduction in Section 6.2, a reaction thickness of 4 layers in the low temperature case.

Subsequently, the gigantic signal increase sets off at a calcium coverage of 5 ML similar to the experiments at low temperature utilizing PTCDA as substrate, though with lower amplitude here. The metallic over layer is built up faster since less diffusion and reaction are happening on the cooled sample. Hence, an earlier onset of the gigantic signal increase seems to be correlated with the metallic over layer. As the final amplitude for the cold sample is reduced, compared to the specimens investigated at ambient temperature, an influence of temperature dependent material properties, *e.g.*, stiffness, of one of the sample components, *i.e.*, detector polymer, organic thin film, and metallic cover layer, is plausible. A detailed investigation dedicated to this behavior is given in Section 6.8.

Since the obtained heat of adsorption does not match the heat of sublimation, which is the expected reference value, at least during a range of constant values, a discussion of absolute values is not reasonable.

6.6 Adsorption of Copper

This section covers a selection of experiments in which copper has been adsorbed on various surfaces utilizing the calorimeter presented in Chapter 2 evaluating the option for the electron beam evaporator according to the procedure given in Section 6.3.

Copper was chosen as an example for metals exhibiting a medium vapor pressure, see Section 6.1, being liquid at operation temperature. Reactions of copper with molecules exhibiting a porphin-like inner structure, *e.g.*, tetraphenyl porphyrin or phthalocyanine, have previously been investigated^[88,198,199]. Studies utilizing adsorption calorimetry have been performed before^[14,16,17,21,22,53] and provide estimates about the behavior.

6.6.1 Experiment: Adsorption of Copper

Copper evaporated from a medium size molybdenum crucible¹⁶ in an electron beam evaporator¹⁷ mounted on the molecular beam housing is converted into pulses and adsorbed on several substrates. One monolayer is defined as $1.77 \cdot 10^{19}$ Atoms/m² in this case. The deposition rate related to the adsorption on PTCDA has been adjusted to 0.05 ML/s while the deposition rate related to the adsorption on phthalocyanine amounted to 0.1 ML/s. Pulse lengths of 0.20 s respectively 0.10 s result in doses of about $3 \cdot 10^{12}$ copper atoms per pulse which is equivalent to 5 picomole per pulse in both cases. The experiments have been conducted as described in Section 6.3 with the parameters mentioned there and in Appendix A. Since the evaporator lacks a sensor for the temperature of the crucible, it is taken from the manual of the evaporator^[234] as 1500 K.

6.6.2 Results: Adsorption of Copper

Due to vanishing signal intensity from the hot plate and tremendous scatter in the mass spectrometer data, even involving a considerable amount of dark counts, the sticking probability was assumed to be unity for measurements involving the adsorption of copper. Significant signal intensity for the mass spectrometer channel during the radiation measurements using the barium fluoride window further supports this assumption since it proves that the spectrometer is in principle able to measure a signal corresponding to desorbing copper.

¹⁶ 'C Mo M' from FOCUS GmbH *via* Omicron NanoTechnology GmbH.

¹⁷ 'EFM-4' from FOCUS GmbH *via* Omicron NanoTechnology GmbH.

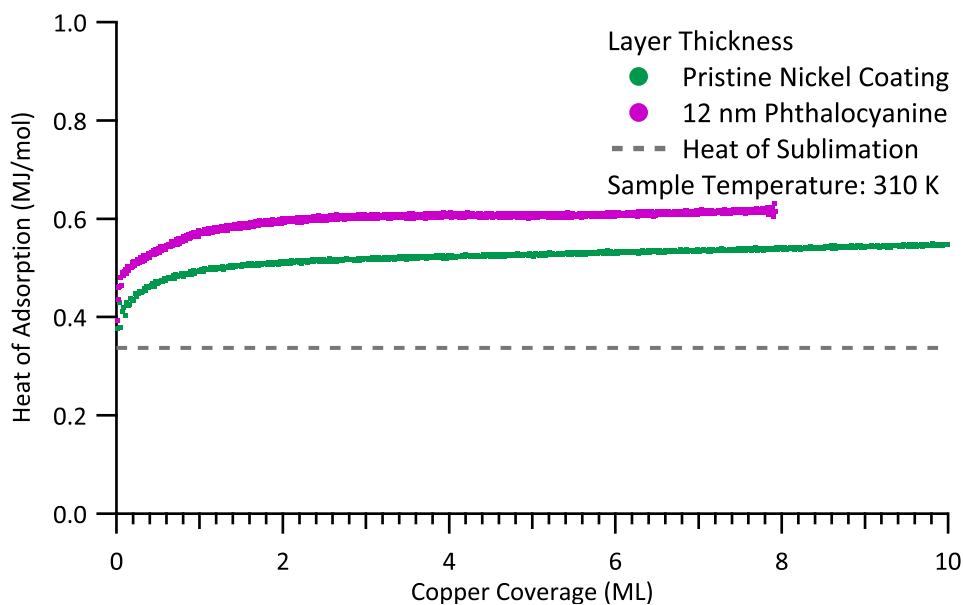


Figure 6.26: Adsorption of Copper: Heats of Adsorption — The derived heats of adsorption (dots) of copper dosed on thin surface layers of different materials are plotted together with the calculated heat of sublimation reference (dashed line) as a function of coverage. Each trace represents a single experiment. The obtained heat of adsorption of pristine detector (pine) and the sample coated with phthalocyanine (lilac) exhibits an initial increase. The phthalocyanine coated sample exhibits a plateau. Both specimens indicate a subsequent increase of the released heat. A constant unity sticking probability is assumed.

Figure 6.26 illustrates the results of heat measurements for adsorption of copper on two surfaces. One is given by an untreated, *i.e.*, pristine nickel coated, detector disc and the other one carries a thin vapor deposited film of phthalocyanine (12 nm).

The pristine specimen (pine) shows an initial heat of adsorption of 400 kJ/mol at the beginning which increases to 510 kJ/mol at a copper coverage of 2 ML. The detector coated with 12 nm of phthalocyanine (lilac) exhibits a heat of adsorption for the initial pulses of 420 kJ/mol increasing to 600 kJ/mol within 2 ML where it remains stable for up to 6 ML. Subsequently, the obtained heat for both samples increases with coverage without saturation in the studied range.

6.6.3 Discussion: Adsorption of Copper

The coverage independent high sticking probability of copper on the here used organic substrate is consistent with values reported for adsorption studies on a polymer substrate^[53] and on single crystal substrates^[16,22].

The initially low heat of adsorption together with the leveling off at about 1 ML indicate diffusion of the weakly bound copper atoms on the surface and growth of islands and clusters on the substrate^[16,53,235]. As the internal reference value is not matched, a discussion of absolute values is not constructive. Data of adsorption on thicker substrate layers has not been obtained so far. However, the absence of a reaction with free base phthalocyanine, which would be indicated by a high obtained heat, is surprising. Reaction of thick layers of phthalocyanine on a Cu(111) surface, *i.e.*, a very similar but presumably less reactive system, is known^[88], at least for elevated temperatures. The temperature effect could be compensated by the more reactive nature of an individual atom compared to one embedded in a crystal and thus a reaction could be expected.

Generally, the usage of the electron beam evaporator is possible which was the main goal of this measurement. Due to the necessary high fluxes, the filament¹⁸ inside the evaporator is glazed with copper after two to three crucible fillings and needs to be replaced. The copper deposition on the filament reached a diameter of up to 1 mm close to the mounting posts while the center of the filament remained clean, as shown in Figure 6.27.

Considering that the filament is mounted on cooled ceramic feedthroughs, its ends are significantly colder than its middle which is typically operated around 2200 K to achieve high thermionic emission currents^[236]. Since the vapor pressure of copper^[187] exceeds 1 Torr at this temperature, it should not condensate on the hot filament. However, condensation is possible on the colder end sections of the filament. This additional material leads to an increase in conductivity and thus to a locally reduced heating power and finally a reduced filament temperature close to the electrical connections. This progressive mechanism is able to explain the thickness gradient on the filament shown in Figure 6.27. It also explains the observation that the filament current had to be increased monotonically during the experiments to maintain a stable deposition rate. The observed amount of copper implies a continuous deposition since it exhibits a thickness which is comparable to the thickness of the copper layer on the cooling shroud, where deposition during operation is standard. Hence, it cannot result from single occasions, such as post

¹⁸ 'W 145300' Thoriated tungsten wire W99Th1, Dia 0.125 mm from Goodfellow GmbH.



Figure 6.27: Copper Glazed Filament — The filament^a on its mounting posts after evaporation of approximately 4 g of copper from a molybdenum crucible^b in the electron beam evaporator^c. Although the filament is incomplete in this picture, it is clearly visible that the thickness of the copper deposit decreases from the mounting posts to the center of the filament, which is the hottest zone during operation.

-
- a ‘W 145300’ Thoriated tungsten wire W99Th1, Dia 0.125 mm from Goodfellow GmbH.
b ‘C Mo M’ from FOCUS GmbH *via* Omicron NanoTechnology GmbH.
c ‘EFM-4’ from FOCUS GmbH *via* Omicron NanoTechnology GmbH.

deposition after the filament has been switched off.

A possible avoidance of this undesired deposition would involve operation conditions outside the specifications of the manual^[234] and is hence not advised. However, there might arise cases in which non-standard operation is required. In such a situation, the filament needs to be aligned to the side of the crucible and not, as recommended by the manual^[234], only approached by the top of the crucible. Such an arrangement might be realized by extension of the mounting posts or the rod carrying the crucible. Usage of this geometry will increase the risk of high voltage arcing, short circuits to the housing of the high voltage, and mechanical destruction of the filament^[234]. Furthermore, the integrated flux monitor is likely to fail. It relies on ions originating from collisions of accelerated electrons with the evaporated species. Due to the changed electron trajectories, these ions might no longer be created. Hence, this measurement unit is lacking its input variable and cannot serve its purpose.

6.7 Adsorption of Zinc

This section covers a selection of experiments in which zinc has been adsorbed on various surfaces, utilizing the calorimeter presented in Chapter 2. Zinc was chosen as an example for metals with a high vapor pressure, see Section 6.1, being liquid at operation temperature.

6.7.1 Experiment: Adsorption of Zinc

Zinc, evaporated from the molecular beam source, is converted into pulses and adsorbed on several substrates. One monolayer is defined as $1.6 \cdot 10^{19}$ Atoms/m² in this case. The deposition rate has been varied between 0.1 ML/s and 0.2 ML/s. A pulse length of 0.20 s results in doses between $6 \cdot 10^{12}$ and $12 \cdot 10^{12}$ zinc atoms per pulse which is equivalent to 15 picomole per pulse for the measurement on the sputtered detector and $2 \cdot 10^{12}$ zinc atoms per pulse for the other experiments which is equivalent to 10 picomole per pulse and 30 picomole per pulse, respectively. The experiments have been conducted as described in Section 6.3 with the parameters mentioned there.

6.7.2 Results: Adsorption of Zinc

Sticking Probabilities

Figure 6.28 presents the obtained coverage dependent sticking probabilities of zinc on two surfaces, one of them investigated at two temperatures. The latter are coated with thin vapor deposited PTCDA films with thicknesses of 12 nm (ambient temperature) and 23 nm (190 K). The third sample has only been cleaned by argon ion bombardment and investigated at ambient temperature.

The cleaned sample (green) exhibits for zinc coverages of up to 1 ML a rather low sticking probability of 0.4 which is slowly increasing to 0.9 at 20 ML. Upon further zinc deposition the probability continues to rise and levels off beyond a coverage of 80 ML at 0.98.

The experiment on a sample cooled to 190 K (orange) shows an initial sticking coefficient of 0.2 rising to 0.85 at 5 ML and reaching unity at about 10 ML without a plateau.

A contrary result is obtained in case zinc is adsorbed on PTCDA at ambient temperature (gold). The initial sticking coefficient is moderate in the entire studied range. Due to a malfunction of the mass spectrometer, likely an unnoticed change of the secondary electron multiplier voltage, the corresponding reference is multiplied

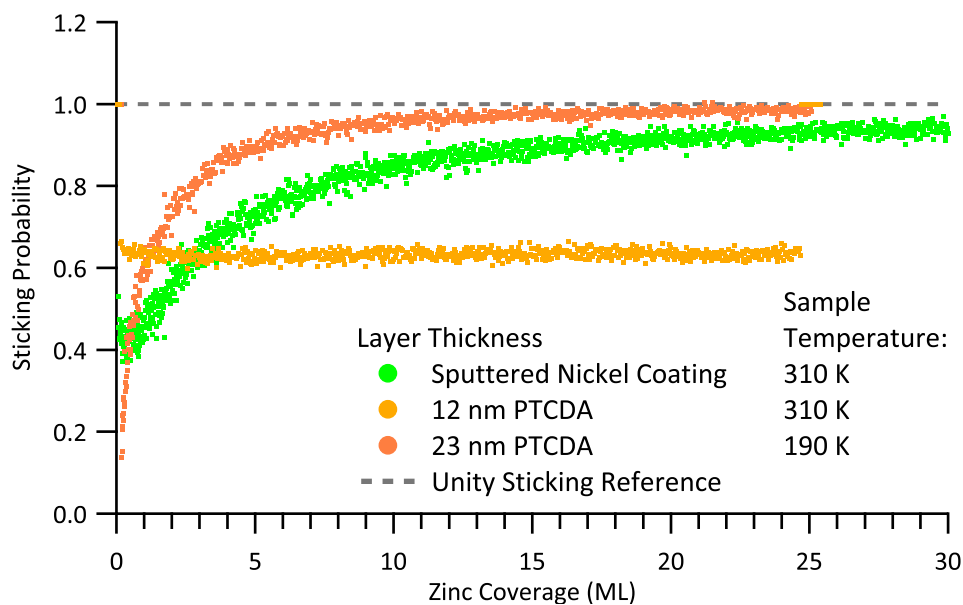


Figure 6.28: Adsorption of Zinc: Sticking Probabilities — The sticking coefficients (dots) of zinc adsorbed on different surfaces and temperatures are plotted together with the unity sticking reference (dashed line) as a function of coverage. Each trace represents a single experiment. The sticking coefficient on the sample cleaned by sputtering (green) is initially low and slowly approaches unity. A similar trend with stronger increase is observed for the cooled surfaces coated with PTCDA (orange). A different behavior is shown upon adsorption on PTCDA (gold) at ambient temperature. The sticking coefficient remains at moderate values over the investigated range. The zero sticking reference is modified by multiplication with a factor of 3.6 to compensate for a malfunction of the mass spectrometer^a.

^a Adjusted to matching background noise level in the signal to avoid pure negative sticking probabilities.

by 3.6. This factor is obtained by matching the noise levels, *i.e.*, mass spectrometer intensity far away from the actual region of interest. Due to this fact the absolute values, also for the heat of adsorption in this case, are rendered meaningless while statements about relative intensities are still possible. This correction is necessary since the uncorrected sticking probabilities would be negative otherwise.

Heats of Adsorption

Figures 6.29 and 6.30 illustrate the results of heat measurements for adsorption of zinc on two surfaces, one of them investigated at two temperatures.

The sample only cleaned by argon ion bombardment has been investigated at ambient temperature and exhibits an obtained heat of adsorption of 80 kJ/mol decreasing to -55 kJ/mol (*sic*) at 0.8 ML. Subsequently, the calculated heat rises to approximately 30 kJ/mol at 5 ML.

The specimen coated with a thin vapor deposited film of PTCDA (12 nm) studied at ambient temperature (gold) remains constant at 10 kJ/mol with a hint of a slightly larger value for the first dosed pulses. A similar sample coated with 23 nm PTCDA held at 190 K (orange) exhibits a released heat of adsorption of 350 kJ/mol and levels out at a value of 131 kJ/mol for a zinc coverage of 5 ML with a very broad and shallow minimum at higher coverages.

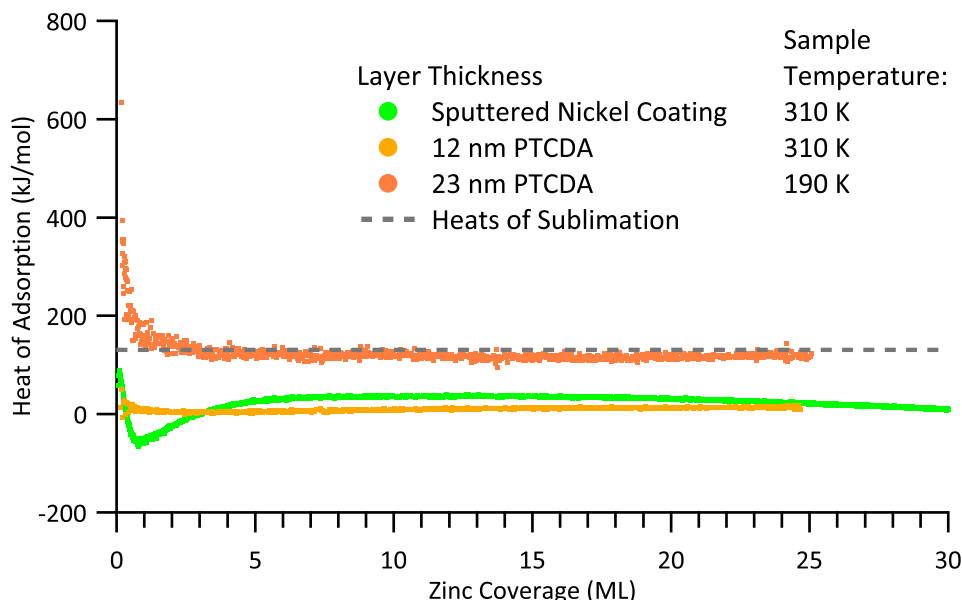


Figure 6.29: Adsorption of Zinc: Heats of Adsorption — The derived heats of adsorption (dots) of zinc dosed on different surfaces and temperatures are plotted together with the unity sticking reference (dashed line) as a function of coverage. Each trace represents a single experiment. The obtained heat of adsorption of the sample cleaned by sputtering (green) and the PTCDA coated samples at ambient (gold) and lowered (orange) temperature exhibit rather constant values for higher coverages. Details for low coverages are given in Figure 6.25.

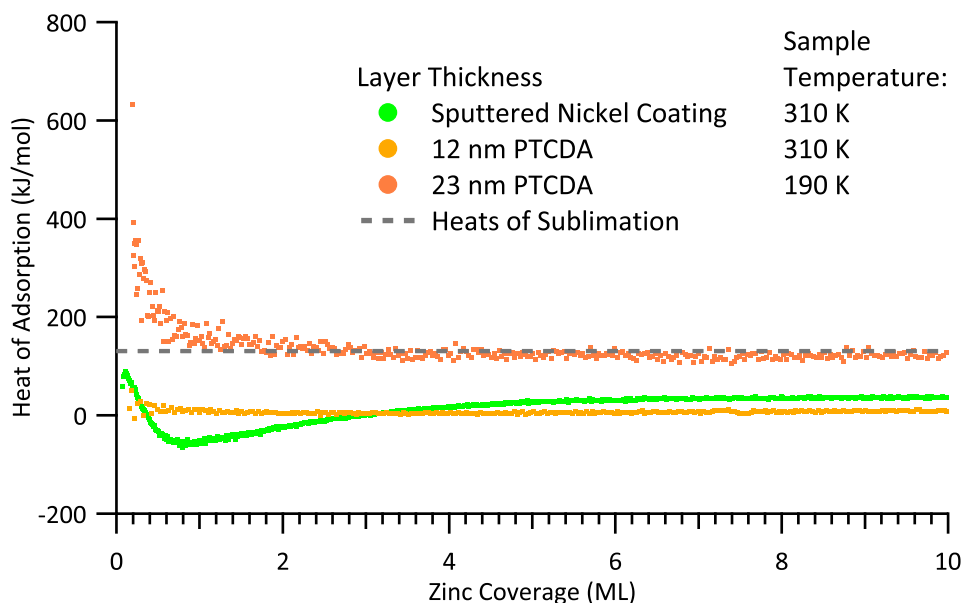


Figure 6.30: Adsorption of Zinc: Low Coverage Heats of Adsorption — The derived heats of adsorption (dots) of zinc dosed on different surfaces and temperatures are plotted together with the unity sticking reference (dashed line) as a function of coverage. Each trace represents a single experiment. The sample cleaned by sputtering (green) exhibits moderate obtained heat of adsorption decreasing into a minimum at one monolayer. Thereafter, it is rising again to an intermediate constant value. The released heats corresponding to the specimens with a coating of PTCDA show a minimal higher released heat during the first pulses compared to the constant rest of the investigated range at ambient (gold) and lowered (orange) temperature.

6.7.3 Discussion: Adsorption of Zinc

The increasing sticking probability of zinc on the sputtered as well as on the cooled sample coated with PTCDA indicates the formation of metallic cover layers in both cases. On the one hand, the fast increase to unity in case of the cooled sample suggests the quick, yet not initial, formation of a closed zinc layer. The slow increase in case of the, most likely, insufficiently sputter cleaned specimen on the other hand supposes the growth of larger clusters on the sample.

On the sputtered sample, the initially high and later dropping heat of adsorption agrees with the growth of clusters on a soiled surface as deduced from the sticking probability measurement. The residue on the nickel surface reacts with the dosed zinc while in parallel large clusters start to grow, eventually covering the whole surface. The constant heat at zinc coverages between 5 ML and 18 ML fits this interpretation. Excessive additional dosage of zinc, to a total coverage of 120 ML,

not shown, surprisingly causes a decrease of the calculated heat to -125 kJ/mol (*sic*) with no indication of saturation.

Inspection of the measured signal initially exhibits a distortion of the signal leading to a change in its polarity. Details on this reproducible effect, see Appendix D.10, are given in Section 6.9.

It should be pointed out that a negative heat of adsorption is physically questionable since this would imply a more stable gas phase than adsorbate phase. Hence, adsorption should not occur. However, this signal inversion has already been observed during the data acquisition and is present in the raw data. This excludes faulty data treatment as origin of this effect.

The heat of adsorption, obtained in case of the cooled, PTCDA coated sample, exhibits an initial maximum. Its extend suggests the reaction of 1 ML of adsorbed zinc with the PTCDA substrate. By analogy to the experiments involving magnesium and calcium, a reaction of the dosed zinc atoms with the anhydride groups in PTCDA or with water condensed on the sample seems possible. The first option is more likely due to the low pressure in the vacuum system and the large amount of reacting zinc which corresponds, according to Section 6.2, to five layers in the substrate.

The consecutively released heat, which matches the heat of sublimation of zinc¹⁹ at coverages between 5 ML and 12 ML, supports the model involving the growth of a dense overlayer. Since no further information about this system is available, the exact nature of the reaction and growth mode remain speculative.

A new behavior is observed for the sample coated with a thin layer of PTCDA at ambient temperature. The constant medium sticking probability is problematic. On the one hand, the result obtained on the sputtered specimen demonstrates that zinc adsorbs on itself with a final sticking coefficient of unity. As the calculated sticking probability is finite, a fraction of the dosed zinc stays on the surface. Consequently, the PTCDA coated sample is converted to a similar state as the cleaned sample. Hence, the sticking probabilities are required to converge. On the other hand, the experimental result shows a constant probability. This is only allowed in the pathological case of absolutely no adsorption on the surface, *i.e.*, a constant null probability, which would leave the specimen unaltered. However, this situation would imply a severely wrong correction factor for the mass spectrometer intensity or an undiscovered operation fault.

The almost constant *not* released heat, *i.e.*, with a value close to zero, is odd as well. One might argue that no material is deposited and hence no heat is released.

¹⁹ This result verifies that this setup is in principle able to fulfill its purpose and that the goal of this work is reached.

However, if this assumption is forced into the model the heat remains constantly zero due to the thermodynamic corrections, see Section 1.2, as the recorded signal purely contains the radiative component. An optical inspection of the sample revealed a spot on the sample with the diameter of the final orifice. This excludes the possible fault of performing the measurement with the infrared transparent window blocking the beam path for matter.

6.8 Gigantic Signal Effect

As mentioned several times in the sections above, the huge increase in the detector signal can be directly observed. Figure 6.31 exemplarily shows this effect for an experiment investigating the adsorption of calcium on sexithiophene. The other discussed systems show an analogue behavior in case an *increase* is observed. The expected radiative contribution to the signal is about $0.1 V_{PP}$, corresponding to approximately half of the initial amplitude. Later in the experiment the measured peak to peak voltage of close to $0.4 V_{PP}$ nominally triples the heat contribution.

A closer inspection reveals that the signal shape is not well reconstructed at higher calcium coverages by the fit using a constant radiation contribution. However, lifting of this constraint allows the fitting routine to match the measured data, as shown in Figure 6.32. Since the coefficients obtained for the radiation component are rising as the experiment proceeds, as shown in Figure 6.33, the increase of the laser-like component is partially compensated. This leads to a reduced resulting heat compared to the use of constant radiation coefficient and rules out a misbehavior of the fitting routine leading to the gigantic signal increase.

One might argue that the temperature control of the evaporator stabilizes the

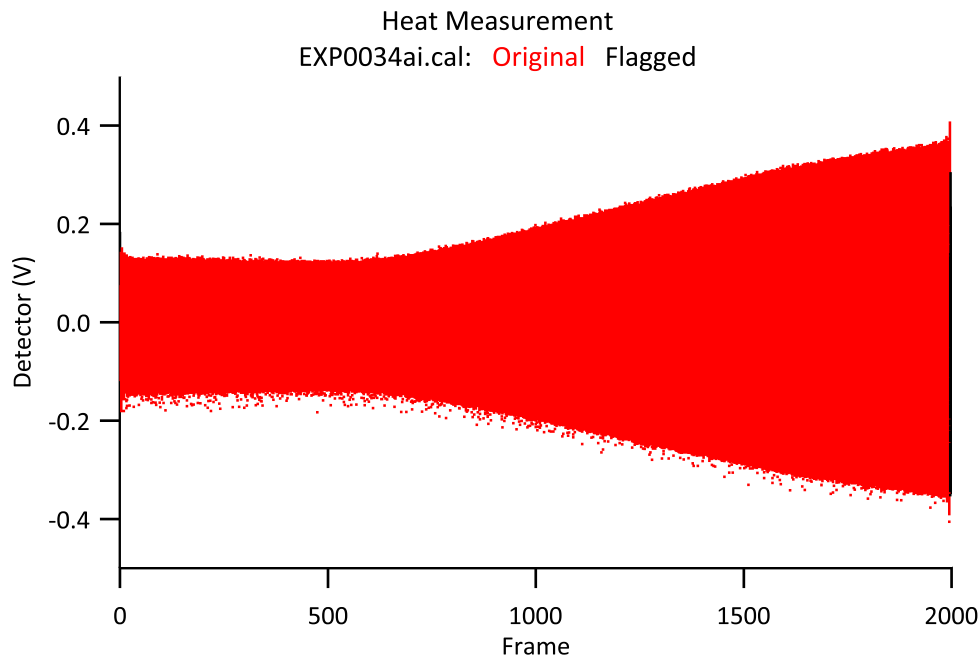


Figure 6.31: Adsorption of Calcium on Sexithiophene: Full Detector Data — The measured calorimetry signal of the experiment, presented in Figure 6.22, corresponding to the thick (310 nm) sexithiophene coating exhibits a readily visible enormous increase in amplitude.

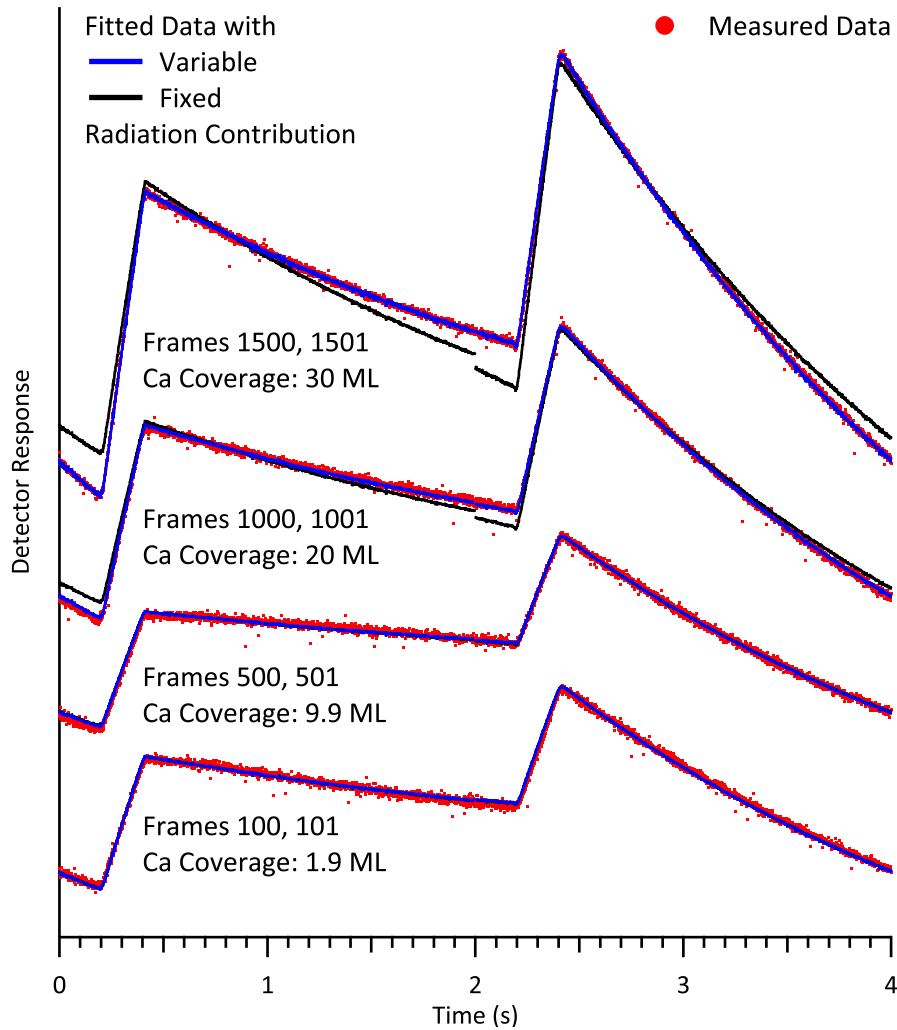


Figure 6.32: Adsorption of Calcium on Sexithiophene: Fitted Detector Data — Selected frames (dots) from Figure 6.31 at different calcium coverages are displayed together with the fitting results for variable (blue lines) and fixed (black lines) radiation contribution to the heat signal. The peak shape is not matched in the latter case at high calcium coverages.

temperature of the thermocouple and not necessarily maintains a stable temperature of the evaporant. Alternatively, a temperature read wrong due to temperature drifts of connections in the thermocouple line would also result in a changed evaporant temperature. A rising temperature of the evaporant would explain increases of the flux, and hence of the dose, as well as of the radiation input into the detector. Both scenarios would imply an alteration of the heating power applied to the crucible.

Inspection of Figure 6.34 clearly demonstrates a constant evaporator temperature together with a constant heating power excluding compensation effects.

Deposition rate measurements before and after the deposition during the calori-

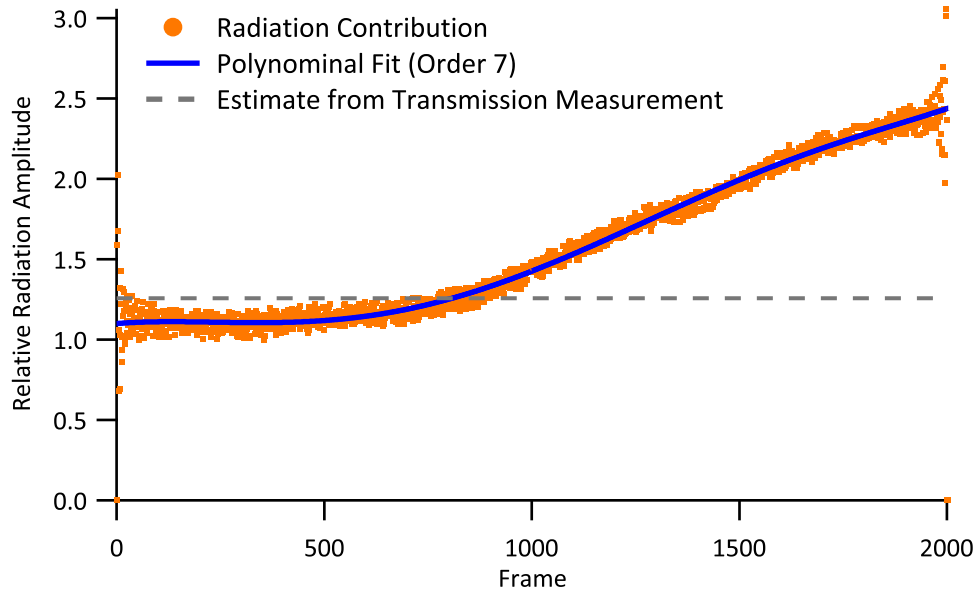


Figure 6.33: Adsorption of Calcium on Sexithiophene: Radiation Contribution — The contribution of the radiative component to the detector signal (orange dots) increases as the experiment proceeds. The corresponding fitted trend (blue) used in the data treatment routine is superimposed as well as the constant value derived from the transmission measurement (gray dashed line).

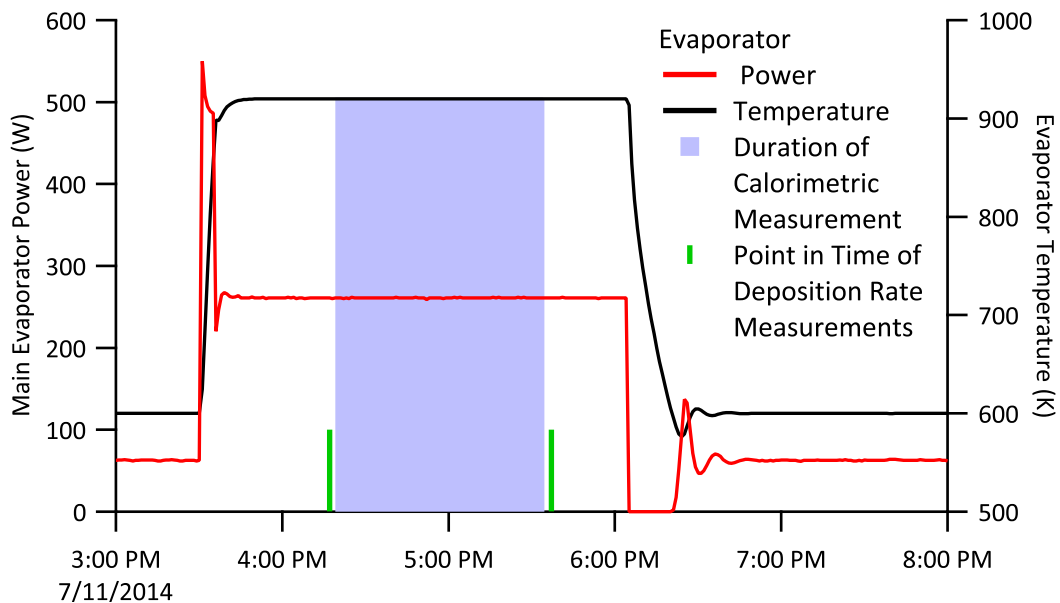


Figure 6.34: Adsorption of Calcium on Sexithiophene: Stability Checks — The heating power (red line) and evaporator temperature (black line) are constant during the calorimetric measurement (shaded blue). The time stamps of the deposition rate measurements before and after the calorimetric measurement are illustrated (green sticks).

metric measurement exhibit very similar rates of 32.6 pm/s and 32.0 pm/s, respectively. Their enclosing positions around the calorimetric measurement in the experimental sequence provide reliable readings. Together, this excludes that the discussed effect originates from increased doses.

Comparison of Figures 6.9, 6.16, 6.18, 6.22, and 6.24 suggests a correlation of the occurrence and the intensity of the gigantic signal effect with the thickness of the organic substrate layer. Especially Figure 6.22 suggests a dependence of the effect on the thickness of the previously deposited layer. Interpretation of Figures 6.18, 6.20, and 6.24 suggests that the intensity of the gigantic signal effect might be related to the stiffness of the sample.

The thin detector sheet is obviously less stiff than the thicker ones resulting in a stronger effect, as shown in Figure 6.18. As the flexural modulus, *i.e.*, stiffness, increases with decreasing temperature^[133], the intensity of the effect should be lower at cryogenic temperatures. The experiments carried out on thick layers of PTCDA (red traces in Figures 6.18 and 6.20) demonstrate this behavior. It should be stated that the experiments involving sexithiophene are not comparable due to different layer thicknesses.

Regarding Figures 6.20 and 6.24 one can conclude that the strength of the gigantic signal effect differs for different materials constituting substrate layers of similar thickness.

Samples coated only on one side or coated on both sides with similar thicknesses were employed to verify an influence of the asymmetry of the detector stack in case only one side is coated. Both kinds of samples exhibit the gigantic signal effect, which leads to the conclusion that a coating of the back side is not able to compensate the effects of the top coating.

Combination of these results suggests an origin of the gigantic signal effect not to be directly related to thermodynamics. Since the deposition of material is necessary and the surface composition seems to determine these effects, one might assume a mechanical cause. Changing mechanical stress in the detector polymer causes a signal as well as temperature changes due to the piezoelectric effect, see Section 1.3.3. This assumption raises the question concerning the origin of the mechanical input. A possible explanation could be the merging of clusters on the surface leading to a lateral compression of the detector polymer. Alternatively, insertion of dosed atoms might lead to a lateral tension in the polymer due to insertion of atoms between islands. Which turns out to be the dominating process depends on the properties of the involved substrate and dosed species as well as the resulting adsorbate system. As the processes result in signals of different polarity^[135], they

might be distinguished. The first case exhibits the same polarity as for thermal radiation and the latter shows a reversed sign. As the data treatment algorithm is independent of absolute polarity²⁰, see Chapter 3, and the discussed effect causes an increase of signal amplitude, one can conclude that the gigantic signal effect might arise from a mechanical lateral compression of the detector. In addition, a reversal of the sensor's polarity, *i.e.*, by upside down mounting of the detector polymer, is not affecting the observed signal in this theory.

²⁰ The absolute polarity can be altered by mounting the detector disc upside down in its holder.

6.9 Inverted Signal Effect

Upon adsorption of zinc on a detector cleaned by sputtering, for experimental parameters see Section 6.7, a severe shape distortion of the recorded detector signal has been observed, ultimately resulting in a change of the signal's polarity. Figure 6.35 illustrates the transition from the positive to the negative intensity.

The radiation measurement with the clean sample, *i.e.*, with a zinc coverage of 0 ML, identifies the detector to be mounted with positive polarity, see Sections 1.3.3 and 2.2. The initial, *i.e.*, at low zinc coverage of 0.2 ML, frames exhibit the typical shape composed of the radiative and the laser-like signal contribution. Upon increasing zinc coverage, between 0.6 ML and 33 ML, the measured heat seems to be released with a time delay. However, further evolution classifies this observation as an artifact arising from a “negative intensity” contribution, partially compensating the original signal at zinc coverages between 45 ML and 84 ML. This contribution dominates the recorded signal at extreme zinc coverages of more than 100 ML. The fitting routine is not able to adapt its result for the measured data at the intermediate coverages, suggesting an additional contribution to the recorded signal. Nevertheless, the peak shape is represented well again at extreme coverages.

Figure 6.36 illustrates the reconstructed power input, see Section 3.10, to the calorimetry detector as a function of time for the laser reference and the radiation measurement of the aforementioned experiment. In accordance with expectation, the power is delivered to the detector during the applied pulses, *i.e.*, while the chopper is in the open state, for the all reference measurements at this time. Exemplarily the laser reference and radiation reference measurements are shown. The relative obtained input powers of 2 μW for the radiation measurement and 12 μW for the laser reference measurement are in agreement with, *i.e.*, are proportional to, the measured peak-to-peak voltages of 0.02 V and 0.12 V, respectively. This basic, manual, data treatment, involving a linear approximation of the detector signal, in this simple case justifies the applicability of the sophisticated reconstruction mechanism for signal shapes which cannot be treated using the simple method.

Reconstruction of the power input of the adsorption of zinc on the sputter cleaned detector exhibits an unexpected behavior illustrated in Figure 6.37. Initially, *i.e.*, for zinc coverages smaller than 0.5 ML, the deposited power correlates with the opening of the shutter. As described in detail above, a deformation of the signal occurs upon dosage of zinc. The compensating nature of this additional effect is clearly visible in Figure 6.37 as white bands during the pulses. It is striking that the white band is limited to the region of the pulses while the red band, indicating positive intensity,

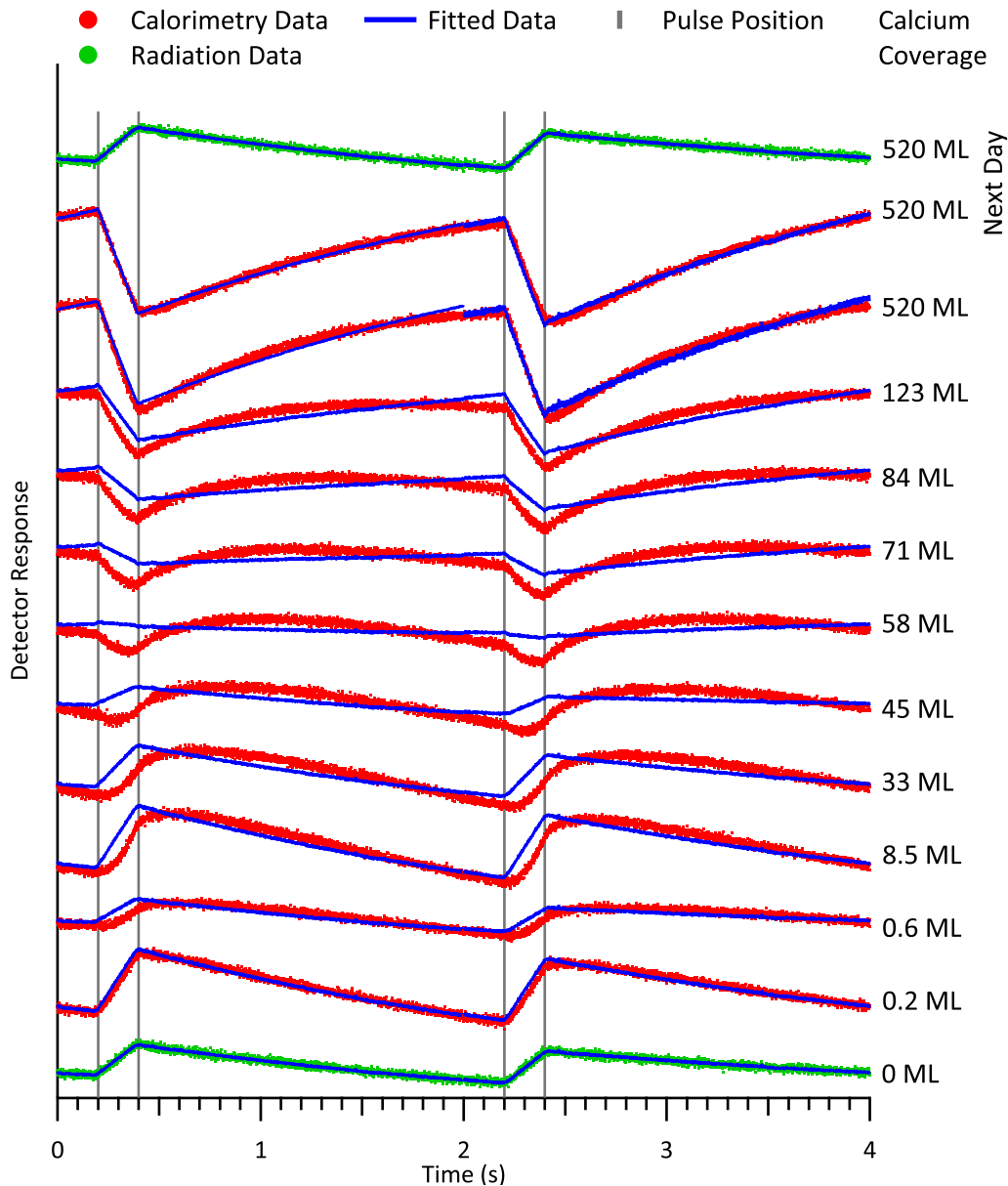


Figure 6.35: Adsorption of Zinc on Sputtered Detector: Coverage Dependent Signal Shape — The response of the detector to single pulses (position between gray lines) of radiation (green) and the molecular beam (red) is displayed for different zinc coverages together with the fitting result. Continuous deposition without calorimetric measurement provided the coverage increase from 123 ML to 520 ML. The evolving deformation of the signal persists until the next day. The second radiation measurement is not affected by the signal inversion.

extends beyond the pulse. This is in strong contrast to the other measurements in this experiment.

The change of the background polarity can be attributed to a combination of

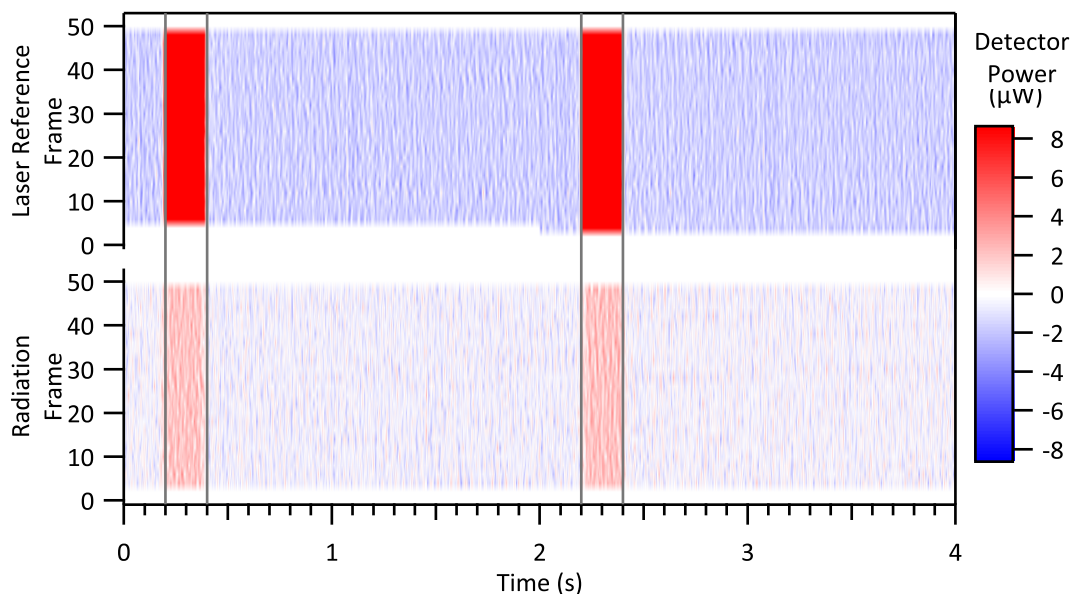


Figure 6.36: Adsorption of Zinc on Sputtered Detector: Reconstructed Power Input for Laser and Radiation Reference — The color coded (red positive, blue negative, white zero) reconstructed power input as a function of temporal position in the frame pair and of the running number of the frame in the measurement is shown together with the nominal pulse position (gray lines). The power input is positive and exclusively located at the nominal pulse positions for both measurements. The negative background input is an artifact due to the offset correction in the used amplifier.

the changed polarity of the peak and the automatic offset correction in the used amplifier.

Leaving the sample at rest for eleven hours improves the quality of the fit for a calorimetric measurement even further, as depicted in Figure 6.35, to an extent mocking an inversion of the detector's polarity. This observation might indicate a relaxation of the deposited zinc layer, *e.g.*, a recrystallization, on the substrate. This effect would require mobility of the topmost zinc atoms at ambient temperature. Altogether, this is in accordance with the results obtained from the sticking measurements on this sample, as the formation of clusters requires mobile surface atoms.

Comparison with the radiation signal from the evaporator and the laser input, which are positive, disproves a theory including an alteration of the detector. These additional measurements on the same sample, shown in the reconstructed form in Figure 6.38, revealed that the signal is inverted only if zinc is deposited on the sample. The comparable amplitude of the radiation measurement implies an

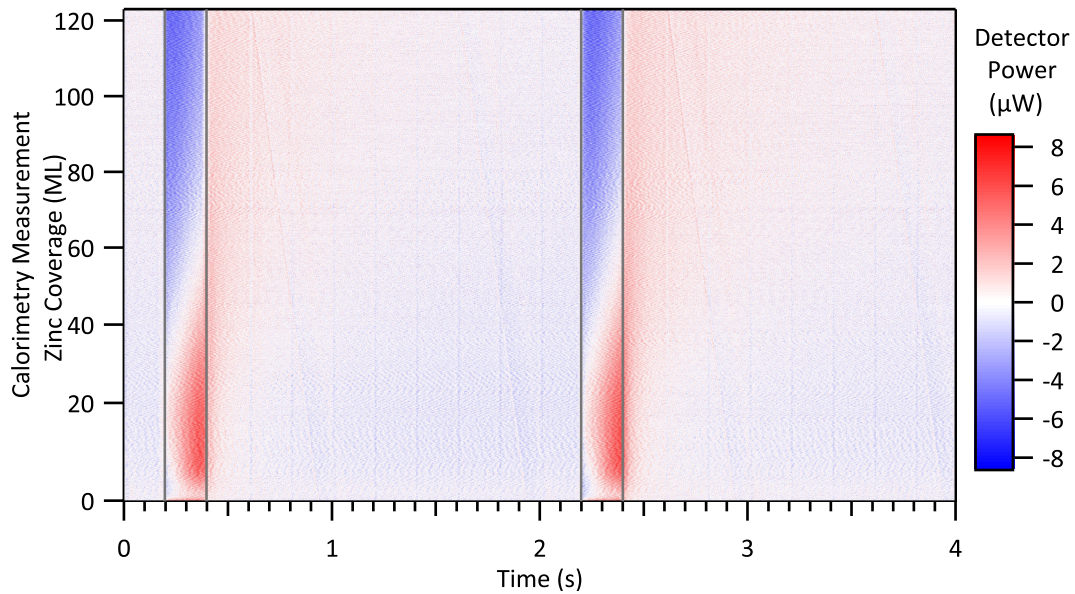


Figure 6.37: Adsorption of Zinc on Sputtered Detector: Reconstructed Power Input for Calorimetric Measurement — The color coded (red positive, blue negative, white zero) reconstructed power input as a function of temporal position in the frame pair and of zinc coverage is shown together with the nominal pulse position (gray lines). The power input exhibits a pronounced contribution outside the nominal pulse positions and the temporal distribution of the power input is continuously modified. Due to the offset correction in the used amplifier, the negative to positive shifting background input is considered to be an artifact.

unchanged sensitivity of the detector for thermal radiation.

These results clearly exclude the possibility of a modification, *i.e.*, a reversal in polarization, of the sensor.

Combination of these results suggests an origin of the inverted signal effect not to be directly related to thermodynamics. Since the deposition of material is necessary and the surface's nature seems to determine this effect, one might assume a mechanical cause. Changing mechanical stress in the detector polymer causes a signal as well as temperature changes due to the piezoelectric effect, see Section 1.3.3. This assumption raises the question concerning the origin of the mechanical input. Analogue to the gigantic signal effect, see Section 6.8, a possible explanation could be the merging of clusters on the surface leading to a lateral compression of the detector polymer. Alternatively, insertion of dosed atoms might lead to a lateral tension in the polymer due to insertion of atoms between islands. Which turns out to be the dominating process depends on the properties of the involved substrate and dosed species as well as the resulting adsorbate system. As the processes result in

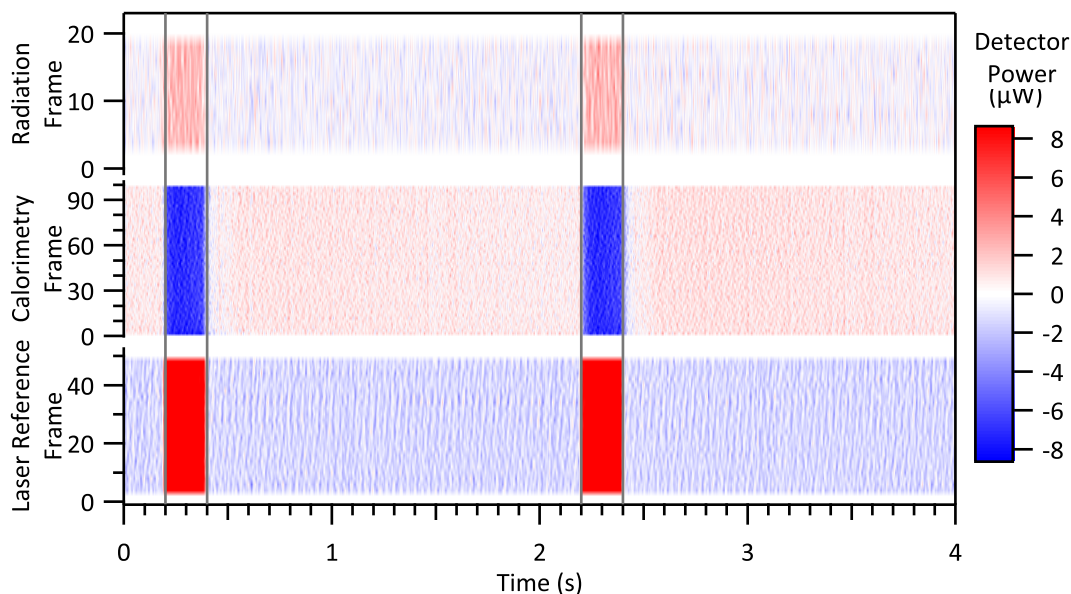


Figure 6.38: Adsorption of Zinc on Sputtered Detector: Reconstructed Power at High Coverages for Various Measurements — The color coded (red positive, blue negative, white zero) reconstructed power input as a function of temporal position in the frame pair and of the running number of the frame in the measurement is shown together with the nominal pulse position (gray lines). The laser and radiation based measurements recorded at a zinc coverage of 520 ML are almost identical to the measurements obtained from the clean sample, see Figure 6.36. The calorimetric measurement performed at the same coverage in between the other two measurements exhibits a power input during the nominal pulse but with inverted polarity. The negative respectively positive background inputs are artifacts due to the offset correction in the used amplifier.

signals of different polarity^[135], they might be distinguished. The first case exhibits the same polarity as for thermal radiation and the latter shows a reversed sign. As the data treatment algorithm is independent of absolute polarity²¹, see Chapter 3, and the discussed effect causes a decrease of signal amplitude and finally a reversal of the polarity, one can conclude that the inverted signal effect might be attributed to mechanical lateral extension of the detector.

²¹ The absolute polarity can be altered by mounting the detector disc upside down in its holder.

6.10 Synopsis of the Results from the Investigated Systems

The choice of materials is explained and motivated using preliminary work. This covers similar systems using adsorption calorimetry or identical systems using complementary techniques. Chemical reactivity as well as toxicity, availability, economical aspects, and scientific relevance are weight against each other. A broad range of interesting combinations resulted therefrom and has been investigated. Subsequently, a method to approximate the reaction thicknesses from crystallographic data is presented. A short introduction to the experimental sequence provides a coarse insight for the handling of the experimental setup, presented in Chapter 2. It also lists the experimental parameters used in the, subsequently presented, investigation of various systems.

The sticking probabilities and adsorption energetics have been studied for most combinations of the chosen adsorbates and substrates. Most experiments suffered from a mismatch of the multilayer enthalpy at elevated coverages to the sublimation enthalpy, which is serving as an internal reference. Nevertheless, several results, especially the one obtained from the adsorption of calcium on a thin coating of sexithiophene at low temperature, see Figure 6.24, reveal that the presented setup is able to perform the experiments it is designed for. This statement is supported by the fact that several intermediate plateau values, *i.e.*, after an occurring reaction and before the gigantic signal effect sets in, match the sublimation enthalpy. These individual concurrences and the results at constant conditions, see Figure D.36, indicate that an excellent reproducibility of the experiments seems generally possible. Due to the secondary perturbations arising from the gigantic and inverted signal effects, this aspect has not been studied in detail yet.

The conclusions for individual systems can be found in Section 6.4.3 concerning the adsorption of magnesium, in Section 6.5.3 concerning the adsorption of calcium, in Section 6.6.3 concerning the adsorption of copper, and in Section 6.7.3 concerning the adsorption of zinc. Most of the investigated systems show the expected behavior. Magnesium and calcium initially react with the substrate and subsequently form a metallic overlayer. Zinc is less reactive but still indicates a reaction while copper is inert. Both substances form a metallic overlayer as well.

Several attempts have been made to adjust the tooling factors, mentioned in Chapter 5, in a way that the multilayer enthalpy matched the heat of sublimation. This strategy was supposed to identify the weak link in the calibration chain. The resulting coefficients are on the one hand not consistent and on the other hand

frequently physically absurd, *e.g.*, reflectivities outside the meaningful range of null to unity, or implied unreasonable large errors not compatible with the obtained data. A discussion of clearly unreasonable quantities is futile and hence not presented here.

The nature of the mismatch together with the results from the calibration measurements, presented in Chapter 5, led to the discovery of the *inverted signal* and *gigantic signal* effects. The origin of these effects has not been ascertained yet. Both effects are only observed in case metal vapor is adsorbing on the sample. The inverted signal occurs in case of samples cleaned by sputtering, *i.e.*, on the bare metallic surface. In contrast, the gigantic signal appears on samples modified by a rather thick film of organic molecules. Furthermore, the strength of the effect seems to be correlated with the substrate layer thickness. The observed amplitudes are in contradiction to physical principles in case of negative amplitudes. In case of extreme positive amplitudes the resulting “detected heat” exceeds the enthalpies of the most exothermic chemical reactions known by far. In addition, this effect takes place at coverages where a reaction with the substrate should not be possible anymore. A reaction with the residual gas in the vacuum system is also unlikely since it should be present during the whole experiment.

Furthermore, the obtained coverage dependent heat should not be a function of substrate thickness as long as a certain minimum thickness is present. The larger reacting quantities, in case of thin substrate layers compared to the thick ones, demonstrate the need for well defined experimental starting points. As a consequence, more attention should be paid to sample preparation and characterization prior to the calorimetric measurement, which has not been possible at the time the experiments have been conducted.

Altogether, these hints suggest an origin of both effects not directly related to thermodynamics. Since the deposition of material is necessary and the surface composition seems to determine these effects, one might assume a mechanical cause. Changing mechanical stress, *e.g.*, by compression or tension, in the detector polymer causes a signal – similar to the one arising from temperature changes – due to the piezoelectric effect, see Section 1.3.3. This assumption, which would explain the gigantic signal effect as well as the inverted signal effect, raises the question concerning the origin of the mechanical input.

Momentum transfer of the deposited atoms to the detector and a resulting deformation can be excluded without any further calculation since this effect would be constant and not developing, as observed. Mechanical strain in the deposited layer could derive from coalescence of clusters in the metallic top layer in case

the voids between the clusters are not filled from the bottom up with a perfect lattice match. As no direct measurements addressing this assumption have been performed, this explanation remains speculative. However, it is supported by the observation that thick layers of deposited material in old vacuum systems tend to peel off after extensive deposition. The same effect was observed on heavily loaded oscillator crystals^[237]. Instead of typical failure due to exceedance of the recommended frequency range some crystals stopped working as the deposited layer partially exfoliated from the sensor.

Macroscopic evidence of these forces was also observed upon purging of the cap on the main evaporator, see Section 2.3.1, after experiments involving the deposition of zinc were completed. The deposit could be easily removed from the cap as the diameter of the zinc part was significantly smaller than the inner diameter of its mold, *i.e.*, the cap. Unfortunately, this specimen was discarded without further documentation.

This behavior has not been reported in literature yet although the spin-coated polymer substrates exhibit similar thicknesses^[55–60] as the molecular thin films investigated in this work. However, the reported coverages of the dosed metal stay below 10 ML, whereas the here observed effects take place at higher coverages.

A possible solution to circumvent the presumed mechanical influence on the detector signal would be based on the use of the detector head designed for single crystals, see Section 2.2, in combination with a cheap, defined dummy for the single crystal. Here, the joint between the dummy and the detector ribbons decouples mechanical stress but still provides thermal contact.

Discs punched-out from 30 μm thick aluminum foil²² exhibit a sufficient stability and chemical inertness due to the passivating oxide layer. Thinner foils are commercially available but their usage is discouraged. The reason for the use of thicker foils is mechanical stability. This will surely sacrifice some sensitivity but will hopefully provide substrate layer thickness independent multilayer enthalpies and thus eliminate the gigantic and inverted signal effects. In addition, the thick aluminum foils are an economical sample substitute for the even thicker – and expensive – single crystal samples and provide safe practice for their handling. The reflectivity of aluminum is rather high but well documented^[136]. These properties, together with the vanishing price per sample, render this option an ideal candidate for single use samples, such as spin-coated polymers or thick molecular films.

Another approach could be based on older work by King^[13], Černý^[117,118], Stuckless^[86,238], and Campbell^[119]. In all groups the employed detector has been based

22 ‘2596.1’ from Carl Roth GmbH + Co. KG.

on, at least for some time, a pyroelectric single crystal, *i.e.*, lithium tantalate, rather than β -polyvinylidene fluoride used in more recent work^[55,86,87,93,114,121] including this one. The expectation is that this stiffer detector material would withstand the mechanical stress and only respond to the heat input. However, these thin single crystalline substrates are expensive and brittle. The first drawback excludes the use as disposable specimen and the latter renders a cleaning of the detector challenging. Furthermore, a reduced sensitivity compared to the polymer detector material is expected.

One possible origin of the minima observed after an initially high heat of adsorption, especially visible in Figure 6.7.2, has been identified as the offset compensation of the employed amplifier. Since a new amplifier is already being built, this assumption could soon be verified or excluded.

The experiments studying the adsorption of calcium on sexithiophene exhibit a similar shape of the sticking probability but with different intensities. This might indicate an issue with the experimental settings of the zero sticking reference measurement. As discussed in Sections 5.7 and 5.8.4, the mass spectrometer exhibits the highest inaccuracy and longs for improvement considering the pulse-to-pulse signal stability and signal shape.

Finally, it should be mentioned that the quality of the experimental results increased along several minor improvements of the experimental setup. However, not all experiments could be repeated on a reasonable time scale as the focus was set rather on the development of the experimental framework than on a detailed investigation of a single metal/substrate combination. Nevertheless, a reinvestigation of the here presented systems with the finally fully operational setup might be fruitful and is thus recommended.

7 Summary and Outlook

By now, abrupt interfaces and diffuse interphases between metals and organic semiconductors have become relevant in the production of organic electronics in consumer products, like organic light emitting diodes (OLED) in cellular phones. However, the description of these contacts focuses on engineering usage. Hence, a complete fundamental and scientific understanding of these electrical joints has not been achieved yet. This situation motivates the usage of nanojoule adsorption calorimetry as a method of studying the energetics of their formation under ultrahigh vacuum conditions. Complementary techniques, such as photoemission spectroscopy, can be used to obtain structural information on the interface or chemical states of the formed reaction products and hence might be used to enhance the results from the calorimetric experiments.

The presented aim of this work includes the construction of the experimental setup, the development of the software used for data evaluation, a full characterization of the experimental setup, and a selection of results from conducted experiments. Each of these individual aspects in the presented dissertation is summarized in a dedicated synopsis at the end of each chapter, see Sections 2.10, 3.15, 4.5, 5.11, and 6.10. Their essential aspects are summarized below.

The amply illustrated experimental setup is dedicated to the investigation of metal adsorption on organic thin films, prepared by physical vapor deposition or by *ex situ* preparation techniques. The concept of the setup also provides the option to study inverse systems, *i.e.*, the adsorption of large organic molecules on thin metal substrates, including single crystals. The individual components of the setup, their usage, and their interaction are discussed in detail.

Two kinds of sample holders provide usage of thin sheet and thin single crystal substrates as well as an adjustable sample temperature. The molecular beam is suitable to accept different kinds of effusive molecular sources. It has been successfully tested concerning operation with a specifically constructed large volume Knudsen cell, providing outstanding long run times at high material throughput, as well as a commercial electron beam evaporator. An integrated valve allows for service routines

on the molecular beam without venting of the main chamber. Additional optical devices guide the laser beam, which is necessary for sensor calibration, to the sample position. Both, the molecular and the laser beam are switched on and off by a mechanical chopper providing almost freely adjustable repetition rate and duty cycle. This process facilitates the pulsed operation required by the measurement principle. Ancillary devices allow for measurement of reference data sets, *e.g.*, the fraction of thermal radiation emitted by the evaporator, which are essential for the evaluation of the recorded calorimetry data. A load lock serves as a facility to transfer samples into the vacuum system as well as for sample storage and to prepare organic thin film substrates.

Possible improvements to be realized on a long term are also suggested, which are primarily related to the handling of air sensitive substances. The design drawings of the individual parts constructed for the experimental setup in the framework of this thesis are documented in the appendix.

The graphical user interface of the treatment procedure for measured data is introduced with great detail along a sample experiment. Numerous options to condition the data, *e.g.*, by digital filtering, are presented and their effects are discussed. The treatment of the individual measurements involved in a calorimetric experiment is demonstrated and possible ways of improving the quality of the results are illustrated. In this context, an *excursus* is made considering the statistical nature of the measurements and the automatic outlier detection algorithm involved in these experiments. Furthermore, the averaging merge of several experimental results into a global result describing the coverage dependent interaction of an adsorptive with an adsorbent is explained. Additionally, the actions of the facilitating operations for experienced, *i.e.*, **lazy**, users are explicated. Finally, calorimetry specific extensions to other software packages are discussed.

The data file formats and the programming background of the data evaluation software are documented. Together with the internal data structuring of the IGOR PRO experiment files, the purpose of each individual data object is described. Subsequently, a brief description of each function used in the program packages is given. Physical and mathematical concepts, which are neither covered by the introduction nor the chapter corresponding to the characterization of the experimental setup but are necessary for the data evaluation, are presented together with the explanation of the functions. Furthermore, a description of two supporting software packages concerning error management and logging of the machine status, which can also be

used for other projects, complete this documentation.

The source code of all three software packages is listed in the appendix and was used to compute most of the presented results in this work. In the majority of cases, data from the characterization measurements have been analyzed with the main program package in a first step. Subsequently, they have been manually processed further according to the particular objective.

Every device involved in the individual measurements in a calorimetric experiment has been intensively characterized. In order to ensure maximal reliability of the obtained results, this process exceeded the standard requirements on a calorimetric experiment by far. If necessary, specific theoretical background to the individual characterizations is given together with the corresponding description of the experiment. The results of each investigation are discussed individually. Additionally, suggestions for improvements, routine checkup experiments, or further experiments are made, if applicable. The characterization of the experimental setup provided valuable findings influencing the sample preparation and measurement routines.

The average reflectivity at the wavelength of the employed laser of the pristine detector material has been determined using a dedicated air-based setup and turned out to be smaller than reported in literature. Cleaning of the sensor material by means of ion bombardment proved to be essential for the preparation of homogeneous molecular thin films on the detector by physical vapor deposition. The deviation of indicated and actual thickness, originating from partial loading of the quartz crystal microbalance's sensor, has been quantified. A contamination arising from the residual gas in the chamber could be excluded since the determined amount obtained by analytical wet chemistry matches the discussed model for the correction factor. The characterization of the coating facility in the load lock comprises the determination of operating temperatures for the crucible, an influence of the thermal load from the crucible on the sensor material, and a quantification of the conversion factor from the reading of the quartz crystal microbalance and the actual thickness of the organic film on the sample substrate. Except for the diode based laser, the specifications of the individual electronic components have been successfully verified. The automatic offset compensation implemented in the amplifier for the pyroelectric signal turned out to be troublesome since it induces artifacts in the measured data. Intensive characterization of the pulsed molecular beam involved determination of the run times of the source for various evaporants, the maximal filling amounts, temperatures of operation, and the temporal stability of the provided flux. After installation of a throttling device, the deposition rate is almost constant on a time scale of

hours. Furthermore, the throttle provides a constant emissivity for electromagnetic radiation and prevents macroscopic particles from being hauled out of the crucible. The chopper generates reproducible, time adjustable events with the targeted slew rate. Laser based measurements are not influenced by the infrared radiation emitted from the crucible since the mount for the mirror in the molecular beam effectively blocks its pathway. The settings of the mass spectrometer have been adjusted to the experimental requirements considering the technical peculiarities of the instrument. Intensive testing has also been performed for the devices involved in the ancillary measurements. The molecule-blocking window exhibits a transmission of the infrared radiation emitted by the evaporator and the laser radiation solely in case of high crucible temperatures. The signal shape resulting from thermal radiation differs significantly from the shape which is obtained using laser radiation. However, it is independent from the temperature of the crucible. The presented theory describing the intensity of the thermal radiation is excellently confirmed and might be used to calculate the contribution of the radiation to the measured signal. This approach might eliminate one of the reference measurements. The correction factors for the mirror setup, used to measure the laser power, and the quartz crystal microbalance, used to obtain the deposition rate, are in agreement with their respective theories. The behavior of the hot plate, used for full reflection of the incoming molecules, requires additional investigations. As expected, a proportionality of the pyroelectric signal to the laser power and to the illuminated area are found. Likewise, the thermal load capacity and the temperature dependent sensitivity of the detector matched their specifications. A round robin test with diverse experimental conditions along the measurement sequence clearly demonstrated that the reconstruction of the power input into the detector can be performed successfully.

In total, the comprehensive characterization of the individual measurement devices give reasons to expect accurate results from the calorimetric experiments.

Finally, several investigated systems covering the adsorption of metal atoms on various surfaces are presented in this thesis. The choice of materials forming an interface is based on the respective toxicity, availability, pricing, and scientific relevance and resulted in a broad range of interesting combinations. In this context, an approximation of the thickness of the reaction zone, *i.e.*, the interphase, from calorimetric data is motivated and presented for the possible material combinations. Furthermore, the experimental sequence is illustrated on the basis of a flow diagram while the used experimental parameters or, respectively, their recommended ranges are stated. Specific conclusions on the results obtained from individual combinations

of substrates and adsorbed metals would exceed the scope of this summary and are given in corresponding sections in this paper.

Although the characterization of the individual components promised accurate results, most of the experiments did not hit the internal standard. The latter is provided by the fact that the enthalpy of adsorption is identical to the enthalpy of resublimation at high coverages of the metal. It is striking to note that the experiments are quite well reproducible and that some of the results from material combinations exhibit a plateau region in which the measured enthalpy matches the standard and deviates at higher coverages. These reproducible regions of constant enthalpy and the experiment covering the adsorption of calcium on a thin layer of sexithiophene at low temperature clearly demonstrate that the observed mismatch does neither originate from systematic errors in the experimental setup nor from the data treatment procedure but from an unknown secondary effect. This hypothesis is further supported by the presence of an unexpected dependency of that secondary effect at high metal coverages on the thickness of the substrate layer. A mechanical deformation of the sensor and a therefrom resulting piezoelectric signal are suspected to cause this effect. However, a verification thereof was not possible in the given laboratory time. Mechanical strain in the forming metallic film is suspected as a possible origin of the deformation. In order to verify or falsify this hypothesis, a process changeover towards investigation of thin sheet samples is recommended since they are mechanically decoupled from the sensor. Discs cut from aluminum foil, coated with the organic component, might serve as a substitute for the expensive single crystals. This proceeding provides the opportunity to practice the handling with the sensitive single crystals.

Most of the investigated systems exhibit the expected behavior at low to medium metal coverages. Initially, magnesium and calcium react with the functional groups of the substrate molecules and grow into a closed top layer at elevated coverages. Zinc reveals a reduced yet still present reactivity while copper shows no reaction along the examined cases. Organic thin films, prepared by physical vapor deposition, exhibit the expected reactivity towards the deposited metal atoms. The anhydride groups of perylene tetracarboxylic anhydride show the largest reaction enthalpies. Complexation by the pyrrole units of the porphyrin release slightly less energy and the reaction of the sulfur atoms in the thiophene units with the deposited metal is least exothermic.

In summary, these experiments led to several specific deductions. Most important for this work, the experiments proved that the constructed experimental setup is

capable of measuring correct heats of sublimation at moderate coverages. Since these values serve as internal reference values, the heats of reaction at lower coverages are expected to be correct. Collaterally, unexpected effects depending on the vertical sample constitution were discovered and possible origins and practices to avoid them were discussed but could not be investigated further in the given amount of time. In addition to the selection of presented experiments, treated data sets from further experiments are documented in the appendix as supporting information.

In the near future, the recommended experiments should be conducted and the dependent alterations should be executed. Subsequently, the setup is ready to be used on a regular basis for calorimetric experiments, *i.e.*, it is fulfilling its purpose. Interesting scenarios comprise alkaline and alkaline earth metals in combination with large organic molecules used in organic electronics, *e.g.*, oligothiophenes, phthalocyanines, porphyrines, fullerenes, and many more, including their (polymer) derivatives as well as their blends.

The usage of high purity materials and their handling in an inert atmosphere is desirable as an intermediate extension of the experimental setup. On the same time scale the planned manipulator for preparation of single crystal samples should be realized. Another productive addition to the vacuum system would be a *vacuum suitcase*, which enables the transfer of specimens to other experimental stations without air contact.

In the long run, upgrades of the experimental setup with complementary techniques are highly recommended. Eligible options would include spectroscopic methods and imaging techniques. Examples for the former are photoemission spectroscopy or Auger spectroscopy to probe chemical states and to detect contamination as well as low energy ion scattering to investigate the growth mode of the adsorbed species. Atomic force microscopy or scanning tunneling microscopy to document surface morphologies before and after deposition processes are among the latter. Under certain circumstances spectroscopic methods are even able to provide knowledge about reaction depths, which are typically obtained by destructive methods, and are thus able to complement the calorimetric measurements.

Nanojoule adsorption calorimetry provides valuable insight into the energetics during adsorption, *i.e.*, during the formation of interfaces and interphases. This thesis describes the fundamental theory and documents the successful implementation of the comprehensive assignment of tasks, *e.g.*, the experimental setup and the software for data treatment as well as the intensive characterization of all mentioned

components. Exemplary scientific discussions of selected trustworthy experiments complete this publication and demonstrate the successful interaction of all modules involved in the framework of this scientific project.

8 Zusammenfassung und Ausblick

Abrupte Grenzflächen und diffuse Grenzschichten (Interphasen) zwischen Metallen und organischen Halbleitern haben mittlerweile eine gewisse Relevanz in der Produktion von organischer Elektronik in Endanwenderprodukten, wie zum Beispiel organische Leuchtdioden (*OLED*) in Mobiltelefonen, gefunden. Die Beschreibung dieser Kontakte fokussiert sich jedoch auf die praktische Anwendung, so dass das grundlegende und wissenschaftliche Verständnis dieser elektrischen Verbindungsstellen noch nicht vollständig ist. Diese Situation motiviert die Verwendung der Nanojoule-Adsorptions-Kalorimetrie als Methode, um die Energetik sich bildender Grenzschichten unter Ultrahochvakuumbedingungen zu untersuchen. Komplementäre Verfahren, wie zum Beispiel Photoemissionsspektroskopie, können genutzt werden, um strukturelle Informationen über die Grenzschicht und chemische Zustände der Reaktionsprodukte zu ermitteln, welche die Ergebnisse der Kalorimetrie zu präzisieren vermögen.

Das präsentierte Ziel dieser Arbeit beinhaltet die Konstruktion des experimentellen Aufbaus, die Entwicklung eines Computerprogramms zur Datenauswertung, eine vollständige Charakterisierung der realisierten Komponenten und eine Auswahl an Ergebnissen von durchgeführten Experimenten. Jeder dieser einzelnen Aspekte in der vorliegenden Dissertation ist detailliert am Ende des jeweiligen Kapitels in englischer Sprache zusammengefasst.

Der ausgiebig illustrierte experimentelle Aufbau ist für Untersuchungen optimiert, in denen Metallatome auf organischen Dünnschichten abgeschieden werden. Diese Schichten können durch Gasphasenabscheidung in oder anderweitig außerhalb der Anlage präpariert werden. Das Konzept beinhaltet auch die Möglichkeit, invertierte Systeme, d.h. die Adsorption von großen organischen Molekülen auf metallischen (Einkristall-) Oberflächen, zu untersuchen. Die einzelnen Komponenten des Aufbaus, ihre Handhabung und ihr Zusammenspiel sind detailliert beschrieben.

Die Probenhalterungen ermöglichen die Verwendung von Dünnschicht- und Einkristallsubstraten bei einstellbarer Proben temperatur. Der Molekularstrahl ist für den Einsatz von verschiedenartigen Effusivquellen geeignet. Er ist sowohl für eine ei-

gens konstruierte Knudsenzelle mit großem Füllvolumen, und dadurch extrem langer Laufzeit bei hohem Materialdurchsatz, als auch für einen kommerziellen Elektronenstrahlverdampfer erfolgreich getestet worden. Ein integriertes Ventil ermöglicht die üblichen Servicearbeiten am Molekularstrahl ohne die Hauptkammer belüften zu müssen. Zusätzlich führen optische Elemente den zur Kalibrierung notwendigen Laserstrahl an die Probenposition. Molekular- und Laserstrahl werden durch einen mechanischen Pulsformer mit nahezu frei einstellbarer Repetitionsrate und Tastverhältnis an- und ausgeschaltet und ermöglichen so den für das Messverfahren notwendigen Pulsbetrieb. Hilfsbausteine ermöglichen die Messung von Referenzdaten, wie beispielsweise den Anteil der thermischen Strahlung des Verdampfers, die für die Auswertung der Kalorimetriedaten nötig sind. Eine Schleuse bietet die Möglichkeit, Proben in das Vakuumsystem zu transferieren, zu lagern und organische Dünnschichten zu präparieren.

Mögliche, längerfristig zu realisierende Verbesserungen sind ebenfalls vorgeschlagen. Dies betrifft im Wesentlichen die Handhabung von luftempfindlichen Chemikalien. Die im Rahmen dieser Arbeit entstandenen Konstruktionszeichnungen der einzelnen Bauteile dieser Anlage sind im Anhang aufgeführt.

Die Benutzeroberfläche des Computerprogramms zur Datenauswertung wird anhand einer exemplarischen Auswertung eines Datensatzes detailliert vorgestellt. Zahlreiche Möglichkeiten um die Daten vor der eigentlichen Auswertung zu optimieren, wie zum Beispiel durch digitales Filtern, sind vorgestellt und ihre Auswirkungen werden besprochen. Die Behandlung der einzelnen Messungen eines Kalorimetrie-Experiments ist beschrieben und Möglichkeiten werden erläutert, um die Qualität der Ergebnisse zu verbessern. In diesem Zusammenhang beleuchtet ein Exkurs die statistische Streuung der einzelnen Datenpunkte und die automatische Erkennung von Ausreißern. Weiterhin wird das mittelnde Zusammenfügen von Einzelexperimenten zu einem Hauptergebnis, das die bedeckungsabhängige Wechselwirkung eines Adsorptivs mit einem Adsorbens beschreibt, erklärt. Zusätzlich sind die arbeitsökonomischen Funktionen für erfahrene Nutzer und nützliche, für Kalorimetrie-Experimente spezifische, Erweiterungen für andere Programmpakete erläutert.

Die Dateiformate und der programmiertechnische Hintergrund des Datenauswertungsprogramms sind, zusammen mit der internen Datenstruktur inklusive des jeweiligen Verwendungszwecks der einzelnen Datenobjekte der IGOR PRO Experiment Datei, beschrieben. Eine knappe Erläuterung aller im Programm verwendeten Funktionen ist anschließend gegeben. Für die Datenauswertung notwendige mathema-

tische und physikalische Konzepte werden hier ebenfalls vorgestellt, soweit sie nicht in der Einleitung oder im Kapitel über die Charakterisierung der Anlage angesiedelt sind. Weiterhin wird durch die Beschreibung von zwei weiteren, unterstützenden Programmpaketen, welche sich auch anderweitig einsetzen lassen, die Dokumentation abgerundet. Ersteres ist für die Behandlung von Fehlermeldungen in Programmen konzipiert, und zweiteres bietet Funktionen, um den protokollierten Maschinenstatus auszuwerten.

Der Quelltext für alle drei Programmpakete ist im Anhang aufgeführt und wurde für den größten Teil der Datenauswertung in dieser Arbeit verwendet. Die meisten Daten aus Charakterisierungsmessungen wurden ebenfalls zunächst mit diesem Programmpaket ausgewertet und dann, entsprechend der Fragestellung, weiter manuell aufbereitet.

Jede für die einzelnen Messungen eines Kalorimetrie-Experiments nötige Vorrichtung wurde intensiv charakterisiert. Um eine größtmögliche Verlässlichkeit der erhaltenen Ergebnisse zu garantieren, geht diese Charakterisierung weit über die in einem Kalorimetrie-Experiment nötigen Anforderungen hinaus. Falls ein weitergehender theoretischer Hintergrund für die einzelnen Aspekte der Auswertungen nötig sein sollte, ist dieser zusammen mit der jeweiligen Beschreibung des Experiments ausgeführt. Die Ergebnisse der einzelnen Untersuchungen werden jeweils für sich diskutiert. Zusätzlich sind gegebenenfalls Vorschläge für weitere Verbesserungen, Prüfroutinen und weiterführende Experimente beschrieben. Die ausgiebige Charakterisierung der Apparatur ermöglichte wertvolle Erkenntnisse, die die Standards in den Abläufen der Probenpräparation und der Messungen beeinflusst und verbessert haben.

Die mittlere Reflektivität des unbehandelten Sensormaterials an Luft wurde mittels eines separaten Aufbaus für die verwendete Laserwellenlänge bestimmt und resultierte kleiner als der entsprechende Literaturwert. Eine Reinigung des Sensormaterials durch Ionenbeschuss erwies sich als essentiell, um homogene molekulare Dünnschichten auf dem Sensor aus der Gasphase abscheiden zu können. Die Abweichung von gemessener und tatsächlicher Schichtdicke, die durch eine teilweise Beladung des Sensors der Quarzmikrowaage entsteht, wurde quantifiziert. Der nasschemische Befund entspricht dem Korrekturfaktor aus dem diskutierten Modell, was eine signifikante Kontamination durch das Restgas in der Kammer ausschließt. Die Charakterisierung der Beschichtungseinrichtung in der Schleusenammer umfasste die Bestimmung von Betriebstemperaturen des Tiegels, den Ausschluss ebendieser auf das Detektormaterial und die Quantifizierung eines Umrechnungsfaktors von

der gemessenen zur tatsächlichen Schichtdicke auf der Probe. Die Spezifikationen der einzelnen elektronischen Baugruppen wurden, mit Ausnahme der Stabilität des Diodenlasers, erfolgreich überprüft. Die automatische Nullpunktkompensation des Verstärkers für das pyroelektrische Signal erwies sich wegen Artefakten in den Messwerten als problematisch. Die intensive Charakterisierung des gepulsten Molekularstrahls umfasst die Laufzeiten der Quelle für verschiedene zu verdampfende Materialien unter Berücksichtigung der ebenfalls bestimmten maximalen Füllmengen und den Betriebstemperaturen, sowie der zeitlichen Stabilität des Flusses. Nach Einbau einer Drossel bleibt die Abscheiderate über Stunden nahezu konstant. Weiterhin ermöglicht die Drossel einen konstanten Emissionsgrad für elektromagnetische Strahlung und verhindert, dass makroskopische Partikel den Tiegel verlassen können. Der Pulsformer erzeugt reproduzierbare, zeitlich einstellbare Ereignisse mit der angestrebten Flankensteilheit. Die Spiegelhalterung blockiert den Weg der Infrarotstrahlung des Tiegels und bewirkt, dass laserbasierte Teilexperimente nicht durch sie gestört werden. Die Einstellungen des Massenspektrometers wurden unter Beachtung der technischen Eigenheiten des Gerätes an die experimentellen Anforderungen angepasst. Die Hilfsexperimente für referenzierende Messwerte wurden ebenfalls ausgiebig getestet. Das molekülblockierende Fenster zeigt für die emittierte Strahlung lediglich bei hohen Tiegeltemperaturen eine ähnliche Transmission wie für die Laserstrahlung. Die von der thermischen Strahlung herrührende Signalförmigkeit unterscheidet sich erheblich von der Form, die bei Verwendung von Laserstrahlung erhalten wird, ist aber unabhängig von der Temperatur des Tiegels. Die präsentierte Theorie bezüglich der Strahlungsintensität wird hervorragend bestätigt und könnte eine Berechnung des Strahlungsanteils am Messsignal unter Einsparung einer Referenzmessung ermöglichen. Die Korrekturparameter für die verwendete Spiegelanordnung, welche für die Leistungsmessung des Lasers verwendet wird, und die Quarzmikrowaage, welche die Abscheiderate ermittelt, ergaben sich in Übereinstimmung mit den entsprechenden Theorien. Das Verhalten der heißen Platte, die eine vollständige Reflexion der ankommenden Moleküle bewirkt, bedarf jedoch weiterer Untersuchungen. Wie erwartet, ist das pyroelektrische Messsignal proportional zur Laserleistung und zur beleuchteten Fläche. Auch die thermische Belastbarkeit und temperaturabhängige Sensitivität des Detektors deckten sich mit den Spezifikationen. Ein Ringversuch mit unterschiedlichen Experimentalbedingungen entlang der Messkette zeigte deutlich, dass die Rekonstruktion des Leistungseintrags in den Detektor erfolgreich bewerkstelligt werden kann.

Insgesamt sind durch die erfolgreiche Charakterisierung der einzelnen Messeinrichtungen genaue Ergebnisse in den Kalorimetrie-Experimenten zu erwarten.

Abschließend befasst sich diese Arbeit mit der Adsorption von Metallatomen auf diversen Oberflächen. Die Materialauswahl der untersuchten Grenzflächen berücksichtigte die jeweilige Giftigkeit, die Verfügbarkeit, den Preis und die wissenschaftliche Relevanz und ergab ein weites Sortiment an interessanten Kombinationen. In diesem Zusammenhang wird eine Abschätzung für die Dicke der Reaktionszone, also der Zwischenphase, aus den Kalorimetriedaten für die möglichen Zusammenstellungen motiviert und präsentiert. Weiterhin wird der Ablauf eines typischen Kalorimetrie-Experiments anhand eines Flussdiagramms illustriert und die üblicherweise verwendeten Parameter, beziehungsweise deren empfohlenen Bereiche, werden genannt. Die individuellen Folgerungen aus den Ergebnissen, die aus den verschiedenen Kombinationen aus Substrat und adsorbiertem Metall hervorgingen, würden den Rahmen dieser Zusammenfassung sprengen und sind daher nur in den entsprechenden Abschnitten in englischer Sprache ausgeführt.

Obwohl die Charakterisierung der einzelnen Komponenten auf akkurate Ergebnisse hoffen ließ, wurde in den meisten Experimenten der interne Standard nicht getroffen. Dieser ist dadurch gegeben, dass die Adsorptionseenthalpie bei hohen Bedeckungsgraden des Metalls dessen Resublimationsenthalpie entspricht. Auffallend ist hierbei jedoch, dass diese Experimente gut reproduzierbar waren, und einige Materialkombinationen eine Plateauregion beinhalten, in der der Standard getroffen wird, und die Abweichung erst später – das heißt, bei höheren Bedeckungsgraden – auftritt. Diese reproduzierbaren Regionen konstanter Enthalpie und insbesondere das Experiment zur Adsorption von Calcium auf einer dünnen Schicht aus Sexithiophen bei tiefer Temperatur zeigen, dass es sich nicht um einen systematischen Fehler im experimentellen Aufbau oder der Datenauswertung handelt, sondern um einen nicht berücksichtigten sekundären Effekt. Zusätzlich unterstützt die unerwartete Abhängigkeit des Verhaltens der Adsorptionseenthalpie bei hohen Metallbedeckungen von der Substratschichtdicke diese Hypothese. Eine mechanische Deformation des Sensors und ein daraus resultierendes piezoelektrisches Signal werden als Ursache für diese Effekte vermutet, konnten im Rahmen der Labortätigkeit aber nicht mehr verifiziert werden. Als Ursache für die Deformation werden mechanische Spannungen im sich bildenden Metallfilm vermutet. Um diese Hypothese zu überprüfen oder zu widerlegen, wird ein Umrüsten der Anlage zur Untersuchung von Einkristallproben empfohlen, da diese mechanisch vom Sensor entkoppelt sind. Als Ersatz für die teuren Einkristalle könnten Scheiben aus Aluminiumfolie dienen, auf die die organische Komponente aufgetragen wird. Dies bietet zudem die Möglichkeit, Erfahrungswerte für den Umgang mit den empfindlichen Einkristallen zu sammeln.

Für geringe bis mittlere Metallbedeckungen zeigen die meisten Systeme das erwartete Verhalten. Magnesium und Calcium reagieren zunächst mit den funktionellen Gruppen der Substratmoleküle und bilden bei höheren Bedeckungen eine geschlossene Deckschicht. Zink zeigt eine geringere, jedoch noch messbare Reaktivität, während sich Kupfer in den untersuchten Fällen inert verhält. Die mittels physikalischer Gasphasenabscheidung erzeugten organischen Filme zeigen die erwartete Reaktivität gegenüber den abgeschiedenen Metallatomen. Die Anhydridgruppen des Perylenderivats liefern die größten Reaktionsenthalpien. Die Komplexierung durch die Pyrroleinheiten des Porphyrins setzt etwas weniger Energie frei, und die Reaktion des Schwefels in den Thiophengruppen mit dem Metall ist am wenigsten exotherm.

Zusammenfassend lässt sich feststellen, dass diese Experimente zu einigen besonderen Schlussfolgerungen führten. Von herausragender Bedeutung für diese Arbeit ist die Tatsache, dass sich mit dem vorgestellten Aufbau korrekte Adsorptionenthalpien bei moderaten Bedeckungen messen lassen. Da diese erhaltenen Werte als interner Standard dienen, ist davon auszugehen, dass auch die bestimmten Reaktionswärmen bei kleineren Bedeckungen korrekt sind. Begleitend zu diesen Ergebnissen wurden unerwartete, von der vertikalen Zusammensetzung der Probe abhängige, Effekte entdeckt und mögliche Ursachen, sowie Ansätze um diese unerwünschten Effekte zu vermeiden, diskutiert, konnten jedoch im gegebenen Zeitrahmen nicht weiter untersucht werden. Zusätzlich zu den im Hauptteil diskutierten Experimenten finden sich weitere ausgewertete Datensätze im Anhang.

In naher Zukunft sollten die empfohlenen Experimente durchgeführt und die davon abhängigen Änderungen ausgeführt werden. Anschließend kann der experimentelle Aufbau seiner Bestimmung nach für die routinemäßige Durchführung von Kalorimetrie-Experimenten genutzt werden. Interessante Fragestellungen beinhalten die Adsorption von Alkalimetallen und Erdalkalimetallen auf großen organischen Molekülen, die unter anderem als organische Halbleiter eingesetzt werden. Als Beispiele für solche Materialien seien Oligothiophene, Phthalocyanine, Porphyrine und Fullerene, sowie deren (polymere) Derivate, als auch deren Mischungen genannt.

Die Verwendung von hochreinen Substanzen und deren Handhabung mittels Inertgastechiken ist als mittelfristige Erweiterung des Experiments wünschenswert. Auf der gleichen Zeitskala sollte ein Manipulator realisiert werden, der zur Präparation von Einkristallen optimiert ist. Eine zusätzliche ergiebige Erweiterung könnte aus einem *Vakuumkoffer* bestehen, mit dem sich Proben zwischen verschiedenen Vakuumanlagen überführen lassen, ohne dass die Probe in Kontakt mit Luft kommt.

Langfristig ist der Ausbau des experimentellen Aufbaus mit komplementären Techniken sehr zu empfehlen. Wünschenswerte Optionen wären spektroskopische Techniken und bildgebende Verfahren. Beispiele für erstere sind Photoemissionspektroskopie oder Augerelektronenspektroskopie um Oxidationszustände unterscheiden und um Kontaminationen erkennen zu können, beziehungsweise niederenergetische Ionenstreuung um die Schichtwachstumsarten zuzuordnen zu können. Zu letzteren zählen beispielsweise Rasterkraftmikroskopie oder Rastertunnelmikroskopie, die zur Dokumentation von Oberflächenmorphologien vor und nach den Beschichtungsprozessen verwendet werden können. Unter gewissen Umständen können Spektroskopiemethoden sogar zur Erstellung von Tiefenprofilen genutzt werden, welche typischerweise durch destruktive Verfahren gewonnen werden, und ergänzen daher hervorragend die kalorimetrischen Messungen.

Die Nanojoule-Adsorptions-Kalorimetrie bietet wertvolle Einsichten in die Energetik einer sich durch Adsorption und Reaktion bildenden scharfen oder graduellen Grenzschicht. Die vorliegende Dissertation beschreibt die zu Grunde liegende Theorie und dokumentiert die erfolgreiche Umsetzung der umfangreichen Aufgabenstellung, wie zum Beispiel den experimentellen Aufbau und das Programm zur Datenauswertung, sowie die intensive Charakterisierung aller genannten Komponenten. Eine beispielhafte wissenschaftliche Diskussion für eine Auswahl an vertrauenswürdigen Experimenten rundet diese Veröffentlichung ab und zeigt das erfolgreiche Zusammenspiel aller beteiligten Module im Rahmen dieses wissenschaftlichen Projekts.

Acknowledgment

First and foremost, I would like to express my gratitude to my two supervisors – Prof. Dr. Jörg Michael GOTTFRIED (Erlangen and Marburg) as well as Prof. Dr. Hans-Peter STEINRÜCK (Erlangen) – for providing me the opportunity to conduct this doctorate within their research groups¹. In this context, I would like to emphasize the immense latitude concerning the construction and realization of this work in conjunction with their willingness to contribute to scientific discussions.

Furthermore, I would like to thank my coworkers – Fabian BEBENSEE (Erlangen), Ole LYTKEN (Erlangen), and Han ZHOU (Marburg) – for the intense and successful cooperation in the calorimetry-teams.

Realization of a scientific setup of this magnitude is a tremendous challenge and was only possible with the contribution of the professionals in the affiliated workshops. Thus, I am indebted to Hans-Peter BÄUMLER (*Elektronikwerkstatt Erlangen*), Friedbert BEPPERLING (*Feinmechanische Werkstatt Marburg*), Michael MILLER (*Zentralwerkstatt Erlangen*), Werner KRÖSCHEL (*Elektronikwerkstatt Erlangen*), Friedhold WÖLFEL (*Feinmechanische Werkstatt Erlangen*) and, explicitly, their individual coworkers. Furthermore, I appreciate the active support of the technicians – Marco HILL (Marburg) and Bernd KRESS (Erlangen) – in both research groups.

I would also like to thank all further coworkers in the work groups in Erlangen and Marburg for the sound working atmosphere and collaboration.

Finally, I apologize to my friends and relatives for sometimes putting the work on this project into the center of my attention and thank them for their understanding.

¹ All namings in alphabetical order, respectively.

Danksagung

Zuallererst danke ich meinen beiden Betreuern – Herrn Prof. Dr. Jörg Michael GOTTFRIED (Erlangen und Marburg) und Herrn Prof. Dr. Hans-Peter STEINRÜCK (Erlangen) – für die Möglichkeit, diese Doktorarbeit in ihren Arbeitskreisen durchführen zu können². In diesem Zusammenhang möchte ich die mir zugestandenen großen Freiheiten bei der Planung und Realisierung dieser Arbeit in Verbindung mit beider Bereitschaft für wissenschaftliche Diskussionen hervorheben.

Weiterhin möchte ich mich bei meinen Mitstreitern – Fabian BEBENSEE (Erlangen), Ole LYTKEN (Erlangen) und Han ZHOU (Marburg) – in den beiden Kalorimetrie-Gruppen für die intensive und erfolgreiche Zusammenarbeit und konstruktiven Diskussionen bedanken.

Eine wissenschaftliche Anlage dieser Größe zu realisieren ist eine gewaltige Herausforderung und konnte nur durch die Mithilfe zahlreicher Profis in den angegliederten Werkstätten bewerkstelligt werden. Daher bin ich Hans-Peter BÄUMLER (Elektronikwerkstatt Erlangen), Friedbert BEPPERLING (Feinmechanische Werkstatt Marburg), Michael MILLER (Zentralwerkstatt Erlangen), Werner KRÖSCHEL (Elektronikwerkstatt Erlangen), Friedhold WÖLFEL (Feinmechanische Werkstatt Erlangen) und ausdrücklich auch den jeweiligen Mitarbeitern zu Dank verpflichtet. Weiterhin bin ich den Technikern beider Arbeitsgruppen – Marco HILL (Marburg) und Bernd KRESS (Erlangen) – für ihre tatkräftige Unterstützung dankbar.

Ich danke auch allen weiteren Mitarbeitern in den Arbeitsgruppen in Erlangen und Marburg für die gute Arbeitsatmosphäre und Zusammenarbeit.

Abschließend möchte ich mich noch bei allen Bekannten, Freunden und Verwandten dafür entschuldigen, dass die Arbeit an diesem Projekt doch sehr im Vordergrund stand und bedanke mich daher für Euer Verständnis.

² Alle Nennungen jeweils in alphabetischer Reihenfolge.

Curriculum Vitae

Personal Data

Name Hans-Jörg DRESCHER
Dipl. Chem. Univ.
Date of Birth July 9th 1979
Place of Birth Erlangen
Nationality German
eMail hansjoerg.drescher@gmail.com

Education

August 2014 – June 2016
Writing-up Ph.D. thesis
January 2012 – July 2014
Continuation of Ph.D. work at
Philipps Universität Marburg, Germany
August 2008 – December 2011
Beginning of PhD work in Physical Chemistry at
*Friedrich-Alexander-Universität
Erlangen-Nürnberg (FAU), Germany*
Construction and Realization of a
Nanojoule-Adsorption-Calorimeter
July 2008
University Diploma Chemistry (excellent) at FAU
(Dipl. Chem. \propto M.Sc.)
2003 – 2008
Study of Chemistry at FAU
2000 – 2002
Study of Mathematics at FAU
1999 – 2002
Study of Physics at FAU
June 1999
General qualification for university entrance (*Abitur*)
at *Gymnasium Herzogenaurach, Germany*

List of Figures

2.1	Assembly of the NAC System	18
2.2	Assembly of the Sample Holder for Crystals	20
2.3	Assembly of the Sample Holder for Thin Films	21
2.4	Assembly of the Detector Stage	24
2.5	Assembly of the Thermal Reservoir	25
2.6	Assembly of the Detector for Crystal Samples	26
2.7	Assembly of the Detector for Polymer Samples	27
2.8	Assembled Heater for Crystal Samples	27
2.9	Assembly of the Spring Suspended Detector Mount	28
2.10	Sample/Ribbon Contact Cases	29
2.11	Assembly of the Molecular Beam	31
2.12	Assembly of the Main Evaporator's Base Flange	32
2.13	Assembly of the Main Evaporator	33
2.14	Schematic of the Heating Wire	34
2.15	Assembly of the Lens Holder	36
2.16	Mirror/Orifice Assembly Vacuum Side	36
2.17	Mirror/Orifice Assembly Air Side	37
2.18	Assembled Mirror/Orifice Stage	38
2.19	Assembly of the Chopper	39
2.20	Assembly of the End Switches	40
2.21	Assembly of the Chopper Blade	41
2.22	Positions of the Chopper Blade	42
2.23	Assembled Chopper	43
2.24	Assembly of the Molecular Beam Valve	44
2.25	Assembled Valve	45
2.26	Assembly of the Deflector Plates	47
2.27	Assembled Deflector Plates	47
2.28	Assembly of the Nozzle	48
2.29	Assembly of the Beam Housing	49
2.30	Welded Beam Housing	51

2.31	Assembly of the Molecular Beam (Top View)	52
2.32	Assembly of the Molecular Beam (Front View)	53
2.33	Assembly of the Molecular Beam (Left View)	54
2.34	Assembly of the Ancillaries Flange	55
2.35	Assembly of the Hot Plate	57
2.36	Assembly of the QCM Section	58
2.37	Assembly of the Mirror Section	58
2.38	Assembly of the Infrared Transparent Window Section	59
2.39	Assembly of the Ancillary Instruments	61
2.40	Assembled Ancillaries Stage	62
2.41	Electrical Potential Between Mass Spectrometer and Sample	63
2.42	Assembly of the Mass Spectrometer Mount	64
2.43	Assembly of the Seat for Optical Meters	66
2.44	Assembly of the Pyrometer Mount	67
2.45	Assembly of the Photometer Mount	68
2.46	Fixed Part of the Fiber Positioner	70
2.47	Moveable Part of the Fiber Positioner	71
2.48	Assembly to Lift the Main Chamber	73
2.49	Upper Assembly for Moving the NAC Machine	74
2.50	Lower Assembly for Moving the NAC Machine	74
2.51	Assembly of the Water Distribution Mount	75
2.52	Assembly to Hold Minicans	75
2.53	Assembly of the Load Lock	77
2.54	Assembly of the Load Lock Housing	78
2.55	Assembly to Support Transfer Rods	79
2.56	Assembly to Support the Load Lock	80
2.57	Assembly of the Load Lock Evaporator	81
2.58	Assembly of the Sample Storage System	82
2.59	Assembly of the Load Lock Sample Transfer System	83
2.60	Assembly of the Main Chamber Sample Transfer	83
2.61	Sample Handover	84
2.62	Sample Retaining Mechanisms	84
2.63	Assembly of the Glove Box Connection	86
2.64	Assembly of the NAC system (Front View)	88
2.65	Assembly of the NAC system (Top View)	89
2.66	The Nanojoule Adsorption Calorimeter	90

3.1	Main Panel of the NAC Data Evaluation Program	102
3.2	Filtered Radiation Reference Measurement	107
3.3	Average Frames of a Filtered Radiation Reference Measurement . .	108
3.4	Time Constant of the Measurement Setup	109
3.5	Effect of the Additional Notch Filter	110
3.6	Effect of the Filtering on the Data	111
3.7	Filtering and Beat in Signal	112
3.8	Constitution of Fit Waves	121
3.9	Constitution of Fit Waves for Deconvolution	122
3.10	Pulse Length Determination	123
3.11	Comparison of Laser Based and Radiation Signal	125
3.12	Statistical Comparison of the References	130
3.13	Statistical Comparison of the References	131
3.14	Fit Contributions Heat Measurement	133
3.15	Effect of Fitted Trends: Noise	140
3.16	Effect of Fitted Trends: Balancing	141
3.17	Influence of Noise in the Deconvolution Reference	145
3.18	Comparison of the Novel and Previous Data Evaluation Approach: Sticking	150
3.19	Comparison of the Novel and Previous Data Evaluation Approach: Calculated Heat	151
3.20	Comparison of the Novel and Previous Data Evaluation Approach: Radiation Contribution	152
5.1	Geometry for the External Reflectivity Measurement	225
5.2	Reflectivity Measurement	226
5.3	Sputtering of a QCM Crystal	229
5.4	Photoemission Spectra of Aluminum Foils	230
5.5	Magnesium Deposition on QCM Crystals	231
5.6	Detector Polymer Degradation upon Coating	242
5.7	Schematic of the Load Lock Evaporator	243
5.8	Stability of the Laser Diode	246
5.9	Voltage Response from the Detector	248
5.10	Deposition Rate and Temperature Stability	250
5.11	Photographs of “Spitted” Evaporant	251
5.12	A photograph of the Steel Wool Plug	251
5.13	Performance of the Inline Valve	253

5.14	Performance of the Chopper: Photo Diode	254
5.15	Performance of the Chopper: Deconvoluted, Diffuse Radiation . . .	255
5.16	Performance of the Chopper: Deconvoluted, Direct Radiation . . .	256
5.17	Crucible Radiation in Laser Measurement	259
5.18	Influence of the Mass Spectrometer's Range Setting	262
5.19	Influence of the Pulse Length on the Mass Spectrometer Signal: Direct Dosing	264
5.20	Influence of the Pulse Length on the Mass Spectrometer Signal: Indirect Dosing	265
5.21	Integrated Mass Spectrometer Signal <i>vs.</i> Pulse Length	266
5.22	Mass Spectrometer Linearity Regarding Deposition Rate	267
5.23	Temperature Dependence of Radiation	269
5.24	Transmission of the Barium Fluoride Window	270
5.25	Wavelength Dependent Parameters	271
5.26	Temperature Dependent Relative Infrared Emission	274
5.27	Infrared Radiation Compared for two Temperatures	275
5.28	Ratio of Deposition Rate in Sample and Ancillary Position	276
5.29	Schematic of the Laser Path	277
5.30	Laser Power Correction Factor	278
5.31	Sticking Reference Correction Factor	282
5.32	Relative Mass Spectrometer Intensity <i>vs.</i> Hot Plate Temperature .	284
5.33	Temperature Dependency of Transient Adsorption	286
5.34	Mass Spectrometer Peak Shape at Different Range Settings	288
5.35	Example of Transient Adsorption: Lead on Molybdenum	289
5.36	Calculated Transient Lifetimes	290
5.37	Peak Shape of the Mass Spectrometer Signal	291
5.38	Detector Linearity Towards Input Power	294
5.39	Illustration for Sample Occlusion	295
5.40	Detector Linearity Towards Active Area	297
5.41	Annealing Effect on the Detector	298
5.42	Thermal Treatment of Detector Polymer	299
5.43	Temperature Dependency of the Detector Sensitivity	300
5.44	Influences of the Detector Structure	302
5.45	Thawing of the Thermal Reservoir	305
5.46	Round Robin Power Input Test	307
5.47	Relative Laser Reference Amplitudes	308
5.48	Histogram of Relative Laser Reference Amplitudes	309

5.49	Scatter of the Laser Reference Amplitudes by Laser Power	310
5.50	Scatter of the Laser Reference Amplitudes by Time	311
6.1	Crystal Structure of the Magnesium Type	319
6.2	Crystal Structure of the Copper Type	320
6.3	Chemical Structure of 3,4,9,10-Perylene-Tetracarboxylic Dianhydride	322
6.4	Chemical Structure of 2,5'-poly(3-Hexylthiophene)	323
6.5	Chemical Structure of α -Sexithiophene	324
6.6	Chemical Structure of 5,10,15,20-Tetraphenyl-21 <i>H</i> ,23 <i>H</i> -Porphin . .	325
6.7	Work Flow of a Calorimetric Experiment	330
6.8	Adsorption of Magnesium: Sticking Probability	334
6.9	Adsorption of Magnesium: Heats of Adsorption	335
6.10	Adsorption of Magnesium: Heats of Adsorption at Low Coverages .	336
6.11	Adsorption of Calcium: Sticking Probabilities (Clean Detector, Tetraphenyl Porphyrin)	340
6.12	Adsorption of Calcium: Sticking Probabilities (PTCDA)	341
6.13	Low Temperature Adsorption of Calcium: Sticking Probabilities (PTCDA)	342
6.14	Adsorption of Calcium: Sticking Probabilities (Sexithiophene) . . .	343
6.15	Low Temperature Adsorption of Calcium: Sticking Probabilities (Sexithiophene)	344
6.16	Adsorption of Calcium: Heats of Adsorption (Clean Detector, Tetraphenyl Porphyrin)	345
6.17	Adsorption of Calcium: Low Coverage Heats of Adsorption (Clean Detector Tetraphenyl Porphyrin)	346
6.18	Adsorption of Calcium: Heats of Adsorption (PTCDA)	347
6.19	Adsorption of Calcium: Low Coverage Heats of Adsorption (PTCDA)	348
6.20	Low Temperature Adsorption of Calcium: Heats of Adsorption (PTCDA)	349
6.21	Low Temperature Adsorption of Calcium: Low Coverage Heats of Adsorption (PTCDA)	350
6.22	Adsorption of Calcium: Heats of Adsorption (Sexithiophene)	351
6.23	Adsorption of Calcium: Low Coverage Heats of Adsorption (Sexithiophene)	352

6.24	Low Temperature Adsorption of Calcium: Heats of Adsorption (Sexithiophene)	353
6.25	Low Temperature Adsorption of Calcium: Low Coverage Heats of Adsorption (Sexithiophene)	354
6.26	Adsorption of Copper: Heats of Adsorption	364
6.27	Copper Glazed Filament	366
6.28	Adsorption of Zinc: Sticking Probabilities	368
6.29	Adsorption of Zinc: Heats of Adsorption	369
6.30	Adsorption of Zinc: Low Coverage Heats of Adsorption	370
6.31	Adsorption of Calcium on Sexithiophene: Full Detector Data	373
6.32	Adsorption of Calcium on Sexithiophene: Fitted Detector Data . .	374
6.33	Adsorption of Calcium on Sexithiophene: Radiation Contribution .	375
6.34	Adsorption of Calcium on Sexithiophene: Stability Checks	375
6.35	Adsorption of Zinc on Sputtered Detector: Coverage Dependent Signal Shape	379
6.36	Adsorption of Zinc on Sputtered Detector: Reconstructed Power Input for Laser and Radiation Reference	380
6.37	Adsorption of Zinc on Sputtered Detector: Reconstructed Power Input for Calorimetric Measurement	381
6.38	Adsorption of Zinc on Sputtered Detector: Reconstructed Power at High Coverages for Various Measurements	382
B.1.1	Design Drawing: Main Evaporator	456
B.1.2	Design Drawing: Internal Valve	465
B.1.3	Design Drawing: Optics Stage	473
B.1.4	Design Drawing: Beam Chopper	483
B.1.5	Design Drawing: Nozzle in Main Chamber	490
B.1.6	Design Drawing: Beam Housing	495
B.2.1	Design Drawing: Sample Holder	512
B.2.2	Design Drawing: Sample Carrier	520
B.2.3	Design Drawing: Detector	525
B.2.4	Design Drawing: Sample Heater	550
B.2.5	Design Drawing: Mass Spectrometer Mount	561
B.2.6	Design Drawing: Ancillaries Stage	568
B.2.7	Design Drawing: Main Chamber Additions	589
B.2.8	Design Drawing: Optical Meters	606

B.2.9	Design Drawing: Fiber Positioner	623
B.3.1	Design Drawing: Mount for Load Lock	639
B.3.2	Design Drawing: Load Lock Housing	647
B.3.3	Design Drawing: Sample Storage	654
B.3.4	Design Drawing: Transfer Rod Support	662
B.4.1	Design Drawing: Glove Box	669
B.4.2	Design Drawing: Evaporator for Synchrotron Applications	673
B.4.3	Design Drawing: Mounting Stand	682
B.4.4	Design Drawing: Threefold Evaporator	690
B.4.5	Design Drawing: Battery Box	701
D.1	Auxiliary Data for Magnesium on Pristine Detector	856
D.2	Averaged Data for Magnesium on Pristine Detector	856
D.3	Sticking Data for Magnesium on Pristine Detector	857
D.4	Enthalpy Data for Magnesium on Pristine Detector	857
D.5	Auxiliary Data for Magnesium on Sputter Cleaned Detector	858
D.6	Averaged Data for Magnesium on Sputter Cleaned Detector	858
D.7	Sticking Data for Magnesium on Sputter Cleaned Detector	859
D.8	Enthalpy Data for Magnesium on Sputter Cleaned Detector	859
D.9	Auxiliary Data for Magnesium on PTCDA	860
D.10	Averaged Data for Magnesium on PTCDA	860
D.11	Sticking Data for Magnesium on PTCDA	861
D.12	Enthalpy Data for Magnesium on PTCDA	861
D.13	Auxiliary Data for Calcium on Sputter Cleaned Detector	862
D.14	Averaged Data for Calcium on Sputter Cleaned Detector	862
D.15	Sticking Data for Calcium on Sputter Cleaned Detector	863
D.16	Enthalpy Data for Calcium on Sputter Cleaned Detector	863
D.17	Auxiliary Data for Calcium on Tetraphenyl Porphyrin	864
D.18	Averaged Data for Calcium on Tetraphenyl Porphyrin	864
D.19	Sticking Data for Calcium on Tetraphenyl Porphyrin	865
D.20	Enthalpy Data for Calcium on Tetraphenyl Porphyrin	865
D.21	Auxiliary Data for Calcium on PTCDA	866
D.22	Averaged Data for Calcium on PTCDA	866
D.23	Sticking Data for Calcium on PTCDA	867
D.24	Enthalpy Data for Calcium on PTCDA	867

D.25	Enthalpy Data for Calcium on PTCDA: Small Layer Thickness . . .	868
D.26	Enthalpy Data for Calcium on PTCDA: Large Layer Thickness . . .	868
D.27	Low Temperature Auxiliary Data for Calcium on PTCDA	869
D.28	Low Temperature Averaged Data for Calcium on PTCDA	869
D.29	Low Temperature Sticking Data for Calcium on PTCDA	870
D.30	Low Temperature Enthalpy Data for Calcium on PTCDA	870
D.31	Auxiliary Data for Calcium on Sexithiophene	871
D.32	Averaged Data for Calcium on Sexithiophene	871
D.33	Sticking Data for Calcium on Sexithiophene	872
D.34	Enthalpy Data for Calcium on Sexithiophene	872
D.35	Enthalpy Data for Calcium on Sexithiophene: Small Layer Thickness	873
D.36	Enthalpy Data for Calcium on Sexithiophene: Medium Layer Thickness	873
D.37	Enthalpy Data for Calcium on Sexithiophene: Large Layer Thickness	874
D.38	Low Temperature Auxiliary Data for Calcium on Sexithiophene . . .	875
D.39	Low Temperature Averaged Data for Calcium on Sexithiophene . . .	875
D.40	Low Temperature Sticking Data for Calcium on Sexithiophene . . .	876
D.41	Low Temperature Enthalpy Data for Calcium on Sexithiophene . . .	876
D.42	Auxiliary Data for Zinc on Sputter Cleaned Detector	877
D.43	Averaged Data for Zinc on Sputter Cleaned Detector	877
D.44	Sticking Data for Zinc on Sputter Cleaned Detector	878
D.45	Enthalpy Data for Zinc on Sputter Cleaned Detector	878
D.46	Auxiliary Data for Zinc on PTCDA	879
D.47	Averaged Data for Zinc on PTCDA	879
D.48	Sticking Data for Zinc on PTCDA	880
D.49	Enthalpy Data for Zinc on PTCDA	880
D.50	Low Temperature Auxiliary Data for Zinc on PTCDA	881
D.51	Low Temperature Averaged Data for Zinc on PTCDA	881
D.52	Low Temperature Sticking Data for Zinc on PTCDA	882
D.53	Low Temperature Enthalpy Data for Zinc on PTCDA	882
E.1	Laser Reference Previous Evaluation Approach	884
E.2	Radiation Reference Previous Evaluation Approach	885

E.3	Desorption Reference Previous Evaluation Approach	886
E.4	Heat Measurement Previous Evaluation Approach	887
E.5	Energy Calculation Previous Evaluation Approach	888
E.6	Filtered Laser Reference Measurement	890
E.7	Filter Residue Laser Reference Measurement	891
E.8	Averaged Filtered Laser Reference	892
E.9	Detail Filtered Radiation Reference Measurement	893
E.10	Average Frames of Filtered Laser Reference Measurement	894
E.11	Filtered Radiation Reference Measurement	895
E.12	Filter Residue Radiation Reference Measurement	896
E.13	Averaged Filtered Radiation Reference Measurement	897
E.14	Detail Filtered Radiation Reference Measurement	898
E.15	Average Frames of Filtered Radiation Reference Measurement	899
E.16	Filtered Heat Measurement	900
E.17	Filter Residue Heat Measurement	901
E.18	Averaged Filtered Heat Measurement	902
E.19	Detail Filtered Heat Measurement	903
E.20	Average Frames of Filtered Heat Measurement	904

List of Tables

2.1	Positions for Ancillary Measurements	60
5.1	Thick Layer Deposition Parameters	235
5.2	Thick Layer Deposition Results	236
5.3	Load Lock Evaporator Parameters	238
5.4	Sample/Detector Structure	240
5.5	Relative Response of a Coated Detector	240
5.6	Tooling Factor of the Evaporator Quartz Crystal Microbalance in the Load Lock	244
5.7	Main Evaporator Fill Amounts	252
5.8	Contribution of Ions to the Molecular Beam	258
5.9	Operation Parameters of the Hot Plate	284
5.10	Properties of Pyroelectric Materials	303
6.1	Properties of Selected Solid Elements	318
6.2	<i>Ersatz</i> Thicknesses and Area Densities	328
6.3	Reaction Equivalents	328
6.4	Data Acquisition Parameters	331
A.1	Operation Parameters: Magnesium	451
A.2	Operation Parameters: Calcium	451
A.3	Operation Parameters: Copper	452
A.4	Operation Parameters: Zinc	452
A.5	Operation Parameters: Perylenetetracarboxylic Dianhydride	453
A.6	Operation Parameters: Phthalocyanine	453
A.7	Operation Parameters: Sexithiophene	454
A.8	Operation Parameters: 5,10,15,20-Tetraphenyl Porphyrin	454

Bibliography

- [1] Rothenberg, G. *Catalysis*. Wiley-VCH Verlag GmbH & Co. KGaA, 1st Edition, **2008**.
- [2] Černý, S.; Ponec, V.; and Hládek, L. Calorimetric Heats of Adsorption of Hydrogen on Molybdenum Films. *Journal of Catalysis*, **1966**, *5*(1), 27. doi:10.1016/S0021-9517(66)80122-7.
- [3] Smutek, M. and Černý, S. Calorimetric Studies of Hydrocarbon Adsorption on Metal Films: III. Methane, Ethane, and Propane on Molybdenum. *Journal of Catalysis*, **1977**, *47*(2), 179. doi:10.1016/0021-9517(77)90165-8.
- [4] Černý, S.; Smutek, M.; Buzek, F.; and Curřínová, A. Calorimetric Studies of Hydrocarbon Adsorption on Metal Films: I. Cyclopropane on Platinum and Molybdenum. *Journal of Catalysis*, **1977**, *47*(2), 159. doi:10.1016/0021-9517(77)90163-4.
- [5] Černý, S.; Smutek, M.; and Buzek, F. Calorimetric Studies of Hydrocarbon Adsorption on Metal Films: II. Ethylene, Acetylene, Propylene, Methylacetylene and Allene on Molybdenum. *Journal of Catalysis*, **1977**, *47*(2), 166. doi:10.1016/0021-9517(77)90164-6.
- [6] Pálfi, S.; Lisowski, W.; Smutek, M.; and Černý, S. Calorimetric Studies of Hydrocarbon Adsorption on Metal Films: V. Hydrocarbons on Platinum. *Journal of Catalysis*, **1984**, *88*(2), 300. doi:10.1016/0021-9517(84)90006-X.
- [7] Černý, S. and Pientka, Z. Heat of Interaction of Carbon Monoxide with Dysprosium. *Surface Science*, **1987**, *191*(3), 449. doi:10.1016/S0039-6028(87)81189-5.
- [8] Bastel, Z. and Černý, S. Calorimetric and XPS Study of the Effect of Copper on the Sorption Properties of Dysprosium. *Applied Surface Science*, **1993**, *68*(2), 275. doi:10.1016/0169-4332(93)90132-U.
- [9] Černý, S. Adsorption Microcalorimetry in Surface Science Studies – Sixty Years of Its Development into a Modern Powerful Method. *Surface Science Reports*, **1996**, *26*(1-2), 1. doi:10.1016/S0167-5729(96)00008-8.
- [10] Černý, S. Adsorption Calorimetry on Filaments, Vacuum-Evaporated Films, and Single Crystals of Metals. *Thermochimica Acta*, **1998**, *312*(1-2), 3. doi:10.1016/S0040-6031(97)00435-8.
- [11] Brown, W. A.; Kose, R.; and King, D. A. Femtomole Adsorption Calorimetry on Single-Crystal Surfaces. *Chemical Reviews*, **1998**, *98*(2), 797. doi:10.1021/cr9700890.
- [12] Stuckless, J. T.; Al-Sarraf, N.; Wartnaby, C.; and King, D. A. Calorimetric Heats of Adsorption for CO on Nickel Single Crystal Surfaces. *The Journal of Chemical Physics*, **1993**, *99*(3), 2202. doi:10.1063/1.465282.

- [13] Dixon-Warren, S. J.; Kovář, M.; Wartnaby, C. E.; and King, D. A. Pyroelectric Single Crystal Adsorption Microcalorimetry at Low Temperatures: Oxygen on Ni{100}. *Surface Science*, **1994**, *307-309*, 16. doi:10.1016/0039-6028(94)90363-8.
- [14] Stuckless, J. T.; Starr, D. E.; Bald, D. J.; and Campbell, C. T. Metal Adsorption Calorimetry and Adhesion Energies on Clean Single-Crystal Surfaces. *Journal of Chemical Physics*, **1997**, *107*(14), 5547. doi:10.1063/1.474230.
- [15] Stuckless, J. T.; Starr, D. E.; Bald, D. J.; and Campbell, C. T. Calorimetric Measurements of the Energetics of Pb Adsorption and Adhesion to Mo(100). *Physical Review B*, **1997**, *56*(20), 13496. doi:10.1103/PhysRevB.56.13496.
- [16] Ranney, J. T.; Starr, D. E.; Musgrove, J. E.; Bald, D. J.; and Campbell, C. T. A Microcalorimetric Study of the Heat of Adsorption of Copper on Well-Defined Oxide Thin Film Surfaces : MgO(100), p(2 × 1) Oxide on Mo(100) and Disordered W Oxide. *Faraday Discussions*, **1999**, *144*, 195. doi:10.1039/A902649E.
- [17] Larsen, J. H.; Starr, D. E.; and Campbell, C. T. Enthalpies of Adsorption of Metal Atoms on Single-Crystalline Surfaces by Microcalorimetry. *The Journal of Chemical Thermodynamics*, **2001**, *33*(3), 333. doi:10.1006/jcht.2000.0747.
- [18] Starr, D. E.; Ranney, J. T.; Larsen, J. H.; Musgrove, J. E.; and Campbell, C. T. Measurement of the Energetics of Metal Film Growth on a Semiconductor: Ag/Si(100)-(2 × 1). *Physical Review Letters*, **2001**, *87*(10), 106102. doi:10.1103/PhysRevLett.87.106102.
- [19] Starr, D. E. and Campbell, C. T. Low-Temperature Adsorption Microcalorimetry: Pb on MgO(100). *The Journal Of Physical Chemistry B*, **2001**, *105*(18), 3776. doi:10.1021/jp003411a.
- [20] Starr, D. E.; Bald, D. J.; Musgrove, J. E.; Ranney, J. T.; and Campbell, C. T. Microcalorimetric Measurements of the Heat of Adsorption of Pb on Well-Defined Oxides: MgO(100) and p(2 × 1)-Oxide on Mo(100). *Journal of Chemical Physics*, **2001**, *114*(8), 3752. doi:10.1063/1.1337097.
- [21] Campbell, C. T. and Starr, D. E. Metal Adsorption and Adhesion Energies on MgO(100). *Journal of the American Chemical Society*, **2002**, *124*(31), 9212. doi:10.1021/ja020146t.
- [22] Starr, D. E.; Diaz, S. F.; Musgrove, J. E.; Ranney, J. T.; Bald, D. J.; Nelen, L.; Ihm, H.; and Campbell, C. T. Heat of Adsorption of Cu and Pb on Hydroxyl-Covered MgO(100). *Surface Science*, **2002**, *515*(1), 13. doi:10.1016/S0039-6028(02)01915-5.
- [23] Ihm, H.; Ajo, H. M.; Gottfried, J. M.; Bera, P.; and Campbell, C. T. Calorimetric Measurement of the Heat of Adsorption of Benzene on Pt(111). *The Journal Of Physical Chemistry B*, **2004**, *108*(38), 14627. doi:10.1021/jp040159o.
- [24] Zhu, J.; Diaz, S.; Heeb, L.; and Campbell, C. T. Adsorption Of Pb on NiAl(110): Energetics and Structure. *Surface Science*, **2005**, *574*(1), 34. doi:10.1016/j.susc.2004.10.014.

- [25] Tait, S. L.; Dohnálek, Z.; Campbell, C. T.; and Kay, B. D. n-Alkanes on Pt(111) and on C(0001)/Pt(111): Chain Length Dependence of Kinetic Desorption Parameters. *The Journal of Chemical Physics*, **2006**, *125*, 234308. doi:10.1063/1.2400235.
- [26] Gottfried, M.; Vestergaard, E. K.; Bera, P.; and Campbell, C. T. Heat of Adsorption of Naphthalene on Pt(111) Measured by Adsorption Calorimetry. *The Journal Of Physical Chemistry B*, **2006**, *110*, 17539. doi:10.1021/jp062659i.
- [27] Zhu, J.; Farmer, J. A.; Ruzycki, N.; Xu, L.; Campbell, C. T.; and Henkelman, G. Calcium Adsorption on MgO(100): Energetics, Structure, and Role of Defects. *Journal of the American Chemical Society*, **2008**, *130*, 2314. doi:10.1021/ja077865y.
- [28] Fiorin, V.; Borthwick, D.; and King, D. A. Microcalorimetry of O₂ and NO on Flat and Stepped Platinum Surfaces. *Surface Science*, **2009**, *603*(10-10), 1360. doi:10.1016/j.susc.2008.08.034.
- [29] Farmer, J. A.; Campbell, C. T.; Xu, L.; and Henkelman, G. Defect Sites and Their Distributions on MgO(100) by Li and Ca Adsorption Calorimetry. *Journal of the American Chemical Society*, **2009**, *131*(8), 3098. doi:10.1021/ja808986b.
- [30] Farmer, J. A.; Ruzycki, N.; Zhu, J.; and Campbell, C. T. Lithium Adsorption on MgO(100) and Its Defects: Charge Transfer, Structure, and Energetics. *Physical Review B*, **2009**, *80*(3), 035418. doi:10.1103/PhysRevB.80.035418.
- [31] Lytken, O.; Lew, W.; and Campbell, C. T. Catalytic Reaction Energetics by Single Crystal Adsorption Calorimetry: Hydrocarbons on Pt(111). *Chemical Society Reviews*, **2008**, *37*(10), 2172. doi:10.1039/B719543P.
- [32] Lytken, O.; Lew, W.; Harris, J. J. W.; Vestergaard, E. K.; Gottfried, J. M.; and Campbell, C. T. Energetics of Cyclohexene Adsorption and Reaction on Pt(111) by Low-Temperature Microcalorimetry. *Journal of the American Chemical Society*, **2008**, *130*(31), 10247. doi:10.1021/ja801856s.
- [33] Farmer, J. A.; Baricuatro, J. H.; and Campbell, C. T. Ag Adsorption on Reduced CeO₂(111) Thin Films. *The Journal Of Physical Chemistry C*, **2010**, *114*(40), 17166. doi:10.1021/jp104593y.
- [34] Farmer, J. A. and Campbell, C. T. Ceria Maintains Smaller Metal Catalyst Particles by Strong Metal-Support Bonding. *Science*, **2010**, *329*(5994), 933. doi:10.1126/science.1191778.
- [35] Schießer, A.; Hörtz, P.; and Schäfer, R. Thermodynamics and Kinetics of CO and Benzene Adsorption on Pt(111) Studied with Pulsed Molecular Beams and Microcalorimetry. *Surface Science*, **2010**, *604*, 2098. doi:10.1016/j.susc.2010.09.001.
- [36] Lew, W.; Crowe, M. C.; Campbell, C. T.; Carrasco, J.; and Michaelides, A. The Energy of Hydroxyl Coadsorbed with Water on Pt(111). *The Journal Of Physical Chemistry C*, **2011**, *115*(46), 23008. doi:10.1021/jp207350r.
- [37] Lew, W.; Crowe, M. C.; Karp, E.; Lytken, O.; Farmer, J. A.; Árnadóttir, L.; Schoenbaum, C.; and Campbell, C. T. The Energy of Adsorbed Hydroxyl on Pt(111) by Microcalorimetry. *The Journal Of Physical Chemistry C*, **2011**, *115*(23), 11586. doi:10.1021/jp201632t.

- [38] Karp, E. M.; Silbaugh, T. L.; Crowe, M. C.; and Campbell, C. T. The Energetics of Adsorbed Methanol and Methoxy on Pt(111) by Microcalorimetry. *Journal of the American Chemical Society*, **2012**, *134*(50), 20388. doi:10.1021/ja307465u.
- [39] Karp, E. and Campbell, C. T. Energetics of Oxygen Adatoms, Hydroxyl Species, and Water Dissociation on Pt(111). *The Journal Of Physical Chemistry C*, **2012**, *116*(49), 25772. doi:10.1021/jp3066794.
- [40] Liao, K.; Fiorin, V.; Jenkins, S. J.; and King, D. A. Microcalorimetry of Oxygen Adsorption on fcc Co(110). *Physical Chemistry Chemical Physics*, **2012**, *14*(20), 7528. doi:10.1039/C2CP40549K.
- [41] Karp, E.; Silbaugh, T. L.; and Campbell, C. T. Energetics of Adsorbed CH₃ and CH on Pt(111) by Calorimetry: Dissociative Adsorption of CH₃I. *The Journal Of Physical Chemistry C*, **2013**, *117*(12), 6325. doi:10.1021/jp400902f.
- [42] Sharp, J. C.; Yao, Y. X.; and Campbell, C. T. Silver Nanoparticles on Fe₃O₄(111): Energetics by Ag Adsorption Calorimetry and Structure by Surface Spectroscopies. *The Journal Of Physical Chemistry C*, **2013**, *117*(47), 24932. doi:10.1021/jp408956x.
- [43] Silbaugh, T. L.; Karp, E. M.; and Campbell, C. T. Surface Kinetics and Energetics from Single Crystal Adsorption Calorimetry Lineshape Analysis: Methyl from Methyl Iodide on Pt(111). *Journal of Catalysis*, **2013**, *308*, 114. doi:10.1016/j.jcat.2013.05.030.
- [44] Liao, K.; Fiorin, V.; Gunn, D. S. D.; Jenkins, S. J.; and King, D. A. Single-Crystal Adsorption Calorimetry and Density Functional Theory of CO Chemisorption on fcc Co{110}. *Physical Chemistry Chemical Physics*, **2013**, *15*(11), 4059. doi:10.1039/C3CP43836H.
- [45] Silbaugh, T. L.; Karp, E. M.; and Campbell, C. T. Energetics of Formic Acid Conversion to Adsorbed Formates on Pt(111) by Transient Calorimetry. *Journal of the American Chemical Society*, **2014**, *136*(10), 3964. doi:10.1021/ja412878u.
- [46] Karp, E. M.; Silbaugh, T. L.; and Campbell, C. T. Bond Energies of Molecular Fragments to Metal Surfaces Track Their Bond Energies to H Atom. *Journal of the American Chemical Society*, **2014**, *136*(11), 4137. doi:10.1021/ja500997n.
- [47] Silbaugh, T. L.; Giorgi, J. B.; Xu, Y.; Tillekaratne, A.; Zaera, F.; and Campbell, C. T. Adsorption Energy of *tert*-Butyl on Pt(111) by Dissociation of *tert*-Butyl Iodide: Calorimetry and DFT. *The Journal Of Physical Chemistry C*, **2014**, *118*(1), 427. doi:10.1021/jp4097716.
- [48] Hörtz, P.; Ruff, P.; and Schäfer, R. A Temperature Dependent Investigation of the Adsorption of CO on Pt(111) using Low-Temperature Single Crystal Adsorption Calorimetry. *Surface Science*, **2015**, *639*, 66. doi:10.1016/j.susc.2015.04.018.
- [49] Grant, A. W.; Ngo, L. T.; Stegelman, K.; and Campbell, C. T. Cyclohexane Dehydrogenation and H₂ Adsorption on Pt Particles on ZnO(0001)-O. *The Journal Of Physical Chemistry B*, **2003**, *107*(5), 1180. doi:10.1021/jp021907h.

-
- [50] Ngo, L. T.; Xu, L.; Grant, A. W.; and Campbell, C. T. Benzene Adsorption and Dehydrogenation on Pt/ZnO(0001)-O Model Catalysts. *The Journal Of Physical Chemistry B*, **2003**, *107*(5), 1174. doi:10.1021/jp021903c.
- [51] Flores-Camacho, J. M.; Fischer-Wolfarth, J.-H.; Peter, M.; Campbell, C. T.; Schauer-
mann, S.; and Freund, H.-J. Adsorption Energetics of CO on Supported Pd Nanopar-
ticles as a Function of Particle Size by Single Crystal Microcalorimetry. *Physical
Chemistry Chemical Physics*, **2011**, *37*, 16800. doi:10.1039/C1CP21677E.
- [52] Peter, M.; Camacho, J. M. F.; Adamovski, S.; Ono, L. K.; Dostert, K.-H.; O'Brien,
C. P.; Cuenya, B. R.; Schauer-
mann, S.; and Freund, H.-J. Trends in the Binding
Strength of Surface Species on Nanoparticles: How Does the Adsorption Energy
Scale with the Particle Size? *Angewandte Chemie, International Edition*, **2013**,
52(19), 5175. doi:10.1002/anie.201209476.
- [53] Murdey, R. and Stuckless, J. T. Calorimetry of Polymer Metallization: Copper,
Calcium, and Chromium on PMDA-ODA Polyimide. *Journal of the American
Chemical Society*, **2003**, *125*(13), 3995. doi:10.1021/ja028829w.
- [54] Hon, S. S.; Richter, J.; and Stuckless, J. T. A Calorimetric Study of the Heat of
Reaction of Calcium Atoms with the Vinylene Group of MEH-PPVh. *Chemical
Physics Letters*, **2004**, *385*(1-2), 92. doi:10.1016/j.cplett.2003.12.055.
- [55] Diaz, S.; Zhu, J.; Harris, J.; Goetsch, P.; Merte, L.; and Campbell, C. T. Heats of Ad-
sorption of Pb on Pristine and Electron-Irradiated Poly(Methyl Methacrylate) by Mi-
crocalorimetry. *Surface Science*, **2005**, *598*(1-3), 22. doi:10.1016/j.susc.2005.09.015.
- [56] Zhu, J.; Goetsch, P.; Ruzycki, N.; and Campbell, C. T. Adsorption Energy, Growth
Mode, and Sticking Probability of Ca on Poly(Methyl Methacrylate) Surfaces with
and without Electron Damage. *Journal of the American Chemical Society*, **2007**,
129, 6432. doi:10.1021/ja067437c.
- [57] Zhu, J.; Bebensee, F.; Hieringer, W.; Zhao, W.; Baricuatro, J. H.; Farmer, J. A.;
Bai, Y.; Steinrück, H.-P.; Gottfried, J. M.; and Campbell, C. T. Formation of the
Calcium/Poly(3-Hexylthiophene) Interface: Structure and Energetics. *Journal of
the American Chemical Society*, **2009**, *131*(37), 13498. doi:10.1021/ja904844c.
- [58] Bebensee, F.; Zhu, J.; Baricuatro, J. H.; Farmer, J. A.; Bai, Y.; Steinrück, H.-
P.; Campbell, C. T.; and Gottfried, J. M. Interface Formation between Calcium
and Electron-Irradiated Poly(3-Hexylthiophene). *Langmuir*, **2010**, *26*(12), 9632.
doi:10.1021/la100209v.
- [59] Sharp, J. C.; Bebensee, F.; Baricuatro, J. H.; Steinrück, H.-P.; Gottfried, J. M.;
and Campbell, C. T. Calcium Thin Film Growth on a Cyano-Substituted Poly(p-
Phenylene Vinylene): Interface Structure and Energetics. *The Journal Of Physical
Chemistry C*, **2013**, *117*(45), 23781. doi:10.1021/jp407825f.
- [60] Ju, H.; Ye, Y.; Feng, X.; Pan, H.; Zhu, J.; Ruzycki, N.; and Campbell, C. T.
Low-Temperature Growth Improves Metal/Polymer Interfaces: Vapor-Deposited
Ca on PMMA. *The Journal Of Physical Chemistry C*, **2014**, *118*(12), 6352.
doi:10.1021/jp500628w.

- [61] Sharp, J. C.; Feng, X. F.; Farmer, J. A.; Guo, Y. X.; Bebensee, F.; Baricuatro, J. H.; Zillner, E.; Zhu, J. F.; Steinrück, H.-P.; Gottfried, J. M.; and Campbell, C. T. Calcium Thin Film Growth on Polyfluorenes: Interface Structure and Energetics. *The Journal Of Physical Chemistry C*, **2014**, *118*(6), 2953. doi:10.1021/jp4105954.
- [62] Forrest, S. R. Ultrathin Organic Films Grown by Organic Molecular Beam Deposition and Related Techniques. *Chemical Reviews*, **1997**, *97*(6), 1793. doi:10.1021/cr941014o.
- [63] Witte, G. and Wöll, C. Growth of Aromatic Molecules on Solid Substrates for Applications in Organic Electronics. *Journal of Materials Research*, **2004**, *19*(7), 1889. doi:10.1557/JMR.2004.0251.
- [64] Kowarik, S.; Gerlach, A.; and Schreiber, F. Organic Molecular Beam Deposition: Fundamentals, Growth Dynamics, and *in situ* Studies. *Journal of Physics Condensed Matter*, **2008**, *20*(18), 184008. doi:10.1088/0953-8984/20/18/184005.
- [65] Klauk, H., Editor. *Organic Electronics*. Wiley-VCH, Weinheim, 1st Edition, **2009**.
- [66] So, F., Editor. *Organic Electronics: Materials, Processing, Devices, and Applications*. CRC Press/Taylor and Francis, Boca Raton, FL., **2009**.
- [67] Sacher, E.; Pireaux, J.-J.; and Kowalczyk, S. P., Editors. *Metallization of Polymers*. American Chemical Society: Washington, DC, **1990**. doi:10.1021/bk-1990-0440.
- [68] Braun, W.; Gavrilu, G.; Gorgoi, M.; and Zahn, D. R. T. Influence of the Molecular Structure on the Interface Formation between Magnesium and Organic Semiconductors. *Radiation Physics and Chemistry*, **2006**, *75*(11), 1869. doi:10.1016/j.radphyschem.2005.07.057.
- [69] Gavrilu, G.; Zahn, D. R. T.; and Braun, W. High Resolution Photoemission Spectroscopy: Evidence for Strong Chemical Interaction between Mg and 3,4,9,10-Perylene-Tetracarboxylic Dianhydride. *Applied Physics Letters*, **2006**, *89*, 162102. doi:10.1063/1.2356305.
- [70] Ju, H.; Feng, X.; Ye, Y.; Zhang, L.; Pan, H.; Campbell, C. T.; and Zhu, J. Ca Carboxylate Formation at the Calcium/Poly(Methyl Methacrylate) Interface. *The Journal Of Physical Chemistry C*, **2012**, *116*(38), 20456. doi:10.1021/jp307010x.
- [71] Bebensee, F.; Schmid, M.; Steinrück, H.-P.; Campbell, C. T.; and Gottfried, J. M. Toward Well-Defined Metal-Polymer Interfaces: Temperature-Controlled Suppression of Subsurface Diffusion and Reaction at the Calcium/Poly(3-Hexylthiophene) Interface. *Journal of the American Chemical Society*, **2010**, *132*(35), 12163. doi:10.1021/ja104029r.
- [72] Murr, J. and Ziegler, C. Interaction of Na with Sexithiophene Thin Films. *Physical Review B*, **1998**, *57*(12), 7299. doi:10.1103/PhysRevB.57.7299.
- [73] Feng, X.; Zhao, W.; Ju, H.; Zhang, L.; Ye, Y.; Zhang, W.; and Zhu, J. Electronic Structures and Chemical Reactions at the Interface between Li and Regioregular Poly(3-Hexylthiophene). *Organic Electronics*, **2012**, *13*(6), 1060. doi:10.1016/j.orgel.2012.02.007.

- [74] Baier, F.; Ludowig, F.; Soukopp, A.; Väterlein, C.; Laubender, J.; Bäuerle, P.; Sokolowski, M.; and Umbach, E. A Combined Photoelectron Spectroscopy and Capacity-Voltage Investigation of the Aluminum/Oligothiophene Interface. *Optical Materials*, **1999**, *12*(2-3), 285. doi:10.1016/S0925-3467(99)00066-X.
- [75] Lazzaroni, R.; Lögdlund, M.; Calderone, A.; Brédas, J.; Dannetun, P.; Fauquet, C.; Fredriksson, C.; Stafström, S.; and Salaneck, W. Chemical and Electronic Aspects of Metal/Conjugated Polymer Interfaces – Implications for Electronic Devices. *Synthetic Metals*, **1995**, *71*(1-3), 2159. doi:10.1016/0379-6779(94)03203-I.
- [76] Dannetun, P.; Boman, M.; Stafström, S.; Salaneck, W. R.; Lazzaroni, R.; Fredriksson, C.; Brédas, J. L.; Zamboni, R.; and Taliani, C. The Chemical and Electronic Structure of the Interface between Aluminum and Polythiophene Semiconductors. *Journal of Chemical Physics*, **1993**, *99*(1), 664. doi:10.1063/1.466217.
- [77] Hirose, Y.; Kahn, A.; Aristov, V.; Soukiassian, P.; Bulovic, V.; and Forrest, S. R. Chemistry and Electronic Properties of Metal-Organic Semiconductor Interfaces: Al, Ti, In, Sn, Ag, and Au on PTCDA. *Physical Review B*, **1996**, *54*(19), 13748. doi:10.1103/PhysRevB.54.13748.
- [78] Lachkar, A.; Selmani, A.; and Sacher, E. Metallization of Polythiophenes – II. Interaction of Vapor-Deposit Cr, V, and Ti with Poly(3-Hexylthiophene) (P3HT). *Synthetic Metals*, **1995**, *72*(1), 73. doi:10.1016/0379-6779(94)02319-T.
- [79] Popovici, D.; Piyakis, K.; Meunier, M.; and Sacher, E. Angle-Resolved X-Ray Photoelectron Spectroscopy Comparison of Copper/Teflon AF1600 and Aluminum/Kapton Metal Diffusion. *Journal of Applied Physics*, **1998**, *83*(1), 108. doi:10.1063/1.366706.
- [80] Koprinarov, I.; Lippitz, A.; Friedrich, J.; Unger, W.; and Wöll, C. Surface Analysis of DC Oxygen Plasma Treated or Chromium Evaporated Poly(Ethylene Terephthalate) Foils by Soft X-Ray Absorption Spectroscopy (NEXAFS). *Polymer*, **1997**, *38*(8), 2005. doi:10.1016/S0032-3861(96)00964-0.
- [81] Lippitz, A.; Koprinarov, I.; Friedrich, J.; Unger, W.; Weiss, K.; and Wöll, C. Surface Analysis of Metallized Poly(Bisphenol A Carbonate) Films by X-Ray Absorption Spectroscopy (NEXAFS). *Polymer*, **1996**, *37*(14), 3157. doi:10.1016/0032-3861(96)89419-5.
- [82] Pireaux, J. J.; Vermeersch, M.; Grégoire, C.; Thiry, P. A.; Caudano, R.; and Clarke, T. C. The Aluminum-Polyimide Interface: An Electron-Induced Vibrational Spectroscopy Approach. *The Journal of Chemical Physics*, **1988**, *88*(5), 3353. doi:10.1063/1.453930.
- [83] Pireaux, J. J.; Thiry, P. A.; Caudano, R.; and Pfluger, P. Surface Analysis of Polyethylene and Hexatriacontane by High Resolution Electron Energy Loss Spectroscopy. *The Journal of Chemical Physics*, **1986**, *84*(11), 6452. doi:10.1063/1.450852.
- [84] DiNardo, N. J.; Demuth, J. E.; and Clarke, T. C. Electron Vibrational Spectroscopy of Thin Polyimide Films. *The Journal of Chemical Physics*, **1986**, *85*(11), 6739. doi:10.1063/1.451405.

- [85] Salvan, G.; Paez, B. A.; Silaghi, S.; and Zahn, D. R. Deposition of Silver, Indium, and Magnesium onto Organic Semiconductor Layers: Reactivity, Indiffusion, and Metal Morphology. *Microelectronic Engineering*, **2005**, *82*(3-4), 228. doi:10.1016/j.mee.2005.07.029.
- [86] Stuckless, J. T.; Frei, N. A.; and Campbell, C. T. A Novel Single-Crystal Adsorption Calorimeter and Additions for Determining Metal Adsorption and Adhesion Energies. *Review Of Scientific Instruments*, **1998**, *69*(6), 2427. doi:10.1063/1.1148971.
- [87] Sellers, J. R. V.; James, T. E.; Hemmingson, S. L.; Farmer, J. A.; and Campbell, C. T. Adsorption Calorimetry During Metal Vapor Deposition on Single Crystal Surfaces: Increased Flux, Reduced Optical Radiation, and Real-Time Flux and Reflectivity Measurements. *Review Of Scientific Instruments*, **2013**, *84*, 123901. doi:10.1063/1.4832980.
- [88] Chen, M.; Röckert, M.; Xiao, J.; Drescher, H.-J.; Steinrück, H.-P.; Lytken, O.; and Gottfried, J. M. Coordination Reactions and Layer Exchange Processes at a Buried Metal-Organic Interface. *The Journal Of Physical Chemistry C*, **2014**, *118*(16), 8501. doi:10.1021/jp5019235.
- [89] Sachs, M.; Gellert, M.; Chen, M.; Drescher, H.-J.; Kachel, S. R.; Zhou, H.; Zugermeier, M.; Gorgoi, M.; Roling, B.; and Gottfried, J. M. LiNi_{0.5}Mn_{1.5}O₄ High-Voltage Cathode Coated with Li₄Ti₅O₁₂: A Hard X-ray Photoelectron Spectroscopy (HAXPES) Study. *Physical Chemistry Chemical Physics*, **2015**, *17*(47), 31790. doi:10.1039/C5CP03837E.
- [90] Chen, M.; Klein, B.; Krug, C.; Zugermeier, M.; Zhou, H.; Drescher, H.-J.; Gorgoi, M.; and Gottfried, J. M. Formation of a Metal/Organic Interphase Monitored Using a Well-Defined Porphyrin Metalation Reaction: A Hard X-Ray Photoelectron Spectroscopy (HAXPES) Study, **In Preparation**.
- [91] Amende, M.; Schernich, S.; Sobota, M.; Nikiforidis, I.; Hieringer, W.; Assenbaum, D.; Gleichweit, C.; Drescher, H.-J.; Papp, C.; Steinrück, H.-P.; Görling, A.; Wasserscheid, P.; Laurin, M.; and Libuda, J. Dehydrogenation Mechanism of Liquid Organic Hydrogen Carriers: Dodecahydro-N-Ethylcarbazole on Pd(111). *Chemistry - A European Journal*, **2013**, *19*(33), 10854. doi:10.1002/chem.201301323.
- [92] Starr, D. E. and Campbell, C. T. Large Entropy Difference between Terrace and Step Sites on Surfaces. *Journal of the American Chemical Society*, **2008**, *130*(23), 7321. doi:10.1021/ja077540h.
- [93] Etzel, K. D.; Bickel, K. R.; and Schuster, R. A Microcalorimeter for Measuring Heat Effects of Electrochemical Reactions with Submonolayer Conversions. *Review of Scientific Instruments*, **2010**, *81*(3), 034101. doi:10.1063/1.3309785.
- [94] Campbell, C. T. and Sellers, J. R. The Entropies of Adsorbed Molecules. *Journal of the American Chemical Society*, **2012**, *134*(43), 18109. doi:10.1021/ja3080117.
- [95] Campbell, C. T. and Sellers, J. R. Enthalpies and Entropies of Adsorption on Well-Defined Oxide Surfaces: Experimental Measurements. *Chemical Reviews*, **2013**, *113*(6), 4106. doi:10.1021/cr300329s.

-
- [96] Zhu, J.; Kinne, M.; Fuhrmann, T.; Denecke, R.; and Steinrück, H.-P. *In situ* High-Resolution XPS Studies on Adsorption of NO on Pt(111). *Surface Science*, **2003**, *529*(3), 384. doi:10.1016/S0039-6028(03)00298-X.
- [97] Kinne, M.; Fuhrmann, T.; Whelan, C. M.; Zhu, J. F.; Pantförder, J.; Probst, M.; Held, G.; Denecke, R.; and Steinrück, H.-P. Kinetic Parameters of CO Adsorbed on Pt(111) Studied by *in situ* High Resolution X-Ray Photoelectron Spectroscopy. *Journal of Chemical Physics*, **2002**, *117*(23), 10852. doi:10.1063/1.1522405.
- [98] Langmuir, I. The Evaporation, Condensation, and Reflection of Molecules and the Mechanism of Adsorption. *Physical Review*, **1916**, *8*(2), 149. doi:10.1103/PhysRev.8.149.
- [99] Redhead, P. A. Thermal Desorption Of Gases. *Vacuum*, **1962**, *12*(4), 203. doi:10.1016/0042-207X(62)90978-8.
- [100] Pétermann, L. A. Thermal Desorption Kinetics of Chemisorbed Gases. *Progress in Surface Science*, **1972**, *3*(1), 1. doi:10.1016/0079-6816(72)90005-6.
- [101] Falconer, J. L. and Schwarz, J. A. Temperature-Programmed Desorption and Reaction: Applications to Supported Catalysts. *Catalysis Reviews: Science and Engineering*, **1983**, *25*(2), 141. doi:10.1080/01614948308079666.
- [102] de Jong, A. and Niemantsverdriet, J. Thermal Desorption Analysis: Comparative Test of Ten Commonly Applied Procedures. *Surface Science*, **1990**, *233*(2), 355. doi:10.1016/0039-6028(90)90649-S.
- [103] Habenschaden, E. and Küppers, J. Evaluation of Flash Desorption Spectra. *Surface Science*, **1984**, *138*(1), L147. doi:10.1016/0039-6028(84)90488-6.
- [104] King, D. A. Thermal Desorption from Metal Surfaces: A Review. *Surface Science*, **1975**, *47*(1), 384. doi:10.1016/0039-6028(75)90302-7.
- [105] Drescher, H.-J. Konstruktion und Charakterisierung eines Detektors für die Adsorptionsmikrokalorimetrie. Diploma thesis, Universität Erlangen-Nürnberg, **2008**.
- [106] Bebensee, F. Metal-Polymer Interfaces Studied with Adsorption Microcalorimetry and Photoelectron Spectroscopy. Ph.D. thesis, Friedrich-Alexander-Universität Erlangen-Nürnberg, **2010**.
- [107] Sircar, S.; Mohr, R.; Ristic, C.; and Rao, M. B. Isotheric Heat of Adsorption: Theory and Experiment. *The Journal Of Physical Chemistry B*, **1999**, *103*(31), 6539. doi:10.1021/jp9903817.
- [108] Shen, D.; Bülow, M.; Siperstein, F.; Engelhard, M.; and Myers, A. L. Comparison of Experimental Techniques for Measuring Isotheric Heat of Adsorption. *Adsorption*, **2000**, *6*(4), 275. doi:10.1023/A:1026551213604.
- [109] Askalany, A. A. and Saha, B. B. Derivation of Isotheric Heat of Adsorption for Non-Ideal Gases. *International Journal of Heat and Mass Transfer*, **2015**, *89*, 186. doi:10.1016/j.ijheatmasstransfer.2015.05.018.

- [110] Lytken, O.; Drescher, H.-J.; Kose, R.; Gottfried, J. M.; (Ed.), G. B.; and (Ed.), B. H. *Surface Science Techniques*, Volume 51, Chapter 2 - Adsorption Calorimetry on Well-Defined Surfaces. Springer Berlin Heidelberg, **2013**, pp. 35–55. doi:10.1007/978-3-642-34243-1_2.
- [111] Crowe, M. C. and Campbell, C. T. Adsorption Microcalorimetry: Recent Advances in Instrumentation and Application. *Annual Review of Analytical Chemistry*, **2011**, *4*, 41. doi:10.1146/annurev-anchem-061010-113841.
- [112] Schauermaun, S.; Silbaugh, T. L.; and Campbell, C. T. Single-Crystal Adsorption Calorimetry on Well-Defined Surfaces: From Single Crystals to Supported Nanoparticles. *The Chemical Record*, **2014**, *14*, 759. doi:10.1002/tcr.201402022.
- [113] Edinger, K.; Gotszalk, T.; and Rangelow, I. W. Novel High Resolution Scanning Thermal Probe. *Journal of Vacuum Science & Technology B*, **2001**, *19*(6), 2856. doi:10.1116/1.1420580.
- [114] Coufal, H. J.; Grygier, R. K.; Horne, D. E.; and Fromm, J. E. Pyroelectric Calorimeter for Photothermal Studies of Thin Films and Adsorbates. *Journal of Vacuum Science & Technology A*, **1987**, *5*(5), 2875. doi:10.1116/1.574258.
- [115] Borroni-Bird, C. E. and King, D. A. An Ultrahigh Vacuum Single Crystal Adsorption Microcalorimeter. *Review of Scientific Instruments*, **1991**, *62*(9), 2177. doi:10.1063/1.1142525.
- [116] Borroni-Bird, C. E.; Al-Sarraf, N.; Anderson, S.; and King, D. Single Crystal Adsorption Microcalorimetry. *Chemical Physics Letters*, **1991**, *183*(6), 516. doi:10.1016/0009-2614(91)80168-W.
- [117] Dvořák, L.; Kovář, M.; and Černý, S. A new Approach to Adsorption Microcalorimetry Based on a LiTaO₃ Pyroelectric Temperature Sensor and a Pulsed Molecular Beam. *Thermochimica Acta*, **1994**, *245*, 163. doi:10.1016/0040-6031(94)85076-3.
- [118] Kovář, M.; Dvořák, L.; and Černý, S. Application of Pyroelectric Properties of LiTaO₃ Single Crystal to Microcalorimetric Measurement of the Heat of Adsorption. *Applied Surface Science*, **1994**, *74*(1), 51. doi:10.1016/0169-4332(94)90099-X.
- [119] Ajo, H. M.; Ihm, H.; Moilanen, D. E.; and Campbell, C. T. Calorimeter for Adsorption Energies of Larger Molecules on Single Crystal Surfaces. *Review Of Scientific Instruments*, **2004**, *75*(11), 4471. doi:10.1063/1.1794391.
- [120] Murdey, R.; Liang, S. J. S.; and Stuckless, J. T. An Atom-Transparent Photon Block for Metal-Atom Deposition from High-Temperature Ovens. *Review Of Scientific Instruments*, **2005**, *76*, 023911. doi:10.1063/1.1855315.
- [121] Lew, W.; Lytken, O.; Farmer, J. A.; Crowe, M. C.; and Campbell, C. T. Improved Pyroelectric Detectors for Single Crystal Adsorption Calorimetry from 100 to 350 K. *Review Of Scientific Instruments*, **2010**, *81*(2), 24102. doi:10.1063/1.3290632.
- [122] Fischer-Wolfarth, J.-H.; Hartmann, J.; Farmer, J. A.; Flores-Camacho, J. M.; Campbell, C. T.; Schauermaun, S.; and Freund, H.-J. An Improved Single Crystal Adsorption Calorimeter for Determining Gas Adsorption and Reaction Energies on

- Complex Model Catalysts. *Review Of Scientific Instruments*, **2011**, *82*(2), 24102. doi:10.1063/1.3544020.
- [123] Comsa, G. and David, R. Dynamical Parameters of Desorbing Molecules. *Surface Science Reports*, **1985**, *5*(4), 145. doi:10.1016/0167-5729(85)90009-3.
- [124] Campbell, C. T. Ultrathin Metal Films And Particles on Oxide Surfaces: Structural, Electronic, and Chemisorptive Properties. *Surface Science Reports*, **1997**, *27*(1-3), 1. doi:10.1016/S0167-5729(96)00011-8.
- [125] Diaz, S.; Zhu, J.; Shamir, N.; and Campbell, C. T. Pyroelectric Heat Detector for Measuring Adsorption Energies on Thicker Single Crystals. *Sensors and Actuators B: Chemical*, **2005**, *107*(1), 454. doi:10.1016/j.snb.2004.11.037.
- [126] Hörtz, P. and Schäfer, R. A Compact Low-Temperature Single Crystal Adsorption Calorimetry Setup for Measuring Coverage Dependent Heats of Adsorption at Cryogenic Temperatures. *Review of Scientific Instruments*, **2014**, *85*, 074101. doi:10.1063/1.4890435.
- [127] Fischer-Wolfarth, J.-H.; Farmer, J. A.; Flores-Camacho, J. M.; Genest, A.; Yudanov, I. V.; Rösch, N.; Campbell, C. T.; Schauermaun, S.; and Freund, H.-J. Particle-Size Dependent Heats of Adsorption of CO on Supported Pd Nanoparticles as Measured with a Single-Crystal Microcalorimeter. *Physical Review B*, **2010**, *81*(24), 241416. doi:10.1103/PhysRevB.81.241416.
- [128] Das-Gupta, D. K. Pyroelectricity in Polymers. *Ferroelectrics*, **1991**, *118*(1), 165. doi:10.1080/00150199108014757.
- [129] Das-Gupta, D. K. On the Nature of Pyroelectricity in Polyvinylidene Fluoride. *Ferroelectrics*, **1981**, *33*(1), 75. doi:10.1080/00150198108008072.
- [130] Damjanovic, D. Ferroelectric, Dielectric, and Piezoelectric Properties of Ferroelectric Thin Films and Ceramics. *Reports on Progress in Physics*, **1998**, *61*(9), 1267. doi:10.1088/0034-4885/61/9/002.
- [131] Porter, S. G. A Brief Guide to Pyroelectric Detectors. *Ferroelectrics*, **1981**, *33*(1), 193. doi:10.1080/00150198108008086.
- [132] Zhang, Q.; Bharti, V.; and Kavarnos, G. *Encyclopedia of Smart Materials*, Chapter Poly(Vinylidene Fluoride) (PVDF) and Its Copolymers. John Wiley and Sons, Inc., **2002**, pp. 807–825. doi:10.1002/0471216275.esm063.
- [133] Solvay Plastics. *Solef[®] PVDF – Design and Processing Guide*.
- [134] Kochervinskiĭ, V. V. Piezoelectricity in Crystallizing Ferroelectric Polymers: Poly(Vinylidene Fluoride) and Its Copolymers (A Review). *Crystallography Reports*, **2003**, *48*(4), 649. doi:10.1134/1.1595194.
- [135] AMP, AMP, Inc. Valley Forge, PA. *Definition of Piezo Film Polarity – Application Note 65773*, b Edition, **1994**.
- [136] Polyanskiy, M. N. Refractive Index Database. In *Aluminum*. Available at <http://refractiveindex.info>, **2015**, p. Reflection.

- [137] Polyanskiy, M. N. Refractive Index Database. In *Silver*. Available at <http://refractiveindex.info>, **2015**, p. Reflection.
- [138] Polyanskiy, M. N. Refractive Index Database. In *Gold*. Available at <http://refractiveindex.info>, **2015**, p. Reflection.
- [139] Lu, C.-S. and Lewis, O. Investigation of Film-Thickness Determination by Oscillating Quartz Resonators with Large Mass Load. *Journal of Applied Physics*, **1972**, *43*(11), 4385. doi:10.1063/1.1660931.
- [140] Lu, C.-S. Mass Determination with Piezoelectric Quartz Crystal Resonators. *Journal of Vacuum Science & Technology*, **1975**, *12*(1), 578. doi:10.1116/1.568614.
- [141] Sauerbrey, G. Verwendung von Schwingquarzen zur Wägung Dünner Schichten und zur Mikrowägung. *Zeitschrift für Physik*, **1959**, *155*, 206. doi:10.1007/BF01337937.
- [142] Intellevation Ltd., 5 Dalziel Road, Hillington Park, Glasgow, G52 4NN. *Model IL150 Thickness Monitor Instruction Manual*, 4.1 Edition.
- [143] Mueller, R. M. and White, W. Direct Gravimetric Calibration of a Quartz Crystal Microbalance. *Review Of Scientific Instruments*, **1968**, *39*(3), 291. doi:10.1063/1.1683352.
- [144] Cumpson, P. and Seah, M. The Quartz Crystal Microbalance; Radial/Polar Dependence of Mass Sensitivity – Both on and off the Electrodes. *Measurement Science and Technology*, **1990**, *1*(7), 544. doi:10.1088/0957-0233/1/7/002.
- [145] Lu, F.; Lee, H.; and Lim, S. Quartz Crystal Microbalance with Rigid Mass Partially Attached on Electrode Surfaces. *Sensors and Actuators A*, **2004**, *112*, 203. doi:10.1016/j.sna.2004.01.018.
- [146] King, D. A. and Wells, M. G. Molecular Beam Investigation Of Adsorption Kinetics on Bulk Metal Targets: Nitrogen on Tungsten. *Surface Science*, **1972**, *29*(2), 454. doi:10.1016/0039-6028(72)90232-4.
- [147] Pauls, S. W. and Campbell, C. T. Magic-Angle Thermal Desorption Mass Spectroscopy. *Surface Science*, **1990**, *226*(3), 250. doi:10.1016/0039-6028(90)90490-Y.
- [148] Teyssedre, G.; Bernes, A.; and Lacabanne, C. Temperature Dependence of the Pyroelectric Coefficient in Polyvinylidene Fluoride. *Ferroelectrics*, **1994**, *160*, 67. doi:10.1080/00150199408007696.
- [149] Levinstein, H. J.; Ballman, A. A.; and Capio, C. D. Domain Structure and Curie Temperature of Single-Crystal Lithium Tantalate. *Journal of Applied Physics*, **1966**, *37*(12), 4585. doi:10.1063/1.1708088.
- [150] Tolkien, J. R. R. *The Hobbit, or There and Back Again*. George Allen & Unwin, **1937**.
- [151] Toptica Photonics, Lochhamer Schlag 19 D-82166 Graefelfing/Munich. *iBeam / iPulse Manual*, m-014 version 04 Edition, **2008**.

-
- [152] LumaSense Technologies, 3033 Scott Blvd. Santa Clara, CA 95054-3316. *IP 140 IMPAC-Pyrometer Operation Manual*, **2009**.
- [153] Kurt J. Lesker Company, 15/16 Burgess Road Hastings, East Sussex TN35 4NR, England. *Global Vacuum Product Guide - CF Flanged Zero Length Kodial Glass Viewports*, 9 Edition.
- [154] Malenfant, P. R. L.; Dimitrakopoulos, C. D.; Gelorme, J. D.; Kosbar, L. L.; Graham, T. O.; Curioni, A.; and Andreoni, W. N-Type Organic Thin-Film Transistor with High Field-Effect Mobility Based on a N,N-Dialkyl-3,4,9,10-Perylene Tetracarboxylic Diimide Derivative. *Applied Physics Letters*, **2002**, *80*(14), 2517. doi:10.1063/1.1467706.
- [155] WaveMetrics, Inc., PO Box 2088 Lake Oswego, OR 97035 USA. *IGOR Pro*, 6.34 Edition, **2013**.
- [156] Thomson, W. On the Equilibrium of Vapour at a Curved Surface of Liquid. *Philosophical Magazine Series 4*, **1871**, *42*(282), 448. doi:10.1080/14786447108640606.
- [157] Linstrom, P. J. *A Guide to the NIST Chemistry WebBook*. National Institute of Standards and Technology.
- [158] Wedler, G. *Lehrbuch der Physikalischen Chemie*. Wiley-VCH Verlag GmbH & Co. KGaA, 5th Edition, **2004**.
- [159] Atkins, P. and de Paula, J. *Atkins' Physical Chemistry*. Oxford University Press, 10th Edition, **2014**.
- [160] Debye, P. Zur Theorie der Spezifischen Wärmen. *Annalen der Physik*, **1912**, *344*(14), 789. doi:10.1002/andp.19123441404.
- [161] Mecea, V. Is Quartz Crystal Microbalance Really a Mass Sensor? *Sensors and Actuators A*, **2006**, *128*(2), 270. doi:10.1016/j.sna.2006.01.023.
- [162] Polyanskiy, M. N. Refractive Index Database. In *Copper*. Available at <http://refractiveindex.info>, **2015**, p. Transmission.
- [163] Polyanskiy, M. N. Refractive Index Database. In *Nickel*. Available at <http://refractiveindex.info>, **2015**, p. Transmission.
- [164] Tsai, B. K.; Allen, D. W.; Hanssen, L. M.; Wilthan, B.; and Zeng, J. A Comparison of Optical Properties between High Density and Low Density Sintered PTFE. *Proc. of SPIE*, **2008**, *7065*, 1. doi:10.1117/12.798138.
- [165] Polyanskiy, M. N. Refractive Index Database. In *Nickel*. Available at <http://refractiveindex.info>, **2015**, p. Reflection.
- [166] Hollemann-Wiberg. *Lehrbuch der Anorganischen Chemie*. Walter de Gruyter, Berlin/New York, 101st Edition, **1996**. doi:10.1002/ange.19961082135.
- [167] SPECS Surface Nano Analysis GmbH, Voltastrasse 5 13355 Berlin Germany. *Useful Information and Facts about the Practice of Sputtering*.

- [168] Heras, J. M. and Albano, E. V. Adsorption of Water on Gold Films – A Work Function and Thermal Desorption Mass Spectrometry Study. *Zeitschrift für Physikalische Chemie*, **1982**, *129*, 11. doi:10.1524/zpch.1982.129.1.011.
- [169] Sigma-Aldrich Chemie GmbH, Riedstrasse 2 D - 89555 Steinheim. *Material Safety Data Sheet – Poly(Propylene Glycol) (#202347)*, 5.1st Edition.
- [170] Powell, C. J. and Jablonski, A. *NIST Electron Inelastic-Mean-Free-Path Database - Version 2*. National Institute of Standards and Technology, Gaithersburg, MD, **2010**.
- [171] Yoshida, T.; Tanaka, T.; Yoshida, H.; Funabiki, T.; and Yoshida, S. Study of Dehydration of Magnesium Hydroxide. *The Journal of Physical Chemistry*, **1995**, *99*, 10890. doi:10.1021/j100027a033.
- [172] Krim, J. and Daly, C. Quartz Monitors and Microbalances. In Glocker, D. A.; Shah, S. I.; and Westwood, W. D., Editors, *Handbook of Thin Film Process Technology*, Chapter D4.0. Bristol, UK ; Philadelphia : Institute of Physics Pub., **1995**, pp. 1–6.
- [173] Sallamie, N. and Shaw, J. Heat Capacity Prediction for Polynuclear Aromatic Solids Using Vibration Spectra. *Fluid Phase Equilibria*, **2005**, *237*, 100. doi:10.1016/j.fluid.2005.07.022.
- [174] N.N. Heat Capacity of the Elements at 25 °C. In Haynes, W. M., Editor, *CRC Handbook of Chemistry and Physics 95th Edition (Internet Version)*. CRC Press/Taylor and Francis, Boca Raton, FL., **2015**, p. 4.05.
- [175] Gaur, U.; fai Lau, S.; Wunderlich, B. B.; and Wunderlich, B. Heat Capacity and Other Thermodynamic Properties of Linear Macromolecules – VIII. Polyesters and Polyamides. *Journal of Physical and Chemical Reference Data Reprints*, **1983**, *12*(1), 65. doi:10.1063/1.555678.
- [176] N.N. Physical Constants of Inorganic Compounds. In Haynes, W. M., Editor, *CRC Handbook of Chemistry and Physics 95th Edition (Internet Version)*. CRC Press/Taylor and Francis, Boca Raton, FL., **2015**, p. 4.02.
- [177] N.N. Physical Properties of Selected Polymers. In Haynes, W. M., Editor, *CRC Handbook of Chemistry and Physics 95th Edition (Internet Version)*. CRC Press/Taylor and Francis, Boca Raton, FL., **2015**, p. 4.02.
- [178] Ogawa, T.; Kuwamoto, K.; Isoda, S.; Kobayashi, T.; and Karl, N. 3,4,9,10-Perylenetetracarboxylic Dianhydride (PTCDA) by Electron Crystallography. *Acta Crystallographica*, **1999**, *B55*, 123. doi:10.1107/S0108768198009872.
- [179] Klein, B. Charakterisierung eines Magnesiumatomstrahls. Bachelor thesis, Philipps-Universität Marburg, **2012**.
- [180] Dresser, M. The Saha-Langmuir Equation and Its Application. *Journal of Applied Physics*, **1968**, *39*(1), 338. doi:10.1063/1.1655755.
- [181] N.N. Electron Work Function of the Elements. In Haynes, W. M., Editor, *CRC Handbook of Chemistry and Physics 95th Edition (Internet Version)*. CRC Press/Taylor and Francis, Boca Raton, FL., **2015**, p. 12.21.

-
- [182] N.N. Ionization Energies of Atoms and Atomsomic Ions. In Haynes, W. M., Editor, *CRC Handbook of Chemistry and Physics 95th Edition (Internet Version)*. CRC Press/Taylor and Francis, Boca Raton, FL., **2015**, p. 10.5.
- [183] Hiden Analytical Limited, 420 European Boulevard Warrinton WA5 7UN England. *MASoft Version 5 User Manual*.
- [184] Korth Kristalle GmbH, Am Jägersberg 3 24161 Altenholz (Kiel) Germany. *Materials Details: Barium Fluoride*.
- [185] Qioptiq Photonics GmbH & Co. KG, Koenigsallee 23 37081 Goettingen Germany. *Data Sheet - Coating: RAGV - Silver Reflection Coating*, **2012**.
- [186] Zhou, Z. and Burns, R. P. Thermal Desorption Spectroscopy of Magnesium from a Chemical Vapor Deposited Aluminum Oxide Surface. *Applied Surface Science*, **1993**, 72(4), 329. doi:10.1016/0169-4332(93)90370-Q.
- [187] Henzler, M. and Göpel, W. *Oberflächenphysik des Festkörpers*. Teubner Verlag, **1994**. doi:10.1007/978-3-322-84875-8.
- [188] Bronstein; Semendjajew; Musiol; and Mühlig. *Taschenbuch der Mathematik*. Verlag Harri Deutsch, **2001**.
- [189] Teysse, G. and Lacabanne, C. Study of the Thermal and Dielectric Behavior of P(VDF-TrFE) Copolymers in Relation with their Electroactive Properties. *Ferroelectrics*, **1995**, 171, 125. doi:10.1080/00150199508018427.
- [190] Hanlon, J. F. *Handbook of Package Engineering*. Chapter 3 Films and Foils. Technomic Publishing Co, 1st Edition, **1992**.
- [191] Johnson, P. B. and Christy, R. W. Optical Constants of Transition Metals: Ti, V, Cr, Mn, Fe, Co, Ni, and Pd. *Physical Review B*, **1974**, 9, 5056. doi:10.1103/PhysRevB.9.5056.
- [192] Rakić, A. D.; Djurišić, A. B.; Elazar, J. M.; and Majewski, M. L. Optical Properties of Metallic Films for Vertical-Cavity Optoelectronic Devices. *Applied Optics*, **1998**, 37(22), 5271. doi:10.1364/AO.37.005271.
- [193] Sturges, H. A. The Choice of a Class Interval. *Journal of the American Statistical Association*, **1926**, 21(153), 65. doi:10.1080/01621459.1926.10502161.
- [194] Sigma-Aldrich Chemie GmbH, Riedstrasse 2 D - 89555 Steinheim. *Material Safety Data Sheet – Magnesium (#254118)*, 5.1st Edition.
- [195] Sigma-Aldrich Chemie GmbH, Riedstrasse 2 D - 89555 Steinheim. *Material Safety Data Sheet – Calcium (#327387)*, 5.4th Edition.
- [196] Hon, S. S.-M. Calcium Vapour Deposition on Semiconducting Polymers Studied by Adsorption Calorimetry and Visible Light Absorption. Ph.D. thesis, The University of British Columbia, Vancouver, Canada, **2008**.
- [197] Sigma-Aldrich Chemie GmbH, Riedstrasse 2 D - 89555 Steinheim. *Material Safety Data Sheet – Copper (#254177)*, 5.1st Edition.

- [198] Xiao, J.; Ditze, S.; Chen, M.; Buchner, F.; Stark, M.; Drost, M.; Steinrück, H.-P.; Gottfried, J. M.; and Marbach, H. Temperature-Dependent Chemical and Structural Transformations from 2H-Tetraphenylporphyrin to Copper(II)-Tetraphenylporphyrin on Cu(111). *The Journal Of Physical Chemistry C*, **2012**, *116*(22), 12275. doi:10.1021/jp301757h.
- [199] Li, Y.; Xiao, J.; Shubina, T. E.; Chen, M.; Shi, Z.; Schmid, M.; Steinrück, H.-P.; Gottfried, J. M.; and Lin, N. Coordination and Metalation Bifunctionality of Cu with 5,10,15,20-Tetra(4-Pyridyl)Porphyrin: Toward a Mixed-Valence Two-Dimensional Coordination Network. *Journal of the American Chemical Society*, **2012**, *134*(14), 6101. doi:10.1021/ja300593w.
- [200] Shubina, T. E.; Marbach, H.; Flechtner, K.; Kretschmann, A.; Jux, N.; Buchner, F.; Steinrück, H.-P.; Clark, T.; and Gottfried, J. M. Principle and Mechanism of Direct Porphyrin Metalation: Joint Experimental and Theoretical Investigation. *Journal of the American Chemical Society*, **2007**, *129*(30), 9476. doi:10.1021/ja072360t.
- [201] Sigma-Aldrich Chemie GmbH, Riedstrasse 2 D - 89555 Steinheim. *Material Safety Data Sheet – Zinc (#267635)*, 5.0th Edition.
- [202] Kretschmann, A.; Walz, M.-M.; Flechtner, K.; Steinrück, H.-P.; and Gottfried, J. M. Tetraphenylporphyrin Picks up Zinc Atoms from a Silver Surface. *Chemical Communications*, **2007**, (6), 568. doi:10.1039/B614427F.
- [203] Sigma-Aldrich Chemie GmbH, Riedstrasse 2 D - 89555 Steinheim. *Material Safety Data Sheet – Lead (#695912)*, 5.1st Edition.
- [204] Sigma-Aldrich Chemie GmbH, Riedstrasse 2 D - 89555 Steinheim. *Material Safety Data Sheet – Perylene-3,4,9,10-Tetracarboxylic Dianhydride (#P11255)*, 5.0th Edition.
- [205] Ostrick, J. R.; Dodabalapur, A.; Torsi, L.; Lovinger, A. J.; Kwock, E. W.; Miller, T. M.; Galvin, M.; Berggren, M.; and Katz, H. E. Conductivity-Type Anisotropy in Molecular Solids. *Journal of Applied Physics*, **1997**, *81*(10), 6804. doi:10.1063/1.365238.
- [206] Möller, S.; Perlov, C.; Jackson, W.; Taussig, C.; and Forrest, S. R. A Polymer/Semiconductor Write-Once Read-Many-Times Memory. *Nature*, **2003**, *426*, 166. doi:10.1038/nature02070.
- [207] Tahir, M.; Sayyad, M. H.; Wahab, F.; Azizc, F.; Ullah, I.; and Khan, G. Enhancement in Electrical Properties of ITO/PEDOT:PSS/PTCDA/Ag by Using Calcium Buffer Layer. *Physica B: Condensed Matter*, **2015**, *446-467*, 38. doi:10.1016/j.physb.2015.03.020.
- [208] Friend, R. H.; Gymer, R. W.; Holmes, A. B.; Burroughes, J. H.; Marks, R. N.; Taliani, C.; Bradley, D. D. C.; Santos, D. A. D.; Brédas, J. L.; Lögdlund, M.; and Salaneck, W. R. Electroluminescence in Conjugated Polymers. *Nature*, **1999**, *379*, 121. doi:10.1038/16393.
- [209] Coakley, K. M. and McGehee, M. D. Conjugated Polymer Photovoltaic Cells. *Chemistry of Materials*, **2004**, *16*(23), 4533. doi:10.1021/cm049654n.

- [210] Garnier, F.; Hajlaoui, R.; Yassara, A.; and Srivastava, P. All-Polymer Field-Effect Transistor Realized by Printing Techniques. *Science*, **1994**, *265*(5179), 1684. doi:10.1126/science.265.5179.1684.
- [211] Fahlman, M. and Salaneck, W. Surfaces and Interfaces in Polymer-Based Electronics. *Surface Science*, **2002**, *500*(1-3), 904. doi:10.1016/S0039-6028(01)01554-0.
- [212] Salaneck, W.; Lögdlund, M.; Fahlman, M.; Greczynska, G.; and Kugler, T. The Electronic Structure of Polymer-Metal Interfaces Studied by Ultraviolet Photoelectron Spectroscopy. *Materials Science and Engineering: R: Reports*, **2001**, *34*(3), 121. doi:10.1016/S0927-796X(01)00036-5.
- [213] Gomathi, N. and Neogi, S. Surface Modification of Polypropylene Using Argon Plasma: Statistical Optimization of the Process Variables. *Applied Surface Science*, **2009**, *255*(17), 7590. doi:10.1016/j.apsusc.2009.04.034.
- [214] Geyter, N. D.; Morent, R.; and Leys, C. Surface Characterization of Plasma-Modified Polyethylene by Contact Angle Experiments and ATR-FTIR Spectroscopy. *Surface and Interface Analysis*, **2007**, *40*(3-4), 608. doi:10.1002/sia.2611.
- [215] Burkert, S.; Kuntzsch, M.; Bellmann, C.; Uhlmann, P.; and Stamm, M. Tuning of Surface Properties of Thin Polymer Films by Electron Beam Treatment. *Applied Surface Science*, **2009**, *255*(12), 6256. doi:10.1016/j.apsusc.2009.01.096.
- [216] Massey, S.; Cloutier, P.; Bazin, M.; Sanche, L.; and Roy, D. Chemical Modification of Polystyrene by Low-Energy (<100 eV) Electron Irradiation Studied by Mass Spectrometry. *Journal of Applied Polymer Science*, **2008**, *108*(5), 3163. doi:10.1002/app.27892.
- [217] Zekonyte, J.; Erichsen, J.; Zaporajtchenko, V.; and Faupel, F. Mechanisms of Argon Ion-Beam Surface Modification of Polystyrene. *Surface Science*, **2003**, *532-535*, 1040. doi:10.1016/S0039-6028(03)00130-4.
- [218] Sahre, K.; Eichhorn, K.-J.; Simon, F.; Pleul, D.; Jankea, A.; and Gerlach, G. Characterization of Ion-Beam Modified Polyimide Layers. *Surface and Coatings Technology*, **2001**, *139*(2-3), 257. doi:10.1016/j.nimb.2007.08.040.
- [219] Zaporajtchenko, V.; Zekonyte, J.; and Faupel, F. Effects of Ion Beam Treatment on Atomic and Macroscopic Adhesion of Copper to Different Polymer Materials. *Nuclear Instruments and Methods in Physics Research Section B: Beam Interactions with Materials and Atoms*, **2007**, *265*(1), 139. doi:10.1016/j.nimb.2007.08.040.
- [220] Sigma-Aldrich Chemie GmbH, Riedstrasse 2 D - 89555 Steinheim. *Material Safety Data Sheet - 5,10,15,20-Tetraphenyl-21H,23H-Porphine (#247367)*, 5.3rd Edition.
- [221] Chen, M.; Feng, X.; Zhang, L.; Ju, H.; Xu, Q.; Zhu, J.; Gottfried, J. M.; Ibrahim, K.; Qian, H.; and Wang, J. Direct Synthesis of Nickel(II) Tetraphenylporphyrin and Its Interaction with a Au(111) Surface: A Comprehensive Study. *The Journal Of Physical Chemistry B*, **2010**, *114*(21), 9908. doi:10.1021/jp102031m.
- [222] Gottfried, J. M.; Flechtner, K.; Kretschmann, A.; Lukasczyk, T.; and Steinrück, H.-P. Direct Synthesis of a Metalloporphyrin Complex on a Surface. *Journal of the American Chemical Society*, **2006**, *128*(17), 5644. doi:10.1021/ja0610333.

- [223] Krause, B.; Dürr, A. C.; Ritley, K.; Schreiber, F.; Dosch, H.; and Smilgies, D. Structure and Growth Morphology of an Archetypal System for Organic Epitaxy: PTCDA on Ag(111). *Physical Review B*, **2002**, *66*, 235404. doi:10.1103/PhysRevB.66.235404.
- [224] Amar, N.; Gould, R.; and Saleh, A. Structural and Electrical Properties of the α -form of Metal-Free Phthalocyanine (α -H₂Pc) Semiconducting Thin Films. *Current Applied Physics*, **2002**, *2*(6), 455. doi:10.1016/S1567-1739(02)00156-6.
- [225] Horowitz, G.; Bachet, B.; Yassar, A.; Lang, P.; Demanze, F.; Fave, J.-L.; and Garnier, F. Growth and Characterization of Sexithiophene Single Crystals. *Chemistry of Materials*, **1995**, *7*, 1337. doi:10.1021/cm00055a010.
- [226] Ashida, M.; Yanagi, H.; Hayashi, S.; and Takemoto, K. Epitaxial Growth and Molecular Orientation of Tetraphenylporphyrin Thin Film Vacuum-Evaporated on KCl. *Acta Crystallographica Section B*, **1991**, *47*(1), 87. doi:10.1107/S0108768190008904.
- [227] Zhou, H. Interaction of Ca/6T at Metal-Organic Interface Studied by Adsorption Microchlorimetry and Photoelectron Spectroscopy. Ph.D. thesis, Philipps-Universität-Marburg, **In Preparation**.
- [228] Bender, M.; Yakovkin, I. N.; and Freund, H.-J. Adsorption and Reaction of Magnesium on Cr₂O₃(0001)/Cr(110). *Surface Science*, **1996**, *365*(2), 394. doi:10.1016/0039-6028(96)00742-X.
- [229] Buchner, F.; Flechtner, K.; Bai, Y.; Zillner, E.; Kellner, I.; Steinrück, H.-P.; Marbach, H.; and Gottfried, J. M. Coordination of Iron Atoms by Tetraphenylporphyrin Monolayers and Multilayers on Ag(111) and Formation of Iron-Tetraphenylporphyrin. *The Journal Of Physical Chemistry C*, **2008**, *112*(39), 15458. doi:10.1021/jp8052955.
- [230] Gottfried, J. M. Surface Chemistry of Porphyrins and Phthalocyanines. *Surface Science Reports*, **2015**, *70*(3), 259. doi:10.1016/j.surfrep.2015.04.001.
- [231] Kolbeck, C.; Niedermaier, I.; Deyko, A.; Lovelock, K. R. J.; Taccardi, N.; Wei, W.; Wasserscheid, P.; Maier, F.; and Steinrück, H.-P. Influence of Substituents and Functional Groups on the Surface - Composition of Ionic Liquids. *Chemistry - A European Journal*, **2014**, *20*(14), 3954. doi:10.1002/chem.201304549.
- [232] Steinrück, H.-P. Recent Developments in the Study of Ionic Liquid Interfaces using X-Ray Photoelectron Spectroscopy and Potential Future Directions. *Physical Chemistry Chemical Physics*, **2012**, *14*(15), 510. doi:10.1039/C2CP24087D.
- [233] Gardella, J. A. J. Recent Advances in Ion and Electron Spectroscopy of Polymer Surfaces. *Applied Surface Science*, **1988**, *31*(1), 72. doi:10.1016/0169-4332(88)90025-6.
- [234] Omicron NanoTechnology, Limburger Strasse 75 65232 Tausnusstein Germany. *Instruction Manual UHV Evaporator EFM 2/3/3s/4 etc.*, version 3.9 Edition, **2008**.
- [235] Faupel, F.; Willecke, R.; and Thran, A. Diffusion of Metals in Polymers. *Materials Science and Engineering: R: Reports*, **1998**, *22*(1), 1. doi:10.1016/S0927-796X(97)00020-X.

-
- [236] Schneider, P. Thermionic Emission of Thoriated Tungsten. *The Journal of Chemical Physics*, **1958**, *28*(4), 675. doi:10.1063/1.1744212.
- [237] Notes on Extending Crystal Life. Available at <http://www.intellectrics.com/xtalcrystals.htm>, **2014**.
- [238] Stuckless, J. T.; Frei, N. A.; and Campbell, C. T. Pyroelectric Detector for Single-Crystal Adsorption Microcalorimetry: Analysis of Pulse Shape and Intensity. *Sensors and Actuators B: Chemical*, **2000**, *62*(1), 13. doi:10.1016/S0925-4005(99)00371-8.
- [239] N.N. Crystallographic Data on Minerals. In Haynes, W. M., Editor, *CRC Handbook of Chemistry and Physics 95th Edition (Internet Version)*. CRC Press/Taylor and Francis, Boca Raton, FL., **2015**, p. 4.11.
- [240] Kersey, J. B. and Jerner, R. C. The Effect of Firing Temperature on Properties Natural Steatite and Pyrophyllite. *Journal of Materials Science*, **1972**, *7*(6), 621. doi:10.1007/BF00549373.
- [241] Chase, M. J. *NIST-JANAF Thermochemical Tables*, Volume Monograph 9. Journal of Physical and Chemical Reference Data, 4th Edition, **1998**.
- [242] Ho, C. Y.; Powell, R. W.; and Liley, P. E. Thermal Conductivity of the Elements: A Comprehensive Review. *Journal of Physical and Chemical Reference Data*, **1974**, *3*(Supplement 1), 1.
- [243] Chekhovskoi, V.; Gusev, Y.; and Tarasov, V. Experimental Study of the Specific Heat and Enthalpy of Copper in the Range 300 - 2000 K. *High Temperatures - High Pressures*, **2000**, *34*(3), 291. doi:10.1068/htjr022.

Nanojoule Adsorption Calorimetry

Design, Construction, Novel Evaluation

Approach, Software Development,

Characterization, and Exemplary Measurements

D i s s e r t a t i o n

zur Erlangung des
Doktorgrades der Naturwissenschaften
(Dr. rer. nat.)

dem Fachbereich Chemie
der Philipps-Universität Marburg

vorgelegt von

Hans-Jörg Drescher

Diplom Chemiker Universität

aus Erlangen

Marburg an der Lahn
2016

Contents

Selbständigkeitserklärung	iii
Abstract	v
Kurzzusammenfassung	vii
Contents	ix
Abbreviations	xix
1 Introduction	1
1.1 Enthalpy of Adsorption	3
1.1.1 Deduction from Desorption Kinetics	3
1.1.2 Derivation from Adsorption-Desorption Equilibria	5
1.1.3 Direct Measurement by Adsorption Calorimetry	5
1.2 Theoretical Background	7
1.3 Involved Principles	10
1.3.1 Beam Source	10
1.3.2 Infrared Radiation	10
1.3.3 Pyroelectric Detector	11
1.3.4 Detector Calibration	13
1.3.5 Pulsing	14
1.3.6 Deposition Rate Measurement	14
1.3.7 Sticking Measurement	15
2 Experimental Setup	17
2.1 Sample Holder	20
2.2 Detector Stage	23
2.3 Molecular Beam	30
2.3.1 Main Evaporator	30
2.3.2 Optics Stage	35
2.3.3 Beam Chopper	39

2.3.4	Inline Valve	44
2.3.5	Parts in the Main Chamber	46
2.3.6	Beam Housing	49
2.3.7	Assembled Beam	52
2.4	Ancillaries Stage	55
2.4.1	Hot Plate	56
2.4.2	Quartz Crystal Microbalance	57
2.4.3	Mirror	58
2.4.4	Infrared Transparent Window	59
2.4.5	Assembled Ancillaries	60
2.5	Main Chamber Additions	63
2.5.1	Mass Spectrometer	63
2.5.2	Optical Meters	65
2.5.3	Fiber Positioner	69
2.5.4	Miscellaneous Additions	72
2.6	Load Lock	76
2.7	Sample Handling	82
2.8	Glove Box	85
2.9	Assembled System	87
2.10	Synopsis of the Experimental Setup	91
3	Data Evaluation	93
3.1	User Interface	94
3.1.1	Menu	94
3.1.2	Main Panel	101
3.1.3	Interactive Windows	101
3.2	Loading Data	104
3.3	Data Filtering	106
3.3.1	High Pass Filter	106
3.3.2	Line Notch Filter	108
3.3.3	Extra Notch Filter	109
3.3.4	Nyquist Cut Off Filter	109
3.3.5	Effects on the Calorimetry Data	110
3.4	Quartz Crystal Microbalance Measurements	113
3.4.1	Sample Coating	113
3.4.2	Calorimetry Deposition Rate Measurement	114

3.5	Measured References	117
3.5.1	Deconvolution	120
3.5.2	Clean Sample	121
3.5.3	Coated Sample	121
3.5.4	Laser Reference	122
3.5.5	Transmission of Infrared Transparent Window	124
3.5.6	Radiation Contribution	124
3.5.7	Zero Sticking	125
3.6	Statistics	126
3.7	Automatic Outlier Removal	128
3.8	Calorimetry Measurement	132
3.8.1	Heat Measurement	132
3.8.2	Sticking Measurement	134
3.8.3	Enthalpy Calculation	136
3.9	Fitted Trends	138
3.10	Deconvolution of Measurements	143
3.11	Averaging Experiments	146
3.12	Lazy Operations	148
3.13	Comparison to Previous Approach	149
3.14	Status Display	154
3.15	Synopsis of the Data Evaluation	155
4	Software	157
4.1	File Formats	158
4.1.1	Deposition Files	158
4.1.2	Calorimetry Files	160
4.1.3	Auxiliary Files	161
4.1.4	Logging Files	162
4.2	NAC Program Package	163
4.2.1	Definitions	164
4.2.2	Initialization	166
4.2.3	Graphical User Interface	178
4.2.4	Data Processing	186
4.2.5	Fitting Functions	194
4.2.6	File Input/Output	199
4.2.7	Controls Handling	202
4.2.8	Statistics Functions	208

4.2.9	Experiment Averaging Functions	210
4.2.10	Miscellaneous	213
4.2.11	Extensions to the Status Package	215
4.2.12	Version History	215
4.2.13	Known Issues	215
4.3	Error Handling Package	216
4.3.1	Definitions	216
4.3.2	Initialization	217
4.3.3	Error Handling	217
4.3.4	Graphical User Interface	218
4.3.5	Version History	218
4.3.6	Known Issues	218
4.4	Status Report Package	219
4.4.1	Definitions	219
4.4.2	File Input/Output	220
4.4.3	User Interface	220
4.4.4	Tools	221
4.4.5	Version History	221
4.4.6	Known Issues	221
4.5	Synopsis of the Software Packages	222
5	Characterizing Experiments	223
5.1	External Reflectivity Measurement	224
5.2	Sputtering	228
5.3	Partially Loaded Quartz Crystal Microbalance	233
5.4	Sample Preparation in the Load Lock	238
5.4.1	Evaporator	238
5.4.2	Effects of Coating	239
5.4.3	Thermal Degrading During Deposition	241
5.4.4	Tooling of the Quartz Crystal Microbalance in the Load Lock	242
5.5	Additional Instrumentation	245
5.5.1	Digital Acquisition Card	245
5.5.2	Laser Stability	245
5.5.3	Amplifier	247
5.6	Molecular Beam	249
5.6.1	Main Evaporator	249
5.6.2	Inline Valve	252

5.6.3	Chopper	253
5.6.4	Deflector Plates	257
5.6.5	Evaporator Radiation in Reference Measurements	258
5.7	Mass Spectrometer	260
5.7.1	Intensity Estimation	260
5.7.2	Mass Spectrometer Settings	261
5.7.3	Mass Spectrometer Peak Shape <i>vs.</i> Pulse Length	263
5.8	Ancillaries Stage	268
5.8.1	Infrared Transparent Window	268
5.8.2	Quartz Crystal Microbalance	275
5.8.3	Mirror	277
5.8.4	Hot Plate	279
5.9	Pyroelectric Detector	293
5.9.1	Linearity Regarding Input Power	293
5.9.2	Linearity Regarding Active Area	294
5.9.3	External Heat Treatment of β -Polyvinylidene Fluoride	297
5.9.4	Temperature Influence on Detector Sensitivity	299
5.9.5	Detailed Detector Composition	301
5.9.6	Thermal Insulation of the Detector Stage	304
5.9.7	Deconvolution Test	305
5.10	Statistical Considerations	308
5.11	Synopsis of the Characterization Experiments	312
6	Investigated Systems	315
6.1	Choice of Materials	317
6.1.1	Magnesium	318
6.1.2	Calcium	319
6.1.3	Copper	320
6.1.4	Zinc	321
6.1.5	Lead	321
6.1.6	Unaltered Detector Material	321
6.1.7	Sputter Cleaned Detector Material	322
6.1.8	3,4,9,10-Perylene-Tetracarboxylic Dianhydride	322
6.1.9	Poly(3-Hexylthiophene)	323
6.1.10	Sexithiophene	324
6.1.11	Tetraphenyl Porphyrin	325
6.2	Reaction Thicknesses	326

6.3	Measurement Procedure	329
6.4	Adsorption of Magnesium	333
6.4.1	Experiment	333
6.4.2	Results	333
6.4.3	Discussion	336
6.5	Adsorption of Calcium	339
6.5.1	Experiment	339
6.5.2	Results	340
6.5.3	Discussion	355
6.6	Adsorption of Copper	363
6.6.1	Experiment	363
6.6.2	Results	363
6.6.3	Discussion	365
6.7	Adsorption of Zinc	367
6.7.1	Experiment	367
6.7.2	Results	367
6.7.3	Discussion	370
6.8	Gigantic Signal Effect	373
6.9	Inverted Signal Effect	378
6.10	Synopsis of the Results from the Investigated Systems	383
7	Summary and Outlook	387
8	Zusammenfassung und Ausblick	395
	Acknowledgment	403
	Danksagung	404
	<i>Curriculum Vitae</i>	405
	List of Figures	407
	List of Tables	417
	Bibliography	419

Contents	441
A Operating Parameters	450
A.1 Magnesium	451
A.2 Calcium	451
A.3 Copper	452
A.4 Zinc	452
A.5 Perylenetetracarboxylic Dianhydride	453
A.6 Phthalocyanine	453
A.7 Sexithiophene	454
A.8 5,10,15,20-Tetraphenyl-Porphyrin	454
B Design Drawings	455
B.1 Molecular Beam	455
B.1.1 Main Evaporator	456
B.1.2 Internal Valve	465
B.1.3 Optics Stage	473
B.1.4 Beam Chopper	483
B.1.5 Nozzle in Main Chamber	490
B.1.6 Beam Housing	495
B.2 Main Chamber	511
B.2.1 Sample Holder	512
B.2.2 Sample Carrier	520
B.2.3 Detector	525
B.2.4 Sample Heater	550
B.2.5 Mass Spectrometer Mount	561
B.2.6 Ancillaries Stage	568
B.2.7 Main Chamber Additions	589
B.2.8 Optical Meters	606
B.2.9 Fiber Positioner	623
B.3 Load Lock	638
B.3.1 Mount for Load Lock	639
B.3.2 Load Lock Housing	647
B.3.3 Sample Storage	654
B.3.4 Transfer Rod Support	662
B.4 Miscellaneous	668
B.4.1 Glove Box	669

B.4.2	Evaporator for Synchrotron Applications	673
B.4.3	Mounting Stand	682
B.4.4	Threefold Evaporator	690
B.4.5	Battery Box	701
C	Program Codes	703
C.1	NAC Package	704
C.1.1	Definitions	704
C.1.2	Initialization	706
C.1.3	Graphical User Interface	710
C.1.4	Data Processing	740
C.1.5	Fitting Functions	770
C.1.6	Input/Output	775
C.1.7	Controls Handling	793
C.1.8	Statistics Functions	813
C.1.9	Experiment Averaging Functions	819
C.1.10	Miscellaneous	827
C.1.11	Extensions to the Status Package	837
C.1.12	Version History	837
C.2	Error Handling Package	841
C.2.1	Definitions	841
C.2.2	Initialization	841
C.2.3	Error Handling	841
C.2.4	Graphical User Interface	844
C.2.5	Version History	844
C.3	Machine Status Package	846
C.3.1	Definitions	846
C.3.2	File Input/Output	846
C.3.3	User Interface	849
C.3.4	Tools	852
C.3.5	Version History	853
D	Overview of the Investigated Systems	855
D.1	Magnesium Adsorbed on Pristine Detector	856
D.2	Magnesium Adsorbed on Sputter Cleaned Detector	858
D.3	Magnesium Adsorbed on PTCDA	860
D.4	Calcium Adsorbed on Sputter Cleaned Detector	862

D.5	Calcium Adsorbed on Tetraphenyl Porphyrin	864
D.6	Calcium Adsorbed on PTCDA	866
D.7	Calcium Adsorbed on PTCDA at Low Temperature	869
D.8	Calcium Adsorbed on Sexithiophene	871
D.9	Calcium Adsorbed on Sexithiophene at Low Temperature	875
D.10	Zinc Adsorbed on Sputter Cleaned Detector	877
D.11	Zinc Adsorbed on PTCDA	879
D.12	Zinc Adsorbed on PTCDA at Low Temperature	881
E	Supplementary Information	883
E.1	Previous Data Evaluation Approach	883
E.2	Filtering	889
E.2.1	Laser Reference Measurement	890
E.2.2	Radiation Reference Measurement	895
E.2.3	Calorimetry Measurement	900
	List of Figures	905
	List of Tables	915
	Bibliography	917

A Operating Parameters

This chapter collects the used parameters for the laboratory equipment such as setting for the mass spectrometer (QMS), the quartz crystal microbalance (QCM) controller, evaporation temperatures, and so on. References for heat capacities and standard enthalpies are given in the program code, see Appendix C.1.

CAS provides the *Chemical Abstracts Service* registry number of the substance.

Specification provides order number, purity, and vendor.

Modification gives further information about the used crystal structure or phase.

Designator consists of a short name of the substance, *e.g.*, the element's symbol, and the plane designator for the exposed surface according to MILLER notation, *e.g.*, (0001).

Unit cell lists a , b , c , α , β , γ representing the parameters of the unit cell and Z the number of molecules in it.

Layer thickness shows the thickness calculation for a monomolecular layer from cell parameters in the bulk phase.

Layer density presents the calculation for the number of molecules in the designated plane per area.

Density indicates the density set for the QCM controller.

Acoustic impedance expresses the acoustic impedance used by the QCM controller.

Mass to charge ratio denotes the setting for the mass filter in the mass spectrometer for the sticking measurements.

Emission current states the set emission current for the ion source of the QMS.

Ionization energy quotes the utilized ionization energy employed in the ion source of the QMS.

Evaporation recommends crucible, evaporator, and parameters.

A.1 Magnesium

CAS: 7439-95-4

Specification: '254118' 99.98 % from Sigma-Aldrich Co. LLC.

Modification: HCP

Designator: Mg(0001)

Unit cell^[239]: $a = 320.94$ pm, $b = 320.94$ pm, $c = 521.08$ pm

$$\alpha = 90^\circ, \beta = 90^\circ, \gamma = 120^\circ, Z = 2$$

Layer thickness: $d = c/2 = 260.54$ pm

Layer density: $1/A = (a^2 \sin(\gamma))^{-1} = 1.1210 \cdot 10^{19}$ 1/m²

Density^[142]: 1.74 g/cm³

Acoustic impedance^[142]: $11.4 \cdot 10^5$ g/cm²s

Mass to charge ratio: $m/z = 24$, Abundance ≈ 79 %

Emission current: 1000 μ A

Ionization energy: 30 eV

Evaporation: Stainless steel crucible in main evaporator at 800 K

A.2 Calcium

CAS: 7440-70-2

Specification: '327387' 99 % from Sigma-Aldrich Co. LLC.

Modification: CCP (fcc)

Designator: Ca(111)

Unit cell^[239]: $a = 558.84$ pm, $b = 558.84$ pm, $c = 558.84$ pm

$$\alpha = 90^\circ, \beta = 90^\circ, \gamma = 90^\circ, Z = 4$$

Layer thickness: $d = \sqrt{3}/3a = 322.65$ pm

Layer density: $1/A = (1/2a^2 \sin(2/3\pi))^{-1} = 7.3948 \cdot 10^{18}$ 1/m²

Density^[142]: 1.55 g/cm³

Acoustic impedance^[142]: $3.30 \cdot 10^5$ g/cm²s

Mass to charge ratio: $m/z = 40$, Abundance ≈ 97 %

Emission current: 1000 μ A

Ionization energy: 50 eV

Evaporation: Stainless steel crucible in main evaporator at 850 K

A.3 Copper

CAS: 7440-50-8

Specification: '490DFL016-G-S5' OFHC(99.99%) from Pfeiffer Vacuum GmbH

Modification: CCP (fcc)

Designator: Cu(111)

Unit cell: $a = 361.49$ pm, $b = 361.49$ pm, $c = 361.49$ pm

$$\alpha = 90^\circ, \beta = 90^\circ, \gamma = 90^\circ, Z = 4$$

Layer thickness: $d = \sqrt{3}/3a = 208.71$ pm

Layer density: $1/A = (1/2a^2 \sin(2/3\pi))^{-1} = 1.7673 \cdot 10^{19}$ 1/m²

Density^[142]: 8.93 g/cm³

Acoustic impedance^[142]: $20.20 \cdot 10^5$ g/cm²s

Mass to charge ratio: $m/z = 63$, Abundance $\approx 69\%$

Emission current: 1000 μ A

Ionization energy: 70 eV

Evaporation: Molybdenum crucible (medium size) in electron beam evaporator
(800 V, 30 mA, ≈ 1500 K^[234])

A.4 Zinc

CAS: 7440-66-6

Specification: '8780' p.a. from Merck KGaA discontinued

Modification: HCP

Designator: Zn(0001)

Unit cell: $a = 266.49$ pm, $b = 266.49$ pm, $c = 494.68$ pm

$$\alpha = 90^\circ, \beta = 90^\circ, \gamma = 120^\circ, Z = 2$$

Layer thickness: $d = c/2 = 247.34$ pm

Layer density: $1/A = (a^2 \sin(\gamma))^{-1} = 1.6260 \cdot 10^{19}$ 1/m²

Density^[142]: 7.04 g/cm³

Acoustic impedance^[142]: $17.17 \cdot 10^5$ g/cm²s

Mass to charge ratio: $m/z = 64$, Abundance $\approx 49\%$

Emission current: 1000 μ A

Ionization energy: 50 eV

Evaporation: Stainless steel crucible in main evaporator at 760 K

A.5 Perylenetetracarboxylic Dianhydride

CAS: 128-69-8

Specification: 'P11255' 97% from Sigma-Aldrich Co. LLC.

Modification^[178]: α -phase

Designator: PTCDA

Unit cell^[178,223]: $a = 374$ pm, $b = 1196$ pm, $c = 1734$ pm

$$\alpha = 90^\circ, \beta = 98.8^\circ, \gamma = 90^\circ, Z = 2$$

Density: 1.69 g/cm³ (calculated from [178])

Acoustic impedance^[142]: $8.8 \cdot 10^5$ g/cm²s (Quartz)

Evaporation: Quartz crucible in load lock evaporator at 540 K

A.6 Phthalocyanine

CAS: 574-93-6

Specification: '253103' 98% from Sigma-Aldrich Co. LLC.

Modification^[224]: α -phase

Designator: 2HPc

Unit cell^[224]: $a = 1985$ pm, $b = 472$ pm, $c = 1480$ pm

$$\alpha = 90^\circ, \beta = 122^\circ, \gamma = 90^\circ, Z = 2$$

Density: 1.45 g/cm³ (calculated from [224])

Acoustic impedance^[142]: $8.8 \cdot 10^5$ g/cm²s (Quartz)

Evaporation: Quartz crucible in load lock evaporator at 550 K

A.7 Sexithiophene

CAS: 88493-55-4

Specification: '594687' from Sigma-Aldrich Co. LLC.

Designator: 6T

Unit cell^[225]: $a = 4470.8$ pm, $b = 785.1$ pm, $c = 602.9$ pm

$$\alpha = 90^\circ, \beta = 90.76^\circ, \gamma = 90^\circ, Z = 4$$

Density^[225]: 1.55 g/cm³

Acoustic impedance^[142]: $8.8 \cdot 10^5$ g/cm²s (Quartz)

Evaporation: Quartz crucible in load lock evaporator at 410 K

A.8 5,10,15,20-Tetraphenyl-Porphyrin

CAS: 917-23-7

Specification: 'PO890001' 98 % from Porphyrin Systems GbR

Designator: 2HTPP

Unit cell^[226]: $a = 1200$ pm, $b = 1900$ pm, $c = 1470$ pm

$$\alpha = 90^\circ, \beta = 91^\circ, \gamma = 90^\circ, Z = 4$$

Density: 1.22 g/cm³ (calculated from [226])

Acoustic impedance^[142]: $8.8 \cdot 10^5$ g/cm²s (Quartz)

Evaporation: Quartz crucible in load lock evaporator at 550 K

B Design Drawings

This appendix contains all the technical drawings used to build the setup. Unless otherwise stated, images are scaled by 71 % to fit a page, chamfers are 1X45°, threads are cut to maximum depth, and one piece each is to be manufactured. Dimensions are given in millimeters and decimal degrees. Tubes are designated by $\varnothing_{\text{outer}} \times d_{\text{wall}}$ and parts are made from 1.4301 if not stated otherwise. This stainless steel can be replaced by 1.4541 or 1.4547 but not *vice versa*.

B.1 Molecular Beam

Details about the molecular beam are discussed in Section 2.3. The following pages contain the technical drawings of the parts related to the molecular beam:

Main Evaporator High volume effusive source for the adsorbate in a NAC experiment (Appendix B.1.1).

Internal Valve Home built device to separate the molecular beam from the main chamber (Appendix B.1.2).

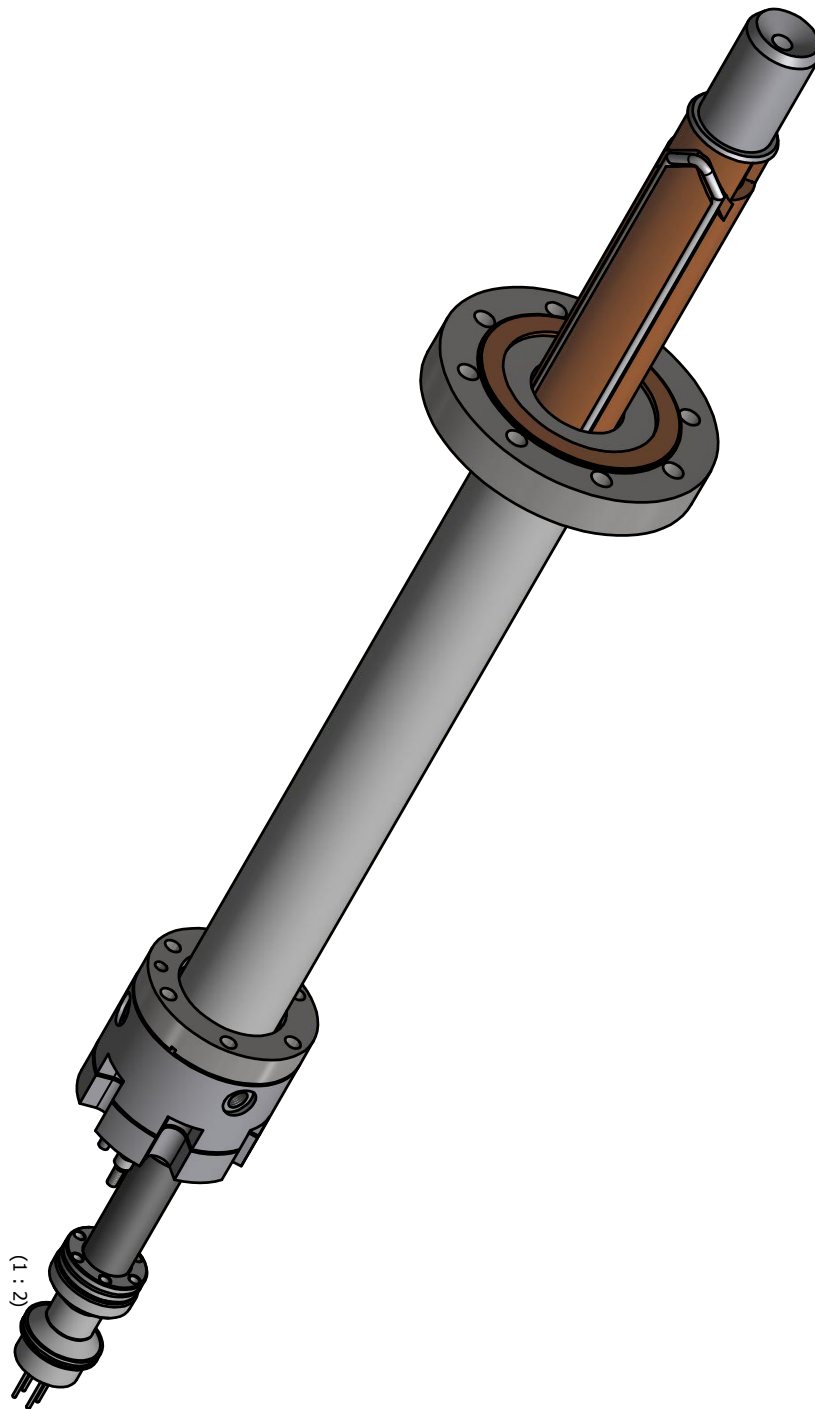
Optics Stage Parts to defocus the laser beam and reflect it onto the sample (Appendix B.1.3).

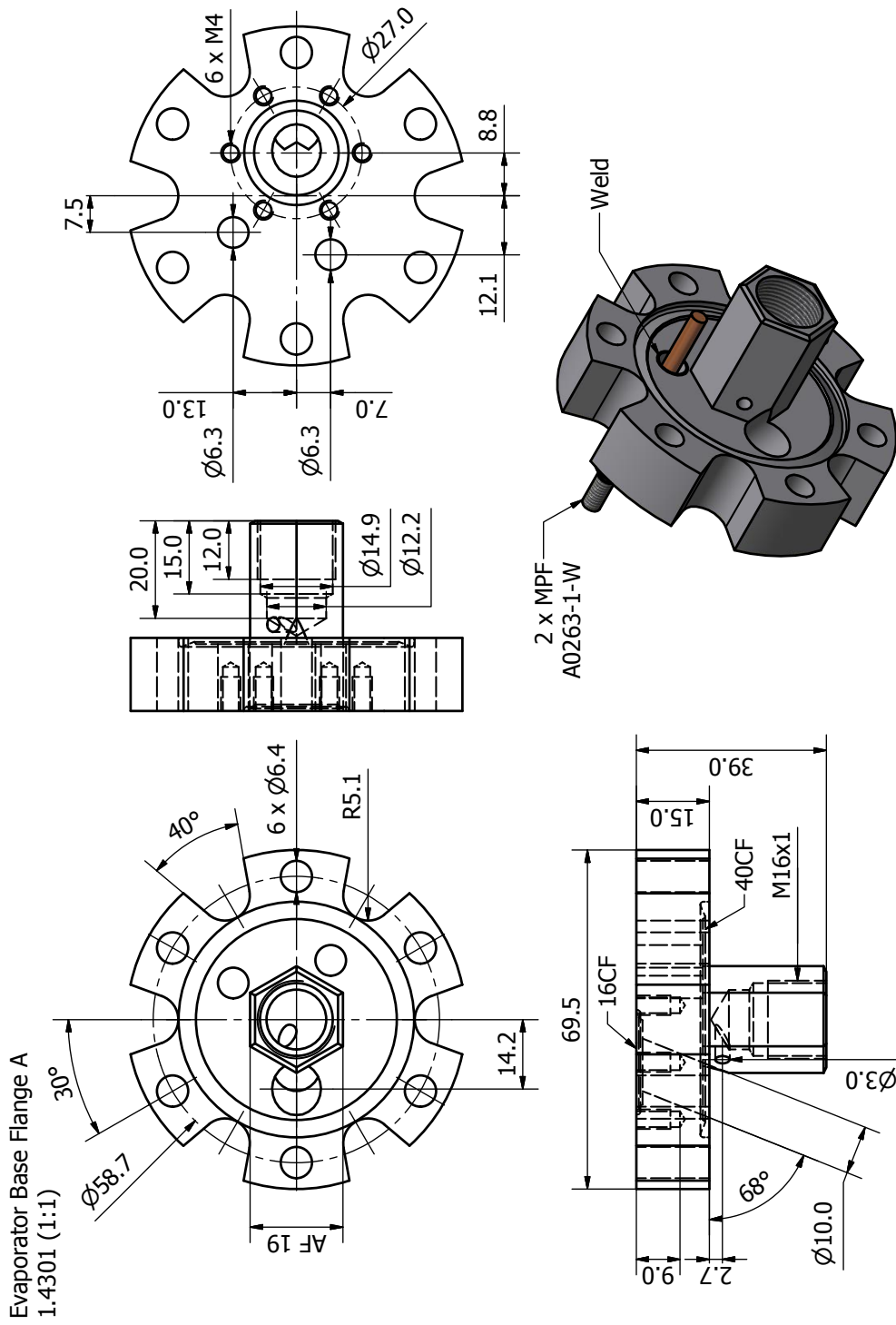
Beam Chopper Device used to pulse the adsorbate flux (Appendix B.1.4).

Nozzle in Main Chamber Beam defining orifice of the molecular flux mounted on the beam housing (Appendix B.1.5).

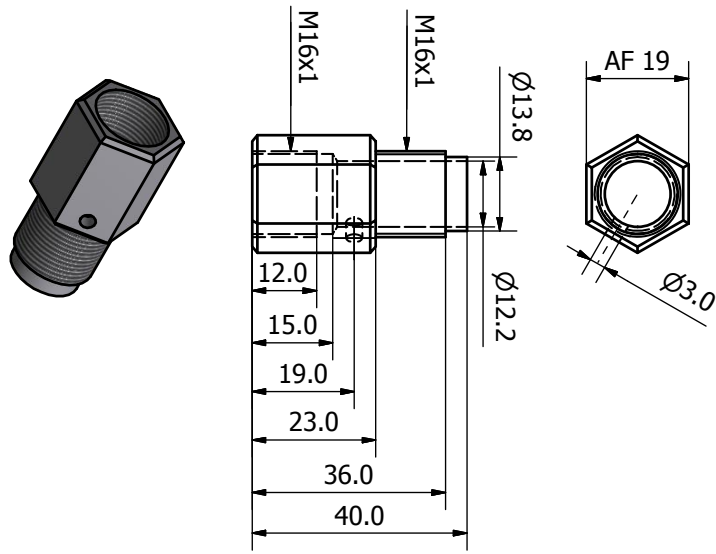
Beam Housing Structural components of the molecular beam (Appendix B.1.6).

B.1.1 Main Evaporator

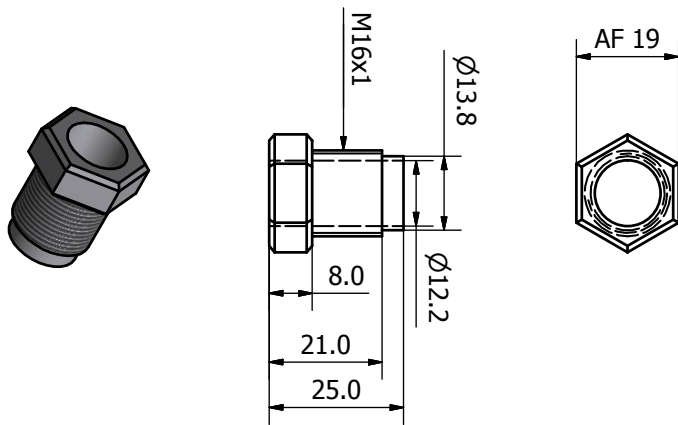




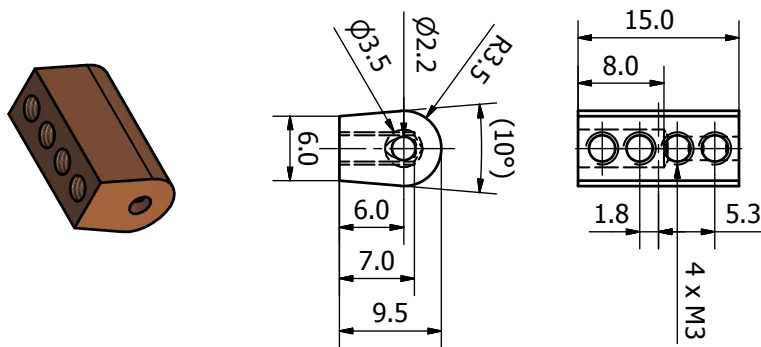
Evaporator Base Flange B
1.4301 (1:1)



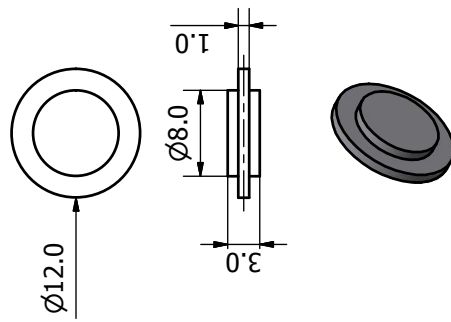
Evaporator Base Flange C
1.4301 (1:1)



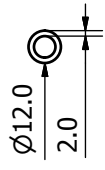
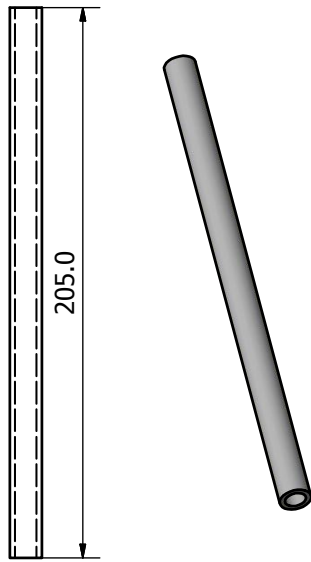
Evaporator Connector
OFHC-Cu (2:1) 4 pieces



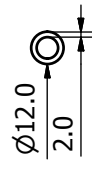
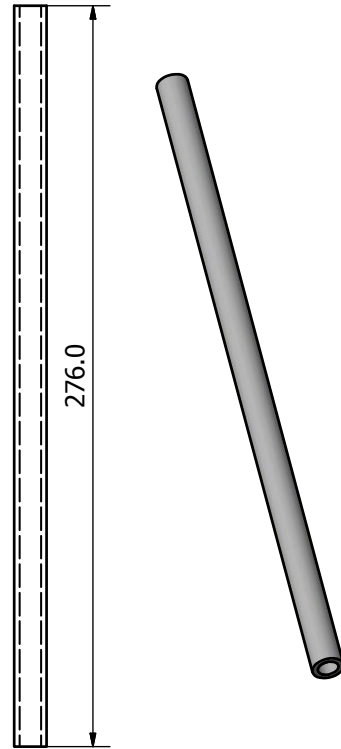
Evaporator Crucible A
1.4541 (2:1)



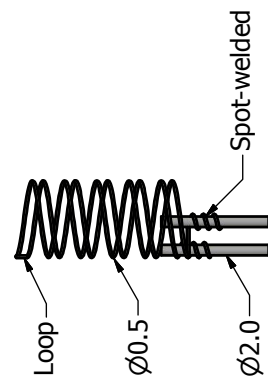
Evaporator Crucible B
1.4541 (1:2)

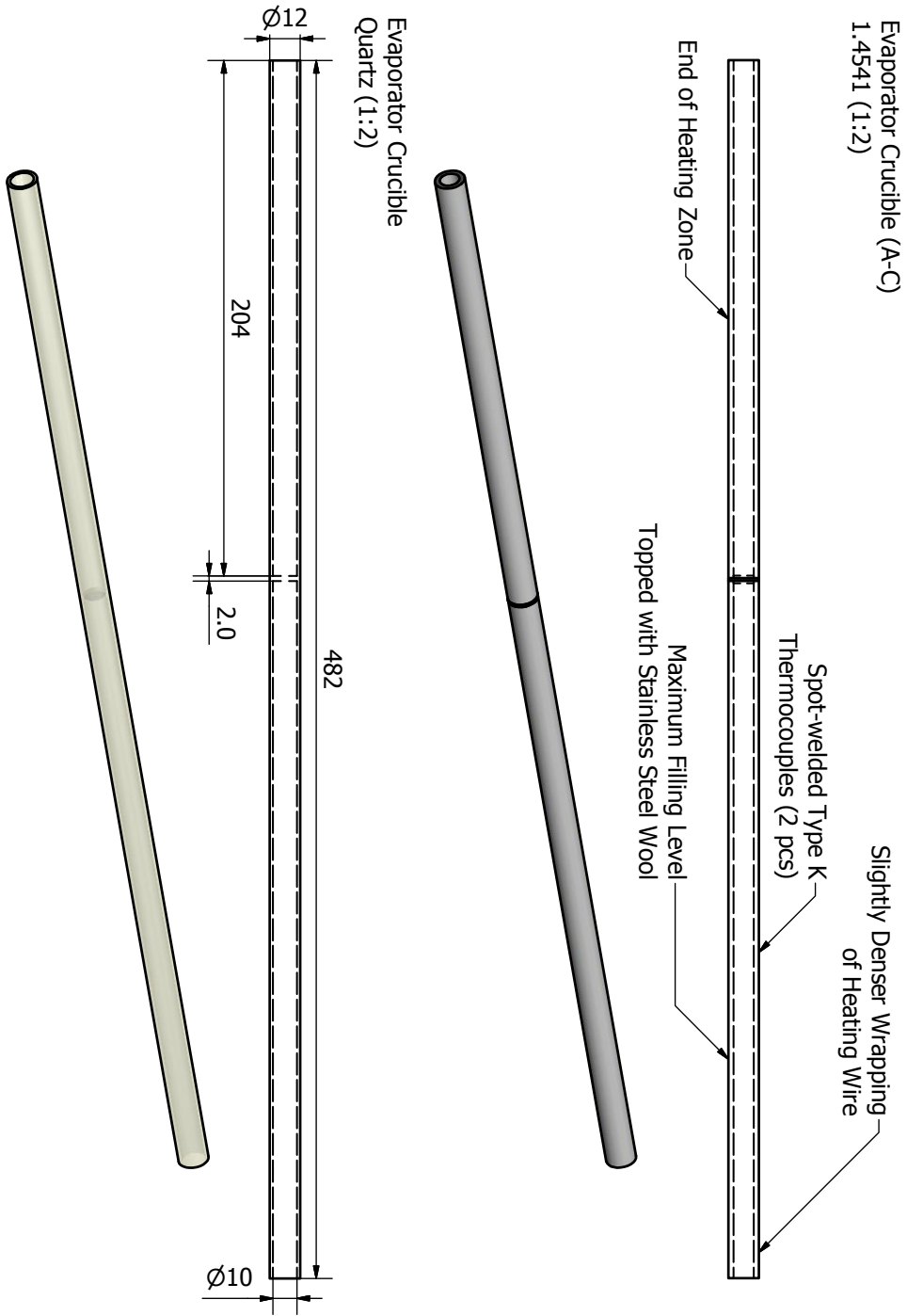


Evaporator Crucible C
1.4541 (1:2)

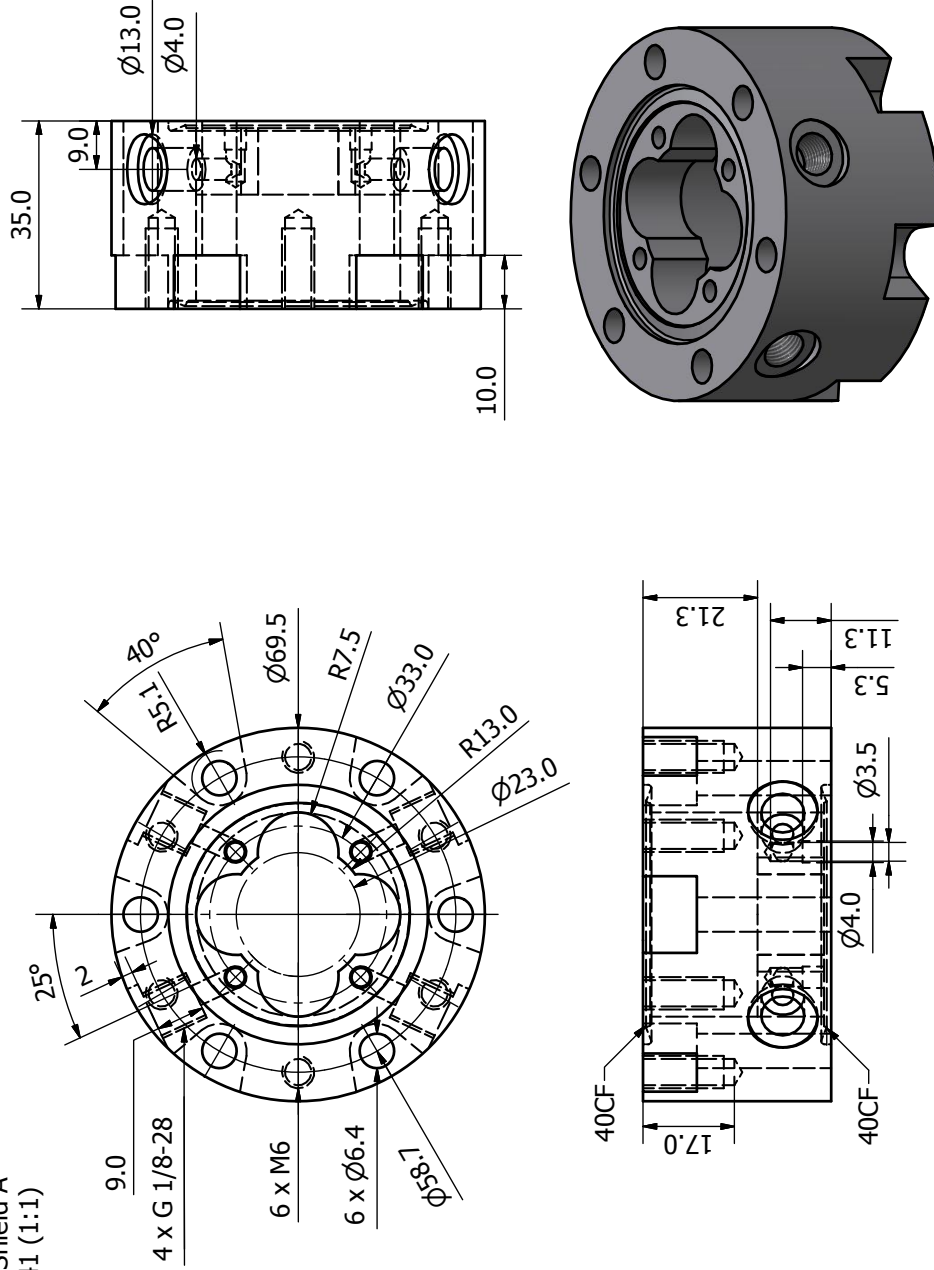


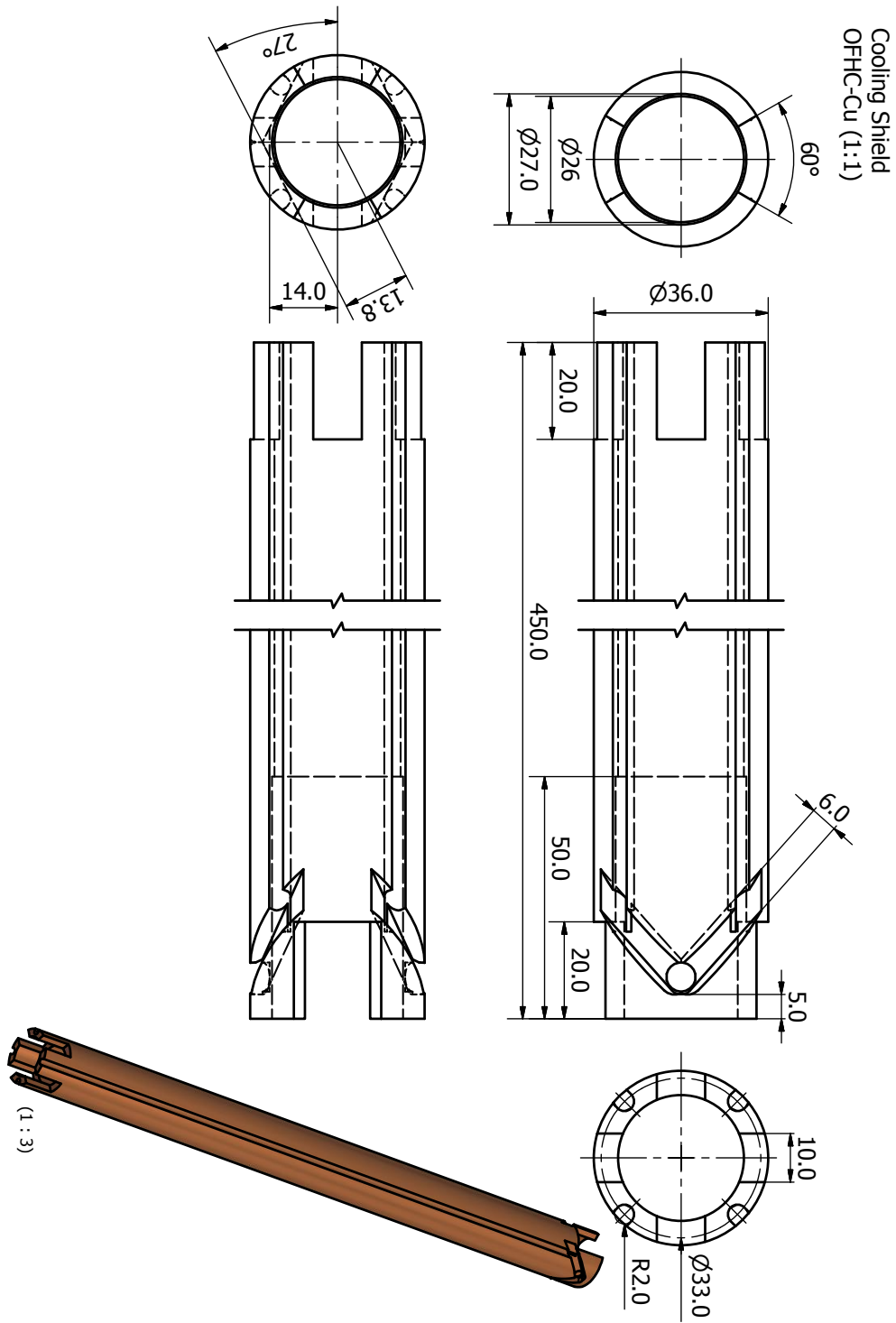
Filament
Tantalum (schematic)



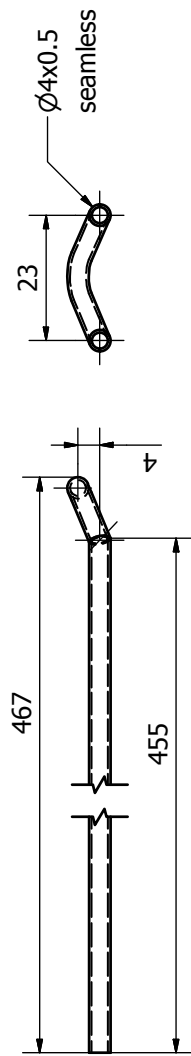


Heat Shield A
1.4541 (1:1)

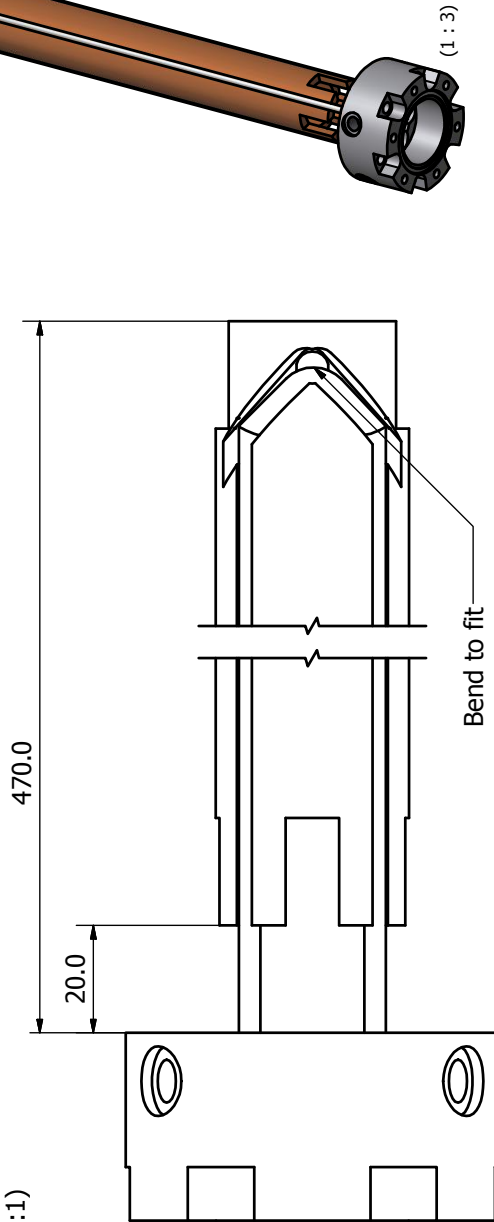




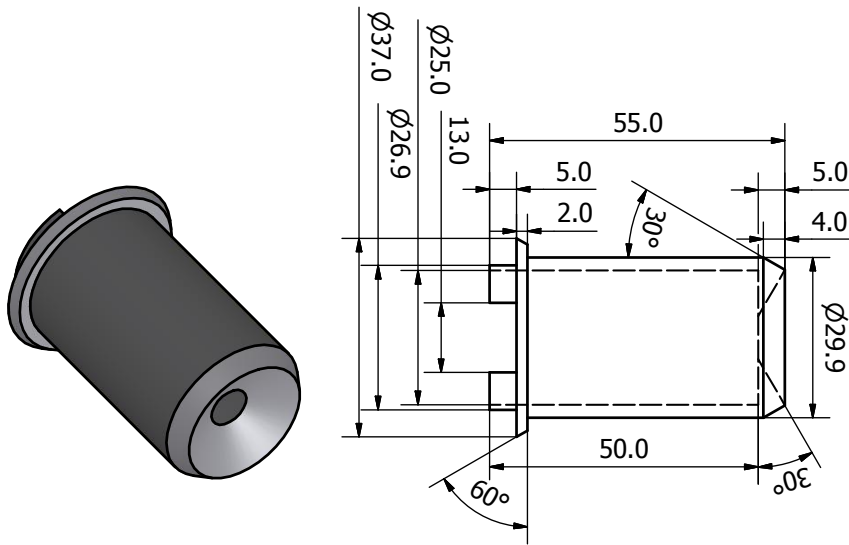
Heat Shield C
1.4541 (1:1)



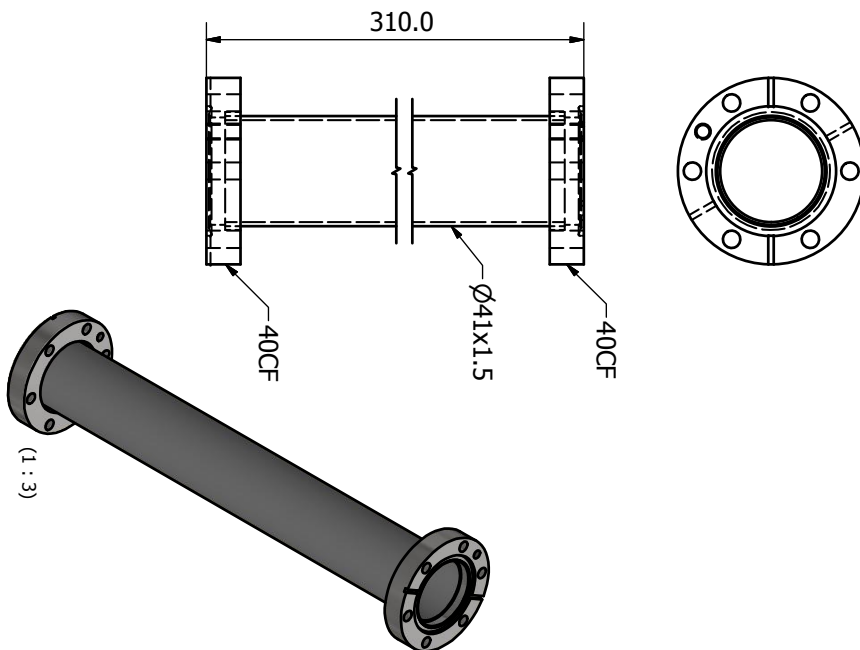
Heat Shield Assembly
(1:1)



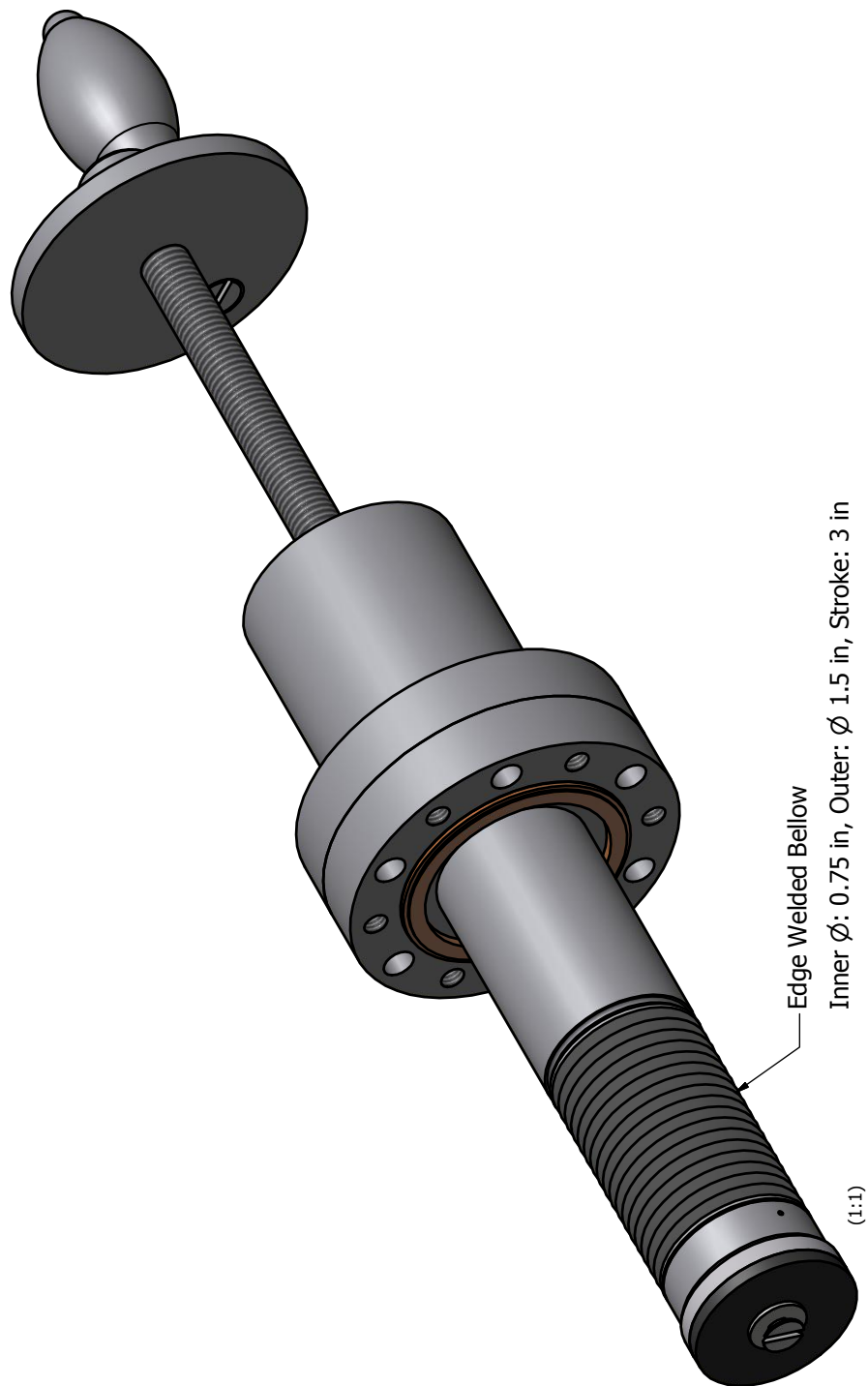
Heat Shield Cap
1.4541 (1:1)

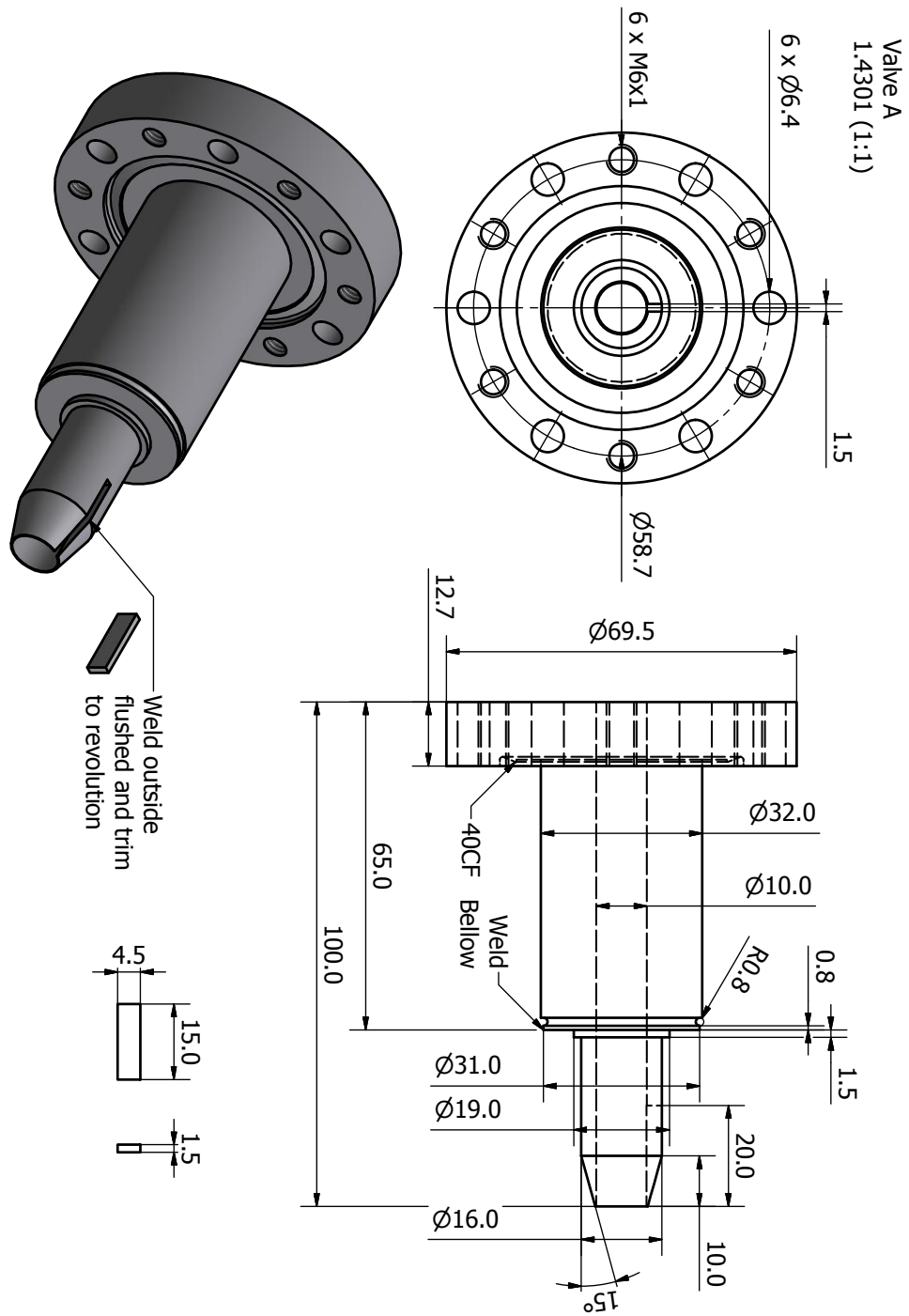


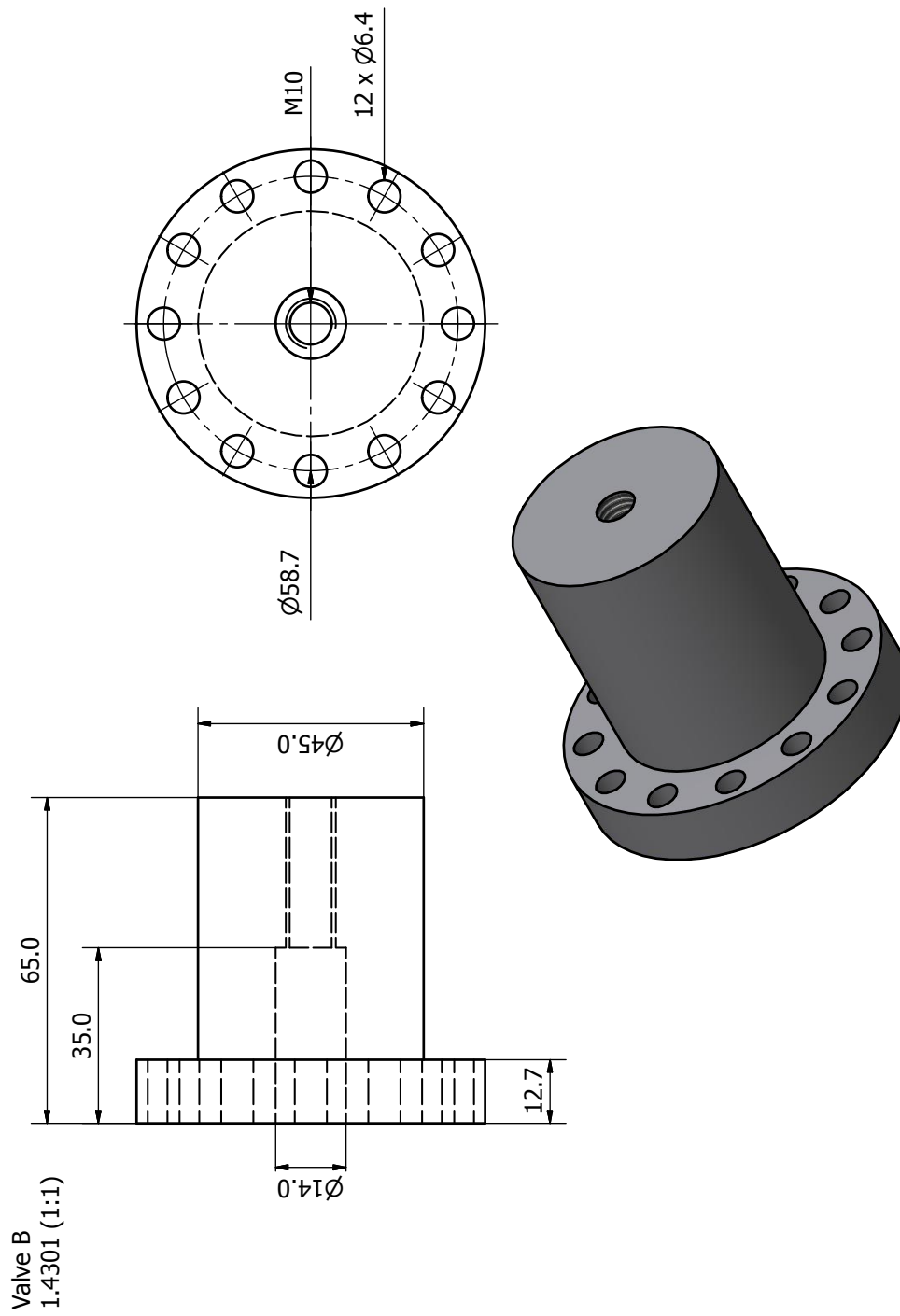
Mounting Tube
1.4301 (1:2)

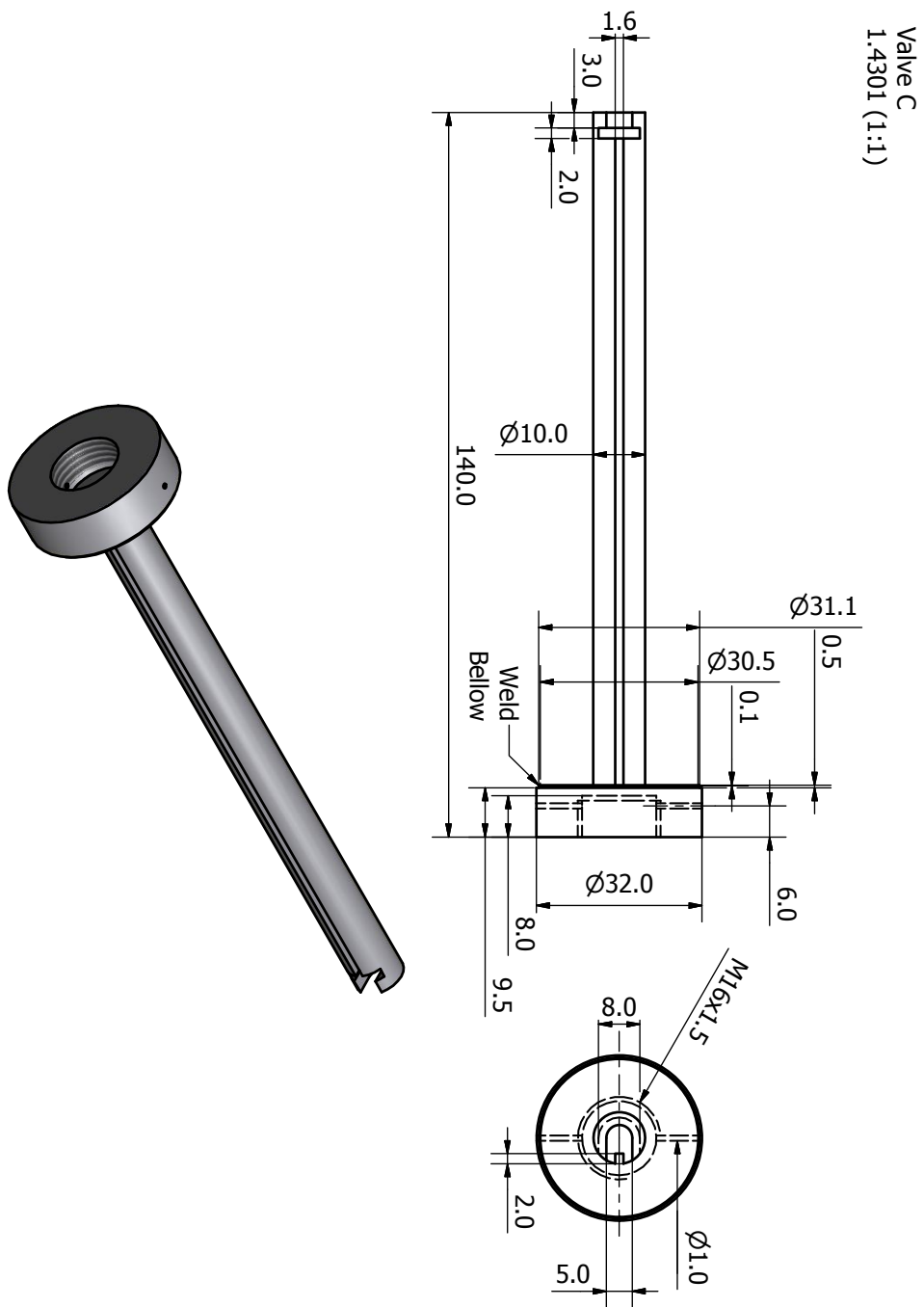


B.1.2 Internal Valve

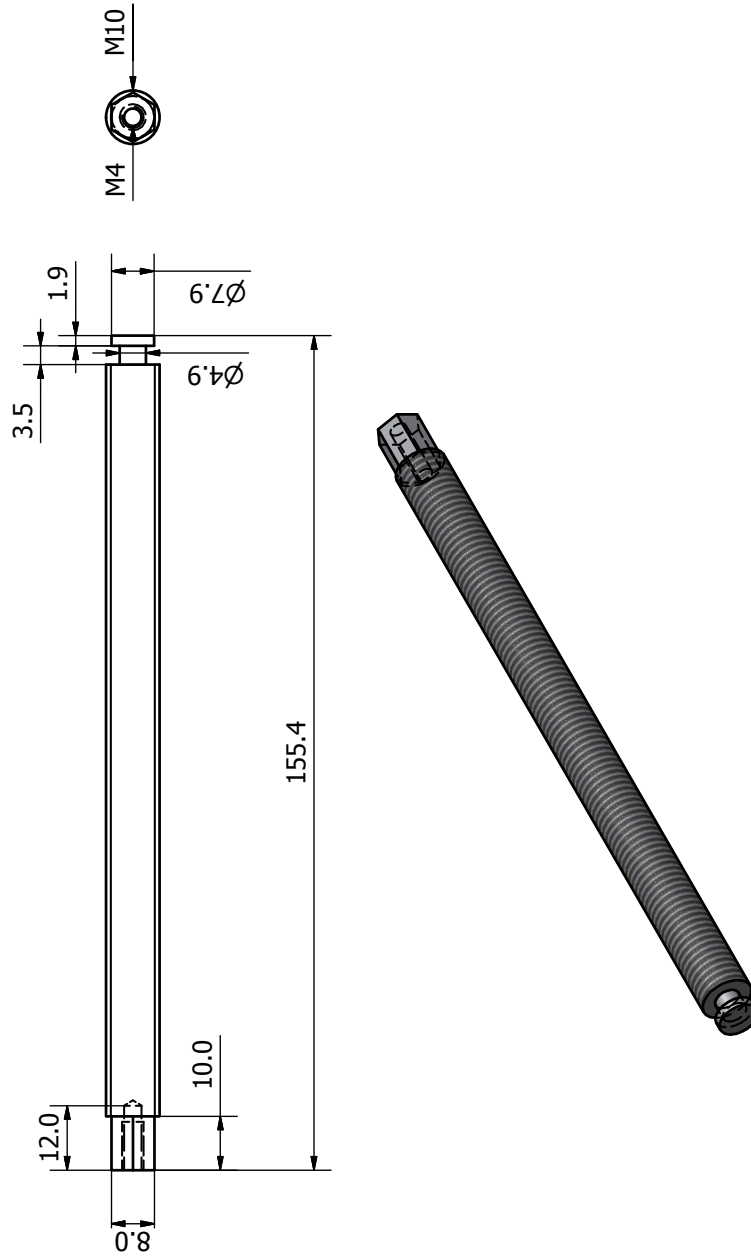




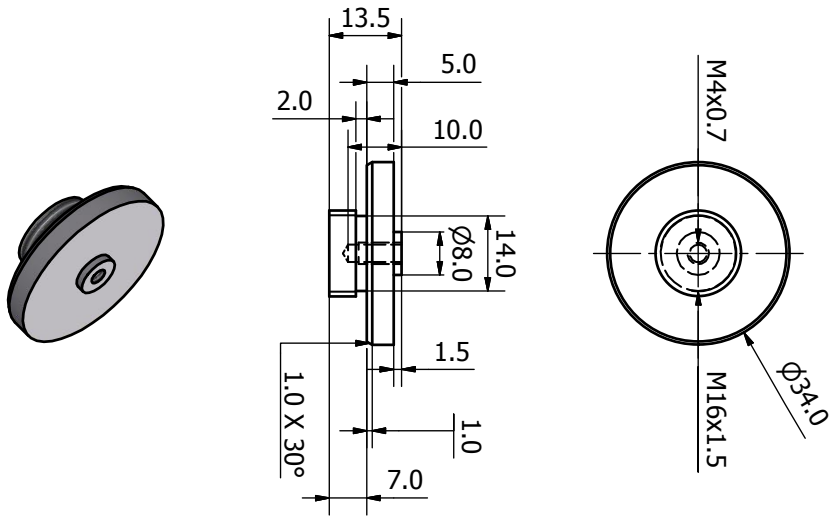




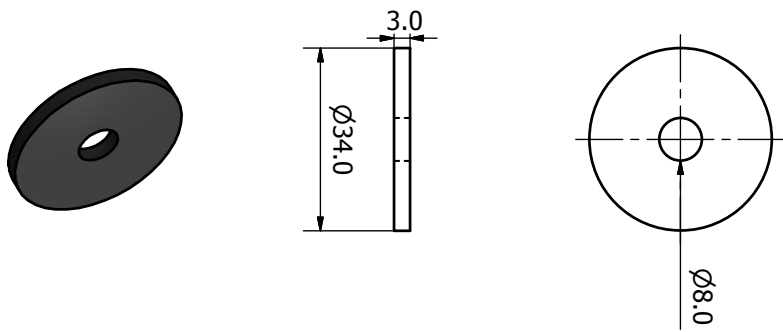
Valve D
Threaded Rod Stainless Steel (1:1)



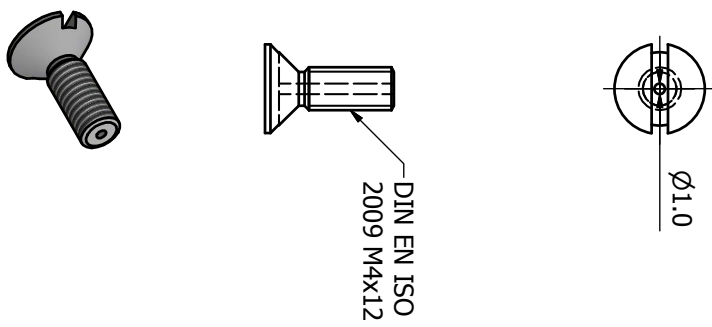
Valve E
1.4301 (1:1)

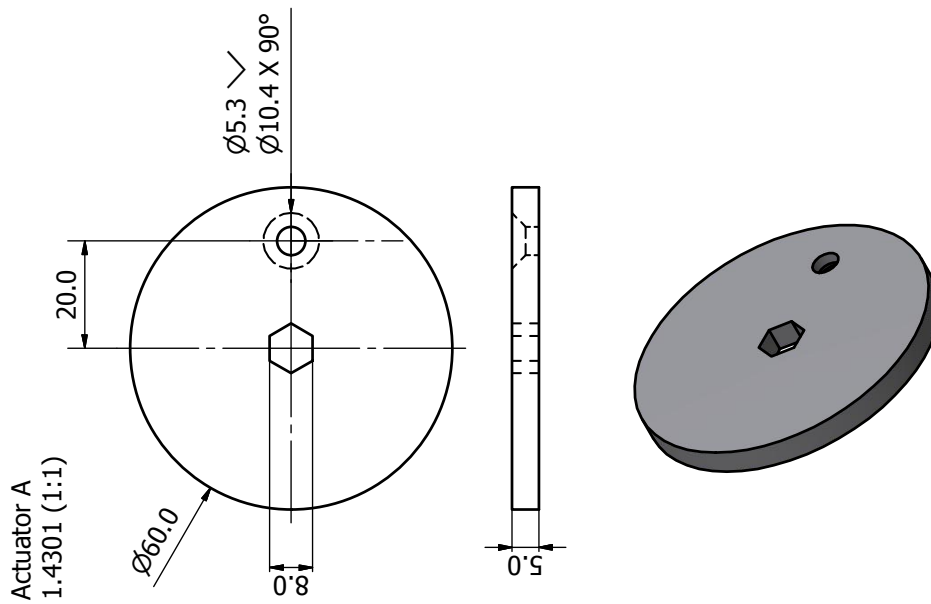
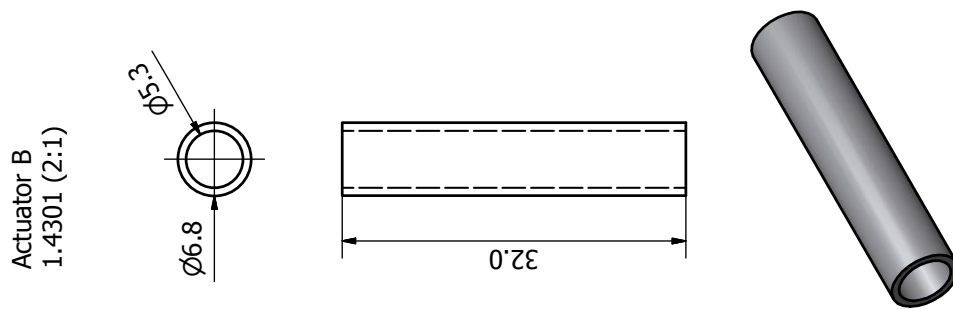
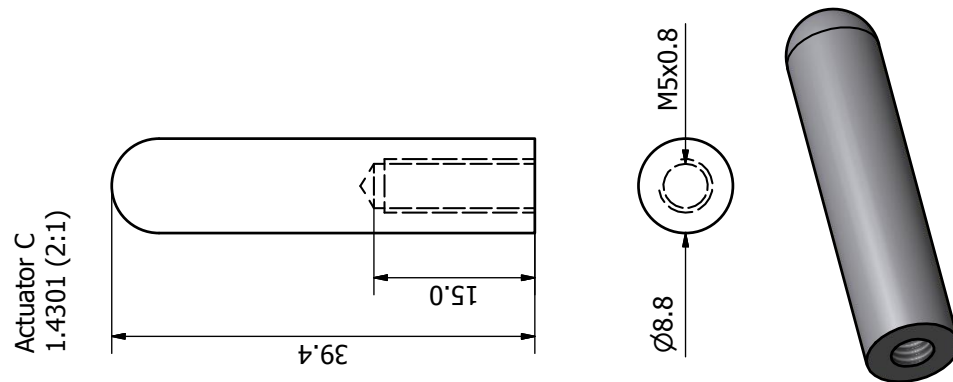


Valve F
Viton (1:1)

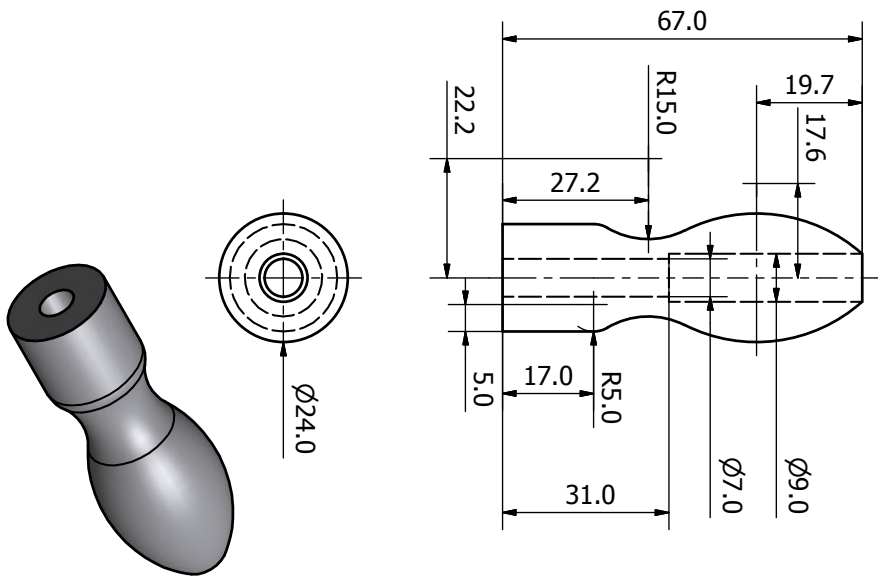


Valve Screw
Stainless Steel (2:1)

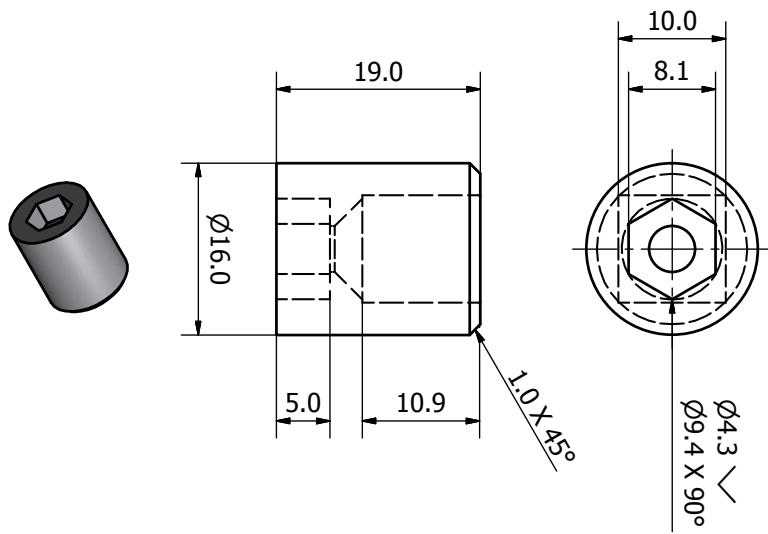




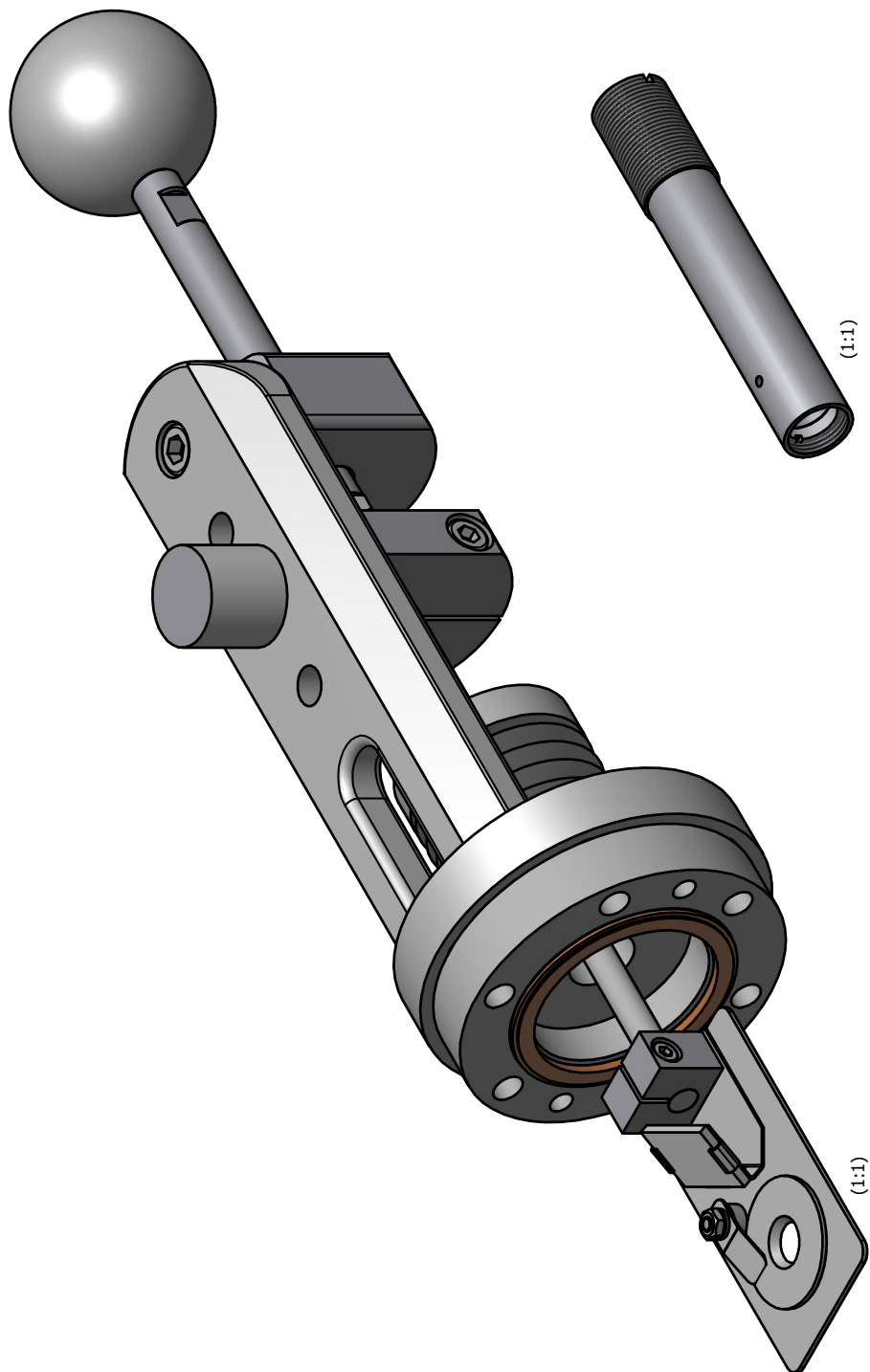
Actuator D
1.4301 (1:1)

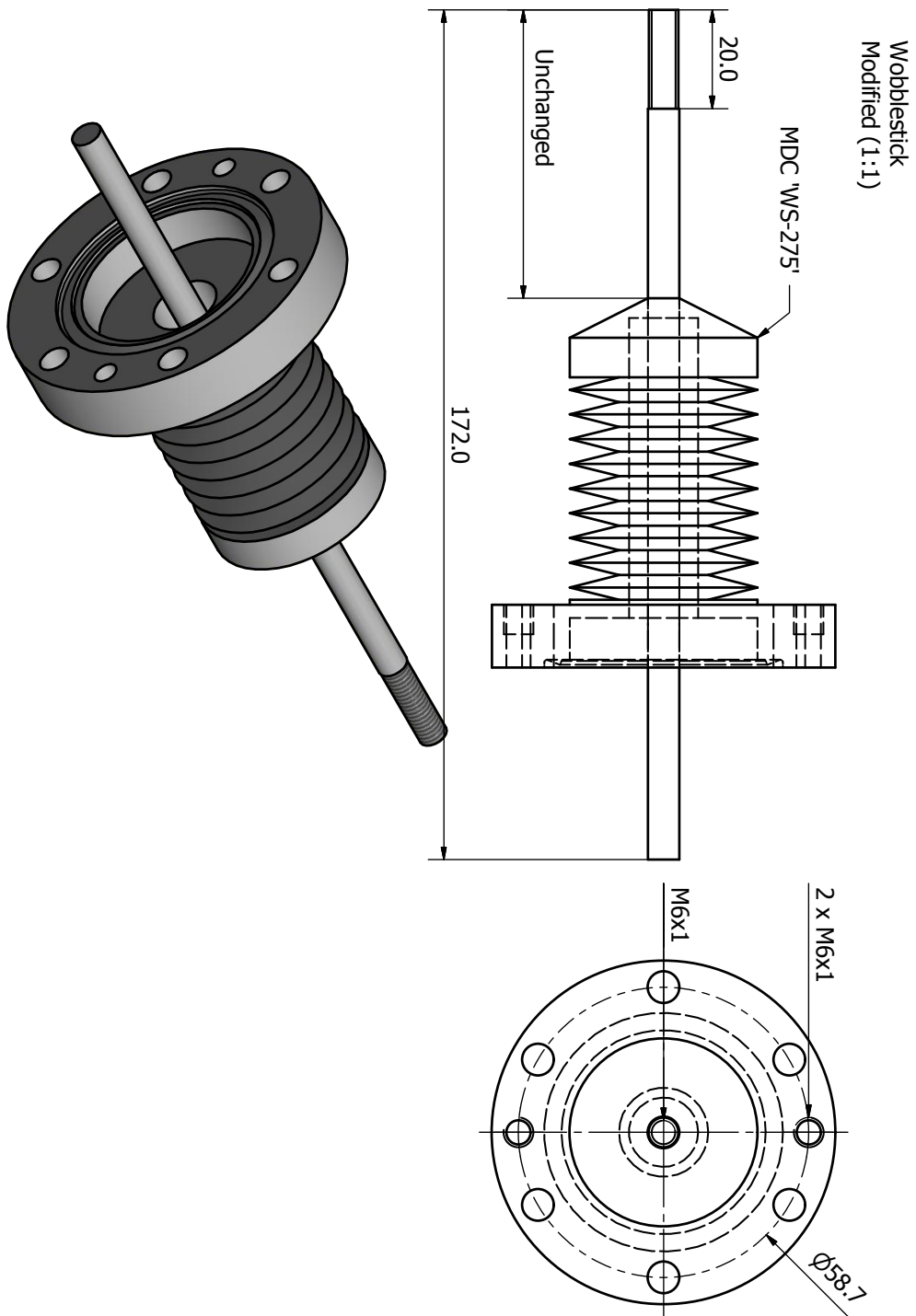


Actuator E
1.4301 (2:1)

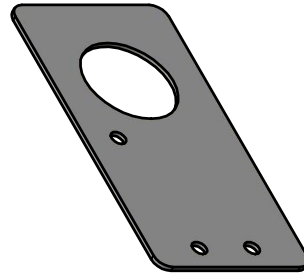
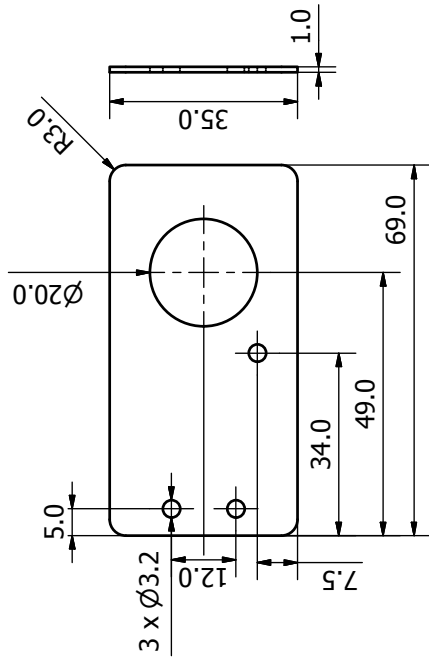


B.1.3 Optics Stage

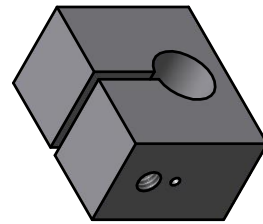
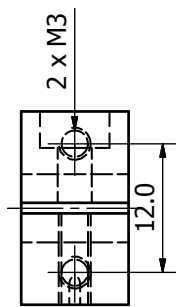
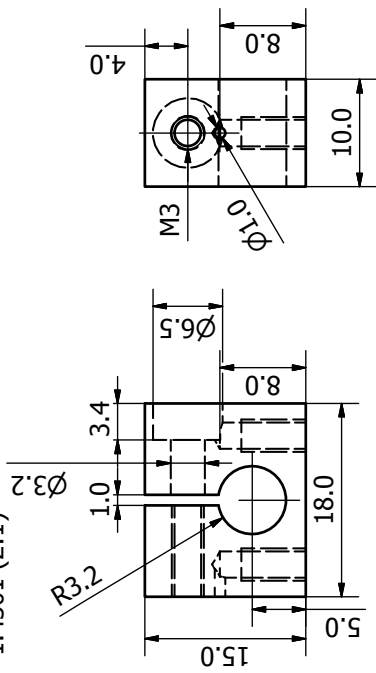




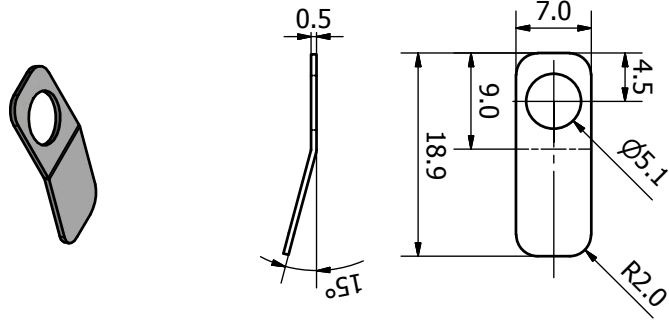
Orifice Holder A
1.4301 (1:1)



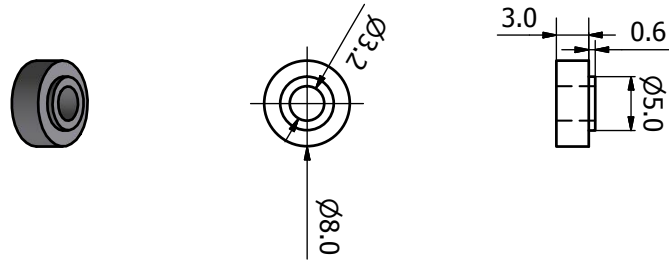
Mount
1.4301 (2:1)



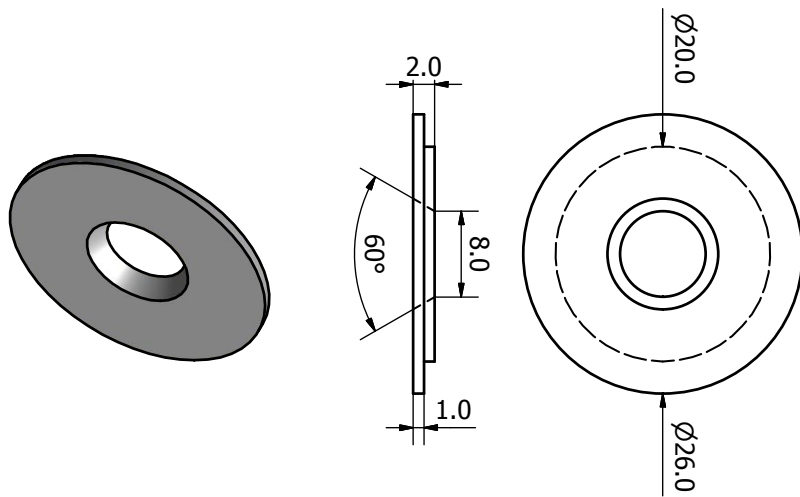
Orifice Holder B
1.4301 (2:1)



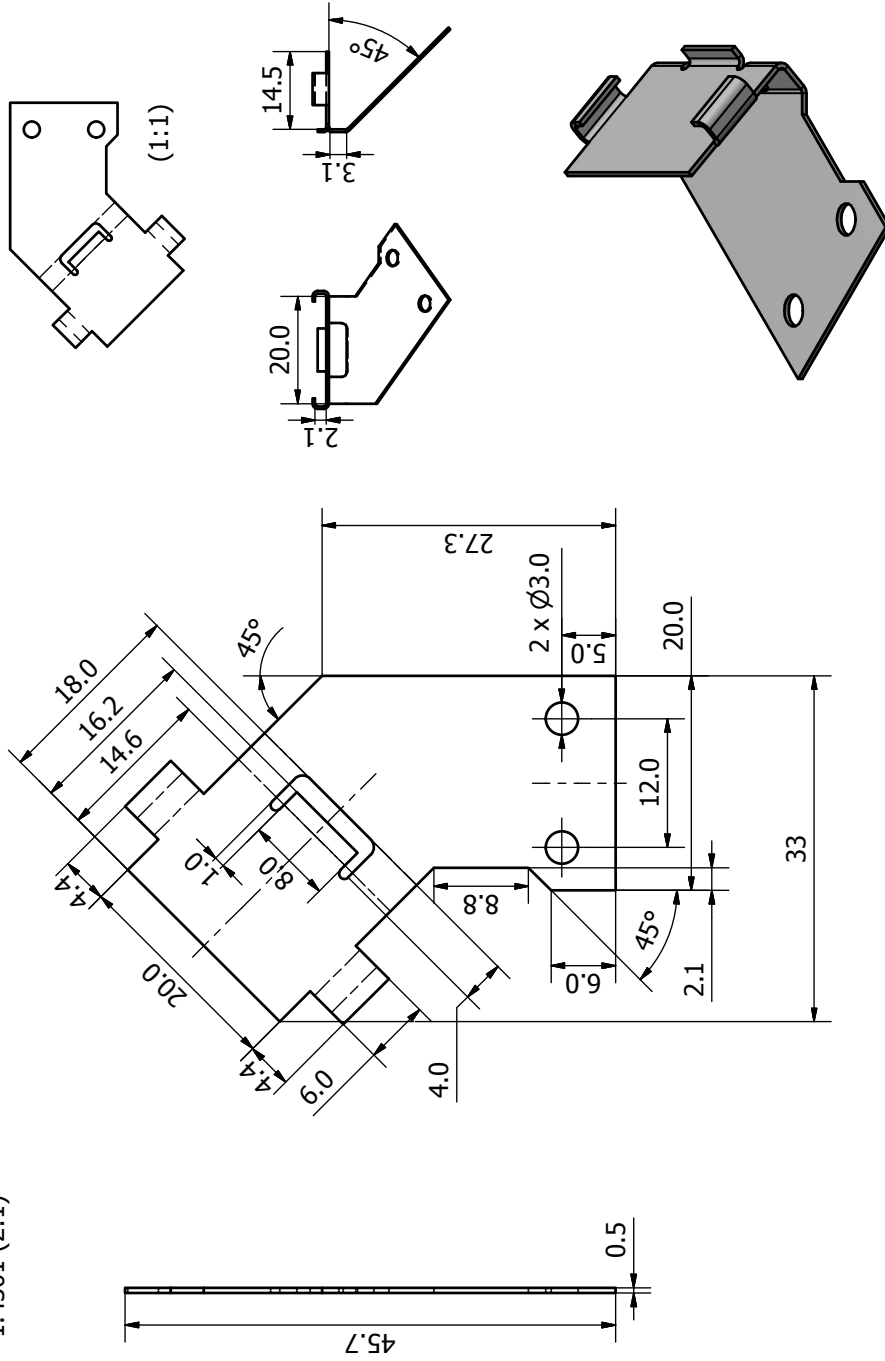
Orifice Holder C
1.4301 (2:1)



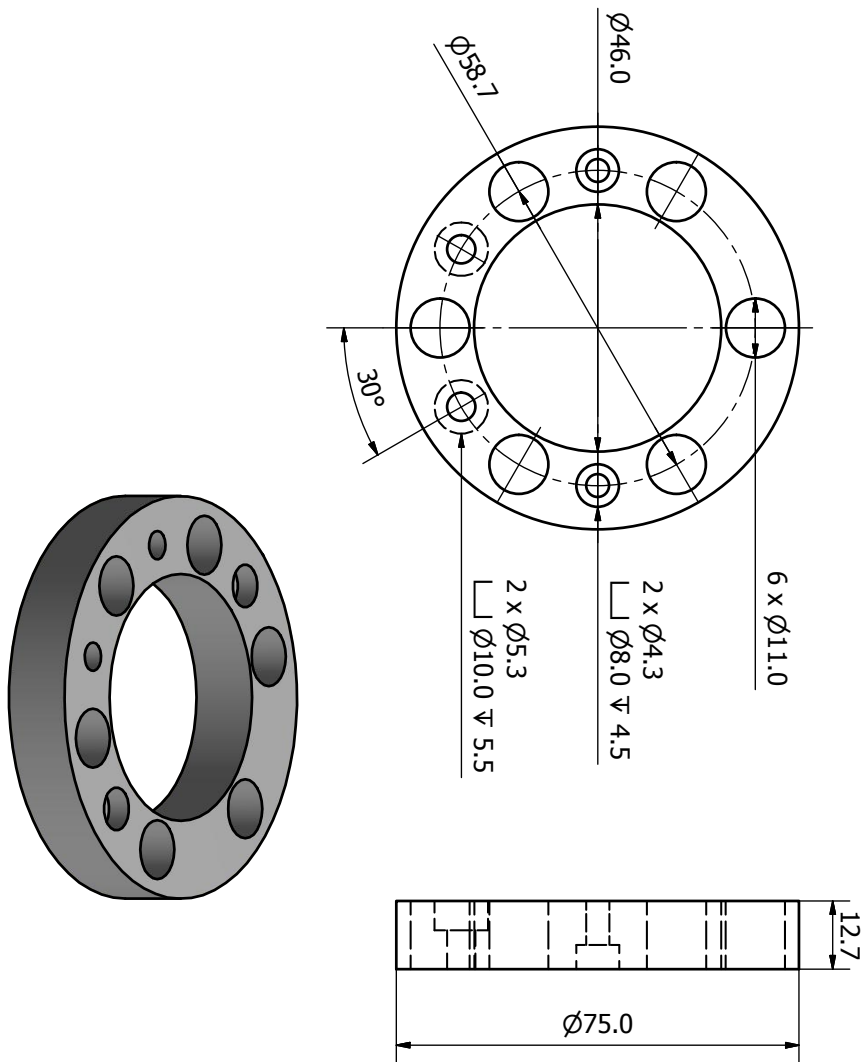
Orifice
1.4541 (2:1) 5 pieces



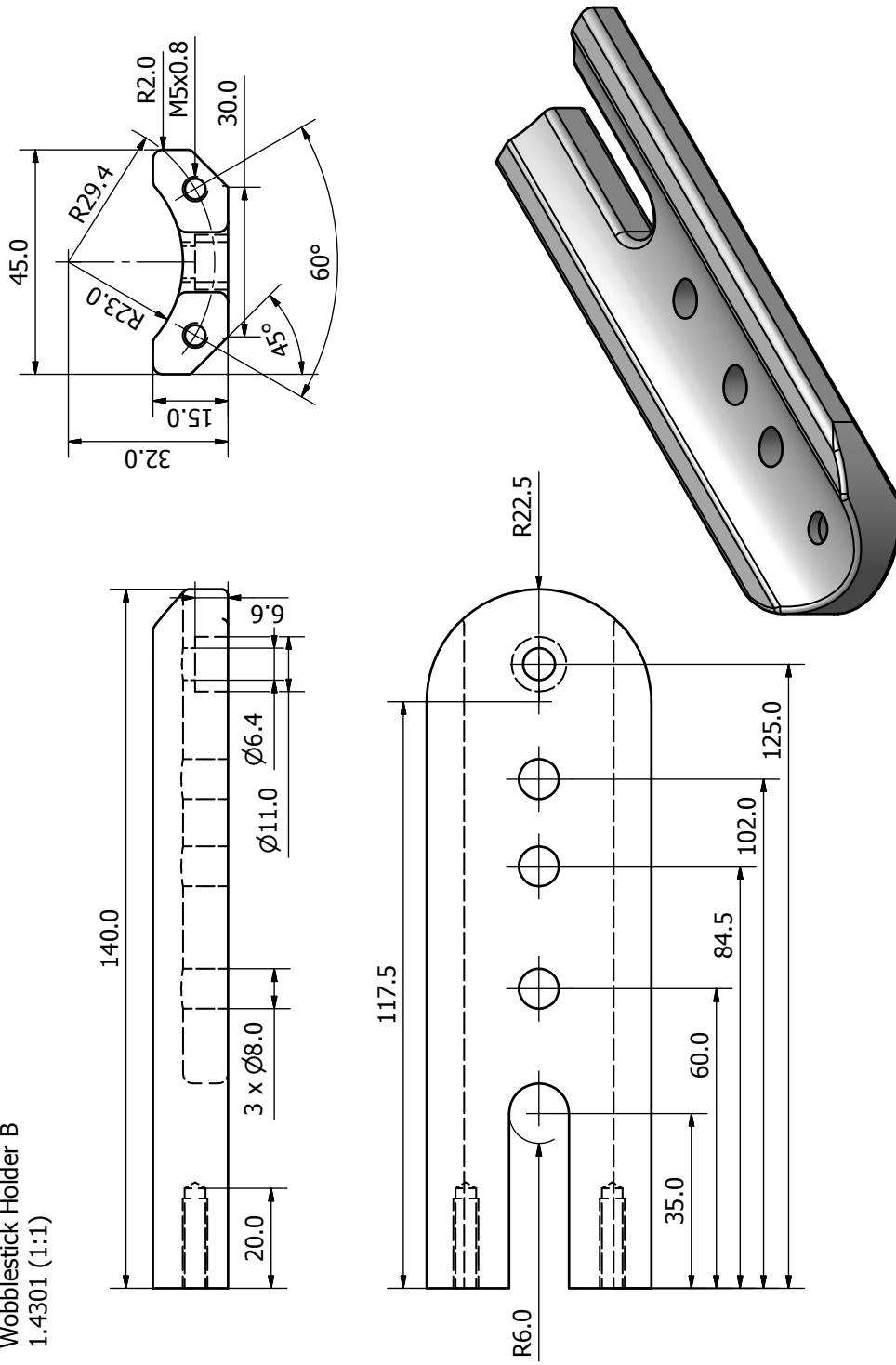
Orifice Holder B
1.4301 (2:1)



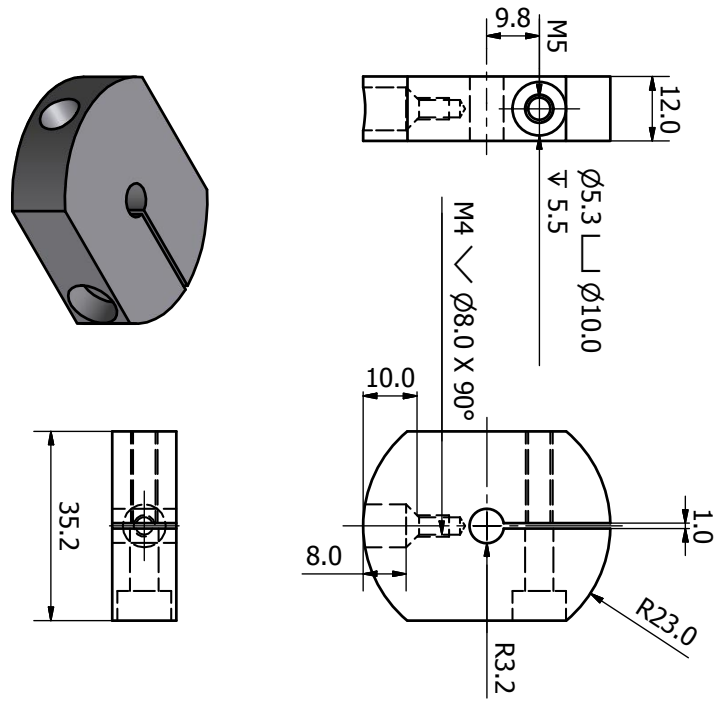
Wobblestick Holder A
1.4301 (1:1)



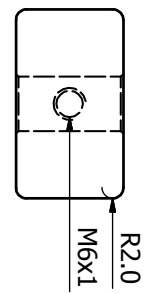
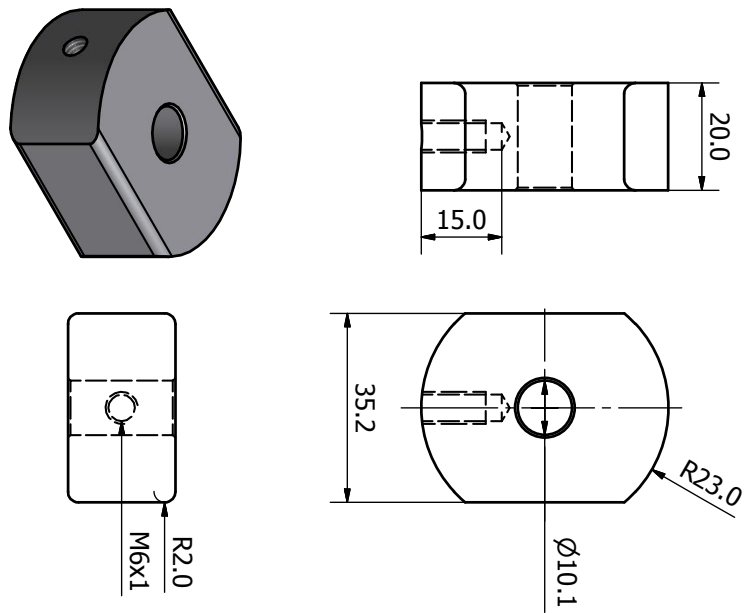
Wobblestick Holder B
1.4301 (1:1)

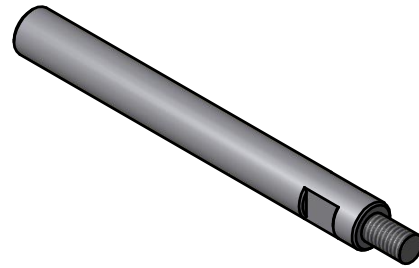
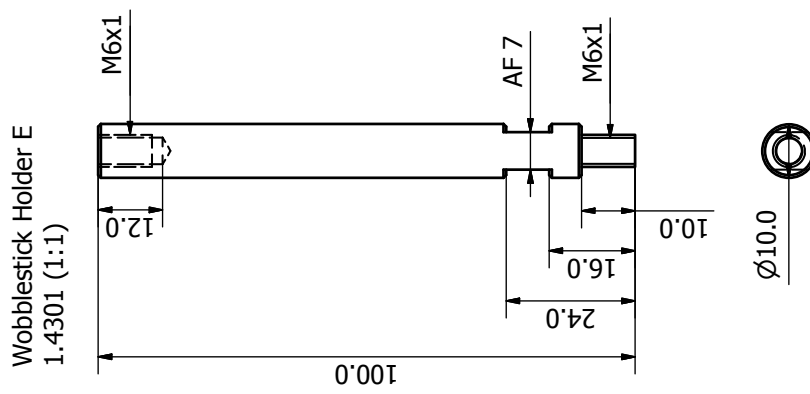
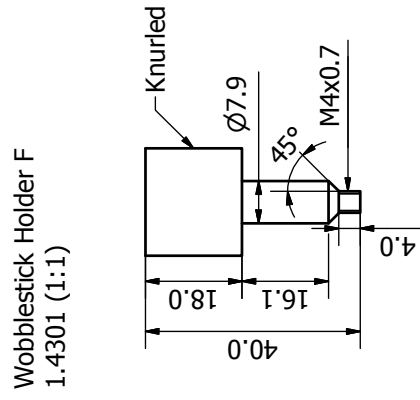


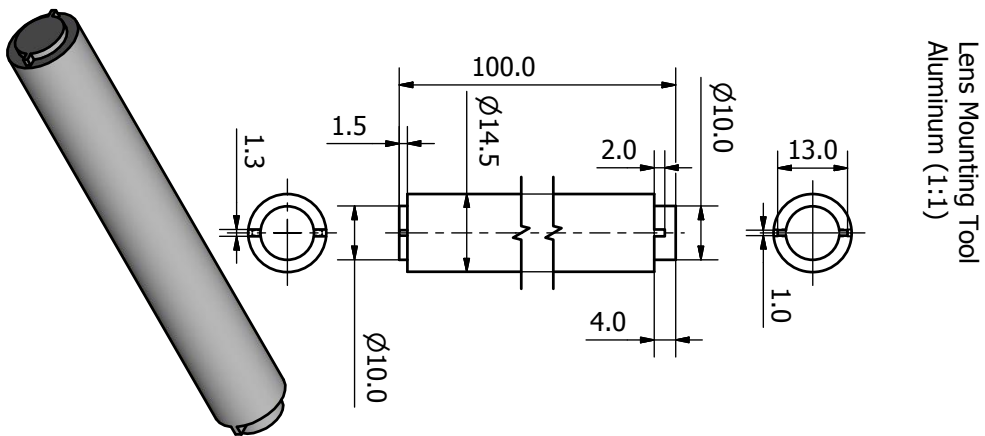
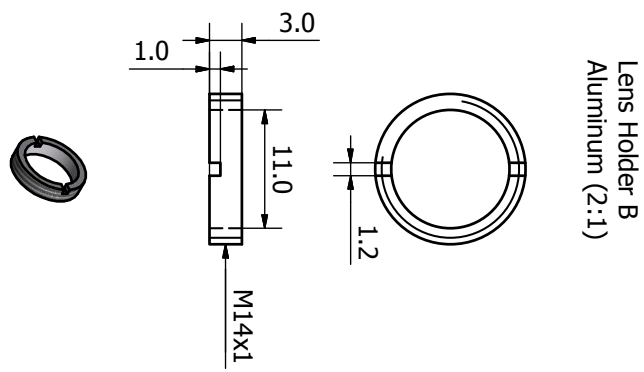
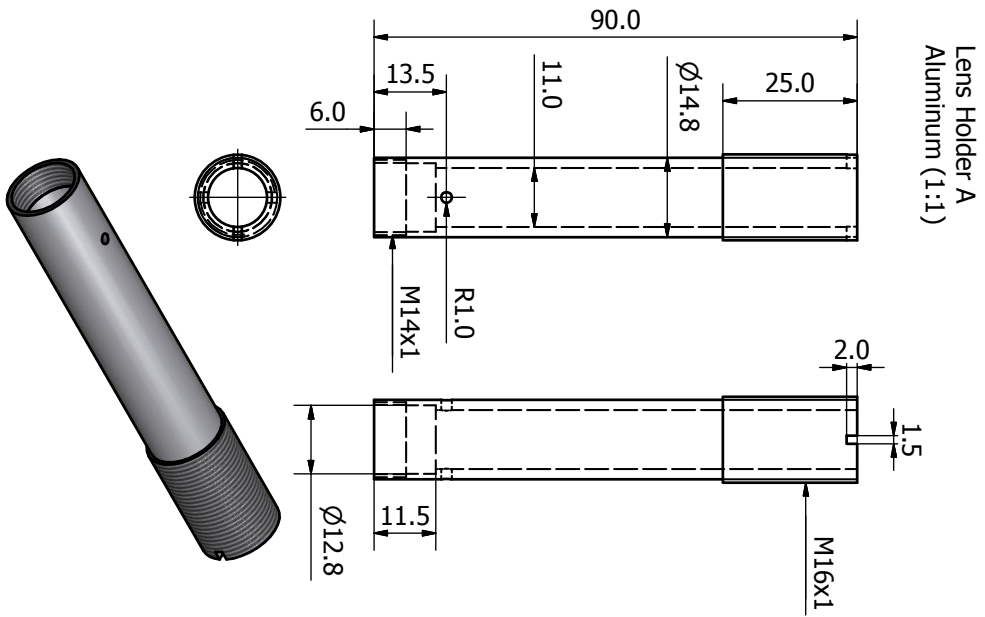
Wobblestick Holder C
1.4301 (1:1)



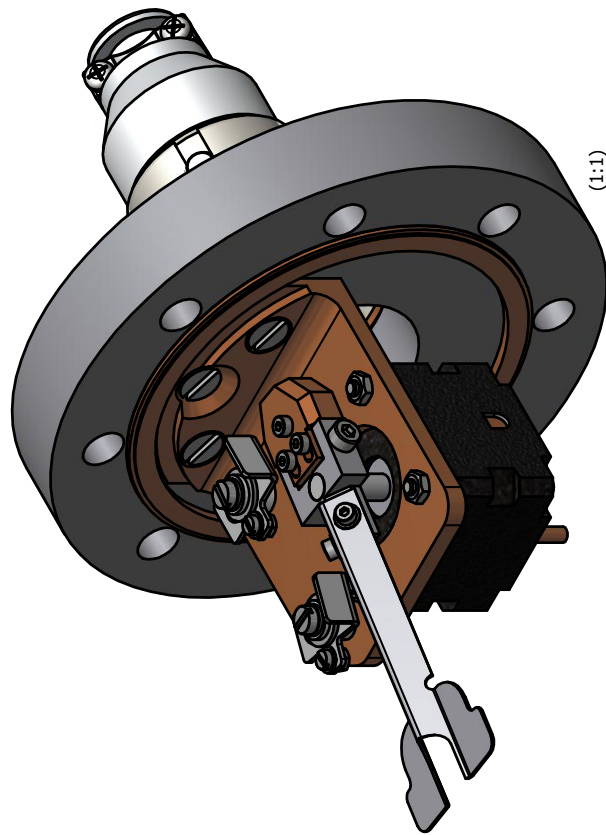
Wobblestick Holder D
1.4301 (1:1)

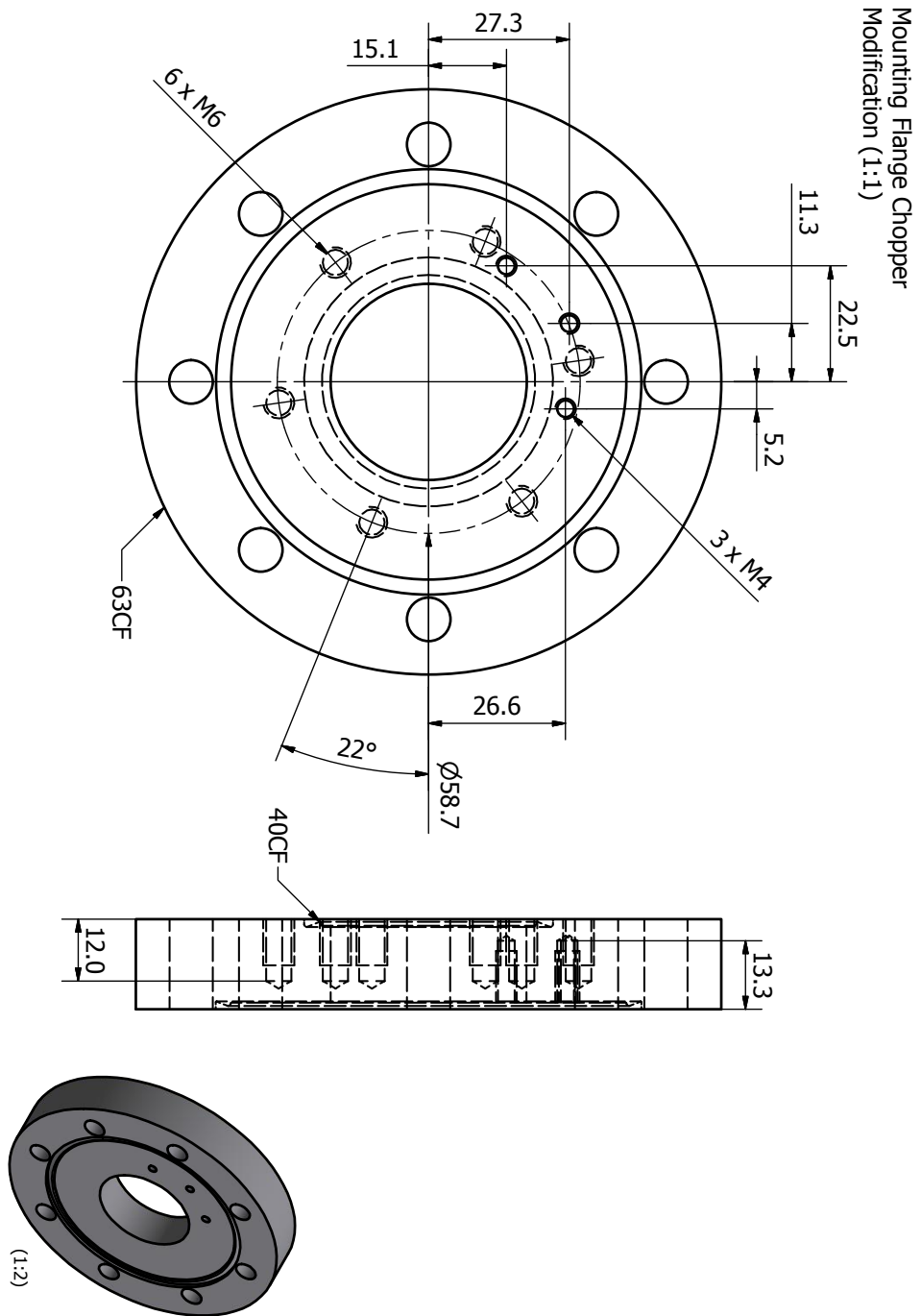




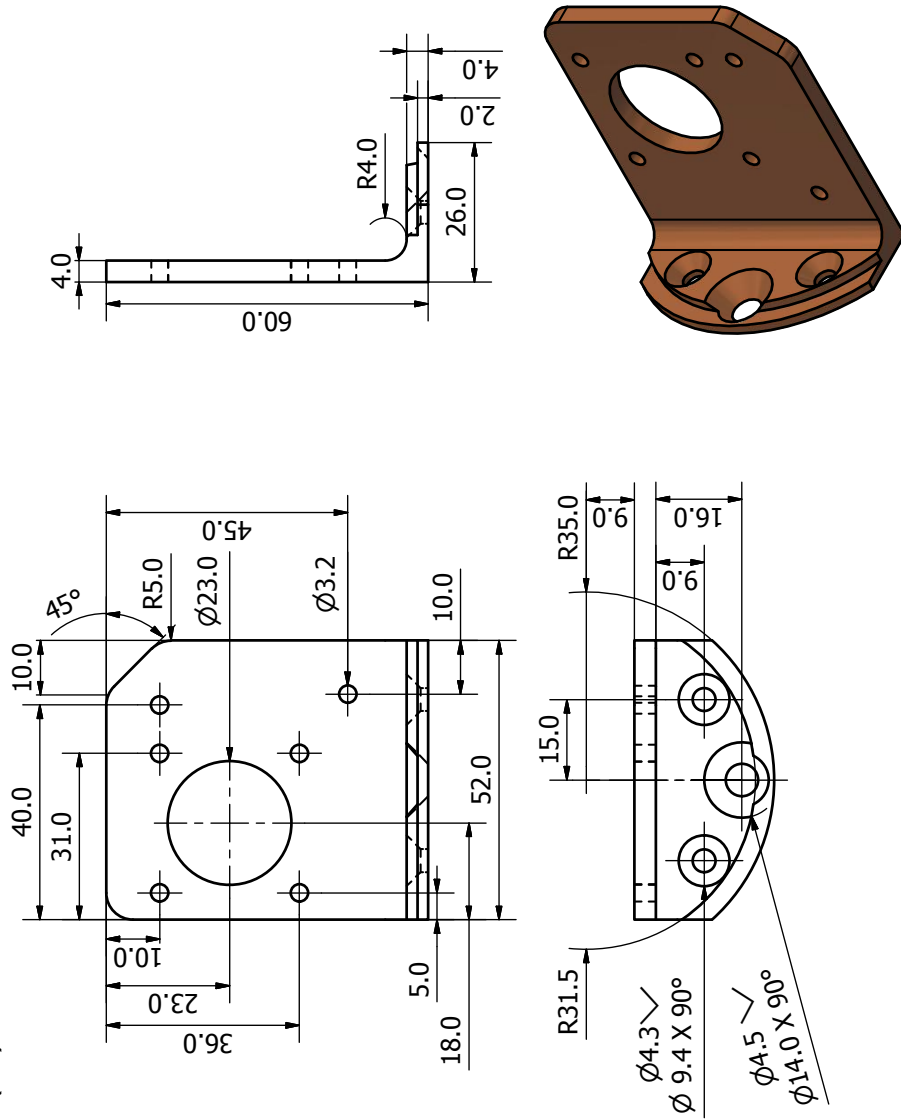


B.1.4 Beam Chopper

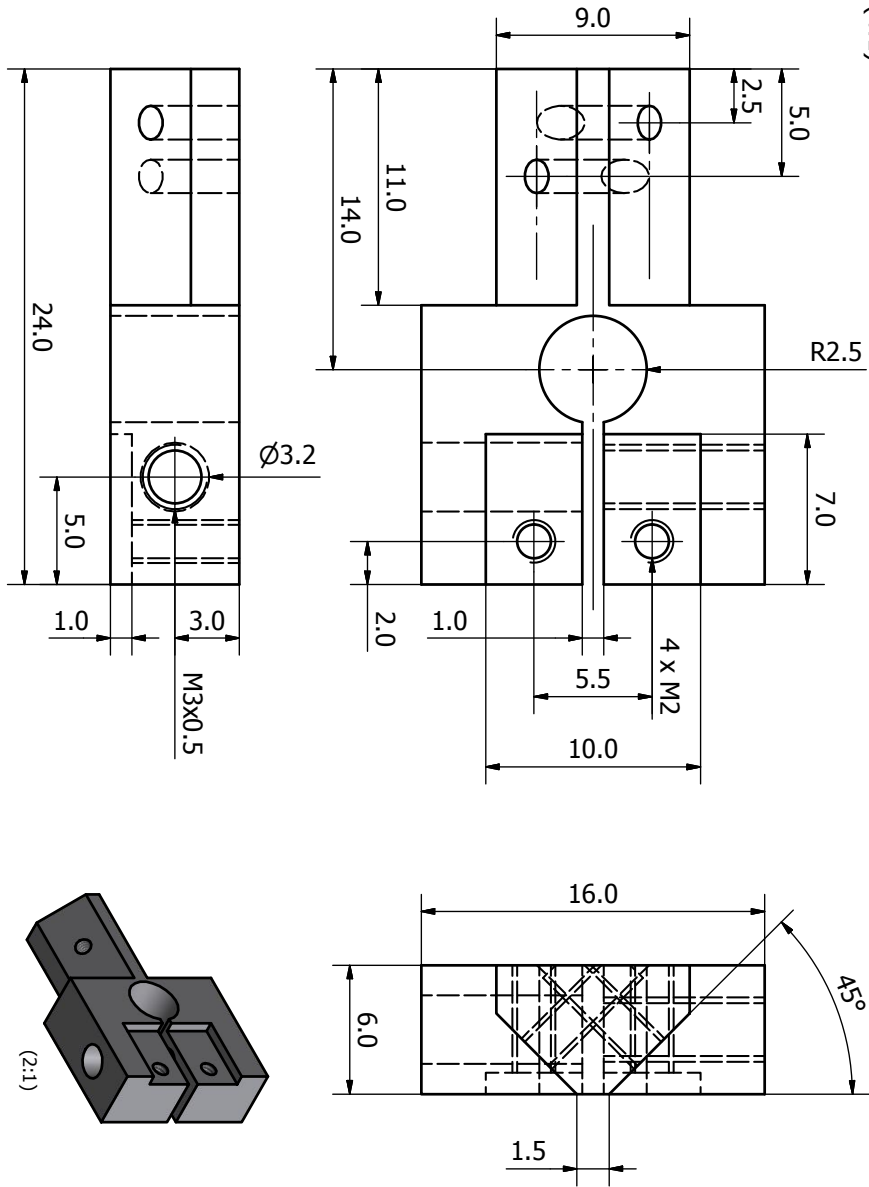




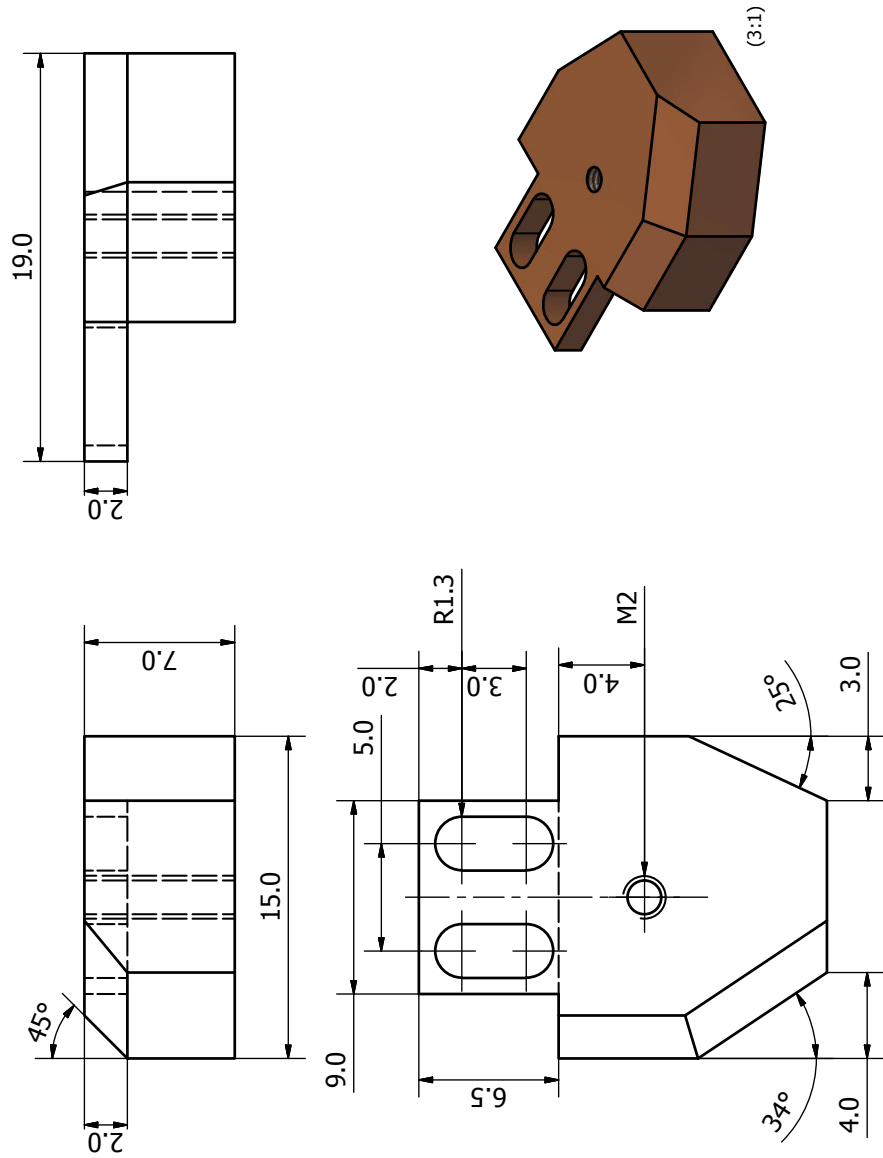
Mounting Chopper
Copper (1:1)

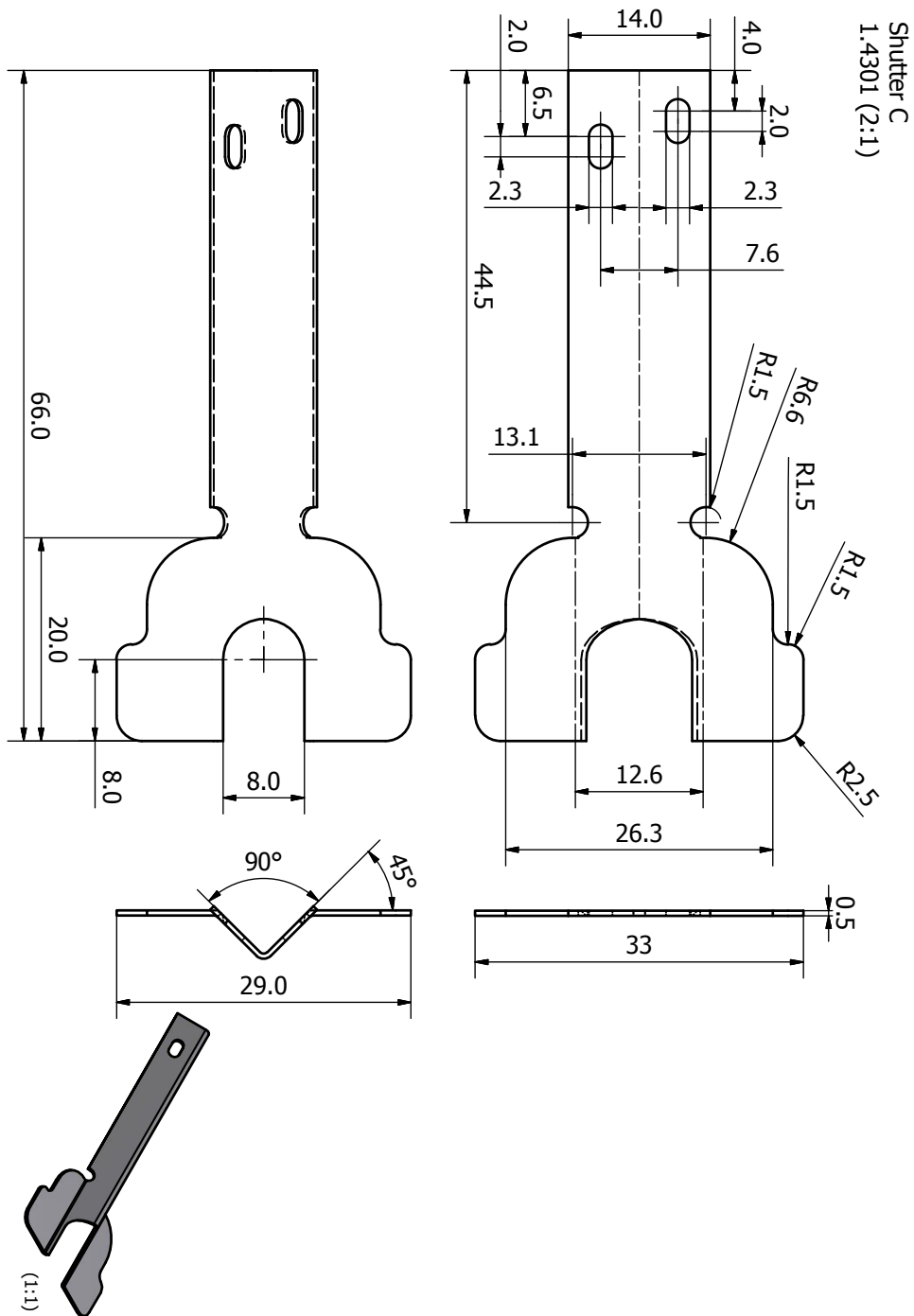


Shutter A
1.4301 (4:1)

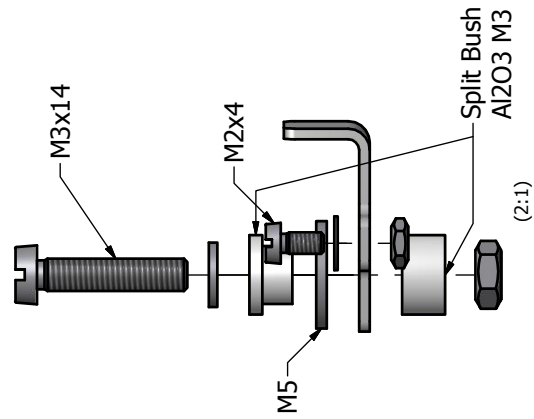
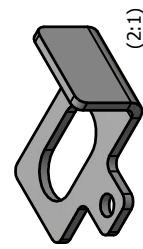
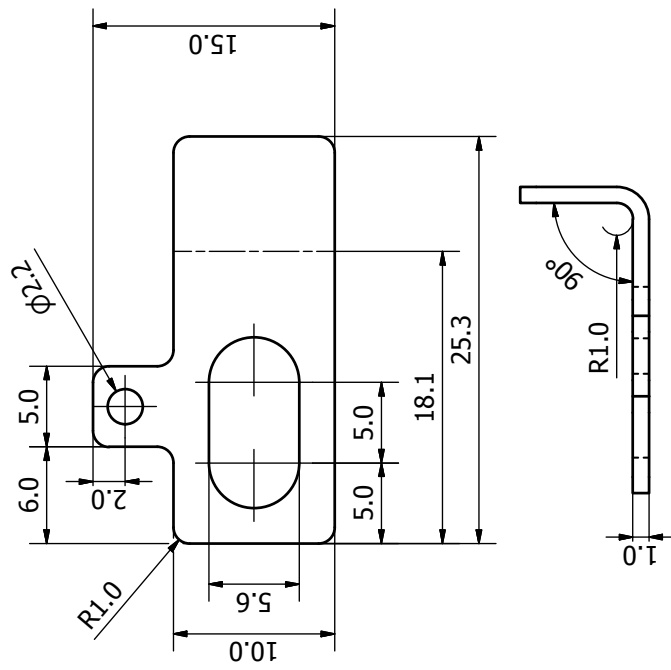


Shutter B
Copper (4:1)

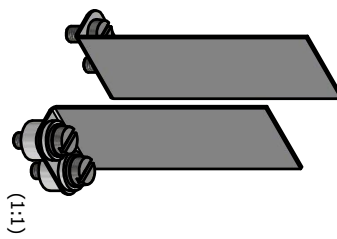
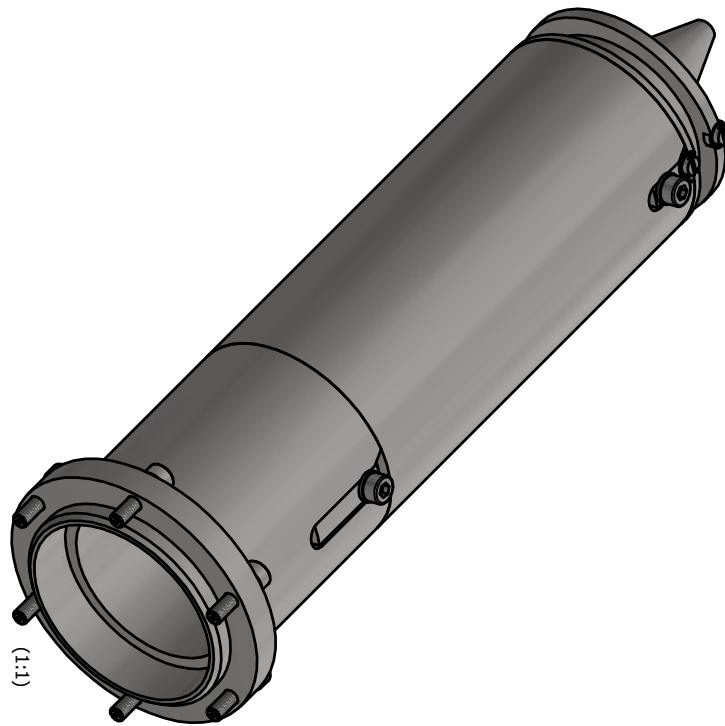


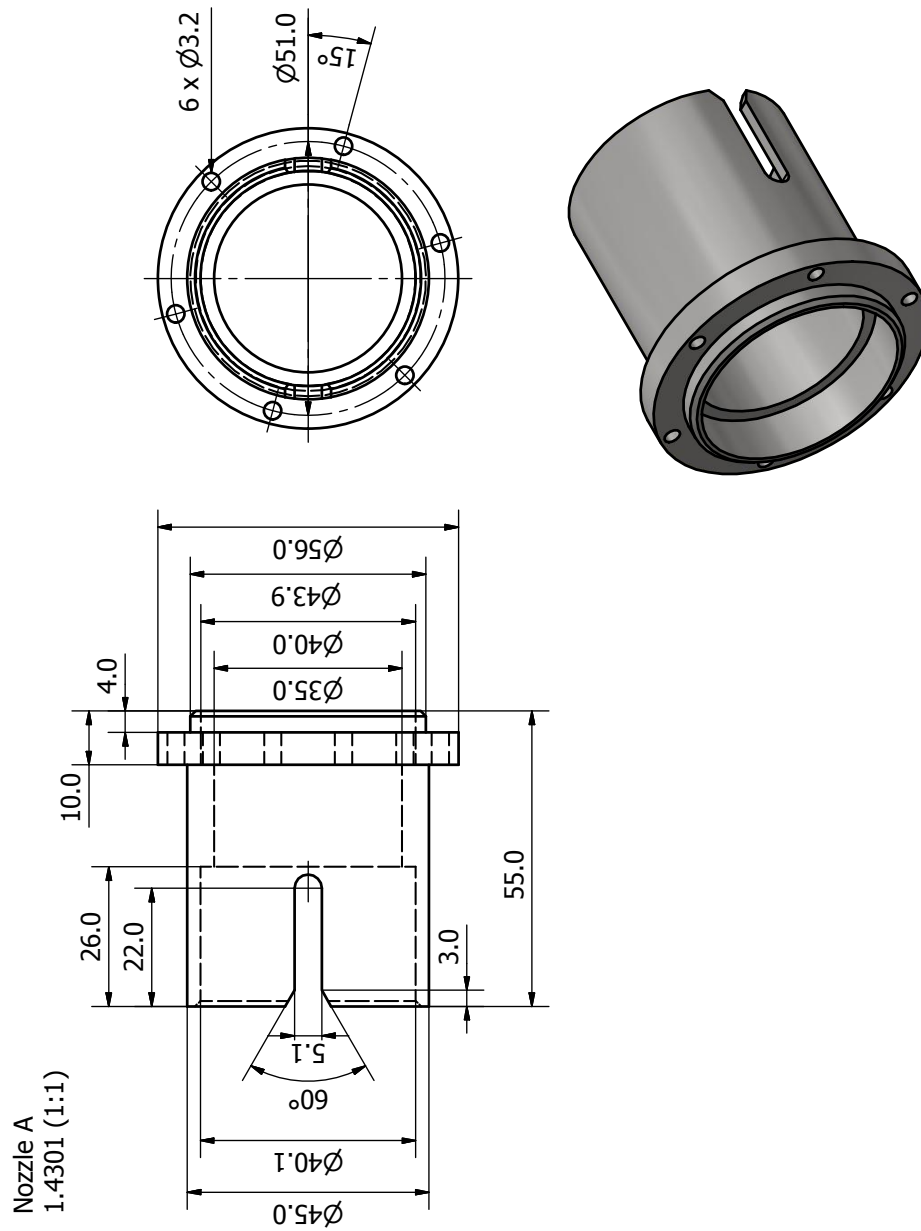


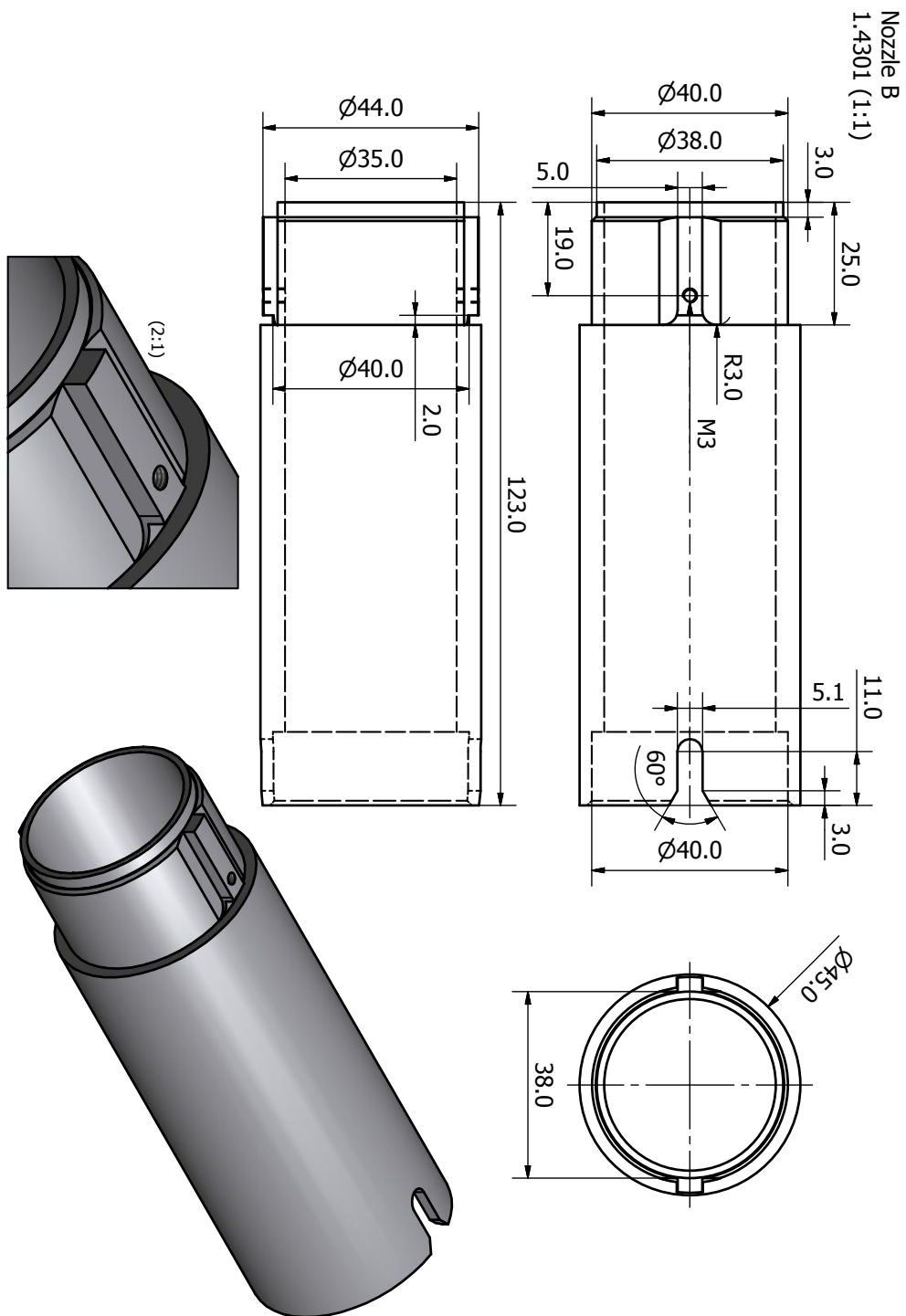
Shutter End Switch
1.4301 (3:1) 2 pieces

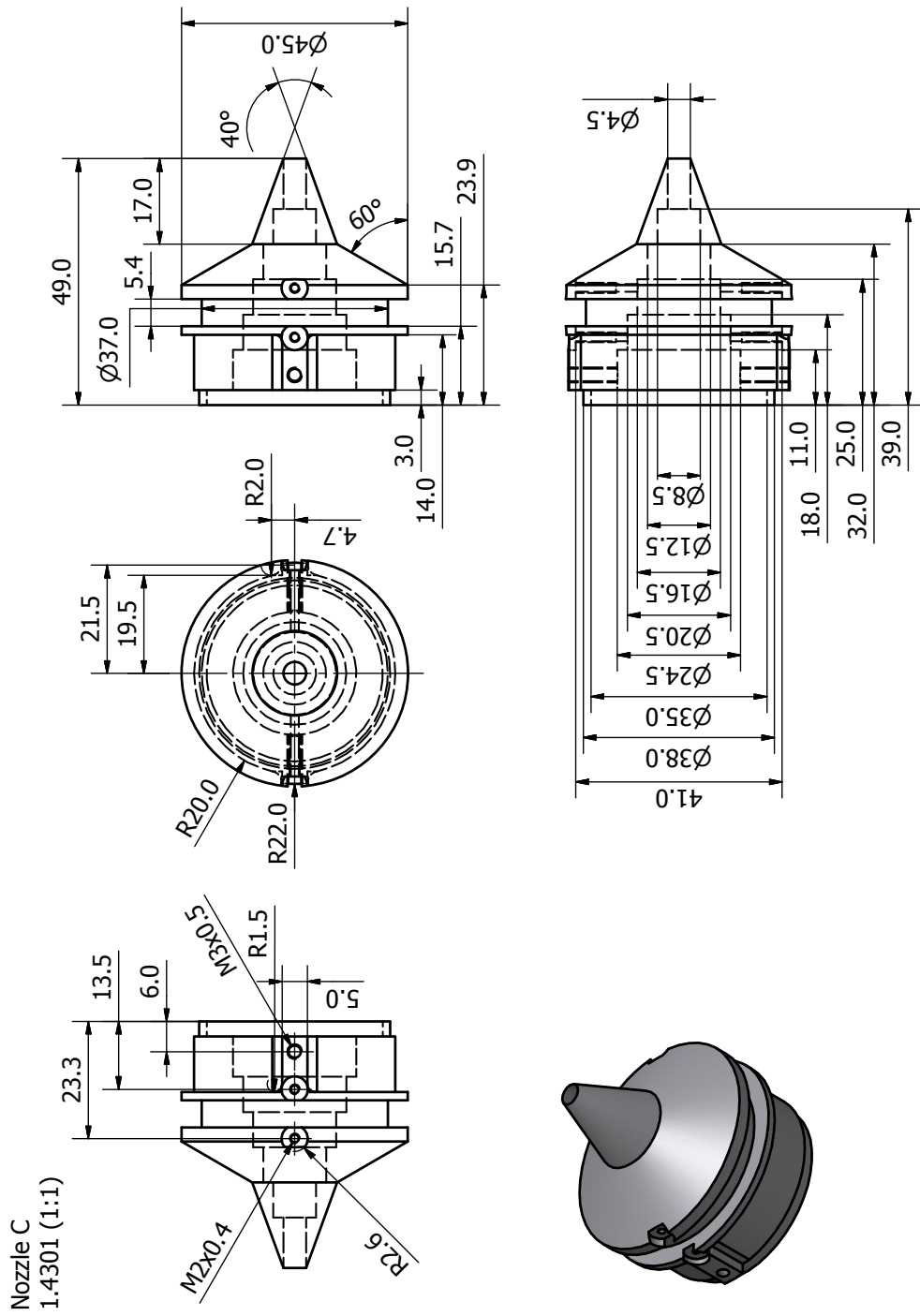


B.1.5 Nozzle in Main Chamber

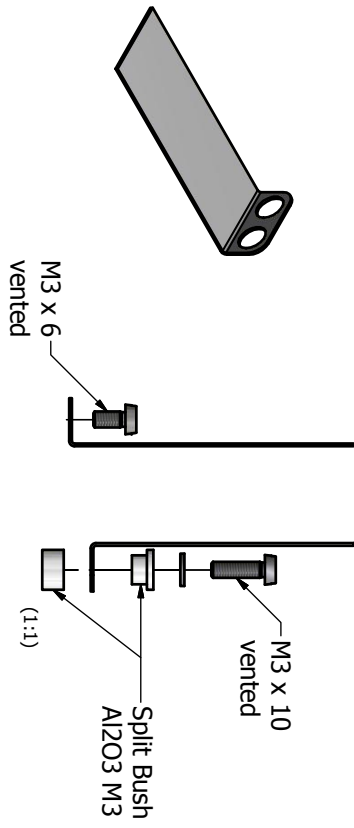
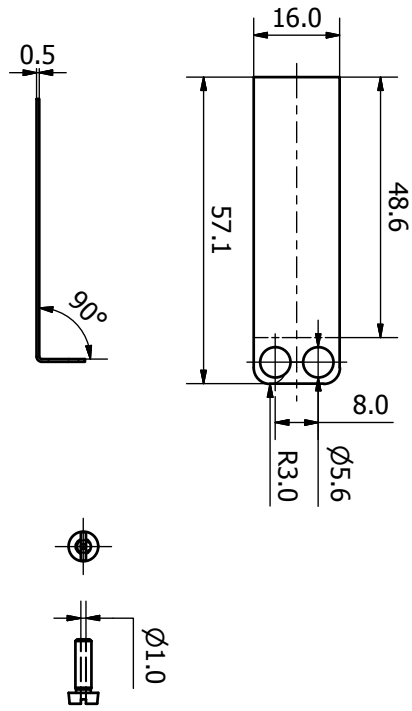




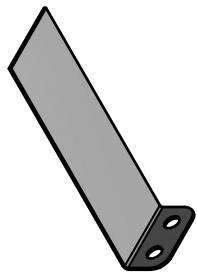
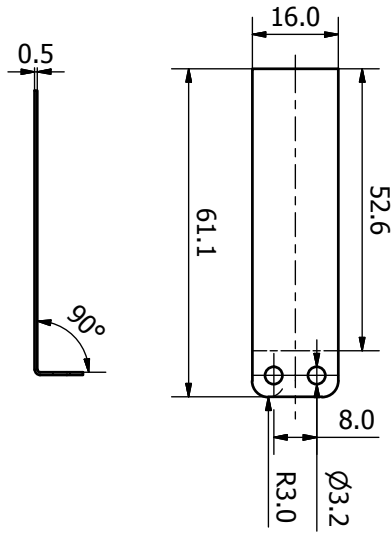




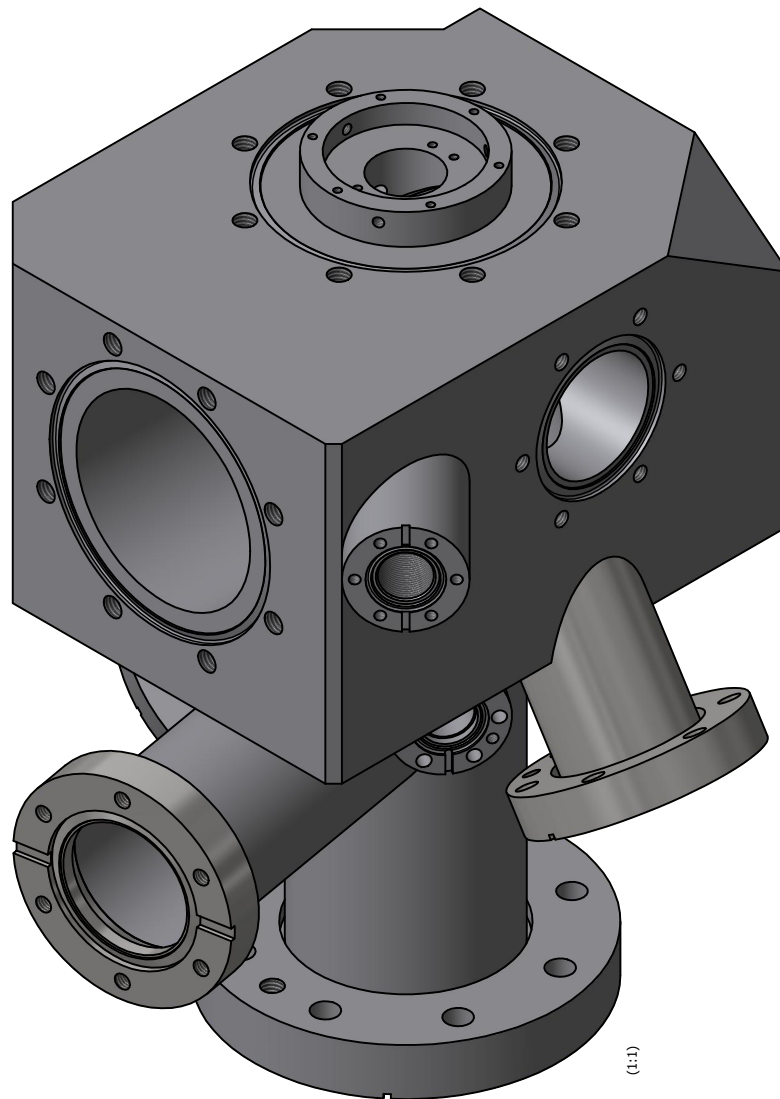
Deflector A
1.4301 (1:1)



Deflector B
1.4301 (1:1)

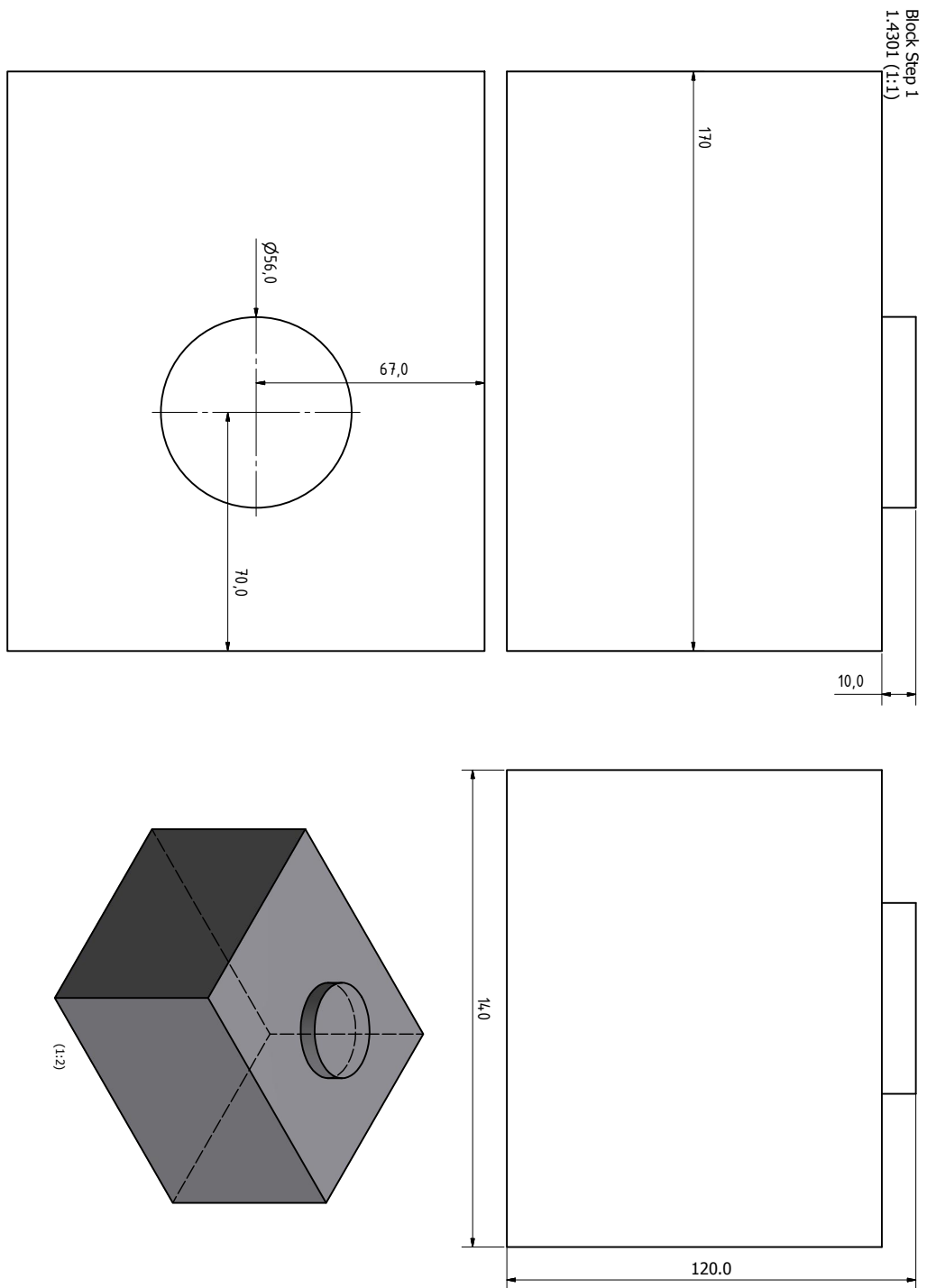


B.1.6 Beam Housing

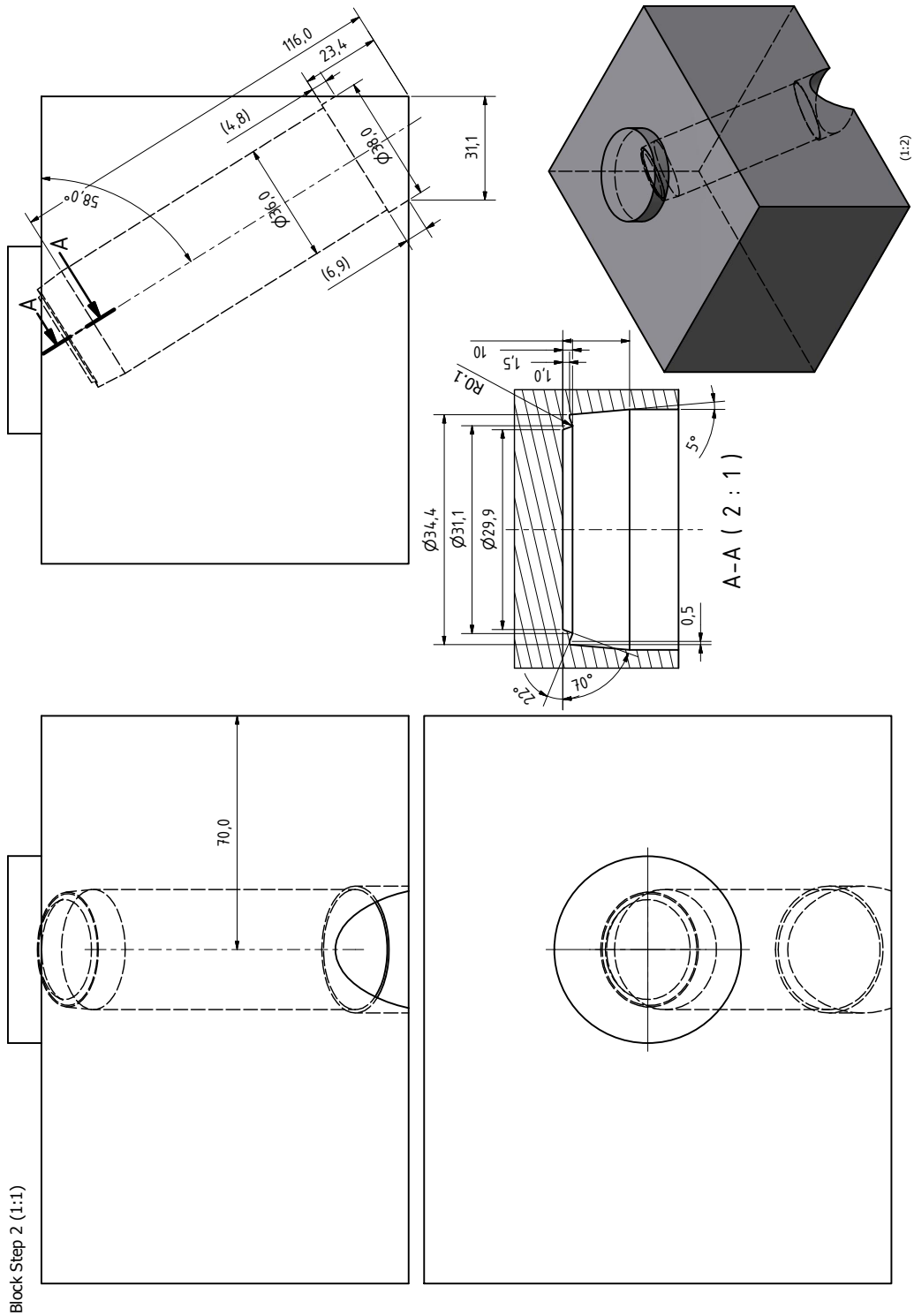


Beam Housing

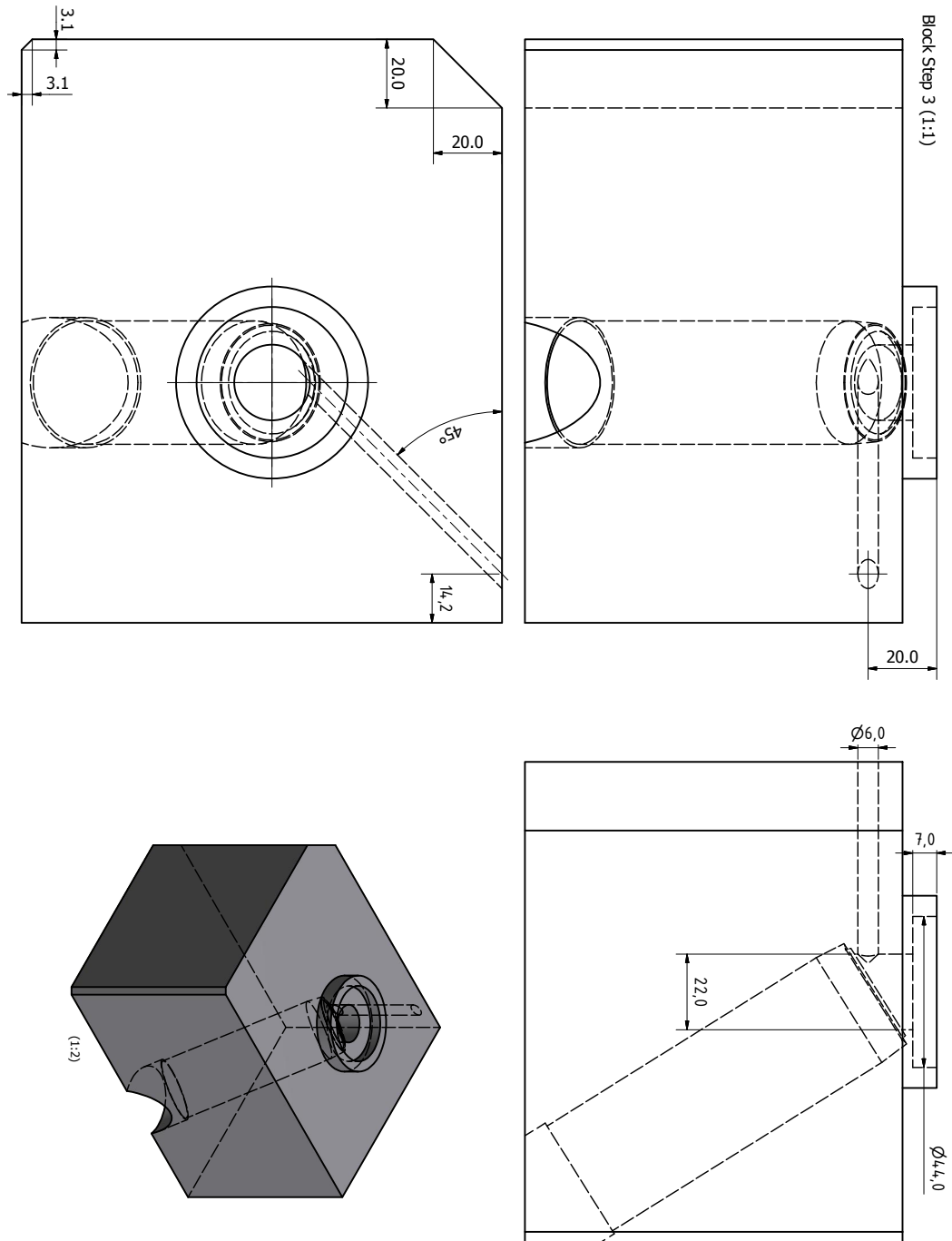
Scaled by 50 %.



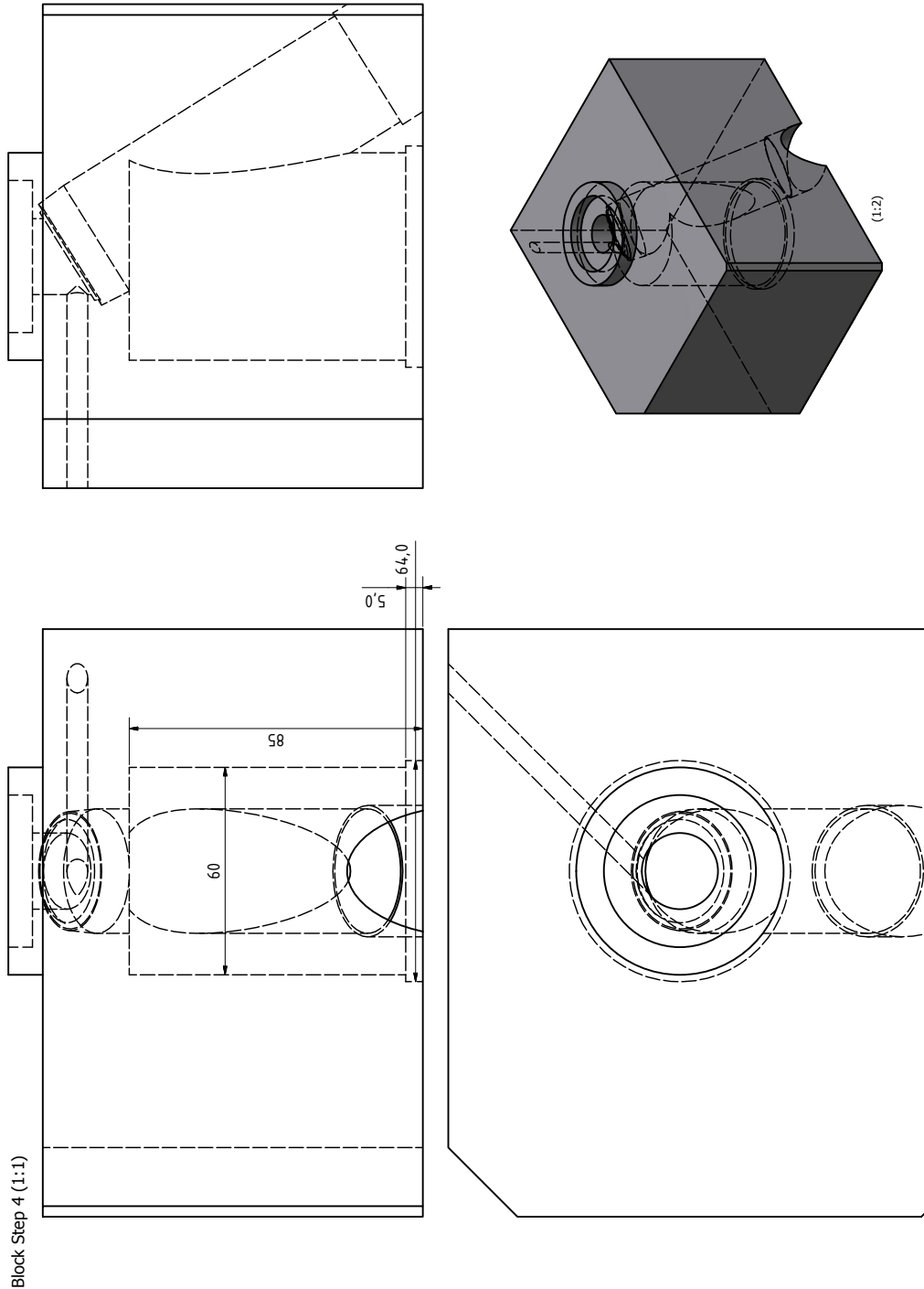
Scaled by 50 %.



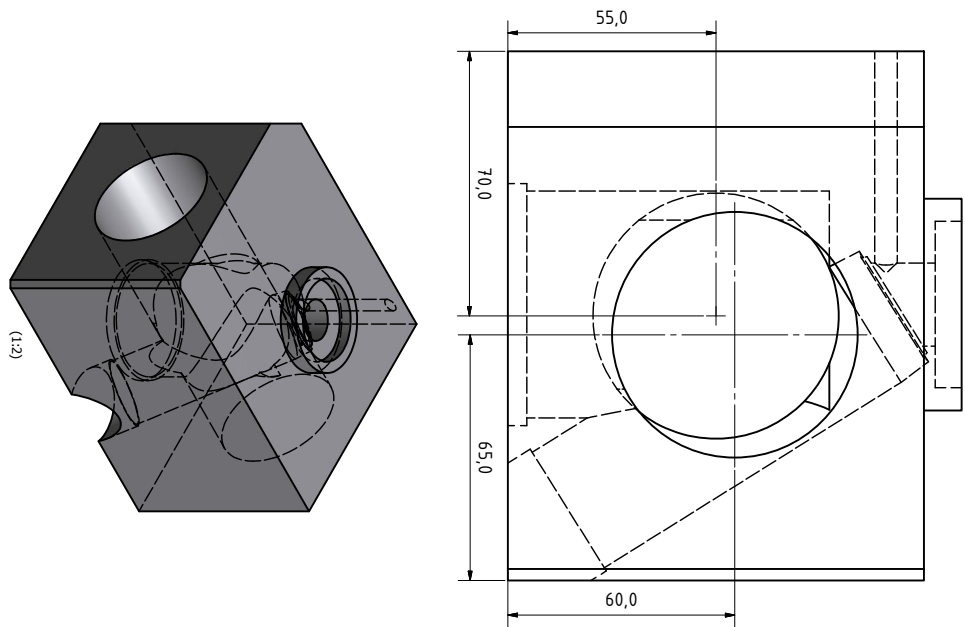
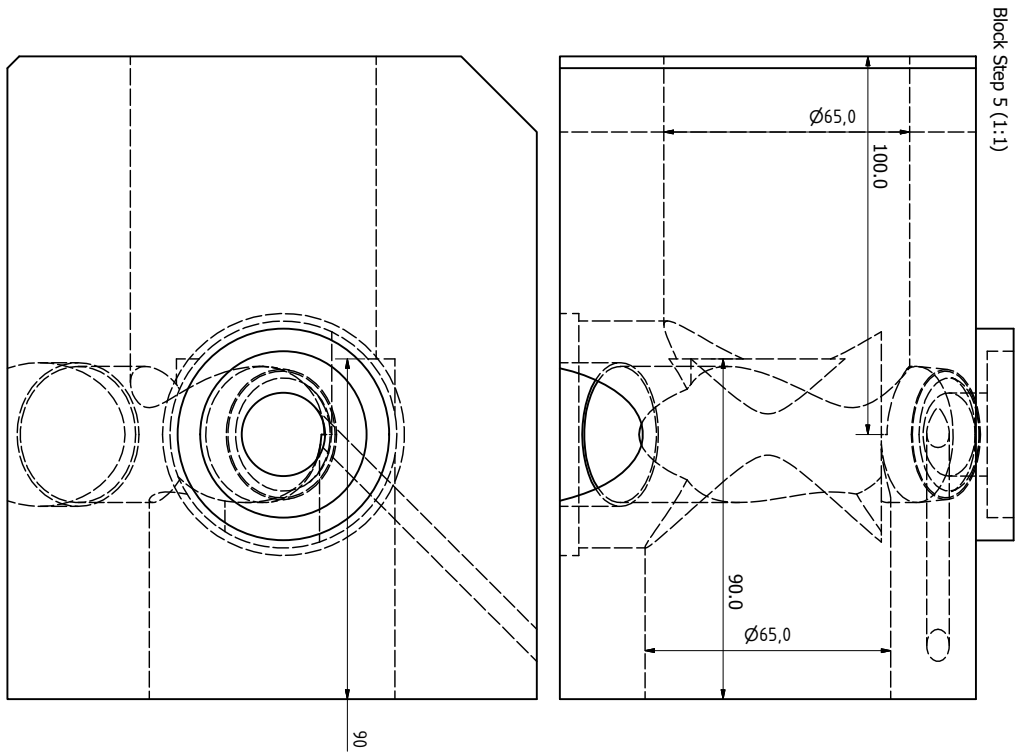
Scaled by 50 %.



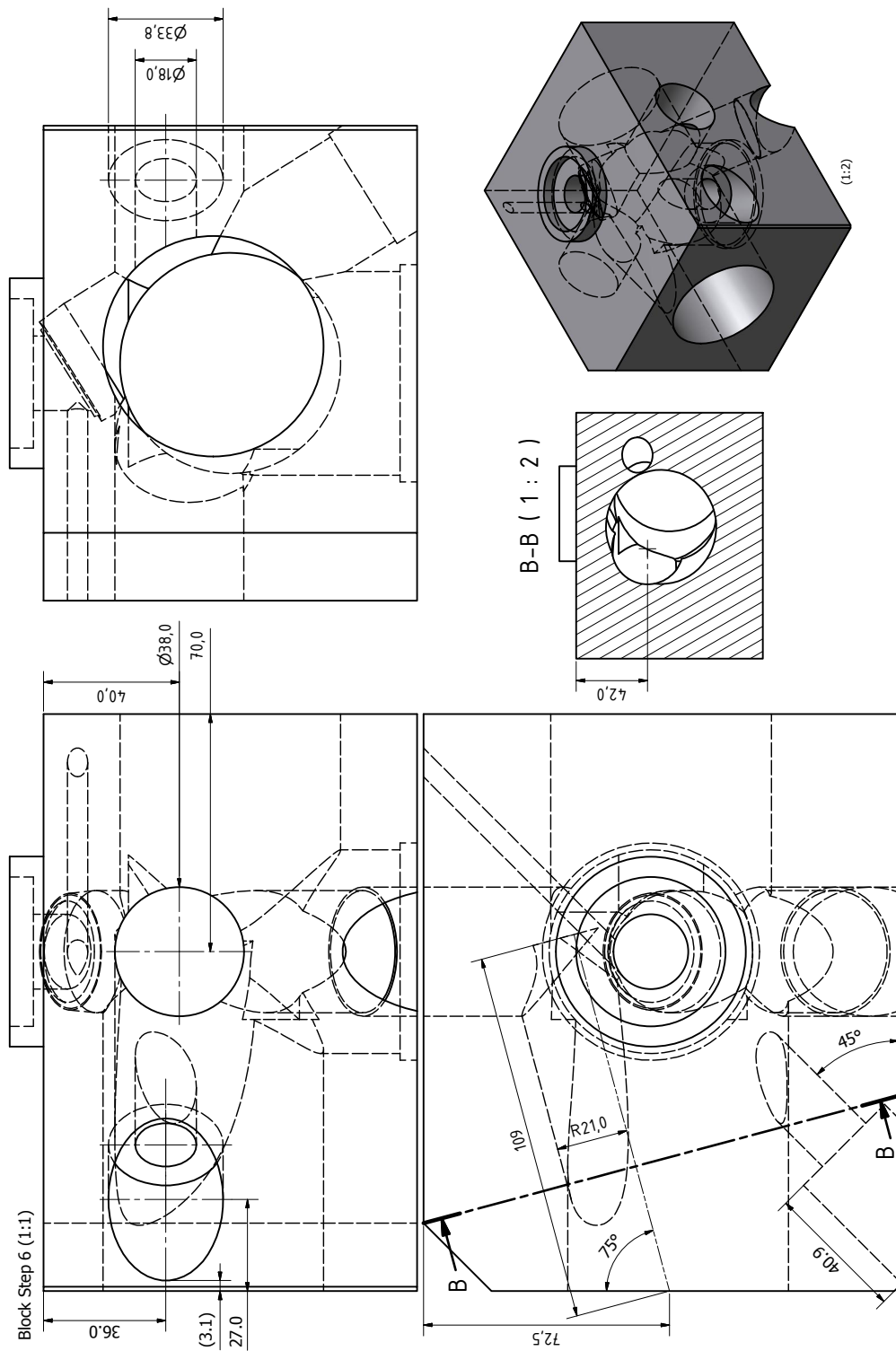
Scaled by 50 %.



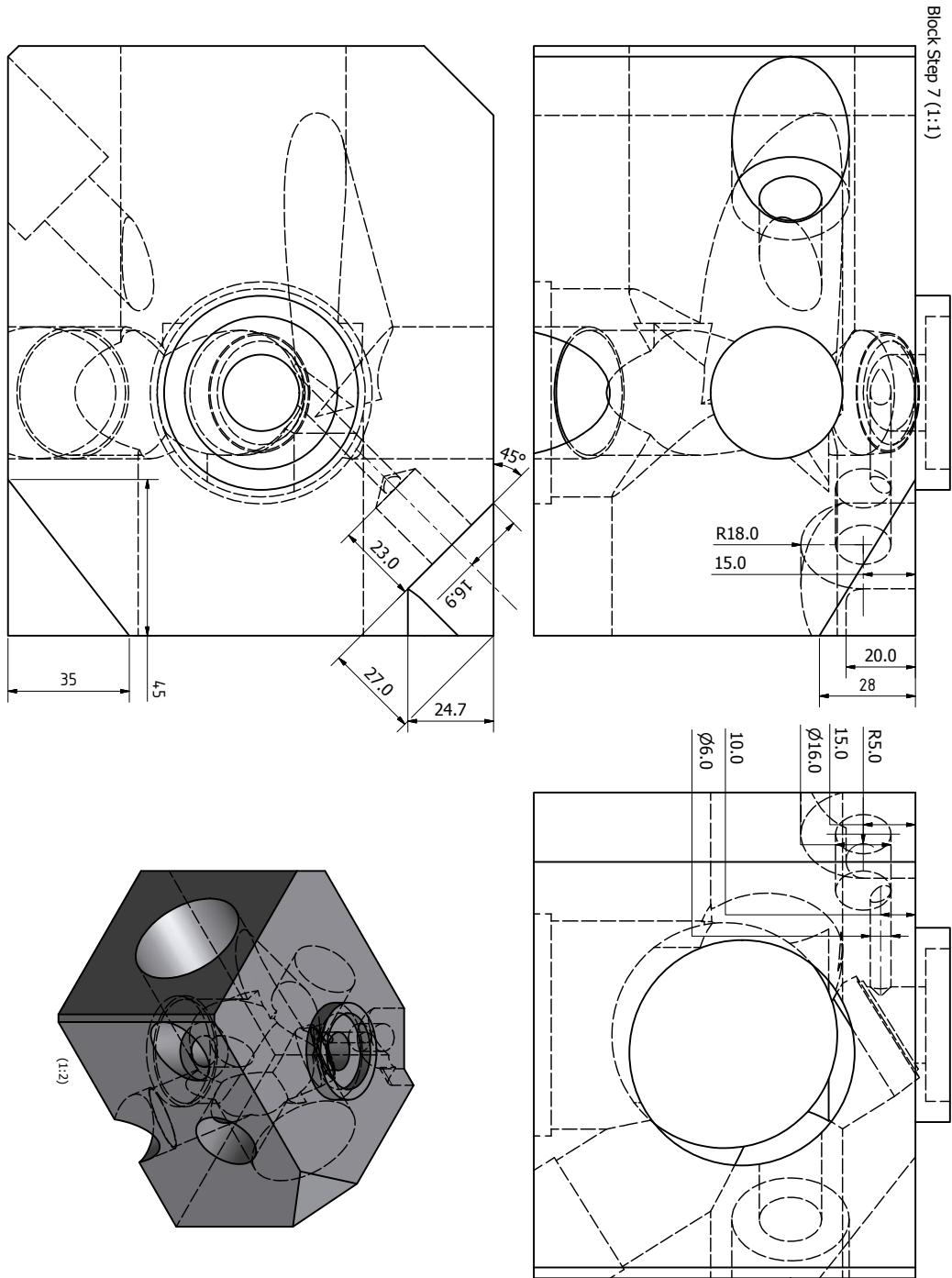
Scaled by 50 %.



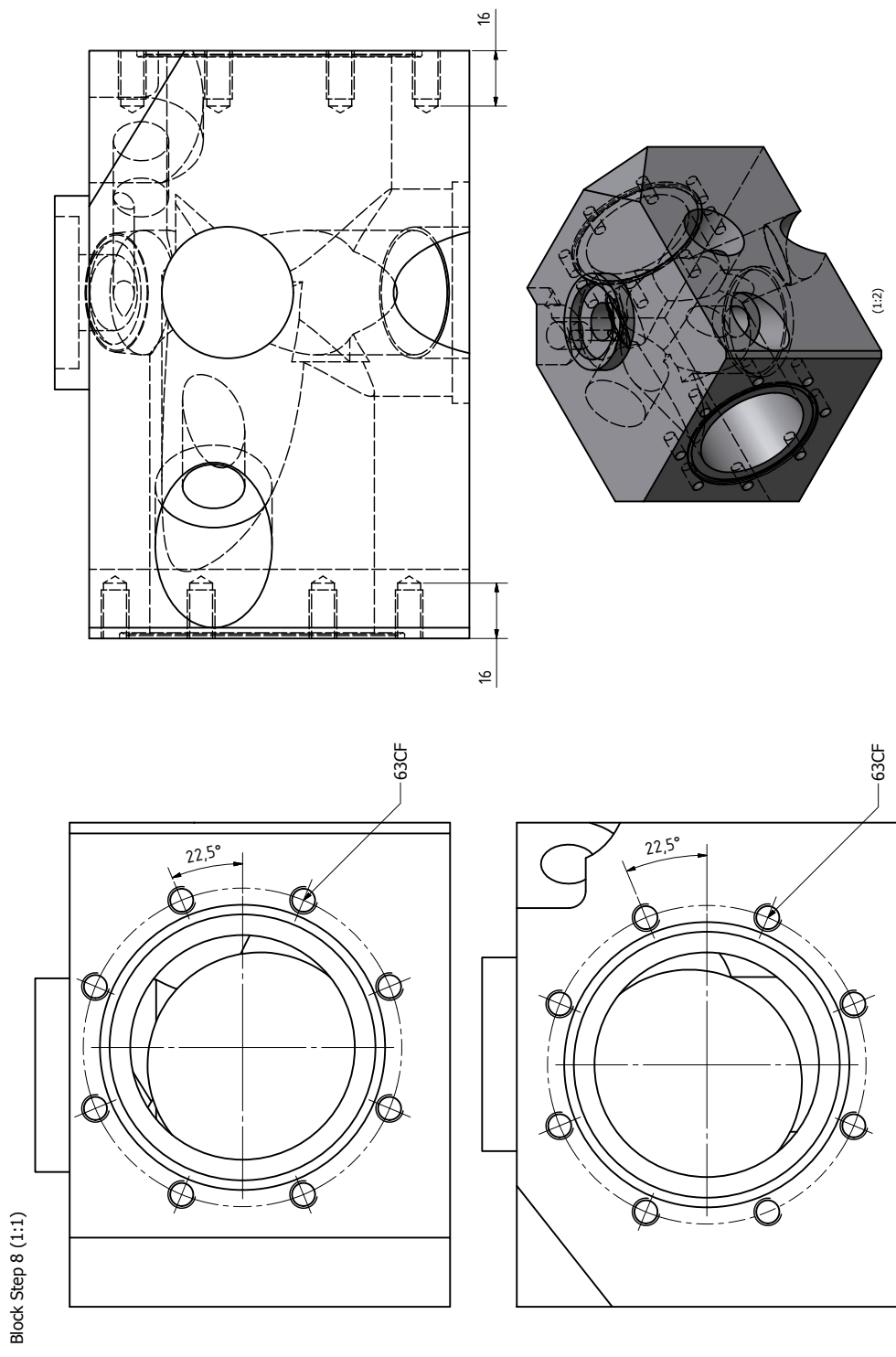
Scaled by 50 %.



Scaled by 50%.

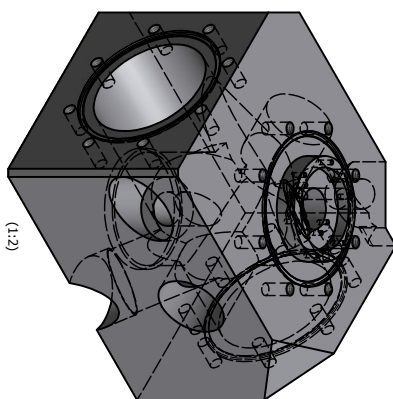
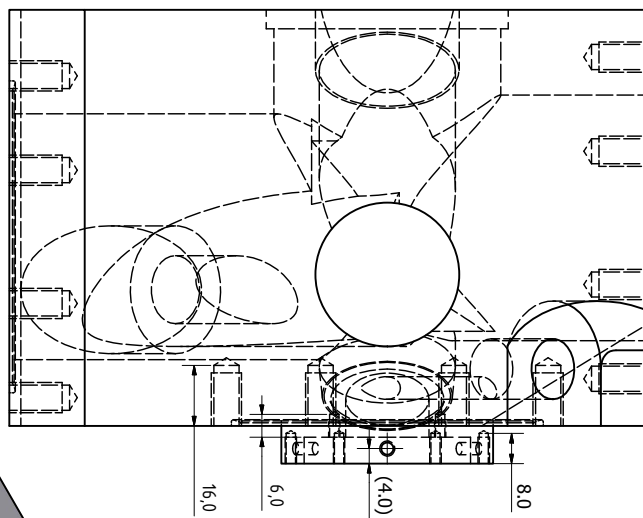
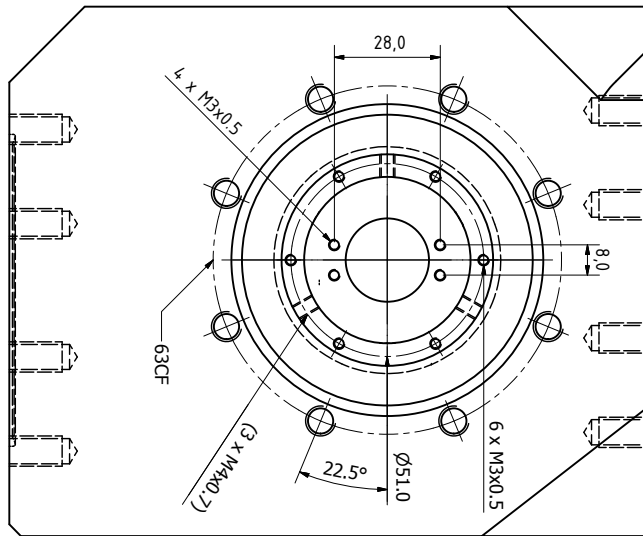


Scaled by 50 %.

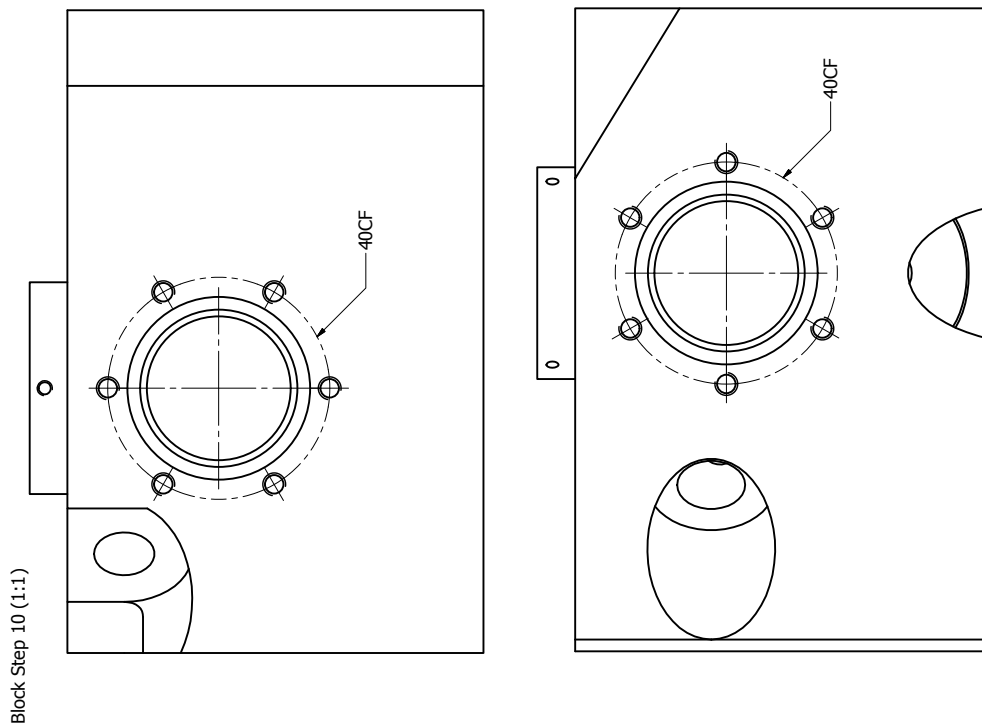
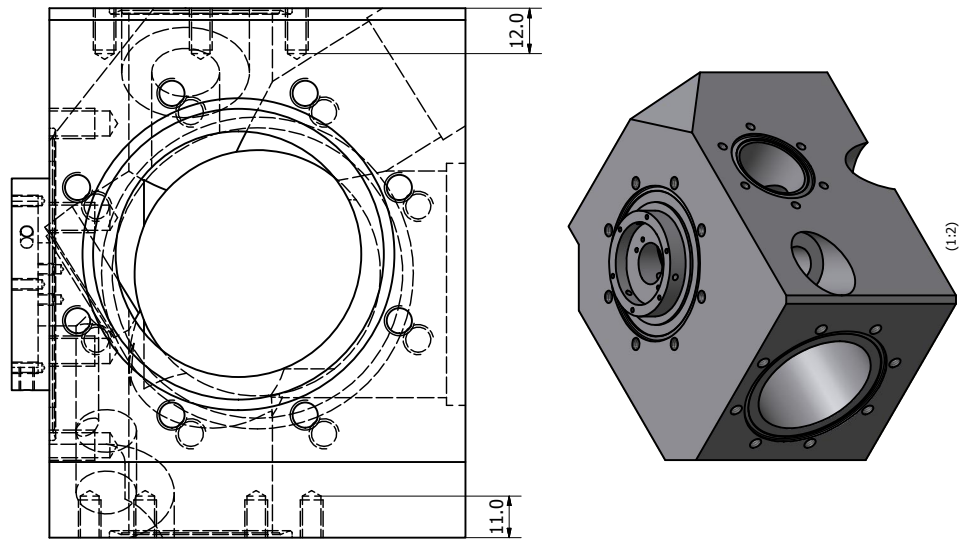


Scaled by 50 %.

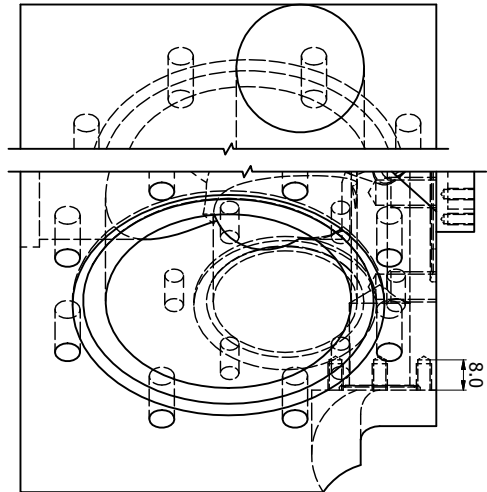
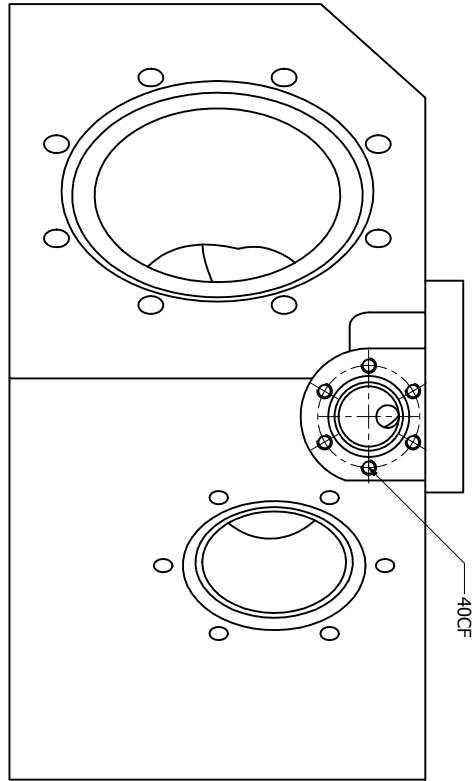
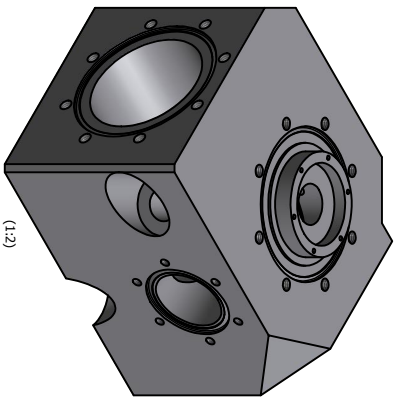
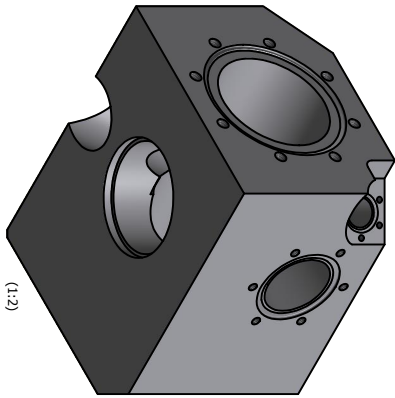
Block Step 9 (1:1)



Scaled by 50 %.

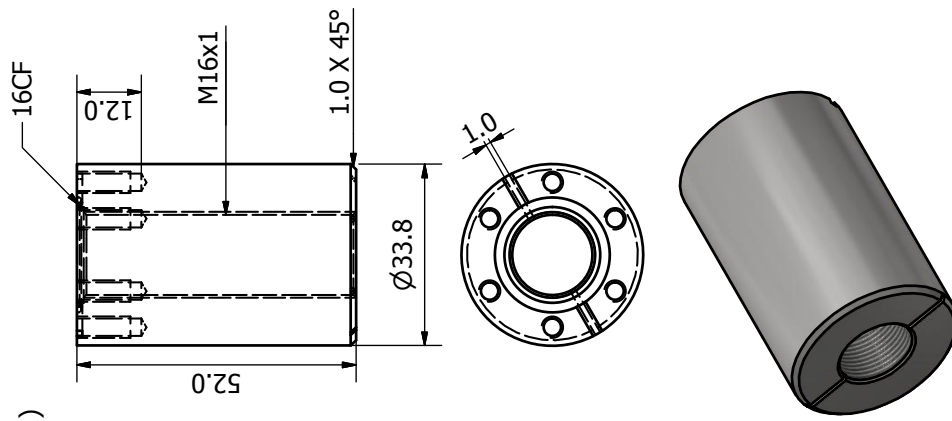


Scaled by 50%.

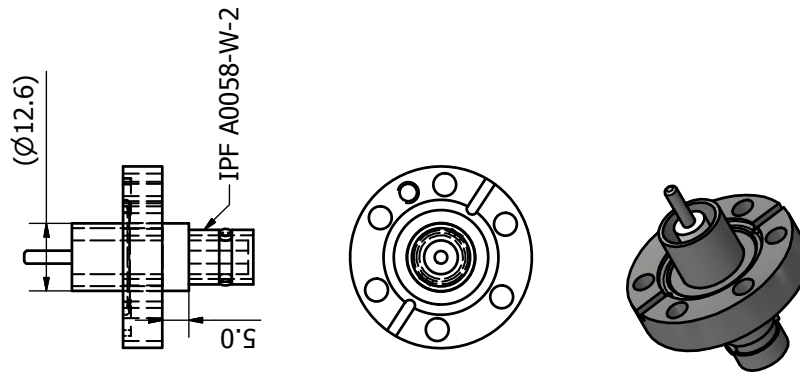


Scaled by 50 %.

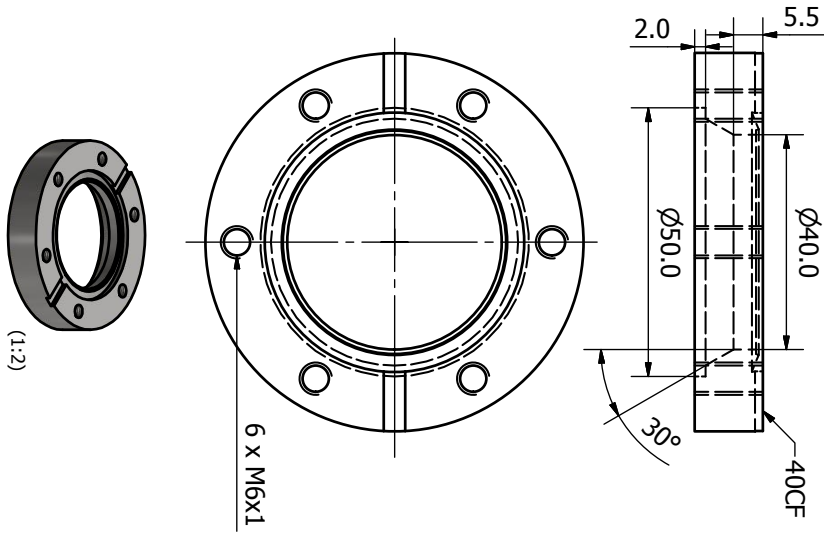
Laser Port
1.4301 (1:1)



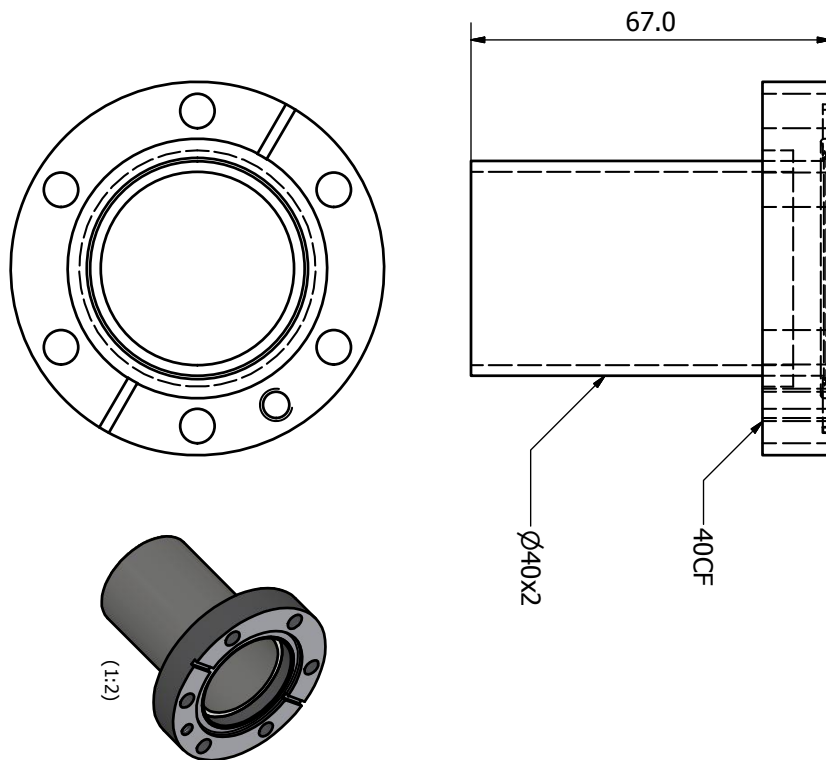
Deflector Feed Through
Modification (1:1)



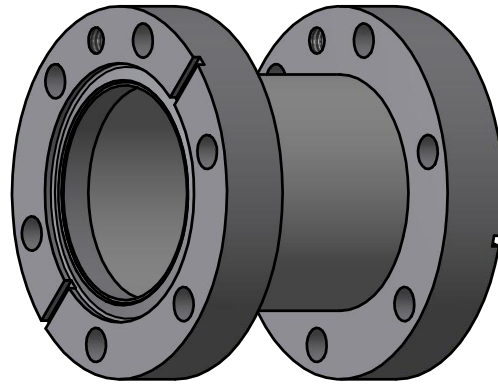
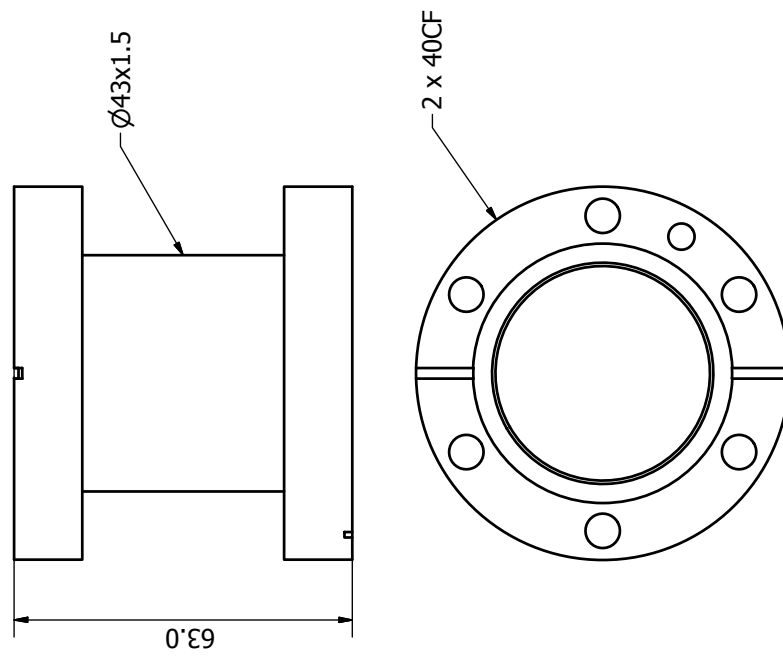
40CF-TX50
1.4301 (1:1)

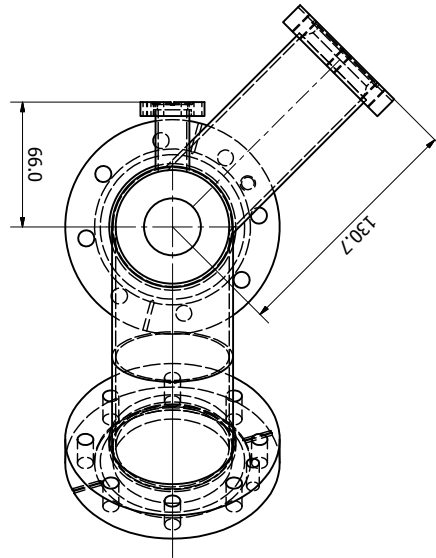
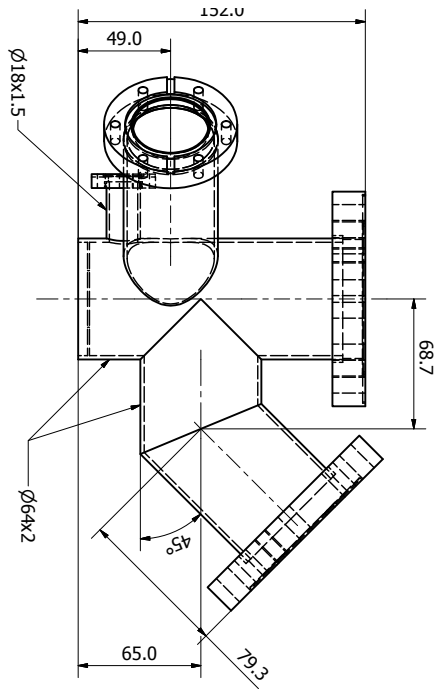


Valve Port
1.4301 (1:1)

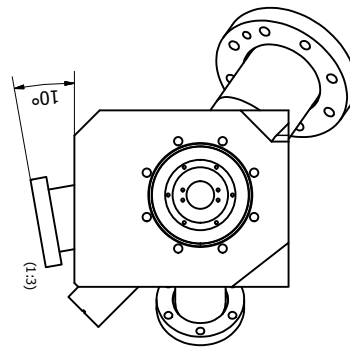
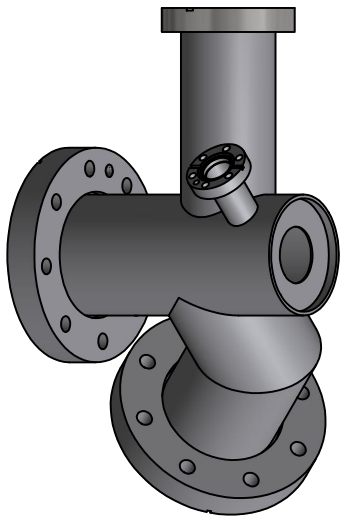
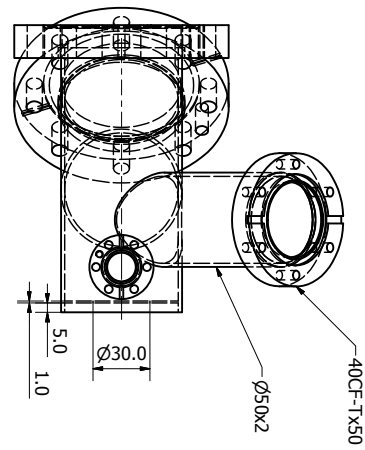


Adapter Nipple 40CF
for e-Beam Evaporator EFM-4
1.4301 (1:1)





Beam Housing
1.4301 (1:2)



Scaled by 50 %.

B.2 Main Chamber

Details about the extensions to the main chamber are discussed in Sections 2.1, 2.2, and 2.9. The following pages contain the technical drawings of the parts related to the main chamber:

Sample Holder Mount options for thin film as well as sheet material samples (Appendix B.2.1).

Sample Carrier Parts to carry the sample holders during transfer in the chambers (Appendix B.2.2).

Detector The main instrument in an NAC experiment (Appendix B.2.3).

Sample Heater Option to heat sheet material samples in the detector setup (Appendix B.2.4).

QMS Mount Part to mount the mass spectrometer to the main chamber (Appendix B.2.5).

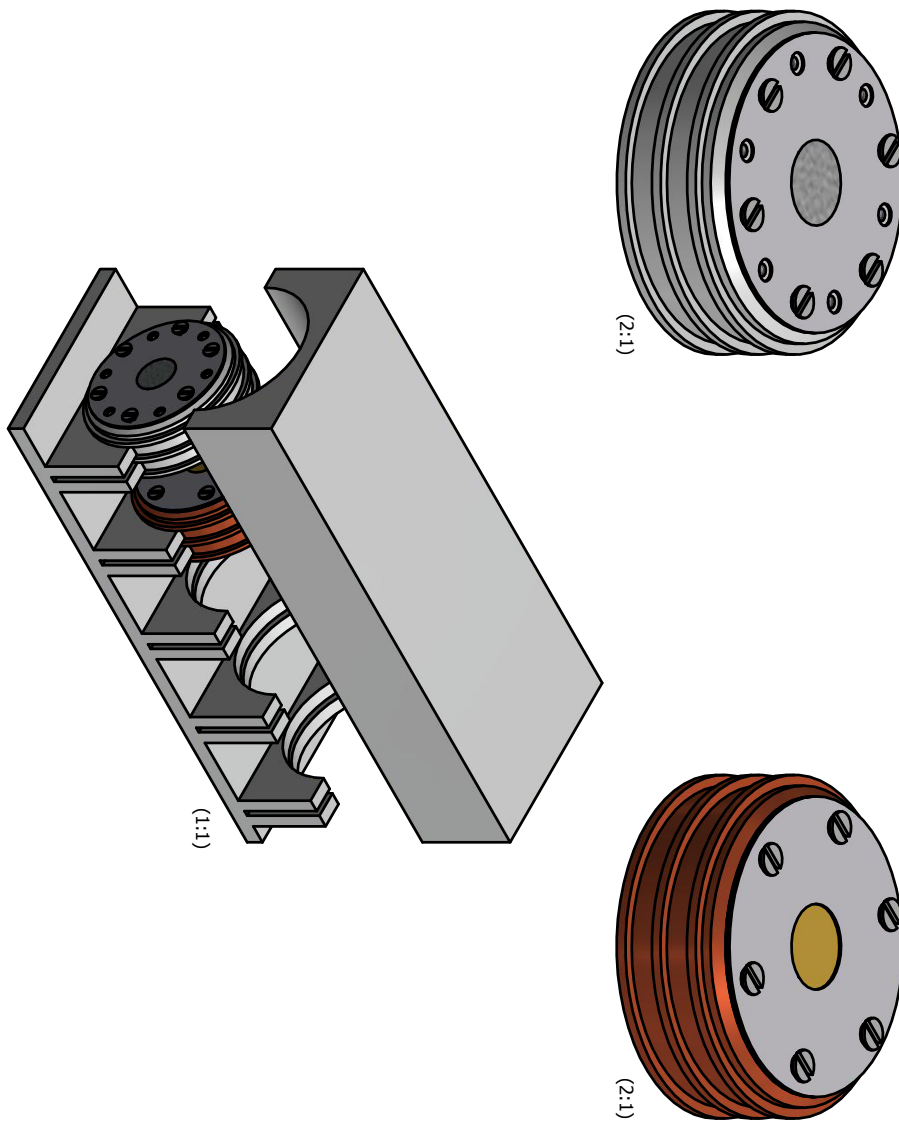
Ancillaries Stage Assembly of the instruments for the ancillary measurements (Appendix B.2.6).

Main Chamber Additions Several minor devices related to the main chamber (Appendix B.2.7).

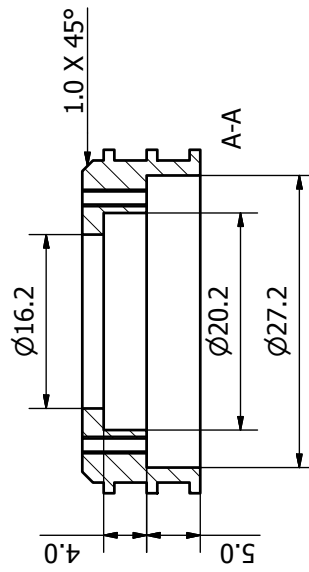
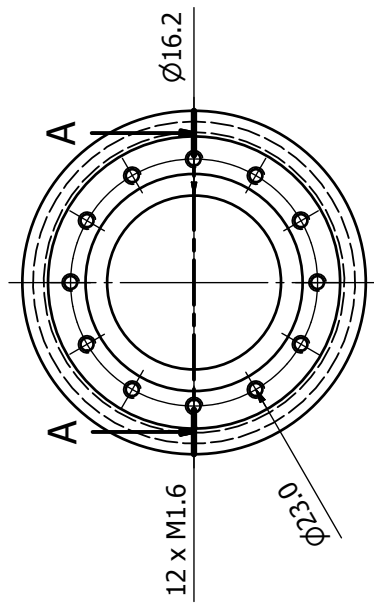
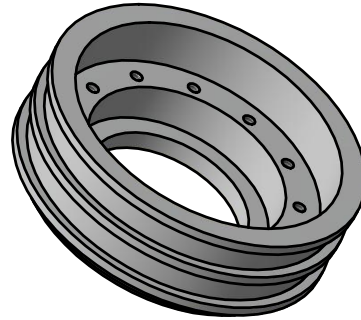
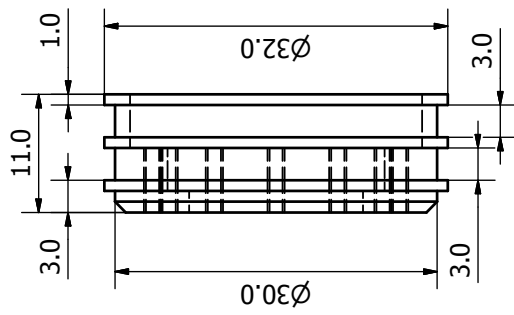
Optical Meters Mounting options for a pyrometer and a photometer (Appendix B.2.8).

Fiber Positioner Tool to align the output of the laser guiding fiber to the optics of the molecular beam (Appendix B.2.2).

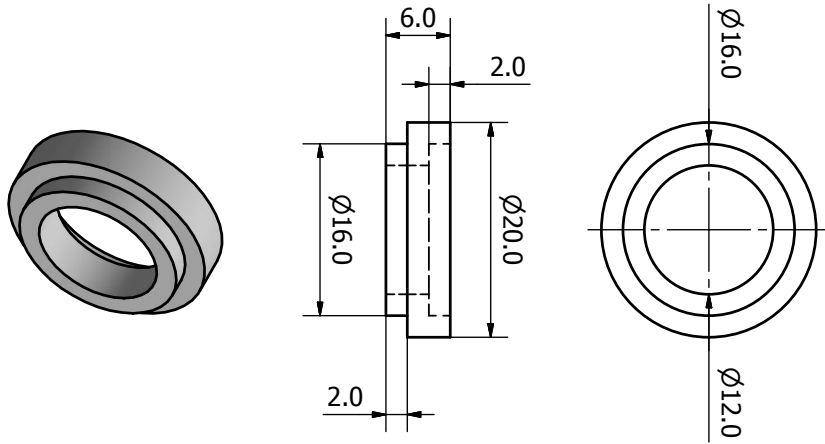
B.2.1 Sample Holder



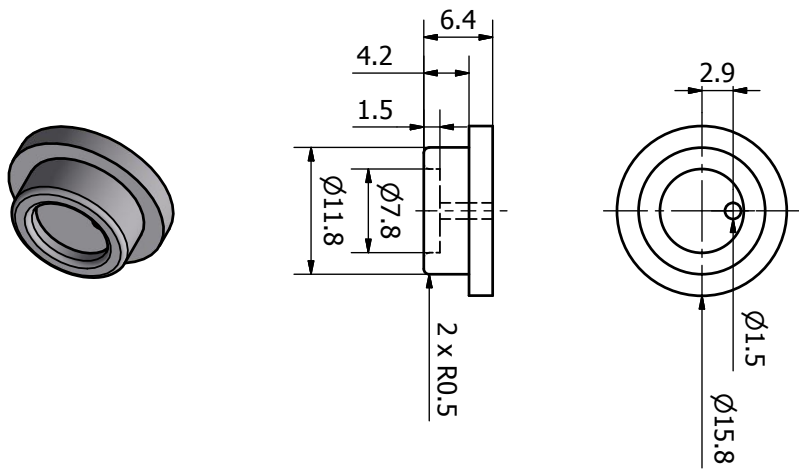
Sample Holder A Thin Film
Aluminum (2:1)



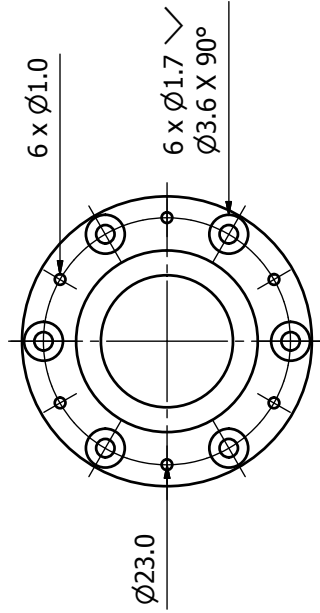
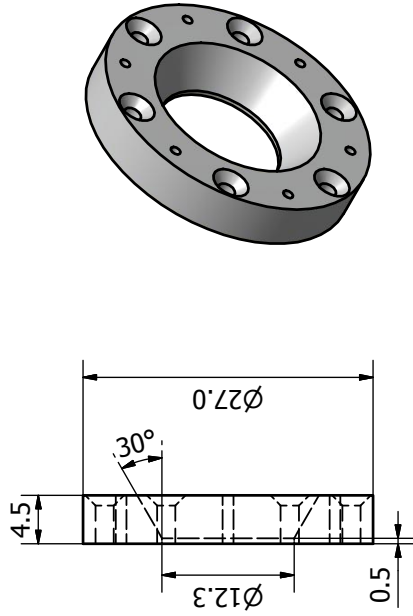
Sample Holder B Thin Film
Macor (2:1)



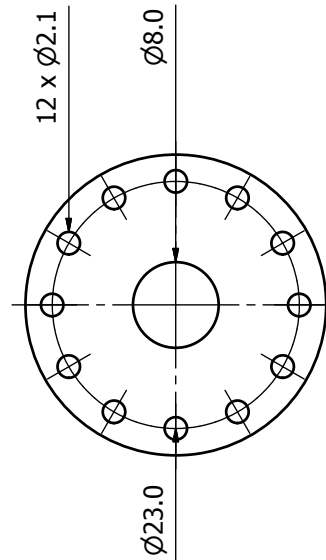
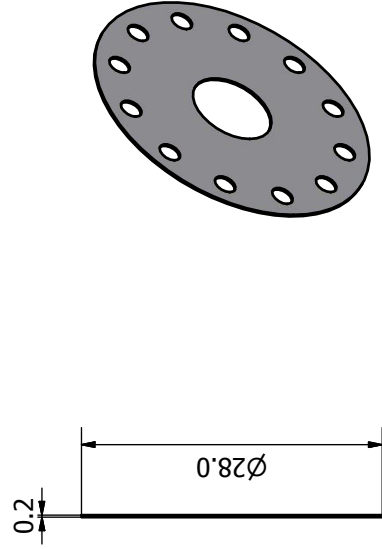
Sample Holder C Thin Film
Aluminum (2:1)



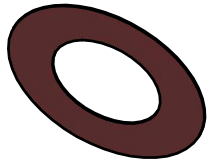
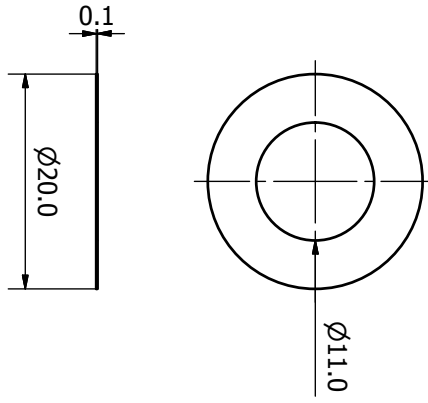
Sample Holder D Thin Film
Aluminum (2:1)



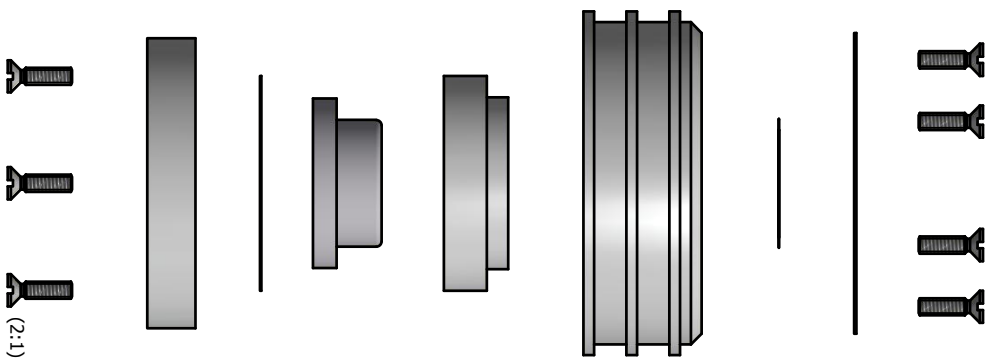
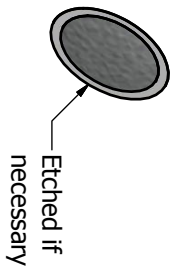
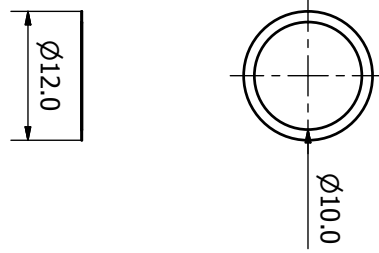
Sample Holder E Thin Film
Aluminum (2:1)

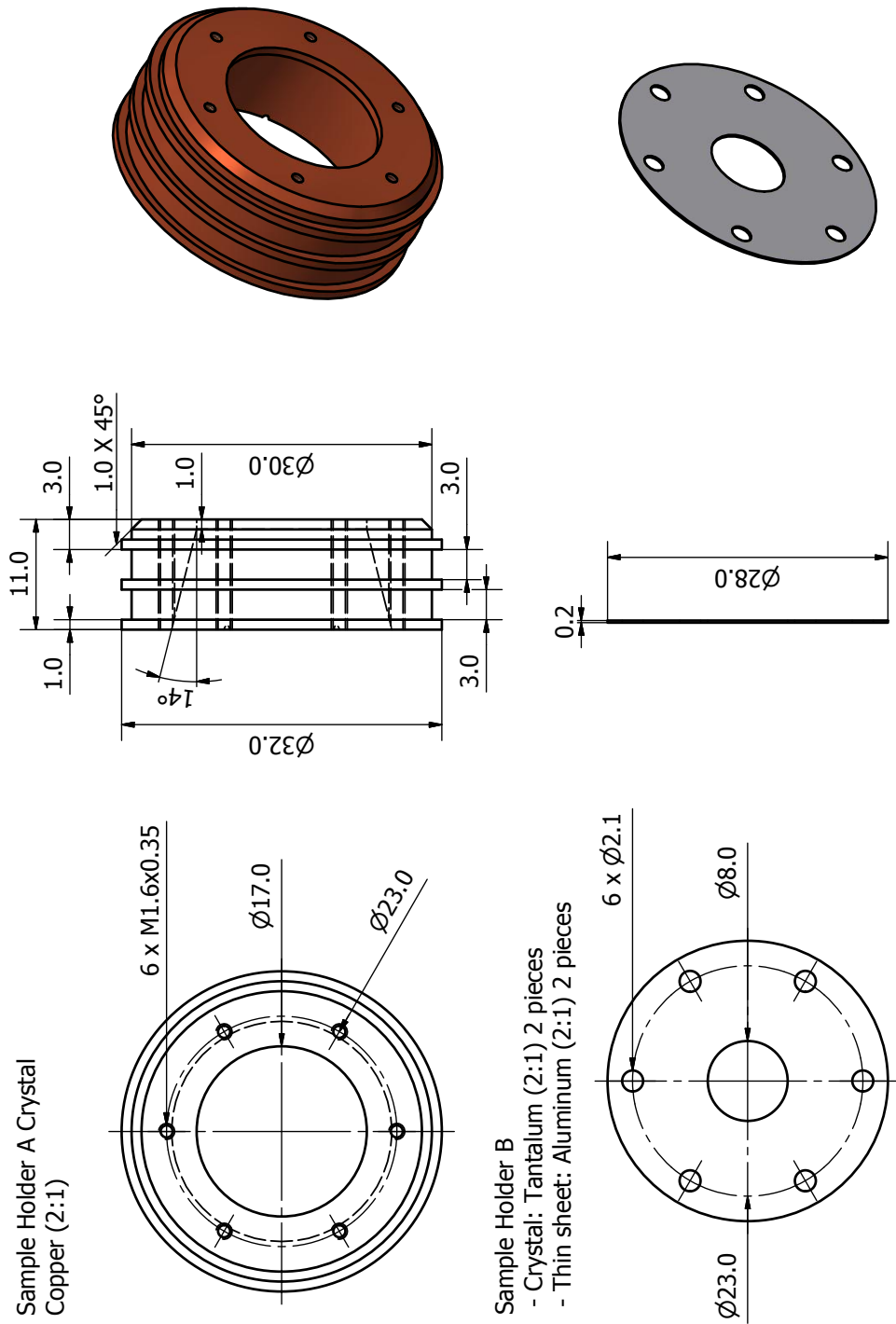


Sample Holder F Thin Film
Kapton (2:1)

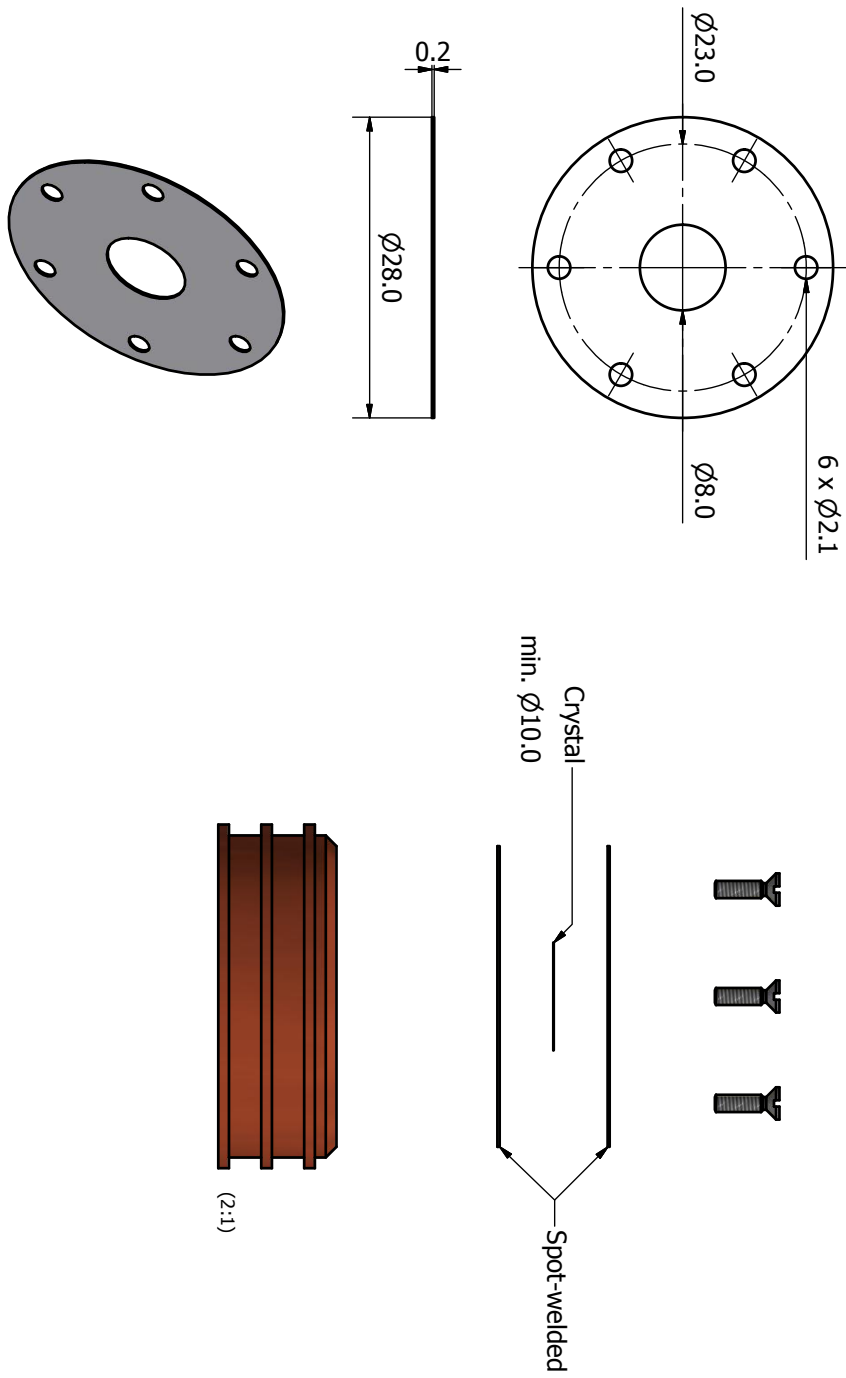


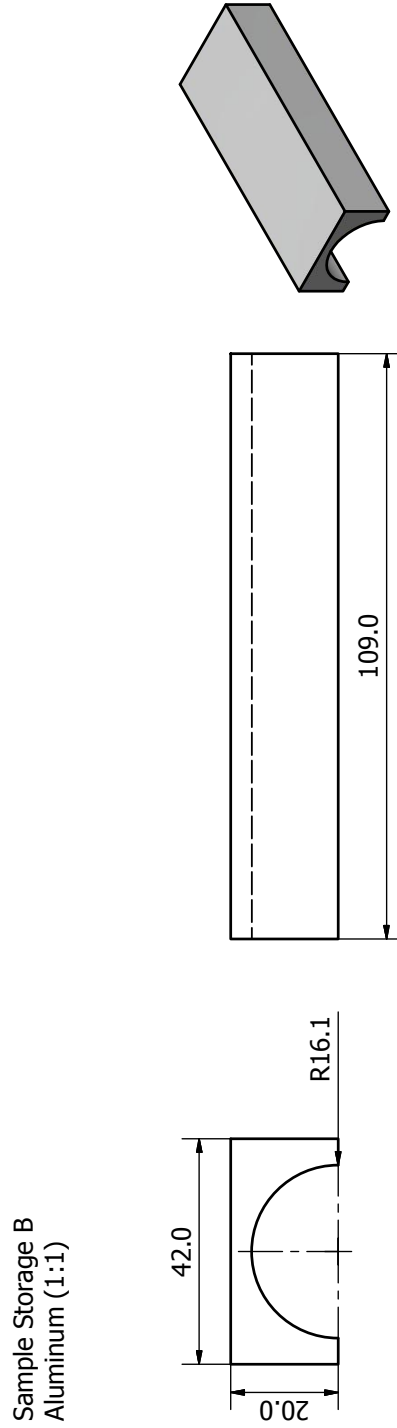
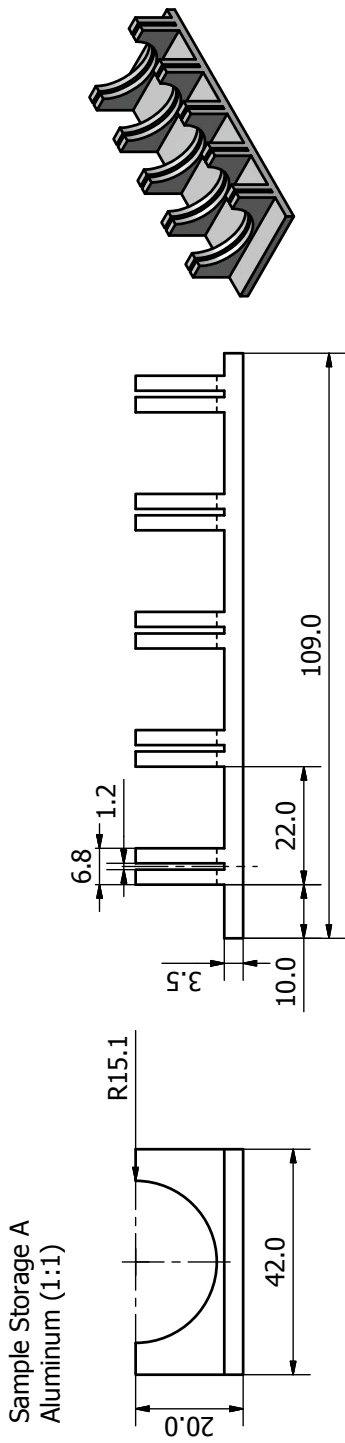
Detector Foil Thin Film
Metalized, poled PVDF (2:1)





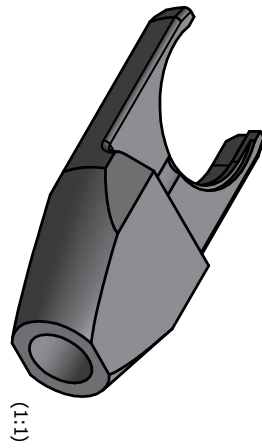
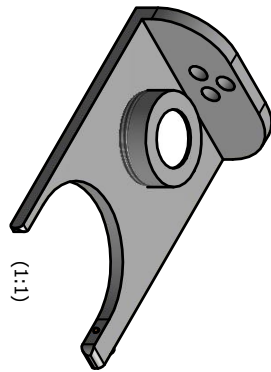
Sample Holder B Crystal
Tantalum (2:1) 2 pieces



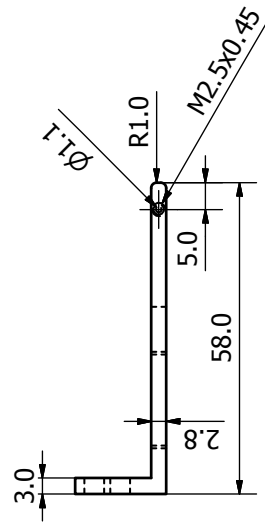
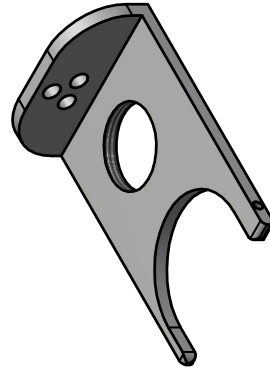
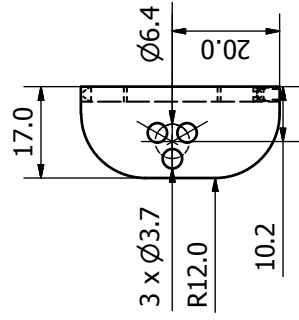
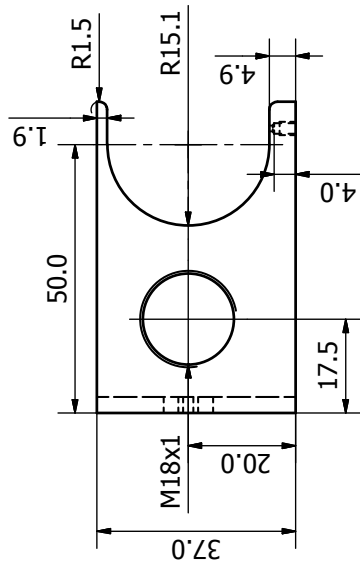


Design by O. LYTKEN.

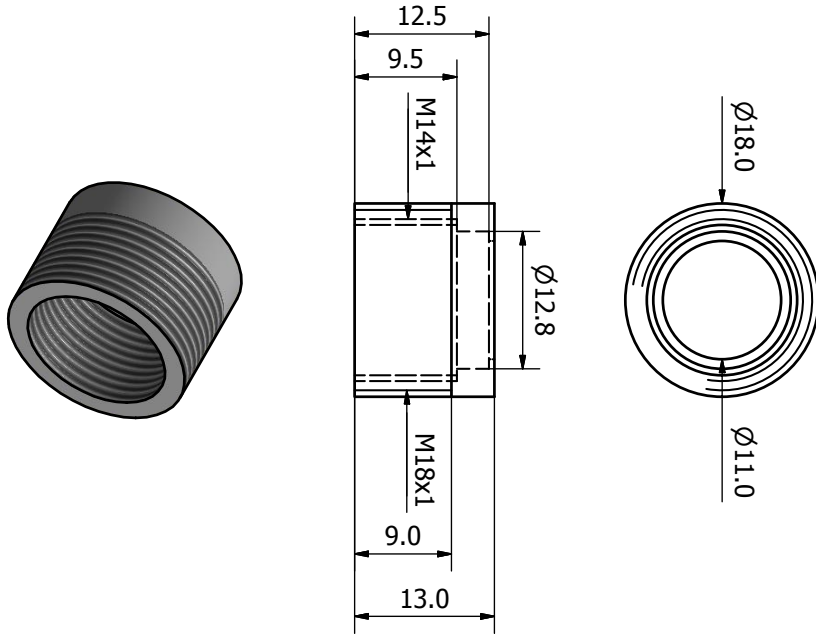
B.2.2 Sample Carrier



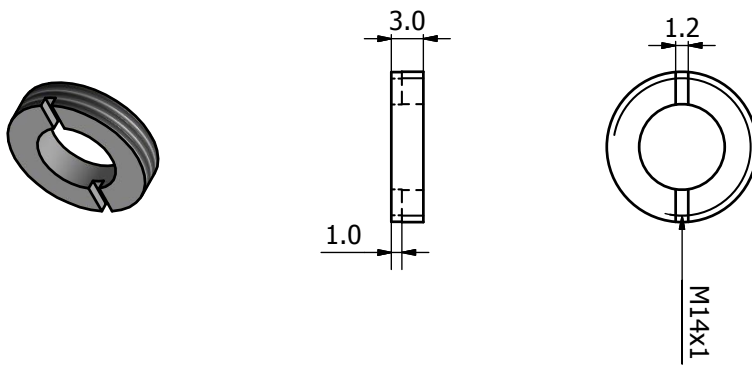
Main Chamber Sample Transfer A
1.4301 (1:1)



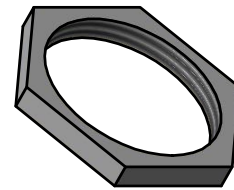
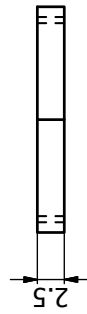
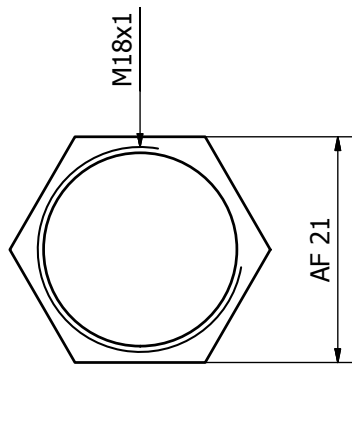
Main Chamber Sample Transfer B
1.4301 (2:1)



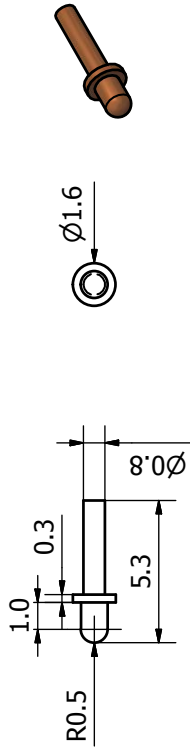
Main Chamber Sample Transfer C
1.4301 (2:1)



Main Chamber Sample Transfer D
1.4301 (2:1)



Main Chamber Sample Transfer E
E-Cu (5:1)



Vented Screw
Stainless Steel (5:1)

DIN 913 M2.5x3



Main Chamber Sample Transfer E

Spring

Stainless Steel (5:1)

ØWire 0.3

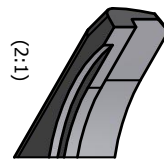
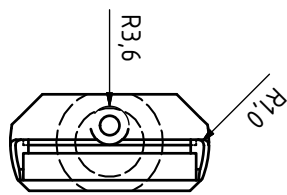
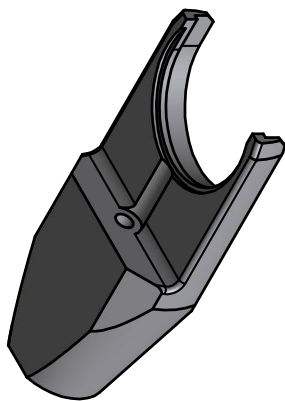
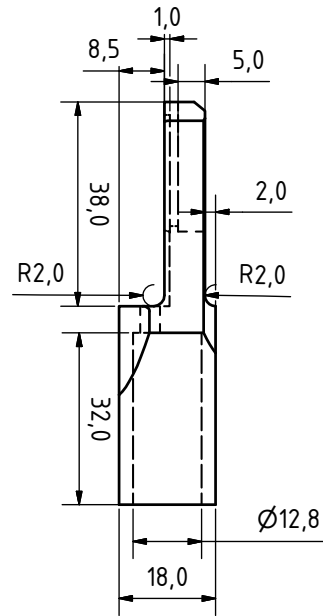
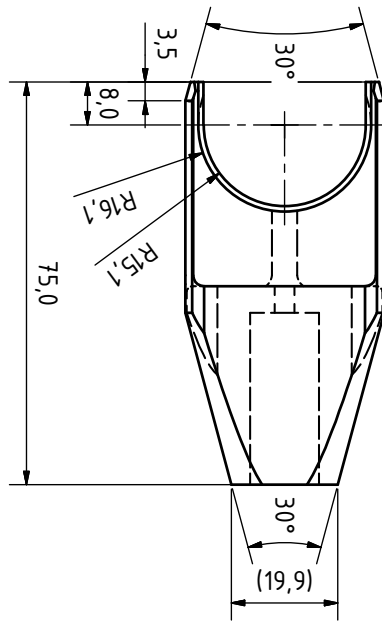
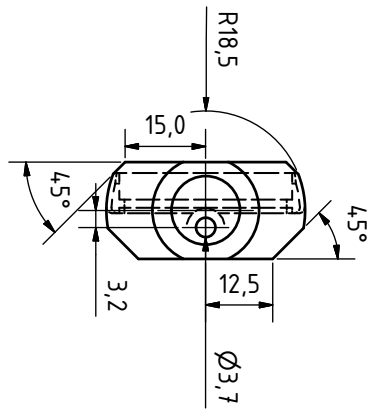
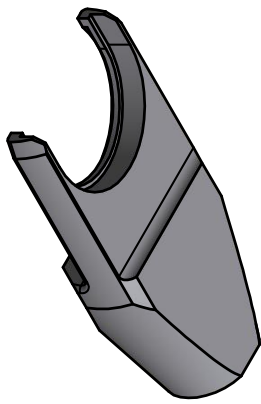
ØInner 1,2

Pitch 0.75mm

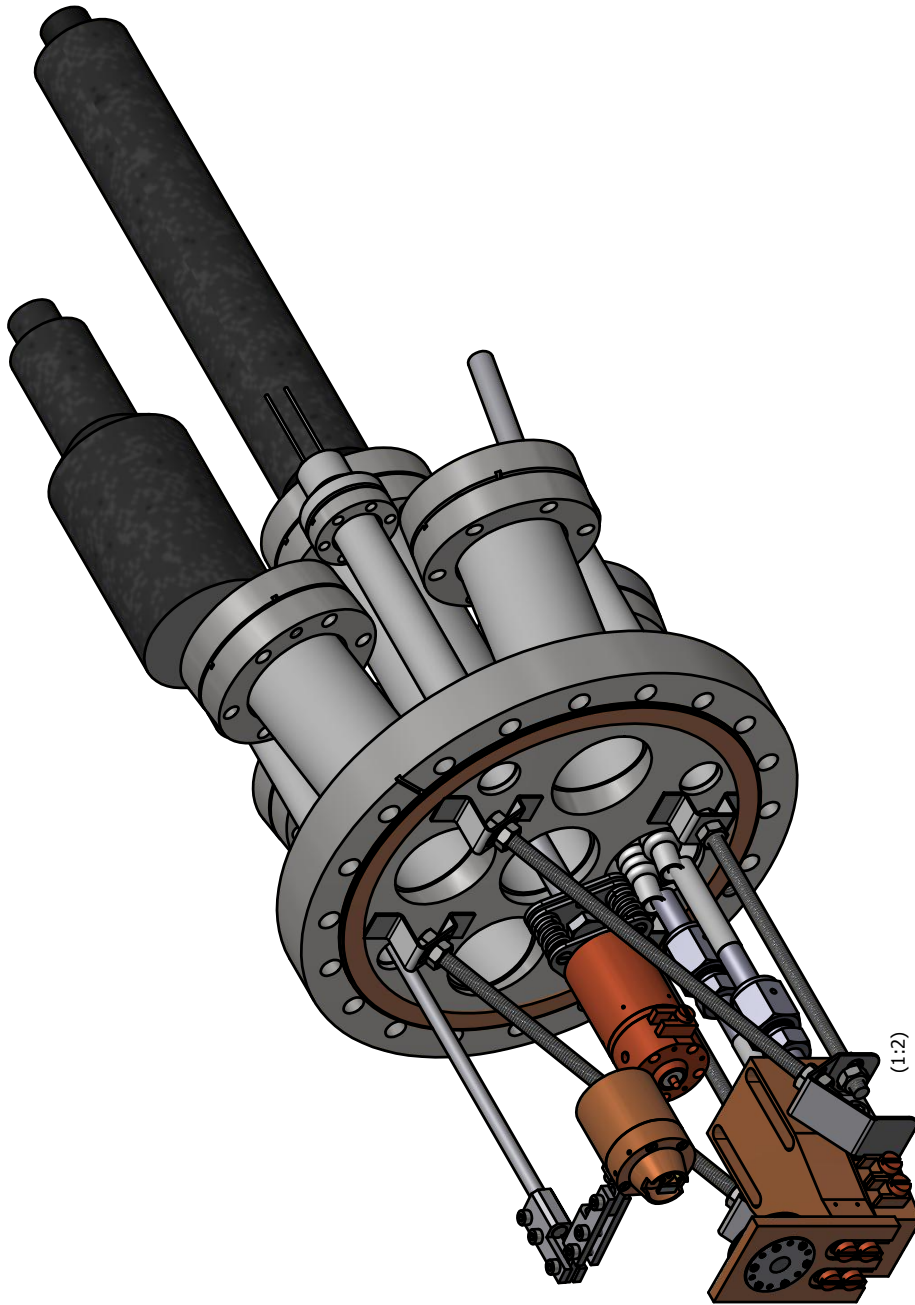
Coils 5



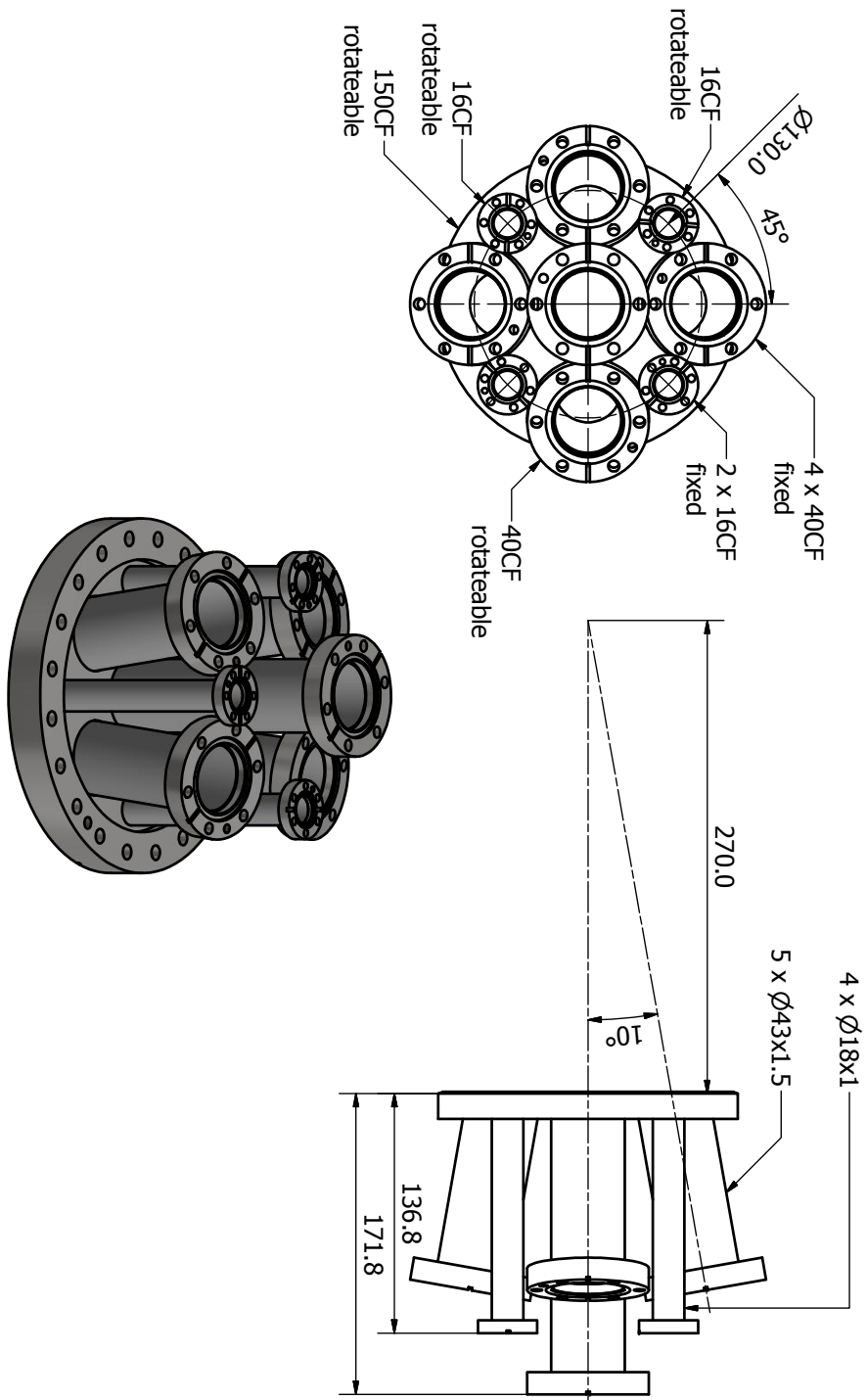
Load Lock Sample Transfer
1.4301 (1:1)



B.2.3 Detector

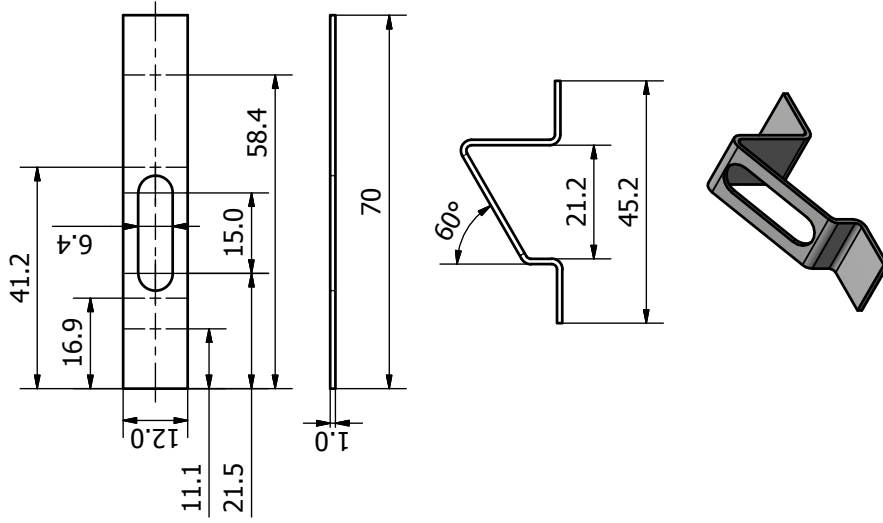


Detector Base Flange
1.4301 (1:3)

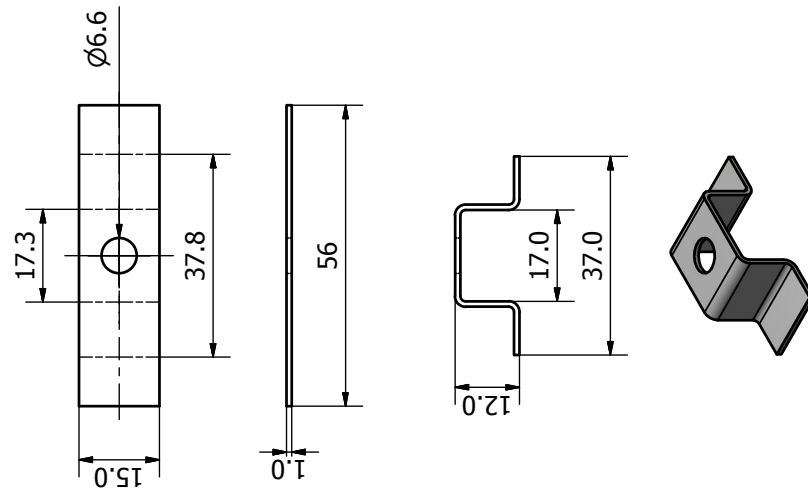


Part of diploma thesis^[105].

Detector Mount B
1.4301 (1:1) 2 pieces

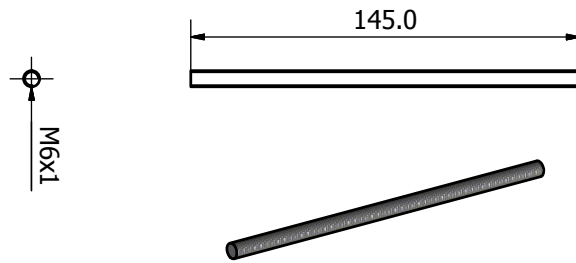


Detector Mount A
1.4301 (1:1) 2 pieces

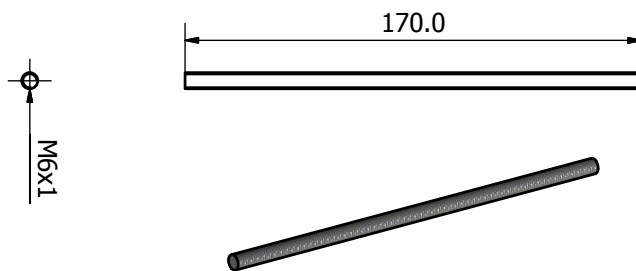


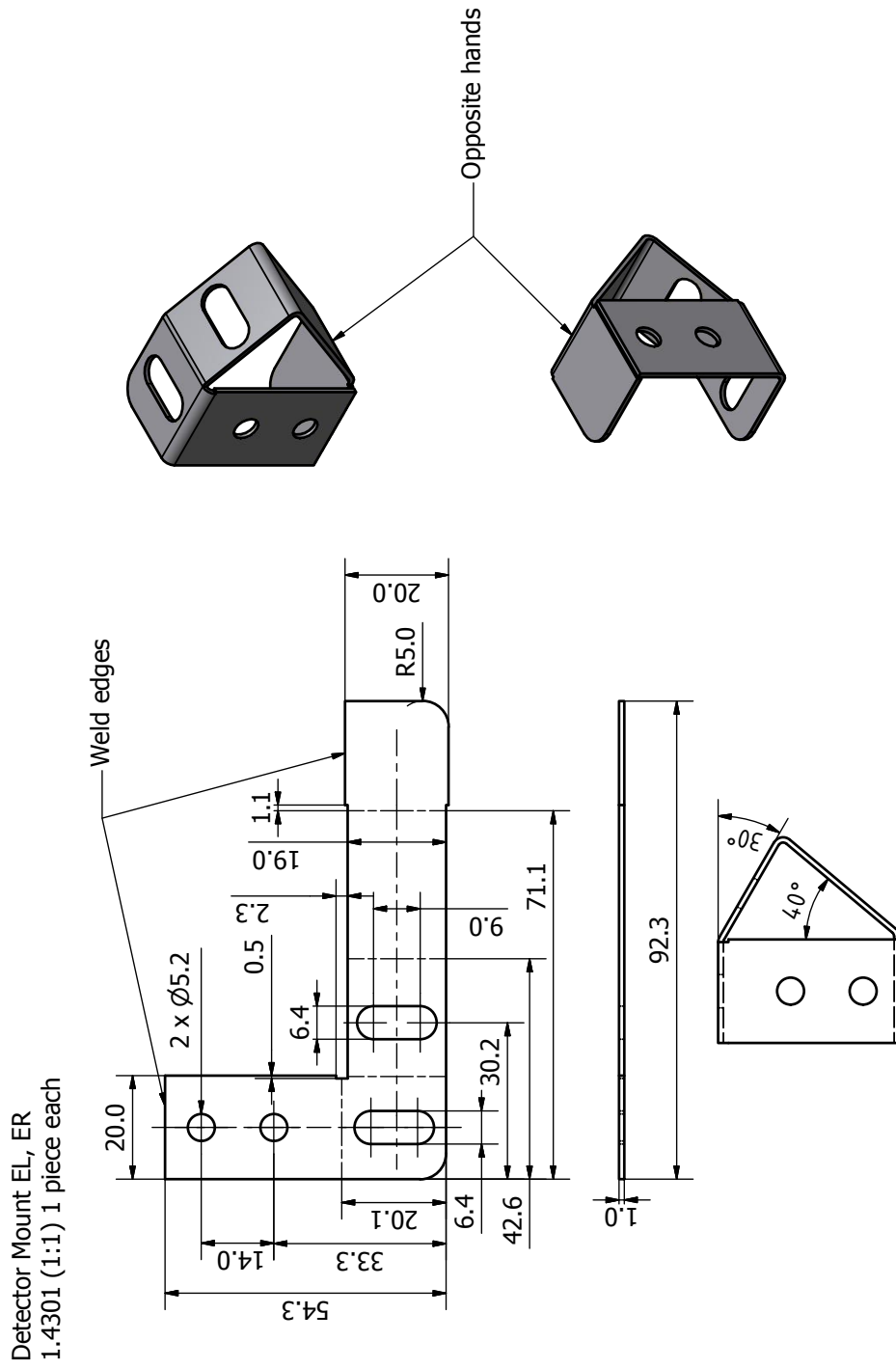
Part of diploma thesis^[105].

Detector Mount C
1.4301 (1:2) 2 pieces

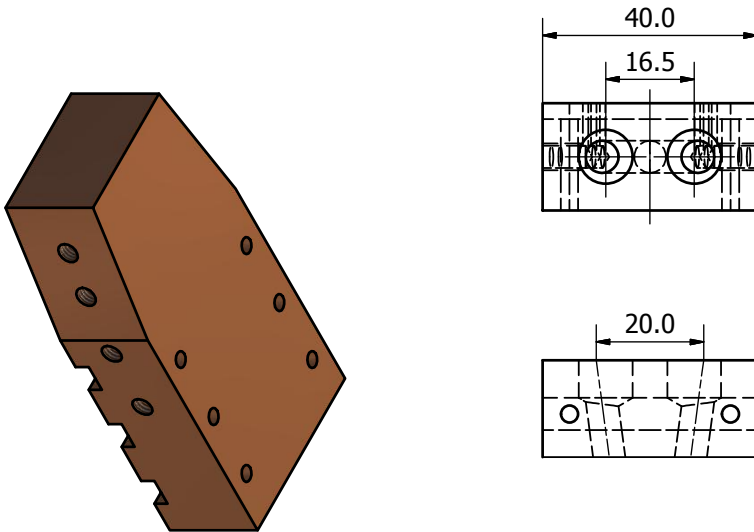
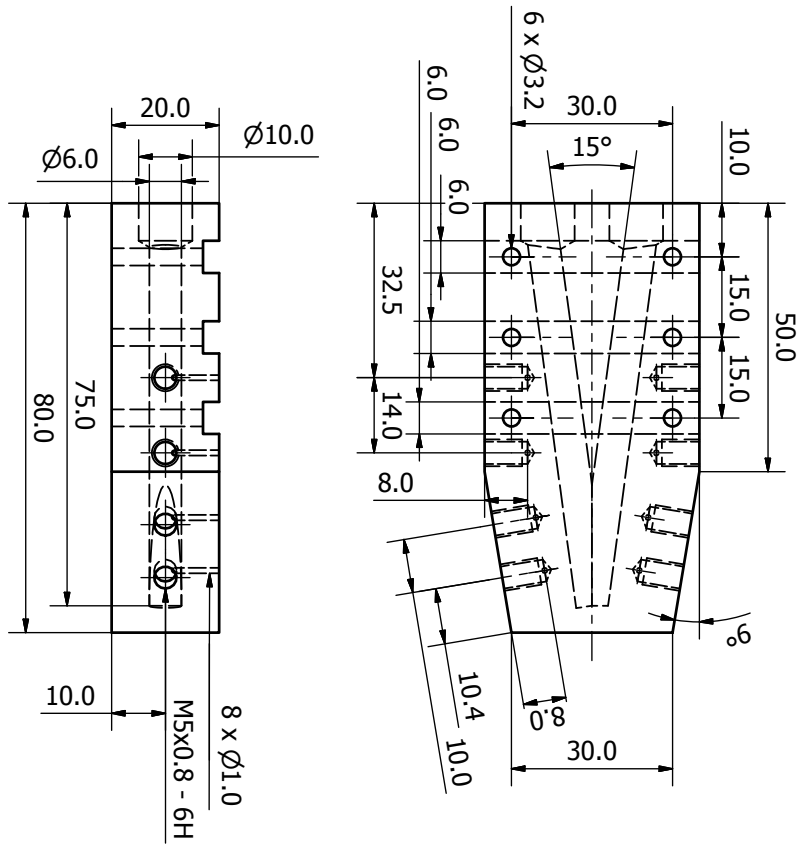


Detector Mount D
1.4301 (1:2) 2 pieces

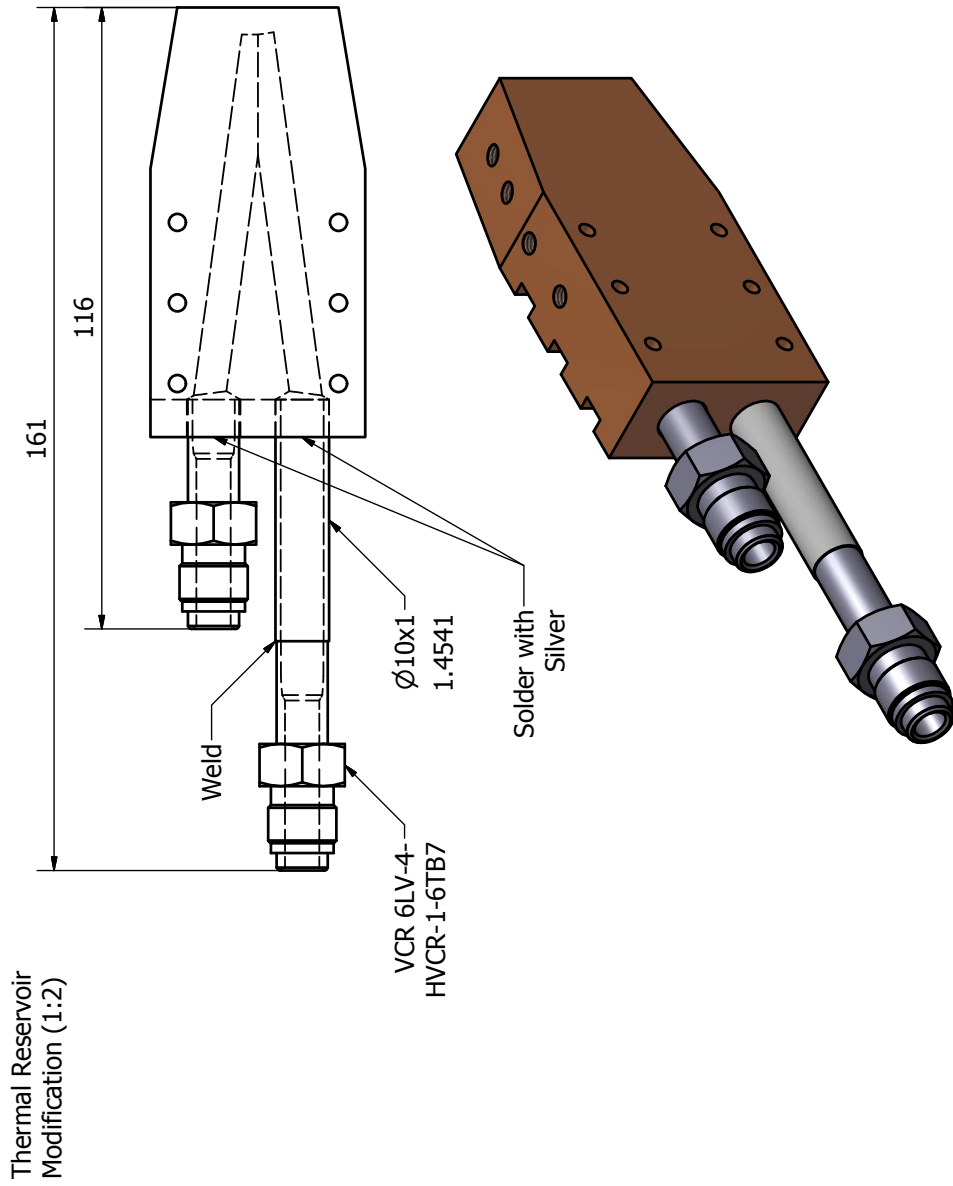




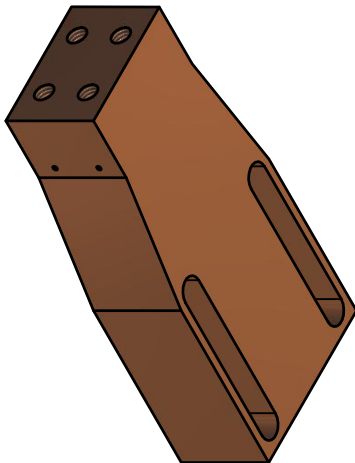
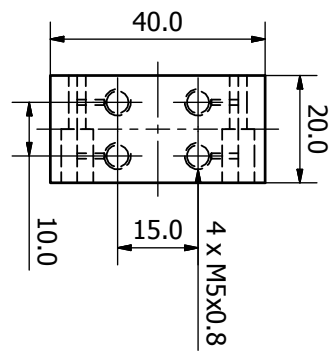
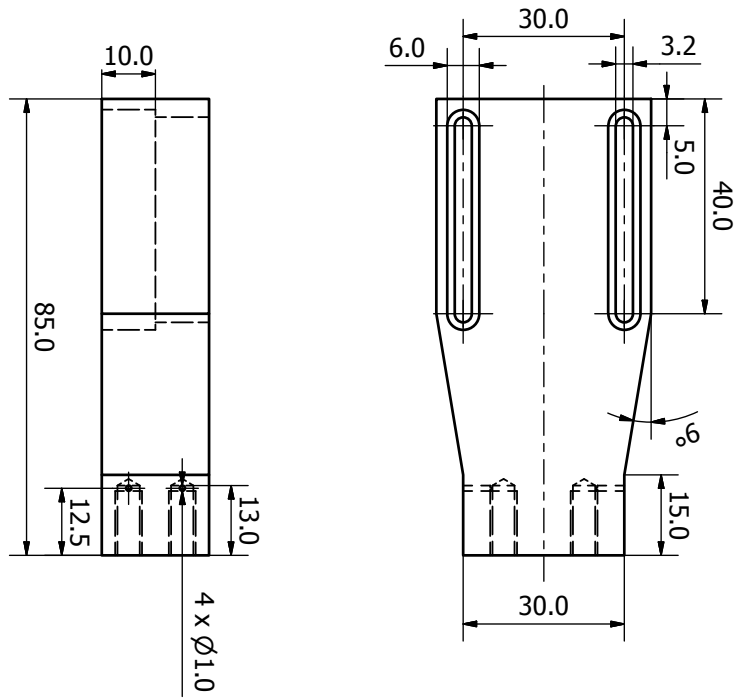
Thermal Reservoir A
Copper (1:1)



Part of diploma thesis^[105].

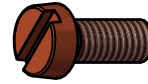
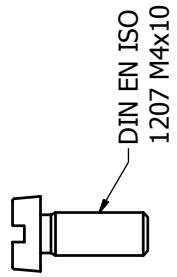


Thermal Reservoir B
Copper (1:1)

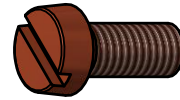
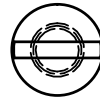
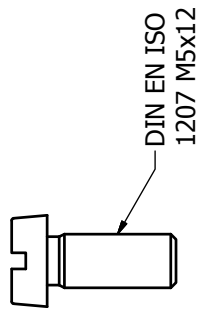


Part of diploma thesis^[105].

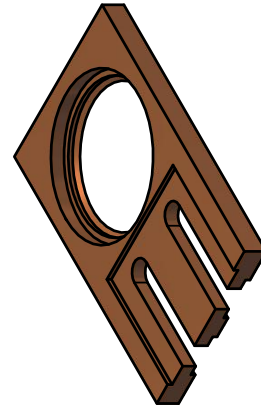
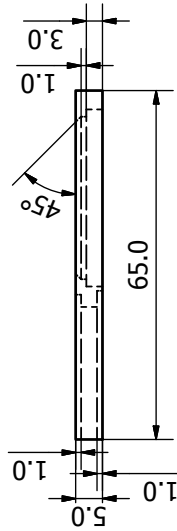
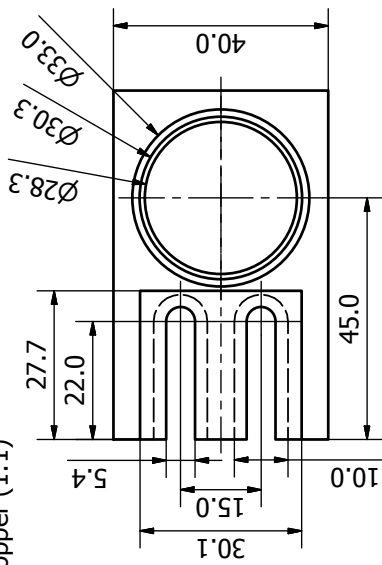
Thermal Reservoir Db
Copper (2:1) 4 pieces



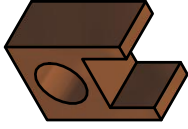
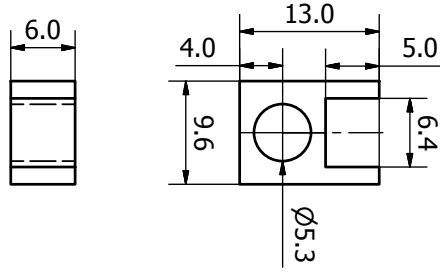
Thermal Reservoir Da
Copper (2:1) 8 pieces



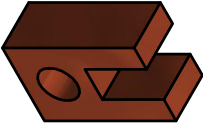
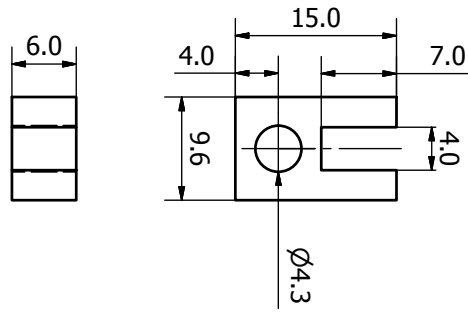
Thermal Reservoir C
Copper (1:1)



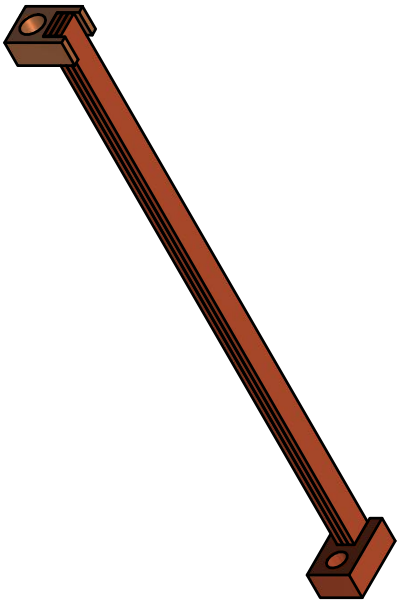
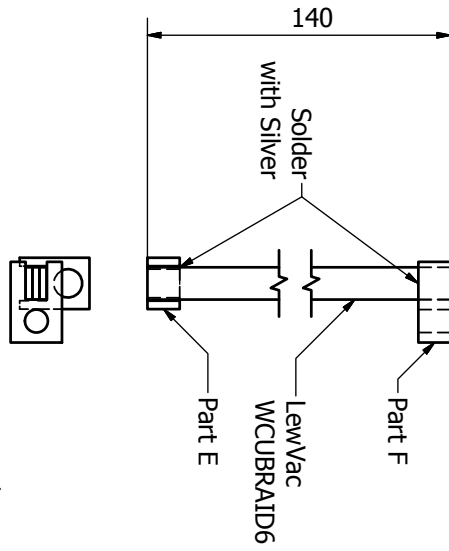
Thermal Reservoir E
Copper (2:1)

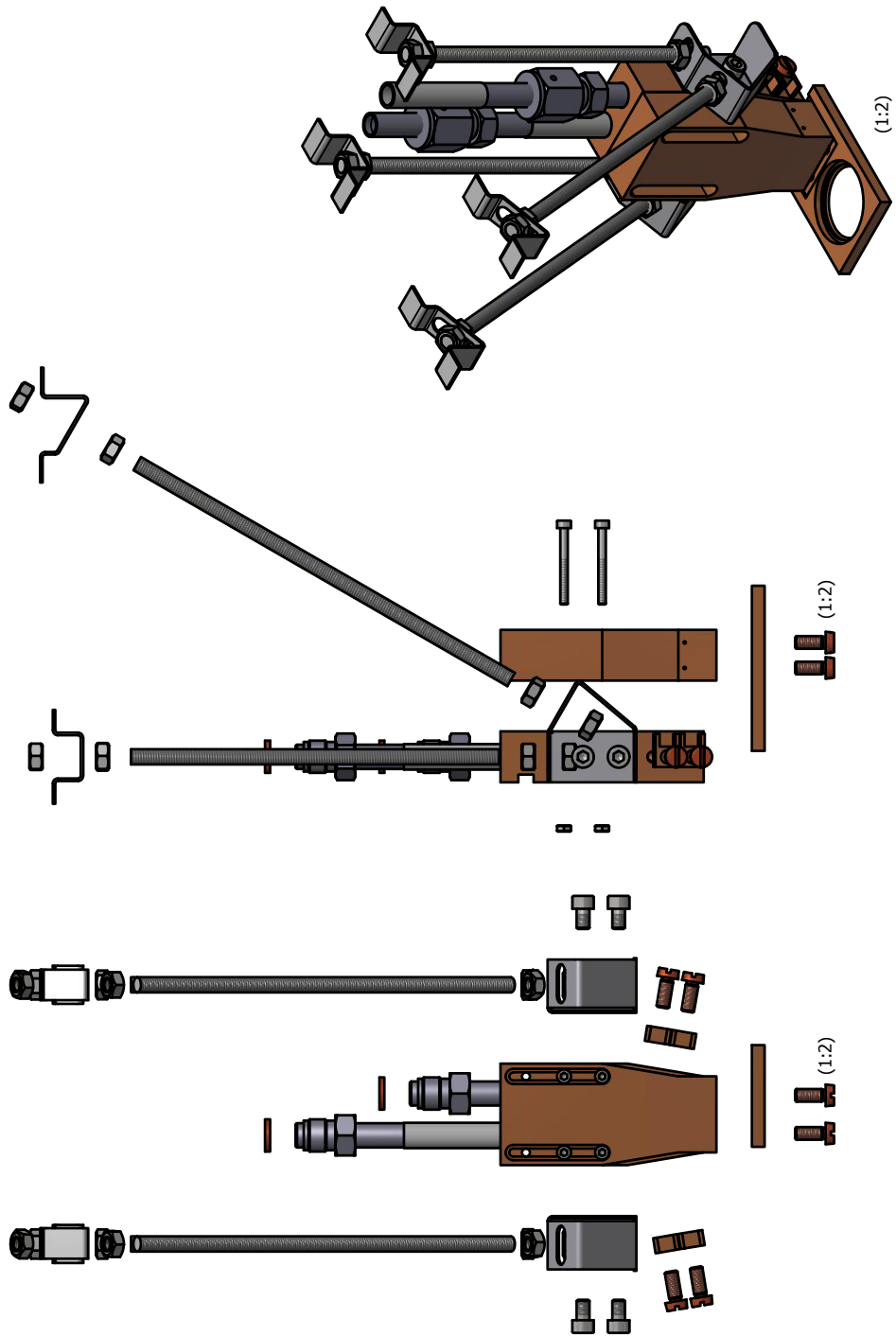


Thermal Reservoir E
Copper (2:1)

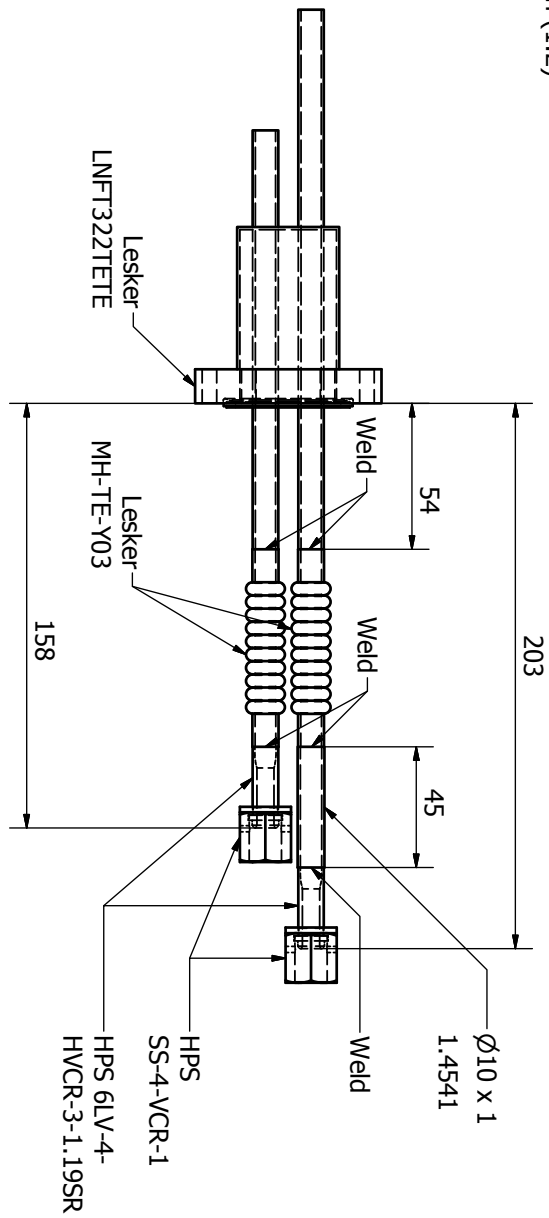


Cooling Braids
(1:1) 4 pieces





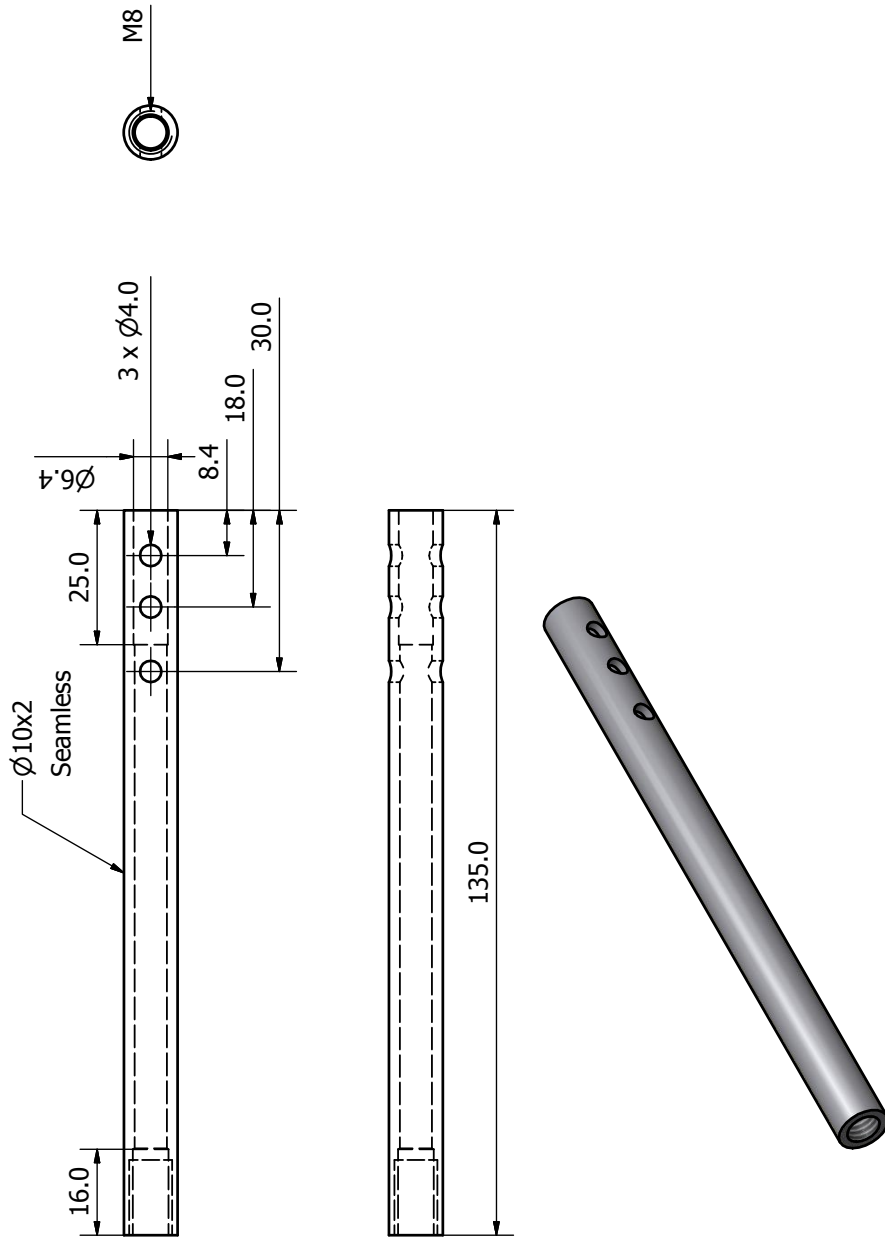
Cooling Feedthrough
Modification (1:2)



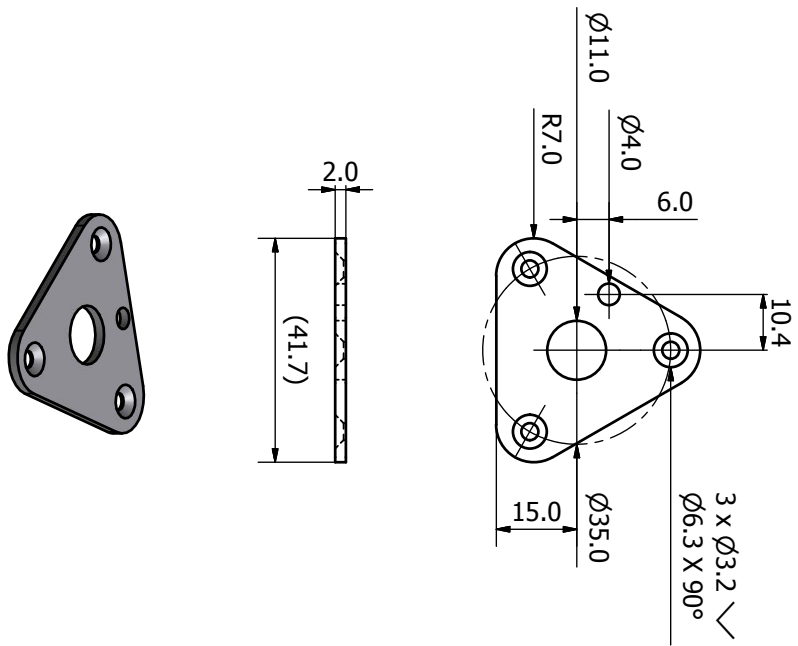
Ancillaries VCR Gasket
OFFHC-Copper (1:1) 2 pieces



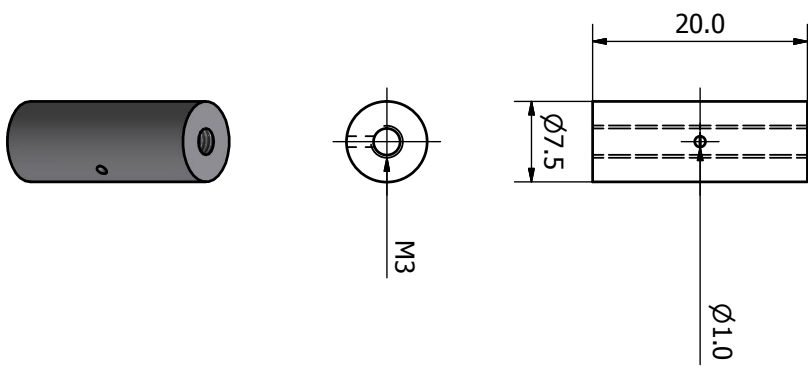
Head Mount A
1.4301 (1:1)



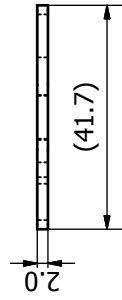
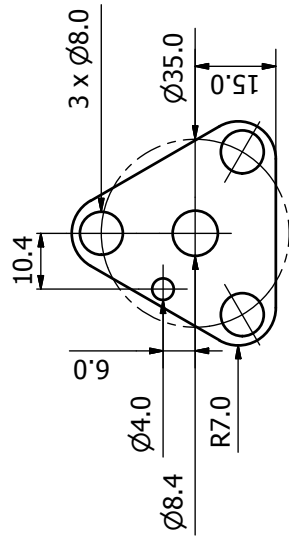
Head Mount B
1.4301 (1:1)



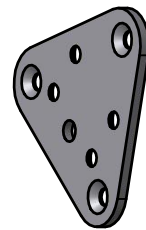
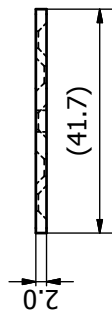
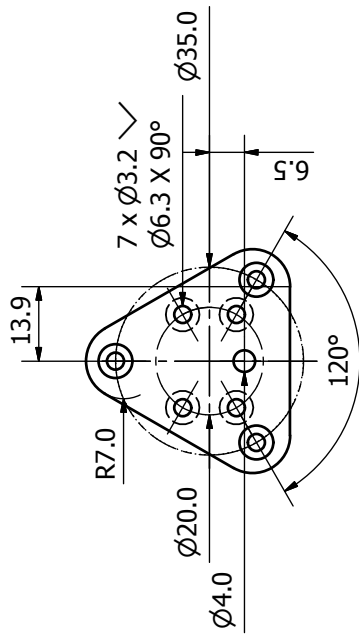
Head Mount C
1.4301 (2:1) 3 pieces

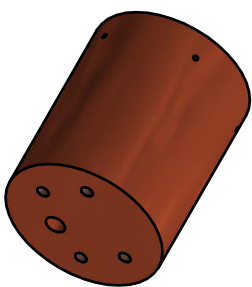
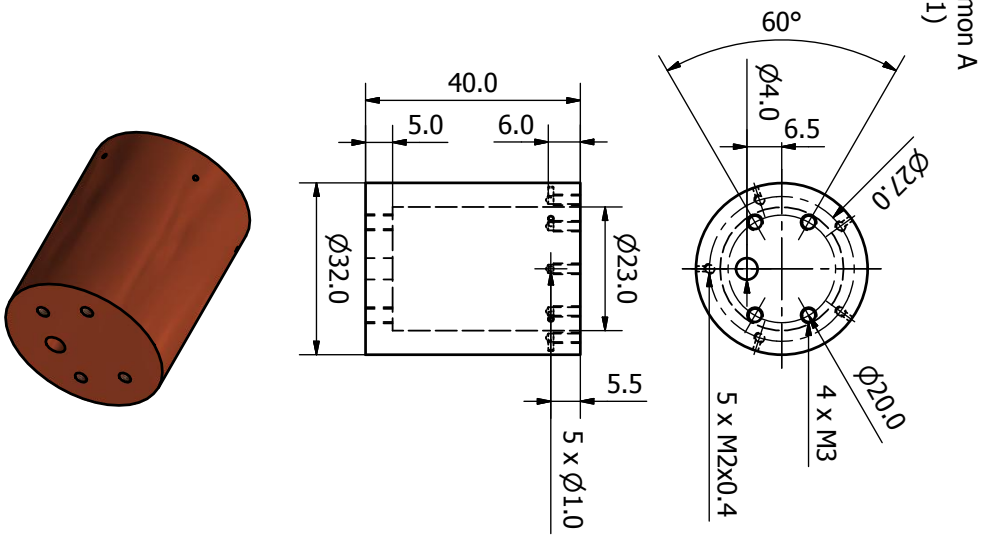
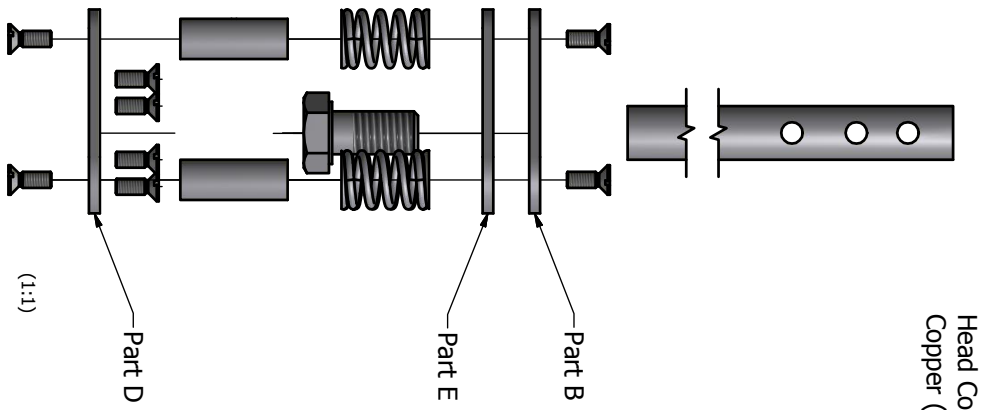
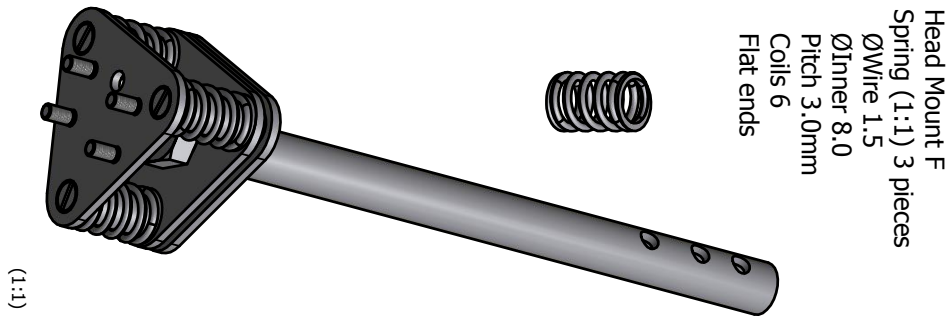


Head Mount E
1.4301 (1:1)

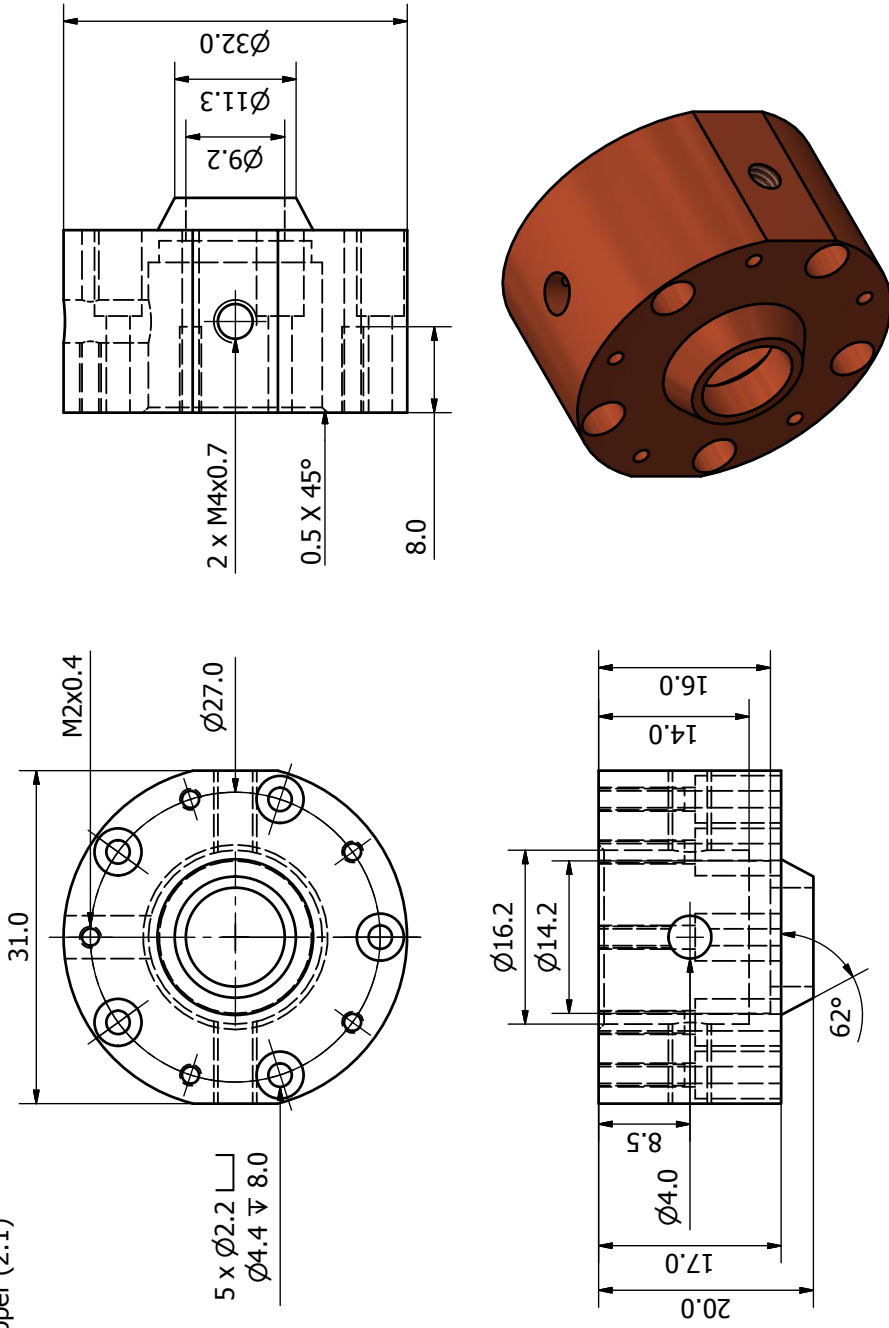


Head Mount D
1.4301 (1:1)

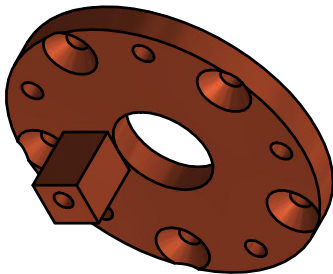
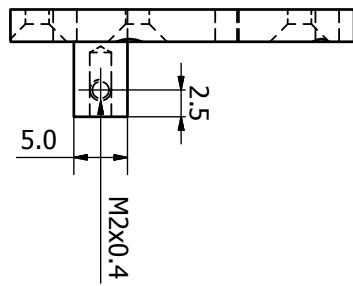
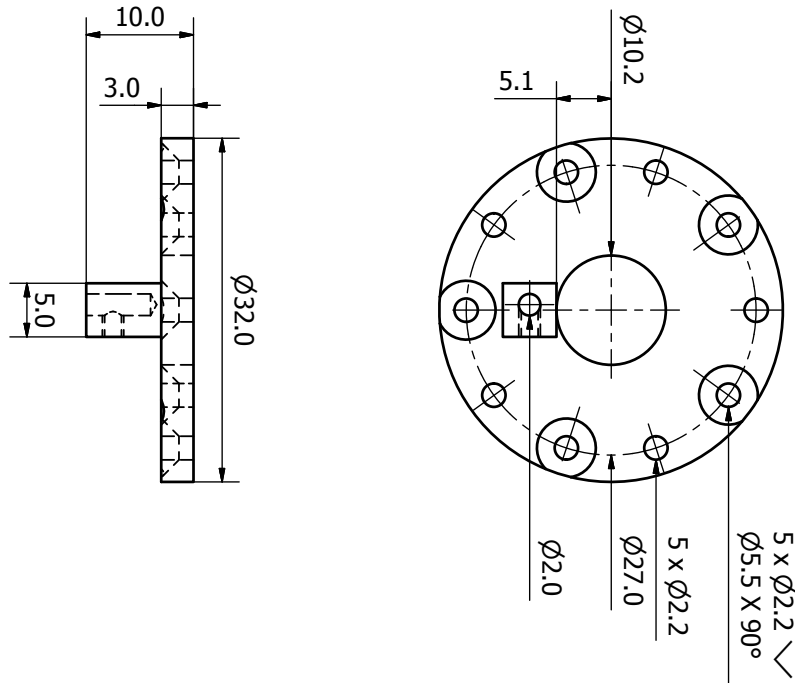


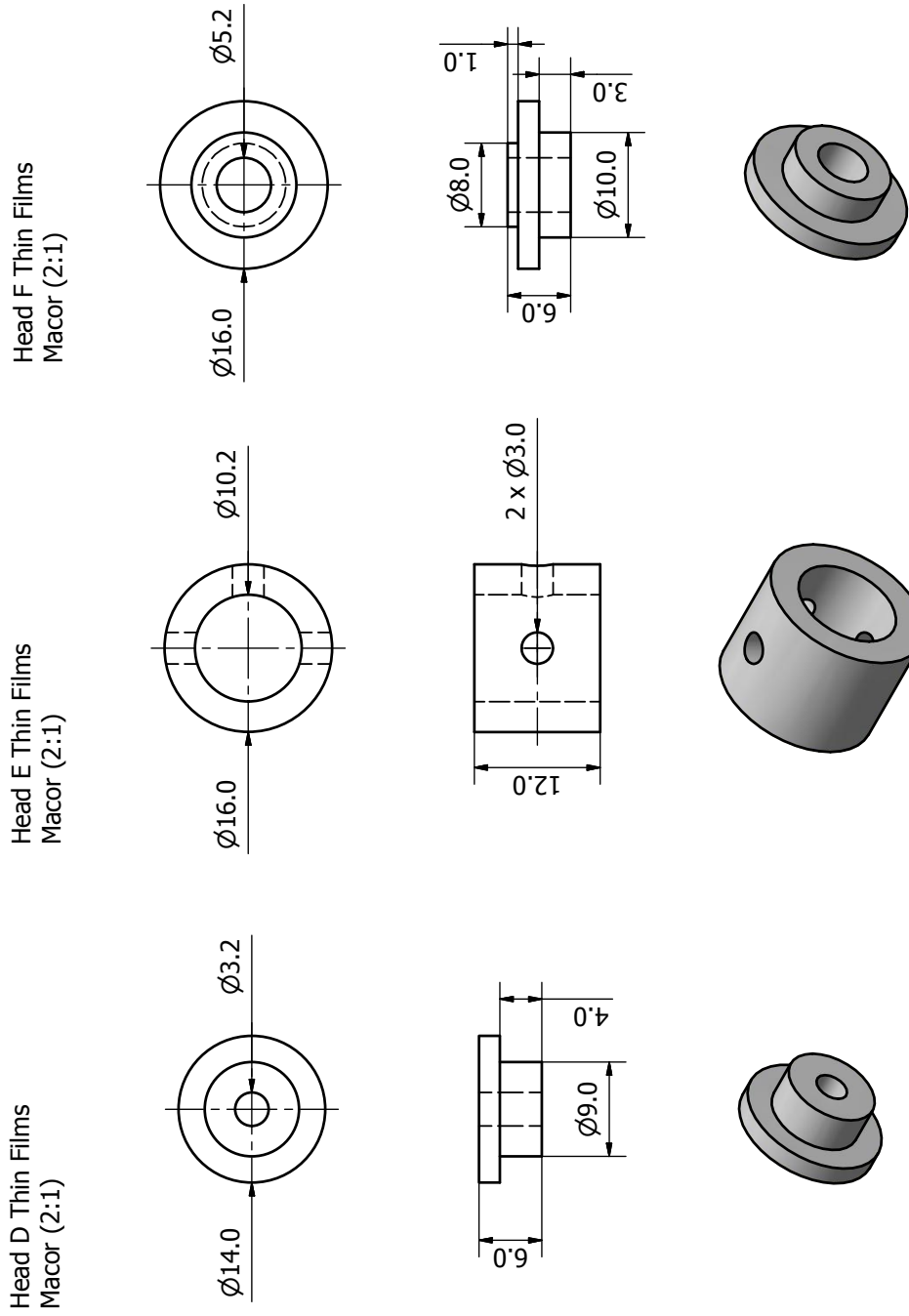


Head B Thin Films
Copper (2:1)

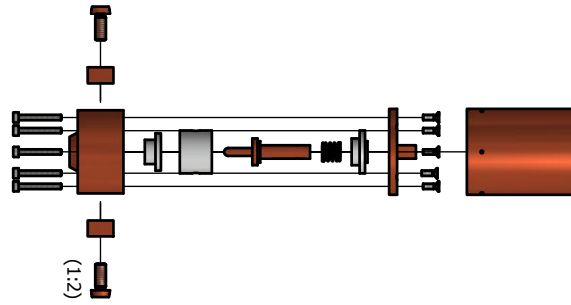
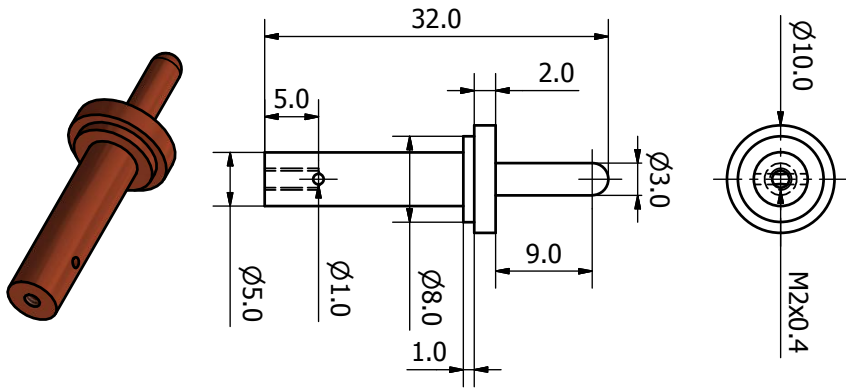


Head C Thin Films
Copper (2:1)

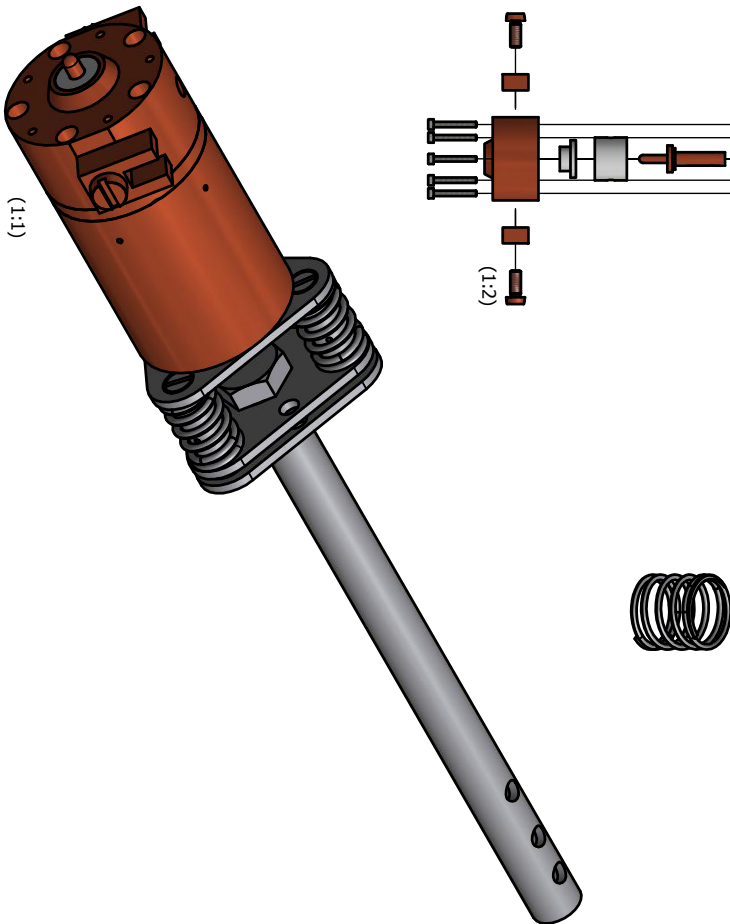


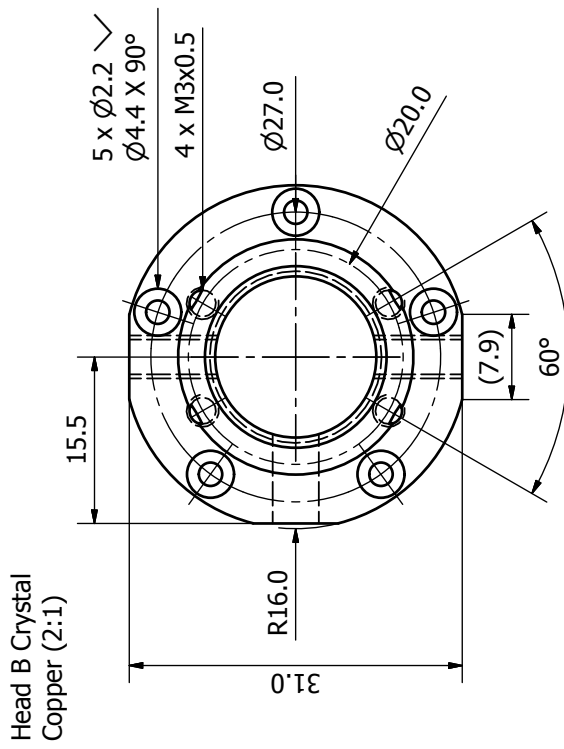
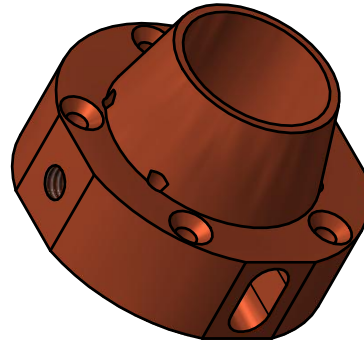
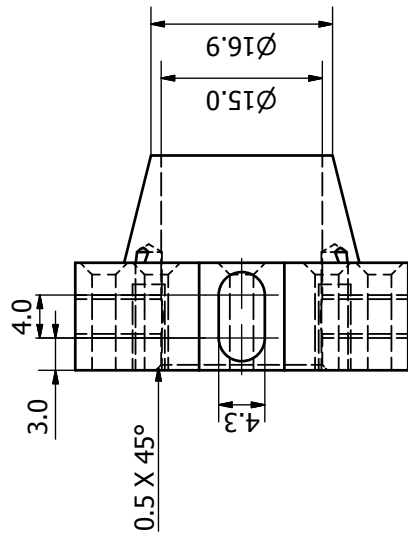


Head G Thin Films
Copper (2:1)

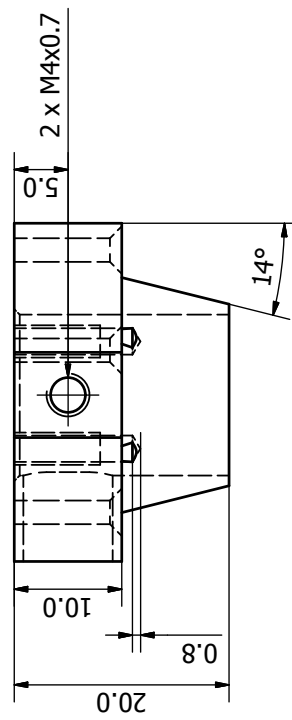


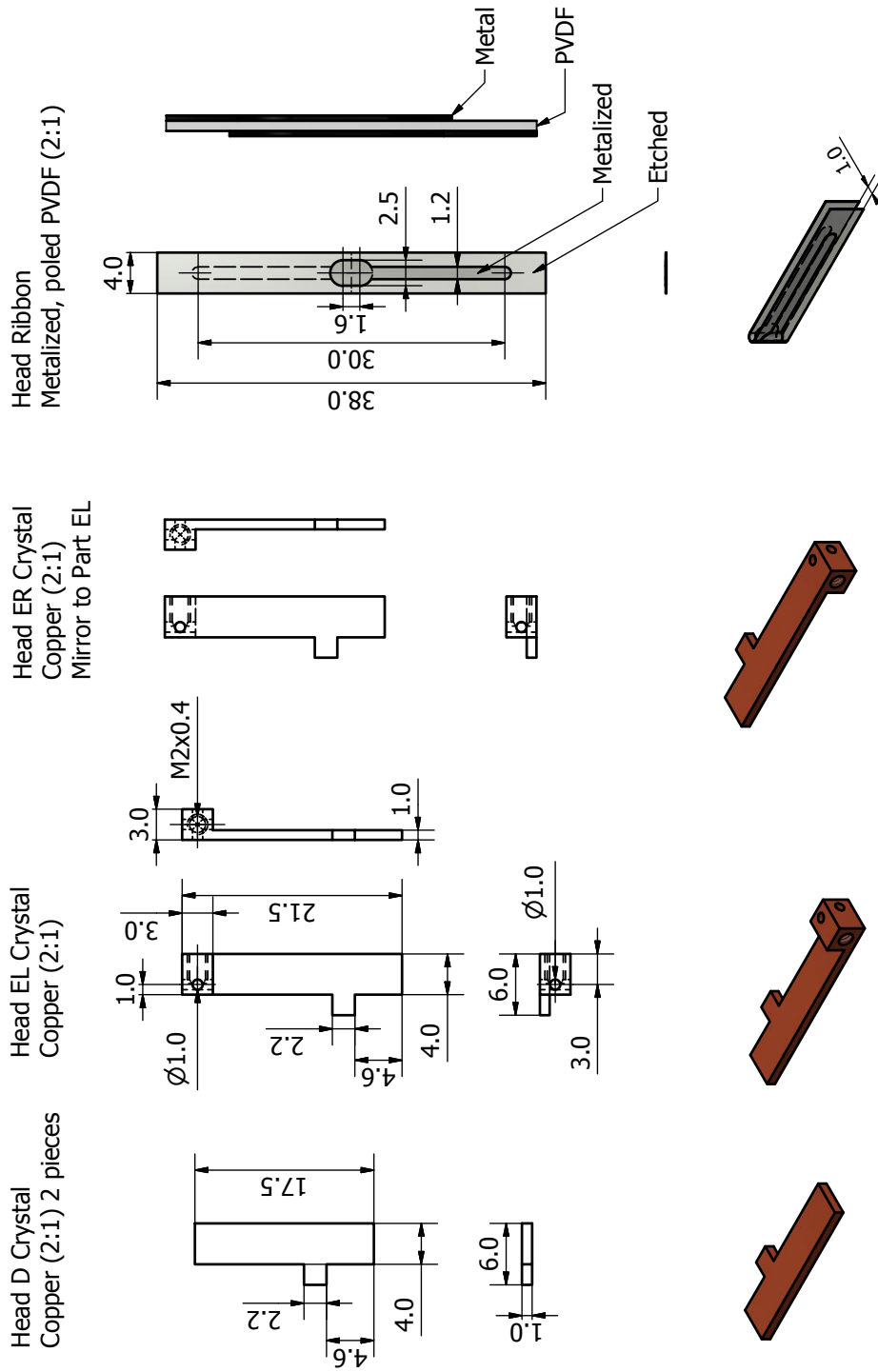
Head H Thin Films
Spring (2:1)
 ϕ Wire 0,5
 ϕ Inner 6.0
Pitch 2.5mm
Coils 5

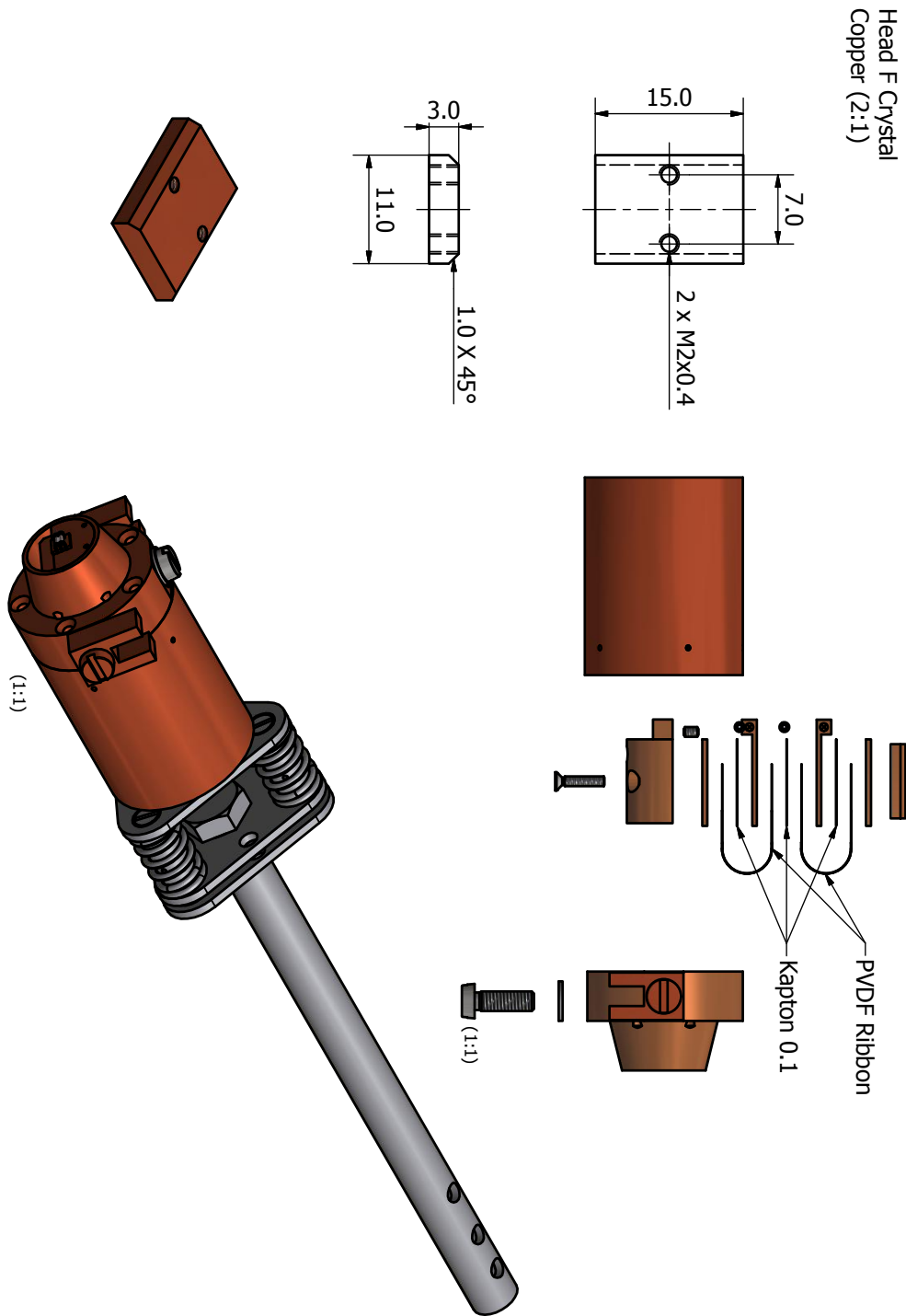


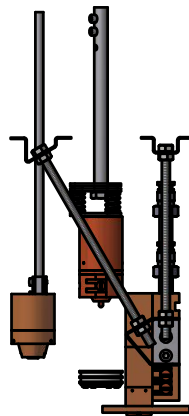
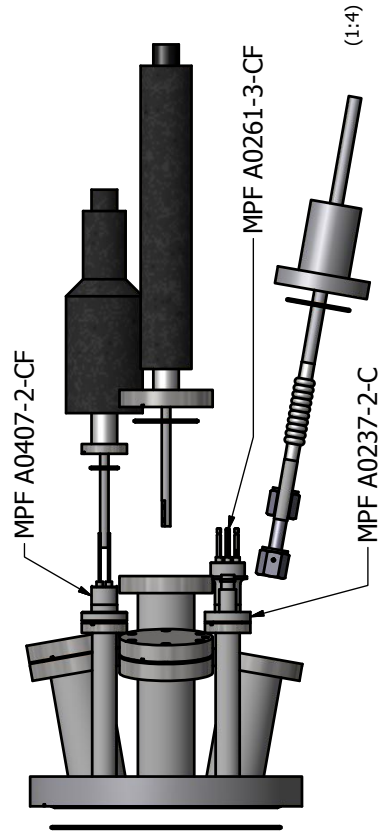


Head B Crystal
Copper (2:1)





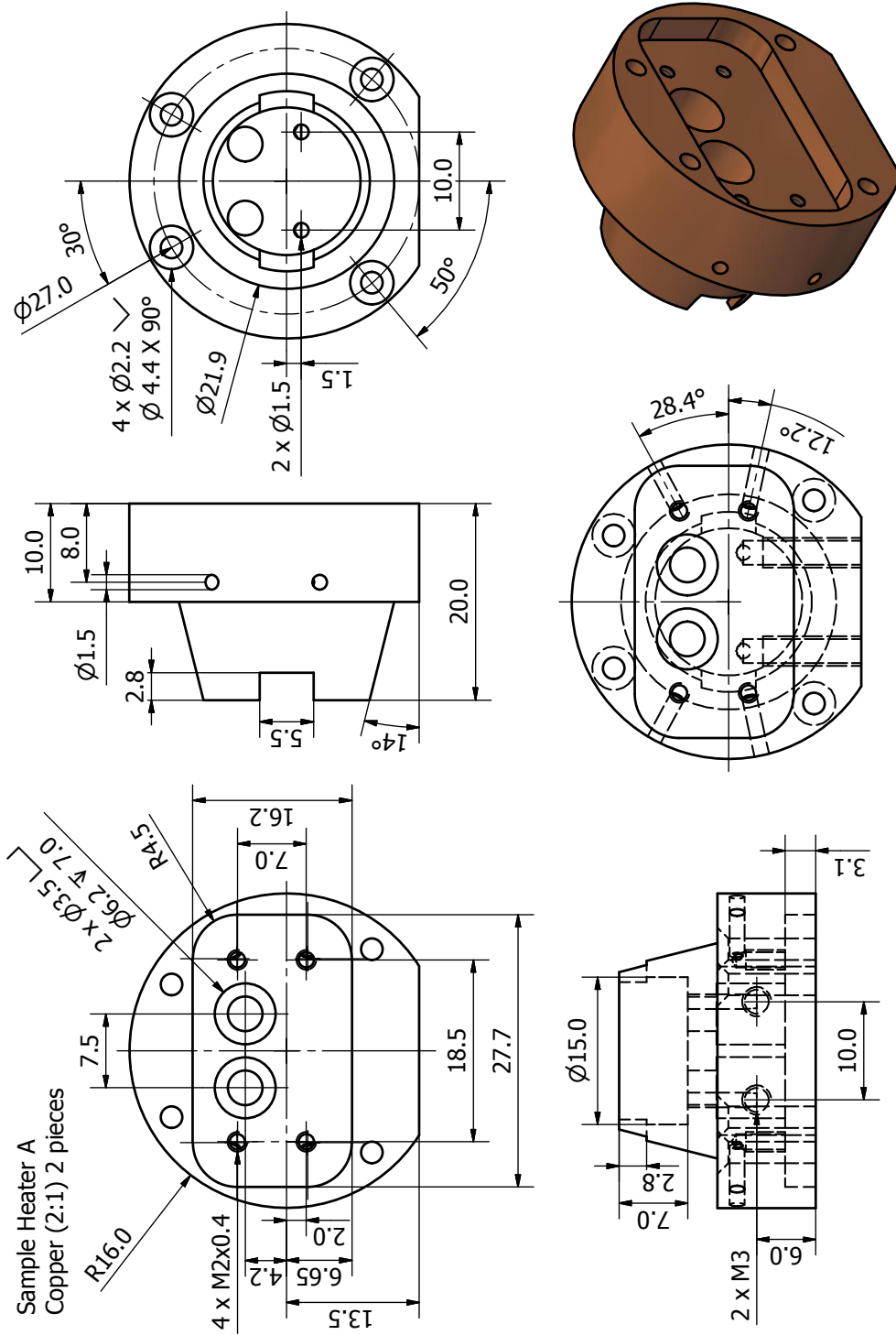




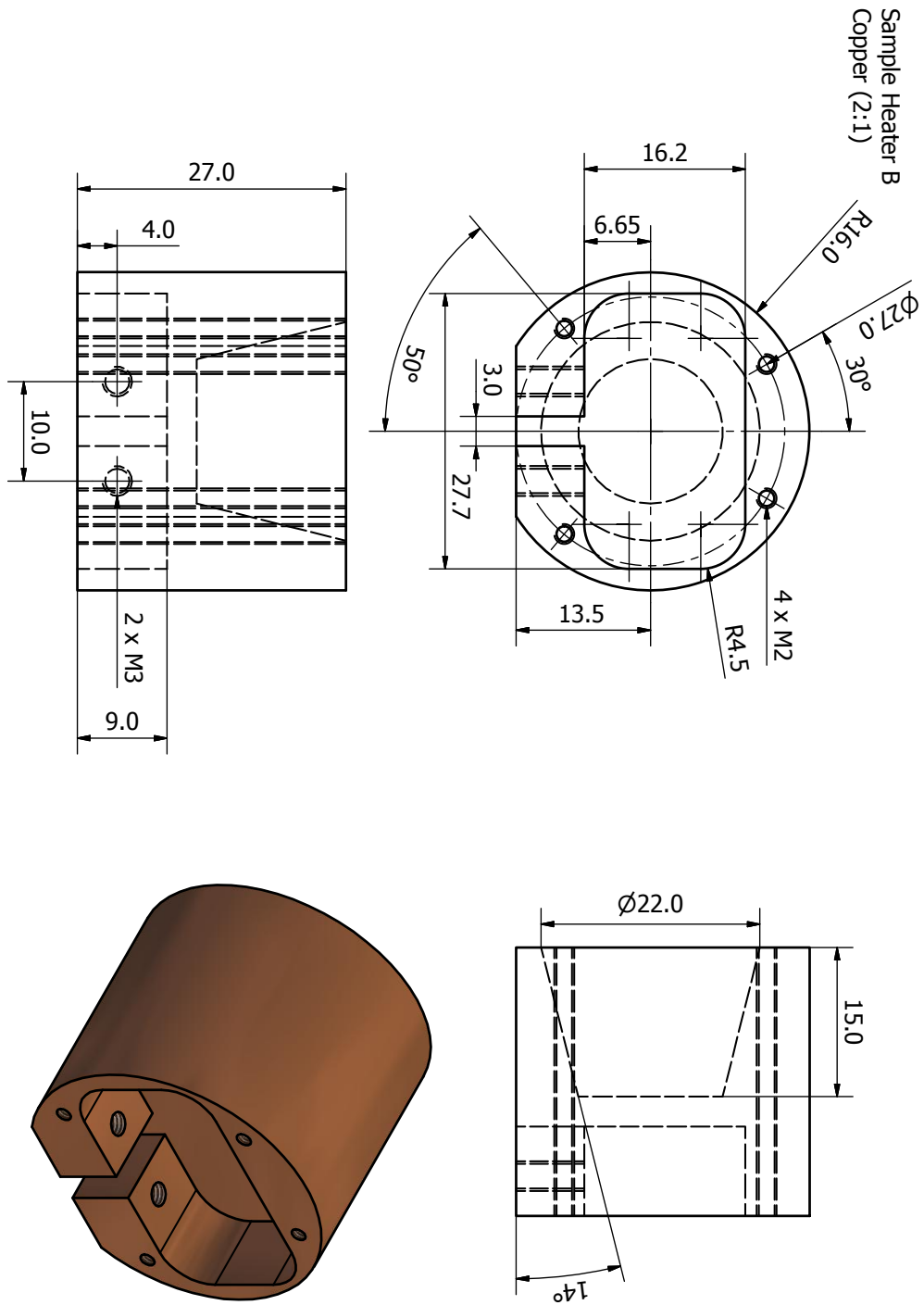
B.2.4 Sample Heater



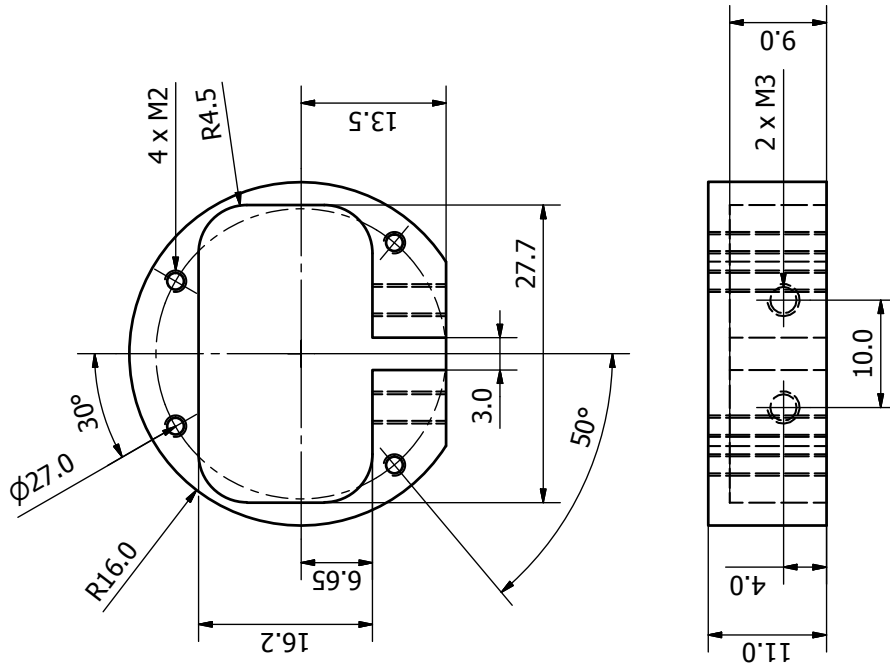
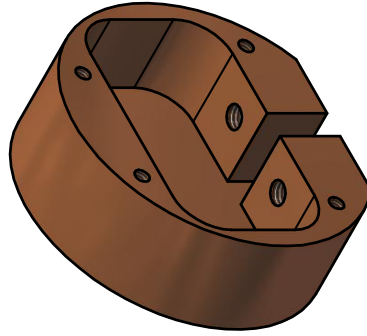
Design by O. LYTKEN.



Design by O. LYTKEN.



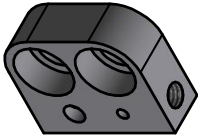
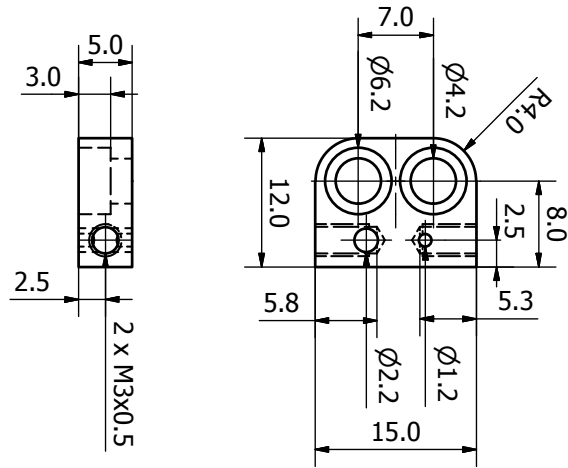
Design by O. LYTKEN.



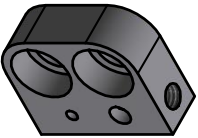
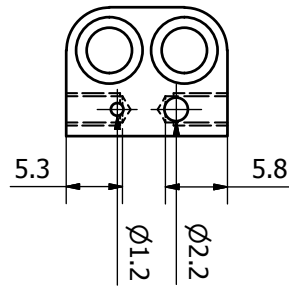
Sample Heater BB
Copper (2:1)

Design by O. LYTKEN.

Sample Heater CL
1.4301 (2:1) 2 pieces

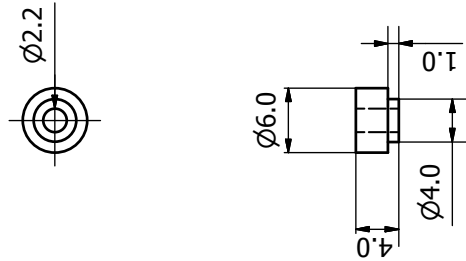


Sample Heater CR
1.4301 (2:1) 2 pieces
Opposite hand from CL

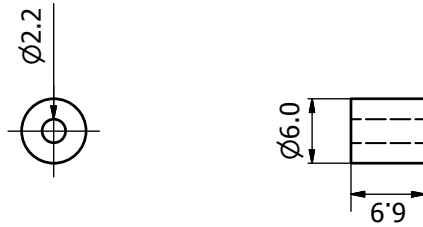


Design by O. LYTKEN.

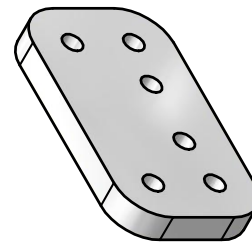
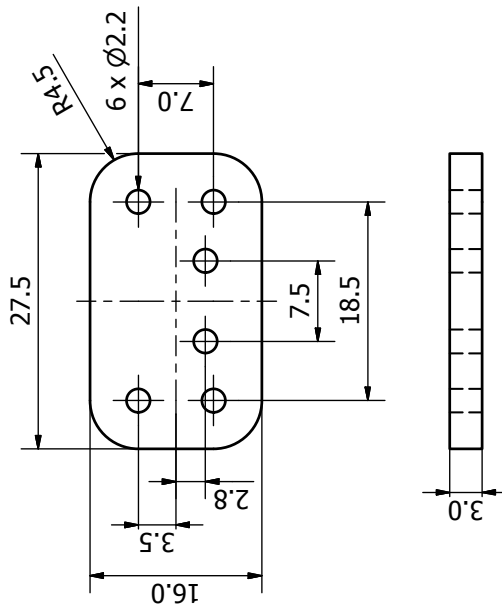
Sample Heater F
Macor (2:1) 8 pieces



Sample Heater E
Macor (2:1) 4 pieces

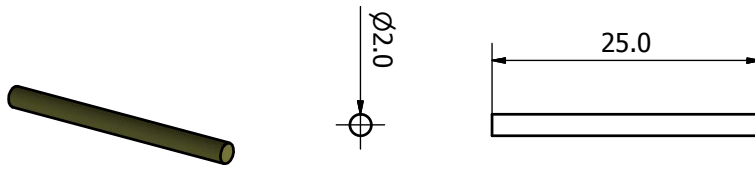


Sample Heater D
Macor (2:1) 2 pieces

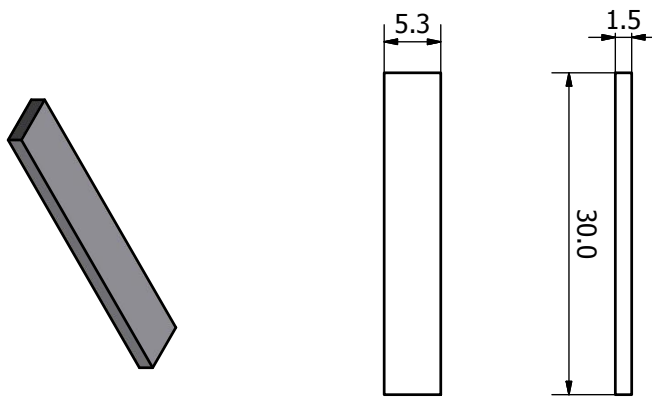


Design by O. LYTKEN.

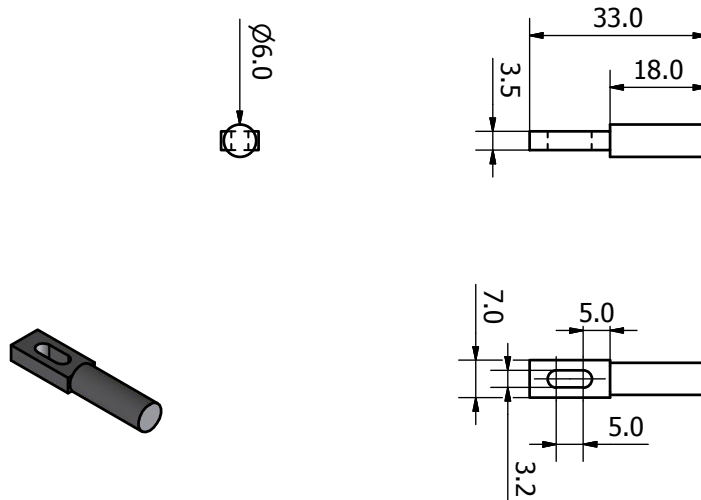
Sample Heater G
Tantalum (2:1) 4 pieces



Sample Heater H
1.4301 (2:1)
Alignment piece

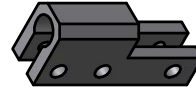
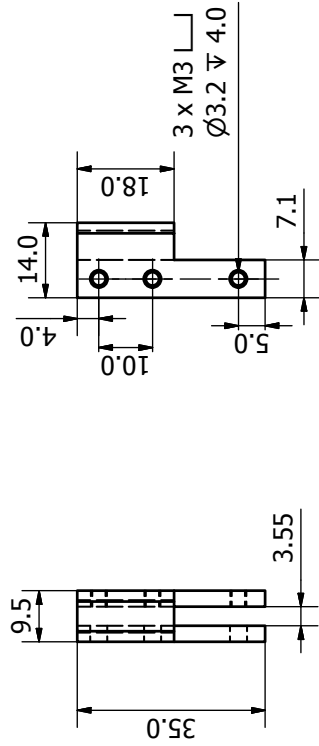


Sample Heater I
1.4301 (1:1)

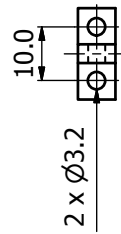
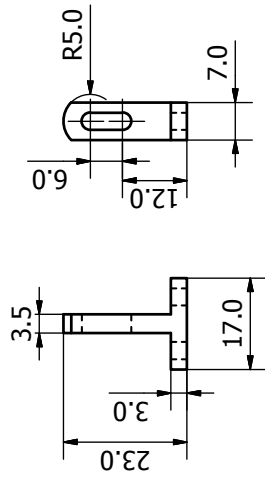


Design by O. LYTKEN.

Sample Heater K
1.4301 (1:1) 2 pieces

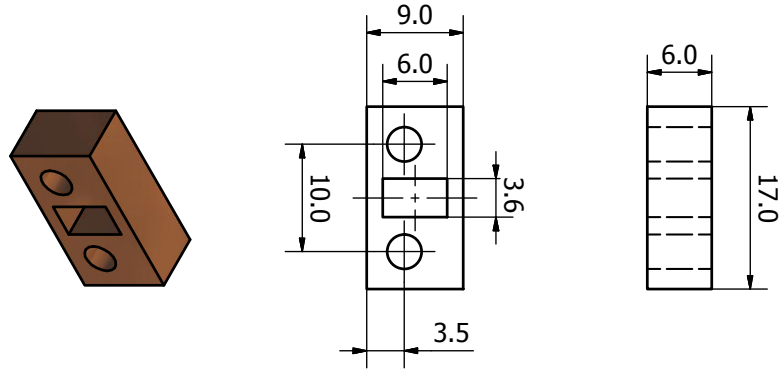


Sample Heater J
1.4301 (1:1)

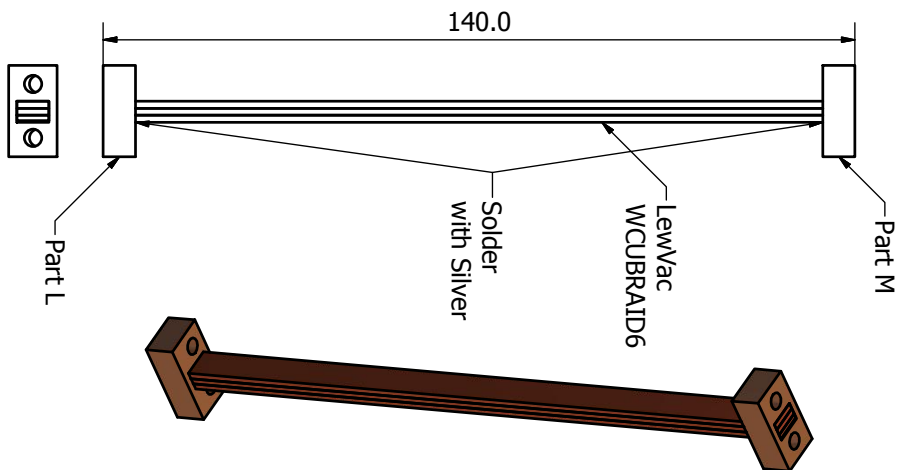
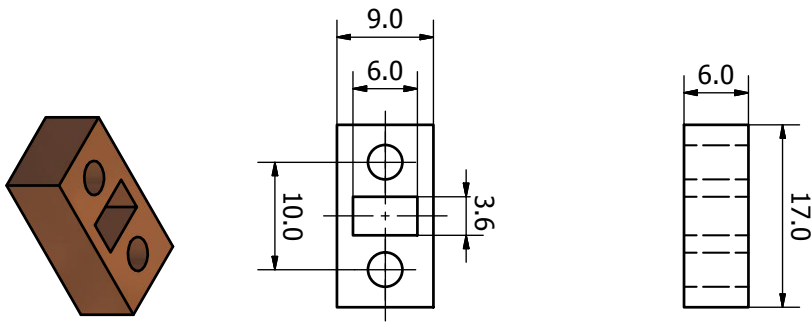


Design by O. LYTKEN.

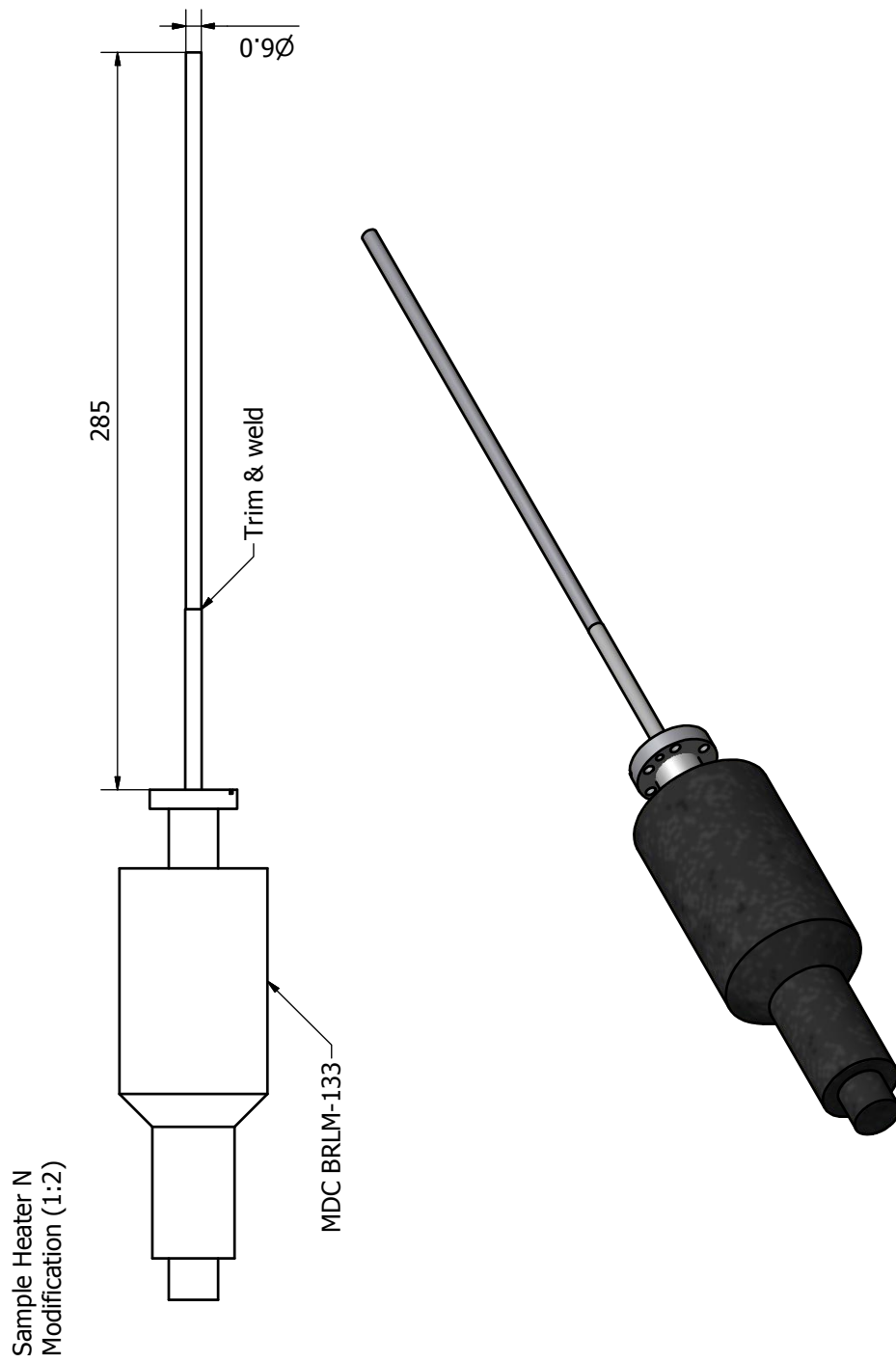
Sample Heater L
Copper (2:1)



Sample Heater M
Copper (2:1)

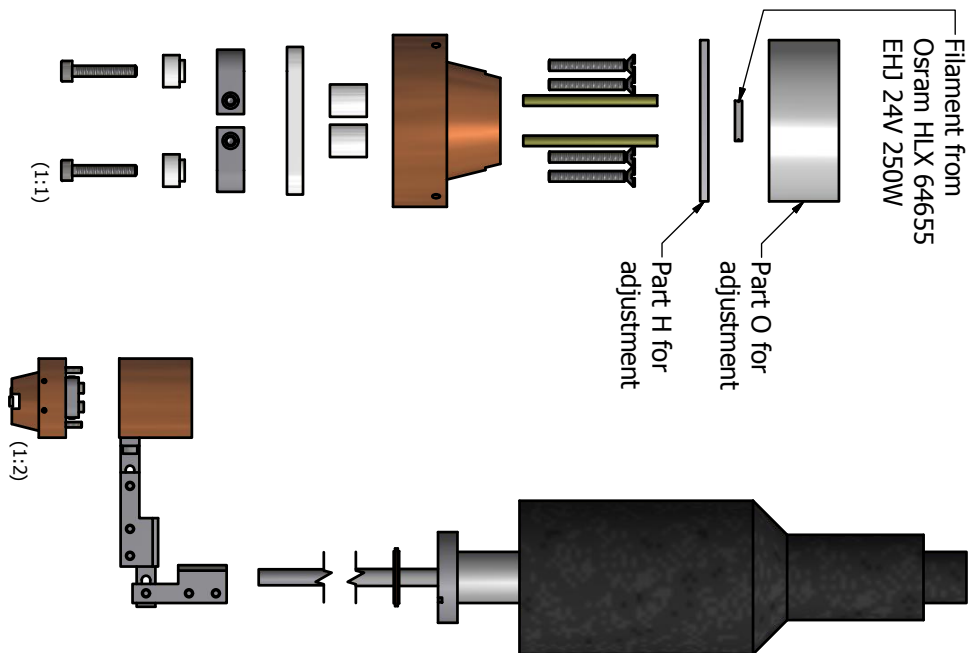
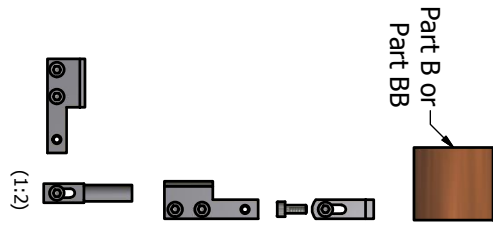
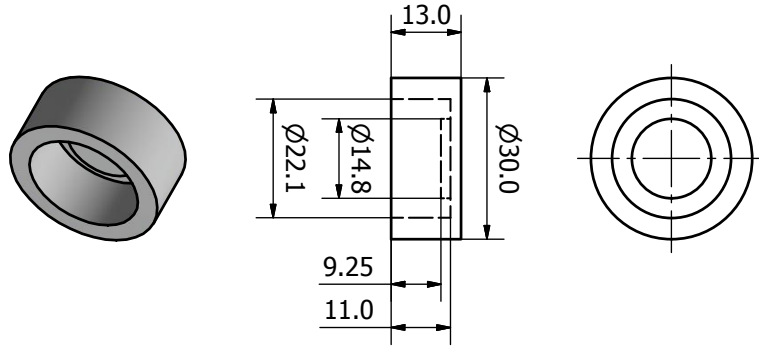


Design by O. LYTKEN.



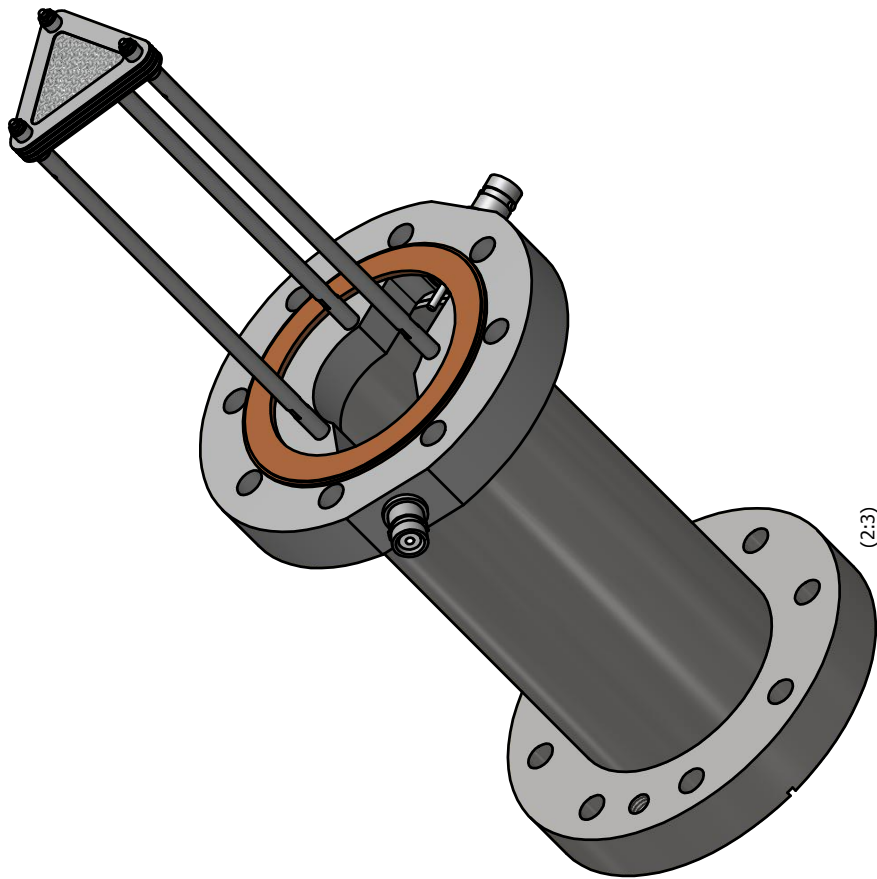
Design by O. LYTKEN.

Sample Heater O
 Aluminum (1:1)
 Alignment piece



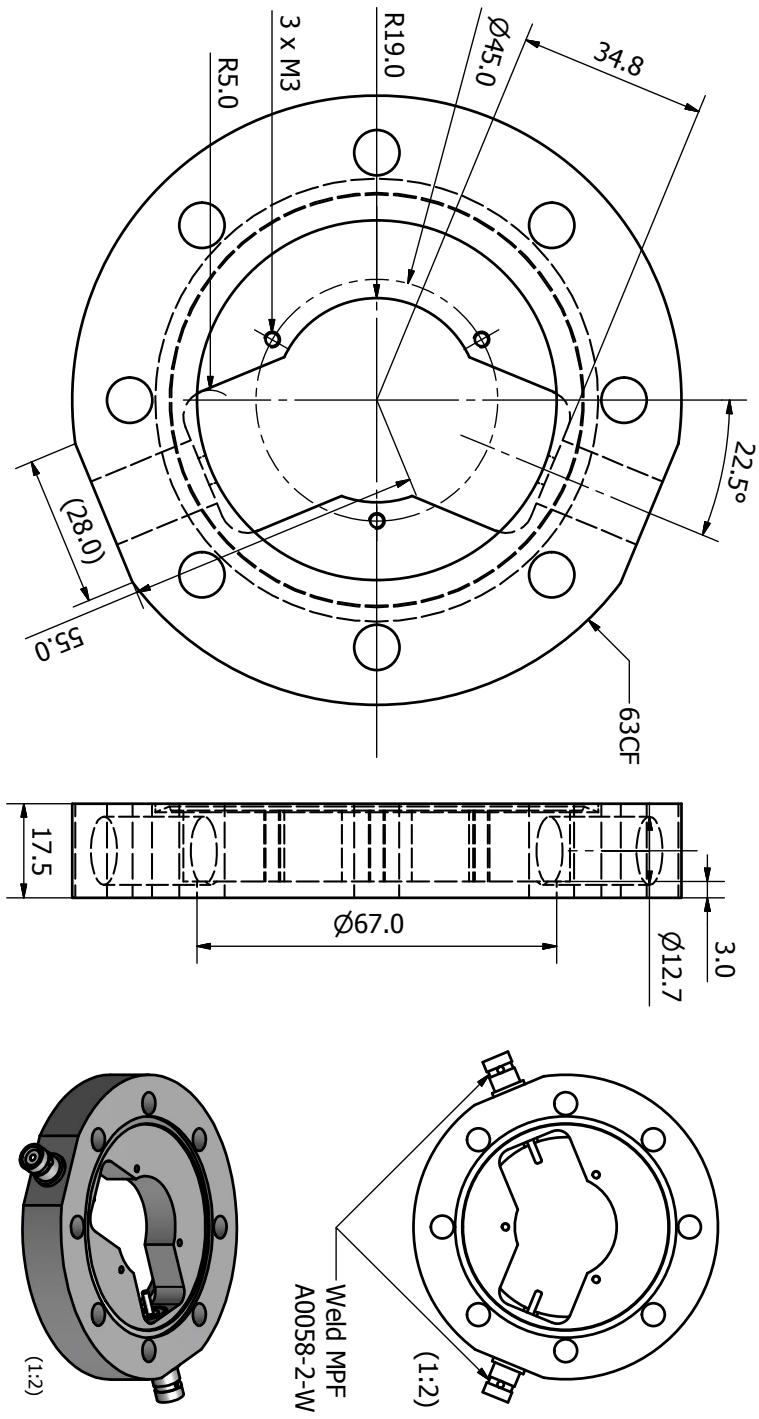
Design by O. LYTKEN.

B.2.5 Mass Spectrometer Mount

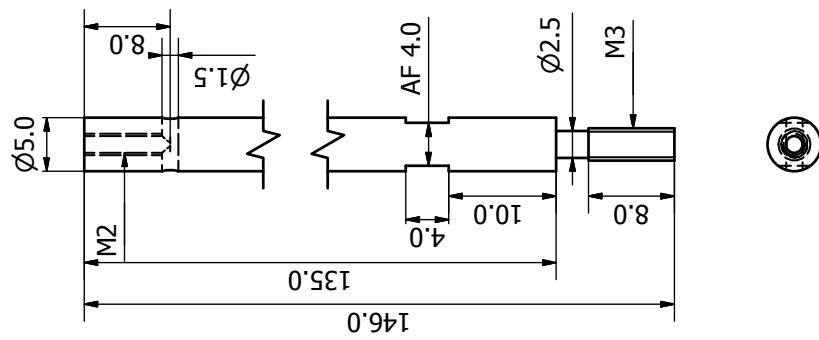


(2:3)

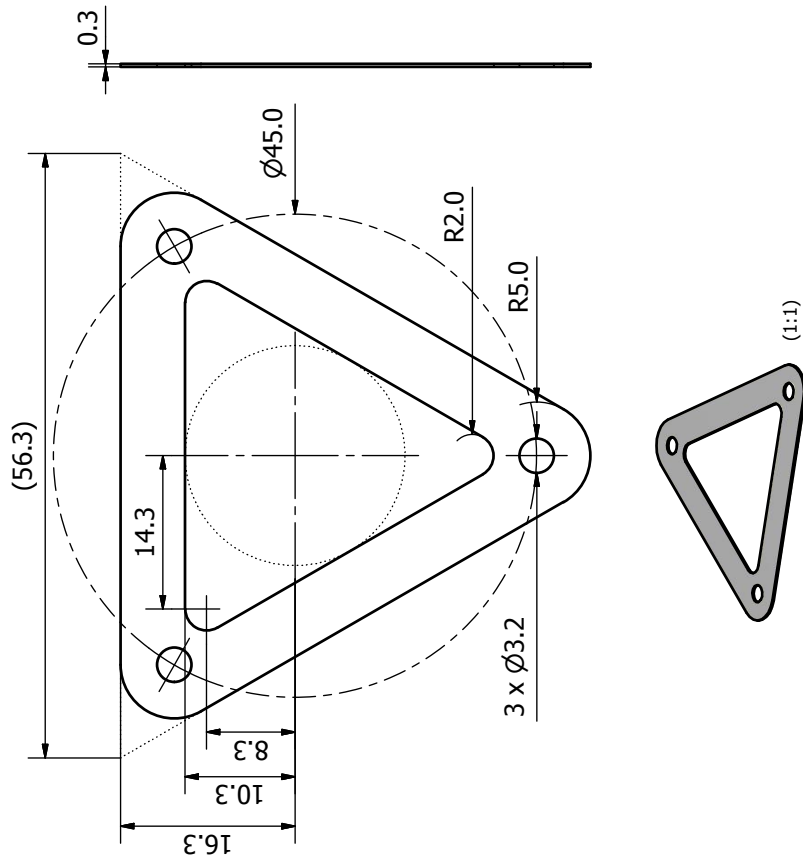
QMS Mounting Flange
1.4301 (1:1)



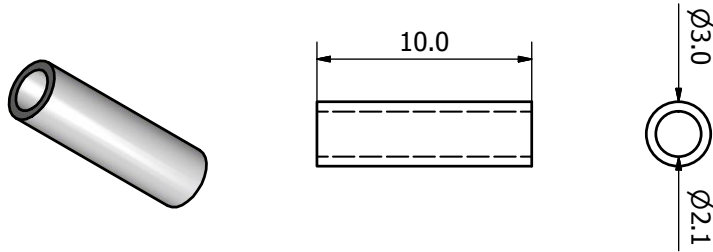
QMS Mounting Rod
1.4301 (2:1) 3 pieces



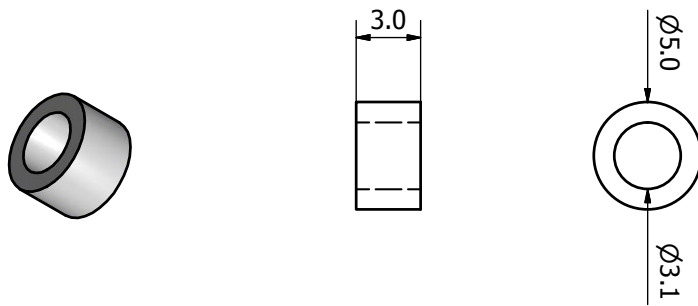
QMS Grid Holder
1.4301 (2:1) 8 pieces



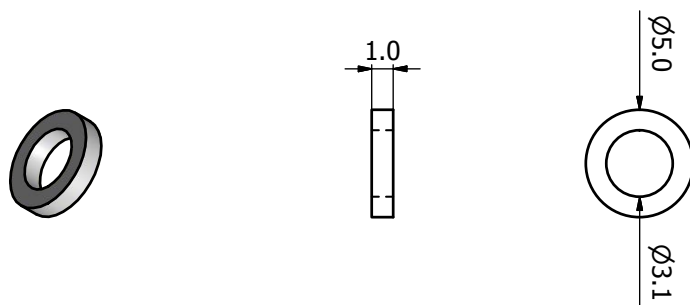
Grid Isolation A
A1203 (4:1) 3 pieces



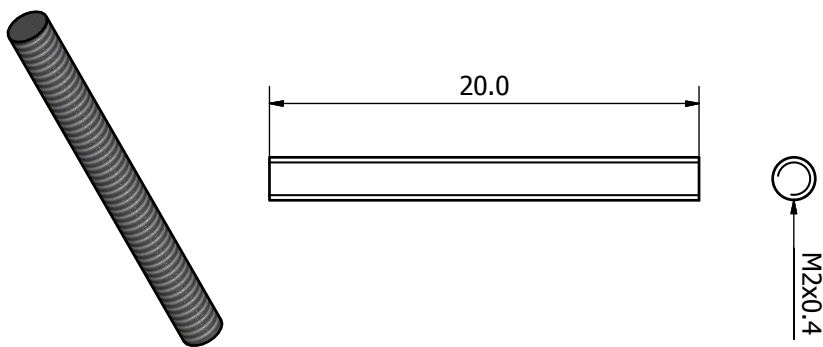
Grid Isolation B
A1203 (4:1) 6 pieces

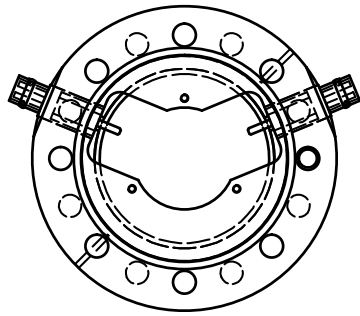
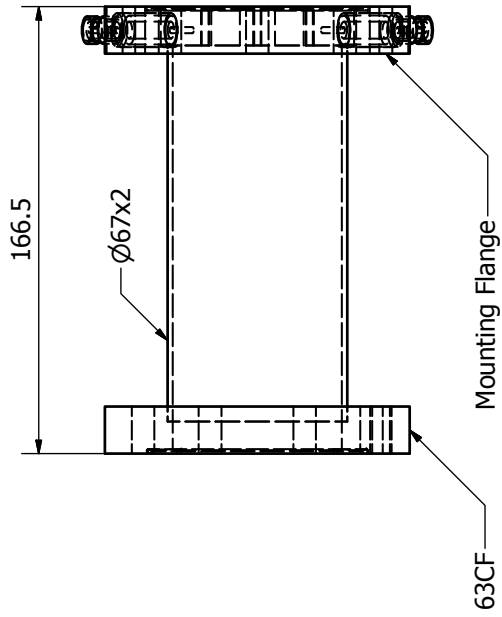


Grid Isolation C
A1203 (4:1) 9 pieces

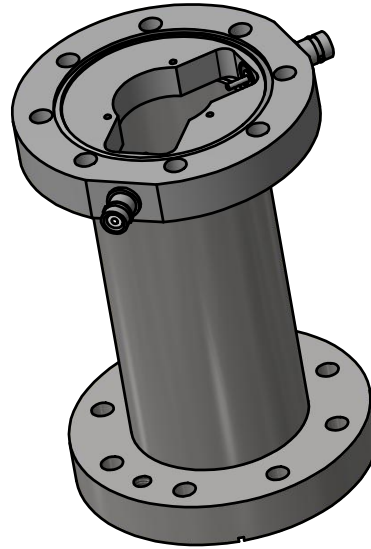


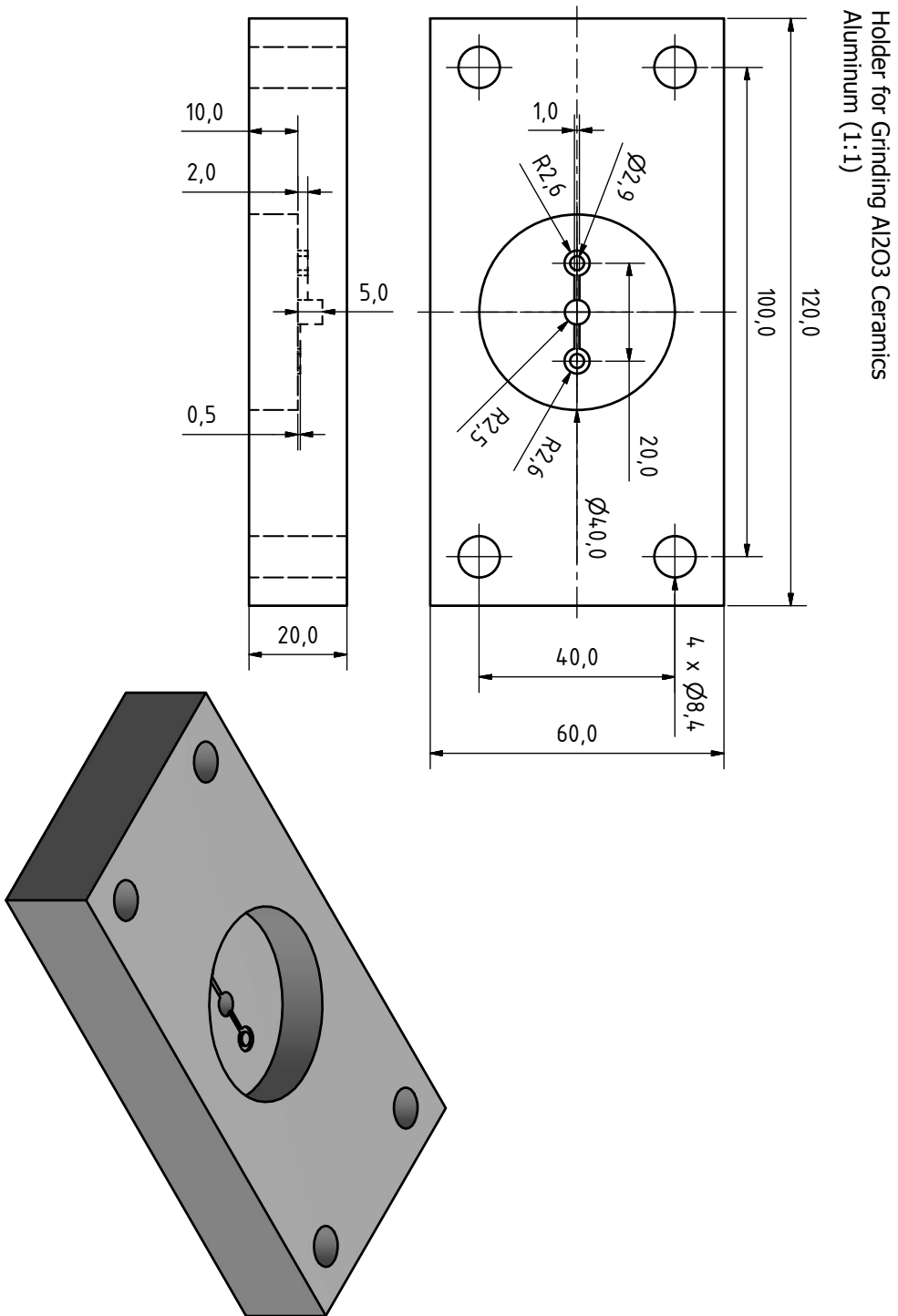
Grid Isolation D
1.4301 (4:1) 3 pieces

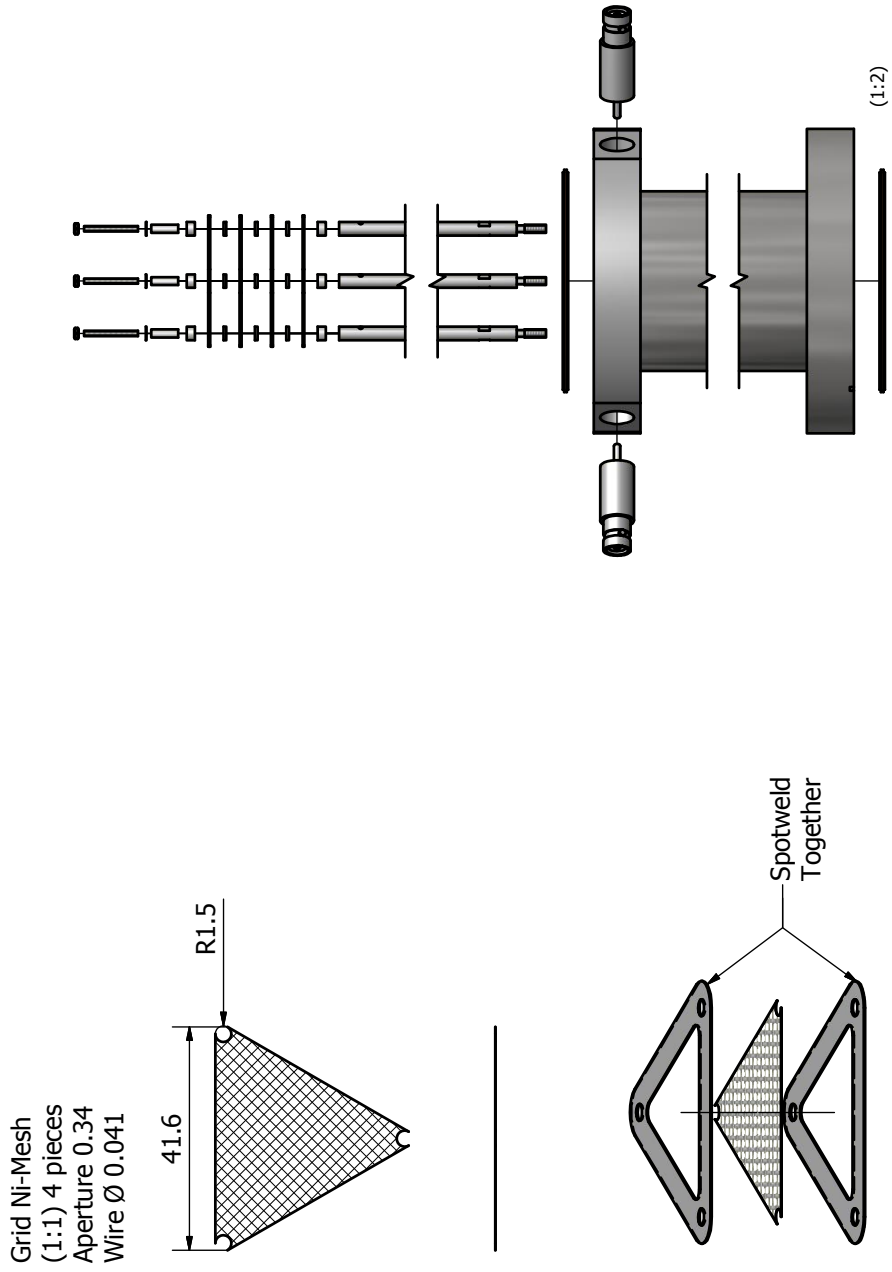




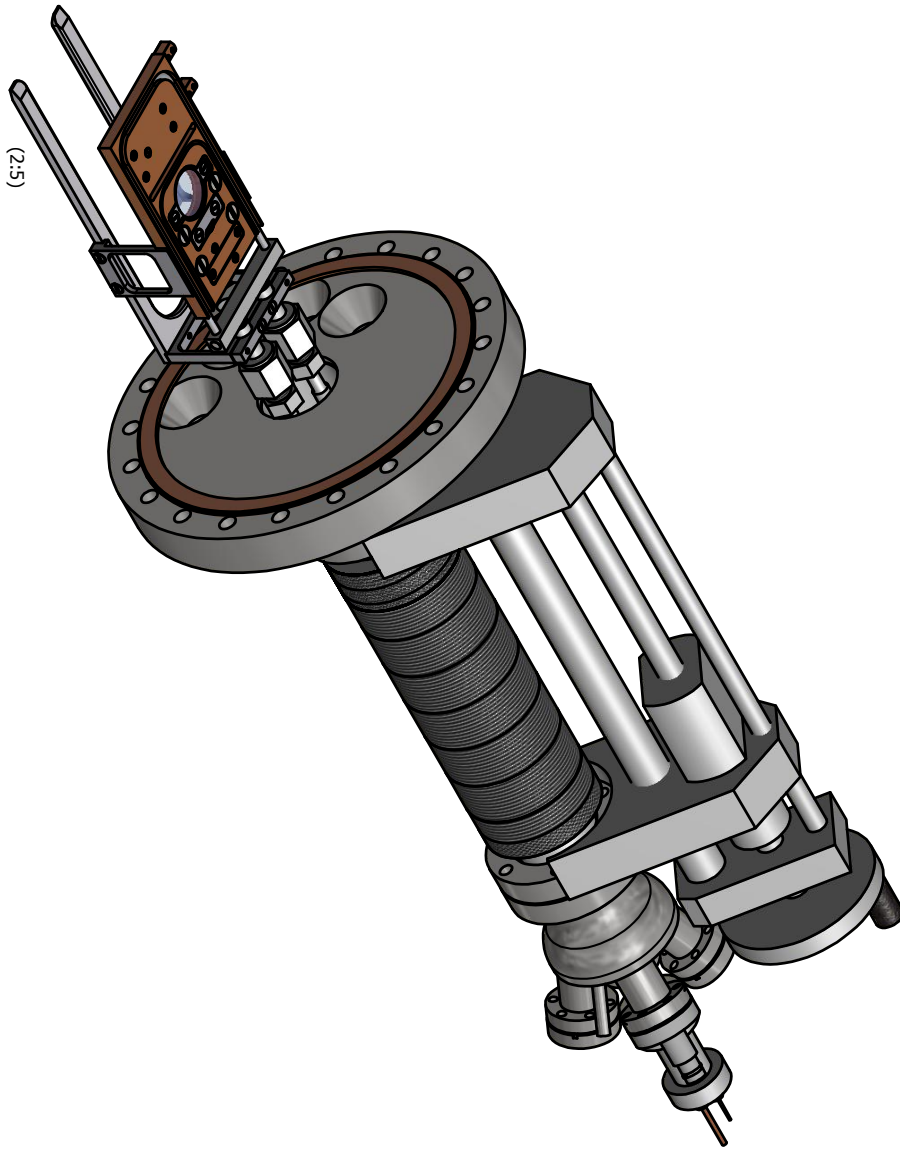
Nipple for QMS
(1:2)

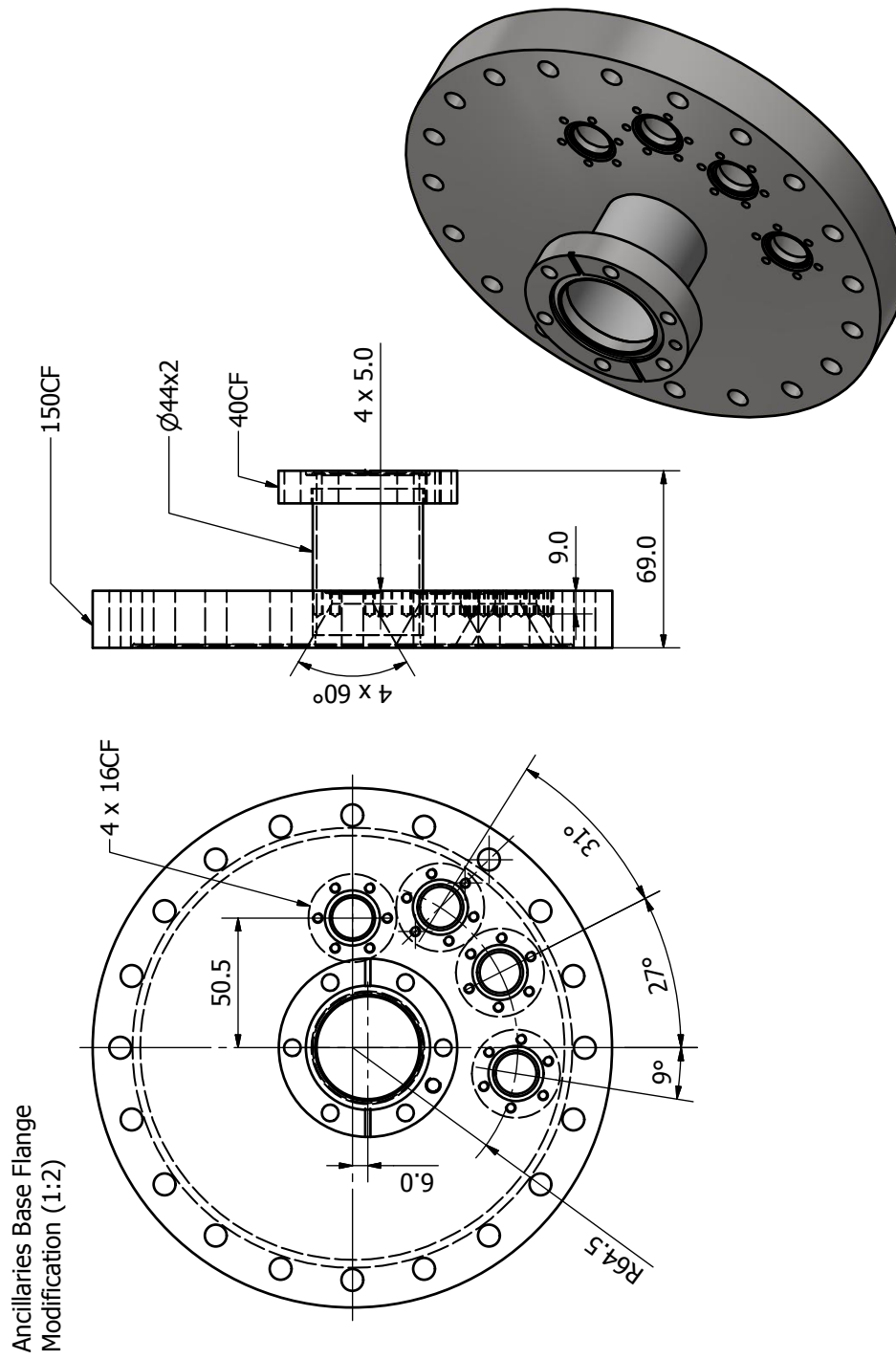


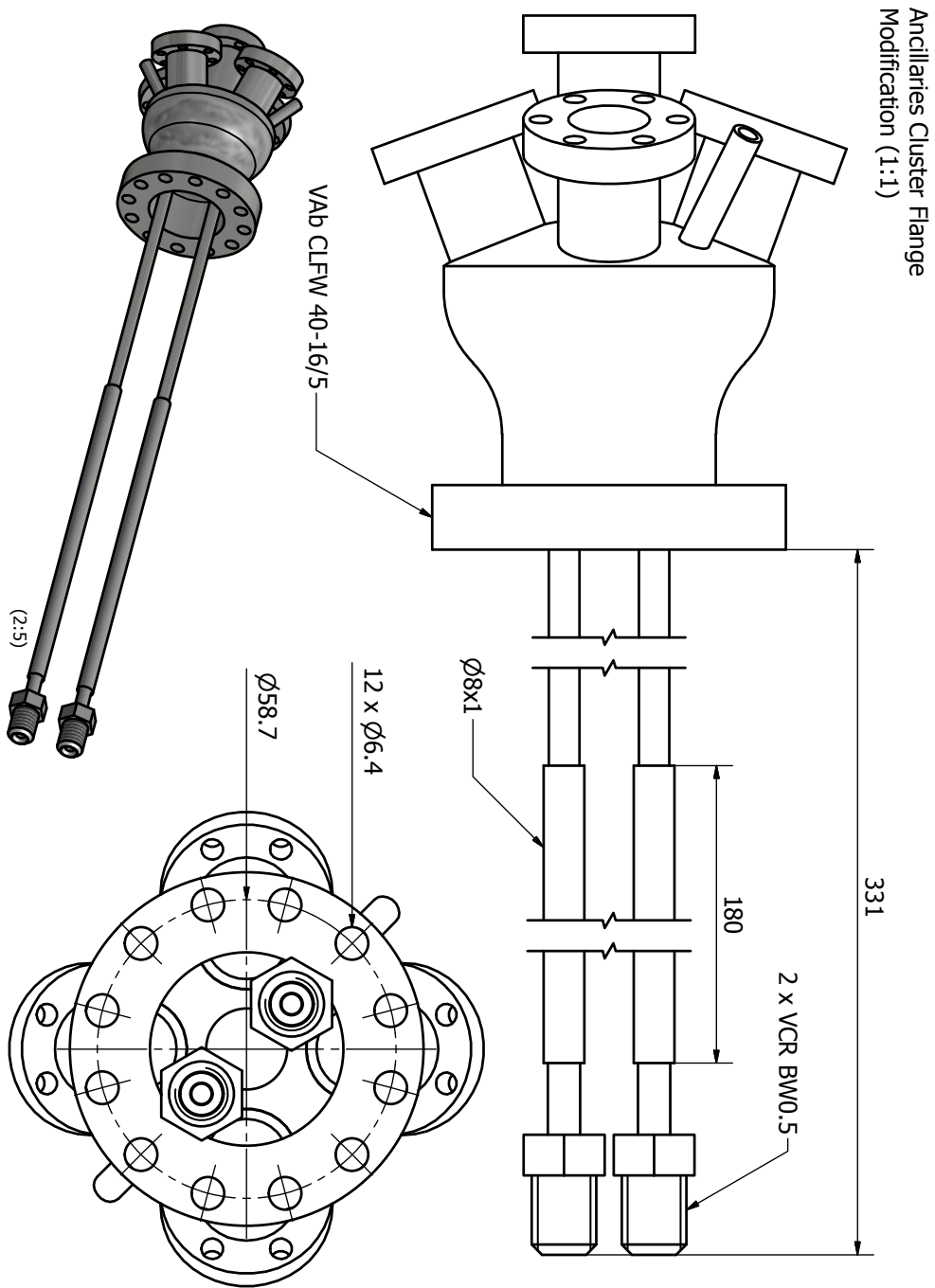


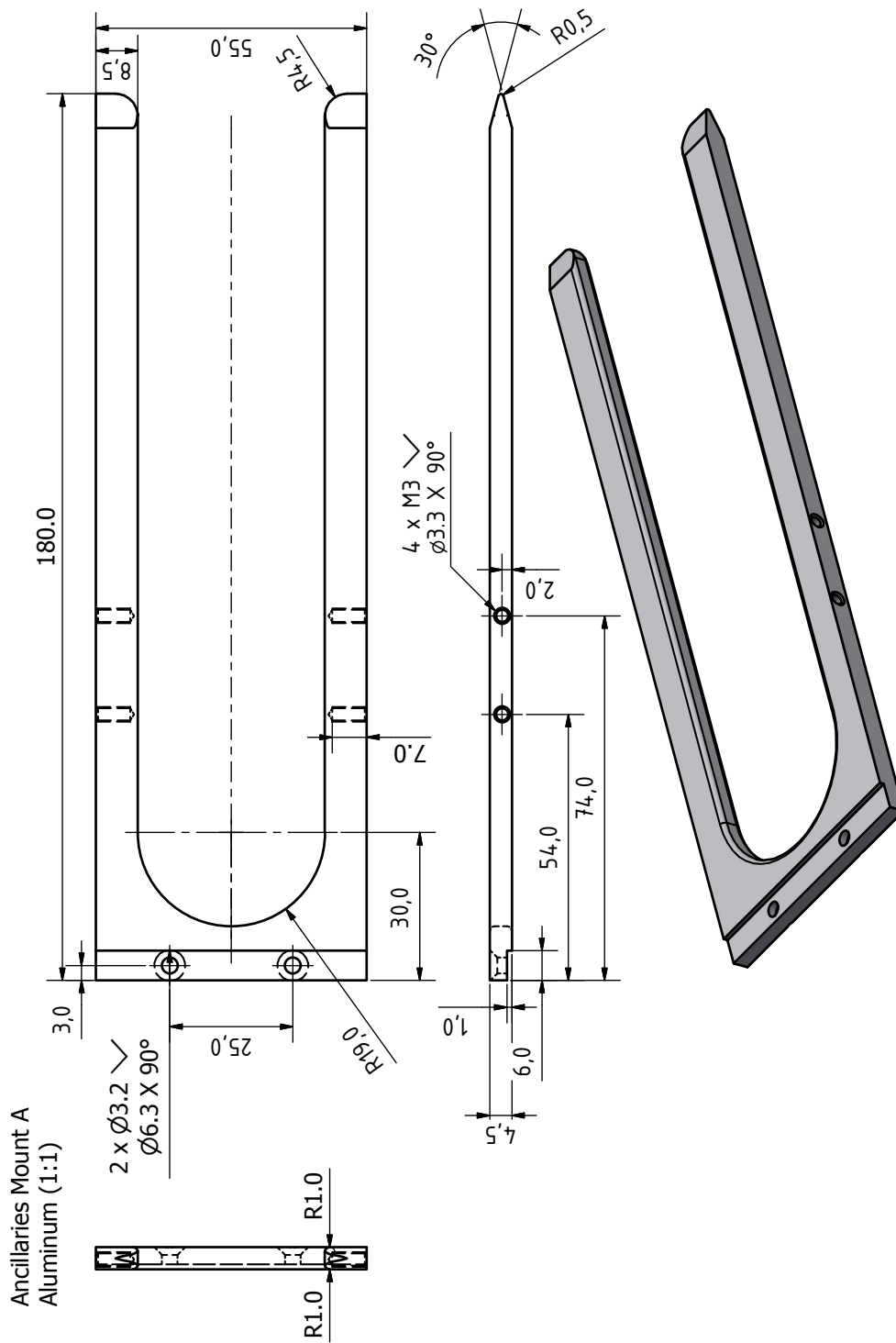


B.2.6 Ancillaries Stage

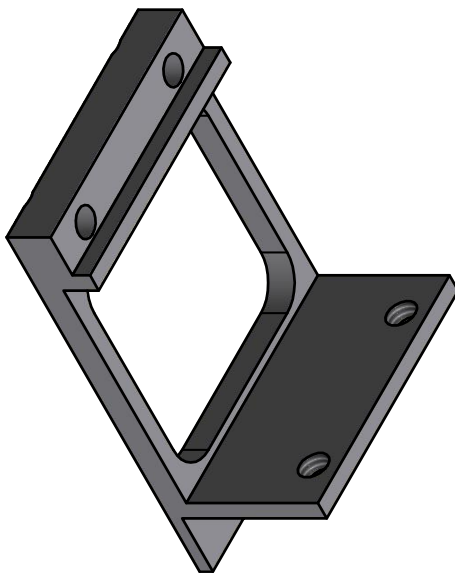
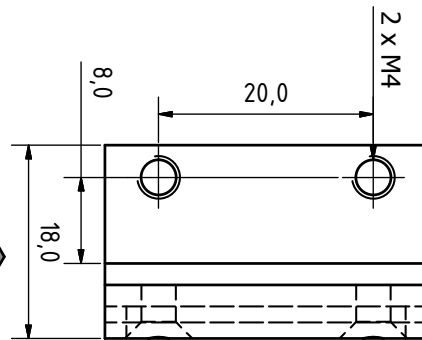
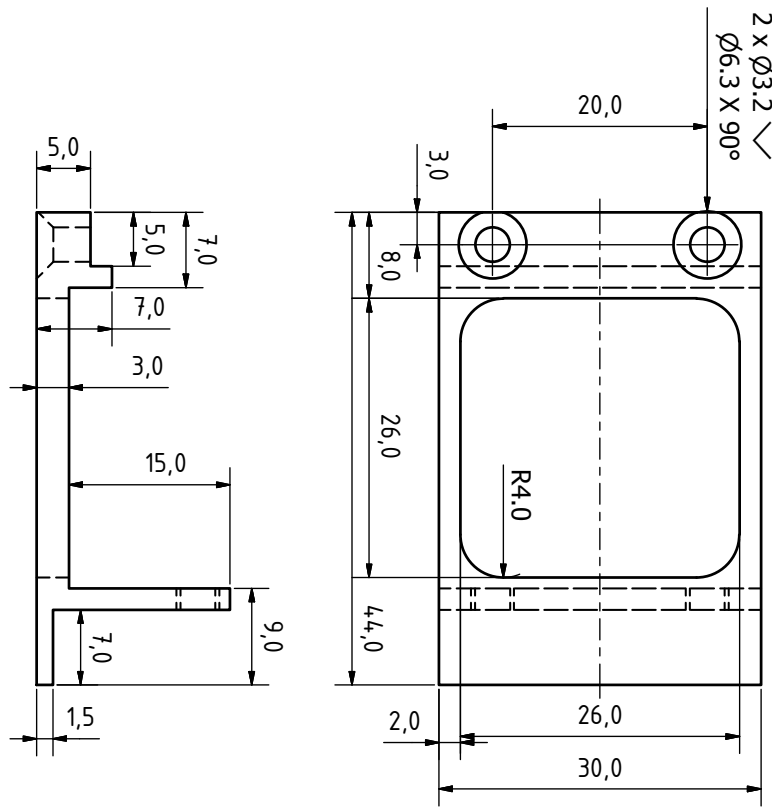


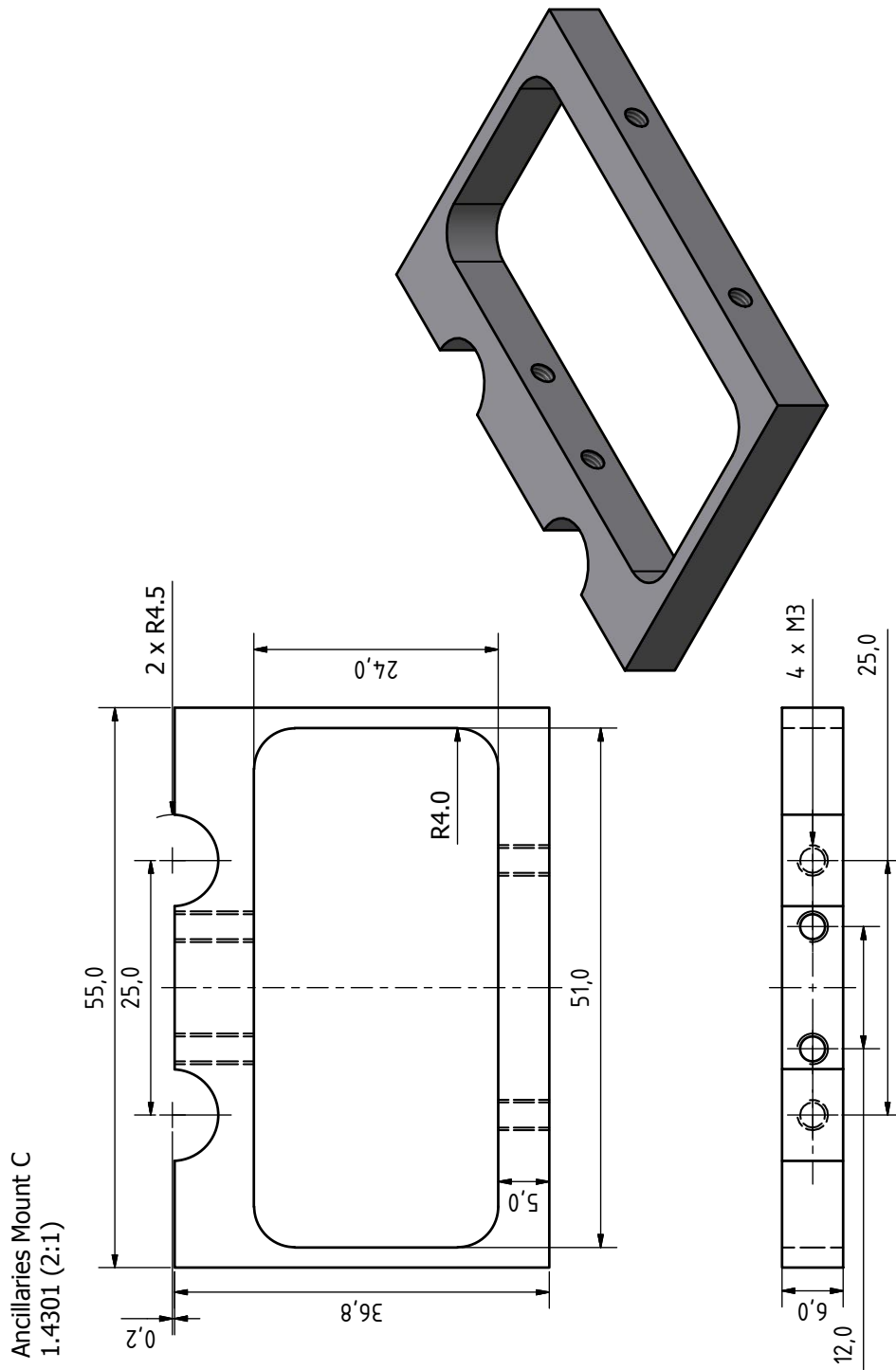


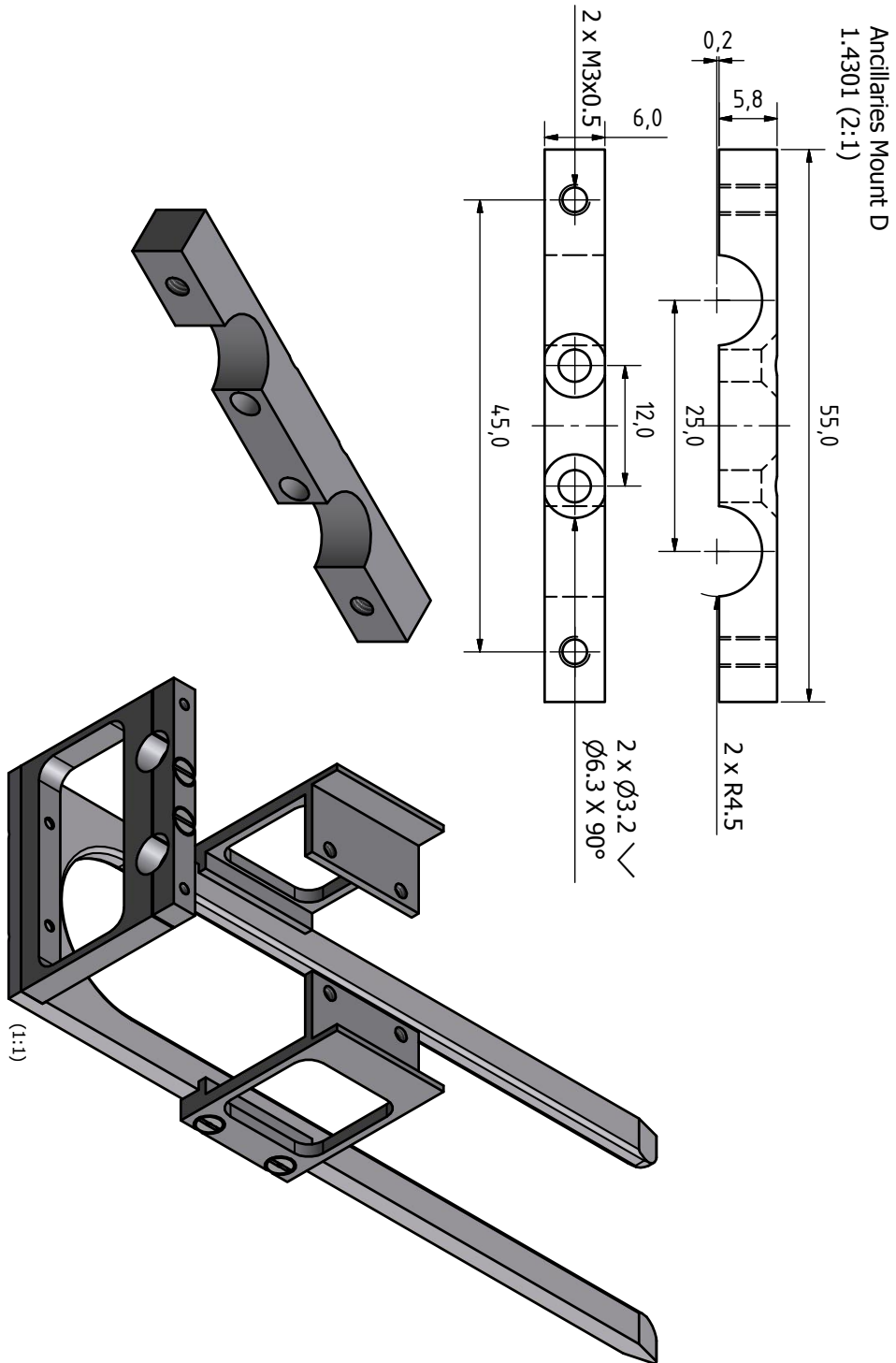


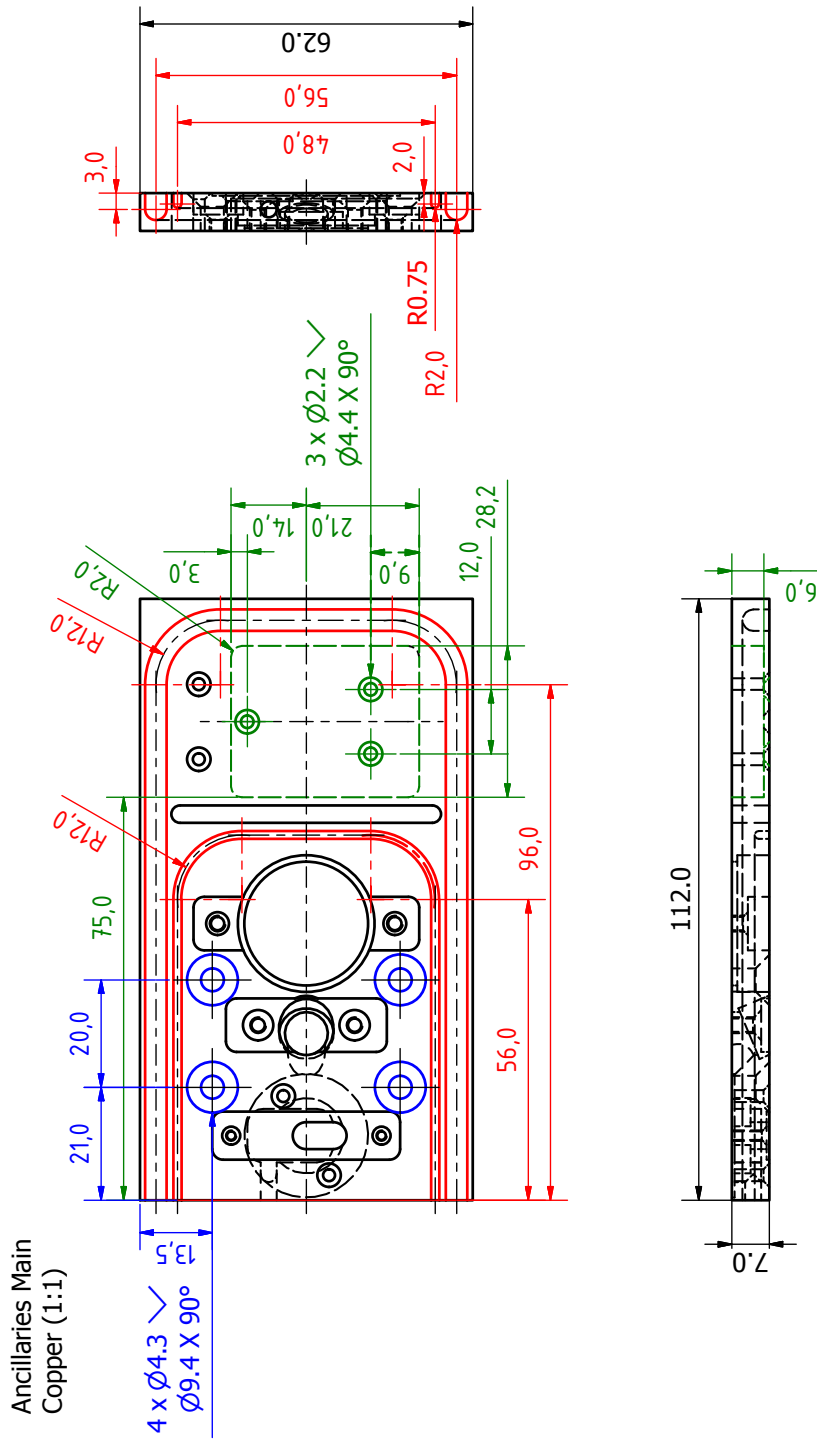


Ancillaries Mount B
1.4301 (2:1) 2 pieces

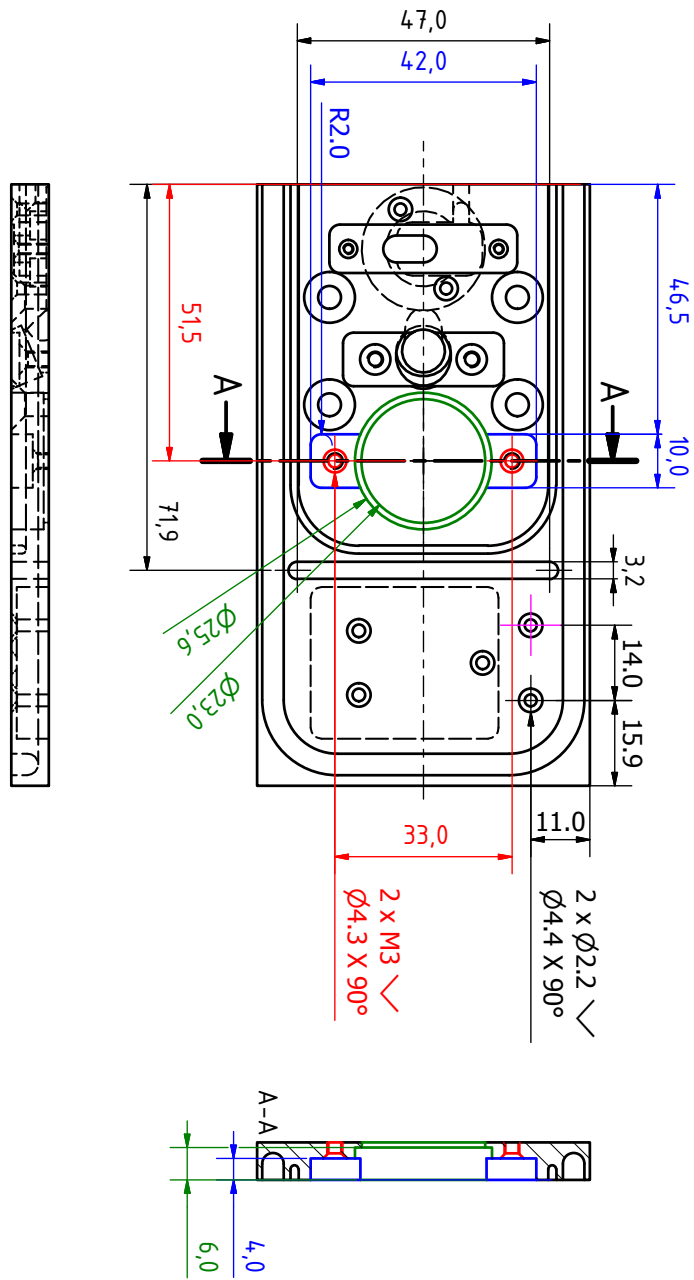




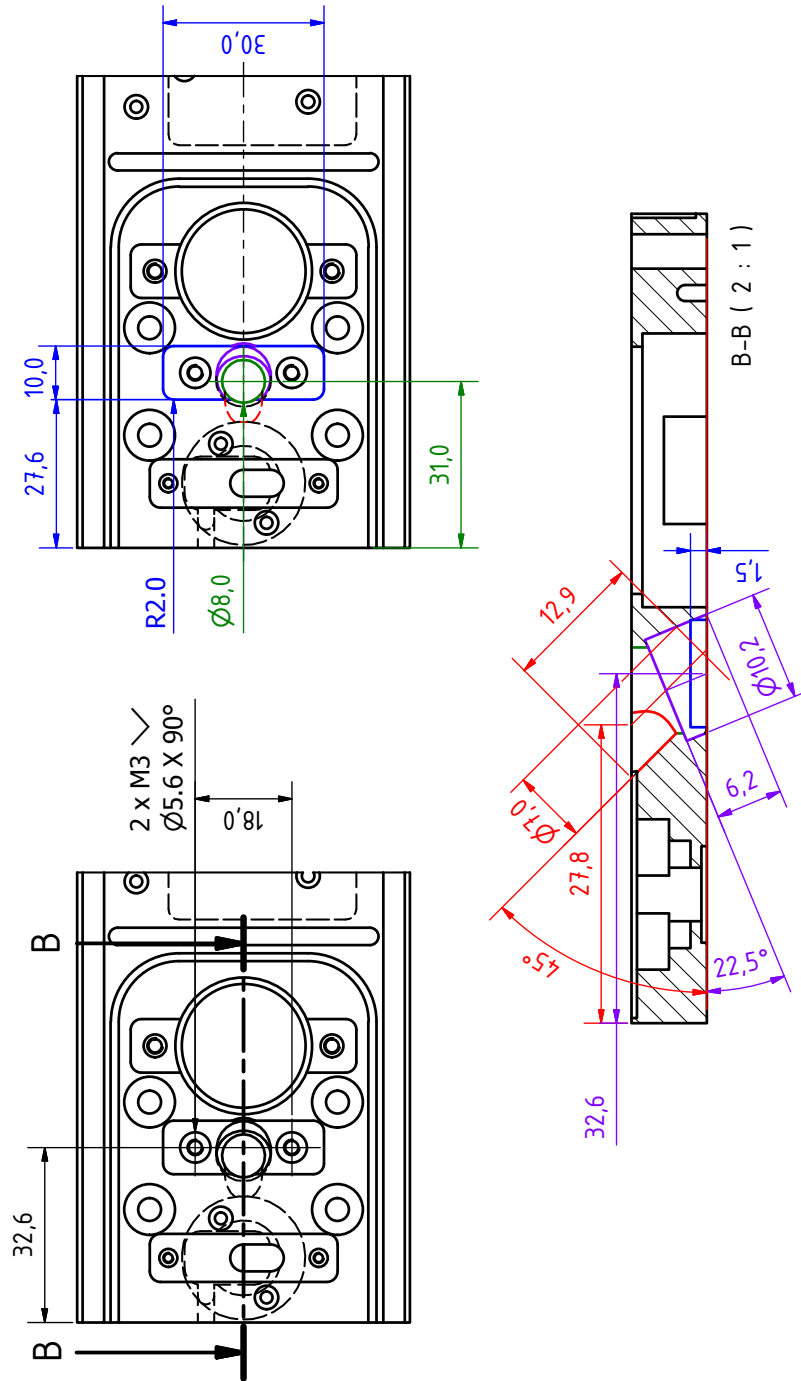




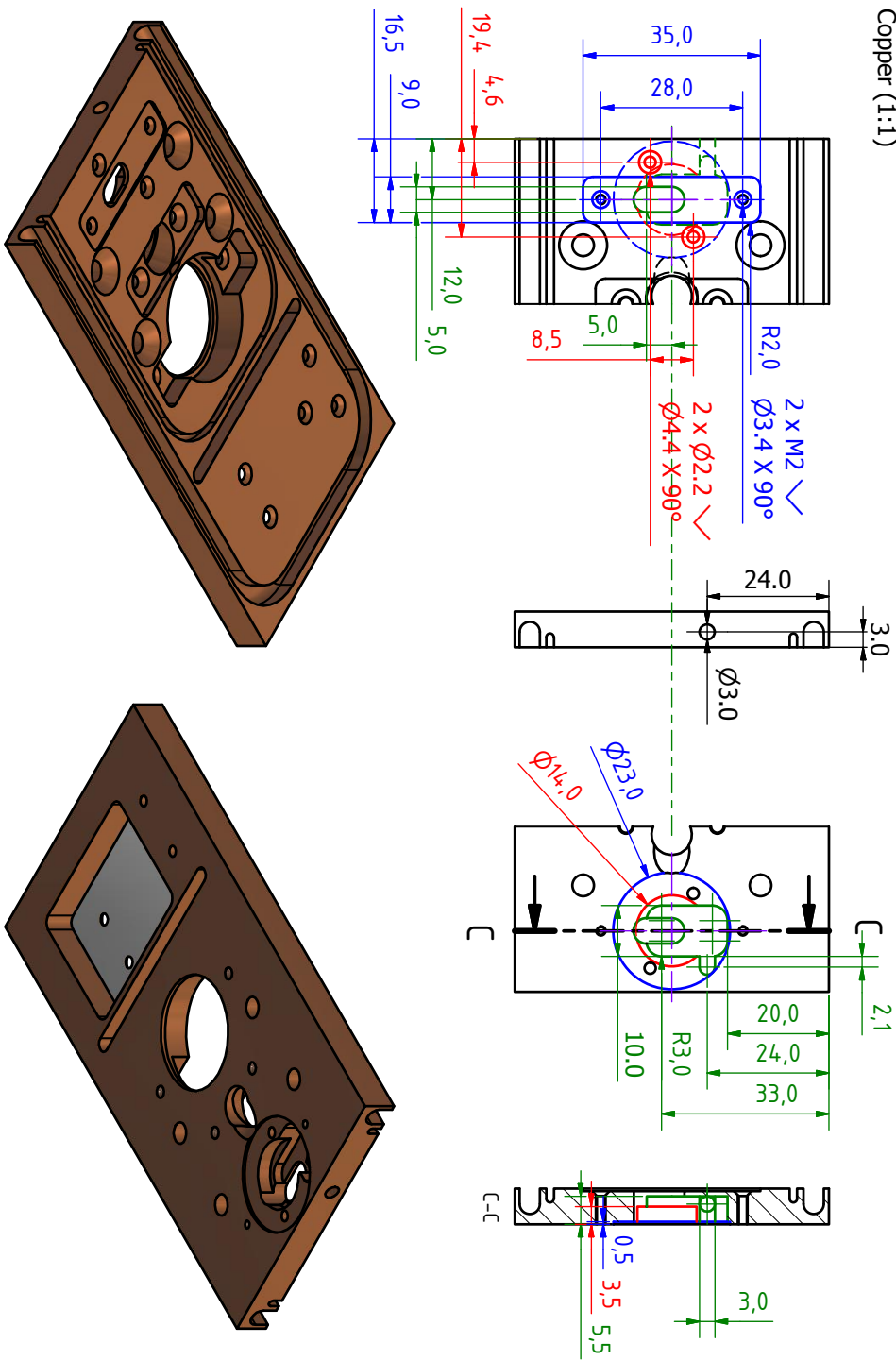
Ancillaries Main
Copper (1:1)

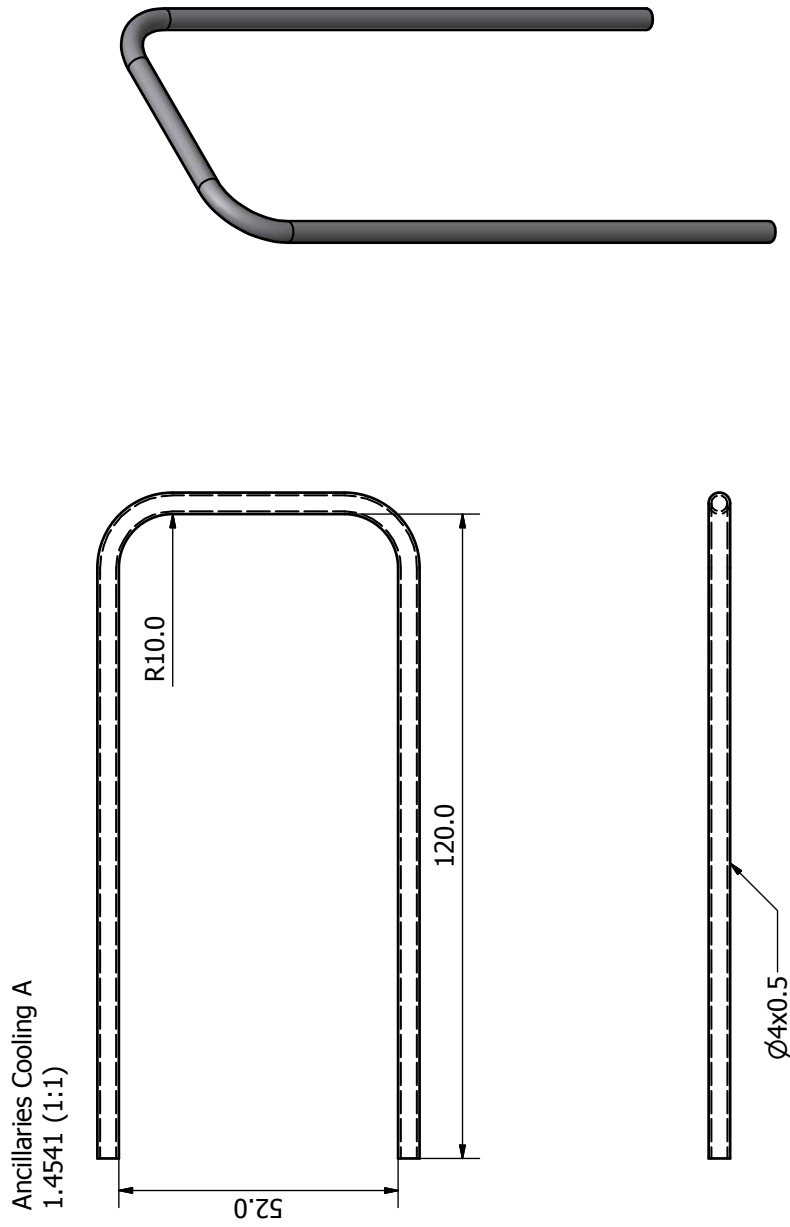


Ancillaries Main
Copper (1:1)

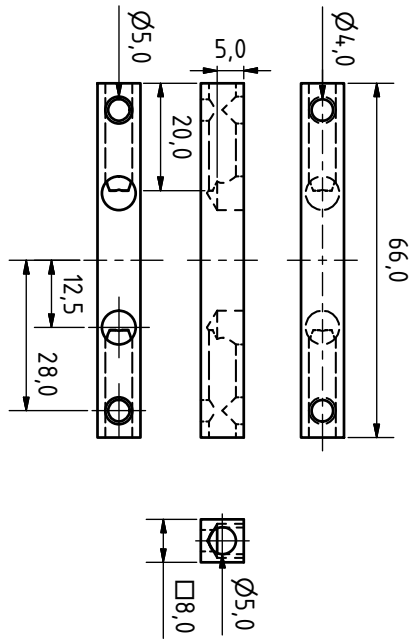


Ancillaries Main
Copper (1:1)

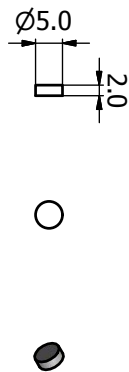




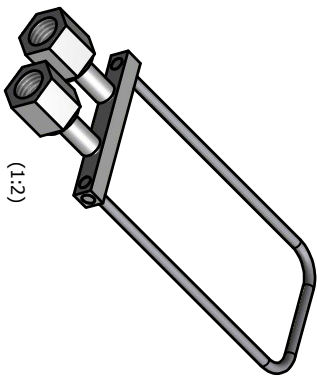
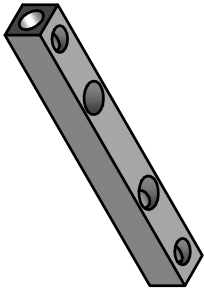
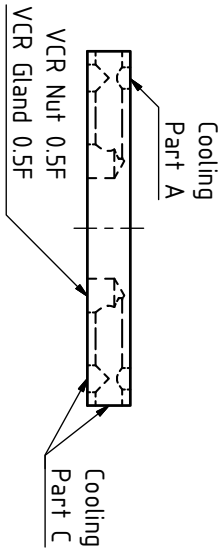
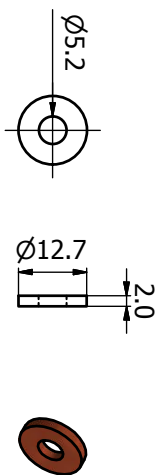
Ancillaries Cooling B
1.4541 (1:1)

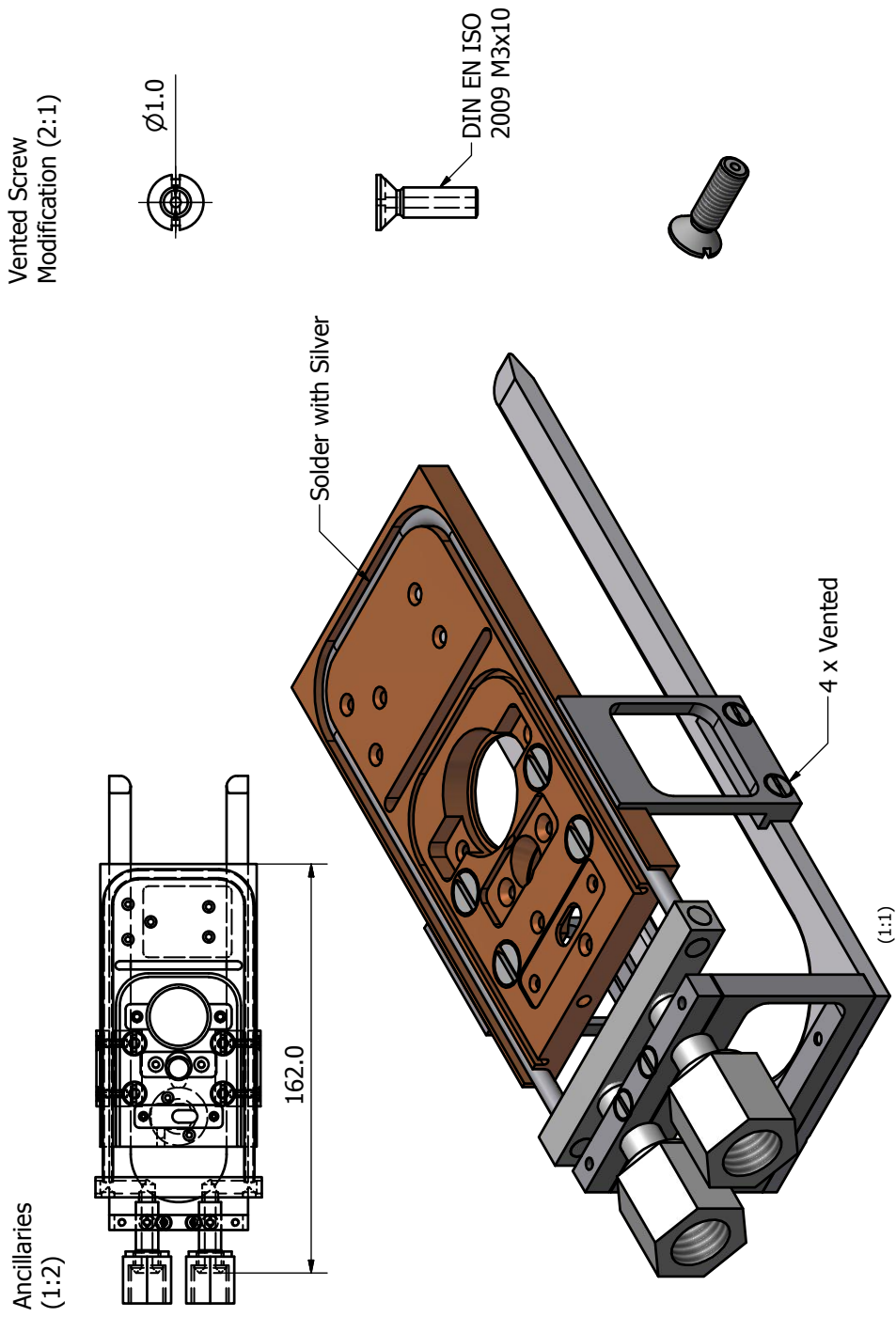


Ancillaries Cooling C
1.4541 (1:1) 4 pieces

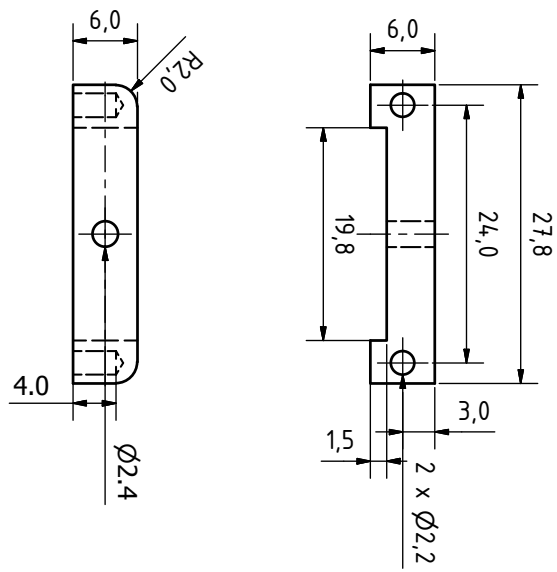


Ancillaries VCR Gasket
OFHC-Copper (1:1) 2 pieces

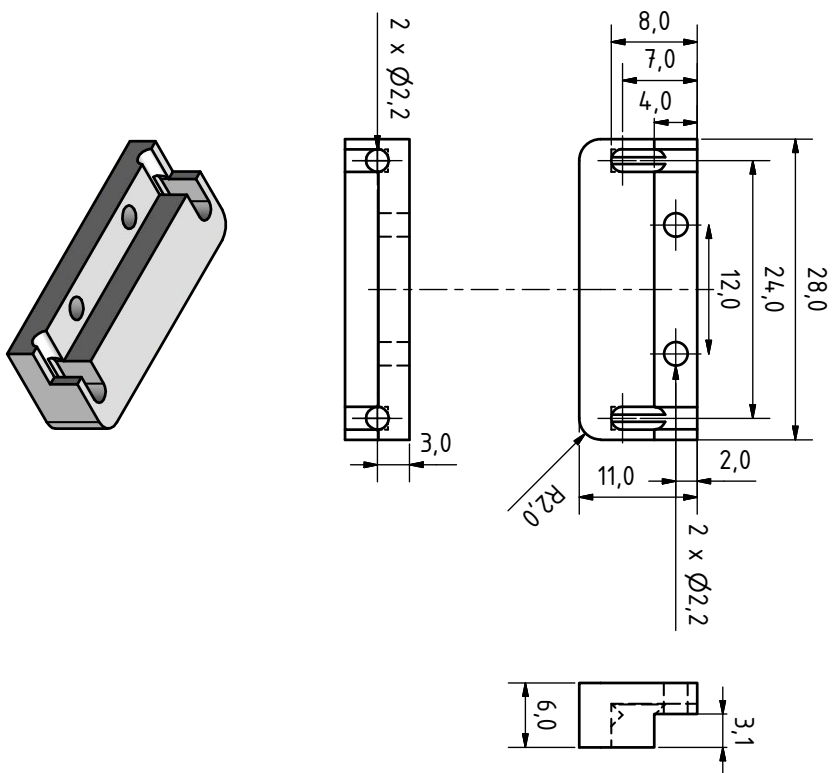




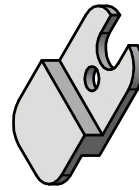
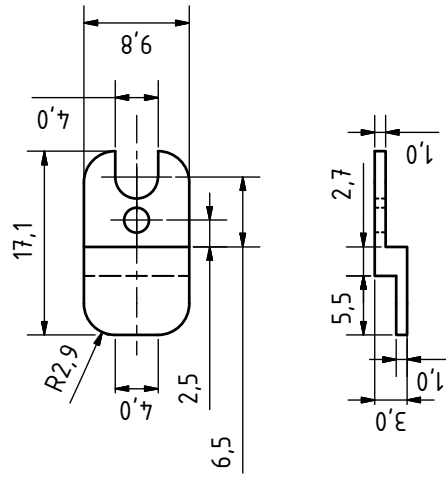
Ancillaries Isolation A
Macor (2:1)



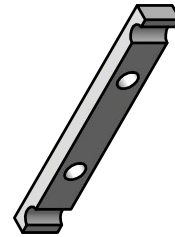
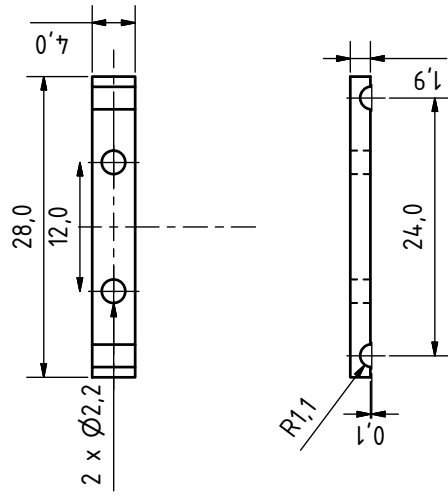
Ancillaries Isolation B
Macor (2:1)



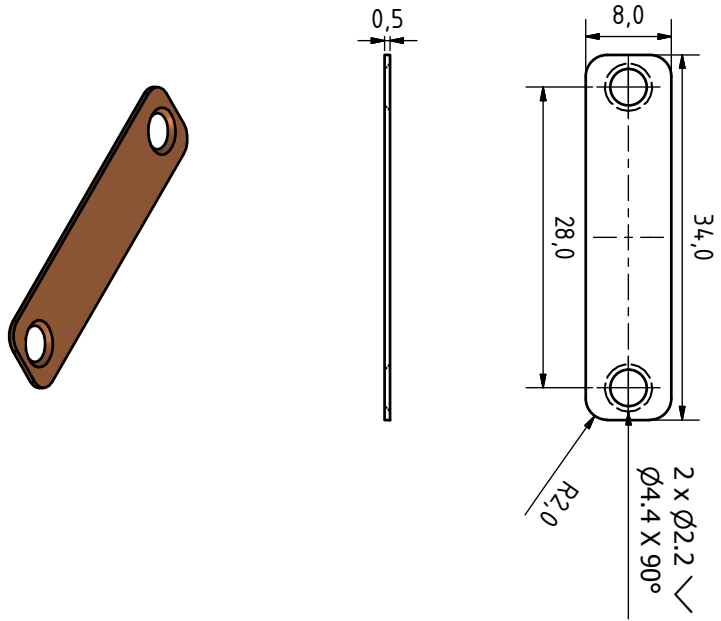
Ancillaries Isolation D
Macor (2:1)



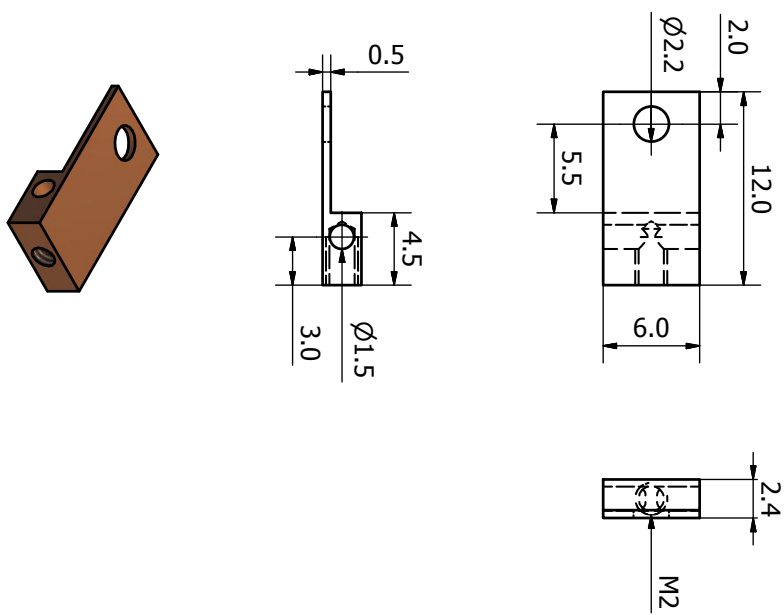
Ancillaries Isolation C
Macor (2:1)



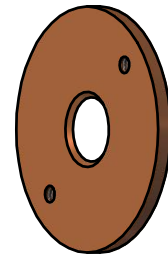
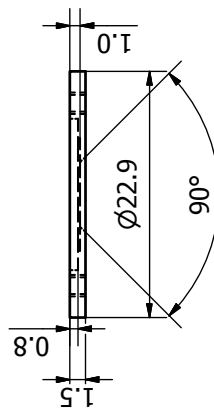
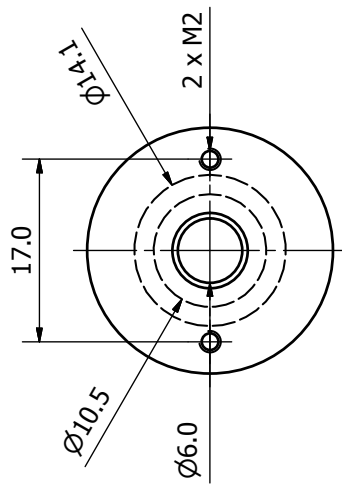
Ancillaries Fastener A
Copper (2:1)



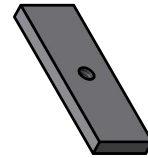
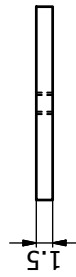
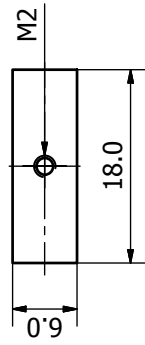
Ancillaries Fastener B
Copper (3:1)



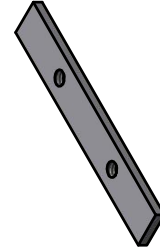
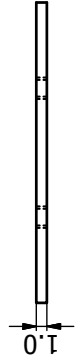
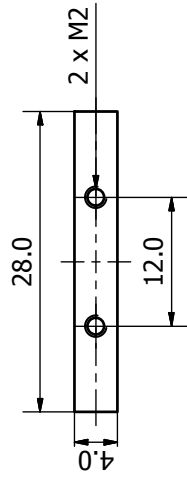
Ancillaries Fastener C
CuBe2 (2:1)



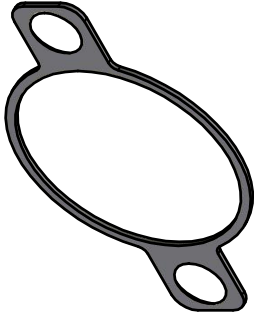
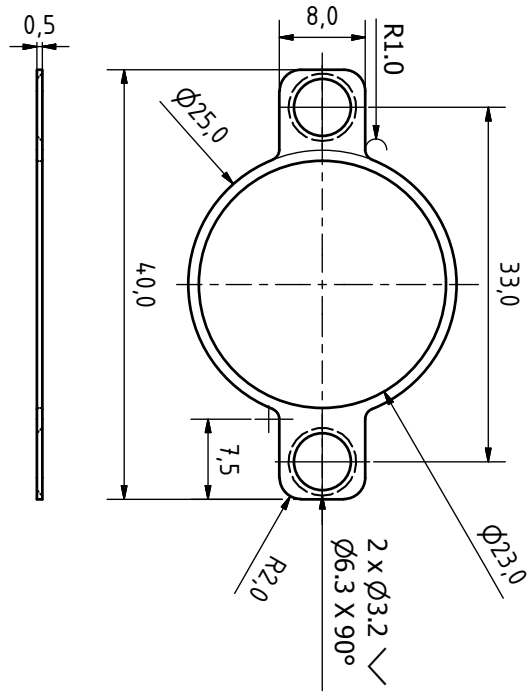
Ancillaries Fastener D
1.4301 (2:1)



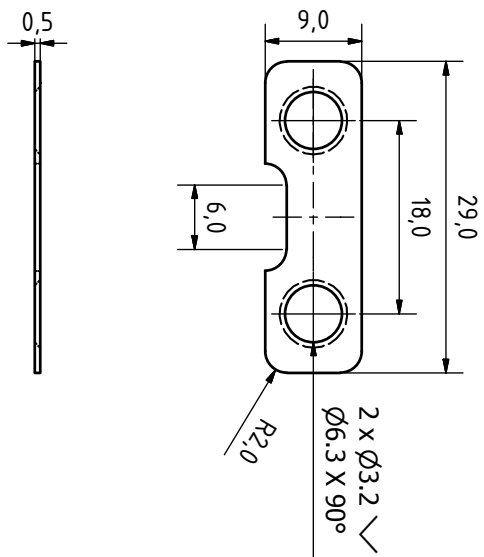
Ancillaries Fastener E
1.4301 (2:1)



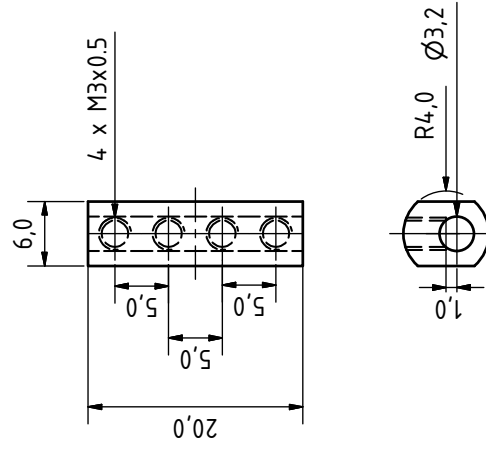
Ancillaries Fastener F
1.4301 (2:1)



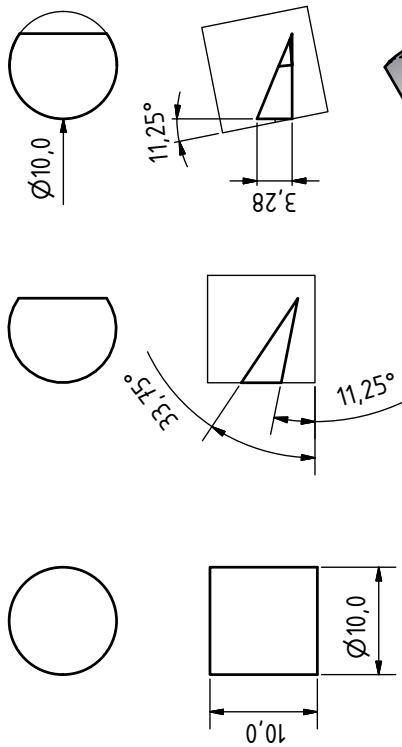
Ancillaries Fastener G
1.4301 (2:1)



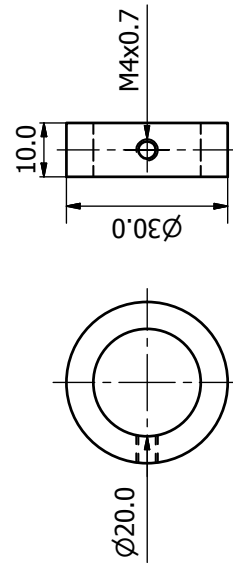
Ancillaries Connector A
Copper (2:1) 4 pieces



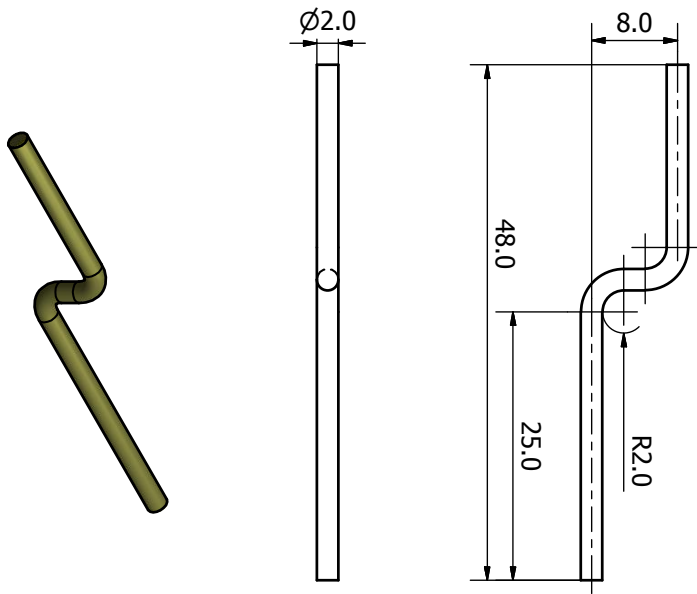
Ancillaries Fastener H
1.4301 (2:1)



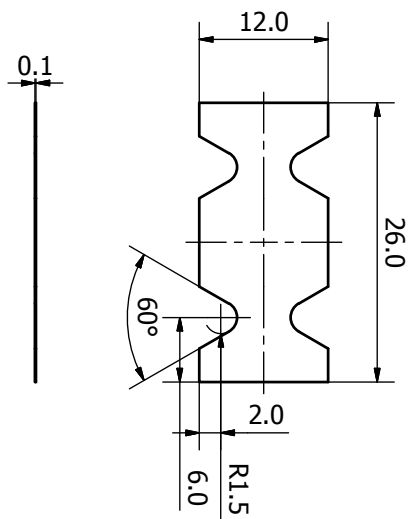
Linear Shift Stop
Aluminum (1:1) 2 pieces



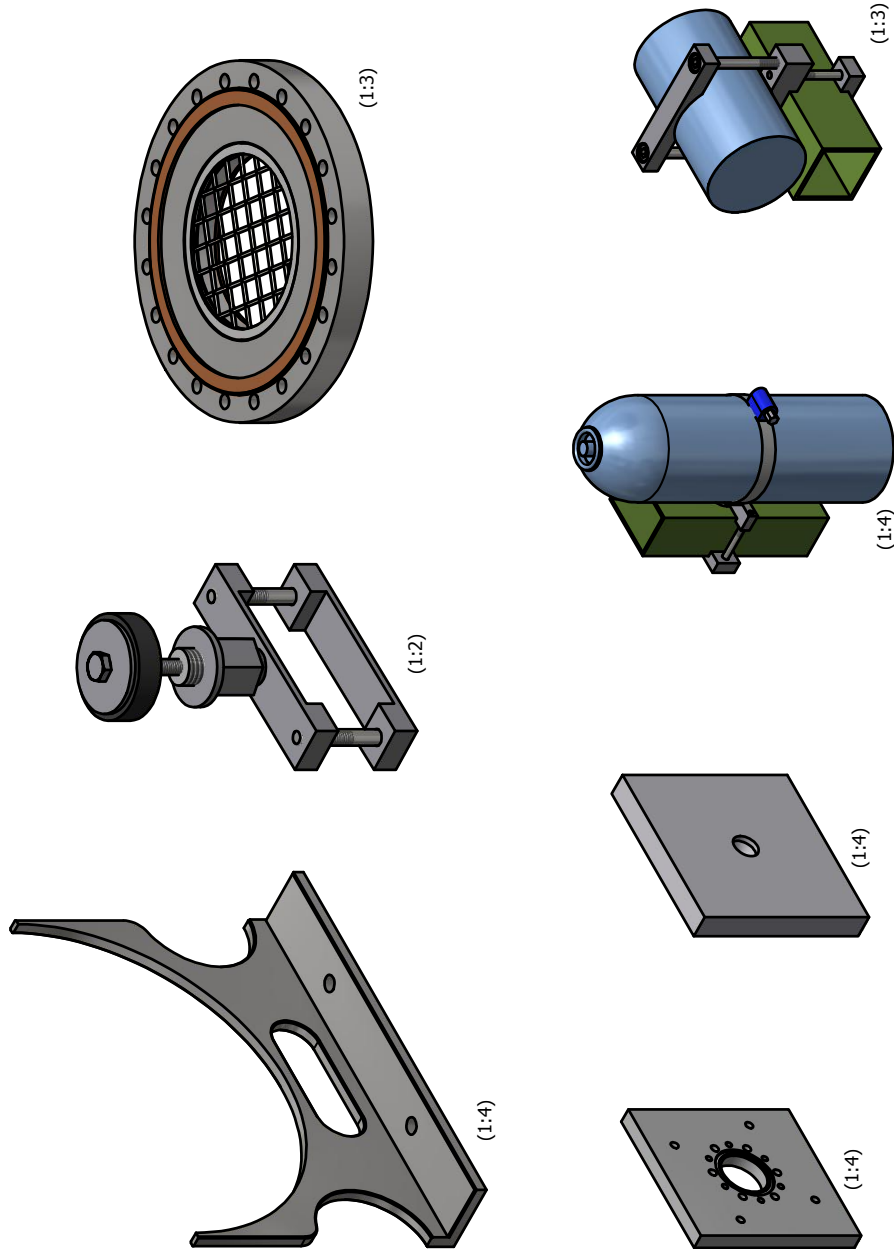
Ancillaries Connector B
Tantalum (2:1) 2 pieces

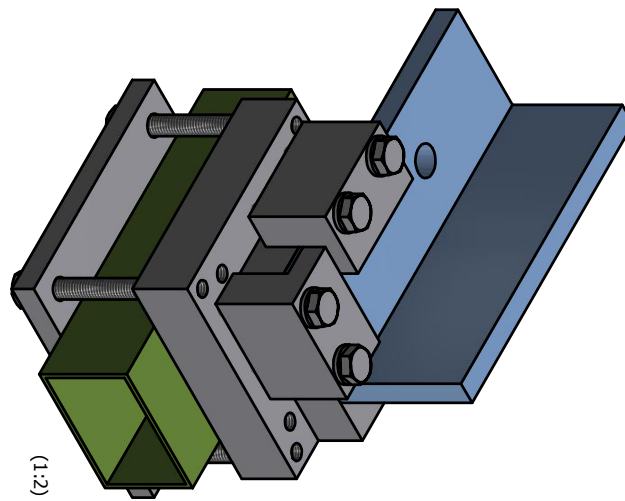
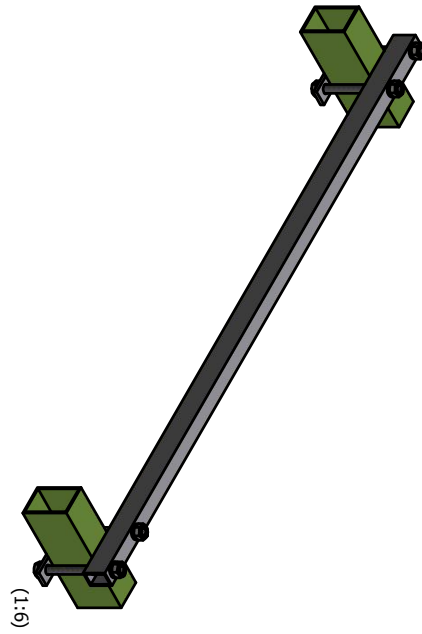


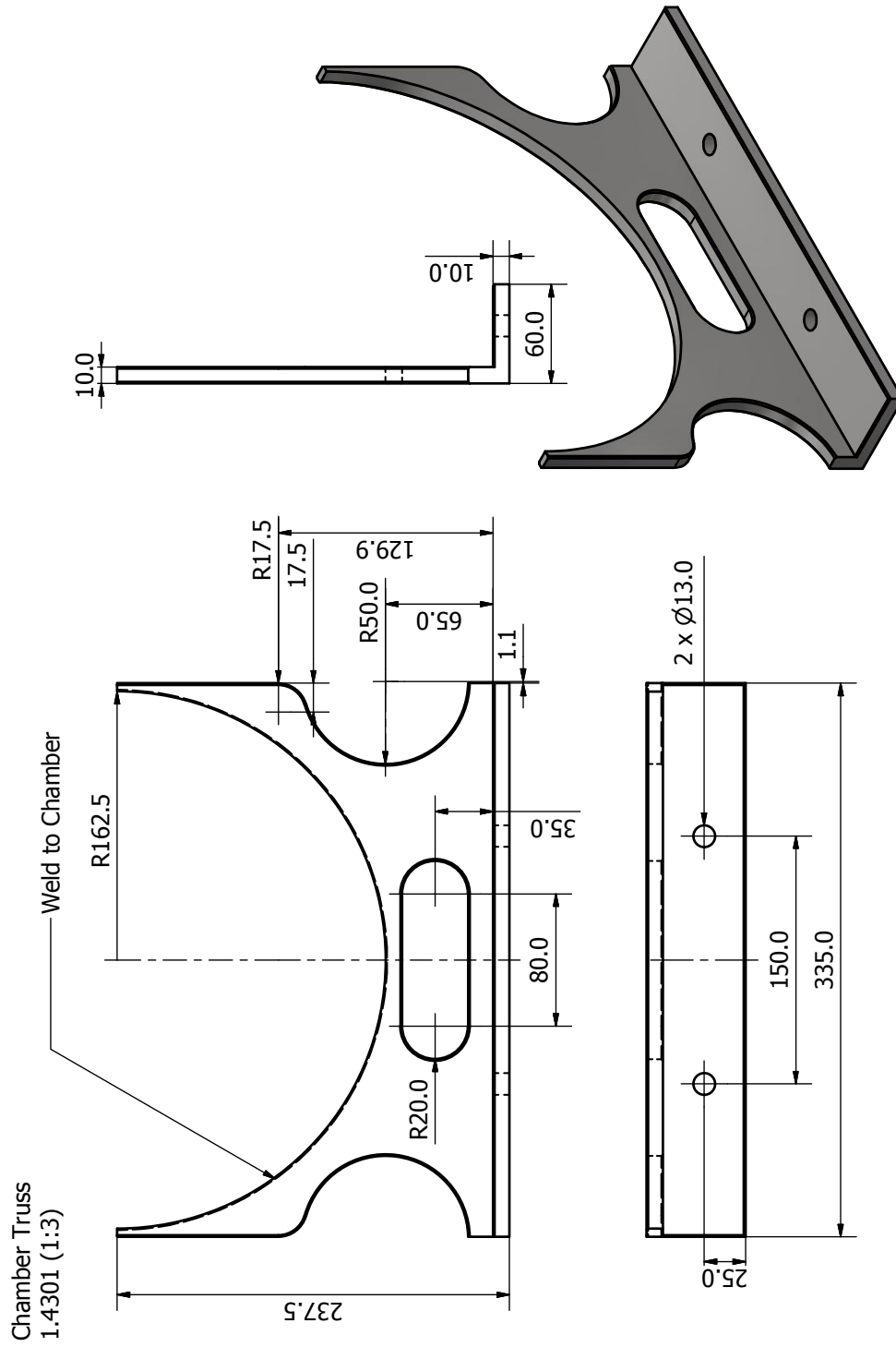
Ancillaries Baffle
Tantalum (2:1)



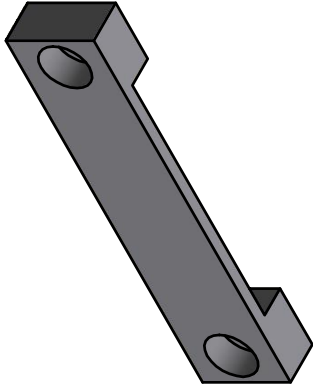
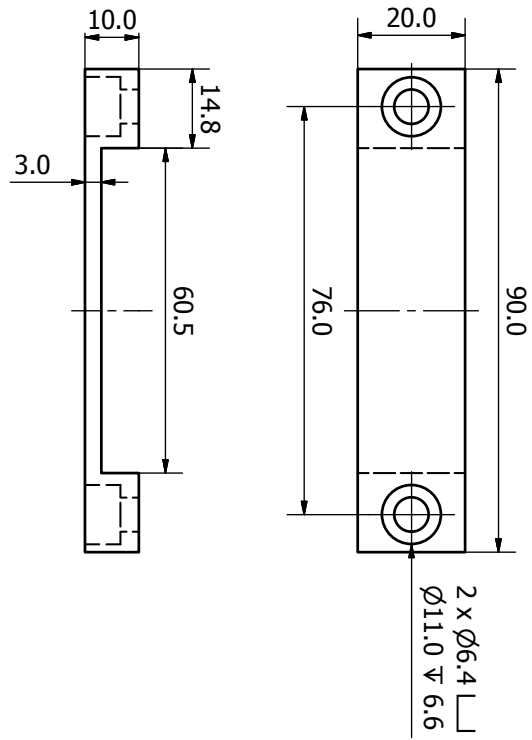
B.2.7 Main Chamber Additions



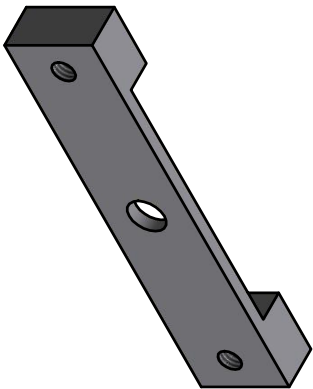
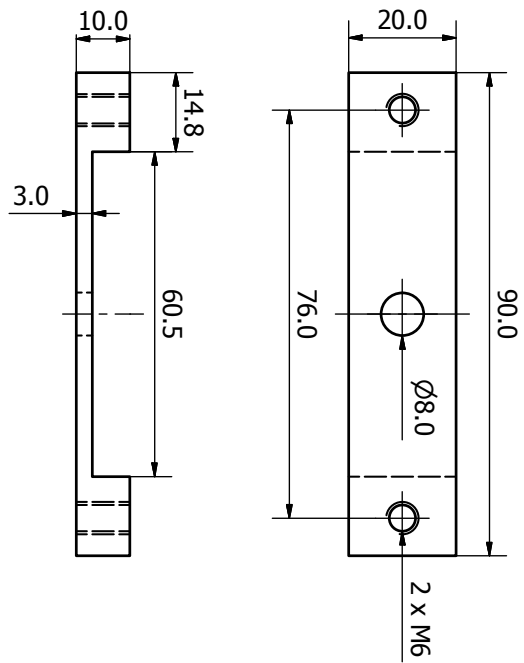




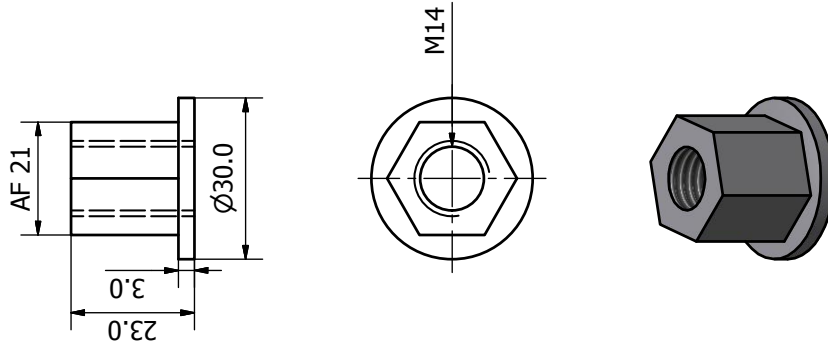
Chamber Support A
1.4301 (1:1) 4 pieces



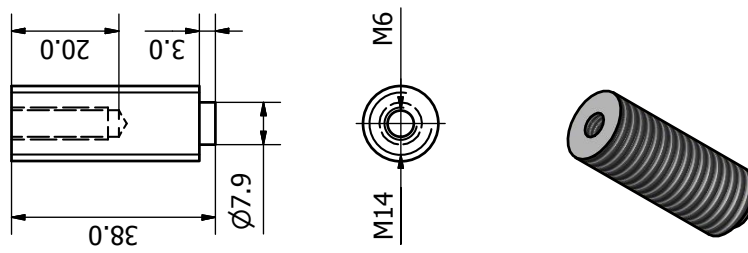
Chamber Support B
1.4301 (1:1) 4 pieces



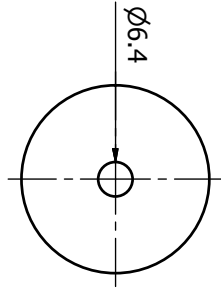
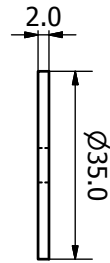
Chamber Support D
1.4301 (1:1) 4 pieces



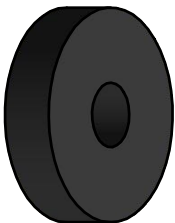
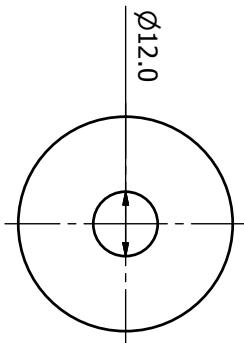
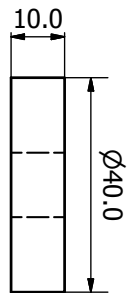
Chamber Support C
1.4301 (1:1) 4 pieces



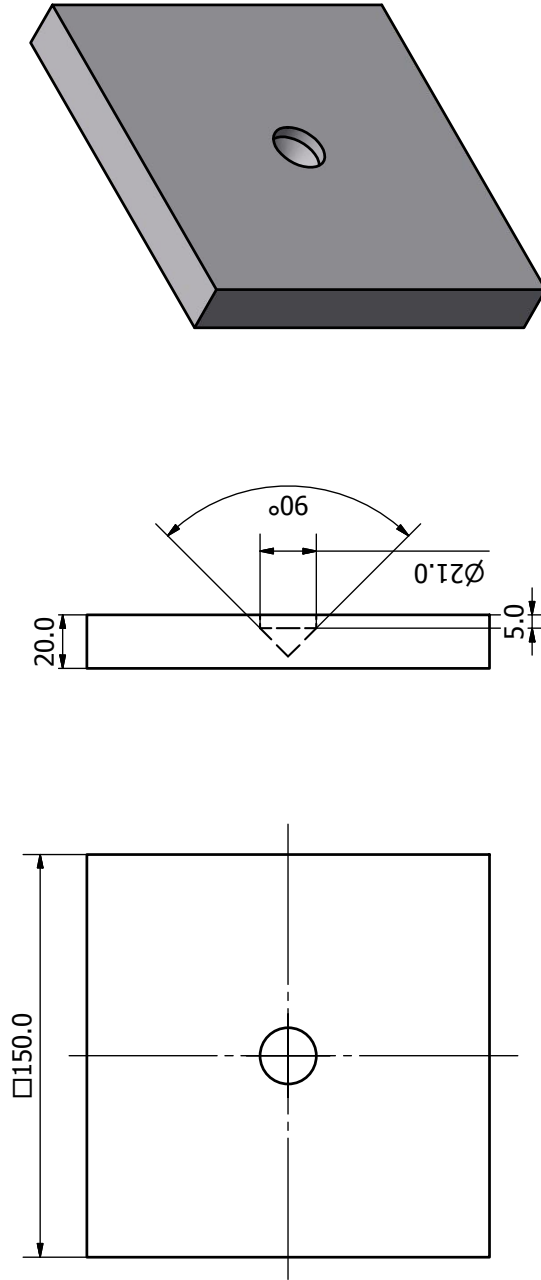
Chamber Support E
1.4301 (1:1) 4 pieces



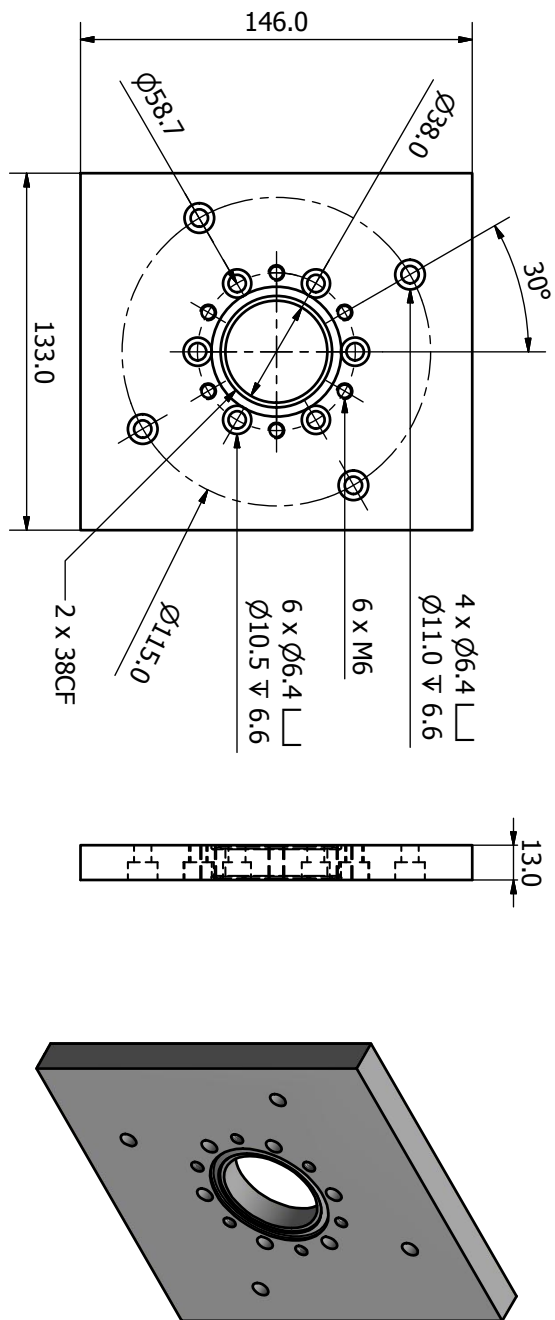
Chamber Support F
Rubber (1:1) 4 pieces

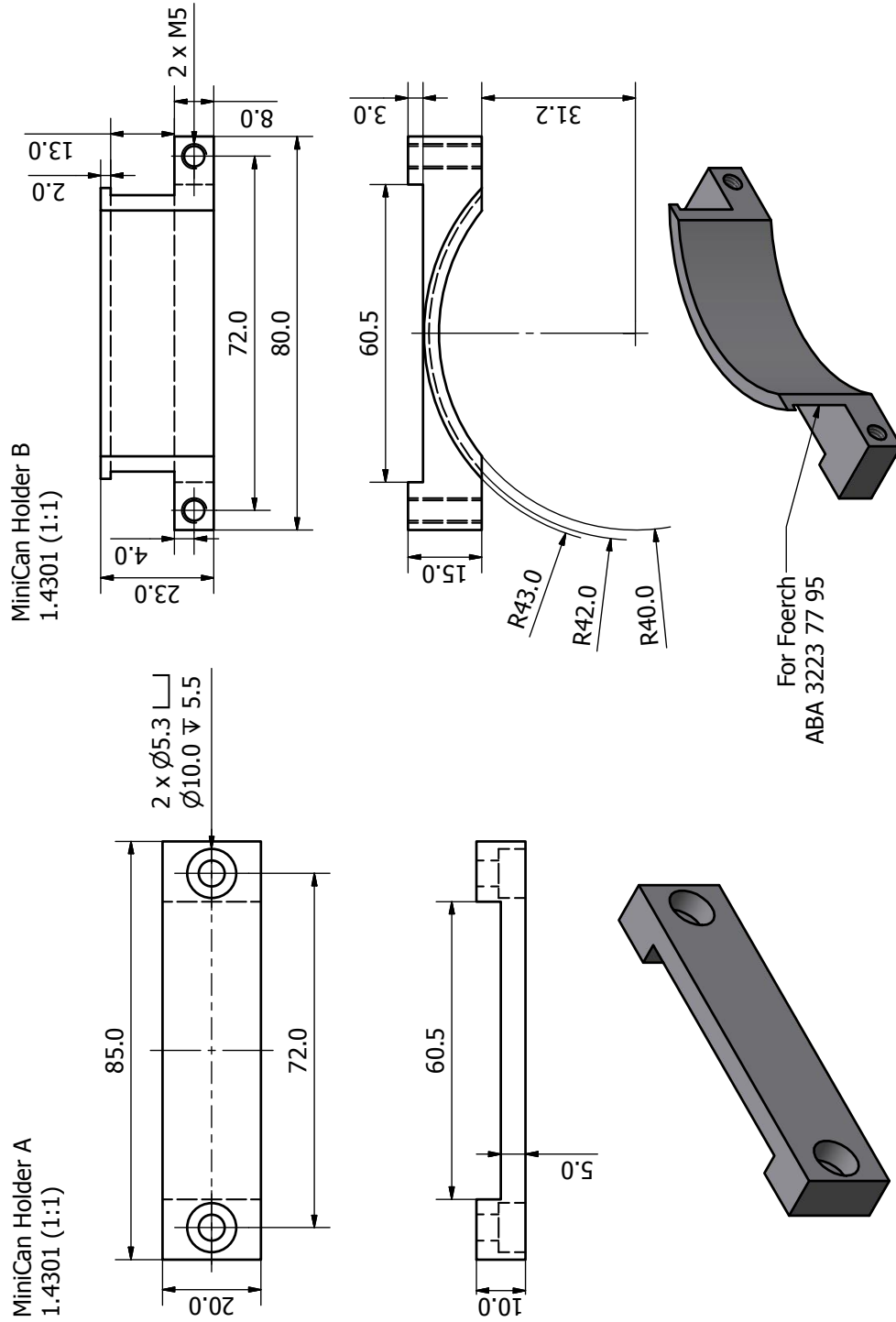


Frame Rests
Aluminum (1:2) 4 pieces

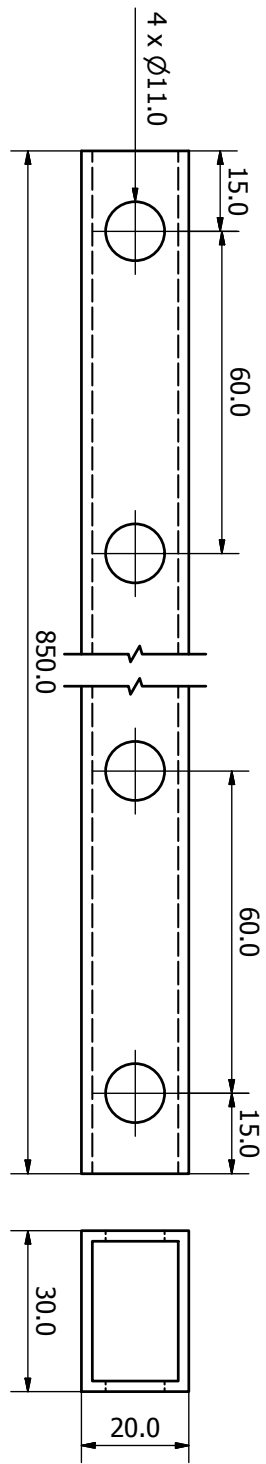


Mounting Plate XY-Stage
1.4301 (1:2)

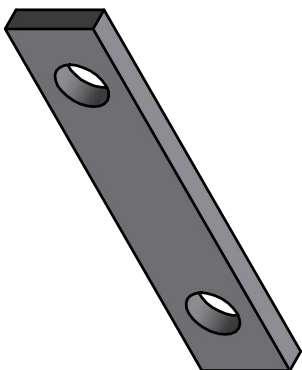
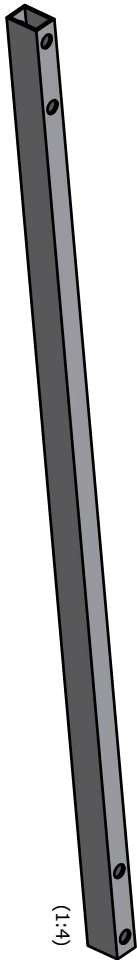
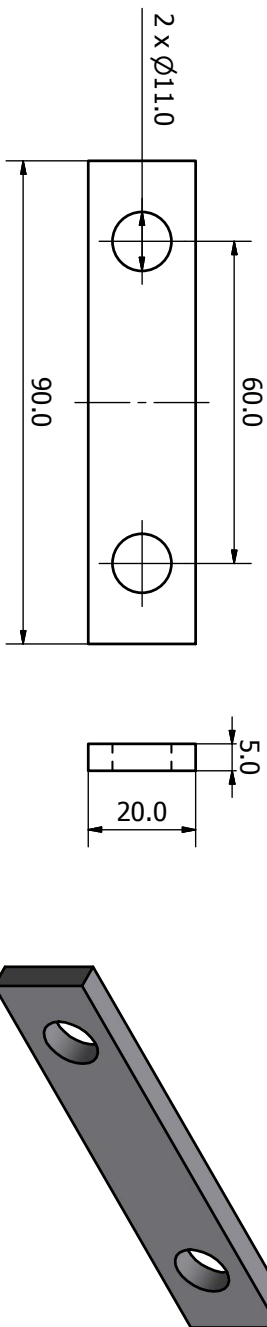




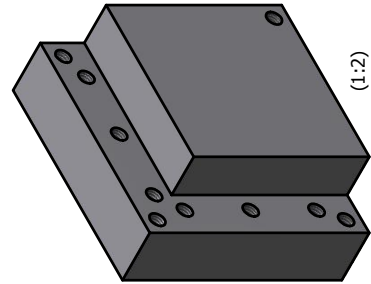
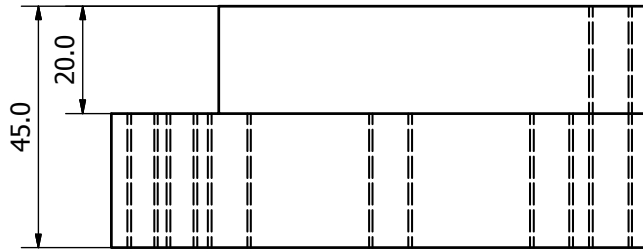
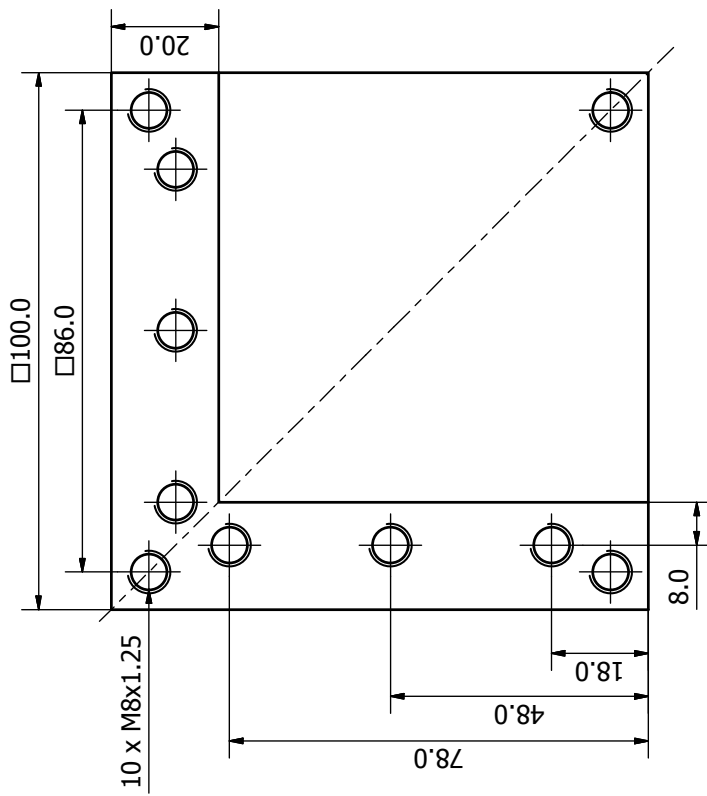
Moving - Bar A
1.0503 (1:1) 3 pieces



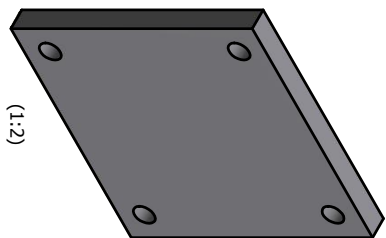
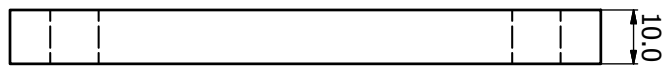
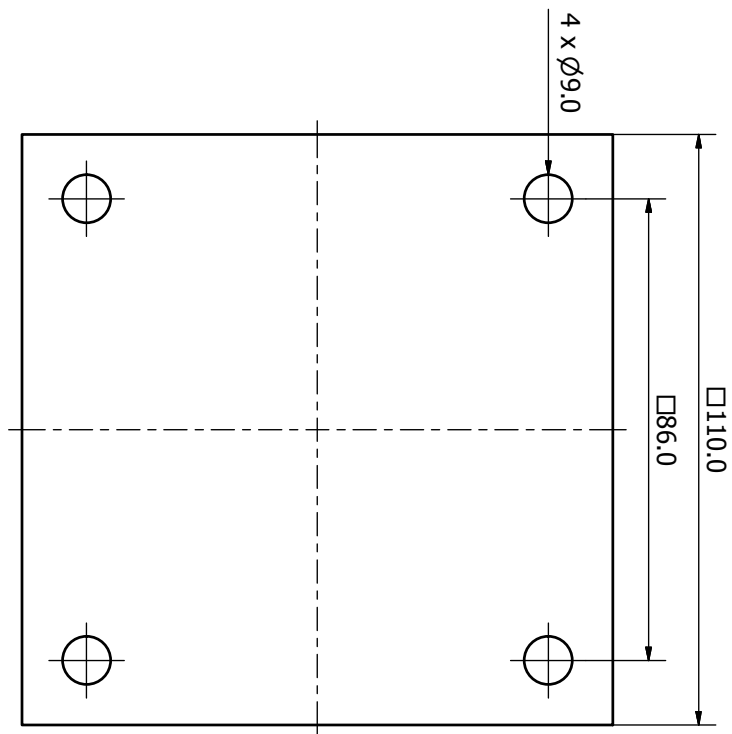
Moving - Bar B
1.0503 (1:1) 6 pieces

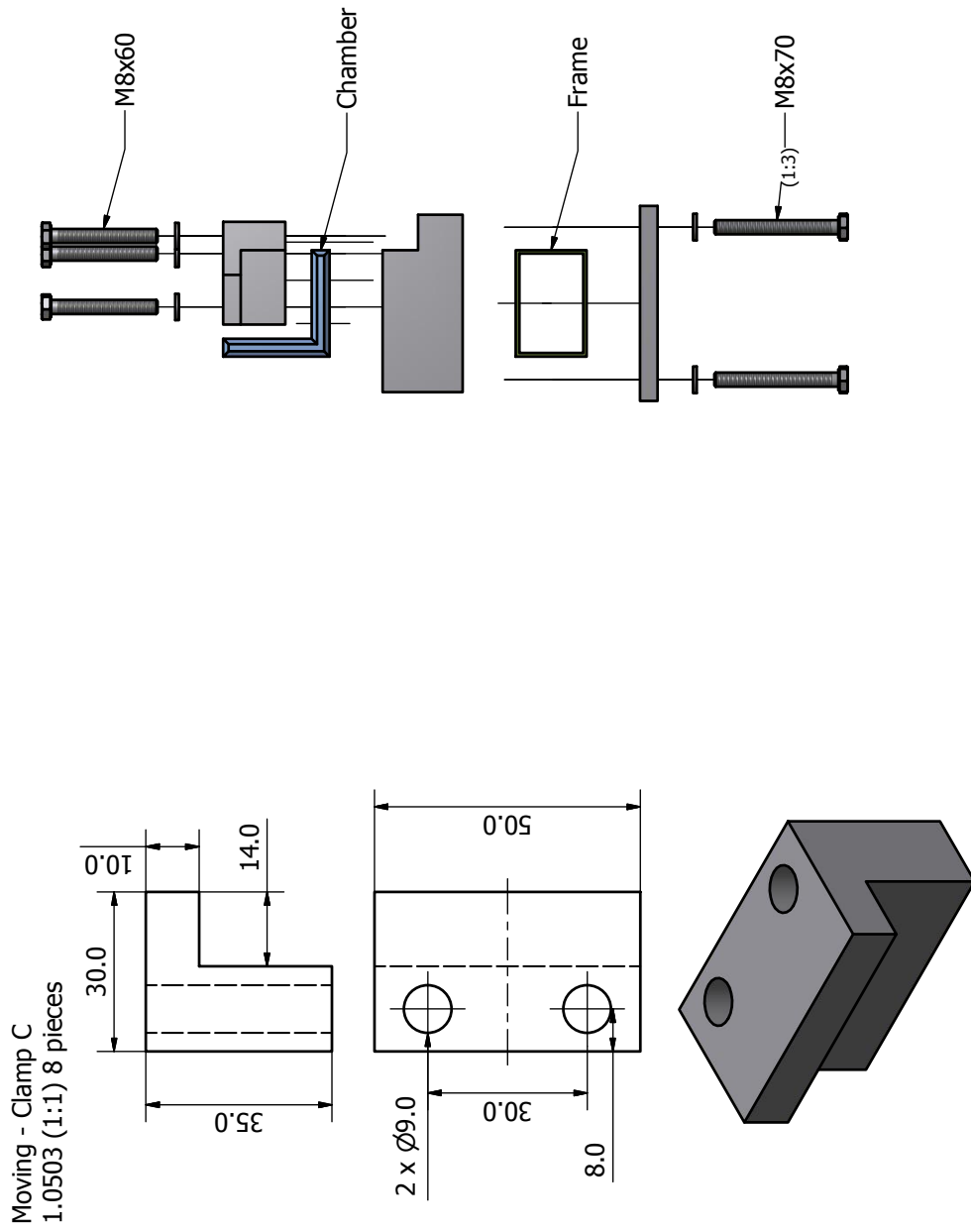


Moving - Clamp A
1.0503 (1:1) 4 pieces

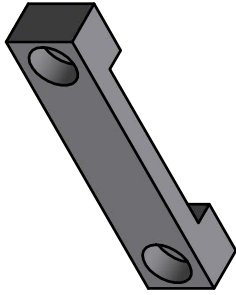
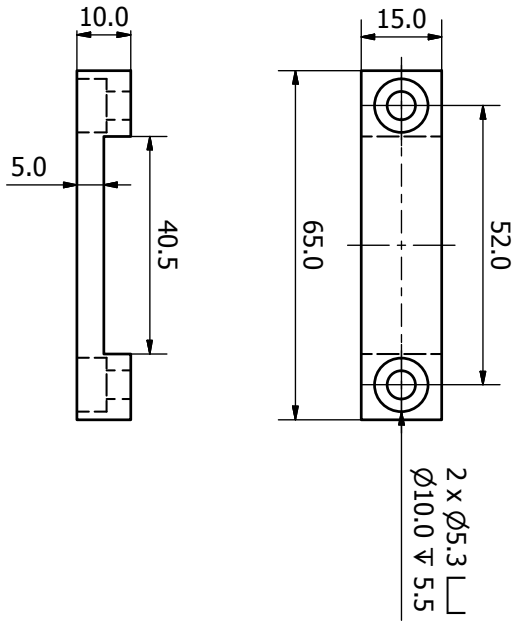


Moving - Clamp B
1.0503 (1:1) 4 pieces

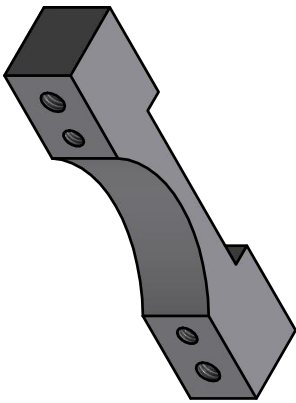
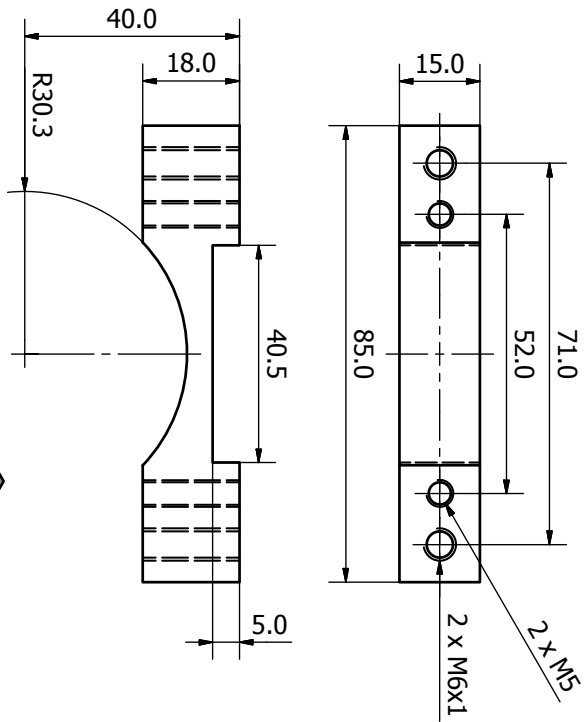




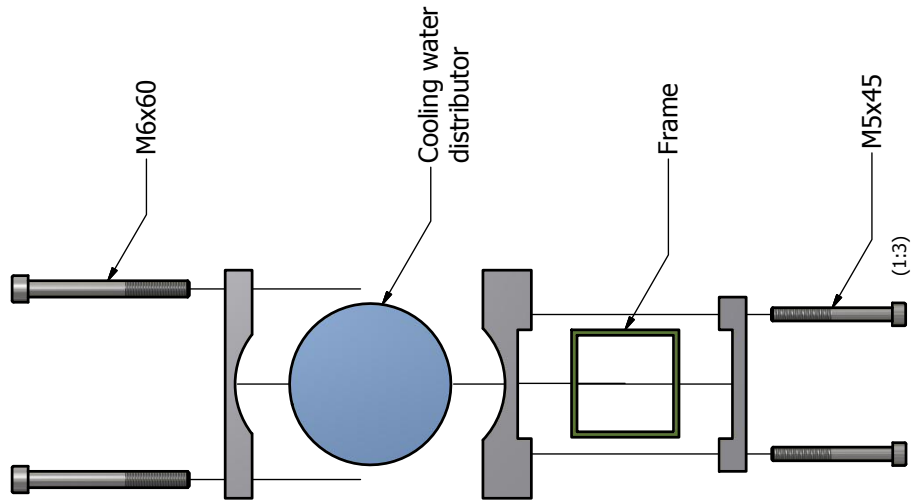
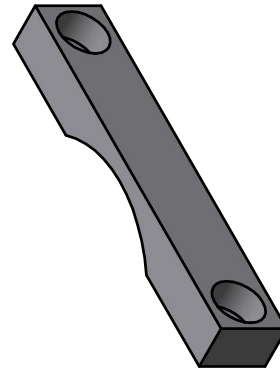
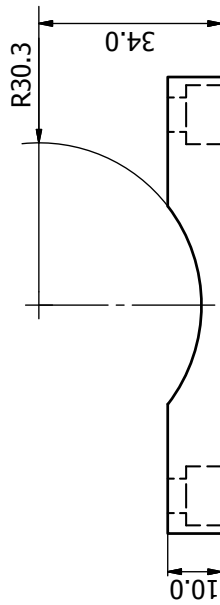
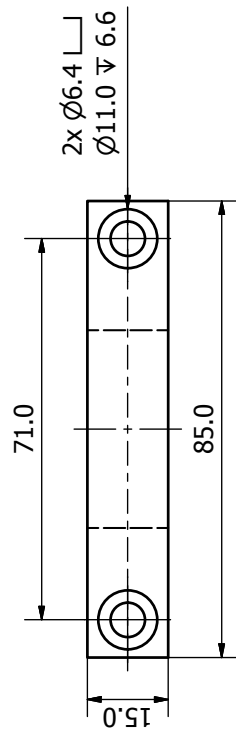
Holder Water Distributor A
1.4301 (1:1) 4 pieces



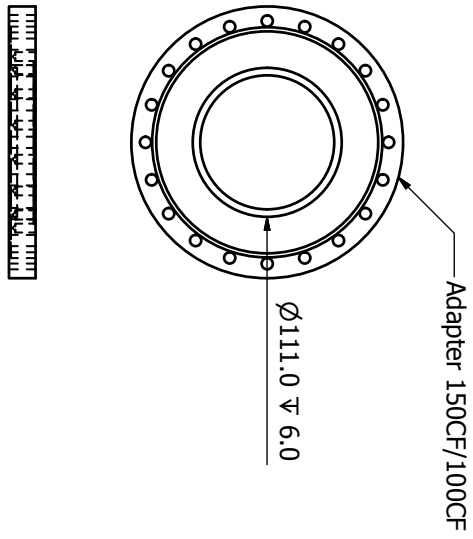
Holder Water Distributor B
1.4301 (1:1) 4 pieces



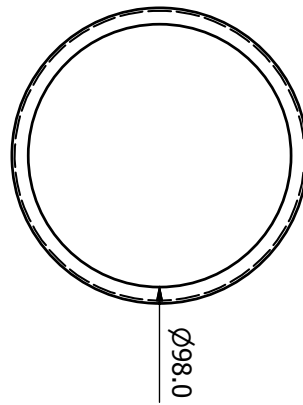
Holder Water Distributor C
1.4301 (1:1) 4 pieces



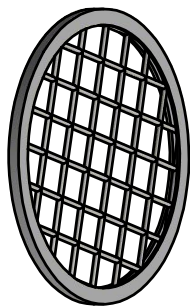
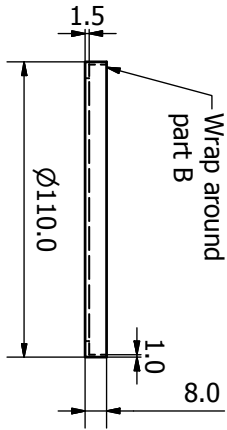
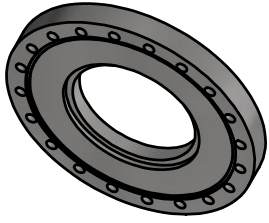
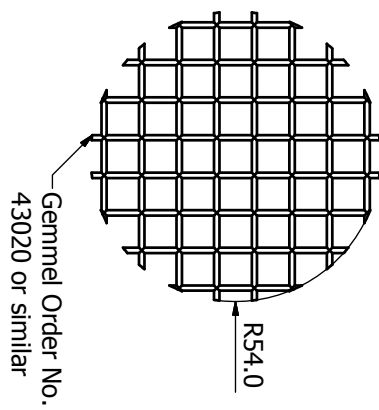
150CF/100CF Adapter for Heavy Duty Safety Grid Modification (1:4)

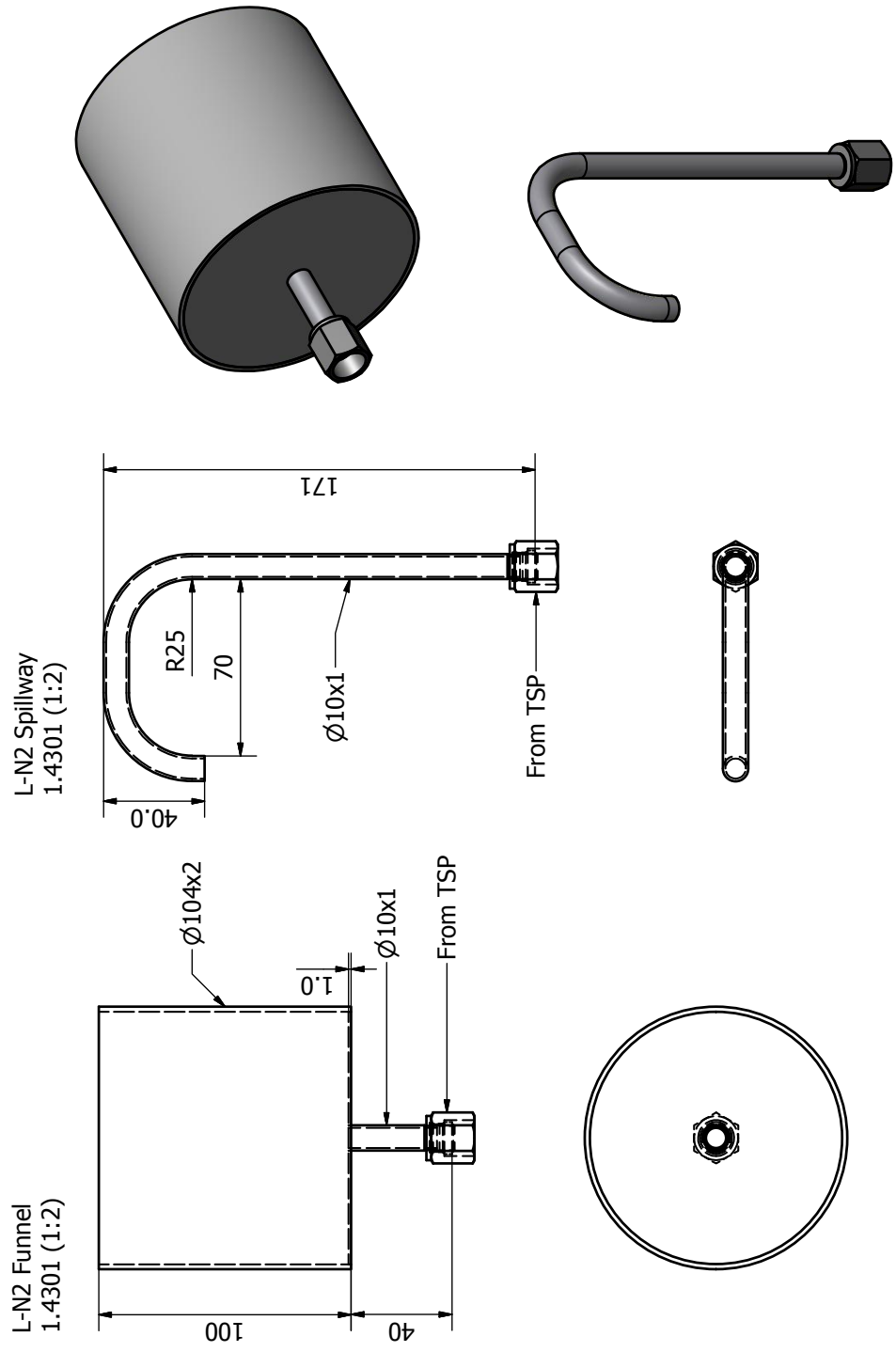


Heavy Duty Safety Grid A 1.4301 (1:2)

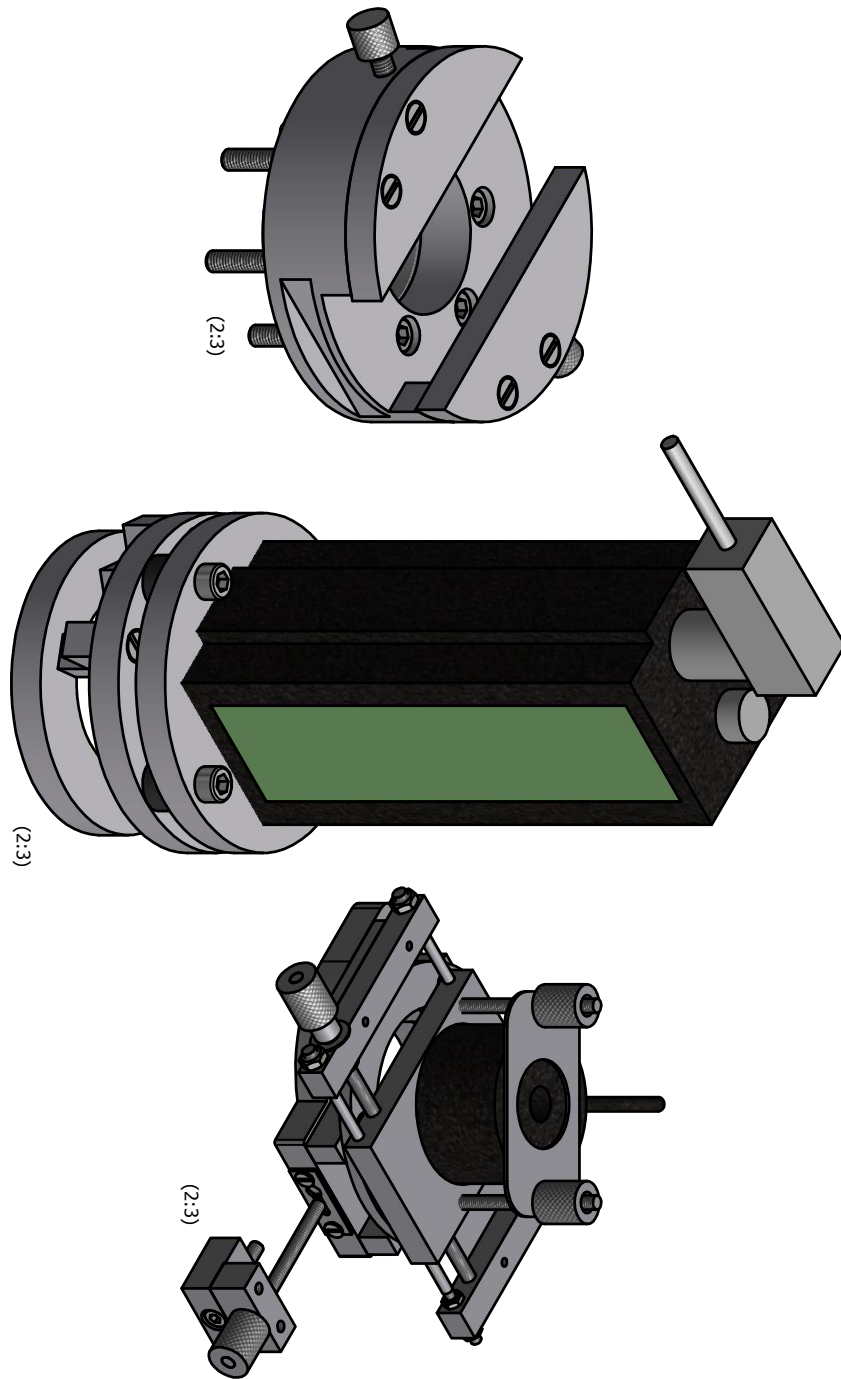


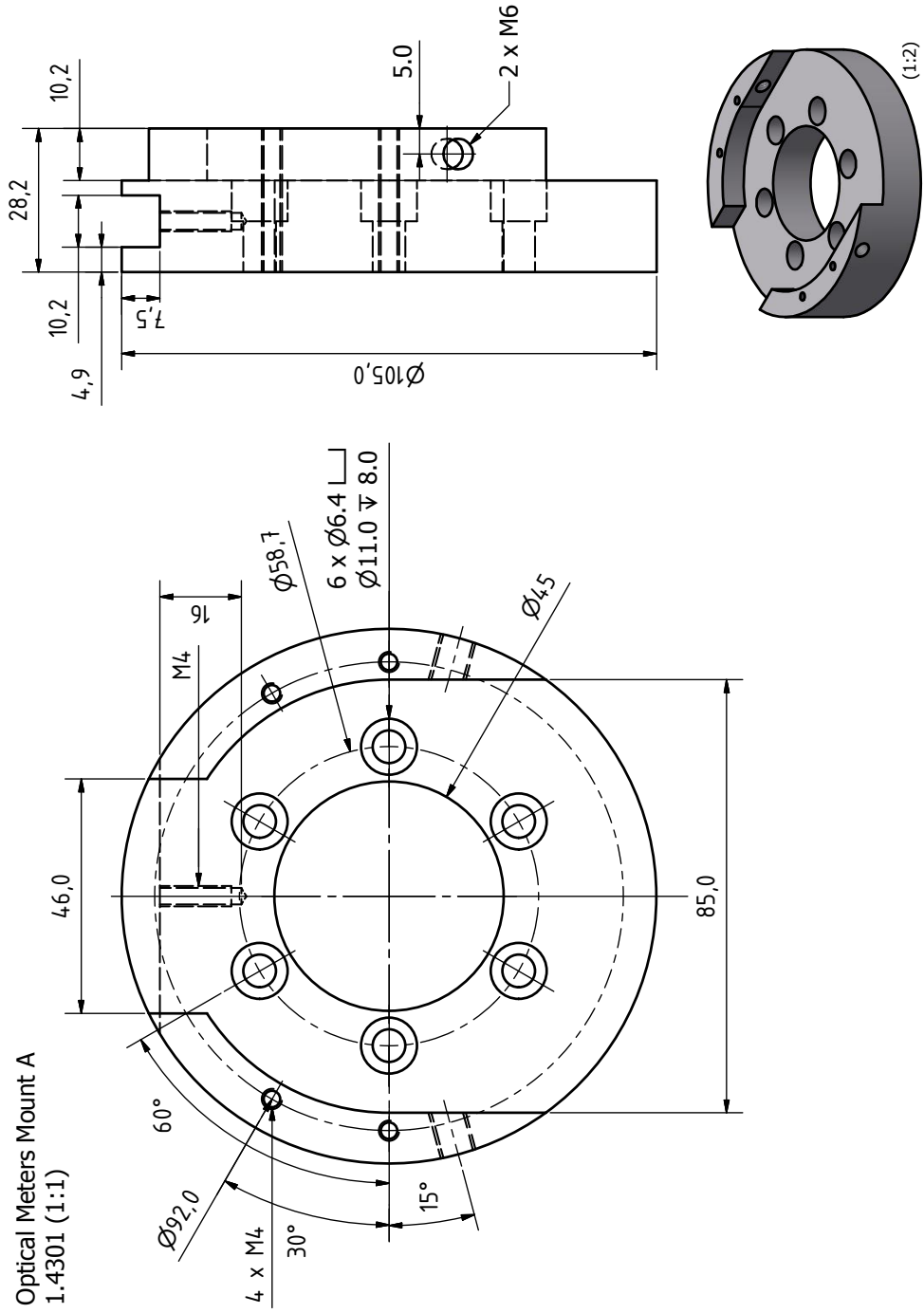
Heavy Duty Safety Grid B 1.4301 (1:2)

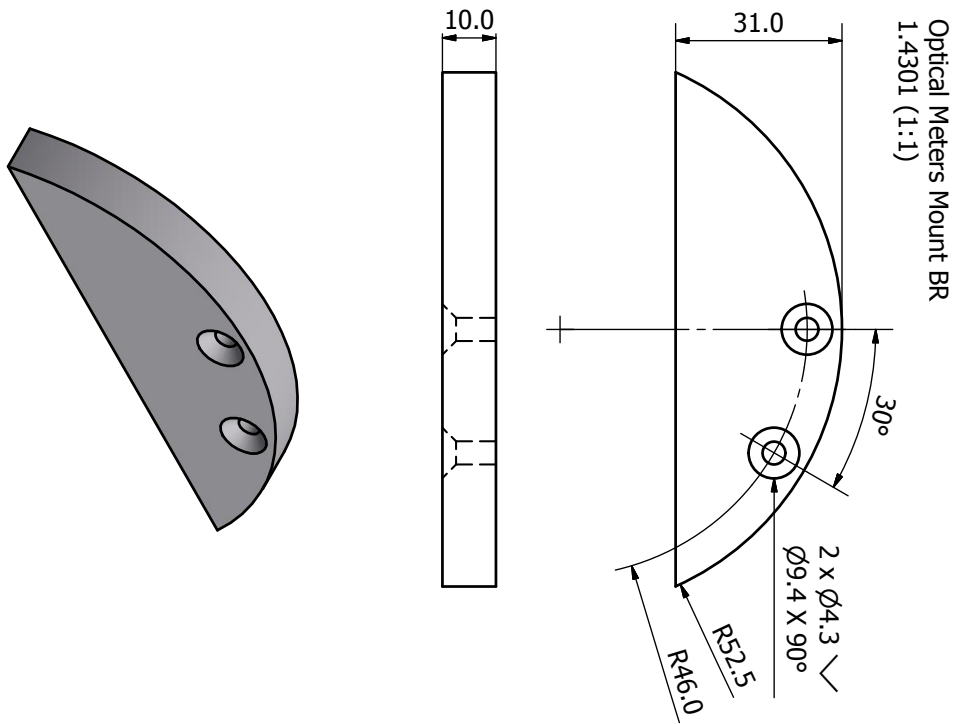
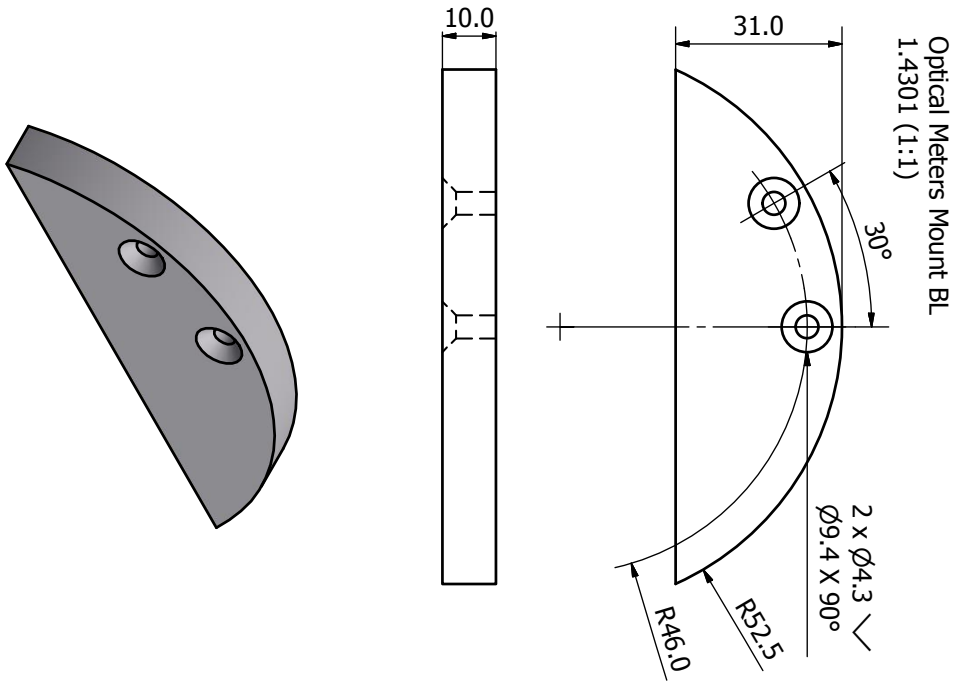


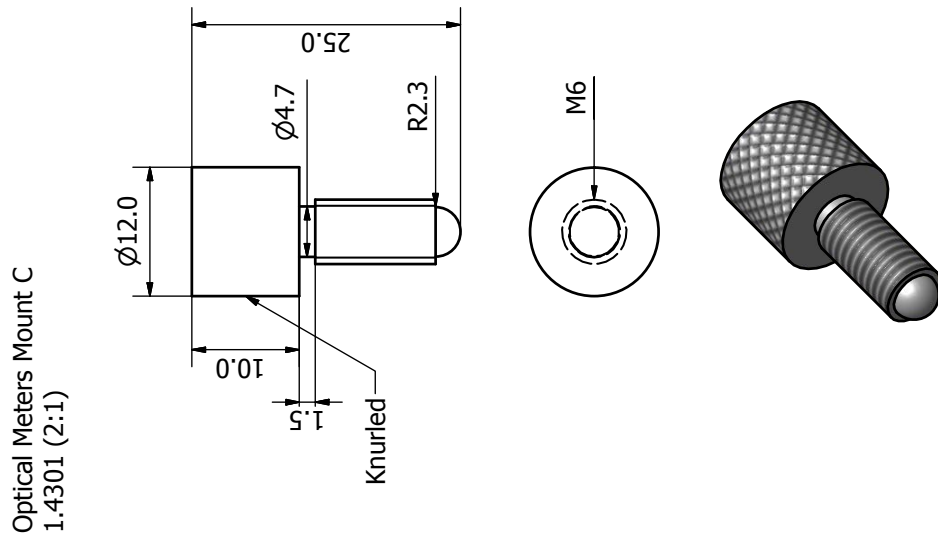
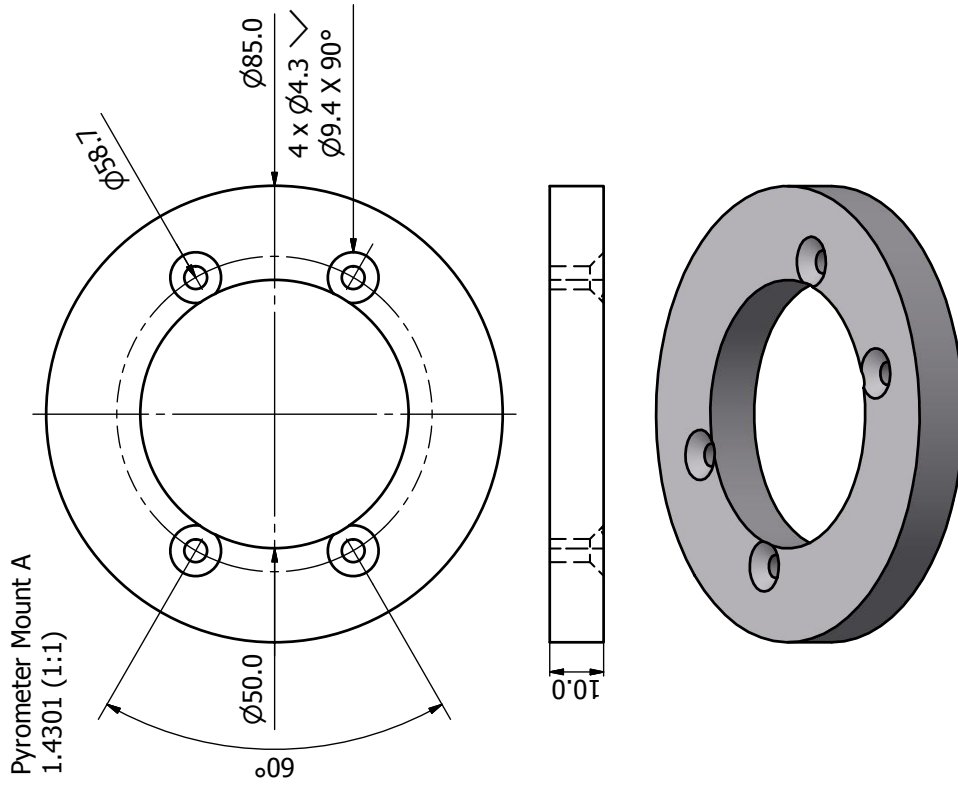


B.2.8 Optical Meters

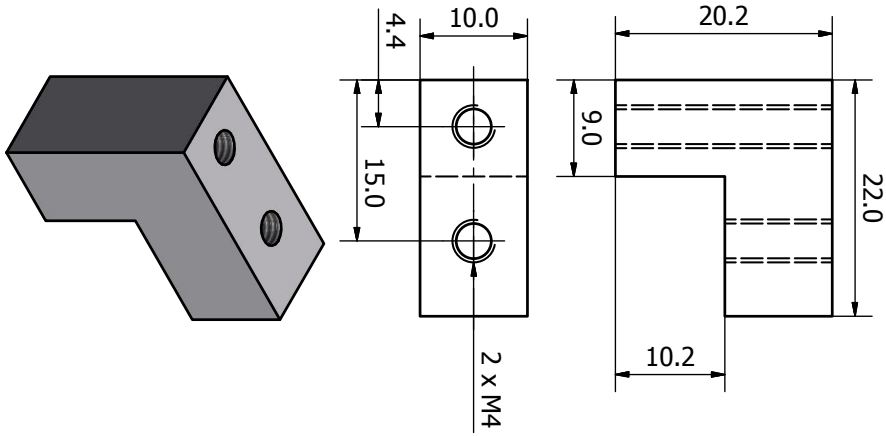




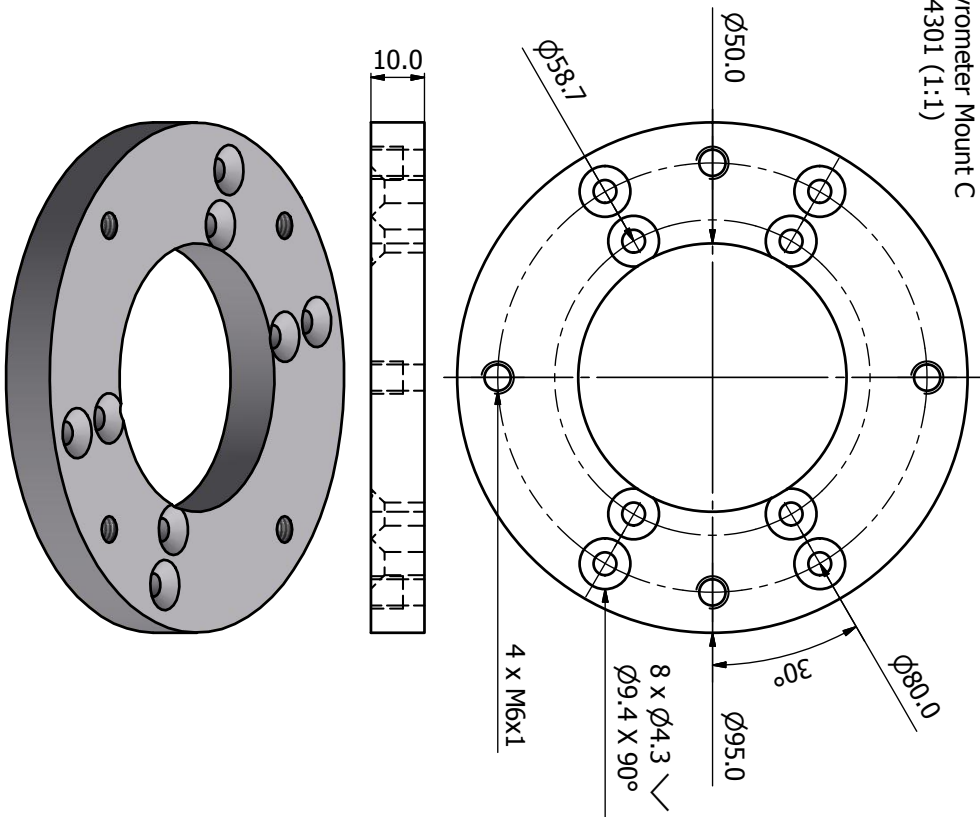




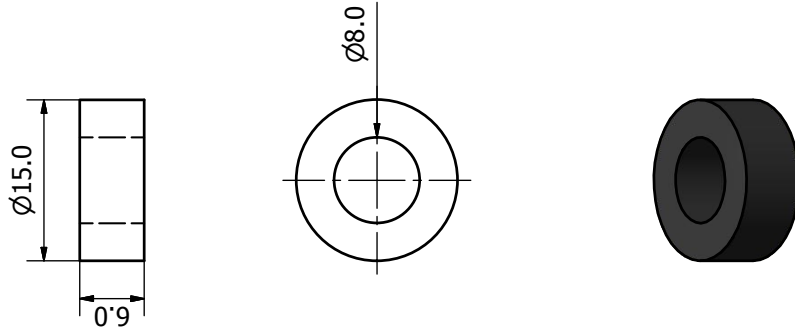
Pyrometer Mount B
1.4301 (2:1) 4 pieces



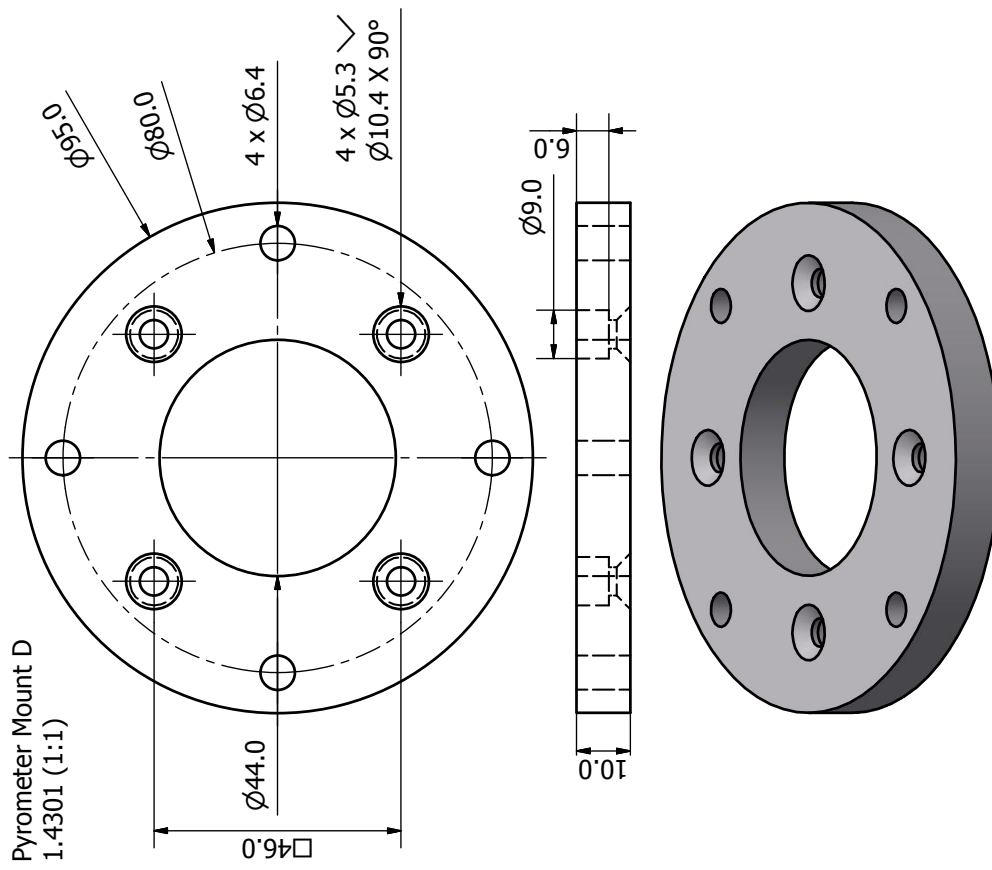
Pyrometer Mount C
1.4301 (1:1)



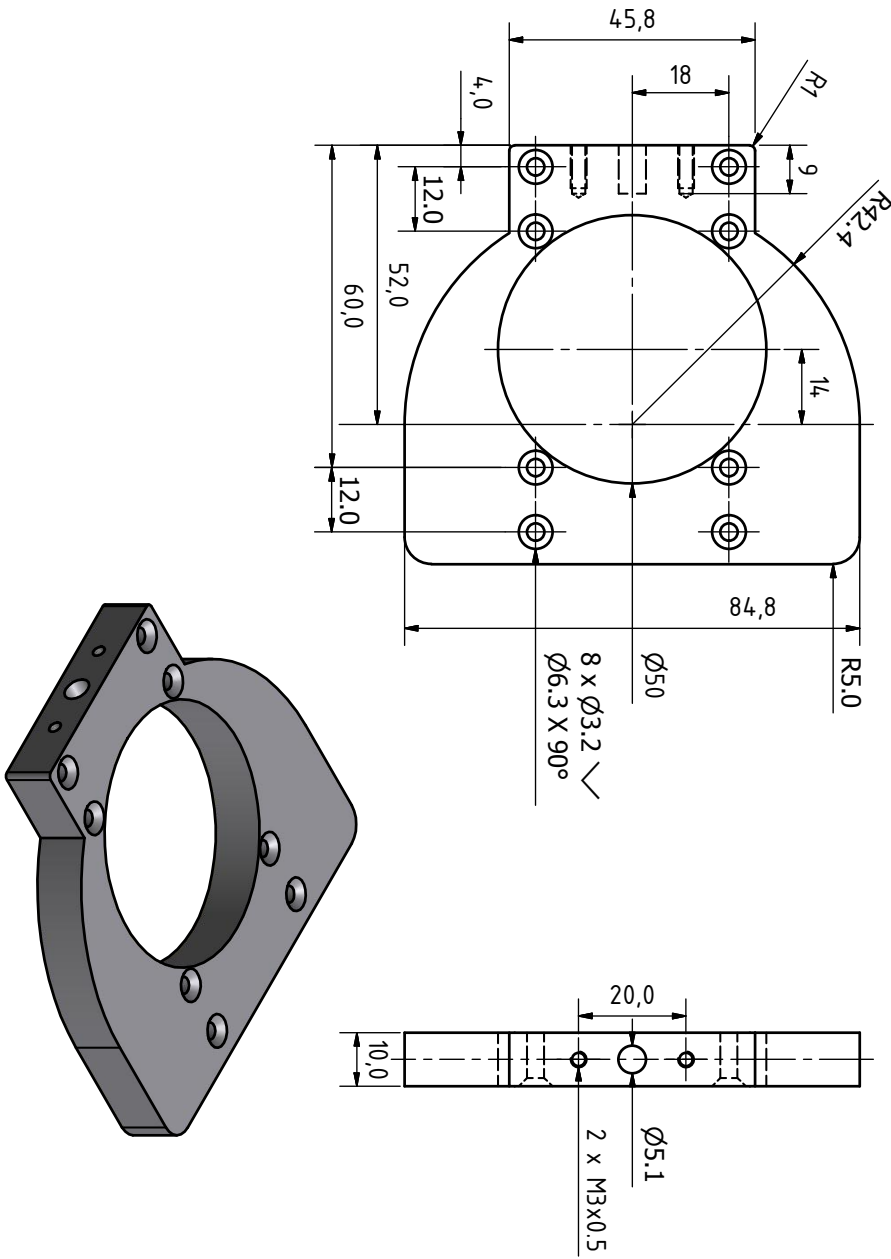
Pyrometer Mount E
Rubber (2:1) 4 pieces



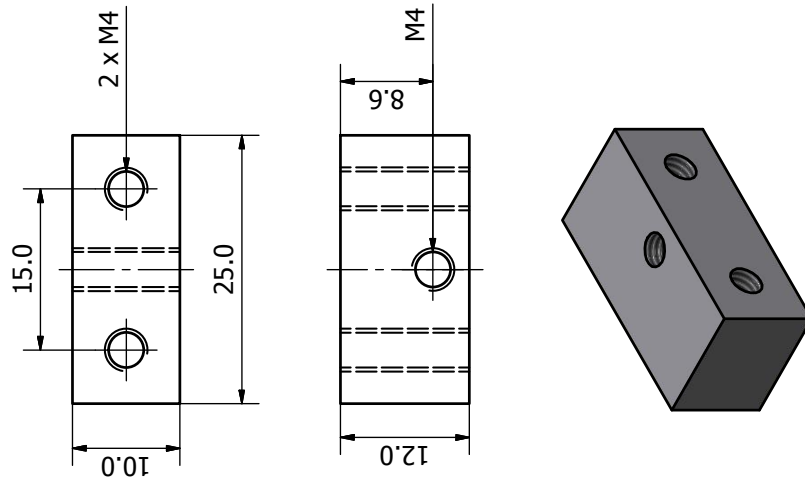
Pyrometer Mount D
1.4301 (1:1)



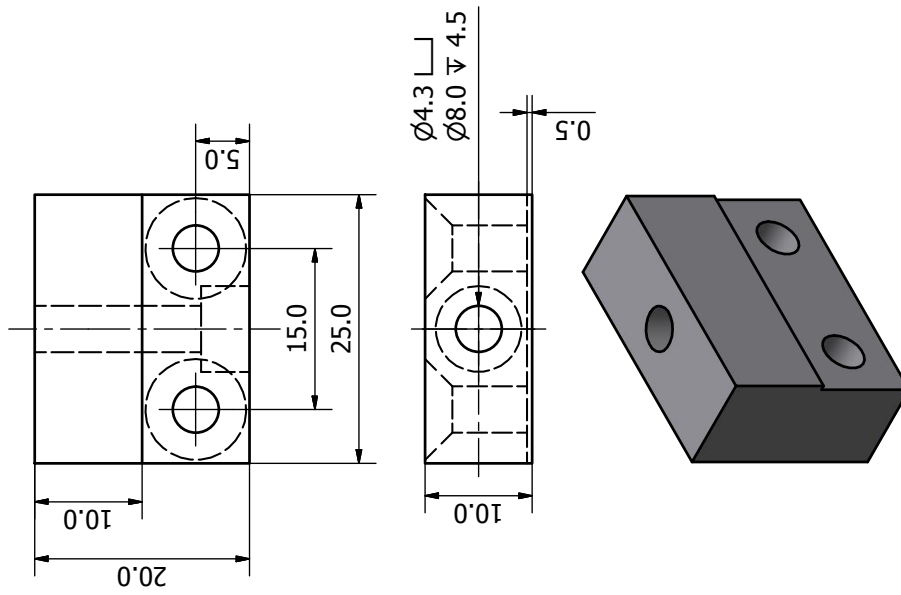
Photometer Mount A
1.4301 (1:1)



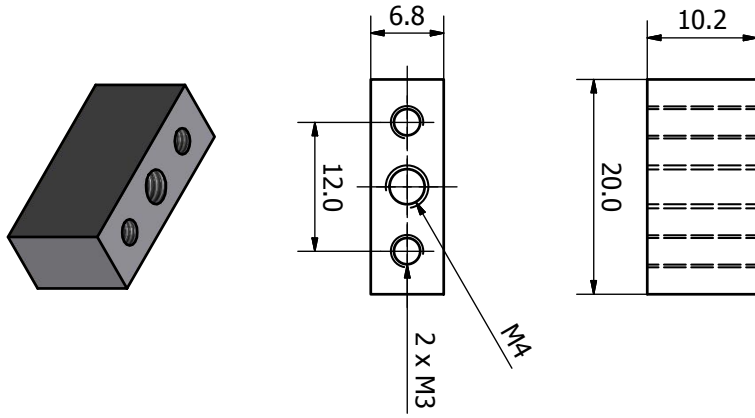
Photometer Mount Ba
1.4301 (2:1)



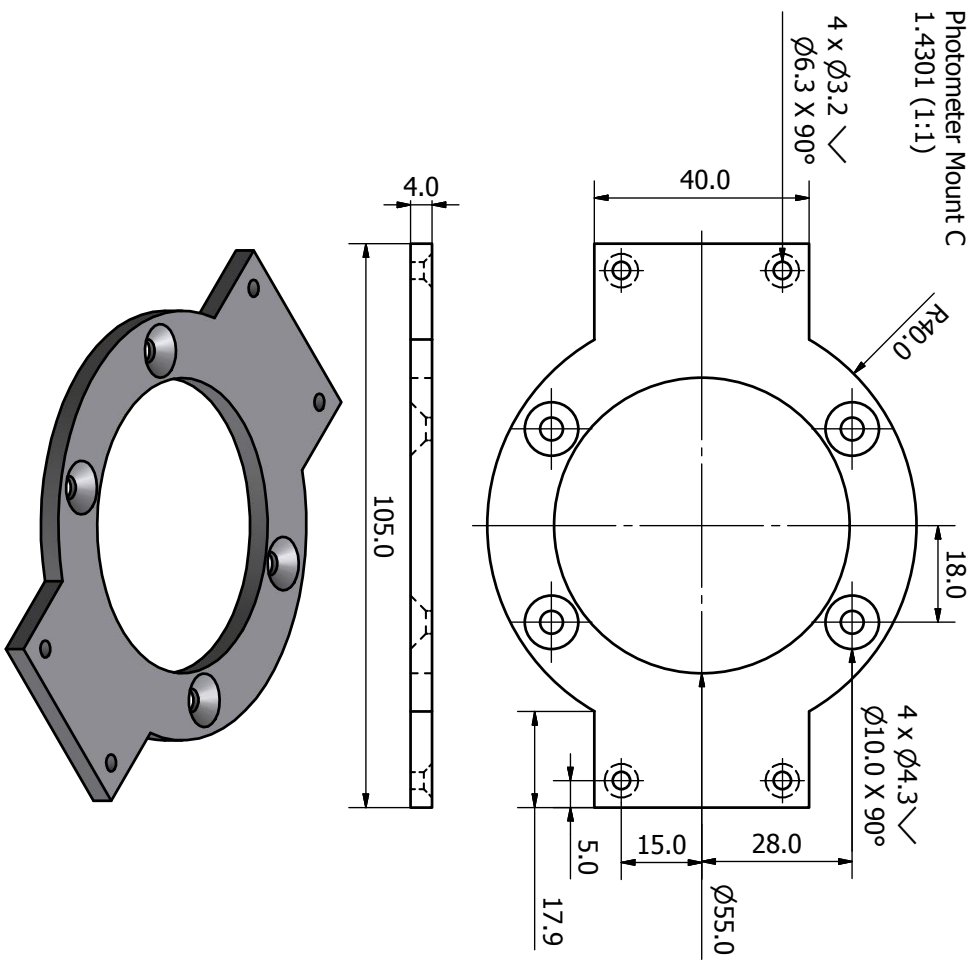
Photometer Mount Ba
1.4301 (2:1)



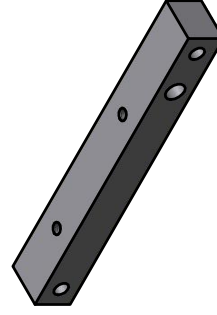
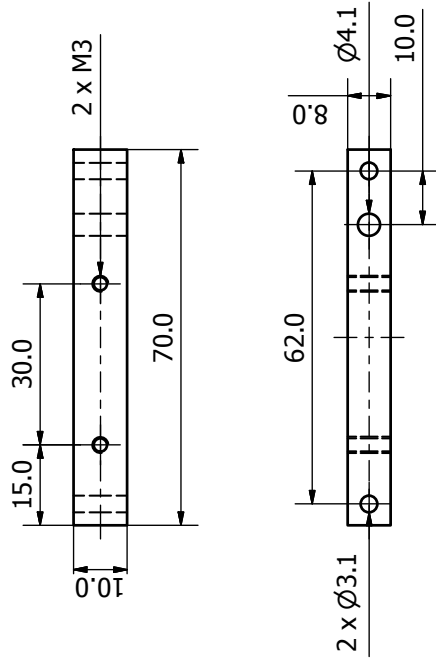
Photometer Mount Bc
1.4301 (2:1) 4 pieces



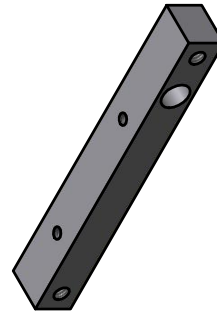
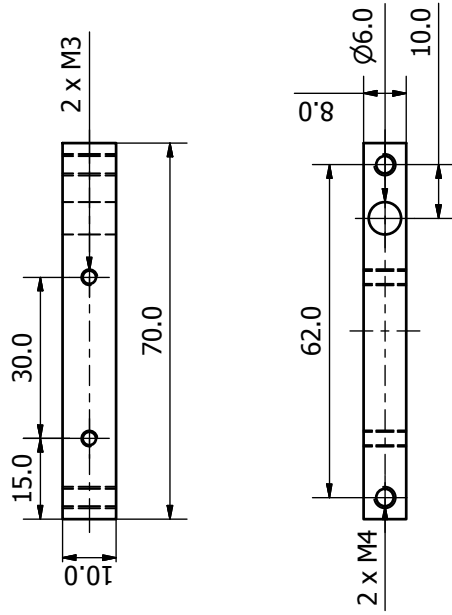
Photometer Mount C
1.4301 (1:1)



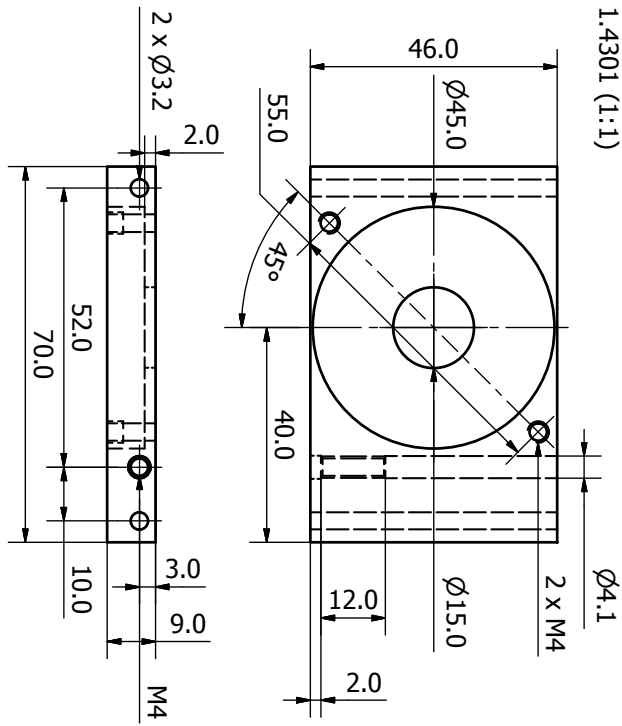
Photometer Mount Db
1.4301 (1:1)



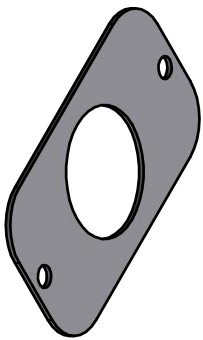
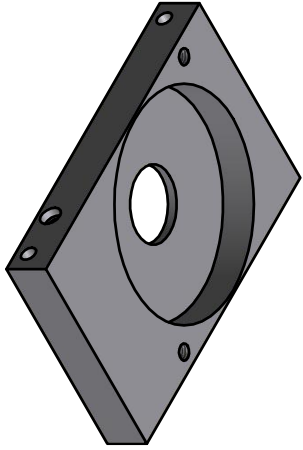
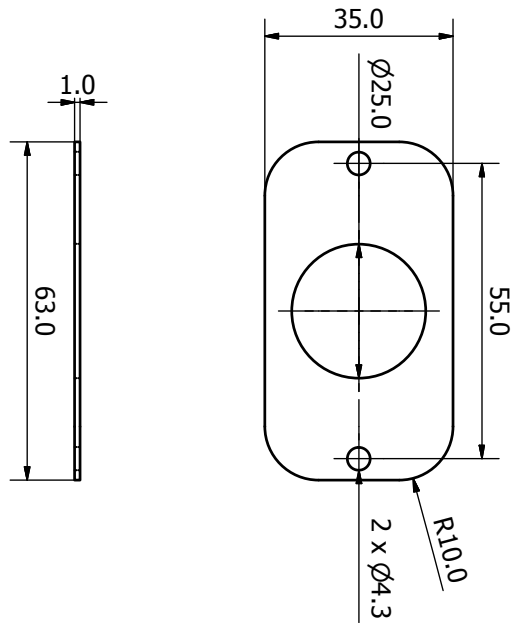
Photometer Mount Da
1.4301 (1:1)



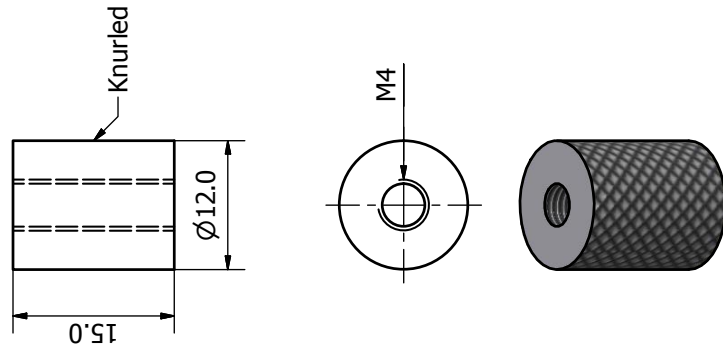
Photometer Mount E
1.4301 (1:1)



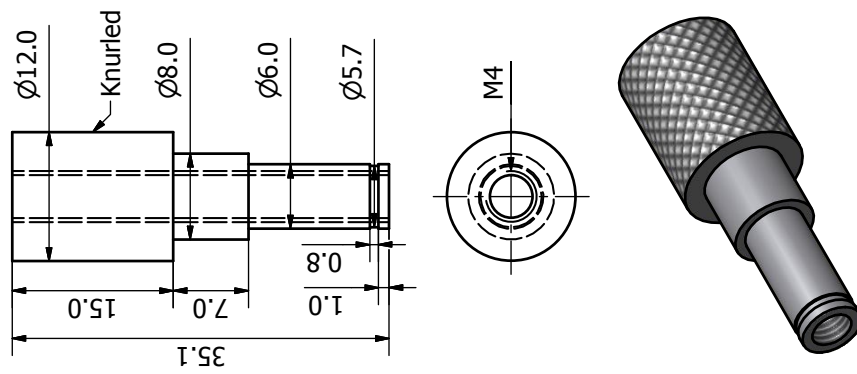
Photometer Mount F
1.4301 (1:1)



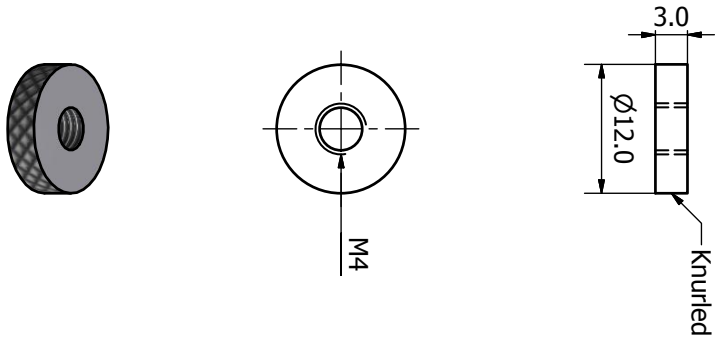
Photometer Mount Gb
1.4301 (2:1)



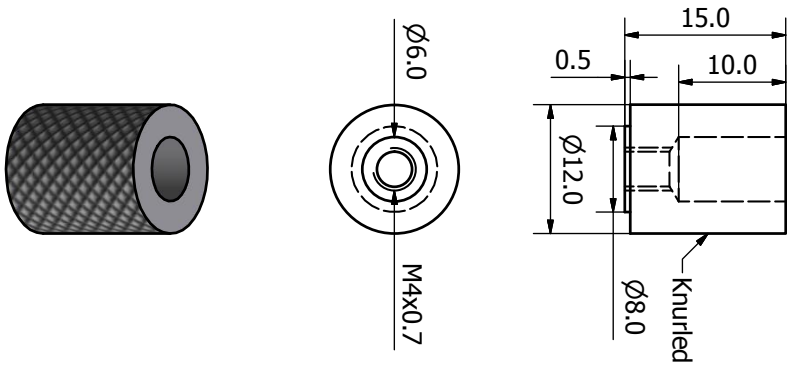
Photometer Mount Ga
1.4301 (2:1)



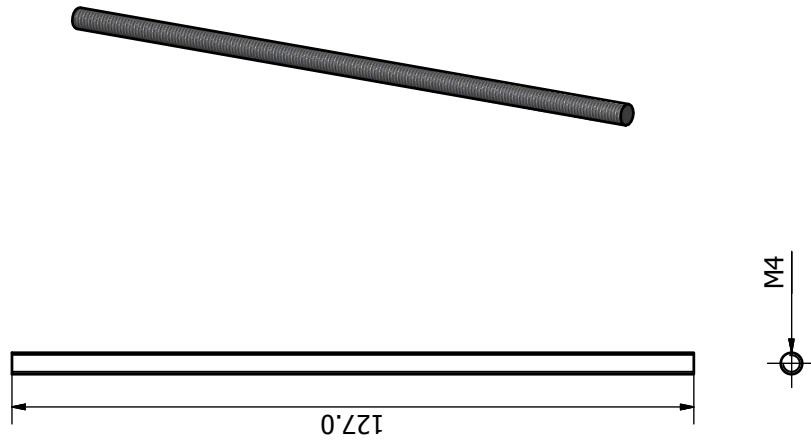
Photometer Mount Gc
1.4301 (2:1) 2 pieces



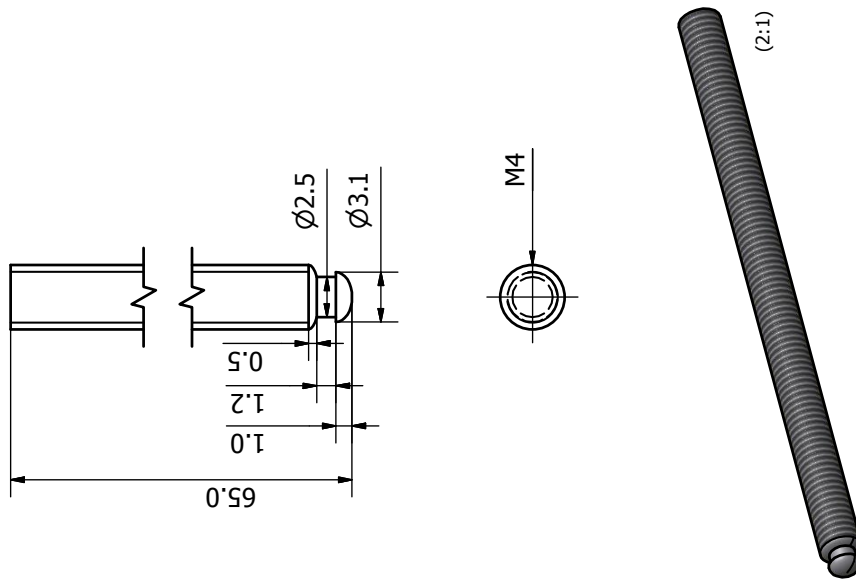
Photometer Mount Gc
1.4301 (2:1) 2 pieces

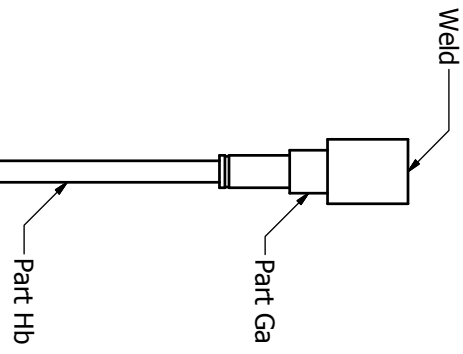
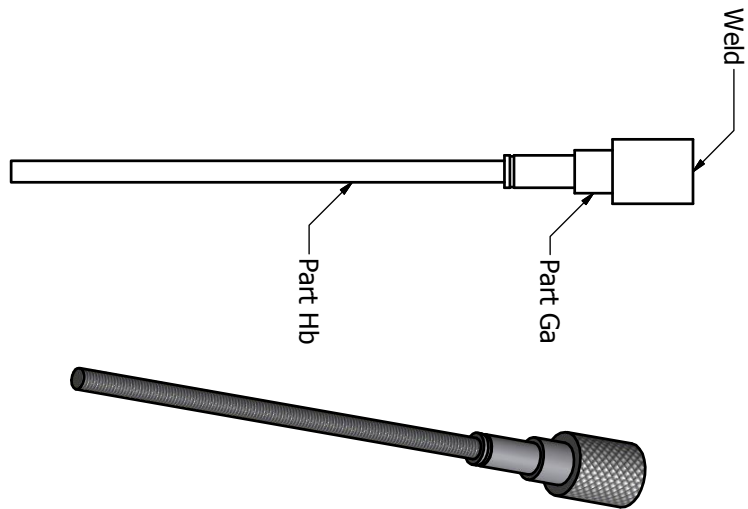
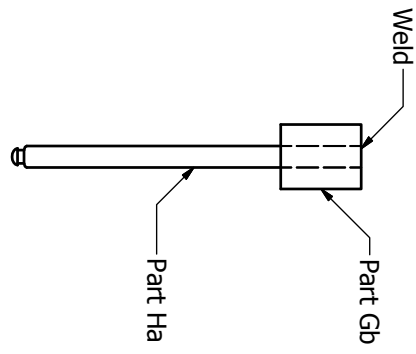
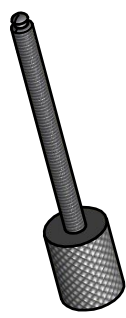


Photometer Mount Hb
1.4301 (1:1)

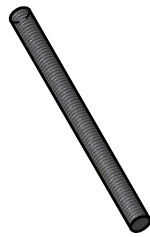
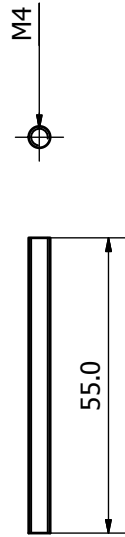


Photometer Mount Ha
1.4301 (3:1)





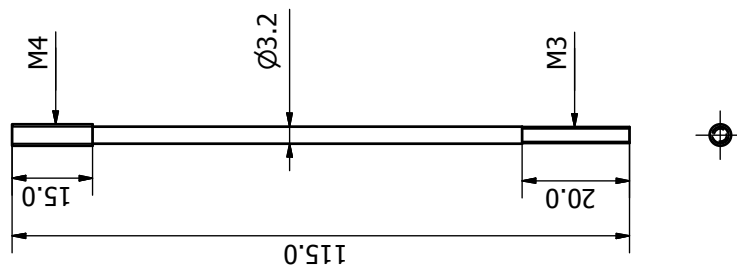
Photometer Mount Hd
1.4301 (1:1) 2 pieces



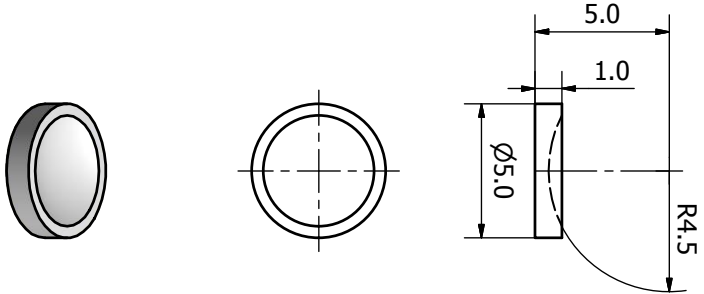
Photometer Mount J
Spring (2:1)
ØWire 0.8
ØInner 4.0
Pitch 2.0mm
Coils 5



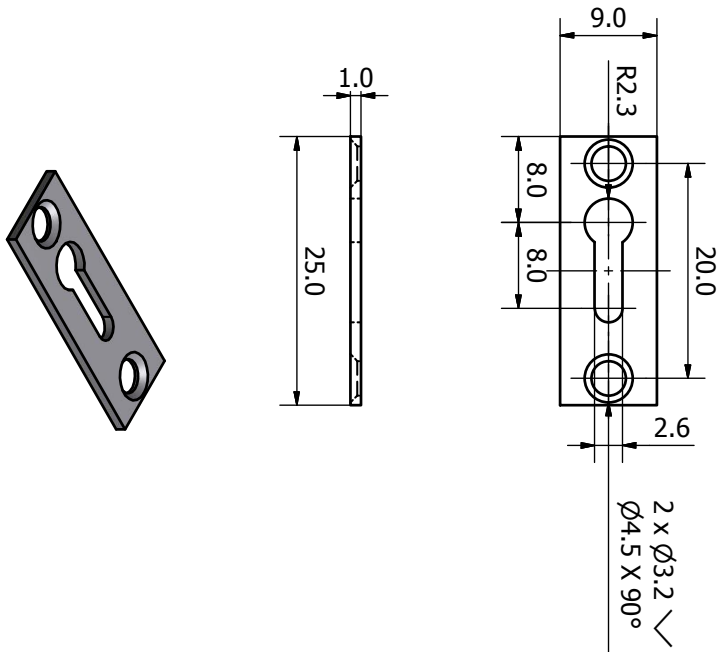
Photometer Mount Hc
1.4301 (1:1) 2 pieces



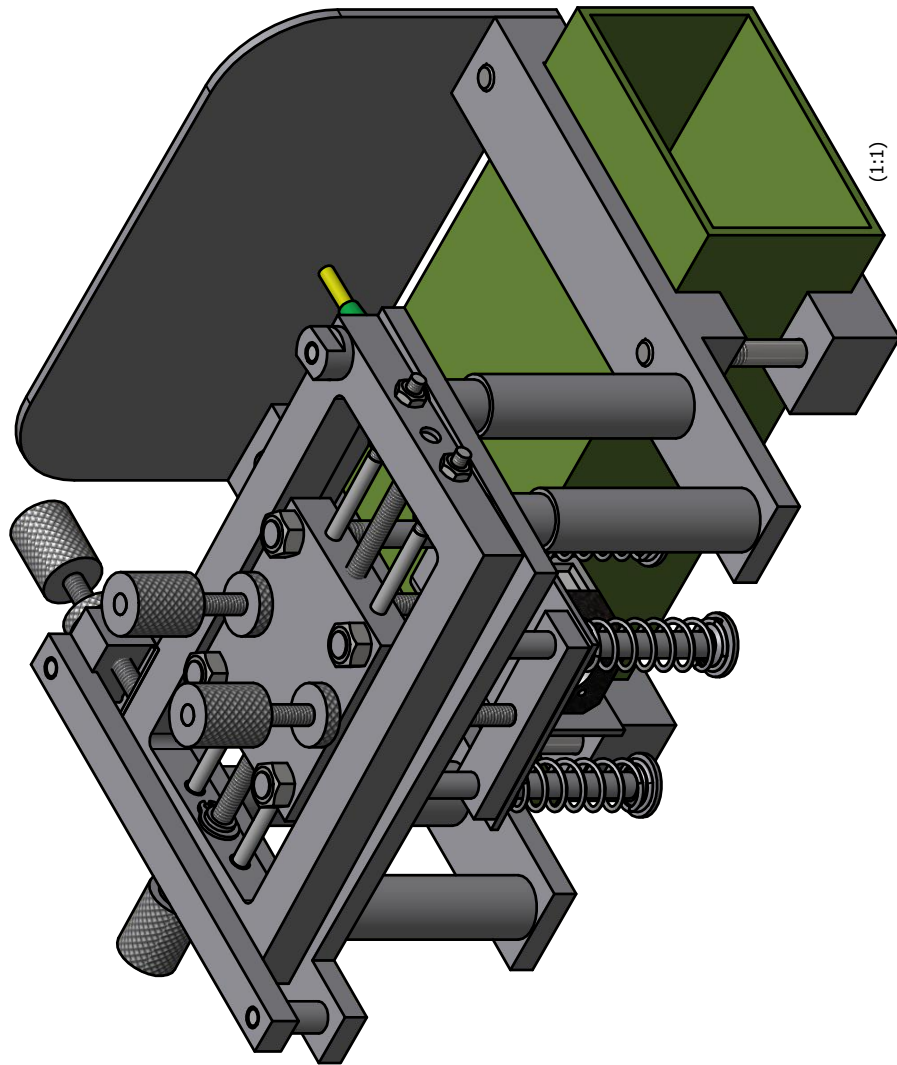
Photometer Mount K
1.4301 (5:1)



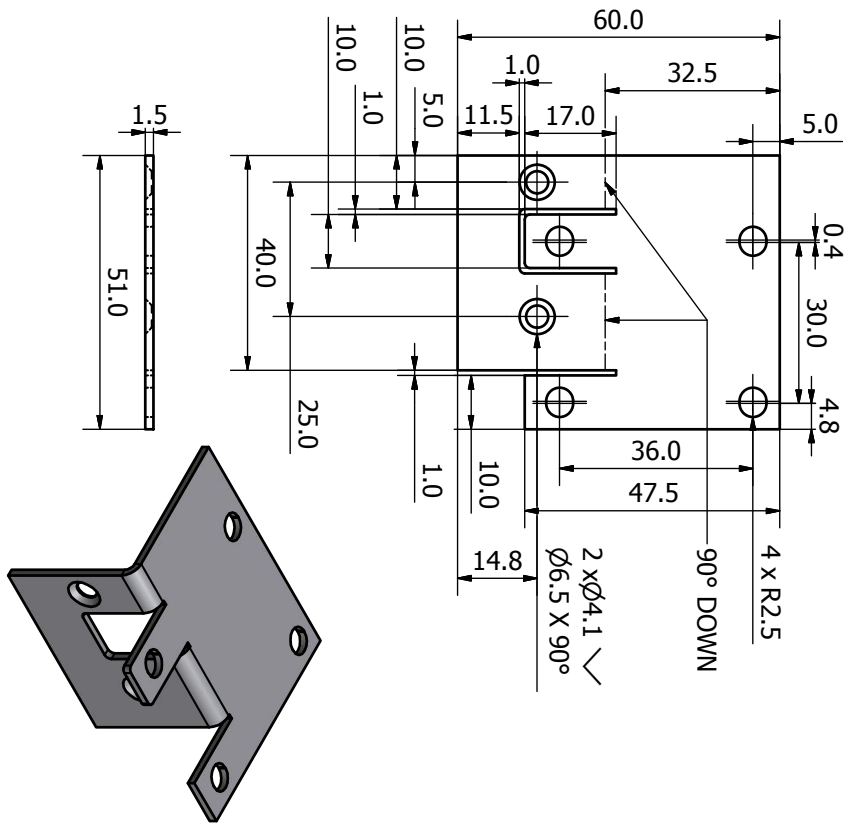
Photometer Mount L
1.4301 (2:1)



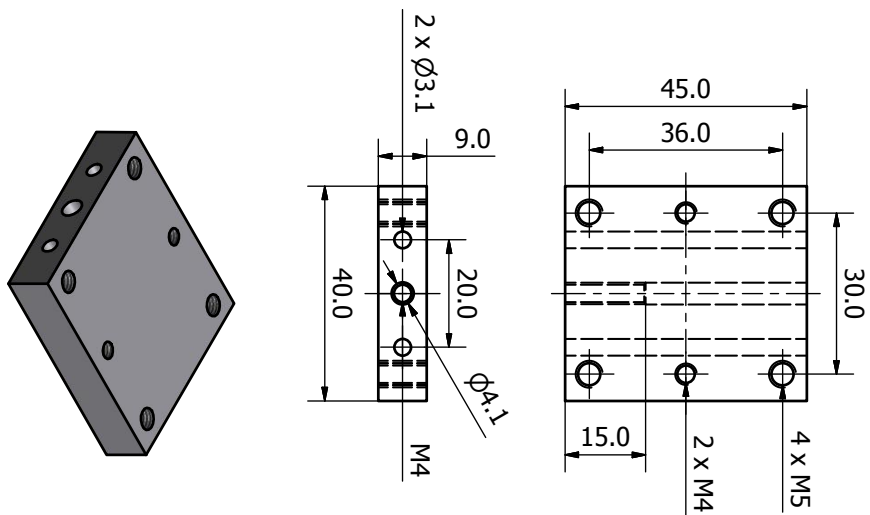
B.2.9 Fiber Positioner

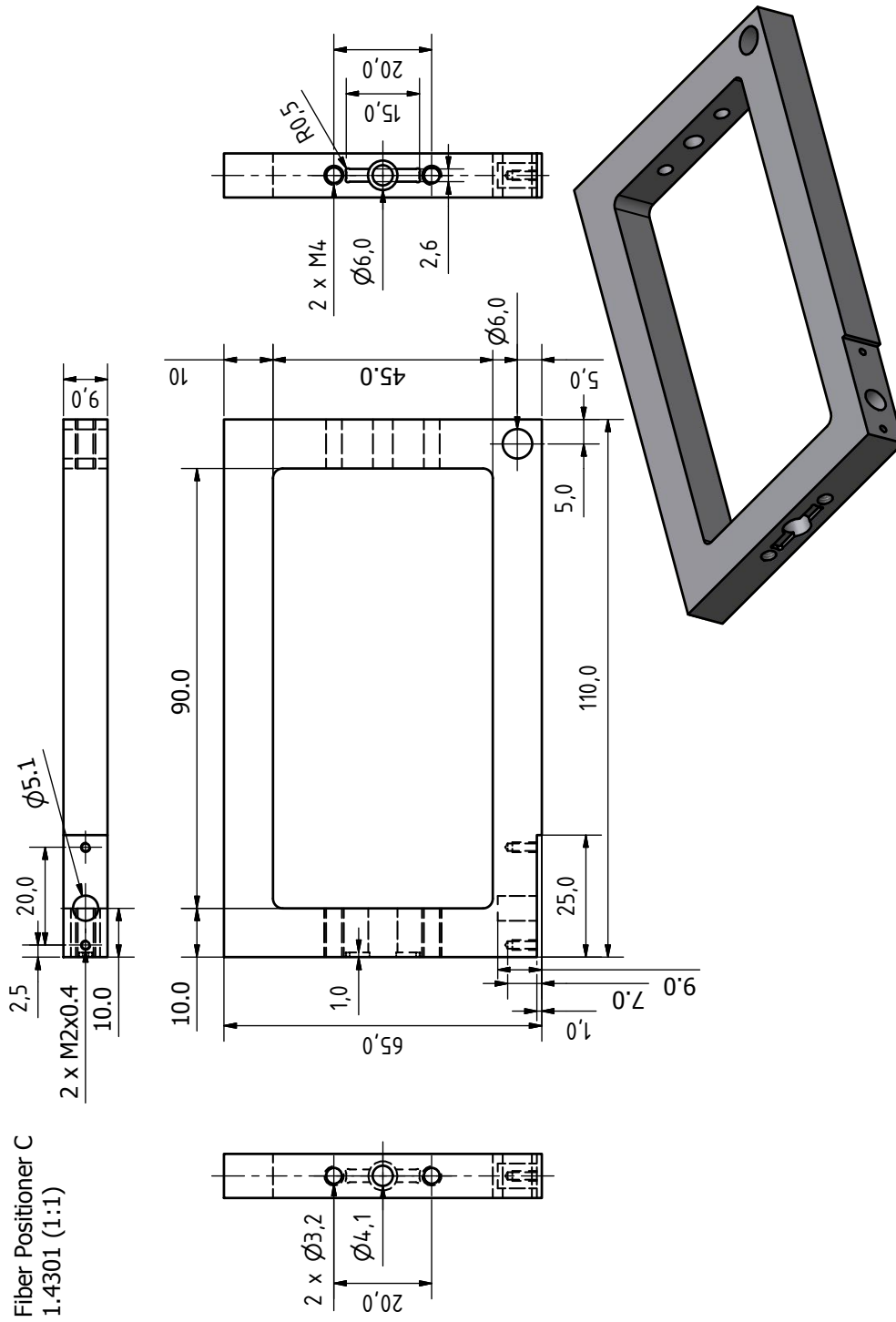


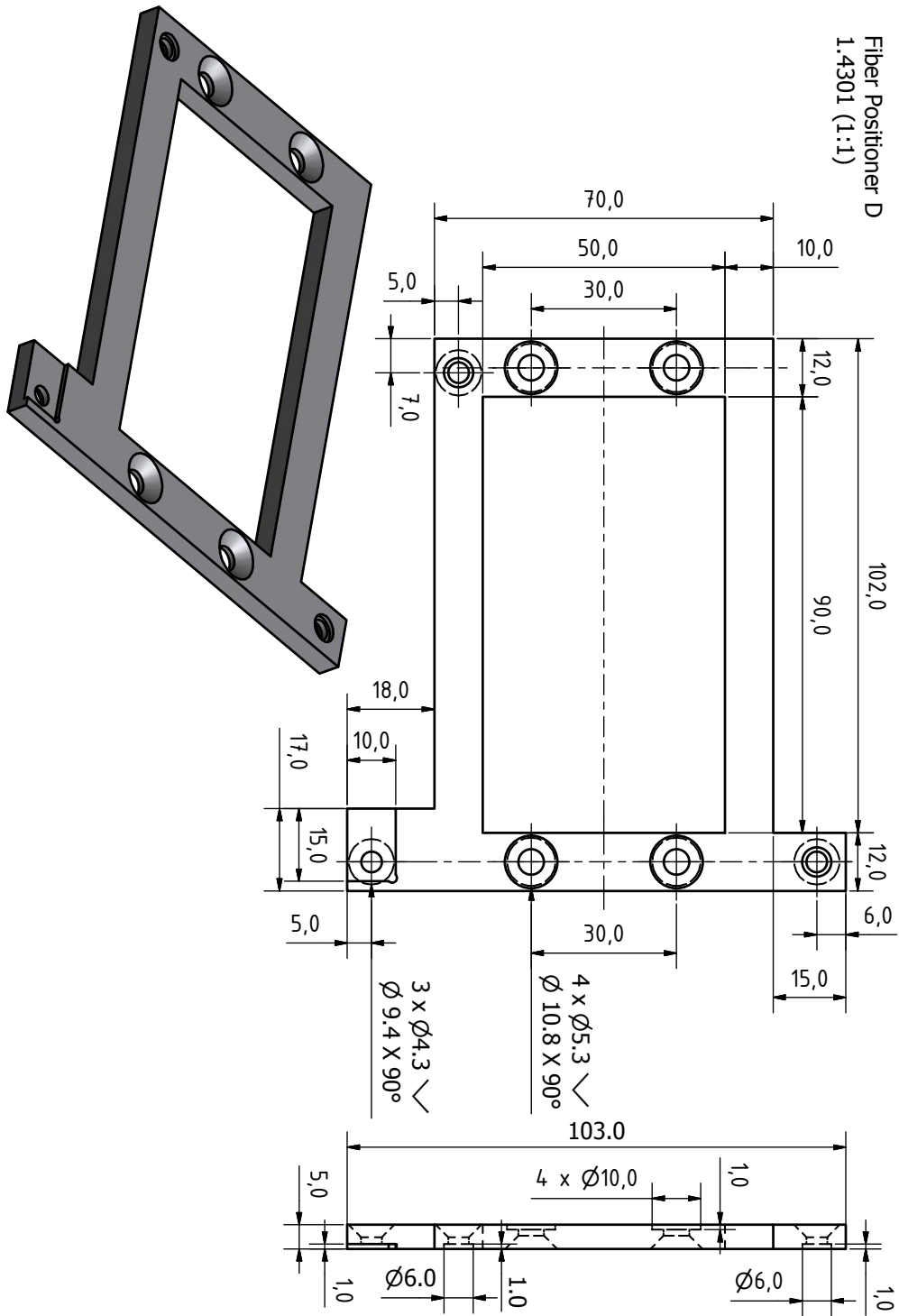
Fiber Positioner A
1.4301 (1:1)



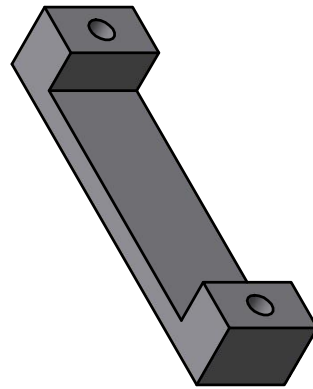
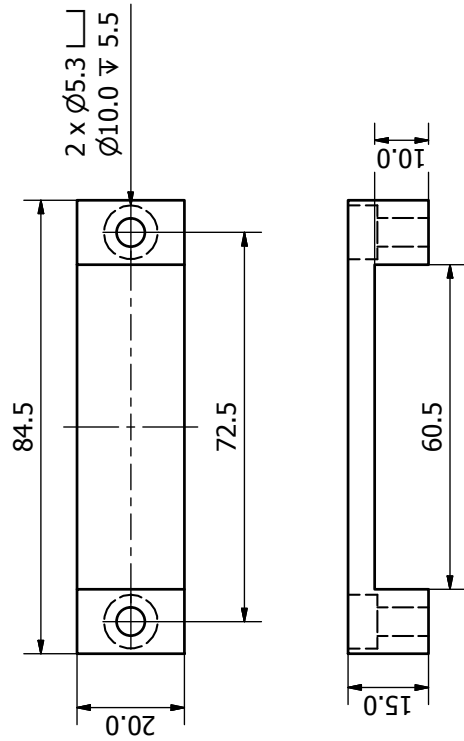
Fiber Positioner B
1.4301 (1:1)



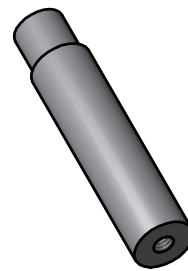
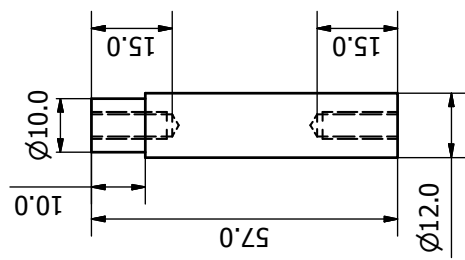




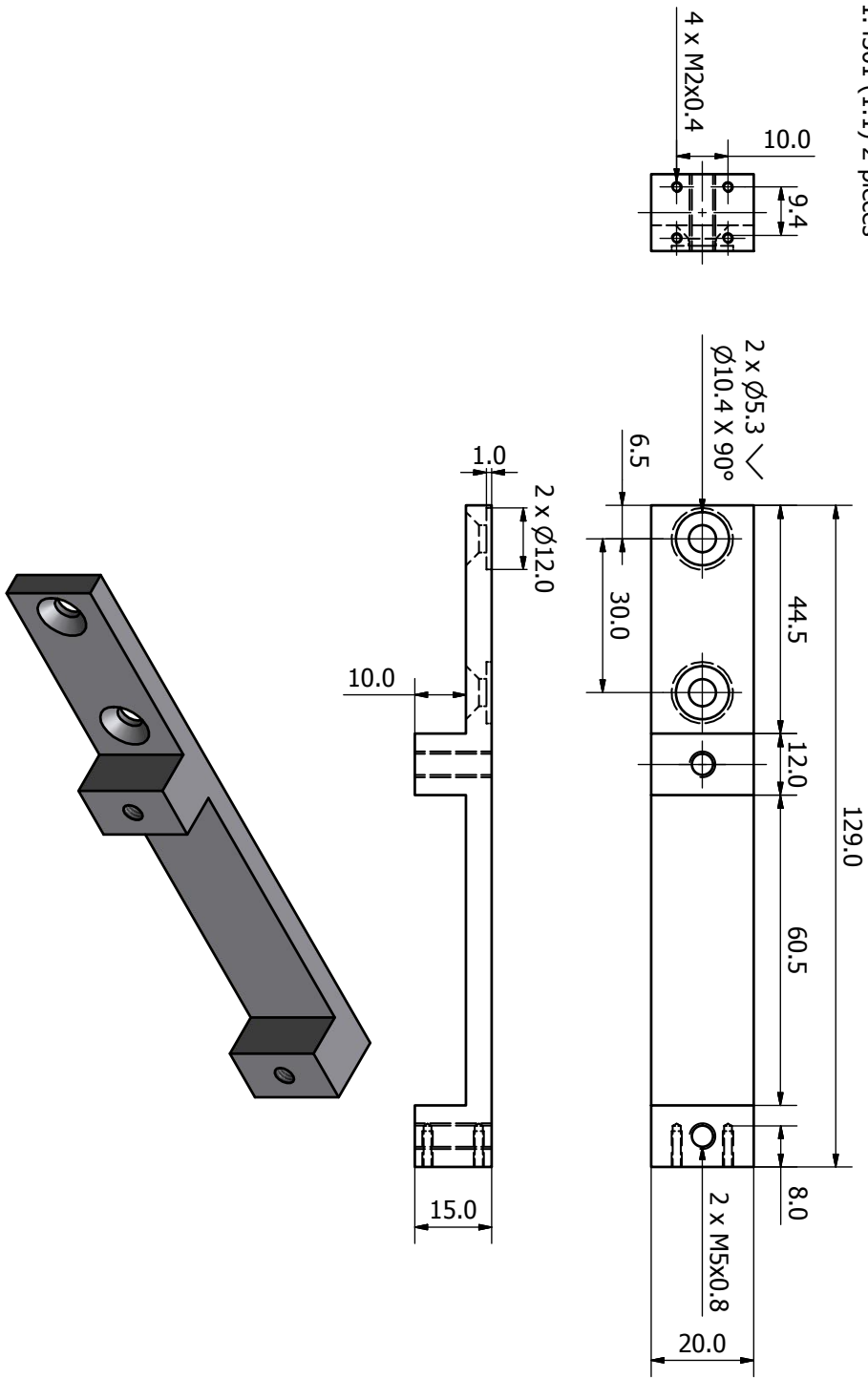
Fiber Positioner F
1.4301 (1:1) 2 pieces

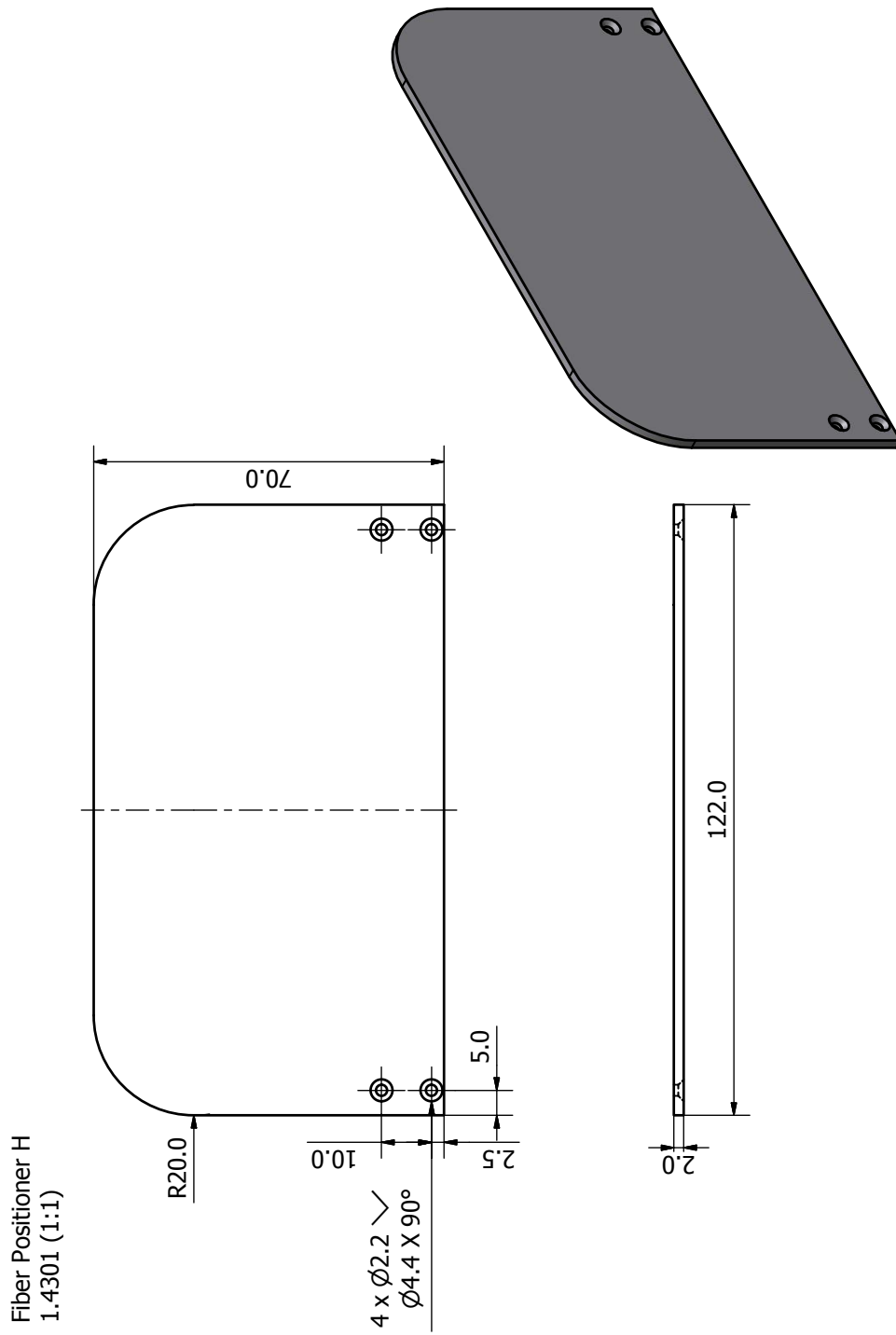


Fiber Positioner E
1.4301 (1:1) 4 pieces

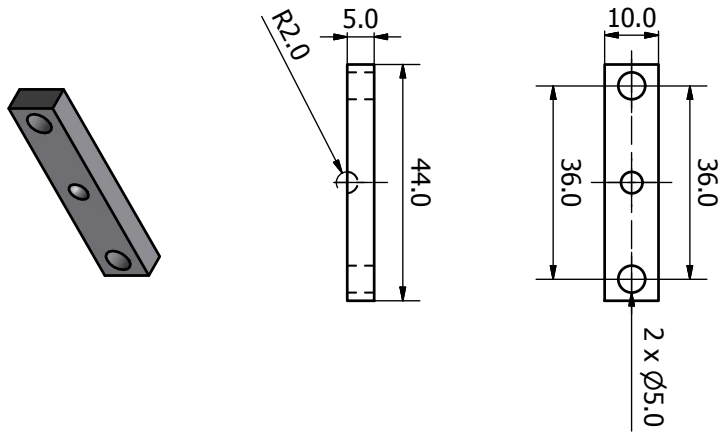


Fiber Positioner G
1.4301 (1:1) 2 pieces

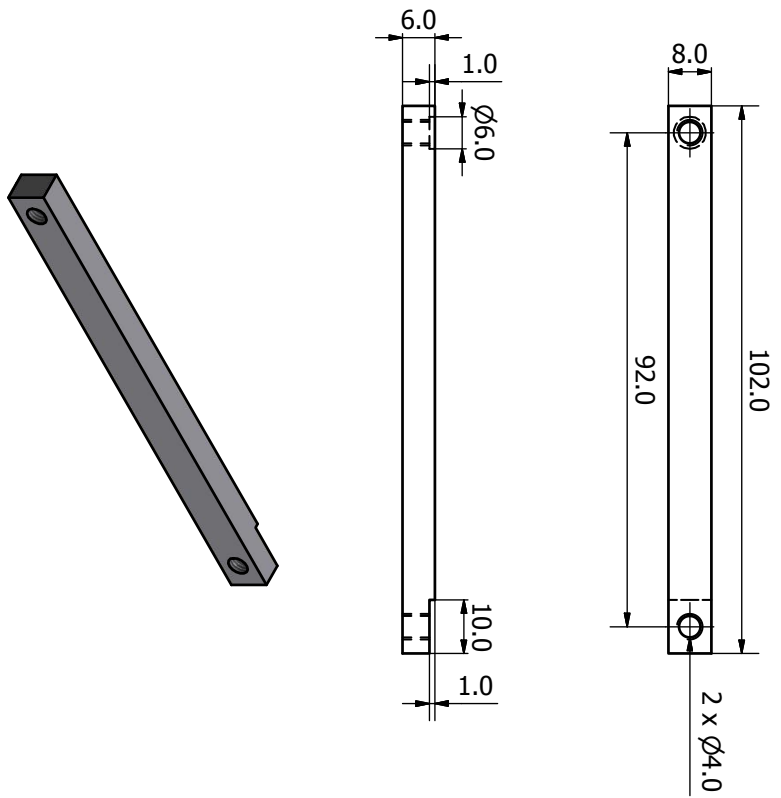




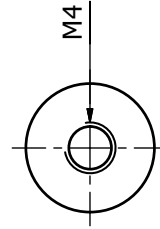
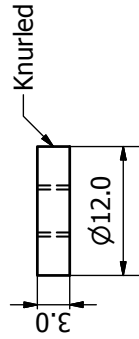
Fiber Positioner J
1.4301 (1:1)



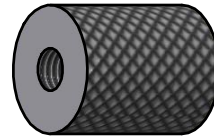
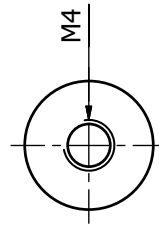
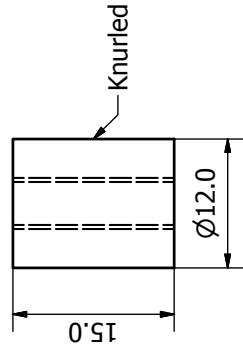
Fiber Positioner K
1.4301 (1:1)



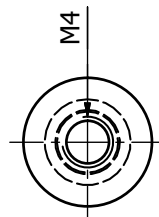
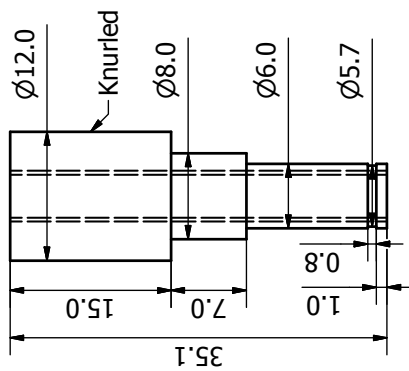
Fiber Positioner Lc
1.4301 (2:1) 3 pieces



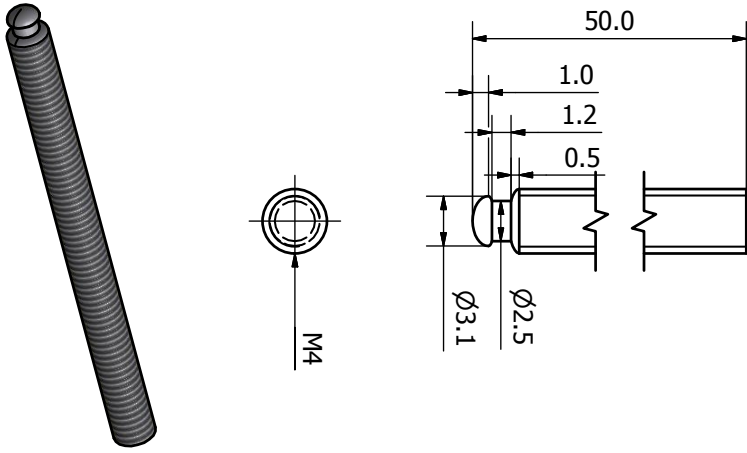
Fiber Positioner Lb
1.4301 (2:1) 3 pieces



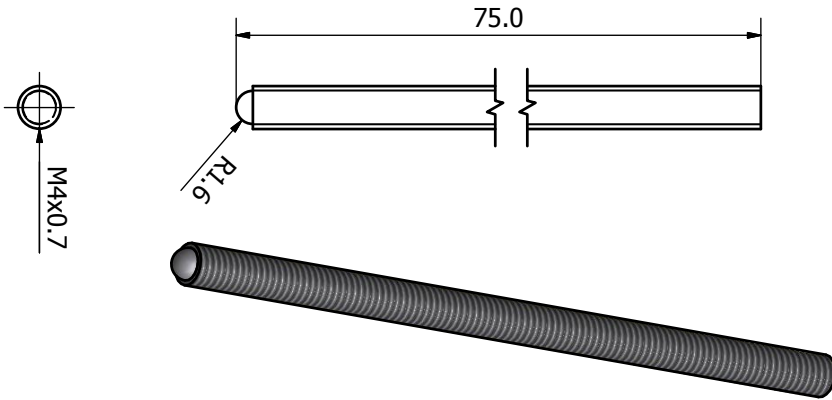
Fiber Positioner La
1.4301 (2:1)



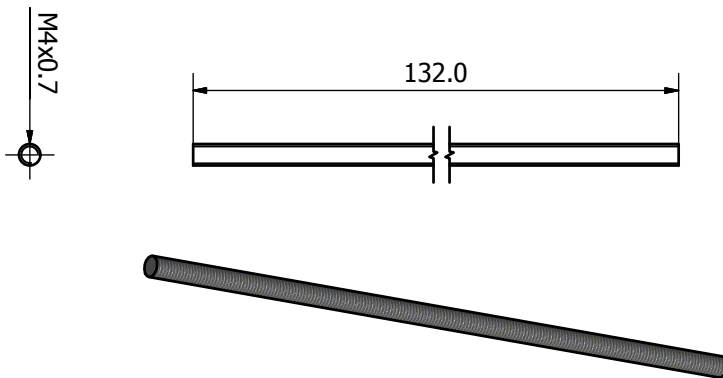
Fiber Positioner Ld
1.4301 (2:1) 3 pieces

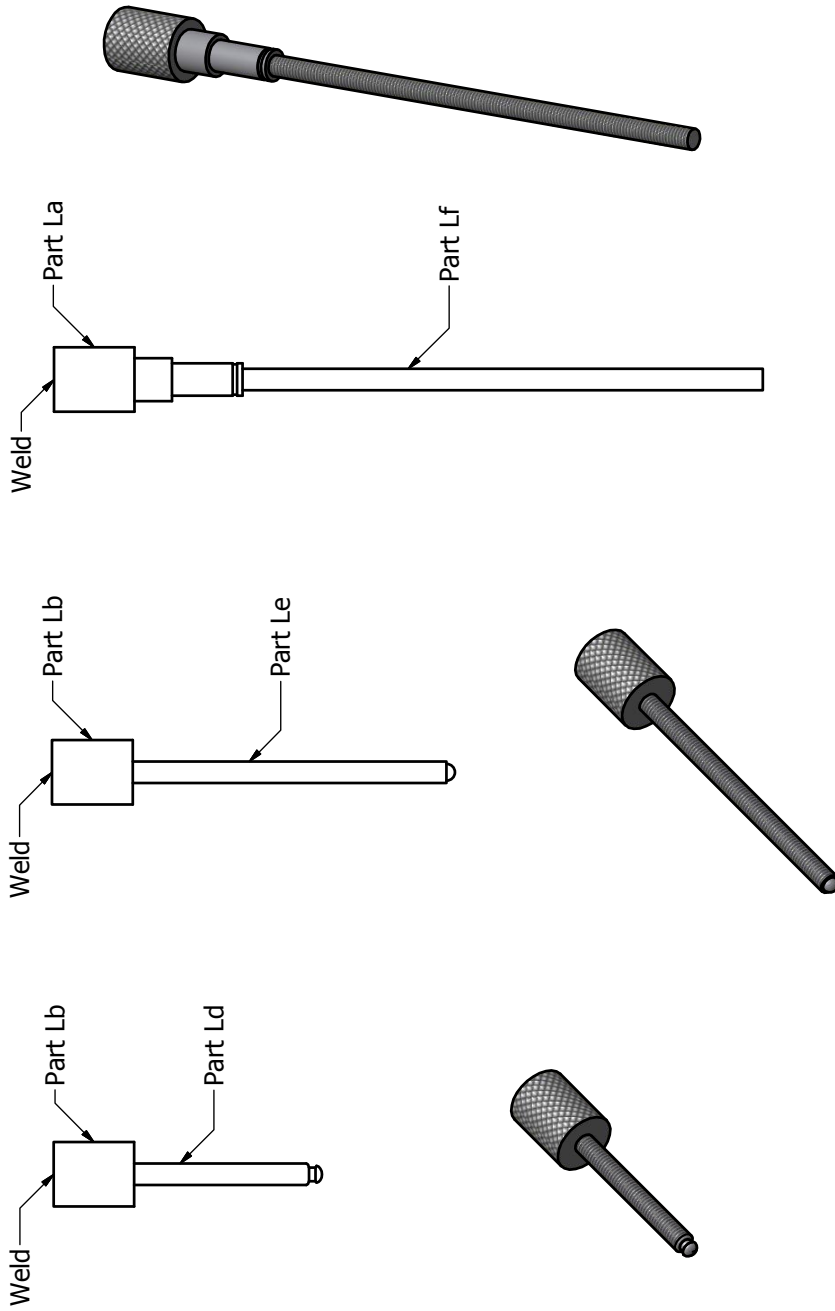


Fiber Positioner Le
1.4301 (2:1) 2 pieces

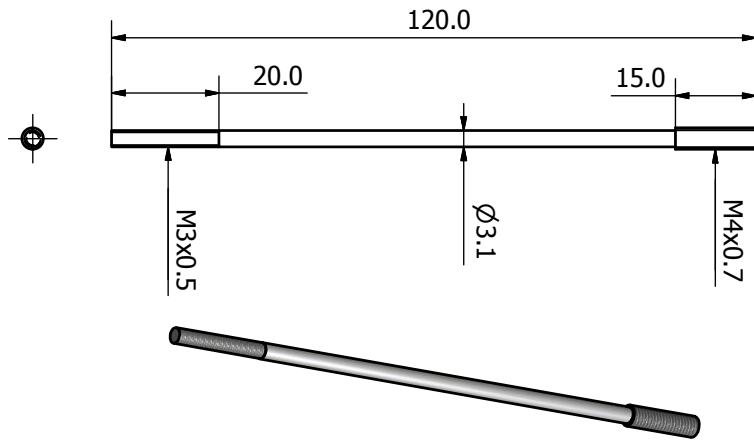


Fiber Positioner Lf
1.4301 (1:1)

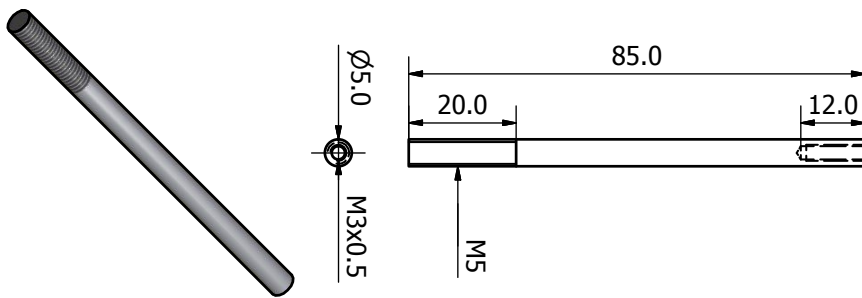




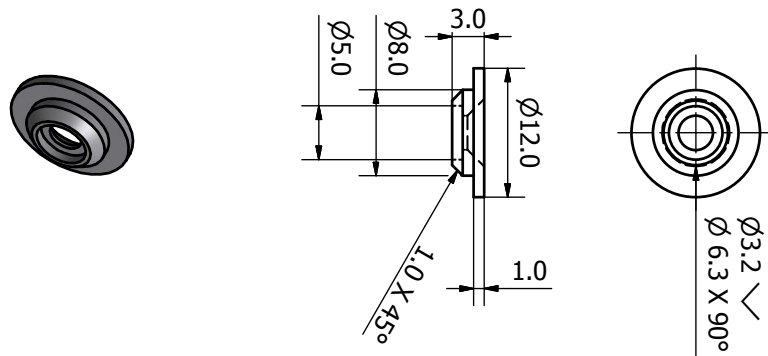
Fiber Positioner Lg
1.4301 (1:1) 2 pieces

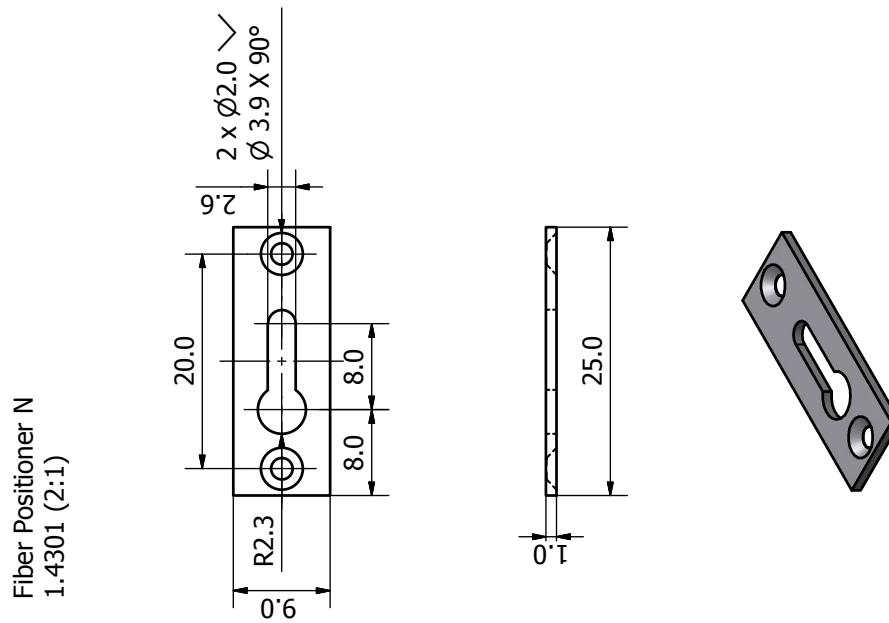
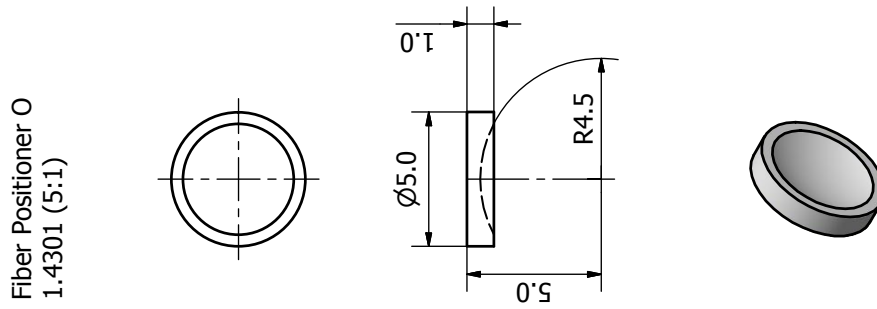
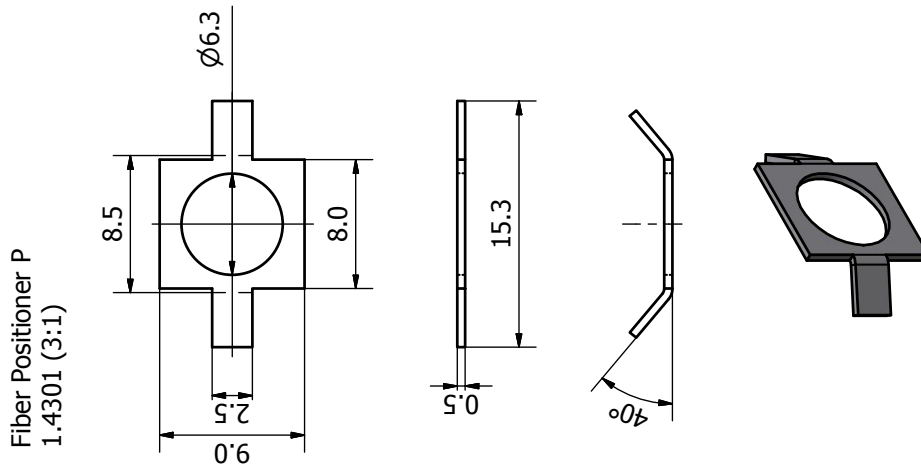


Fiber Positioner Ma
1.4301 (1:1) 4 pieces

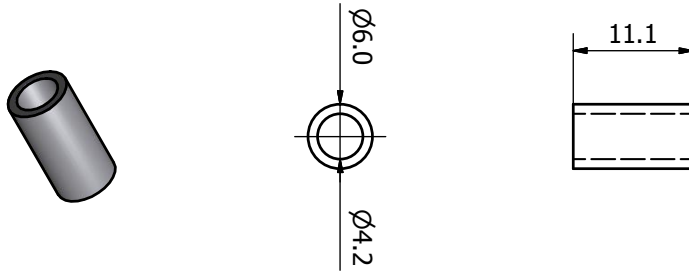


Fiber Positioner Mb
1.4301 (2:1) 4 pieces

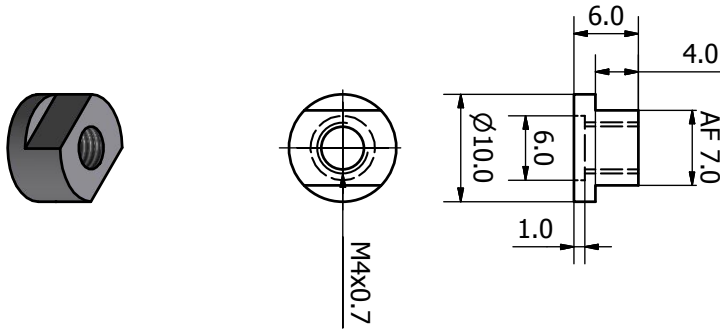




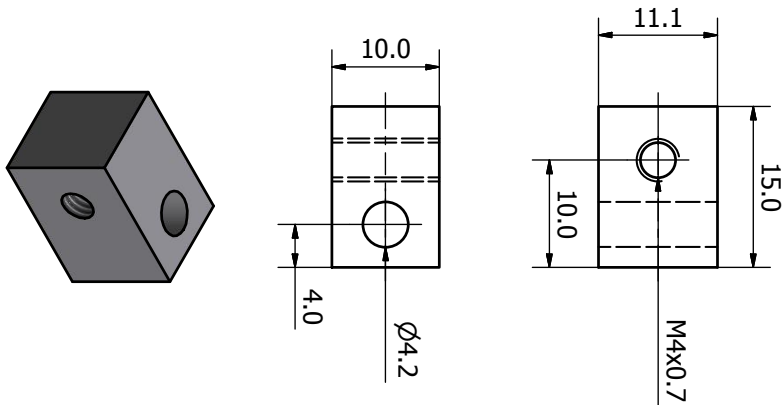
Fiber Positioner Ra
1.4301 (2:1) 2 pieces

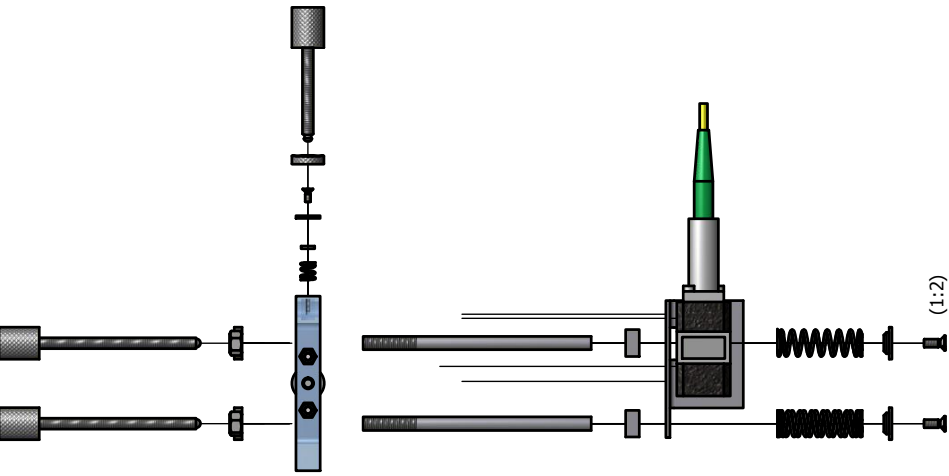


Fiber Positioner Rb
1.4301 (2:1)

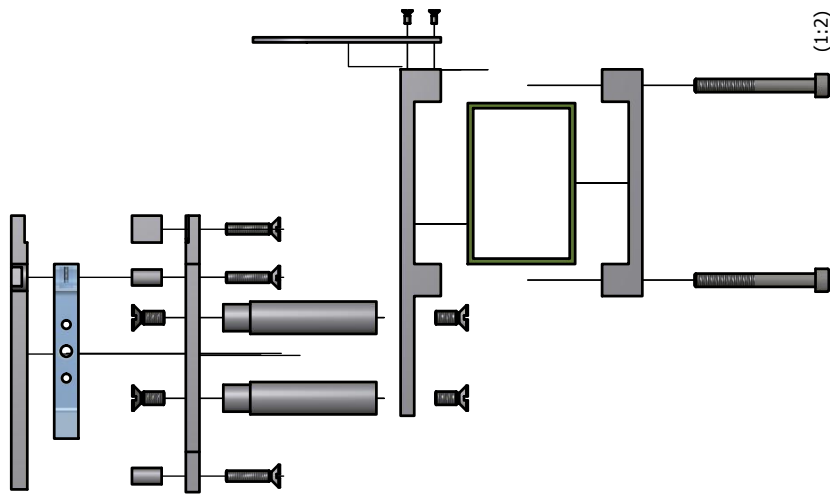


Fiber Positioner Rc
1.4301 (2:1)

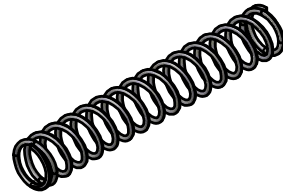




Fiber Positioner Sa
Spring (2:1)
ØWire 0.8
ØInner 4.0
Pitch 2.0mm
Coils 5



Fiber Positioner Sb
Spring (1:1) 4 pieces
ØWire 1.0
ØInner 8.0
Pitch 4.0mm
Coils 20



B.3 Load Lock

Details about the extensions to the load lock chamber are discussed in Section 2.6. The following pages contain the technical drawings of the parts used in the load lock assembly:

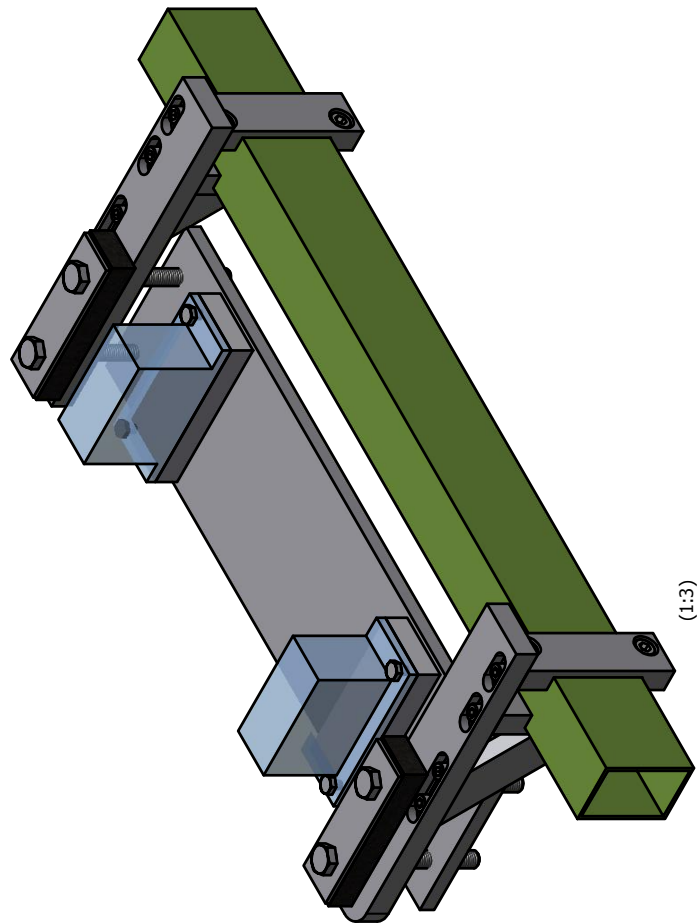
Mount for Load Lock Assembly to support on the turbo molecular pump supporting the load lock (Appendix B.3.1).

Load Lock Housing Structural parts of the load lock (Appendix B.3.2).

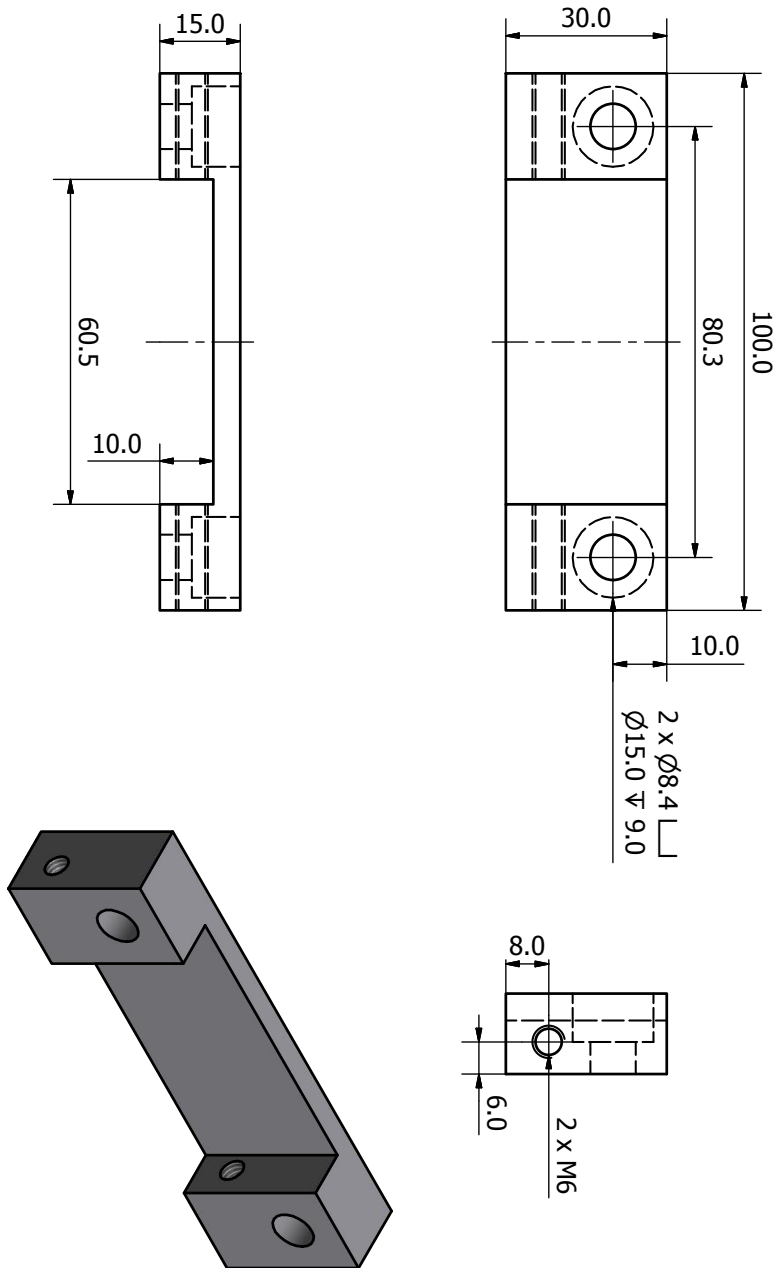
Sample Storage Assembly to store samples (Appendix B.3.3).

Transfer Rod Support Utility to support transfer rods (Appendix B.3.4).

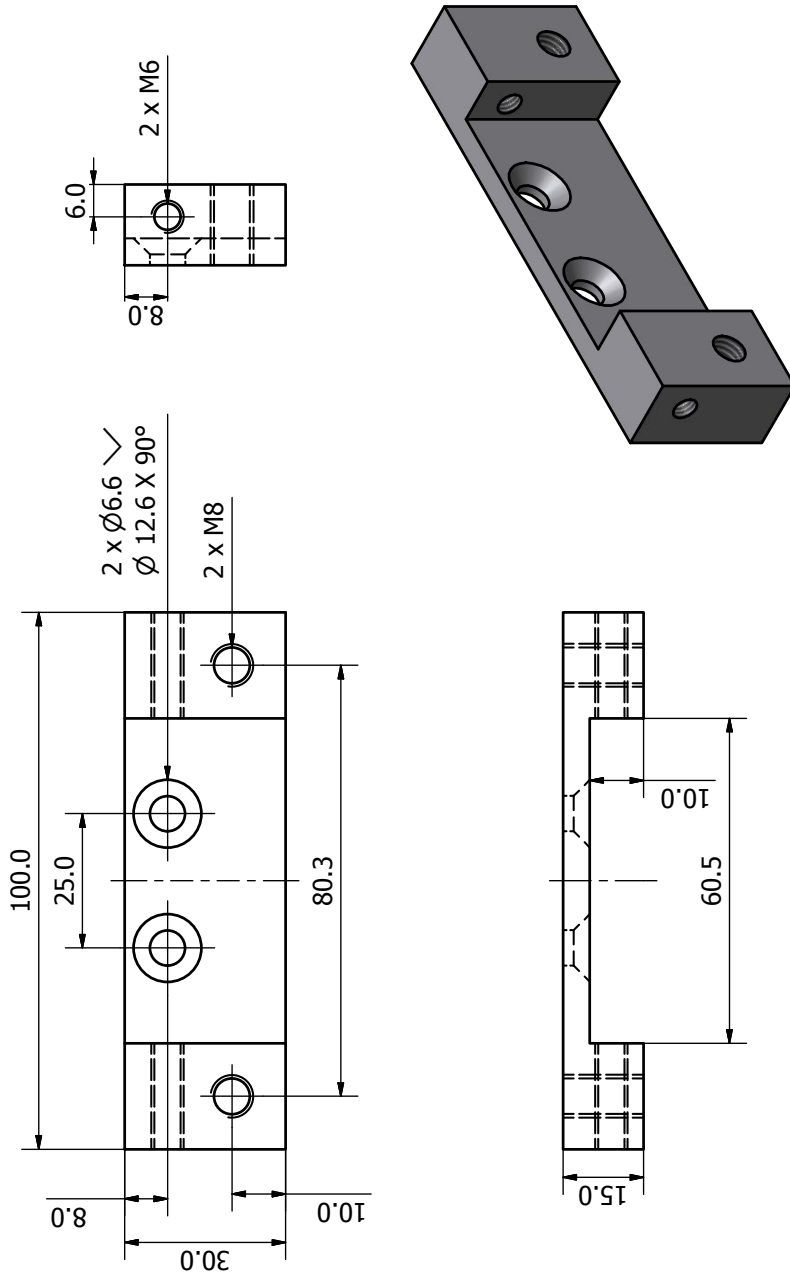
B.3.1 Mount for Load Lock



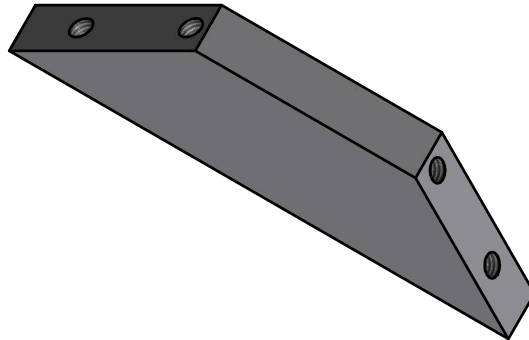
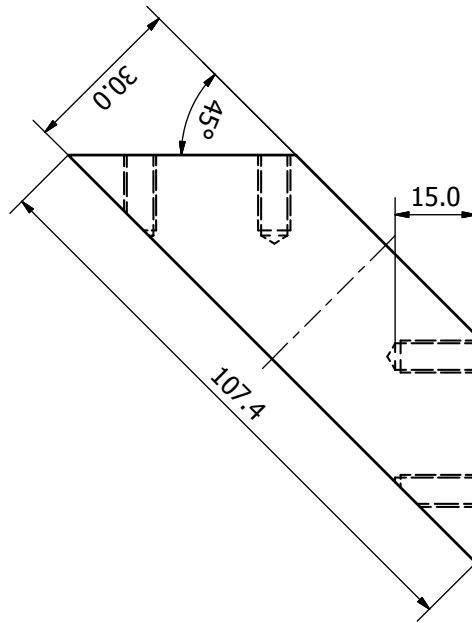
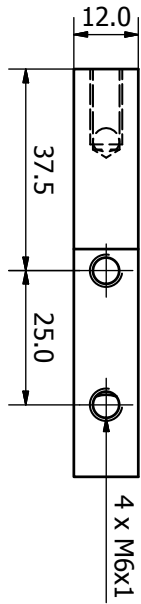
Mount Loadlock Pump A
1.4301 (1:1) 2 pieces



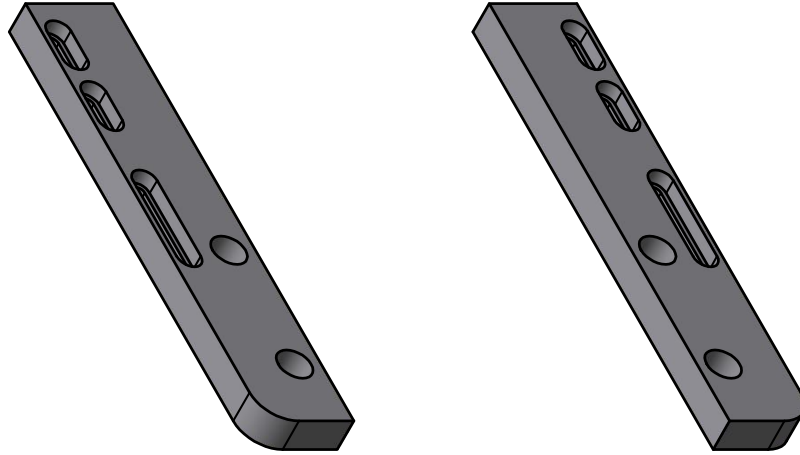
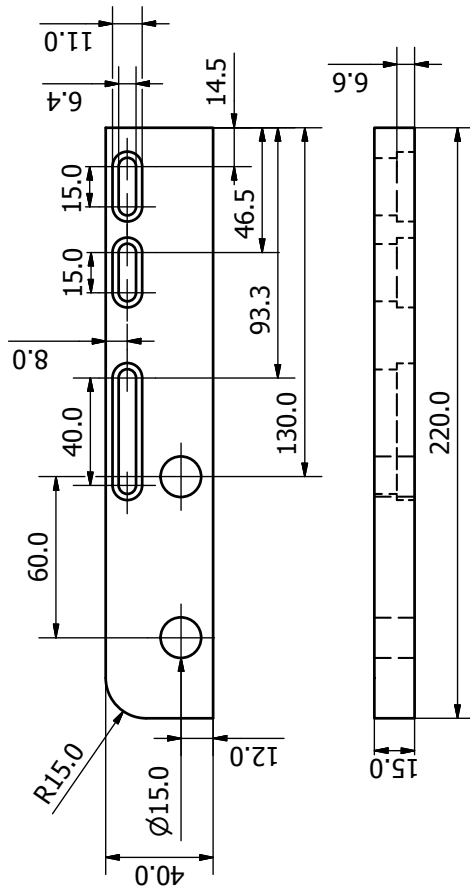
Mount Loadlock Pump B
1.4301 (1:1) 2 pieces



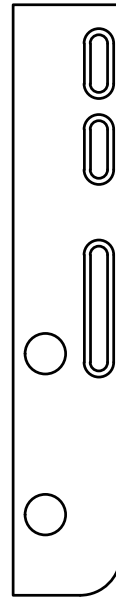
Mount Loadlock Pump C
1.4301 (1:1) 2 pieces

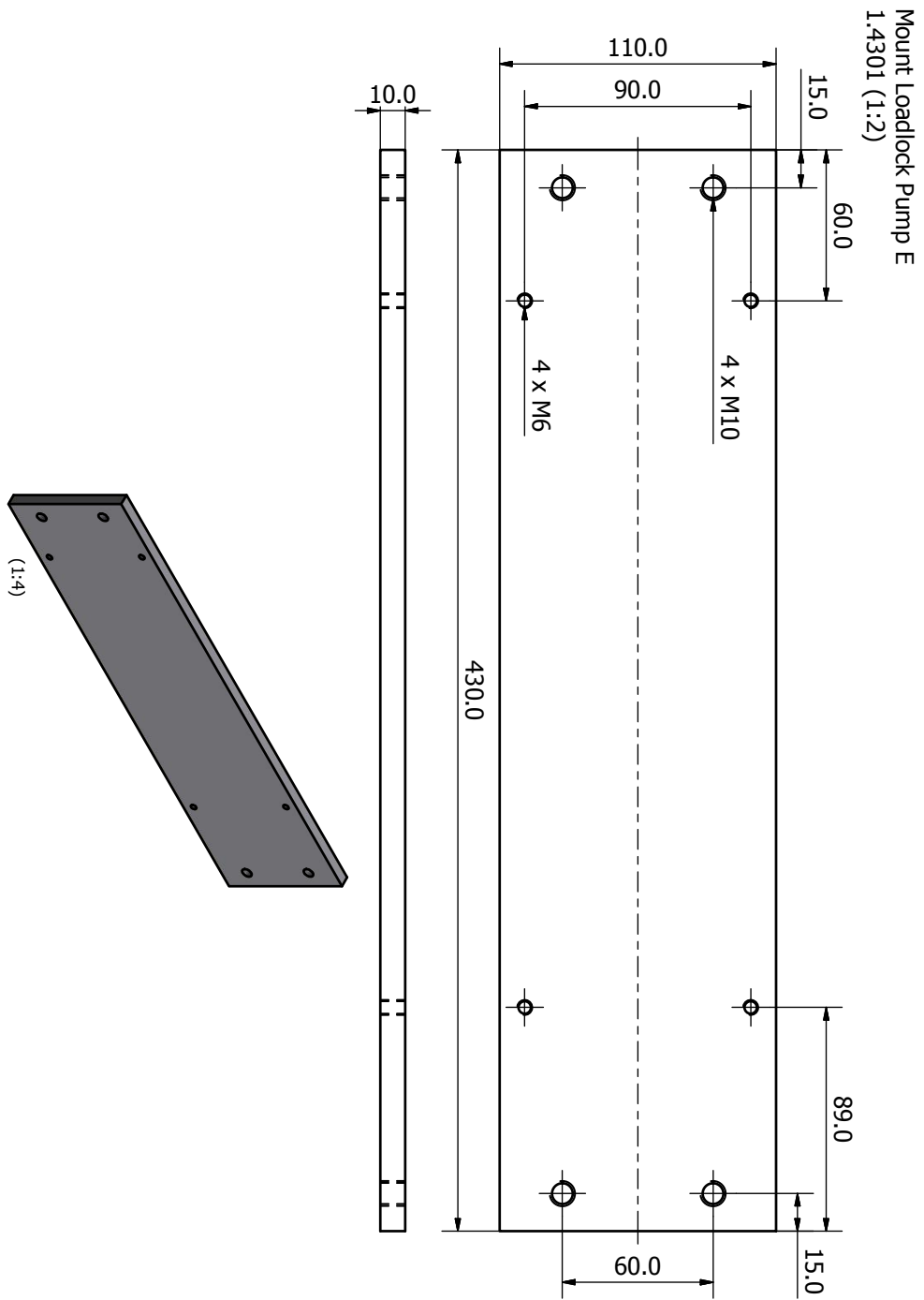


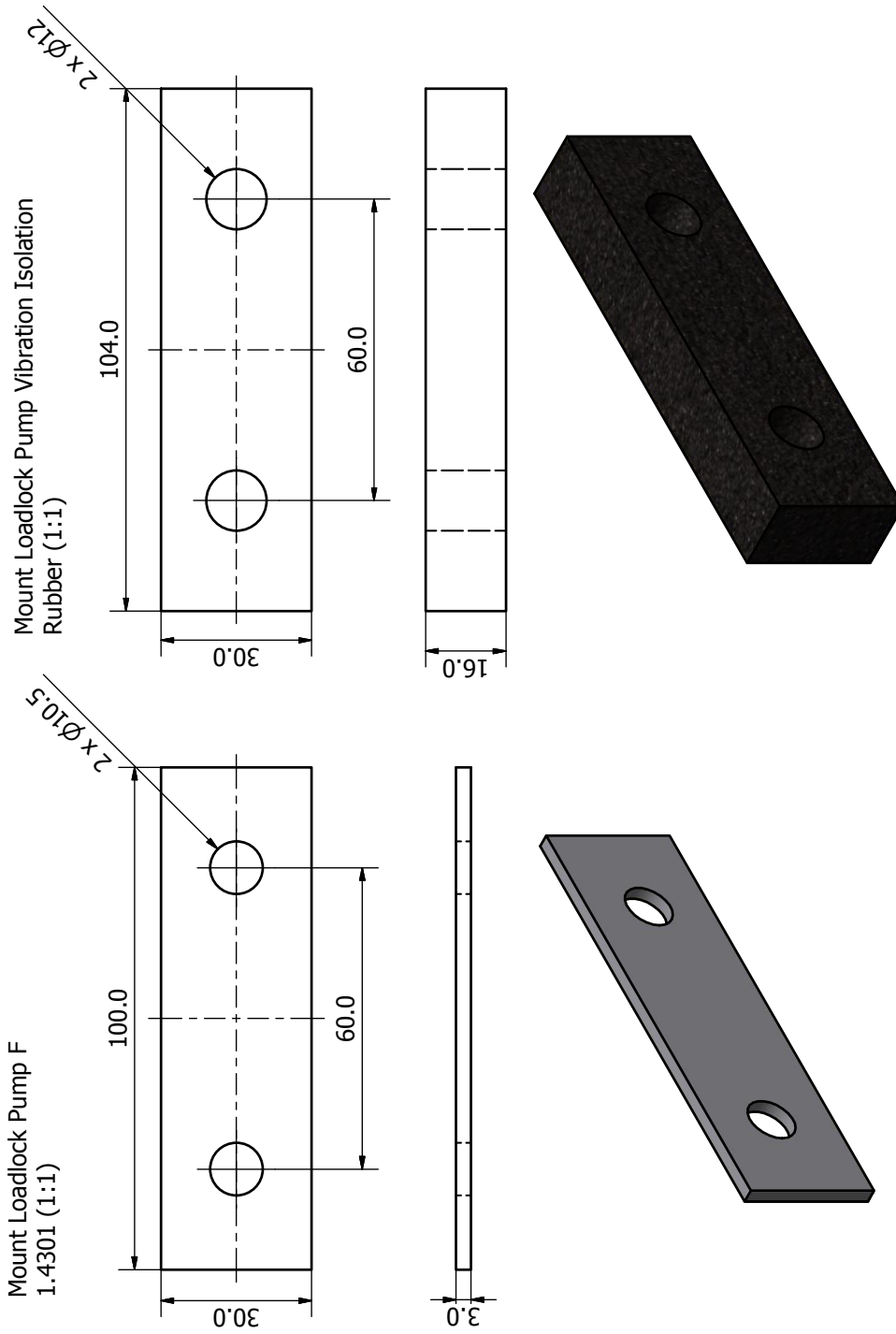
Mount Loadlock Pump DL
1.4301 (1:2)

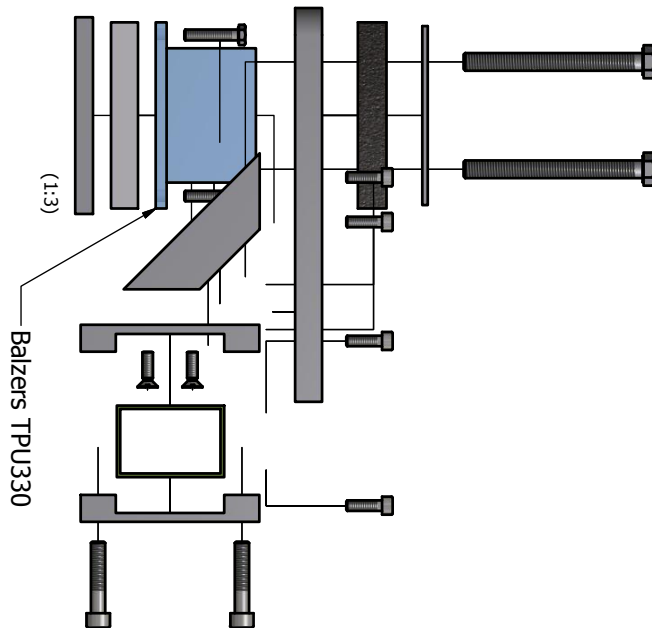
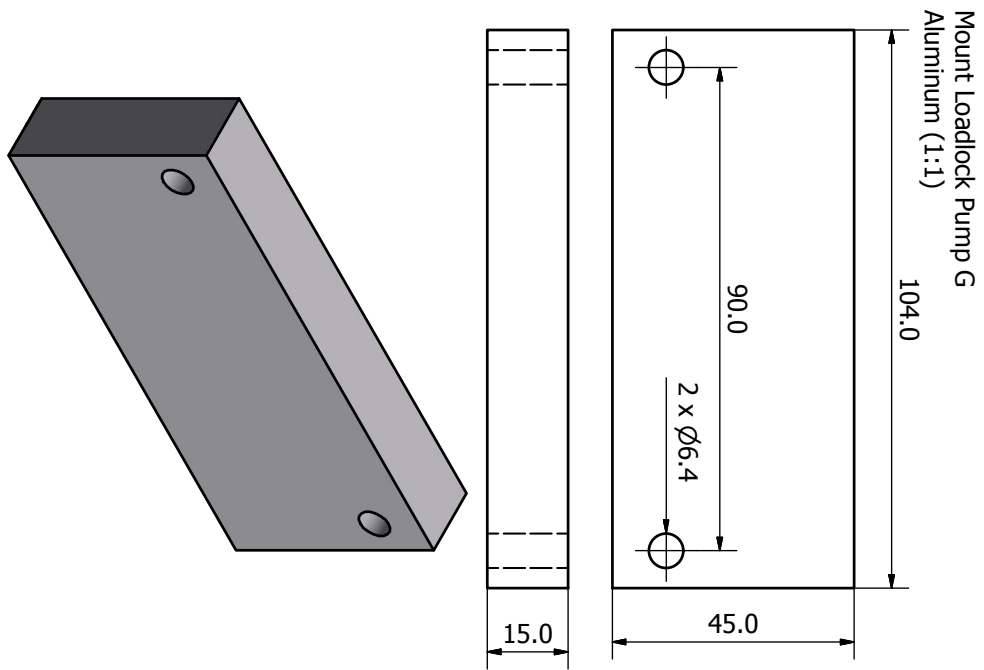


Mount Loadlock Pump DR
1.4301 (1:2) Mirror inverted from DL

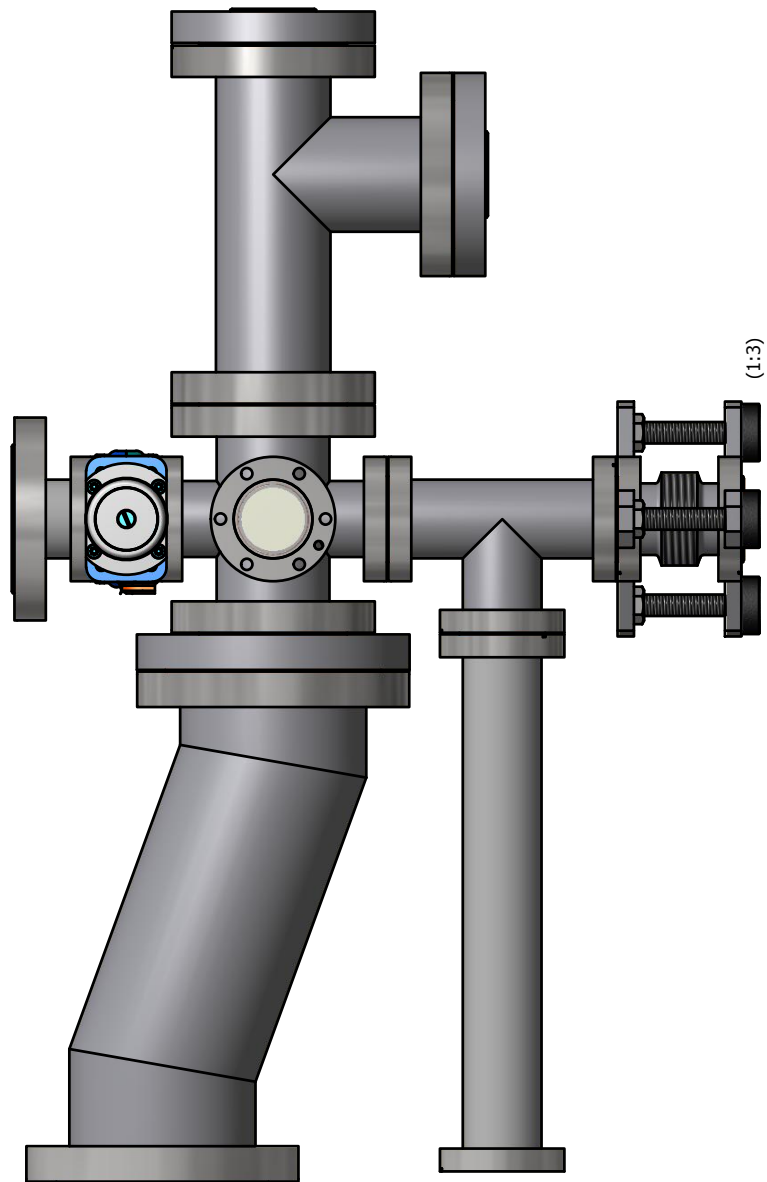


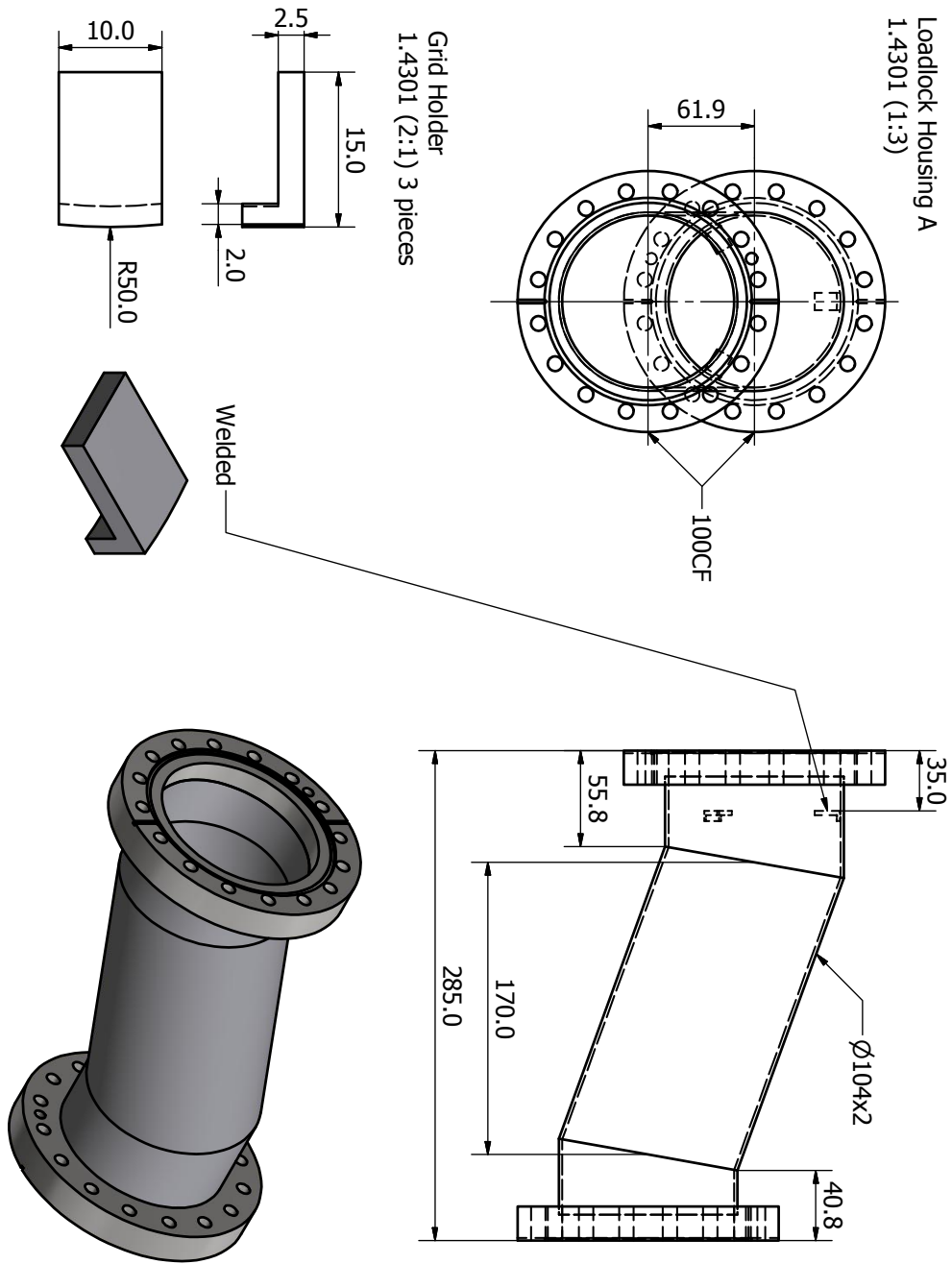


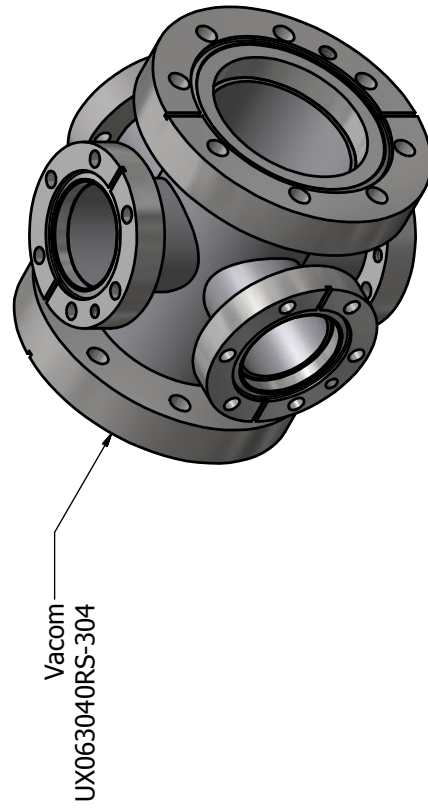
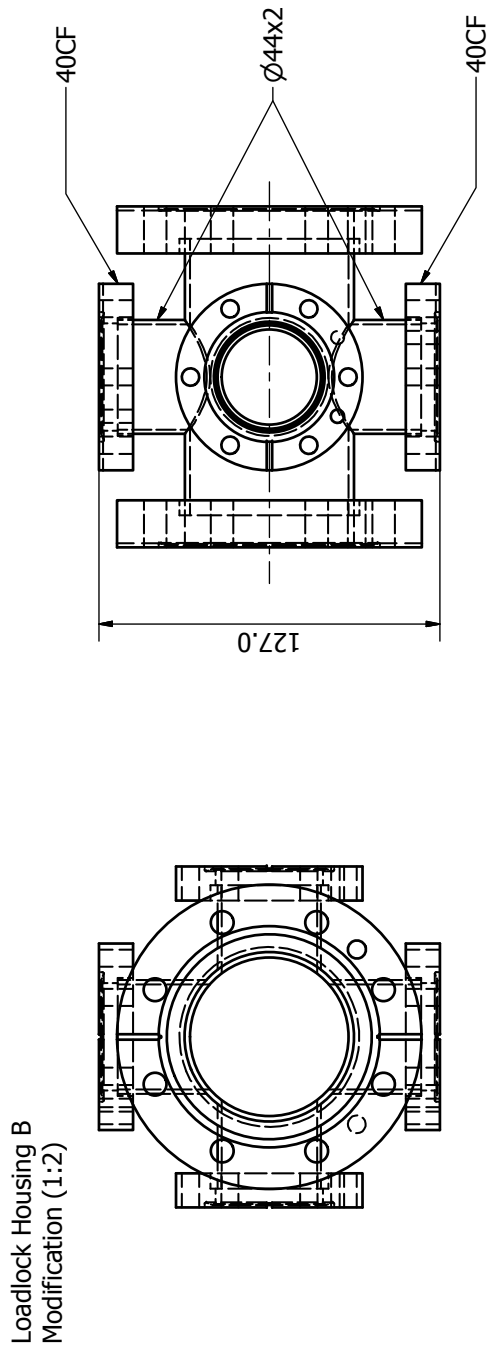


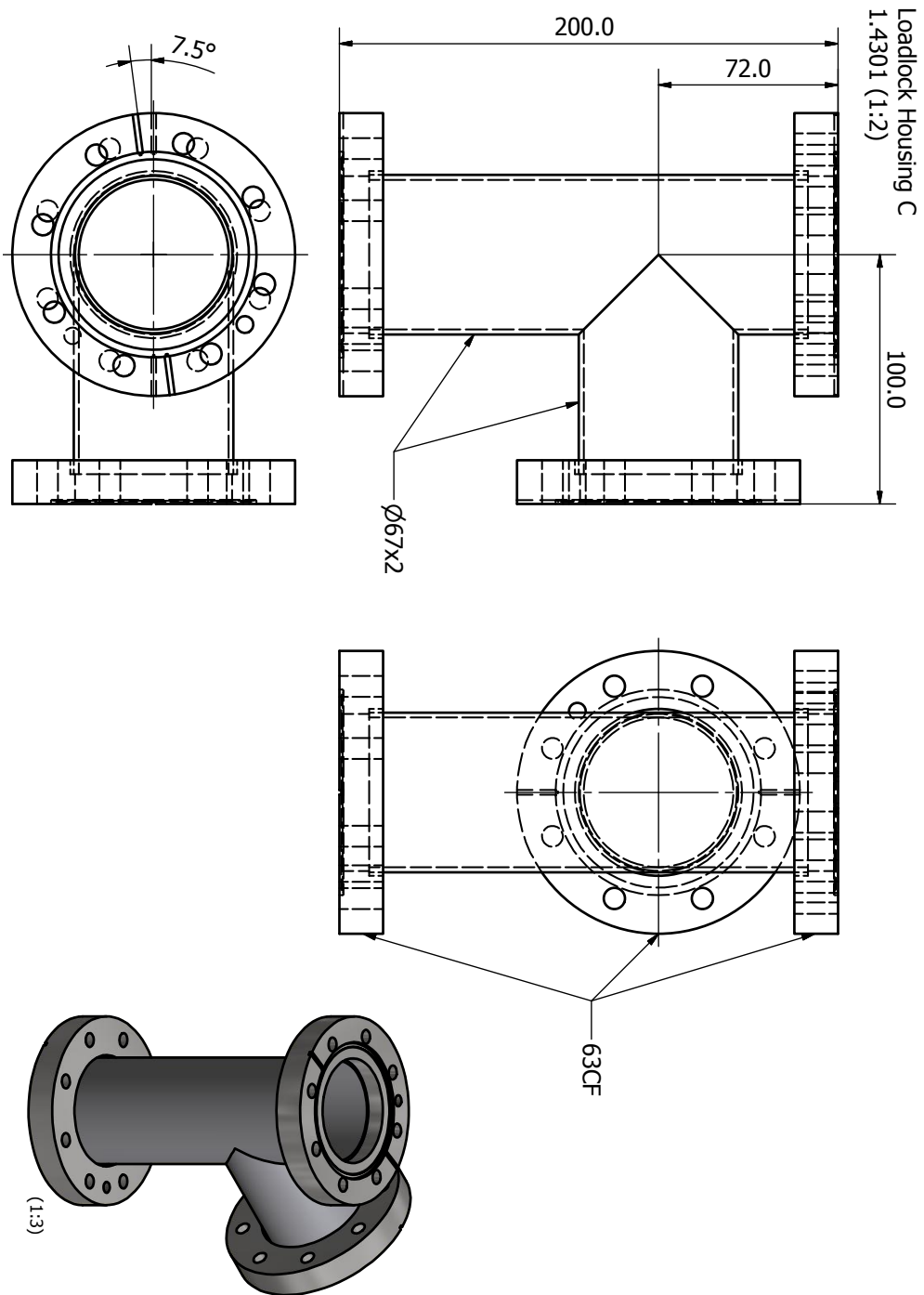


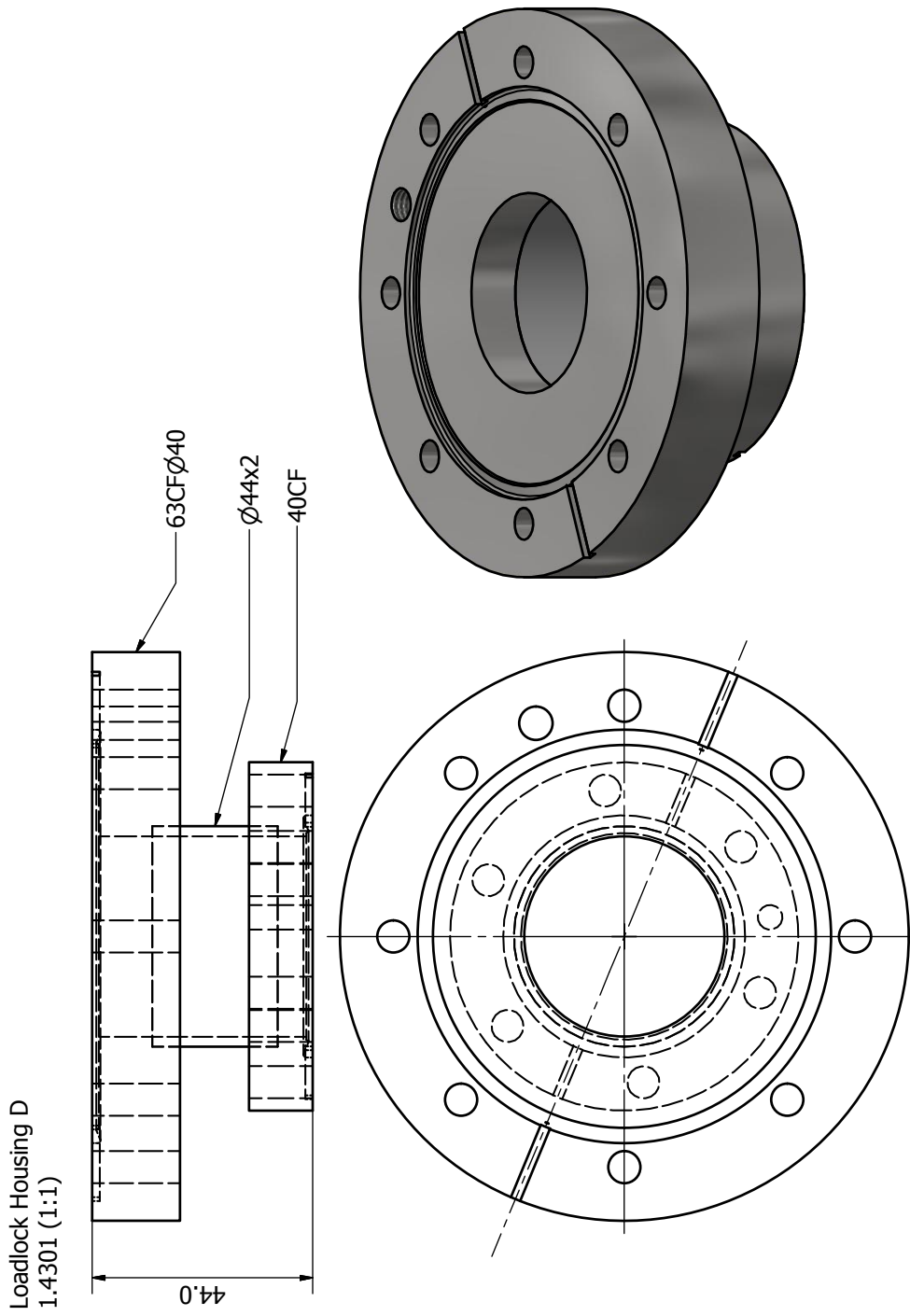
B.3.2 Load Lock Housing



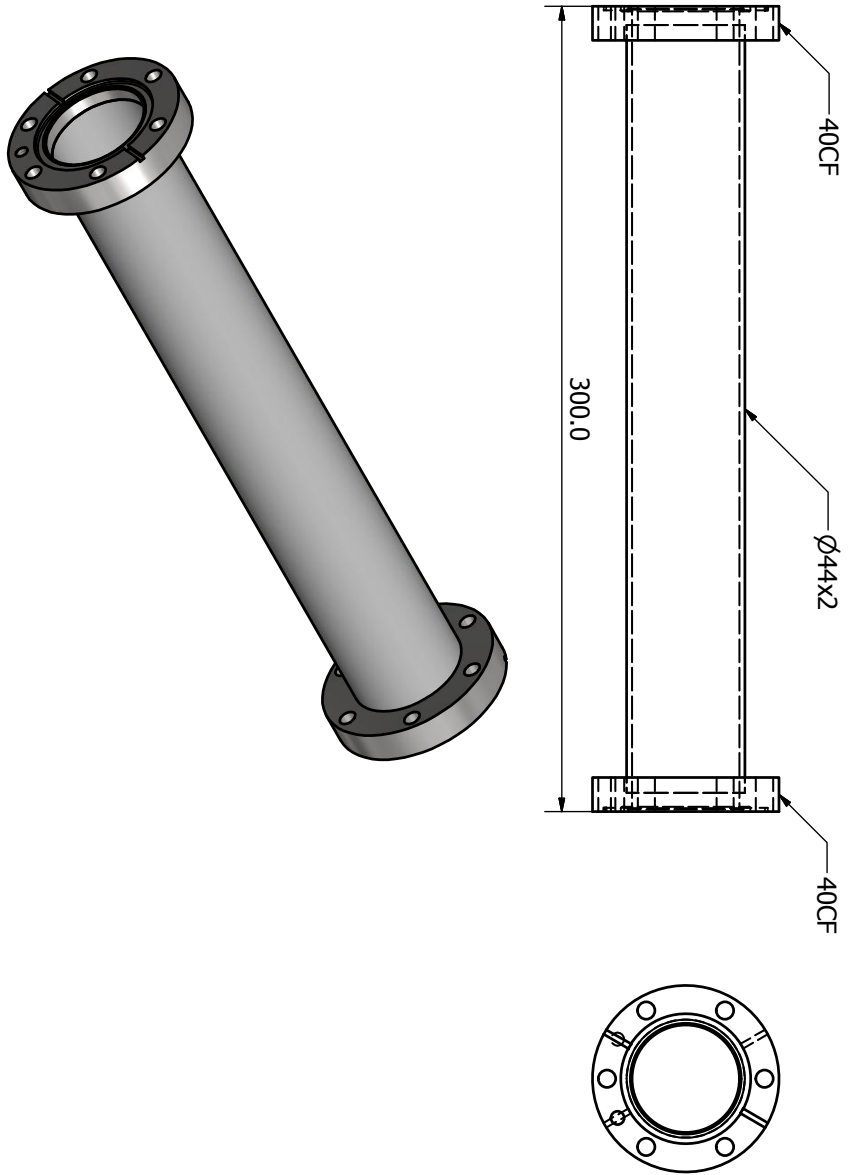




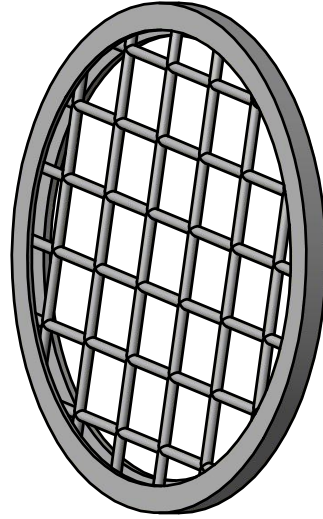
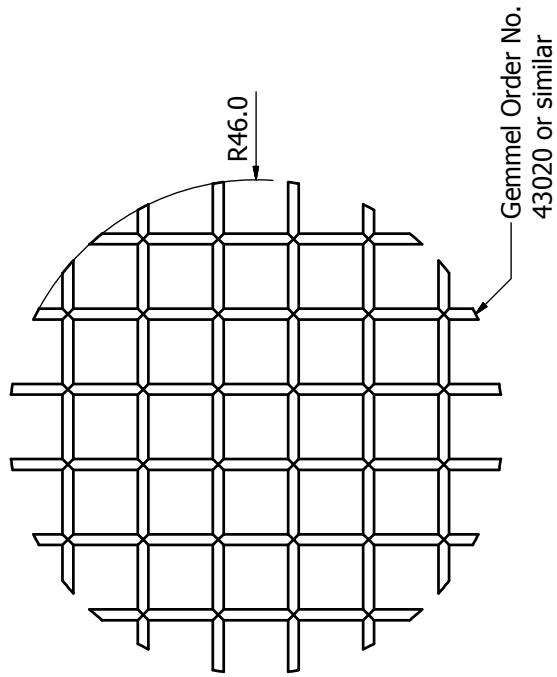




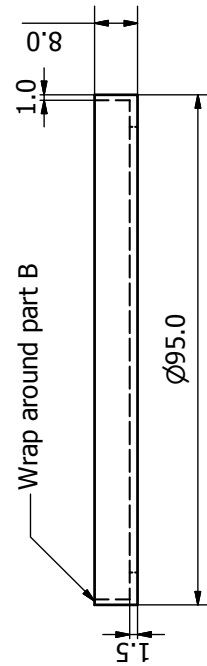
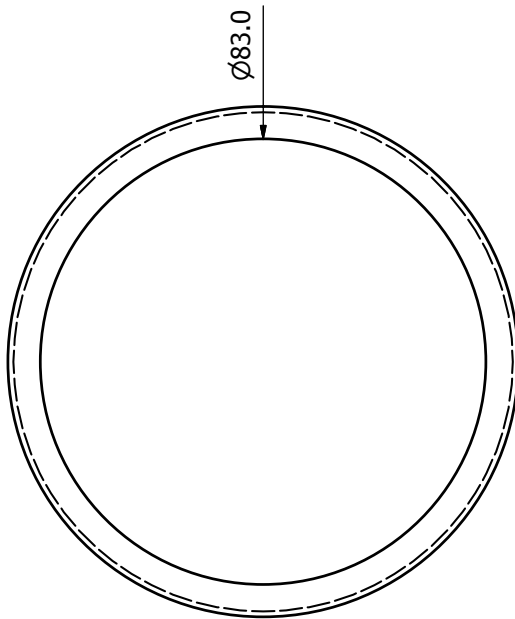
Loadlock Housing E
1.4301 (1:2)



TMP Heavy Duty Safety Grid B
1.4301 (1:1)



TMP Heavy Duty Safety Grid A
1.4301 (1:1)

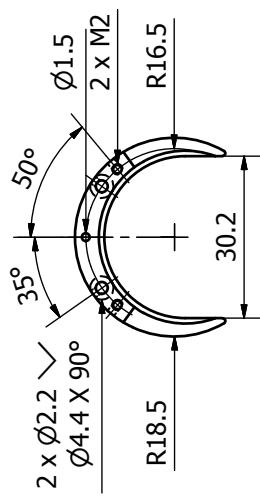


B.3.3 Sample Storage

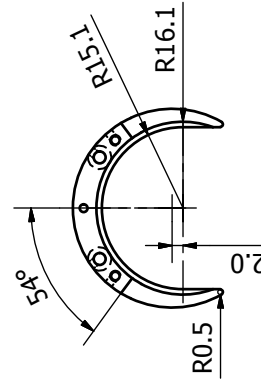
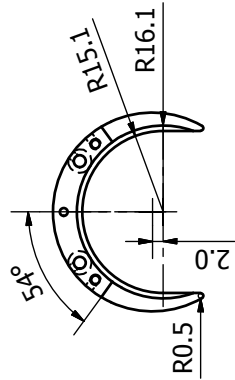
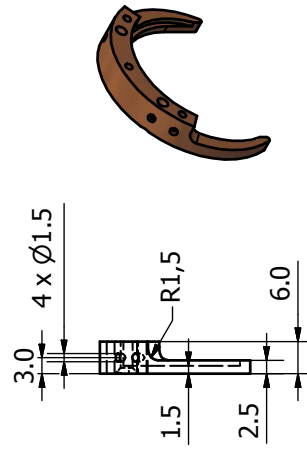
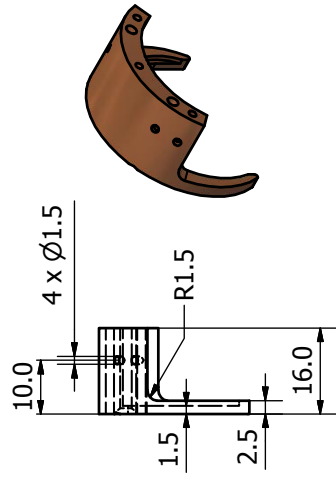
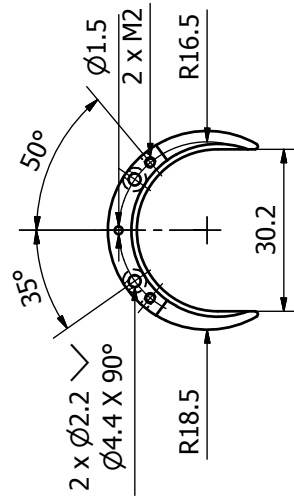


Design by O. LYTKEN.

Sample Storage A
CuBe2 (1:1) 4 pieces

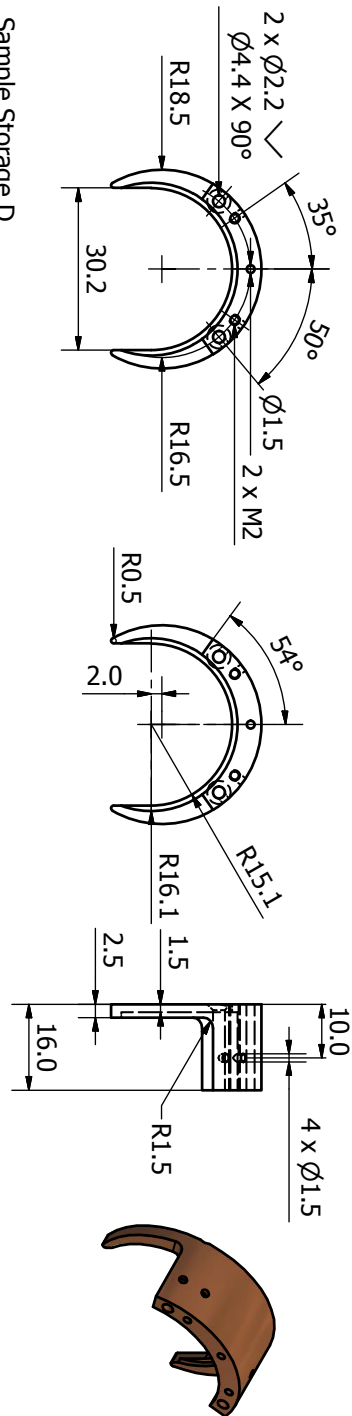


Sample Storage B
CuBe2 (1:1)

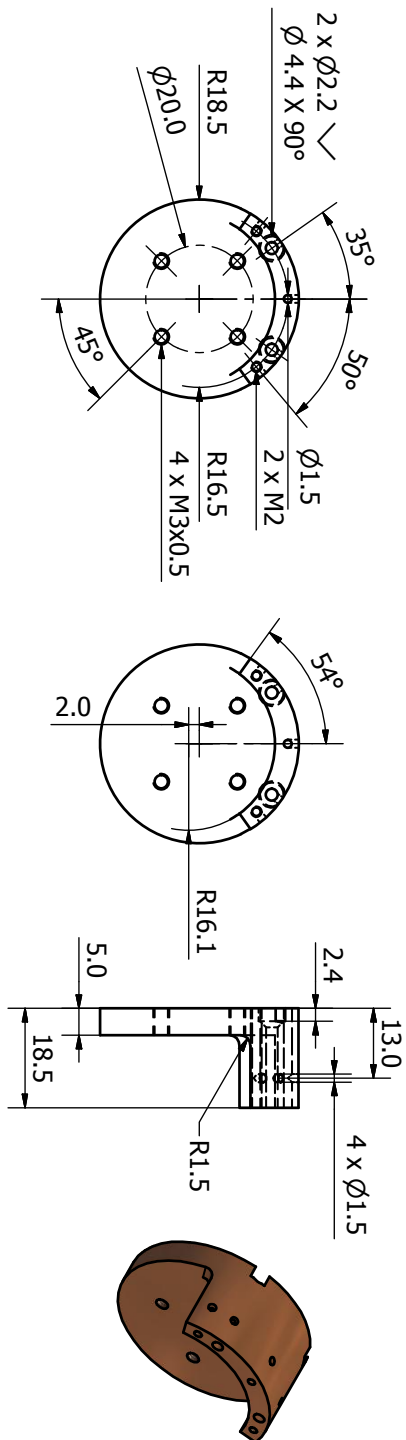


Design by O. LYTKEN.

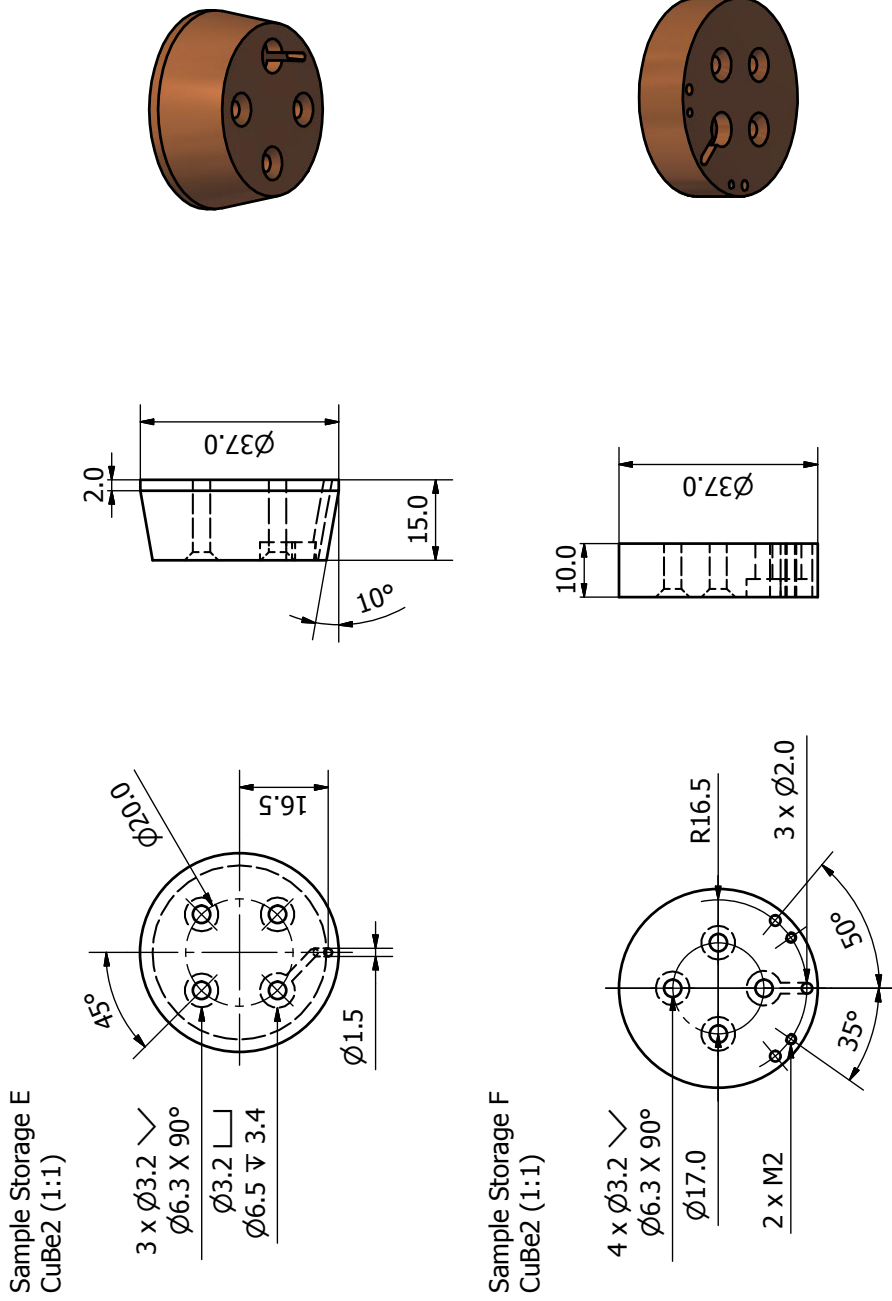
Sample Storage C
CuBe2 (1:1) 5 pieces



Sample Storage D
CuBe2 (1:1) 5 pieces

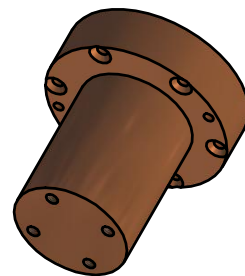
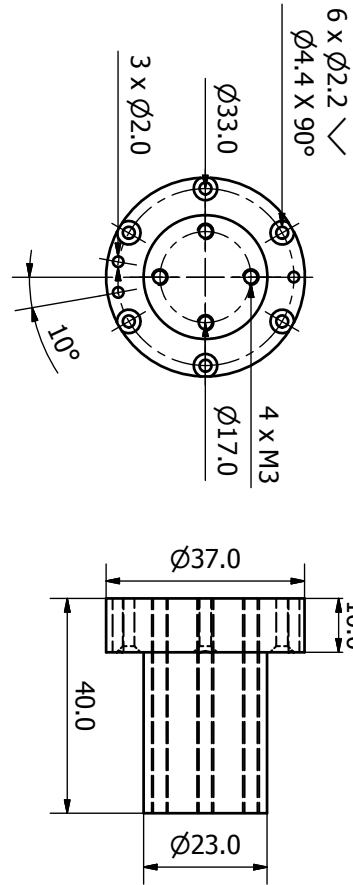


Design by O. LYTKEN.

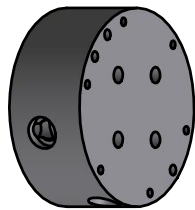
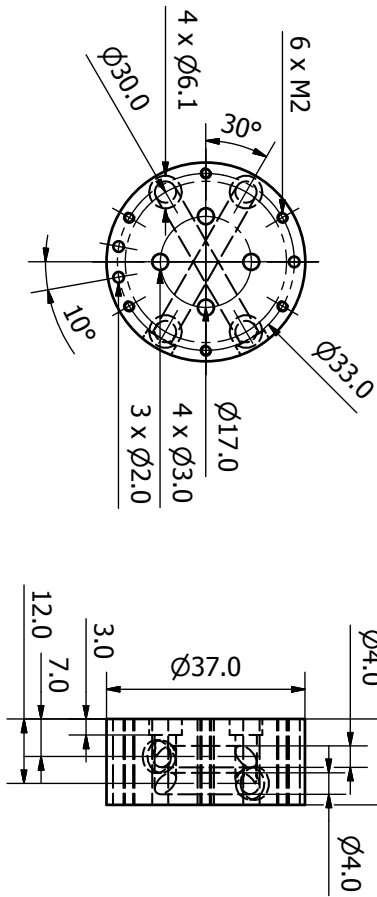


Design by O. LYTKEN.

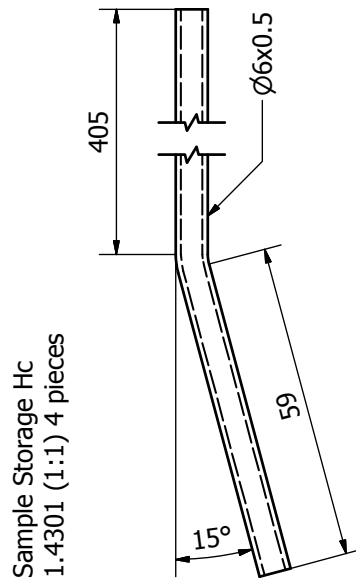
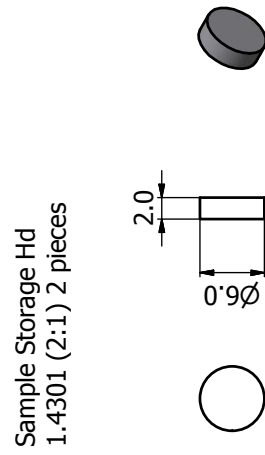
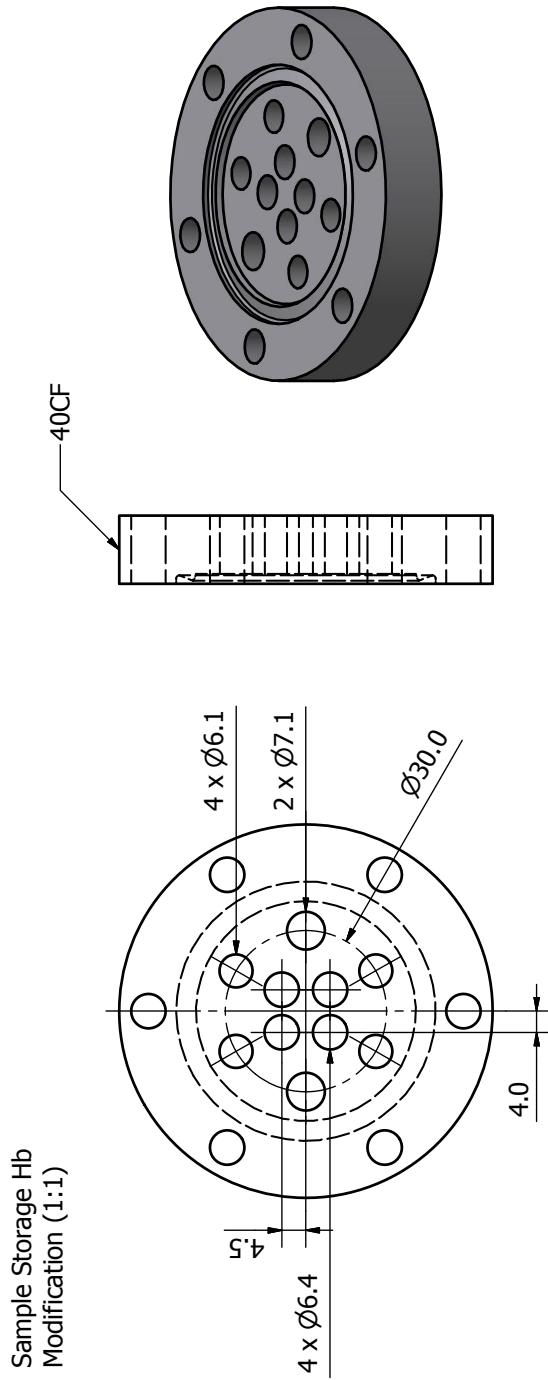
Sample Storage G
CuBe2 (1:1)



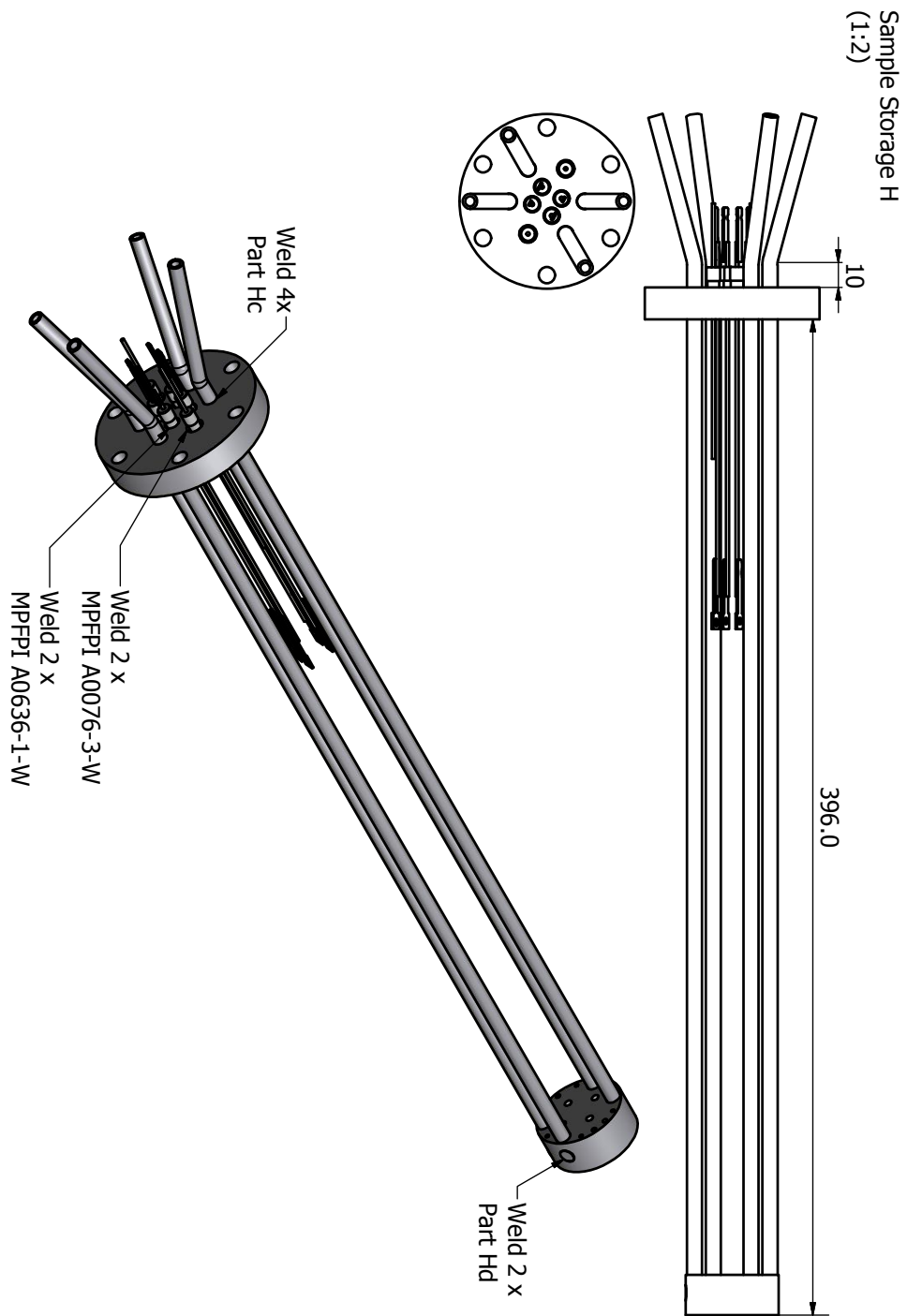
Sample Storage Ha
1.4301 (1:1)



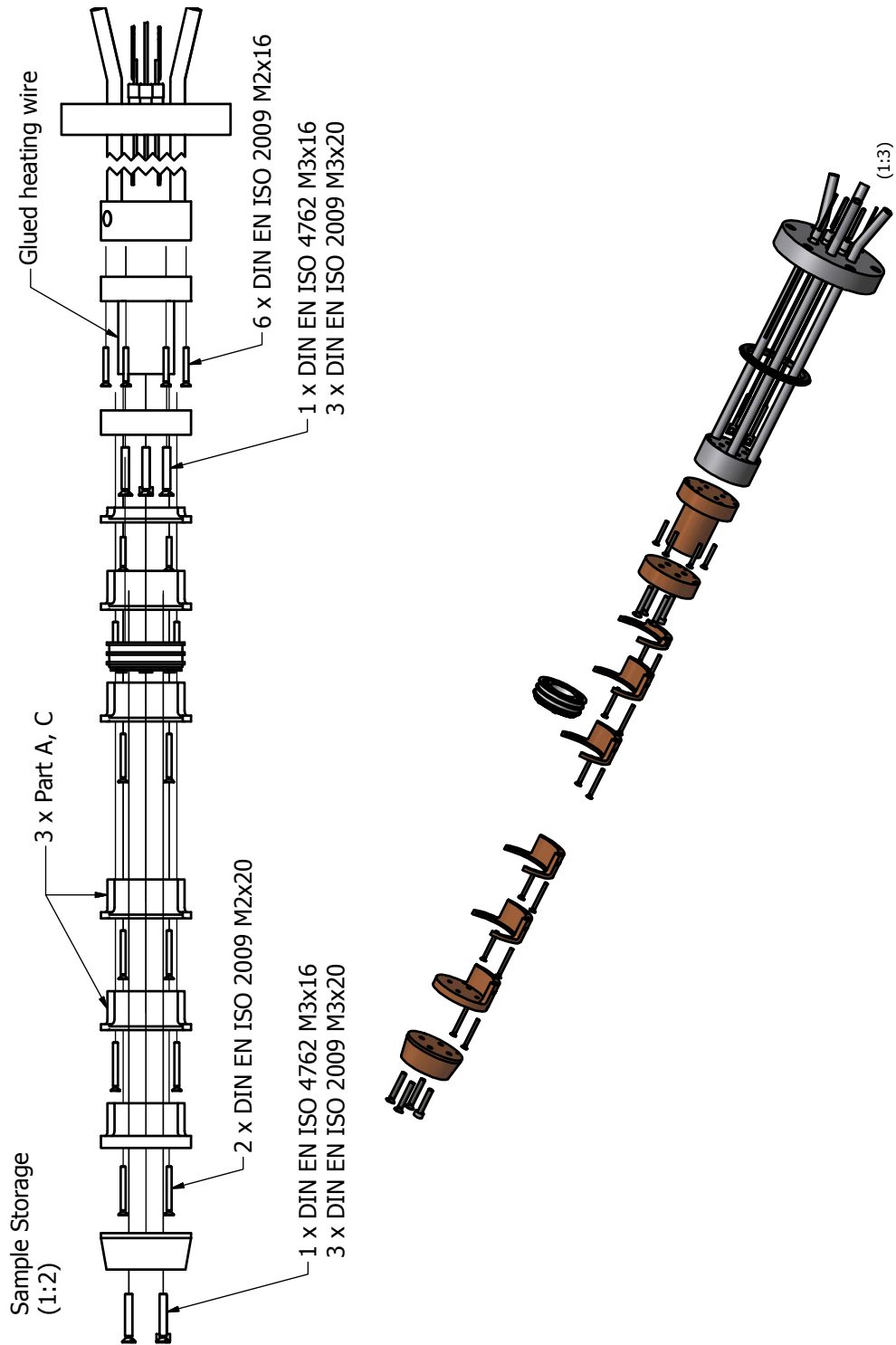
Design by O. LYTKEN.



Design by O. LYTKEN.



Design by O. LYTKEN.

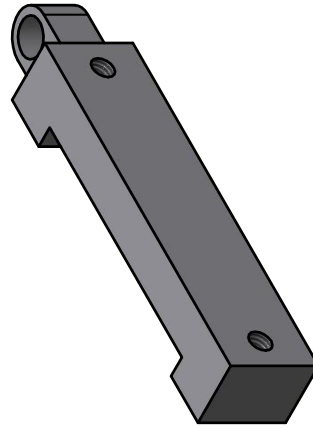
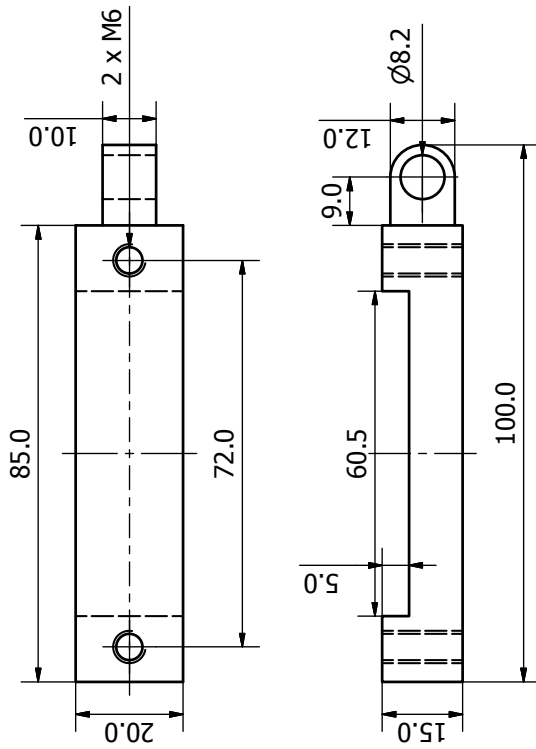


Design by O. LYTKEN.

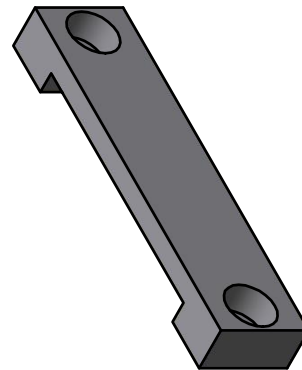
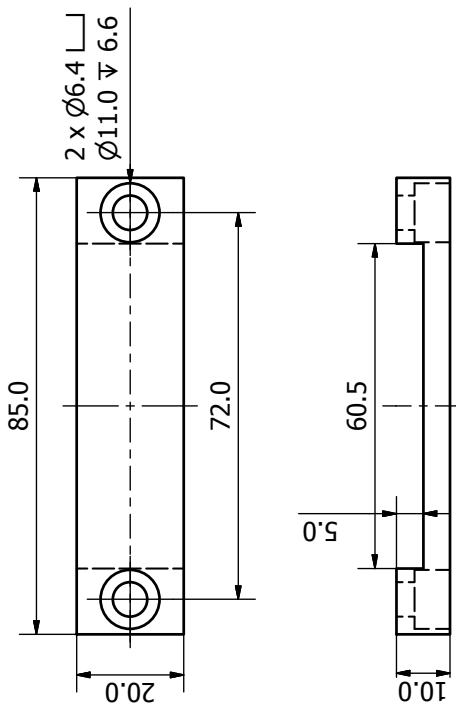
B.3.4 Transfer Rod Support



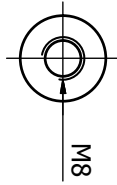
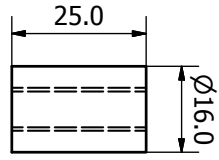
Transfer Rod Support B
1.4301 (1:1) 2 pieces



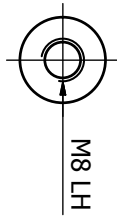
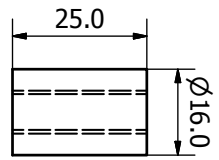
Transfer Rod Support A
1.4301 (1:1) 2 pieces



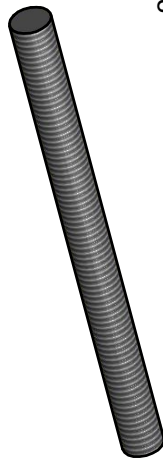
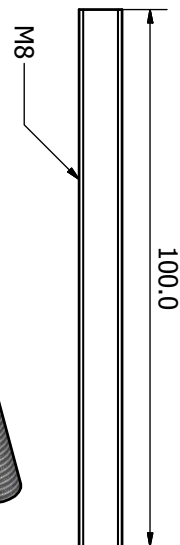
Transfer Rod Support C_R
1.4301 (1:1) 2 pieces



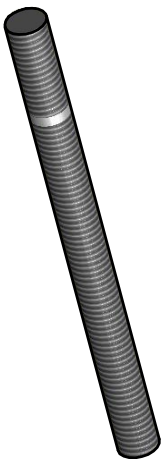
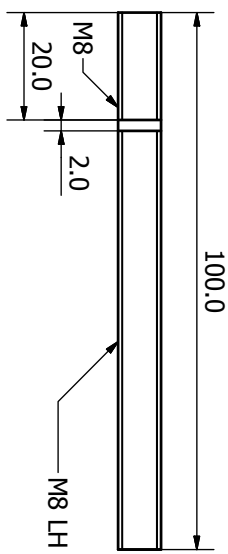
Transfer Rod Support C_L
1.4301 (1:1) 2 pieces

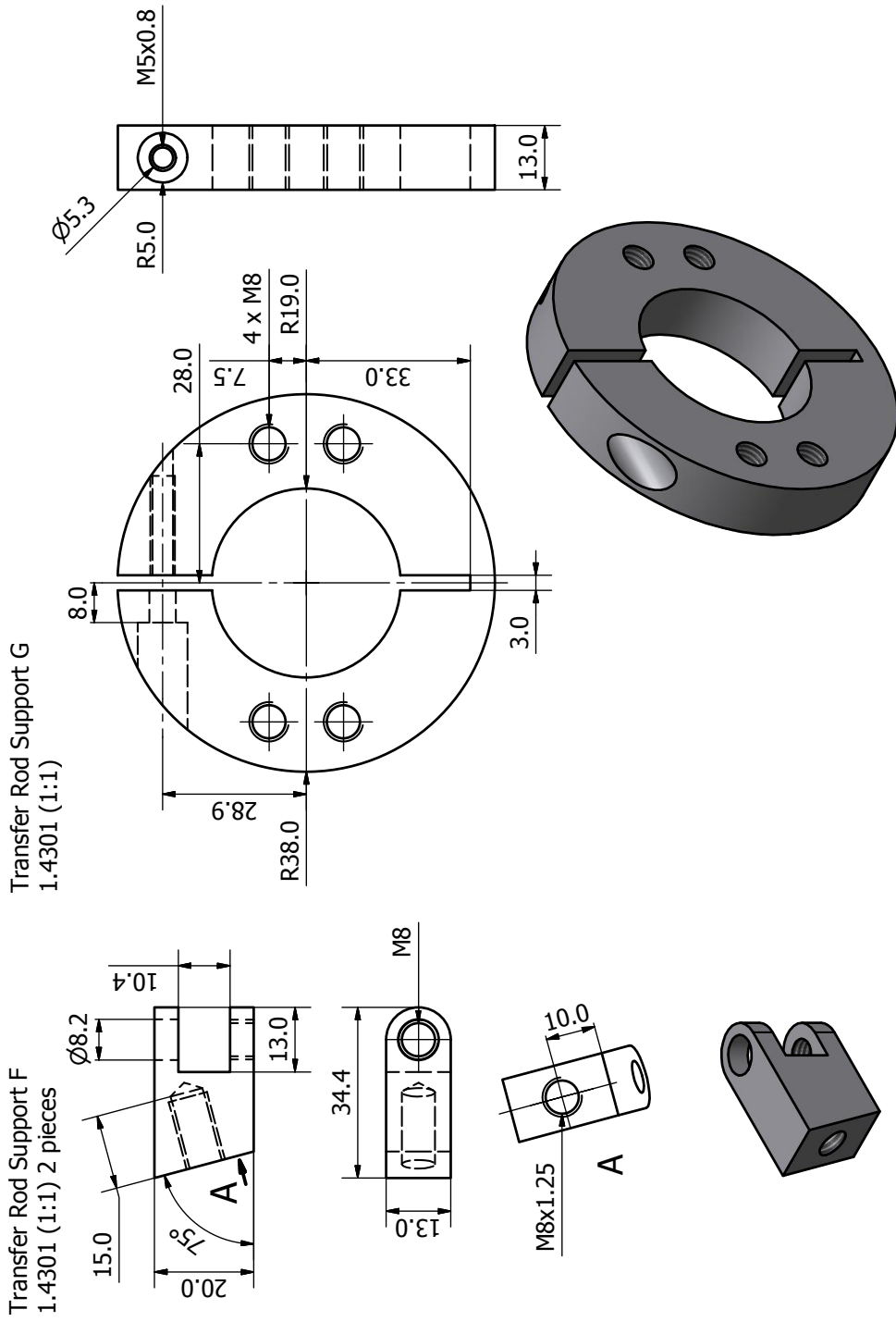


Transfer Rod Support D
1.4301 (1:1) 2 pieces

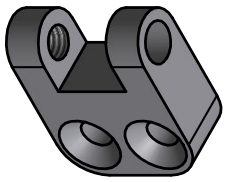
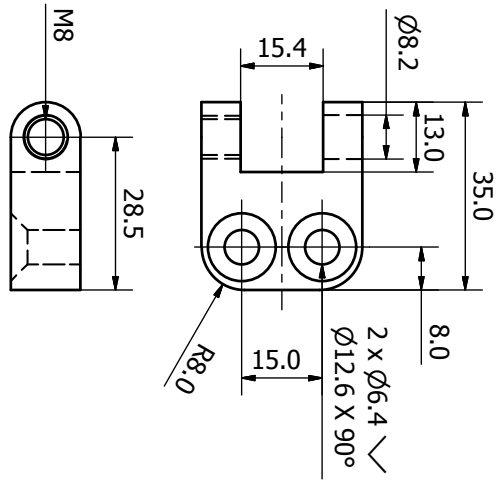


Transfer Rod Support E
1.4301 (1:1) 2 pieces

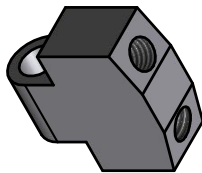
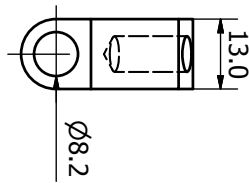
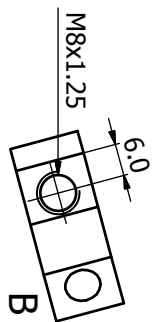
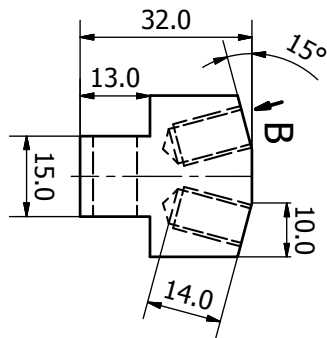




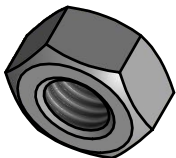
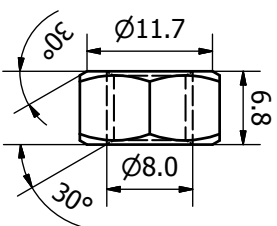
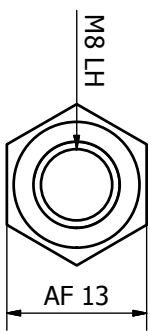
Transfer Rod Support H
1.4301 (1:1)



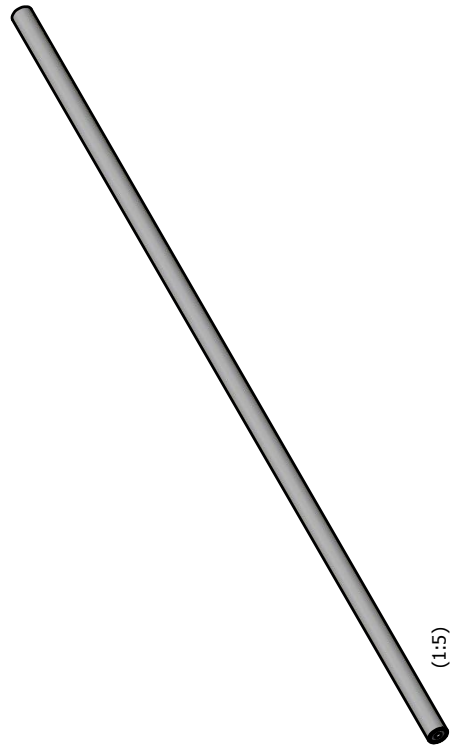
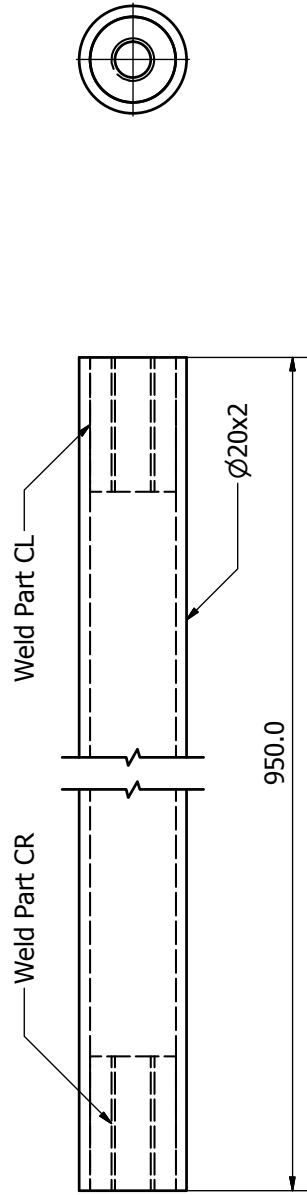
Transfer Rod Support I
1.4301 (1:1)



Transfer Rod Support J
1.4301 (1:1) 2 pieces



Transfer Rod Support K
1.4301 (1:1) 2 pieces



B.4 Miscellaneous

This section contains technical drawing not directly related to the NAC machine.

Glove Box Contains the modifications of a glove box intended to use for refilling the main evaporator with air-sensitive substances (Appendix B.4.1).

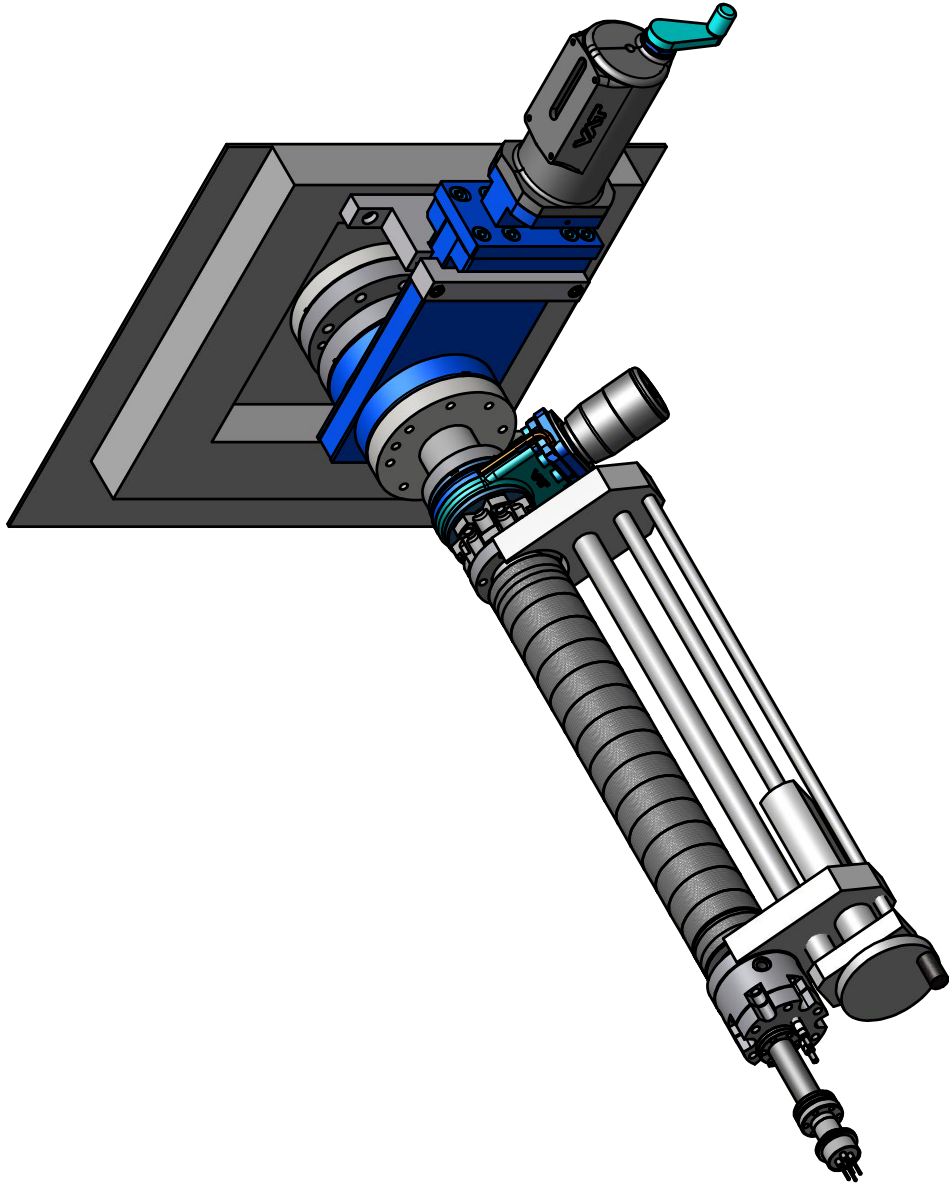
Evaporator for Synchrotron Applications A separable evaporator for up to three substances in standard or low effusion crucibles (Appendix B.4.2).

Mounting Stand A tool to hold CF components in place during repairs (Appendix B.4.3).

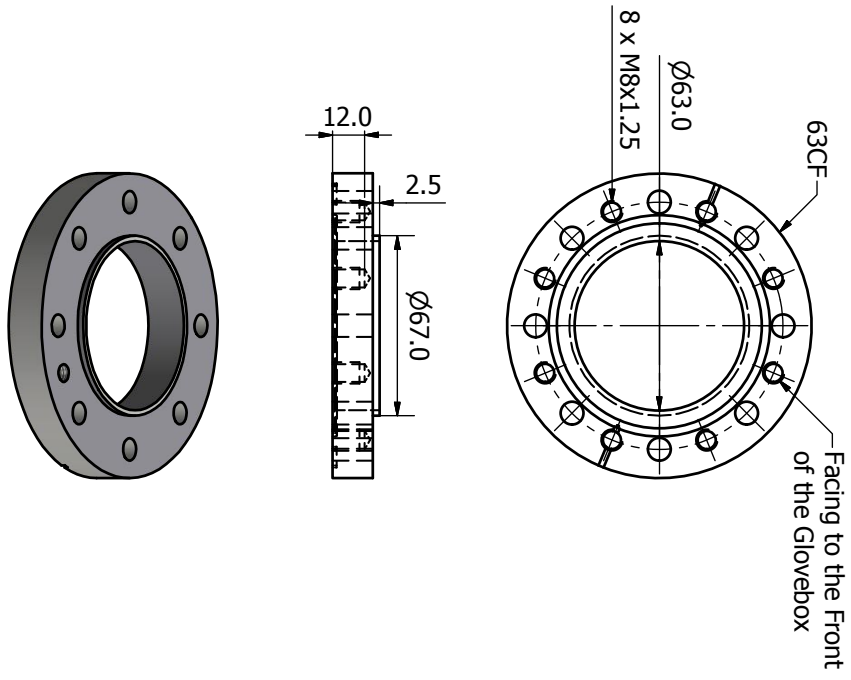
Threefold Evaporator Originally designed for three large volume crucibles on individual flanges in the NAC main chamber, now partially used in the load lock (Appendix B.4.4).

Battery Box The component layer and circuit board for a ripple free high DC voltage supply powered by batteries (Appendix B.4.5).

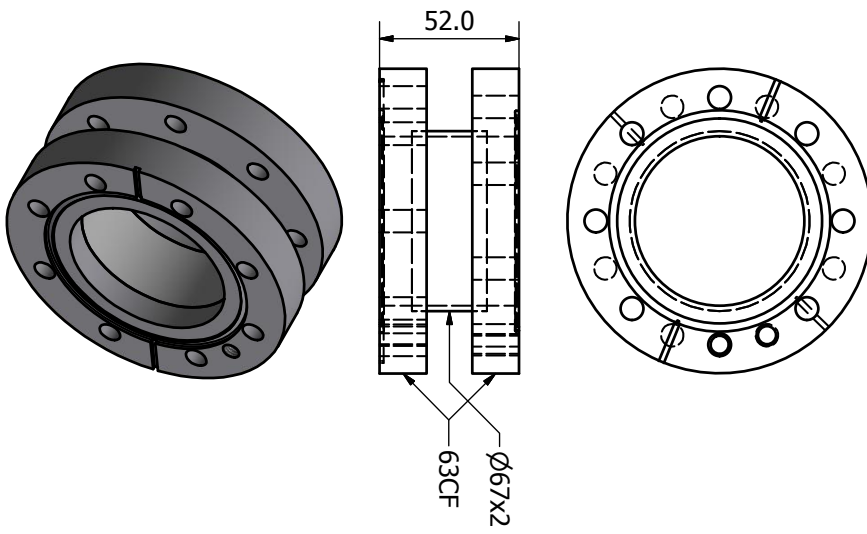
B.4.1 Glove Box



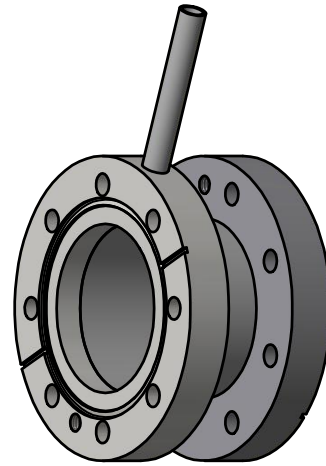
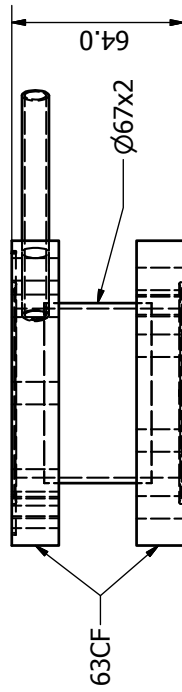
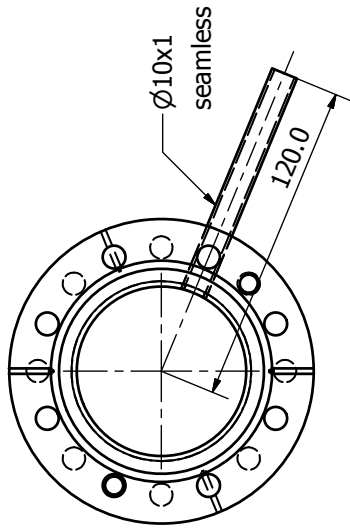
Floor Flange
Modification (1:2)



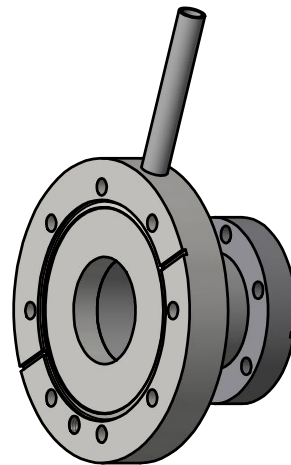
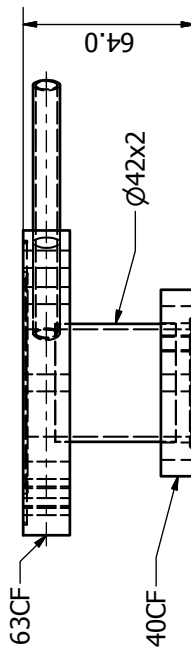
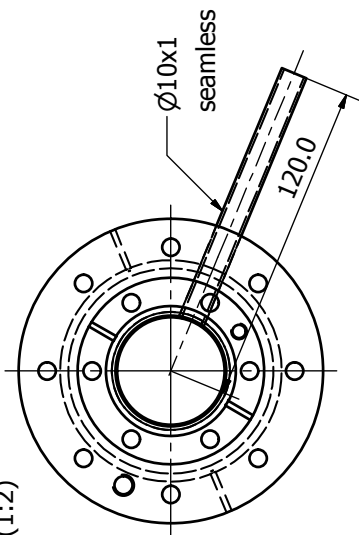
Short Nipple 63
1.4301 (1:2)

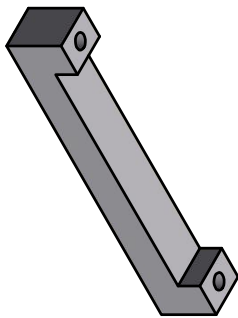
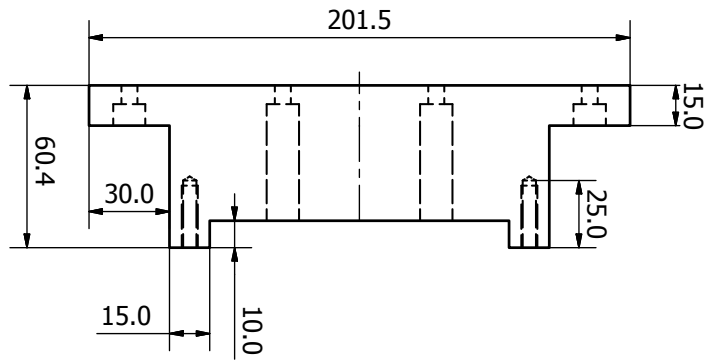
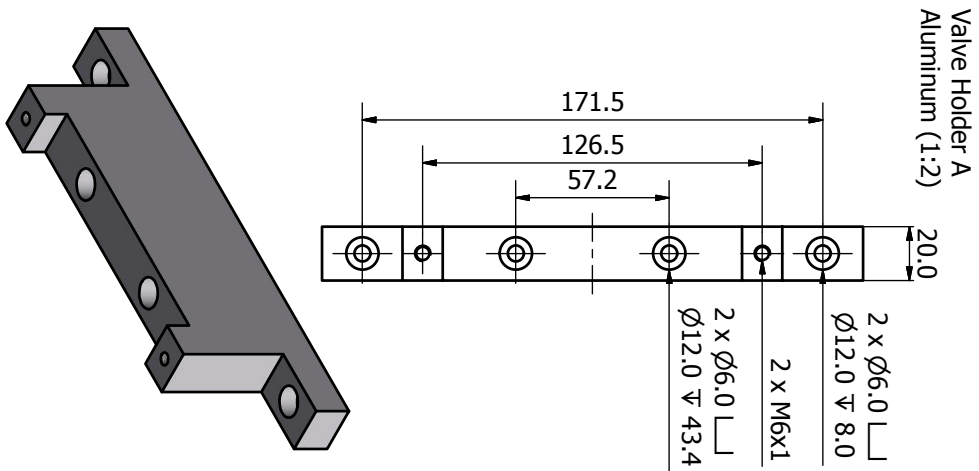


Vented Nipple 63CF
1.4301 (1:2)

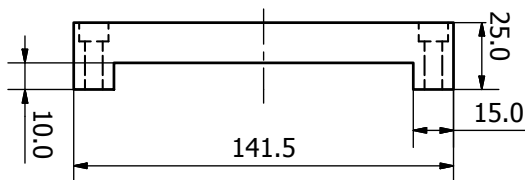
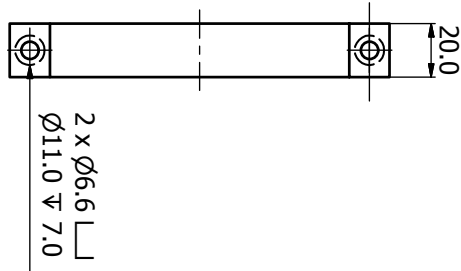


Vented Nipple 40CF
1.4301 (1:2)

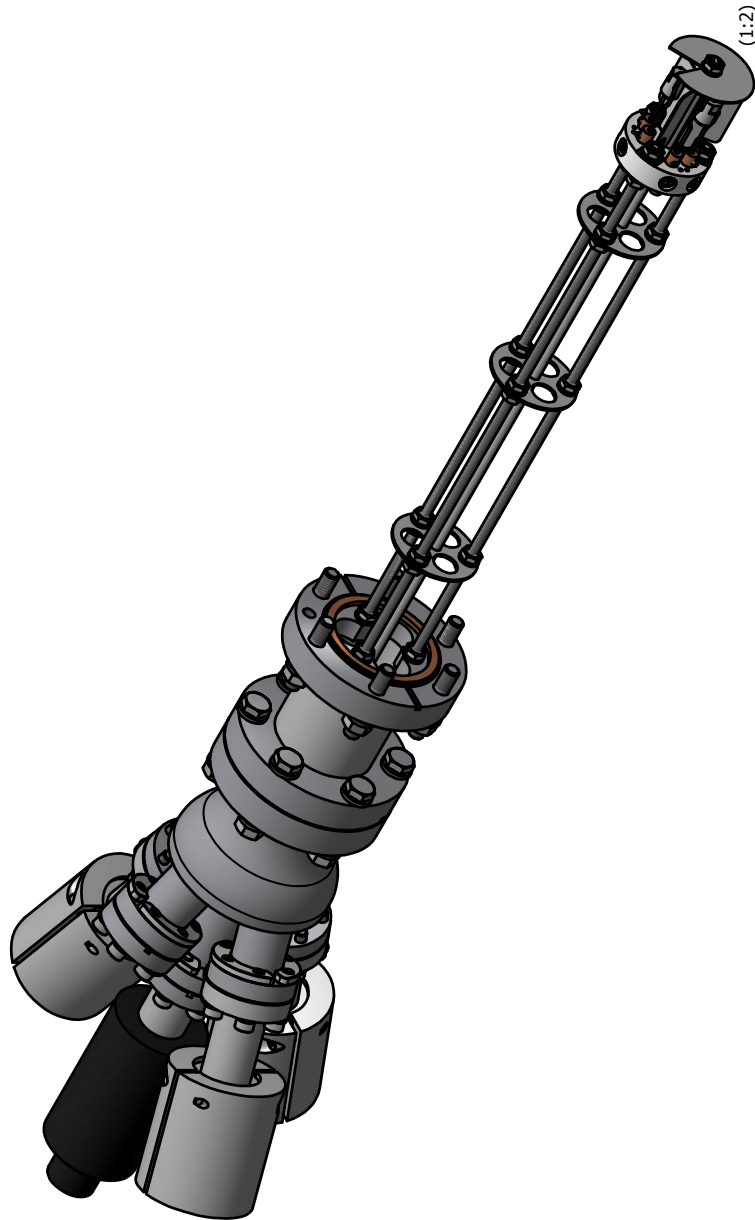


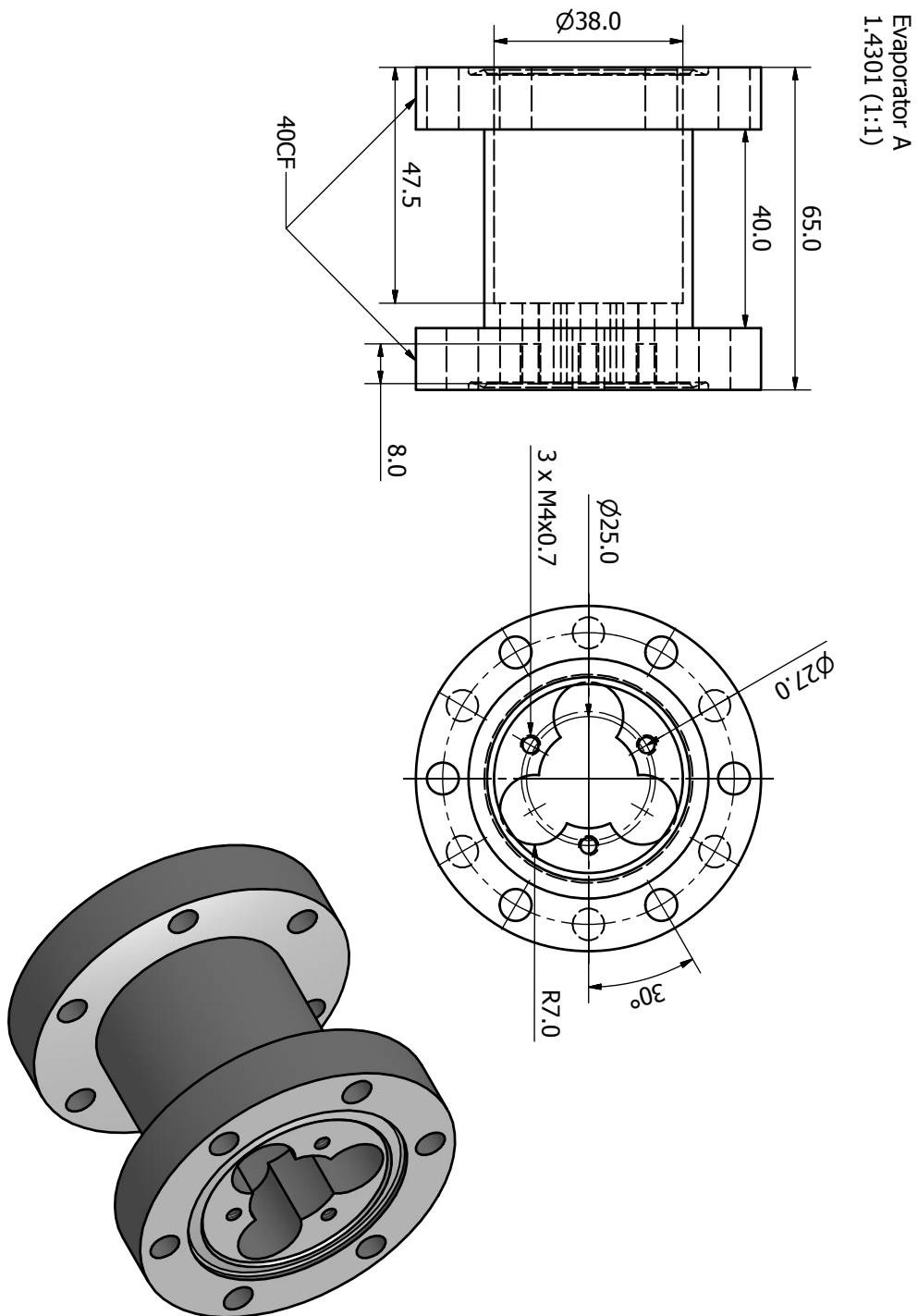


Valve Holder B
Aluminum (1:2)

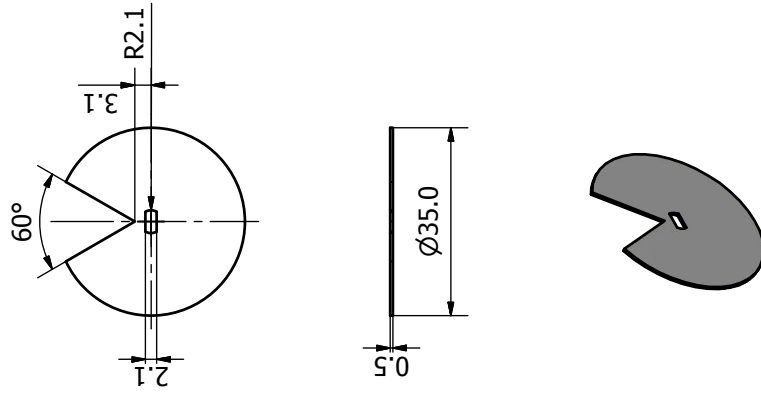


B.4.2 Evaporator for Synchrotron Applications

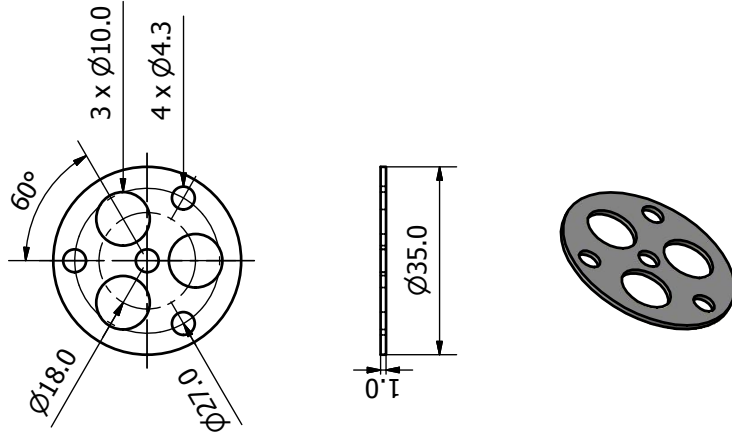




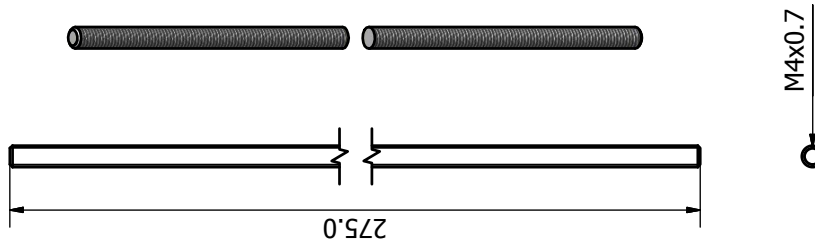
Evaporator D
1.4301 (1:1)



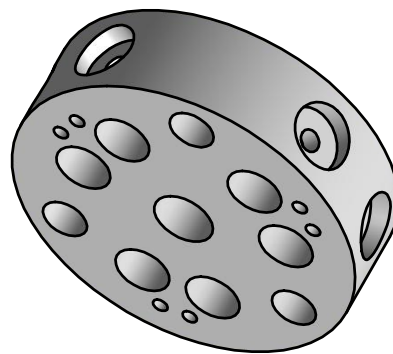
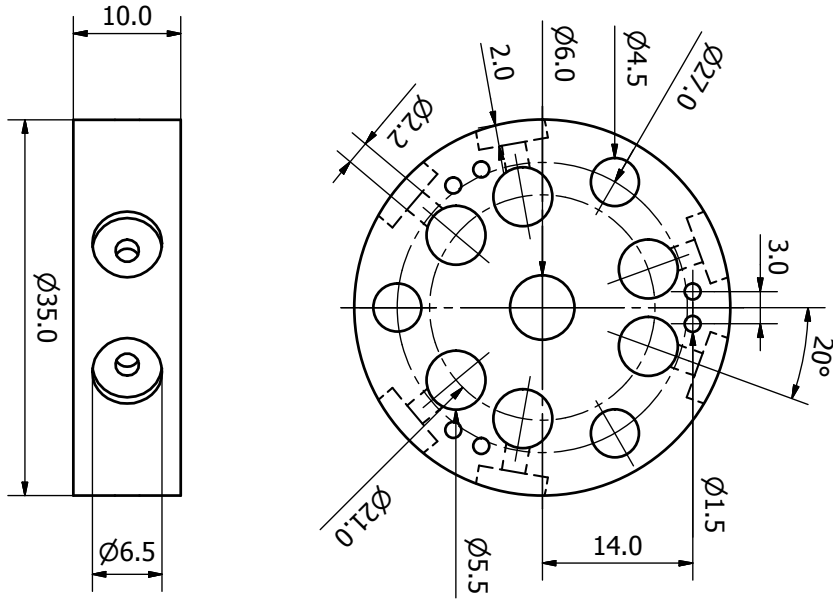
Evaporator C
1.4301 (1:1) 3 pieces



Evaporator B
1.4301 (1:1) 3 pieces



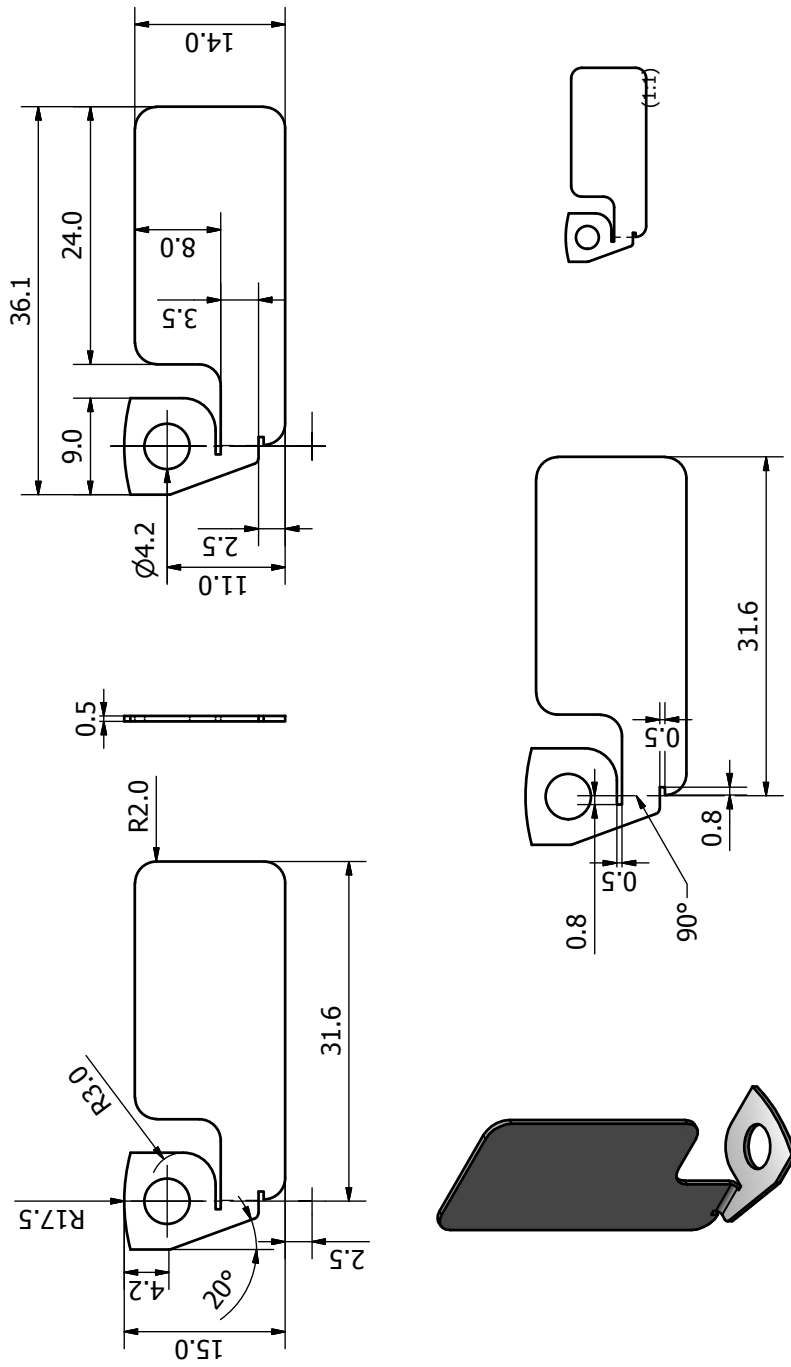
Evaporator E
Fired Pyrophyllite (2:1)



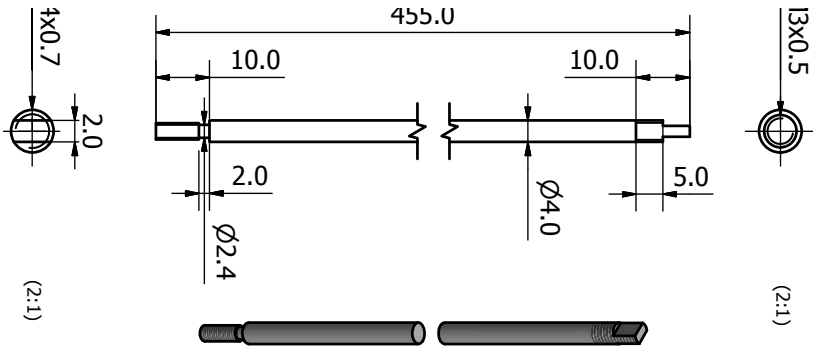
Heat treatment
 Ramp: RT to 400°C within 8h
 Ramp: 400°C to 1300°C within 9h
 Hold: 1300°C for 1h
 Ramp: 1300 °C to RT within 13 h

Heat treatment taken from Reference [240].

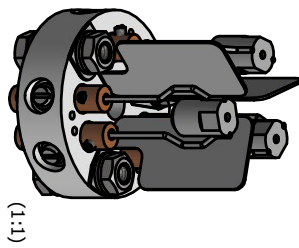
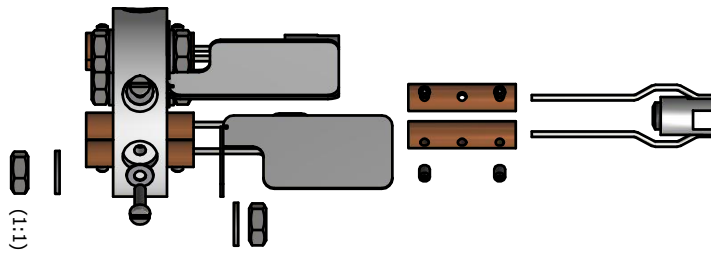
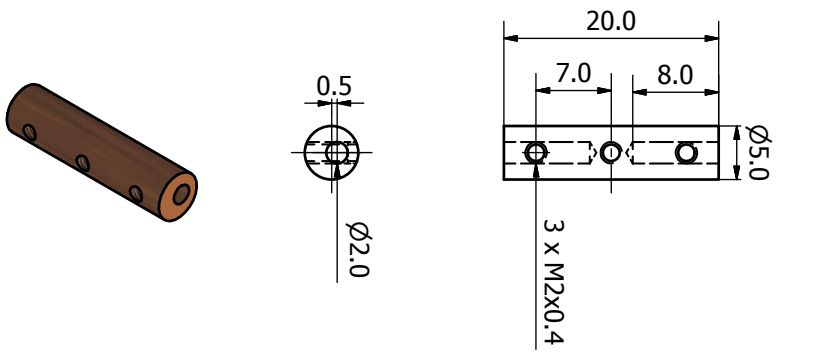
Evaporator F
1.4541 (2:1) 3 pieces



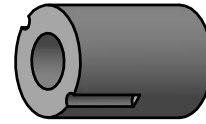
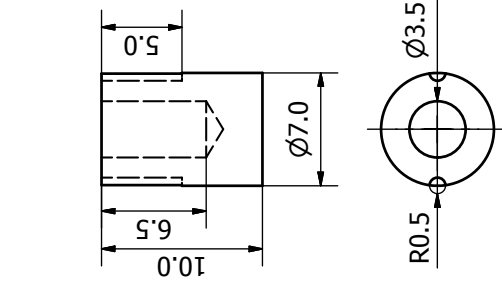
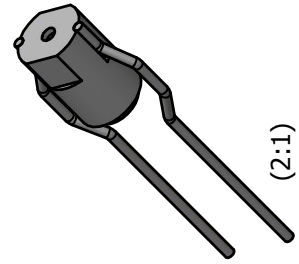
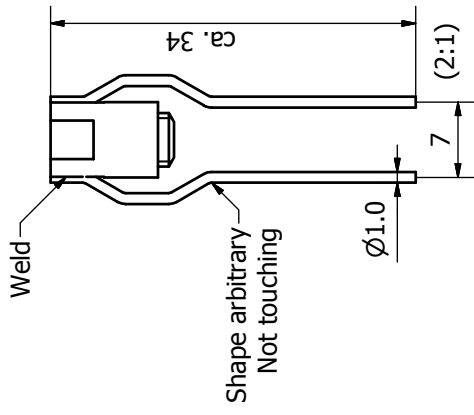
Evaporator G
1.4301 (1:1)



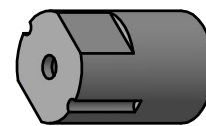
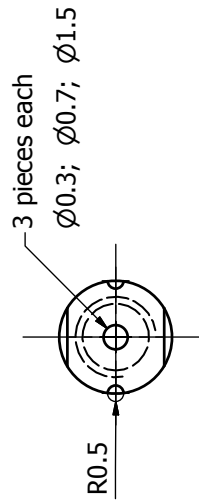
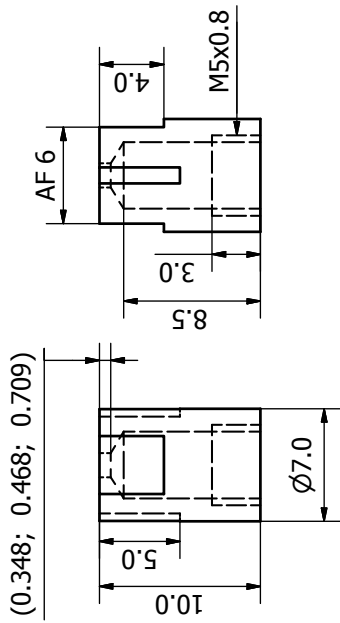
Evaporator H
Copper (2:1) 6 pieces



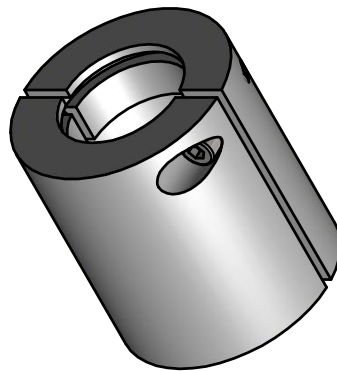
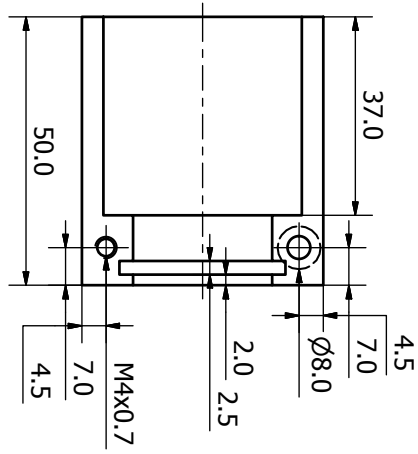
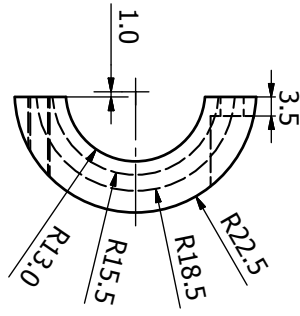
Evaporator Crucible B
1.4301 (3:1) 3 pieces

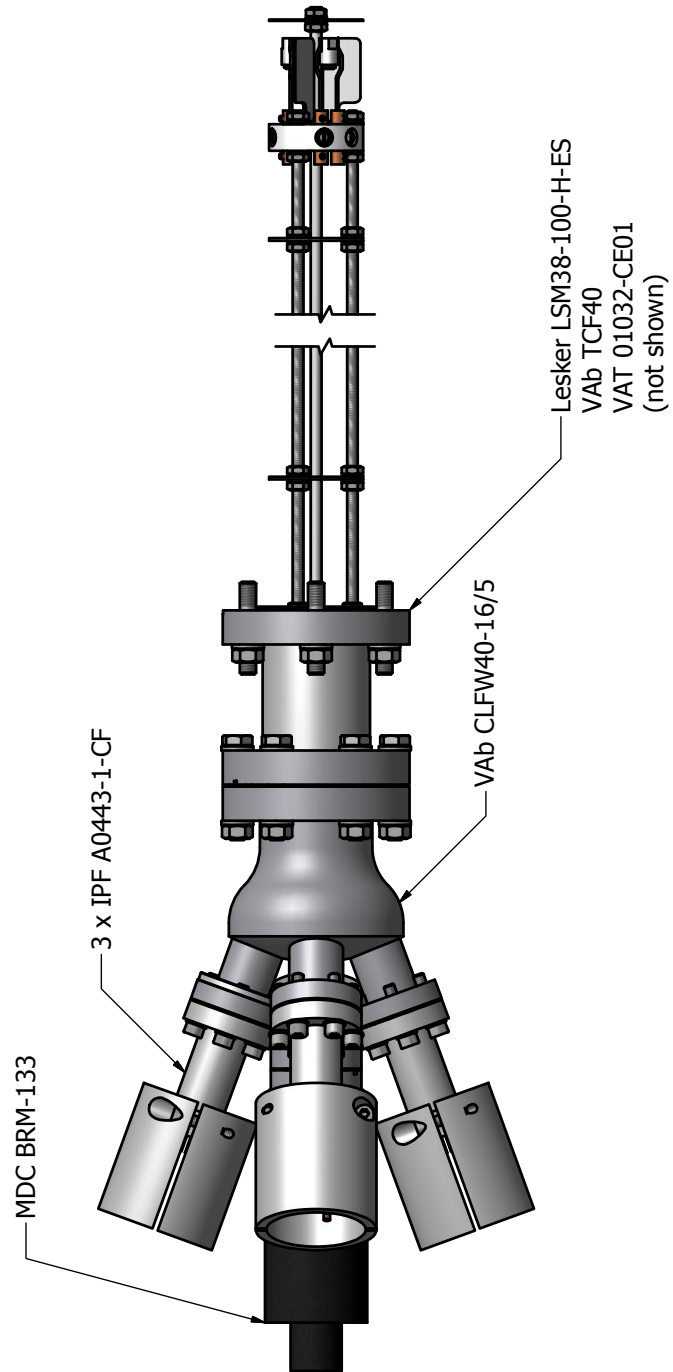


Evaporator Crucible A
1.4301 (3:1) 3 x 3 pieces

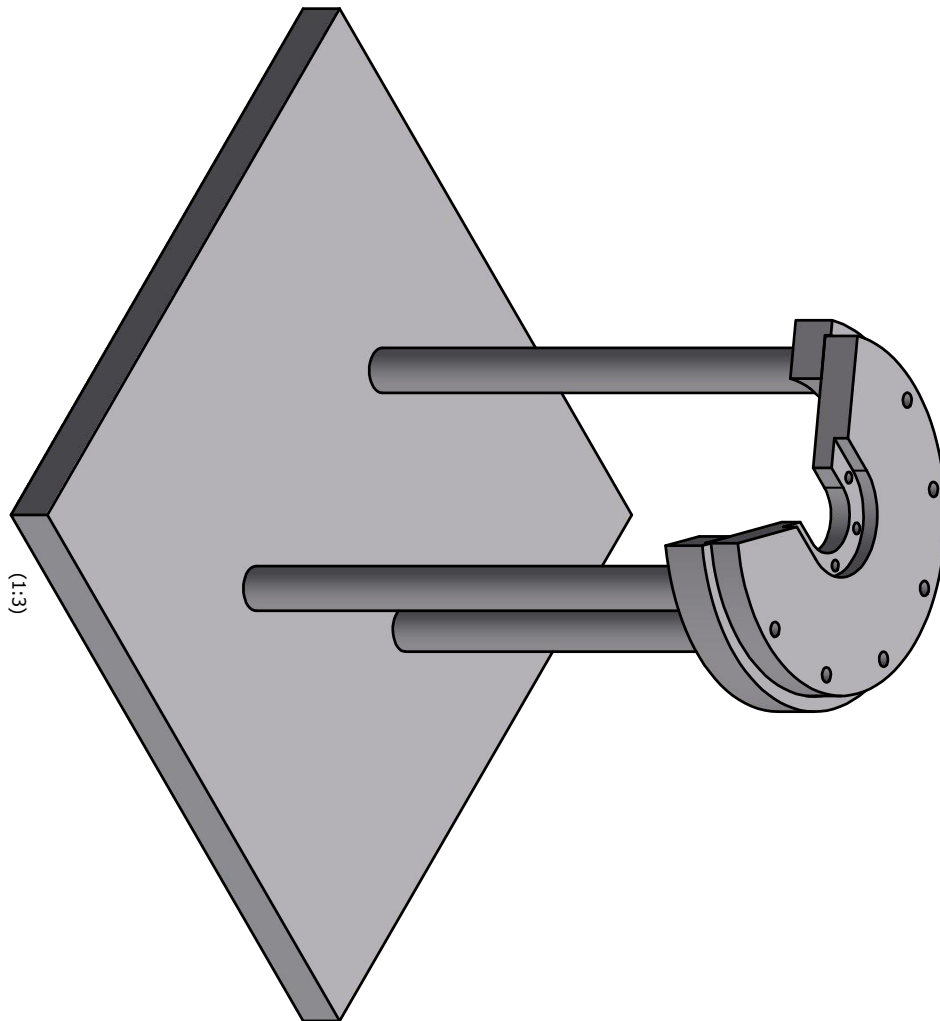


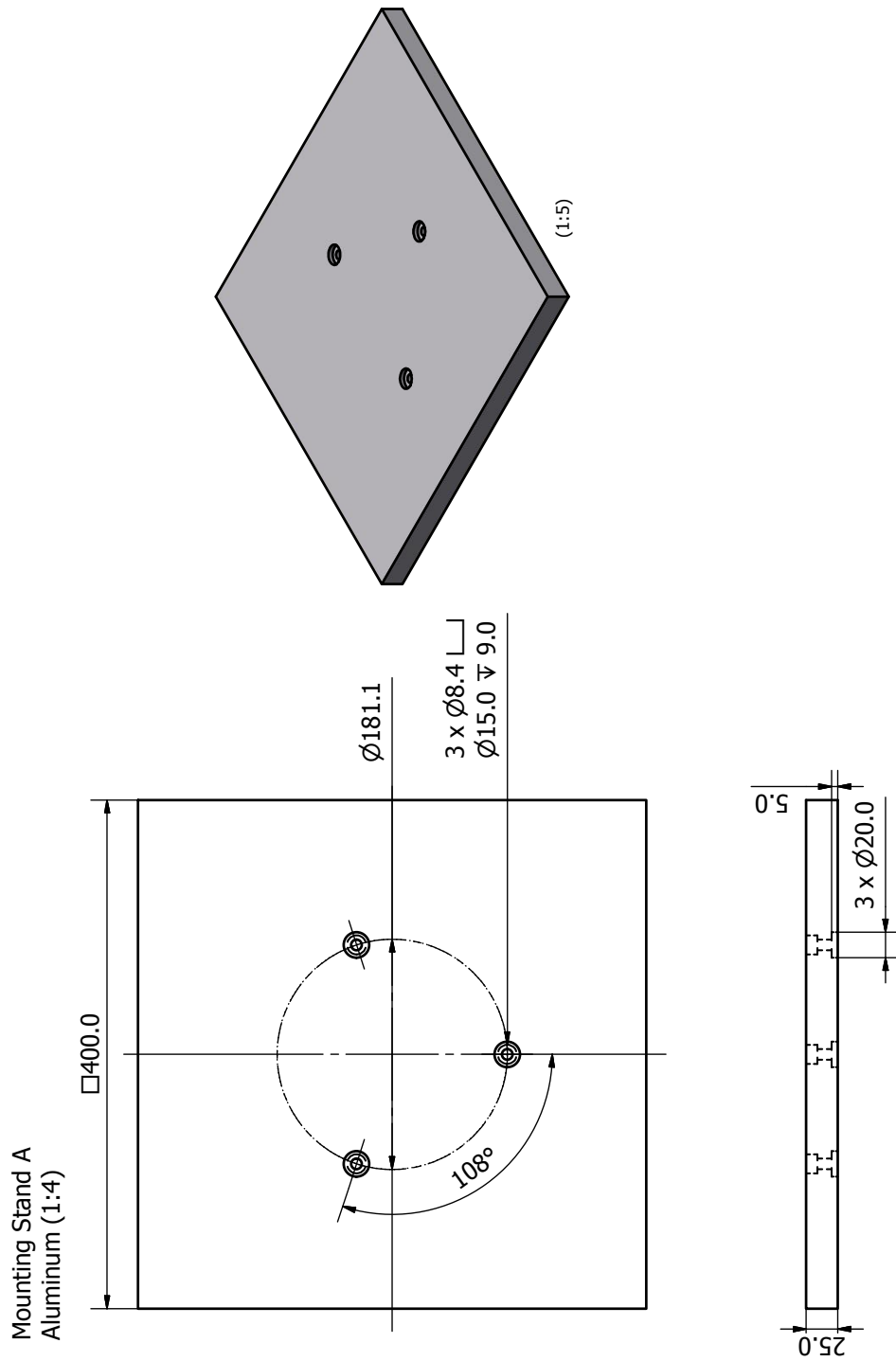
Evaporator Feedthrough Protection
Aluminum (2:1) 3 pairs (6 pieces)
Fits most MPF-16CF feedthroughs



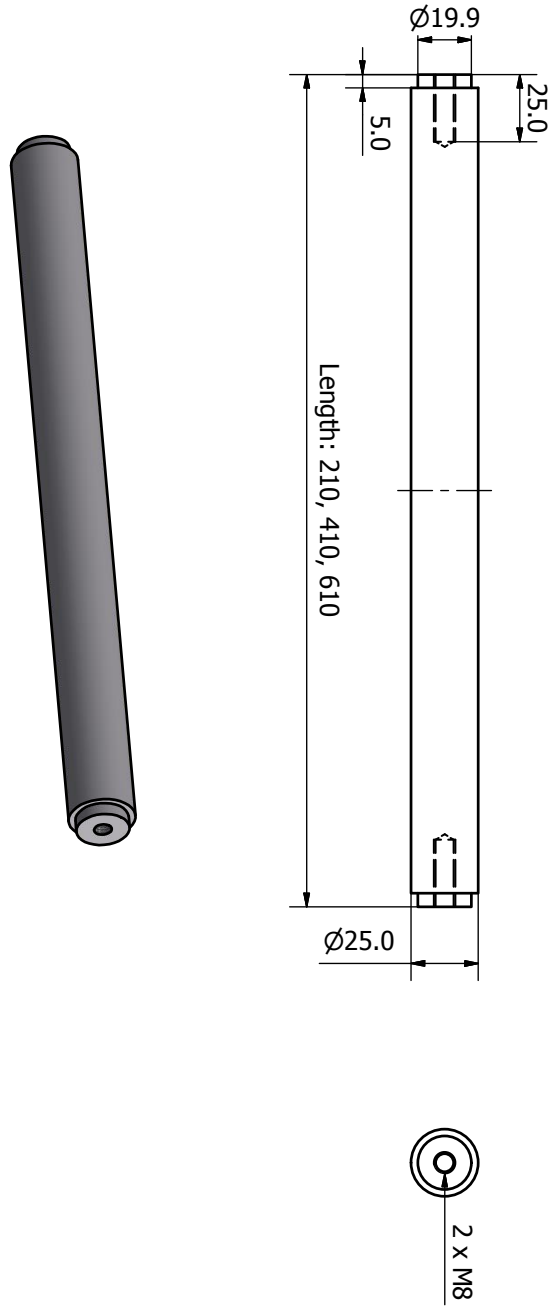


B.4.3 Mounting Stand

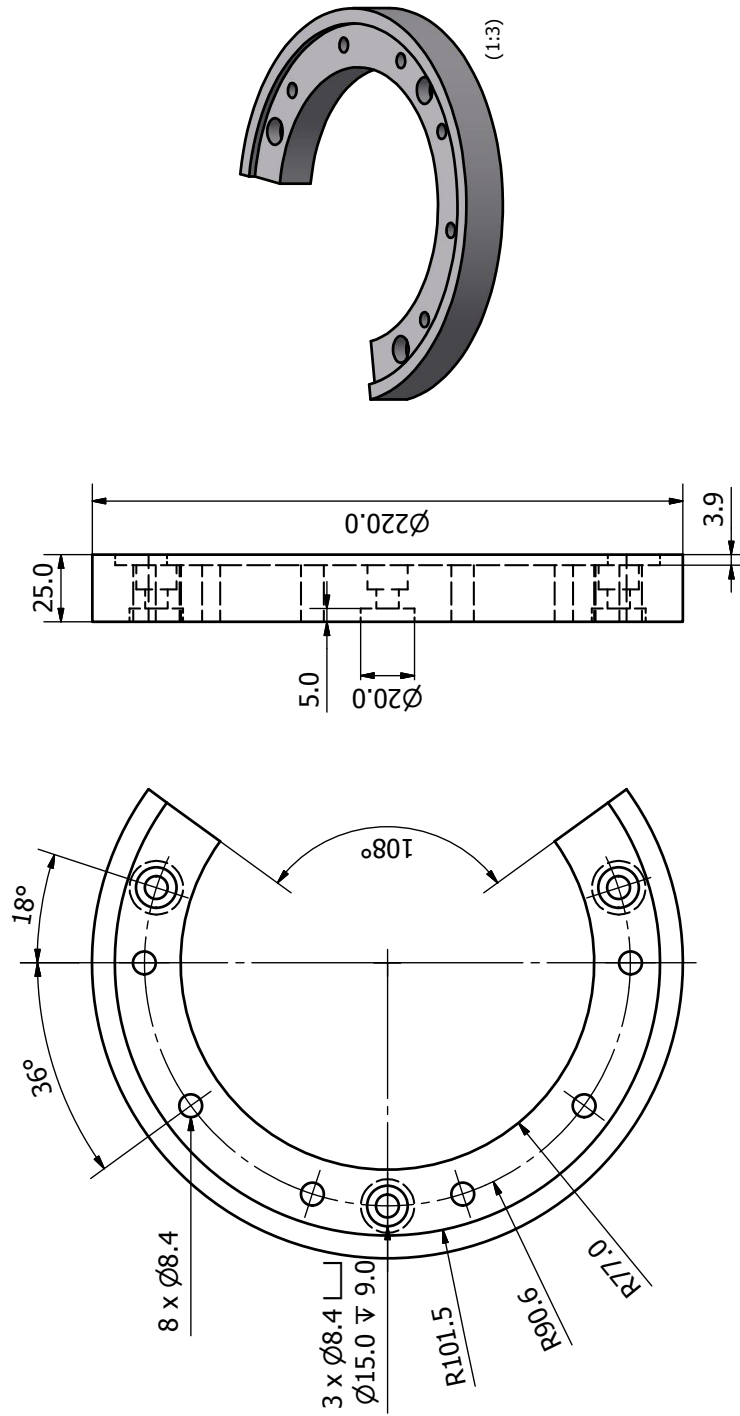




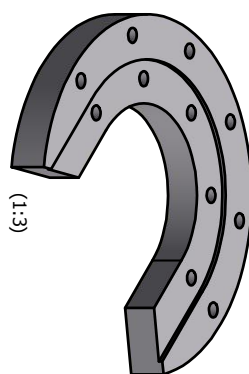
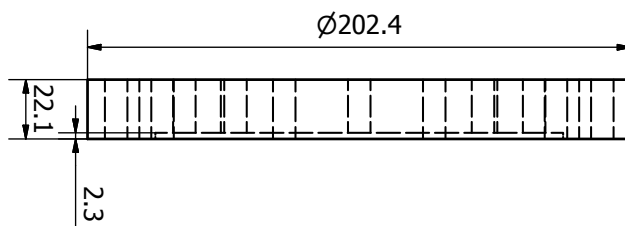
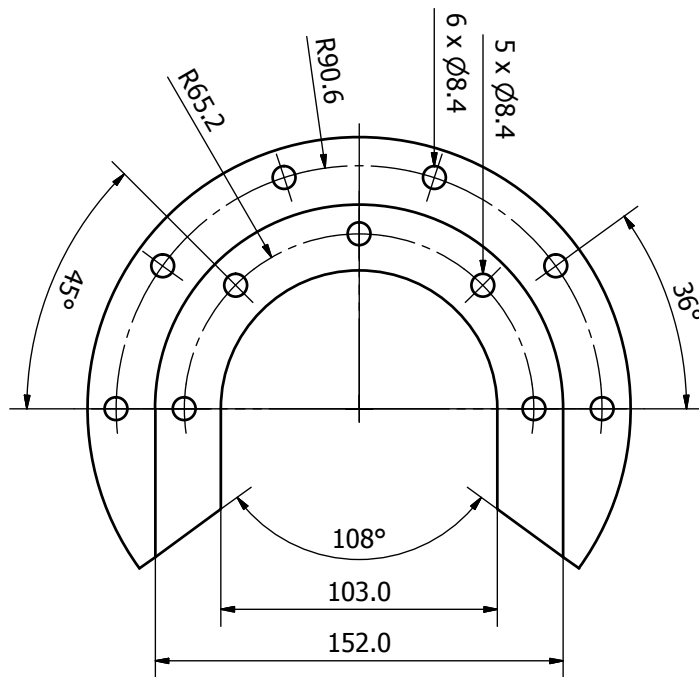
Mounting Stand B
Aluminum (1:2) 3 pieces each



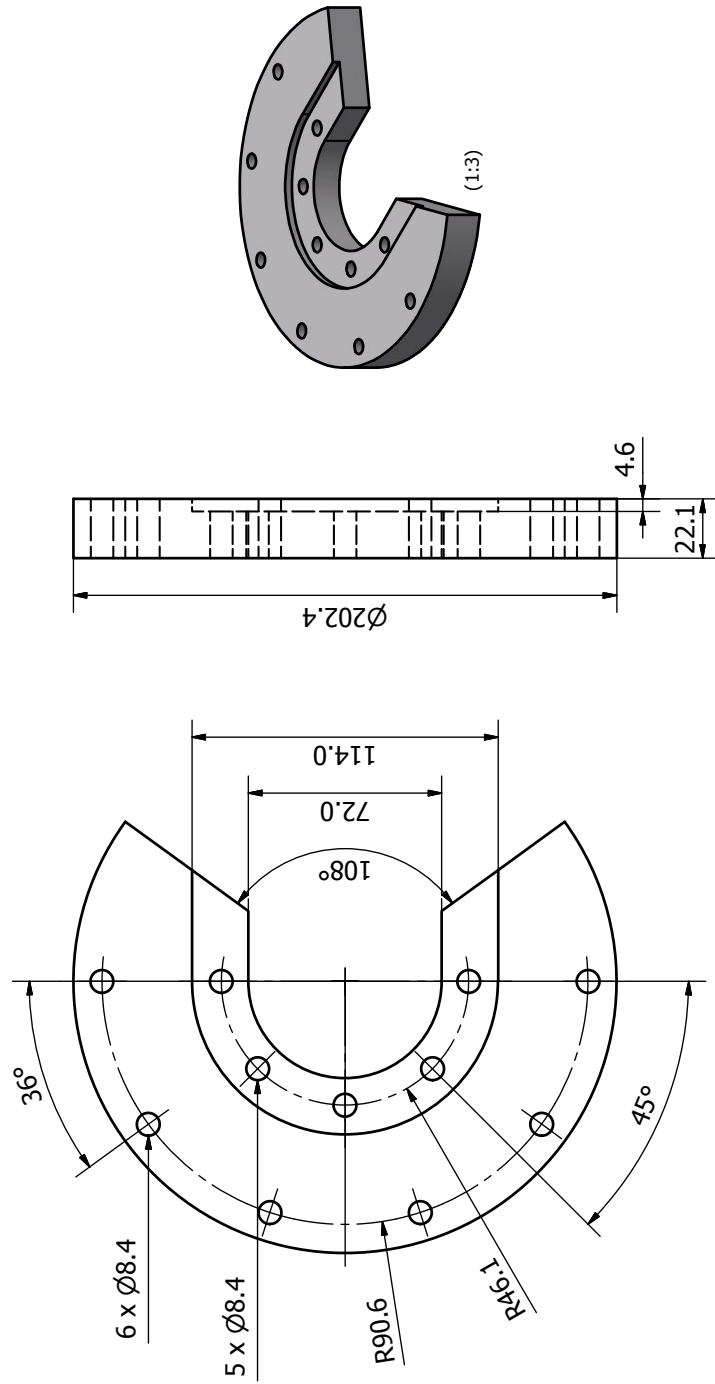
Mounting Stand C
Aluminum (1:2)



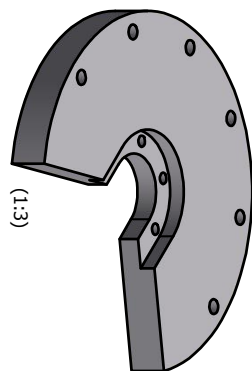
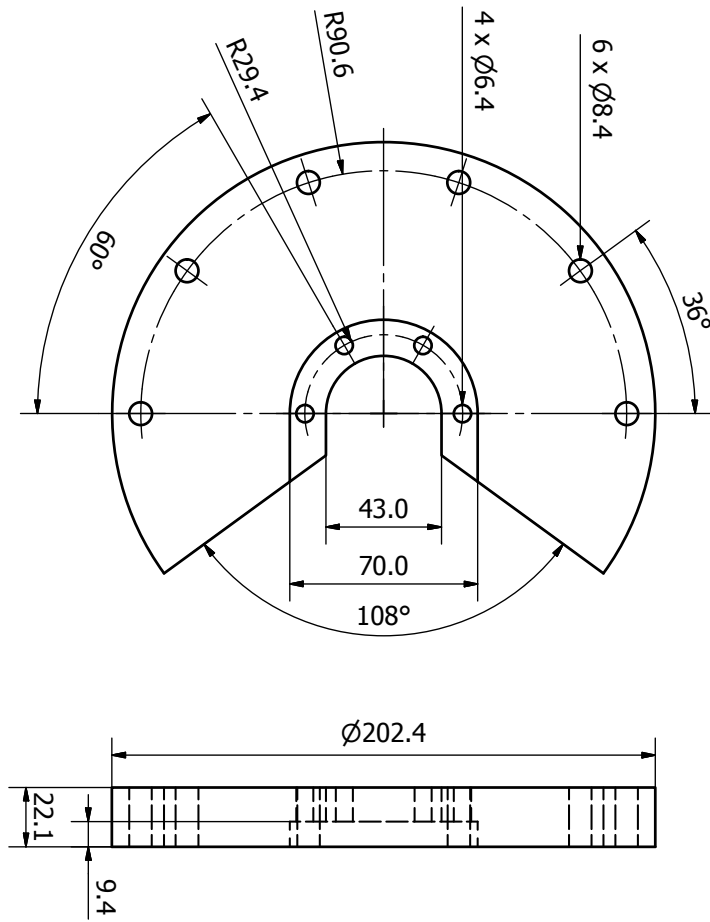
Mounting Stand D
Aluminum (1:2)



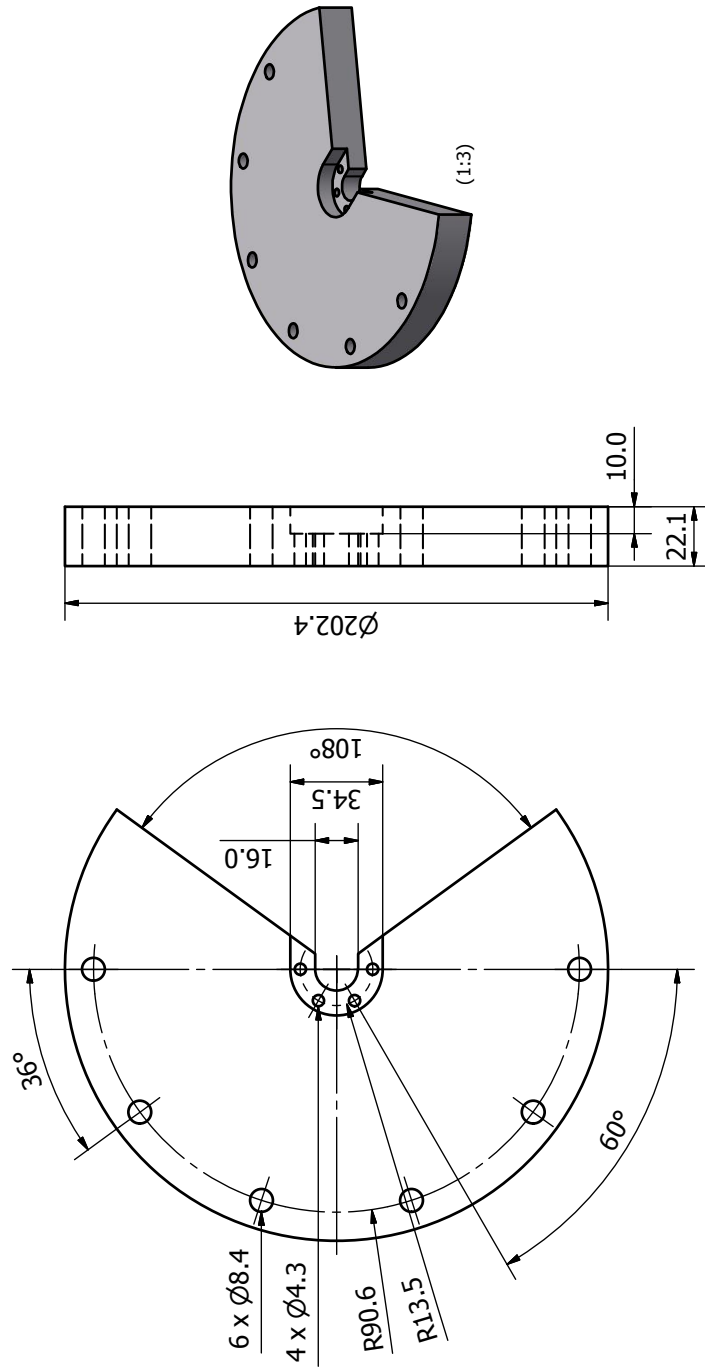
Mounting Stand E
Aluminum (1:2)



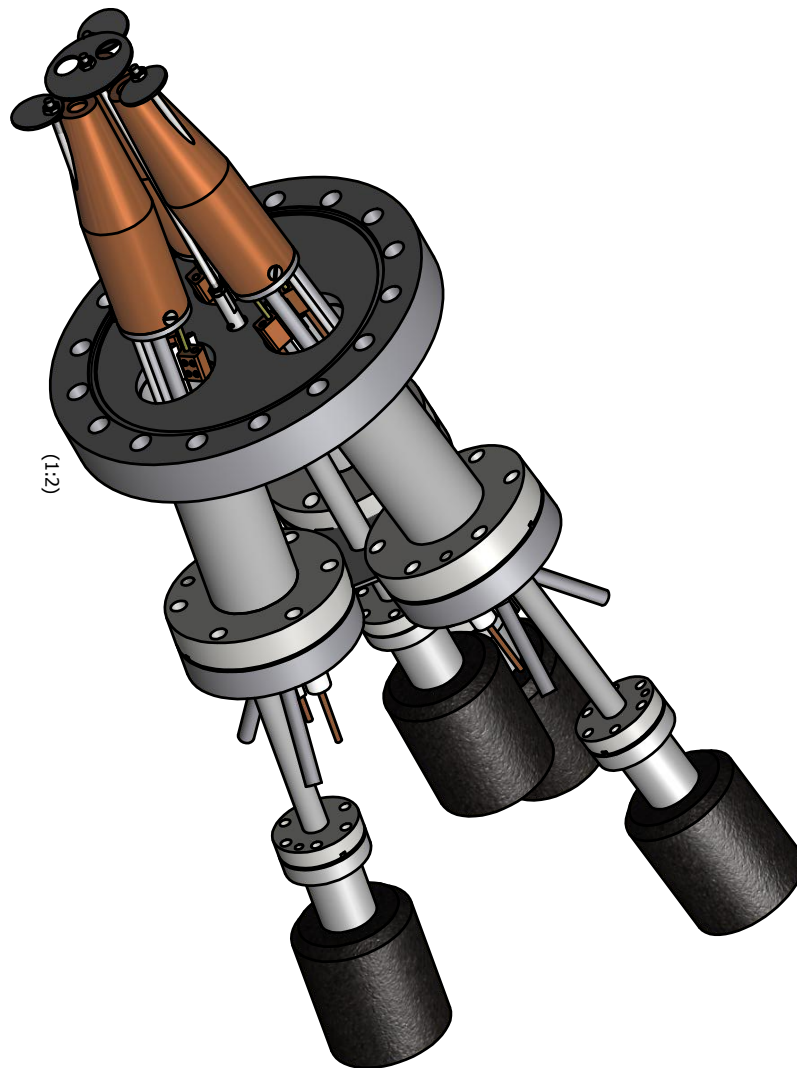
Mounting Stand F
Aluminum (1:2)



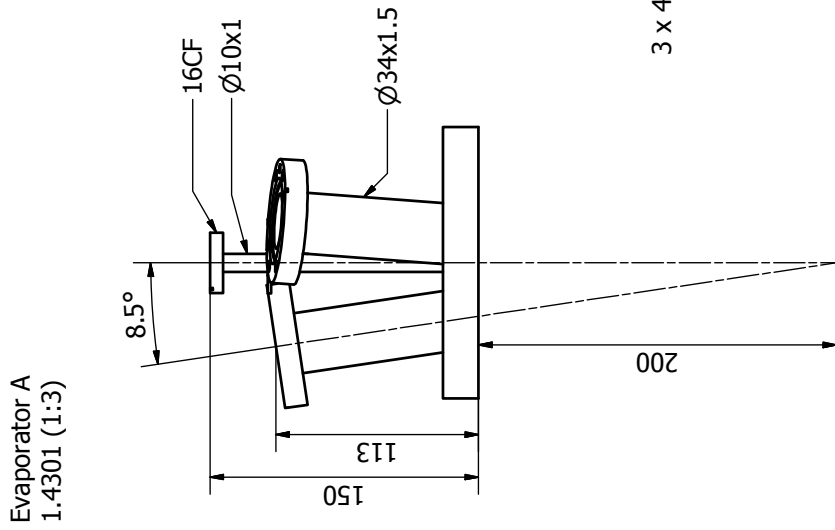
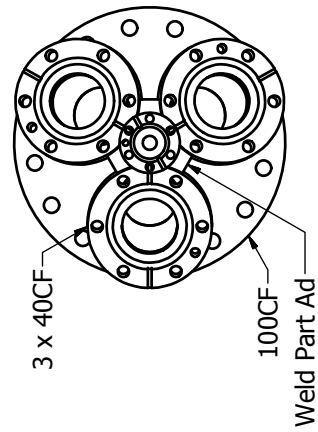
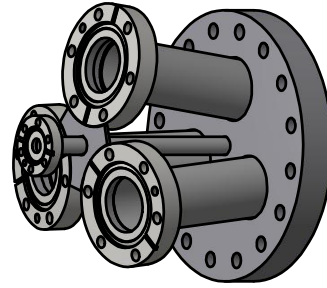
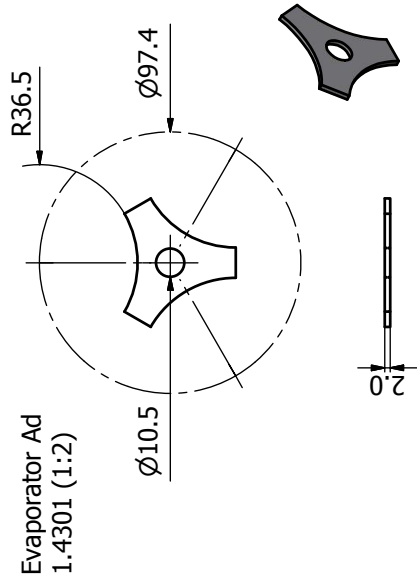
Mounting Stand G
Aluminum (1:2)



B.4.4 Threefold Evaporator

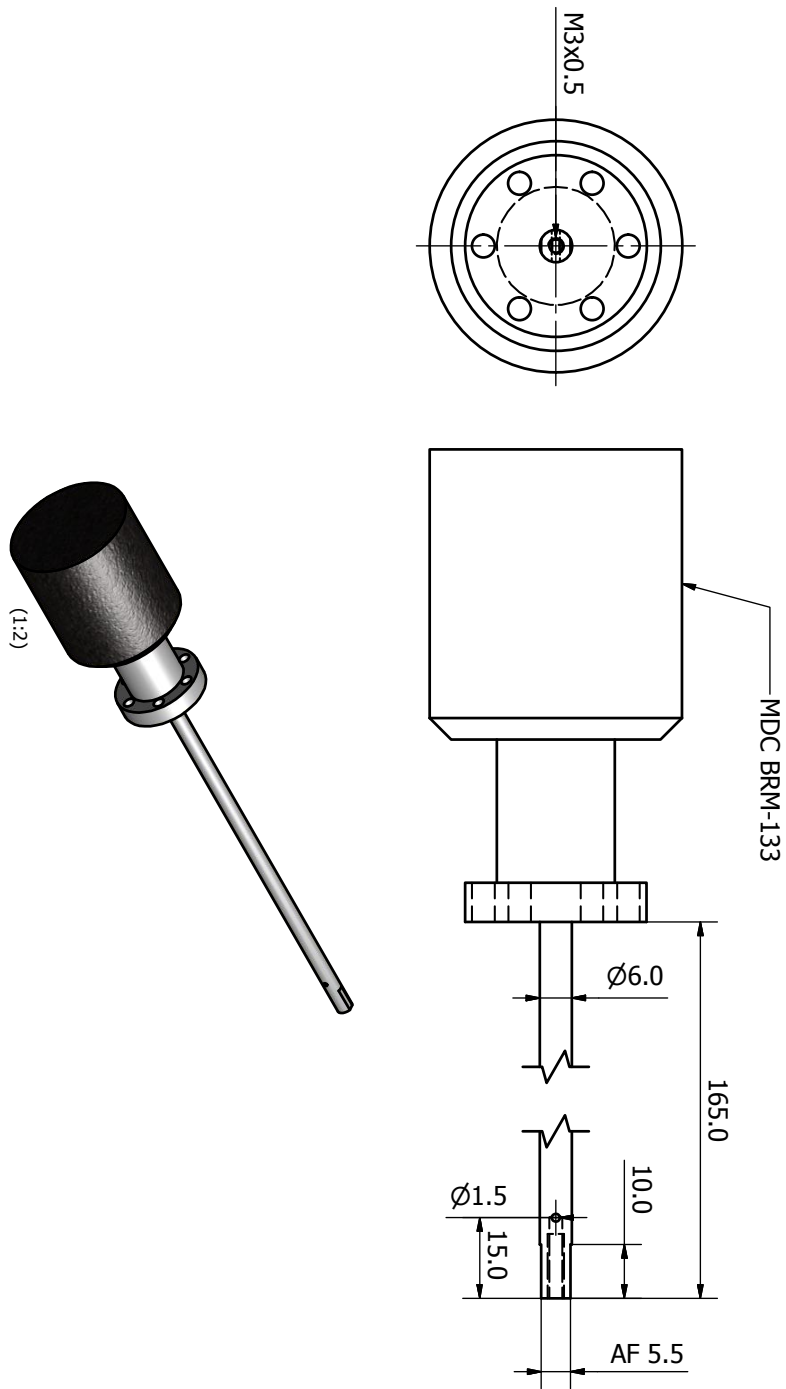


Design by O. LYTKEN.

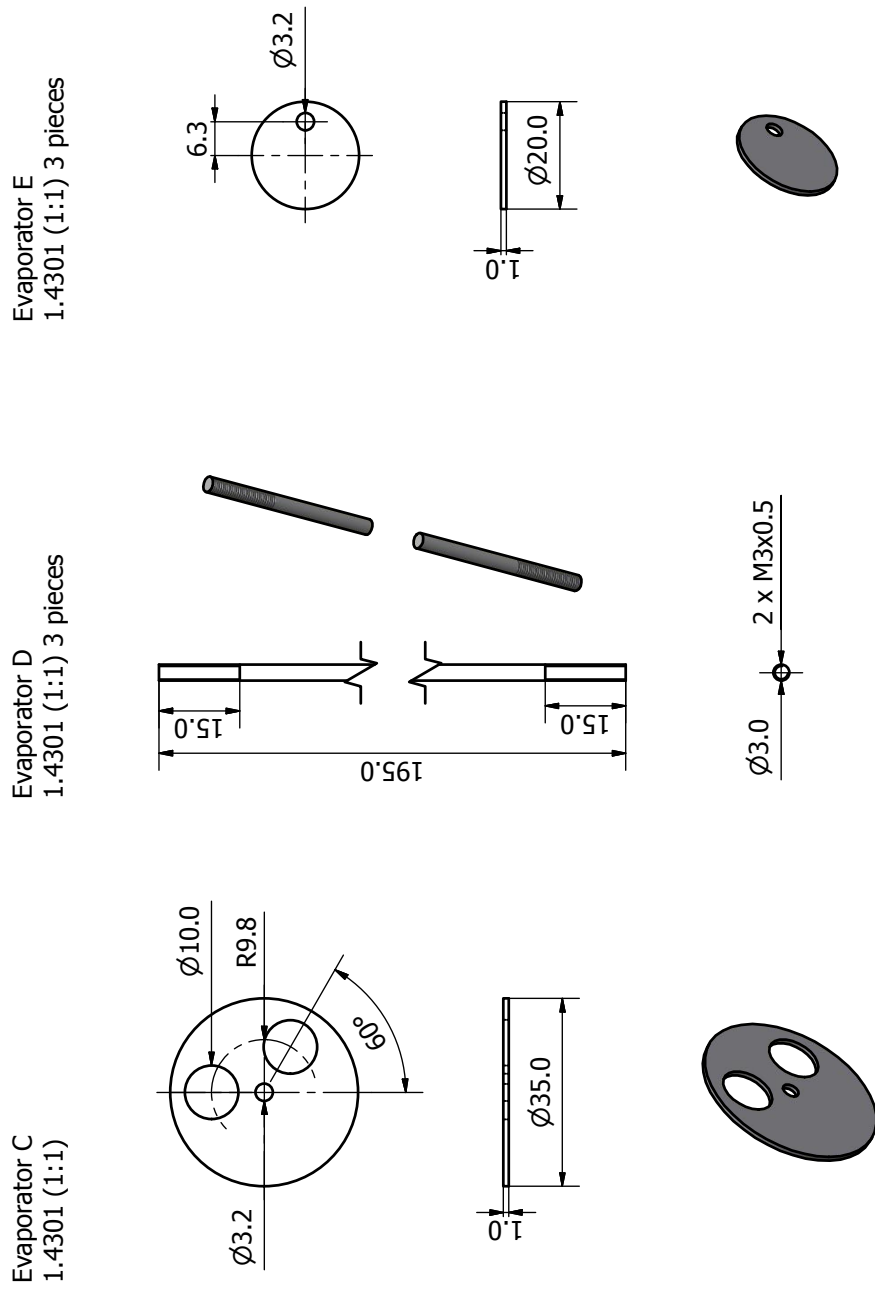


Design by O. LYTKEN.

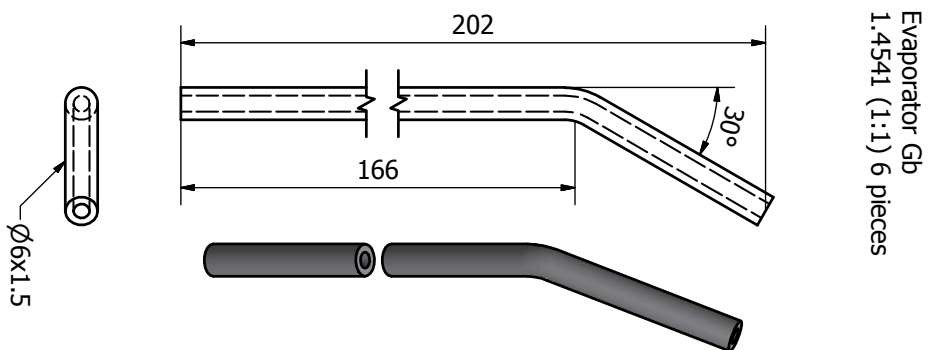
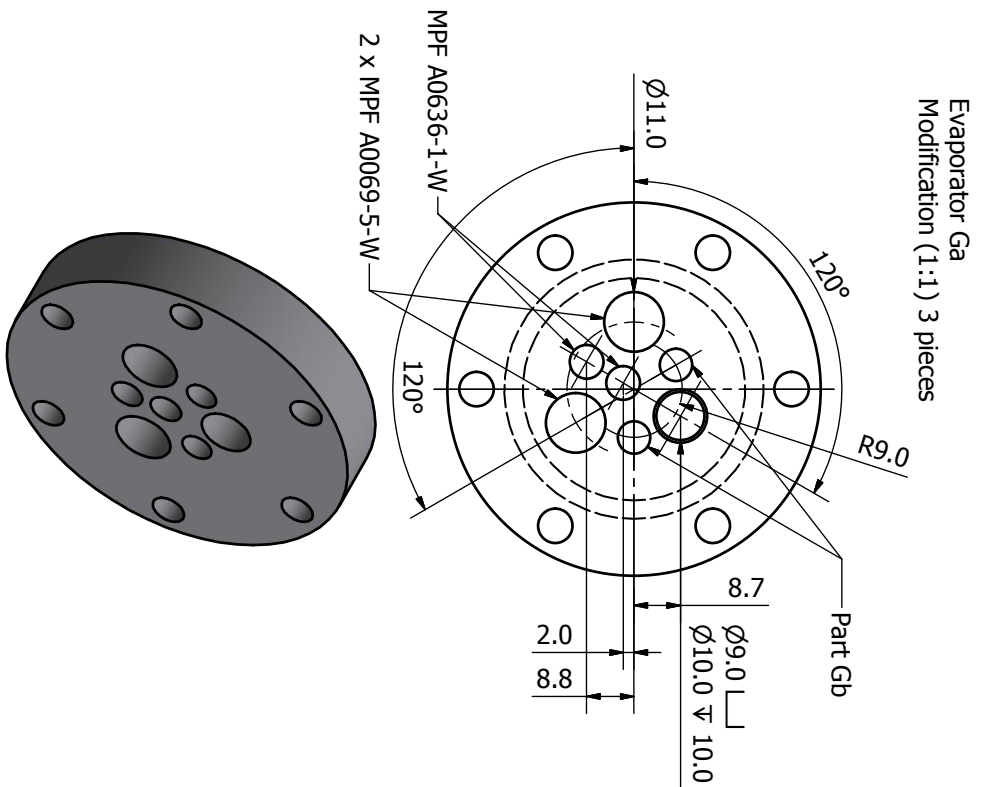
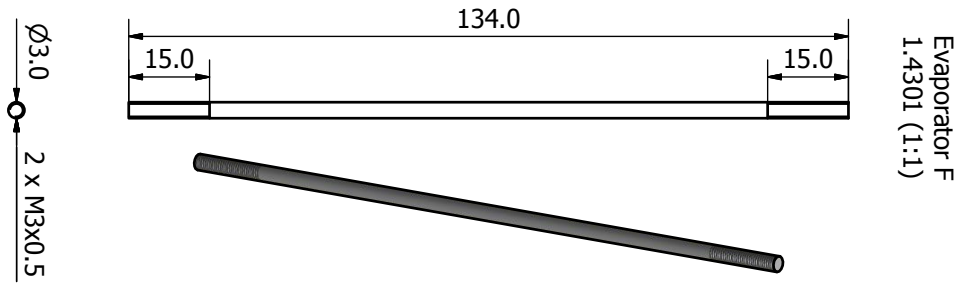
Evaporator B
Modification (1:1)



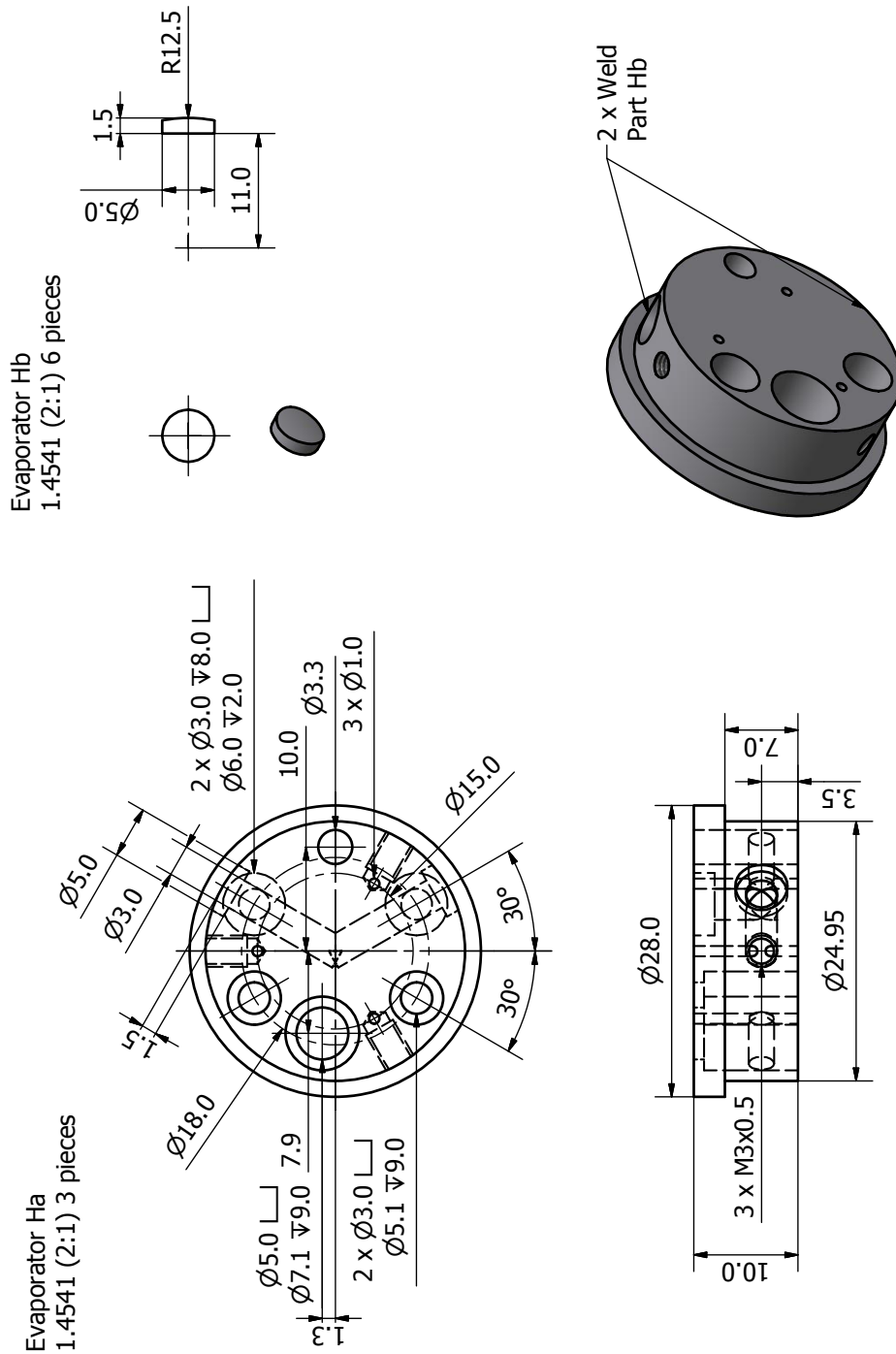
Design by O. LYTKEN.



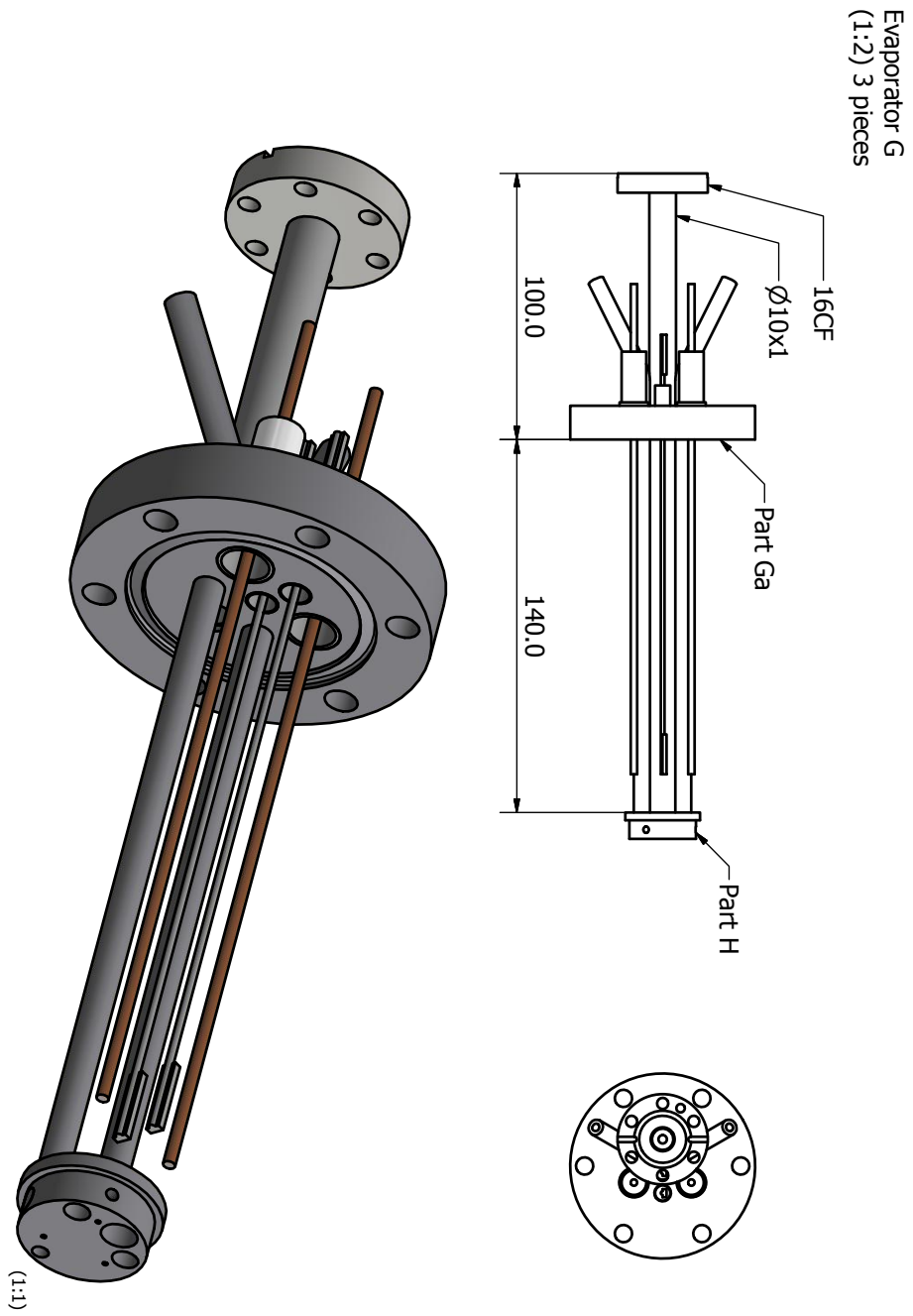
Design by O. LYTKEN.



Design by O. LYTKEN.

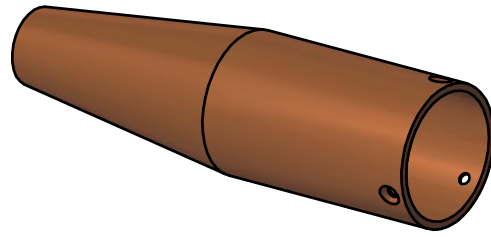
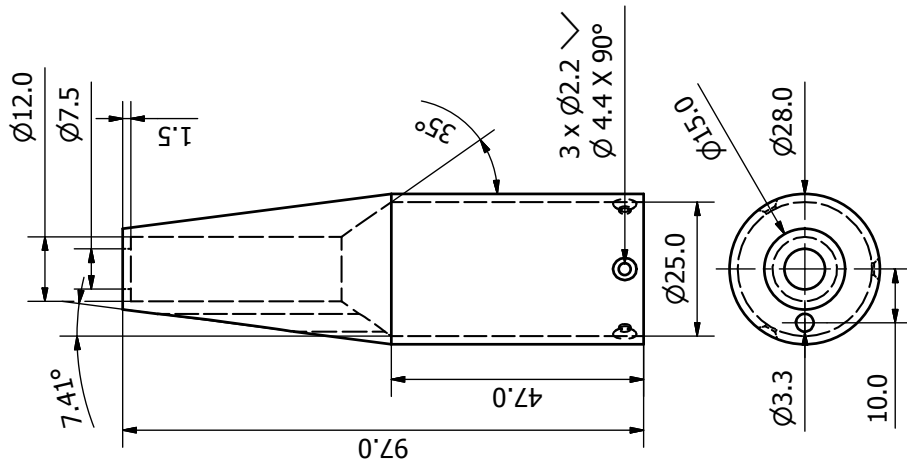


Design by O. LYTKEN.



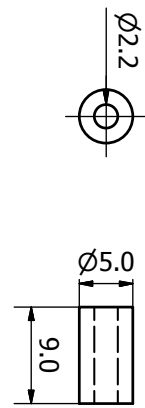
Design by O. LYTKEN.

Evaporator I
Copper (1:1) 3 pieces

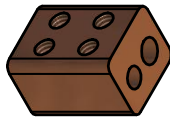
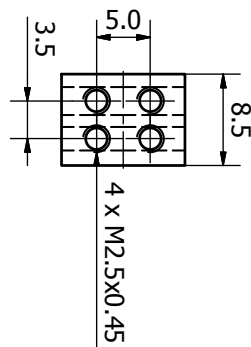
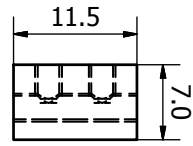


Design by O. LYTKEN.

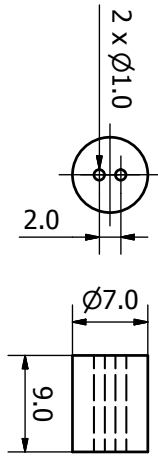
Evaporator J
Macor (2:1) 6 pieces



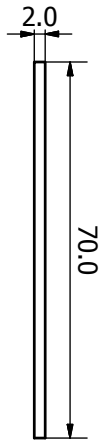
Evaporator M
CuBe2 (2:1) 6 pieces



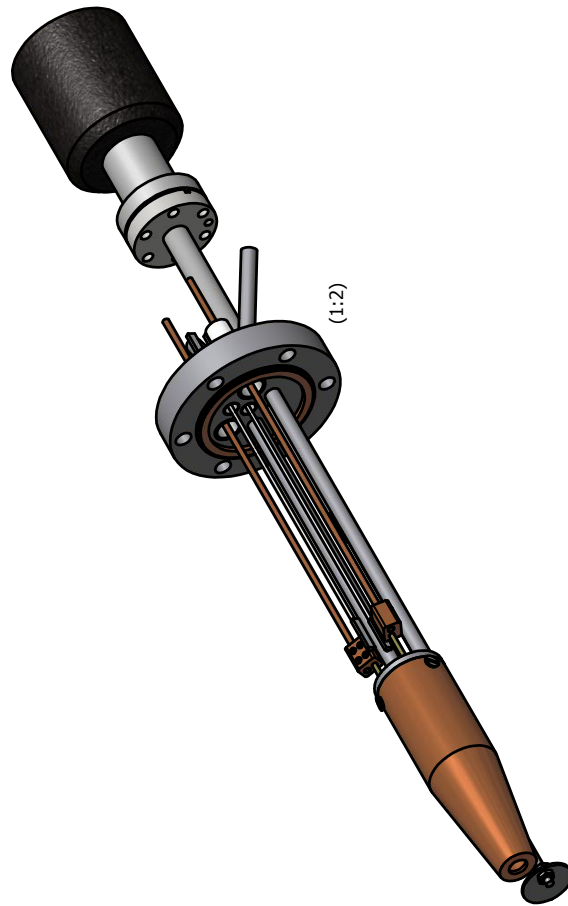
Evaporator K
Macor (2:1) 3 pieces



Evaporator L
Tantalum (2:1) 6 pieces

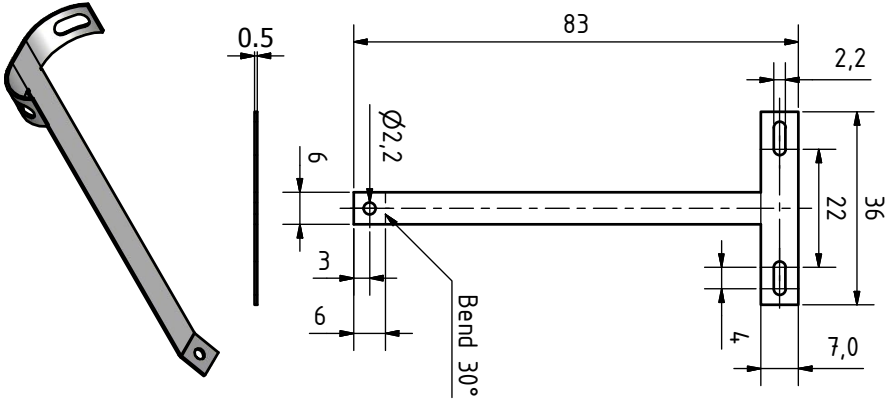


Design by O. LYTKEN.

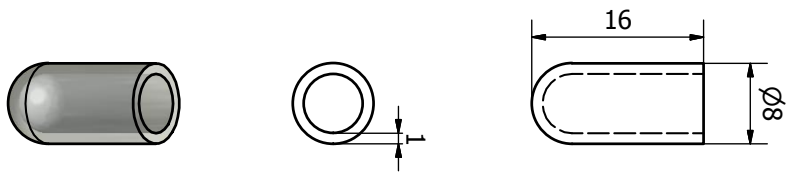


Design by O. LYTKEN.

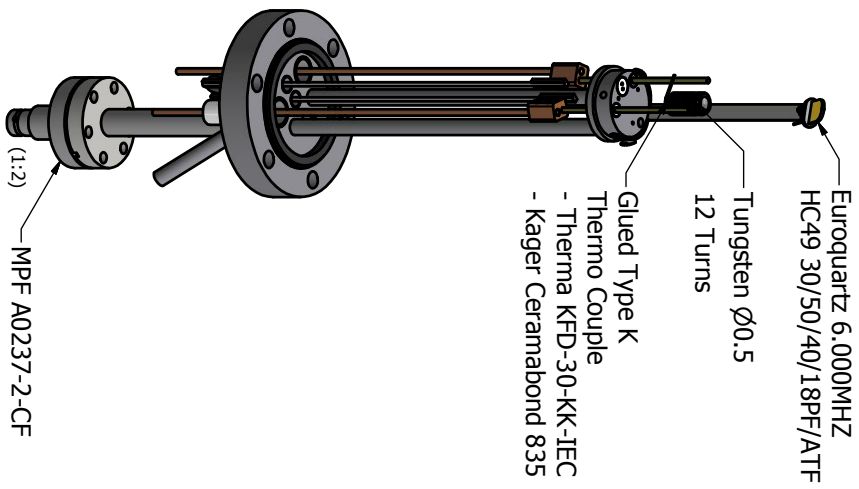
Evaporator QCM extension
1.4301 (1:1)



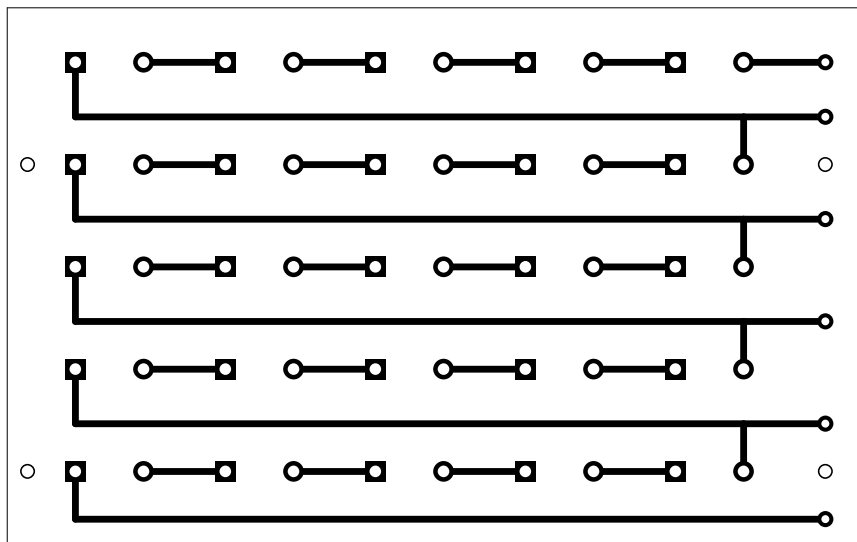
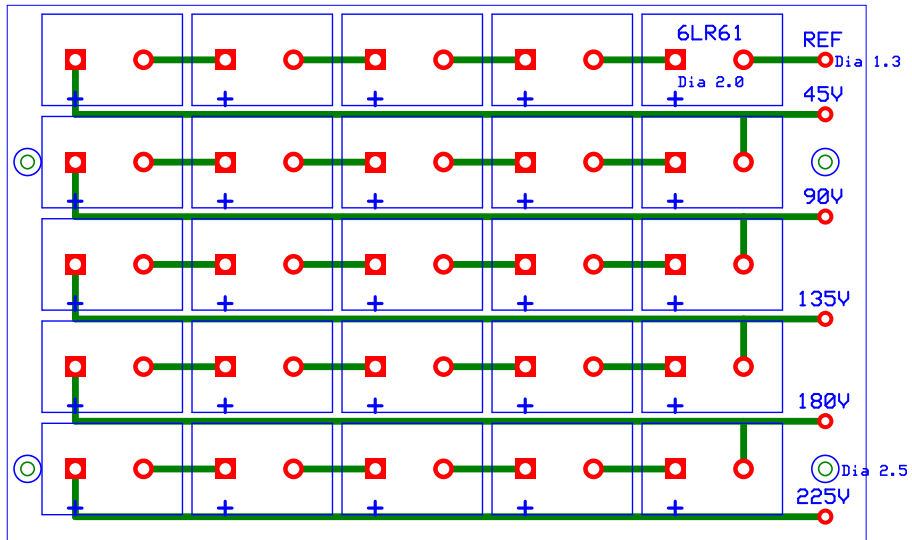
Evaporator Crucible
Quartz (1:1)



Load Lock Evaporator



B.4.5 Battery Box



C Program Codes

This appendix covers the entire IGOR PRO program codes written for the data treatment for the calorimetry instrument. Comments to the individual functions can be found in Chapter 4.

As the results¹, presented in Chapter 6, are not fully understood in detail yet, the complete program code is included in order to provide a possibility to track down conceptual errors.

In addition to the printed version, the program files also contain the L^AT_EX-Code used for formatting the listings in comments. Regular comments in the program follow the ‘//’ sequence. Enhanced structuring comments follow a ‘//(@ . . . @)’ scheme and are ignored by IGOR PRO as well. Most of the functions, *i.e.*, all functions with the keyword **Static**, are only accessible by the package itself. Other functions can be called from the command line. Nevertheless, this is rarely necessary and should be avoided.

¹ Especially the gigantic signal effect and the inverted signal effect.

C.1 NAC Package

Details about the NAC software package are discussed in Section 4.2. Subsequently, the source code of this package is listed.

```
1 //NAC_3-14.ipf//
```

C.1.1 Definitions

```
//
```

Compiler Settings

```
#pragma rtGlobals=3 // Use modern global access method.
```

```
#pragma Version=3.15
```

```
6 #pragma IgorVersion=6.2
```

```
//
```

Constants

```
StrConstant NAC_DataPathStr="Z:Marburg:Data:Calorimetry:Measurements:"
```

```
//StrConstant NAC_DataPathStr="C:"
```

```
StrConstant NAC_Version="3.15"
```

```
11 //Serious Error Codes}
```

```
Constant NAC_UnknownVersion=42015
```

```
Constant NAC_DataFolderError=42014
```

```
Constant NAC_IncompatibleExperiment=42013
```

```
Constant NAC_CorruptExperiment=42012
```

```
16 Constant NAC_NoDataLoaded=42011
```

```
Constant NAC_NotImplementedYet=42010
```

```
Constant NAC_LaserPowerMissing=42009
```

```
Constant NAC_PulseLengthDetectionFailed=42008
```

```
Constant NAC_UnknownFitFunction=42007
```

```
21 Constant NAC_AuxFileLoadFailed=42006
```

```
Constant NAC_AuxFileNotFound=42005
```

```
Constant NAC_NotApplicable=42003
```

```
Constant NAC_DataMismatch=42002
```

```
Constant NAC_UnknownMeasurement=42001
```

```
26 //Well Handled Error Codes
```

```
Constant NAC_ReEntry=42101
```

```
Constant NAC_NoSuchWindow=42102
```

```
Constant NAC_AvgAlreadyInitialized=42103
```

```
Constant NAC_WindowAlreadyExists=42105
```

```
31 Constant NAC_NothingToProcess=42106
```

```
Constant NAC_FitWavesMissing=42107
```

```
Constant NAC_AverageWavesMissing=42110
```

```
Constant NAC_WrongCursor=42111
```

```
Constant NAC_StickingMissing=42112
```

```
36 Constant NAC_AdsorptionMissing=42113
```

```
Constant NAC_DoseMissing=42113
```

```
Constant NAC_ParameterOutsideRange=42114
```

```
Constant NAC_NotInitialized=42115
```

```
//Other Constants
```

```
41 Constant NAC_RatioTypeReflectivity=1
```

```
Constant NAC_RatioTypeTransmission=2
```

```
Constant NAC_RatioTypeSensitivity=3
```

```
Constant R_Gas=8.3144621 // J / mol K
```

```
46 Constant N_Avo=6.02214085774e23 // 1 / mol
```

```
//
```

Menu

```
Menu "NAC", dynamic
```

```
"Initialize", /Q, NAC_Initialize()
```

```
"Show Control Panel/1" , /Q, Error_Clear(); NAC_ShowControlPanel()
```

```
"_"
```

```
51 SubMenu "Data Manipulation"
```

```
"Remove Detector Baseline", /Q, Error_Clear(); NAC_RemoveBaseLine()
```

```
"Invert Polarity", /Q, Error_Clear(); NAC_Invert()
```

```

"Correct for Gain", /Q, Error_Clear(); NAC_CorrectGain()
"Unload Measurement", /Q, Error_Clear(); NAC_Unload()
56 "Remove Experiment Structure", /Q, Error_Clear(); NAC_RemoveNAC()
End
"Display Statistics", /Q, Error_Clear(); NAC_DisplayStatistics("All")
SubMenu "Auto Flag"
  "All", /Q, Error_Clear(); NAC_AutoFlagAll(); NAC_GetAllStatistics(); ↵
  ↵ NAC_DisplayStatistics("All")
61 "Deconvolution", /Q, Error_Clear(); NAC_AutoFlag("Deconvolution"); ↵
  ↵ NAC_GetStatistics("Deconvolution"); NAC_DisplayStatistics("Deconvolution")
  "Before Deposition", /Q, Error_Clear(); NAC_AutoFlag("BeforeCoating"); ↵
  ↵ NAC_GetStatistics("BeforeCoating"); NAC_DisplayStatistics("BeforeCoating")
  "After Deposition", /Q, Error_Clear(); NAC_AutoFlag("AfterCoating"); ↵
  ↵ NAC_GetStatistics("AfterCoating"); NAC_DisplayStatistics("AfterCoating")
  "Laser Reference", /Q, Error_Clear(); NAC_AutoFlag("LaserReference"); ↵
  ↵ NAC_GetStatistics("LaserReference"); NAC_DisplayStatistics("LaserReference" ↵
  ↵ ")
  "Transmission", /Q, Error_Clear(); NAC_AutoFlag("Transmission"); ↵
  ↵ NAC_GetStatistics("Transmission"); NAC_DisplayStatistics("Transmission")
66 "Radiation", /Q, Error_Clear(); NAC_AutoFlag("Radiation"); NAC_GetStatistics ↵
  ↵ ("Radiation"); NAC_DisplayStatistics("Radiation")
  "Zero Sticking", /Q, Error_Clear(); NAC_AutoFlag("ZeroSticking"); ↵
  ↵ NAC_GetStatistics("ZeroSticking"); NAC_DisplayStatistics("ZeroSticking")
End
SubMenu "Reset Flag List"
  "All", /Q, Error_Clear(); NAC_ResetFlagList("All")
71 "Deconvolution", /Q, Error_Clear(); NAC_ResetFlagList("Deconvolution")
  "Before Deposition", /Q, Error_Clear(); NAC_ResetFlagList("BeforeCoating")
  "After Deposition", /Q, Error_Clear(); NAC_ResetFlagList("AfterCoating")
  "Laser Reference", /Q, Error_Clear(); NAC_ResetFlagList("LaserReference")
  "Transmission", /Q, Error_Clear(); NAC_ResetFlagList("Transmission")
76 "Radiation", /Q, Error_Clear(); NAC_ResetFlagList("Radiation")
  "Zero Sticking", /Q, Error_Clear(); NAC_ResetFlagList("ZeroSticking")
  "Heat", /Q, Error_Clear(); NAC_ResetFlagList("Heat")
  "Sticking", /Q, Error_Clear(); NAC_ResetFlagList("Sticking")
End
81 SubMenu "Copy Flag List"
  "Heat -> Sticking", /Q, Error_Clear(); NAC_CopyFlagList("Heat", "Sticking")
  "Sticking -> Heat", /Q, Error_Clear(); NAC_CopyFlagList("Sticking", "Heat")
End
SubMenu "Fitted Trends"
86 "Fit Radiation", /Q, Error_Clear(); NAC_CreateTrend("Radiation")
  "Fit Desorption", /Q, Error_Clear(); NAC_CreateTrend("Desorption")
End
"_"
"Update Experiment Version/5", /Q, NAC_UpdateVersion()
91 "Concatenate Calorimetry Files", /Q, Error_Clear(); NAC_Concat()
  "Trim Calorimetry Files", /Q, Error_Clear(); NAC_Trim()
  "_"
SubMenu "Settings"
  NAC_MenuAutoFlag(), /Q, NAC_ToggleAutoFlagging()
96 NAC_MenuLoadSupport(), /Q, NAC_ToggleLoadSupport()
  NAC_MenuStoreFiltered(), /Q, NAC_ToggleStoreFiltered()
  NAC_MenuAutoUpdateAverages(), /Q, NAC_ToggleAutoUpdateAverages()
  NAC_MenuShowBoxPlotData(), /Q, NAC_ToggleShowBoxPlotData()
End
101 "_"
SubMenu "Average Experiments"
  "Load Results/2", /Q, Error_Clear(); NAC_Results_Load()
  "Average Loaded Experiments", /Q, Error_Clear(); NAC_Results_Average()
  "Remove Loaded Experiment", /Q, Error_Clear(); NAC_Results_Remove()
106 "Display Averaged Results", /Q, Error_Clear(); NAC_Results_Display()
End
"_"
"Display NAC-Status", /Q, Error_Clear(); NAC_DisplayStatus()
End

```

111 //

C.1.2 Initialization

//

Function NAC_Initialize

```

Function NAC_Initialize()
  NewPath /O /Q CalDataPath NAC_DataPathStr
  Error_Init()
116  Error_Clear()
  If (DataFolderExists("root:NAC"))
    Error_Message(KillWins("NAC"), ",KillWins", "NAC_Initialize", "NAC")
    Error_Message(KillDependencies(), "KillDependencies", "NAC_Initialize", "NAC"
    ↵ ")
    KillDataFolder /Z root:NAC
121  If (V_Flag)
    Return Error_Message(NAC_DataFolderError, "InProc", "NAC_Initialize", "NAC"
    ↵ ")
    EndIf
  EndIf
  Error_Message(Variables(), "Variables", "NAC_Initialize", "NAC")
126  Error_Message(Dependencies(), "Dependencies", "NAC_Initialize", "NAC")
  Error_Message(NAC_Panels(), "Panels", "NAC_Initialize", "NAC")
  ExperimentModified 0
  Return NoError
End
131 //
```

Function Variables

```

Static Function Variables()
String RateMeasurements="RateCalorimetry;RateCoating;"
String CalorimetryMeasurements="LaserReference;Transmission;BeforeCoating;↵
  ↵ AfterCoating;Deconvolution;Radiation;Heat;Sticking;ZeroSticking;"
Variable i
136 DFRef OldDF=GetDataFolderDFR()
  NewDatafolder /S root:NAC
  // User interface
  NewDatafolder /S root:NAC:GUI
  Variable /G WWidth=400, WHeight=275, MarginTop=45
141  Variable /G ReEntryFlagWin=0, ReEntryCursor=0, ReEntryPosProc=0
  Variable /G ProgressValue
  Variable /G PositiveRange, NegativeRange
  Variable /G PositiveRangeSticking, NegativeRangeSticking
  Variable /G RangeDeconvolution
146  Variable /G LoadSupportFiles=0
  Variable /G StoreFilteredWaves=0
  Variable /G ShowBoxPlotData=1
  String /G PositiveName="", NegativeName=""
  String /G PositiveNameSticking="", NegativeNameSticking=""
151  String /G NameRangeDeconvolution=""
  Make /N=0 StatsLabelPos
  Make /N=0 /T StatsLabels
  // Machine specific parameters
  NewDatafolder /S root:NAC:Machine
156  String /G LaserPowerCorrectionList="1.28;1.38682;1.31814;1.15762;" // Laser ↵
    ↵ Power Correction Factors // Add new one in the begining // Exp. 2013-12-22
  String /G ReflectivityCleanList="0.444 Ni/PVDF;0.436 Ni/PVDF old;0.89 Al/PVDF;"↵
    ↵ // Reflectivities of Clean Samples // Number must come first! // ↵
    ↵ External Measurement R( HD-PTFE)=0.948 R(LD-PTFE)=R(Spetralon)=0.978 !!
  Variable /G LaserPowerCorrection=Str2Num(StringFromList(0, ↵
    ↵ LaserPowerCorrectionList, ";"))
  Variable /G ReflectivityClean=Str2Num(StringFromList(0, ReflectivityCleanList, ↵
    ↵ ";"))
  Variable /G BeamDiameter=0.0045 // Construction Nozzle
161  Variable /G QCMDiameter=0.006 // Data sheet
  Variable /G QCMToolingCalorimetry=1.09042 // Sauerbrey sensitivity
  Variable /G QCMToolingCoating=0.604 // Exp. 2013-06-19 EXCEL
  Variable /G QMSToolingCalorimetry=0.959158 // Exp. 2013-12-20 Tooling QMS
  Variable /G RateFittingWindow=60 // Data Points
```



```

166 Variable /G DeconvolutionWindow=0.012 // Empirical; Lower:Noisy -- Higher: ↵
    ↵ Artefacts...
Variable /G PulseLengthDetectionWindow=0.1
Variable /G HighpassFrequency=0.175
Variable /G LineNotchFrequency=50
Variable /G SecondNotchFrequency=0
171 Variable /G NyquistFrequency=500, ProcessRate
Variable /G TrimTrendRange=5 // Neglect TrimTrendRange data points at start ↵
    ↵ and end for trends
NewDatafolder /S root:NAC:Enthalpies
Variable /G MultiLayerPosLow=NaN, MultiLayerPosHigh=NaN
Variable /G MultiLayerEnthalpy, MultiLayerEnthalpyError
176 Variable /G SubtractAdsorbed=NaN, SubtractDesorbed=NaN
Make /N=2 MultiLayerReference=0, ThicknessRange=NaN, StickingLimit=1
Make /N=0 Coverage, Enthalpy, Sticking, Thickness
Setscale /P x, 0, 1, "Frame", Coverage, Enthalpy, Sticking
Setscale /P d, 0, 0, "ML", Coverage
181 Setscale /P d, 0, 0, "J/mol", Enthalpy, MultiLayerReference
Setscale /P d, 0, 0, "", Sticking
SetScale /P x 0, 1, "m", ThicknessRange
NewDatafolder /S root:NAC:Experiment // Common settings in an experiment
String /G ProjectVersion=NAC_Version
186 String /G ExperimentName
Variable /G SampleRate=0
Variable /G DataPointsPerFrame=0
Variable /G OpenCloseSteps=0
Variable /G ChopperPeriod=0, ChopperDelay=0, NominalPulseLength=0
191 Variable /G PulseLength=0
Variable /G LengthDetectFailed
Variable /G TemperatureSample=NaN, TemperatureSource=NaN
Variable /G AutoFlag=1, AutoFlagged=0
Variable /G UseFittedRadiation=0, UseFittedDesorption=0
196 Variable /G MirrorContamination=1//0.84898 // Usually ==1 // EXP0020 Mirror ↵
    ↵ Contamination
Variable /G SwitchDeadTime=0
Variable /G UseEmptyCrucibleReference=0
Variable /G EmptyCrucibleTemperature=NaN
For (i=0;i<ItemsInList(CalorimetryMeasurements);i+=1)
201 NewDatafolder /S $"root:NAC:"+StringFromList(i,CalorimetryMeasurements)
NewDatafolder $"root:NAC:"+StringFromList(i,CalorimetryMeasurements)+": ↵
    ↵ Auxiliaries"
If (!StringMatch(StringFromList(i,CalorimetryMeasurements),"Sticking"))
    Make /T /N=1 Header={"Not Loaded"}
EndIf
206 String /G FileName="Not Loaded"
Variable /G Loaded=0
Make /N=0 DisplayRaw, DisplayFit
Make /N=0 /B /U FlagList
Variable /G NumberOfFrames, EffectiveFrames
211 Variable /G CurrentFrame=0
Variable /G BrowseDeconvolutionIndex=0
Wave FlagList
StrSwitch (StringFromList(i,CalorimetryMeasurements))
    Case "Heat":
216 Case "Sticking":
        Break
    Default:
        NewDatafolder /S $"root:NAC:"+StringFromList(i,CalorimetryMeasurements) ↵
        ↵ +":Statistics"
        Make /N=0 Amplitude, Position, ChiSq, Outlier
221 Make /N=1 Medians=NaN
        Make /N=2 Quartiles=NaN, Whiskers=NaN, WhiskerLimits=NaN
        Wave Amplitude, Outlier
        SetScale /P x, 0, 1, "Frame", Amplitude, FlagList, ChiSq, Outlier
        SetScale /P d, 0, 2, "Relative Amplitude", Amplitude
226 Variable /G AutoFlagged=0, StdDev=NaN
    EndSwitch
EndFor
For (i=0;i<ItemsInList(RateMeasurements);i+=1)

```

```
NewDatafolder /S $"root:NAC:"+StringFromList(i,RateMeasurements)
231 NewDatafolder $"root:NAC:"+StringFromList(i,RateMeasurements)+":Auxiliaries"
    Make /T /N=1 Header={"Not Loaded"}
    String /G FileName="Not Loaded"
    Variable /G Loaded=0
    String /G Substance="", SubstanceName=""
236 Make /N=2 FittedRateAvg, FittedRateErrorPos, FittedRateErrorNeg
    Variable /G BaselineTo, BaselineFrom
    Variable /G UseBaseline
    Variable /G DepositionRate=0
    Variable /G BaselineBefore=0, ApparentRate=0, BaselineAfter=0
241 Variable /G TotalThickness=0, ThicknessMonoLayers=0, Duration=0
    Variable /G Density, MolarMass, MonolayerDensity
    Variable /G FittedFrom=NaN, FittedTo=NaN
    Variable /G FittedAvg=NaN, FittedSDev=NaN
EndFor
246 NVar ReflectivityClean=root:NAC:Machine:ReflectivityClean
    SetDatafolder root:NAC:Deconvolution
    Variable /G Reflectivity=ReflectivityClean
    Variable /G LaserPower
    Variable /G SampleRate=0
251 Variable /G DataPointsPerFrame=0
    Variable /G OpenCloseSteps=0
    Variable /G ChopperPeriod=0, ChopperDelay=0, NominalPulseLength=0
    Variable /G PulseLength=0
    Variable /G AverageFrames=1
256 Variable /G RemoveFixedRadiation, RemoveFittedRadiation, UseFittedFitWave=1
    Variable /G SwitchDeadTime=0
    Variable /G Sensitivity=1, UseSensitivity=1
    SetDatafolder root:NAC:BeforeCoating
    Variable /G Reflectivity=ReflectivityClean
261 Variable /G LaserPower
    SetDatafolder root:NAC:AfterCoating
    Variable /G Reflectivity=NaN
    Variable /G LaserPower
    SetDatafolder root:NAC:LaserReference
266 Variable /G Reflectivity=ReflectivityClean
    Variable /G LaserPower
    SetDatafolder root:NAC:Transmission
    Variable /G Transmission
    Variable /G LaserPower
271 SetDatafolder root:NAC:Radiation
    SetDatafolder root:NAC:ZeroSticking
    SetDatafolder root:NAC:Heat
    Variable /G InitOffset=0, InitAdsorption=1e-6, InitRadiation=1
    Variable /G InitAdsorptionShift=0, InitRadiationShift=0
276 Variable /G HoldOffset=0, HoldAdsorption=0, HoldRadiation=0
    Variable /G HoldAdsorptionShift=1, HoldRadiationShift=1, LinkShifts=1
    Make /N=0 Offset, Adsorption, Radiation, ShiftAds, ShiftRad, ChiSq, ↵
        ↵ fit_Radiation, orig_Radiation
    SetScale /I x, 0, 1, "Frame", Offset, Adsorption, Radiation, ShiftAds, ShiftRad ↵
        ↵ , ChiSq, fit_Radiation, orig_Radiation
    SetDatafolder root:NAC:Sticking
281 Variable /G InitOffset=0, InitDesorption=0.5
    Variable /G InitShift=0
    Variable /G HoldOffset=0, HoldDesorption=0, HoldShift=1
    Make /N=0 Offset, Desorption, Shift, ChiSq, fit_Desorption, orig_Desorption
    SetScale /I x, 0, 1, "Frame", Offset, Desorption, Shift, ChiSq, fit_Desorption, ↵
        ↵ orig_Desorption
286 Make /N=2 StickingLimit=1
    SetDatafolder root:NAC:RateCoating:
    Variable /G UseTotalRange=1
    SetDatafolder root:NAC:RateCalorimetry:
    Variable /G DosePerPulse=0, MoleDosePerPulse=0
291 Variable /G RateMonoLayer=0
    SetDatafolder root:NAC:
    SetScale d 0, 0, "s", :Heat:ShiftAds, :Heat:ShiftRad, :Sticking:Shift
    SetScale d 0, 0, "J", :Heat:Adsorption
    SetDataFolder OldDF
```

```

296   CreateDebyeIntegral()
      Return NoError
End
//

```

Function Dependencies

```

Static Function Dependencies()
301 Variable i
String Measurements="LaserReference;Transmission;BeforeCoating;AfterCoating;↵
    ↵ Radiation;Heat;Sticking;ZeroSticking;Deconvolution;"
SetFormula root:NAC:Machine:ProcessRate "2*NyquistFrequency" // Hz
SetFormula root:NAC:Experiment:EmptyCrucibleTemperature "Mean(root:NAC:↵
    ↵ Radiation:Auxiliaries:Source)"
SetFormula root:NAC:BeforeCoating:Reflectivity "root:NAC:Machine:↵
    ↵ ReflectivityClean" // d.l.
306 SetFormula root:NAC:LaserReference:Reflectivity "root:NAC:Machine:↵
    ↵ ReflectivityClean" // d.l.
SetFormula root:NAC:Deconvolution:Reflectivity "root:NAC:Machine:↵
    ↵ ReflectivityClean" // d.l.
SetFormula root:NAC:Deconvolution:PulseLength "root:NAC:Deconvolution:↵
    ↵ NominalPulseLength"
SetFormula root:NAC:RateCalorimetry:DepositionRate "root:NAC:RateCalorimetry:↵
    ↵ UseBaseline ? (root:NAC:RateCalorimetry:ApparentRate - (root:NAC:↵
    ↵ RateCalorimetry:BaselineBefore+root:NAC:RateCalorimetry:BaselineAfter)/2) :↵
    ↵ (root:NAC:RateCalorimetry:ApparentRate)" // m/s
SetFormula root:NAC:RateCalorimetry:RateMonoLayer "root:NAC:RateCalorimetry:↵
    ↵ DepositionRate * (root:NAC:RateCalorimetry:Density*1e3) / (root:NAC:↵
    ↵ RateCalorimetry:MolarMass*1e-3) / (root:NAC:RateCalorimetry:↵
    ↵ MonoLayerDensity) * N_Avo" // ML/s
311 SetFormula root:NAC:RateCalorimetry:DosePerPulse "root:NAC:RateCalorimetry:↵
    ↵ RateMonoLayer * root:NAC:Experiment:PulseLength" // ML/Pulse
SetFormula root:NAC:RateCalorimetry:MoleDosePerPulse "root:NAC:RateCalorimetry:↵
    ↵ DepositionRate * root:NAC:Experiment:PulseLength * (root:NAC:↵
    ↵ RateCalorimetry:Density*1e3) / (root:NAC:RateCalorimetry:MolarMass*1e-3) * ↵
    ↵ (root:NAC:Machine:BeamDiameter/2)^2*pi" // m/s*s/Pulse*kg/m^3/(kg/mol)*m↵
    ↵ ^2=mol/Pulse <-- relevant quantity
SetFormula root:NAC:RateCoating:Duration "root:NAC:RateCoating:Timeline[root:↵
    ↵ NAC:RateCoating:BaselineFrom] - root:NAC:RateCoating:Timeline[root:NAC:↵
    ↵ RateCoating:BaselineTo]" // s
SetFormula root:NAC:RateCoating:DepositionRate "root:NAC:RateCoating:↵
    ↵ UseBaseline ? root:NAC:RateCoating:ApparentRate - (root:NAC:RateCoating:↵
    ↵ BaselineBefore+root:NAC:RateCoating:BaselineAfter)/2 : root:NAC:RateCoating↵
    ↵ :ApparentRate" // m/s
SetFormula root:NAC:RateCoating:TotalThickness "root:NAC:RateCoating:↵
    ↵ UseTotalRange ? ((root:NAC:RateCoating:Thickness[root:NAC:RateCoating:↵
    ↵ BaselineFrom] - root:NAC:RateCoating:Thickness[root:NAC:RateCoating:↵
    ↵ BaselineTo]) * root:NAC:Machine:QCMToolingCoating) : (root:NAC:RateCoating:↵
    ↵ DepositionRate*root:NAC:RateCoating:Duration)" // m
316 SetFormula root:NAC:Enthalpies:SubtractAdsorbed "NAC_CorrAdsorbed(root:NAC:↵
    ↵ RateCalorimetry:Substance,root:NAC:Experiment:TemperatureSample,root:NAC:↵
    ↵ Experiment:TemperatureSource)" // J/mol
SetFormula root:NAC:Enthalpies:SubtractDesorbed "NAC_CorrDesorbed(root:NAC:↵
    ↵ RateCalorimetry:Substance,root:NAC:Experiment:TemperatureSample,root:NAC:↵
    ↵ Experiment:TemperatureSource)" // J/mol
SetFormula root:NAC:Enthalpies:MultiLayerEnthalpy "Mean(root:NAC:Enthalpies:↵
    ↵ Enthalpy, root:NAC:Enthalpies:MultilayerPosLow, root:NAC:Enthalpies:↵
    ↵ MultilayerPosHigh)" // J/mol
SetFormula root:NAC:Enthalpies:MultiLayerEnthalpyError "Sqrt(Variance(root:NAC:↵
    ↵ Enthalpies:Enthalpy, root:NAC:Enthalpies:MultilayerPosLow, root:NAC:↵
    ↵ Enthalpies:MultilayerPosHigh))" // J/mol
SetFormula root:NAC:Enthalpies:MultiLayerReference "NAC_RefEnthalpy(root:NAC:↵
    ↵ RateCalorimetry:Substance,root:NAC:Experiment:TemperatureSample)" // J/mol
321 SetFormula root:NAC:Enthalpies:Thickness "root:NAC:Enthalpies:Coverage / (root:↵
    ↵ NAC:RateCalorimetry:Density*1e3) * (root:NAC:RateCalorimetry:MolarMass*1e-3)↵
    ↵ * (root:NAC:RateCalorimetry:MonoLayerDensity)/N_Avo" // m
For (i=0;i<ItemsInList(Measurements, ";");i+=1)
SetFormula $"root:NAC:"+StringFromList(i,Measurements, ";")+":EffectiveFrames"↵
    ↵ "root:NAC:"+StringFromList(i,Measurements, ";")+":NumberOfFrames-Sum(root:↵
    ↵ NAC:"+StringFromList(i,Measurements, ";")+":FlagList)" //Frames

```

```

    EndFor
    Return NoError
326 End
    //
Function CreateDebyeIntegral
Static Function CreateDebyeIntegral()
    Make /D /N=5000 root:NAC:Enthalpies:Debye_Integral
    Make /FREE /D /N=5000 Temp
331 Wave Debye_Integral=root:NAC:Enthalpies:Debye_Integral
    SetScale /I x, 1e-6, 20, "", Temp, Debye_Integral // Theta/T
    MultiThread Temp=x^4*Exp(x)/(Exp(x)-1)^2
    MultiThread Debye_Integral=Area(Temp,0,x)
    KillWaves Temp
336 End
    //
Function KillDependencies
Static Function KillDependencies() // Necessary only for dependencies including ↵
    ↵ wave references
Variable i
String Measurements="LaserReference;Transmission;ReflecBefore;BeforeCoating;↵
    ↵ ReflecAfter;AfterCoating;Radiation;Heat;Sticking;ZeroSticking;Deconvolution↵
    ↵ ;"
341 If (DataFolderExists("root:NAC"))
    SetFormula root:NAC:Experiment:EmptyCrucibleTemperature ""
    SetFormula root:NAC:Sticking:FlagList ""
    SetFormula root:NAC:Enthalpies:MultiLayerEnthalpy ""
    SetFormula root:NAC:Enthalpies:MultiLayerReference ""
346 SetFormula root:NAC:Enthalpies:Thickness ""
    SetFormula root:NAC:Enthalpies:MultiLayerEnthalpy ""
    If (DataFolderExists("root:NAC:RateCoat"))
        SetFormula root:NAC:RateCoat:TotalThickness ""
        SetFormula root:NAC:RateCoat:Duration ""
351 ElseIf (DataFolderExists("root:NAC:RateCoating"))
        SetFormula root:NAC:RateCoating:TotalThickness ""
        SetFormula root:NAC:RateCoating:Duration ""
    EndIf
    If (Exists("root:NAC:Enthalpies:MultiLayerEnthalpyError"))
356 SetFormula root:NAC:Enthalpies:MultiLayerEnthalpyError ""
    EndIf
    For (i=0;i<ItemsInList(Measurements, ";");i+=1)
        If (DataFolderExists("root:NAC:"+StringFromList(i,Measurements, ";")))
            SetFormula $"root:NAC:"+StringFromList(i,Measurements, ";")+":↵
    ↵ EffectiveFrames" ""
361 EndIf
    EndFor
    EndIf
    Return NoError
366 //

```

C.1.3 Graphical User Interface

```

//
Function NAC_RemoveNAC
Function NAC_RemoveNAC()
    If (DataFolderExists("root:NAC"))
        DoAlert 1, "Delete the NAC data folder and discard all included data?"
371 If (V_Flag!=1)
            Error_Message(UserAbort, "InProc", "NAC_RemoveNAC", "")
            Return NaN
        EndIf
        Error_Message(KillWins("NAC"), "KillWins", "NAC_RemoveNAC", "")
376 Error_Message(KillDependencies(), "KillDependencies", "NAC_RemoveNAC", "")
        KillDataFolder /Z root:NAC
        If (V_Flag)
            Error_Message(NAC_DataFolderError, "InProc", "NAC_RemoveNAC", "")
            Return NaN
        EndIf
    EndIf

```

```

381     EndIf
      Else
        Error_Message(NAC_NotInitialized, "InProc", "NAC_RemoveNAC", "")
      EndIf
      Return NoError
386 End
    //
Function NAC_Unload
Function NAC_Unload()
  String NameList="Deconvolution;BeforeCoating;RateCoating;AfterCoating;↵
    ↵ LaserReference;Transmission;Radiation;RateCalorimetry;ZeroSticking;Heat;↵
    ↵ Sticking"
  String Name=""
391  Variable i, j
    If (!DataFolderExists("root:NAC"))
      Return NaN
    EndIf
    For (i=0;i<ItemsInList(NameList);i+=1)
396      NVar Loaded="$root:NAC:"+StringFromList(i, NameList, ";")+":Loaded"
        If (Loaded)
          Name+=StringFromList(i, NameList, ";")+";"
        EndIf
    EndFor
401  NameList="Cancel;" + Name
    Name=""
    Prompt Name, "Measurement: ", popup, NameList
    DoPrompt /HELP="" "Remove Measurement", Name
    If (!V_Flag && !StringMatch(Name, "Cancel"))
406      DFRef OldDF=GetDataFolderDFR()
        SetDataFolder "$root:NAC:"+Name
        StrSwitch (Name)
          Case "Heat":
            Case "Sticking":
411              NameList="Heat;Sticking;"
                KillWins("NAC_Desorption")
                KillWins("NAC_Adsorption")
                KillWins("NAC_Radiation_VsFrame")
                Break
            Case "BeforeCoating":
            Case "AfterCoating":
416              NVar Reflec=root:NAC:AfterCoating:Reflectivity
                Reflec=NaN
                NameList=Name+";"
            Break
421          Case "LaserReference":
            Case "Transmission":
                KillWins("NAC_Heat")
                KillWins("NAC_Adsorption")
426              NameList=Name+";"
                NVar Trans=root:NAC:Transmission:Transmission
                Trans=NaN
                Break
            Case "ZeroSticking":
431              KillWins("NAC_Sticking")
                KillWins("NAC_Desorption")
                NameList=Name+";"
                Break
            Default:
436              NameList=Name+";"
                Break
        EndSwitch
        For (j=0; j<ItemsInList(NameList); j+=1)
441          Name=StringFromList(j, NameList)
            KillWins("NAC_" + Name)
            SetDataFolder "$root:NAC:"+Name+":Auxiliaries"
            KillWaves /A
            SetDataFolder "$root:NAC:"+Name
            NVar Loaded

```

```

446     SVar FileName
      Make /O /T /N=1 Header={"Not Loaded"}
      FileName="Not Loaded"
      Loaded=0
      StrSwitch (Name)
451         Case "RateCalorimetry":
            SetFormula root:NAC:RateCalorimetry:DepositionRate ""
            SetFormula root:NAC:RateCalorimetry:RateMonoLayer ""
            SetFormula root:NAC:RateCalorimetry:DosePerPulse ""
            SetFormula root:NAC:RateCalorimetry:MoleDosePerPulse ""
456         Break
            Case "RateCoating":
                SetFormula root:NAC:RateCoating:Duration ""
                SetFormula root:NAC:RateCoating:DepositionRate ""
                SetFormula root:NAC:RateCoating:TotalThickness ""
461         Break
            Case "BeforeCoating":
            Case "AfterCoating":
            Case "LaserReference":
            Case "Transmission":
466         Case "Deconvolution":
            NVar LaserPower
            LaserPower=0
            Break
            Default:
471         Break
      EndSwitch
      StrSwitch (Name)
            Case "RateCoating":
            Case "RateCalorimetry":
476         SVar Substance, SubstanceName
            Substance=""
            SubstanceName=""
            NVar DepositionRate, BaselineBefore, ApparentRate, BaselineAfter, ↗
            TotalThickness, ThicknessMonoLayers, Duration, Density, MolarMass, ↗
            ↘ MonolayerDensity
                NVar FittedFrom, FittedTo, FittedAvg, FittedSDev
481         BaselineBefore=0
            ApparentRate=0
            BaselineAfter=0
            TotalThickness=0
            ThicknessMonoLayers=0
486         Duration=0
            Density=NaN
            MolarMass=NaN
            MonolayerDensity=0
            FittedFrom=NaN
491         FittedTo=NaN
            FittedAvg=NaN
            FittedSDev=NaN
            DepositionRate=0
            Wave Thickness, Timeline, Thickness_FitHigh, Thickness_FitMid, ↗
            ↘ Thickness_FitLow, Timeline_FitHigh, Timeline_FitMid, Timeline_FitLow
496         KillWaves Thickness, Timeline, Thickness_FitHigh, Thickness_FitMid, ↗
            ↘ Thickness_FitLow, Timeline_FitHigh, Timeline_FitMid, Timeline_FitLow
            Break
            Default:
                Wave DisplayFit, DisplayRaw, FlagList, Detector
501         ReDimension /N=0 DisplayFit, DisplayRaw, FlagList
            KillWaves /Z Detector
            NVar NumberOfFrames, CurrentFrame, BrowseDeconvolutionIndex
            NumberOfFrames=0
            CurrentFrame=0
            BrowseDeconvolutionIndex=0
506         Break
      EndSwitch
      StrSwitch (Name)
            Case "RateCoating":
            Break

```

```

511     Case "RateCalorimetry":
        NVar DosePerPulse, MoleDosePerPulse, RateMonoLayer
        DosePerPulse=0
        MoleDosePerPulse=0
        RateMonoLayer=0
516     Break
        Case "Heat":
        Case "Sticking":
            Break
        Default:
521     NVar AutoFlagged="$root:NAC:"+Name+":Statistics:AutoFlagged", ↵
        ↵ AutoFlaggedExp=root:NAC:Experiment:AutoFlagged
            Wave StatAmp="$root:NAC:"+Name+":Statistics:Amplitude", StatWhi="$root:↵
        ↵ NAC:"+Name+":Statistics:Whiskers", StatWhiLim="$root:NAC:"+Name+":↵
        ↵ Statistics:WhiskerLimits"
            Wave StatQuart="$root:NAC:"+Name+":Statistics:Quartiles", StatPos="$↵
        ↵ root:NAC:"+Name+":Statistics:Position", StatMed="$root:NAC:"+Name+":↵
        ↵ Statistics:Medians"
            Wave StatChiSq="$root:NAC:"+Name+":Statistics:ChiSq", StatOutlier="$↵
        ↵ root:NAC:"+Name+":Statistics:Outlier"
526     AutoFlagged=0
        AutoFlaggedExp=0
        ReDimension /N=0 StatAmp, StatPos, StatChiSq, StatOutlier
        StatMed=NaN
        StatQuart=NaN
        StatWhi=NaN
531     StatWhiLim=NaN
        Break
    EndSwitch
    StrSwitch (Name)
        Case "Heat":
536     Wave Radiation, Adsorption, Offset, ShiftAds, ShiftRad, ChiSq, ↵
        ↵ fit_Radiation
            Wave Enthalpy=root:NAC:Enthalpies:Enthalpy
            ReDimension /N=0 Radiation, Adsorption, Enthalpy, Offset, ShiftAds, ↵
        ↵ ShiftRad, fit_Radiation
            ReDimension /N=(NumberOfFrames) ChiSq
            NVar UseFR=root:NAC:Experiment:UseFittedRadiation
541     ChiSq=0
            UseFR=0
            CheckBox FittedRad Disable=2, Win=NAC_Control
            Break
        Case "Sticking":
546     Wave Desorption, Offset, Shift, ChiSq, fit_Desorption
            Wave Sticking=root:NAC:Enthalpies:Sticking
            Wave Coverage=root:NAC:Enthalpies:Coverage, Thickness=root:NAC:↵
        ↵ Enthalpies:Thickness
            NVar UseFD=root:NAC:Experiment:UseFittedDesorption
            ReDimension /N=(0) Desorption, Offset, Shift, Sticking, Coverage, ChiSq↵
        ↵ , fit_Desorption, Thickness
551     ReDimension /N=(NumberOfFrames) ChiSq
            ChiSq=0
            UseFD=0
            CheckBox FittedDes Disable=2, Win=NAC_Control
            Break
556     Case "LaserReference":
            NVar Failed=root:NAC:Experiment:LengthDetectFailed
            Failed=0
            Break
        Default:
561     Break
    EndSwitch
    StrSwitch (Name)
        Case "BeforeCoating":
            KillWaves /Z root:NAC:Experiment:FitReflectivityOdd, root:NAC:↵
        ↵ Experiment:FitReflectivityEven
566     Break
        Case "LaserReference":

```

```

        KillWaves /Z root:NAC:Experiment:FitLaserReferenceOdd, root:NAC:↵
↵ Experiment:FitLaserReferenceEven
        Break
        Case "Radiation":
571     KillWaves /Z root:NAC:Experiment:FitRadiationOdd, root:NAC:Experiment:↵
↵ FitRadiationEven
        Break
        Case "ZeroSticking":
        KillWaves /Z root:NAC:Experiment:FitStickingOdd, root:NAC:Experiment:↵
↵ FitStickingEven
        Break
576     Case "Deconvolution":
        KillWaves /Z root:NAC:Experiment:DeconvolutionOdd, root:NAC:Experiment:↵
↵ FitDeconvolutionEven
        Break
        Default:
        Break
581     EndSwitch
        If (StringMatch(Name, "Heat"))
            NVar TemperatureSource=root:NAC:Experiment:TemperatureSource, ↵
↵ TemperatureSample=root:NAC:Experiment:TemperatureSample
            TemperatureSource=NaN
            TemperatureSample=NaN
586     EndIf
        StrSwitch (Name)
            Case "RateCalorimetry":
                SetFormula root:NAC:RateCalorimetry:DepositionRate "root:NAC:↵
↵ RateCalorimetry:UseBaseline ? (root:NAC:RateCalorimetry:ApparentRate - (↵
↵ root:NAC:RateCalorimetry:BaselineBefore+root:NAC:RateCalorimetry:↵
↵ BaselineAfter)/2) : (root:NAC:RateCalorimetry:ApparentRate)" // m/s
                SetFormula root:NAC:RateCalorimetry:RateMonoLayer "root:NAC:↵
↵ RateCalorimetry:DepositionRate * (root:NAC:RateCalorimetry:Density*1e3) / (↵
↵ root:NAC:RateCalorimetry:MolarMass*1e-3) / (root:NAC:RateCalorimetry:↵
↵ MonolayerDensity) * N_Avo" // ML/s
591     SetFormula root:NAC:RateCalorimetry:DosePerPulse "root:NAC:↵
↵ RateCalorimetry:RateMonoLayer * root:NAC:Experiment:PulseLength" // ML/↵
↵ Pulse
                SetFormula root:NAC:RateCalorimetry:MoleDosePerPulse "root:NAC:↵
↵ RateCalorimetry:DepositionRate * root:NAC:Experiment:PulseLength * (root:↵
↵ NAC:RateCalorimetry:Density*1e3) / (root:NAC:RateCalorimetry:MolarMass*1e↵
↵ -3) * (root:NAC:Machine:BeamDiameter/2)^2*pi" // m/s*s/Pulse*kg/m^3/(kg/↵
↵ mol)*m^2=mol/Pulse <-- relevant quantity
                Case "RateCoating":
                    SetFormula root:NAC:RateCoating:Duration "root:NAC:RateCoating:Timeline↵
↵ [root:NAC:RateCoating:BaselineFrom] - root:NAC:RateCoating:Timeline[root:↵
↵ NAC:RateCoating:BaselineTo]" // s
                    SetFormula root:NAC:RateCoating:DepositionRate "root:NAC:RateCoating:↵
↵ UseBaseline ? root:NAC:RateCoating:ApparentRate - (root:NAC:RateCoating:↵
↵ BaselineBefore+root:NAC:RateCoating:BaselineAfter)/2 : root:NAC:RateCoating↵
↵ :ApparentRate" // m/s
596     SetFormula root:NAC:RateCoating:TotalThickness "root:NAC:RateCoating:↵
↵ UseTotalRange ? ((root:NAC:RateCoating:Thickness[root:NAC:RateCoating:↵
↵ BaselineFrom] - root:NAC:RateCoating:Thickness[root:NAC:RateCoating:↵
↵ BaselineTo]) * root:NAC:Machine:QCMToolingCoating) : (root:NAC:RateCoating:↵
↵ DepositionRate*root:NAC:RateCoating:Duration)" // m
                Default:
                Break
            EndSwitch
        EndFor
601     SetDataFolder OldDF
        EndIf
        Return NoError
    End
    //
Function NAC_CorrectGain
606 Function NAC_CorrectGain()
        String NameList="Deconvolution;Before Coating;After Coating;Laser Reference;↵
↵ Transmission;Radiation;Zero Sticking;Heat;Sticking"

```



```

String Name=""
Variable i, Gain=1
If (!DataFolderExists("root:NAC"))
611   Return NaN
EndIf
For (i=0;i<ItemsInList(NameList);i+=1)
  NVar Loaded="$root:NAC:"+ReplaceString(" ", StringFromList(i, NameList, ";"),↵
  ↵ " ")+"Loaded"
  If (Loaded)
616   Name+=StringFromList(i, NameList, ";")+";"
  EndIf
EndFor
NameList="Cancel;" + Name
Name=""
621 Prompt Name, "Measurement: ", popup, NameList
Prompt Gain, "Gain Correction: "
DoPrompt /HELP="" "Enter Gain for Measurement", Name, Gain
If (!V_Flag && (Gain!=0) && !StringMatch(Name,"Cancel"))
  Wave Detector="$root:NAC:"+ReplaceString(" ", Name+":Detector", "")
626   Detector /= Gain
  Print "root:NAC:"+Name+":Detector devided by " + Num2Str(Gain)+"      Data ↵
  ↵ needs to be processed again."
  Note Detector, "Values devided by " + Num2Str(Gain)
EndIf
End
631 //
Function NAC_MenuAutoFlag
Function /S NAC_MenuAutoFlag()
  If (Exists("root:NAC:Experiment:AutoFlag")!=2)
    Return "( Auto Flagging"
  EndIf
636 NVar AutoFlag=root:NAC:Experiment:AutoFlag
  If (AutoFlag)
    Return "! Auto Flagging"
  Else
    Return "Auto Flagging"
641 EndIf
End
//
Function NAC_MenuLoadSupport
Function /S NAC_MenuLoadSupport()
  If (Exists("root:NAC:GUI:LoadSupportFiles")!=2)
646   Return "( Load Supporting Files"
  EndIf
  NVar LoadSupport=root:NAC:GUI:LoadSupportFiles
  If (LoadSupport)
    Return "! Load Supporting Files"
651 Else
    Return "Load Supporting Files"
  EndIf
End
//
Function NAC_MenuStoreFiltered
656 Function /S NAC_MenuStoreFiltered()
  If (Exists("root:NAC:GUI:StoreFilteredWaves")!=2)
    Return "( Store Filter Residue Waves"
  EndIf
  NVar LoadSupport=root:NAC:GUI:StoreFilteredWaves
661  If (LoadSupport)
    Return "! Store Filter Residue Waves"
  Else
    Return "Store Filter Residue Waves"
  EndIf
666 End

```

//

Function NAC_MenuAutoUpdateAverages

```
Function /S NAC_MenuAutoUpdateAverages ()
  If (Exists("root:NAC_Average:Settings:AutoRecalculate")!=2)
    Return "( Automatically Recalculate Averaged Experiments "
671  EndIf
  NVar AutoRecalculate=root:NAC_Average:Settings:AutoRecalculate
  If (AutoRecalculate)
    Return "! Automatically Recalculate Averaged Experiments "
  Else
676  Return "Automatically Recalculate Averaged Experiments "
  EndIf
End
//
```

Function NAC_MenuShowBoxPlotData

```
Function /S NAC_MenuShowBoxPlotData ()
681  If (Exists("root:NAC:GUI:ShowBoxPlotData")!=2)
    Return "( Show Data Points in Box Plots "
  EndIf
  NVar ShowBoxPlotData=root:NAC:GUI:ShowBoxPlotData
  If (ShowBoxPlotData)
686  Return "! Show Data Points in Box Plots "
  Else
    Return "Show Data Points in Box Plots "
  EndIf
End
691 //
```

Function SetDeconvolutionGraphRanges

```
Static Function SetDeconvolutionGraphRanges(Name, Type)
String Name, Type
Variable Tmp, TmpRange
String WindowList, WName
696 String WinSubList="_Deconv;_BrowseDeconv;_AvgDeconv;"
Variable V1, V2
  StrSwitch (Name)
    Case "Deconvolution":
    Case "RateCalorimetry":
701  Case "RateCoating":
    Return NAC_NotApplicable
    Break
    Case "Sticking":
    Case "ZeroSticking":
706  Return NAC_NotImplementedYet
    Break
  Default:
    WindowList="BeforeCoating;AfterCoating;LaserReference;Transmission;↵
↵ Radiation;Heat;"
    NVar Range=root:NAC:GUI:RangeDeconvolution
711  SVar DefRange=root:NAC:GUI:NameRangeDeconvolution
    Break
  EndSwitch
  NVar Loaded="$root:NAC:"+Name+":Loaded"
  If (!Loaded)
716  Return NAC_NoDataLoaded
  EndIf
  StrSwitch (Type)
    Case "AverageEven":
721  Wave DispWave="$root:NAC:Deconvolution:"+Name+" AvgEven "
    Break
    Case "AverageOdd":
    Wave DispWave="$root:NAC:Deconvolution:"+Name+" AvgOdd "
    Break
726  Case "Deconvolution":
    Wave DispWave="$root:NAC:"+Name+":Deconvolution "
    Break
  Default:
```

```

        Return NAC_NotApplicable
        Break
731 EndSwitch
    Tmp=Max(Abs(WaveMin(DispWave)), Abs(WaveMax(DispWave)))
    TmpRange=((Tmp>0) ? Ceil(Tmp/10^Floor(Log(Abs(Tmp)))) : Floor(Tmp/10^Floor(Log(↵
↵ Abs(Tmp)))) ) * 10^Floor(Log(Abs(Tmp)))
    If ((TmpRange>Range) || StringMatch(Name, DefRange))
        Range=TmpRange
736 DefRange=Name
    EndIf
    For (V1=0; V1<ItemsInList(WindowList); V1+=1)
        For (V2=0; V2<ItemsInList(WinSubList); V2+=1)
            WName="NAC_" + StringFromList(V1, WindowList, ";") + StringFromList(V2, WinSubList ↵
↵ ", ";")
741 DoWindow $WName
            If (V_Flag)
                If (StringMatch(StringFromList(V2, WinSubList, ";"), "_Deconv")
                    ModifyImage /W=$WName Deconvolution ctab= {-Range, Range, RedWhiteBlue ↵
↵ , 1}
            Else
746 If (Range==0)
                SetAxis /W=$WName left *, *
            Else
                SetAxis /W=$WName left -Range, Range
            EndIf
751 EndIf
        EndIf
    EndFor
    EndFor
    Return NoError
756 End
//

```

Function SetGraphRanges

```

Static Function SetGraphRanges(Name[, ProcessWave])
String Name, ProcessWave
Variable Tmp, Range
761 String WindowList, WName
String WinSubList="_Full;_Flag;_Frames;_Avg;"
Variable V1, V2
    StrSwitch (Name)
        Case "Deconvolution":
766 Case "RateCalorimetry":
        Case "RateCoating":
            Return NAC_NotApplicable
            Break
        Case "Sticking":
771 Case "ZeroSticking":
            WindowList="Sticking;ZeroSticking;"
            NVar Pos=root:NAC:GUI:PositiveRangeSticking, Neg=root:NAC:GUI:↵
↵ NegativeRangeSticking
            SVar DefPos=root:NAC:GUI:PositiveNameSticking, DefNeg=root:NAC:GUI:↵
↵ NegativeNameSticking
            Break
776 Default:
            WindowList="BeforeCoating;AfterCoating;LaserReference;Transmission;↵
↵ Radiation;Heat;"
            NVar Pos=root:NAC:GUI:PositiveRange, Neg=root:NAC:GUI:NegativeRange
            SVar DefPos=root:NAC:GUI:PositiveName, DefNeg=root:NAC:GUI:NegativeName
            Break
781 EndSwitch
    NVar Loaded="$root:NAC:"+Name+": Loaded"
    If (!Loaded)
        Return NAC_NoDataLoaded
    EndIf
786 If (ParamIsDefault(ProcessWave))
        Wave DispWave="$root:NAC:"+Name+": Detector"
    Else
        Wave DispWave="$root:NAC:"+Name+": "+ProcessWave
    EndIf

```

```

EndIf
791 Tmp=WaveMin(DispWave)
Range=((Tmp>0) ? Ceil(Tmp/10^Floor(Log(Abs(Tmp)))) : Floor(Tmp/10^Floor(Log(Abs(
↳ (Tmp)))) ) * 10^Floor(Log(Abs(Tmp)))
If ((Range<Neg) || StringMatch(Name,DefNeg))
    Neg=Range
    DefNeg=Name
796 EndIf
Tmp=WaveMax(DispWave)
Range=((Tmp>0) ? Ceil(Tmp/10^Floor(Log(Abs(Tmp)))) : Floor(Tmp/10^Floor(Log(Abs(
↳ (Tmp)))) ) * 10^Floor(Log(Abs(Tmp)))
If ((Range>Pos) || StringMatch(Name,DefPos))
    Pos=Range
801 DefPos=Name
EndIf
For (V1=0;V1<ItemsInList(WindowList);V1+=1)
    For (V2=0;V2<ItemsInList(WinSubList);V2+=1)
        WName="NAC_"+StringFromList(V1,WindowList,",";")+StringFromList(V2,WinSubList,
↳ ",")
806 DoWindow $WName
        If (V_Flag)
            If (Neg==Pos)
                SetAxis /W=$WName left *, *
            Else
811 GetAxis /W=$WName /Q left
                If ((V_min!=Neg) || (V_max!=Pos))
                    SetAxis /W=$WName left Neg, Pos
                EndIf
            EndIf
816 EndIf
        EndFor
    EndFor
Return NoError
End
821 //

```

Function DisplayTrend

```

Static Function DisplayTrend(Name, ShowTrend)
String Name
Variable ShowTrend
String WName
826 NVar WWidth=root:NAC:GUI:WWidth, WHeight=root:NAC:GUI:WHeight, MarginTop=root:NAC:
↳ :GUI:MarginTop
String FolderName
StrSwitch (Name)
    Case "Heat":
        Name="Radiation"
831 Case "Radiation":
        If (WaveExists(root:NAC:Heat:Radiation) && WaveExists(root:NAC:Heat:
↳ fit_Radiation))
            Wave Original=root:NAC:Heat:orig_Radiation
            Wave Trend=root:NAC:Heat:fit_Radiation
        Else
836 Return NAC_NothingToProcess
        EndIf
        FolderName="Heat"
        Break
    Case "Sticking":
        Name="Desorption"
841 Case "Desorption":
        If (WaveExists(root:NAC:Sticking:Desorption) && WaveExists(root:NAC:
↳ Sticking:fit_Desorption))
            Wave Original=root:NAC:Sticking:orig_Desorption
            Wave Trend=root:NAC:Sticking:fit_Desorption
846 Else
            Return NAC_NothingToProcess
        EndIf
        FolderName="Sticking"
        Break

```

```

851     Default:
        Return NAC_NotApplicable
        Break
    EndSwitch
    WName="NAC_"+Name+"_Trend"
856   If (NumPnts(Trend) == 0)
        Return NAC_NothingToProcess
    EndIf
    DoWindow $WName
    If (V_Flag)
861     DoWindow /F $WName
        If (ShowTrend)
            ModifyGraph /W=$WName HideTrace($"fit_"+Name)=0
        Else
            ModifyGraph /W=$WName HideTrace($"fit_"+Name)=2
866     EndIf
        Return NAC_WindowAlreadyExists
    EndIf
    Display /N=$WName /K=1 /W=(50, 50, 50+WWidth, 50+WHeight) Original, Trend as "↵
    ↵ Trends for "+Name
    ModifyGraph /W=$WName Mode($"orig_"+Name)=2, LSize($"orig_"+Name)=2, Margin(Top↵
    ↵ )=MarginTop, zColor($"orig_"+Name)={"root:NAC:"+FolderName+":Flaglist↵
    ↵ ",-1,1,YellowHot,1}
871   ModifyGraph /W=$WName Mode($"fit_"+Name)=0, LSize($"fit_"+Name)=2, RGB($"fit_"+↵
    ↵ Name)=(0,0,65280)
    If (ShowTrend)
        ModifyGraph /W=$WName HideTrace($"fit_"+Name)=0
    Else
        ModifyGraph /W=$WName HideTrace($"fit_"+Name)=2
876   EndIf
    Label /W=$WName Left "Intensity (a.u.)"
    Label /W=$WName Bottom "\u"
    Return NoError
End
881 //
Function DisplayFittedRate

Static Function DisplayFittedRate(Name)
String Name
String WName="NAC_"+Name+"_FittedRate"
Variable AxisMax, Conv
886 NVar WWidth=root:NAC:GUI:WWidth, WHeight=root:NAC:GUI:WHeight, MarginTop=root:NAC↵
    ↵ :GUI:MarginTop
    StrSwitch (Name)
        Case "RateCoating":
        Case "RateCalorimetry":
            Break
891     Default:
        Return NAC_NotApplicable
        Break
    EndSwitch
    If (!WaveExists($"root:NAC:"+Name+":FittedRate"))
896     Error_Message(CalcQCMRate(Name), "CalcQCMRate", "DisplayFittedRate", Name)
    EndIf
    DoWindow $WName
    Wave FittedRate=$"root:NAC:"+Name+":FittedRate"
    Wave FittedRateAvg=$"root:NAC:"+Name+":FittedRateAvg"
901   Wave FittedRateErrorPos=$"root:NAC:"+Name+":FittedRateErrorPos", ↵
    ↵ FittedRateErrorNeg=$"root:NAC:"+Name+":FittedRateErrorNeg"
    If (Stringmatch(WaveUnits(FittedRate,0),"*s*"))
        AxisMax=Ceil(RightX(FittedRate)*10) / 10
        Conv=1
    ElseIf (Stringmatch(WaveUnits(FittedRate,0),"*m*"))
906     AxisMax=Ceil(RightX(FittedRate)*30) / 30
        Conv=60
    ElseIf (Stringmatch(WaveUnits(FittedRate,0),"*h*"))
        AxisMax=Ceil(RightX(FittedRate)*2) / 2
        Conv=60*60
911   ElseIf (Stringmatch(WaveUnits(FittedRate,0),"*d*"))

```

```

    AxisMax=Ceil(RightX(FittedRate)*0.5) / 0.5
    Conv=60*60*24
EndIf
SetScale /I x, 0, AxisMax, WaveUnits(FittedRate,0), FittedRateAvg, ↵
    ↵ FittedRateErrorPos, FittedRateErrorNeg
916 FittedRateAvg=Mean(FittedRate)
    If (V_Flag)
        DoWindow /F $WName
        Label /W=$WName Left "Deposition Rate (\\U)"
        Label /W=$WName Bottom "Runtime (\\u)"
921 SetAxis /W=$WName Bottom 0, AxisMax
        SetAxis /W=$WName Left Min(0, WaveMin(FittedRate)), Max(2*WaveMax(↵
            ↵ FittedRateAvg), 1.25*WaveMax(FittedRate))
        Return NAC_WindowAlreadyExists
    EndIf
    Display /N=$WName /K=1 /W=(50, 50, 50+WWidth, 50+WHeight) FittedRate, ↵
        ↵ FittedRateAvg, FittedRateErrorPos, FittedRateErrorNeg as "Fitted Deposition↵
            ↵ Rate for "+Name
926 ModifyGraph /W=$WName Mode(FittedRate)=2, LSize(FittedRate)=2, Margin(Top)=↵
        ↵ MarginTop
    ModifyGraph /W=$WName Mode(FittedRateAvg)=0, LSize(FittedRateAvg)=1.5, LStyle(↵
        ↵ FittedRateAvg)=2, rgb(FittedRateAvg)=(21760,21760,21760)
    ModifyGraph /W=$WName Mode(FittedRateErrorPos)=0, LSize(FittedRateErrorPos)=1, ↵
        ↵ LStyle(FittedRateErrorPos)=1, rgb(FittedRateErrorPos)=(0,0,0)
    ModifyGraph /W=$WName Mode(FittedRateErrorNeg)=0, LSize(FittedRateErrorNeg)=1, ↵
        ↵ LStyle(FittedRateErrorNeg)=1, rgb(FittedRateErrorNeg)=(0,0,0)
931 ModifyGraph margin(left)=43,margin(bottom)=43, margin(right)=14
    Label /W=$WName Left "Deposition Rate (\\U)"
    Label /W=$WName Bottom "Runtime (\\u)"
    SetAxis /W=$WName Bottom 0, AxisMax
    SetAxis /W=$WName Left Min(0, WaveMin(FittedRate)), Max(2*WaveMax(FittedRateAvg↵
        ↵ ), 1.25*WaveMax(FittedRate))
    NVar FittedFrom="$root:NAC:"+Name+":FittedFrom", FittedTo="$root:NAC:"+Name+":↵
        ↵ FittedTo"
936 NVar BaselineTo="$root:NAC:"+Name+":BaselineTo", BaselineFrom="$root:NAC:"+Name↵
        ↵ +":BaselineFrom"
    NVar RateFittingWindow=root:NAC:Machine:RateFittingWindow
    If (NumType(BaselineTo)==0)
        FittedFrom=BaselineTo/Conv+DimDelta(FittedRate, 0)
    EndIf
941 If (NumType(BaselineFrom)==0)
        FittedTo=BaselineFrom/Conv-DimDelta(FittedRate, 0)
    EndIf
    Cursor /N=1 /W=$WName A FittedRate FittedFrom
    Cursor /N=1 /W=$WName B FittedRate FittedTo
946 SVar FileName="$root:NAC:"+Name+":Filename"
    NVar AvgWindow=root:NAC:Machine:RateFittingWindow
    Error_Message(UpdateFittedRate(Name), "UpdateFittedRate", "DisplayFittedRate", ↵
        ↵ Name)
    SetWindow $WName Hook("$NAC_"+Name+"Csr")=NAC_WinHookFittedRate
    Return NoError
951 End
    //

```

Function DisplayVsCoverage

```

Static Function DisplayVsCoverage(Name)
String Name
String WName="NAC_"+Name+"_VsCov"
956 NVar WWidth=root:NAC:GUI:WWidth, WHeight=root:NAC:GUI:WHeight, MarginTop=root:NAC↵
    ↵ :GUI:MarginTop
    StrSwitch (Name)
        Case "Heat":
        Case "Sticking":
            Break
961 Default:
            Return NAC_NotApplicable
            Break
    EndSwitch
    DoWindow $WName

```

```

966   If (V_Flag)
       DoWindow /F $WName
       Return NAC_WindowAlreadyExists
   EndIf
   Wave Coverage=root:NAC:Enthalpies:Coverage, Range=root:NAC:Enthalpies:↵
       ↵ ThicknessRange
971   StrSwitch (Name)
       Case "Sticking":
           Wave Sticking=root:NAC:Enthalpies:Sticking
           If ((NumPnts(Sticking)==0) || (NumPnts(root:NAC:Enthalpies:Coverage)==0))
               Return NAC_NothingToProcess
976       EndIf
           NVar TemperatureSample=root:NAC:Experiment:TemperatureSample
           Display /N=$WName /K=1 /W=(2*WWidth+220, 50, 3*WWidth+220, 50+WHeight) ↵
           ↵ Sticking vs root:NAC:Enthalpies:Coverage as "Sticking vs Coverage"
           AppendToGraph /W=$WName root:NAC:Enthalpies:StickingLimit
           ModifyGraph /W=$WName Margin(Top)=MarginTop, mode(Sticking)=2, lsize(↵
           ↵ Sticking)=2
981       ModifyGraph /W=$WName Mode(StickingLimit)=0, LSize(StickingLimit)=1, LStyle↵
           ↵ (StickingLimit)=2, rgb(StickingLimit)=(30464,30464,30464)
           Label /W=$WName Left "Sticking Probability"
           SVar Substance=root:NAC:RateCalorimetry:Substance, Substrate=root:NAC:↵
           ↵ RateCoating:Substance
           String Msg="\JCSticking Measurement for "+Substance+" on "
           If (StrLen(Substance))
986               Msg+=Substrate
           Else
               Msg+="\ "PVDF\ "
           EndIf
           Msg=Msg + " @ " +Num2Str(Round(TemperatureSample)) + " K"
991       TextBox /W=$WName /A=MT /C/E/F=0 /X=0/Y=5 /N=TBSum /B=1 Msg
           Break
       Case "Heat":
           If ((NumPnts(root:NAC:Enthalpies:Enthalpy)==0) || (NumPnts(root:NAC:↵
           ↵ Enthalpies:Coverage)==0))
               Return NAC_NothingToProcess
996       EndIf
           Wave Enthalpy=root:NAC:Enthalpies:Enthalpy
           NVar PosLow=root:NAC:Enthalpies:MultiLayerPosLow, PosHigh=root:NAC:↵
           ↵ Enthalpies:MultiLayerPosHigh
           Display /N=$WName /K=1 /W=(2*WWidth+220, 400, 3*WWidth+220, 400+WHeight) ↵
           ↵ Enthalpy vs root:NAC:Enthalpies:Coverage as "Heat of Adsorption vs Coverage" ↵
           ↵ "
           AppendToGraph /W=$WName root:NAC:Enthalpies:MultiLayerReference
1001       ModifyGraph /W=$WName Margin(Top)=MarginTop, Mode(Enthalpy)=2, LSize(↵
           ↵ Enthalpy)=2
           ModifyGraph /W=$WName Mode(MultiLayerReference)=0, LSize(↵
           ↵ MultiLayerReference)=1, LStyle(MultiLayerReference)=2, rgb(↵
           ↵ MultiLayerReference)=(30464,30464,30464)
           Label /W=$WName Left "Heat of Adsorption (\U)"
           SetWindow $WName Hook("$HeatCsr")=NAC_WinHookCal
           Cursor /N=1 /W=$WName A Enthalpy PosLow
1006       Cursor /N=1 /W=$WName B Enthalpy PosHigh
           Break
       Default:
           Return NAC_NotApplicable
           Break
1011   EndSwitch
       SetScale /I x, Coverage2Thickness(Floor(WaveMin(Coverage))), Coverage2Thickness ↵
           ↵ (Ceil(WaveMax(Coverage))), "m", Range
       Error_Message(SetRangesCoverage(Name), "DisplayVsCoverage", "SetRangesCoverage ↵
           ↵ ", Name)
       AppendToGraph /W=$WName /B=Thickness Range
       ModifyGraph /W=$WName Margin(Bottom)=60, LblPos(bottom)=60, FreePos(Thickness)↵
           ↵ =27
1016   Label /W=$WName bottom "Coverage"
       Label /W=$WName Thickness " "
       Return NoError
End

```

//

Function SetRangesCoverage

```

1021 Static Function SetRangesCoverage(Name)
String Name
String WName="NAC_"+Name+"_VsCov"
DoWindow $WName
If (!V_Flag)
1026   Return NAC_NoSuchWindow
EndIf
StrSwitch (Name)
Case "Sticking":
Wave Sticking=root:NAC:Enthalpies:Sticking
1031   If ((WaveMin(Sticking)>=0) && (WaveMax(Sticking)<=1))
SetAxis /W=$WName Left 0,1
ElseIf ((WaveMin(Sticking)>=0) && (WaveMax(Sticking)>1))
SetAxis /W=$WName Left 0,Ceil(WaveMax(Sticking)*10)/10
ElseIf ((WaveMin(Sticking)<0) && (WaveMax(Sticking)<=1))
1036   SetAxis /W=$WName Left Floor(WaveMin(Sticking)*10)/10,1
Else
SetAxis /W=$WName Left Floor(WaveMin(Sticking)*10)/10,Ceil(WaveMax(
↵ Sticking)*10)/10
EndIf
Break
1041 Case "Heat":
Wave Enthalpy=root:NAC:Enthalpies:Enthalpy
Wave RefEnthalpy=root:NAC:Enthalpies:MultiLayerReference
If (WaveMin(Enthalpy)>=0 )
SetAxis /W=$WName Left 0, Ceil(Max(WaveMax(Enthalpy), RefEnthalpy[0])/1e5↵
↵ )*1e5
1046 Else
SetAxis /W=$WName Left Floor(WaveMin(Enthalpy)/1e5)*1e5, Ceil(Max(WaveMax↵
↵ (Enthalpy), RefEnthalpy[0])/1e5)*1e5
EndIf
Break
Default:
1051   Return NAC_NotApplicable
EndSwitch
Return NoError
End
//

```

Function DisplayVsPulse

```

1056 Static Function DisplayVsPulse(Name)
String Name
String WName, NameList, LabelList
NVar WWidth=root:NAC:GUI:WWidth, WHeight=root:NAC:GUI:WHeight, MarginTop=root:NAC↵
↵ :GUI:MarginTop
Variable WOfs=0, Ret=0
1061 DFref OldDF=GetDataFolderDFR()
StrSwitch (Name)
Case "Heat":
Variable i
NameList="Adsorption;Radiation;"
1066   LabelList="Adsorption Enthalpy (\U);Relative Radiation Contribution;"
Break
Case "Sticking":
NameList="Desorption;"
LabelList="Relative Desorption Intensity;"
1071   WOfs=-1
Break
Default:
Return NAC_NotApplicable
Break
1076 EndSwitch
SetDataFolder $"root:NAC:"+Name
SVar FileName=$"root:NAC:"+Name+":FileName"
Variable Test=0
For (i=0;i<ItemsInList(NameList);i+=1)

```



```

1081     Name=StringFromList(i, NameList, ";")
        WName="NAC_"+Name+"_VsPulse"
        DoWindow $WName
        Test=0
        If (V_Flag)
1086         DoWindow /F $WName
            Error_Message(NAC_WindowAlreadyExists, "InProc", "DisplayVsPulse", Name)
            Test=1
        EndIf
        If (NumPnts($Name)<=0)
1091         Error_Message(NAC_NothingToProcess, "InProc", "DisplayVsPulse", Name)
            Test=1
        EndIf
        If (!Test)
            Wave DispWave=$Name
1096         Display /N=$WName /K=1 /W=((i+1+WOfs)*(WWidth)+(i+1+WOfs)*50+50, 525, (i+2+↵
            ↵ WOfs)*WWidth+(i+1+WOfs)*50+50, 525+WHeight) DispWave as "Fit Results for "+↵
            ↵ Name
            ModifyGraph /W=$WName Margin(Top)=MarginTop, mode($Name)=2, lsize($Name)=2
            Label /W=$WName left StringFromList(i,LabelList, ";")
            Label /W=$WName bottom "\u"
            StrSwitch (Name)
1101             Case "Adsorption":
                TextBox /W=$WName /A=MT /C/E/F=0 /X=0/Y=5 /N=Caption /A=MC /B=1 "\↵
            ↵ JCAdsorption (\Laser\") Contribution to the Heat Signal\r"+FileName
                Break
                Case "Radiation":
                TextBox /W=$WName /A=MT /C/E/F=0 /X=0/Y=5 /N=Caption /A=MC /B=1 "\↵
            ↵ JCRadiation Contribution to the Heat Signal\r"+FileName
1106             Break
                Case "Desorption":
                If ((WaveMin(DispWave)>=0) && (WaveMax(DispWave)<=1))
                    SetAxis /W=$WName Left 0,1
                ElseIf ((WaveMin(DispWave)>=0) && (WaveMax(DispWave)>1))
1111                 SetAxis /W=$WName Left 0,Ceil(WaveMax(DispWave)*10)/10
                ElseIf ((WaveMin(DispWave)<0) && (WaveMax(DispWave)<=1))
                    SetAxis /W=$WName Left Floor(WaveMin(DispWave)*10)/10,1
                Else
                    SetAxis /W=$WName Left Floor(WaveMin(DispWave)*10)/10,Ceil(WaveMax(↵
            ↵ DispWave)*10)/10
1116             EndIf
                AppendToGraph /W=$WName root:NAC:Sticking:StickingLimit
                ModifyGraph /W=$WName Mode(StickingLimit)=0, LSize(StickingLimit)=1, ↵
            ↵ LStyle(StickingLimit)=2, rgb(StickingLimit)=(30464,30464,30464)
                TextBox /W=$WName /A=MT /C/E/F=0 /X=0/Y=5 /N=Caption /A=MC /B=1 "\↵
            ↵ JCSticking Contribution to the Heat Signal\r"+FileName
                Break
1121             Default:
                Break
            EndSwitch
        EndIf
        EndFor
1126     SetDataFolder OldDF
        Return NoError
End
//

```

Function DisplayNonFlagged

```

Static Function DisplayNonFlagged(Name)
1131 String Name
String WName="NAC_"+Name+"_Frames"
Variable i
    StrSwitch (Name)
1136     Case "Deconvolution":
    Case "BeforeCoating":
    Case "AfterCoating":
    Case "LaserReference":
    Case "Transmission":
    Case "Radiation":

```

```

1141     Case "ZeroSticking":
        Case "Heat":
        Case "Sticking":
            Break
        Case "RateCoating":
1146     Case "RateCalorimetry":
            Return NAC_NotApplicable
            Break
        Default:
            Return NAC_UnknownMeasurement
1151     Break
EndSwitch
NVar Loaded="$root:NAC:"+Name+":Loaded"
If (!Loaded)
    Return NAC_NoDataLoaded
1156 EndIf
DoWindow $WName
If (V_Flag)
    DoWindow /F $WName
    Return NAC_WindowAlreadyExists
1161 EndIf
NVar WWidth=root:NAC:GUI:WWidth, WHeight=root:NAC:GUI:WHeight, MarginTop=root:↵
    ↵ NAC:GUI:MarginTop
NVar ProcessRate=root:NAC:Machine:ProcessRate
SVar FileName="$root:NAC:"+Name+":FileName"
DFref OldDF=GetDataFolderDFR()
1166 SetDataFolder "$root:NAC:"+Name
If (StringMatch(Name,"Deconvolution"))
    NVar ChopperPeriod=root:NAC:Deconvolution:ChopperPeriod
Else
    NVar ChopperPeriod=root:NAC:Experiment:ChopperPeriod
1171 EndIf
Wave Detector, FlagList
Display /N=$WName /K=1 /W=(150+2*WWidth, 525, 150+3*WWidth, 525+WHeight) as "↵
    ↵ All Non-Flagged Frames for "+Name
ModifyGraph /W=$WName Margin(Top)=MarginTop
For (i=0;i<NumPnts(FlagList);i+=1)
1176     AppendToGraph /W=$WName Detector[][i]/TN="$Frame"+Num2Str(i)
        ModifyGraph /W=$WName rgb("$Frame"+Num2Str(i))=(0,SelectNumber(Mod(i,2)↵
            ↵ ,0,52224),SelectNumber(Mod(i,2),65280,0)), HideTrace("$Frame"+Num2Str(i))=↵
            ↵ FlagList[i]
EndFor
SetWindow $WName Hook("$Frame"+Name+"Csr")=NAC_WinHookCal
Cursor /N=1 /W="$NAC_"+Name+"_Frames" A Frame0 0
1181 TextBox /W=$WName /A=MT /C/E/F=0 /X=0/Y=5 /N=Caption /A=MC /B=1 "\JCALL Non-↵
    ↵ Flagged Frames for "+Name+" Measurement\r\JC"+FileName+": \K(0,0,65280)↵
    ↵ Even Frames\K(0,0,0) \K(0,52224,0)Odd Frames"
SetDataFolder OldDF
Return NoError
End
//

```

Function CheckButtons

```

1186 Static Function CheckButtons(Name, WName)
String Name, WName
NVar CurrentFrame="$root:NAC:"+Name+":CurrentFrame", NumberOfFrames="$root:NAC:"+↵
    ↵ Name+":NumberOfFrames"
Wave FlagList="$root:NAC:"+Name+":FlagList"
DoWindow $WName
1191 If (!V_Flag)
    Return NAC_NoSuchWindow
EndIf
If (FlagList[CurrentFrame])
    Button "$Flag_"+Name Title="Unflag", Win=$WName
1196 Else
    Button "$Flag_"+Name Title="Flag", Win=$WName
EndIf
Button "$NAV_"+Name+"_Fi" Disable=2*(CurrentFrame<1), Win=$WName
Button "$NAV_"+Name+"_M1" Disable=2*(CurrentFrame<1), Win=$WName

```

```

1201 Button $"NAV_" + Name + "_M2" Disable=2*(CurrentFrame<2), Win=$WName
Button $"NAV_" + Name + "_P2" Disable=2*(CurrentFrame>NumberOfFrames-3), Win=$WName
Button $"NAV_" + Name + "_P1" Disable=2*(CurrentFrame>NumberOfFrames-2), Win=$WName
Button $"NAV_" + Name + "_La" Disable=2*(CurrentFrame>NumberOfFrames-2), Win=$WName
DoWindow /F $"NAC_" + Name + "_Full"
1206 Return NoError
End
//
Function DisplayFlagWindow
Static Function DisplayFlagWindow(Name)
String Name
1211 NVar WWidth=root:NAC:GUI:WWidth, WHeight=root:NAC:GUI:WHeight, MarginTop=root:NAC:
    ↪ :GUI:MarginTop
NVar Loaded=$"root:NAC:" + Name + ":Loaded"
String WName="NAC_" + Name + "_Flag"
Variable Error=NoError
NVar CurrentFrame=$"root:NAC:" + Name + ":CurrentFrame"
1216 If (!Loaded)
    Return NAC_NoDataLoaded
EndIf
DoWindow $WName
If (V_Flag)
1221 DoWindow /F $WName
    Return NAC_WindowAlreadyExists
EndIf
NVar NoP=$"root:NAC:" + Name + ":NumberOfFrames"
Display /N=$WName /K=1 /W=(100+WWidth, 525, 100+2*WWidth, 525+WHeight) $"root:↪
    ↪ NAC:" + Name + ":DisplayRaw", $"root:NAC:" + Name + ":DisplayFit" as "Flagging for ↪
    ↪ "+Name
1226 ModifyGraph /W=$WName rgb(DisplayFit)=(0,0,0), Margin(Top)=MarginTop
ModifyGraph Mode(DisplayRaw)=2, LSize(DisplayRaw)=1.5
Button $"NAV_" + Name + "_Fi" Proc=NAC_NavProc, Size={30,20}, Title="|<<", Win=↪
    ↪ $WName, Pos={10,5}
Button $"NAV_" + Name + "_M2" Proc=NAC_NavProc, Size={30,20}, Title="<<", Win=↪
    ↪ $WName, Pos={45,5}
Button $"NAV_" + Name + "_M1" Proc=NAC_NavProc, Size={30,20}, Title="<", Win=$WName ↪
    ↪ , Pos={80,5}
1231 SetVariable $"NAV_" + Name Proc=NAC_CurrentFrameProc, Limits={0, NoP-1, 1}, Size↪
    ↪ ={95,20}, Title="Frame:", Value=CurrentFrame, Pos={115,8}
Button $"NAV_" + Name + "_P1" Proc=NAC_NavProc, Size={30,20}, Title=">", Win=$WName ↪
    ↪ , Pos={220,5}
Button $"NAV_" + Name + "_P2" Proc=NAC_NavProc, Size={30,20}, Title=">>", Win=↪
    ↪ $WName, Pos={255,5}
Button $"NAV_" + Name + "_La" Proc=NAC_NavProc, Size={30,20}, Title=">>|", Win=↪
    ↪ $WName, Pos={290,5}
Button $"Flag_" + Name Proc=NAC_FlagProc, Size={45,20}, Title="Flag", Win=$WName, ↪
    ↪ Pos={325,5}
1236 Button $"Range_" + Name Proc=NAC_RangeProc, Size={45,20}, Title="Range", Win=↪
    ↪ $WName, Pos={375,5}
Button $"Clear_" + Name Proc=NAC_ClearProc, Size={45,20}, Title="Clear", Win=↪
    ↪ $WName, Pos={425,5}
Button $"Kill_" + Name Proc=NAC_KillFrameProc, Size={45,20}, Title="Kill !", Win=↪
    ↪ $WName, Pos={475,5}
TextBox /W=$WName /A=MT /C/E/F=0 /X=0/Y=5 /N=Caption /A=MC /B=1 "\r\JCFrame "+↪
    ↪ Num2Str(0) + " for "+Name+ " Measurement"
Error_Message(UpdateFlagWin(Name), "UpdateFlagWin", "DisplayFlagWindow", Name)
1241 Return NoError
End
//
Function UpdateFlagWin
Static Function UpdateFlagWin(Name)
String Name
1246 Variable i
String WName, Info
NVar ReEntry=root:NAC:GUI:ReEntryFlagWin
If (ReEntry)
    Return NAC_ReEntry

```

```

1251   Endif
      ReEntry=1
      WName="NAC_"+Name+"_Flag"
      DoWindow $WName
      If (!V_Flag)
1256     ReEntry=0
          Return NAC_NoSuchWindow
      Endif
      DFRef OldDF=GetDataFolderDFR()
      SetDataFolder $"root:NAC:"+Name
1261     NVar CurrentFrame
      If (StringMatch(Name,"Deconvolution"))
          NVar ChopperPeriod=root:NAC:Deconvolution:ChopperPeriod
      Else
          NVar ChopperPeriod=root:NAC:Experiment:ChopperPeriod
1266     Endif
      Wave DisplayRaw, DisplayFit, Detector, FlagList
      DisplayRaw=Detector[p][CurrentFrame]
      String FitName
      StrSwitch (Name)
1271     Case "ZeroSticking":
          FitName="Sticking"
          Break
          Case "LaserReference":
          FitName="Laser"
1276     Break
          Default:
          FitName=Name
          Break
      EndSwitch
1281     StrSwitch (Name)
          Case "ZeroSticking":
          Case "BeforeCoating":
          Case "AfterCoating":
          Case "LaserReference":
1286     Case "Transmission":
          Case "Radiation":
          Case "Deconvolution":
              If (Exists("Average"+SelectString(Mod(CurrentFrame,2),"Even","Odd"))==1)
                  Wave Avg=$"Average"+SelectString(Mod(CurrentFrame,2),"Even","Odd")
1291     If (NumPnts(Avg)>0)
                    DisplayFit=Avg
                Else
                    DisplayFit=NaN
                Endif
1296     Endif
          Break
          Case "Heat":
              Wave ChiSq
              If (ChiSq[CurrentFrame]>0)
1301     Wave Radiation, Adsorption, ShiftRad, ShiftAds, Offset
                  Make /FREE /N=5 /D FitCoef={Offset[CurrentFrame], Adsorption[CurrentFrame]
                  ↵ }, ShiftAds[CurrentFrame], Radiation[CurrentFrame], ShiftRad[CurrentFrame]}
                  If (Mod(CurrentFrame,2))
                      CalorimetryOdd(FitCoef,DisplayFit,DisplayFit)
                  Else
1306     CalorimetryEven(FitCoef,DisplayFit,DisplayFit)
                  Endif
                  Else
                      DisplayFit=NaN
                  Endif
1311     Break
          Case "Sticking":
              Wave ChiSq
              If (ChiSq[CurrentFrame]>0)
                  Wave Desorption, Shift, Offset
1316     Make /FREE /N=5 /D FitCoef={Offset[CurrentFrame], Desorption[CurrentFrame]
                  ↵ }, Shift[CurrentFrame]}
                  If (Mod(CurrentFrame,2))

```

```

        StickingOdd(FitCoef, DisplayFit, DisplayFit)
    Else
        StickingEven(FitCoef, DisplayFit, DisplayFit)
1321    EndIf
    Else
        DisplayFit=NaN
    EndIf
    Break
1326    Default:
        ReEntry=0
        Return NAC_UnknownMeasurement
        Break
EndSwitch
1331    Error_Message(CheckButtons(Name, WName), "CheckButtons", "UpdateFlagWin", Name)
    TextBox /W=$WName /A=MT /C/E/F=0 /X=0/Y=5 /N=Caption /A=MC /B=1 "\r\JCFrame "+↵
        ↵ Num2Str(CurrentFrame)+" for "+Name+" Measurement"
    If (FlagList[CurrentFrame])
        ModifyGraph /W=$WName rgb(DisplayRaw)=(34816,34816,34816)
    Else
1336        ModifyGraph /W=$WName rgb(DisplayRaw)=(0,SelectNumber(Mod(CurrentFrame,2)↵
            ↵ ,0,52224),SelectNumber(Mod(CurrentFrame,2),65280,0))
    EndIf
    SetDataFolder OldDF
    DoWindow $"NAC_"+Name+"_Full"
    If (V_Flag)
1341        Cursor /N=1 /W=$"NAC_"+Name+"_Full" A $"Frame"+Num2Str(CurrentFrame) ↵
            ↵ ChopperPeriod/2
    EndIf
    String TList=TraceNameList("NAC_"+Name+"_Frames", ";", 1)
    DoWindow $"NAC_"+Name+"_Frames"
    If (V_Flag)
1346        Cursor /N=1 /W=$"NAC_"+Name+"_Frames" A $"Frame"+Num2Str(CurrentFrame) ↵
            ↵ ChopperPeriod/2
        ModifyGraph /W=$"NAC_"+Name+"_Frames" rgb($"Frame"+Num2Str(CurrentFrame))↵
            ↵ =(65280,0,0)
        For (i=0;i<ItemsInList(TList);i+=1)
            Info=TraceInfo("NAC_"+Name+"_Frames", "Frame"+Num2Str(i), 0)
            If (Str2Num(Info[StrSearch(Info, "hideTrace(x)=", 0)+13,StrSearch(Info, ↵
                ↵ ";", StrSearch(Info, "hideTrace(x)=", 0))-1]) !=FlagList[i])
1351                ModifyGraph /W=$"NAC_"+Name+"_Frames" HideTrace($"Frame"+Num2Str(i))=↵
                    ↵ FlagList[i]
            EndIf
            If (!StringMatch(Info[StrSearch(Info, "rgb(x)=", 0)+7,StrSearch(Info, ";", ↵
                ↵ StrSearch(Info, "rgb(x)=", 0))-1], "(0,"+num2str(SelectNumber(Mod(i,2)↵
                ↵ ,0,52224))+","+Num2Str(SelectNumber(Mod(i,2),65280,0))+")" ) )
                ModifyGraph /W=$"NAC_"+Name+"_Frames" rgb($"Frame"+Num2Str(i))=(0,↵
                ↵ SelectNumber(Mod(i,2),0,52224),SelectNumber(Mod(i,2),65280,0))
            EndIf
1356        EndFor
        ModifyGraph /W=$"NAC_"+Name+"_Frames" rgb($"Frame"+Num2Str(CurrentFrame))↵
            ↵ =(65280,0,0)
    EndIf
    DoWindow /F $"NAC_"+Name+"_Full"
    DoWindow /F $"NAC_"+Name+"_Flag"
1361    DoWindow /F $"NAC_"+Name+"_Frames"
    ReEntry=0
    SetDataFolder OldDF
    Return NoError
End
1366 //

```

Function KillWins

```

Static Function KillWins(Name)
String Name
String WindowsList=WinList(Name+"*",";","WIN:71")
Variable i
1371    For (i=0;i<ItemsInList(WindowsList);i+=1)
        KillWindow $(StringFromList(i,WindowsList))
    EndFor

```

```

Return NoError
End
1376 //
Function DisplayAverage
Static Function DisplayAverage(Name)
String Name
NVar WWidth=root:NAC:GUI:WWidth, WHeight=root:NAC:GUI:WHeight
DFRef OldDF=GetDataFolderDFR()
1381 String WName="NAC_"+Name+"_Avg"
If ((Exists("root:NAC:"+Name+":AverageOdd")!=1) && (Exists("root:NAC:"+Name+":
↳ AverageEven")!=1))
Return NAC_AverageWavesMissing
Endif
DoWindow $WName
1386 If (V_Flag)
DoWindow /F $WName
Return NAC_WindowAlreadyExists
Endif
SetDataFolder $"root:NAC:"+Name
1391 SVar FileName
Wave AverageOdd, AverageEven
String GraphTitle="Average for "+Name+" Measurement"
Display /N=$WName /K=1 /W=(500, 525, 500+WWidth, 525+WHeight) AverageOdd, ↵
↳ AverageEven as Name +" Measurement"
ModifyGraph /W=$WName rgb(AverageOdd)=(0,52224,0)
1396 ModifyGraph /W=$WName rgb(AverageEven)=(0,0,65280)
TextBox /W=$WName /A=MT /C/E/F=0 /X=0 /Y=5 /N=Caption /A=MC /B=1 "\JC"+↵
↳ GraphTitle+"\r\JC"+FileName+": \K(0,0,65280)Even Frame\K(0,0,0) \K↵
↳ (0,52224,0)Odd Frame"
Label /W=$WName bottom "Time (\u)"
Label /W=$WName left "Detector (\U)"
SetDataFolder OldDF
1401 Return NoError
End
//
Function DisplayDeconvolutedAverage
Static Function DisplayDeconvolutedAverage(Name)
String Name
1406 NVar WWidth=root:NAC:GUI:WWidth, WHeight=root:NAC:GUI:WHeight
DFRef OldDF=GetDataFolderDFR()
String WName="NAC_"+Name+"_AvgDeconv"
If ((Exists("root:NAC:Deconvolution:"+Name+"AvgOdd")!=1) && (Exists("root:NAC:↵
↳ Deconvolution:"+Name+":AvgEven")!=1))
Return NAC_NothingToProcess
1411 Endif
DoWindow $WName
If (V_Flag)
DoWindow /F $WName
Error_Message(SetDeconvolutionGraphRanges(Name, "AverageEven"), "↵
↳ SetDeconvolutionGraphRanges", "DisplayDeconvolutedAverage", Name)
1416 Error_Message(SetDeconvolutionGraphRanges(Name, "AverageOdd"), "↵
↳ SetDeconvolutionGraphRanges", "DisplayDeconvolutedAverage", Name)
Return NAC_WindowAlreadyExists
Endif
SetDataFolder root:NAC:Deconvolution
SVar FileName=$"root:NAC:"+Name+":FileName"
1421 Wave AverageOdd=$Name+"AvgOdd", AverageEven=$Name+"AvgEven"
Display /N=$WName /K=1 /W=(50, 525, 50+WWidth, 525+WHeight) AverageOdd, ↵
↳ AverageEven as Name +" Measurement"
ModifyGraph /W=$WName rgb($Name+"AvgOdd")=(0,52224,0)
ModifyGraph /W=$WName rgb($Name+"AvgEven")=(0,0,65280)
TextBox /W=$WName /A=MT /C/E/F=0 /X=0 /Y=5 /N=Caption /A=MC /B=1 "\↵
↳ JCDeconvoluted Average for "+Name+" Measurement\r\JC"+FileName+": \K↵
↳ (0,0,65280)Even Frame\K(0,0,0) \K(0,52224,0)Odd Frame"
1426 Label /W=$WName bottom "Time (\u)"
Label /W=$WName left "Power (\U)"
SetDataFolder OldDF

```

```

    Error_Message(SetDeconvolutionGraphRanges(Name, "AverageEven"), "↵
    ↵ SetDeconvolutionGraphRanges", "DisplayDeconvolutedAverage", Name)
    Error_Message(SetDeconvolutionGraphRanges(Name, "AverageOdd"), "↵
    ↵ SetDeconvolutionGraphRanges", "DisplayDeconvolutedAverage", Name)
1431 Return NoError
End
//
Function DisplayDeconvolution

Static Function DisplayDeconvolution(Name)
String Name
1436 NVar WWidth=root:NAC:GUI:WWidth, WHeight=root:NAC:GUI:WHeight
DFRef OldDF=GetDataFolderDFR()
String WName="NAC_"+Name+"_Deconv"
    If ((Exists("root:NAC:"+Name+":Deconvolution")!=1))
        Return NAC_FitWavesMissing
1441 Endif
DoWindow $WName
If (V_Flag==1)
    DoWindow /F $WName
    Error_Message(SetDeconvolutionGraphRanges(Name, "Deconvolution"), "↵
    ↵ SetDeconvolutionGraphRanges", "DisplayDeconvolution", Name)
1446 Return NAC_WindowAlreadyExists
EndIf
SetDataFolder $"root:NAC:"+Name
SVar FileName
NVar ChopperPeriod=root:NAC:Experiment:ChopperPeriod
1451 Wave Deconvolution
String GraphTitle="Deconvolution for "+Name+" Measurement"
Variable Range, MRange
Display /N=$WName /K=1 /W=(1000, 100, 1000+WWidth, 100+WHeight) as Name + " ↵
    ↵ Measurement"
AppendImage /W=$WName Deconvolution
1456 MRange=Max(Abs(WaveMin(Deconvolution)), Abs(WaveMax(Deconvolution)))
Range=Ceil(MRange/10^Floor(Log(MRange)))*10^Floor(Log(MRange))
ModifyImage /W=$WName Deconvolution ctab= {-Range, Range, RedWhiteBlue, 1}, ↵
    ↵ Interpolate=-1
ModifyGraph /W=$WName StandOff=0, Margin(left)=50
SetAxis /W=$WName Bottom 0, ChopperPeriod
1461 TextBox /W=$WName /A=LT /C/E/F=0 /N=Caption /A=MC /B=1 "\JC"+GraphTitle+"\r\JC↵
    ↵ "+FileName
ColorScale/C/N=CSale /Z=1 /A=RT /E=2 /F=0 /B=1 Width=130, Height=10, lblLatPos↵
    ↵ =80, lblMargin=30, Image=Deconvolution, Vert=0
Label /W=$WName bottom "Time (\u)"
SetWindow $WName hook($"NAC_"+Name+"Csr")=NAC_WinHookDeconvolution
Cursor /N=1 /W=$WName /I /N=1 A Deconvolution ChopperPeriod/2, 0
1466 SetDataFolder OldDF
Error_Message(SetDeconvolutionGraphRanges(Name, "Deconvolution"), "↵
    ↵ SetDeconvolutionGraphRanges", "DisplayDeconvolution", Name)
Return NoError
End
//
Function DisplayDeconvolutedFrame

1471 Static Function DisplayDeconvolutedFrame(Name)
String Name
NVar WWidth=root:NAC:GUI:WWidth, WHeight=root:NAC:GUI:WHeight
DFRef OldDF=GetDataFolderDFR()
String WName="NAC_"+Name+"_BrowseDeconv"
1476 If ((Exists("root:NAC:Deconvolution:"+Name+"BrowseOdd")!=1) || (Exists("root:↵
    ↵ NAC:Deconvolution:"+Name+"BrowseEven")!=1))
    Return NAC_NothingToProcess
Endif
DoWindow $WName
If (V_Flag)
1481 DoWindow /F $WName
    Error_Message(SetDeconvolutionGraphRanges(Name, "Deconvolution"), "↵
    ↵ SetDeconvolutionGraphRanges", "DisplayMeasurement", Name)
    Return NAC_WindowAlreadyExists

```

```

EndIf
SetDataFolder root:NAC:Deconvolution
1486 NVar Period=root:NAC:Experiment:ChopperPeriod
SVar FileName
Wave BrowseOdd=$Name+"BrowseOdd", BrowseEven=$Name+"BrowseEven"
Display /N=$WName /K=1 /W=(1000, 450, 1000+WWidth, 450+WHeight) BrowseOdd, ↵
↳ BrowseEven as Name + " Deconvoluted Frame"
ModifyGraph /W=$WName rgb($Name+"BrowseOdd")=(0,52224,0), rgb($Name+"BrowseEven" ↵
↳ ")=(0,0,65280)
1491 Error_Message(DoDeconvolutionTextBox(Name), "DoDeconTextBox", " ↵
↳ DisplayDeconvolutedFrame", Name)
Label /W=$WName bottom "Time (\u)"
Label /W=$WName left "Power (\U)"
SetDataFolder OldDF
Error_Message(SetDeconvolutionGraphRanges(Name, "Deconvolution"), " ↵
↳ SetDeconvolutionGraphRanges", "DisplayDeconvolutedFrame", Name)
1496 Return NoError
End
//

```

Function DisplayMeasurement

```

Static Function DisplayMeasurement(Name)
String Name
1501 String WName="NAC_"+Name+"_Full"
NVar WWidth=root:NAC:GUI:WWidth, WHeight=root:NAC:GUI:WHeight, MarginTop=root:NAC ↵
↳ :GUI:MarginTop
NVar Loaded=$"root:NAC:"+Name+":Loaded"
DFRef OldDF=GetDataFolderDFR()
Variable i
1506 If (!Loaded)
Return NAC_NoDataLoaded
EndIf
DoWindow $WName
If (V_Flag==1)
1511 DoWindow /F $WName
Error_Message(SetGraphRanges(Name), ",SetGraphRanges", "DisplayMeasurement", ↵
↳ Name)
Return NAC_WindowAlreadyExists
EndIf
SetDataFolder $"root:NAC:"+Name
1516 SVar FileName
Wave Detector, FlagList
NVar NumberOfFrames, CurrentFrame
StrSwitch (Name)
Case "Deconvolution":
1521 NVar ChopperPeriod=root:NAC:Deconvolution:ChopperPeriod
Break
Default:
NVar ChopperPeriod=root:NAC:Experiment:ChopperPeriod
Break
1526 EndSwitch
Display /N=$WName /K=1 /W=(50, 525, 50+WWidth, 525+WHeight) as Name + " ↵
↳ Measurement"
ModifyGraph /W=$WName Margin(Top)=MarginTop
For (i=0;i<NumberOfFrames;i+=1)
AppendToGraph /W=$WName Detector[][i]/TN=$"Frame"+Num2Str(i)
1531 ModifyGraph rgb($"Frame"+Num2Str(i))=(65280*(FlagList[i]==0),0,0), Offset($" ↵
↳ Frame"+Num2Str(i))={ChopperPeriod*i,0}
EndFor
Label /W=$WName bottom "Time (\u)"
Label /W=$WName left "Detector (\U)"
TextBox /W=$WName /A=MT /C/E/F=0 /X=0 /Y=5 /N=Caption /A=MC /B=1 ("\JC"+Name+" ↵
↳ Measurement\r\JC"+FileName)+": \K(65280,0,0)Original \K(0,0,0)Flagged"
1536 SetWindow $WName hook($"Frame"+Name+"Csr")=NAC_WinHookCal
Cursor /N=1 /W=$WName A $"Frame"+Num2Str(CurrentFrame) ChopperPeriod/2
SetDataFolder OldDF
Error_Message(SetGraphRanges(Name), "SetGraphRanges", "DisplayMeasurement", ↵
↳ Name)
Return NoError

```



```

1541 End
    //
Function DisplayRateFile
    Static Function DisplayRateFile(Name)
    String Name
    String WName="NAC_"+Name+"_Full"
1546 NVar WWidth=root:NAC:GUI:WWidth, WHeight=root:NAC:GUI:WHeight, MarginTop=root:NAC:
        ↵ :GUI:MarginTop
    NVar Loaded="$root:NAC:"+Name+":Loaded"
    DFREF OldDF=GetDataFolderDFR()
    DoWindow $WName
    If (V_Flag)
1551     DoWindow /F $WName
        Return NAC_WindowAlreadyExists
    EndIf
    If (!Loaded)
1556     Return NAC_NoDataLoaded
    EndIf
    SetDataFolder $"root:NAC:"+Name
    Wave Thickness, TimeLine
    NVar BaselineTo, BaselineFrom, Loaded
    SVar Substance
1561 Display /N=$WName /K=1 /W=(50, 525, WWidth+50, WHeight+525) Thickness vs ↵
        ↵ Timeline as Name + " Measurement"
    ModifyGraph /W=$WName Mode=3, Marker=19, Margin(Top)=MarginTop
    Make /O/N=2 Thickness_FitLow, Thickness_FitMid, Thickness_FitHigh
    Make /O/N=2 Timeline_FitLow, Timeline_FitMid, Timeline_FitHigh
    AppendToGraph /W=$WName Thickness_FitLow vs Timeline_FitLow
1566 AppendToGraph /W=$WName Thickness_FitMid vs Timeline_FitMid
    AppendToGraph /W=$WName Thickness_FitHigh vs Timeline_FitHigh
    ModifyGraph /W=$WName rgb(Thickness_FitLow)=(0,0,0), lsize(Thickness_FitLow)↵
        ↵ =1.5
    ModifyGraph /W=$WName rgb(Thickness_FitMid)=(0,0,65280), lsize(Thickness_FitMid)↵
        ↵ )=1.5
    ModifyGraph /W=$WName rgb(Thickness_FitHigh)=(0,0,0), lsize(Thickness_FitHigh)↵
        ↵ =1.5
1571 Label /W=$WName bottom "Time (\u)"
    Label /W=$WName left "QCM Thickness (\u)"
    SetWindow $WName hook($"NAC_"+Name+"Csr")=NAC_WinHookRate
    Cursor /N=1 /W=$WName /N=1 A Thickness BaselineTo
    Cursor /N=1 /W=$WName /N=1 B Thickness BaselineFrom
1576 SetAxis /W=$WName left Floor(WaveMin(Thickness)*1e9)/1e9, Ceil(WaveMax(↵
        ↵ Thickness)*1e9)/1e9
    ErrorMessage(FitQCMRate(Name), "FitQCMRate", "DisplayRateFile", Name)
    ErrorMessage(DoRateTextBoxes(Name), "DoRateTextBoxes", "DisplayRateFile", Name)↵
        ↵ )
    SetDataFolder OldDF
    Return NoError
1581 End
    //
Function UpdateFittedRate
    Static Function UpdateFittedRate(Name)
    String Name
    DFREF OldDF=GetDataFolderDFR()
1586 String WName, ExpName=""
        DoUpdate
        WName="NAC_"+Name+"_FittedRate"
        DoWindow $WName
        If (V_Flag)
1591     DoWindow /F $WName
        Else
            Return NAC_NoSuchWindow
        EndIf
    SetDataFolder $"root:NAC:"+Name
1596 StrSwitch (Name)
        Case "RateCalorimetry":
            ExpName="Calorimetry"

```

```

Case "RateCoating":
  If (!StrLen(ExpName))
1601   ExpName="Coating"
  EndIf
  NVar FittedFrom, FittedTo
  NVar AvgWindow=root:NAC:Machine:RateFittingWindow
  SVar FileName, SubstanceName
1606   Wave FittedRate, FittedRateAvg, FittedRateErrorPos, FittedRateErrorNeg
  String Msg=""
  WaveStats /Q /R=(FittedFrom,FittedTo) FittedRate
  Msg+="\JCFitted "+ExpName+" Deposition Rate for "+FileName+" ("+"↵
↵ SubstanceName+"):↵r"
  Msg+="\JCTooling: "+Num2Str(CalcQCMTooling(Name))+ " No base line ↵
↵ correction↵r\JCFitting window "+Num2Str(AvgWindow)+" pnts↵r"
1611   Msg+="\JCRange from "+Num2Str(FittedFrom)+" "+WaveUnits(FittedRate,0)+" to ↵
↵ "+Num2Str(FittedTo)+" "+WaveUnits(FittedRate,0)+"↵r"
  Msg+="Average: "+Num2Str(V_Avg*1e12)+" pm/s +/-"+Num2Str(V_SDev/V_Avg*100)↵
↵ "+" %"
  TextBox /W=$WName /A=MT /C/E/F=0 /X=0 /Y=5 /N=RateInfo /A=MC /B=1 Msg
  FittedRateAvg=V_Avg
  FittedRateErrorPos=V_Avg+V_SDev
1616   FittedRateErrorNeg=V_Avg-V_SDev
  Break
  Default:
  SetDataFolder OldDF
  Return NAC_NotApplicable
1621   Break
EndSwitch
SetDataFolder OldDF
Return NoError
End
1626 //

```

Function DoRateTextBoxes

```

Static Function DoRateTextBoxes(Name)
String Name
DFREF OldDF=GetDataFolderDFR()
String WName
1631 String Msg=""
  DoUpdate
  WName="NAC_"+Name+"_Full"
  DoWindow $WName
  If (V_Flag)
1636   DoWindow /F $WName
  Else
  Return NAC_NoSuchWindow
  EndIf
  SetDataFolder $"root:NAC:"+Name
1641 StrSwitch (Name)
  Case "RateCalorimetry":
  NVar DepositionRate, BaselineBefore, ApparentRate, BaselineAfter, ↵
↵ UseBaseline
  TextBox /W=$WName /A=MT /C/E/F=0 /X=0 /Y=5 /N=TBSum /B=1 "\JCDeposition ↵
↵ Rate Measurement for Calorimetry Measurement↵r\JC"+Num2Str(Round(↵
↵ DepositionRate*1e17)/1e5)+ " pm/s"
  Msg="\JLBaseline (Before): "+Num2Str(Round(BaselineBefore*1e17)/1e5)+ " pm/↵
↵ s↵r"
1646   Msg+="\JLApparent Deposition Rate: "+Num2Str(Round(ApparentRate*1e17)/1e5)↵
↵ "+" pm/s↵r"
  Msg+="\JLBaseline (After): "+Num2Str(Round(BaselineAfter*1e17)/1e5)+ " pm/s↵
↵ r"
  Msg+="\JLBaseline Correction: "+SelectString(UseBaseline, "No", "Yes")
  TextBox /W=$WName /A=LT /C/F=0 /X=5 /Y=5 /N=TBDet /B=1 Msg
  Break
1651 Case "RateCoating":
  NVar TotalThickness, UseTotalRange, BaselineTo, BaselineFrom, UseBaseline, ↵
↵ BaselineBefore, BaselineAfter, ApparentRate, DepositionRate
  Wave Timeline, Thickness

```

```

    TextBox /W=$WName /A=MT /C/E/F=0/X=0 /Y=5 /N=TBSum /B=1 "\JCThickness ↵
↵ Measurement for Sample Coating\r\JC"+Num2Str(Round(TotalThickness*1e14)/1e5↵
↵ )+ " nm"
    If (UseTotalRange)
1656     Msg="\JLStart: "+Num2Str(TimeLine[BaselineTo])+ " s / "+Num2Str(Round(↵
↵ Thickness[BaselineTo]*1e14)/1e5)+" nm\r"
    Msg+="\JLEnd: "+Num2Str(TimeLine[BaselineFrom])+ " s / "+Num2Str(Round(↵
↵ Thickness[BaselineFrom]*1e14)/1e5)+" nm\r"
    Msg+="\JLDuration: "+Num2Str(TimeLine[BaselineFrom]-TimeLine[BaselineTo])↵
↵ +" s\r"
    Msg+="\JLUse Total Range: "+SelectString(UseTotalRange , "No", "Yes")
1661     TextBox /W=$WName /A=LT /C /F=0 /X=5 /Y=5 /N=TBDet /B=1 Msg
    Else
    Msg="\JLBaseline (Before): "+Num2Str(Round(BaselineBefore*1e17)/1e5)+ " ↵
↵ pm/s\r"
    Msg+="\JLApparent Deposition Rate: "+Num2Str(Round(ApparentRate*1e17)/1e5↵
↵ )+" pm/s\r"
    Msg+="\JLBaseline (after): "+Num2Str(Round(BaselineAfter*1e17)/1e5)+" pm/↵
↵ s\r"
    Msg+="\JLBaseline Correction: "+SelectString(UseBaseline , "No", "Yes")↵
↵ +"r"
1666     Msg+="\JLRate : "+Num2Str(Round(DepositionRate*1e17)/1e5)+" pm/s\r"
    Msg+="\JLDuration: "+Num2Str(TimeLine[BaselineFrom]-TimeLine[BaselineTo])↵
↵ +" s"
    TextBox /W=$WName /A=LT /C/F=0 /X=5 /Y=5 /N=TBDet /B=1 Msg
    EndIf
    Break
1671     Default:
        SetDataFolder OldDF
        Return NAC_NotApplicable
        Break
    EndSwitch
1676     SetDataFolder OldDF
    Return NoError
End
//

```

Function DoHeatTextBox

```

Static Function DoHeatTextBox()
1681 DFREF OldDF=GetDataFolderDFR()
String WName, Msg
    DoUpdate
    WName="NAC_Heat_VsCov"
    DoWindow $WName
1686     If (V_Flag)
        DoWindow /F $WName
    Else
        Return NAC_NoSuchWindow
    EndIf
1691     NVar Enthalpy=root:NAC:Enthalpies:MultiLayerEnthalpy, TemperatureSample=root:↵
↵     NAC:Experiment:TemperatureSample
    NVar EnthalpyError=root:NAC:Enthalpies:MultiLayerEnthalpyError
    NVar Thickness=root:NAC:RateCoating:TotalThickness
    SVar Substance=root:NAC:RateCalorimetry:Substance, Substrate=root:NAC:↵
↵     RateCoating:SubstanceName
    Msg="\JCCalorimetry Measurement for "+Substance+" on "
1696     If (StrLen(Substrate))
        Msg=Msg + Substrate +" ("
        If (Thickness >1e-6)
            Msg=Msg+ Num2Str(Round(Thickness*1e8)/100) +" um)"
        Else
1701             Msg=Msg+ Num2Str(Round(Thickness*1e9)) +" nm)"
        EndIf
    Else
        Msg=Msg + "\"PVDF\""
    EndIf
1706     Msg=Msg + " @ " +Num2Str(Round(TemperatureSample)) +" K"
    Msg=Msg+"\r\JCMultilayer Enthalpy: "+Num2Str(Round(Enthalpy/10)/100)+" +/- "+↵
↵     Num2Str(Round(EnthalpyError/10)/100)+"kJ/mol Lit.: "+Num2Str(↵

```

```

    ↪ NAC_RefEnthalpy(Substance, TemperatureSample)/1000)+" kJ/mol"
    TextBox /W=$WName /A=MT /C/E/F=0 /X=0 /Y=5 /N=TBSum /B=1 Msg
    SetDataFolder OldDF
    Return NoError
1711 End
    //
Function DoDeconvolutionTextBox
    Static Function DoDeconvolutionTextBox(Name)
    String Name
    String WName
1716 DoUpdate
    WName="NAC_"+Name+"_BrowseDeconv"
    DoWindow $WName
    If (V_Flag)
        DoWindow /F $WName
1721 Else
        Return NAC_NoSuchWindow
    EndIf
    NVar FrameIndex=$"root:NAC:"+Name+":BrowseDeconvolutionIndex"
    SVar FileName=$"root:NAC:"+Name+":FileName"
1726 Wave Deconvolution=$"root:NAC:"+Name+":Deconvolution"
    String Caption="\JCDeconvoluted Frames " + Num2Str(FrameIndex*DimDelta(↪
        ↪ Deconvolution, 1)) + " to " + Num2Str((FrameIndex+2)*DimDelta(↪
        ↪ , 1)-1)
    Caption+=" for "+Name+" Measurement\r\JC" + FileName + ":"
    Caption+=" \K(0,0,65280)Even Frame" + SelectString(DimDelta(Deconvolution, 1)↪
        ↪ >1, "", "s") + " \K(0,52224,0)Odd Frame" + SelectString(DimDelta(↪
        ↪ Deconvolution, 1)>1, "", "s")
    TextBox /W=$WName /A=MT /C/E/F=0 /X=0 /Y=5 /N=Caption/A=MC /B=1 Caption
1731 Return NoError
    End
    //
Function NAC_ShowControlPanel
    Function NAC_ShowControlPanel()
    If (DataFolderExists("root:NAC"))
1736 DoWindow NAC_Control
        If (V_Flag==0)
            Error_Message(DataPanel(), "DataPanel", "NAC_Panels", "Data")
        Else
            DoWindow /F NAC_Control
1741 EndIf
        Else
            Error_Message(NAC_Initialize(), "NAC_Initialize", "NAC_ShowControlPanel", "")
        EndIf
        Return NoError
1746 End
    //
Function NAC_Panels
    Static Function NAC_Panels()
    Error_Message(DataPanel(), "DataPanel", "NAC_Panels", "Data")
    Return NoError
1751 End
    //
Function NAC_DataPanel
    Static Function DataPanel()
    Variable yOfs, i, Left
    String ExpListLoad="Deconvolution;BeforeCoating;RateCoating;AfterCoating;↪
        ↪ LaserReference;Transmission;Radiation;RateCalorimetry;ZeroSticking;Heat;↪
        ↪ Sticking;"
1756 String Name
    yOfs=10
    NewPanel /N=NAC_Control /K=2 /W=(10,10,1250,815) as "NAC Data Evaluation ↪
        ↪ Version "+NAC_Version
    ModifyPanel /W=NAC_Control fixedsize=1
    SetDrawLayer UserBack

```

```

1761 Left=170
ValDisplay SampleRate, Pos={Left,yOfs+0}, BodyWidth=80, Frame=2, Title="Sample ↵
  ↳ Rate (1/s): ", Value="#root:NAC:Experiment:SampleRate"
ValDisplay ChopperPeriod, Pos={Left,yOfs+20}, BodyWidth=80, Frame=2, Title="↵
  ↳ Chopper Halfperiod (s): ", Value="#root:NAC:Experiment:ChopperPeriod"
ValDisplay ChopperDelay, Pos={Left,yOfs+40}, BodyWidth=80, Frame=2, Title="↵
  ↳ Chopper Delay (s): ", Value="#root:NAC:Experiment:ChopperDelay"
ValDisplay ChopperOpenCloseSteps, Pos={Left,yOfs+60}, BodyWidth=80, Frame=2, ↵
  ↳ Title="Chopper Steps: ", Value="#root:NAC:Experiment:OpenCloseSteps"
1766 ValDisplay NominalPulseLength, Pos={Left,yOfs+80}, BodyWidth=80, Frame=2, Title↵
  ↳ ="Nominal Pulse Length (s): ", Value="#root:NAC:Experiment:↵
  ↳ NominalPulseLength"
SetVariable PulseLength, Pos={Left,yOfs+100}, BodyWidth=80, Frame=2, Limits↵
  ↳ ={0.001, Inf, 0.001}, Title="Pulse Length (s): ", Value=root:NAC:Experiment↵
  ↳ :PulseLength
ValDisplay Transmission, Pos={Left,yOfs+120}, BodyWidth=80, Frame=2, Title="↵
  ↳ Transmission: ",Value="#root:NAC:Transmission:Transmission"
Left+=250
ValDisplay BeamDia, Pos={Left,yOfs+0}, BodyWidth=80, Frame=2, Title="Beam ↵
  ↳ Diameter (m): ", Value="#root:NAC:Machine:BeamDiameter"
1771 ValDisplay QCMDia, Pos={Left,yOfs+20}, BodyWidth=80, Frame=2, Title="QCM ↵
  ↳ Diameter (m): ", Value="#root:NAC:Machine:QCMDiameter"
ValDisplay QCMToolCoat, Pos={Left,yOfs+40}, BodyWidth=80, Frame=2, Title="QCM ↵
  ↳ Tooling Coating: ", Value="#root:NAC:Machine:QCMToolingCoating"
ValDisplay QMSToolCal, Pos={Left,yOfs+60}, BodyWidth=80, Frame=2, Title="QMS ↵
  ↳ Tooling Calorimetry: ", Value="#root:NAC:Machine:QMSToolingCalorimetry"
//ValDisplay LaserPowCorr, Pos={Left,yOfs+80}, BodyWidth=80, Frame=2, Title="\↵
  ↳ Laser\" Power Correction: ", Value="#root:NAC:Machine:LaserPowerCorrection"
PopupMenu LaserPowCorr, Pos={Left,yOfs+77}, BodyWidth=80, Frame=0, Mode=1, proc↵
  ↳ =NAC_LaserPowerCorrectionPopUp, Title="\Laser\" Power Correction: ", Value↵
  ↳ ="#root:NAC:Machine:LaserPowerCorrectionList"
1776 SetVariable MirrorPowCorr, Pos={Left,yOfs+100}, BodyWidth=80, Frame=2, Title="↵
  ↳ Mirror Contamination: ", Value=root:NAC:Experiment:MirrorContamination
//SetVariable ReflectClean, Pos={Left,yOfs+120}, BodyWidth=80, Frame=2, Limits↵
  ↳ ={0.001, 0.999, 0.005}, Title="Reflectivity Clean Sample: ",Value=root:NAC:↵
  ↳ Machine:ReflectivityClean
PopupMenu ReflectClean, Pos={Left,yOfs+117}, BodyWidth=80, Frame=0, Mode=1, ↵
  ↳ proc=NAC_ReflectivityCleanPopUp, Title="Reflectivity Clean Sample: ", Value↵
  ↳ ="#root:NAC:Machine:ReflectivityCleanList"
Left+=250
ValDisplay HiPass, Pos={Left,yOfs+0}, BodyWidth=80, Frame=2, Title="High Pass ↵
  ↳ Cutoff (Hz): ",Value="#root:NAC:Machine:HighPassFrequency"
1781 ValDisplay LineNotch, Pos={Left,yOfs+20}, BodyWidth=80, Frame=2, Title="Mains ↵
  ↳ Frequency (Hz): ",Value="#root:NAC:Machine:LineNotchFrequency"
SetVariable SecondNotch, Pos={Left,yOfs+40}, BodyWidth=80, Frame=2, Limits={1, ↵
  ↳ 1e4, 1}, Title="Extra Notch Filter (Hz): ", Value=root:NAC:Machine:↵
  ↳ SecondNotchFrequency
ValDisplay Nyquist, Pos={Left,yOfs+60}, BodyWidth=80, Frame=2, Title="Nyquist ↵
  ↳ Cutoff (Hz): ",Value="#root:NAC:Machine:NyquistFrequency"
SetVariable DeconvWin, Pos={Left,yOfs+80}, BodyWidth=80, Frame=2, Limits={0, 1,↵
  ↳ 1e-3}, Title="Deconvolution Window (s): ", Value=root:NAC:Machine:↵
  ↳ DeconvolutionWindow
SetVariable RateFitWin, Pos={Left,yOfs+100}, BodyWidth=80, Frame=2, Limits={0, ↵
  ↳ Inf, 1e-10}, Title="Dep. Rate Fitting Window (pnts): ", Value=root:NAC:↵
  ↳ Machine:RateFittingWindow
1786 SetVariable CoatingThickness, Pos={Left,yOfs+120}, BodyWidth=80, Frame=2, ↵
  ↳ Limits={0, Inf, 1e-10}, Title="Coating Thickness (m): ", Value=root:NAC:↵
  ↳ RateCoating:TotalThickness
Left+=250
SetVariable DepositionRate, Pos={Left,yOfs+0}, BodyWidth=80, Frame=2, Limits↵
  ↳ ={0, Inf, 1e-12}, Title="Calorimetry Dep. Rate (m/s): ", Value=root:NAC:↵
  ↳ RateCalorimetry:DepositionRate
ValDisplay QCMToolCal, Pos={Left,yOfs+20}, BodyWidth=80, Frame=2, Title="QCM ↵
  ↳ Tooling Calorimetry: ", Value="#root:NAC:Machine:QCMToolingCalorimetry"
SetVariable RateML, Pos={Left,yOfs+40}, BodyWidth=80, Frame=2, Limits={0.001, ↵
  ↳ Inf, 0.001}, Title="Calorimetry Dep. Rate (ML/s): ", Value=root:NAC:↵
  ↳ RateCalorimetry:RateMonoLayer
1791 SetVariable DoseML, Pos={Left,yOfs+60}, BodyWidth=80, Frame=2, Limits={0.001, ↵
  ↳ Inf, 0.001}, Title="Calorimetry Dose (ML/Pulse): ", Value=root:NAC:↵

```

```

    ↪ RateCalorimetry:DosePerPulse
SetVariable DoseMole, Pos={Left,yOfs+80}, BodyWidth=80, Frame=2, Limits={1e-15,↪
    ↪ Inf, 1e-12}, Title="Calorimetry Dose (Mole/Pulse): ", Value=root:NAC:↪
    ↪ RateCalorimetry:MoleDosePerPulse
SetVariable MLDensity, Pos={Left,yOfs+100}, BodyWidth=80, Frame=2, Limits={1, ↪
    ↪ Inf, 1e15}, Title="Sample ML Density (1/m^2): ", Value=root:NAC:↪
    ↪ RateCalorimetry:MonolayerDensity
Left+=250
SetVariable TemperatureSample, Pos={Left,yOfs+0}, BodyWidth=80, Frame=2, Limits↪
    ↪ ={1, 2000, 1}, Title="Sample Temperature (K): ", Value=root:NAC:Experiment:↪
    ↪ TemperatureSample, proc=NAC_ReCalcHeat
1796 SetVariable TemperatureSource, Pos={Left,yOfs+20}, BodyWidth=80, Frame=2, ↪
    ↪ Limits={1, 2000, 1}, Title="Source Temperature (K): ", Value=root:NAC:↪
    ↪ Experiment:TemperatureSource, proc=NAC_ReCalcHeat
SetVariable SubAds, Pos={Left,yOfs+40}, BodyWidth=80, Frame=2, Limits={0, Inf, ↪
    ↪ 10}, Title="Subtract Adsorption (J/mol): ", Value=root:NAC:Enthalpies:↪
    ↪ SubtractAdsorbed, proc=NAC_ReCalcHeat
SetVariable SubDes, Pos={Left,yOfs+60}, BodyWidth=80, Frame=2, Limits={0, Inf, ↪
    ↪ 10}, Title="Subtract Desorption (J/mol): ", Value=root:NAC:Enthalpies:↪
    ↪ SubtractDesorbed, proc=NAC_ReCalcHeat
ValDisplay MultEntRef, Pos={Left,yOfs+80}, BodyWidth=80, Frame=2, Limits={0, ↪
    ↪ Inf, 10}, Title="Multilayer Reference (J/mol): ", Value=#"root:NAC:↪
    ↪ Enthalpies:MultiLayerReference[0]"
ValDisplay MultEnth, Pos={Left,yOfs+100}, BodyWidth=80, Frame=2, Limits={0, Inf↪
    ↪ , 10}, Title="Multilayer Enthalpy (J/mol): ", Value=#"root:NAC:Enthalpies:↪
    ↪ MultiLayerEnthalpy"
1801 ValDisplay MultEnthErr, Pos={Left,yOfs+120}, BodyWidth=80, Frame=2, Limits={0, ↪
    ↪ Inf, 10}, Title="Multilayer Enthalpy Error (J/mol): ", Value=#"root:NAC:↪
    ↪ Enthalpies:MultiLayerEnthalpyError"
yOfs+=160
left=40
DrawLine 10,yOfs-10,1220,yOfs-10
TitleBox T_Lazy size={110,30}, fcolor=(0, 0, 0), pos={10,yOfs}, frame=0, fstyle↪
    ↪ =1, fixedsize=1, anchor=MT, title="\JC \r\JCLazy"
1806 TitleBox T_DeConv size={85,30}, fcolor=(0, 0, 0), pos={left+100,yOfs}, frame=0,↪
    ↪ fstyle=1, fixedsize=1, anchor=MT, title="\JC \r\JCDeconvolution"
TitleBox T_BeforeCoating size={80,30}, fcolor=(0, 0, 0), pos={left+200,yOfs}, ↪
    ↪ frame=0, fstyle=1, fixedsize=1, anchor=MT, title="\JCBefore\r\JCCoating"
TitleBox T_Coating size={80,30}, fcolor=(0, 0, 0), pos={left+300,yOfs}, frame↪
    ↪ =0, fstyle=1, fixedsize=1, anchor=MT, title="\JCThickness\r\JCCoating"
TitleBox T_AfterCoating size={80,30}, fcolor=(0, 0, 0), pos={left+400,yOfs}, ↪
    ↪ frame=0, fstyle=1, fixedsize=1, anchor=MT, title="\JCAfter\r\JCCoating"
TitleBox T_LaserReference size={80,30}, fcolor=(0, 0, 0), pos={left+500,yOfs}, ↪
    ↪ frame=0, fstyle=1, fixedsize=1, anchor=MT, title="\JC"Laser"\r\↪
    ↪ JCReference"
1811 TitleBox T_Transmission size={80,30}, fcolor=(0, 0, 0), pos={left+600,yOfs}, ↪
    ↪ frame=0, fstyle=1, fixedsize=1, anchor=MT, title="\JC \r\JCTransmission"
TitleBox T_Radiation size={80,30}, fcolor=(0, 0, 0), pos={left+700,yOfs}, frame↪
    ↪ =0, fstyle=1, fixedsize=1, anchor=MT, title="\JC \r\JCRadiation"
TitleBox T_QCMCal size={100,30}, fcolor=(0, 0, 0), pos={left+800-10,yOfs}, ↪
    ↪ frame=0, fstyle=1, fixedsize=1, anchor=MT, title="\JCDeposition Rate\r\↪
    ↪ JCCalorimetry"
TitleBox T_ZeroSticking size={80,30}, fcolor=(0, 0, 0), pos={left+900,yOfs}, ↪
    ↪ frame=0, fstyle=1, fixedsize=1, anchor=MT, title="\JCZero\r\JCSticking"
TitleBox T_Heat size={80,30}, fcolor=(0, 0, 0), pos={left+1000,yOfs}, frame=0, ↪
    ↪ fstyle=1, fixedsize=1, anchor=MT, title="\JC \r\JCHeat"
1816 TitleBox T_Sticking size={80,30}, fcolor=(0, 0, 0), pos={left+1100,yOfs}, frame↪
    ↪ =0, fstyle=1, fixedsize=1, anchor=MT, title="\JC \r\JCSticking"
yOfs+=40
Button LoadLazy pos={10,yOfs-2}, Proc=NAC_LoadLazyButton, size={110,20}, title↪
    ↪ ="Load"
TitleBox T_Header size={120, 25}, fcolor=(0, 0, 0), pos={10,yOfs+25}, frame=0, ↪
    ↪ fstyle=1, fixedsize=1, anchor=LT, title="File Header:"
TitleBox T_FileName size={120, 25}, fcolor=(0, 0, 0), pos={10,yOfs+50}, frame↪
    ↪ =0, fstyle=1, fixedsize=1, anchor=LT, title="File Name:"
1821 TitleBox T_Disp size={120, 25}, fcolor=(0, 0, 0), pos={10,yOfs+75}, frame=0, ↪
    ↪ fstyle=1, fixedsize=1, anchor=LT, title="Full Data:"
TitleBox T_Flag size={120, 25}, fcolor=(0, 0, 0), pos={10,yOfs+100}, frame=0, ↪
    ↪ fstyle=1, fixedsize=1, anchor=LT, title="Flagging:"

```

```

Button ProcessLazy pos={10,yOfs+123}, Proc=NAC_ProcessLazyButton, size↵
↳ ={110,20}, title="Process"
Button StatisticsLazy pos={10,yOfs+148}, Proc=NAC_StatisticsLazyButton, size↵
↳ ={110,20}, title="Statistics"
TitleBox T_Decon size={120, 25}, fcolor=(0, 0, 0), pos={10,yOfs+175}, frame=0, ↵
↳ fstyle=1, fixedsize=1, anchor=LT, title="Deconvolution:"
1826 TitleBox T_Res size={120, 25}, fcolor=(0, 0, 0), pos={10,yOfs+200}, frame=0, ↵
↳ fstyle=1, fixedsize=1, anchor=LT, title="Result:"
For (i=0;i<ItemsInList(ExpListLoad);i+=1)
left=(i+1)*100+40
Name=StringFromList(i,ExpListLoad)
StrSwitch (Name)
1831 Case "Heat":
Button $"Load"+Name pos={left,yOfs-2}, Proc=NAC_LoadButton, size↵
↳ ={180,20}, title="Load"
Button $"Header"+Name pos={left,yOfs+23}, Proc=NAC_HeaderButton, size↵
↳ ={180,20}, title="Show"
SetVariable $"FileName"+Name bodyWidth=180, disable=2, pos={left+130,yOfs↵
↳ +50}, title=" ", value=$"root:NAC:"+Name+":FileName"
Break
1836 Case "Sticking":
Break
Default:
Button $"Load"+Name pos={left,yOfs-2}, Proc=NAC_LoadButton, size={80,20},↵
↳ title="Load"
Button $"Header"+Name pos={left,yOfs+23}, Proc=NAC_HeaderButton, size↵
↳ ={80,20}, title="Show"
1841 SetVariable $"FileName"+Name bodyWidth=80, disable=2, pos={left+30,yOfs↵
↳ +50}, title=" ", value=$"root:NAC:"+Name+":FileName"
EndSwitch
StrSwitch (Name)
Case "RateCalorimetry":
Case "RateCoating":
1846 Button $"Display"+Name pos={left,yOfs+73}, Proc=NAC_DisplayRateFile, size↵
↳ ={80,20}, title="Display"
Default:
Button $"Display"+Name pos={left,yOfs+73}, Proc=NAC_DisplayFullButton, ↵
↳ size={80,20}, title="Display"
Break
EndSwitch
1851 StrSwitch (Name)
Case "RateCalorimetry":
Case "RateCoating":
Button $"Process"+Name pos={left,yOfs+123}, Proc=NAC_ProcessButton, size↵
↳ ={80,20}, title="Process"
Button $"Result"+Name pos={left,yOfs+198}, Proc=NAC_ResultButton, size↵
↳ ={80,20}, title="Present"
1856 Break
Case "Heat":
Button $"Flag"+Name pos={left,yOfs+98}, Proc=NAC_DisplayFlagButton, size↵
↳ ={80,20}, title="Flag"
Button $"Process"+Name pos={left,yOfs+123}, Proc=NAC_ProcessButton, size↵
↳ ={80,20}, title="Process"
Button $"Result"+Name pos={left,yOfs+198}, Proc=NAC_ResultButton, size↵
↳ ={80,20}, title="Present"
1861 Button $"DeConvAvg"+Name pos={left,yOfs+173}, Proc=↵
↳ NAC_DeconvoluteAverageButton, size={38,20}, title="Avg"
Button $"DeConvAll"+Name pos={left+42,yOfs+173}, Proc=↵
↳ NAC_DeconvoluteAllButton, size={38,20}, title="All"
Break
Case "Sticking":
Button $"Flag"+Name pos={left,yOfs+98}, Proc=NAC_DisplayFlagButton, size↵
↳ ={80,20}, title="Flag"
1866 Button $"Process"+Name pos={left,yOfs+123}, Proc=NAC_ProcessButton, size↵
↳ ={80,20}, title="Process"
Button $"Result"+Name pos={left,yOfs+198}, Proc=NAC_ResultButton, size↵
↳ ={80,20}, title="Present"
Button $"DeConvAvg"+Name pos={left,yOfs+173}, Proc=↵
↳ NAC_DeconvoluteAverageButton, size={38,20}, title="Avg", disable=2

```

```

        Button $"DeConvAll"+Name pos={left+42,yOfs+173}, Proc=↵
↵ NAC_DeconvoluteAllButton, size={38,20}, title="All", disable=2
        Break
1871    Default:
        Button $"Flag"+Name pos={left,yOfs+98}, Proc=NAC_DisplayFlagButton, size↵
↵ ={80,20}, title="Flag"
        Button $"Process"+Name pos={left,yOfs+123}, Proc=NAC_ProcessButton, size↵
↵ ={80,20}, title="Process"
        Button $"Statistics"+Name pos={left,yOfs+148}, Proc=NAC_StatisticsButton,↵
↵ size={80,20}, title="Statistics"
        StrSwitch (Name)
1876    Case "ZeroSticking":
        Break
        Case "Deconvolution":
        Button $"DeConvFull"+Name pos={left,yOfs+173}, Proc=↵
↵ NAC_DeconvoluteFullButton, size={80,20}, title="Everything"
        Break
1881    Default:
        Button $"DeConvAvg"+Name pos={left,yOfs+173}, Proc=↵
↵ NAC_DeconvoluteAverageButton, size={38,20}, title="Avg"
        Button $"DeConvAll"+Name pos={left+42,yOfs+173}, Proc=↵
↵ NAC_DeconvoluteAllButton, size={38,20}, title="All"
        EndSwitch
        Button $"Result"+Name pos={left,yOfs+198}, Proc=NAC_ResultButton, size↵
↵ ={80,20}, title="Present"
1886    Break
        EndSwitch
    EndFor
    yofs+=225
    TitleBox T_Subst size={120,20}, fcolor=(0, 0, 0), pos={10,yOfs+0}, frame=0, ↵
↵ fstyle=1, fixedsize=1, anchor=LT, title="Substance:"
1891    TitleBox T_NumFrame size={120,20}, fcolor=(0, 0, 0), pos={10,yOfs+20}, frame=0,↵
↵ fstyle=1, fixedsize=1, anchor=LT, title="Total Frames:"
    TitleBox T_EffFrame size={120,20}, fcolor=(0, 0, 0), pos={10,yOfs+40}, frame=0,↵
↵ fstyle=1, fixedsize=1, anchor=LT, title="Processed Frames:"
    TitleBox T_LaserPow size={120,20}, fcolor=(0, 0, 0), pos={10,yOfs+60}, frame=0,↵
↵ fstyle=1, fixedsize=1, anchor=LT, title="\Laser\" Power (W):"
    TitleBox T_Reflec size={120,20}, fcolor=(0, 0, 0), pos={10,yOfs+80}, frame=0, ↵
↵ fstyle=1, fixedsize=1, anchor=LT, title="Reflectivity:"
    For (i=0;i<ItemsInList(ExpListLoad);i+=1)
1896    left=(i+1)*100+40
        Name=StringFromList(i,ExpListLoad)
        If (StringMatch(Name,"Rate*"))
            SetVariable $"Substance"+Name bodyWidth=80, disable=2, pos={left+30,yOfs↵
↵ +0}, title=" ", value=$"root:NAC:"+Name+":Substance"
        Else
1901    ValDisplay $"NumFrames"+Name, pos={left+30,yOfs+20}, bodyWidth=80, frame=2,↵
↵ title="",value=#("root:NAC:"+Name+":NumberOfFrames")
            ValDisplay $"NonFFrames"+Name, pos={left+30,yOfs+40}, bodyWidth=80, frame↵
↵ =2, title="",value=#("root:NAC:"+Name+":EffectiveFrames")
        EndIf
        If ((!StringMatch(Name,"Rate*") && StringMatch(Name,"*Coating")) || ↵
↵ StringMatch(Name,"Laser*") || StringMatch(Name,"Transmission") || ↵
↵ StringMatch(Name,"Deconvolution"))
            SetVariable $"LaserPow"+Name, pos={left+30,yOfs+60}, bodyWidth=80, title=" ↵
↵ ", Limits={0,Inf,1e-6}, Value=$("root:NAC:"+Name+":LaserPower")
1906    Endif
        If (StringMatch(Name,"BeforeCoating") || StringMatch(Name,"Laser*") || ↵
↵ StringMatch(Name,"Deconvolution"))
            SetVariable $"Reflec"+Name, pos={left+30,yOfs+80}, bodyWidth=80, frame=2, ↵
↵ title=" ", limits={0,1,0.01}, value=$("root:NAC:"+Name+":Reflectivity")
        ElseIf (StringMatch(Name,"AfterCoating"))
            ValDisplay ReflecAfterCoating, pos={left+30,yOfs+80}, bodyWidth=80, frame↵
↵ =2, title="", value=#"root:NAC:AfterCoating:Reflectivity"
1911    Endif
    EndFor
    yofs+=120
    DrawLine 10,yOfs-10,1220,yOfs-10

```



```

TitleBox T_Fitting size={120,20}, fcolor=(0, 0, 0), pos={10,y0fs+0}, frame=0, ↵
  ↵ fstyle=1, fixedsize=1, anchor=LT, title="Fitting:"
1916 ValDisplay Progress, Pos={40,y0fs+20}, BodyWidth=110, frame=2, title=" ", ↵
  ↵ Disable=1, fixedsize=1, BarMisc={0,0}, value=#"root:NAC:GUI:ProgressValue"
CheckBox AutoFlag, Pos={30,y0fs+62}, BodyWidth=110, Frame=2, Side=1, Title=" ↵
  ↵ Auto Flag: ", Variable=root:NAC:Experiment:AutoFlag
left=140
TitleBox T_DeConAverage size={100,20}, fcolor=(0, 0, 0), pos={left+0,y0fs+4}, ↵
  ↵ frame=0, fstyle=0, fixedsize=1, anchor=LT, title="Average Frames"
SetVariable DeConAverage, Pos={Left+15,y0fs+20}, BodyWidth=65, Frame=2, Limits↵
  ↵ ={1,Inf,1}, Title=" ", Value=root:NAC:Deconvolution:AverageFrames
1921 TitleBox T_DeConRemRad size={100,20}, fcolor=(0, 0, 0), pos={left+0,y0fs+44}, ↵
  ↵ frame=0, fstyle=0, fixedsize=1, anchor=LT, title="Remove Radiation"
CheckBox RemRadFix proc=NAC_DCRproc, Pos={left-10,y0fs+62}, BodyWidth=30, Frame↵
  ↵ =2, Side=1, fixedsize=1, Title="Fixed", Variable=root:NAC:Deconvolution:↵
  ↵ RemoveFixedRadiation
CheckBox RemRadFit proc=NAC_DCRproc, Pos={left+35,y0fs+62}, BodyWidth=30, Frame↵
  ↵ =2, Side=1, fixedsize=1, Title="Fitted", Variable=root:NAC:Deconvolution:↵
  ↵ RemoveFittedRadiation
TitleBox T_DeConUseFit size={100,20}, fcolor=(0, 0, 0), pos={left+0,y0fs+84}, ↵
  ↵ frame=0, fstyle=0, fixedsize=1, anchor=LT, title="Use Fitted"
CheckBox UseFit Pos={left+30,y0fs+102}, BodyWidth=80, Frame=2, Side=1, ↵
  ↵ fixedsize=1, Title="Fit Wave: ", Variable=root:NAC:Deconvolution:↵
  ↵ UseFittedFitWave
1926 CheckBox UseSens Pos={left+35,y0fs+122}, BodyWidth=80, Frame=2, Side=1, ↵
  ↵ fixedsize=1, Title="Use Sensitivity", Variable=root:NAC:Deconvolution:↵
  ↵ UseSensitivity
SetVariable DeConSens, Pos={Left+15,y0fs+140}, BodyWidth=65, Frame=2, Limits={-↵
  ↵ Inf,Inf,0.01}, Title=" ", Value=root:NAC:Deconvolution:Sensitivity
left+=200
CheckBox UseTotalRateCoating proc=NAC_UseTotalRangeProc, disable=0, pos={left↵
  ↵ +30,y0fs+0}, BodyWidth=80, Side=1, Title="Total Range: ", variable=root:NAC↵
  ↵ :RateCoating:UseTotalRange
CheckBox UseBLRateCoating proc=NAC_UseBaselineProc, disable=0, pos={left+30,↵
  ↵ y0fs+20}, BodyWidth=80, Side=1, Title="Baseline: ", variable=root:NAC:↵
  ↵ RateCoating:UseBaseline
1931 NVar UseTotalRange=root:NAC:RateCoating:UseTotalRange
If (UseTotalRange)
  CheckBox UseBLRateCoating Disable=2
EndIf
left+=400
1936 TitleBox T_EmptyCrucible size={100,20}, fcolor=(0, 0, 0), pos={left+0,y0fs+4}, ↵
  ↵ frame=0, fstyle=0, fixedsize=1, anchor=LT, title="Use Empty Crucible"
CheckBox UseEmptyCrucible proc=NAC_UseEmptyCrucibleProc, disable=0, pos={left↵
  ↵ +30,y0fs+20}, Side=1, Title="Reference: ", variable=root:NAC:Experiment:↵
  ↵ UseEmptyCrucibleReference
TitleBox T_EmptyCrucibleTempA size={100,20}, fcolor=(0, 0, 0), pos={left+0,y0fs↵
  ↵ +46}, frame=0, fstyle=0, fixedsize=1, anchor=LT, title="Reference"
TitleBox T_EmptyCrucibleTempB size={100,20}, fcolor=(0, 0, 0), pos={left+0,y0fs↵
  ↵ +62}, frame=0, fstyle=0, fixedsize=1, anchor=LT, title="Temperature (K):"
ValDisplay EmptyCrucibleTemperature, Pos={Left+30,y0fs+80}, BodyWidth=80, Frame↵
  ↵ =2, Title=" ", Value=#"root:NAC:Experiment:EmptyCrucibleTemperature"
1941 left+=100
CheckBox UseBLRateCalorimetry proc=NAC_UseBaselineProc, disable=0, pos={left↵
  ↵ +30,y0fs+20}, Side=1, Title="Baseline: ", variable=root:NAC:RateCalorimetry↵
  ↵ :UseBaseline
left+=200
TitleBox T_HeatOffset size={100,20}, fcolor=(0, 0, 0), pos={left+0,y0fs+4}, ↵
  ↵ frame=0, fstyle=0, fixedsize=1, anchor=LT, title="Offset | Hold"
SetVariable HeatOffset, Pos={left+15,y0fs+20}, BodyWidth=65, Frame=2, Limits={-↵
  ↵ Inf, Inf, 0.001}, Title=" ", Value=root:NAC:Heat:InitOffset
1946 CheckBox HoldHeatOffset, Pos={left+65,y0fs+22}, BodyWidth=10, Frame=2, Title=" ↵
  ↵ ", Variable=root:NAC:Heat:HoldOffset
TitleBox T_HeatAmp size={100,20}, fcolor=(0, 0, 0), pos={left+0,y0fs+44}, frame↵
  ↵ =0, fstyle=0, fixedsize=1, anchor=LT, title="Heat Amp | Hold"
SetVariable HeatAmp, Pos={left+15,y0fs+60}, BodyWidth=65, Frame=2, Limits={-↵
  ↵ Inf, Inf, 1e-7}, Title=" ", Value=root:NAC:Heat:InitAdsorption
CheckBox HoldHeatAmp, Pos={left+65,y0fs+62}, BodyWidth=10, Frame=2, Title=" ", ↵
  ↵ Variable=root:NAC:Heat:HoldAdsorption

```

```

TitleBox T_HeatShift size={100,20}, fcolor=(0, 0, 0), pos={left+0,y0fs+84}, ↵
  ↵ frame=0, fstyle=0, fixedsize=1, anchor=LT, title="Heat Shift | Hold"
1951 SetVariable HeatShift, Pos={left+15,y0fs+100}, BodyWidth=65, Frame=2, Limits={-↵
  ↵ Inf, Inf, 0.001}, Title=" ", Value=root:NAC:Heat:InitAdsorptionShift
CheckBox HoldHeatShift, Pos={left+65,y0fs+102}, BodyWidth=10, Frame=2, Title=" ↵
  ↵ ", Variable=root:NAC:Heat:HoldAdsorptionShift
TitleBox T_RadAmp size={100,20}, fcolor=(0, 0, 0), pos={left+0,y0fs+124}, frame↵
  ↵ =0, fstyle=0, fixedsize=1, anchor=LT, title="Rad Amp | Hold"
SetVariable RadAmp, Pos={left+15,y0fs+140}, BodyWidth=65, Frame=2, Limits={-Inf↵
  ↵ , Inf, 0.01}, Title=" ", Value=root:NAC:Heat:InitRadiation
CheckBox HoldRadAmp, Pos={left+65,y0fs+142}, BodyWidth=10, Frame=2, Title=" ", ↵
  ↵ Variable=root:NAC:Heat:HoldRadiation
1956 TitleBox T_RadShift size={100,20}, fcolor=(0, 0, 0), pos={left+0,y0fs+164}, ↵
  ↵ frame=0, fstyle=0, fixedsize=1, anchor=LT, title="Rad Shift | Hold"
SetVariable RadShift, Pos={left+15,y0fs+180}, BodyWidth=65, Frame=2, Limits={-↵
  ↵ Inf,Inf,0.001}, Title=" ", Value=root:NAC:Heat:InitRadiationShift
CheckBox HoldRadShift, Pos={left+65,y0fs+182}, BodyWidth=10, Frame=2, Title=" ↵
  ↵ ", Variable=root:NAC:Heat:HoldRadiationShift
CheckBox FittedRad, Pos={left+31,y0fs+207}, BodyWidth=10, Frame=2, Side=1, ↵
  ↵ Disable=2, Title="Use Trend: ", Variable=root:NAC:Experiment:↵
  ↵ UseFittedRadiation
CheckBox LockShifts, Pos={left+31,y0fs+227}, BodyWidth=40, Frame=2, Side=1, ↵
  ↵ Disable=0, Title="Link Heat & Radiation Shifts: ", Variable=root:NAC:Heat:↵
  ↵ LinkShifts
1961 left+=100
TitleBox T_StickingOffset size={100,20}, fcolor=(0, 0, 0), pos={left+0,y0fs+4},↵
  ↵ frame=0, fstyle=0, fixedsize=1, anchor=LT, title="Offset | Hold"
SetVariable StickingOffset, Pos={left+15,y0fs+20}, BodyWidth=65, Frame=2, ↵
  ↵ Limits={-Inf,Inf,0.001}, Title=" ", Value=root:NAC:Sticking:InitOffset
CheckBox HoldDesorptionOffset, Pos={left+65,y0fs+22}, BodyWidth=10, Frame=2, ↵
  ↵ Title=" ", Variable=root:NAC:Sticking:HoldOffset
TitleBox T_StickingAmp size={100,20}, fcolor=(0, 0, 0), pos={left+0,y0fs+44}, ↵
  ↵ frame=0, fstyle=0, fixedsize=1, anchor=LT, title="Desorption | Hold"
1966 SetVariable StickingAmp, Pos={left+15,y0fs+60}, BodyWidth=65, Frame=2, Limits↵
  ↵ ={-Inf,Inf,0.01}, Title=" ", Value=root:NAC:Sticking:InitDesorption
CheckBox HoldDesorptionAmp, Pos={left+65,y0fs+62}, BodyWidth=10, Frame=2, Title↵
  ↵ =" ", Variable=root:NAC:Sticking:HoldDesorption
TitleBox T_StickingShift size={100,20}, fcolor=(0, 0, 0), pos={left+0,y0fs+84},↵
  ↵ frame=0, fstyle=0, fixedsize=1, anchor=LT, title="Shift | Hold"
SetVariable StickingShift, Pos={left+15,y0fs+100}, BodyWidth=65, Frame=2, ↵
  ↵ Limits={-Inf,Inf,0.001}, Title=" ", Value=root:NAC:Sticking:InitShift
CheckBox HoldDesorptionShift, Pos={left+65,y0fs+102}, BodyWidth=10, Frame=2, ↵
  ↵ Title=" ", Variable=root:NAC:Sticking:HoldShift
1971 CheckBox FittedDes, Pos={left+31,y0fs+207}, BodyWidth=10, Frame=2, Side=1, ↵
  ↵ Disable=2, Title="Use Trend: ", Variable=root:NAC:Experiment:↵
  ↵ UseFittedDesorption
y0fs+=230
Return NoError
End
//

```

C.1.4 Data Processing

```

1976 //
Function NAC_AutoFlagAll
Function NAC_AutoFlagAll()
String ExpList="Deconvolution;BeforeCoating;AfterCoating;LaserReference;↵
  ↵ Transmission;Radiation;ZeroSticking;"
String Name
Variable i
1981 NVar AutoFlagged=root:NAC:Experiment:AutoFlagged
  For (i=0;i<ItemsInList(ExpList);i+=1)
    Name=StringFromList(i, ExpList, ";")
    NAC_AutoFlag(Name)
    Error_Message(UpdateFlagWin(Name), "UpdateFlagWin", "NAC_AutoFlagAll", Name)
1986 EndFor
  AutoFlagged=1
End

```

```

//
Function Coverage2Thickness
Static Function Coverage2Thickness(Coverage)
1991 Variable Coverage
NVar Density=root:NAC:RateCalorimetry:Density,MolarMass=root:NAC:RateCalorimetry:↵
↵ MolarMass, MonolayerDensity=root:NAC:RateCalorimetry:MonolayerDensity
Return Coverage / (Density*1e3)*(MolarMass*1e-3)*(MonolayerDensity)/N_Avo
End
//
Function ProcessProc
1996 Static Function ProcessProc(Name[, NoDecon])
String Name
Variable NoDecon
String WName="NAC_"+Name+"_Avg"
Variable Tmp, DoDecon
2001 If (ParamIsDefault(NoDecon))
NoDecon=0
EndIf
DoDecon=!NoDecon
StrSwitch (Name)
2006 Case "RateCalorimetry":
Case "RateCoating":
NVar Loaded=$"root:NAC:"+Name+":Loaded"
If (!Loaded)
Return NAC_NoDataLoaded
2011 EndIf
Break
Case "Deconvolution":
Case "BeforeCoating":
Case "AfterCoating":
2016 Case "LaserReference":
Case "Transmission":
Case "Radiation":
Case "Heat":
Case "Sticking":
2021 Case "ZeroSticking":
NVar Loaded=$"root:NAC:"+Name+":Loaded"
If (!Loaded)
Return NAC_NoDataLoaded
EndIf
2026 NVar EffectiveFrames=$"root:NAC:"+Name+":EffectiveFrames"
If (EffectiveFrames<=0)
Return NAC_NothingToProcess
EndIf
Error_Message(Averaging(Name), "Averaging", "ProcessProc", Name)
2031 Error_Message(DisplayAverage(Name), "DisplayAverage", "ProcessProc", Name)
Break
Default:
Return NAC_UnknownMeasurement
EndSwitch
2036 Tmp=0
StrSwitch (Name)
Case "AfterCoating":
If ((Exists("root:NAC:Experiment:FitReflectivityOdd")!=1) || (Exists("root:↵
↵ NAC:Experiment:FitReflectivityEven")!=1))
Tmp=1
2041 EndIf
Break
Case "Transmission":
If ((Exists("root:NAC:Experiment:FitLaserReferenceOdd")!=1) || (Exists("↵
↵ root:NAC:Experiment:FitLaserReferenceEven")!=1))
Tmp=1
2046 EndIf
Break
Case "Heat":
If ((Exists("root:NAC:Experiment:FitLaserReferenceOdd")!=1) || (Exists("↵
↵ root:NAC:Experiment:FitLaserReferenceEven")!=1))

```

```

    Tmp=1
2051   EndIf
      If ((Exists("root:NAC:Experiment:FitRadiationOdd")!=1) || (Exists("root:NAC:
↳ :Experiment:FitRadiationEven")!=1))
        Tmp=1
        EndIf
        Break
2056   Case "Sticking":
      NVar HoldDesorption=root:NAC:Sticking:HoldDesorption
      If ((Exists("root:NAC:Experiment:FitStickingOdd")!=1) || (Exists("root:NAC:
↳ Experiment:FitStickingEven")!=1) && !HoldDesorption)
        Tmp=1
        EndIf
2061   Break
      Default:
        Break
    EndSwitch
    If (Tmp)
2066   Error_Message(SetGraphRanges(Name), "SetGraphRanges", "ProcessProc", Name)
      Return NAC_FitWavesMissing
    EndIf
    Execute /Z/Q "ModifyBrowser Collapse=GetBrowserLine(\"root:NAC\")"
    StrSwitch (Name)
2071   Case "Deconvolution":
      Error_Message(NormalizeFitWave(Name), "NormalizeFitWave", "ProcessProc",
↳ Name)
        Break
      Case "BeforeCoating":
        NVar ReflectivityClean=root:NAC:BeforeCoating:Reflectivity, ReflecCoat=root
↳ :NAC:AfterCoating:Reflectivity, ReflecLaser=root:NAC:LaserReference:
↳ Reflectivity
2076   Error_Message(NormalizeFitWave(Name), "NormalizeFitWave", "ProcessProc",
↳ Name)
        ReflecCoat=1-(GetRatio(NAC_RatioTypeReflectivity))*(1-ReflectivityClean)
        If (NumType(ReflecCoat)==0)
          ReflecLaser=ReflecCoat
        Else
2081   ReflecLaser=ReflectivityClean
        EndIf
        Break
      Case "AfterCoating":
        NVar ReflectivityClean=root:NAC:BeforeCoating:Reflectivity, ReflecCoat=root
↳ :NAC:AfterCoating:Reflectivity
2086   NVar ReflecLaser=root:NAC:LaserReference:Reflectivity, Sensitivity=root:NAC
↳ :Deconvolution:Sensitivity
        Error_Message(NormalizeFitWave(Name), "NormalizeFitWave", "ProcessProc",
↳ Name)
        ReflecCoat=1-GetRatio(NAC_RatioTypeReflectivity)*(1-ReflectivityClean)
        Sensitivity=GetRatio(NAC_RatioTypeSensitivity)
        If (NumType(ReflecCoat)==0)
2091   ReflecLaser=ReflecCoat
        Else
          ReflecLaser=ReflectivityClean
        EndIf
        Break
2096   Case "LaserReference":
        NVar Sensitivity=root:NAC:Deconvolution:Sensitivity
        Error_Message(GetPulseLength(), "GetPulseLength", "ProcessProc", Name)
        Error_Message(NormalizeFitWave(Name), "NormalizeFitWave", "ProcessProc",
↳ Name)
        Sensitivity=GetRatio(NAC_RatioTypeSensitivity)
2101   Break
      Case "Transmission":
        NVar Transmission=root:NAC:Transmission:Transmission, Radiation=root:NAC:
↳ Heat:InitRadiation
        NVar Hold=root:NAC:Heat:HoldRadiation
        Transmission=GetRatio(NAC_RatioTypeTransmission)
2106   If (!Hold)
          Radiation=1/Transmission

```

```

        EndIf
        Break
    Case "Radiation":
2111     Error_Message(NormalizeFitWave(Name), "NormalizeFitWave", "ProcessProc", ↵
        ↵ Name)
        Break
    Case "ZeroSticking":
        Error_Message(Averaging(Name), "Averaging", "ProcessProc", Name)
        Error_Message(NormalizeFitWave(Name), "NormalizeFitWave", "ProcessProc", ↵
        ↵ Name)
2116     Break
    Case "Heat":
        If ((Exists("root:NAC:Experiment:FitLaserReferenceOdd")==1) && (Exists("↵
        ↵ root:NAC:Experiment:FitLaserReferenceEven")==1)&& (Exists("root:NAC:↵
        ↵ Experiment:FitRadiationOdd")==1) && (Exists("root:NAC:Experiment:↵
        ↵ FitRadiationEven")==1))
            Error_Message(FitHeat(), "FitHeat", "ProcessProc", Name)
            CheckBox FittedRad Disable=0, Win=NAC_Control
2121     EndIf
            Break
    Case "Sticking":
        If (((Exists("root:NAC:Experiment:FitStickingOdd")==1) && (Exists("root:NAC↵
        ↵ :Experiment:FitStickingEven")==1)) || HoldDesorption)
            Error_Message(FitDesorption(), "FitDesorption", "ProcessProc", Name)
2126     CheckBox FittedDes Disable=0, Win=NAC_Control
            EndIf
            Break
    Case "RateCalorimetry":
    Case "RateCoating":
2131     Wave Thickness="$root:NAC:"+Name+":Thickness"
            If (WaveExists(Thickness))
                NVar AvgWindow=root:NAC:Machine:RateFittingWindow
                If (NumPnts(Thickness) > AvgWindow)
                    Error_Message(CalcQCMRate(Name), "CalcQCMRate", "ProcessProc", Name)
2136     Error_Message(DisplayFittedRate(Name), "DisplayFittedRate", "↵
        ↵ ProcessProc", Name)
                EndIf
            EndIf
            Break
    Default:
2141     Execute /Z/Q "ModifyBrowser Expand=GetBrowserLine(\"root:NAC\")"
            Return NAC_UnknownMeasurement
            Break
EndSwitch
StrSwitch (Name)
2146     Case "RateCalorimetry":
    Case "RateCoating":
        Break
    Case "BeforeCoating":
    Case "AfterCoating":
2151     Case "LaserReference":
    Case "Transmission":
    Case "Radiation":
    Case "Heat":
        If (DoDecon)
2156     Error_Message(DeconvolutionProcAverage(Name), "DeconvolutionProcAverage", ↵
        ↵ "NAC_DeconvoluteAverageButton", Name)
            Error_Message(DisplayDeconvolutedAverage(Name), "↵
        ↵ DisplayDeconvolutedAverage", "NAC_DeconvoluteAverageButton", Name)
            EndIf
        Case "Deconvolution":
    Case "Sticking":
2161     Case "ZeroSticking":
            Break
        Default:
            Execute /Z/Q "ModifyBrowser Expand=GetBrowserLine(\"root:NAC\")"
            Return NAC_UnknownMeasurement
2166     Break
EndSwitch

```

```

StrSwitch (Name)
  Case "RateCalorimetry":
  Case "RateCoating":
2171   Error_Message(UpdateFittedRate(Name), "UpdateFittedRate", "ProcessProc", ↵
    ↵ Name)
    Break
  Case "Deconvolution":
    Break
  Default:
2176   Error_Message(SetGraphRanges(Name, ProcessWave="AverageOdd"), "↵
    ↵ SetGraphRanges", "ProcessProc", Name+" Odd")
    Error_Message(SetGraphRanges(Name, ProcessWave="AverageEven"), "↵
    ↵ SetGraphRanges", "ProcessProc", Name+" Even")
    Break
EndSwitch
String FlagWindows=WinList("NAC*_Flag",",", "WIN:1")
2181 Variable i
For (i=0;i<ItemsInList(FlagWindows);i+=1)
  Error_Message(UpdateFlagWin(StringFromList(i,FlagWindows)), "UpdateFlagWin", ↵
    ↵ "ProcessProc", Name)
EndFor
StrSwitch (Name)
2186   Case "Heat":
  Case "Sticking":
    NVar TemperatureSource=root:NAC:Experiment:TemperatureSource, ↵
    ↵ TemperatureSample=root:NAC:Experiment:TemperatureSample
    If ((NumType(TemperatureSource)!=0) || (NumType(TemperatureSample)!=0))
      Variable TSource=TemperatureSource, TSample=TemperatureSample
2191     Prompt TSample, "Sample Temperature (K): "
      Prompt TSource, "Source Temperature (K): "
      DoPrompt /HELP="" "Parameters missing:", TSample, TSource
      TemperatureSource=TSource
      TemperatureSample=TSample
2196     If (V_Flag)
        Execute /Z/Q "ModifyBrowser Expand=GetBrowserLine(\"root:NAC\")"
        Return UserAbort
      ElseIf ((NumType(TemperatureSource)!=0) || (NumType(TemperatureSample)↵
    ↵ !=0))
        Execute /Z/Q "ModifyBrowser Expand=GetBrowserLine(\"root:NAC\")"
2201        Return NAC_NotApplicable
      EndIf
      DoUpdate
      EndIf
      Error_Message(CalcHeat(), "CalcHeat", "ProcessProc", Name)
2206     Error_Message(DisplayVsPulse("Heat"), "DisplayVsPulse", "ProcessProc", Name↵
    ↵ )
    Error_Message(DisplayVsPulse("Sticking"), "DisplayVsPulse", "ProcessProc", ↵
    ↵ Name)
    NVar Dose=root:NAC:RateCalorimetry:DosePerPulse
    If ((Dose>0) || (NumType(Dose)==0))
      Error_Message(DisplayVsCoverage("Heat"), "DisplayVsCoverage", "↵
    ↵ ProcessProc", Name)
2211     Error_Message(DisplayVsCoverage("Sticking"), "DisplayVsCoverage", "↵
    ↵ ProcessProc", Name)
    EndIf
    Error_Message(DoHeatTextBox(), "CalcHeat", "ProcessProc", Name)
    Error_Message(SetGraphRanges(Name), "SetGraphRanges", "ProcessProc", Name)
    Error_Message(UpdateFlagWin(Name), "UpdateFlagWin", "ProcessProc", Name)
2216   Break
  Case "RateCalorimetry":
  Case "RateCoating":
  Case "Deconvolution":
    Break
2221   Default:
    Error_Message(SetGraphRanges(Name), "SetGraphRanges", "ProcessProc", Name)
    Error_Message(UpdateFlagWin(Name), "UpdateFlagWin", "ProcessProc", Name)
    Break
EndSwitch
2226 DoUpdate

```

```

    DoWindow /F $WName
    Execute /Z/Q "ModifyBrowser Expand=GetBrowserLine(\"root:NAC\")"
    Return NoError
End
2231 //
Function DeconvoluteFrame
Static Function DeconvoluteFrame(Data, Index, Result, Parity)
Wave Data
Variable Index
Wave Result
2236 String Parity
NVar Delay=root:NAC:Experiment:ChopperDelay, Period=root:NAC:Experiment:
    ↪ ChopperPeriod
NVar Win=root:NAC:Machine:DeconvolutionWindow, Fitted=root:NAC:Deconvolution:
    ↪ UseFittedFitWave
Variable YOffset=0
Variable Step, Shift
2241 Make /N=1 /D /FREE FitCoef
    Step=DimDelta(Data,0)
    Make /FREE /D /N=(DimSize(Data,0)) Process, Diff=0, Int=0, Subtr=0
    SetScale /P x, DimOffset(Data,0), Step, "", Process, Diff, Int
    Process=Data[p][Index]
2246 If (Fitted)
    StrSwitch (Parity)
        Case "Odd":
            For (Shift=0;Shift<Period+9*Win;Shift+=Step)
                FitCoef={1e-6} // Offset, Amp, Shift
                SetScale /P x, -Shift, Step, "", Process, Subtr
                FuncFit /N /Q /W=2 DeconvolutionFuncOddFitted FitCoef Process(-Win,+Win
                ↪ )
                DeconvolutionFuncOddFitted(FitCoef,Subtr,Subtr)
                Process -=Subtr[p]
                Diff[Shift/Step]=FitCoef[0]
2256            EndFor
            Break
        Case "Even":
            For (Shift=0;Shift<Period+9*Win;Shift+=Step)
                FitCoef={1e-6} // Offset, Amp, Shift
                SetScale /P x, -Shift, Step, "", Process, Subtr
                FuncFit /N /Q /W=2 DeconvolutionFuncEvenFitted FitCoef Process(-Win,+
                ↪ Win)
                DeconvolutionFuncEvenFitted(FitCoef,Subtr,Subtr)
                Process -=Subtr[p]
                Diff[Shift/Step]=FitCoef[0]
2266            EndFor
            Break
    EndSwitch
Else
    StrSwitch (Parity)
2271    Case "Odd":
        For (Shift=0;Shift<Period+9*Win;Shift+=Step)
            FitCoef={1e-6}
            SetScale /P x, -Shift, Step, "", Process, Subtr
            FuncFit /N /Q /W=2 DeconvolutionFuncOdd FitCoef Process(-Win,+Win)
2276            DeconvolutionFuncOdd(FitCoef,Subtr,Subtr)
            Process -=Subtr[p]
            Diff[Shift/Step]=FitCoef[0]
        EndFor
        Break
2281    Case "Even":
        For (Shift=0;Shift<Period+9*Win;Shift+=Step)
            FitCoef={1e-6} // Offset, Amp, Shift
            SetScale /P x, -Shift, Step, "", Process, Subtr
            FuncFit /N /Q /W=2 DeconvolutionFuncEven FitCoef Process(-Win,+Win)
2286            DeconvolutionFuncEven(FitCoef,Subtr,Subtr)
            Process -=Subtr[p]
            Diff[Shift/Step]=FitCoef[0]
        EndFor

```

```

                Break
2291      EndSwitch
      EndIf
      Integrate /P Diff /D=Int
      SetScale /P x, -5*Win, Step, "", Int
      Result[][Index]=Int[p]
2296      SetScale d, 0, 0, "W", Result
      Killwaves Process, Int, Diff, Subtr
      Return NoError
End
//
Function DeconvolutionProcAverage
2301 Static Function DeconvolutionProcAverage(Name)
String Name
Variable Sens
  If (!WaveExists(root:NAC:Experiment:FitDeconvolutionOdd) || !WaveExists(root:↵
    ↵ NAC:Experiment:FitDeconvolutionEven))
    Return NAC_FitWavesMissing
2306  EndIf
  StrSwitch (Name)
    Case "RateCalorimetry":
    Case "RateCoating":
    Case "Deconvolution":
2311      Return NAC_NotApplicable
    Break
    Case "Sticking":
    Case "ZeroSticking":
2316      Return NAC_NotImplementedYet
    Break
    Case "BeforeCoating":
    Case "AfterCoating":
      Sens=1
    Break
2321  Case "LaserReference":
  Case "Transmission":
  Case "Radiation":
  Case "Heat":
    NVar Sensitivity=root:NAC:Deconvolution:Sensitivity, UseSens=root:NAC:↵
    ↵ Deconvolution:UseSensitivity
2326    If ((UseSens) && (NumType(Sensitivity)==0))
      Sens=Sensitivity
    Else
      Sens=1
    Endif
2331    Break
  Default:
    Return NAC_UnknownMeasurement
    Break
  EndSwitch
2336 DFRef OldDF=GetDataFolderDFR()
NVar EffectiveFrames="$root:NAC:"+Name+":EffectiveFrames"
NVar Average=root:NAC:Deconvolution:AverageFrames
NVar DPpP=root:NAC:Experiment:DataPointsPerFrame, Win=root:NAC:Machine:↵
  ↵ DeconvolutionWindow, Rate=root:NAC:Machine:ProcessRate, CP=root:NAC:↵
  ↵ Experiment:ChopperPeriod
If (!(EffectiveFrames>0))
2341  Return NAC_NothingToProcess
EndIf
If (!WaveExists("$root:NAC:"+Name+":AverageOdd") || !WaveExists("$root:NAC:"+↵
  ↵ Name+":AverageEven"))
  Error_Message(Averaging(Name), "Averaging", "DeconvolutionProcAverage", Name)
EndIf
2346 NVar ProgressValue=root:NAC:GUI:ProgressValue
NVar RemRadFix=root:NAC:Deconvolution:RemoveFixedRadiation, RadAmpFix=root:NAC:↵
  ↵ :Heat:InitRadiation
If (RemRadFix)
  If (WaveExists(root:NAC:Experiment:FitRadiationOdd) && WaveExists(root:NAC:↵
    ↵ Experiment:FitRadiationEven))

```



```

Wave RadOdd=root:NAC:Experiment:FitRadiationOdd, RadEven=root:NAC:
  Experiment:FitRadiationEven
2351 Else
  Return NAC_FitWavesMissing
EndIf
EndIf
ValDisplay Progress Disable=0, Limits={0,2,0}, win=NAC_Control
2356 ProgressValue=0
DoUpdate /W=NAC_Control
SetDataFolder $"root:NAC:"+Name
Make /O /N=(DPpP+10*Win*Rate) $"root:NAC:Deconvolution:"+Name+"AvgOdd"=0, $"
  root:NAC:Deconvolution:"+Name+"AvgEven"=0
Make /FREE /N=(DPpP+10*Win*Rate) DeconvWave=0
2361 Wave AverageOdd=$"root:NAC:"+Name+":AverageOdd", AverageEven=$"root:NAC:"+Name
  "+" :AverageEven"
Wave ResultAvgOdd=$"root:NAC:Deconvolution:"+Name+"AvgOdd", ResultAvgEven=$"
  root:NAC:Deconvolution:"+Name+"AvgEven"
SetScale /P x -5*Win, 1/Rate, "s", DeconvWave, ResultAvgOdd, ResultAvgEven
DeconvWave=(Pnt2X(DeconvWave,p)<0) ? AverageEven[X2Pnt(AverageEven,CP+x)] : ((
  Pnt2X(DeconvWave,p)>=CP) ? AverageEven[X2Pnt(AverageEven,x-CP)] :
  AverageOdd(x))
If (RemRadFix)
2366 DeconvWave -=RadAmpFix*RadOdd(x)
EndIf
DeconvWave/=Sens
Error_Message(DeconvoluteFrame(DeconvWave, 0, ResultAvgOdd, "Odd"), "
  DeconvoluteFrame", "DeconvolutionProcAverage", Name)
ProgressValue=1
2371 DoUpdate /W=NAC_Control
SetScale /P x -5*Win, 1/Rate, "s", DeconvWave
DeconvWave=(Pnt2X(DeconvWave,p)<0) ? AverageOdd[X2Pnt(AverageOdd,CP+x)] : ((
  Pnt2X(DeconvWave,p)>=CP) ? AverageOdd[X2Pnt(AverageOdd,x-CP)] : AverageEven
  (x))
If (RemRadFix)
  DeconvWave -=RadAmpFix*RadEven(x)
2376 EndIf
DeconvWave/=Sens
Error_Message(DeconvoluteFrame(DeconvWave, 0, ResultAvgEven, "Even"), "
  DeconvoluteFrame", "DeconvolutionProcAverage", Name)
DeletePoints /M=0 DPpP+5*Win*Rate, 5*Win*Rate, ResultAvgEven, ResultAvgOdd
DeletePoints /M=0 0, 5*Win*Rate, ResultAvgEven, ResultAvgOdd
2381 SetScale /P x 0, 1/Rate, "s", ResultAvgOdd, ResultAvgEven
SetScale /P d 0, 0, "W", ResultAvgOdd, ResultAvgEven
ProgressValue=2
DoUpdate /W=NAC_Control
2386 ValDisplay Progress win=NAC_Control, Disable=1
Killwaves DeconvWave
SetDataFolder OldDF
Error_Message(SetDeconvolutionGraphRanges(Name, "AverageEven"), "
  SetDeconvolutionGraphRanges", "DeconvolutionProcAverage", Name)
Error_Message(SetDeconvolutionGraphRanges(Name, "AverageOdd"), "
  SetDeconvolutionGraphRanges", "DeconvolutionProcAverage", Name)
Return NoError
2391 End
//

```

Function DeconvolutionProc

```

Static Function DeconvolutionProc(Name)
String Name
Variable Sens
2396 If (!WaveExists(root:NAC:Experiment:FitDeconvolutionOdd) || !WaveExists(root:
  NAC:Experiment:FitDeconvolutionEven))
  Return NAC_FitWavesMissing
EndIf
StrSwitch (Name)
2401 Case "RateCalorimetry":
Case "RateCoating":
Case "Deconvolution":
  Return NAC_NotApplicable

```

```

        Break
    Case "Sticking":
2406    Case "ZeroSticking":
        // Merge with LC etc. and select DECON function
        Return NAC_NotImplementedYet
        Break
    Case "BeforeCoating":
2411    Case "AfterCoating":
        Sens=1
        Break
    Case "LaserReference":
    Case "Transmission":
2416    Case "Radiation":
    Case "Heat":
        NVar UseSens=root:NAC:Deconvolution:UseSensitivity, Sensitivity=root:NAC:↵
        ↵ Deconvolution:Sensitivity
        If ((UseSens) && (NumType(Sensitivity)==0))
            Sens=Sensitivity
2421        Else
            Sens=1
        Endif
        Break
    Default:
2426    Return NAC_UnknownMeasurement
        Break
EndSwitch
DFRef OldDF=GetDataFolderDFR()
NVar EffectiveFrames="$root:NAC:"+Name+":EffectiveFrames"
2431 NVar Average=root:NAC:Deconvolution:AverageFrames
NVar DPpP=root:NAC:Experiment:DataPointsPerFrame, Win=root:NAC:Machine:↵
    ↵ DeconvolutionWindow, Rate=root:NAC:Machine:ProcessRate
Variable CntOdd, CntEven, i
If (!(EffectiveFrames>0))
    Return NAC_NothingToProcess
2436 EndIf
If (!WaveExists("$root:NAC:"+Name+":AverageOdd") || !WaveExists("$root:NAC:"+↵
    ↵ Name+":AverageEven"))
    Error_Message(Averaging(Name), "Averaging", "DeconvolutionProc", Name)
EndIf
NVar ProgressValue=root:NAC:GUI:ProgressValue
2441 NVar RemRadFix=root:NAC:Deconvolution:RemoveFixedRadiation, RemRadFit=root:NAC:↵
    ↵ Deconvolution:RemoveFittedRadiation
NVar RadAmpFix=root:NAC:Heat:InitRadiation
If (RemRadFix || RemRadFit)
    If (WaveExists(root:NAC:Experiment:FitRadiationOdd) && WaveExists(root:NAC:↵
        ↵ Experiment:FitRadiationEven))
        Wave RadOdd=root:NAC:Experiment:FitRadiationOdd, RadEven=root:NAC:↵
        ↵ Experiment:FitRadiationEven
2446    Else
        Return NAC_FitWavesMissing
    EndIf
EndIf
SetDataFolder "$root:NAC:"+Name
2451 Wave AverageOdd, AverageEven
Make /FREE /N=(DPpP+10*Win*Rate) AvgOdd, AvgEven
Wave FlagList, Detector
NVar Win=root:NAC:Machine:DeconvolutionWindow
Wave RadAmpFit=root:NAC:Heat:Radiation
2456 Variable AvgRadOdd, AvgRadEven
AvgOdd=0
AvgEven=0
AvgRadOdd=0
AvgRadEven=0
2461 CntOdd=0
CntEven=0
Make /O /N=(DPpP+10*Win*Rate, Ceil(Ceil(NumPnts(FlagList)/2)/Average)*2) ↵
    ↵ DeconPrep=0
Make /O /N=(Ceil(Ceil(NumPnts(FlagList)/2)/Average)*2) DeconFlag=0
SetScale /P x, -5*Win, 1/Rate, "", AvgOdd, AvgEven, DeconPrep

```

```

2466 Variable Idx=0, j=0
For (i=0; i<NumPnts(FlagList)-1;)
  For (j=i; j<i+Average*2; j+=2)
    If (j<NumPnts(FlagList)-2)
      If (!FlagList[j])
2471       AvgEven+=Detector[DPpP*j+p-5*Win*Rate]
          If (RemRadFit)
              AvgRadEven+=RadAmpFit[j]
          EndIf
          CntEven+=1
2476       EndIf
          If (!FlagList[j+1])
              AvgOdd+=Detector[DPpP*(j+1)+p-5*Win*Rate]
              If (RemRadFit)
                  AvgRadOdd+=RadAmpFit[j+1]
2481             EndIf
              CntOdd+=1
          EndIf
      EndIf
  EndFor
2486 i+=2*Average
  If (CntEven>0)
    AvgEven/=CntEven
    If (RemRadFix)
      AvgEven -= RadAmpFix*RadEven(x)
2491    ElseIf (RemRadFit)
      AvgRadEven/=CntEven
      AvgEven -= AvgRadEven*RadEven(x)
    EndIf
    DeconPrep[][Idx]=AvgEven[p]
2496 Else
    DeconFlag[Idx]=1
  EndIf
  If (CntOdd>0)
    AvgOdd/=CntOdd
2501    If (RemRadFix)
      AvgOdd -= RadAmpFix*RadOdd(x)
    ElseIf (RemRadFit)
      AvgRadOdd/=CntOdd
      AvgOdd -= AvgRadOdd*RadOdd(x)
2506    EndIf
    DeconPrep[][Idx+1]=AvgOdd[p]
  Else
    DeconFlag[Idx+1]=1
  EndIf
2511 AvgOdd=0
  AvgEven=0
  CntOdd=0
  CntEven=0
  Idx+=2
2516 EndFor
DeconPrep/=Sens
Make /O /N=(DPpP+10*Win*Rate,DimSize(DeconPrep,1)) Deconvolution=0
SetScale /P x 0, 1/Rate, "s", Deconvolution
SetScale /P y 0, Average, "Frame", Deconvolution
2521 SetScale /P d 0, 0, "W", Deconvolution
NVar Fitted=root:NAC:Deconvolution:UseFittedFitWave
ValDisplay Progress Disable=0, Limits={0,DimSize(DeconPrep,1)-1,0}, win=
↳ NAC_Control
ProgressValue=0
DoUpdate /W=NAC_Control
2526 For (i=0; i<DimSize(DeconPrep,1)-1; i+=2)
  If (!DeconFlag[i])
    DeconvoluteFrame(DeconPrep, i, Deconvolution, "Even")
  EndIf
  ProgressValue=i
2531 DoUpdate /W=NAC_Control
  If (!DeconFlag[i+1])
    DeconvoluteFrame(DeconPrep, i+1, Deconvolution, "Odd")
  EndIf
EndFor

```

```

        EndIf
        ProgressValue=i+1
2536    DoUpdate /W=NAC_Control
    EndFor
    DeletePoints /M=0 DPpP+5*Win*Rate, 5*Win*Rate, Deconvolution
    DeletePoints /M=0 0, 5*Win*Rate, Deconvolution
    KillWaves AvgOdd, AvgEven, DeconPrep
2541    Make /O /N=(DPpP) $"root:NAC:Deconvolution:"+Name+"BrowseOdd "=0
    Make /O /N=(DPpP) $"root:NAC:Deconvolution:"+Name+"BrowseEven "=0
    Wave BrowseOdd=$"root:NAC:Deconvolution:"+Name+"BrowseOdd"
    Wave BrowseEven=$"root:NAC:Deconvolution:"+Name+"BrowseEven"
    SetScale /P x 0, 1/Rate, "s", BrowseOdd, BrowseEven
2546    SetScale /P d 0, 0, "W", BrowseOdd, BrowseEven
    ValDisplay Progress win=NAC_Control, Disable=1
    ProgressValue=0
    SetDataFolder OldDF
    Error_Message(SetDeconvolutionGraphRanges(Name, "Deconvolution"), "↵
        ↵ SetDeconvolutionGraphRanges", "DeconvolutionProc", Name)
2551    Return NoError
    End
    //
Function CalcQCMRate
    Static Function CalcQCMRate(Name)
    String Name
2556    Variable i, Delta
        If (!WaveExists($"root:NAC:"+Name+":Thickness"))
            Return NAC_NoDataLoaded
        EndIf
        Wave Thickness=$"root:NAC:"+Name+":Thickness"
2561    Wave Timeline=$"root:NAC:"+Name+":Timeline"
        NVar AvgWindow=root:NAC:Machine:RateFittingWindow
        Duplicate /FREE Timeline DeltaWave
        Differentiate DeltaWave
        Delta=Mean(DeltaWave)
2566    Make /O /N=(Floor(NumPnts(Thickness)/AvgWindow)) $"root:NAC:"+Name+":FittedRate↵
        ↵ "
        Wave FittedRate=$"root:NAC:"+Name+":FittedRate"
        Make /FREE /N=(AvgWindow) AvgWave, TimeWave
        Make /FREE /D /N=2 FitCoef
        For (i=0;i<Floor(NumPnts(Thickness)/AvgWindow);i+=1)
2571    AvgWave=Thickness[i*AvgWindow+p]*CalcQCMTooling(Name)
        TimeWave=Timeline[i*AvgWindow+p]
        CurveFit /Q Line kWcWave=FitCoef AvgWave /X=TimeWave
        FittedRate[i]=FitCoef[1]
        EndFor
2576    String Unit="s"
        Variable Scale=AvgWindow*Delta
        If (NumPnts(FittedRate)*Scale > 600)
            Unit="min"
            Scale/=60
2581    If (NumPnts(FittedRate)*Scale > 120)
                Unit="h"
                Scale/=60
                If (NumPnts(FittedRate)*Scale > 48)
                    Unit="d"
2586    Scale/=24
            EndIf
        EndIf
        EndIf
        SetScale /P x 0, Scale, Unit, FittedRate
2591    SetScale d 0, 0, "m/s", FittedRate
        KillWaves AvgWave, FitCoef, TimeWave, DeltaWave
        Return NoError
    End
    //
Function NAC_CorrAdsorbed
2596    Function NAC_CorrAdsorbed(Material, Sample, Source)

```

```

String Material
Variable Sample, Source
  If (StrSearch(Material,"(",0,2)>0)
    Material=Material[0,StrSearch(Material,"(",0,2)-1]
2601  EndIf
    Make /FREE /D /N=2001 Cv
    SetScale /P x, 0, 1, "K", Cv
    Cv=CvGas(Material, x)
    Return Area(Cv, Sample, Source) + 1/2*R_Gas*Source - R_Gas*Sample
2606 End
    //
Function NAC_CorrDesorbed
Function NAC_CorrDesorbed(Material, Sample, Source)
String Material
Variable Sample, Source
2611  If (StrSearch(Material,"(",0,2)>0)
    Material=Material[0,StrSearch(Material,"(",0,2)-1]
    EndIf
    Make /FREE /D /N=2001 C
    SetScale /P x, 0, 1, "K", C
2616  C=CvGas(Material, x)+1/2*R_Gas
    Return Area(C, Sample, Source)
End
//
Function CvGas
Static Function CvGas(Material, Temperature) // J / molK
2621 String Material
Variable Temperature
Variable A, B, C, D, E, F, G, H
  // NIST values given for Cp !
  StrSwitch (Material)
2626  Case "Li":
    Case "Lithium":
      If (Temperature<1620.12)
        A=5/2*R_Gas // [J/molK]
      ElseIf (Temperature<6000)
2631  A=23.33408; B=-2.772423; C=0.767421; D=-0.003595; E=-0.035246; F↵
↵ =151.5035; G=166.1885; H=159.3004 // [241]
      EndIf
      Break
    Case "Mg":
    Case "Magnesium":
2636  If (Temperature<1366.104)
        A=5/2*R_Gas // [J/molK]
      ElseIf (Temperature<2200)
        A=20.77306; B=0.035592; C=-0.031917; D=0.009109; E=0.000461; F=140.9071; ↵
↵ G=173.7799; H=147.1002 // [241]
      ElseIf (Temperature<6000)
2641  A=47.60848; B=-15.40875; C=2.875965; D=-0.120806; E=-27.01764; F↵
↵ =97.40017; G=177.2305; H=147.1002 // [241]
      EndIf
      Break
    Case "Ca":
    Case "Calcium":
2646  If (Temperature<1774)
        A=5/2*R_Gas // [J/molK]
      ElseIf (Temperature<6000)
        A=121.5470; B=-74.95390; C=19.17230; D=-1.400821; E=-64.51340; F↵
↵ =42.23540; G=217.4470; H=177.8000 // [241]
      EndIf
2651  Break
    Case "Cu":
    Case "Copper":
      If (Temperature<2843.261)
        A=5/2*R_Gas // [J/molK]
2656  ElseIf (Temperature<6000)

```

```

    A=-80.48635; B=49.35865; C=-7.578061; D=0.404960; E=133.3382; F=519.9331; ↵
    ↵ G=193.5351; H=337.6003 // [241]
    EndIf
    Break
    Case "Zn":
2661    Case "Zinc":
        If (Temperature<1180.173)
            A=5/2*R_Gas // [J/molK]
            ElseIf (Temperature<6000)
                A=18.20166; B=2.313999; C=-0.736547; D=0.079950; E=1.073557; F=126.9388; ↵
                ↵ G=184.6977; H=130.4203 // [241]
2666    EndIf
            Break
        Default:
            Return NaN
    EndSwitch
2671    Variable t=Temperature/1000
    Return A - R_Gas + B*t + C*t^2 + D*t^3 + E/t^2 // Correction Cv=Cp-R in A
End
//

```

Function CpCondensed

```

Static Function CpCondensed(Material, Temperature[, Phase]) // J / molK
2676 String Material
    Variable Temperature
    String Phase
    Variable A, B, C, D, E, F, G, H, Theta=-1, Scale=1
    If (StrSearch(Material, "(,0,2)>0)
2681     Material=Material[0,StrSearch(Material, "(,0,2)-1]
    EndIf
    If (Temperature<=0)
        Return NaN
    EndIf
2686    If (ParamIsDefault(Phase))
        Phase=""
    EndIf
    // Debye temperatures with references can be found at
    // http://www.knowledgedoor.com/2/elements_handbook/debye_temperature.html
2691    StrSwitch (Material)
        Case "Li":
            Case "Lithium":
                If (Temperature < 298)
                    Theta=448 // [242]
2696                    Scale=24.6232/22.3048
                    ElseIf (Temperature < 453) // Graph looks odd
                        A=169.5520; B=-882.7110; C=1977.438; D=-1487.312; E=-1.609635; F ↵
                        ↵ =-31.24825; G=413.6466; H=0 // [241]
                        ElseIf (Temperature < 700) // Liquid Region 1
                            A=32.46972; B=-2.635975; C=-6.327128; D=4.230359; E=0.005686; F ↵
                            ↵ =-7.117319; G=74.29361; H=2.380002 // [241]
2701                        ElseIf (Temperature < 1620) // Liquid Region 1
                            A=26.00896; B=5.632375; C=-4.013227; D=0.873686; E=0.34415; F=-4.19969; G ↵
                            ↵ =66.36284; H=2.380002 // [241]
                        Else
                            Return NaN
                        EndIf
2706                    Break
                Case "Ca":
                    Case "Calcium":
                        If (Temperature < 298)
                            Theta=230 // [242]
2711                            Scale=25.9338/24.2120
                            ElseIf ((Temperature < 1115) && (StringMatch(Phase, "alpha") || StringMatch ↵
                            ↵ (Phase, ""))) // alpha-Phase (default)
                                A=19.77517; B=10.10813; C=14.50338; D=-5.529491; E=0.178031; F=-5.862997; ↵
                                ↵ G=62.91606; H=0 // [241]
                                ElseIf ((Temperature < 716) && StringMatch(Phase, "beta")) // beta-Phase ↵
                                ↵ Region 1

```

```

    A=11.11735; B=38.52364; C=-8.891419; D=-9.618305; E=0.391850; F↵
↵ =-2.563503; G=47.71852; H=1.056001 //[241]
2716 ElseIf ((Temperature < 1115) && StringMatch(Phase, "beta")) // beta-Phase ↵
↵ Region 2
    A=-40.63785; B=126.7765; C=-69.73891; D=17.93162; E=5.409494; F=24.49192; ↵
↵ G=-15.67297; H=1.056001 //[241]
    ElseIf (Temperature < 1774) // Liquid Phase -- Not trustworthy
        A=35.00004; B=1.119602e-10; C=-8.292981e-11; D=1.878880e-11; E=1.912569e↵
↵ -12; F=-2.646946; G=87.86609; H=7.788015 //[241]
    Else
2721     Return NaN
        EndIf
        Break
    Case "Cu":
    Case "Copper":
2726     If (Temperature < 298)
            theta=310 //[242]
            Scale=24.4693/23.6360
            ElseIf (Temperature < 1358)
                A=17.72891; B=28.09870; C=-31.25289; D=13.97243; E=0.068611; F=-6.056591; ↵
↵ G=47.89592; H=0 //[241]
2731 //     ElseIf (Temperature<2843.2) // Liquid Phase -- not trustworthy
//         A=32.84450; B=-0.000084; C=0.000032; D=-0.000004; E=-0.000028; F↵
↵ =-1.804901; G=73.92310; H=11.85730 //[241]
            ElseIf (Temperature<2843.2) // Liquid Phase
                A=49.5541644568037; B=-14.5015987758264; C=6.62989966065709; D↵
↵ =-1.09508006359702; E=3.30874559839901 //[243]
            Else
2736     Return NaN
                EndIf
                Break
    Case "Mg":
    Case "Magnesium":
2741     If (Temperature < 298)
            theta=330 //[242]
            Scale=24.8532/23.4694
            ElseIf (Temperature < 923)
                A=26.54083; B=-1.533048; C=8.062443; D=0.572170; E=-0.174221; F↵
↵ =-8.501596; G=63.90181; H=0 //[241]
2746     ElseIf (Temperature<1366)
                A=34.30901; B=-7.471034e-10; C=6.146212e-10; D=-1.598238e-10; E=-1.152011↵
↵ e-11; F=-5.439367; G=75.98311; H=4.790011 //[241]
            Else
                Return NaN
            EndIf
2751     Break
    Case "Zn":
    Case "Zinc":
        If (Temperature < 298)
            theta=237 //[242]
2756     Scale=25.3904/24.1676
            ElseIf (Temperature < 693)
                A=25.60123; B=-4.405292; C=20.42206; D=-7.399697; E=-0.045801; F↵
↵ =-7.755964; G=72.91373; H=0 //[241]
            ElseIf (Temperature<1180)
                A=31.38004; B=-9.647635e-9; C=6.798541e-9; D=-1.574453e-9; E↵
↵ =-3.249003-10; F=-3.590873; G=86.68160; H=6.519007 //[241]
2761     Else
                Return NaN
            EndIf
            Break
        Default:
2766     Return NaN
            Break
    EndSwitch
    If (Theta<0) // Use NIST data
        Variable t
2771     t=Temperature/1000

```

```

Return A + B*t + C*t^2 + D*t^3 + E/t^2 // Shomate equation probably not OK ↗
↳ for low temperature (T < 298K)
Else
  If (Exists("root:NAC:Enthalpies:Debye_Integral")!=1)
    Return NaN
2776 EndIf
Wave Debye_Integral=root:NAC:Enthalpies:Debye_Integral
If (Theta/Temperature>19) // Use Debye-theory
  Return 9*R_Gas*(Temperature/theta)^3*Debye_Integral(19) * Scale //SCALED ↗
↳ to match NIST data at boundary!!
Else
2781 Return 9*R_Gas*(Temperature/theta)^3*Debye_Integral(theta/Temperature) * ↗
↳ Scale //SCALED to match NIST data at boundary!!
EndIf
EndIf
End
//
Function NAC_RefEnthalpy
2786 Function NAC_RefEnthalpy(Material, T_Sample)
String Material
Variable T_Sample
Variable Hf0_Gas, T_Ref=298, Hf0_Solid
If (StrSearch(Material,"(",0,2)>0)
2791 Material=Material[0,StrSearch(Material,"(",0,2)-1]
EndIf
If ((NumType(T_Sample)!=0) )
  Return NaN
EndIf
2796 If (Exists("root:NAC:Enthalpies:Debye_Integral")!=1)
  Return NaN
EndIf
StrSwitch (Material)
  Case "Ca":
2801 Case "Calcium":
  Hf0_Gas=177.8e3 // J/mol CRC 05_02_90
  Break
  Case "Cu":
  Case "Copper":
2806 Hf0_Gas=337.4e3 // J/mol CRC 05_02_90
  Break
  Case "Li":
  Case "Lithium":
2811 Hf0_Gas=159.3e3 // J/mol CRC 05_02_90
  Break
  Case "Li2":
  Case "Dilithium":
  Hf0_Gas=215.9e3 // J/mol CRC 05_02_90
  Break
2816 Case "Mg":
  Case "Magnesium":
  Hf0_Gas=147.1e3 // J/mol CRC 05_02_90
  Break
2821 Case "Zn":
  Case "Zinc":
  Hf0_Gas=130.4e3 // J/mol CRC 05_02_90
  Break
  Default:
  Return NaN
2826 EndSwitch
If (Abs(T_Sample-T_Ref)<1)
  Return Hf0_Gas
EndIf
Make /FREE /D /N=(Abs(Ceil(T_Sample)-T_Ref)+1) Cp_Solid, Cp_Gas
2831 SetScale /I x T_Ref, Ceil(T_Sample), Cp_Solid, Cp_Gas
Cp_Solid=CpCondensed(Material,x)
Cp_Gas=CvGas(Material,x)+R_Gas
Return Hf0_Gas+Area(Cp_Solid, T_Sample, T_Ref)-Area(Cp_Gas, T_Sample, T_Ref)
End

```



```

2836 //
Function CalcHeat
Static Function CalcHeat()
DFRef OldDF=GetDataFolderDFR()
  If (NumPnts(root:NAC:Enthalpies:Sticking)==0)
    Return NAC_StickingMissing
2841 EndIf
  If (NumPnts(root:NAC:Heat:Adsorption)==0)
    Return NAC_AdsorptionMissing
  EndIf
  NVar Dose=root:NAC:RateCalorimetry:MoleDosePerPulse
2846 If ((Dose <=0) || (NumType(Dose)!=0))
    Return NAC_DoseMissing
  EndIf
  Wave Enthalpy=root:NAC:Enthalpies:Enthalpy, Adsorption=root:NAC:Heat:Adsorption ↵
    ↵ , Sticking=root:NAC:Enthalpies:Sticking
  Wave FlagHeat=root:NAC:Heat:FlagList, FlagSticking=root:NAC:Sticking:FlagList
2851 NVar SubAbs=root:NAC:Enthalpies:SubtractAdsorbed, SubRef=root:NAC:Enthalpies:↵
    ↵ SubtractDesorbed
  Enthalpy!=(FlagHeat[p] || FlagSticking[p]) ? 1/(Sticking[p]*Dose) * Adsorption[↵
    ↵ p] - (Sticking[p]*Dose)*SubAbs - SubRef*Dose*(1-Sticking[p]) : NaN
  Error_Message(SetRangesCoverage("Heat"), "CalcHeat", "SetRangesCoverage", "Heat ↵
    ↵ ")
  Return NoError
End
2856 //
Function CalcCoverage
Static Function CalcCoverage()
DFRef OldDF=GetDataFolderDFR()
Variable i
  If (Exists("root:NAC:Enthalpies:Sticking")!=1)
2861 Return NAC_StickingMissing
  EndIf
  NVar PulseLength=root:NAC:Experiment:PulseLength, Dose=root:NAC:RateCalorimetry ↵
    ↵ :DosePerPulse, UseTrend=root:NAC:Experiment:UseFittedDesorption
  If ((PulseLength<=0) || (Dose<=0) || (NumType(Dose)!=0))
    Return NAC_DoseMissing
2866 EndIf
  SetDataFolder root:NAC:Sticking
  If (UseTrend)
    Wave Desorption=fit_Desorption
  Else
2871 Wave Desorption
  EndIf
  Wave Sticking=root:NAC:Enthalpies:Sticking, Coverage=root:NAC:Enthalpies:↵
    ↵ Coverage, Range=root:NAC:Enthalpies:ThicknessRange
  NVar NumberOfFrames
  If (!NumPnts(Sticking))
2876 SetDataFolder OldDF
    Return NAC_StickingMissing
  EndIf
  Sticking=1-Desorption
  Coverage[0]=Dose*Sticking[0]
2881 For (i=1;i<NumberOfFrames;i+=1)
    Coverage[i]=Coverage[i-1]+Dose*(Sticking[i]+Sticking[i-1])/2
  EndFor
  SetScale /I x, 0, Ceil(WaveMax(Coverage)), "ML", root:NAC:Enthalpies:↵
    ↵ MultiLayerReference
  SetScale /I x, 0, Ceil(WaveMax(Coverage)), "ML", root:NAC:Enthalpies:↵
    ↵ StickingLimit
2886 SetScale /I x, Coverage2Thickness(Floor(WaveMin(Coverage))), ↵
    ↵ Coverage2Thickness(Ceil(WaveMax(Coverage))), "m", Range
  SetDataFolder OldDF
  Error_Message(SetRangesCoverage("Sticking"), "CalcCoverage", "SetRangesCoverage ↵
    ↵ ", "Sticking")
  Return NoError
End

```

```

2891 //
Function FitHeat
Static Function FitHeat()
Variable ExPVTime, tmptime, i
Variable V_FitError, V_FitQuitReason
DFRef OldDF=GetDataFolderDFR()
2896 //Checking
SetDataFolder root:NAC:Heat
Wave Offset, Adsorption, ShiftAds, Radiation, ShiftRad, ChiSq, FlagList, ↵
↳ Detector, fit_Radiation
Wave Enthalpy=root:NAC:Enthalpies:Enthalpy
NVar NumberOfFrames=NumberOfFrames, DataPointsPerFrame=root:NAC:Experiment:↵
↳ DataPointsPerFrame
2901 NVar InitOffset, InitAdsorption, InitRadiation, InitAdsorptionShift, ↵
↳ InitRadiationShift
NVar HoldOffset, HoldAdsorption, HoldRadiation, HoldAdsorptionShift, ↵
↳ HoldRadiationShift
NVar ProgressValue=root:NAC:GUI:ProgressValue
NVar ChopperPeriod=root:NAC:Experiment:ChopperPeriod
NVar UseFittedRad=root:NAC:Experiment:UseFittedRadiation
2906 NVar SwitchDeadTime=root:NAC:Experiment:SwitchDeadTime
NVar LinkShifts=root:NAC:Heat:LinkShifts
If (UseFittedRad && !NumPnts(fit_Radiation))
UseFittedRad=0
EndIf
2911 ReDimension /N=(NumberOfFrames) Radiation, Adsorption, Offset, ShiftAds, ↵
↳ ShiftRad, ChiSq, Enthalpy
Adsorption=0
ShiftAds=0
Radiation=0
ShiftRad=0
2916 Offset=0
ChiSq=0
Enthalpy=0
Variable HAS, HRS, LS
If (InitRadiationShift>ChopperPeriod/4)
2921 InitRadiationShift=0
Error_Message(NAC_ParameterOutsideRange, "FitHeat", "InProc", "↵
↳ InitRadiationShift set to zero")
EndIf
If (InitAdsorptionShift>ChopperPeriod/4)
2926 Error_Message(NAC_ParameterOutsideRange, "FitHeat", "InProc", "↵
↳ InitAdsorptionShift set to zero")
EndIf
If (LinkShifts)
If (!HoldAdsorptionShift && !HoldRadiationShift)
Variable Tmp=(InitRadiationShift+InitAdsorptionShift)/2
2931 InitRadiationShift=Tmp
InitAdsorptionShift=Tmp
LS=1
EndIf
If (HoldAdsorptionShift || HoldRadiationShift)
2936 HAS=1
HRS=1
LS=0
If (HoldAdsorptionShift && !HoldRadiationShift)
InitRadiationShift=InitAdsorptionShift
2941 EndIf
If (!HoldAdsorptionShift && HoldRadiationShift)
InitAdsorptionShift=InitRadiationShift
EndIf
EndIf
2946 Else
HAS=HoldAdsorptionShift
HRS=HoldRadiationShift
LS=0
EndIf

```

```

2951 Variable CP=0.125*ChopperPeriod
String HoldCoef=Num2Str(HoldOffset)+Num2Str(HoldAdsorption)+Num2Str(HAS)+↵
↳ Num2Str(HoldRadiation || UseFittedRad)+Num2Str(HRS)
Make /FREE /D /N=5 FitCoef, InitCoef={InitOffset, InitAdsorption, ↵
↳ InitAdsorptionShift, InitRadiation, InitRadiationShift}
Make /FREE /D /N=(5,6) FitConstrM={{0,0,0,0,0,0},{0,0,0,0,0,0},{!HAS,-!HAS,0,0,↵
↳ LS,-LS},{0,0,0,0,0,0},{0,0,!HRS,-!HRS,-LS,LS}}
Make /FREE /D /N=6 FitConstrV={CP,CP,CP,CP, 0.0001, 0.0001}
2956 Make /FREE /N=(DataPointsPerFrame) CurrentPeak
Setscale /P x, 0, DimDelta(Detector, 0), CurrentPeak
ProgressValue=0
ValDisplay Progress Disable=0, Limits={0,NumberOfFrames-1,1}, win=NAC_Control
DoUpdate /W=NAC_Control
2961 For (i=0;i<NumberOfFrames;i+=1)
  If (!FlagList[i])
    CurrentPeak=Detector[p][i]
    FitCoef=InitCoef
    If (UseFittedRad)
2966     FitCoef[3]=fit_Radiation[i]
    EndIf
    FuncFit /N=1 /W=2 /Q /H=HoldCoef $"Calorimetry"+SelectString(Mod(i,2),"Even↵
↳ ","Odd"), FitCoef, CurrentPeak(SwitchDeadTime, ChopperPeriod) /C={↵
↳ FitConstrM,FitConstrV}
    If (V_FitError)
2971     Offset[i]=0
     Adsorption[i]=0
     ShiftAds[i]=0
     Radiation[i]=0
     ShiftRad[i]=0
     ChiSq[i]=-V_FitError
2976     V_FitError=0
     V_FitQuitReason=0
     FlagList[i]=1
    Else
2981     Offset[i]=FitCoef[0]
     Adsorption[i]=FitCoef[1]
     ShiftAds[i]=FitCoef[2]
     Radiation[i]=FitCoef[3]
     ShiftRad[i]=FitCoef[4]
     ChiSq[i]=V_ChiSq
2986     EndIf
     ProgressValue=i
     DoUpdate /W=NAC_Control
    Else
2991     Offset[i]=0
     Adsorption[i]=0
     ShiftAds[i]=0
     Radiation[i]=0
     ShiftRad[i]=0
     ChiSq[i]=0
2996     EndIf
  EndFor
KillWaves FitCoef, CurrentPeak, InitCoef, FitConstrV, FitConstrM
If (!UseFittedRad)
  Duplicate /O Radiation root:NAC:Heat:orig_Radiation
3001 EndIf
DoWindow NAC_Heat_Full
If (V_Flag)
  For (i=0;i<NumPnts(FlagList);i+=1)
    If (FlagList[i])
3006     ModifyGraph /W=NAC_Heat_Full rgb($"Frame"+Num2Str(i))=(0,0,0)
    EndIf
  EndFor
EndIf
ValDisplay Progress win=NAC_Control, Disable=1
3011 ProgressValue=0
SetDataFolder OldDF
Return NoError
End

```

```

//
Function FitDesorption
3016 Static Function FitDesorption()
Variable ExpVTime, tmptime, i
Variable V_FitError, V_fitOptions=4, V_FitQuitReason
DFRef OldDF=GetDataFolderDFR()
//Checking
3021 SetDataFolder root:NAC:Sticking
Wave Offset, Desorption, Shift, ChiSq, FlagList, Detector
Wave Coverage=root:NAC:Enthalpies:Coverage, Sticking=root:NAC:Enthalpies:↵
↵ Sticking, Thickness=root:NAC:Enthalpies:Thickness
NVar NumberOfFrames=NumberOfFrames, DataPointsPerFrame=root:NAC:Experiment:↵
↵ DataPointsPerFrame
NVar InitOffset, InitDesorption, InitShift
3026 NVar HoldOffset, HoldDesorption, HoldShift
NVar ProgressValue=root:NAC:GUI:ProgressValue
NVar ChopperPeriod=root:NAC:Experiment:ChopperPeriod
String HoldCoef=Num2Str(HoldOffset)+Num2Str(HoldDesorption)+Num2Str(HoldShift)
NVar UseFittedDes=root:NAC:Experiment:UseFittedDesorption
3031 Wave Coverage=root:NAC:Enthalpies:Coverage
Redimension /N=(NumberOfFrames) Desorption, Offset, Shift, ChiSq, Sticking, ↵
↵ Coverage, Thickness
SetScale /I x, 0, NumberOfFrames-1, "", root:NAC:Sticking:StickingLimit
ChiSq=0
Sticking=0
3036 If (HoldDesorption)
Desorption=InitDesorption
Shift=InitShift
Offset=InitOffset
Error_Message(CalcCoverage(), "CalcCoverage", "FitDesorption", "")
3041 SetDataFolder OldDF
Return NAC_NothingToProcess
EndIf
If (UseFittedDes)
Wave fit_Desorption=root:NAC:Sticking:fit_Desorption
3046 Desorption=fit_Desorption
Error_Message(CalcCoverage(), "CalcCoverage", "FitDesorption", "")
SetDataFolder OldDF
Return NAC_NothingToProcess
EndIf
3051 Sticking=0
Desorption=1
Coverage=0
Shift=0
Offset=0
3056 Make /FREE /D /N=3 FitCoef, InitCoef={InitOffset, InitDesorption, InitShift}
Make /FREE /D /N=(3,2) FitConstrM={{0,0},{0,0},{!HoldShift,-!HoldShift}}
Make /FREE /D /N=2 FitConstrV=0.125*ChopperPeriod
Make /FREE /N=(DataPointsPerFrame) CurrentPeak
Setscale /P x, 0, DimDelta(Detector, 0), CurrentPeak
3061 ProgressValue=0
ValDisplay Progress Disable=0, Limits={0,NumberOfFrames-1,1}, win=NAC_Control
DoUpdate /W=NAC_Control
For (i=0;i<NumberOfFrames;i+=1)
If (!FlagList[i])
3066 CurrentPeak=Detector[p][i]
FitCoef=InitCoef
FuncFit /N=1 /W=2 /Q /H=HoldCoef $"Sticking"+SelectString(Mod(i,2),"Even",↵
↵ Odd"), FitCoef, CurrentPeak /C={FitConstrM,FitConstrV}
If (V_FitError)
3071 Offset[i]=0
Desorption[i]=1
Shift[i]=0
ChiSq[i]=-V_FitError
V_FitError=0
V_FitQuitReason=0
3076 FlagList[i]=1
ModifyGraph /W=$"NAC_Sticking_Full" rgb($"Frame"+Num2Str(i))=(0,0,0)

```

```

    Else
      Offset[i]=FitCoef[0]
      Desorption[i]=FitCoef[1]
3081      Shift[i]=FitCoef[2]
      ChiSq[i]=V_ChiSq
    EndIf
    ProgressValue=i
    DoUpdate /W=NAC_Control
3086  Else
    Offset[i]=0
    Desorption[i]=0
    Shift[i]=0
    ChiSq[i]=0
3091  EndIf
  EndFor
  Error_Message(CalcCoverage(), "CalcCoverage", "FitDesorption", "")
  KillWaves FitCoef, InitCoef, CurrentPeak, FitConstrV, FitConstrM
  Duplicate /O Desorption root:NAC:Sticking:orig_Desorption
3096  ValDisplay Progress win=NAC_Control, Disable=1
  ProgressValue=0
  SetDataFolder OldDF
  Return NoError
End
3101 //

```

Function Averaging

```

Static Function Averaging(Name)
String Name
DFRef OldDF=GetDataFolderDFR()
NVar Loaded="$root:NAC:"+Name+":Loaded"
3106  If (!Loaded)
    Return NAC_NoDataLoaded
  EndIf
  SetDataFolder "$root:NAC:"+Name
  If (StringMatch(Name,"Deconvolution"))
3111    NVar DataPoints=root:NAC:Deconvolution:DataPointsPerFrame
  Else
    NVar DataPoints=root:NAC:Experiment:DataPointsPerFrame
  EndIf
  NVar ProcessRate=root:NAC:Machine:ProcessRate
3116  NVar NumberOfFrames
  Wave Detector, FlagList
  Variable i, CountOdd=0, CountEven=0
  Make /O /N=(DataPoints) AverageOdd=0, AverageEven=0
  SetScale /P x, 0, 1/ProcessRate, "s", AverageOdd, AverageEven
3121  SetScale d, -10, 10, "V", AverageOdd, AverageEven
  If (NumberOfFrames==0)
    AverageOdd=NaN
    AverageEven=NaN
    SetDataFolder OldDF
3126  Return NAC_NothingToProcess
  EndIf
  For (i=0; i<NumberOfFrames; i+=1)
    If (FlagList[i]==0)
      If (Mod(i,2))
3131        AverageOdd+=Detector[p][i]
        CountOdd+=1
      Else
        AverageEven+=Detector[p][i]
        CountEven+=1
3136      EndIf
    EndIf
  EndFor
  AverageOdd/=CountOdd
  AverageEven/=CountEven
3141  SetDataFolder OldDF
  Return NoError
End

```

```

//
Function NormalizeFitWave
Static Function NormalizeFitWave(Name)
3146 String Name
      StrSwitch (Name)
        Case "BeforeCoating":
        Case "AfterCoating":
        Case "LaserReference":
3151 Case "Deconvolution":
          NVar LaserPower=$"root:NAC:"+Name+":LaserPower"
          If (NumType(LaserPower) || (LaserPower==0))
            Return NAC_LaserPowerMissing
          EndIf
3156 Break
        Case "ZeroSticking":
        Case "Radiation":
          Break
        Case "Heat":
3161 Case "Sticking":
        Case "Transmission":
        Case "RateCalorimetry":
        Case "RateCoating":
          Return NAC_NotApplicable
3166 Break
        Default:
          Return NAC_UnknownMeasurement
          Break
      EndSwitch
3171 If ((Exists("root:NAC:"+Name+":AverageOdd")!=1) || (Exists("root:NAC:"+Name+":
  ↳ AverageEven")!=1))
      Return NAC_AverageWavesMissing
      EndIf
      Wave AverageOdd=$"root:NAC:"+Name+":AverageOdd", AverageEven=$"root:NAC:"+Name
  ↳ "+:AverageEven"
      StrSwitch (Name)
3176 Case "BeforeCoating":
        Name="Reflectivity"
        Break
        Case "AfterCoating":
        Name="Sensitivity"
3181 Break
        Case "ZeroSticking":
        Name="Sticking"
        Break
        Default:
3186 EndSwitch
      NVar ChopperPeriod=root:NAC:Experiment:ChopperPeriod, Nyquist=root:NAC:Machine:
  ↳ NyquistFrequency, Delay=root:NAC:Experiment:ChopperDelay
      Variable SRate=2*Nyquist, DPpP=2*Nyquist*ChopperPeriod, Tmp
      Make /O /N=(DPpP*2) $"root:NAC:Experiment:Fit"+Name+"Odd", $"root:NAC:
  ↳ Experiment:Fit"+Name+"Even"
      Wave FitOdd=$"root:NAC:Experiment:Fit"+Name+"Odd", FitEven=$"root:NAC:
  ↳ Experiment:Fit"+Name+"Even"
3191 SetScale /P x, -ChopperPeriod/2, 1/SRate, "s", FitEven, FitOdd
      SetScale d, 0, 1, "V", FitEven, FitOdd
      FitEven[]=(p>=3/2*DPpP) ? AverageOdd[p-3/2*DPpP] : ((p>=1/2*DPpP) ? AverageEven
  ↳ [p-1/2*DPpP] : AverageOdd[p+1/2*DPpP])
      FitOdd[]=(p>=3/2*DPpP) ? AverageEven[p-3/2*DPpP] : ((p>=1/2*DPpP) ? AverageOdd[
  ↳ p-1/2*DPpP] : AverageEven[p+1/2*DPpP])
      StrSwitch (Name)
3196 Case "Reflectivity":
        Case "Sensitivity":
          FitOdd/=LaserPower
          FitEven/=LaserPower
          SetScale d, 0, 0, "V/W", FitOdd, FitEven
3201 Break
        Case "LaserReference":

```

```

NVar PulseLength=root:NAC:Experiment:PulseLength, LaserPowerCorrection=root↵
↵ :NAC:Machine:LaserPowerCorrection, MirrorCorr=root:NAC:Experiment:↵
↵ MirrorContamination
NVar Reflectivity=root:NAC:LaserReference:Reflectivity
FitOdd/=LaserPower*LaserPowerCorrection*MirrorCorr*(1-Reflectivity)*↵
3206 ↵ PulseLength // Normalize to 1 J input energy
FitEven/=LaserPower*LaserPowerCorrection*MirrorCorr*(1-Reflectivity)*↵
↵ PulseLength
SetScale d, 0, 0, "V/J", FitOdd, FitEven
Break
Case "Sticking":
NVar QMSTooling=root:NAC:Machine:QMSToolingCalorimetry
3211 FitOdd*=QMSTooling
FitEven*=QMSTooling
Break
Case "Radiation":
Break
3216 Case "Deconvolution":
If (ChopperPeriod>0)
NVar LineNotch=root:NAC:Machine:LineNotchFrequency, MirrorCorr=root:NAC:↵
↵ Experiment:MirrorContamination
NVar LaserPowerCorrection=root:NAC:Machine:LaserPowerCorrection, ↵
↵ Reflectivity=root:NAC:Deconvolution:Reflectivity
NVar Delay=root:NAC:Deconvolution:ChopperDelay
3221 Duplicate /FREE AverageEven TempWaveEven
Duplicate /FREE AverageOdd TempWaveOdd
If (LineNotch>0)
Make /O /C /FREE /N=0 TempCWave
3226 FFT /DEST=TempCWave TempWaveEven
TempCWave[X2Pnt(TempCWave, LineNotch),*]=0
IFFT /Dest=TempWaveEven TempCWave
Make /O /C /FREE /N=0 TempCWave
FFT /DEST=TempCWave TempWaveOdd
TempCWave[X2Pnt(TempCWave, LineNotch),*]=0
3231 IFFT /Dest=TempWaveOdd TempCWave
Killwaves TempCWave
EndIf
TempWaveEven/=LaserPower*LaserPowerCorrection*MirrorCorr*(1-Reflectivity)↵
↵ //Normalize to 1W constant input power
TempWaveOdd/=LaserPower*LaserPowerCorrection*MirrorCorr*(1-Reflectivity)
3236 Duplicate /R=(Delay-1.4*ChopperPeriod,Delay+1.4*ChopperPeriod) /O ↵
↵ TempWaveEven root:NAC:Experiment:FitDeconvolutionEven
Duplicate /R=(Delay-1.4*ChopperPeriod,Delay+1.4*ChopperPeriod) /O ↵
↵ TempWaveOdd root:NAC:Experiment:FitDeconvolutionOdd
Wave FitOdd=root:NAC:Experiment:FitDeconvolutionOdd, FitEven=root:NAC:↵
↵ Experiment:FitDeconvolutionEven
SetScale /P x, -1.4*ChopperPeriod, DimDelta(FitOdd,0), WaveUnits(FitOdd ↵
↵ ,0), FitOdd
SetScale /P x, -1.4*ChopperPeriod, DimDelta(FitEven,0), WaveUnits(FitEven ↵
↵ ,0), FitEven
3241 Duplicate /O FitOdd root:NAC:Experiment:FitDeconvolutionOddFitted
Duplicate /O FitEven root:NAC:Experiment:FitDeconvolutionEvenFitted
Wave FitOddFitted=root:NAC:Experiment:FitDeconvolutionOddFitted, ↵
↵ FitEvenFitted=root:NAC:Experiment:FitDeconvolutionEvenFitted
Make /D /FREE /N=4 FitCoef
FitCoef={Abs(WaveMin(FitEven)) > Abs(WaveMax(FitEven)) ? -1e3 : 1e3, ↵
↵ 0.001 ,Abs(WaveMin(FitEven)) > Abs(WaveMax(FitEven)) ? -1e6 : 1e6, 0.5}
3246 FuncFit /NTHR=0 /Q /W=2 DeconvolutionFunction FitCoef FitEven(-↵
↵ ChopperPeriod/2,ChopperPeriod/2)
Duplicate /R=(Delay-1.4*ChopperPeriod+FitCoef[1],Delay+1.4*ChopperPeriod+↵
↵ FitCoef[1]) /O TempWaveEven root:NAC:Experiment:FitDeconvolutionEven
FitEven-=FitCoef[0]
FitCoef[0]=0
FitCoef[1]=0
3251 FitEvenFitted=DeconvolutionFunction(FitCoef,x)
FitCoef={Abs(WaveMin(FitEven)) > Abs(WaveMax(FitEven)) ? -1e3 : 1e3, ↵
↵ 0.001 ,Abs(WaveMin(FitEven)) > Abs(WaveMax(FitEven)) ? -1e6 : 1e6, 0.5}
FuncFit /NTHR=0 /Q /W=2 DeconvolutionFunction FitCoef FitOdd(-↵
↵ ChopperPeriod/2,ChopperPeriod/2)

```

```

        Duplicate /R=(Delay-1.4*ChopperPeriod+FitCoef[1],Delay+1.4*ChopperPeriod+
↵ FitCoef[1]) /O TempWaveOdd root:NAC:Experiment:FitDeconvolutionOdd
        FitOdd-=FitCoef[0]
3256     FitCoef[0]=0
        FitCoef[1]=0
        FitOddFitted=DeconvolutionFunction(FitCoef,x)
        SetScale /P x, -1.4*ChopperPeriod, DimDelta(FitEven,0), WaveUnits(FitEven↵
↵ ,0), FitEven
        SetScale /P x, -1.4*ChopperPeriod, DimDelta(FitOdd,0), WaveUnits(FitOdd↵
↵ ,0), FitOdd
3261     SetScale d, 0, 0, "V/W", FitOdd, FitEven
        KillWaves TempWaveEven, TempWaveOdd
        Endif
        Break
    Default:
3266     Return NAC_UnknownMeasurement
        Break
EndSwitch
StrSwitch (Name)
    Case "Deconvolution":
3271     Break
    Default:
        Tmp=Mean(FitOdd,0,0.9*Delay)
        FitOdd-=Tmp
        Tmp=Mean(FitEven,0,0.9*Delay)
3276     FitEven-=Tmp
        Break
    EndSwitch
    Return NoError
End
3281 //

```

Function GetRatio

```

Static Function GetRatio(Type)
Variable Type
Variable IntBefore, IntAfter, LaserBefore, LaserAfter, Ratio
String S_Fit, S_Before, S_After
3286     Switch (Type)
        Case NAC_RatioTypeReflectivity:
            S_Before="BeforeCoating"
            S_After="AfterCoating"
            Break
3291     Case NAC_RatioTypeTransmission:
            S_Before="LaserReference"
            S_After="Transmission"
            Break
3296     Case NAC_RatioTypeSensitivity:
            S_Before="AfterCoating"
            S_After="LaserReference"
            Break
        Default:
            Error_Message(NAC_NotApplicable, "InProc", "GetRatio", "Type:"+Num2Str(Type↵
↵ ))
3301     Return NaN
    EndSwitch
    NVar LP_B="$root:NAC:"+S_Before+":LaserPower", LP_A="$root:NAC:"+S_After+":↵
↵ LaserPower"
    LaserBefore=LP_B
    LaserAfter=LP_A
3306     If ((Exists("root:NAC:"+S_Before+":AverageOdd")!=1) || (Exists("root:NAC:"+↵
↵ S_Before+":AverageEven")!=1))
        Error_Message(NAC_AverageWavesMissing, "InProc", "GetRatio", "Type:"+Num2Str(↵
↵ Type))
        Return NaN
    EndIf
    If ((Exists("root:NAC:"+S_After+":AverageOdd")!=1) || (Exists("root:NAC:"+↵
↵ S_After+":AverageEven")!=1))
3311     Error_Message(NAC_AverageWavesMissing, "InProc", "GetRatio", "Type:"+Num2Str(↵
↵ Type))

```



```

    Return NaN
  EndIf
  If (!LaserBefore || !LaserAfter)
    Error_Message(NAC_LaserPowerMissing, "InProc", "GetRatio", "Type:"+Num2Str(↵
    ↵ Type))
3316   Return NaN
  EndIf
  If (NumType(LaserAfter) || (LaserAfter==0))
    Variable LP
    Prompt LP, "Laser Power: "
3321   DoPrompt /HELP="" "Missing Laser Power for AfterCoating", LP
    If (V_Flag)
      Error_Message(NAC_LaserPowerMissing, "InProc", "GetRatio", "Type:"+Num2Str(↵
      ↵ Type))
      Return NaN
    Else
3326     LP_A=LP
      LaserAfter=LP
    EndIf
  EndIf
  EndIf
  Wave BeforeOdd=$"root:NAC:"+S_Before+":AverageOdd", BeforeEven=$"root:NAC:"+↵
  ↵ S_Before+":AverageEven"
3331   Wave AfterOdd=$"root:NAC:"+S_After+":AverageOdd", AfterEven=$"root:NAC:"+↵
  ↵ S_After+":AverageEven"
  Duplicate /FREE AfterOdd DataOdd, TmpOdd
  Duplicate /FREE AfterEven DataEven, TmpEven
  Duplicate BeforeOdd, root:NAC:FitRatioOdd
  Duplicate BeforeEven, root:NAC:FitRatioEven
3336   Wave FitRatioOdd=root:NAC:FitRatioOdd, FitRatioEven=root:NAC:FitRatioEven
  FitRatioOdd/=LaserBefore
  FitRatioEven/=LaserBefore
  DataOdd/=LaserAfter
  DataEven/=LaserAfter
3341   Make /FREE /D /N=2 FitCoef
  NVar ChopperDelay=root:NAC:Experiment:ChopperDelay
  NVar ChopperPeriod=root:NAC:Experiment:ChopperPeriod, SwitchDeadTime=root:NAC:↵
  ↵ Experiment:SwitchDeadTime
  Variable FitFrom, FitTo
  String HoldCoef
3346   FitCoef={0,1e-6}
  FitFrom=SwitchDeadTime
  FitTo=ChopperPeriod
  FuncFit /W=2 /N=1 /Q RatioOdd, FitCoef, DataOdd(FitFrom,FitTo) /D=TmpOdd
  Ratio=FitCoef[1]
3351   FuncFit /W=2 /N=1 /Q RatioEven, FitCoef, DataEven(FitFrom,FitTo) /D=TmpEven
  Ratio=(Ratio+FitCoef[1])/2
  KillWaves FitCoef, TmpOdd, TmpEven, root:NAC:FitRatioOdd, root:NAC:FitRatioEven
  Return Ratio
End
3356 //
Function GetPulseLength
Static Function GetPulseLength()
String Name
Variable LengthOdd, LengthEven
NVar Length=root:NAC:Experiment:PulseLength, NomLength=root:NAC:Experiment:↵
↵ NominalPulseLength
3361 NVar Delay=root:NAC:Experiment:ChopperDelay//, NomLength=root:NAC:Experiment:↵
↵ NominalPulseLength
NVar Failed=root:NAC:Experiment:LengthDetectFailed, Win=root:NAC:Machine:↵
↵ PulseLengthDetectionWindow
DFRef OldDF=GetDataFolderDFR()
  If ((Exists("root:NAC:LaserReference:AverageOdd")!=1) || (Exists("root:NAC:↵
  ↵ LaserReference:AverageEven")!=1))
    Return NAC_FitWavesMissing
3366   EndIf
  SetDataFolder root:NAC
  Failed=0

```

```

Wave AvgOdd=root:NAC:LaserReference:AverageOdd, AvgEven=root:NAC:LaserReference↵
↵ :AverageEven
Variable InterBefore, SlopeBefore, InterPulseBeg, SlopePulseBeg, InterPulseEnd,↵
↵ SlopePulseEnd, InterAfter, SlopeAfter
3371 If ((Win>Delay) || (Win>Length))
      Win=0.8*Min(Delay,Length)
      EndIf
      Make /FREE /D /N=2 FitCoef
      CurveFit /N=1 /Q /W=2 line, kWcWave=FitCoef AvgEven(Delay-Win, Delay-0.2*Win)
3376 InterBefore=FitCoef [0]
      SlopeBefore=FitCoef [1]
      CurveFit /N=1 /Q /W=2 line, kWcWave=FitCoef AvgEven(Delay+0.2*Win, Delay+Win)
      InterPulseBeg=FitCoef [0]
      SlopePulseBeg=FitCoef [1]
3381 CurveFit /N=1 /Q /W=2 line, kWcWave=FitCoef AvgEven(Delay+Length-Win, Delay+↵
↵ Length-0.2*Win)
      InterPulseEnd=FitCoef [0]
      SlopePulseEnd=FitCoef [1]
      CurveFit /N=1 /Q /W=2 line, kWcWave=FitCoef AvgEven(Delay+Length+0.2*Win, Delay↵
↵ +Length+Win)
3386 InterAfter=FitCoef [0]
      SlopeAfter=FitCoef [1]
      LengthEven=(InterAfter-InterPulseEnd)/(SlopePulseEnd-SlopeAfter) - (InterBefore↵
↵ -InterPulseBeg)/(SlopePulseBeg-SlopeBefore)
      CurveFit /N=1 /Q /W=2 line, kWcWave=FitCoef AvgOdd(Delay-Win,Delay-0.2*Win)
      InterBefore=FitCoef [0]
      SlopeBefore=FitCoef [1]
3391 CurveFit /N=1 /Q /W=2 line, kWcWave=FitCoef AvgOdd(Delay+0.2*Win,Delay+Win)
      InterPulseBeg=FitCoef [0]
      SlopePulseBeg=FitCoef [1]
      CurveFit /N=1 /Q /W=2 line, kWcWave=FitCoef AvgEven(Delay+Length-Win,Delay+↵
↵ Length-0.2*Win)
      InterPulseEnd=FitCoef [0]
3396 SlopePulseEnd=FitCoef [1]
      CurveFit /N=1 /Q /W=2 line, kWcWave=FitCoef AvgOdd(Delay+Length+0.2*Win,Delay+↵
↵ Length+Win)
      InterAfter=FitCoef [0]
      SlopeAfter=FitCoef [1]
      LengthOdd=(InterAfter-InterPulseEnd)/(SlopePulseEnd-SlopeAfter) - (InterBefore↵
↵ -InterPulseBeg)/(SlopePulseBeg-SlopeBefore)
3401 If ((LengthEven/LengthOdd>1.05) || (LengthEven/LengthOdd<0.95) || (((LengthEven+↵
↵ LengthOdd)/2)/NomLength>1.05) || (((LengthEven+LengthOdd)/2)/NomLength↵
↵ <0.95))
      Length=NomLength
      Failed=1
      Else
      Length=(LengthEven+LengthOdd)/2
3406 EndIf
      SetDataFolder OldDF
      If (Failed)
      Return NAC_PulseLengthDetectionFailed
      Else
3411 Return NoError
      EndIf
End
//

```

Function GetRadiationContribution

```

Static Function GetRadiationContribution(Name)
3416 String Name
      NVar SampleTemp=root:NAC:Experiment:TemperatureSample
      NVar SourceTemp=root:NAC:Experiment:TemperatureSource
      NVar RefSourceTemp=root:NAC:Experiment:EmptyCrucibleTemperature
      Variable OnErrors=0
3421 StrSwitch (Name)
      Case "Heat":
      Case "Radiation":
      Break
      Default:

```

```

3426     Return NAC_NotApplicable
EndSwitch
If ((NumType(SampleTemp)!=0) || NumType(SourceTemp))
  OnErrors+=Error_Message(NAC_NoDataLoaded, "InProc", "GetRadiationContribution↵
↵ ", "Heat")
EndIf
3431 If ((NumType(RefSourceTemp)!=0) || (Exists("root:NAC:Radiation:Auxiliaries:↵
↵ Sample")!=1))
  OnErrors+=Error_Message(NAC_NoDataLoaded, "InProc", "GetRadiationContribution↵
↵ ", "Radiation")
EndIf
If (OnErrors)
  Return NaN
3436 EndIf
Wave RefSampleTemp=root:NAC:Radiation:Auxiliaries:Sample
If (Abs(SampleTemp-Mean(RefSampleTemp))> 5)
  Error_Message(NAC_IncompatibleExperiment, "InProc", "GetRadiationContribution↵
↵ ", "Sample Temperature Mismatch")
  Return NaN
3441 EndIf
Return (SourceTemp^4-SampleTemp^4)/(RefSourceTemp^4-SampleTemp^4)
End

//
Function FitQCMRate
3446 Static Function FitQCMRate(Name) // ErrorHandling
String Name
String Type=""
DFREF OldDF=GetDataFolderDFR()
  SetDataFolder $"root:NAC:"+Name+":"
3451 NVar BaselineTo, BaselineFrom
NVar BaselineBefore, ApparentRate, BaselineAfter, DepositionRate, UseBaseline
Wave Thickness, Timeline
Make /FREE /D /N=2 Coef
If (BaselineTo <= 10)
3456   BaselineBefore=0
   Make /O /N=0 Thickness_FitLow
   Make /O /N=0 TimeLine_FitLow
Else
3461   Duplicate /O /R=[0, BaselineTo-5] Thickness, Thickness_FitLow
   Duplicate /O /R=[0, BaselineTo-5] Timeline, Timeline_FitLow
   Duplicate /FREE /R=[0, BaselineTo-5] Thickness, TempThick
   Duplicate /FREE /R=[0, BaselineTo-5] Timeline, TempTime
   CurveFit /Q /W=2 /line kWWave=Coef TempThick /X=TempTime /D=Thickness_FitLow
   BaselineBefore=Coef[1]*CalcQCMTooling(Name)
3466 EndIf
If (NumPnts(Thickness)-BaselineFrom <=10)
  BaselineAfter=0
  Make /O /N=0 Thickness_FitHigh
  Make /O /N=0 TimeLine_FitHigh
3471 Else
  Duplicate /O /R=[BaselineFrom+5,*] Thickness, Thickness_FitHigh
  Duplicate /O /R=[BaselineFrom+5,*] Timeline, Timeline_FitHigh
  Duplicate /FREE /R=[BaselineFrom+5,*] Thickness, TempThick
  Duplicate /FREE /R=[BaselineFrom+5,*] Timeline, TempTime
3476 CurveFit /Q /W=2 /line kWWave=Coef TempThick /X=TempTime /D=Thickness_FitHigh
  BaselineAfter=Coef[1]*CalcQCMTooling(Name)
EndIf
Duplicate /O /R=[BaselineTo+5, BaselineFrom-5] Thickness, Thickness_FitMid
Duplicate /O /R=[BaselineTo+5, BaselineFrom-5] Timeline, Timeline_FitMid
3481 Duplicate /FREE /R=[BaselineTo+5, BaselineFrom-5] Thickness, TempThick
Duplicate /FREE /R=[BaselineTo+5, BaselineFrom-5] Timeline, TempTime
CurveFit /Q /W=2 /line kWWave=Coef TempThick /X=TempTime /D=Thickness_FitMid
ApparentRate=Coef[1]*CalcQCMTooling(Name)
KillWaves /Z Coef, TempThick, TempTime
3486 SetDataFolder OldDF
DoUpdate
Error_Message(CalcHeat(), "CalcHeat", "FitQCMRate", Name)

```

```

    Error_Message( CalcCoverage(), "CalcCoverage", "FitQCMRate", Name)
    Error_Message( DoHeatTextBox(), "DoHeatTextBox", "FitQCMRate", Name)
3491    Return NoError
End
//
Function CalcQCMTooling
Static Function CalcQCMTooling(Name)
String Name
3496    StrSwitch (Name)
        Case "RateCalorimetry":
            NVar GeometryQCM=root:NAC:Machine:QCMToolingCalorimetry
            Return GeometryQCM
            Break
3501    Case "Mecea":
            NVar BeamDiameter=root:NAC:Machine:BeamDiameter, QCMDiameter=root:NAC:↵
            ↵ Machine:QCMDiameter
            Make /FREE /D /N=400 G
            Setscale x, -QCMDiameter, QCMDiameter, "", G
            G=Gauss(x,0,1.0669*QCMDiameter/6) // V.M. Mecea / Sensors and Actuators A↵
            ↵ 128 (2006) 270-277
3506    Return 1/Area(G,-BeamDiameter/2, BeamDiameter/2)
            Break
        Case "Sauerbrey":// "RateCalorimetry":// "Sauerbrey":
            NVar BeamDiameter=root:NAC:Machine:BeamDiameter, QCMDiameter=root:NAC:↵
            ↵ Machine:QCMDiameter, GeometryQCM=root:NAC:Machine:QCMToolingCalorimetry
            // Calculates the tooling due to a partially loaded QCM according to ↵
            ↵ Sauerbrey, ZfP 155, 206-222 (1959)
3511    // Coefficients from a sigmoidal fit from Fig. 5
            Return 1/(-0.022841+1.0392/(1+exp(-(BeamDiameter/QCMDiameter-0.43809)↵
            ↵ /0.12912)))/ *GeometryQCM
            Break
        Case "RateCoating":
            NVar GeometryQCM=root:NAC:Machine:QCMToolingCoating
3516    Return GeometryQCM
            Break
        Default:
            Error_Message(NAC_NotApplicable, "InProc", "CalcQCMTooling", Name)
            Return NaN
3521    EndSwitch
End
//
NAC_CreateTrend
Function NAC_CreateTrend(Name)
String Name
3526 String FitList="Cancel;Averaging;Loaded Average;Line;Polynom;Smooth;Gauss;Lorentz↵
        ↵ ;Sine;Exp;Sigmoid;Power;"
String FitType, Mode, WName
Variable Error
If (!DataFolderExists("root:NAC:"))
    Error_Message(NAC_NotInitialized, "InProc", "NAC_CreateTrend", "")
3531    Return NaN
EndIf
StrSwitch (Name)
    Case "Radiation":
3536    Wave Source=root:NAC:Heat:orig_Radiation
        Wave Dest=root:NAC:Heat:fit_Radiation
        Wave Flag=root:NAC:Heat:FlagList
        NVar UseTrend=root:NAC:Experiment:UseFittedRadiation
        Break
    Case "Sticking":
3541    Name="Desorption"
    Case "Desorption":
        Wave Source=root:NAC:Sticking:orig_Desorption
        Wave Dest=root:NAC:Sticking:fit_Desorption
        Wave Flag=root:NAC:Sticking:FlagList
3546    NVar UseTrend=root:NAC:Experiment:UseFittedDesorption
        Break

```

```

Case "Deconvolution":
Case "BeforeCoating":
Case "AfterCoating":
3551 Case "LaserReference":
Case "Transmission":
Case "Radiation":
Case "ZeroSticking":
Case "RateCalorimetry":
3556 Case "RateCoating":
    Error_Message(NAC_NotApplicable, "InProc", "NAC_CreateTrend", Name)
    Return NaN
Default:
    Error_Message(NAC_UnknownMeasurement, "InProc", "NAC_CreateTrend", Name)
3561 Return NaN
EndSwitch
WName="NAC_"+Name+"_Trend"
If (NumPnts(Source)==0)
    Error_Message(NAC_NothingToProcess, "InProc", "NAC_CreateTrend", Name)
3566 Return NaN
EndIf
Duplicate /O Source Dest
Dest=(!Flag[p]) ? Source : NaN
Error=Error_Message(DisplayTrend(Name, 0), "DisplayTrend", "NAC_CreateTrend", ↵
    ↵ Name)
3571 If ((Error !=NoError) && (Error!=NAC_WindowAlreadyExists))
    Return NaN
EndIf
TextBox /W=$WName /A=MT /C/E/F=0 /X=0/Y=5 /N=Caption/A=MC /B=1 "\JCTrend for "+↵
    ↵ Name+"\r\JC \K(65280,0,0)Original Data"
DoUpdate
3576 Do
    Duplicate /O /FREE Source Process
    Process=(!Flag[p]) ? Source : NaN
    Prompt FitType, "Type", Popup, FitList
    DoPrompt /HELP="" "Create Fitted Trend for "+Name, FitType
3581 If (V_Flag || StringMatch(FitType,"Cancel"))
        Error_Message(UserAbort, "InProc", "NAC_CreateTrend", Name)
        UseTrend=0
        ModifyGraph /W=$WName HideTrace($"fit_"+Name)=1
        Return NaN
3586 EndIf
NVar Trim=root:NAC:Machine:TrimTrendRange
StrSwitch (FitType)
    Case "Loaded Average":
        String FileName=""
3591 Error_Message(LoadTrend(Name,FileName), "InProc", "NAC_CreateTrend", Name↵
    ↵ )
        FitType+=" from "+ FileName
        StrSwitch (Name)
            Case "Radiation":
                Variable RemOfs=2, Low=Ceil(0.1*NumPnts(Flag)), High=Floor(0.9*↵
    ↵ NumPnts(Flag))
3596 String NoYes="No;Yes"
        Prompt RemOfs, "Scale Contribution", Popup, NoYes
        Prompt Low, "Start Frame"
        Prompt High, "End Frame"
        DoPrompt /HELP="" "Create Fitted Trend for "+Name, RemOfs, Low, High
3601 If (V_Flag || (RemOfs!=2))
            Error_Message(UserAbort, "InProc", "NAC_CreateTrend", Name)
            Return NaN
        EndIf
        If (Low>High)
3606 Variable Tmp=Low
            Low=High
            High=Tmp
        EndIf
        Low=Limit(Low, 0, NumPnts(Flag)-1)
3611 High=Limit(High, 0, NumPnts(Flag)-1)
        Duplicate /Free Source, TempWave

```

```

        TempWave/=Process
        Dest*=Mean(TempWave,Low,High)
        FitType+="\K(0,0,0)\rScaled to Match Frames "+Num2Str(Low)+" to "+↵
↵ Num2Str(High)+" by "+Num2Str(Mean(TempWave,Low,High))
3616        Break
        Default:
        Break
        EndSwitch
        Break
3621        Case "Averaging":
        Variable Temp=Mean(Source, Pnt2X(Source, Trim), Pnt2X(Source, NumPnts(↵
↵ Source)-Trim-1))
        Dest=Temp
        StrSwitch (Name)
        Case "Radiation":
3626        NVar Value=root:NAC:Heat:InitRadiation
        NVar Hold=root:NAC:Heat:HoldRadiation
        Break
        Case "Desorption":
3631        NVar Value=root:NAC:Sticking:InitDesorption
        NVar Hold=root:NAC:Sticking:HoldDesorption
        Break
        EndSwitch
        Value=Temp
        Hold=1
3636        Break
        Case "Line":
        Make /N=2 /FREE /D FitCoef
        CurveFit /N /X /Q /W=2 Line, kwCWave=FitCoef Process[Trim,NumPnts(Source)↵
↵ -Trim-1]
        Dest=FitCoef[0]+FitCoef[1]*x
3641        Break
        Case "Exp":
        Make /N=3 /FREE /D FitCoef
        CurveFit /N /X /Q /W=2 Exp, kwCWave=FitCoef Process[Trim,NumPnts(Source)-↵
↵ Trim-1]
        Dest=FitCoef[0]+FitCoef[1]*exp(-FitCoef[2]*x)
3646        Break
        Case "Gauss":
        Make /N=4 /FREE /D FitCoef
        CurveFit /N /X /Q /W=2 Gauss, kwCWave=FitCoef Process[Trim,NumPnts(Source)↵
↵ )-Trim-1]
        Dest=FitCoef[0]+FitCoef[1]*exp(-((x-FitCoef[2])/FitCoef[3])^2)
3651        Break
        Case "Lorentz":
        Make /N=4 /FREE /D FitCoef
        CurveFit /N /X /Q /W=2 Lor, kwCWave=FitCoef Process[Trim,NumPnts(Source)-↵
↵ Trim-1]
        Dest=FitCoef[0]+FitCoef[1]/((x-FitCoef[2])^2+FitCoef[3])
3656        Break
        Case "Sine":
        Make /N=4 /FREE /D FitCoef
        CurveFit /N /X /Q /W=2 sin, kwCWave=FitCoef Process[Trim,NumPnts(Source)-↵
↵ Trim-1]
        Dest=FitCoef[0]+FitCoef[1]*sin(FitCoef[2]*x+FitCoef[3])
3661        Break
        Case "DblExp":
        Make /N=5 /FREE /D FitCoef
        CurveFit /N /X /Q /W=2 DblExp, kwCWave=FitCoef Process[Trim,NumPnts(↵
↵ Source)-Trim-1]
        Dest=FitCoef[0]+FitCoef[1]*Exp(-FitCoef[2]*x)+FitCoef[3]*Exp(-FitCoef[4]*↵
↵ x)
3666        Break
        Case "Sigmoid":
        Make /N=4 /FREE /D FitCoef
        CurveFit /N /X /Q /W=2 Sigmoid, kwCWave=FitCoef Process[Trim,NumPnts(↵
↵ Source)-Trim-1]
        Dest=FitCoef[0]+FitCoef[1]/(1+Exp(-(x-FitCoef[2])/FitCoef[3]))
3671        Break

```

```

Case "Power":
  Make /N=3 /FREE /D FitCoef
  CurveFit /N /X /Q /W=2 Power, kwCWave=FitCoef Process[Trim,NumPnts(Source)
  )-Trim-1]
  Dest=FitCoef [0]+FitCoef [1]*x^FitCoef [2]
3676 Break
Case "Polynom":
  Variable Para=0
  String ParaList="3;4;5;6;7;8;9;10;11;12;13;14;15;16;17;18;19;20"
  Prompt Para, "Number of Polynom Coefficients (Order +1): ", Popup, ↵
  ParaList
3681 DoPrompt /HELP="" "Create Fitted Trend for "+Name, Para
  If (V_Flag)
    Error_Message(UserAbort, "InProc", "NAC_CreateTrend", Name)
    UseTrend=0
    ModifyGraph /W=$WName HideTrace($"fit_"+Name)=1
3686 Return NaN
  EndIf
  Para+=2
  Make /N=(Para) /FREE /D /O FitCoef
  CurveFit /N /X=1 /Q /W=2 Poly Para, kwCWave=FitCoef Process[Trim,NumPnts(
  Source)-Trim-1]
3691 Dest=Poly(FitCoef,x)
  FitType+="(" + "Coefficients: " + Num2Str(Para) +)"
  Break
Case "Smooth":
  String ModeList="Binominal;BoxCar;Median;"
3696 Variable WinSize=25
  Prompt Mode, "Smoothing Method: ", Popup, ModeList
  Prompt WinSize, "Smoothing Window Size: "
  DoPrompt /HELP="" "Create Smoothed Trend for "+Name, Mode, WinSize
  WinSize=Ceil(WinSize)
3701 If ((WinSize<1) || V_Flag)
    Error_Message(UserAbort, "InProc", "NAC_CreateTrend", Name)
    UseTrend=0
    ModifyGraph /W=$WName HideTrace($"fit_"+Name)=1
    Return NaN
3706 EndIf
  Dest [0,Trim]=Process [2*Trim+1-p]
  Dest [NumPnts(Process)-Trim-1,NumPnts(Process)-1]=Process [NumPnts(Process)
  -Trim-1-(NumPnts(Process)-p)]
  StrSwitch (Mode)
3711 Case "Binominal":
    Smooth WinSize, Dest
    Break
  Case "BoxCar":
    Smooth /B WinSize, Dest
    Break
3716 Case "Median":
    Smooth /M=0 WinSize, Dest
    Break
  Default:
    Error_Message(NAC_UnknownFitFunction, "InProc", "NAC_CreateTrend", ↵
  Name)
3721 UseTrend=0
    ModifyGraph /W=$WName HideTrace($"fit_"+Name)=1
    Return NaN
    Break
  EndSwitch
3726 FitType+="(" + Mode + ", Win:" + Num2Str(WinSize) +)"
  Break
  Default:
    Make /O /N=0 Dest
    Error_Message(NAC_UnknownFitFunction, "InProc", "NAC_CreateTrend", Name)
3731 UseTrend=0
    ModifyGraph /W=$WName HideTrace($"fit_"+Name)=1
    Return NaN
    Break
  EndSwitch

```

```

3736     TextBox /W=$WName /A=MT /C/E/F=0 /X=0/Y=5 /N=Caption/A=MC /B=1 "\JCTrend for ↵
↵ "+Name+"\r\JC \K(65280,0,0)Original Data\K(0,0,0) \K(0,0,52224) " + ↵
↵ FitType
ModifyGraph /W=$WName HideTrace($"fit_"+Name)=0
Error=Error_Message(DisplayTrend(Name, 1), "DisplayTrend", "NAC_CreateTrend", ↵
↵ Name)
If ((Error !=NoError) && (Error!=NAC_WindowAlreadyExists))
    Return NaN
3741     EndIf
DoUpdate
DoAlert /T="NAC Fitted Trends" 2, "Acceptable Match?"
While (V_Flag==2)
StrSwitch (Name)
3746     Case "Radiation":
        CheckBox FittedRad Disable=2*(V_Flag!=1), Win=NAC_Control
        Break
        Case "Desorption":
        CheckBox FittedDes Disable=2*(V_Flag!=1), Win=NAC_Control
3751     Break
        Default:
        Break
EndSwitch
If (V_Flag==3)
3756     Error_Message(UserAbort, "InProc", "NAC_CreateTrend", Name)
UseTrend=0
ModifyGraph /W=$WName HideTrace($"fit_"+Name)=1
Return NaN
EndIf
3761     StrSwitch (FitType)
        Case "Averaging":
        UseTrend=0
        Break
        Default:
3766     UseTrend=1
EndSwitch
Return NaN
End
//

```

C.1.5 Fitting Functions

```

3771 //
Function CpShomate
Function CpShomate(w,T) : FitFunc
    Wave w
    Variable T
    //CurveFitDialog/ These comments were created by the Curve Fitting dialog. ↵
    ↵ Altering them will
3776 //CurveFitDialog/ make the function less convenient to work with in the Curve ↵
    ↵ Fitting dialog.
    //CurveFitDialog/ Equation:
    //CurveFitDialog/ f(t) = A + B*t + C*t^2 + D*t^3 + E/t^2
    //CurveFitDialog/ End of Equation
    //CurveFitDialog/ Independent Variables 1
3781 //CurveFitDialog/ T
    //CurveFitDialog/ Coefficients 5
    //CurveFitDialog/ w[0] = A
    //CurveFitDialog/ w[1] = B
    //CurveFitDialog/ w[2] = C
3786 //CurveFitDialog/ w[3] = D
    //CurveFitDialog/ w[4] = E
    t=T/1000
    Return w[0] + w[1]*t + w[2]*t^2 + w[3]*t^3 + w[4]/t^2
End
3791 //
Function HShomate
Function HShomate(w,T) : FitFunc
    Wave w

```



```

Variable T
//CurveFitDialog/ These comments were created by the Curve Fitting dialog. ↵
  ↳ Altering them will
3796 //CurveFitDialog/ make the function less convenient to work with in the Curve ↵
  ↳ Fitting dialog.
//CurveFitDialog/ Equation:
//CurveFitDialog/ t=T/1000
//CurveFitDialog/ f(T) = (A*t + B/2*t^2 + C/3*t^3 + D/4*t^4 - E/t + F - H) * ↵
  ↳ 1000
//CurveFitDialog/ End of Equation
3801 //CurveFitDialog/ Independent Variables 1
//CurveFitDialog/ T
//CurveFitDialog/ Coefficients 7
//CurveFitDialog/ w[0] = A
//CurveFitDialog/ w[1] = B
3806 //CurveFitDialog/ w[2] = C
//CurveFitDialog/ w[3] = D
//CurveFitDialog/ w[4] = E
//CurveFitDialog/ w[5] = F
//CurveFitDialog/ w[6] = H
3811 t=T/1000
Return (w[0]*t + w[1]/2*t^2 + w[2]/3*t^3 + w[3]/4*t^4 - w[4]/t + w[5] - w[6]) *↵
  ↳ 1000
End
//

```

Function DeconvolutionFunction

```

Function DeconvolutionFunction(w,t):FitFunc
3816 Wave w
Variable t
Variable A0=w[0], t0=w[1], A=w[2], tau=w[3]
If (t<t0)
  Return A0
3821 Else
  Return A0+A*(1-exp(-(t-t0)*tau))
EndIf
End
//

```

Function DampedOscillation

```

3826 Function DampedOscillation(w, x):Fitfunc
Wave w
Variable x
//CurveFitDialog/ These comments were created by the Curve Fitting dialog. ↵
  ↳ Altering them will
//CurveFitDialog/ make the function less convenient to work with in the Curve ↵
  ↳ Fitting dialog.
3831 //CurveFitDialog/ Equation:
//CurveFitDialog/ f(x) = (x0 +Amp*exp(-x/tau)*cos(x/sigma-phi)
//CurveFitDialog/ End of Equation
//CurveFitDialog/ Independent Variables 1
//CurveFitDialog/ x
3836 //CurveFitDialog/ Coefficients 5
//CurveFitDialog/ w[0] = x0
//CurveFitDialog/ w[1] = Amp
//CurveFitDialog/ w[2] = tau
//CurveFitDialog/ w[3] = sigma
3841 //CurveFitDialog/ w[4] = phi
Return w[0]+w[1]*exp(-x/w[2])*cos(x/w[3]-w[4])
End
//

```

Function DeconvolutionFuncEven

```

Function DeconvolutionFuncEven(wc,wy,wx):Fitfunc
3846 Wave wc, wy, wx
Wave DCE=root:NAC:Experiment:FitDeconvolutionEven
MultiThread wy=wc[0]*DCE(x)
End

```

```
//
Function DeconvolutionFuncOdd
3851 Function DeconvolutionFuncOdd(wc,wy,wx):Fitfunc
Wave wc, wy, wx
Wave DCO=root:NAC:Experiment:FitDeconvolutionOdd
MultiThread wy=wc[0]*DCO(x)
End
3856 //
Function DeconvolutionFuncEvenFitted
Function DeconvolutionFuncEvenFitted(wc,wy,wx):Fitfunc
Wave wc, wy, wx
Wave DCE=root:NAC:Experiment:FitDeconvolutionEvenFitted
MultiThread wy=wc[0]*DCE(x)
3861 End
//
Function DeconvolutionFuncOddFitted
Function DeconvolutionFuncOddFitted(wc,wy,wx):Fitfunc
Wave wc, wy, wx
Wave DCO=root:NAC:Experiment:FitDeconvolutionOddFitted
3866 MultiThread wy=wc[0]*DCO(x)
End
//
Function CalorimetryEven
Function CalorimetryEven(wc,wy,wx):Fitfunc
Wave wc, wy, wx
3871 Wave LE=root:NAC:Experiment:FitLaserReferenceEven, RE=root:NAC:Experiment:↵
↵ FitRadiationEven
MultiThread wy=wc[0]+wc[1]*LE(x-wc[2])+wc[3]*RE(x-wc[4])
End
//
Function CalorimetryOdd
Function CalorimetryOdd(wc,wy,wx):Fitfunc
3876 Wave wc, wy, wx
Wave LO=root:NAC:Experiment:FitLaserReferenceOdd, RO=root:NAC:Experiment:↵
↵ FitRadiationOdd
MultiThread wy=wc[0]+wc[1]*LO(x-wc[2])+wc[3]*RO(x-wc[4])
End
//
Function RatioEven
3881 Function RatioEven(wc,wy,wx):Fitfunc
Wave wc, wy, wx
Wave RE=root:NAC:FitRatioEven
MultiThread wy=wc[0]+wc[1]*RE(x)
End
3886 //
Function RatioOdd
Function RatioOdd(wc,wy,wx):Fitfunc
Wave wc, wy, wx
Wave RO=root:NAC:FitRatioOdd
MultiThread wy=wc[0]+wc[1]*RO(x)
3891 End
//
Function LaserReferenceEven
Function LaserReferenceEven(wc,wy,wx):Fitfunc
Wave wc, wy, wx
Wave LE=root:NAC:Experiment:FitLaserReferenceEven
3896 MultiThread wy=wc[0]+wc[1]*LE(x-wc[2])
End
```

```

//
Function LaserReferenceOdd
Function LaserReferenceOdd(wc,wy,wx):Fitfunc
Wave wc, wy, wx
3901 Wave L0=root:NAC:Experiment:FitLaserReferenceOdd
      MultiThread wy=wc[0]+wc[1]*L0(x-wc[2])
End
//
Function StickingEven
Function StickingEven(wc,wy,wx):Fitfunc
3906 Wave wc, wy, wx
Wave SE=root:NAC:Experiment:FitStickingEven
      MultiThread wy=wc[0]+wc[1]*SE(x-wc[2])
End
//
Function StickingOdd
3911 Function StickingOdd(wc,wy,wx):Fitfunc
Wave wc, wy, wx
Wave S0=root:NAC:Experiment:FitStickingOdd
      MultiThread wy=wc[0]+wc[1]*S0(x-wc[2])
End
3916 //
Function StatLaserReferenceEven
Function StatLaserReferenceEven(wc,wy,wx):Fitfunc
Wave wc, wy, wx
Wave Avg=root:NAC:LaserReference:AverageEven
      MultiThread wy=wc[0]+wc[1]*Avg(x)
3921 End
//
Function StatLaserReferenceOdd
Function StatLaserReferenceOdd(wc,wy,wx):Fitfunc
Wave wc, wy, wx
Wave Avg=root:NAC:LaserReference:AverageOdd
3926 MultiThread wy=wc[0]+wc[1]*Avg(x)
End
//
Function StatTransmissionEven
Function StatTransmissionEven(wc,wy,wx):Fitfunc
Wave wc, wy, wx
3931 Wave Avg=root:NAC:Transmission:AverageEven
      MultiThread wy=wc[0]+wc[1]*Avg(x)
End
//
Function StatTransmissionOdd
Function StatTransmissionOdd(wc,wy,wx):Fitfunc
3936 Wave wc, wy, wx
Wave Avg=root:NAC:Transmission:AverageOdd
      MultiThread wy=wc[0]+wc[1]*Avg(x)
End
//
Function StatBeforeCoatingEven
3941 Function StatBeforeCoatingEven(wc,wy,wx):Fitfunc
Wave wc, wy, wx
Wave Avg=root:NAC:BeforeCoating:AverageEven
      MultiThread wy=wc[0]+wc[1]*Avg(x)
End
3946 //
Function StatBeforeCoatingOdd
Function StatBeforeCoatingOdd(wc,wy,wx):Fitfunc
Wave wc, wy, wx

```

```
Wave Avg=root:NAC:BeforeCoating:AverageOdd
  MultiThread wy=wc[0]+wc[1]*Avg(x)
3951 End
  //
Function StatAfterCoatingEven
Function StatAfterCoatingEven(wc,wy,wx):Fitfunc
Wave wc, wy, wx
Wave Avg=root:NAC:AfterCoating:AverageEven
3956 MultiThread wy=wc[0]+wc[1]*Avg(x)
End
  //
Function StatAfterCoatingOdd
Function StatAfterCoatingOdd(wc,wy,wx):Fitfunc
Wave wc, wy, wx
3961 Wave Avg=root:NAC:AfterCoating:AverageOdd
  MultiThread wy=wc[0]+wc[1]*Avg(x)
End
  //
Function StatDeconvolutionEven
Function StatDeconvolutionEven(wc,wy,wx):Fitfunc
3966 Wave wc, wy, wx
Wave Avg=root:NAC:Deconvolution:AverageEven
  MultiThread wy=wc[0]+wc[1]*Avg(x)
End
  //
Function StatDeconvolutionOdd
3971 Function StatDeconvolutionOdd(wc,wy,wx):Fitfunc
Wave wc, wy, wx
Wave Avg=root:NAC:Deconvolution:AverageOdd
  MultiThread wy=wc[0]+wc[1]*Avg(x)
End
3976 //
Function StatRadiationEven
Function StatRadiationEven(wc,wy,wx):Fitfunc
Wave wc, wy, wx
Wave Avg=root:NAC:Radiation:AverageEven
  MultiThread wy=wc[0]+wc[1]*Avg(x)
3981 End
  //
Function StatRadiationOdd
Function StatRadiationOdd(wc,wy,wx):Fitfunc
Wave wc, wy, wx
Wave Avg=root:NAC:Radiation:AverageOdd
3986 MultiThread wy=wc[0]+wc[1]*Avg(x)
End
  //
Function StatZeroStickingEven
Function StatZeroStickingEven(wc,wy,wx):Fitfunc
Wave wc, wy, wx
3991 Wave Avg=root:NAC:ZeroSticking:AverageEven
  MultiThread wy=wc[0]+wc[1]*Avg(x)
End
  //
Function StatZeroStickingOdd
Function StatZeroStickingOdd(wc,wy,wx):Fitfunc
3996 Wave wc, wy, wx
Wave Avg=root:NAC:ZeroSticking:AverageOdd
  MultiThread wy=wc[0]+wc[1]*Avg(x)
End
```

//

C.1.6 Input/Output

4001 //

LoadCalFile

```

Static Function LoadCalFile(Name, FileNameOpen) // Loads a calorimeter file
String Name, FileNameOpen
Variable i=0, j=0, temp
String TempString="", FileHeader="", Extension=""
4006 String MiscFiles="Miscellaneous Files (*.tst, *.las, *.qms):.tst,.las,.qms;"
//String AllCalFiles= "All Calorimetry Files (*.ref, *.las, .tst, *.win, *.cln, ↵
↵ *.dcv, *.usd, *.cot, *.amp, *.rad, *.cal, *.qms, *.stk):.ref,.las,.tst,.win↵
↵ *.cln,.dcv,.usd,.cot,.cot,.amp,.rad,.cal,.qms,.stk;" // String too long
String AllCalFiles= "All Calorimetry Files:.ref,.las,.tst,.win,.cln,.dcv,.usd,.↵
↵ cot,.cot,.amp,.rad,.cal,.qms,.stk;"
String AllFiles="All Files (*.*):.*;"
Variable RefNum, NumberOfLines=0
4011 DRef OldDF=GetDataFolderDFR()
StrSwitch (Name)
  Case "LaserReference":
    TempString="Laser Reference Files (*.ref):.ref;"
    Break
4016 Case "Transmission":
    TempString="Window Transmission Files (*.win):.win;"
    Break
  Case "BeforeCoating":
    TempString="Clean Sample Files (*.cln, *.usd):.cln,.usd;"
4021 Break
  Case "AfterCoating":
    TempString="Coated Sample Files (*.cot):.cot;"
    Break
4026 Case "Radiation":
    TempString="Radiation Files (*.rad):.rad;"
    Break
  Case "Heat":
    TempString="Heat Files (*.cal):.cal;"
    Break
4031 Case "ZeroSticking":
    TempString="Zero Sticking Files (*.stk):.stk;"
    Break
  Case "Deconvolution":
    TempString="Deconvolution Files (*.dcv):.dcv;"
4036 Break
  Case "Trim":
  Case "Concat1":
  Case "Concat2":
    Break
4041 Case "RateCoating":
  Case "RateCalorimetry":
    Return NAC_NotApplicable
    Break
  Default:
4046 Return NAC_UnknownMeasurement
    Break
EndSwitch
StrSwitch (Name)
  Case "Trim":
4051 Case "Concat1":
  Case "Concat2":
    FilenameOpen=""
    TempString=AllCalFiles+AllFiles
    Break
4056 Default:
  NVar LoadSupport=root:NAC:GUI:LoadSupportFiles
  If (LoadSupport)
    TempString=MiscFiles+TempString+AllCalFiles+AllFiles
  Else

```

```

4061     TempString=TempString+MiscFiles+AllCalFiles+AllFiles
        EndIf
        Break
    EndSwitch
    PathInfo CalDataPath
4066    If (!V_Flag)
        NewPath /0 /Q /Z CalDataPath, NAC_DataPathStr
        If (!V_Flag)
            NewPath /0 /Q CalDataPath
            If (V_Flag)
4071         Return UserCancel
            EndIf
        EndIf
    EndIf
    SetDataFolder root:NAC
4076    Open /R /P=CalDataPath /F=TempString RefNum as FileNameOpen
    If (CmpStr(S_FileName, "")==0)
        SetDataFolder OldDF
        Return LoadAborted
    EndIf
4081    TempString="\r"
    Make /T /N=1 /FREE TempHeader
    TempHeader[0]=S_FileName
    Do
        If (CmpStr(TempString, "\r") !=0)
4086         ReDimension /N=(NumPnts(TempHeader)+1) TempHeader
            TempHeader[NumPnts(TempHeader)-1]=TempString
        EndIf
        FReadLine RefNum, TempString
        NumberOfLines=NumberOfLines+1
4091    While (!StringMatch(TempString, "Calorimetry*MassSpec*"))
        ReDimension /N=(NumPnts(TempHeader)+1) TempHeader
        TempHeader[NumPnts(TempHeader)-1]="End of Header"
        Close RefNum
        TempHeader=ReplaceString("(", TempHeader, "[")
4096    TempHeader=ReplaceString(")", TempHeader, "]")
        TempHeader=ReplaceString("\r", TempHeader, "")
        Variable NFrames, SRate, CPeriod, PLength, OCSteps, CDelay, LPower, SDTime, Tmp
        ↵ , CGain, QGain, Refl=NaN
        String Prop, Unit, Value, STmp
        For (i=0; (i<NumPnts(TempHeader)) && (!StringMatch(TempHeader[i], "Notes:")); i
        ↵ +=1)
4101         STmp=TempHeader[i]
            If (StringMatch(TempHeader[i], "*[*]") && StringMatch(TempHeader[i], "*[*]*") )
                Prop=STmp[0, StrSearch(STmp, "[", 0)-1]
                Unit=STmp[StrSearch(STmp, "[", 0)+1, StrSearch(STmp, "]", 0)-1]
            Else
4106         Prop=STmp[0, StrSearch(STmp, ":", 0)-1]
                Unit=""
            EndIf
            Value=STmp[StrSearch(STmp, ":", 0)+1, inf]
            Unit=ReplaceString(" ", Unit, "")
4111         For( ;StringMatch(Prop, "* "); )
                Prop=Prop[0, StrLen(Prop)-2]
            EndFor
            For( ;StringMatch(Prop, " *"); )
                Prop=Prop[1, StrLen(Prop)-1]
            EndFor
4116         Value=ReplaceString(" ", Value, "")
            Tmp=GetPrefix(Unit)*Str2Num(Value)
            StrSwitch (Prop)
            Case "Pulses Acquired":
4121             Case "Frames Acquired":
                    NFrames=Tmp
                    Break
            Case "Pulse Pairs Acquired":
            Case "Frame Pairs Acquired":
4126             NFrames=Tmp*2
                    Break

```

```

    Case "Data Points per Second":
    Case "Sample Rate":
      SRate=Tmp
4131      Break
    Case "Chopper Period":
      CPeriod=Tmp/2
      Break
    Case "Pulse Length":
4136      PLength=Tmp
      Break
    Case "Open/Close":
      OCSteps=Tmp
      Break
4141    Case "Chopper Delay":
      CDelay=Tmp
      Break
    Case "Laser Power":
      If (StringMatch(Unit, "*W*" ))
4146        LPower=Tmp
      Else
        LPower=Tmp/1e6
      EndIf
      Break
4151    Case "Switch Dead Time":
      SDTime=Tmp+0.020
      Break
    Case "Reflectivity":
4156      Refl=Tmp
      Break
    Case "Calorimetry Gain":
      CGain=Tmp
      Break
    Case "QMS Gain":
4161      QGain=Tmp
      Break
    EndSwitch
  EndFor
  TempString=""
4166  StrSwitch (Name)
    Case "Trim":
    Case "ConCat1":
    Case "ConCat2":
      SetDataFolder root:NAC:TempSet
4171      Break
    Case "Deconvolution":
      SetDataFolder root:NAC:Deconvolution
      Break
    Default:
4176      SetDataFolder root:NAC:Experiment
      Break
    EndSwitch
  NVar SampleRate, ChopperPeriod, NominalPulseLength, OpenCloseSteps, ↵
  ↵ ChopperDelay, DataPoints=DataPointsPerFrame, PulseLength, SwitchDeadTime
  StrSwitch (Name)
4181    Case "Deconvolution":
    Case "BeforeCoating":
    Case "LaserReference":
      NVar Reflectivity="$root:NAC:"+Name+":Reflectivity"
      Break
4186    Default:
    EndSwitch
  If ((ChopperPeriod!=0) && (ChopperPeriod!=CPeriod))
    TempString+="ChopperPeriod, "
  EndIf
4191  If ((OpenCloseSteps!=0) && (OpenCloseSteps!=OCSteps))
    TempString+="CopperSteps, "
  EndIf
  If ((ChopperDelay!=0) && (ChopperDelay!=CDelay))
    TempString+="CopperDelay, "

```

```

4196     EndIf
        If ((NominalPulseLength!=0) && (NominalPulseLength!=PLength))
            TempString+="PulseLength, "
        EndIf
//     If ((NominalPulseLength!=0) && (SwitchDeadTime!=SDTime))
4201 //     TempString+="SwitchDeadTime, "
//     EndIf
TempString=RemoveEnding(TempString, ", ")
Variable Deconv=StringMatch(Name,"Deconvolution")
If (!Deconv && StrLen(TempString))
4206     SetDataFolder OldDF
        Error_Message(NAC_DataMismatch, "LoadCalFile", "InProc", TempString)
        NVar LoadSupport=root:NAC:GUI:LoadSupportFiles
        If (!LoadSupport)
            Return NAC_DataMismatch
4211     EndIf
        EndIf
String OpenPath=S_FileName
LoadWave /O/A /B=("C=1,F=0,N=CalData; C=1,F=0,N=QMSData;") /J /Q /L={↵
    ↵ NumberOfLines,NumberOfLines+1,NFrames*SRate*CPeriod,0,2} S_FileName
Wave CalData, QMSData
4216 WaveStats /Q CalData
    /// Replace with input dialogue
String Corrupt=""
If ((V_numNaNs!=0) || (!Deconv && (nFrames*SRate*CPeriod!=V_npnts)))
    Corrupt+="[CH1]"
4221 EndIf
WaveStats /Q QMSData
If ((V_numNaNs!=0) || (!Deconv && (nFrames*SRate*CPeriod!=V_npnts)))
    If (StrLen(Corrupt))
        Corrupt+=" & "
4226 EndIf
    Corrupt+="[CH2]"
EndIf
If (StrLen(Corrupt))
    DoAlert /T="Corrupt Data File" 1, S_FileName+" contains corrupt channels "+↵
    ↵ Corrupt+"!\r\rContinue load?"
4231     If (V_Flag>1)
        SetDataFolder OldDF
        Return LoadAborted
        EndIf
EndIf
4236 SampleRate=SRate
ChopperPeriod=CPeriod
OpenCloseSteps=OCSteps
ChopperDelay=CDelay
NominalPulseLength=PLength
4241 PulseLength=PLength
SwitchDeadTime=SDTime
If (NumType(Refl)==0)
    Reflectivity=Refl
Else
4246     StrSwitch (Name)
        Case "Deconvolution":
            SetFormula root:NAC:Deconvolution:Reflectivity "root:NAC:Machine:↵
            ↵ ReflectivityClean" // d.l.
            Break
        Case "BeforeCoating":
4251         SetFormula root:NAC:BeforeCoating:Reflectivity "root:NAC:Machine:↵
            ↵ ReflectivityClean" // d.l.
            Break
        Case "LaserReference":
            SetFormula root:NAC:LaserReference:Reflectivity "root:NAC:Machine:↵
            ↵ ReflectivityClean" // d.l.
            Break
4256     EndSwitch
EndIf
String NameList
NVar PRate=root:NAC:Machine:ProcessRate

```



```

DataPoints=PRate*CPeriod
4261 SetScale /P x, 0, 1/SRate, "s", CalData, QMSData //Sets the x-scale to be ↗
      ↳ seconds
SetScale d, -10, 10, "V", CalData, QMSData //Sets the data-scale to be ↗
      ↳ Volts
StrSwitch (Name)
  Case "Heat":
4266   NameList="Heat;Sticking;"
      KillWins("NAC_Desorption")
      KillWins("NAC_Adsorption")
      KillWins("NAC_Radiation_VsFrame")
      Break
  Case "Trim":
4271   NameList="TrimA;TrimB;"
      Break
  Case "Concat1":
      NameList="ConcatA;ConcatC;"
      Break
4276   Case "Concat2":
      NameList="ConcatB;ConcatD;"
      Break
  Case "BeforeCoating":
  Case "AfterCoating":
4281   NVar Reflec=root:NAC:AfterCoating:Reflectivity
      Reflec=NaN
      NameList=Name+";"
      Break
4286   Case "LaserReference":
  Case "Transmission":
      KillWins("NAC_Heat")
      KillWins("NAC_Adsorption")
      NameList=Name+";"
      NVar Trans=root:NAC:Transmission:Transmission
4291   Trans=NaN
      Break
  Case "ZeroSticking":
      KillWins("NAC_Sticking")
      KillWins("NAC_Desorption")
4296   NameList=Name+";"
      Break
  Default:
      NameList=Name+";"
      Break
4301 EndSwitch
NewPath /O /Q CalDataPath RemoveEnding(OpenPath,S_FileName)
PathInfo CalDataPath
String Path=S_Path
SVar ExpName=root:NAC:Experiment:ExperimentName
4306 If (!Strlen(ExpName))
      ExpName=Path[StrSearch(Path, ":", StrLen(Path)-2,3)+1, StrLen(Path)-2]
EndIf
For (j=0; j<ItemsInList(NameList); j+=1)
  Name=StringFromList(j,NameList)
4311 KillWins("NAC_"+Name)
      SetDataFolder $"root:NAC:"+Name
      NVar NumberOfFrames, Loaded, CurrentFrame, BrowseDeconvolutionIndex
      CurrentFrame=0
      BrowseDeconvolutionIndex=0
4316 SVar FileName
      Wave DisplayFit, DisplayRaw, FlagList
      StrSwitch (Name)
        Case "Sticking":
        Case "ConcatC":
4321   Case "ConcatD":
        Case "TrimB":
          Break
        Default:
          Wave /T Header
4326   Break

```

```

EndSwitch
StrSwitch (Name)
  Case "ConcatC":
  Case "ConcatD":
4331  Case "Sticking":
  Case "ZeroSticking":
  Case "TrimB":
    Duplicate /O QMSdata $"root:NAC:"+Name+":Detector"
    Break
4336  Case "TrimA":
  Case "ConcatA":
  Case "ConcatB":
  Default:
    Wave /T Header
4341  Duplicate /O Caldata $"root:NAC:"+Name+":Detector"
    Wave Detector=$"root:NAC:"+Name+":Detector"
    Break
EndSwitch
StrSwitch (Name)
4346  Case "Sticking":
  Case "TrimB":
  Case "ConcatC":
  Case "ConcatD":
    Break
4351  Default:
    Duplicate /O TempHeader $"root:NAC:"+Name+":Header"
    Break
EndSwitch
FileName=S_FileName
4356  StrSwitch (Name)
  Case "BeforeCoating":
  Case "AfterCoating":
  Case "LaserReference":
  Case "Transmission":
4361  Case "Deconvolution":
    NVar LaserPower
    LaserPower=LPower
    Break
  Default:
4366  Break
EndSwitch
NumberOfFrames=NFrames
StrSwitch (Name)
4371  Case "TrimA":
  Case "TrimB":
  Case "ConcatA":
  Case "ConcatB":
  Case "ConcatC":
  Case "ConcatD":
4376  Case "Heat":
  Case "Sticking":
    Break
  Default:
    NVar AutoFlagged=$"root:NAC:"+Name+":Statistics:AutoFlagged", ↵
    ↵ AutoFlaggedExp=root:NAC:Experiment:AutoFlagged
4381  Wave StatAmp=$"root:NAC:"+Name+":Statistics:Amplitude", StatWhi=$"root:↵
    ↵ NAC:"+Name+":Statistics:Whiskers", StatWhiLim=$"root:NAC:"+Name+":↵
    ↵ Statistics:WhiskerLimits"
    Wave StatQuart=$"root:NAC:"+Name+":Statistics:Quartiles", StatPos=$"root:↵
    ↵ NAC:"+Name+":Statistics:Position", StatMed=$"root:NAC:"+Name+":Statistics:↵
    ↵ Medians"
    Wave StatChiSq=$"root:NAC:"+Name+":Statistics:ChiSq", StatOutlier=$"root:↵
    ↵ NAC:"+Name+":Statistics:Outlier"
    AutoFlagged=0
    AutoFlaggedExp=0
4386  ReDimension /N=0 StatAmp, StatPos, StatChiSq, StatOutlier
    StatMed=NaN
    StatQuart=NaN
    StatWhi=NaN

```

```

4391     StatWhiLim=NaN
        Break
    EndSwitch
    StrSwitch (Name)
        Case "Heat":
            Wave Radiation, Adsorption, Offset, ShiftAds, ShiftRad, ChiSq, ↵
            ↵ fit_Radiation
4396         Wave Enthalpy=root:NAC:Enthalpies:Enthalpy
            ReDimension /N=0 Radiation, Adsorption, Enthalpy, Offset, ShiftAds, ↵
            ↵ ShiftRad, fit_Radiation
                ReDimension /N=(NumberOfFrames) ChiSq
                NVar UseFR=root:NAC:Experiment:UseFittedRadiation
                ChiSq=0
4401         UseFR=0
            CheckBox FittedRad Disable=2, Win=NAC_Control
            Break
        Case "Sticking":
4406         Wave Desorption, Offset, Shift, ChiSq, fit_Desorption
            Wave Sticking=root:NAC:Enthalpies:Sticking
            Wave Coverage=root:NAC:Enthalpies:Coverage, Thickness=root:NAC:Enthalpies ↵
            ↵ :Thickness
                NVar UseFD=root:NAC:Experiment:UseFittedDesorption
                ReDimension /N=(0) Desorption, Offset, Shift, Sticking, Coverage, ChiSq, ↵
            ↵ fit_Desorption, Thickness
                ReDimension /N=(NumberOfFrames) ChiSq
4411         ChiSq=0
            UseFD=0
            CheckBox FittedDes Disable=2, Win=NAC_Control
            Break
        Case "LaserReference":
4416         NVar Failed=root:NAC:Experiment:LengthDetectFailed
            Failed=0
            Break
        Default:
            Break
4421    EndSwitch
    StrSwitch (Name)
        Case "BeforeCoating":
            KillWaves /Z root:NAC:Experiment:FitReflectivityOdd, root:NAC:Experiment: ↵
            ↵ FitReflectivityEven
                Break
4426         Case "LaserReference":
            KillWaves /Z root:NAC:Experiment:FitLaserReferenceOdd, root:NAC: ↵
            ↵ Experiment:FitLaserReferenceEven
                Break
            Case "Radiation":
            KillWaves /Z root:NAC:Experiment:FitRadiationOdd, root:NAC:Experiment: ↵
            ↵ FitRadiationEven
                Break
4431         Case "ZeroSticking":
            KillWaves /Z root:NAC:Experiment:FitStickingOdd, root:NAC:Experiment: ↵
            ↵ FitStickingEven
                Break
4436         Case "Deconvolution":
            KillWaves /Z root:NAC:Experiment:DeconvolutionOdd, root:NAC:Experiment: ↵
            ↵ FitDeconvolutionEven
                Break
        Default:
            Break
    EndSwitch
4441    StrSwitch (Name)
        Case "TrimA":
        Case "TrimB":
        Case "ConcatA":
        Case "ConcatB":
4446         Case "ConcatC":
        Case "ConcatD":
            Break
        Default:

```

```

4451     NVar NyquistFrequency=root:NAC:Machine:NyquistFrequency
NVar LineFrequency=root:NAC:Machine:LineNotchFrequency
NVar NotchFrequency=root:NAC:Machine:SecondNotchFrequency
NVar HighPassFrequency=root:NAC:Machine:HighPassFrequency
NVar Store=root:NAC:GUI:StoreFilteredWaves
FlagList=0
4456     Loaded=1
CurrentFrame=0
ReDimension /N=(DataPoints) DisplayFit, DisplayRaw
SetScale /P x, 0, 1/PRate, "s", DisplayFit, DisplayRaw
Wave Detector="$root:NAC:"+Name+":Detector"
4461     If ((SRate!=2*NyquistFrequency) || (HighPassFrequency>0) || (↵
↵ LineFrequency>2) || (NotchFrequency>2))
↵ FFT Detector // Double precision is not increasing quality of ↵
↵ backtransformed data
If (Store)
Duplicate /O Detector "$root:NAC:"+Name+":Filtered"
Wave /C FilteredC="$root:NAC:"+Name+":Filtered"
4466     EndIf
Wave /C DetectorTemp="$root:NAC:"+Name+":Detector"
If ((LineFrequency>2) && (LineFrequency<=NyquistFrequency-2))
DetectorTemp[X2Pnt(DetectorTemp,LineFrequency-0.5),X2Pnt(Detector,↵
↵ LineFrequency+0.5)]=0
EndIf
4471     If ((NotchFrequency>2) && (NotchFrequency<=NyquistFrequency-2))
DetectorTemp[X2Pnt(DetectorTemp,NotchFrequency-1),X2Pnt(Detector,↵
↵ NotchFrequency+1)]=0
EndIf
If (SRate!=2*NyquistFrequency)
ReDimension /C /N=(X2Pnt(DetectorTemp,NyquistFrequency)+1) ↵
↵ DetectorTemp
4476     EndIf
StrSwitch (Name)
Case "Deconvolution":
Case "ZeroSticking":
4481     Case "Sticking":
Break
Default:
If (HighPassFrequency>0)
DetectorTemp[1,X2Pnt(DetectorTemp,HighPassFrequency)]=0
EndIf
4486     Break
EndSwitch
If (Store)
FilteredC==DetectorTemp
IFFT DetectorTemp
4491     IFFT FilteredC
Wave Filtered="$root:NAC:"+Name+":Filtered"
Else
IFFT DetectorTemp
EndIf
4496     If (SRate!=2*NyquistFrequency)
Detector*=2*NyquistFrequency/SRate
If (Store)
Filtered*=2*NyquistFrequency/SRate
EndIf
4501     EndIf
EndIf
StrSwitch (Name)
Case "Heat":
4506     Case "Sticking":
Break
Default:
Wave Amplitude="$root:NAC:"+Name+":Statistics:Amplitude", ChiSq="$↵
↵ root:NAC:"+Name+":Statistics:ChiSq", Outlier="$root:NAC:"+Name+":Statistics↵
↵ :Outlier"
ReDimension /N=0 Amplitude, ChiSq, Outlier
Break
4511     EndSwitch

```

```

    ReDimension /N=(NumberOfFrames) FlagList
    ReDimension /N=(DataPoints,NumberOfFrames) Detector
    Header=ReplaceString("\t", Header, " ")
    KillWaves /Z $"root:NAC:"+Name+":AverageEven", $"root:NAC:"+Name+":↵
↵ AverageOdd"
4516    Wave DisplayFit=$"root:NAC:"+Name+":DisplayFit"
        DisplayFit=NaN
        Error_Message(UpdateFlagWin(Name), "UpdateFlagWin", "LoadCalFile", Name)
        Break
    EndSwitch
4521    Error_Message(LoadAuxFile(Name, S_FileName), "LoadAuxFile", "LoadCalFile", ↵
↵ Name)
    If (StringMatch(Name, "Heat"))
        If (Exists("root:NAC:Heat:Auxiliaries:Source")==1)
            Wave Source=root:NAC:Heat:Auxiliaries:Source
            NVar TemperatureSource=root:NAC:Experiment:TemperatureSource
4526            TemperatureSource=Mean(Source)
        Else
            TemperatureSource=NaN
        EndIf
        If (Exists("root:NAC:Heat:Auxiliaries:Sample")==1)
4531            Wave Sample=root:NAC:Heat:Auxiliaries:Sample
            NVar TemperatureSample=root:NAC:Experiment:TemperatureSample
            TemperatureSample=Mean(Sample)
        Else
            TemperatureSample=NaN
4536        EndIf
    EndIf
    If (Exists("root:NAC:"+Name+":Auxiliaries:Motor_FB")==1)
        Wave /T Motor=$"root:NAC:"+Name+":Auxiliaries:Motor_FB"
        Wave FlagList=$"root:NAC:"+Name+":FlagList"
4541        If (Deconv)
            NVar DataPoints=root:NAC:Deconvolution:DataPointsPerFrame
        Else
            NVar DataPoints=root:NAC:Experiment:DataPointsPerFrame
        EndIf
4546        FlagList=!StringMatch(Motor[Floor(p/2)], "Y*")
        StrSwitch (Name)
            Case "TrimA":
            Case "TrimB":
            Case "ConcatA":
4551            Case "ConcatB":
            Case "ConcatC":
            Case "ConcatD":
            Case "Deconvolution":
                Break
4556            Case "Heat":
            Case "Sticking":
                For (i=NumPnts(FlagList)-1; (FlagList[i]==1) && (i>1); i--1)
                    EndFor
                    If (i>0)
4561                        FlagList[i]=1
                        FlagList[i-1]=1
                    EndIf
                    Break
            Default:
4566                For (i=0; (FlagList[i]==1) && (i<NumPnts(FlagList)-1); i+=1) //
                    EndFor
                    If (i<NumPnts(FlagList)-1)
                        FlagList[i]=1
                        FlagList[i+1]=1
4571                    EndIf
                    For (i=NumPnts(FlagList)-1; (FlagList[i]==1) && (i>1); i--1)
                    EndFor
                    If (i>0)
4576                        FlagList[i]=1
                        FlagList[i-1]=1
                    EndIf
                    Break

```

```

        EndSwitch
    EndIf
4581 EndFor
    KillWaves /Z CalData, QMSData
    SetVariable PulseLength, Win=NAC_Control, Limits={0.001, CPeriod, 0.001}
    SetDataFolder OldDF
    Return NoError
4586 End
//
LoadRateFile

Static Function LoadRateFile(Name, FileName)
String Name, FileName
Variable RefNum, HeaderLines, NumberOfLines, LDensity, LMolarMass, ↵
    ↵ LMonolayerDensity, i
4591 String TempString, FileHeader="", LSubstance, LSubstanceName
String MiscRateFiles= "Miscellaneous QCM Files (*.qcm):.qcm;"
String AllRateFiles= "All QCM Files (*.flx *.tck *.qcm):.flx,.tck,.qcm;"
String AllFiles="All Files (*.*):.*;"
DFRef OldDF=GetDataFolderDFR()
4596   StrSwitch (Name)
        Case "Deconvolution":
        Case "BeforeCoating":
        Case "AfterCoating":
        Case "LaserReference":
4601     Case "Transmission":
        Case "Radiation":
        Case "ZeroSticking":
        Case "Sticking":
        Case "Heat":
4606     Return NAC_NotApplicable
        Break
        Case "RateCalorimetry":
            TempString="Calorimetry Deposition Rate Files (*.flx):.flx;"
            Break
4611     Case "RateCoating":
            TempString="Coating Thickness Files (*.tck):.tck;"
            Break
        Default:
            Return NAC_UnknownMeasurement
4616 EndSwitch
NVar LoadSupport=root:NAC:GUI:LoadSupportFiles
If (LoadSupport)
    TempString=MiscRateFiles+TempString+AllRateFiles+AllFiles
Else
4621     TempString=TempString+MiscRateFiles+AllRateFiles+AllFiles
EndIf
PathInfo CalDataPath
If (!V_Flag)
    NewPath /O /Q /Z CalDataPath, NAC_DataPathStr
4626     If (!V_Flag)
        NewPath /O /Q CalDataPath
        If (V_Flag)
            Return UserCancel
        EndIf
4631     EndIf
EndIf
SetDataFolder $"root:NAC:"+Name
Open /R /P=CalDataPath /F=TempString RefNum as FileName
If (CmpStr(S_FileName,"")==0)
4636     SetDataFolder OldDF
    Return UserAbort
EndIf
FReadLine RefNum, TempString
Do
4641     If (CmpStr(TempString,"\r")!=0)
        FileHeader=FileHeader+TempString
        HeaderLines=HeaderLines+1
        If (StringMatch(TempString,"Density*"))

```

```

        sscanf TempString,"Density:\t%f", LDensity
4646    EndIf
        If (StringMatch(TempString,"Molar Mass*"))
            sscanf TempString,"Molar Mass:\t%f", LMolarMass
        EndIf
        If (StringMatch(TempString,"ML atom density*"))
4651    sscanf TempString,"ML atom density:\t%f", LMonolayerDensity
        EndIf
        If (StringMatch(TempString,"Substance*"))
            LSubstance=TempString[11,strlen(TempString)-2]
            LSubstanceName=GetSubstanceName(LSubstance)
4656    EndIf
        EndIf
        FReadLine RefNum, TempString
        NumberOfLines=NumberOfLines+1
        While (!StringMatch(TempString, "*Time*"))
4661    Close RefNum
        Error_Message(LoadAuxFile(Name,S_FileName,Delta=1), "LoadAuxFile", "↵
            ↵ LoadRateFile", Name)
        If (!WaveExists("$root:NAC:"+Name+":Auxiliaries:Thickness"))
            SetDataFolder OldDF
            Return ErrorHandled
4666    EndIf
        Duplicate /O "$root:NAC:"+Name+":Auxiliaries:Thickness", "$root:NAC:"+Name+":↵
            ↵ Thickness"
        Duplicate /O "$root:NAC:"+Name+":Auxiliaries:Timeline", "$root:NAC:"+Name+":↵
            ↵ Timeline"
        KillWaves /Z "$root:NAC:"+Name+":Auxiliaries:Thickness", "$root:NAC:"+Name+":↵
            ↵ Auxiliaries:Timeline"
        KillWins("NAC_"+Name)
4671    String WName="NAC_"+Name+"_Full"
        Wave /T Header
        ReDimension /N=(HeaderLines+2) Header
        Header[0]=S_FileName
        For (i=0; i<HeaderLines;i=i+1)
4676    Header[i+1]=StringFromList(i,FileHeader,"\r\n")
        EndFor
        Header[HeaderLines+1]="End of Header"
        Header=ReplaceString("\t", Header, " ")
        NVar MonolayerDensity, MolarMass, Density
4681    SVar Substance, LoadName=FileName, SubstanceName
        MonolayerDensity=LMonolayerDensity
        MolarMass=LMolarMass
        Density=LDensity
        LoadName=S_FileName[StrSearch(S_FileName, ":", Inf, 3)+1,Inf]
4686    Substance=LSubstance
        SubstanceName=LSubstanceName
        Wave Thickness
        If (StringMatch(Substance,"PTCDA*"))
            If (Density==3.37)
4691    Density=1.69
                Thickness/=1.69/3.37
                Note Thickness "Wrong density has been corrected"
            EndIf
        EndIf
4696    Variable Ref, NP
        NVar BaselineTo, BaselineFrom
        Ref=Thickness[0]+2.5e-10
        NP=NumPnts(Thickness)
        i=0
4701    Do
            i=i+1
            While ((i<NP/4)&&(Thickness[i]<Ref))
                BaselineTo=i
            Ref=Thickness[NP-1]-2.5e-10
4706    i=NP
        Do
            i=i-1
            While ((i>NP*3/4)&&(Thickness[i]>Ref))

```

```

BaselineFrom=i
4711 NVar Loaded
Loaded=1
NewPath /O /Q CalDataPath S_FileName[0,StrSearch(S_FileName, ":", Inf, 3)]
SetDataFolder OldDF
Error_Message(DisplayRateFile(Name), "DisplayRateFile", "LoadRateFile", Name)
4716 Return NoError
End
//
LoadAuxFile

Static Function LoadAuxFile(Name, FileName, [Delta])
String Name, FileName
4721 Variable Delta
Variable RefNum, NumberOfLines, i
String TempString, HeaderLine, UnitList="", NameList="", ListItem, xUnit, dUnit
DFRef OldDF=GetDataFolderDFR()
If (ParamIsDefault(Delta))
4726 Delta=2
xUnit="Frame"
Else
Delta=1
xUnit="s"
4731 EndIf
If (StringMatch(FileName, ":*.*"))
Open /R /P=CalDataPath RefNum as FileName
Else
4736 FileName=FileName[0,StrSearch(FileName, ".", Inf, 3)-1]
TempString=IndexedFile(CalDataPath, -1, ".aux")
If (!StringMatch(TempString, "*" + FileName + "*"))
Return NAC_AuxFileNotFound
EndIf
Open /R /P=CalDataPath RefNum as FileName+".aux"
4741 EndIf
FReadLine RefNum, TempString
Do
FReadLine RefNum, TempString
NumberOfLines=NumberOfLines+1
4746 While (!stringmatch(TempString, "Time*") && !stringmatch(TempString, "*Pair ↵
↵ Time*"))
Close RefNum
HeaderLine=TempString
TempString=""
For (i=0; i<ItemsInList(HeaderLine, "\t"); i+=1)
4751 ListItem=StringFromList(i, HeaderLine, "\t")
If (StringMatch(ListItem, "Frame pair time*") || StringMatch(ListItem, "Pulse ↵
↵ pair time*"))
TempString+="C=1,N='_skip_'; "
ElseIf (StringMatch(ListItem, "N/A*"))
TempString+="C=1,N='_skip_'; "
4756 ElseIf (StringMatch(ListItem, "*[TXT]*"))
TempString+="C=1,F=-2,N="+ListItem[0,StrSearch(ListItem, "[", Inf, 3)-1]+";↵
↵ "
NameList+=ListItem[0,StrSearch(ListItem, "[", Inf, 3)-1]+";"
UnitList+="TXT;"
ElseIf (StringMatch(ListItem, "Time*"))
4761 TempString+="C=1,F=0,T=2,N=Timeline; "
NameList+="Timeline;"
UnitList+="s;"
ElseIf (StringMatch(ListItem, "Crystal Frequency*"))
4766 TempString+="C=1,F=0,T=2,N=Frequency; "
NameList+="Frequency;"
UnitList+="Hz;"
Else
TempString+="C=1,F=0,T=2,N="+ListItem[0,StrSearch(ListItem, "[", Inf, 3)↵
↵ -1]+"; "
UnitList+=ListItem[StrSearch(ListItem, "[", 0, 2)+1,StrSearch(ListItem, ↵
↵ "]" , Inf, 3)-1]+";"
4771 NameList+=ListItem[0,StrSearch(ListItem, "[", Inf, 3)-1]+";"

```



```

    EndIf
  EndFor
  SetDataFolder $"root:NAC:"+Name+":Auxiliaries"
  LoadWave /O /A /B=TempString /J /L={0,NumberOfLines+2,0,0,0} /Q S_FileName
4776 If (V_flag==0)
    SetDataFolder OldDF
    Return NAC_AuxFileLoadFailed
  EndIf
  NameList=ReplaceString(" ", NameList, "")
4781 For (i=0;i<ItemsInList(NameList,"");i+=1)
    Wave Process=$StringFromList(i,NameList,";")
    StrSwitch (StringFromList(i,UnitList,";"))
      Case "mBar":
4786       Process*=100
        dUnit="Pa"
        Break
      Case "Torr":
        Process*=101325/760
4791       dUnit="Pa"
        Break
      Case "nm":
        Process/=1e9
        dUnit="m"
        Break
4796       Case "C":
        Case "degC":
          Process+=273.15
          dUnit="K"
          Break
4801       Case "F":
        Case "degF":
          Process=(Process + 459.67)*5/9
          dUnit="K"
          Break
4806       Default:
        dUnit=StringFromList(i,UnitList,";")
        Break
    EndSwitch
    SetScale d, 0, 0, dUnit, $StringFromList(i,NameList,";")
4811 SetScale /P x, 0, Delta, xUnit, $StringFromList(i,NameList,";")
  EndFor
  SetDataFolder OldDF
  Return NoError
End
4816 //

```

Function LoadTrend

```

Static Function LoadTrend(Name, FileName)
String Name, &FileName
Variable RefNum, i
String ExpName, Corrupt=""
4821 StrSwitch(Name)
  Case "Radiation":
    Wave Fit=root:NAC:Heat:fit_Radiation
    NVar Frames=root:NAC:Heat:NumberOfFrames
    Break
4826  Case "Desorption":
    Wave Fit=root:NAC:Sticking:fit_Desorption
    NVar Frames=root:NAC:Sticking:NumberOfFrames
    Break
  Default:
4831    Return NAC_NotApplicable
    Break
  EndSwitch
  Open /D /R /F="Igor Experiment Files (*.pxp):.pxp;" RefNum
  If (!StrLen(S_FileName))
4836    Return UserAbort
  EndIf
  DRef OldDF=GetDataFolderDFR

```

```

SetDataFolder root:
LoadData /L=1 /O /Q /S="NAC_Average:" /J="AveragedSticking;AveragedRadiation" /↵
↳ T=NAC_Import S_FileName
4841 RefNum=GetRTError(1)
ExpName=PossiblyQuoteName(S_FileName[StrSearch(S_FileName, ":", Inf ,3)+1,↵
↳ StrSearch(S_FileName, ".", Inf ,3)-1])
FileName=S_FileName[StrSearch(S_FileName, ":", Inf ,3)+1,StrSearch(S_FileName, ↵
↳ ".", Inf ,3)-1]
StrSwitch(Name)
  Case "Radiation":
4846   If (Exists("root:NAC_Import:AveragedSticking")!=1)
       Corrupt+="AveragedSticking(W), "
       EndIf
       Break
  Case "Desorption":
4851   If (Exists("root:NAC_Import:AveragedRadiation")!=1)
       Corrupt+="AveragedRadiation(W), "
       EndIf
       Break
  Default:
4856   Break
EndSwitch
If (StrLen(Corrupt))
  Corrupt=RemoveEnding(Corrupt, ", ")
  KillDataFolder NAC_Import
4861  SetDataFolder OldDF
  Return NAC_CorruptExperiment
EndIf
StrSwitch(Name)
  Case "Radiation":
4866   Wave Radiation=root:NAC_Import:AveragedRadiation
       Wave Fit=root:NAC:Heat:fit_Radiation, Cov=root:NAC:Enthalpies:Coverage
       ReDimension /N=(Frames) Fit
       SetScale /P x,0,1, "Fame", Fit
       Fit=Radiation(Cov[p])
4871   NVar UseTrend=root:NAC:Experiment:UseFittedRadiation
       Break
  Case "Desorption":
       NVar Dose=root:NAC:RateCalorimetry:DosePerPulse
       Wave Desorption=root:NAC_Import:AveragedSticking
4876   Desorption=1-Desorption
       ReDimension /N=(Frames) Fit
       SetScale /P x,0,1, "Fame", Fit
       Fit=0
       For (i=1;i<Frames;i+=1)
4881   Fit[i]=Desorption(Limit(Dose*(i-Sum(Fit, 0, i-1)), 0, RightX(Desorption))↵
↳ )
       EndFor
       NVar UseTrend=root:NAC:Experiment:UseFittedDesorption
       Break
  Default:
4886   Break
EndSwitch
Fit[0]=Fit[1]
Error_Message(DisplayTrend(Name, 1), "DisplayTrend", "NAC_LoadTrend", Name)
UseTrend=1
4891 SetDataFolder OldDF
KillDataFolder NAC_Import
Return NoError
End
//
NAC_ConCat
4896 Function NAC_ConCat() //// Error handling
DFRef OldDF=GetDataFolderDFR()
String ExpList="ConcatA;ConcatB;ConcatC;ConcatD;"
String NewFileName, AuxWavesA, AuxWavesB, ColumnNames=""
Variable i, j, Fail=0
4901 If (!DataFolderExists("root:NAC:"))

```

```

    NAC_initialize()
  EndIf
  For (i=0;i<ItemsInList(ExpList,"");i+=1)
    KillDataFolder /Z $"root:NAC:"+StringFromList(i,ExpList,"");
4906   NewDataFolder /S $"root:NAC:"+StringFromList(i,ExpList,"");
    NewDataFolder $"root:NAC:"+StringFromList(i,ExpList,"")+":Auxiliaries"
    String /G FileName="Not Loaded"
    Make /T /N=1 Header={"Not Loaded"}
    Make /N=0 DisplayFit, DisplayRaw
4911   Make /N=0 /B /U FlagList
    Variable /G NumberOfFrames, EffectiveFrames, LaserPower
    Variable /G Loaded=0, CurrentFrame=0, Gain=0
  EndFor
  NewDataFolder /S root:NAC:TempSet
4916   Variable /G SampleRate=0, OpenCloseSteps=0, ChopperPeriod=0
    Variable /G NominalPulseLength=0, DataPointsPerFrame=0
    Variable /G LengthDetectFailed, ChopperDelay=0, PulseLength=0, SwitchDeadTime=0
    Fail=Error_Message(LoadCalFile("Concat1",""), "LoadCalFile", "NAC_ConCat", "↵
    ↵ File A")
  If (!Fail)
4921   SVar FileNameA=root:NAC:ConcatA:FileName
    Fail=Error_Message(LoadCalFile("Concat2",FileNameA[StrSearch(FileNameA, ".", ↵
    ↵ Inf, 3)+1,Inf]), "LoadCalFile", "NAC_ConCat", "File B")
  EndIf
  If (!Fail)
4926   SVar FileNameB=root:NAC:ConcatB:FileName
    Fail=(!Stringmatch(FileNameB,"*"+FileNameA[StrSearch(FileNameA, ".", Inf, 3)↵
    ↵ +1,Inf]))*2
  EndIf
  If (!Fail)
    Fail=StringMatch(FileNameA, FileNameB)*3
  EndIf
4931   If (Fail)
    SetDataFolder OldDF
    For (i=0;i<ItemsInList(ExpList,"");i+=1)
      KillDataFolder $"root:NAC:"+StringFromList(i,ExpList,"");
    EndFor
4936   KillDataFolder root:NAC:TempSet
    Return Fail
  EndIf
  For (i=0;StringMatch(FileNameA[0,i],FileNameB[0,i]);i+=1) // find first not ↵
    ↵ machting character
  EndFor
4941   NewFileName=FileNameA[0,StrSearch(FileNameA, ".", Inf, 3)-1]+"_"+FileNameB[i,↵
    ↵ Inf]
  SetDataFolder root:NAC
  Wave DetectorA=root:NAC:ConcatA:Detector, DetectorC=root:NAC:ConcatC:Detector
  Wave DetectorB=root:NAC:ConcatB:Detector, DetectorD=root:NAC:ConcatD:Detector
  Wave /T HeaderA=root:NAC:ConcatA:Header, HeaderB=root:NAC:ConcatB:Header
4946   Duplicate HeaderA root:NAC:ConcatA:NewHeader
  Wave /T NewHeader=root:NAC:ConcatA:NewHeader
  NVar FramesA=root:NAC:ConcatA:NumberOfFrames, FramesB=root:NAC:ConcatB:↵
    ↵ NumberOfFrames
  NVar GainA=root:NAC:ConcatA:Gain, GainB=root:NAC:ConcatB:Gain, GainC=root:NAC:↵
    ↵ ConcatC:Gain, GainD=root:NAC:ConcatD:Gain
  For (i=0;(!StringMatch(HeaderA[i],"Experiment Finished*")) && (i<NumPnts(↵
    ↵ HeaderA)) ;i+=1) // Test for corrupt Header?
4951   EndFor
  If (i<NumPnts(HeaderA))
    NewHeader[i]=ReplaceString("Finished", HeaderA[i], "Interrupted")
    InsertPoints i+1, 2, NewHeader
  EndIf
4956   For (j=0;(!StringMatch(HeaderB[j],"Experiment Started*")) && (j<NumPnts(HeaderB↵
    ↵ )) ;j+=1)
  EndFor
  If (j<NumPnts(HeaderB))
    NewHeader[i+1]=ReplaceString("Started", HeaderB[j], "Continued")
  EndIf

```

```

4961 For (j=0;(!StringMatch(HeaderB[j],"Experiment Finished*")) && (j<NumPnts(↵
↵ HeaderB));j+=1)
EndFor
If (j<NumPnts(HeaderB))
NewHeader[i+2]=HeaderB[j]
EndIf
4966 For (i=0;(StringMatch(NewHeader[i],"* Pairs Acquired*")) && (i<NumPnts(↵
↵ NewHeader)); i+=1)
EndFor
If (i<NumPnts(NewHeader))
NewHeader[i]="Frame Pairs Acquired: "+Num2Str((FramesA+FramesB))
EndIf
4971 For (i=0;(!StringMatch(NewHeader[i],"Calorimetry Gain*")) && (i<NumPnts(↵
↵ NewHeader)); i+=1)
EndFor
If (i<NumPnts(NewHeader))
NewHeader[i]="Calorimetry Gain: 1"
EndIf
4976 For (i=0;(!StringMatch(NewHeader[i],"QMS Gain*")) && (i<NumPnts(NewHeader)) ;i↵
↵ +=1)
EndFor
If (i<NumPnts(NewHeader))
NewHeader[i]="QMS Gain: 1"
EndIf
4981 For (i=0;(!StringMatch(NewHeader[i],"Notes*")) && (i<NumPnts(NewHeader)) ;i+=1)
EndFor
If (i<NumPnts(NewHeader))
If ((GainA!=1) || (GainB!=1) || (GainC!=1) || (GainD!=1))
InsertPoints i+1, 4, NewHeader
4986 NewHeader[i+1]="Gains changed to 1"
NewHeader[i+2]="Old Values("+FileNameA+"): GainCal:"+Num2Str(GainA)+" ↵
↵ GainQMS:"+Num2Str(GainC)
NewHeader[i+3]="Old Values("+FileNameB+"): GainCal:"+Num2Str(GainB)+" ↵
↵ GainQMS:"+Num2Str(GainD)
NewHeader[i+4]="Original Notes from "+FileNameA
EndIf
4991 EndIf
NewHeader[NumPnts(NewHeader)-1]="Original Notes from "+FileNameB
For (i=0;(!StringMatch(HeaderB[i],"Notes*")) && (i<NumPnts(HeaderB)) ;i+=1)
EndFor
If (i<NumPnts(HeaderB))
4996 For (j=i+1;j<NumPnts(HeaderB)-1;j+=1)
InsertPoints NumPnts(NewHeader), 1, NewHeader
NewHeader[NumPnts(NewHeader)-1]=HeaderB[j]
EndFor
EndIf
5001 DeletePoints 0, 1, NewHeader
InsertPoints NumPnts(NewHeader), 2, NewHeader
NewHeader[numpnts(NewHeader)-2]="
NewHeader[numpnts(NewHeader)-1]="Calorimetry"+num2char(9)+"MassSpec"
Save /E=0 /M="\r\n" /P=CalDataPath /O /G NewHeader as NewFileName
5006 Save /A=1 /J /M="\r\n" /P=CalDataPath /G DetectorA, DetectorC as NewFileName
Save /A=2 /J /M="\r\n" /P=CalDataPath /G DetectorB, DetectorD as NewFileName
Error_Message(LoadAuxFile("ConcatA", FileNameA), "LoadAuxFile", "NAC_ConCat", " ↵
↵ Auxfile A") //// ErrorChecking
Error_Message(LoadAuxFile("ConcatB", FileNameB), "LoadAuxFile", "NAC_ConCat", " ↵
↵ Auxfile B")
SetDatafolder root:NAC:ConcatA:Auxiliaries
5011 AuxWavesA=WaveList(";", ";", "")
For (i=0;i<ItemsInList(AuxWavesA);i+=1)
ColumnNames+=StringFromList(i, AuxWavesA, ";")+["+WaveUnits($StringFromList(↵
↵ i, AuxWavesA, ";"), -1)+"]\t"
EndFor
ColumnNames=ColumnNames[0,StrLen(ColumnNames)-2]
5016 NewFileName=NewFileName[0,StrSearch(NewFileName,".",3)]+"aux"
SetDatafolder root:NAC:ConcatB:Auxiliaries
AuxWavesB=WaveList(";", ";", "")
Fail=0
For (i=0;i<ItemsInList(AuxWavesB);i+=1)

```

```

5021     Fail=Fail || !StringMatch(AuxWavesA, "*" + StringFromList(i, AuxWavesB, ";") ↵
    ↵ + "*"")
EndFor
ColumnNames=ReplaceString("Timeline", ColumnNames, "Time")
If (!Fail && (ItemsInList(AuxWavesA, ";") == ItemsInList(AuxWavesB, ";")))
5026     NewHeader[NumPnts(NewHeader)-1]=ColumnNames
     Save /E=0 /M="\r\n" /P=CalDataPath /O /G NewHeader as NewFileName
     SetDataFolder root:NAC:ConcatA:Auxiliaries
     Save /A=1 /J /M="\r\n" /P=CalDataPath /G /B AuxWavesA as NewFileName
     SetDataFolder root:NAC:ConcatB:Auxiliaries
     Save /A=2 /J /M="\r\n" /P=CalDataPath /G /B AuxWavesA as NewFileName
5031 Else
     Print "Auxiliary waves mismatch!"
EndIf
SetDataFolder OldDF
For (i=0; i < ItemsInList(ExpList, ";"); i += 1)
5036     KillDataFolder $"root:NAC:" + StringFromList(i, ExpList, ";")
EndFor
KillDataFolder root:NAC:TempSet
Return NoError
End
5041 //
NAC_Trim
Function NAC_Trim()      //// Error handling
DFRef OldDF=GetDataFolderDFR()
String ExpList="TrimA;TrimB;"
String NewFileName, InvertStr, ColumnNames="", AuxWaves
5046 Variable i
Variable TrimFrom, TrimTo
If (!DataFolderExists("root:NAC:"))
    NAC_Initialize()
EndIf
5051 For (i=0; i < ItemsInList(ExpList, ";"); i += 1)
    KillDataFolder /Z $"root:NAC:" + StringFromList(i, ExpList, ";")
    NewDataFolder /S $"root:NAC:" + StringFromList(i, ExpList, ";")
    NewDataFolder $"root:NAC:" + StringFromList(i, ExpList, ";") + ":Auxiliaries"
    String /G FileName="Not Loaded"
5056     Make /T /N=1 Header={"Not Loaded"}
     Make /N=0 DisplayFit, DisplayRaw
     Make /N=0 /B /U FlagList
     Variable /G Gain=0
     Variable /G NumberOfFrames, EffectiveFrames, LaserPower
5061     Variable /G Loaded=0, CurrentFrame=0
EndFor
NewDataFolder /S root:NAC:TempSet
Variable /G SampleRate=0, OpenCloseSteps=0, ChopperPeriod=0
Variable /G NominalPulseLength=0, DataPointsPerFrame=0, SwitchDeadTime=0
5066 Variable /G LengthDetectFailed, ChopperDelay=0, PulseLength=0
If (Error_Message(LoadCalFile("Trim", ""), "LoadCalFile", "NAC_Trim", "") != 0)
    SetDataFolder OldDF
    KillDataFolder root:NAC:TrimA
    KillDataFolder root:NAC:TrimB
5071     KillDataFolder root:NAC:TempSet
     Return -1
EndIf
SetDataFolder root:NAC
Do
5076     TrimFrom=0
     TrimTo=NumberOfFrames-1
     Prompt TrimFrom, "From Frame (even):"
     Prompt TrimTo, "To Frame (odd):"
     DoPrompt /HELP="" "Trim file "+ FileName, TrimFrom, TrimTo
5081 While (((TrimFrom < 0) || (TrimTo < 0) || (TrimTo > NumberOfFrames-1) || (TrimFrom > ↵
    ↵ NumberOfFrames-1) || (Mod(TrimFrom, 2) == 1) || (Mod(TrimTo, 2) == 0)) && (V_flag ↵
    ↵ == 0))
If (V_Flag != 0)
    SetDataFolder OldDF
    KillDataFolder root:NAC:TrimA

```

```

KillDataFolder root:NAC:TrimB
5086 KillDataFolder root:NAC:TempSet
Return -1
EndIf
If (TrimFrom>TrimTo)
i=TrimTo
5091 TrimTo=TrimFrom
TrimFrom=i
EndIf
Wave DetectorA=root:NAC:TrimA:Detector, DetectorB=root:NAC:TrimB:Detector
SVar FileName=root:NAC:TrimA:FileName
5096 Wave /T Header=root:NAC:TrimA:Header
NewFileName=FileName[0,StrSearch(FileName, ".", Inf, 3)-1]
If (TrimFrom == 0)
NewFileName+="_S"
Else
5101 NewFileName+="_"+Num2Str(TrimFrom/2)
EndIf
If (TrimTo == NumberOfFrames-1)
NewFileName+="_E"
Else
5106 NewFileName+="_"+Num2Str((TrimTo-1)/2)
EndIf
NVar DataPointsPerFrame=root:NAC:TempSet:DataPointsPerFrame
NVar NumberOfFrames=root:NAC:TrimA:NumberOfFrames
DeletePoints (TrimTo+1)*DataPointsPerFrame, (NumberOfFrames-TrimTo)*
DataPointsPerFrame-1, DetectorA, DetectorB
5111 DeletePoints 0, TrimFrom*DataPointsPerFrame, DetectorA, DetectorB
NewFileName+=FileName[StrSearch(FileName, ".", Inf, 3),Inf]
For (i=0;!StringMatch(Header[i],"* Pairs Acquired*");i+=1)
EndFor
Header[i]="Frame Pairs Acquired: "+Num2Str((TrimTo-TrimFrom+1)/2)
5116 For (i=0;!StringMatch(Header[i],"Calorimetry Gain*");i+=1)
EndFor
Header[i]="Calorimetry Gain: 1"
For (i=0;!StringMatch(Header[i],"QMS Gain*");i+=1)
EndFor
5121 Header[i]="QMS Gain: 1"
NVar GainA=root:NAC:TrimA:Gain, GainB=root:NAC:TrimB:Gain
For (i=0;i<NumPnts(Header);i+=1)
If (StringMatch(Header[i],"Notes*"))
InsertPoints i+1, 4, Header
5126 Header[i+1]="Trimmed from frame pair "+Num2Str(TrimFrom/2)+" to frame pair
"+Num2Str((TrimTo-1)/2)
Header[i+2]="Gain changed to 1"
Header[i+3]="Old Values: GainCal:"+Num2Str(GainA)+" GainQMS:"+Num2Str(GainB
)
Header[i+4]="Original Notes from "+FileName
EndIf
EndFor
5131 DeletePoints 0, 1, Header
InsertPoints NumPnts(Header)-1, 1, Header
Header[NumPnts(Header)-2]="
Header[NumPnts(Header)-1]="Calorimetry"+num2char(9)+"MassSpec"
5136 Save /E=0 /M="\r\n" /P=CalDataPath /O /G Header as NewFileName
Save /A=1 /J /M="\r\n" /P=CalDataPath /G DetectorA, DetectorB as NewFileName
Error_Message(LoadAuxFile("TrimA", FileName), "LoadAuxFile", "NAC_Trim", "")
Error_Message(LoadAuxFile("TrimB", FileName), "LoadAuxFile", "NAC_Trim", "")
Error_Message(LoadAuxFile("TrimC", FileName), "LoadAuxFile", "NAC_Trim", "")
Error_Message(LoadAuxFile("TrimD", FileName), "LoadAuxFile", "NAC_Trim", "")
Error_Message(LoadAuxFile("TrimE", FileName), "LoadAuxFile", "NAC_Trim", "")
Error_Message(LoadAuxFile("TrimF", FileName), "LoadAuxFile", "NAC_Trim", "")
Error_Message(LoadAuxFile("TrimG", FileName), "LoadAuxFile", "NAC_Trim", "")
Error_Message(LoadAuxFile("TrimH", FileName), "LoadAuxFile", "NAC_Trim", "")
Error_Message(LoadAuxFile("TrimI", FileName), "LoadAuxFile", "NAC_Trim", "")
Error_Message(LoadAuxFile("TrimJ", FileName), "LoadAuxFile", "NAC_Trim", "")
Error_Message(LoadAuxFile("TrimK", FileName), "LoadAuxFile", "NAC_Trim", "")
Error_Message(LoadAuxFile("TrimL", FileName), "LoadAuxFile", "NAC_Trim", "")
Error_Message(LoadAuxFile("TrimM", FileName), "LoadAuxFile", "NAC_Trim", "")
Error_Message(LoadAuxFile("TrimN", FileName), "LoadAuxFile", "NAC_Trim", "")
Error_Message(LoadAuxFile("TrimO", FileName), "LoadAuxFile", "NAC_Trim", "")
Error_Message(LoadAuxFile("TrimP", FileName), "LoadAuxFile", "NAC_Trim", "")
Error_Message(LoadAuxFile("TrimQ", FileName), "LoadAuxFile", "NAC_Trim", "")
Error_Message(LoadAuxFile("TrimR", FileName), "LoadAuxFile", "NAC_Trim", "")
Error_Message(LoadAuxFile("TrimS", FileName), "LoadAuxFile", "NAC_Trim", "")
Error_Message(LoadAuxFile("TrimT", FileName), "LoadAuxFile", "NAC_Trim", "")
Error_Message(LoadAuxFile("TrimU", FileName), "LoadAuxFile", "NAC_Trim", "")
Error_Message(LoadAuxFile("TrimV", FileName), "LoadAuxFile", "NAC_Trim", "")
Error_Message(LoadAuxFile("TrimW", FileName), "LoadAuxFile", "NAC_Trim", "")
Error_Message(LoadAuxFile("TrimX", FileName), "LoadAuxFile", "NAC_Trim", "")
Error_Message(LoadAuxFile("TrimY", FileName), "LoadAuxFile", "NAC_Trim", "")
Error_Message(LoadAuxFile("TrimZ", FileName), "LoadAuxFile", "NAC_Trim", "")
SetDatafolder root:NAC:TrimA:Auxiliaries
AuxWaves=WaveList(";", ";", "")
5141 For (i=0;i<ItemsInList(AuxWaves);i+=1)
ColumnNames+=StringFromList(i, AuxWaves, ";")+ "["+WaveUnits($StringFromList(i,
AuxWaves, ";"), -1)+"]\t"
DeletePoints (TrimTo+1)/2, (NumberOfFrames-TrimTo)/2, $StringFromList(i,
AuxWaves, ";")
DeletePoints 0, TrimFrom/2, $StringFromList(i, AuxWaves, ";")
EndFor
5146 ColumnNames=ReplaceString("Timeline", ColumnNames, "Time")
ColumnNames=ColumnNames[0,StrLen(ColumnNames)-2]

```

```

NewFileName=NewFileName[0,StrSearch(NewFileName,".",3)]+"aux"
Header[NumPnts(Header)-1]=ColumnNames
Save /E=0 /M="\r\n" /P=CalDataPath /O /G Header as NewFileName
5151 Save /A=1 /J /M="\r\n" /P=CalDataPath /G /B AuxWaves as NewFileName
SetDataFolder OldDF
For (i=0;i<ItemsInList(ExpList,";");i+=1)
    KillDataFolder $"root:NAC:"+StringFromList(i,ExpList,";")
EndFor
5156 KillDataFolder root:NAC:TempSet
End
//

```

C.1.7 Controls Handling

//

NAC_LaserPowerCorrectionPopUp

```

Function NAC_LaserPowerCorrectionPopUp(ctrlName, popNum, popStr) : ↵
    ↵ PopupMenuControl
5161 String ctrlName
    Variable popNum
    String popStr
    NVar LaserPowerCorrection=root:NAC:Machine:LaserPowerCorrection
    LaserPowerCorrection=Str2Num(popStr)
5166 End
//

```

NAC_ReflectivityCleanPopUp

```

Function NAC_ReflectivityCleanPopUp(ctrlName, popNum, popStr) : PopupMenuControl
    String ctrlName
    Variable popNum
5171 String popStr
    NVar ReflectivityClean=root:NAC:Machine:ReflectivityClean
    ReflectivityClean=Str2Num(popStr)
End
//

```

Function NAC_WinHookDeconvolution

```

5176 Function NAC_WinHookDeconvolution(Data)
STRUCT WMWinHookStruct &Data
String Name
Variable Type
    Switch (Data.EventCode)
5181 Case 7:
        Break
    Default:
        Return NoError
        Break
5186 EndSwitch
NVar ReEntry=root:NAC:GUI:ReEntryCursor
If (ReEntry)
    Error_Message(NAC_ReEntry, "InProc", "NAC_WinHookDeconvolution", "")
    Return NaN
5191 EndIf
ReEntry=1
DFRef OldDF=GetDataFolderDFR()
Name=Data.WinName
Name=Name[StrSearch(Name,"_",0,2)+1,StrSearch(Name,"_",Inf,3)-1]
5196 String WName="NAC_"+Name+"_BrowseDeconv"
StrSwitch (Name)
    Case "ZeroSticking":
    Case "Sticking":
        Error_Message(NAC_NotImplementedYet, "InProc", "NAC_WinHookDeconvolution", ↵
            ↵ Name)
5201 Break
    Case "Deconvolution":
    Case "RateCalorimetry":
    Case "RateCoating":
        Error_Message(NAC_NotApplicable, "InProc", "NAC_WinHookDeconvolution", Name ↵
            ↵ )

```

```

5206     Break
        Case "BeforeCoating":
        Case "AfterCoating":
        Case "LaserReference":
        Case "Transmission":
5211     Case "Radiation":
        Case "Heat":
            StrSwitch (Data.CursorName)
                Case "A":
                    DoWindow $WName
5216     NVar FrameIndex="$root:NAC:"+Name+":BrowseDeconvolutionIndex"
            Wave Deconvolution="$root:NAC:"+Name+":Deconvolution"
            If ((FrameIndex!=Data.yPointNumber) && (Data.yPointNumber<DimSize(↵
↵ Deconvolution,1)-1))
                If (!V_Flag)
                    Error_Message(DisplayDeconvolutedFrame(Name), "↵
↵ DisplayDeconvolutedFrame", "NAC_WinHookDeconvolution", Name)
5221     DoUpdate
            EndIf
            FrameIndex=Data.yPointNumber
            Wave BrowseOdd="$root:NAC:Deconvolution:"+Name+"BrowseOdd"
            Wave BrowseEven="$root:NAC:Deconvolution:"+Name+"BrowseEven"
5226     If (Mod(FrameIndex,2))
                BrowseOdd=Deconvolution[p][FrameIndex]
                BrowseEven=Deconvolution[p][FrameIndex+1]
            Else
                BrowseOdd=Deconvolution[p][FrameIndex+1]
5231     BrowseEven=Deconvolution[p][FrameIndex]
            EndIf
            Error_Message(DoDeconvolutionTextBox(Name), "DoDeconTextBox", "↵
↵ NAC_WinHookDeconvolution", Name)
            DoUpdate
            EndIf
5236     Break
        Default:
            Break
            EndSwitch
            Break
5241     Default:
            Error_Message(NAC_UnknownMeasurement, "InProc", "NAC_WinHookDeconvolution",↵
↵ Name)
            Break
            EndSwitch
            ReEntry=0
5246     Return NoError
End
//
Function NAC__WinHookRate
Function NAC_WinHookRate(Data)
STRUCT WMWinHookStruct &Data
5251 String Name
        Switch (Data.EventCode)
            Case 7:
                Break
            Default:
5256     Return NoError
                Break
        EndSwitch
        NVar ReEntry=root:NAC:GUI:ReEntryCursor
        If (ReEntry)
5261     Error_Message(NAC_ReEntry, "InProc", "NAC_WinHookRate", "")
            Return NaN
        EndIf
        ReEntry=1
        DFRef OldDF=GetDataFolderDFR()
5266     Name=Data.WinName
        Name=Name[StrSearch(Name, "_", 0, 2)+1,StrSearch(Name, "_", Inf, 3)-1]
        StrSwitch (Name)

```



```

Case "BeforeCoating":
Case "AfterCoating":
5271 Case "LaserReference":
Case "Transmission":
Case "Radiation":
Case "ZeroSticking":
Case "Heat":
5276 Case "Sticking":
Case "Deconvolution":
    Error_Message(NAC_NotApplicable, "InProc", "NAC_WinHookRate", Name)
    Break
Case "RateCalorimetry":
5281 Case "RateCoating":
    SetDataFolder $"root:NAC:"+Name
    NVar BaselineTo, BaselineFrom
    Wave Thickness
    StrSwitch (Data.CursorName)
5286     Case "A":
        If (Pnt2x(Thickness,Data.PointNumber)>BaselineFrom)
            BaselineTo=BaselineFrom
            BaselineFrom=Pnt2x(Thickness,Data.PointNumber)
        Else
5291         BaselineTo=Pnt2x(Thickness,Data.PointNumber)
        EndIf
        Break
        Case "B":
5296         If (Pnt2x(Thickness,Data.PointNumber)<BaselineTo)
            BaselineFrom=BaselineTo
            BaselineTo=Pnt2x(Thickness,Data.PointNumber)
        Else
            BaselineFrom=Pnt2x(Thickness,Data.PointNumber)
        EndIf
5301         Break
        Default:
            SetDataFolder OldDF
            Error_Message(NAC_WrongCursor, "InProc", "NAC_WinHookRate", Name)
            Return NaN
5306         Break
    EndSwitch
    Cursor /N=1 /W=$Data.WinName A Thickness BaselineTo
    Cursor /N=1 /W=$Data.WinName B Thickness BaselineFrom
    Error_Message(FitQCMRate(Name), "FitQCMRate", "NAC_WinHookRate", Name)
5311 Error_Message(DoRateTextBoxes(Name), "DoRateTextBoxes", "NAC_WinHookRate",
    ↵ Name)
    SetDataFolder OldDF
    Break
    Default:
5316     Error_Message(NAC_UnknownMeasurement, "InProc", "NAC_WinHookRate", Name)
    Break
EndSwitch
ReEntry=0
Return NoError
End
5321 //
Function NAC__WinHookFittedRate
Function NAC_WinHookFittedRate(Data)
STRUCT WMWinHookStruct &Data
String Name
    Switch (Data.EventCode)
5326     Case 7:
        Break
    Default:
        Return NoError
        Break
5331 EndSwitch
NVar ReEntry=root:NAC:GUI:ReEntryCursor
If (ReEntry)
    Error_Message(NAC_ReEntry, "InProc", "NAC_WinHookRate", "")

```

```

Return NaN
5336 EndIf
ReEntry=1
DFRef OldDF=GetDataFolderDFR()
Name=Data.WinName
Name=Name[StrSearch(Name, "_", 0, 2)+1,StrSearch(Name, "_", Inf, 3)-1]
5341 StrSwitch (Name)
Case "BeforeCoating":
Case "AfterCoating":
Case "LaserReference":
Case "Transmission":
5346 Case "Radiation":
Case "ZeroSticking":
Case "Heat":
Case "Sticking":
Case "Deconvolution":
5351 Error_Message(NAC_NotApplicable, "InProc", "NAC_WinHookRate", Name)
Break
Case "RateCalorimetry":
Case "RateCoating":
SetDataFolder $"root:NAC:"+Name
5356 NVar FittedFrom, FittedTo
Wave FittedRate
StrSwitch (Data.CursorName)
Case "A":
If (Pnt2x(FittedRate,Data.PointNumber)>FittedTo)
5361 FittedFrom=FittedTo
FittedTo=Pnt2x(FittedRate,Data.PointNumber)
Else
FittedFrom=Pnt2x(FittedRate,Data.PointNumber)
Endif
5366 Break
Case "B":
If (Pnt2x(FittedRate,Data.PointNumber)<FittedFrom)
FittedTo=FittedFrom
FittedFrom=Pnt2x(FittedRate,Data.PointNumber)
5371 Else
FittedTo=Pnt2x(FittedRate,Data.PointNumber)
EndIf
Break
Default:
5376 SetDataFolder OldDF
Error_Message(NAC_WrongCursor, "InProc", "NAC_WinHookRate", Name)
ReEntry=0
Return NaN
Break
5381 EndSwitch
Cursor /N=1 /W=$Data.WinName A FittedRate FittedFrom
Cursor /N=1 /W=$Data.WinName B FittedRate FittedTo
Error_Message(UpdateFittedRate(Name), "UpdateFittedRate", "NAC_WinHookRate",
↵ ", Name)
SetDataFolder OldDF
5386 Break
Default:
Error_Message(NAC_UnknownMeasurement, "InProc", "NAC_WinHookRate", Name)
Break
EndSwitch
5391 ReEntry=0
Return NoError
End
//

```

Function NAC__WinHookCal

```

Function NAC_WinHookCal(Data)
5396 STRUCT WMWinHookStruct &Data
String Name
Variable Type
Switch (Data.EventCode)
Case 7:

```

```

5401     Break
        Default:
            Return NoError
            Break
    EndSwitch
5406 NVar ReEntry=root:NAC:GUI:ReEntryCursor
    If (ReEntry)
        Error_Message(NAC_ReEntry, "InProc", "NAC_WinHookCal", "")
        Return NaN
    EndIf
5411 ReEntry=1
    DRef OldDF=GetDataFolderDFR()
    Name=Data.WinName
    Name=Name[StrSearch(Name, "_", 0, 2)+1,StrSearch(Name, "_", Inf, 3)-1]
    StrSwitch (Name)
5416     Case "RateCalorimetry":
        Case "RateCoating":
            Error_Message(NAC_NotApplicable, "InProc", "NAC_WinHookProc", Name)
            Break
5421     Case "BeforeCoating":
        Case "AfterCoating":
        Case "LaserReference":
        Case "Transmission":
        Case "Radiation":
5426     Case "ZeroSticking":
        Case "Heat":
        Case "Sticking":
        Case "Deconvolution":
            Break
        Default:
5431     Error_Message(NAC_UnknownMeasurement, "InProc", "NAC_WinHookCal", Data.↵
↵ WinName)
            Break
    EndSwitch
    If (StringMatch(Data.WinName,"*Full*"))
        Type=0
5436 ElseIf (StringMatch(Data.WinName,"*Frames*"))
        Type=1
    ElseIf (StringMatch(Data.WinName,"*Heat_VsCov*"))
        Type=2
    Else
5441     Error_Message(NAC_NoSuchWindow, "InProc", "NAC_WinHookCal", Data.WinName)
        ReEntry=0
        Return NaN
    EndIf
    Switch (Type)
5446     Case 0:
        StrSwitch (Data.CursorName)
            Case "A":
                If (StringMatch(Name,"Deconvolution"))
                    NVar ChopperPeriod=root:NAC:Deconvolution:ChopperPeriod
5451                Else
                    NVar ChopperPeriod=root:NAC:Experiment:ChopperPeriod
                EndIf
                NVar CurrentFrame="$root:NAC:"+Name+":CurrentFrame"
                sscanf Data.TraceName, "Frame%f", CurrentFrame
5456                Cursor /N=1 /W=$Data.WinName A $"Frame"+Num2Str(CurrentFrame) ↵
↵ ChopperPeriod/2
                Break
            Default:
                SetDataFolder OldDF
                Error_Message(NAC_WrongCursor, "InProc", "NAC_WinHookCal", Name)
5461                Return NaN
                Break
        EndSwitch
        Error_Message(UpdateFlagWin(Name), "UpdateFlagWin", "NAC_WinHookCal", Name)
        Break
5466     Case 1:
        NVar CurrentFrame="$root:NAC:"+Name+":CurrentFrame "

```

```

    sscanf Data.TraceName, "Frame%f", CurrentFrame
    Error_Message(UpdateFlagWin(Name), "UpdateFlagWin", "NAC_WinHookCal", Name)
    Break
5471 Case 2:
    NVar PosLow=root:NAC:Enthalpies:MultiLayerPosLow, PosHigh=root:NAC:
    ↘ Enthalpies:MultiLayerPosHigh
    Variable Tmp=0
    If (NumType(PosHigh)!=0)
        PosHigh=Ceil(NumPnts(root:NAC:Enthalpies:Coverage)*0.9)
5476     Tmp=1
    EndIf
    If (NumType(PosLow)!=0)
        PosLow=Floor(NumPnts(root:NAC:Enthalpies:Coverage)*2/3)
        Tmp=1
5481    EndIf
    If (!Tmp)
        StrSwitch (Data.CursorName)
            Case "A":
                If (Data.PointNumber <= PosHigh)
5486                 PosLow=Data.PointNumber
                Else
                    PosLow=PosHigh
                    PosHigh=Data.PointNumber
                EndIf
            Break
            Case "B":
                If (Data.PointNumber >= PosLow)
                    PosHigh=Data.PointNumber
                Else
5496                 PosHigh=PosLow
                    PosLow=Data.PointNumber
                EndIf
            Break
        Default:
            Break
5501    EndSwitch
    EndIf
    If (NumType(PosHigh)!=0)
        PosHigh=Ceil(NumPnts(root:NAC:Enthalpies:Coverage)*0.9)
5506    EndIf
    If (NumType(PosLow)!=0)
        PosLow=Floor(NumPnts(root:NAC:Enthalpies:Coverage)*3/4)
    EndIf
    If (PosLow==PosHigh)
5511        PosHigh=Ceil(NumPnts(root:NAC:Enthalpies:Coverage)*0.9)
    EndIf
    If (!(PosLow <= PosHigh))
        Tmp=PosLow
        PosLow=PosHigh
5516        PosHigh=Tmp
    EndIf
    Cursor /N=1 /W=$Data.WinName A Enthalpy PosLow
    Cursor /N=1 /W=$Data.WinName B Enthalpy PosHigh
    Error_Message(DoHeatTextBox(), "DoHeatTextBox", "NAC_WinHookCal", Name)
5521    Break
    Default:
        Break
    EndSwitch
    SetDataFolder OldDF
5526    ReEntry=0
    Return NoError
End
//
Function NAC_ToggleAutoFlagging
Function NAC_ToggleAutoFlagging()
5531    NVar AutoFlag=root:NAC:Experiment:AutoFlag
    AutoFlag=!AutoFlag
End

```

```

//
Function NAC__ToggleLoadSupport
Function NAC_ToggleLoadSupport ()
5536   NVar LoadSupport=root:NAC:GUI:LoadSupportFiles
      LoadSupport=!LoadSupport
End
//
Function NAC__ToggleStoreFiltered
Function NAC_ToggleStoreFiltered ()
5541   NVar StoreFiltered=root:NAC:GUI:StoreFilteredWaves
      StoreFiltered=!StoreFiltered
End
//
Function NAC__ToggleAutoUpdateAverages
Function NAC_ToggleAutoUpdateAverages ()
5546   NVar AutoRecalculate=root:NAC_Average:Settings:AutoRecalculate
      AutoRecalculate=!AutoRecalculate
End
//
Function NAC__ToggleShowBoxPlotData
Function NAC_ToggleShowBoxPlotData ()
5551   String ExpList="Deconvolution;BeforeCoating;AfterCoating;LaserReference;↵
      ↵ Transmission;Radiation;ZeroSticking;"
      String Name, NameList
      NVar ShowBoxPlotData=root:NAC:GUI:ShowBoxPlotData
      Variable i
      ShowBoxPlotData=!ShowBoxPlotData
5556   DoWindow NAC_Statistics
      If (V_Flag)
          DOWindow /F NAC_Statistics
      Else
          Return NaN
5561   EndIf
      NameList=" "+TraceNameList("NAC_Statistics", ";", 1)
      For (i=0; i<ItemsInList(ExpList, ";"); i+=1)
          Name=StringFromList(i, ExpList, ";")
          If (StringMatch(NameList, "*" + Name + "*"))
5566   ModifyGraph hideTrace($Name)=!ShowBoxPlotData
          EndIf
      EndFor
End
//
Function NAC__ResetFlagList
5571   Function NAC_ResetFlagList(ExpName)
      String ExpName
      String Name
      Variable i, j
      If (!DataFolderExists("root:NAC:"))
5576   Error_Message(NAC_NotInitialized, "InProc", "NAC_ResetFlagList", "")
          Return NaN
      EndIf
      If (StringMatch(ExpName, "All"))
          ExpName="Deconvolution;BeforeCoating;AfterCoating;LaserReference;Transmission↵
          ↵ ;Radiation;ZeroSticking;Heat;Sticking;"
5581   NVar AutoFlagged=root:NAC:Experiment:AutoFlagged
          AutoFlagged=0
      Else
          NVar Loaded=$"root:NAC:"+ExpName+":Loaded"
          If (!Loaded)
5586   Return NaN
          EndIf
          ExpName=ExpName+";"
      EndIf
      For (j=0; j<ItemsInList(ExpName, ";"); j+=1)

```

```

5591     Name=StringFromList(j, ExpName, ";")
        If (Exists("root:NAC:"+Name+":Auxiliaries:Motor_FB")==1)
            Wave FlagList="$root:NAC:"+Name+":FlagList"
            Wave /T MotorFB="$root:NAC:"+Name+":Auxiliaries:Motor_FB"
            FlagList=!StringMatch(MotorFB[Floor(p/2)],"Y")
5596     StrSwitch (Name)
            Case "Heat":
            Case "Sticking":
                For (i=NumPnts(FlagList)-1; (FlagList[i]==1) && (i>1); i--=1)
                    EndFor
5601     If (i>0)
            FlagList[i]=1
            FlagList[i-1]=1
            EndIf
            Break
5606     Default:
            NVar AutoFlagged="$root:NAC:"+Name+":Statistics:AutoFlagged"
            AutoFlagged=0
            For (i=0; (FlagList[i]==1) && (i<NumPnts(FlagList)-1); i+=1) //
            EndFor
5611     If (i<NumPnts(FlagList)-1)
            FlagList[i]=1
            FlagList[i+1]=1
            EndIf
            For (i=NumPnts(FlagList)-1; (FlagList[i]==1) && (i>1); i--=1)
5616     EndFor
            If (i>0)
                FlagList[i]=1
                FlagList[i-1]=1
            EndIf
            Break
5621     EndSwitch
            Error_Message(UpdateFlagWin(Name), "UpdateFlagWin", "NAC_ResetFlagList", ↵
            ↵ Name)
            DoWindow "$NAC_"+Name+"_Full"
            If (V_Flag)
5626     KillWindow "$NAC_"+Name+"_Full"
            Error_Message(DisplayMeasurement(Name), "DisplayMeasurement", "↵
            ↵ NAC_ResetFlagList", Name)
            EndIf
            EndIf
            EndFor
5631 End
        //
NAC_LoadLazyButton

Function NAC_LoadLazyButton(CtrlName):ButtonControl
String CtrlName
String AllExpFiles = "All Calorimetry Files (*.ref *.las *.win *.cln *.dcv *.usd ↵
    ↵ *.cot *.amp *.rad *.cal *.qms *.stk *.tck *.flx):.ref,.las,.win,.cln,.dcv,.↵
    ↵ usd,.cot,.cot,.amp,.rad,.cal,.qms,.stk,.tck,.flx;"
5636 String ListBeforeCoating="", ListRateCoating="", ListAfterCoating="", ↵
    ↵ ListLaserReference="", ListTransmission="", ListRadiation="", ↵
    ↵ ListRateCalorimetry="", ListZeroSticking="", ListHeat=""
String NameBeforeCoating="", NameRateCoating="", NameAfterCoating="", ↵
    ↵ NameLaserReference="", NameTransmission="", NameRadiation="", ↵
    ↵ NameRateCalorimetry="", NameZeroSticking="", NameHeat=""
String ListDeconvolution="", NameDeconvolution=""
String Name, DirList, Item
Variable i, j
5641 DFRef OldDF=GetDataFolderDFR()
        Error_Clear()
        Button $CtrlName disable=2, win=NAC_Control
        PathInfo CalDataPath
        If (!V_Flag)
5646     NewPath /O /Q /Z CalDataPath, NAC_DataPathStr
            If (!V_Flag)
                NewPath /O /Q CalDataPath
                If (V_Flag)

```

```

        Return UserCancel
5651     EndIf
        EndIf
    EndIf
    SetDataFolder root:NAC
    Open /R/D /P=CalDataPath /F=AllExpFiles j
5656     If (CmpStr(S_FileName, "")==0)
        Button $CtrlName disable=0, win=NAC_Control
        SetDataFolder OldDF
        Error_Message(UserAbort, "InProc", "NAC_LoadLazyButton", "Lazy")
        Return NaN
5661     EndIf
    NewPath /O /Q CalDataPath S_FileName[0,StrSearch(S_FileName, ":", Inf , 1)-1]
    DirList=IndexedFile(CalDataPath,-1,"????")
    For (i=0;i<ItemsInList(DirList);i+=1)
        Item=StringFromList(i,DirList,";")
5666     StrSwitch (LowerStr(Item[StrSearch(Item, ".", Inf , 1)+1,Inf]))
        Case "cIn":
        Case "usd":
            ListBeforeCoating+=Item+";"
            Break
5671     Case "tck":
            ListRateCoating+=Item+";"
            Break
        Case "cot":
            ListAfterCoating+=Item+";"
5676     Break
        Case "ref":
            ListLaserReference+=Item+";"
            Break
5681     Case "dcv":
            ListDeconvolution+=Item+";"
            Break
        Case "win":
            ListTransmission+=Item+";"
            Break
5686     Case "rad":
            ListRadiation+=Item+";"
            Break
        Case "flx":
            ListRateCalorimetry+=Item+";"
5691     Break
        Case "stk":
            ListZeroSticking+=Item+";"
            Break
5696     Case "cal":
            ListHeat+=Item+";"
            Break
        Default:
            Break
    EndSwitch
5701     EndFor
    ListBeforeCoating=SortList(ListBeforeCoating, ";", 4) + "Don't Load"
    ListRateCoating=SortList(ListRateCoating, ";", 4) + "Don't Load"
    ListAfterCoating=SortList(ListAfterCoating, ";", 4) + "Don't Load"
5706     ListLaserReference=SortList(ListLaserReference, ";", 4) + "Don't Load"
    ListDeconvolution=SortList(ListDeconvolution, ";", 4) + "Don't Load"
    ListTransmission=SortList(ListTransmission, ";", 4) + "Don't Load"
    ListRadiation=SortList(ListRadiation, ";", 4) + "Don't Load"
    ListRateCalorimetry=SortList(ListRateCalorimetry, ";", 4) + "Don't Load"
    ListZeroSticking=SortList(ListZeroSticking, ";", 4) + "Don't Load"
5711     ListHeat=SortList(ListHeat, ";", 4) + "Don't Load"
    Prompt NameDeconvolution, SelectString(ItemsInList(ListDeconvolution, ";")>2, ↵
    ↵ " ", ">>> ")+"Deconvolution Reference (" + Num2Str(ItemsInList(↵
    ↵ ListDeconvolution, ";")-1)+")"+SelectString(ItemsInList(ListDeconvolution ↵
    ↵ ", ";")>2, " ", " <<<"), popup, ListDeconvolution
    Prompt NameBeforeCoating, SelectString(ItemsInList(ListBeforeCoating, ";")>2, ↵
    ↵ " ", ">>> ")+"Reflectivity Clean (" + Num2Str(ItemsInList(ListBeforeCoating ↵
    ↵ ", ";")-1)+")"+SelectString(ItemsInList(ListBeforeCoating, ";")>2, " ", " ↵

```

```

    ↪ <<<"), popup, ListBeforeCoating
Prompt NameRateCoating, SelectString(ItemsInList(ListRateCoating, ";")>2, "", ↪
    ↪ ">>> ")+"Coating Thickness (" +Num2Str(ItemsInList(ListRateCoating, ";")-1) ↪
    ↪ +")"+SelectString(ItemsInList(ListRateCoating, ";")>2, "", " <<<"), popup, ↪
    ↪ ListRateCoating
Prompt NameAfterCoating, SelectString(ItemsInList(ListAfterCoating, ";")>2, "", ↪
    ↪ ">>> ")+"Reflectivity Coated (" +Num2Str(ItemsInList(ListAfterCoating, ";") ↪
    ↪ -1)+")"+SelectString(ItemsInList(ListAfterCoating, ";")>2, "", " <<<"), ↪
    ↪ popup, ListAfterCoating
5716 Prompt NameLaserReference, SelectString(ItemsInList(ListLaserReference, ";")>2, ↪
    ↪ "", ">>> ")+"Laser Reference (" +Num2Str(ItemsInList(ListLaserReference ↪
    ↪ , ";")-1)+")"+SelectString(ItemsInList(ListLaserReference, ";")>2, "", " ↪
    ↪ <<<"), popup, ListLaserReference
Prompt NameTransmission, SelectString(ItemsInList(ListTransmission, ";")>2, "", ↪
    ↪ ">>> ")+"Transmission Measurement (" +Num2Str(ItemsInList(ListTransmission ↪
    ↪ , ";")-1)+")"+SelectString(ItemsInList(ListTransmission, ";")>2, "", " <<<") ↪
    ↪ , popup, ListTransmission
Prompt NameRadiation, SelectString(ItemsInList(ListRadiation, ";")>2, "", ">>> ↪
    ↪ ")+"Radiation Measurement (" +Num2Str(ItemsInList(ListRadiation, ";")-1)+")"+ ↪
    ↪ SelectString(ItemsInList(ListRadiation, ";")>2, "", " <<<"), popup, ↪
    ↪ ListRadiation
Prompt NameRateCalorimetry, SelectString(ItemsInList(ListRateCalorimetry, ";") ↪
    ↪ >2, "", ">>> ")+"Deposition Rate Calorimetry (" +Num2Str(ItemsInList( ↪
    ↪ ListRateCalorimetry, ";")-1)+")"+SelectString(ItemsInList( ↪
    ↪ ListRateCalorimetry, ";")>2, "", " <<<"), popup, ListRateCalorimetry
Prompt NameZeroSticking, SelectString(ItemsInList(ListZeroSticking, ";")>2, "", ↪
    ↪ ">>> ")+"Zero Sticking Measurement (" +Num2Str(ItemsInList(ListZeroSticking ↪
    ↪ , ";")-1)+")"+SelectString(ItemsInList(ListZeroSticking, ";")>2, "", " <<<") ↪
    ↪ , popup, ListZeroSticking
5721 Prompt NameHeat, SelectString(ItemsInList(ListHeat, ";")>2, "", ">>> ")+" ↪
    ↪ Calorimetry Measurement (" +Num2Str(ItemsInList(ListHeat, ";")-1)+")"+ ↪
    ↪ SelectString(ItemsInList(ListHeat, ";")>2, "", " <<<"), popup, ListHeat
If ((ItemsInList(ListDeconvolution, ";")>2) || (ItemsInList(ListBeforeCoating ↪
    ↪ , ";")>2) || (ItemsInList(ListRateCoating, ";")>2) || (ItemsInList( ↪
    ↪ ListAfterCoating, ";")>2) || (ItemsInList(ListLaserReference, ";")>2) || ( ↪
    ↪ ItemsInList(ListTransmission, ";")>2) || (ItemsInList(ListRadiation, ";")>2) ↪
    ↪ || (ItemsInList(ListRateCalorimetry, ";")>2) || (ItemsInList( ↪
    ↪ ListZeroSticking, ";")>2) || (ItemsInList(ListHeat, ";")>2))
Button LoadLazy fcolor=(65280,0,0)
DoPrompt /HELP="" "Ambiguous Filenames", NameDeconvolution, NameBeforeCoating ↪
    ↪ , NameRateCoating, NameAfterCoating, NameLaserReference, NameTransmission, ↪
    ↪ NameRadiation, NameRateCalorimetry, NameZeroSticking, NameHeat
Button LoadLazy fcolor=(0,0,0)
5726 Else
DoPrompt /HELP="" "Load Options", NameDeconvolution, NameBeforeCoating, ↪
    ↪ NameRateCoating, NameAfterCoating, NameLaserReference, NameTransmission, ↪
    ↪ NameRadiation, NameRateCalorimetry, NameZeroSticking, NameHeat
EndIf
If (V_Flag)
SetDataFolder OldDF
5731 Button $CtrlName disable=0, win=NAC_Control
Return NaN
EndIf
If ((StrLen(NameDeconvolution)>0) && !StringMatch(NameDeconvolution, "_none_") ↪
    ↪ && !StringMatch(NameDeconvolution, "Don't Load"))
Error_Message(LoadCalFile("Deconvolution", NameDeconvolution), "LoadCalFile", ↪
    ↪ "NAC_LoadLazyButton", "Deconvolution")
5736 DoUpdate
EndIf
If ((StrLen(NameBeforeCoating)>0) && !StringMatch(NameBeforeCoating, "_none_") ↪
    ↪ && !StringMatch(NameBeforeCoating, "Don't Load"))
Error_Message(LoadCalFile("BeforeCoating", NameBeforeCoating), "LoadCalFile", ↪
    ↪ "NAC_LoadLazyButton", "BeforeCoating")
DoUpdate
5741 EndIf
If ((StrLen(NameRateCoating)>0) && !StringMatch(NameRateCoating, "_none_") && ! ↪
    ↪ StringMatch(NameRateCoating, "Don't Load"))
Error_Message(LoadRateFile("RateCoating", NameRateCoating), "LoadRateFile", " ↪
    ↪ NAC_LoadLazyButton", "RateCoating")

```



```

    DoUpdate
  EndIf
5746 If ((StrLen(NameAfterCoating)>0) && !StringMatch(NameAfterCoating,"_none_") && ↵
    ↵ !StringMatch(NameAfterCoating, "Don't Load"))
    Error_Message(LoadCalFile("AfterCoating", NameAfterCoating), "LoadCalFile", "↵
    ↵ NAC_LoadLazyButton", "AfterCoating")
    DoUpdate
  EndIf
5751 If ((StrLen(NameLaserReference)>0) && !StringMatch(NameLaserReference,"_none_")↵
    ↵ && !StringMatch(NameLaserReference, "Don't Load"))
    Error_Message(LoadCalFile("LaserReference", NameLaserReference), "LoadCalFile↵
    ↵ ", "NAC_LoadLazyButton", "LaserReference")
    DoUpdate
  EndIf
5756 If ((StrLen(NameTransmission)>0) && !StringMatch(NameTransmission,"_none_") && ↵
    ↵ !StringMatch(NameTransmission, "Don't Load"))
    Error_Message(LoadCalFile("Transmission", NameTransmission), "LoadCalFile", "↵
    ↵ NAC_LoadLazyButton", "Transmission")
    DoUpdate
  EndIf
5761 If ((StrLen(NameRadiation)>0) && !StringMatch(NameRadiation,"_none_") && !↵
    ↵ StringMatch(NameRadiation, "Don't Load"))
    Error_Message(LoadCalFile("Radiation", NameRadiation), "LoadCalFile", "↵
    ↵ NAC_LoadLazyButton", "Radiation")
    DoUpdate
  EndIf
5766 If ((StrLen(NameRateCalorimetry)>0) && !StringMatch(NameRateCalorimetry,"_none_↵
    ↵ ") && !StringMatch(NameRateCalorimetry, "Don't Load"))
    Error_Message(LoadRateFile("RateCalorimetry", NameRateCalorimetry), "↵
    ↵ LoadRateFile", "NAC_LoadLazyButton", "RateCalorimetry")
    DoUpdate
  EndIf
5771 If ((StrLen(NameZeroSticking)>0) && !StringMatch(NameZeroSticking, "_none_") &&↵
    ↵ !StringMatch(NameZeroSticking, "Don't Load"))
    Error_Message(LoadCalFile("ZeroSticking", NameZeroSticking), "LoadCalFile", "↵
    ↵ NAC_LoadLazyButton", "ZeroSticking")
    DoUpdate
  EndIf
5776 If ((StrLen(NameHeat)>0) && !StringMatch(NameHeat,"_none_") && !StringMatch(↵
    ↵ NameHeat, "Don't Load"))
    Error_Message(LoadCalFile("Heat",NameHeat), "LoadCalFile", "↵
    ↵ NAC_LoadLazyButton", "Heat")
    DoUpdate
  EndIf
5781 SetDataFolder OldDF
    PathInfo CalDataPath
    String Path=S_Path
    SVar ExpName=root:NAC:Experiment:ExperimentName
    If (StrLen(ExpName))
      ExpName=Path[StrSearch(Path, ":", StrLen(Path)-2,3)+1, StrLen(Path)-2]
    EndIf
    Button $CtrlName disable=0, win=NAC_Control
    Return NaN
End
//
NAC_StatisticsLazyButton
Function NAC_StatisticsLazyButton(CtrlName) : ButtonControl
5786 String CtrlName
    NAC_GetAllStatistics()
    NAC_DisplayStatistics("All")
End
//
NAC_ProcessLazyButton
5791 Function NAC_ProcessLazyButton(CtrlName) : ButtonControl
String CtrlName
NVar AutoFlag=root:NAC:Experiment:AutoFlag, AutoFlagged=root:NAC:Experiment:↵
    ↵ AutoFlagged

```

```

Error_Clear()
5796 Button $CtrlName disable=2, win=NAC_Control
DoUpdate
Error_Message(ProcessProc("Deconvolution", NoDecon=AutoFlag), "ProcessProc", "↵
↳ NAC_ProcessLazyButton", "Deconvolution")
Error_Message(ProcessProc("BeforeCoating", NoDecon=AutoFlag), "ProcessProc", "↵
↳ NAC_ProcessLazyButton", "BeforeCoating")
Error_Message(ProcessProc("RateCoating", NoDecon=AutoFlag), "ProcessProc", "↵
↳ NAC_ProcessLazyButton", "RateCoating")
Error_Message(ProcessProc("AfterCoating", NoDecon=AutoFlag), "ProcessProc", "↵
↳ NAC_ProcessLazyButton", "AfterCoating")
5801 Error_Message(ProcessProc("LaserReference", NoDecon=AutoFlag), "ProcessProc", "↵
↳ NAC_ProcessLazyButton", "LaserReference")
Error_Message(ProcessProc("Transmission", NoDecon=AutoFlag), "ProcessProc", "↵
↳ NAC_ProcessLazyButton", "Transmission")
Error_Message(ProcessProc("Radiation", NoDecon=AutoFlag), "ProcessProc", "↵
↳ NAC_ProcessLazyButton", "Radiation")
Error_Message(ProcessProc("RateCalorimetry", NoDecon=AutoFlag), "ProcessProc", ↵
↳ "NAC_ProcessLazyButton", "RateCalorimetry")
Error_Message(ProcessProc("ZeroSticking", NoDecon=AutoFlag), "ProcessProc", "↵
↳ NAC_ProcessLazyButton", "ZeroSticking")
5806 If (AutoFlag && !AutoFlagged)
NAC_GetAllStatistics()
NAC_AutoFlagAll()
Error_Message(ProcessProc("Deconvolution"), "ProcessProc", "↵
↳ NAC_ProcessLazyButton", "Deconvolution")
Error_Message(ProcessProc("BeforeCoating"), "ProcessProc", "↵
↳ NAC_ProcessLazyButton", "BeforeCoating")
5811 Error_Message(ProcessProc("AfterCoating"), "ProcessProc", "↵
↳ NAC_ProcessLazyButton", "AfterCoating")
Error_Message(ProcessProc("LaserReference"), "ProcessProc", "↵
↳ NAC_ProcessLazyButton", "LaserReference")
Error_Message(ProcessProc("Transmission"), "ProcessProc", "↵
↳ NAC_ProcessLazyButton", "Transmission")
Error_Message(ProcessProc("Radiation"), "ProcessProc", "NAC_ProcessLazyButton↵
↳ ", "Radiation")
Error_Message(ProcessProc("ZeroSticking"), "ProcessProc", "↵
↳ NAC_ProcessLazyButton", "ZeroSticking")
5816 EndIf
NAC_GetAllStatistics()
NAC_DisplayStatistics("All")
Error_Message(ProcessProc("Heat"), "ProcessProc", "NAC_ProcessLazyButton", "↵
↳ Heat")
Error_Message(ProcessProc("Sticking"), "ProcessProc", "NAC_ProcessLazyButton", ↵
↳ "Sticking")
5821 Button $CtrlName disable=0, win=NAC_Control
Return NaN
End
//

```

NAC_DeconvoluteFullButton

```

Function NAC_DeconvoluteFullButton(CtrlName):ButtonControl
5826 String CtrlName
Error_Clear()
Button $CtrlName disable=2, win=NAC_Control
DoUpdate
DoAlert /T="Deconvolution", 1, "This might take some time...\r\r\rContinue?"
5831 If (V_Flag!=1)
Error_Message(UserAbort, "InProc", "NAC_DeconvoluteFullButton", "")
Return NaN
EndIf
Error_Message(DeconvolutionProc("BeforeCoating"), "DeconvolutionProc", "↵
↳ NAC_DeconvoluteFullButton", "BeforeCoating")
5836 Error_Message(DisplayDeconvolution("BeforeCoating"), "DisplayDeconvolution", "↵
↳ NAC_DeconvoluteFullButton", "BeforeCoating")
Error_Message(DisplayDeconvolutedFrame("BeforeCoating"), "↵
↳ DisplayDeconvolutedFrame", "NAC_DeconvoluteFullButton", "BeforeCoating")
Error_Message(DeconvolutionProc("AfterCoating"), "DeconvolutionProc", "↵
↳ NAC_DeconvoluteFullButton", "AfterCoating")

```

```

Error_Message(DisplayDeconvolution("AfterCoating"), "DisplayDeconvolution", "↵
↳ NAC_DeconvoluteFullButton", "AfterCoating")
Error_Message(DisplayDeconvolutedFrame("AfterCoating"), "↵
↳ DisplayDeconvolutedFrame", "NAC_DeconvoluteFullButton", "AfterCoating")
5841 Error_Message(DeconvolutionProc("LaserReference"), "DeconvolutionProc", "↵
↳ NAC_DeconvoluteFullButton", "LaserReference")
Error_Message(DisplayDeconvolution("LaserReference"), "DisplayDeconvolution", "↵
↳ NAC_DeconvoluteFullButton", "LaserReference")
Error_Message(DisplayDeconvolutedFrame("LaserReference"), "↵
↳ DisplayDeconvolutedFrame", "NAC_DeconvoluteFullButton", "LaserReference")
Error_Message(DeconvolutionProc("Transmission"), "DeconvolutionProc", "↵
↳ NAC_DeconvoluteFullButton", "Transmission")
Error_Message(DisplayDeconvolution("Transmission"), "DisplayDeconvolution", "↵
↳ NAC_DeconvoluteFullButton", "Transmission")
5846 Error_Message(DisplayDeconvolutedFrame("Transmission"), "↵
↳ DisplayDeconvolutedFrame", "NAC_DeconvoluteFullButton", "Transmission")
Error_Message(DeconvolutionProc("Radiation"), "DeconvolutionProc", "↵
↳ NAC_DeconvoluteFullButton", "Radiation")
Error_Message(DisplayDeconvolution("Radiation"), "DisplayDeconvolution", "↵
↳ NAC_DeconvoluteFullButton", "Radiation")
Error_Message(DisplayDeconvolutedFrame("Radiation"), "DisplayDeconvolutedFrame↵
↳ ", "NAC_DeconvoluteFullButton", "Radiation")
Error_Message(DeconvolutionProc("Heat"), "DeconvolutionProc", "↵
↳ NAC_DeconvoluteFullButton", "Heat")
5851 Error_Message(DisplayDeconvolution("Heat"), "DisplayDeconvolution", "↵
↳ NAC_DeconvoluteFullButton", "Heat")
Error_Message(DisplayDeconvolutedFrame("Heat"), "DisplayDeconvolutedFrame", "↵
↳ NAC_DeconvoluteFullButton", "Heat")
Button $CtrlName disable=0, win=NAC_Control
Return NaN
End
5856 //
NAC_KillFrameProc

Function NAC_KillFrameProc(CtrlName):ButtonControl
String CtrlName
String Name=CtrlName[5,Inf]
String WName="NAC_"+Name+"_Flag"
5861 Error_Clear()
NVar CurrentFrame="$root:NAC:"+Name+":CurrentFrame"
Wave FlagList="$root:NAC:"+Name+":FlagList", Detector="$root:NAC:"+Name+":↵
↳ Detector"
FlagList[CurrentFrame]=1
Detector[][CurrentFrame]=0
5866 ModifyGraph /W="$NAC_"+Name+"_Frames" hideTrace($"Frame"+Num2Str(CurrentFrame))↵
↳ =FlagList[CurrentFrame]
Error_Message(UpdateFlagWin(Name), "UpdateFlagWin", "NAC_KillFrameProc", Name)
Error_Message(SetGraphRanges(Name), "SetGraphRanges", "NAC_KillFrameProc", Name↵
↳ )
Return NaN
End
5871 //
NAC_FlagProc

Function NAC_FlagProc(CtrlName):ButtonControl
String CtrlName
String Name=CtrlName[5,Inf]
String WName="NAC_"+Name+"_Flag"
5876 Error_Clear()
NVar CurrentFrame="$root:NAC:"+Name+":CurrentFrame"
Wave FlagList="$root:NAC:"+Name+":FlagList"
FlagList[CurrentFrame]=!FlagList[CurrentFrame]
Error_Message(DisplayMeasurement(Name), "DisplayMeasurement", "NAC_FlagProc", ↵
↳ Name)
5881 Error_Message(DisplayNonFlagged(Name), "DisplayNonFlagged", "NAC_FlagProc", ↵
↳ Name)
ModifyGraph /W="$NAC_"+Name+"_Frames" hideTrace($"Frame"+Num2Str(CurrentFrame))↵
↳ =FlagList[CurrentFrame]

```

```

ModifyGraph /W=$"NAC_"+Name+"_Full" rgb($"Frame"+Num2Str(CurrentFrame)) ↵
↵ =(65280*(FlagList[CurrentFrame]==0),0,0)
Error_Message(UpdateFlagWin(Name), "UpdateFlagWin", "NAC_FlagProc", Name)
Return NaN
5886 End
//
NAC_ClearProc

Function NAC_ClearProc(CtrlName):ButtonControl
String CtrlName
String Name=CtrlName[6,Inf]
5891 String WName="NAC_"+Name+"_Flag"
Wave FlagList=$"root:NAC:"+Name+":FlagList"
Variable i
NVar NoP=$"root:NAC:"+Name+":NumberOfFrames"
Error_Clear()
5896 StrSwitch (Name)
    Case "Desorption":
    Case "Sticking":
    Case "Heat":
        Break
5901 Default:
    NVar AutoFlagged=$"root:NAC:"+Name+":Statistics:AutoFlagged"
    AutoFlagged=0
    Break
EndSwitch
5906 FlagList=0
For (i=0;i<NoP;i+=1)
    ModifyGraph /W=$"NAC_"+Name+"_Frames" hideTrace($"Frame"+Num2Str(i))=0
    ModifyGraph /W=$"NAC_"+Name+"_Full" rgb($"Frame"+Num2Str(i))=(65280,0,0)
EndFor
5911 Error_Message(UpdateFlagWin(Name), "UpdateFlagWin", "NAC_ClearProc", Name)
Return NaN
End
//
NAC_RangeProc

Function NAC_RangeProc(CtrlName):ButtonControl  //// ERROR if full data is not ↵
↵ displayed yet
5916 String CtrlName
String Name=CtrlName[6,Inf]
String WName="NAC_"+Name+"_Flag"
Variable From, To, Flag, i, Pattern
Error_Clear()
5921 If (StringMatch(Name,"Deconvolution"))
    NVar DataPoints=root:NAC:Deconvolution:DataPointsPerFrame
Else
    NVar DataPoints=root:NAC:Experiment:DataPointsPerFrame
EndIf
5926 NVar NoP=$"root:NAC:"+Name+":NumberOfFrames"
Wave FlagList=$"root:NAC:"+Name+":FlagList"
Do
    From=(From<0) ? 0 : From
    From=(From>=NoP) ? NoP-1 : From
5931 To=(To<0) ? 0 : To
    To=(To>=NoP) ? NoP-1 : To
    Prompt Flag, "Flag / Unflag:", popup, "Flag;Unflag"
    Prompt Pattern, "Pattern:", popup, "All;Even;Odd"
    Prompt From, "From Frame: "
5936 Prompt To, "To Frame: "
    DoPrompt /HELP="" "Range Flagging", Flag, Pattern, From, To
    If (From > To)
        i=From
        From=To
5941 To=i
    EndIf
While (((From<0) || (From>=NoP) || (To<0) || (To>=NoP)) && !V_Flag)
If (V_Flag)
    Return UserAbort

```

```

5946 EndIf
Error_Message(DisplayMeasurement(Name), "DisplayMeasurement", "NAC_RangeProc", ↵
↳ Name)
Error_Message(DisplayNonFlagged(Name), "DisplayNonFlagged", "NAC_RangeProc", ↵
↳ Name)
For (i=From;i<=To;i+=1)
FlagList[i]=((Pattern==1) && Mod(Flag,2)) || ((Pattern==2) && (mod(i,2)==0) ↵
↳ && Mod(Flag,2)) || ((Pattern==3) && (mod(i,2)==1) && Mod(Flag,2))
5951 ModifyGraph /W="$NAC_"+Name+"_Frames" hideTrace($"Frame"+Num2Str(i))=FlagList ↵
↳ [i]
ModifyGraph /W="$NAC_"+Name+"_Full" rgb($"Frame"+Num2Str(i))=(65280*(FlagList ↵
↳ [i]==0),0,0)
EndFor
Error_Message(CheckButtons(Name, WName), "CheckButtons", "NAC_RangeProc", Name)
Error_Message(UpdateFlagWin(Name), "UpdateFlagWin", "NAC_RangeProc", Name)
5956 Return NaN
End
//
NAC_NavProc
Function NAC_NavProc(CtrlName):ButtonControl
String CtrlName
5961 String Name=CtrlName[4,StrLen(CtrlName)-4]
NVar CurrentFrame="$root:NAC:"+Name+":CurrentFrame"
NVar ReEntry=root:NAC:GUI:ReEntryPosProc
If (ReEntry)
Return NAC_ReEntry
5966 EndIf
ReEntry=1
Error_Clear()
StrSwitch (CtrlName[StrLen(CtrlName)-2,Inf])
Case "Fi":
5971 CurrentFrame=0
Break
Case "M2":
CurrentFrame-=2
Break
5976 Case "M1":
CurrentFrame-=1
Break
Case "P1":
CurrentFrame+=1
5981 Break
Case "P2":
CurrentFrame+=2
Break
Case "La":
5986 NVar NumberOfFrames="$root:NAC:"+Name+":NumberOfFrames"
CurrentFrame=NumberOfFrames-1
Break
Default:
Break
5991 EndSwitch
Error_Message(UpdateFlagWin(Name), "UpdateFlagWin", "NAC_NavProc", Name)
DoWindow /F "$NAC_"+Name+"_Frames"
ReEntry=0
Return NaN
5996 End
//
NAC_CurrentFrameProc
Function NAC_CurrentFrameProc(CtrlName,ValNum,ValStr,VarName):SetVariableControl
String CtrlName
Variable ValNum
6001 String ValStr, VarName
String Name=CtrlName[4,Inf]
NVar CurrentFrame="$root:NAC:"+Name+":CurrentFrame"
Error_Clear()
CurrentFrame=Floor(ValNum)

```

```

6006   Error_Message(UpdateFlagWin(Name), "UpdateFlagWin", "NAC_CurrentFrameProc", ↵
      ↵ Name)
      Return NaN
End
//
NAC_UseEmptyCrucibleProc
Function NAC_UseEmptyCrucibleProc(CtrlName,Checked):CheckBoxControl
6011 String CtrlName
      Variable Checked
      NVar RadHold=root:NAC:Heat:HoldRadiation
      NVar Radiation=root:NAC:Heat:InitRadiation
      Error_Clear()
6016   DoUpdate
      If (Checked)
          RadHold=1
          Radiation=GetRadiationContribution("Radiation")
      Else
6021   RadHold=0
      EndIf
      Return NaN
End
//
NAC_UseBaselineProc
6026 Function NAC_UseBaselineProc(CtrlName,Checked):CheckBoxControl
      String CtrlName
      Variable Checked
      String Name=CtrlName[5,Inf], Type
      Error_Clear()
6031   DoUpdate
      Error_Message(DoRateTextBoxes(Name), "DoRateTextBoxes", "NAC_UseBaselineProc", ↵
          ↵ Name)
      Return NaN
End
//
NAC_UseTotalRangeProc
6036 Function NAC_UseTotalRangeProc(CtrlName,Checked):CheckBoxControl
      String CtrlName
      Variable Checked
      String Name=CtrlName[8,Inf], Type
      Error_Clear()
6041   DoUpdate
      Error_Message(DoRateTextBoxes(Name), "DoRateTextBoxes", "NAC_UseTotalRangeProc ↵
          ↵ ", Name)
      If (Checked)
          CheckBox $"UseBL"+Name Disable=2, Win=NAC_Control
      Else
6046   CheckBox $"UseBL"+Name Disable=0, Win=NAC_Control
      EndIf
      Return NaN
End
//
NAC_DCRproc
6051 Function NAC_DCRproc(CtrlName,Checked):CheckBoxControl
      String CtrlName
      Variable Checked
      String Name=CtrlName[6,Inf]
      NVar RemFit=root:NAC:Deconvolution:RemoveFittedRadiation, RemFix=root:NAC:↵
          ↵ Deconvolution:RemoveFixedRadiation
6056   Error_Clear()
      DoUpdate
      StrSwitch (Name)
          Case "Fit":
              If (RemFix && Checked)
6061   RemFix=0
              EndIf

```

```

        Break
    Case "Fix":
        If (RemFit && Checked)
6066         RemFit=0
            EndIf
            Break
        Default:
            Break
6071 EndSwitch
    Return NaN
End
//
NAC_ReCalcHeat
Function NAC_ReCalcHeat(ctrlName,varNum,varStr,varName) : SetVariableControl
6076 String ctrlName
    Variable varNum // value of variable as number
    String varStr // value of variable as string
    String varName // name of variable
    Error_Clear()
6081 Error_Message(CalcHeat(), "NAC_ReCalcHeat", "CalcHeat", "")
    Return NaN
End
//
NAC_HeaderButton
Function NAC_HeaderButton(CtrlName):ButtonControl
6086 String CtrlName
    String Name=CtrlName[6,Inf], WName="NAC_"+Name+"_Header"
    NVar Loaded=$"root:NAC:"+Name+":Loaded"
    Error_Clear()
    DoWindow $WName
6091 If (!Loaded)
        Error_Message(NAC_NoDataLoaded, "InProc", "NAC_HeaderButton", Name)
        Return NaN
    EndIf
    If (V_Flag)
6096 DoWindow /F $WName
        Error_Message(NAC_WindowAlreadyExists, "InProc", "NAC_HeaderButton", Name)
        Return NaN
    EndIf
    Edit /N=$WName /W=(600,100,1000,700) /K=1 $"root:NAC:"+Name+":Header" As "File ↵
        ↵ Header: "+Name
6101 ModifyTable Alignment=0, Autosize={0,0,-1,0,0}
    Return NaN
End
//
NAC_LoadButton
Function NAC_LoadButton(CtrlName):ButtonControl
6106 String CtrlName
    String Name
    Variable Ret
    Error_Clear()
    Button $CtrlName disable=2, win=NAC_Control
6111 DoUpdate /W=NAC_Control
    Name=CtrlName[4,Inf]
    If (StringMatch(Name,"Rate*"))
        Error_Message(LoadRateFile(Name,""), "InProc", "NAC_LoadButton", Name)
    Else
6116 Error_Message(LoadCalFile(Name,""), "InProc", "NAC_LoadButton", Name)
    EndIf
    Button $CtrlName disable=0, win=NAC_Control
    Return NaN
End
6121 //
NAC_DisplayFullButton
Function NAC_DisplayFullButton(CtrlName):ButtonControl

```

```
String CtrlName
String Name
Error_Clear()
6126 Button $CtrlName disable=2, win=NAC_Control
DoUpdate /W=NAC_Control
Name=CtrlName[7,Inf]
If (StringMatch(Name,"Rate*"))
    Error_Message(DisplayRateFile(Name), "DisplayRateFile", "↵
    ↵ NAC_DisplayFullButton", Name)
6131 Else
    Error_Message(DisplayMeasurement(Name), "DisplayMeasurement", "↵
    ↵ NAC_DisplayFullButton", Name)
EndIf
Button $CtrlName Disable=0, Win=NAC_Control
Return NaN
6136 End
//
NAC_DisplayFlagButton
Function NAC_DisplayFlagButton(CtrlName):ButtonControl
String CtrlName
String Name=CtrlName[4,Inf]
6141 Variable Error
Error_Clear()
If (StringMatch(Name,"*Rate*"))
    Error_Message(NAC_NotApplicable, "InProc", "NAC_DisplayFlagButton", Name)
Return NaN
6146 Endif
Button $CtrlName disable=2, win=NAC_Control
DoUpdate /W=NAC_Control
Error_Message(DisplayMeasurement(Name), "DisplayMeasurement", "↵
    ↵ NAC_DisplayFlagButton", Name)
Error_Message(DisplayFlagWindow(Name), "DisplayFlagWindow", "↵
    ↵ NAC_DisplayFlagButton", Name)
6151 Error_Message(DisplayNonFlagged(Name), "DisplayNonFlagged", "↵
    ↵ NAC_DisplayFlagButton", Name)
If (!StringMatch(Name,"Deconvolution"))
    Error_Message(SetGraphRanges(Name), "SetGraphRanges", "NAC_DisplayFlagButton↵
    ↵ ", Name)
EndIf
Button $CtrlName disable=0, win=NAC_Control
6156 Return NaN
End
//
NAC_ProcessButton
Function NAC_ProcessButton(CtrlName) : ButtonControl
String CtrlName
6161 String Name=CtrlName[7,Inf]
Error_Clear()
Button $CtrlName disable=2, win=NAC_Control
DoUpdate
Error_Message(ProcessProc(Name, NoDecon=1), "ProcessProc", "NAC_ProcessButton",↵
    ↵ Name)
6166 Button $CtrlName disable=0, win=NAC_Control
End
//
NAC_StatisticsButton
Function NAC_StatisticsButton(CtrlName) : ButtonControl
String CtrlName
6171 String Name=CtrlName[10,Inf]
Error_Clear()
If (StringMatch(Name,"*Rate*"))
    Error_Message(NAC_NotApplicable, "InProc", "NAC_StatisticsButton", Name)
Return NaN
6176 Endif
Button $CtrlName disable=2, win=NAC_Control
DoUpdate
```



```

    NAC_GetStatistics(Name)
    NAC_DisplayStatistics(Name)
6181 Button $CtrlName disable=0, win=NAC_Control
End
//
NAC_DeconvoluteAverageButton
Function NAC_DeconvoluteAverageButton(CtrlName) : ButtonControl
String CtrlName
6186 String Name=CtrlName[9,Inf]
    Error_Clear()
    If (StringMatch(Name,"*Rate*"))
        Error_Message(NAC_NotApplicable, "InProc", "NAC_DeconvoluteAverageButton", ↵
            ↵ Name)
        Return NaN
6191 Endif
    Button $CtrlName disable=2, win=NAC_Control
    DoUpdate
    Error_Message(DeconvolutionProcAverage(Name), "DeconvolutionProcAverage", "↵
        ↵ NAC_DeconvoluteAverageButton", Name)
    Error_Message(DisplayDeconvolutedAverage(Name), "DisplayDeconvolutedAverage", "↵
        ↵ NAC_DeconvoluteAverageButton", Name)
6196 Button $CtrlName disable=0, win=NAC_Control
    Return NaN
End
//
NAC_DeconvoluteAllButton
Function NAC_DeconvoluteAllButton(CtrlName):ButtonControl
6201 String CtrlName
String Name=CtrlName[9,Inf]
    Error_Clear()
    If (StringMatch(Name,"*Rate*"))
        Error_Message(NAC_NotApplicable, "InProc", "NAC_DeconvoluteAverageButton", ↵
            ↵ Name)
6206 Return NaN
    Endif
    Button $CtrlName disable=2, win=NAC_Control
    DoUpdate
    Error_Message(DeconvolutionProc(Name), "DeconvolutionProc", "↵
        ↵ NAC_DeconvoluteAllButton", Name)
6211 Error_Message(DisplayDeconvolution(Name), "DisplayDeconvolution", "↵
        ↵ NAC_DeconvoluteAllButton", Name)
    Error_Message(DisplayDeconvolutedFrame(Name), "DisplayDeconvolutedFrame", "↵
        ↵ NAC_DeconvoluteAllButton", Name)
    Button $CtrlName disable=0, win=NAC_Control
    Return NaN
End
6216 //
NAC_ResultButton
Function NAC_ResultButton(CtrlName):ButtonControl
String CtrlName
String Name=CtrlName[6,inf]
NVar Loaded=$"root:NAC:"+Name+":Loaded"
6221 Error_Clear()
    If (!Loaded)
        Error_Message(NAC_NoDataLoaded, "InProc", "NAC_ResultButton", Name)
        Return NaN
    Endif
6226 Button $CtrlName disable=2, win=NAC_Control
    DoUpdate /W=NAC_Control
    StrSwitch (Name)
        Case "RateCalorimetry":
        Case "RateCoating":
6231 Error_Message(DisplayFittedRate(Name), "DisplayFittedRate", "↵
            ↵ NAC_ResultButton", Name)
            Break
        Case "Deconvolution":

```

```

        NVar NoP=$"root:NAC:"+Name+":NumberOfFrames"
        If (NoP>0)
6236     Error_Message(DisplayAverage(Name), "DisplayAverage", "NAC_ResultButton", ↵
        ↵ Name)
        EndIf
        Break
        Case "BeforeCoating":
        Case "AfterCoating":
6241     Case "LaserReference":
        Case "Transmission":
        Case "Radiation":
        Case "ZeroSticking":
6246     NVar NoP=$"root:NAC:"+Name+":NumberOfFrames"
        If (NoP>0)
        Error_Message(DisplayAverage(Name), "DisplayAverage", "NAC_ResultButton", ↵
        ↵ Name)
        Error_Message(DisplayDeconvolutedAverage(Name), " ↵
        ↵ DisplayDeconvolutedAverage", "NAC_ResultButton", Name)
        Error_Message(DisplayDeconvolution(Name), "DisplayDeconvolution", " ↵
        ↵ NAC_ResultButton", Name)
        Error_Message(DisplayDeconvolutedFrame(Name), "DisplayDeconvolutedFrame", ↵
        ↵ "NAC_ResultButton", Name)
6251     EndIf
        Break
        Case "Heat":
        Case "Sticking":
6256     NVar NoP=$"root:NAC:"+Name+":NumberOfFrames"
        If (NoP>0)
        Error_Message(DisplayAverage(Name), "DisplayAverage", "NAC_ResultButton", ↵
        ↵ Name)
        Error_Message(DisplayDeconvolutedAverage(Name), " ↵
        ↵ DisplayDeconvolutedAverage", "NAC_ResultButton", Name)
        Error_Message(DisplayDeconvolution(Name), "DisplayDeconvolution", " ↵
        ↵ NAC_ResultButton", Name)
        Error_Message(DisplayDeconvolutedFrame(Name), "DisplayDeconvolutedFrame", ↵
        ↵ "NAC_ResultButton", Name)
6261     Error_Message(DisplayVsPulse(Name), "DisplayVsPulse", "NAC_ResultButton", ↵
        ↵ Name)
        Error_Message(DisplayVsCoverage(Name), "DisplayVsCoverage", " ↵
        ↵ NAC_ResultButton", Name)
        Error_Message(DisplayTrend(Name,1), "DisplayVsCoverage", " ↵
        ↵ NAC_ResultButton", Name)
        EndIf
        Break
6266     Default:
        Error_Message(NAC_UnknownMeasurement, "InProc", "NAC_ResultButton", Name)
        Break
        EndSwitch
        Button $CtrlName disable=0, win=NAC_Control
6271     Return NaN
End
//

```

Function NAC_CopyFlagList

```

Function NAC_CopyFlagList(From, To)
String From, To
6276     If (!DataFolderExists("root:NAC:"))
        Error_Message(NAC_NotInitialized, "InProc", "NAC_DisplayStatistics", "")
        Return NaN
        EndIf
        If ((NumPnts($"root:NAC:"+From+":FlagList")==0) || (NumPnts($"root:NAC:"+To+": ↵
        ↵ FlagList")==0) )
6281     Error_Message(NAC_NothingToProcess, "InProc", "NAC_CopyFlagList", "")
        Return NaN
        EndIf
        Wave WFrom=$"root:NAC:"+From+":FlagList", WTo=$"root:NAC:"+To+":FlagList"
        WTo=WFrom
6286     Return NaN
End

```

//

C.1.8 Statistics Functions

//

Function NAC_GetAllStatistics

```

Function NAC_GetAllStatistics()
6291   If (!DataFolderExists("root:NAC:"))
       Error_Message(NAC_NotInitialized, "InProc", "NAC_GetAllStatistics", "")
       Return NaN
   EndIf
6296   NAC_GetStatistics("Deconvolution")
       NAC_GetStatistics("BeforeCoating")
       NAC_GetStatistics("AfterCoating")
       NAC_GetStatistics("LaserReference")
       NAC_GetStatistics("Transmission")
       NAC_GetStatistics("Radiation")
6301   NAC_GetStatistics("ZeroSticking")
End
//

```

Function NAC_GetStatistics

```

Function NAC_GetStatistics(Name)
String Name
6306   If (!DataFolderExists("root:NAC:"))
       Error_Message(NAC_NotInitialized, "InProc", "NAC_GetStatistics", "")
       Return NaN
   EndIf
DFRef OldDF=GetDataFolderDFR()
6311   StrSwitch (Name)
       Case "Deconvolution":
       Case "BeforeCoating":
       Case "AfterCoating":
       Case "LaserReference":
6316   Case "Transmission":
       Case "Radiation":
       Case "ZeroSticking":
           Break
       Case "RateCalorimetry":
6321   Case "RateCoating":
       Case "Heat":
       Case "Sticking":
           Error_Message(NAC_NotApplicable, "InProc", "NAC_AutoFlag", Name)
           Return NaN
6326   Break
       Default:
           Error_Message(NAC_UnknownMeasurement, "InProc", "NAC_AutoFlag", Name)
           Return NaN
           Break
6331   EndSwitch
NVar Loaded="$root:NAC:"+Name+":Loaded"
If (!Loaded)
   Error_Message(NAC_NoDataLoaded, "InProc", "NAC_GetStatistics", Name)
   Return NaN
6336   EndIf
If ((Exists("root:NAC:"+Name+":AverageOdd")!=1) || (Exists("root:NAC:"+Name+":↵
↵ AverageEven")!=1))
   If (!Error_Message(Averaging(Name), "Averaging", "NAC_GetStatistics", Name))
       Error_Message(NAC_AverageWavesMissing, "InProc", "NAC_GetStatistics", Name)
       Return NaN
6341   EndIf
   EndIf
NVar NumberOfFrames="$root:NAC:"+Name+":NumberOfFrames", StdDev="$root:NAC:"+↵
↵ Name+":Statistics:StdDev"
If (NumberOfFrames==0)
   Error_Message(NAC_NothingToProcess, "InProc", "NAC_GetStatistics", Name)
6346   SetDataFolder OldDF
       Return NaN
   EndIf

```

```

SetDataFolder $"root:NAC:"+Name
Wave Detector, FlagList
6351 Wave Amplitude=$"root:NAC:"+Name+":Statistics:Amplitude", ChiSq=$"root:NAC:"+Name+":Statistics:ChiSq", Outlier=$"root:NAC:"+Name+":Statistics:Outlier"
Variable InitOffs=0, InitAmp=1, InitShift=0
Variable V_FitError, V_fitOptions=4, V_FitQuitReason
Variable i
StrSwitch (Name)
6356 Case "Deconvolution":
NVar ChopperPeriod=root:NAC:Deconvolution:ChopperPeriod, DataPointsPerFrame=
↳ =root:NAC:Deconvolution:DataPointsPerFrame
Break
Default:
NVar ChopperPeriod=root:NAC:Experiment:ChopperPeriod, DataPointsPerFrame=
↳ root:NAC:Experiment:DataPointsPerFrame
6361 Break
EndSwitch
NVar ProgressValue=root:NAC:GUI:ProgressValue
Wave Medians=$"root:NAC:"+Name+":Statistics:Medians", Quartiles=$"root:NAC:"+Name+":Statistics:Quartiles", Whiskers=$"root:NAC:"+Name+":Statistics:WhiskerLimits"
↳ Whiskers", WhiskerLimits=$"root:NAC:"+Name+":Statistics:WhiskerLimits"
Make /D /FREE /N=2 FitCoef, InitCoef={InitOffs, InitAmp}
6366 Make /FREE /N=(DataPointsPerFrame) CurrentPeak
Redimension /N=(NumberOfFrames) Amplitude, ChiSq, Outlier
Setscale /P x, 0, DimDelta(Detector, 0), CurrentPeak
ProgressValue=0
ValDisplay Progress Disable=0, Limits={0,NumberOfFrames-1,1}, win=NAC_Control
6371 DoUpdate /W=NAC_Control
For (i=0;i<NumberOfFrames;i+=1)
If (!FlagList[i])
CurrentPeak=Detector[p][i]
FitCoef=InitCoef
6376 FuncFit /N=1 /W=2 /Q $("Stat"+Name>SelectString(Mod(i,2),"Even","Odd")),
↳ FitCoef, CurrentPeak
If (V_FitError)
Amplitude[i]=NaN
FlagList[i]=1
ChiSq[i]=-V_FitError
6381 Else
Amplitude[i]=FitCoef[1]
ChiSq[i]=V_ChiSq
EndIf
ChiSq[i]=V_ChiSq
6386 ProgressValue=i
DoUpdate /W=NAC_Control
Else
Amplitude[i]=NaN
ChiSq[i]=0
6391 EndIf
EndFor
ValDisplay Progress win=NAC_Control, Disable=1
ProgressValue=0
Medians=Quantile(Amplitude,0.5)
6396 StdDev=Sqrt(Variance(Amplitude))
Quartiles[0]=Quantile(Amplitude,0.25)
Quartiles[1]=Quantile(Amplitude,0.75)
WhiskerLimits[0]=Quartiles[0]-1.5*Abs(Quartiles[1]-Quartiles[0])
WhiskerLimits[1]=Quartiles[1]+1.5*Abs(Quartiles[1]-Quartiles[0])
6401 Whiskers[0]=GetWhisker(Amplitude, WhiskerLimits[0])
Whiskers[1]=GetWhisker(Amplitude, WhiskerLimits[1])
Outlier=(Amplitude > WhiskerLimits[1]) || (Amplitude < WhiskerLimits[0])?
↳ Amplitude : NaN
SetDataFolder OldDF
Return NoError
6406 End
//

```

Function NAC_DisplayStatistics

```
Function NAC_DisplayStatistics(ExpNames)
```

```

String ExpNames
String ExpList="Deconvolution;BeforeCoating;AfterCoating;LaserReference;↵
    ↵ Transmission;Radiation;ZeroSticking;"
6411 String LabelsList="Deconvolution;Before\rCoating;After\rCoating;Detector\↵
    ↵ rCalibration;Transmission;Radiation;ZeroSticking;"
String DisplayList="", DisplayLabels="", Name, WName
Variable NumExp=0
Variable i, RMax=-Inf, RMin=Inf
    If (!DataFolderExists("root:NAC:"))
6416     Error_Message(NAC_NotInitialized, "InProc", "NAC_DisplayStatistics", "")
        Return NaN
    EndIf
NVar WWidth=root:NAC:GUI:WWidth, WHeight=root:NAC:GUI:WHeight
    If (StringMatch(ExpNames, "All"))
6421     ExpNames=ExpList
    EndIf
    For (i=0; i<ItemsInList(ExpList, ";"); i+=1)
        If (StringMatch(ExpNames, "*" + StringFromList(i, ExpList, ";") + "*"))
            If (NumPnts("$root:NAC:" + StringFromList(i, ExpList, ";") + ":Statistics:↵
                ↵ Amplitude") > 0)
6426                 NumExp+=1
                    DisplayList += StringFromList(i, ExpList, ";") + ";"
                    DisplayLabels += StringFromList(i, LabelsList, ";") + ";"
                EndIf
            EndIf
6431        EndFor
        If (NumExp == 0)
            Error_Message(NAC_NothingToProcess, "InProc", "NAC_DisplayStatistics", "")
            Return NaN
        EndIf
6436        DoWindow NAC_Statistics
        If (V_Flag)
            KillWindow NAC_Statistics
        EndIf
        If (NumExp > 4)
6441            Display /N=NAC_Statistics /K=1 /W=(50,50,180+ItemsInList(DisplayList, ";") * 80, ↵
                ↵ 100+WHeight) as "NAC Statistics"
        Else
            Display /N=NAC_Statistics /K=1 /W=(50,50,280+ItemsInList(DisplayList, ";") * 80, ↵
                ↵ 50+WHeight) as "NAC Statistics"
        EndIf
        Wave LabelsPos=root:NAC:GUI:StatsLabelPos
6446        Wave /T Labels=root:NAC:GUI:StatsLabels
        Redimension /N=(NumExp) LabelsPos, Labels
        For (i=0; i<ItemsInList(DisplayList, ";"); i+=1)
            Name=StringFromList(i, DisplayList, ";")
            SVar FileName="$root:NAC:" + Name + ":FileName"
6451            Wave Amplitude="$root:NAC:" + Name + ":Statistics:Amplitude"
            NVar ShowBoxPlotData=root:NAC:GUI:ShowBoxPlotData
            Duplicate /O Amplitude "$root:NAC:" + Name + ":Statistics:Position"
            Wave Position="$root:NAC:" + Name + ":Statistics:Position"
            Wave Medians="$root:NAC:" + Name + ":Statistics:Medians"
6456            Wave Quartiles="$root:NAC:" + Name + ":Statistics:Quartiles"
            Wave Whiskers="$root:NAC:" + Name + ":Statistics:Whiskers"
            Wave WhiskerLimits="$root:NAC:" + Name + ":Statistics:WhiskerLimits"
            Wave Outlier="$root:NAC:" + Name + ":Statistics:Outlier"
            Position=i
6461            LabelsPos[i]=i
            Labels[i]=StringFromList(i, DisplayLabels, ";")
            If (NumType(WaveMin(Amplitude)) == 0)
                RMin=Min(RMin, WaveMin(Amplitude))
            EndIf
6466            If (NumType(WaveMax(Amplitude)) == 0)
                RMax=Max(RMax, WaveMax(Amplitude))
            EndIf
            AppendToGraph /W=NAC_Statistics Amplitude /TN=$Name vs Position
            AppendToGraph /W=NAC_Statistics Medians /TN="$Median"+Name vs Position
6471            AppendToGraph /W=NAC_Statistics Quartiles /TN="$Quartiles"+Name vs Position
            AppendToGraph /W=NAC_Statistics Whiskers /TN="$Whiskers"+Name vs Position

```

```

AppendToGraph /W=NAC_Statistics WhiskerLimits /TN="$WhiskerLimits"+Name vs ↵
↵ Position
AppendToGraph /W=NAC_Statistics Outlier /TN="$Outlier"+Name vs Position
ModifyGraph /W=NAC_Statistics Mode($Name)=3, Mode($"Median"+Name)=3, Mode($"↵
↵ Quartiles"+Name)=3, Mode($"Whiskers"+Name)=3, Mode($"WhiskerLimits"+Name)↵
↵ =3, Mode($"Outlier"+Name)=3
6476 ModifyGraph /W=NAC_Statistics Marker($Name)=8, Marker($"Median"+Name)=9, ↵
↵ Marker($"Quartiles"+Name)=9, Marker($"Whiskers"+Name)=9, Marker($"↵
↵ WhiskerLimits"+Name)=9, Marker($"Outlier"+Name)=19
ModifyGraph /W=NAC_Statistics MSize($Name)=2, MSize($"Median"+Name)=20, MSize↵
↵ ($"Quartiles"+Name)=20, MSize($"Whiskers"+Name)=20, MSize($"WhiskerLimits"+↵
↵ Name)=10, MSize($"Outlier"+Name)=3
ModifyGraph /W=NAC_Statistics MrkThick($"Median"+Name)=3, MrkThick($"↵
↵ Quartiles"+Name)=2, MrkThick($"Whiskers"+Name)=2, MrkThick($"WhiskerLimits↵
↵ "+Name)=0.5
ModifyGraph /W=NAC_Statistics RGB($Name)=(0,0,0), RGB($"Median"+Name)↵
↵ =(0,52224,0), RGB($"Quartiles"+Name)=(0,0,65280), RGB($"Whiskers"+Name)↵
↵ =(52224,52224,52224), RGB($"WhiskerLimits"+Name)=(0,0,0), RGB($"Outlier"+↵
↵ Name)=(65280,0,0)
6481 ModifyGraph /W=NAC_Statistics hideTrace($Name)=!ShowBoxPlotData
WName="NAC_"+Name+"_Statistics"
DoWindow $WName
If (V_Flag!=0)
DoWindow /F $WName
Else
6486 Display /N=$WName /K=1 /W=(800,50+i*20,800+WWidth, 50+WHeight+i*20) as "↵
↵ Statistics for "+ReplaceString("\r", StringFromList(i, DisplayLabels, ";"),↵
↵ " ")
AppendtoGraph /W=$WName Amplitude[0,*,2]/TN=$Name+"Even", Amplitude[1,*,2]/↵
↵ TN=$Name+"Odd", Outlier/TN=$Name+"Outlier"
ModifyGraph /W=$WName Mode=3, Marker=19, MSize=3
ModifyGraph RGB($Name+"Even")=(0,0,65280), RGB($Name+"Odd")=(0,52224,0), ↵
↵ RGB($Name+"Outlier")=(65280,0,0)
ModifyGraph /W=$WName Grid(Left)=1, GridStyle(left)=0, GridRGB(Left)↵
↵ =(0,0,0)
6491 EndIf
NVar StdDev="$root:NAC:"+Name+":Statistics:StdDev"
TextBox /W=$WName /C /N=Title /A=MT /E /F=0 /X=0 /Y=5 /J /B=1 "\JCAmplitudes↵
↵ for "+Name+" Measurement\r\JC"+FileName+": \K(0,0,65280)Even \K(0,0,0) \↵
↵ K(0,52224,0)Odd \K(0,0,0) \K(65280,0,0)Outlier\K(0,0,0) Frames Standard ↵
↵ Deviation: "+Num2Str(StdDev)
EndFor
For (i=0;i<ItemsInList(DisplayList,"");i+=1)
6496 Name=StringFromList(i, DisplayList, ";")
WName="NAC_"+Name+"_Statistics"
SetAxis /W=$WName Left, Floor(RMin*20)/20, Ceil(RMax*20)/20
EndFor
Name=StringFromList(0, DisplayList, ";")
6501 If (NumExp>4)
TextBox /W=NAC_Statistics /C /N=Legend /A=MB /E /F=0 /X=0 /Y=5 /J /B=1 "\s↵
↵ ("+Name+") Data \s(Outlier"+Name+") Outlier \s(Median"+Name)↵
↵ +" Median \s(Quartiles"+Name+") Quartiles \s(Whiskers"+Name)↵
↵ +" Whiskers \s(WhiskerLimits"+Name+") Outlier Limit"
Else
TextBox /W=NAC_Statistics /C /N=Legend /A=RC /E /F=0 /X=5 /Y=0 /J /B=1 "\s↵
↵ ("+Name+") Data\r\s(Outlier"+Name+") Outlier\r\s(Median"+Name) Median\r↵
↵ \s(Quartiles"+Name+) Quartiles\r\s(Whiskers"+Name+) Whiskers\r\s(↵
↵ WhiskerLimits"+Name+) Outlier Limit"
EndIf
6506 TextBox /W=NAC_Statistics /C /N=text0/F=0/A=MT/X=0/Y=5/E /B=1 "Statistics: Box↵
↵ Plots"
SetAxis /W=NAC_Statistics Bottom -0.5, ItemsInList(DisplayList,"") - 0.25
Label /W=NAC_Statistics bottom " "
ModifyGraph /W=NAC_Statistics Grid(Left)=1, GridStyle(left)=0, GridRGB(Left)↵
↵ =(0,0,0)
ModifyGraph /W=NAC_Statistics UserTicks(Bottom)={LabelsPos, Labels}
6511 Return NaN
End

```

```

//
Function NAC_AutoFlag
Function NAC_AutoFlag(Name)
String Name
6516 Variable i
      If (!DataFolderExists("root:NAC:"))
          Error_Message(NAC_NotInitialized, "InProc", "NAC_DisplayStatistics", "")
          Return NaN
      EndIf
6521 StrSwitch (Name)
          Case "Deconvolution":
          Case "BeforeCoating":
          Case "AfterCoating":
          Case "LaserReference":
6526 Case "Transmission":
          Case "Radiation":
          Case "ZeroSticking":
              Break
          Case "RateCalorimetry":
          Case "RateCoating":
6531 Case "Heat":
          Case "Sticking":
              Error_Message(NAC_NotApplicable, "InProc", "NAC_AutoFlag", Name)
              Return NaN
              Break
6536 Default:
          Error_Message(NAC_UnknownMeasurement, "InProc", "NAC_AutoFlag", Name)
          Return NaN
          Break
6541 EndSwitch
NVar DataPoints="$root:NAC:"+Name+":EffectiveFrames", AutoFlagged="$root:NAC:"+
  ↳ Name+":Statistics:AutoFlagged"
If ((DataPoints==0) || AutoFlagged)
    Error_Message(NAC_NothingToProcess, "InProc", "NAC_AutoFlag", Name)
    Return NaN
6546 EndIf
Wave Amplitude="$root:NAC:"+Name+":Statistics:Amplitude", Whiskers="$root:NAC"+
  ↳ :"+Name+":Statistics:Whiskers"
Wave FlagList="$root:NAC:"+Name+":FlagList"
For (i=0;i<NumPnts(Amplitude);i+=1)
    If ((Amplitude[i]>Whiskers[1]) || (Amplitude[i]<Whiskers[0]))
6551     FlagList[i]=1
    EndIf
EndFor
DoWindow $"NAC_"+Name+"_Full"
If (V_Flag!=0)
6556 KillWindow $"NAC_"+Name+"_Full"
    Error_Message(DisplayMeasurement(Name), "DisplayMeasurement", "NAC_AutoFlag",
  ↳ Name)
EndIf
DoWindow $"NAC_"+Name+"_Flag"
If (V_Flag!=0)
6561 KillWindow $"NAC_"+Name+"_Flag"
    Error_Message(DisplayFlagWindow(Name), "DisplayFlagWindow", "NAC_AutoFlag",
  ↳ Name)
EndIf
DoWindow $"NAC_"+Name+"_Frames"
If (V_Flag!=0)
6566 KillWindow $"NAC_"+Name+"_Frames"
    Error_Message(DisplayNonFlagged(Name), "DisplayNonFlagged", "NAC_AutoFlag",
  ↳ Name)
EndIf
AutoFlagged=1
Return NaN
6571 End

```

//

Quantile

```
Function Quantile(Input, Level)
Wave Input
Variable Level
6576 Variable i
      Duplicate /FREE Input Sorted
      For (i=NumPnts(Sorted)-1;i>=0;i--1)
        If (NumType(Sorted[i])!=0)
          DeletePoints i, 1, Sorted
6581      EndIf
      EndFor
      If (NumPnts(Sorted)<=0)
        Return NaN
      EndIf
6586      If (Level<=0)
        Return WaveMin(Sorted)
      ElseIf (Level>=1)
        Return WaveMax(Sorted)
      Else
6591      Sort Sorted, Sorted
        Return (Sorted[Floor((NumPnts(Sorted)-1)*Level)]+Sorted[Ceil((NumPnts(Sorted)-
        ↵ -1)*Level)))/2
      EndIf
End
//
```

GetWhisker

```
6596 Function GetWhisker(Input, Threshold)
Wave Input
Variable Threshold
Variable i
      Duplicate /FREE Input Sorted
6601      Sort Sorted, Sorted
      For (i=NumPnts(Sorted)-1;i>=0;i--1)
        If (NumType(Sorted[i])!=0)
          DeletePoints i, 1, Sorted
        EndIf
6606      EndFor
      If (NumPnts(Sorted)==0)
        Return NaN
      EndIf
      If (Threshold>=Quantile(Sorted, 0.5))
6611      If (Sorted[NumPnts(Sorted)-1]<Threshold)
        Return Sorted[NumPnts(Sorted)-1]
      EndIf
      For (i=NumPnts(Sorted)-1;i>0;i--1)
        If ((Sorted[i]>=Threshold) && (Sorted[i-1]<Threshold))
6616      Return Sorted[i-1]
        EndIf
      EndFor
      Else
        If (Sorted[0]>Threshold)
6621      Return Sorted[0]
        EndIf
        For (i=0;i<NumPnts(Sorted);i+=1)
          If ((Sorted[i]<Threshold) && (Sorted[i+1]>=Threshold))
            Return Sorted[i+1]
6626      EndIf
        EndFor
      EndIf
      KillWaves Sorted
      Return NaN
6631 End
```


//

C.1.9 Experiment Averaging Functions

//

Function Results_Initialize

```

Function Results_Initialize()
  If (DataFolderExists("root:NAC_Average"))
6636     Return NAC_AvgAlreadyInitialized
  EndIf
  DFRef OldDF=GetDataFolderDFR()
  NewPath /O /Q CalDataPath NAC_DataPathStr
  NewDataFolder /S root:NAC_Average
6641  NewDataFolder root:NAC_Average:Experiments
  Make /N=0 AveragedEnthalpy, AveragedSticking, AveragedRadiation, ↵
    ↵ DepositionRates, Thicknesses, MultiLayerEnthalpies, ↵
    ↵ MultiLayerEnthalpyErrors
  Make /N=0 /T Experiments
  Make /O /N=2 StickingLimit=1, EnthalpyLimit
  SetScale d, 0, 0, "J/mol", AveragedEnthalpy, EnthalpyLimit
6646  SetScale d, 0, 0, "m/s", DepositionRates
  SetScale d, 0, 0, "m", Thicknesses
  Variable /G ReferenceEnthalpy=NaN
  SetFormula EnthalpyLimit, "root:NAC_Average:ReferenceEnthalpy"
  String /G System=""
6651  NewDataFolder /S root:NAC_Average:Settings
  Variable /G BinSize=0.05 // ML
  Variable /G WWidth=400, WHeight=300, MarginTop=45
  Variable /G Processed=0, AutoRecalculate=1, AutoDisplay=1
  Variable /G LegendLines=8
6656  String /G ProjectVersion=NAC_Version
  String Temp=""
  SetDataFolder OldDF
  Prompt Temp, "System Descriptor: "
  DoPrompt /HELP="" "NAC Average", Temp
6661  System=Temp
  If (V_Flag)
    Return UserAbort
  EndIf
  Return NoError
6666 End
//

```

Function NAC_Results_Load

```

Function NAC_Results_Load()
  Variable RefNum, i
  String ExpName, Corrupt="", FileName
6671  If (!DataFolderExists("root:NAC_Average"))
    If (Error_Message(Results_Initialize(), "NAC_Results_Load", "ResultsInitialize↵
      ↵ ", ""))
      ExperimentModified 0
      Return ErrorHandled
    EndIf
6676  EndIf
  Open /D /R /MULT=1 /F="Igor Experiment Files (*.pxp):.pxp;" RefNum
  If (!StrLen(S_FileName))
    Error_Message(UserAbort, "InProc", "NAC_Results_Load", "")
    Return NaN
6681  EndIf
  DFRef OldDF=GetDataFolderDFR
  SetDataFolder root:
  For (i=0;i<ItemsInList(S_FileName, "\r");i+=1)
    FileName=StringFromList(i, S_FileName, "\r")
6686  LoadData /L=4 /O /Q /S="NAC:Experiment:" /J="ProjectVersion" /T=NAC_Import ↵
    ↵ FileName
    If (GetRTError(1))
      Error_Message(NAC_IncompatibleExperiment, "InProc", "NAC_Results_Load", ↵
        ↵ FileName[StrSearch(FileName, ":", Inf, 3)+1, Inf])
      Continue
    EndIf
  EndFor

```

```

EndIf
6691 SVar Version=root:NAC_Import:ProjectVersion
StrSwitch (Version)
  Case "3.6 beta":
  Case "3.7 beta":
  Case "3.8 alpha":
6696   Case "3.8 beta":
  Case "3.9 alpha":
  Case "3.9 beta":
  Case "3.10 alpha":
  Case "3.10 beta":
6701   Case "3.10 gamma":
  Case "3.10 delta":
  Case "3.10 epsilon":
  Case "3.11":
    LoadData /L=2 /O /Q /S="NAC:FluxCalorimetry:" /J="DosePerPulse;Flux" /T=↵
  ↵ NAC_Import FileName
6706   LoadData /L=2 /O /Q /S="NAC:FluxCoating:" /J="TotalThickness" /T=↵
  ↵ NAC_Import FileName
    ReName root:NAC_Import:Flux DepositionRate
    Break
  Case "3.12":
  Case "3.13":
6711   Case "3.14":
    LoadData /L=2 /O /Q /S="NAC:RateCalorimetry:" /J="DosePerPulse;↵
  ↵ DepositionRate" /T=NAC_Import FileName
    LoadData /L=2 /O /Q /S="NAC:RateCoating:" /J="TotalThickness" /T=↵
  ↵ NAC_Import FileName
    Break
  Default:
6716   Error_Message(NAC_UnknownVersion, "InProc", "NAC_Results_Load", Version)
    KillDataFolder NAC_Import
    Continue
EndSwitch
LoadData /L=1 /O /Q /S="NAC:Enthalpies:" /J="Enthalpy;Coverage;↵
  ↵ MultiLayerReference" /T=NAC_Import FileName
6721 LoadData /L=1 /O /Q /S="NAC:Heat:" /J="orig_Radiation" /T=NAC_Import FileName
LoadData /L=1 /O /Q /S="NAC:Sticking:" /J="orig_Desorption" /T=NAC_Import ↵
  ↵ FileName
LoadData /L=2 /O /Q /S="NAC:Enthalpies:" /J="MultiLayerEnthalpy;↵
  ↵ MultiLayerEnthalpyError" /T=NAC_Import FileName
ExpName=PossiblyQuoteName(FileName[StrSearch(FileName, ":", Inf ,3)+1,↵
  ↵ StrSearch(FileName, ".", Inf ,3)-1])
If (Exists("root:NAC_Import:DosePerPulse")!=2)
6726   Corrupt+="DosePerPulse(V), "
EndIf
If (Exists("root:NAC_Import:TotalThickness")!=2)
   Corrupt+="TotalThicknes(V), "
EndIf
6731 If (Exists("root:NAC_Import:DepositionRate")!=2)
   Corrupt+="DepositionRate(V), "
EndIf
If (Exists("root:NAC_Import:MultiLayerEnthalpy")!=2)
   Corrupt+="MultiLayerEnthalpy(V), "
6736 EndIf
If (Exists("root:NAC_Import:MultiLayerEnthalpyError")!=2)
   Corrupt+="MultiLayerEnthalpyError(V), "
EndIf
If (Exists("root:NAC_Import:Enthalpy")!=1)
6741   Corrupt+="Enthalpy(W), "
EndIf
If (Exists("root:NAC_Import:orig_Desorption")!=1)
   Corrupt+="orig_Desorption(W), "
EndIf
6746 If (Exists("root:NAC_Import:orig_Radiation")!=1)
   Corrupt+="orig_Radiation(W), "
EndIf
If (Exists("root:NAC_Import:Coverage")!=1)
   Corrupt+="Coverage(W), "

```

```

6751 EndIf
    If (Exists("root:NAC_Import:MultiLayerReference")!=1)
        Corrupt+="MultiLayerReference(W), "
    EndIf
    If (Exists("root:NAC_Import:Enthalpy")==1 && Exists("root:NAC_Import:Sticking"
6756 ↵ ")==1)
    If (NumPnts(root:NAC_Import:Enthalpy) != NumPnts(root:NAC_Import:Sticking) ↵
        ↵ )
            Corrupt+="Data Mismatch (E/S), "
            EndIf
            If (NumPnts(root:NAC_Import:Enthalpy) == 0)
                Corrupt+="No Data (E), "
6761 Endif
            If (NumPnts(root:NAC_Import:Sticking)==0)
                Corrupt+="No Data (S), "
            Endif
        EndIf
6766 If (StrLen(Corrupt))
            Corrupt=RemoveEnding(Corrupt, ", ")
            Error_Message(NAC_CorruptExperiment, "InProc", "NAC_Results_Load", ExpName ↵
        ↵ "+": "+Corrupt)
            KillDataFolder NAC_Import
            SetDataFolder OldDF
6771 Return NaN
        EndIf
        If (!DataFolderExists("root:NAC_Average:Experiments:"+ExpName))
            NewDataFolder $"root:NAC_Average:Experiments:"+Expname
            Variable /G $"root:NAC_Average:Experiments:"+ExpName+":DosePerPulse"
6776 Variable /G $"root:NAC_Average:Experiments:"+ExpName+":SubstrateThickness"
            Variable /G $"root:NAC_Average:Experiments:"+ExpName+":DepositionRate"
            Variable /G $"root:NAC_Average:Experiments:"+ExpName+":MultiLayerEnthalpy"
            Variable /G $"root:NAC_Average:Experiments:"+ExpName+": ↵
        ↵ MultiLayerEnthalpyError"
        EndIf
6781 NVar DoseImp=root:NAC_Import:DosePerPulse, ThicknessImp=root:NAC_Import: ↵
        ↵ TotalThickness, RateImp=root:NAC_Import:DepositionRate
        NVar MultiLayerEnthalpyImp=root:NAC_Import:MultiLayerEnthalpy, ↵
        ↵ MultiLayerEnthalpyErrorImp=root:NAC_Import:MultiLayerEnthalpyError
        NVar Dose=$"root:NAC_Average:Experiments:"+ExpName+":DosePerPulse"
        NVar SubstrateThickness=$"root:NAC_Average:Experiments:"+ExpName+": ↵
        ↵ SubstrateThickness"
        NVar Rate=$"root:NAC_Average:Experiments:"+ExpName+":DepositionRate"
6786 NVar MultiLayerEnthalpy=$"root:NAC_Average:Experiments:"+ExpName+": ↵
        ↵ MultiLayerEnthalpy"
        NVar MultiLayerEnthalpyError=$"root:NAC_Average:Experiments:"+ExpName+": ↵
        ↵ MultiLayerEnthalpyError"
        Duplicate /O root:NAC_Import:Enthalpy $"root:NAC_Average:Experiments:"+ ↵
        ↵ ExpName+":Enthalpy"
        Duplicate /O root:NAC_Import:orig_Desorption $"root:NAC_Average:Experiments ↵
        ↵ :"+ExpName+":Sticking"
        Duplicate /O root:NAC_Import:orig_Radiation $"root:NAC_Average:Experiments:"+ ↵
        ↵ ExpName+":Radiation"
6791 Duplicate /O root:NAC_Import:Coverage $"root:NAC_Average:Experiments:"+ ↵
        ↵ ExpName+":Coverage"
        Duplicate /O root:NAC_Import:MultiLayerReference $"root:NAC_Average: ↵
        ↵ Experiments:"+ExpName+":MultiLayerReference"
        Wave Sticking=$"root:NAC_Average:Experiments:"+ExpName+":Sticking"
        Sticking=1-Sticking
        Dose=DoseImp
6796 SubstrateThickness=ThicknessImp
        Rate=RateImp
        MultiLayerEnthalpy=MultiLayerEnthalpyImp
        MultiLayerEnthalpyError=MultiLayerEnthalpyErrorImp
        KillDataFolder NAC_Import
6801 EndFor
        SetDataFolder OldDF
        NVar Processed=root:NAC_Average:Settings:Processed, AutoRecalc=root:NAC_Average ↵
        ↵ :Settings:AutoRecalculate, AutoDisplay=root:NAC_Average:Settings: ↵
        ↵ AutoDisplay

```

```

        Processed=0
        If (AutoRecalc)
6806     NAC_Results_Average()
        EndIf
        Return NaN
    End
    //
Function NAC_Results_Average
6811 Function NAC_Results_Average()
    String ExpName
    Variable i, j, MaxCoverage=0
    DFRRef OldDF=GetDataFolderDFR()
    Variable NumExp, Cont, NP
6816     If (!DataFolderExists("root:NAC_Average"))
        Error_Message(Results_Initialize(), "NAC_Results_Load", "ResultsInitialize", "↵
        ↵ Average")
        EndIf
        SetDataFolder root:NAC_Average
        NVar BinSize=root:NAC_Average:Settings:BinSize, RefEnthalpy=root:NAC_Average:↵
        ↵ ReferenceEnthalpy
6821     NumExp=CountObjects("root:NAC_Average:Experiments",4)
        If (NumExp<=0)
            Error_Message(NAC_NothingToProcess, "InProc","NAC_Results_Average","Average")
            SetDataFolder OldDF
            Return NaN
6826     EndIf
        Make /D /O /N=(NumExp) RefEnthalpies=0, Doses
        Wave /T Experiments
        Wave DepositionRates, Thicknesses, MultiLayerEnthalpies, ↵
        ↵ MultiLayerEnthalpyErrors
        ReDimension /N=(NumExp) Experiments, DepositionRates, Thicknesses, ↵
        ↵ MultiLayerEnthalpies, MultiLayerEnthalpyErrors
6831     For (i=0; i<NumExp;i+=1)
        ExpName=PossiblyQuoteName(GetIndexedObjName("root:NAC_Average:Experiments:", ↵
        ↵ 4,i))
        Cont = (Exists("root:NAC_Average:Experiments:"+ExpName+":Coverage")==1) && (↵
        ↵ Exists("root:NAC_Average:Experiments:"+ExpName+":MultiLayerReference")==1)
        Cont = Cont && (Exists("root:NAC_Average:Experiments:"+ExpName+":Sticking")↵
        ↵ ==1) && (Exists("root:NAC_Average:Experiments:"+ExpName+":Enthalpy")==1)
        Cont = Cont && (Exists("root:NAC_Average:Experiments:"+ExpName+":DosePerPulse↵
        ↵ ")==2)
6836     Cont = Cont && (Exists("root:NAC_Average:Experiments:"+ExpName+":↵
        ↵ MultiLayerEnthalpy")==2) && (Exists("root:NAC_Average:Experiments:"+↵
        ↵ ExpName+":MultiLayerEnthalpyError")==2)
        If (!Cont)
            DoAlert /T="NAC Averaging" 0, "Experiment Structure for "+ ExpName+" is ↵
            ↵ corrupt!\r\r Removal is recommended."
            Error_Message(NAC_CorruptExperiment, "InProc","NAC_Results_Average",ExpName↵
            ↵ )
            SetDataFolder OldDF
6841     Return NaN
        EndIf
        Wave Coverage="$root:NAC_Average:Experiments:"+ExpName+":Coverage", Ref="$↵
        ↵ root:NAC_Average:Experiments:"+ExpName+":MultiLayerReference"
        NVar Dose="$root:NAC_Average:Experiments:"+ExpName+":DosePerPulse", ↵
        ↵ DepositionRate="$root:NAC_Average:Experiments:"+ExpName+":DepositionRate"
        NVar Thickness="$root:NAC_Average:Experiments:"+ExpName+":SubstrateThickness"
6846     NVar MultiLayerEnthalpy="$root:NAC_Average:Experiments:"+ExpName+":↵
        ↵ MultiLayerEnthalpy", MultiLayerEnthalpyError="$root:NAC_Average:Experiments↵
        ↵ :"+ExpName+":MultiLayerEnthalpyError"
        Experiments[i]=ExpName
        DepositionRates[i]=DepositionRate
        Thicknesses[i]=Thickness
        MultiLayerEnthalpies[i]=MultiLayerEnthalpy
6851     MultiLayerEnthalpyErrors[i]=MultiLayerEnthalpyError
        RefEnthalpies[i]=Ref[0]
        Doses[i]=Dose
        If (WaveMax(Coverage)>MaxCoverage)

```

```

        MaxCoverage=WaveMax(Coverage)
6856     EndIf
    EndFor
    WaveStats /Q RefEnthalpies
    If (Abs(V_SDev/V_Avg)>0.05)
        If (Abs(V_Min-V_Avg)>Abs(V_Max-V_Avg))
6861     ExpName=GetIndexedObjName("root:NAC_Average:Experiments:", 4,V_MinLoc)
        Else
            ExpName=GetIndexedObjName("root:NAC_Average:Experiments:", 4,V_MaxLoc)
        EndIf
        DoAlert /T="NAC Averaging" 0, "Experiment Incompatible: "+ ExpName+"\r\r ↵
        ↵ Removal is recommended."
6866     Error_Message(NAC_IncompatibleExperiment, "InProc","NAC_Results_Average",↵
        ↵ ExpName)
        SetDataFolder OldDF
        RefEnthalpy=NaN
        Return NaN
    EndIf
6871     RefEnthalpy=V_Avg
    Make /FREE /D /N=(Ceil(MaxCoverage/BinSize)*10) SumPoints=0
    Make /O /N=(Ceil(MaxCoverage/BinSize)*10) AveragedEnthalpy=0, AveragedSticking↵
    ↵ =0, AveragedRadiation=0
    SetScale /P x, 0, 0.1*BinSize, "ML", AveragedEnthalpy, AveragedSticking, ↵
    ↵ AveragedRadiation, SumPoints
    For (i=0; i<NumExp;i+=1)
6876     ExpName=PossiblyQuoteName(GetIndexedObjName("root:NAC_Average:Experiments:", ↵
    ↵ 4,i))
        Wave Sticking="$root:NAC_Average:Experiments:"+ExpName+":Sticking"
        Wave Radiation="$root:NAC_Average:Experiments:"+ExpName+":Radiation"
        Wave Enthalpy="$root:NAC_Average:Experiments:"+ExpName+":Enthalpy"
        Wave Coverage="$root:NAC_Average:Experiments:"+ExpName+":Coverage"
6881     NP=NumPnts(Sticking) // Remove flagegd frames at the begining
        For (j=0; (j<NP) && ((Sticking[j]==1 && Enthalpy[j]==0) || NumType(Enthalpy[↵
    ↵ j])!=0);j+=1)
            EndFor
            If (j>0)
6886             DeletePoints /M=0 0, j, Sticking, Radiation, Enthalpy, Coverage
            EndIf
            NP=NumPnts(Sticking) // Remove flagegd frames at the end
            For (j=NP-1; (j>0) && ((Sticking[j]==1 && Enthalpy[j]==0) || NumType(↵
    ↵ Enthalpy[j])!=0);j-=1)
                EndFor
                If (j<NP-1)
6891                 DeletePoints /M=0 j+1, Inf, Sticking, Radiation, Enthalpy, Coverage
                EndIf
                AveragedEnthalpy+= (x<=WaveMax(Coverage)) ? Interp(x, Coverage, Enthalpy) : 0
                AveragedSticking+= (x<=WaveMax(Coverage)) ? Interp(x, Coverage, Sticking) : 0
                AveragedRadiation+= (x<=WaveMax(Coverage)) ? Interp(x, Coverage, Radiation) : ↵
    ↵ 0
6896             SumPoints+=(x<=WaveMax(Coverage)) ? 1 :0
        EndFor
        AveragedEnthalpy/=SumPoints
        AveragedSticking/=SumPoints
        AveragedRadiation/=SumPoints
6901     ReSample /DOWN=10/WINF=None AveragedEnthalpy, AveragedSticking, ↵
    ↵ AveragedRadiation
        SetScale /P x, 0, BinSize, "ML", AveragedEnthalpy, AveragedSticking, ↵
    ↵ AveragedRadiation
        SetScale d, 0, 0, "J/mol", AveragedEnthalpy
        NVar Processed=root:NAC_Average:Settings:Processed, AutoDisplay=root:↵
    ↵ NAC_Average:Settings:AutoDisplay
        Processed=1
6906     SetDataFolder OldDF
        If (AutoDisplay)
            NAC_Results_Display()
        EndIf
        Return NaN
6911 End

```

```

//
Function NAC_Results_Remove
Function NAC_Results_Remove()
  If (!DataFolderExists("root:NAC_Average"))
    Error_Message(Results_Initialize(), "NAC_Results_Load","ResultsInitialize"
    ↪ ",")
6916  EndIf
  String ExpList = "", ExpName
  Variable i
  Variable NumExp=CountObjects("root:NAC_Average:Experiments",4)
  For (i=0; i< NumExp; i+=1)
6921  ExpList+=GetIndexedObjName("root:NAC_Average:Experiments:", 4,i)+";"
  EndFor
  ExpList="Cancel;" + ExpList
  Prompt ExpName, "Remove Experiment: ", popup, ExpList
  DoPrompt /HELP="" "NAC Average", ExpName
6926  If (V_Flag || StringMatch(ExpName,"Cancel"))
    Return NaN
  EndIf
  NVar Processed=root:NAC_Average:Settings:Processed, AutoRecalc=root:NAC_Average
    ↪ :Settings:AutoRecalculate, AutoDisplay=root:NAC_Average:Settings:
    ↪ AutoDisplay
  DoWindow NAC_ResultEnthalpy
6931  If (V_Flag)
    RemoveFromGraph /W=NAC_ResultEnthalpy $ExpName
  EndIf
  DoWindow NAC_ResultSticking
  If (V_Flag)
6936  RemoveFromGraph /W=NAC_ResultSticking $ExpName
  EndIf
  DoWindow NAC_ResultRadiation
  If (V_Flag)
6941  RemoveFromGraph /W=NAC_ResultRadiation $ExpName
  EndIf
  KillDataFolder $"root:NAC_Average:Experiments:" + PossiblyQuoteName(ExpName)
  Processed=0
  If (AutoRecalc)
    NAC_Results_Average()
6946  EndIf
  Return NaN
End
//
Function NAC_Results_Display
Function NAC_Results_Display()
6951  If (!DataFolderExists("root:NAC_Average"))
    Error_Message(Results_Initialize(), "NAC_Results_Load","ResultsInitialize"
    ↪ ",")
  EndIf
  Variable i, j, NumExp, Cont, MaxCoverage=0
  String ExpName, Color
6956  NVar WWidth=root:NAC_Average:Settings:WWidth, WHeight=root:NAC_Average:Settings
    ↪ :WHeight, MarginTop=root:NAC_Average:Settings:MarginTop
  NVar RefEnthalpy=root:NAC_Average:ReferenceEnthalpy
  NVar Processed=root:NAC_Average:Settings:Processed
  SVar System=root:NAC_Average:System
  NumExp=CountObjects("root:NAC_Average:Experiments",4)
6961  If ((NumExp<=0) || !Processed)
    Error_Message(NAC_AverageWavesMissing, "InProc","NAC_Results_Average","
    ↪ Results")
    Return NaN
  EndIf
  Cont=1
6966  For (i=0; i<NumExp;i+=1)
    ExpName=PossiblyQuoteName(GetIndexedObjName("root:NAC_Average:Experiments:",
    ↪ 4,i))
    Cont=Cont && (Exists("root:NAC_Average:Experiments:"+ExpName+":Sticking")==1)
    ↪ && (Exists("root:NAC_Average:Experiments:"+ExpName+":Enthalpy")==1) && (

```

```

    ↪ Exists("root:NAC_Average:Experiments:"+ExpName+":Coverage")==1)
  If (!Cont)
    DoAlert /T="NAC Averaging" 0, "Experiment Structure for "+ ExpName+" is ↪
    ↪ corrupt!\r\r Removal is recommended."
6971   Error_Message(NAC_CorruptExperiment, "InProc","NAC_Results_Average",ExpName↪
    ↪ )
    SetDataFolder OldDF
    Return NaN
  EndIf
  Wave Coverage="$root:NAC_Average:Experiments:"+ExpName+":Coverage"
6976   If (WaveMax(Coverage)>MaxCoverage)
    MaxCoverage=WaveMax(Coverage)
  EndIf
EndFor
If (Exists("root:NAC_Average:AveragedEnthalpy")!=1)
6981   Error_Message(NAC_AdsorptionMissing, "InProc","NAC_Results_Display","Average↪
    ↪ ")
  Return NaN
EndIf
If (Exists("root:NAC_Average:AveragedSticking")!=1)
6986   Error_Message(NAC_StickingMissing, "InProc","NAC_Results_Display","Average")
  Return NaN
EndIf
If (Exists("root:NAC_Average:AveragedRadiation")!=1)
//   Error_Message(NAC_StickingMissing, "InProc","NAC_Results_Display","Average↪
    ↪ ")
//   Return NaN
6991   EndIf
  Make /O /N=2 root:NAC_Average:RadiationLimit=1
  Wave AveragedEnthalpy=root:NAC_Average:AveragedEnthalpy, AveragedSticking=root:↪
    ↪ NAC_Average:AveragedSticking, AveragedRadiation=root:NAC_Average:↪
    ↪ AveragedRadiation
  Wave StickingLimit=root:NAC_Average:StickingLimit, EnthalpyLimit=root:↪
    ↪ NAC_Average:EnthalpyLimit, RadiationLimit=root:NAC_Average:RadiationLimit
  String WName, NameList="NAC_ResultEnthalpy;NAC_ResultSticking;↪
    ↪ NAC_ResultRadiation", LabelList="Enthalpy;Sticking;Radiation;", WLabel
6996   NVar LegendLines=root:NAC_Average:Settings:LegendLines
  Make /T /N=(LegendLines) /FREE LegendTextLines=""
  String LegendText=""
  SetScale /I x 0, Ceil(MaxCoverage*5)/5, "ML" StickingLimit, EnthalpyLimit, ↪
    ↪ RadiationLimit
  For (i=0;i<ItemsInList(NameList);i+=1)
7001   WName=StringFromList(i,NameList,";")
    WLabel=StringFromList(i,LabelList,";")
    DoWindow $WName
    If (V_Flag)
      KillWindow $WName
7006   EndIf
    Display /N=$WName /K=1 /W=(i*WWidth+150+i*30, 500, (i+1)*WWidth+150+i*30, ↪
    ↪ 500+WHeight) as "Averaged "+WLabel
    ModifyGraph /W=$WName margin(Top)=MarginTop
    For (j=0; j<NumExp; j+=1)
      ExpName=GetIndexedObjName("root:NAC_Average:Experiments:", 4,j)
7011   AppendToGraph /W=$WName $"root:NAC_Average:Experiments:"+PossiblyQuoteName(↪
    ↪ ExpName)+":"+WLabel/TN=$ExpName vs $"root:NAC_Average:Experiments:"+↪
    ↪ PossiblyQuoteName(ExpName)+":Coverage"
      ModifyGraph /W=$WName Mode($ExpName)=2, LSize($ExpName)=1.5, RGB($ExpName)↪
    ↪ =(HSL2RGB(j*210/NumExp+50, 240, 100, 0), HSL2RGB(j*210/NumExp+50, 240, 100,↪
    ↪ 1), HSL2RGB(j*210/NumExp+50, 240, 100, 2))
    EndFor
    AppendToGraph /W=$WName $"root:NAC_Average:Averaged"+WLabel/TN=Average, $"↪
    ↪ root:NAC_Average:"+WLabel+"Limit"/TN=Reference
    ModifyGraph LStyle(Reference)=7, LSize(Reference)=1.5, RGB(Reference)↪
    ↪ =(17408,17408,17408), Mode(Average)=2, LSize(Average)=2, RGB(Average)↪
    ↪ =(0,0,0)
7016   EndFor
  For (j=0; j<NumExp; j+=1)
    ExpName=PossiblyQuoteName(GetIndexedObjName("root:NAC_Average:Experiments:", ↪
    ↪ 4,j))

```

```

NVar Thickness="$root:NAC_Average:Experiments:"+ExpName+":SubstrateThickness"
// LegendTextLines[Mod(j,LegendLines)]+="\s("+ExpName+") "+ExpName
7021 Color="( "+Num2Str(HSL2RGB(j*210/NumExp+50, 240, 100, 0))+", "+Num2Str(HSL2RGB(
↳ (j*210/NumExp+50, 240, 100, 1))+", "+Num2Str(HSL2RGB(j*210/NumExp+50, 240,
↳ 100, 2))+")"
LegendTextLines[Mod(j,LegendLines)]+="\k"+Color+"\k"+Color+"\W519\k
↳ (0,0,0)\t"+ExpName+"\t"
EndFor
For (i=0;i<LegendLines;i+=1)
If (StrLen(LegendTextLines[i]))
7026 LegendText+=RemoveEnding(LegendTextLines[i],"\t")+"\r"
EndIf
EndFor
If (NumExp<=LegendLines)
LegendText+="\k(0,0,0)\k(0,0,0)\W519\k(0,0,0)\tAverage\r\s(Reference)\
↳ tReference"
7031 Else
LegendText+="\k(0,0,0)\k(0,0,0)\W519\k(0,0,0)\tAverage\t\s(Reference)\
↳ tReference"
EndIf
Legend /W=NAC_ResultEnthalpy /C /N=text0 /B=1 /F=0 /A=RT /H={0,2,10} /T
↳ ={28,100,128} LegendText
Legend /W=NAC_ResultSticking /C /N=text0 /B=1/F=0 /A=RB /H={0,2,10} /T
↳ ={28,100,128} LegendText
7036 Legend /W=NAC_ResultRadiation /C /N=text0 /B=1/F=0 /A=RT /H={0,2,10} /T
↳ ={28,100,128} LegendText
TextBox /W=NAC_ResultEnthalpy /C/N=text1/F=0/Z=1/H={0,2,10}/A=MT/X=0/Y=5/E=2 /B
↳ =1 "\Z14Enthalpies for "+System
TextBox /W=NAC_ResultSticking /C/N=text1/F=0/Z=1/H={0,2,10}/A=MT/X=0/Y=5/E=2 /B
↳ =1 "\Z14Sticking for "+System
TextBox /W=NAC_ResultRadiation /C/N=text1/F=0/Z=1/H={0,2,10}/A=MT/X=0/Y=5/E=2 /
↳ B=1 "\Z14Radiation for "+System
7041 SetAxis /W=NAC_ResultEnthalpy /A /N=1 /E=3 Left
SetAxis /W=NAC_ResultSticking /A /N=1 /E=3 Left
SetAxis /W=NAC_ResultRadiation Left 0, 3
Label /W=NAC_ResultEnthalpy Left "Heat of Adsorption (\U)"
Label /W=NAC_ResultSticking Left "Sticking Probability"
Label /W=NAC_ResultRadiation Left "Radiation Contribution"
7046 WName="NAC_ResultAverages"
DoWindow $WName
If (V_Flag)
DoWindow /F $WName
Else
7051 Display /N=$WName /K=1 /W=(WWidth+180, 130, 2*WWidth+180, 130+WHeight) as "
↳ Averages"
ModifyGraph /W=$WName margin(Top)=MarginTop
AppendToGraph /W=$WName /L root:NAC_Average:AveragedEnthalpy, root:
↳ NAC_Average:EnthalpyLimit
AppendToGraph /W=$WName /R root:NAC_Average:AveragedSticking, root:
↳ NAC_Average:StickingLimit
ModifyGraph /W=$WName LStyle(EnthalpyLimit)=7, LSize(EnthalpyLimit)=1.25, RGB
↳ (EnthalpyLimit)=(65280,0,0)
7056 ModifyGraph /W=$WName LStyle(StickingLimit)=7, LSize(StickingLimit)=1.25, RGB
↳ (StickingLimit)=(0,0,65280)
ModifyGraph /W=$WName Mode(AveragedEnthalpy)=2, LSize(AveragedEnthalpy)=2,
↳ RGB(AveragedEnthalpy)=(65280,0,0)
ModifyGraph /W=$WName Mode(AveragedSticking)=2, LSize(AveragedSticking)=2,
↳ RGB(AveragedSticking)=(0,0,65280)
SetAxis /W=$WName /A /N=1 /E=3 Left
SetAxis /W=$WName /A /N=1 /E=3 Right
7061 Label /W=$WName Left "\k(52224,0,0)Heat of Adsorption (\U)"
Label /W=$WName Right "\k(0,0,52224)Sticking Probability"
TextBox /W=$WName /C/N=text1/F=0/Z=1/H={0,2,10}/A=MT/X=0/Y=5/E=2 /B=1 "\Z14
↳ "+System
EndIf
WName="NAC_ResultAuxilaray"
7066 DoWindow $WName
If (V_Flag)
KillWindow $WName

```



```

EndIf
Display /N=$WName /K=1 /W=(150, 130, WWidth+150, 130+WHeight) as "Auxiliary ↵
↳ Information"
7071 ModifyGraph /W=$WName margin(Top)=MarginTop
AppendToGraph /W=$WName /L root:NAC_Average:DepositionRates vs root:NAC_Average↵
↳ :Experiments
AppendToGraph /W=$WName /R root:NAC_Average:Thicknesses vs root:NAC_Average:↵
↳ Experiments
ModifyGraph /W=$WName Mode=3, Marker(DepositionRates)=18, Marker(Thicknesses)↵
↳ =18, marker(DepositionRates)=19, MSize=3, rgb(DepositionRates)=(52224,0,0),↵
↳ rgb(Thicknesses)=(0,0,52224)
SetAxis /W=$WName /A /N=1 /E=1 Left
7076 SetAxis /W=$WName /A /N=1 /E=1 Right
Label /W=$WName Left "\\K(52224,0,0)Calorimetry Deposition Rate (\\U)"
Label /W=$WName Right "\\K(0,0,52224)Substrate Thickness (\\U)"
Label /W=$WName Bottom "Experiment"
If (NumPnts(root:NAC_Average:Experiments)>4)
7081 ModifyGraph /W=$WName tkLblRot(Bottom)=90
EndIf
TextBox /W=$WName /C/N=text1/F=0/Z=1/H={0,2,10}/A=MT/X=0/Y=5/E=2 /B=1 "\\Z14"+↵
↳ System
Return NoError
End
7086 //
```

C.1.10 Miscellaneous

```
//
```

GetPrefix

```

Static Function GetPrefix(Str)
String Str
If (StrSearch(Str,"ms",0)>=0)
7091 Return 1e-3
EndIf
If (StrSearch(Str,"kHz",0)>=0)
Return 1e3
EndIf
7096 Return 1
End
//
```

Function SauerbreyThickness

```

Function SauerbreyThickness(F0, F, Z, D) //m
Variable F0, F, Z, D
7101 Variable Zq=8.83 // g/cm^2*s
Variable Dq=2.65 // g/cm^3
Variable Nq=1.661e6 // Hz*mm
Return Dq/D * Nq/F*Z /(Pi*Zq)*ATan(Zq/Z*Tan(Pi*((F0-F)/F0)))/1000
End
7106 //
```

Function HSL2RGB

```

Function HSL2RGB(Hue, Sat, Lum, Ch)
//http://en.wikipedia.org/wiki/HSL_and_HSV
// Igor uses 240 as maximum for Hue, Sat & Lum
Variable Hue, Sat, Lum, Ch
7111 Variable H, C, X, m
Variable R, G, B
If (NumType(Hue)!=0)
Return 0
EndIf
7116 Hue=Mod(Hue,240)
Sat=Sat/240
Lum=Lum/240
H=Hue/40
C=(1-Abs(2*Lum-1))*Sat
7121 X=C*(1-Abs(Mod(H,2)-1))
If (H<1)
R=C; G=X; B=0

```

```
    ElseIf (H<2)
        R=X; G=C; B=0
7126    ElseIf (H<3)
        R=0; G=C; B=X
        ElseIf (H<4)
            R=0; G=X; B=C
        ElseIf (H<5)
7131    R=X; G=0; B=C
        Else
            R=C; G=0; B=X
        EndIf
        m=Lum-C/2
7136    Switch (Ch)
        Case 0:
            Return (R+m)*65535
            Break
        Case 1:
7141    Return (G+m)*65535
            Break
        Case 2:
            Return (B+m)*65535
            Break
7146    EndSwitch
End
//
```

Function GetSubstanceName

```
Function /S GetSubstanceName(Substance)
String Substance
7151    If (StringMatch(Substance, "Mg*"))
        Return "Magnesium"
    ElseIf (StringMatch(Substance, "Ca*"))
        Return "Calcium"
    ElseIf (StringMatch(Substance, "Cu*"))
7156    Return "Copper"
    ElseIf (StringMatch(Substance, "Li*"))
        Return "Lithium"
    ElseIf (StringMatch(Substance, "Zn*"))
        Return "Zinc"
7161    ElseIf (StringMatch(Substance, "PTCDA*"))
        Return "PTCDA"
    ElseIf (StringMatch(Substance, "2HPc*"))
        Return "Phtalocyanine"
    ElseIf (StringMatch(Substance, "2HTPP*"))
7166    Return "Tetrphenyl Porphyrin"
    ElseIf (StringMatch(Substance, "6T*"))
        Return "Sexithiophene"
    Else
        Return Substance[0, strsearch(Substance, "(", 0)-1]
7171    EndIf
End
//
```

Function NAC_UpdateVersion

```
Function NAC_UpdateVersion()
DFRef OldDF=GetDataFolderDFR()
7176 String LaserMeasurements="LaserReference;Transmission;ReflecBefore;ReflecAfter;↵
    ↵ Deconvolution;"
String FluxMeasurements="FluxCalorimetry;FluxCoating;"
String OtherMeasurements="Radiation;Heat;Sticking;ZeroSticking;"
String AuxList=""
Variable i, j, Updated=0
7181 String MeasurementsList=LaserMeasurements+OtherMeasurements
String WName, Name
    If (!DataFolderExists("root:NAC:") && !DataFolderExists("root:NAC_Average:"))
        Error_Message(NAC_NotInitialized, "InProc", "NAC_UpdateVersion", "")
        Return NaN
7186    EndIf
    If (DataFolderExists("root:NAC"))
```

```

If (Exists("root:NAC:Experiment:ProjectVersion")!=2)
  Print "Unable to patch from unknown version"
  Return -1
7191 EndIf
SVar Version=root:NAC:Experiment:ProjectVersion
StrSwitch (Version)
  Case "3.6 beta":
    Print "Patching from NAC 3.6 beta"
7196   SetDataFolder root:NAC:GUI
    Variable /G RangeDeconvolution
    String /G NameRangeDeconvolution=""
    For (i=0;i<ItemsInList(MeasurmentsList);i+=1)
      SetDataFolder $"root:NAC:"+StringFromList(i,MeasurmentsList)
7201   Variable /G BrowseDeconvolutionIndex=0
    EndFor
    Version="3.7 beta"
  Case "3.7 beta":
    Print "Patching from NAC 3.7 beta"
7206   For (i=0;i<ItemsInList(MeasurmentsList);i+=1)
      Name=StringFromList(i,MeasurmentsList)
      SetDataFolder $"root:NAC:"+Name
      Rename NumberOfPulses, NumberOfFrames
      Rename EffectivePulses, EffectiveFrames
7211   Rename CurrentPulse, CurrentFrame
      SetFormula $"root:NAC:"+StringFromList(i,MeasurmentsList,";")+":↵
↵ EffectiveFrames" "root:NAC:"+StringFromList(i,MeasurmentsList,";")+":↵
↵ NumberOfFrames-Sum(root:NAC:"+StringFromList(i,MeasurmentsList,";")+":↵
↵ FlagList)"
      WName="NAC_"+Name+"_AvgDeconv"
      DoWindow $WName
      If (V_Flag)
7216   SVar FileName
        TextBox /W=$WName /A=MT /C/E/F=0 /X=0 /Y=5 /N=Caption/A=MC /B=1 "\↵
↵ JCDeconvoluted Average for "+Name+" Measurement\r\JC"+FileName+": \K↵
↵ (0,0,65280)Even Frame\K(0,0,0) \K(0,52224,0)Odd Frame"
      EndIf
      WName="NAC_"+Name+"_Avg"
      DoWindow $WName
7221   If (V_Flag)
        SVar FileName
        TextBox /W=$WName /A=MT /C/E/F=0 /X=0 /Y=5 /N=Caption/A=MC /B=1 "\↵
↵ JCDeconvolution for "+Name+" Measurement\r\JC"+FileName+": \K(0,0,65280)↵
↵ Even Frame\K(0,0,0) \K(0,52224,0)Odd Frame"
      EndIf
      WName="NAC_"+Name+"_Full"
7226   DoWindow $WName
      If (V_Flag)
        KillWindow $WName
        DisplayMeasurement(Name)
      EndIf
7231   WName="NAC_"+Name+"_Pulses"
      DoWindow $WName
      If (V_Flag)
        KillWindow $WName
        DisplayNonFlagged(Name)
7236   EndIf
      WName="NAC_"+Name+"_Flag"
      DoWindow $WName
      If (V_Flag)
        KillWindow $WName
7241   DisplayFlagWindow(Name)
      EndIf
      WName="NAC_"+Name+"_BrowseDeconv"
      DoWindow $WName
      If (V_Flag)
7246   DoWindow /T $WName, Name +" Deconvoluted Frame"
        DoDeconvolutionTextBox(Name)
      EndIf

```

```

        SetDataFolder $"root:NAC:"+StringFromList(i,MeasurmentsList)+":↵
↵ Auxiliaries"
        AuxList=WaveList("*", ";", "")
7251        For (j=0;j<ItemsInList(AuxList, ";");j+=1)
            Wave AuxWave=$StringFromList(j, AuxList, ";")
            If (StringMatch(WaveUnits(AuxWave, 0), "Pulse"))
                SetScale /P x, DimOffset(AuxWave, 0), DimDelta(AuxWave, 0), "Frame↵
↵ ", AuxWave
                EndIf
7256        EndFor
        SetDataFolder $"root:NAC:"+StringFromList(i,MeasurmentsList)+":↵
↵ Statistics"
        Wave Amplitude
        SetScale /P x, 0, 1, "Frame", Amplitude
        EndFor
7261        SetDataFolder root:NAC:Machine
        ReName FluxAveragingWindow FluxFittingWindow
        SetDataFolder root:NAC:Experiment
        ReName DataPointsPerPulse, DataPointsPerFrame
7266        SetDataFolder root:NAC:Deconvolution
        ReName DataPointsPerPulse, DataPointsPerFrame
        WName="NAC_Radiation_Trend"
        DoWindow $WName
        If (V_Flag)
            Label /W=$WName Bottom "Frame"
7271        EndIf
        WName="NAC_Desorption_Trend"
        DoWindow $WName
        If (V_Flag)
            Label /W=$WName Bottom "Frame"
7276        EndIf
        Version="3.8 alpha"
        Case "3.8 alpha":
            Print "Patching from 3.8 NAC alpha"
            PathInfo CalDataPath
7281            String Path=S_Path
            String /G root:NAC:Experiment:ExperimentName=""
            SVar ExpName=root:NAC:Experiment:ExperimentName
            If (!StringMatch(Path, NAC_DataPathStr))
                ExpName=Path[StrSearch(Path, ":", StrLen(Path)-2,3)+1, StrLen(Path)-2]
7286            EndIf
            SVar CoatSubstance=root:NAC:FluxCoating:Substance, CalSubstance=root:NAC:↵
↵ FluxCalorimetry:Substance
            If (StrLen(CoatSubstance))
                String /G root:NAC:FluxCoating:SubstanceName=GetSubstanceName(↵
↵ CoatSubstance)
            Else
7291            String /G root:NAC:FluxCoating:SubstanceName=""
            EndIf
            If (StrLen(CalSubstance))
                String /G root:NAC:FluxCalorimetry:SubstanceName=GetSubstanceName(↵
↵ CalSubstance)
            Else
7296            String /G root:NAC:FluxCoating:SubstanceName=""
            EndIf
            Version="3.8 beta"
            Case "3.8 beta":
                Print "Patching from NAC 3.8 beta"
7301            KillVariables root:NAC:Machine:QCMToolingCoating
            ReName root:NAC:Machine:LasPowCorr, LaserPowerCorrection
            ReName root:NAC:Machine:QCMToolingCal, QCMToolingCalorimetry
            ReName root:NAC:Machine:QCMToolingCoat QCMToolingCoating
            Rename root:NAC:Machine:QMSToolingCal QMSToolingCalorimetry
7306            SVar SubstCoat=root:NAC:FluxCoating:Substance, SubstCal=root:NAC:↵
↵ FluxCalorimetry:Substance
            String /G root:NAC:FluxCoating:SubstanceName=GetSubstanceName(SubstCoat)
            String /G root:NAC:FluxCalorimetry:SubstanceName=GetSubstanceName(↵
↵ SubstCal)

```

```

Error_Message(ProcessProc("Deconvolution"), "ProcessProc", "↵
↵ NAC_UpdateVersion", "Deconvolution")
Print "Deconvolution needs to be performed again"
7311 Version="3.9 alpha"
Case "3.9 alpha":
Print "Patching from NAC 3.9 alpha"
KillDependencies()
If (Exists("root:NAC:Machine:QCMToolingCoat")==2)
7316 KillVariables /Z root:NAC:Machine:QCMToolingCoating
Rename root:NAC:Machine:QCMToolingCoat QCMToolingCoating
EndIf
If (Exists("root:NAC:Machine:QCMToolingCal")==2)
7321 KillVariables /Z root:NAC:Machine:QCMToolingCalorimetry
Rename root:NAC:Machine:QCMToolingCal QCMToolingCalorimetry
EndIf
If (Exists("root:NAC:Machine:QMSToolingCal")==2)
7326 KillVariables /Z root:NAC:Machine:QMSToolingCalorimetry
Rename root:NAC:Machine:QMSToolingCal QMSToolingCalorimetry
EndIf
Variable /G root:NAC:GUI:LoadSupportFiles=0
Variable /G root:NAC:Deconvolution:Sensitivity=1, root:NAC:Deconvolution:↵
↵ UseSensitivity=1
NVar QCMToolingCalorimetry=root:NAC:Machine:QCMToolingCalorimetry, ↵
↵ QMSTooling=root:NAC:Machine:QMSToolingCalorimetry
QCMToolingCalorimetry=1.09042 // Sauerbrey sensitivity
7331 QMSTooling=0.959158
For (i=0;i<ItemsInList(MeasurmentsList);i+=1)
Name=StringFromList(i,MeasurmentsList)
Duplicate /FREE $"root:NAC:"+Name+":FlagList" FlagTemp
Make /O /B /U /N=(NumPnts(FlagTemp)) $"root:NAC:"+Name+":FlagList"
7336 Wave FlagList=$"root:NAC:"+Name+":FlagList"
If (NumPnts(FlagList))
FlagList=FlagTemp
EndIf
SetScale /P x, 0, 1, "Frame", FlagList
7341 EndFor
KillVariables /Z root:NAC:Machine:TransmissionClean FlagTemp
Version="3.9 beta"
Case "3.9 beta":
Print "Patching from NAC 3.9 beta"
7346 Variable /G root:NAC:GUI:StoreFilteredWaves=0, root:NAC:Machine:↵
↵ PulseLengthDetectionWindow=0.05
Version="3.10 alpha"
Case "3.10 alpha":
Print "Patching from NAC 3.10 alpha"
Version="3.10 beta"
7351 Case "3.10 beta":
Print "Patching from NAC 3.10 beta"
If (DataFolderExists("root:NAC:AverageSticking"))
KillDataFolder /Z root:NAC:AverageSticking
EndIf
7356 KillDependencies()
If (Exists("root:NAC:Experiment:TempSource")==2)
Rename root:NAC:Experiment:TempSource TemperatureSource
EndIf
If (Exists("root:NAC:Experiment:TempSample")==2)
7361 Rename root:NAC:Experiment:TempSample TemperatureSample
EndIf
If (Exists("root:NAC:Deconvolution:Average")==2)
Rename root:NAC:Deconvolution:Average AverageFrames
EndIf
7366 If (DataFolderExists("root:NAC:ReflecBefore"))
RenameDataFolder root:NAC:ReflecBefore BeforeCoating
EndIf
If (DataFolderExists("root:NAC:ReflecAfter"))
RenameDataFolder root:NAC:ReflecAfter AfterCoating
7371 EndIf
If (V_Flag)

```

```

        SetWindow NAC_FluxCalorimetry_Full hook(NAC_FluxCoatingCsr)=↵
↵ NAC_WinHookFlux
    EndIf
    DoWindow NAC_FluxCoating_FittedFlux
7376     If (V_Flag)
        SetWindow NAC_FluxCoating_FittedFlux hook(NAC_FluxCalorimetryCsr)=↵
↵ NAC_WinHookFittedFlux
    EndIf
    DoWindow NAC_FluxCalorimetry_FittedFlux
7381     If (V_Flag)
        SetWindow NAC_FluxCalorimetry_FittedFlux hook(NAC_FluxCalorimetryCsr)=↵
↵ NAC_WinHookFittedFlux
    EndIf
    Make /N=2 /O root:NAC:FluxCal:FittedFluxErrorPos , root:NAC:FluxCoat:↵
↵ FittedFluxErrorPos , root:NAC:FluxCal:FittedFluxErrorNeg , root:NAC:FluxCoat:↵
↵ FittedFluxErrorNeg
    Variable /G root:NAC:Machine:SecondNotchFrequency=0
    LaserMeasurements="LaserReference;Transmission;BeforeCoating;AfterCoating↵
↵ ;Deconvolution;"
7386     MeasurementsList=LaserMeasurements+OtherMeasurements
    For (i=0;i<ItemsInList(MeasurmentsList);i+=1)
        Name=StringFromList(i,MeasurmentsList)
        If (!StringMatch(Name,"Heat") && !StringMatch(Name,"Sticking"))
7391             Make /O /N=0 $"root:NAC:"+Name+":Statistics:ChiSq"
                SetScale /P x, 0, 1, "Frame", $"root:NAC:"+Name+":Statistics:ChiSq"
            EndIf
        EndFor
    DoWindow NAC_FluxCoating_Full
7396     If (V_Flag)
        SetWindow NAC_FluxCoating_Full hook(NAC_FluxCoatingCsr)=NAC_WinHookFlux
    EndIf
    DoWindow NAC_FluxCalorimetry_Full
    Version="3.10 gamma"
7401     Case "3.10 gamma":
        Print "Patching from NAC 3.10 gamma"
        LaserMeasurements="LaserReference;Transmission;BeforeCoating;AfterCoating↵
↵ ;Deconvolution;"
        MeasurementsList=LaserMeasurements+OtherMeasurements
        For (i=0;i<ItemsInList(MeasurmentsList);i+=1)
7406             Name=StringFromList(i,MeasurmentsList)
                If (!StringMatch(Name,"Heat") && !StringMatch(Name,"Sticking"))
                    Make /O /N=0 $"root:NAC:"+Name+":Statistics:Outlier"
                    Make /O /N=0 $"root:NAC:"+Name+":Statistics:Medians"
                    SetScale /P x, 0, 1, "Frame", $"root:NAC:"+Name+":Statistics:Medians"
                    SetScale /P x, 0, 1, "Frame", $"root:NAC:"+Name+":Statistics:Outlier"
7411                SetScale /P d, 0, 2, "Relative Amplitude", $"root:NAC:"+Name+":↵
↵ Statistics:Amplitude"
                EndIf
            EndFor
            Variable /G root:NAC:GUI>ShowBoxPlotData=1
            Variable /G root:NAC:Enthalpies:MultiLayerEnthalpyError
7416            SetFormula root:NAC:Enthalpies:MultiLayerEnthalpyError "Sqrt(Variance(↵
↵ root:NAC:Enthalpies:Enthalpy, root:NAC:Enthalpies:MultilayerPosLow, root:↵
↵ NAC:Enthalpies:MultilayerPosHigh))" // J/mol
            Version="3.10 delta"
            Case "3.10 delta":
                Print "Patching from NAC 3.10 delta"
                If (Exists("root:NAC:Machine:ReflecClean")==2)
7421                    ReName root:NAC:Machine:ReflecClean ReflectivityClean
                EndIf
                SetFormula root:NAC:Deconvolution:Reflectivity "root:NAC:Machine:↵
↵ ReflectivityClean" // d.l.
                ReNameDataFolder root:NAC:FluxCoat, FluxCoating
                ReNameDataFolder root:NAC:FluxCal, FluxCalorimetry
7426                String /G LaserPowerCorrectionList="1.38682;1.31814;1.15762;" // Laser ↵
↵ Power Correction Factors // Add new one in the begining
                Version="3.10 epsilon"
                Case "3.10 epsilon":
                    Print "Patching from NAC 3.10 epsilon"

```

```

7431     If (Exists("root:NAC:Sticking:InitSticking")==2)
        ReName root:NAC:Sticking:InitSticking InitDesorption
      EndIf
      If (Exists("root:NAC:Sticking:HoldSticking")==2)
        ReName root:NAC:Sticking:HoldSticking HoldDesorption
      EndIf
7436     String /G root:NAC:Machine:LaserPowerCorrectionList ↵
↵ ="1.28;1.38682;1.31814;1.15762;"
      String /G root:NAC:Machine:ReflectivityCleanList="0.444 Ni/PVDF; 0.89 Al/↵
↵ PVDF;"
      ReName root:NAC:FluxCoating:ApparentFlux ApparentFlux
      ReName root:NAC:FluxCalorimetry:ApparentFlux ApparentFlux
      Version="3.11"
7441     Case "3.11":
      Print "Patching from NAC 3.11"
      ReName root:NAC:Machine:FluxFittingWindow RateFittingWindow
      ReName root:NAC:FluxCalorimetry:FittedFluxErrorNeg FittedRateErrorNeg
      ReName root:NAC:FluxCalorimetry:FittedFluxErrorPos FittedRateErrorPos
7446     ReName root:NAC:FluxCalorimetry:FittedFluxAvg FittedRateAvg
      ReName root:NAC:FluxCalorimetry:ApparentFlux ApparentRate
      ReName root:NAC:FluxCalorimetry:Flux DepositionRate
      ReName root:NAC:FluxCalorimetry:FluxMonoLayer RateMonoLayer
      ReNameDataFolder root:NAC:FluxCalorimetry RateCalorimetry
7451     ReName root:NAC:FluxCoating:FittedFluxErrorNeg FittedRateErrorNeg
      ReName root:NAC:FluxCoating:FittedFluxErrorPos FittedRateErrorPos
      ReName root:NAC:FluxCoating:FittedFluxAvg FittedRateAvg
      ReName root:NAC:FluxCoating:ApparentFlux ApparentRate
      ReName root:NAC:FluxCoating:Flux DepositionRate
7456     ReNameDataFolder root:NAC:FluxCoating RateCoating
      Variable /G root:NAC:Heat:LinkShifts=1
      SetScale d, 0, 0, "J/mol", root:NAC:Enthalpies:MultiLayerReference
      SetScale /P x, 0, DimDelta(root:NAC:Enthalpies:MultiLayerReference,0), "↵
↵ ML", root:NAC:Enthalpies:MultiLayerReference
      SetScale /P x, 0, DimDelta(root:NAC:Enthalpies:StickingLimit,0), "ML", ↵
↵ root:NAC:Enthalpies:StickingLimit
7461     Version="3.12"
      Case "3.12":
      Print "No patch for NAC_Average 3.12 necessary"
      Case "3.13":
      Print "Patching from NAC 3.12"
7466     NVar RefClean=root:NAC:Machine:ReflectivityClean
      If (RefClean==0.439)
        RefClean=0.444
        Print "Reference Reflectivity changed. Data should be processed again."
      EndIf
7471     LaserMeasurements="LaserReference;Transmission;BeforeCoating;AfterCoating ↵
↵ ;Deconvolution;"
      MeasurementsList=LaserMeasurements+OtherMeasurements
      For (i=0;i<ItemsInList(MeasurmentsList);i+=1)
        Name=StringFromList(i,MeasurmentsList)
        If (!StringMatch(Name,"Heat") && !StringMatch(Name,"Sticking"))
7476     If (Exists("root:NAC:"+Name+":Statistics:Outlier")!=1)
          Make /O /N=0 $"root:NAC:"+Name+":Statistics:Outlier"
          SetScale /P x, 0, 1, "Frame", $"root:NAC:"+Name+":Statistics:↵
↵ Outlier"
        EndIf
        If (Exists("root:NAC:"+Name+":Statistics:Medians")!=1)
7481     Make /O /N=0 $"root:NAC:"+Name+":Statistics:Medians"
          SetScale /P x, 0, 1, "Frame", $"root:NAC:"+Name+":Statistics:↵
↵ Medians"
        EndIf
      EndIf
      EndFor
7486     Version="3.14"
      Case "3.14":
      Print "Patching from NAC 3.14"
      Variable /G root:NAC:Experiment:UseEmptyCrucibleReference=0
      Variable /G root:NAC:Experiment:EmptyCrucibleTemperature=NaN
7491     Version="3.15"

```

```

Case "3.15":
  //Print "Patching from NAC 3.14"
  //
  //Print "Patching within NAC 3.15"
7496  //
  // Insert new cases before this line
  Print "Version is up to date: "+Version
  Print "Patching done"
  Updated=1
7501  Break
  Default:
    Print "Unable to patch from version "+Version
    Break
  EndSwitch
7506  If (Updated)
    KillWindow NAC_Control
    Dependencies()
    DataPanel()
    NAC_ReCalcHeat("",nan,"","");
7511  DoHeatTextBox()
  EndIf
EndIf
If (DataFolderExists("root:NAC_Average"))
  If (Exists("root:NAC_Average:Settings:ProjectVersion")!=2)
7516  String /G root:NAC_Average:Settings:ProjectVersion="3.11"
  EndIf
  SVar Version=root:NAC_Average:Settings:ProjectVersion
  Variable NumExp
  StrSwitch (Version)
7521  Case "3.11":
    Print "Patching from NAC_Average prior to 3.12"
    If (Exists("root:NAC_Average:Fluxes")==1)
      Rename root:NAC_Average:Fluxes DepositionRates
    EndIf
7526  NumExp=CountObjects("root:NAC_Average:Experiments",4)
    If (NumExp>0)
      For (i=0; i<NumExp;i+=1)
        Name=PossiblyQuoteName(GetIndexedObjName("root:NAC_Average:↵
↵ Experiments:", 4,i))
        Rename $"root:NAC_Average:Experiments:"+Name+":Flux" DepositionRate
7531  EndFor
      EndIf
      Label /W=NAC_ResultAuxilaray Left "\\K(52224,0,0)Calorimetry Deposition ↵
↵ Rate (\\U)"
      Version="3.12"
    Case "3.12":
7536  Print "No patch for NAC_Average 3.12 necessary"
      Version="3.13"
    Case "3.13":
      Print "Patching from NAC_Average 3.13"
      Variable /G root:NAC_Average:Settings:LegendLines=8
7541  Version="3.14"
    Case "3.14":
  //    Print "Patching within NAC_Average 3.12"
  //    Insert new cases before this line
  //    Print "Version is up to date: "+Version
7546  Print "Patching done"
    Updated=1
    Break
  Default:
    Print "Unable to patch from version "+Version
7551  Break
  EndSwitch
  If (Updated)

  EndIf
7556  EndIf
  SetDataFolder OldDF
  Return NoError

```



```

End
//
Function NAC_Invert
7561 Function NAC_Invert()
String ExpList="Deconvolution;BeforeCoating;AfterCoating;LaserReference;↵
↳ Transmission;Radiation;ZeroSticking;Heat;Sticking;"
String Name, NameList=""
Variable i
If (!DataFolderExists("root:NAC:"))
7566 Error_Message(NAC_NotInitialized, "InProc", "NAC_DisplayStatistics", "")
Return NaN
EndIf
For (i=0;i<ItemsInList(ExpList); i+=1)
If (Exists("root:NAC:"+StringFromList(i, ExpList, ";")+":Detector")==1)
7571 NameList+=StringFromList(i, ExpList, ";")+";"
EndIf
EndFor
If (ItemsInList(NameList)>1)
NameList="Cancel;All;All Calorimetry;All QMS;" + NameList
7576 ElseIf (ItemsInList(NameList)==1)
NameList="Cancel;" + NameList
Else
Error_Message(NAC_NothingToProcess, "InProc", "NAC_Invert", "")
Return NaN
7581 EndIf
Prompt Name, "Invert Signal for", Popup, NameList
DoPrompt /HELP="" "Signal Inversion ", Name
If (V_Flag || StringMatch(Name,"Cancel"))
Error_Message(UserAbort, "InProc", "NAC_Invert", "")
7586 Return NaN
EndIf
StrSwitch (Name)
Case "All":
Break
7591 Case "All Calorimetry":
NameList=RemoveFromList("ZeroSticking;Sticking;", NameList, ";")
Break
Case "All QMS":
NameList=RemoveFromList("Deconvolution;BeforeCoating;AfterCoating;↵
↳ LaserReference;Transmission;Radiation;Heat;", NameList, ";")
7596 Break
Default:
NameList=Name+";"
Break
EndSwitch
7601 NameList=RemoveFromList("Cancel;All;All Calorimetry;All QMS;", NameList, ";")
For (i=0; i<ItemsInList(NameList); i+=1)
Name=StringFromList(i, NameList, ";")
KillWins("NAC_"+Name)
Wave Detector="$root:NAC:"+Name+":Detector"
7606 Detector*=-1
EndFor
Return NaN
End
//
Function NAC_RemoveBaseline
7611 Function NAC_RemoveBaseline()
String ExpList="BeforeCoating;AfterCoating;LaserReference;Transmission;Radiation;↵
↳ ZeroSticking;Heat;Sticking;"
String FitList="Line;Exp;Exp_XOffset;DblExp;DblExp_XOffset;Sigmoid;Power;Damped ↵
↳ Oscillation;"
String Type, Name, NameList="Cancel;"
Variable i
7616 If (!DataFolderExists("root:NAC:"))
Error_Message(NAC_NotInitialized, "InProc", "NAC_DisplayStatistics", "")
Return NaN
EndIf

```

```

DFRef OldDF=GetDataFolderDFR()
7621 For (i=0;i<ItemsInList(ExpList);i+=1)
      If (Exists("root:NAC:"+StringFromList(i,ExpList, ";")+":Detector")==1)
          NameList+=StringFromList(i,ExpList, ";")+";"
      EndIf
    EndFor
7626 Prompt Name, "Remove Baseline from", Popup, NameList
    Prompt Type, "Type", Popup, FitList
    DoPrompt /HELP=" " Remove Detector Baseline ", Name, Type
    If (V_Flag || StringMatch(Name,"Cancel"))
        Error_Message(UserAbort, "InProc", "NAC_RemoveBaseline", "")
7631 Return NaN
    EndIf
    SetDataFolder $"root:NAC:"+Name
    Wave Detector
    Duplicate /O Detector BaselineFit
7636 Wave BaselineFit
    StrSwitch (Type)
      Case "Line":
        CurveFit /Q /W=2 Line, Detector /D=BaselineFit
        Break
7641 Case "Exp":
        CurveFit /Q /W=2 Exp, Detector /D=BaselineFit
        Break
      Case "Exp_XOffset":
        CurveFit /Q /W=2 Exp_XOffset, Detector /D=BaselineFit
7646 Break
      Case "DblExp":
        CurveFit /Q /W=2 DblExp, Detector /D=BaselineFit
        Break
      Case "DblExp_XOffset":
7651 CurveFit /Q /W=2 DblExp_XOffset, Detector /D=BaselineFit
        Break
      Case "Sigmoid":
        CurveFit /Q /W=2 Sigmoid, Detector /D=BaselineFit
        Break
7656 Case "Power":
        CurveFit /Q /W=2 Power, Detector /D=BaselineFit
        Break
      Case "Damped Oscillation":
        Make /O /D /N=5 BaselineCoef={0,1,0.05,0.01,0}
7661 FuncFit /Q /NTHR=0 DampedOscillation BaselineCoef Detector /D=BaselineFit
        Break
      Default:
        BaselineFit=0
        Error_Message(NAC_UnknownFitFunction, "InProc", "NAC_RemoveBaseline", Name)
7666 Return NaN
        Break
    EndSwitch
    Detector-=BaselineFit
    SetDataFolder OldDF
7671 Return NaN

```

```

End
//

```

ZeroOffset

```

Function ZeroOffset(GraphName, [StartX, EndX])
String GraphName
7676 Variable StartX, EndX
String TraceList
Variable i, ofs
    If (Strlen(GraphName))
        DoWindow $GraphName
7681 If (V_Flag!=1)
            Return -1 //No Such Window
        EndIf
    EndIf
    If (ParamIsDefault(StartX))
7686 StartX=-Inf
    EndIf

```

```

EndIf
If (ParamIsDefault(EndX))
  EndX=Inf
EndIf
7691 TraceList=TraceNameList(GraphName, ";", 1)
For (i=0;i<ItemsInList(TraceList, ";");i+=1)
  Wave Process=TraceNameToWaveRef(GraphName, StringFromList(i, TraceList, ";"))
  Ofs=Mean(Process, StartX, EndX)
  ModifyGraph Offset($StringFromList(i, TraceList, ";"))={0, -Ofs}
7696 EndFor
Return 0 // No Error
End
//

```

C.1.11 Extensions to the Status Package

```
//
```

Function Status_DisplayNAC

```

7701 Function NAC_DisplayStatus()
Variable Error
  If (!DataFolderExists("root:Status"))
    Error_Message(NAC_NoDataLoaded, "NAC_DisplayStatus", "InProc", "")
    Return NaN
7706 EndIf
Error_Message(Status_DisplayAll("Temp_1", WindowName="Baffle"), "↵
  ↳ Status_DisplayAll", "NAC_DisplayAll", "Baffle")
Error_Message(Status_DisplayAll("Temp_2", WindowName="Sample"), "↵
  ↳ Status_DisplayAll", "NAC_DisplayAll", "Sample")
Error_Message(Status_DisplayAll("Temp_3", WindowName="Reservoir"), "↵
  ↳ Status_DisplayAll", "NAC_DisplayAll", "Reservoir")
Error_Message(Status_DisplayAll("Temp_4", WindowName="Source"), "↵
  ↳ Status_DisplayAll", "NAC_DisplayAll", "Source")
7711 Error_Message(Status_DisplayAll("Temp_5", WindowName="TSP"), "Status_DisplayAll↵
  ↳ ", "NAC_DisplayAll", "TSP")
Error_Message(Status_DisplayAll("Temp_6", WindowName="QCM"), "Status_DisplayAll↵
  ↳ ", "NAC_DisplayAll", "QCM")
Error_Message(Status_DisplayAll("Temp_7", WindowName="LLEvap"), "↵
  ↳ Status_DisplayAll", "NAC_DisplayAll", "LLEvap")
Error_Message(Status_DisplayAll("Temp_8", WindowName="Block"), "↵
  ↳ Status_DisplayAll", "NAC_DisplayAll", "Block")
Error_Message(Status_DisplayAll("Temp_CJC", WindowName="CJCRef"), "↵
  ↳ Status_DisplayAll", "NAC_DisplayAll", "CJCRef")
7716 Error_Message(Status_DisplayAll("P_1", WindowName="Pirani"), "Status_DisplayAll↵
  ↳ ", "NAC_DisplayAll", "P_1")
Error_Message(Status_DisplayAll("P_2", WindowName="Pirani", Right=1), "↵
  ↳ Status_DisplayAll", "NAC_DisplayAll", "P_2")
Error_Message(Status_DisplayAll("P_I", WindowName="IonGauge"), "↵
  ↳ Status_DisplayAll", "NAC_DisplayAll", "P_I")
Error_Message(Status_DisplayAll("Evap_U", WindowName="EvaporatorVoltage"), "↵
  ↳ Status_DisplayAll", "NAC_DisplayAll", "Evap_U")
Error_Message(Status_DisplayAll("Evap_I", WindowName="EvaporatorCurrent"), "↵
  ↳ Status_DisplayAll", "NAC_DisplayAll", "Evap_I")
7721 ModifyGraph /W=Pirani Log(Left)=1, Log(Right)=1
SetAxis /W=Pirani Left 0.1,1000
SetAxis /W=Pirani Right 0.1,1000
ModifyGraph /W=IonGauge Log(Left)=1
SetAxis /W=IonGauge Left 1e-9,1e-6
7726 Return NoError
End
//

```

C.1.12 Version History

```

//Version Changes
// Version 1.x
7731 // Ole's Version with Odd/Even Pulses
// Version 2.x
// Completely Rewritten with Datafolders
// New Fitting Approach

```

```
// Version 3.0
7736 // Removed Gain Measurement completely
// Changed Internal Data Structure to 2D-Waves [time][pulse#]
// Removed "Flagged" wave: much faster GUI experience
// Basic Error Message System
// Version 3.1
7741 // Error Message System
// Removed Gains from Program
// Function Included in ErrorMessage
// Display for Deconvoluted Averages
// FIXED: Fit Crash on no LaserPower for GetRatio / NormalizeFitWave
7746 // Version 3.2
// Use Fitted Radiation contribution
// Changed Error System
// FIXED: Wrong multilayer average range on start
// FIXED: Missing Ads / Ref correction on source temperature change
7751 // FIXED: Trend not used for Sticking
// Version 3.3
// "Energies" changed to "Enthaplies"
// Experiment averaging implemented
// Version 3.4
7756 // Error Subsystem as independent module
// Flagged pulses yield NaN as enthalpy
// Version 3.5
// Import parsing altered
// LaTeX sectioning included
7761 // Auxilaries typo fixed
// Version 3.6
// Versioninfo for project added
// Statistics for Averages added
// LaserCal renamed to LaserReference
7766 // Version 3.7
// DoWindow /C/N replaced
// New Deconvolution routine
// Deconvolution Browsing implemented
// Wrong filename in deconvoluted data fixed
7771 // Experiment version update implemented
// Persistent cursors
// Version 3.8
// Discrimination between Frames and Pulses
// FIXED "No status loaded" bug
7776 // Changes in "Process Rate"
// Statistics reset upon load implemented
// ExperimentName added
// UpdateExperiment in menu
// Check for sample rate removed
7781 // FIXED "LoadLazy" Bug
// Added "Missing Laser Power" info
// FIXED outdated assignment for .usd files
// FIXED Blank in aux files "ChannelName [Unit]"
// FIXED Missing update for FittedRate info box
7786 // Included Substance in FittedRate info box
// Added SubstanceName for Rate, GetSubstanceName function
// Removed unused DeconvFit
// DeconvolutionFunction simplified
// Deconvolution fit functions modified: offset set to 0, peakstart set to 0 (↙
↳ both from fitted waves)
7791 // Preserved Offset in Highpass filtering
// Units in parentheses
// More substances for GetSubstanceName added
// Correction for wrong PTCDA density implemented
// LasPowCorr renamed to LaserPowerCorrection
7796 // Version 3.9
// Support for supplementary experiments enhanced
// FIXED Missing average in flag window
// FIXED High pass filtering for QMS channel removed
// FIXED Missing SwitchDeadTime for Concat
7801 // Added feature to correct manually for gains in old data
// MISTAKE: Separate deconvolution measurement needed for LT data.
```

```

//     FIXED Error on DisplayStatisticcs from menu
//     FitCoef waves double precision
//     FlagList waves changed to UByte, Unit "Frame"
7806 // Version 3.10 alpha
//     FIXED: NAC_RefEnthalpy("Zn", x) returning NaN
//     FIXED: Sensitivity assumed as 1 if NaN
//     Added Deconvolution to Invert function
//     Added Option to keep filter residue in load function
7811 // Line Notch filter with reduced from 2 Hz to 1 Hz
// Version 3.10 beta
//     Removed "Statistics" section from Menu
//     DisplayStickingAverage() removed
//     FIXED: IFFT of missing residual wave
7816 // FIXED: Pluse length detection failed with shifted pulses, window increased
//     FIXED: Boundaries for monolayer density
//     Applicable checks extended
//     Results Display label changed to "Present"
//     FIXED runtime error in Quartiles if all frames are flagged
7821 // :Experiment:Timeline removed
//     ChiSquared for statistics added
//     ReflecBefore renamed to BeforeCoating
//     ReflecAfter renamed to AfterCoating
//     2nd Notch filter added
7826 // Worlking Version 3.10 gamma
//     Outliers for BoxPlot added
//     Signal Inversion more convenient
//     Option to display data points in box plots added
//     Function to reset the flag list implemented
7831 // Version 3.10 delta
//     Update bugs fixed
//     Reflectivity for deconvolution linked to clean reflectivity
//     Reflectivity import from files prepared
//     FIXED Index bug in Quartile
7836 // FIXED Too many frames automatically flagged for deconvolution
//     Added Unload Measurement
//     Renamed RateCal to RateCalorimetry
//     Renamed RateCoat to RateCoating
//     Selectable LaserPowerCorrection implemented
7841 // Selectable Standard Reflectivities implemented
// Version 3.10 epsilon
//     FIXED Error on removal of not displayed experiments in averages
//     Included Liberal Names for Experiments
//     Simultaneous loadig of multiple experiments for averaging added
7846 // FIXED NAC_RefEnthalpy returning NaN for T_Sample-T_Ref
//     Improved HeatTextBox information
//     FIXED NaN ranges for statistics if all frames are flagged
//     Flagged frames lowlighted in trend creation
//     FIXED Crash on renamed / deleted active folder in loadig routines
7851 // Legend for Averaging movable
//     Init- / Hold-Sticking renamed to -Desorption
//     FIXED Crash on Enthalpy zero data points and sticking finite data points
//     Fixed ChiSq not stored for statistics
//     Fixed CpCondensed / CvGas mixup
7856 // Implemented Loaded Trends
//     Incompatible experiments are loaded on activated Load Supporting Files with ↵
//     ↵ a warning
//     Fixed "Apparent" typo
// Version 3.11
//     Minor beauty fixes
7861 // Version 3.12
//     Renamed Flux to (deposition) RATE (Fluxes are Unit per square meter and ↵
//     ↵ second)
//     Load of averaged experiments Version dependent
//     Renamed NAC_UnknownExperiment to NAC_UnknownMeasurement
//     Implemented linking of heat and radiation shifts
7866 // Removal of main structure implemented (used for meta-experiments)
// Version 3.13
//     Fixed wrong procedure for DisplayRateData-Button
//     Fixed wrong coloring of full data after processing

```

```
//      Looped FittedTrends implemented
7871 //      Minor fixes on Trend Controls
//      Force-Killed ControlPanel is recreated automatically
//      Bigger symbols for "Averaged Results" graphs
//      LegendLines in averaging settings
//      Minor correction of pristine reflectivity
7876 //      Patch error for statistics fixed
//      Version 3.14
//      Data loading speed optimized
//      Reflectivity assignment from files modified
//      Version 3.15
7881 //      Option for calculated radiation contribution added (not verified in ↗
      ↘ experiment)
//      Release
//      Future Versions 4.x
//      Implement Measurement Subsystem
//      Implement Control Subsystem
```

C.2 Error Handling Package

Details about the error handling package are discussed in Section 4.3. Subsequently, the source code of this package is listed.

```
1 //Errors.ipf//
```

C.2.1 Definitions

```
//
```

Compiler Settings

```
#pragma rtGlobals=3 // Use modern global access method.
```

```
#pragma Version=1.0
```

```
6 #pragma IgorVersion=6.2
```

```
//
```

Data Paths

```
StrConstant ErrorDataFolder="root:Errors"
```

```
//
```

Standard Errors

```
Constant NoError=0
```

```
11 Constant NoErrorHandler=43001
```

```
Constant ErrorHandled=43002
```

```
Constant LoadAborted=43003
```

```
Constant UserAbort=43004
```

```
Constant UserCancel=43005
```

```
16 //
```

Constants

```
Constant Error_TalkLevel=3
```

```
//No Errors (0,1), Serious Errors (2,3), Handled Errors (4,5), Exceptions(8,9)
```

```
//Odd: Include procedure name etc.
```

```
//
```

C.2.2 Initialization

```
21 //
```

Function Error_Init

```
Function Error_Init()
```

```
DFRef OldDF=GetDataFolderDFR()
```

```
  If (!DataFolderExists(ErrorDataFolder))
```

```
    NewDataFolder /S $ErrorDataFolder
```

```
26  EndIf
```

```
  Make /O /N=1 /T ErrorList="No Error"
```

```
  SetDataFolder OldDF
```

```
  Error_Panel()
```

```
  DoWindow /F Error_Messages
```

```
31 End
```

```
//
```

C.2.3 Error Handling

```
//
```

Function Error_Clear

```
Function Error_Clear()
```

```
  If (DataFolderExists(ErrorDataFolder))
```

```
36    Wave /T Errors=$ErrorDataFolder+":ErrorList"
```

```
    Redimension /N=1 Errors
```

```
    Errors[0]="No Error"
```

```
    MoveWindow /W=Error_Messages 0, 0, 0, 0
```

```
    DoUpdate
```

```
41  EndIf
```

```
  Return NoError
```

```
End
//
Function Error_Add
Static Function Error_Add(Msg)
46 String Msg
Wave /T Errors=$ErrorDataFolder+":ErrorList"
  If (StringMatch(Errors[0],"No Error"))
    Errors[0]=Msg
  Else
51   ReDimension /N=(NumPnts(Errors)+1) Errors
    Errors[NumPnts(Errors)-1]=Msg
  EndIf
  DoWindow /F Error_Messages
  Return NoError
56 End
//
Function Error_Message
Function Error_Message(ErrorCode, FunctionName, ProcedureName, Argument)
Variable ErrorCode
String FunctionName, ProcedureName, Argument
61 If (!DataFolderExists(ErrorDataFolder))
  Error_Init()
  EndIf
  If (NumType(ErrorCode)) //NaN or INF
    ErrorCode=NoErrorHandler
66 EndIf
  If (Mod(Error_TalkLevel,2)) //// How much talking?
    ProcedureName=FunctionName+"("+Argument+")@"+"ProcedureName+": "
  Else
    ProcedureName=""
71 EndIf
  Switch (Error_TalkLevel)
    Case 8: // Common and well handled exceptions
    Case 9:
      Switch (ErrorCode)
76       Case NAC_ReEntry:
          Error_Add(ProcedureName+ "Procedure ReEntry")
          Break
          Case NAC_WindowAlreadyExists:
            Error_Add(ProcedureName+ "Window Already Exists")
81           Break
            Case ErrorHandler:
              Error_Add(ProcedureName+ "Error Already Handled")
              Break
            Default:
86             Break
          EndSwitch // No Break!
    Case 4: // Expected and well handled errors
    Case 5:
      Switch (ErrorCode)
91       Case NoError:
          Case NoErrorHandler: // Serious Errors to be handled further on
          Case NAC_DataFolderError:
          Case NAC_NotApplicable:
          Case NAC_DataMismatch:
96       Case NAC_UnknownMeasurement:
          Case NAC_ReEntry:
          Case NAC_WindowAlreadyExists:
          Case NAC_AuxFileNotFound:
          Case NAC_AuxFileLoadFailed:
101      Case NAC_PulseLengthDetectionFailed:
          Case NAC_LaserPowerMissing:
          Case NAC_NoDataLoaded:
          Case NAC_NotImplementedYet:
          Case NAC_CorruptExperiment:
106      Case NAC_DataFolderError:
          Case NAC_IncompatibleExperiment:
```



```

Case NAC_UnknownVersion:
Case Status_ChannelNotExistant:
Case Status_NoSuchWindow:
111     Break
Case NAC_NoSuchWindow:
    Error_Add(ProcedureName + "No Such Window")
    Break
Case LoadAborted:
116     Error_Add(ProcedureName + "Load Aborted")
    Break
Case NAC_NothingToProcess:
    Error_Add(ProcedureName + "Nothing To Process")
    Break
121     Case NAC_FitWavesMissing:
        Error_Add(ProcedureName + "Fit Wave Missing")
        Break
Case UserAbort:
    Error_Add(ProcedureName + "User Abort")
126     Break
Case NAC_AverageWavesMissing:
    Error_Add(ProcedureName + "Averaged Waves Missing")
    Break
Case NAC_WrongCursor:
131     Error_Add(ProcedureName + "Wrong Cursor")
    Break
Case NAC_StickingMissing:
    Error_Add(ProcedureName + "Sticking Wave Missing")
    Break
136     Case NAC_AdsorptionMissing:
        Error_Add(ProcedureName + "Adsorption Wave Missing")
        Break
Case NAC_DoseMissing:
    Error_Add(ProcedureName + "Dose not Calculated")
141     Break
Case NAC_AvgAlreadyInitialized:
    Error_Add(ProcedureName + "Average Subsystem Already Initialized")
    Break
Case NAC_ParameterOutsideRange:
146     Error_Add(ProcedureName + "Parameter Outside Allowed Range")
    Break
Case NAC_NotInitialized:
    Error_Add(ProcedureName + "NAC Package not Initialized")
    Break
151     Default:
        Error_Add(ProcedureName + "Unknown Error #" + Num2Str(ErrorCode))
        Break
EndSwitch // No Break!
Case 2: // Should not happen errors
Case 3:
156     Switch (ErrorCode)
        Case NoError:
            Break
        Case NAC_NotApplicable:
            Error_Add(ProcedureName + "Not Applicable !")
            Break
161     Case NAC_DataMismatch:
            Error_Add(ProcedureName + "DataMismatch !")
            Break
166     Case NAC_UnknownMeasurement:
            Error_Add(ProcedureName + "Unknown Measurement !")
            Break
        Case NoErrorHandler:
            Error_Add(ProcedureName + "No Error Handler !")
            Break
171     Case NAC_AuxFileNotFound:
            Error_Add(ProcedureName + "Auxillary File not Found !")
            Break
        Case NAC_AuxFileLoadFailed:
176     Error_Add(ProcedureName + "Failed to Load Auxillary File !")

```

```

        Break
    Case NAC_UnknownFitFunction:
        Error_Add(ProcedureName + "Unknown Fit Function !")
        Break
181   Case NAC_PulseLengthDetectionFailed:
        Error_Add(ProcedureName + "Automatic Pulse Length Detection Failed !")
        Break
    Case NAC_LaserPowerMissing:
186   Error_Add(ProcedureName + "Laser Power Missing !")
        Break
    Case NAC_NoDataLoaded:
        Error_Add(ProcedureName + "No Data Loaded !")
        Break
191   Case NAC_NotImplementedYet:
        Error_Add(ProcedureName + "Not Implemented Yet !")
        Break
    Case NAC_CorruptExperiment:
        Error_Add(ProcedureName + "Corrupt Experiment Structure !")
        Break
196   Case NAC_IncompatibleExperiment:
        Error_Add(ProcedureName + "Incompatible Experiment !")
        Break
    Case NAC_DataFolderError:
        Error_Add(ProcedureName + "Reinitialization failed - close all user ↵
↳ objects and try again !")
201   Break
    Case Status_ChannelNotExistant:
        Error_Add(ProcedureName + "Channel not existant !")
        Break
206   Case Status_NoSuchWindow:
        Error_Add(ProcedureName + "No such window !")
        Break
    Case NAC_UnknownVersion:
        Error_Add(ProcedureName + "Unknown version number !")
        Break
211   Default:
        Break
        EndSwitch // No Break!
        Case 0: // No Error report
        Case 1:
216   Default:
        Break
        EndSwitch
        DoUpdate
        Return ErrorCode
221 End
    //

```

C.2.4 Graphical User Interface

```

//
Function Error_Panel
Function Error_Panel()
    DoWindow Error_Messages
226   If (V_Flag)
        Return NoError
    EndIf
    NewPanel /K=2 /W=(1300,70,1800,220) /N=Error_Messages as "Error Messages"
    ModifyPanel fixedsize=1
231   ListBox Errors Size={500,150}, Pos={0,0}, listWave=$ErrorDataFolder+":ErrorList↵
↳ "
        SetActiveSubwindow _endfloat_
        Return NoError
    End
    //

```

C.2.5 Version History

```

236 // Version Changes

```

```
// Version 1.0
//   FIXED "No popup on a single error"
//   Renamed NAC_UnknownExperiment to NAC_UnknownMeasurement
```

C.3 Machine Status Package

Details about the machine status package are discussed in Section 4.4. Subsequently, the source code of this package is listed.

```
//Status.ipf//
```

2 C.3.1 Definitions

```
//
```

Compiler Settings

```
#pragma rtGlobals=3 // Use modern global access method.  
#pragma Version=1.2  
#pragma IgorVersion=6.2
```

```
7 //
```

Data Paths

```
StrConstant Status_DataFolderStr="root:Status"
```

```
//
```

Constants

```
StrConstant Status_DataPathStr="Z:Marburg:Data:Calorimetry:StatusLogging:"  
StrConstant Status_Version="1.2 alpha"
```

```
12 //
```

Error Codes

```
Constant Status_ChannelNotExistant=44101  
Constant Status_InvalidDateFormat=44102  
Constant Status_NoSuchWindow=44103  
Constant Status_NothingToDisplay=44001  
Constant Status_LoadFailed=44002
```

```
17 //
```

Menu

```
Menu "Status"
```

```
  "Import Machine Status", /Q, Error_Clear(); Status_Import()
```

```
  "Display all Data for a Channel", /Q, Error_Clear(); Status_DisplayChannel()
```

```
22  "Get Runtime for Top Window", /Q, Error_Clear(); Status_GetRuntimeMenu()
```

```
End
```

```
//
```

C.3.2 File Input/Output

```
//
```

Function Status_Import

```
Function Status_Import()
```

```
27 String FileList
```

```
Variable i
```

```
DFRef OldDF=GetDataFolderDFR()
```

```
  If (DataFolderExists(Status_DataFolderStr))
```

```
    SetDataFolder $Status_DataFolderStr
```

```
32  Else
```

```
    NewDataFolder /S $Status_DataFolderStr
```

```
    NewPath /O /Q StatusDataPath Status_DataPathStr
```

```
  EndIf
```

```
  Open /D /MULT=1 /R /P=StatusDataPath /F="Logging Files (*.log):.log;All Files ↵  
    ↵ (*.*):.*;" /M="Machine Status: Select Logging Files for Import" i
```

```
37  If (!StrLen(S_FileName))
```

```
    Error_Message(UserAbort, "InProc", "Status_Import", "")
```

```
    SetDataFolder OldDF
```

```
    Return NaN
```

```
  EndIf
```

```
42  For (i=0; i<ItemsInList(S_FileName, "\r"); i+=1)
```

```

    Error_Message(Status_Load(StringFromList(i, S_FileName, "\r")), "↵
    ↵ Status_Import", "Status_Load", "")
EndFor
SetDataFolder OldDF
Return NaN
47 End
//
Function Status_Load
Function Status_Load(FileName)
String FileName
DFRef OldDF=GetDataFolderDFR()
52 String HeaderLine="", TempString="", ListItem=""
String NameList="", UnitList="", DateString="", dUnit
Variable RefNum, i
    If (DataFolderExists(Status_DataFolderStr))
        SetDataFolder $Status_DataFolderStr
57 Else
        NewDataFolder /S $Status_DataFolderStr
        NewPath /O /Q StatusDataPath Status_DataPathStr
    EndIf
    Open /R /P=StatusDataPath /F="Logging Files (*.log):.log;All Files (*.*):.*;" ↵
        ↵ RefNum as FileName
62 If (StrLen(S_FileName)==0)
        Close RefNum
        Return LoadAborted
    EndIf
    String Day, Month, Year
67 DateString=S_FileName[StrSearch(S_FileName, ":", Inf, 3)+1,StrSearch(S_FileName ↵
        ↵, ".", Inf, 3)-1]
    Switch (StrLen(DateString))
        Case 6:
            Day=DateString[0,1]
            Month=DateString[2,3]
72 Year="20"+DateString[4,5]
            Break
        Case 8:
            Day=DateString[6,7]
            Month=DateString[4,5]
77 Year=DateString[0,3]
            Break
        Case 10:
            Day=DateString[8,9]
            Month=DateString[5,6]
82 Year=DateString[0,3]
            Break
        Default:
            Return Status_InvalidDateFormat
            Break
87 EndSwitch
    DateString=Year+"-"+Month+"-"+Day
    If (DataFolderExists(Status_DataFolderStr+": "+PossiblyQuoteName(DateString)))
        DoAlert /T="Status Import", 1, DateString+" already imported.\r\rOverwrite?"
        If (V_Flag==2)
92 Close RefNum
            Return UserAbort
        EndIf
    EndIf
    NewDataFolder /O/S $(Status_DataFolderStr+": "+PossiblyQuoteName(DateString))
97 TempString=""
    FReadLine RefNum, HeaderLine
    Close RefNum
    For (i=0;i<ItemsInList(HeaderLine, "\t");i+=1)
        ListItem=StringFromList(i,HeaderLine, "\t")
102 If (StringMatch(ListItem, "NC*") || StringMatch(ListItem, "N/C*"))
            TempString+="C=1,N='_skip_' ; "
        ElseIf (StringMatch(ListItem, "N/A*"))
            TempString+="C=1,N='_skip_' ; "
        ElseIf (StringMatch(ListItem, "*[TXT]*"))

```

```

107     TempString+="C=1,F=-2,N="+ListItem[0,StrSearch(ListItem, "[", Inf, 3)-1]+";↵
↵     "
    NameList+=ListItem[0,StrSearch(ListItem, "[", Inf, 3)-1]+";"
    UnitList+="TXT;"
    ElseIf (StringMatch(ListItem,"Time*"))
    TempString+="C=1,F=7,T=4,N=Timeline; "
112     NameList+="Timeline;"
    UnitList+="dat;"
    ElseIf (StringMatch(ListItem,"Temp_CSC*"))
    TempString+="C=1,F=0,T=2,N=Temp_CJC; "
    NameList+="Temp_CJC;"
117     UnitList+=ListItem[StrSearch(ListItem, "[", 0, 2)+1,StrSearch(ListItem, ↵
↵ "]" , Inf, 3)-1]+";"
    ElseIf (StringMatch(ListItem,"I*"))
    TempString+="C=1,F=0,T=2,N=Evap_I; "
    NameList+="Evap_I;"
    UnitList+=ListItem[StrSearch(ListItem, "[", 0, 2)+1,StrSearch(ListItem, ↵
↵ "]" , Inf, 3)-1]+";"
122     ElseIf (StringMatch(ListItem,"U*"))
    TempString+="C=1,F=0,T=2,N=Evap_U; "
    NameList+="Evap_U;"
    UnitList+=ListItem[StrSearch(ListItem, "[", 0, 2)+1,StrSearch(ListItem, ↵
↵ "]" , Inf, 3)-1]+";"
    Else
127     TempString+="C=1,F=0,T=2,N="+ListItem[0,StrSearch(ListItem, "[", Inf, 3)↵
↵ -1]+"; "
    UnitList+=ListItem[StrSearch(ListItem, "[", 0, 2)+1,StrSearch(ListItem, ↵
↵ "]" , Inf, 3)-1]+";"
    NameList+=ListItem[0,StrSearch(ListItem, "[", Inf, 3)-1]+";"
    EndIf
EndFor
132 LoadWave /O /A /B=TempString /J /L={0,1,0,0,0} /Q S_FileName
If (V_flag==0)
    Print "Failed to load status file!"
    SetDataFolder OldDF
    Return Status_LoadFailed
137 EndIf
For (i=0;i<ItemsInList(NameList, ";"); i+=1)
    Wave Process=$StringFromList(i,NameList, ";")
    StrSwitch(StringFromList(i,UnitList, ";"))
    Case "mBar":
142     Process*=100
        dUnit="Pa"
        Break
    Case "Torr":
147     Process*=101325/760
        dUnit="Pa"
        Break
    Case "nm":
152     Process/=1e9
        dUnit="m"
        Break
    Case "C":
    Case "degC":
157     Process+=273.15
        dUnit="K"
        Break
    Case "F":
    Case "degF":
162     Process=(Process + 459.67)*5/9
        dUnit="K"
        Break
    Default:
167     dUnit=StringFromList(i,UnitList, ";")
        Break
EndSwitch
SetScale d, 0, 0, dUnit, $StringFromList(i,NameList, ";")
SetScale /P x, 0, 1, " ", $StringFromList(i,NameList, ";")
StrSwitch(StringFromList(i, NameList, ";"))

```

```

        Case "Timeline":
            Wave Timeline
172         Timeline+=Date2Secs(Str2Num(Year), Str2Num(Month), Str2Num(Day))
            Break
        Default:
            Break
        EndSwitch
177     EndFor
        SetDataFolder OldDF
        Return NoError
    End
    //

```

C.3.3 User Interface

```

182 //
Function Status_GetRuntimeMenu

Function Status_GetRuntimeMenu()
Variable Threshold
    Prompt Threshold, "Enter Threshold for On State: "
    DoPrompt "Missing Value", Threshold
187     If (!NumType(Threshold) && !V_Flag)
        Status_AddRuntimeText(Status_GetRuntime(Threshold), Threshold)
    EndIf
End
//
Function Status_AddRuntimeText

192 Function Status_AddRuntimeText(Runtime, Threshold, [WindowName])
Variable RunTime, Threshold
String WindowName
String Unit="s"
    If (ParamIsDefault(WindowName))
197         WindowName=""
    EndIf
    If (ItemsInList(WinList(";", "WIN:"+WindowName), ";")!=1)
        Return Status_NoSuchWindow
    EndIf
202 WindowName=StringFromList(0, WinList(";", "WIN:"+WindowName), ";")
    If (Runtime>2*60*60*24)
        Runtime/=60*60*24
        Unit="d"
    ElseIf (Runtime>2*60*60)
207         Runtime/=60*60
        Unit="h"
    ElseIf (Runtime>=5*60)
        Runtime/=60
        Unit="min"
212     EndIf
    Textbox /W=$WindowName /A=MT /E /C /F=0 /X=0 /Y=5 /N=Runtime "Runtime for "+↵
        ↵ WindowName+" (Value >=" + Num2Str(Threshold) + "): " + Num2Str(Runtime) + ↵
        ↵ " " + Unit
    Return NoError
End
//
Function Status_DisplayChannel

217 Function Status_DisplayChannel([Channel, ChannelName, Align])
String Channel, ChannelName
Variable Align // 1 for left axis, 2 for right axis
String ChannelList, TmpS
    If (ParamIsDefault(Align))
222         Align=1
    EndIf
    If (ParamIsDefault(Channel))
        ChannelList=Status_ListChannelNames()
        Prompt TmpS, "Channel to display: ", popup, ChannelList
227     DoPrompt "Status Display", TmpS
        If (V_Flag)

```

```

        Return UserCancel
    EndIf
    Channel=TmpS
232 EndIf
    If (ParamIsDefault(ChannelName))
        ChannelName=Channel
        Prompt TmpS, "Display Name of Channel "+Channel+": "
        Prompt Align, "Select y-Axis: ", popup, "Left;Right"
237 DoPrompt "Status Display", TmpS, Align
        If (V_Flag || !StrLen(TmpS))
            Return UserCancel
        EndIf
        ChannelName=TmpS
242 EndIf
    Status_DisplayAll(Channel, WindowName=ChannelName, Right=Align-1)
End
//
Function Status_Display
Function Status_Display(DateStr, ChannelStr, [Right, New, WindowName])
247 String DateStr, ChannelStr
    Variable Right, New
    String WindowName
    String Wins
    Switch (StrLen(DateStr))
252     Case 6:
        DateStr="20"+DateStr[4,5]+"-"+DateStr[2,3]+"-"+DateStr[0,1]
        Break
        Case 8:
257     DateStr=DateStr[0,3]+"-"+DateStr[4,5]+"-"+DateStr[6,7]
        Break
        Case 10:
            Break
        Default:
262     Return Status_InvalidDateFormat
        Break
    EndSwitch
    If (Exists(Status_DataFolderStr+"."+PossiblyQuoteName(DateStr)+"."+ChannelStr) &
        ↵ !=1)
        Return Status_ChannelNotExistant
    EndIf
267 Wins=WinList("*, ";, "WIN:1")
    If (ParamIsDefault(Right))
        Right=0
    EndIf
    If (ParamIsDefault(New))
272     New=0
    EndIf
    If (ParamIsDefault(WindowName))
        WindowName=""
    EndIf
277 String DateName=PossiblyQuoteName(DateStr)
    String TraceName=ChannelStr+"@"+DateStr
    If (New || (ItemsInList(Wins)==0))
        If (StrLen(WindowName))
            Display /K=1 /N=$WindowName $(Status_DataFolderStr+"."+DateName+"."+↵
            ↵ ChannelStr) /TN=$TraceName vs $(Status_DataFolderStr+"."+DateName+"."↵
            ↵ Timeline") as WindowName
282     Else
            Display /K=1 /N=$WindowName $(Status_DataFolderStr+"."+DateName+"."+↵
            ↵ ChannelStr) /TN=$TraceName vs $(Status_DataFolderStr+"."+DateName+"."↵
            ↵ Timeline")
        EndIf
        Label bottom " "
        Label Left WindowName+" (\U)"
287 ModifyGraph /W=$WindowName nTicks(Bottom)=20
    Else
        If (StrLen(WindowName))
            If (!StringMatch(TraceNameList(WindowName, ";", 1), "*" + TraceName + "*"))

```



```

292     If (Right)
        AppendToGraph /W=$WindowName /R $(Status_DataFolderStr+": "+DateName ↵
↵ +":"+ChannelStr) /TN=$TraceName vs $(Status_DataFolderStr+": "+DateName+": ↵
↵ Timeline")
        ModifyGraph rgb($TraceName)=(0,0,0)
        Label Right WindowName+" (\U)"
        Else
        AppendToGraph /W=$WindowName $(Status_DataFolderStr+": "+DateName+": "+ ↵
↵ ChannelStr) /TN=$TraceName vs $(Status_DataFolderStr+": "+DateName+": ↵
↵ Timeline")
307     Label Left WindowName+" (\U)"
        EndIf
        EndIf
    Else
    If (!StringMatch(TraceNameList("", ";", 1), "*" + TraceName + "*"))
302     If (Right)
        AppendToGraph /R $(Status_DataFolderStr+": "+DateName+": "+ChannelStr) / ↵
↵ TN=$TraceName vs $(Status_DataFolderStr+": "+DateName+": Timeline")
        ModifyGraph rgb($TraceName)=(0,0,0)
        Label Right WindowName+" (\U)"
        Else
307     AppendToGraph $(Status_DataFolderStr+": "+DateName+": "+ChannelStr) /TN= ↵
↵ $TraceName vs $(Status_DataFolderStr+": "+DateName+": Timeline")
        Label Left WindowName+" (\U)"
        EndIf
        EndIf
    EndIf
312 EndIf
    Return NoError
End
//

```

Function Status_DisplayAll

```

Function Status_DisplayAll(ChannelStr, [WindowName, Right])
317 String ChannelStr, WindowName
    Variable Right
    Variable i, Folders, Plot=0
    String Folder
    Folders=CountObjectsDFR($Status_DataFolderStr, 4)
322 For (i=0; i<Folders;i+=1)
    If ((Exists(Status_DataFolderStr+": "+PossiblyQuoteName(GetIndexedObjNameDFR( ↵
↵ $Status_DataFolderStr, 4, i))+":"+ChannelStr)==1) && (Exists( ↵
↵ Status_DataFolderStr+": "+PossiblyQuoteName(GetIndexedObjNameDFR( ↵
↵ $Status_DataFolderStr, 4, i))+":TimeLine")==1))
        Plot+=1
    EndIf
EndFor
327 If (!Plot)
    Return Status_NothingToDisplay
EndIf
If (ParamIsDefault(Right))
    Right=0
332 EndIf
If (ParamIsDefault(WindowName) || !StrLen(WindowName))
    WindowName=ChannelStr
EndIf
WindowName=ReplaceString(" ", WindowName, "_")
337 For (i=0; i<Folders;i+=1)
    DoWindow $WindowName
    If (!V_Flag)
        Error_Message(Status_Display(GetIndexedObjNameDFR($Status_DataFolderStr, 4, ↵
↵ i), ChannelStr, New=1, Right=Right, WindowName=WindowName), " ↵
↵ Status_Display", "Status_DisplayAll", ChannelStr)
    Else
342     Error_Message(Status_Display(GetIndexedObjNameDFR($Status_DataFolderStr, 4, ↵
↵ i), ChannelStr, Right=Right, WindowName=WindowName), "Status_Display", " ↵
↵ Status_DisplayAll", ChannelStr)
    EndIf
EndFor

```

```

    Return NoError
End
347 //
C.3.4 Tools
//
Function Status_GetRuntime
Function Status_GetRuntime(Threshold, [WindowName, ChannelName])
Variable Threshold
String WindowName
352 String ChannelName
Variable i, Runtime=0, Use
String TraceList, Trace, ChannelStr, DateStr
If (ParamIsDefault(WindowName))
    WindowName=""
357 EndIf
If (ParamIsDefault(ChannelName))
    ChannelName=""
EndIf
TraceList=TraceNameList(WindowName, ";", 5)
362 If (!StrLen(TraceList))
    Error_Message(Status_ChannelNotExistant, "Status_GetRuntime", "InProc", ↵
    ↵ WindowName)
    Return NaN
EndIf
For (i=0; i<ItemsInList(TraceList);i+=1)
367 Use=0
Trace=StringFromList(i, TraceList, ";")
ChannelStr=Trace[1, StrSearch(Trace, "@", 0, 0)-1]
If (StrLen(ChannelName))
    If (StringMatch(ChannelStr, ChannelName))
372 Use=1
    EndIf
Else
    Use=1
EndIf
377 If (Use)
    DateStr=Trace[StrSearch(Trace, "@", 0, 0)+1, StrLen(Trace)-2]
    Wave Source=$(Status_DataFolderStr+": "+PossiblyQuoteName(DateStr)+": "+↵
    ↵ PossiblyQuoteName(ChannelStr))
    Wave TimeLine=$(Status_DataFolderStr+": "+PossiblyQuoteName(DateStr)+": ↵
    ↵ TimeLine")
    Duplicate /O /FREE Source Process
382 Process=(Process[p]>=Threshold) ? (TimeLine[Min(p+1, NumPnts(TimeLine)-1)]-↵
    ↵ TimeLine[p]) : 0
    Runtime+=Sum(Process)
EndIf
EndFor
Return Runtime
387 End
//
Function Status_ListChannelNames
Function /S Status_ListChannelNames()
String ChannelList="Timeline;", Folder
Variable i, j, Folders, Channels
392 Folders=CountObjectsDFR($Status_DataFolderStr, 4)
For (i=0; i<Folders; i+=1)
    Folder=GetIndexedObjNameDFR($Status_DataFolderStr, 4, i)
    If (Exists(Status_DataFolderStr+": "+PossiblyQuoteName(Folder)+": Timeline") ==↵
    ↵ 1)
        Channels=CountObjectsDFR($Status_DataFolderStr+": "+PossiblyQuoteName(Folder)↵
        ↵ ), 1)
397 For (j=0; j<Channels; j+=1)
    If (!StringMatch(ChannelList, "*" + GetIndexedObjNameDFR(↵
    ↵ $Status_DataFolderStr+": "+PossiblyQuoteName(Folder), 1, j) + "*" ))
        ChannelList=AddListItem(GetIndexedObjNameDFR($Status_DataFolderStr+": "+↵
        ↵ PossiblyQuoteName(Folder), 1, j), ChannelList, ";", Inf)

```

```
        EndIf
      EndFor
402    EndIf
      EndFor
      ChannelList=RemoveFromList("Timeline", ChannelList , ";")
      Return ChannelList
End
407 //
```

C.3.5 Version History

```
// Version Changes
// Version 1.0
//   First release
// Working Version 1.1
412 //   Unit conversion implemented
//   GetRuntime implemented
//   Additional display options in menu added
//   FIXED Blank in WindowName
//   FIXED wrong format loading waves for special names
```


D Overview of the Investigated Systems

This collection gathers all results obtained from experiments without diagnosed faults, providing supplementary information to Chapter 6. In the figures presenting heat and sticking results, black traces are assigned to averaged data and colored traces represent individual experiments. Additionally, the thickness of the deposited substrate layer and the flux are illustrated for each experiment.

The reference values corresponding to the sticking and the heat measurements are indicated by dashed lines.

Jumps in the traces of averaged data sets arise from inconsistent experiments. This surprising behavior is related to the different layer thicknesses of the substrates and is discussed in Sections 6.8 and 6.9.

Results involving the adsorption of copper are already presented in Section 6.6.

D.1 Magnesium Adsorbed on Pristine Detector

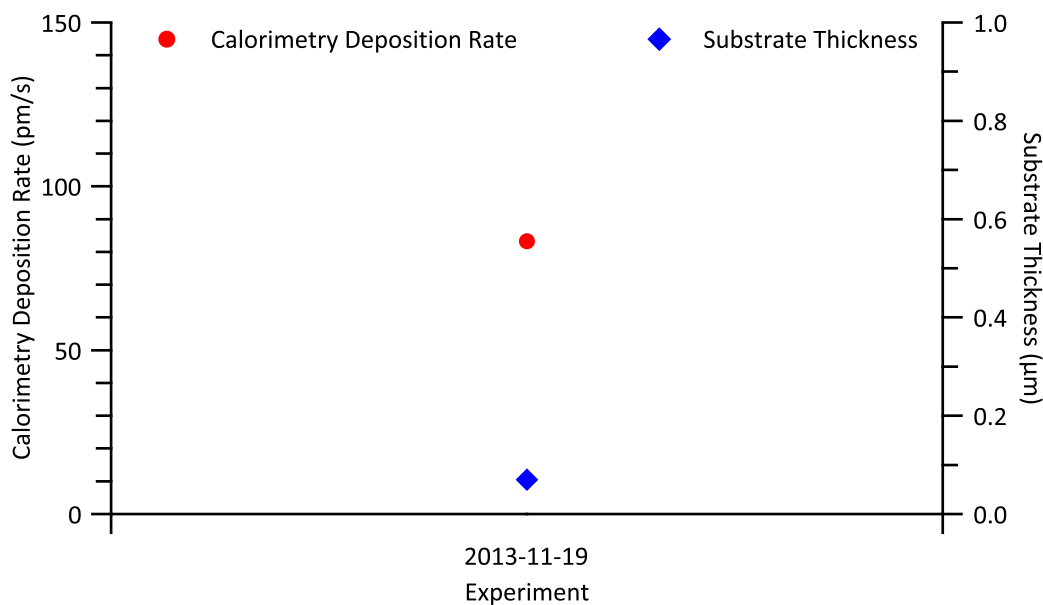


Figure D.1: Auxiliary Data for Magnesium on Pristine Detector — The calorimetry flux (magnesium – red circles) and the thickness of the organic substrate layer (contamination – blue diamonds) are given categorized by experiment.

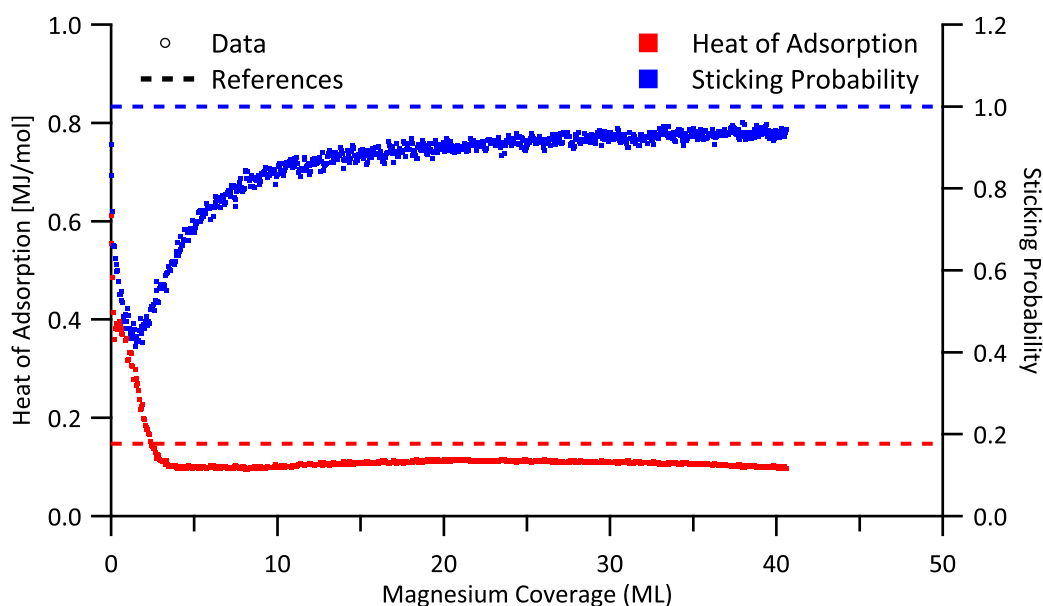


Figure D.2: Averaged Data for Magnesium on Pristine Detector — The averaged results for the heat of adsorption (red) and the sticking probability (blue) obtained from adsorption of magnesium on pristine nickel coated detector surface are given as a function of coverage.

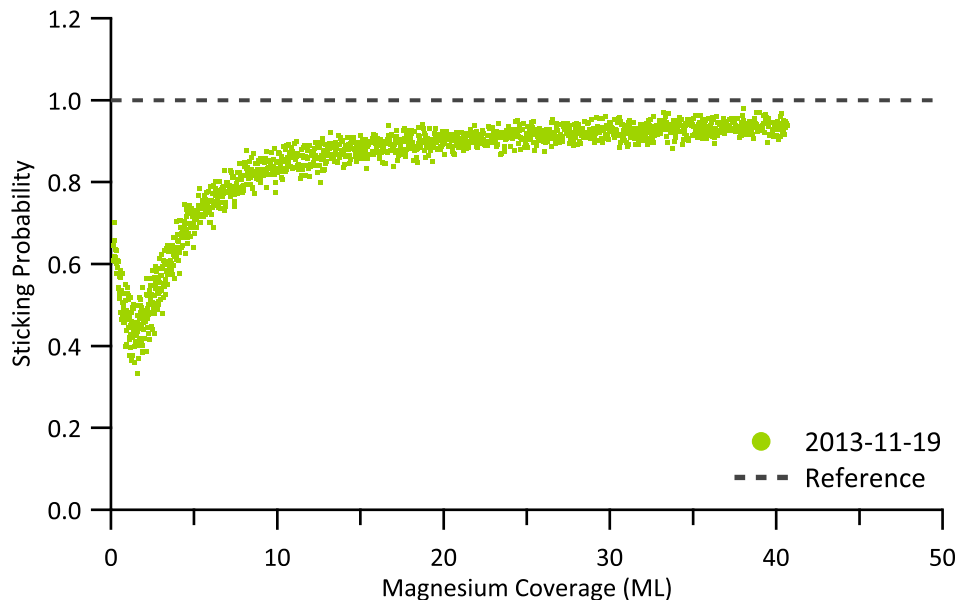


Figure D.3: Sticking Data for Magnesium on Pristine Detector — The obtained sticking probabilities of magnesium dosed on pristine nickel coated detector surface as a function coverage is shown for each individual experiment.

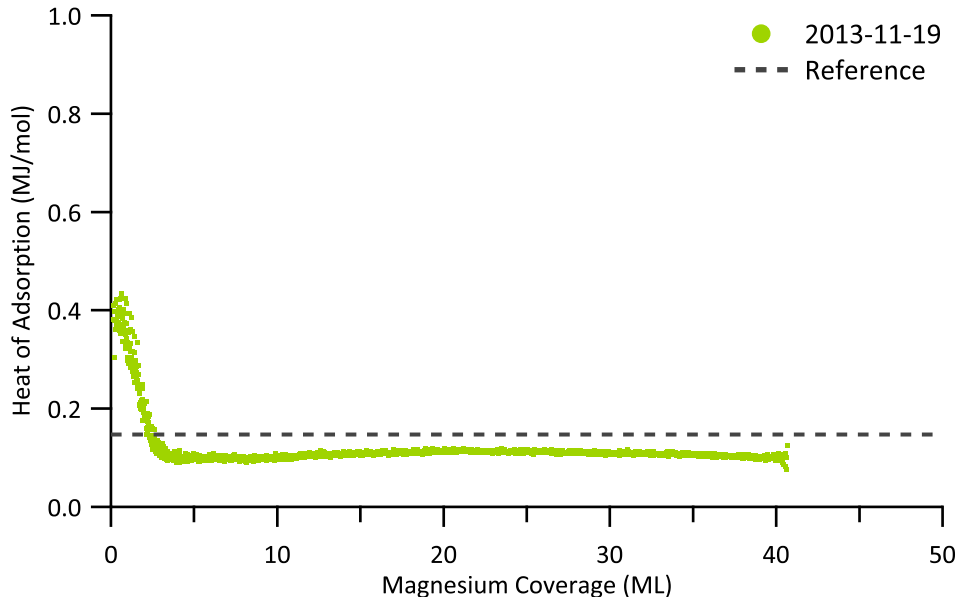


Figure D.4: Enthalpy Data for Magnesium on Pristine Detector — The obtained heat of adsorption of magnesium dosed on pristine nickel coated detector surface as a function coverage is presented for each individual experiment.

D.2 Magnesium Adsorbed on Sputter Cleaned Detector

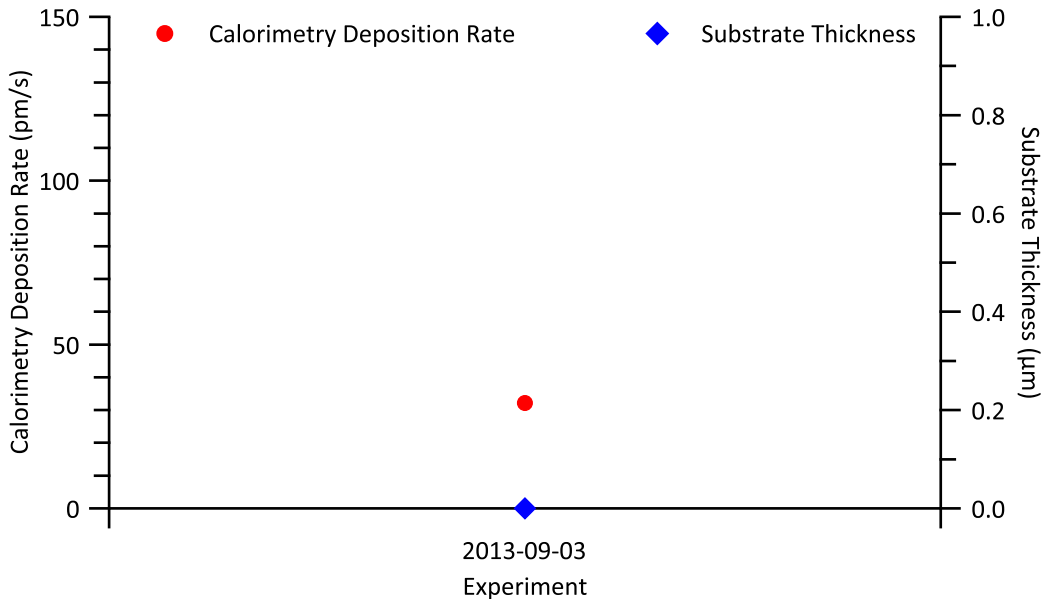


Figure D.5: Auxiliary Data for Magnesium on Sputter Cleaned Detector — The calorimetry flux (magnesium – red circles) and the thickness of the organic substrate layer (absent – blue diamonds) are given categorized by experiment.

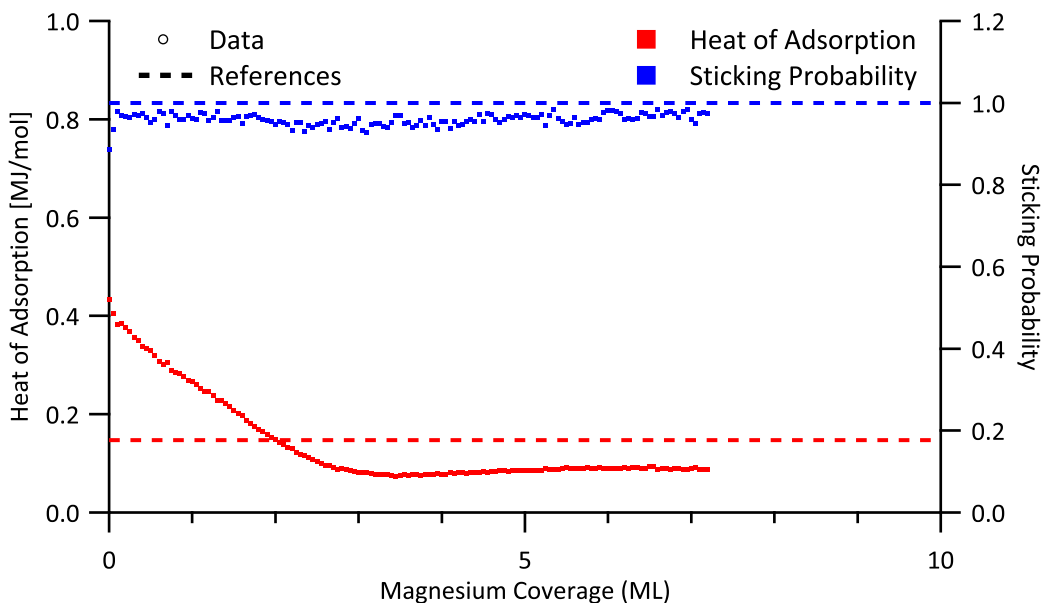


Figure D.6: Averaged Data for Magnesium on Sputter Cleaned Detector — The averaged results for the heat of adsorption (red) and the sticking probability (blue) obtained from adsorption of magnesium on sputter cleaned nickel coated detector surface are given as a function of coverage.

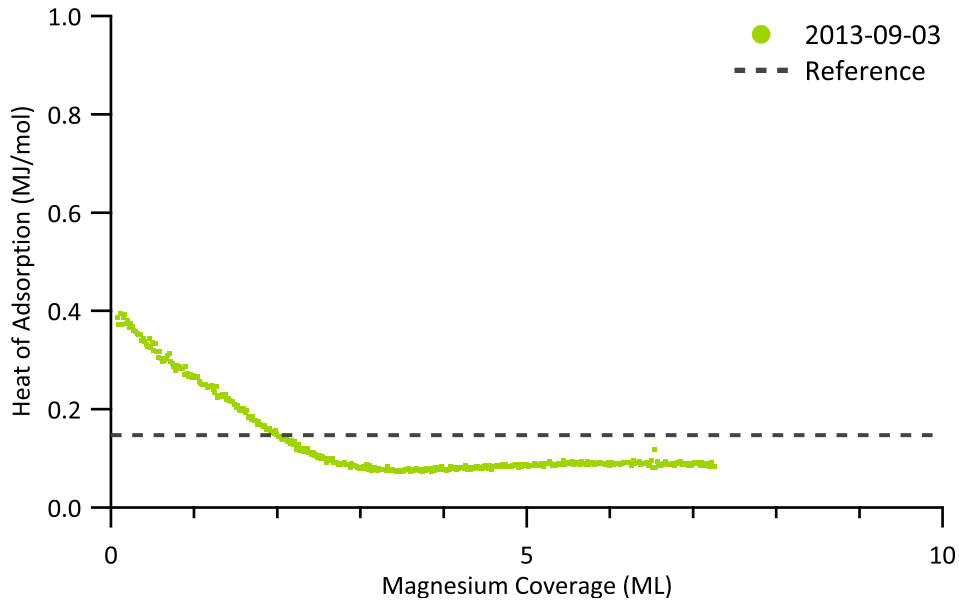


Figure D.7: Sticking Data for Magnesium on Sputter Cleaned Detector — The obtained sticking probabilities of magnesium dosed on sputter cleaned nickel coated detector surface as a function coverage is shown for each individual experiment.

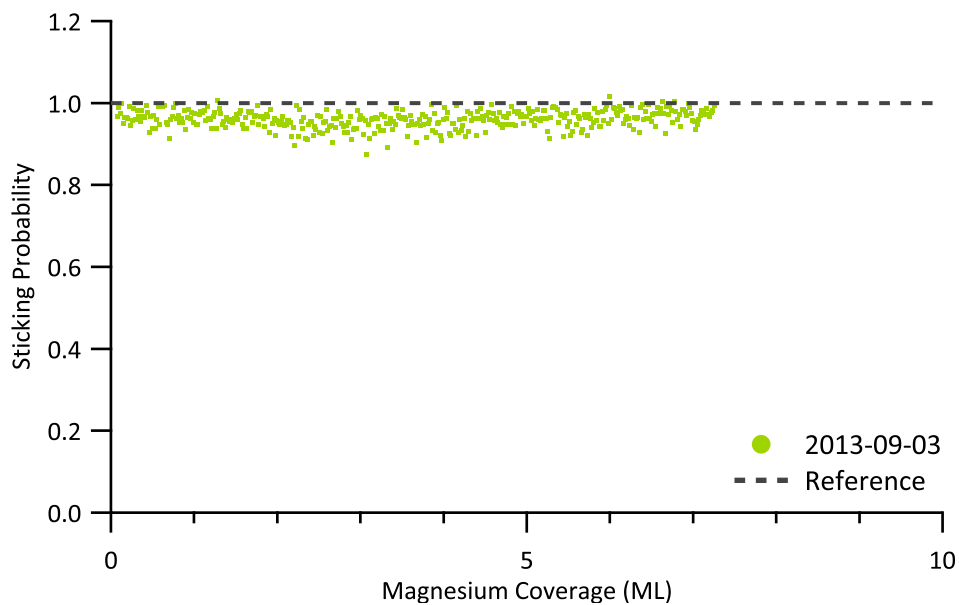


Figure D.8: Enthalpy Data for Magnesium on Sputter Cleaned Detector — The obtained heat of adsorption of magnesium dosed on sputter cleaned nickel coated detector surface as a function coverage is presented for each individual experiment.

D.3 Magnesium Adsorbed on PTCDA

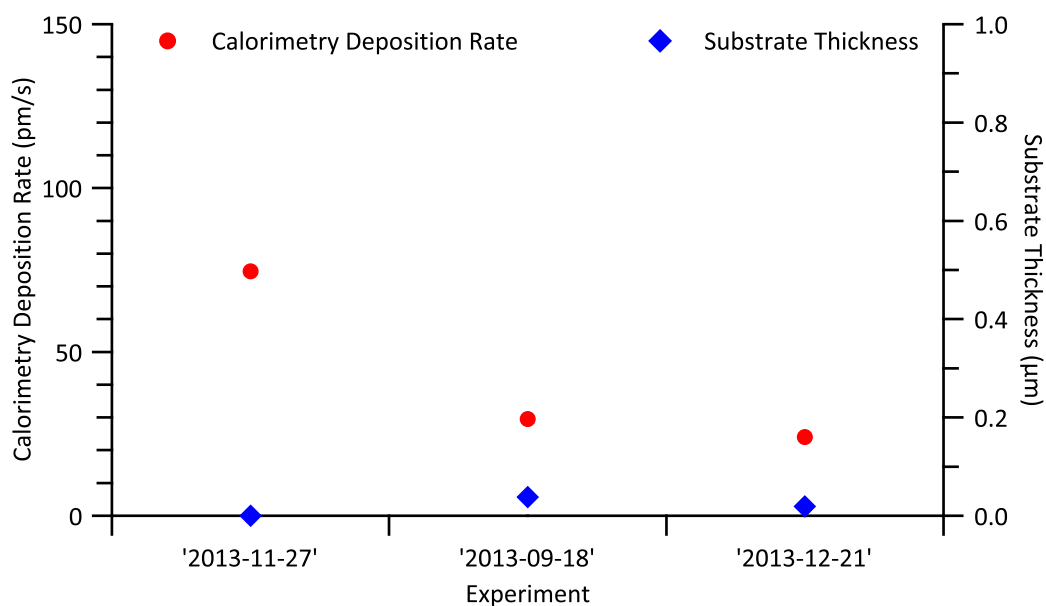


Figure D.9: Auxiliary Data for Magnesium on PTCDA — The calorimetry flux (magnesium – red circles) and the thickness of the organic substrate layer (PTCDA – blue diamonds) are given categorized by experiment.

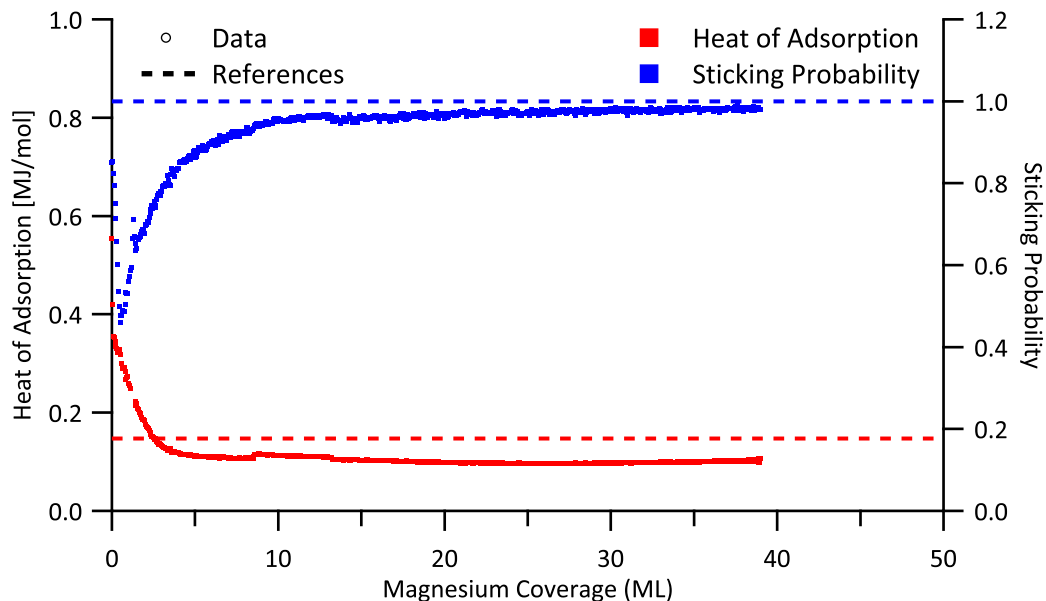


Figure D.10: Averaged Data for Magnesium on PTCDA — The averaged results for the heat of adsorption (red) and the sticking probability (blue) obtained from adsorption of magnesium on PTCDA are given as a function of coverage.

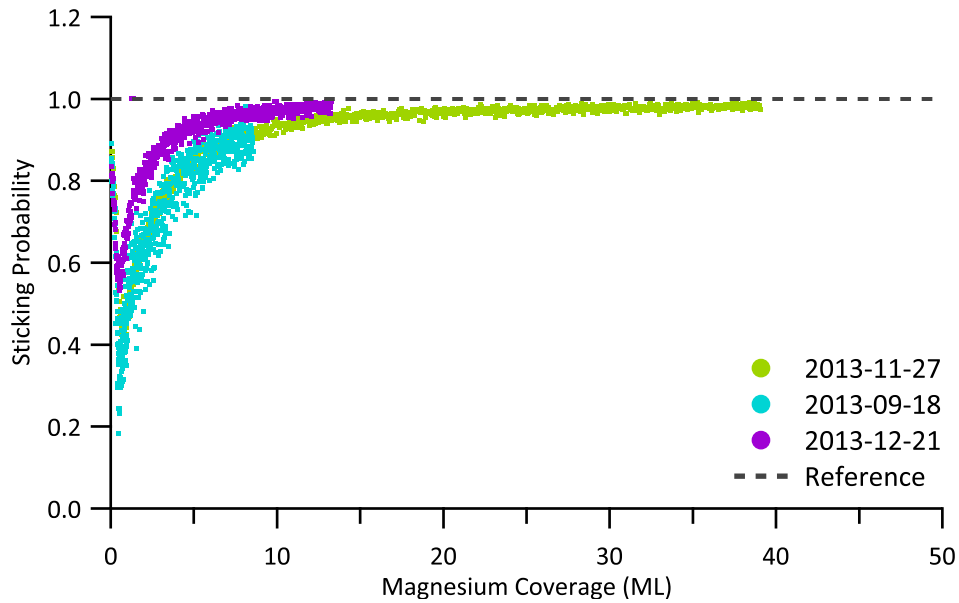


Figure D.11: Sticking Data for Magnesium on PTCDA — The obtained sticking probabilities of magnesium dosed on PTCDA as a function coverage is shown for each individual experiment.

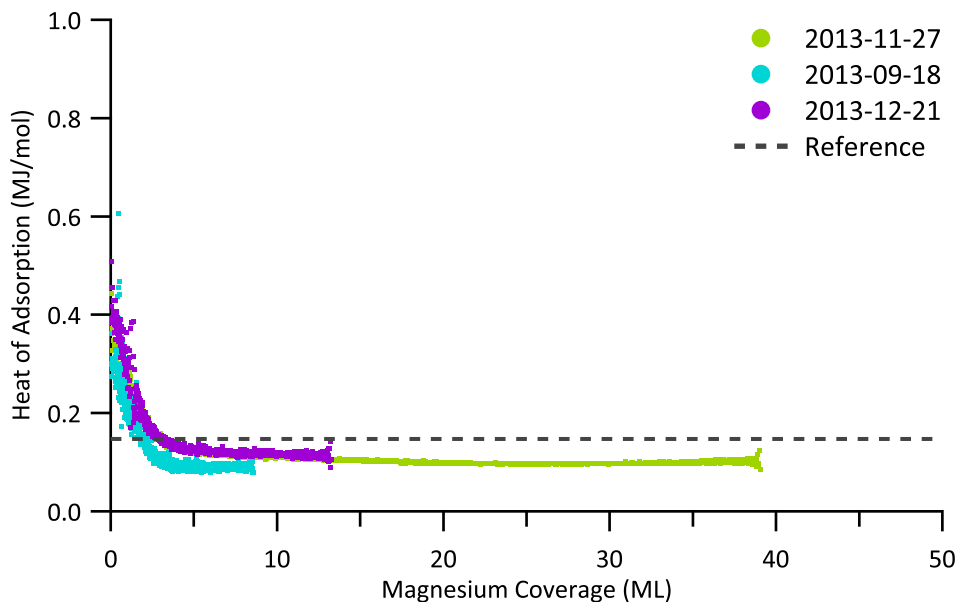


Figure D.12: Enthalpy Data for Magnesium on PTCDA — The obtained heat of adsorption of magnesium dosed on PTCDA as a function coverage is presented for each individual experiment.

D.4 Calcium Adsorbed on Sputter Cleaned Detector

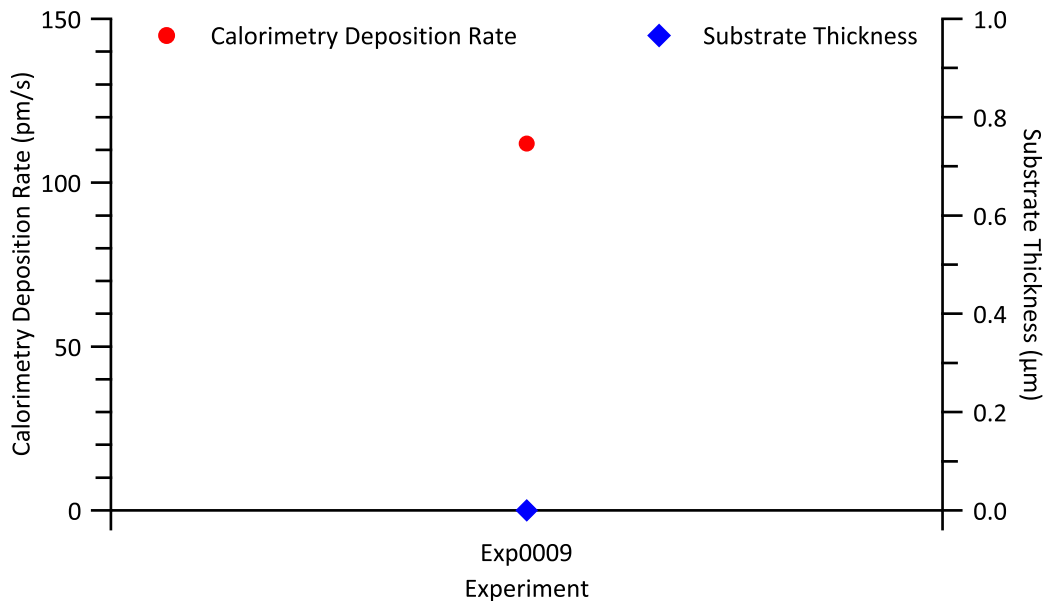


Figure D.13: Auxiliary Data for Calcium on Sputter Cleaned Detector — The calorimetry flux (calcium – red circles) and the thickness of the organic substrate layer (absent – blue diamonds) are given categorized by experiment.

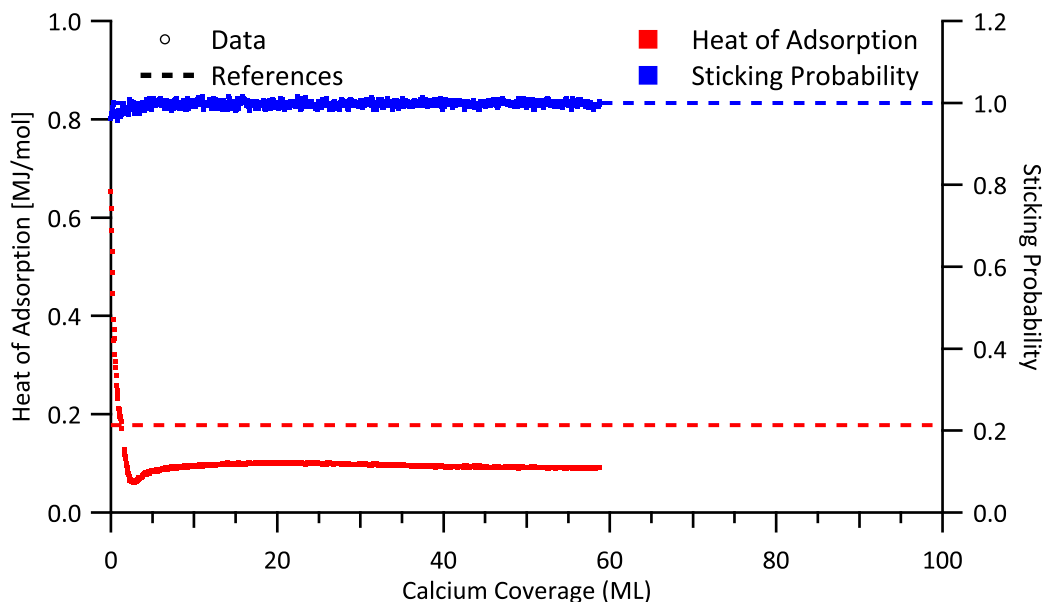


Figure D.14: Averaged Data for Calcium on Sputter Cleaned Detector — The averaged results for the heat of adsorption (red) and the sticking probability (blue) obtained from adsorption of calcium on sputter cleaned nickel coated detector surface are given as a function of coverage.

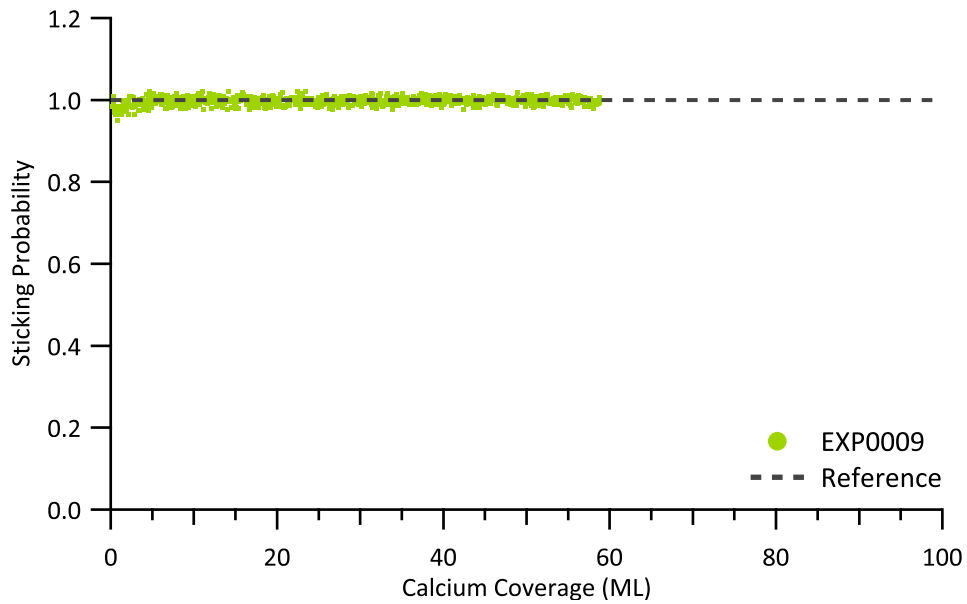


Figure D.15: Sticking Data for Calcium on Sputter Cleaned Detector — The obtained sticking probabilities of calcium dosed on sputter cleaned nickel coated detector surface as a function coverage is shown for each individual experiment.

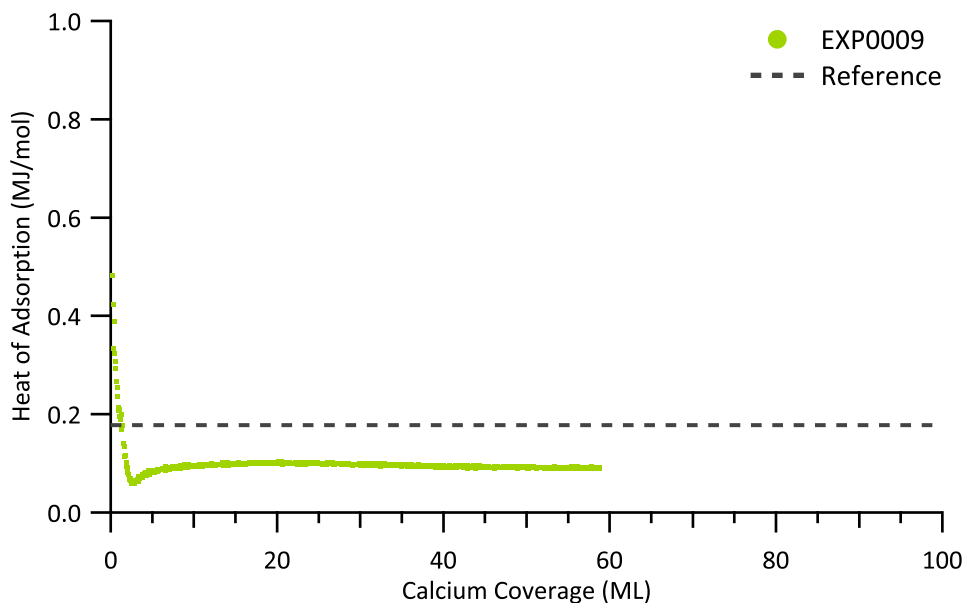


Figure D.16: Enthalpy Data for Calcium on Sputter Cleaned Detector — The obtained heat of adsorption of calcium dosed on sputter cleaned nickel coated detector surface as a function coverage is presented for each individual experiment.

D.5 Calcium Adsorbed on Tetraphenyl Porphyrin

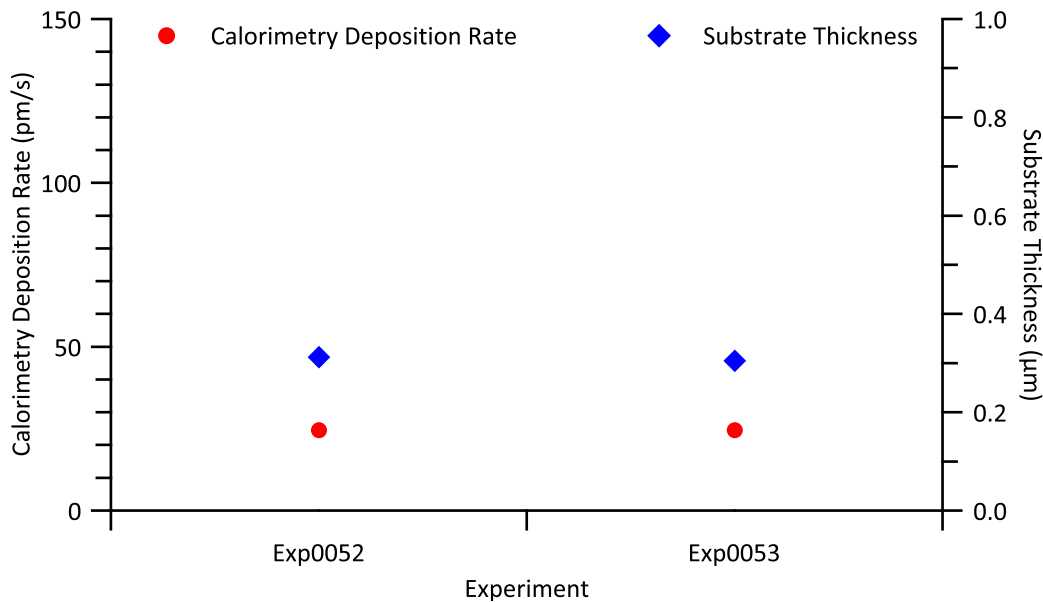


Figure D.17: Auxiliary Data for Calcium on Tetraphenyl Porphyrin — The calorimetry flux (calcium – red circles) and the thickness of the organic substrate layer (tetraphenyl porphyrin – blue diamonds) are given categorized by experiment.

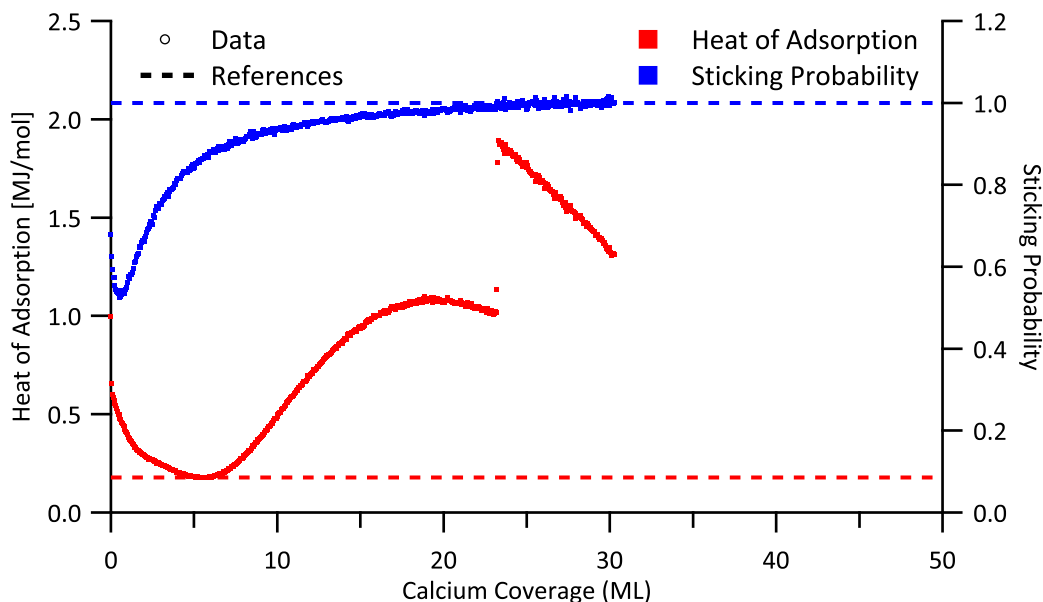


Figure D.18: Averaged Data for Calcium on Tetraphenyl Porphyrin — The averaged results for the heat of adsorption (red) and the sticking probability (blue) obtained from adsorption of calcium on tetraphenyl porphyrin are given as a function of coverage.

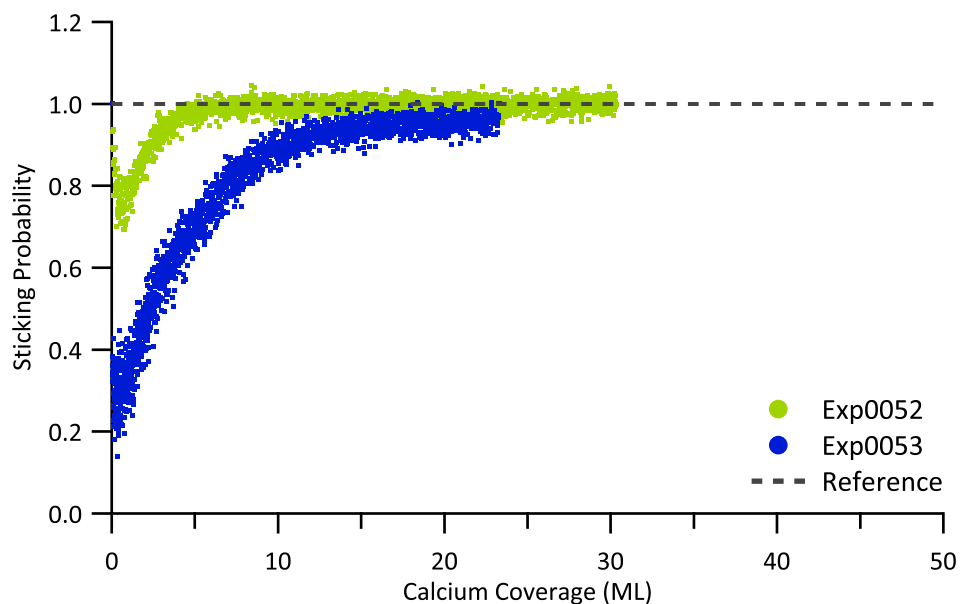


Figure D.19: Sticking Data for Calcium on Tetraphenyl Porphyrin — The obtained sticking probabilities of calcium dosed on tetraphenyl porphyrin as a function coverage is shown for each individual experiment.

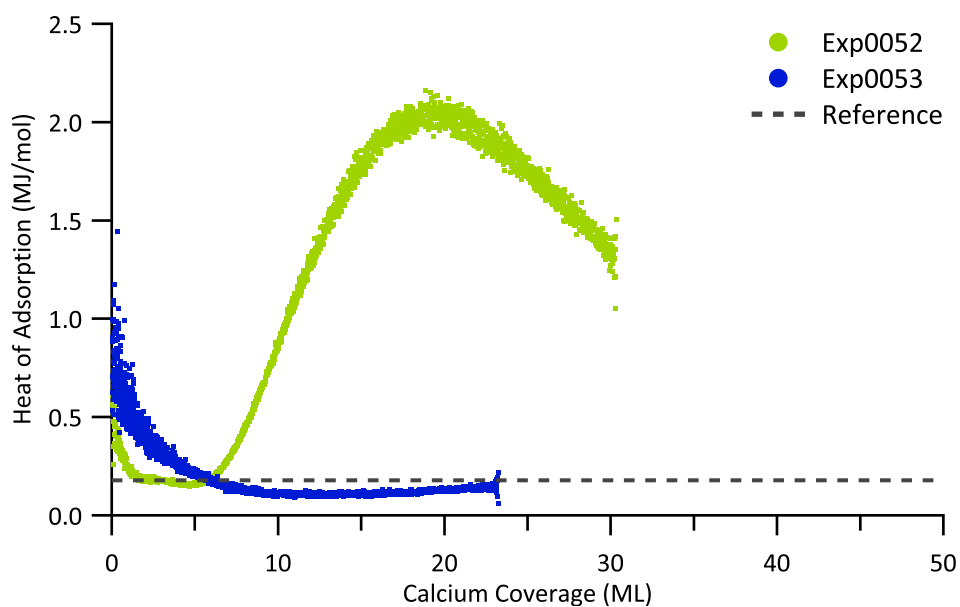


Figure D.20: Enthalpy Data for Calcium on Tetraphenyl Porphyrin — The obtained heat of adsorption of calcium dosed on tetraphenyl porphyrin as a function coverage is presented for each individual experiment.

D.6 Calcium Adsorbed on PTCDA

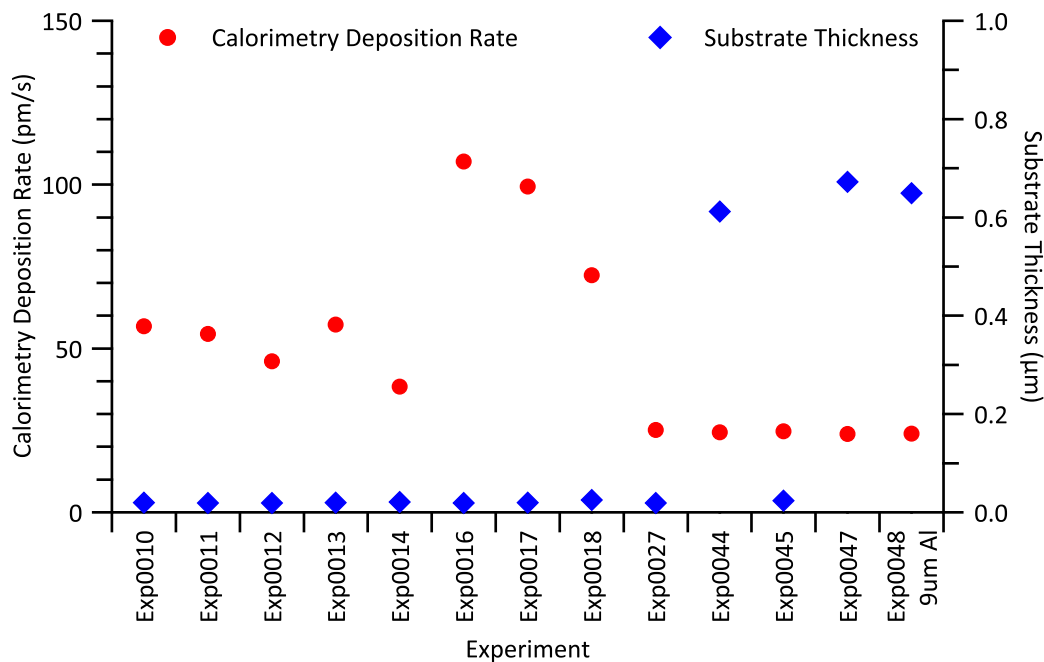


Figure D.21: Auxiliary Data for Calcium on PTCDA — The calorimetry flux (calcium – red circles) and the thickness of the organic substrate layer (PTCDA – blue diamonds) are given categorized by experiment.

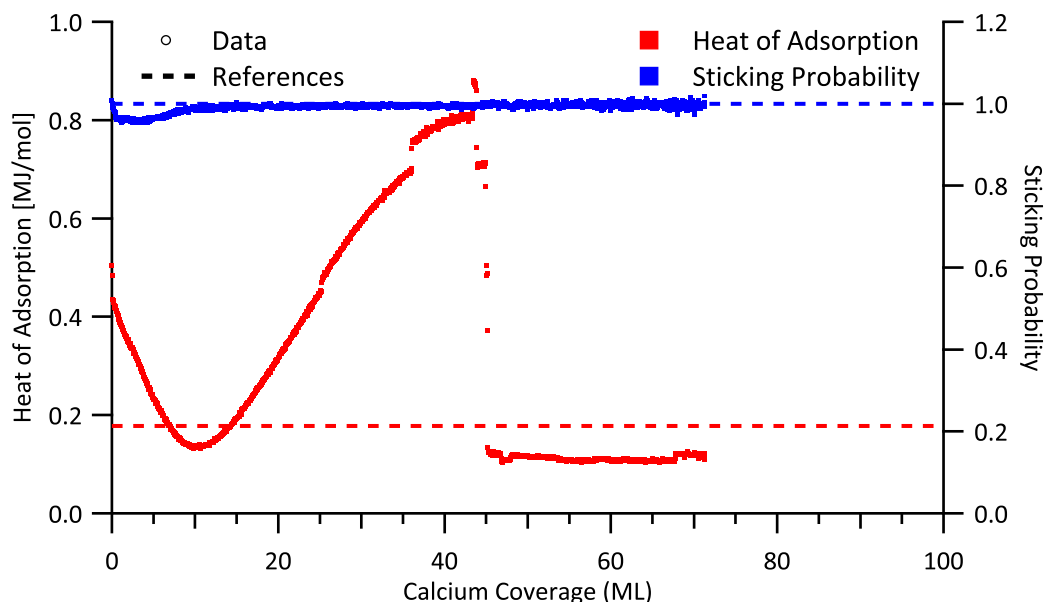


Figure D.22: Averaged Data for Calcium on PTCDA — The averaged results for the heat of adsorption (red) and the sticking probability (blue) obtained from adsorption of calcium on PTCDA are given as a function of coverage.

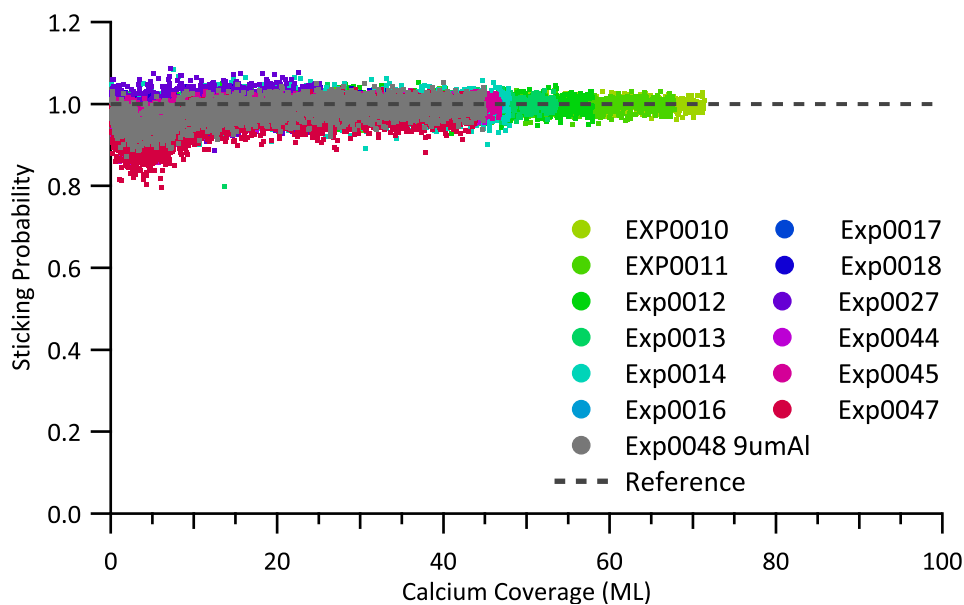


Figure D.23: Sticking Data for Calcium on PTCDA — The obtained sticking probabilities of calcium dosed on PTCDA as a function coverage is shown for each individual experiment.

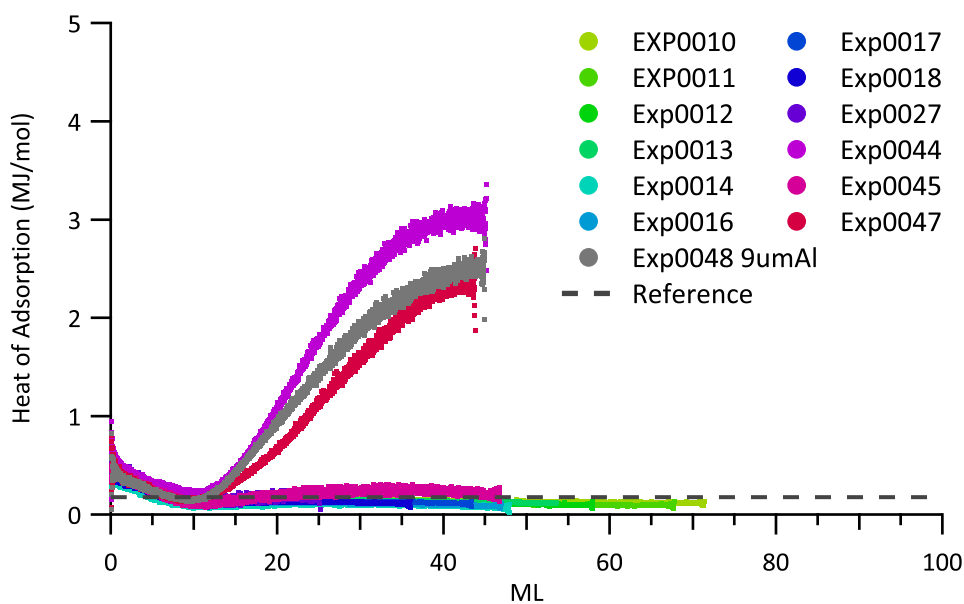


Figure D.24: Enthalpy Data for Calcium on PTCDA — The obtained heat of adsorption of calcium dosed on PTCDA as a function coverage is presented for each individual experiment. Subsets with different substrate layer thicknesses of the displayed experiments are given in Figures D.25 and D.26.

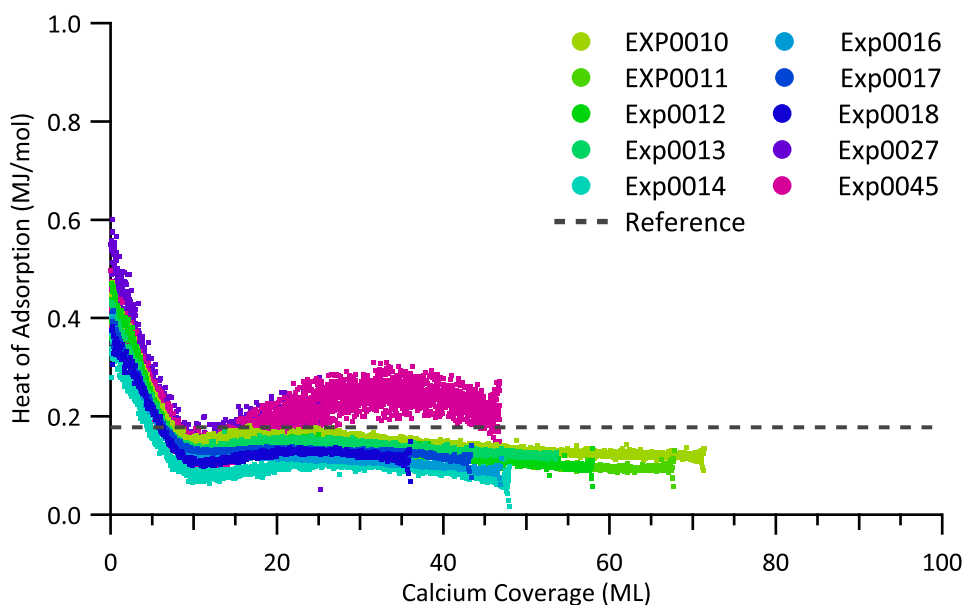


Figure D.25: Enthalpy Data for Calcium on PTCDA: Small Layer Thickness — The obtained heat of adsorption of calcium dosed on sexithiophene as a function coverage is presented for each individual experiment carried out on small substrate layer thicknesses.

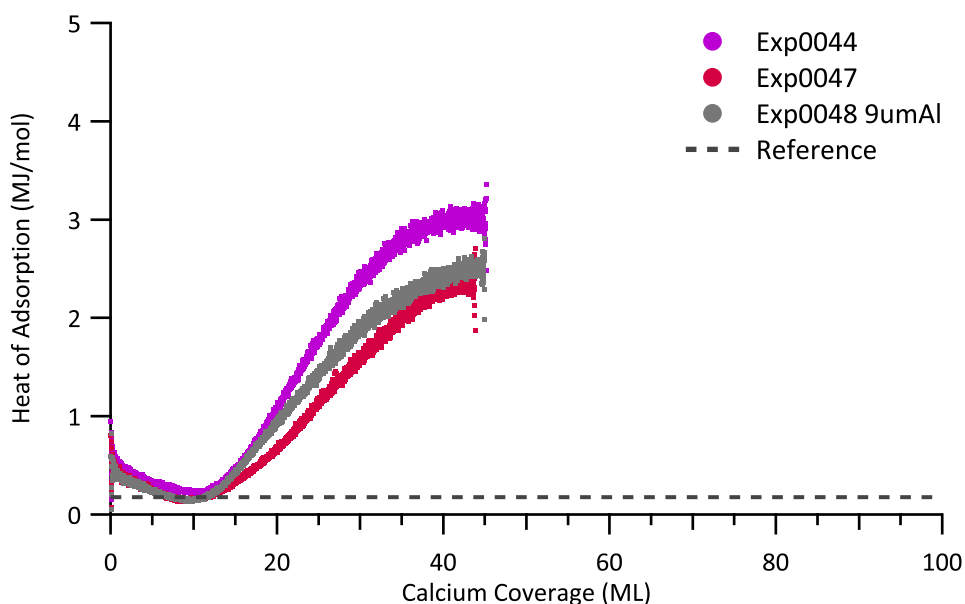


Figure D.26: Enthalpy Data for Calcium on PTCDA: Large Layer Thickness — The obtained heat of adsorption of calcium dosed on sexithiophene as a function coverage is presented for each individual experiment carried out on large substrate layer thicknesses.

D.7 Calcium Adsorbed on PTCDA at Low Temperature

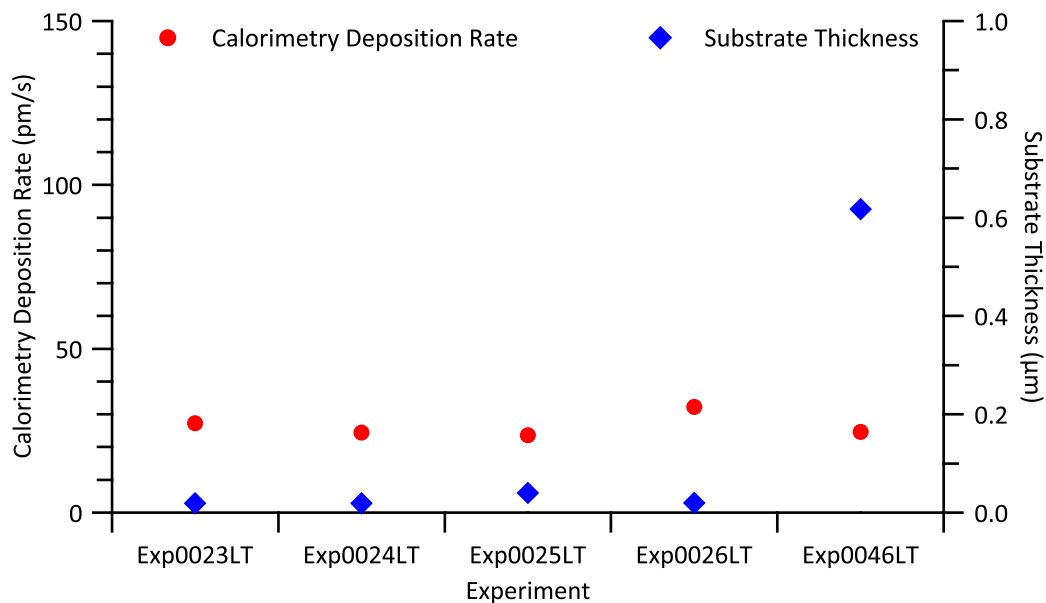


Figure D.27: Low Temperature Auxiliary Data for Calcium on PTCDA — The calorimetry flux (calcium – red circles) and the thickness of the organic substrate layer (PTCDA – blue diamonds) are given categorized by low temperature experiment.

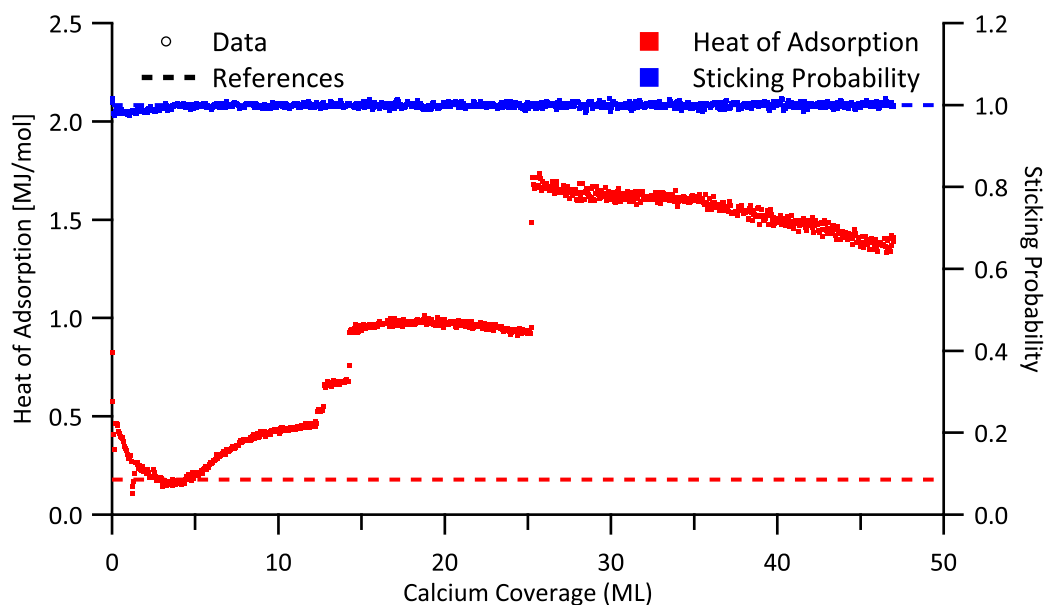


Figure D.28: Low Temperature Averaged Data for Calcium on PTCDA — The averaged results for the heat of adsorption (red) and the sticking probability (blue) obtained from adsorption of calcium on PTCDA at low temperature are given as a function of coverage.

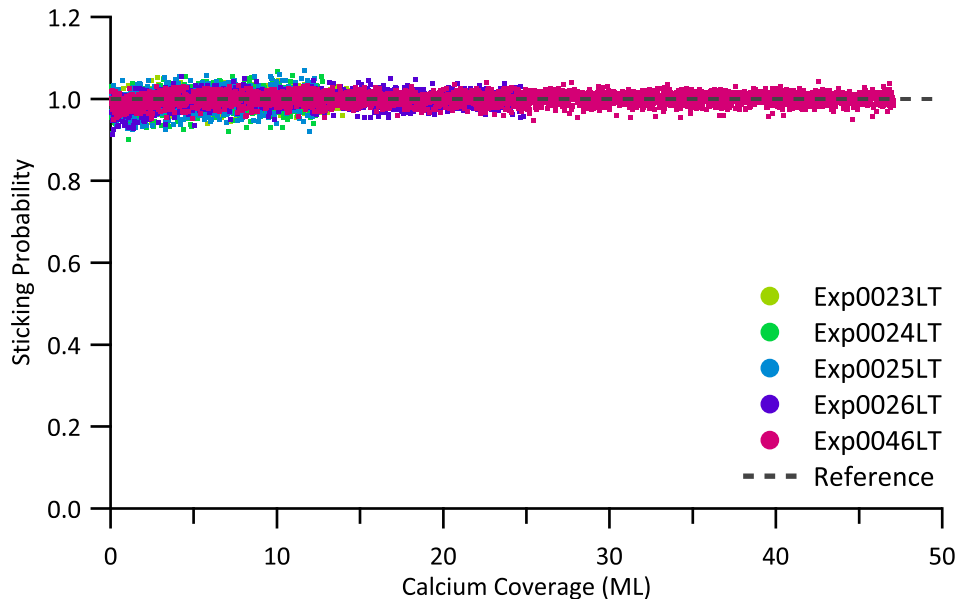


Figure D.29: Low Temperature Sticking Data for Calcium on PTCDA — The obtained sticking probabilities of calcium dosed on PTCDA at low temperature as a function coverage is shown for each individual experiment.

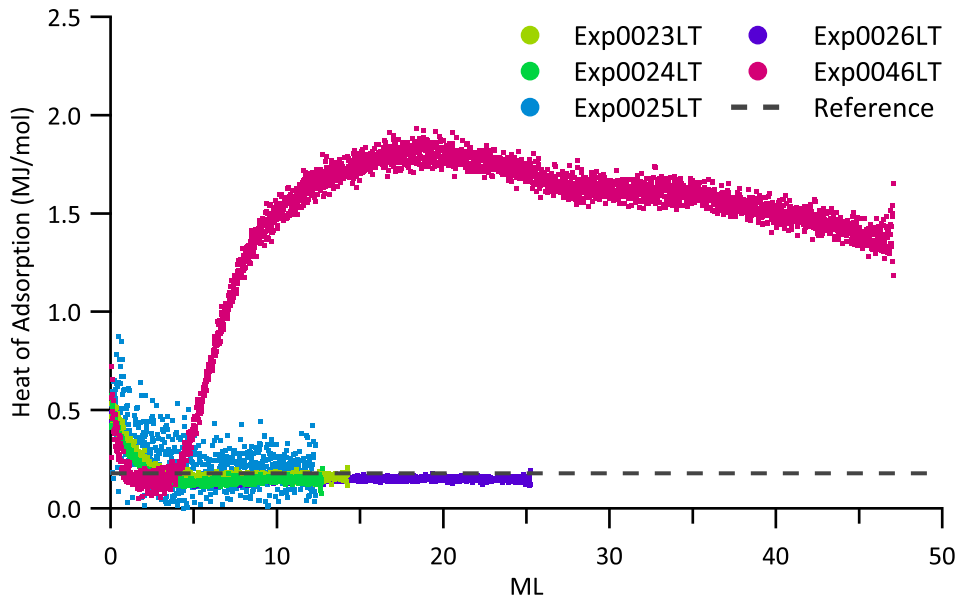


Figure D.30: Low Temperature Enthalpy Data for Calcium on PTCDA — The obtained heat of adsorption of calcium dosed on PTCDA at low temperature as a function coverage is presented for each individual experiment.

D.8 Calcium Adsorbed on Sexithiophene

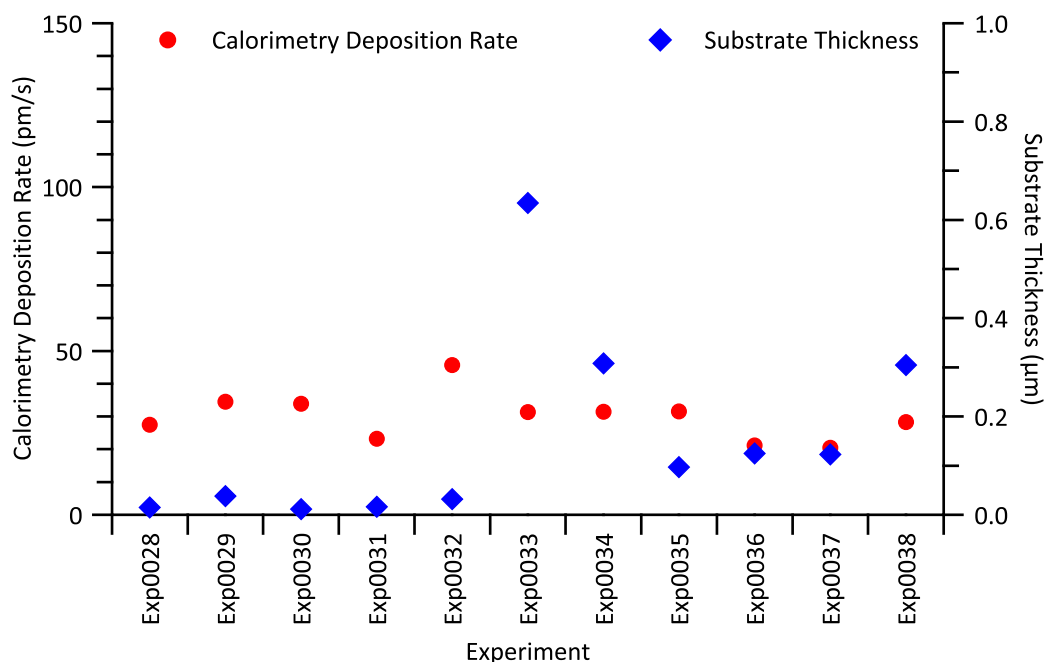


Figure D.31: Auxiliary Data for Calcium on Sexithiophene — The calorimetry flux (calcium – red circles) and the thickness of the organic substrate layer (sexithiophene – blue diamonds) are given categorized by experiment.

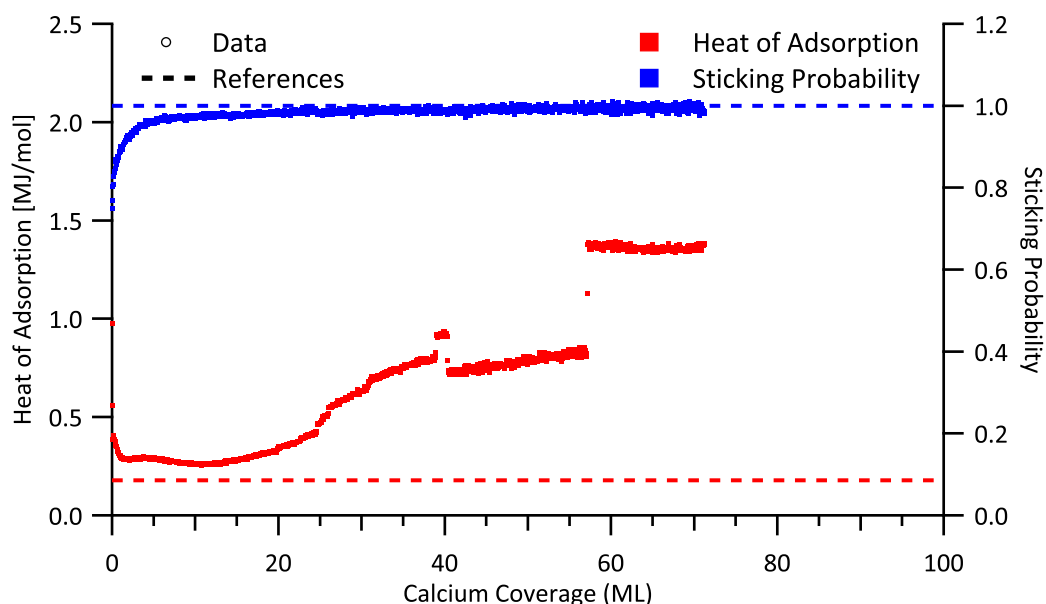


Figure D.32: Averaged Data for Calcium on Sexithiophene — The averaged results for the heat of adsorption (red) and the sticking probability (blue) obtained from adsorption of calcium on sexithiophene are given as a function of coverage.

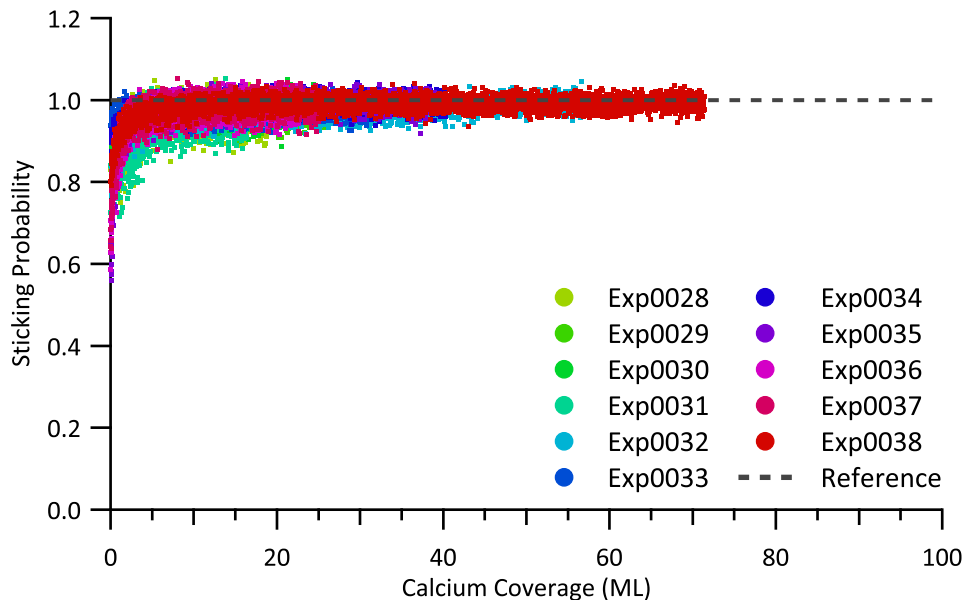


Figure D.33: Sticking Data for Calcium on Sexithiophene — The obtained sticking probabilities of calcium dosed on sexithiophene as a function coverage is shown for each individual experiment.

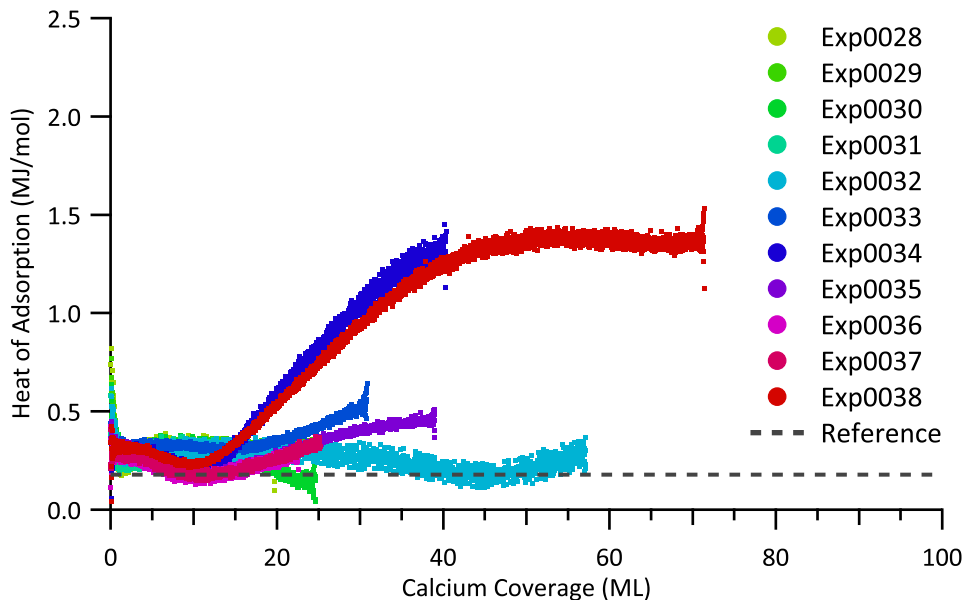


Figure D.34: Enthalpy Data for Calcium on Sexithiophene — The obtained heat of adsorption of calcium dosed on sexithiophene as a function coverage is presented for each individual experiment. Subsets with different substrate layer thicknesses of the displayed experiments are given in Figures D.35, D.36, and D.37.

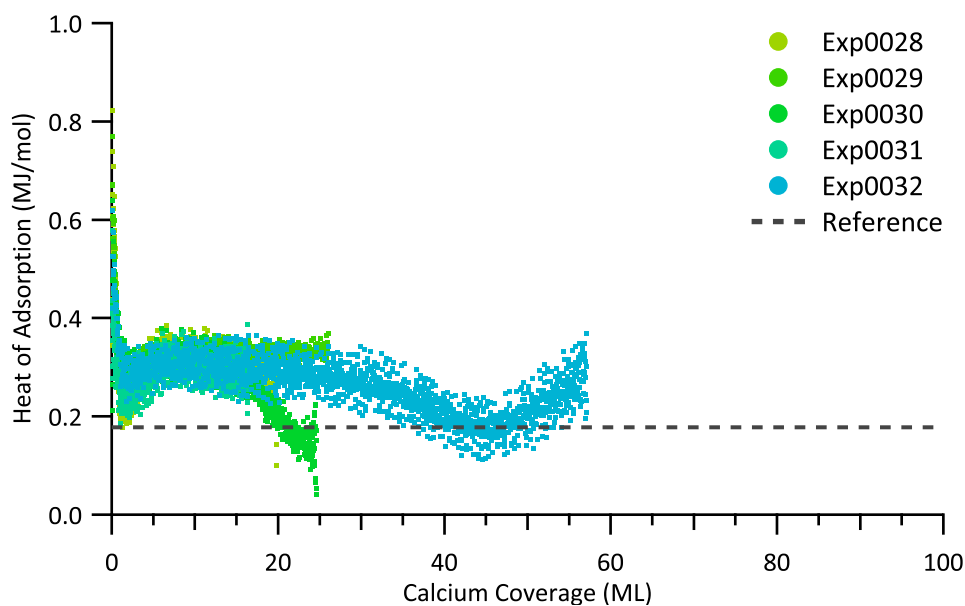


Figure D.35: Enthalpy Data for Calcium on Sexithiophene: Small Layer

Thickness — The obtained heat of adsorption of calcium dosed on sexithiophene as a function coverage is presented for each individual experiment carried out on small substrate layer thicknesses.

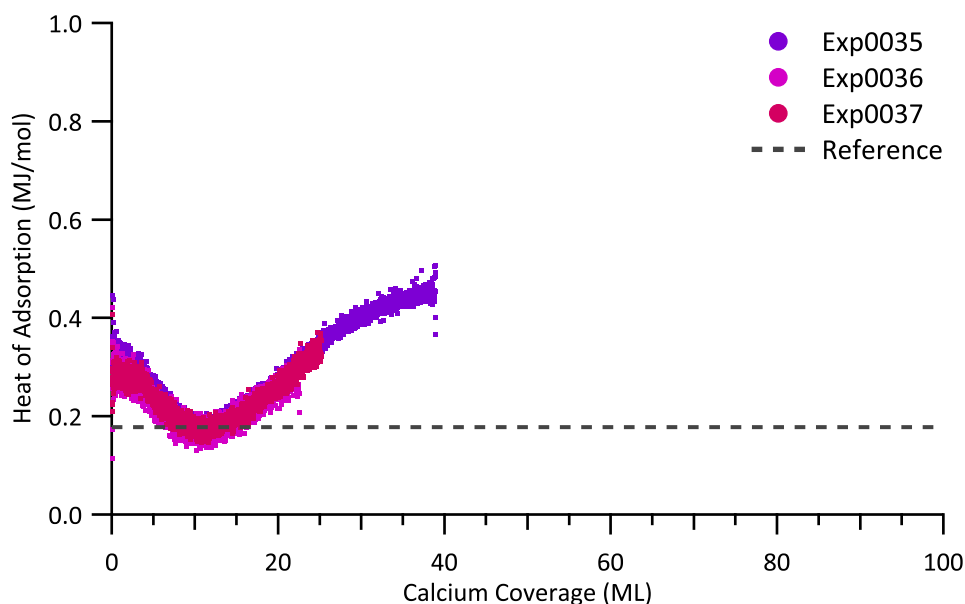


Figure D.36: Enthalpy Data for Calcium on Sexithiophene: Medium Layer

Thickness — The obtained heat of adsorption of calcium dosed on sexithiophene as a function coverage is presented for each individual experiment carried out on medium substrate layer thicknesses.

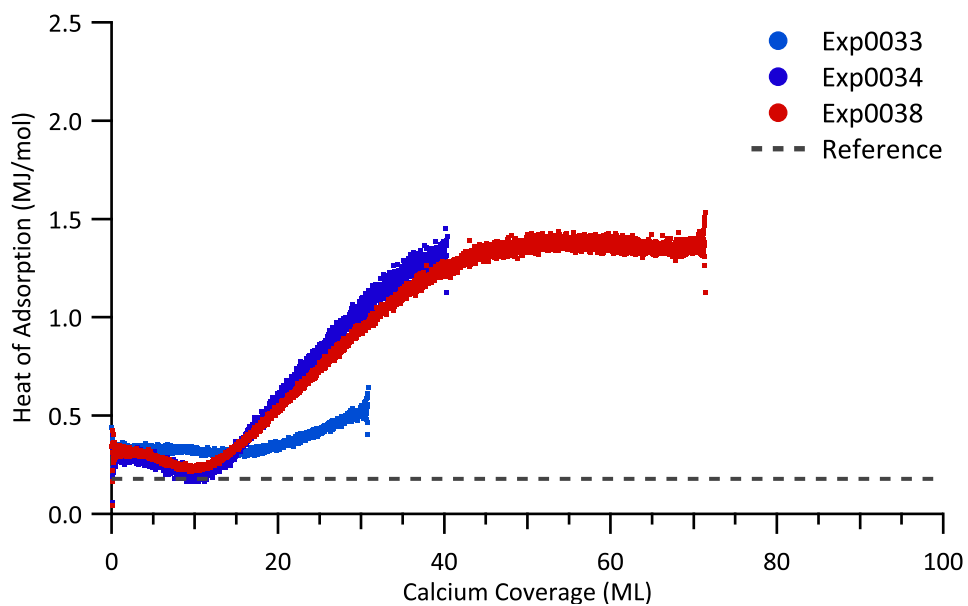


Figure D.37: Enthalpy Data for Calcium on Sexithiophene: Large Layer

Thickness — The obtained heat of adsorption of calcium dosed on sexithiophene as a function coverage is presented for each individual experiment carried out on large substrate layer thicknesses. In case of “Exp0033”, the thickness of the substrate layer is twice as big as in the other two experiments.

D.9 Calcium Adsorbed on Sexithiophene at Low Temperature

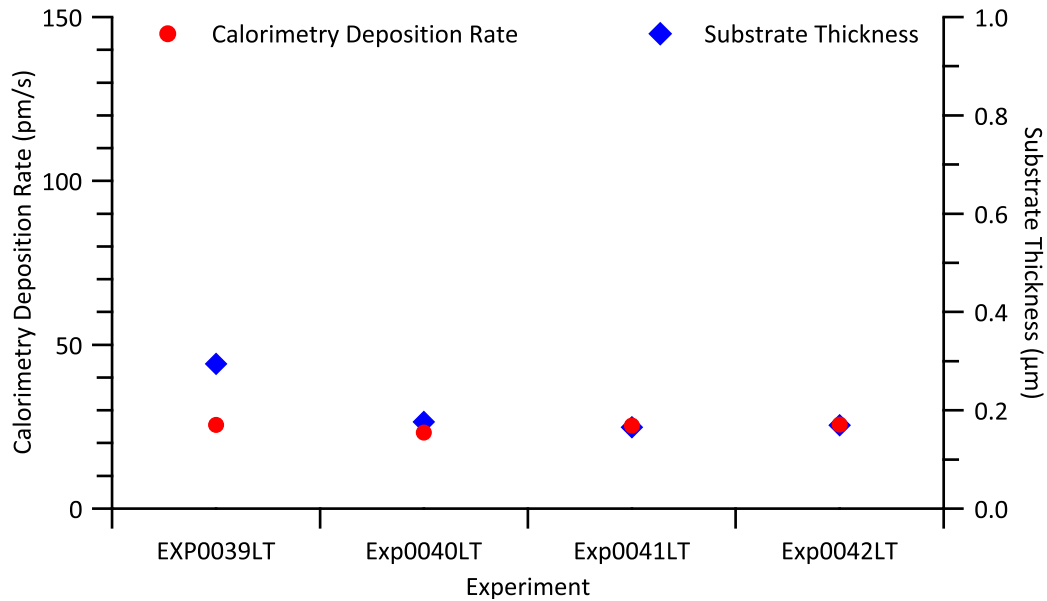


Figure D.38: Low Temperature Auxiliary Data for Calcium on Sexithiophene — The calorimetry flux (calcium – red circles) and the thickness of the organic substrate layer (sexithiophene – blue diamonds) are given categorized by low temperature experiment.

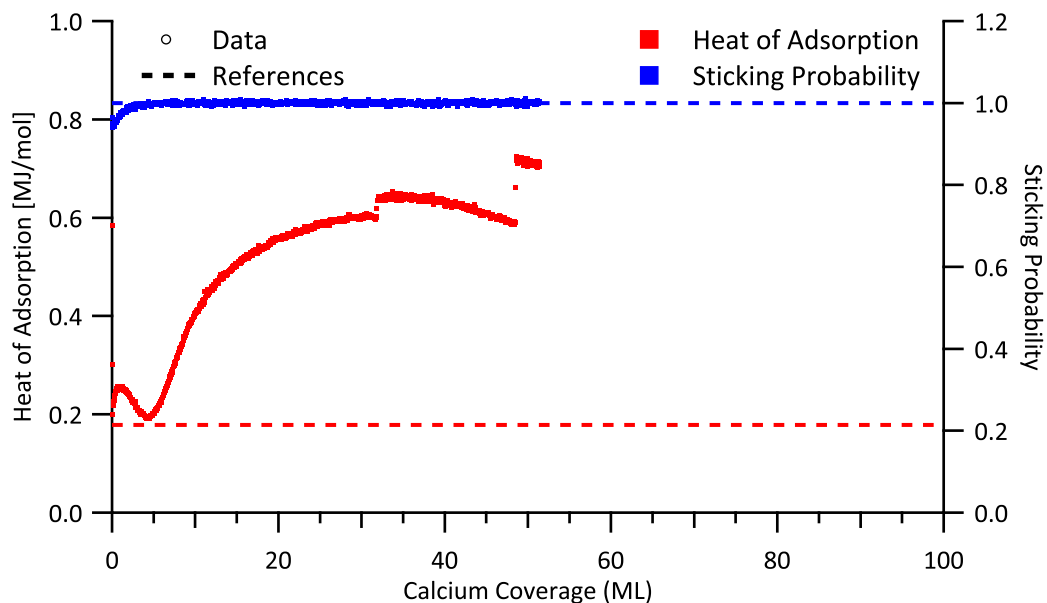


Figure D.39: Low Temperature Averaged Data for Calcium on Sexithiophene — The averaged results for the heat of adsorption (red) and the sticking probability (blue) obtained from adsorption of calcium on sexithiophene at low temperature are given as a function of coverage.

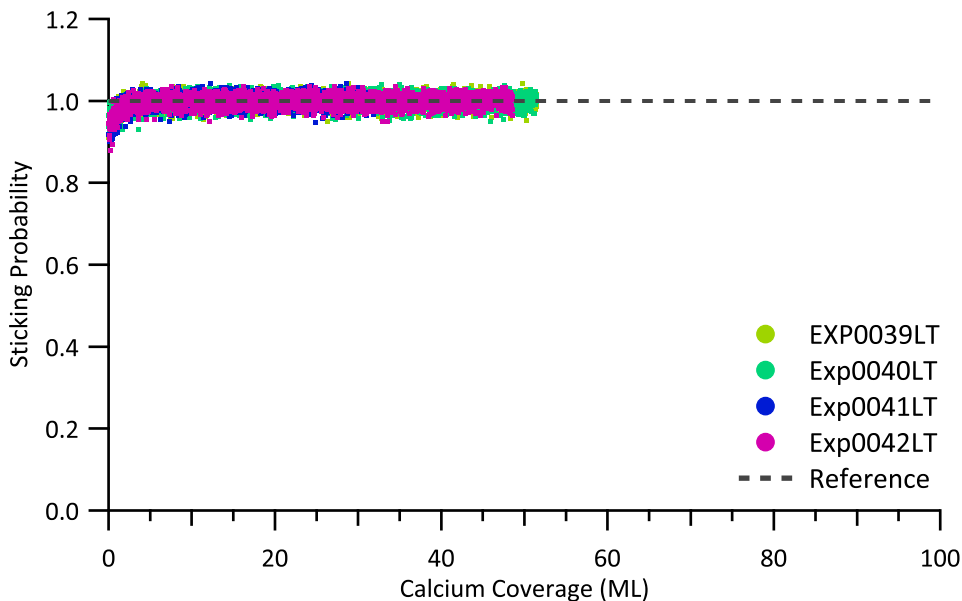


Figure D.40: Low Temperature Sticking Data for Calcium on Sexithiophene — The obtained sticking probabilities of calcium dosed on sexithiophene at low temperature as a function coverage is shown for each individual experiment.

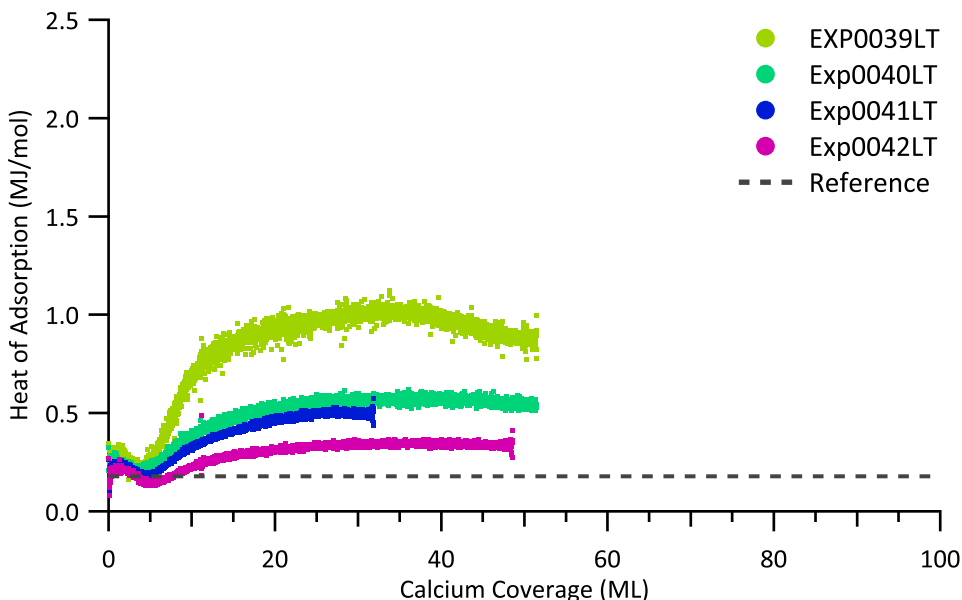


Figure D.41: Low Temperature Enthalpy Data for Calcium on Sexithiophene — The obtained heat of adsorption of calcium dosed on sexithiophene at low temperature as a function coverage is presented for each individual experiment.

D.10 Zinc Adsorbed on Sputter Cleaned Detector

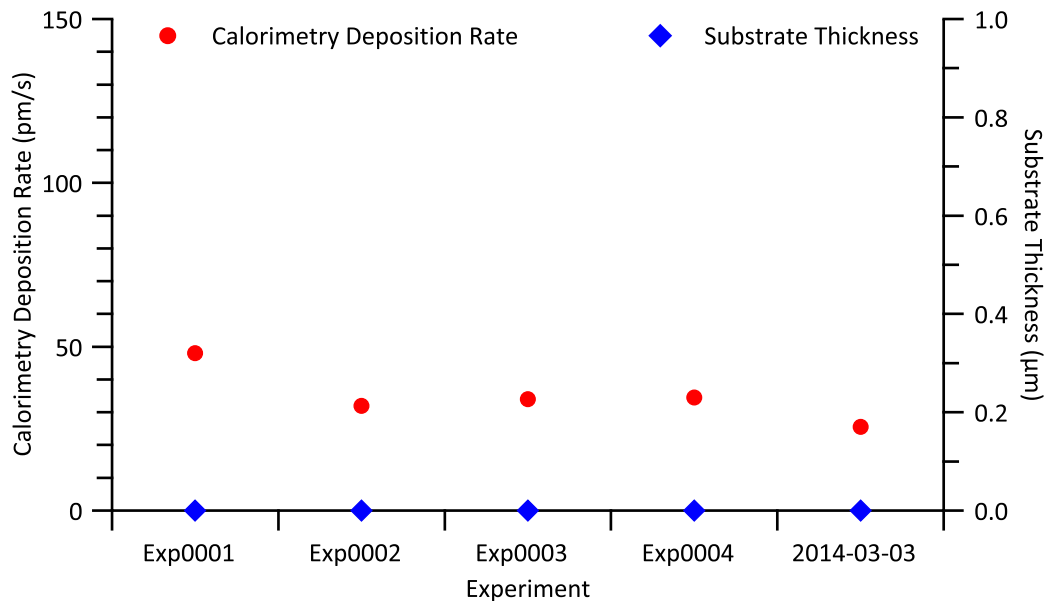


Figure D.42: Auxiliary Data for Zinc on Sputter Cleaned Detector — The calorimetry flux (zinc – red circles) and the thickness of the organic substrate layer (absent – blue diamonds) are given categorized by experiment.

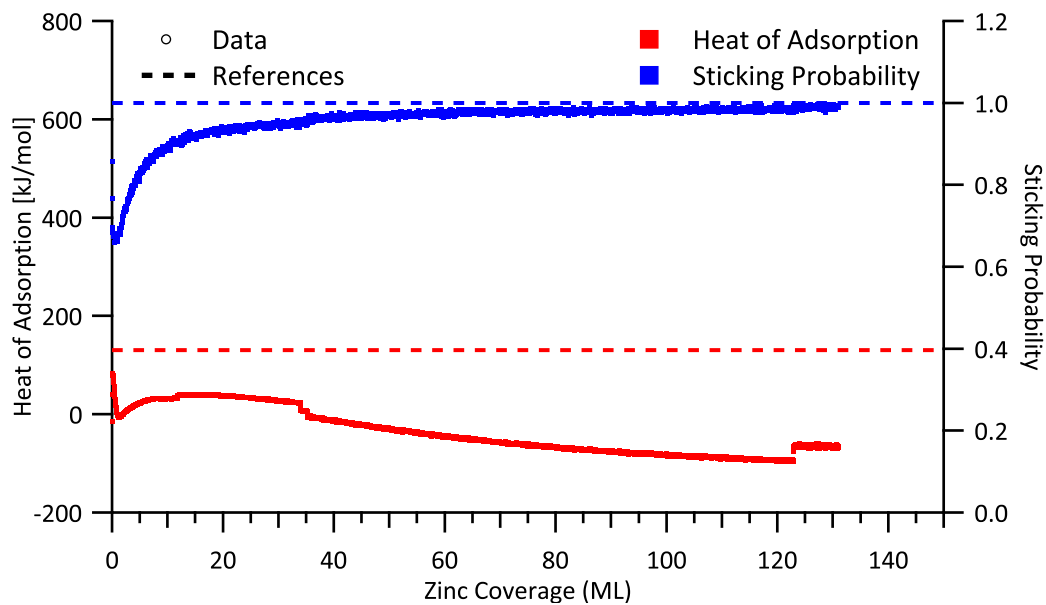


Figure D.43: Averaged Data for Zinc on Sputter Cleaned Detector — The averaged results for the heat of adsorption (red) and the sticking probability (blue) obtained from adsorption of zinc on pristine nickel coated detector surface are given as a function of coverage.

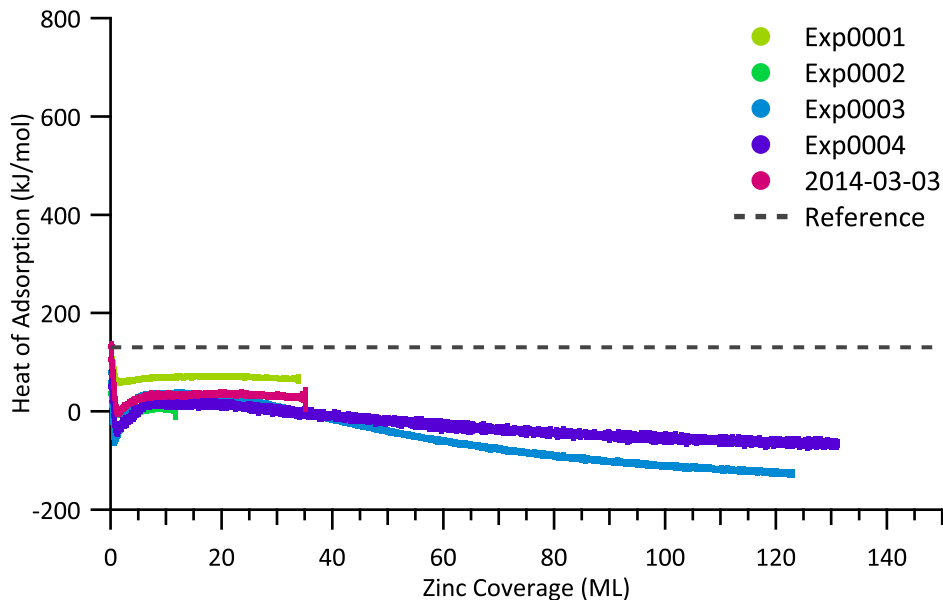


Figure D.44: Sticking Data for Zinc on Sputter Cleaned Detector — The obtained sticking probabilities of zinc dosed on pristine nickel coated detector surface as a function coverage is shown for each individual experiment. The sample in “Exp0001” was stored in the load lock for one week.

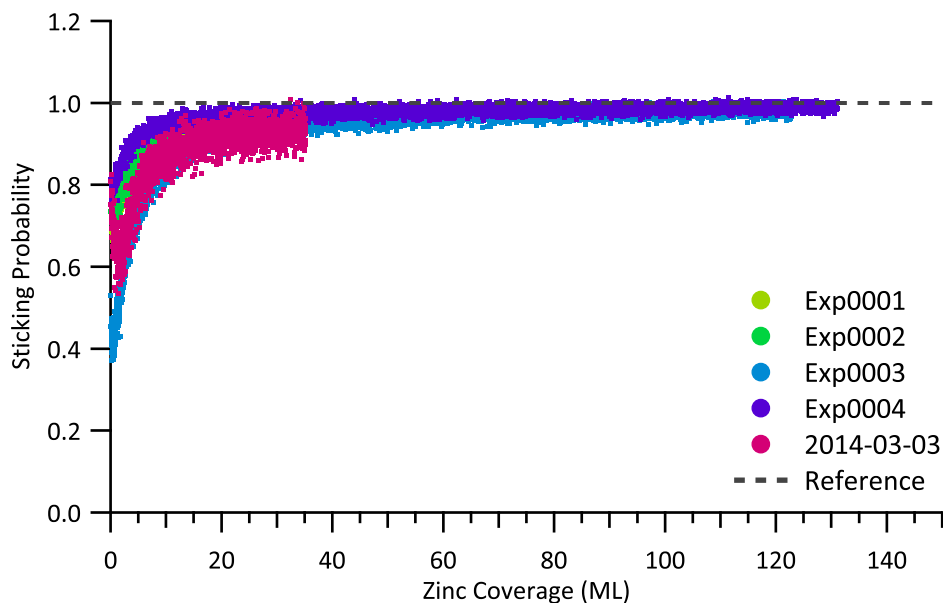


Figure D.45: Enthalpy Data for Zinc on Sputter Cleaned Detector — The obtained heat of adsorption of zinc dosed on pristine nickel coated detector surface as a function coverage is presented for each individual experiment. The sample in “Exp0001” was stored in the load lock for one week.

D.11 Zinc Adsorbed on PTCDA

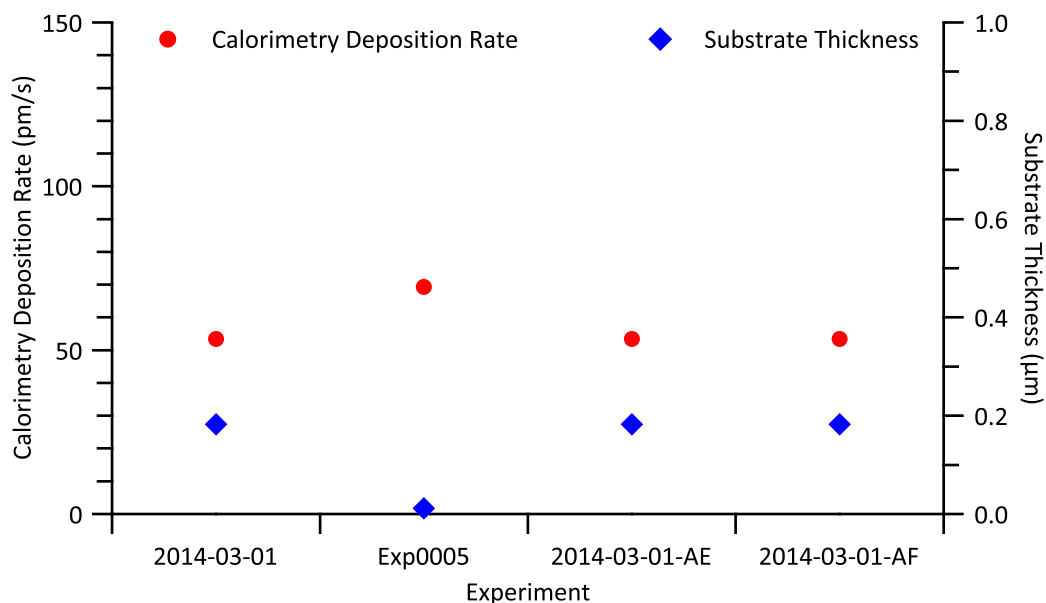


Figure D.46: Auxiliary Data for Zinc on PTCDA — The calorimetry flux (zinc – red circles) and the thickness of the organic substrate layer (PTCDA – blue diamonds) are given categorized by experiment.

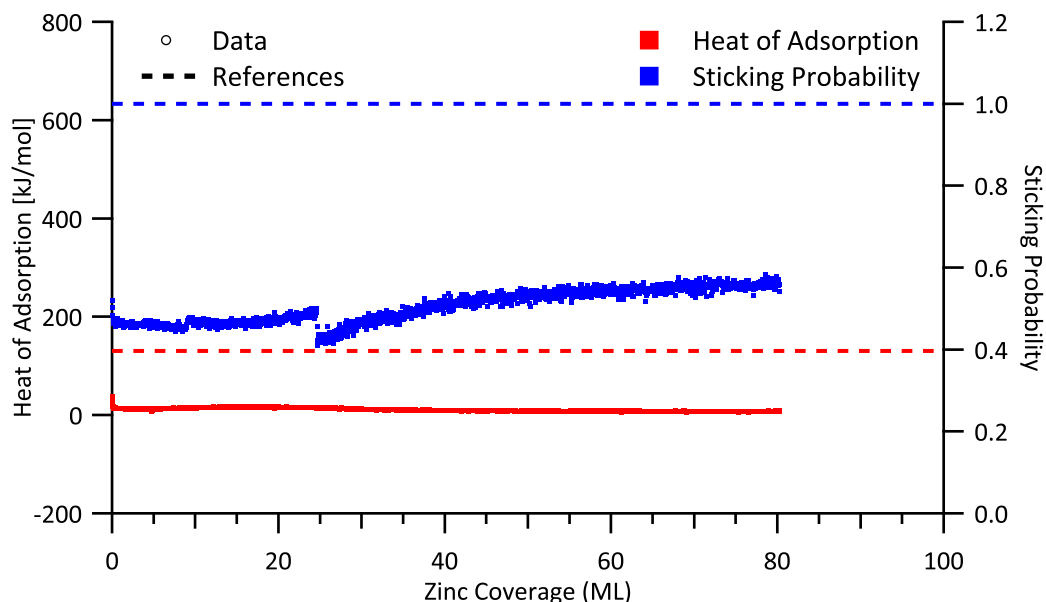


Figure D.47: Averaged Data for Zinc on PTCDA — The averaged results for the heat of adsorption (red) and the sticking probability (blue) obtained from adsorption of zinc on PTCDA are given as a function of coverage.

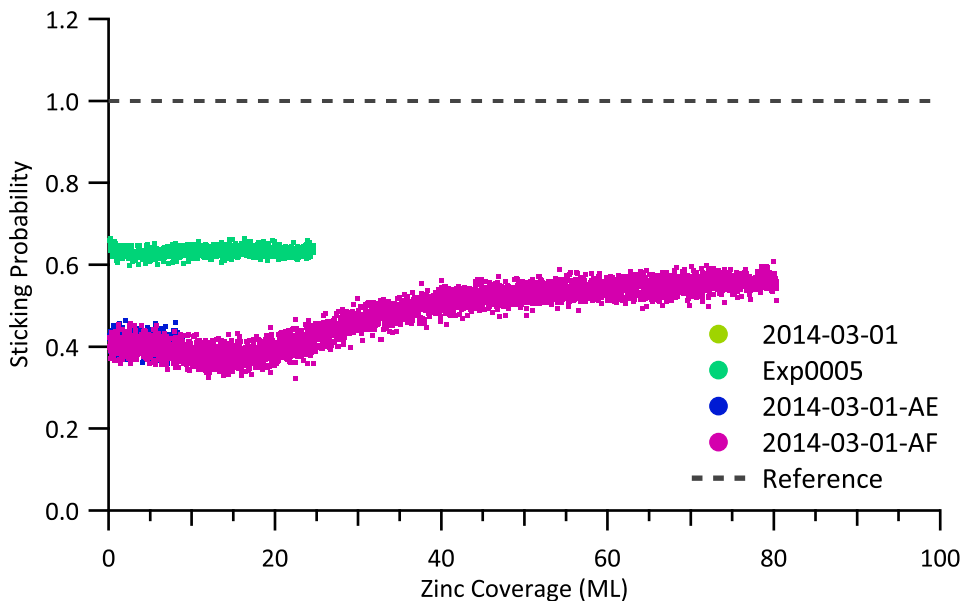


Figure D.48: Sticking Data for Zinc on PTCDA — The obtained sticking probabilities of zinc dosed on PTCDA as a function coverage is shown for each individual experiment.

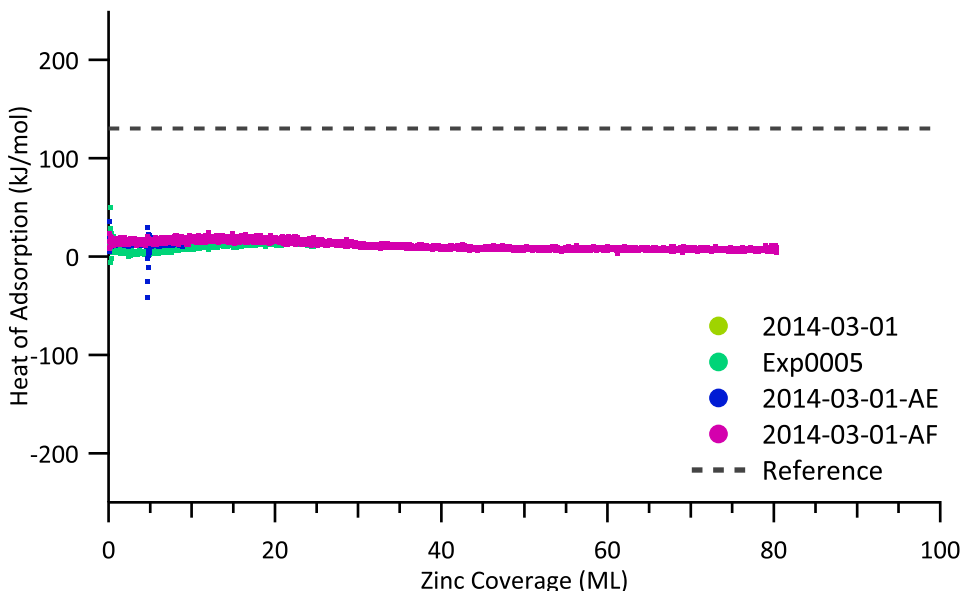


Figure D.49: Enthalpy Data for Zinc on PTCDA — The obtained heat of adsorption of zinc dosed on PTCDA as a function coverage is presented for each individual experiment.

D.12 Zinc Adsorbed on PTCDA at Low Temperature

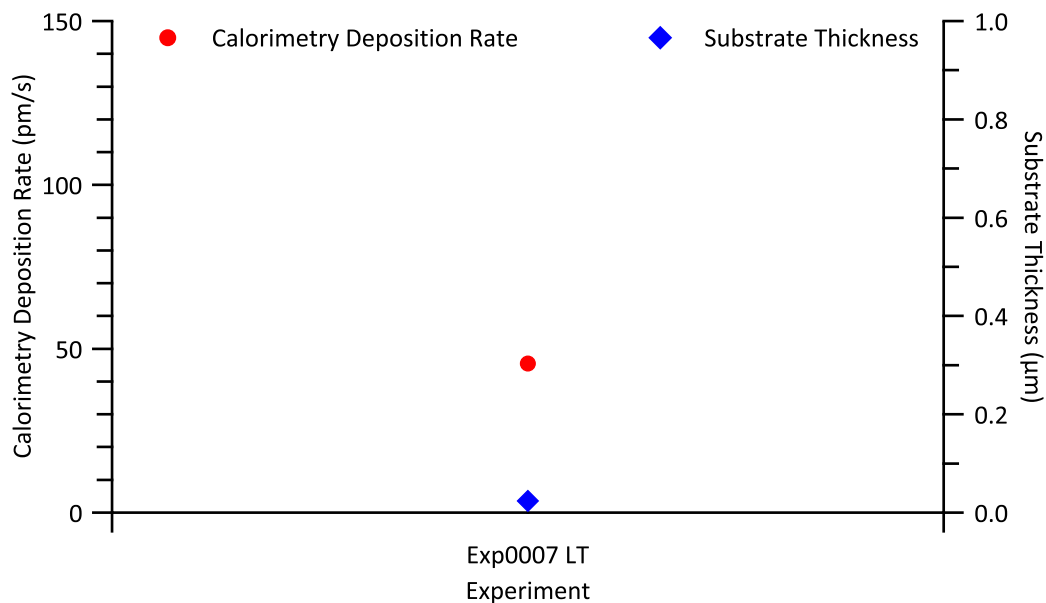


Figure D.50: Low Temperature Auxiliary Data for Zinc on PTCDA — The calorimetry flux (zinc – red circles) and the thickness of the organic substrate layer (PTCDA – blue diamonds) are given categorized by low temperature experiment.

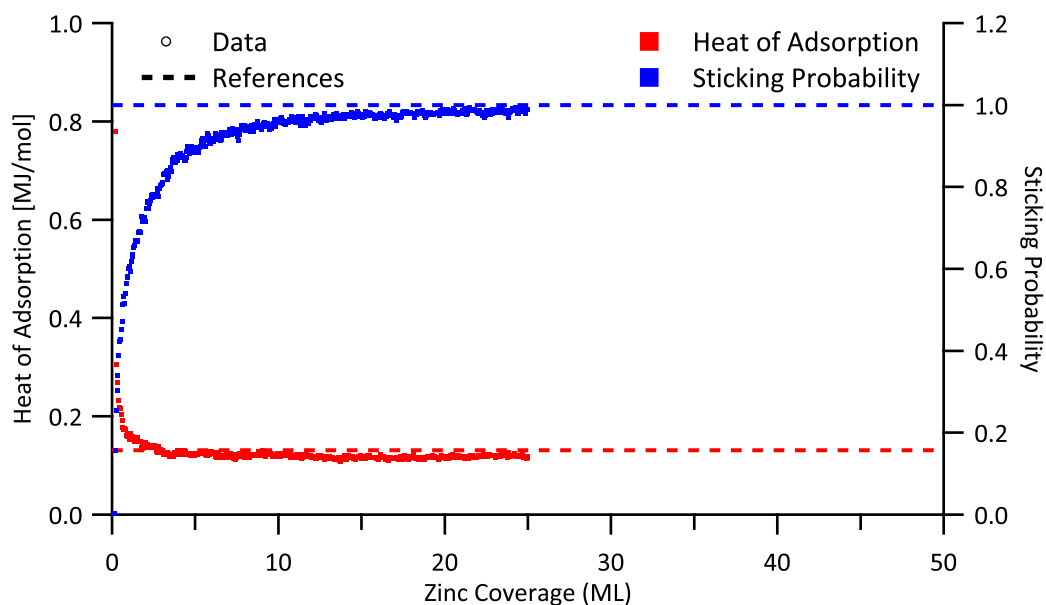


Figure D.51: Low Temperature Averaged Data for Zinc on PTCDA — The averaged results for the heat of adsorption (red) and the sticking probability (blue) obtained from adsorption of zinc on PTCDA at low temperature are given as a function of coverage.

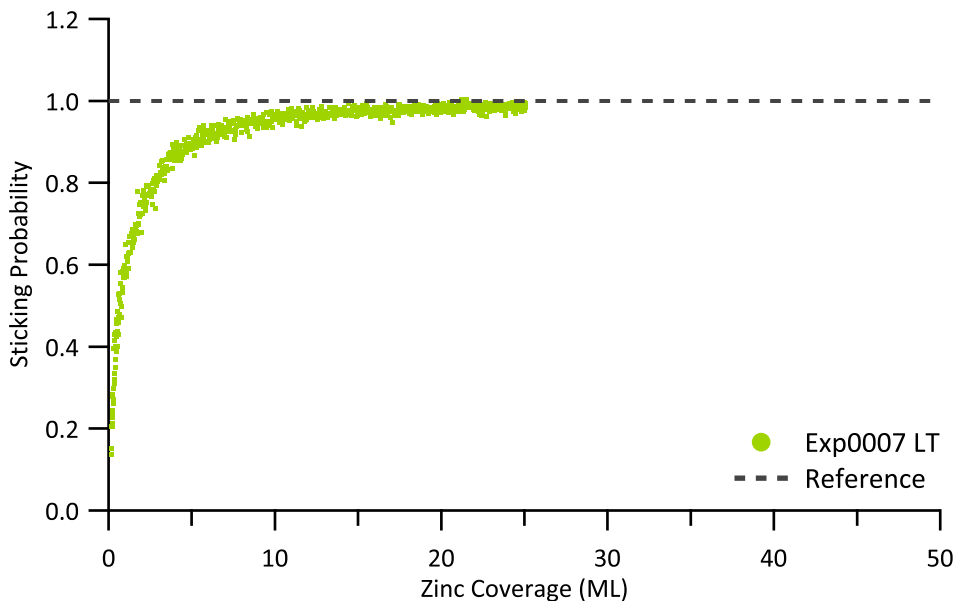


Figure D.52: Low Temperature Sticking Data for Zinc on PTCDA — The obtained sticking probabilities of zinc dosed on PTCDA at low temperature as a function coverage is shown for each individual experiment.

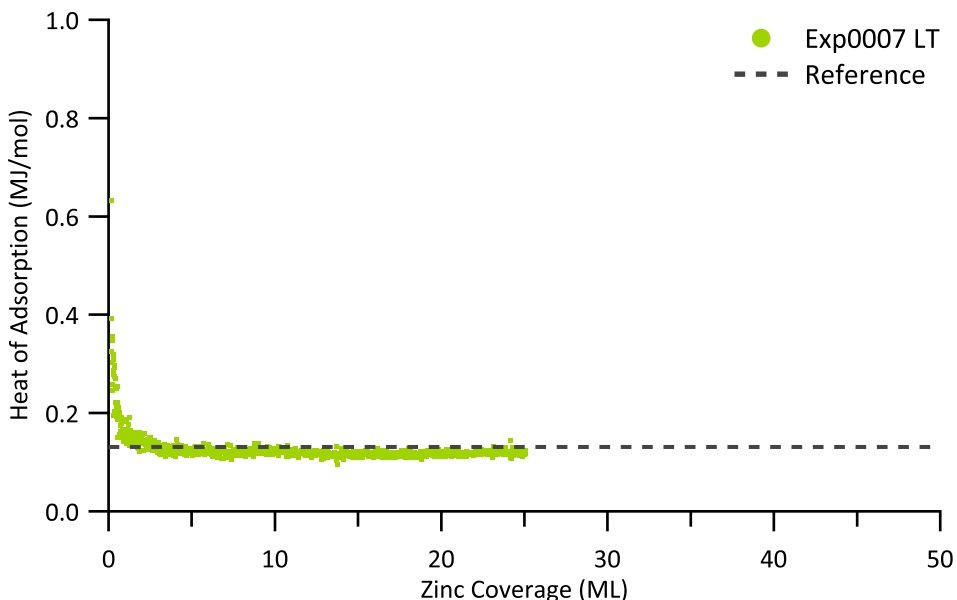


Figure D.53: Low Temperature Enthalpy Data for Zinc on PTCDA — The obtained heat of adsorption of zinc dosed on PTCDA at low temperature as a function coverage is presented for each individual experiment.

E Supplementary Information

This chapter collects additional figures. They demonstrate that the drawn conclusions also apply for analogue measurements discussed in the main parts.

E.1 Previous Data Evaluation Approach

This collection provides intermediary results from the previously used data evaluation approach, see Section 3.13.

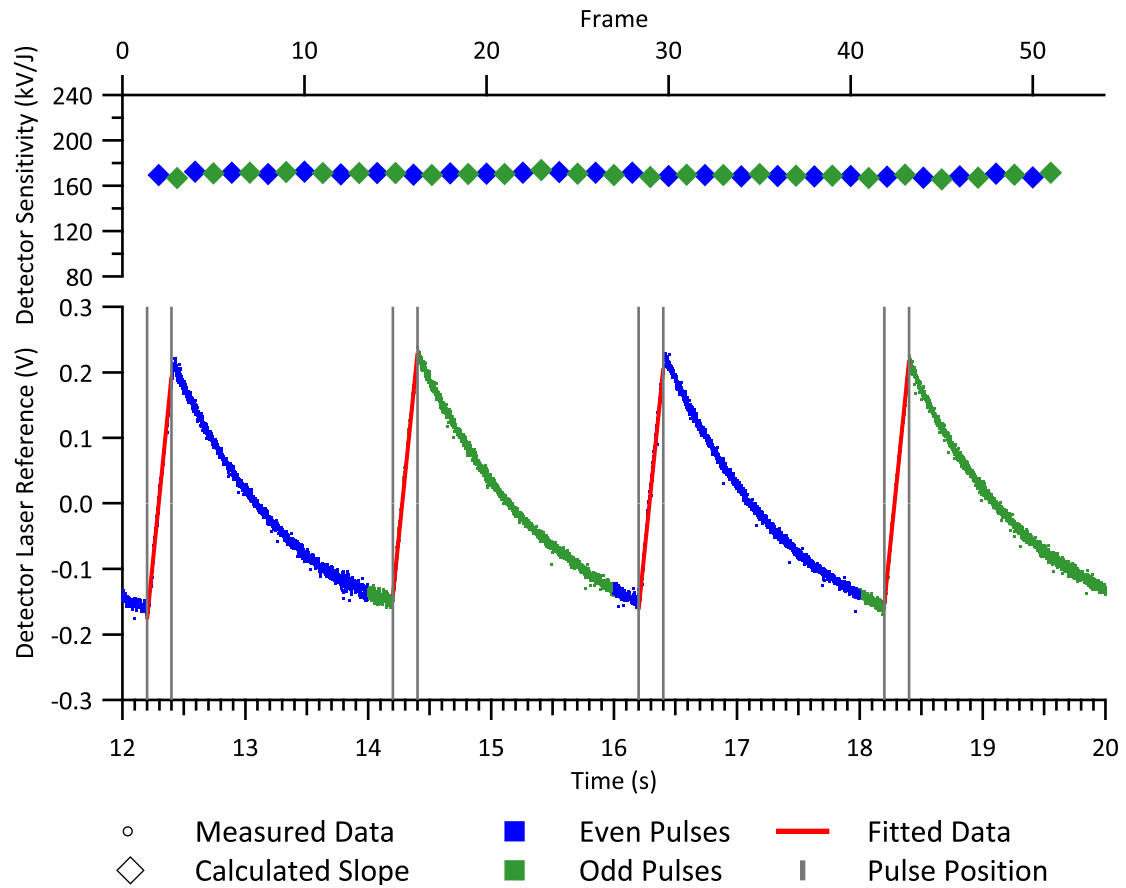


Figure E.1: Laser Reference Previous Evaluation Approach — The lower part of the graph contains exemplary original data of a laser reference measurement, color coded for even (blue dots) and odd (green dots) frames, the pulse position (gray lines), and the linear approximation during the pulse (red line). The upper part of the graph contains the obtained slopes (diamonds) with color coded parity of the whole measurement.

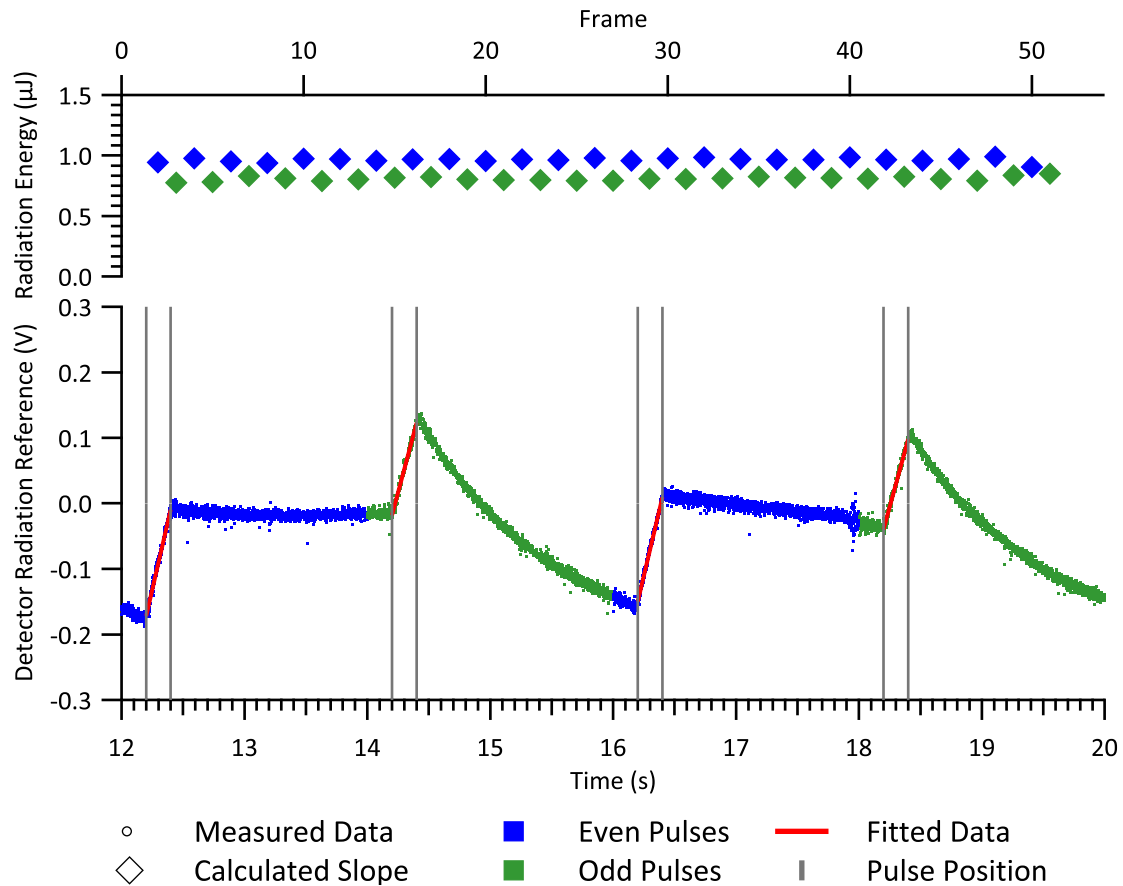


Figure E.2: Radiation Reference Previous Evaluation Approach — The lower part of the graph contains exemplary original data of a radiation reference measurement, color coded for even (blue dots) and odd (green dots) frames, the pulse position (gray lines), and the linear approximation during the pulse (red line). The upper part of the graph contains the obtained slopes (diamonds) with color coded parity of the whole measurement.

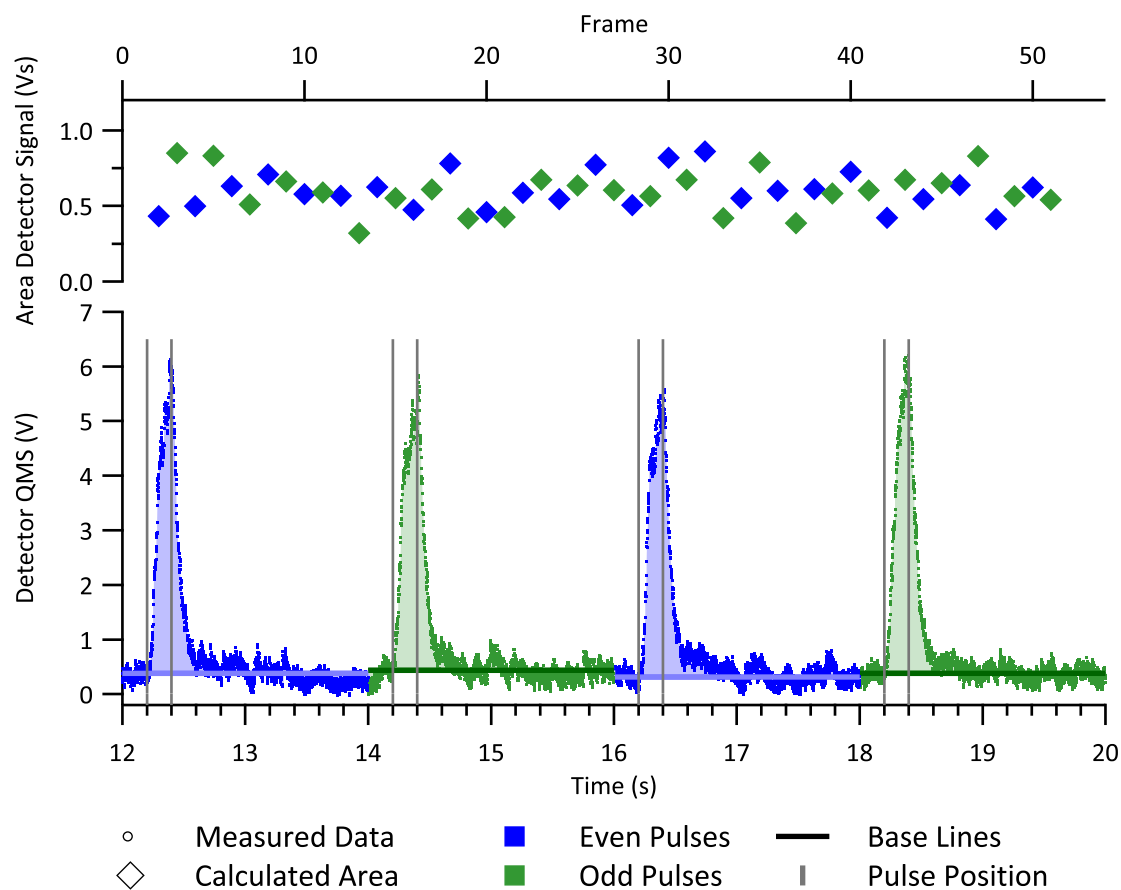


Figure E.3: Desorption Reference Previous Evaluation Approach — The lower part of the graph contains exemplary original data of a sticking reference measurement, color coded for even (blue dots) and odd (green dots) frames, the pulse position (gray lines), the individual baselines (thick lines, color coded), and the area between the baseline and the signal (shaded area, color coded). The upper part of the graph contains the obtained integrated baseline corrected area (diamonds) with color coded parity of the whole measurement.

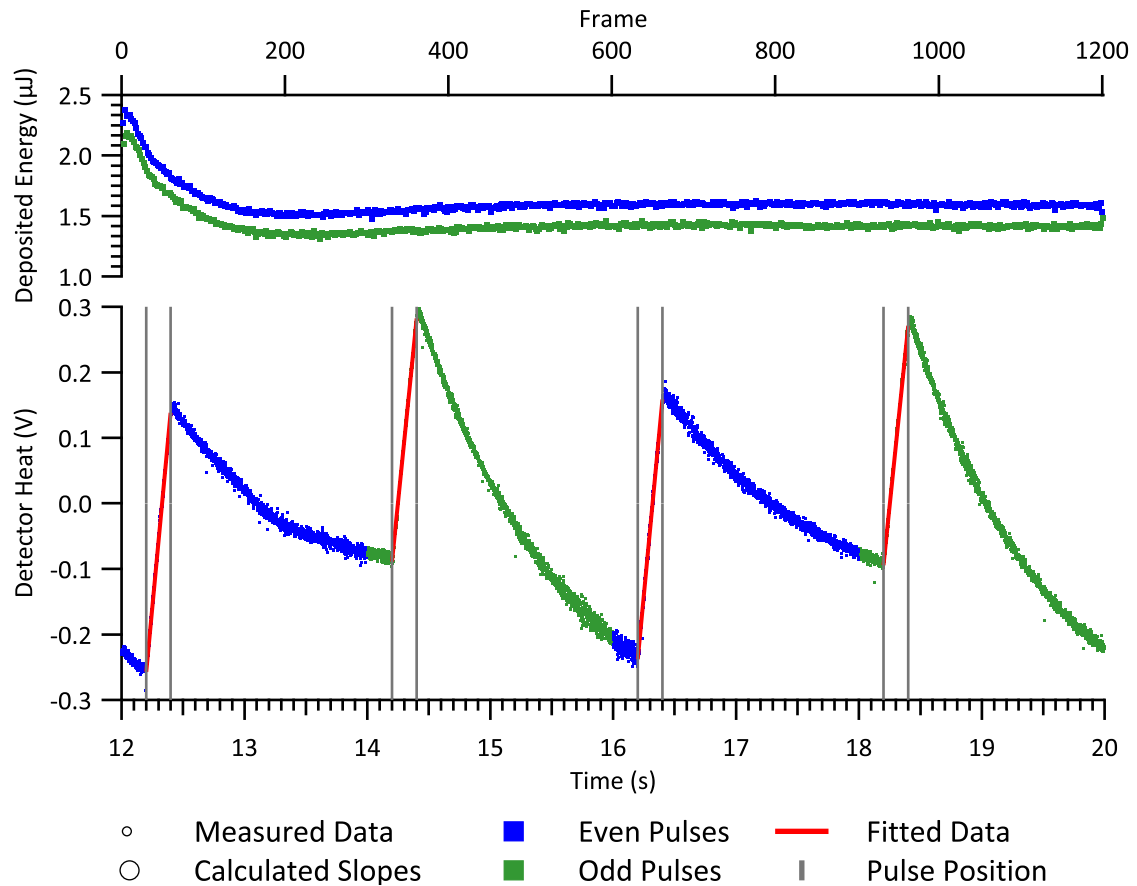


Figure E.4: Heat Measurement Previous Evaluation Approach — The lower part of the graph contains exemplary original data of a calorimetry measurement, color coded for even (small blue dots) and odd (small green dots) frames, the pulse position (gray lines), and the linear approximation during the pulse (red line). The upper part of the graph contains the obtained slopes (large dots) with color coded parity of the whole measurement.

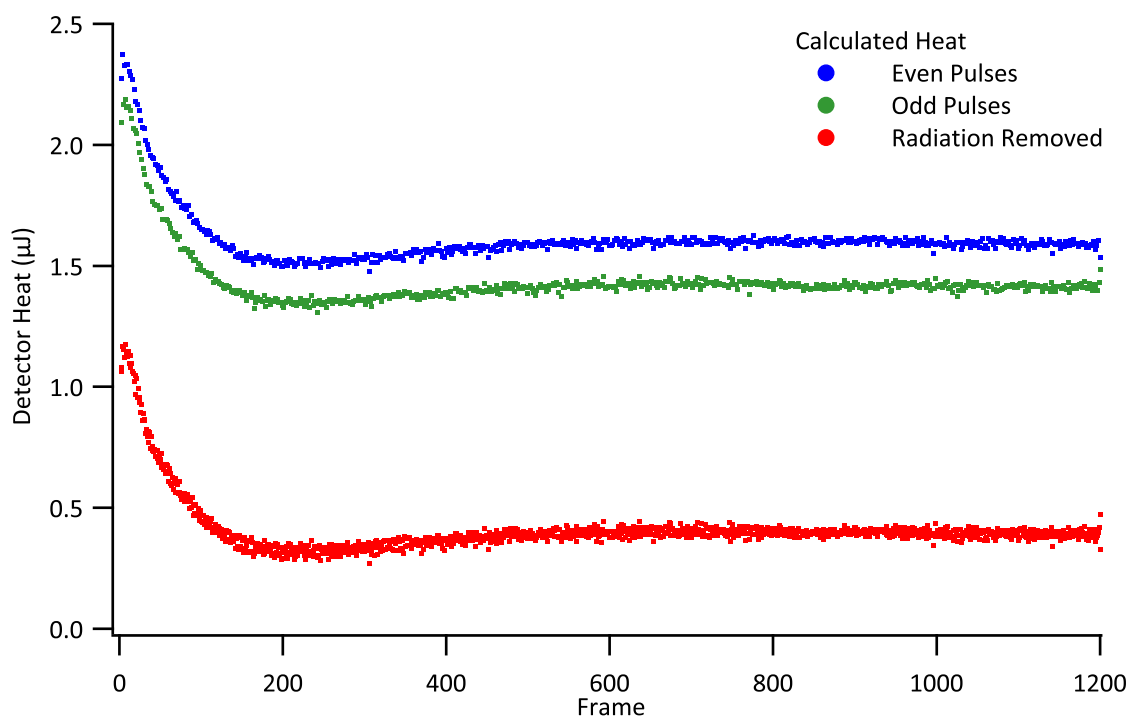


Figure E.5: Energy Calculation Previous Evaluation Approach — The parity dependent original heat from Figure E.4 (even – blue, odd – green) is opposed to the result (red) after subtraction of the parity dependent radiation contribution from Figure E.2 according to the previous approach.

E.2 Filtering

This collection illustrates the choice of the filter frequencies by results of different filters. In these figures black traces are guides to the eye, blue traces original data, and green lines indicate the recommended frequency range. In addition, the results of the filtering algorithm, as discussed in Section 3.3, are provided for all measurements kinds.

E.2.1 Laser Reference Measurement

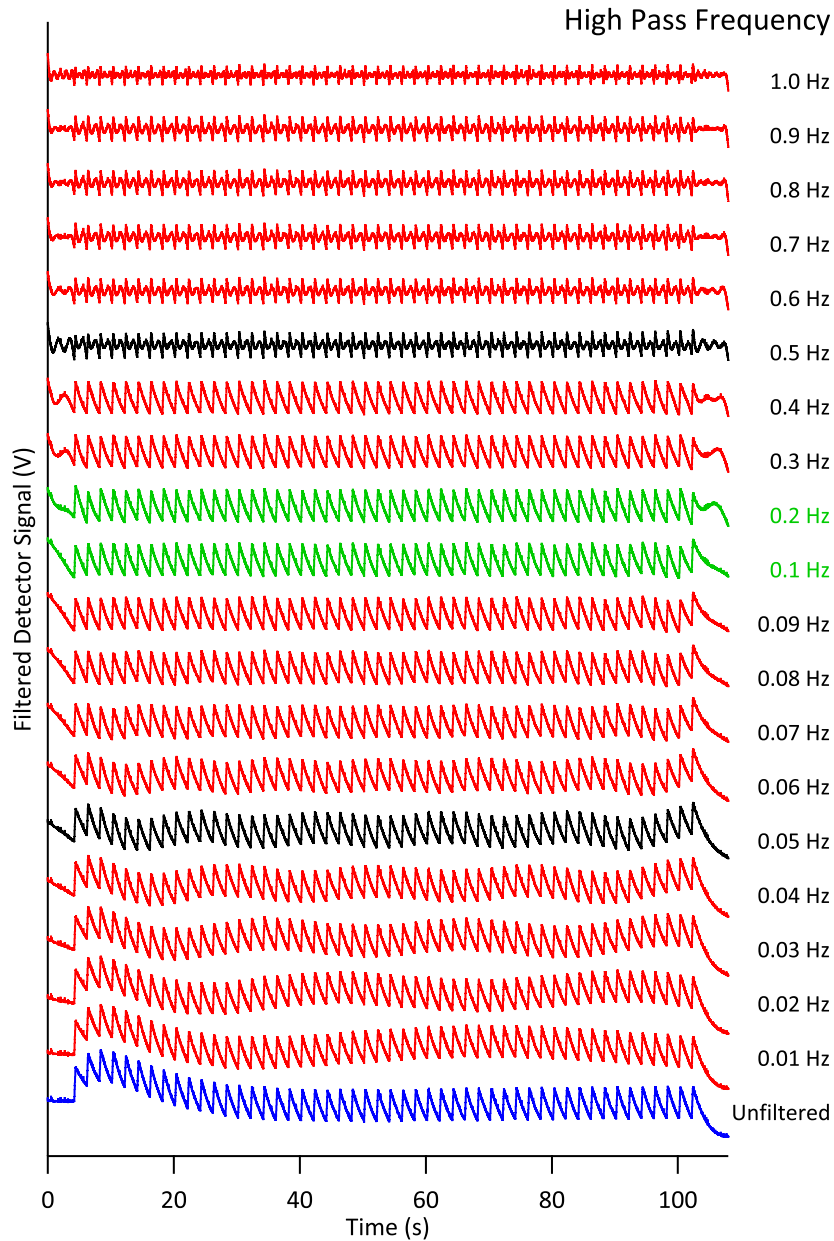


Figure E.6: Filtered Laser Reference Measurement — The obtained 25 consecutive frame pairs at the start of a laser reference measurement are displayed after filtering with a different high pass frequency. The green traces show the range of useful frequencies. The black traces at 0.05 Hz and 0.5 Hz are a guide to the eye while the blue trace represents the unfiltered data for comparison.

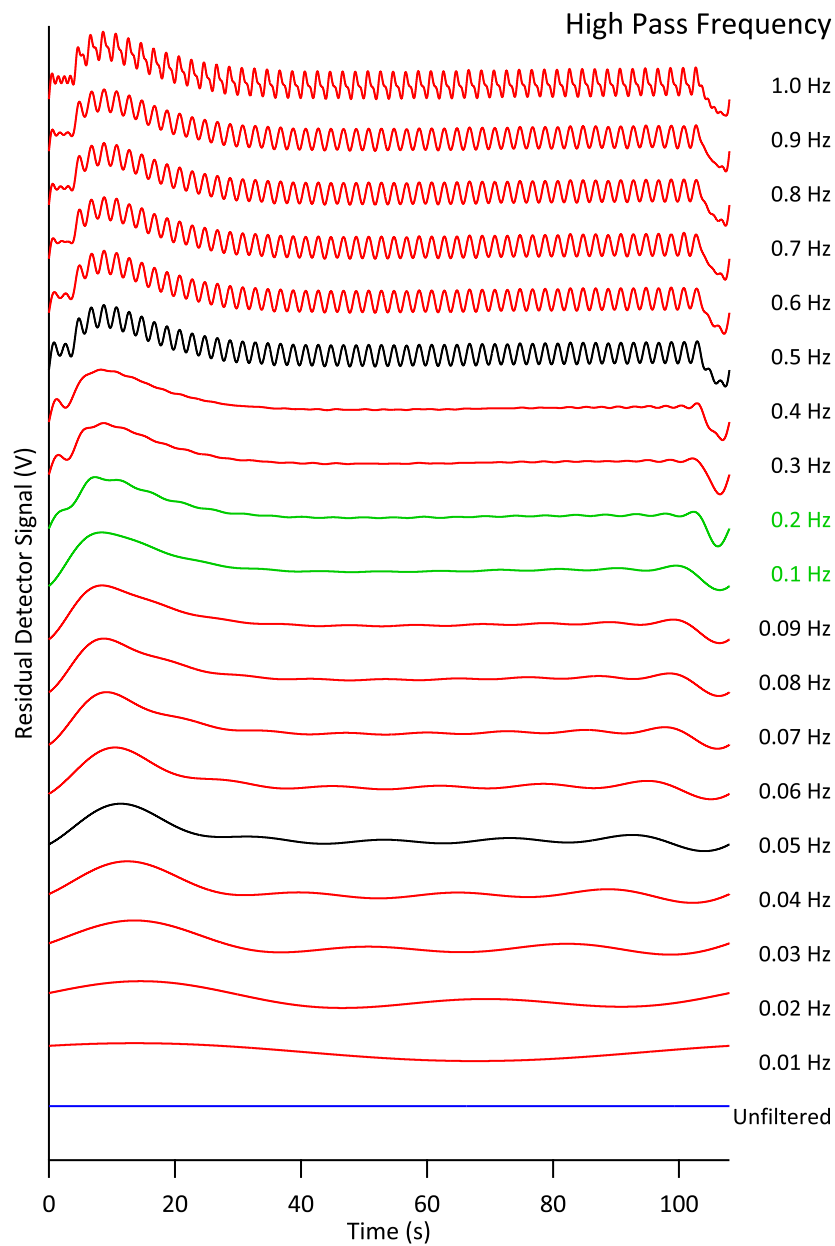


Figure E.7: Filter Residue Laser Reference Measurement — The residues of 25 consecutive frame pairs at the start of a `laser reference` measurement are displayed obtained from filtering with a different high pass frequency. The green traces show the range of useful frequencies. The black traces at 0.05 Hz and 0.5 Hz are a guide to the eye and the blue trace represents the unfiltered data for comparison.

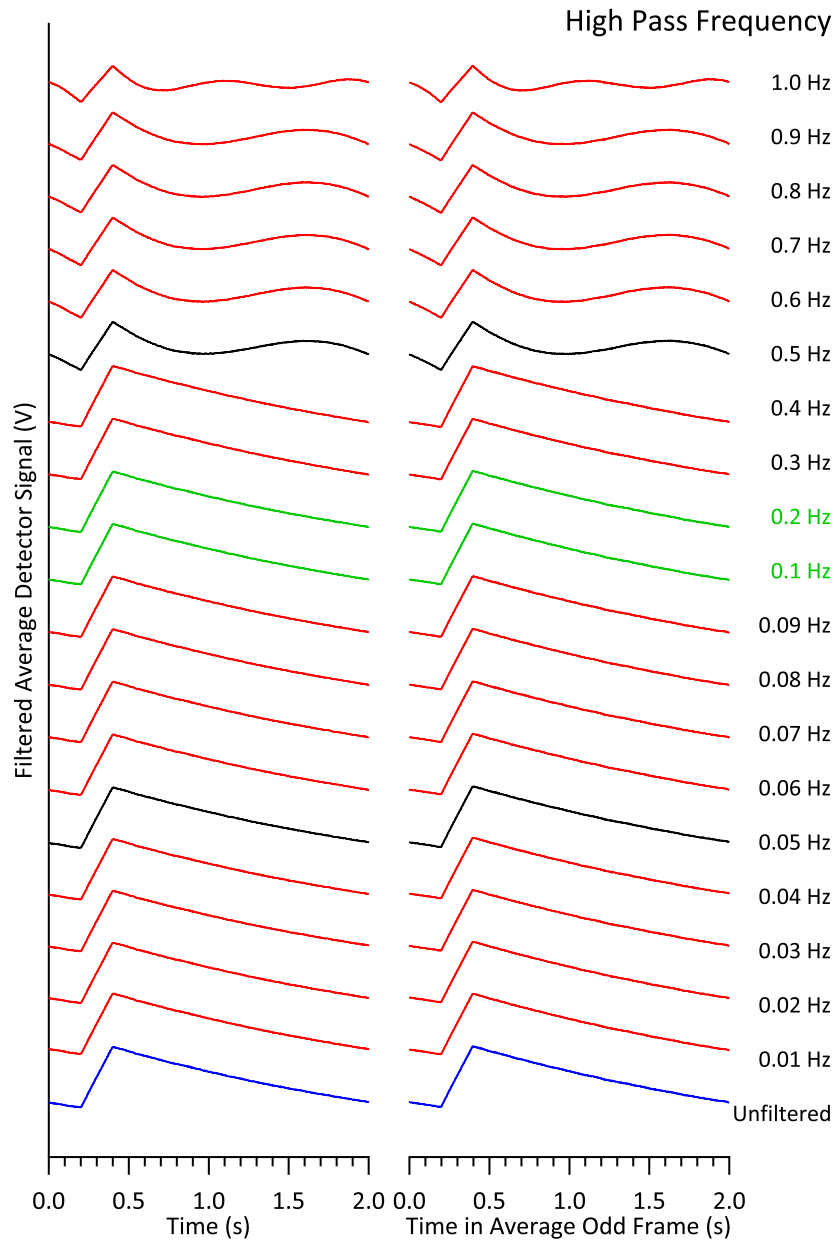


Figure E.8: Averaged Filtered Laser Reference — The averages of 25 consecutive frame pairs at the start of a **laser reference** measurement are displayed after filtering with a different high pass frequency. The green traces show the range of useful frequencies. The black traces at 0.05 Hz and 0.5 Hz are a guide to the eye and the blue trace represents the unfiltered data for comparison.

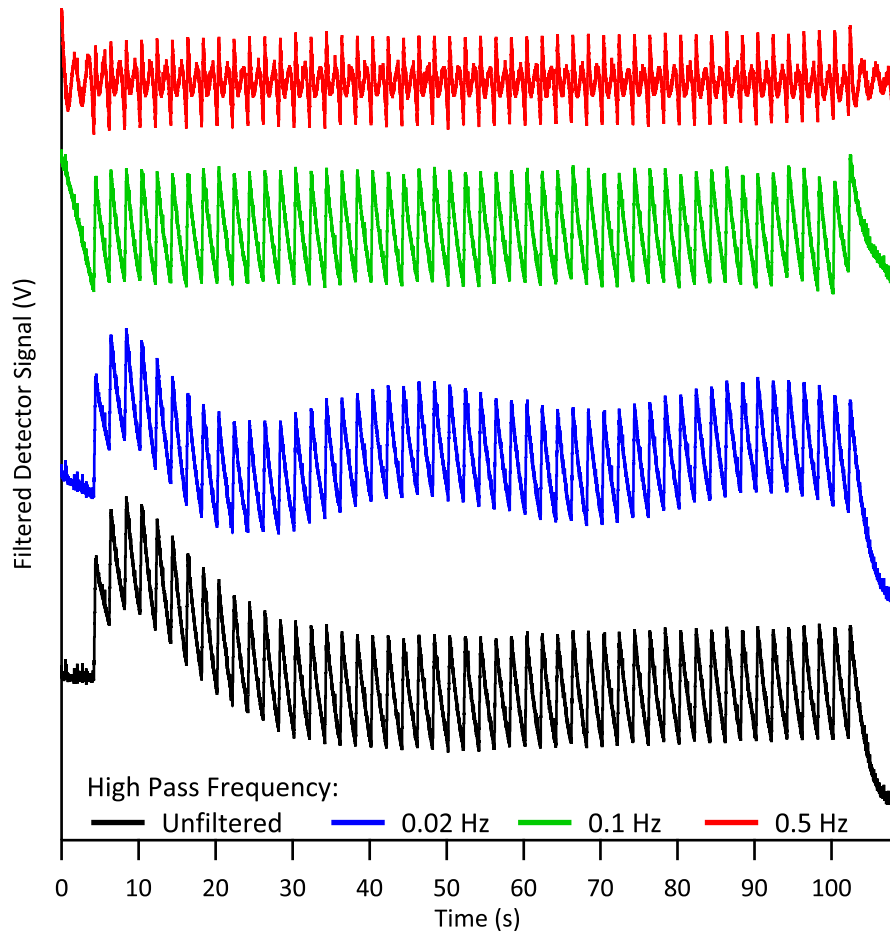


Figure E.9: Detail Filtered Radiation Reference Measurement — A laser reference measurement is displayed together with the results for several filter settings. The unfiltered data (black) exhibits an unwanted slow oscillation. The filtered data set corresponding to a transition frequency of 0.02 Hz (blue) suffers from incomplete removal of the baseline, the data set corresponding to 0.1 Hz (green) matches the ring on in the beginning and shows no contribution of the pulses. An increase of the filter frequency to 0.5 Hz (red) leads to a pronounced contribution of the pulses and thus to a severe distortion of the signal.

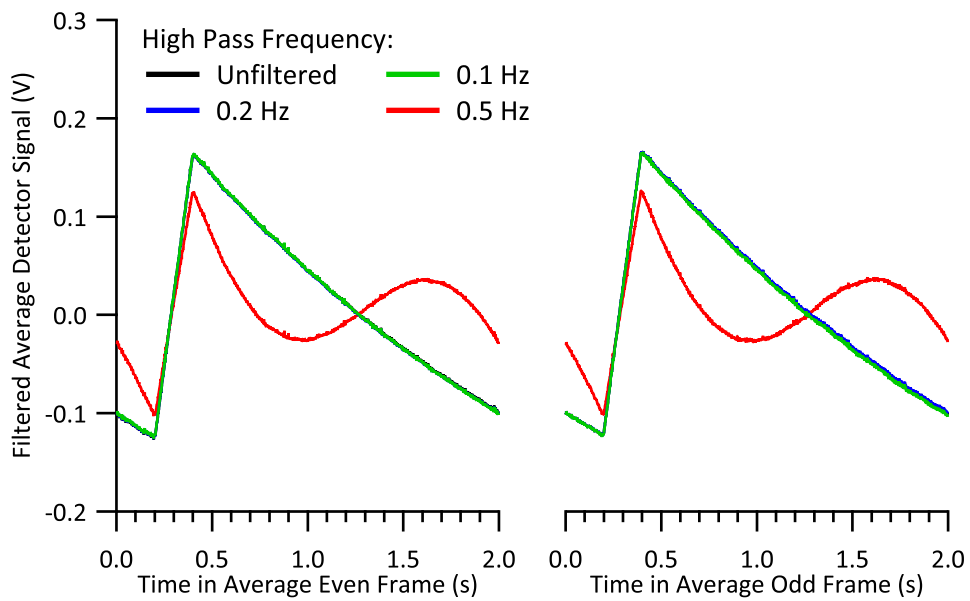


Figure E.10: Average Frames of Filtered Laser Reference Measurement — The average of 12 frame pairs of a `laser reference` measurement is displayed for several filter settings. The unfiltered (black) and filtered waves with a transition frequency of 0.1 Hz (green) and of 0.2 Hz (blue) are almost identical. An increase of the filter frequency to 0.5 Hz (red) leads to a severe distortion of the signal.

E.2.2 Radiation Reference Measurement

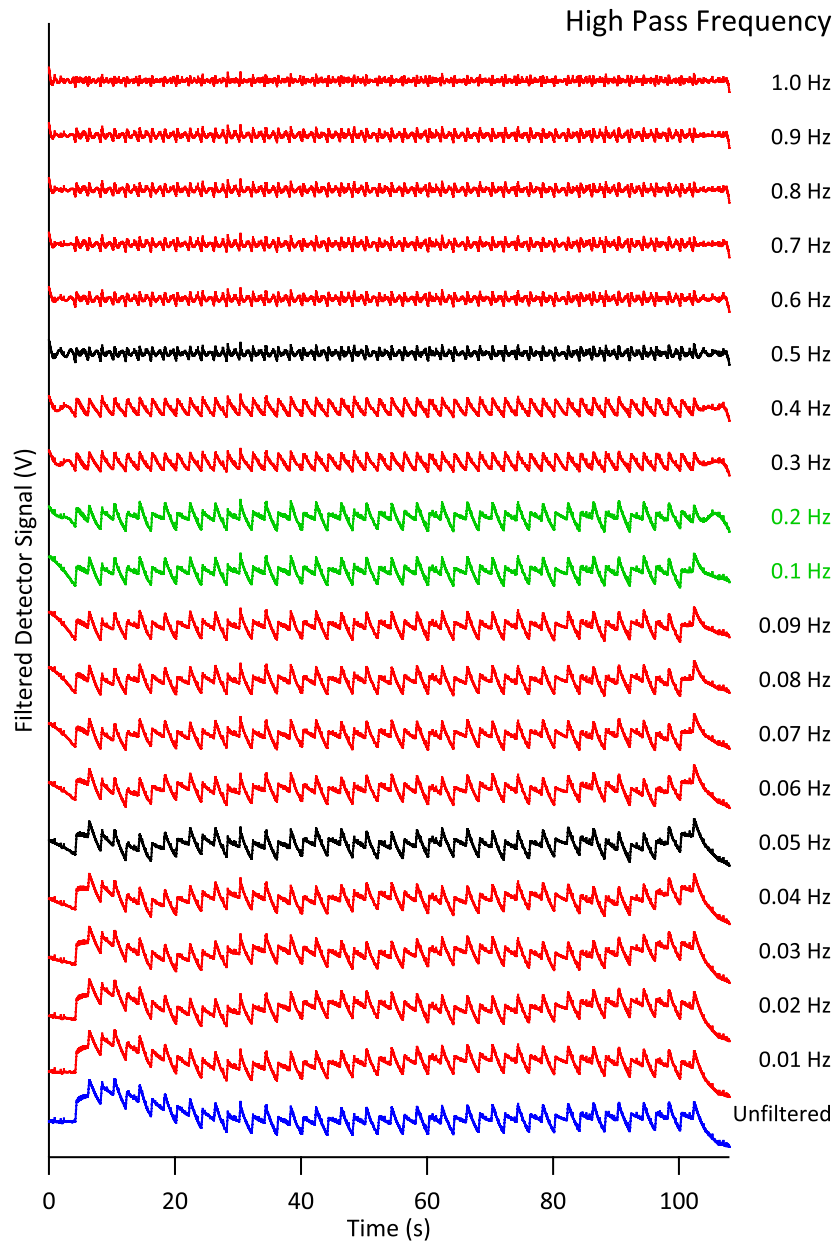


Figure E.11: Filtered Radiation Reference Measurement — The obtained 25 consecutive frame pairs at the start of a radiation reference measurement are displayed after filtering with a different high pass frequency. The green traces show the range of useful frequencies. The black traces at 0.05 Hz and 0.5 Hz are a guide to the eye while the blue trace represents the unfiltered data for comparison.

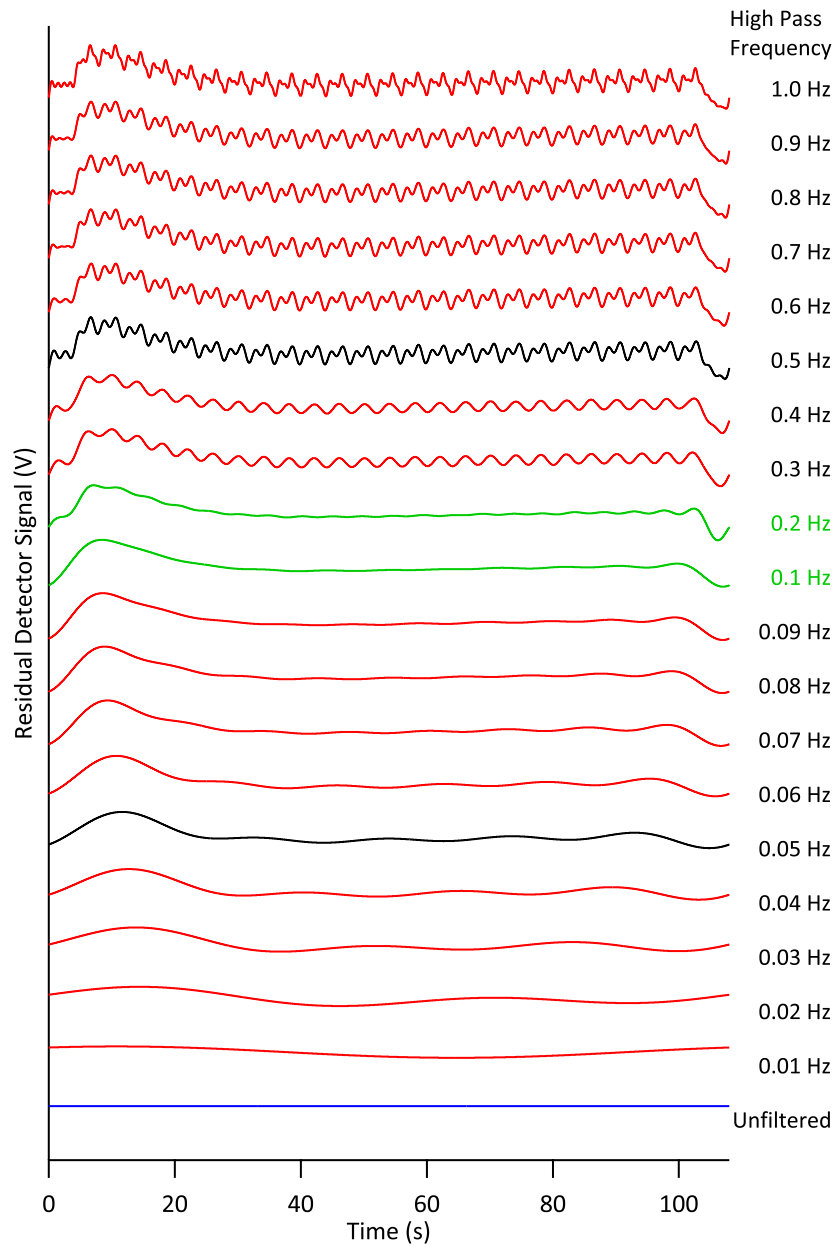


Figure E.12: Filter Residue Radiation Reference Measurement — The residues of 25 consecutive frame pairs at the start of a **radiation** reference measurement are displayed obtained from filtering with a different high pass frequency. The green traces show the range of useful frequencies. The black traces at 0.05 Hz and 0.5 Hz are a guide to the eye and the blue trace represents the unfiltered data for comparison.

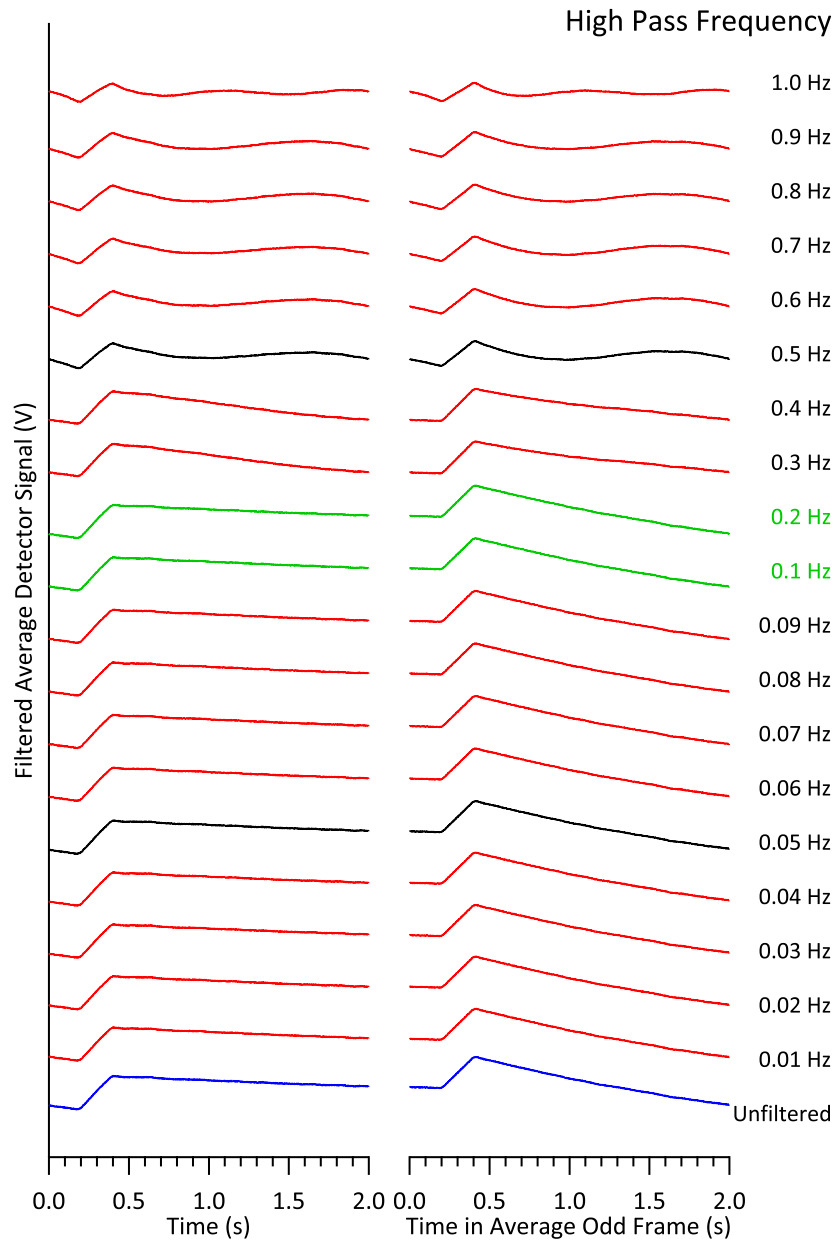


Figure E.13: Averaged Filtered Radiation Reference Measurement — The averages of 25 consecutive frame pairs at the start of a `radiation` reference measurement are displayed after filtering with a different high pass frequency. The green traces show the range of useful frequencies. The black traces at 0.05 Hz and 0.5 Hz are a guide to the eye and the blue trace represents the unfiltered data for comparison.

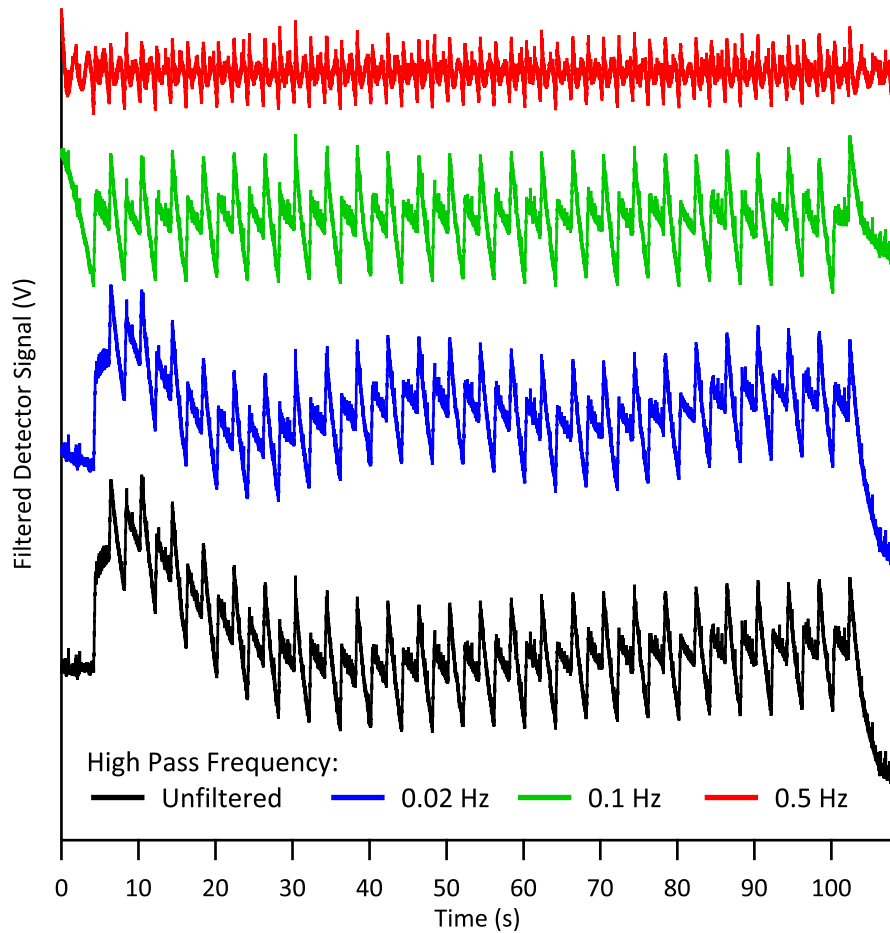


Figure E.14: Detail Filtered Radiation Reference Measurement — A radiation reference measurement is displayed together with the results for several filter settings. The unfiltered data (black) exhibits an unwanted slow oscillation. The filtered data set corresponding to a transition frequency of 0.02 Hz (blue) suffers from incomplete removal of the baseline, the data set corresponding to 0.1 Hz (green) matches the ring on in the beginning and shows no contribution of the pulses. An increase of the filter frequency to 0.5 Hz (red) leads to a pronounced contribution of the pulses and thus to a severe distortion of the signal.

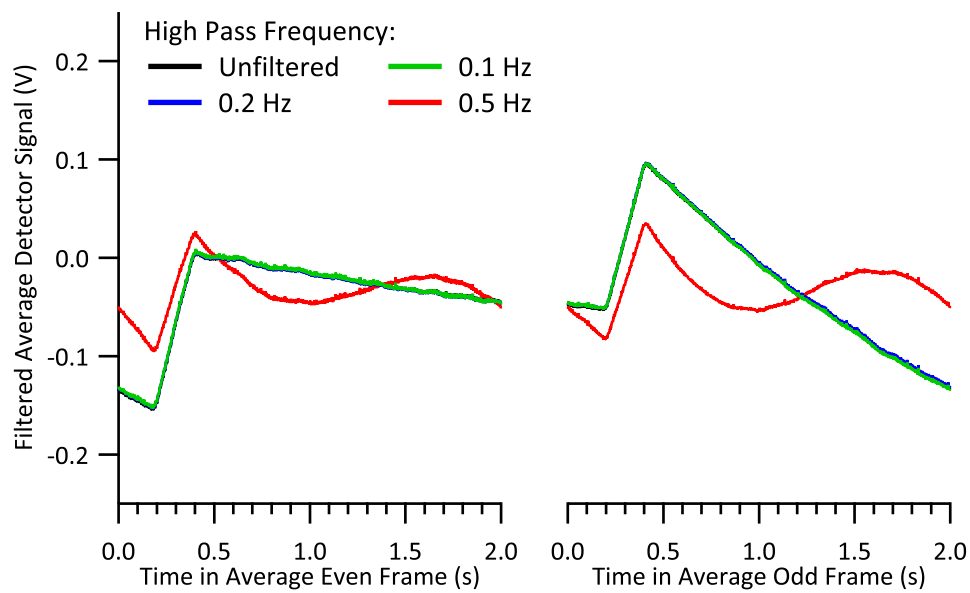


Figure E.15: Average Frames of Filtered Radiation Reference Measurement —

The average of 12 frame pairs of a `radiation` reference measurement is displayed for several filter settings. The unfiltered (black) and filtered waves with a transition frequency of 0.1 Hz (green) and of 0.2 Hz (blue) are almost identical. An increase of the filter frequency to 0.5 Hz (red) leads to a severe distortion of the signal.

E.2.3 Calorimetry Measurement

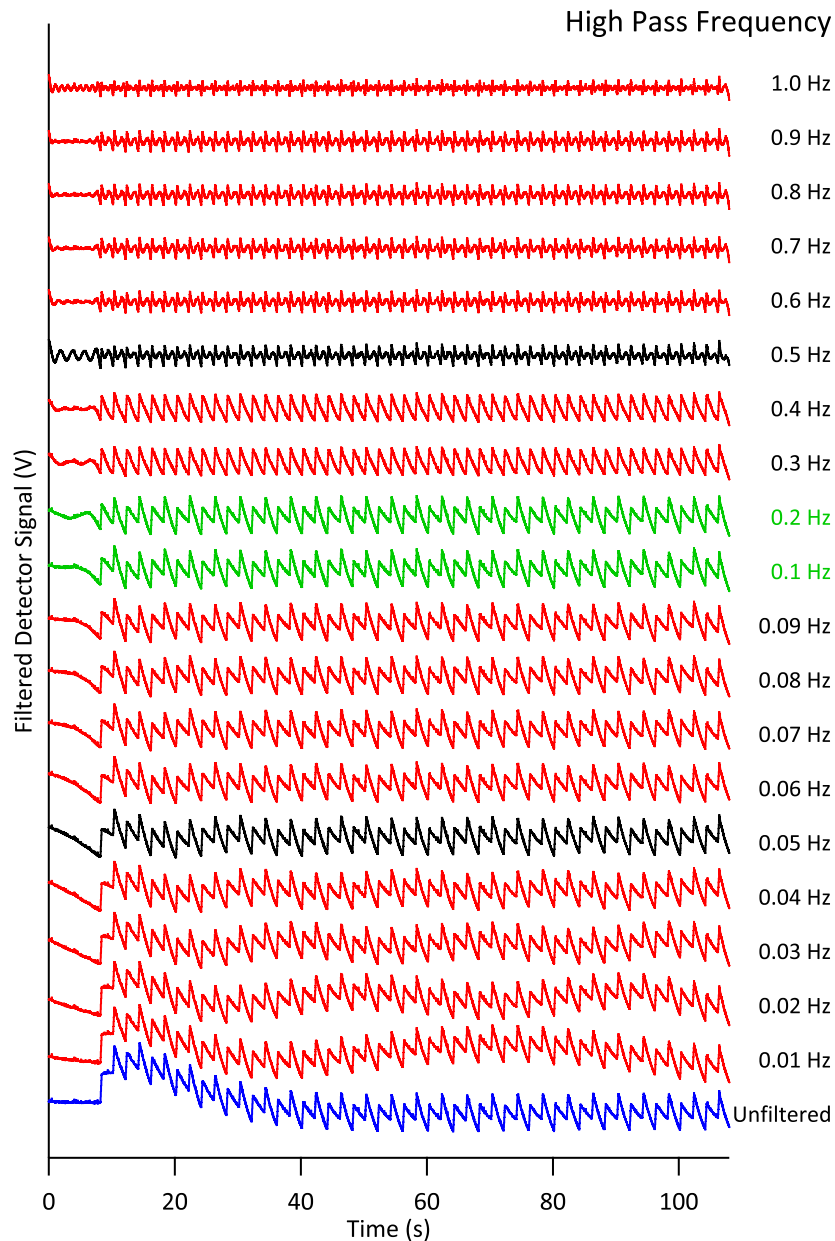


Figure E.16: Filtered Heat Measurement — The obtained 25 consecutive frame pairs at the start of a `heat` measurement are displayed after filtering with a different high pass frequency. The green traces show the range of useful frequencies. The black traces at 0.05 Hz and 0.5 Hz are a guide to the eye while the blue trace represents the unfiltered data for comparison.

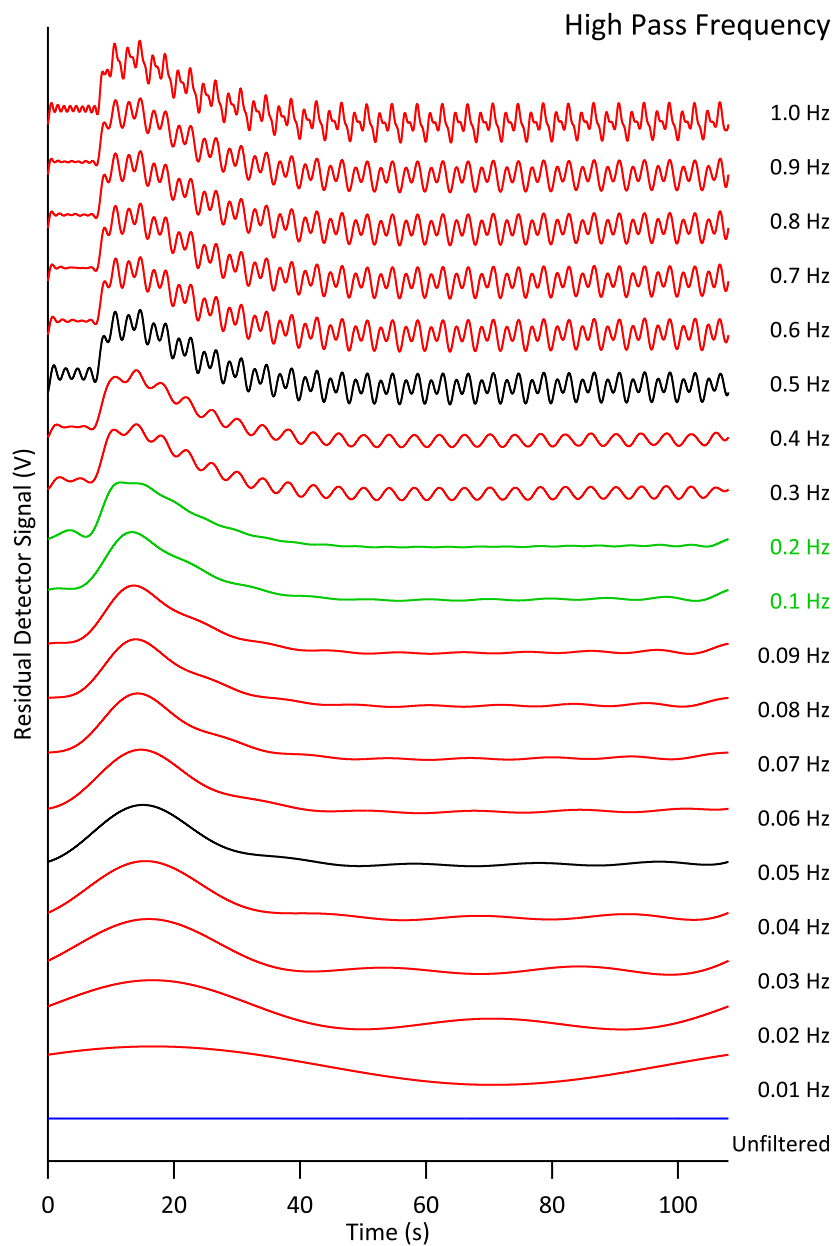


Figure E.17: Filter Residue Heat Measurement — The residues of 25 consecutive frame pairs at the start of a `heat` measurement are displayed obtained from filtering with a different high pass frequency. The green traces show the range of useful frequencies. The black traces at 0.05 Hz and 0.5 Hz are a guide to the eye and the blue trace represents the unfiltered data for comparison.

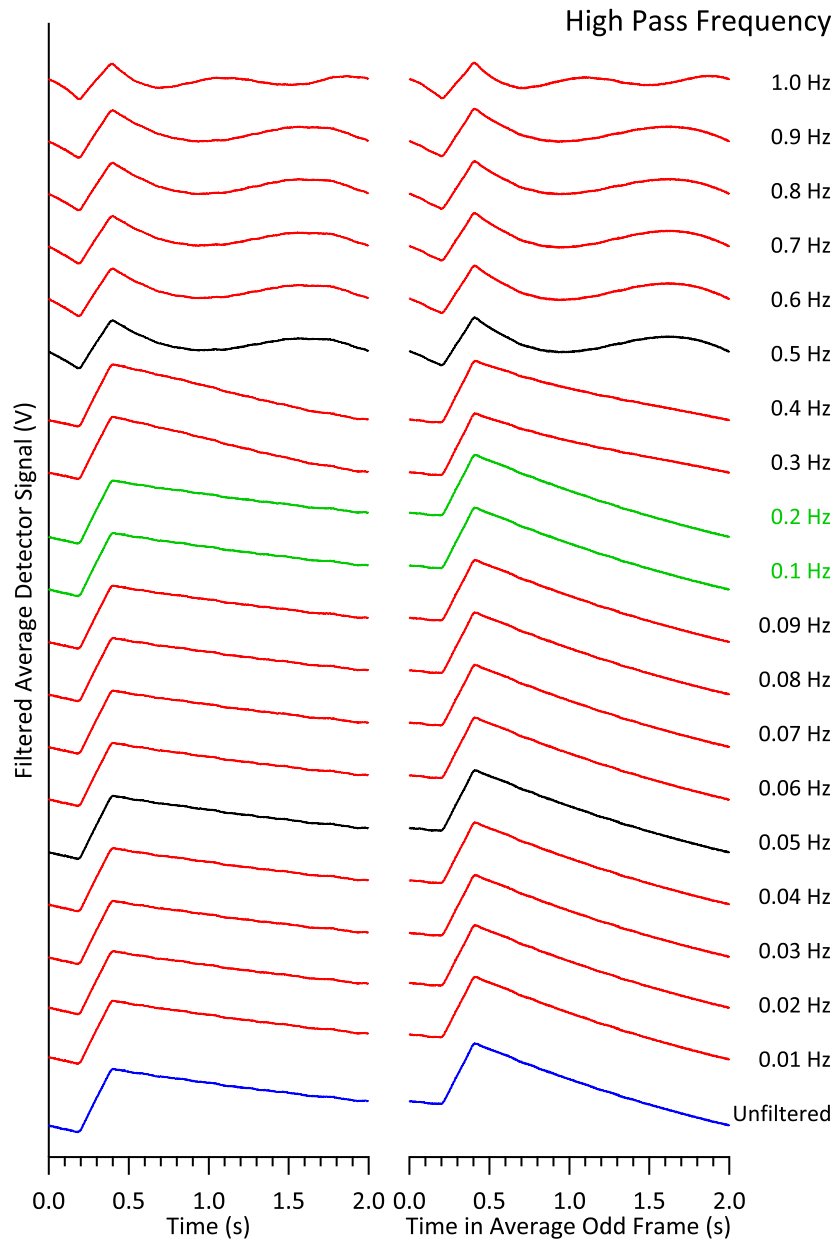


Figure E.18: Averaged Filtered Heat Measurement — The averages of 25 consecutive frame pairs at the start of a `heat` measurement are displayed after filtering with a different high pass frequency. The green traces show the range of useful frequencies. The black traces at 0.05 Hz and 0.5 Hz are a guide to the eye and the blue trace represents the unfiltered data for comparison.

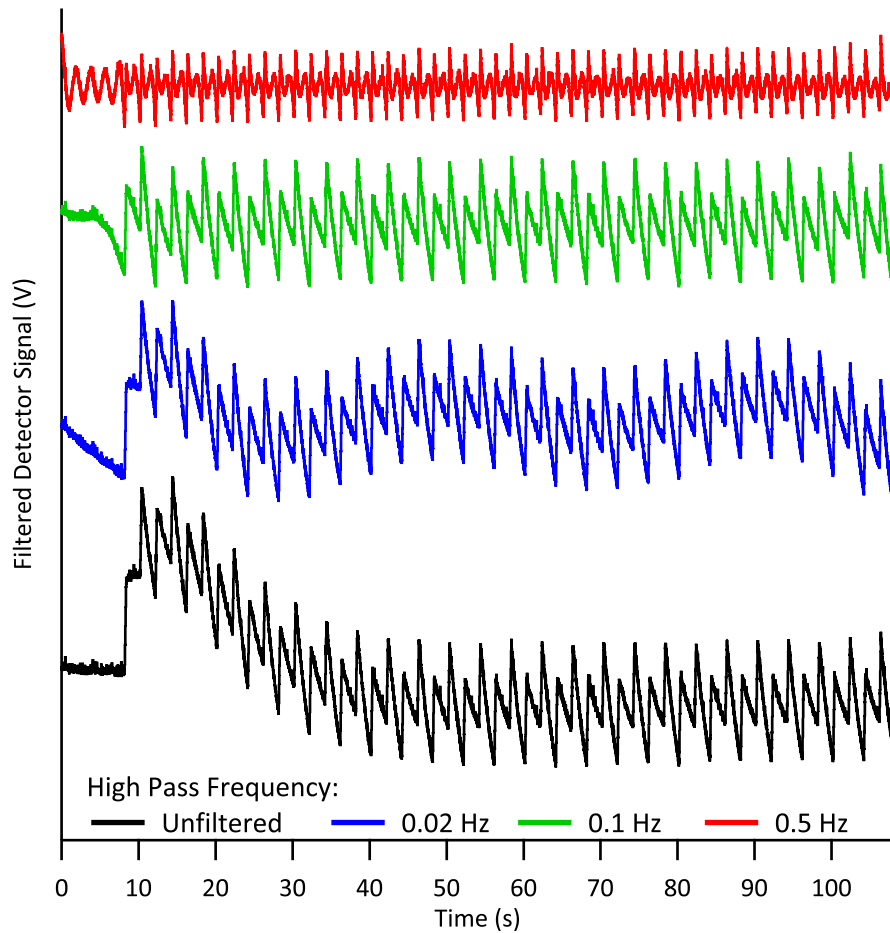


Figure E.19: Detail Filtered Heat Measurement — A heat measurement is displayed together with the results for several filter settings. The unfiltered data (black) exhibits an unwanted slow oscillation. The filtered data set corresponding to a transition frequency of 0.02 Hz (blue) suffers from incomplete removal of the baseline, the data set corresponding to 0.1 Hz (green) matches the ring on in the beginning and shows no contribution of the pulses. An increase of the filter frequency to 0.5 Hz (red) leads to a pronounced contribution of the pulses and thus to a severe distortion of the signal.

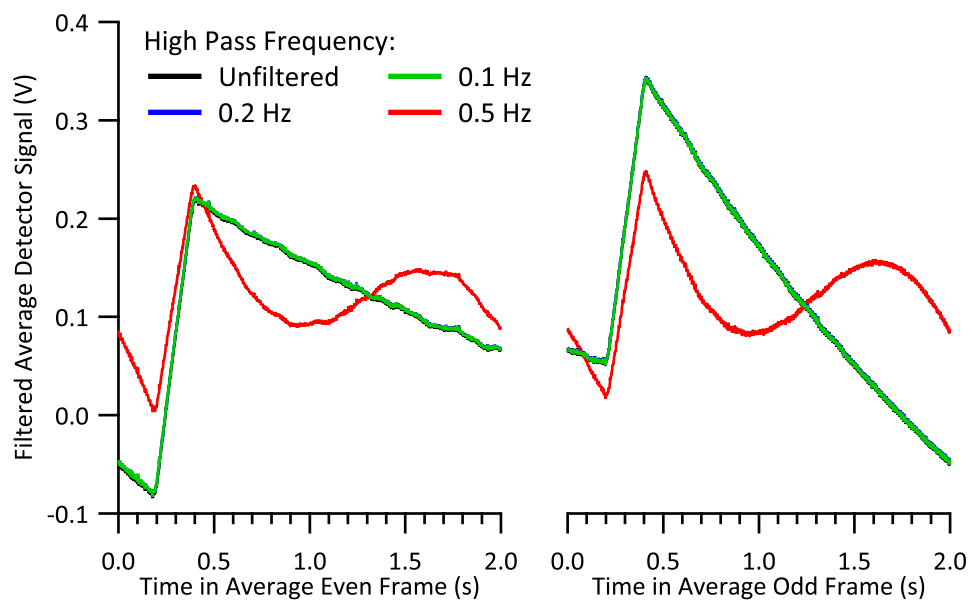


Figure E.20: Average Frames of Filtered Heat Measurement — The average of 12 frame pairs of a `heat` measurement is displayed for several filter settings. The unfiltered (black) and filtered waves with a transition frequency of 0.1 Hz (green) and of 0.2 Hz (blue) are almost identical. An increase of the filter frequency to 0.5 Hz (red) leads to a severe distortion of the signal.

List of Figures

2.1	Assembly of the NAC System	18
2.2	Assembly of the Sample Holder for Crystals	20
2.3	Assembly of the Sample Holder for Thin Films	21
2.4	Assembly of the Detector Stage	24
2.5	Assembly of the Thermal Reservoir	25
2.6	Assembly of the Detector for Crystal Samples	26
2.7	Assembly of the Detector for Polymer Samples	27
2.8	Assembled Heater for Crystal Samples	27
2.9	Assembly of the Spring Suspended Detector Mount	28
2.10	Sample/Ribbon Contact Cases	29
2.11	Assembly of the Molecular Beam	31
2.12	Assembly of the Main Evaporator's Base Flange	32
2.13	Assembly of the Main Evaporator	33
2.14	Schematic of the Heating Wire	34
2.15	Assembly of the Lens Holder	36
2.16	Mirror/Orifice Assembly Vacuum Side	36
2.17	Mirror/Orifice Assembly Air Side	37
2.18	Assembled Mirror/Orifice Stage	38
2.19	Assembly of the Chopper	39
2.20	Assembly of the End Switches	40
2.21	Assembly of the Chopper Blade	41
2.22	Positions of the Chopper Blade	42
2.23	Assembled Chopper	43
2.24	Assembly of the Molecular Beam Valve	44
2.25	Assembled Valve	45
2.26	Assembly of the Deflector Plates	47
2.27	Assembled Deflector Plates	47
2.28	Assembly of the Nozzle	48
2.29	Assembly of the Beam Housing	49
2.30	Welded Beam Housing	51

2.31	Assembly of the Molecular Beam (Top View)	52
2.32	Assembly of the Molecular Beam (Front View)	53
2.33	Assembly of the Molecular Beam (Left View)	54
2.34	Assembly of the Ancillaries Flange	55
2.35	Assembly of the Hot Plate	57
2.36	Assembly of the QCM Section	58
2.37	Assembly of the Mirror Section	58
2.38	Assembly of the Infrared Transparent Window Section	59
2.39	Assembly of the Ancillary Instruments	61
2.40	Assembled Ancillaries Stage	62
2.41	Electrical Potential Between Mass Spectrometer and Sample	63
2.42	Assembly of the Mass Spectrometer Mount	64
2.43	Assembly of the Seat for Optical Meters	66
2.44	Assembly of the Pyrometer Mount	67
2.45	Assembly of the Photometer Mount	68
2.46	Fixed Part of the Fiber Positioner	70
2.47	Moveable Part of the Fiber Positioner	71
2.48	Assembly to Lift the Main Chamber	73
2.49	Upper Assembly for Moving the NAC Machine	74
2.50	Lower Assembly for Moving the NAC Machine	74
2.51	Assembly of the Water Distribution Mount	75
2.52	Assembly to Hold Minicans	75
2.53	Assembly of the Load Lock	77
2.54	Assembly of the Load Lock Housing	78
2.55	Assembly to Support Transfer Rods	79
2.56	Assembly to Support the Load Lock	80
2.57	Assembly of the Load Lock Evaporator	81
2.58	Assembly of the Sample Storage System	82
2.59	Assembly of the Load Lock Sample Transfer System	83
2.60	Assembly of the Main Chamber Sample Transfer	83
2.61	Sample Handover	84
2.62	Sample Retaining Mechanisms	84
2.63	Assembly of the Glove Box Connection	86
2.64	Assembly of the NAC system (Front View)	88
2.65	Assembly of the NAC system (Top View)	89
2.66	The Nanojoule Adsorption Calorimeter	90

3.1	Main Panel of the NAC Data Evaluation Program	102
3.2	Filtered Radiation Reference Measurement	107
3.3	Average Frames of a Filtered Radiation Reference Measurement . .	108
3.4	Time Constant of the Measurement Setup	109
3.5	Effect of the Additional Notch Filter	110
3.6	Effect of the Filtering on the Data	111
3.7	Filtering and Beat in Signal	112
3.8	Constitution of Fit Waves	121
3.9	Constitution of Fit Waves for Deconvolution	122
3.10	Pulse Length Determination	123
3.11	Comparison of Laser Based and Radiation Signal	125
3.12	Statistical Comparison of the References	130
3.13	Statistical Comparison of the References	131
3.14	Fit Contributions Heat Measurement	133
3.15	Effect of Fitted Trends: Noise	140
3.16	Effect of Fitted Trends: Balancing	141
3.17	Influence of Noise in the Deconvolution Reference	145
3.18	Comparison of the Novel and Previous Data Evaluation Approach: Sticking	150
3.19	Comparison of the Novel and Previous Data Evaluation Approach: Calculated Heat	151
3.20	Comparison of the Novel and Previous Data Evaluation Approach: Radiation Contribution	152
5.1	Geometry for the External Reflectivity Measurement	225
5.2	Reflectivity Measurement	226
5.3	Sputtering of a QCM Crystal	229
5.4	Photoemission Spectra of Aluminum Foils	230
5.5	Magnesium Deposition on QCM Crystals	231
5.6	Detector Polymer Degradation upon Coating	242
5.7	Schematic of the Load Lock Evaporator	243
5.8	Stability of the Laser Diode	246
5.9	Voltage Response from the Detector	248
5.10	Deposition Rate and Temperature Stability	250
5.11	Photographs of “Spitted” Evaporant	251
5.12	A photograph of the Steel Wool Plug	251
5.13	Performance of the Inline Valve	253

5.14	Performance of the Chopper: Photo Diode	254
5.15	Performance of the Chopper: Deconvoluted, Diffuse Radiation . . .	255
5.16	Performance of the Chopper: Deconvoluted, Direct Radiation . . .	256
5.17	Crucible Radiation in Laser Measurement	259
5.18	Influence of the Mass Spectrometer's Range Setting	262
5.19	Influence of the Pulse Length on the Mass Spectrometer Signal: Direct Dosing	264
5.20	Influence of the Pulse Length on the Mass Spectrometer Signal: Indirect Dosing	265
5.21	Integrated Mass Spectrometer Signal <i>vs.</i> Pulse Length	266
5.22	Mass Spectrometer Linearity Regarding Deposition Rate	267
5.23	Temperature Dependence of Radiation	269
5.24	Transmission of the Barium Fluoride Window	270
5.25	Wavelength Dependent Parameters	271
5.26	Temperature Dependent Relative Infrared Emission	274
5.27	Infrared Radiation Compared for two Temperatures	275
5.28	Ratio of Deposition Rate in Sample and Ancillary Position	276
5.29	Schematic of the Laser Path	277
5.30	Laser Power Correction Factor	278
5.31	Sticking Reference Correction Factor	282
5.32	Relative Mass Spectrometer Intensity <i>vs.</i> Hot Plate Temperature .	284
5.33	Temperature Dependency of Transient Adsorption	286
5.34	Mass Spectrometer Peak Shape at Different Range Settings	288
5.35	Example of Transient Adsorption: Lead on Molybdenum	289
5.36	Calculated Transient Lifetimes	290
5.37	Peak Shape of the Mass Spectrometer Signal	291
5.38	Detector Linearity Towards Input Power	294
5.39	Illustration for Sample Occlusion	295
5.40	Detector Linearity Towards Active Area	297
5.41	Annealing Effect on the Detector	298
5.42	Thermal Treatment of Detector Polymer	299
5.43	Temperature Dependency of the Detector Sensitivity	300
5.44	Influences of the Detector Structure	302
5.45	Thawing of the Thermal Reservoir	305
5.46	Round Robin Power Input Test	307
5.47	Relative Laser Reference Amplitudes	308
5.48	Histogram of Relative Laser Reference Amplitudes	309

5.49	Scatter of the Laser Reference Amplitudes by Laser Power	310
5.50	Scatter of the Laser Reference Amplitudes by Time	311
6.1	Crystal Structure of the Magnesium Type	319
6.2	Crystal Structure of the Copper Type	320
6.3	Chemical Structure of 3,4,9,10-Perylene-Tetracarboxylic Dianhydride	322
6.4	Chemical Structure of 2,5'-poly(3-Hexylthiophene)	323
6.5	Chemical Structure of α -Sexithiophene	324
6.6	Chemical Structure of 5,10,15,20-Tetraphenyl-21 <i>H</i> ,23 <i>H</i> -Porphin . .	325
6.7	Work Flow of a Calorimetric Experiment	330
6.8	Adsorption of Magnesium: Sticking Probability	334
6.9	Adsorption of Magnesium: Heats of Adsorption	335
6.10	Adsorption of Magnesium: Heats of Adsorption at Low Coverages .	336
6.11	Adsorption of Calcium: Sticking Probabilities (Clean Detector, Tetraphenyl Porphyrin)	340
6.12	Adsorption of Calcium: Sticking Probabilities (PTCDA)	341
6.13	Low Temperature Adsorption of Calcium: Sticking Probabilities (PTCDA)	342
6.14	Adsorption of Calcium: Sticking Probabilities (Sexithiophene) . . .	343
6.15	Low Temperature Adsorption of Calcium: Sticking Probabilities (Sexithiophene)	344
6.16	Adsorption of Calcium: Heats of Adsorption (Clean Detector, Tetraphenyl Porphyrin)	345
6.17	Adsorption of Calcium: Low Coverage Heats of Adsorption (Clean Detector Tetraphenyl Porphyrin)	346
6.18	Adsorption of Calcium: Heats of Adsorption (PTCDA)	347
6.19	Adsorption of Calcium: Low Coverage Heats of Adsorption (PTCDA)	348
6.20	Low Temperature Adsorption of Calcium: Heats of Adsorption (PTCDA)	349
6.21	Low Temperature Adsorption of Calcium: Low Coverage Heats of Adsorption (PTCDA)	350
6.22	Adsorption of Calcium: Heats of Adsorption (Sexithiophene)	351
6.23	Adsorption of Calcium: Low Coverage Heats of Adsorption (Sexithiophene)	352

6.24	Low Temperature Adsorption of Calcium: Heats of Adsorption (Sexithiophene)	353
6.25	Low Temperature Adsorption of Calcium: Low Coverage Heats of Adsorption (Sexithiophene)	354
6.26	Adsorption of Copper: Heats of Adsorption	364
6.27	Copper Glazed Filament	366
6.28	Adsorption of Zinc: Sticking Probabilities	368
6.29	Adsorption of Zinc: Heats of Adsorption	369
6.30	Adsorption of Zinc: Low Coverage Heats of Adsorption	370
6.31	Adsorption of Calcium on Sexithiophene: Full Detector Data	373
6.32	Adsorption of Calcium on Sexithiophene: Fitted Detector Data . .	374
6.33	Adsorption of Calcium on Sexithiophene: Radiation Contribution .	375
6.34	Adsorption of Calcium on Sexithiophene: Stability Checks	375
6.35	Adsorption of Zinc on Sputtered Detector: Coverage Dependent Signal Shape	379
6.36	Adsorption of Zinc on Sputtered Detector: Reconstructed Power Input for Laser and Radiation Reference	380
6.37	Adsorption of Zinc on Sputtered Detector: Reconstructed Power Input for Calorimetric Measurement	381
6.38	Adsorption of Zinc on Sputtered Detector: Reconstructed Power at High Coverages for Various Measurements	382
B.1.1	Design Drawing: Main Evaporator	456
B.1.2	Design Drawing: Internal Valve	465
B.1.3	Design Drawing: Optics Stage	473
B.1.4	Design Drawing: Beam Chopper	483
B.1.5	Design Drawing: Nozzle in Main Chamber	490
B.1.6	Design Drawing: Beam Housing	495
B.2.1	Design Drawing: Sample Holder	512
B.2.2	Design Drawing: Sample Carrier	520
B.2.3	Design Drawing: Detector	525
B.2.4	Design Drawing: Sample Heater	550
B.2.5	Design Drawing: Mass Spectrometer Mount	561
B.2.6	Design Drawing: Ancillaries Stage	568
B.2.7	Design Drawing: Main Chamber Additions	589
B.2.8	Design Drawing: Optical Meters	606

B.2.9	Design Drawing: Fiber Positioner	623
B.3.1	Design Drawing: Mount for Load Lock	639
B.3.2	Design Drawing: Load Lock Housing	647
B.3.3	Design Drawing: Sample Storage	654
B.3.4	Design Drawing: Transfer Rod Support	662
B.4.1	Design Drawing: Glove Box	669
B.4.2	Design Drawing: Evaporator for Synchrotron Applications	673
B.4.3	Design Drawing: Mounting Stand	682
B.4.4	Design Drawing: Threefold Evaporator	690
B.4.5	Design Drawing: Battery Box	701
D.1	Auxiliary Data for Magnesium on Pristine Detector	856
D.2	Averaged Data for Magnesium on Pristine Detector	856
D.3	Sticking Data for Magnesium on Pristine Detector	857
D.4	Enthalpy Data for Magnesium on Pristine Detector	857
D.5	Auxiliary Data for Magnesium on Sputter Cleaned Detector	858
D.6	Averaged Data for Magnesium on Sputter Cleaned Detector	858
D.7	Sticking Data for Magnesium on Sputter Cleaned Detector	859
D.8	Enthalpy Data for Magnesium on Sputter Cleaned Detector	859
D.9	Auxiliary Data for Magnesium on PTCDA	860
D.10	Averaged Data for Magnesium on PTCDA	860
D.11	Sticking Data for Magnesium on PTCDA	861
D.12	Enthalpy Data for Magnesium on PTCDA	861
D.13	Auxiliary Data for Calcium on Sputter Cleaned Detector	862
D.14	Averaged Data for Calcium on Sputter Cleaned Detector	862
D.15	Sticking Data for Calcium on Sputter Cleaned Detector	863
D.16	Enthalpy Data for Calcium on Sputter Cleaned Detector	863
D.17	Auxiliary Data for Calcium on Tetraphenyl Porphyrin	864
D.18	Averaged Data for Calcium on Tetraphenyl Porphyrin	864
D.19	Sticking Data for Calcium on Tetraphenyl Porphyrin	865
D.20	Enthalpy Data for Calcium on Tetraphenyl Porphyrin	865
D.21	Auxiliary Data for Calcium on PTCDA	866
D.22	Averaged Data for Calcium on PTCDA	866
D.23	Sticking Data for Calcium on PTCDA	867
D.24	Enthalpy Data for Calcium on PTCDA	867

D.25	Enthalpy Data for Calcium on PTCDA: Small Layer Thickness . . .	868
D.26	Enthalpy Data for Calcium on PTCDA: Large Layer Thickness . . .	868
D.27	Low Temperature Auxiliary Data for Calcium on PTCDA	869
D.28	Low Temperature Averaged Data for Calcium on PTCDA	869
D.29	Low Temperature Sticking Data for Calcium on PTCDA	870
D.30	Low Temperature Enthalpy Data for Calcium on PTCDA	870
D.31	Auxiliary Data for Calcium on Sexithiophene	871
D.32	Averaged Data for Calcium on Sexithiophene	871
D.33	Sticking Data for Calcium on Sexithiophene	872
D.34	Enthalpy Data for Calcium on Sexithiophene	872
D.35	Enthalpy Data for Calcium on Sexithiophene: Small Layer Thickness	873
D.36	Enthalpy Data for Calcium on Sexithiophene: Medium Layer Thickness	873
D.37	Enthalpy Data for Calcium on Sexithiophene: Large Layer Thickness	874
D.38	Low Temperature Auxiliary Data for Calcium on Sexithiophene . . .	875
D.39	Low Temperature Averaged Data for Calcium on Sexithiophene . . .	875
D.40	Low Temperature Sticking Data for Calcium on Sexithiophene . . .	876
D.41	Low Temperature Enthalpy Data for Calcium on Sexithiophene . . .	876
D.42	Auxiliary Data for Zinc on Sputter Cleaned Detector	877
D.43	Averaged Data for Zinc on Sputter Cleaned Detector	877
D.44	Sticking Data for Zinc on Sputter Cleaned Detector	878
D.45	Enthalpy Data for Zinc on Sputter Cleaned Detector	878
D.46	Auxiliary Data for Zinc on PTCDA	879
D.47	Averaged Data for Zinc on PTCDA	879
D.48	Sticking Data for Zinc on PTCDA	880
D.49	Enthalpy Data for Zinc on PTCDA	880
D.50	Low Temperature Auxiliary Data for Zinc on PTCDA	881
D.51	Low Temperature Averaged Data for Zinc on PTCDA	881
D.52	Low Temperature Sticking Data for Zinc on PTCDA	882
D.53	Low Temperature Enthalpy Data for Zinc on PTCDA	882
E.1	Laser Reference Previous Evaluation Approach	884
E.2	Radiation Reference Previous Evaluation Approach	885

E.3	Desorption Reference Previous Evaluation Approach	886
E.4	Heat Measurement Previous Evaluation Approach	887
E.5	Energy Calculation Previous Evaluation Approach	888
E.6	Filtered Laser Reference Measurement	890
E.7	Filter Residue Laser Reference Measurement	891
E.8	Averaged Filtered Laser Reference	892
E.9	Detail Filtered Radiation Reference Measurement	893
E.10	Average Frames of Filtered Laser Reference Measurement	894
E.11	Filtered Radiation Reference Measurement	895
E.12	Filter Residue Radiation Reference Measurement	896
E.13	Averaged Filtered Radiation Reference Measurement	897
E.14	Detail Filtered Radiation Reference Measurement	898
E.15	Average Frames of Filtered Radiation Reference Measurement	899
E.16	Filtered Heat Measurement	900
E.17	Filter Residue Heat Measurement	901
E.18	Averaged Filtered Heat Measurement	902
E.19	Detail Filtered Heat Measurement	903
E.20	Average Frames of Filtered Heat Measurement	904

List of Tables

2.1	Positions for Ancillary Measurements	60
5.1	Thick Layer Deposition Parameters	235
5.2	Thick Layer Deposition Results	236
5.3	Load Lock Evaporator Parameters	238
5.4	Sample/Detector Structure	240
5.5	Relative Response of a Coated Detector	240
5.6	Tooling Factor of the Evaporator Quartz Crystal Microbalance in the Load Lock	244
5.7	Main Evaporator Fill Amounts	252
5.8	Contribution of Ions to the Molecular Beam	258
5.9	Operation Parameters of the Hot Plate	284
5.10	Properties of Pyroelectric Materials	303
6.1	Properties of Selected Solid Elements	318
6.2	<i>Ersatz</i> Thicknesses and Area Densities	328
6.3	Reaction Equivalents	328
6.4	Data Acquisition Parameters	331
A.1	Operation Parameters: Magnesium	451
A.2	Operation Parameters: Calcium	451
A.3	Operation Parameters: Copper	452
A.4	Operation Parameters: Zinc	452
A.5	Operation Parameters: Perylenetetracarboxylic Dianhydride	453
A.6	Operation Parameters: Phthalocyanine	453
A.7	Operation Parameters: Sexithiophene	454
A.8	Operation Parameters: 5,10,15,20-Tetraphenyl Porphyrin	454

Bibliography

- [1] Rothenberg, G. *Catalysis*. Wiley-VCH Verlag GmbH & Co. KGaA, 1st Edition, **2008**.
- [2] Černý, S.; Ponec, V.; and Hládek, L. Calorimetric Heats of Adsorption of Hydrogen on Molybdenum Films. *Journal of Catalysis*, **1966**, *5*(1), 27. doi:10.1016/S0021-9517(66)80122-7.
- [3] Smutek, M. and Černý, S. Calorimetric Studies of Hydrocarbon Adsorption on Metal Films: III. Methane, Ethane, and Propane on Molybdenum. *Journal of Catalysis*, **1977**, *47*(2), 179. doi:10.1016/0021-9517(77)90165-8.
- [4] Černý, S.; Smutek, M.; Buzek, F.; and Curřínová, A. Calorimetric Studies of Hydrocarbon Adsorption on Metal Films: I. Cyclopropane on Platinum and Molybdenum. *Journal of Catalysis*, **1977**, *47*(2), 159. doi:10.1016/0021-9517(77)90163-4.
- [5] Černý, S.; Smutek, M.; and Buzek, F. Calorimetric Studies of Hydrocarbon Adsorption on Metal Films: II. Ethylene, Acetylene, Propylene, Methylacetylene and Allene on Molybdenum. *Journal of Catalysis*, **1977**, *47*(2), 166. doi:10.1016/0021-9517(77)90164-6.
- [6] Pálfi, S.; Lisowski, W.; Smutek, M.; and Černý, S. Calorimetric Studies of Hydrocarbon Adsorption on Metal Films: V. Hydrocarbons on Platinum. *Journal of Catalysis*, **1984**, *88*(2), 300. doi:10.1016/0021-9517(84)90006-X.
- [7] Černý, S. and Pientka, Z. Heat of Interaction of Carbon Monoxide with Dysprosium. *Surface Science*, **1987**, *191*(3), 449. doi:10.1016/S0039-6028(87)81189-5.
- [8] Bastel, Z. and Černý, S. Calorimetric and XPS Study of the Effect of Copper on the Sorption Properties of Dysprosium. *Applied Surface Science*, **1993**, *68*(2), 275. doi:10.1016/0169-4332(93)90132-U.
- [9] Černý, S. Adsorption Microcalorimetry in Surface Science Studies – Sixty Years of Its Development into a Modern Powerful Method. *Surface Science Reports*, **1996**, *26*(1-2), 1. doi:10.1016/S0167-5729(96)00008-8.
- [10] Černý, S. Adsorption Calorimetry on Filaments, Vacuum-Evaporated Films, and Single Crystals of Metals. *Thermochimica Acta*, **1998**, *312*(1-2), 3. doi:10.1016/S0040-6031(97)00435-8.
- [11] Brown, W. A.; Kose, R.; and King, D. A. Femtomole Adsorption Calorimetry on Single-Crystal Surfaces. *Chemical Reviews*, **1998**, *98*(2), 797. doi:10.1021/cr9700890.
- [12] Stuckless, J. T.; Al-Sarraf, N.; Wartnaby, C.; and King, D. A. Calorimetric Heats of Adsorption for CO on Nickel Single Crystal Surfaces. *The Journal of Chemical Physics*, **1993**, *99*(3), 2202. doi:10.1063/1.465282.

- [13] Dixon-Warren, S. J.; Kovář, M.; Wartnaby, C. E.; and King, D. A. Pyroelectric Single Crystal Adsorption Microcalorimetry at Low Temperatures: Oxygen on Ni{100}. *Surface Science*, **1994**, *307-309*, 16. doi:10.1016/0039-6028(94)90363-8.
- [14] Stuckless, J. T.; Starr, D. E.; Bald, D. J.; and Campbell, C. T. Metal Adsorption Calorimetry and Adhesion Energies on Clean Single-Crystal Surfaces. *Journal of Chemical Physics*, **1997**, *107*(14), 5547. doi:10.1063/1.474230.
- [15] Stuckless, J. T.; Starr, D. E.; Bald, D. J.; and Campbell, C. T. Calorimetric Measurements of the Energetics of Pb Adsorption and Adhesion to Mo(100). *Physical Review B*, **1997**, *56*(20), 13496. doi:10.1103/PhysRevB.56.13496.
- [16] Ranney, J. T.; Starr, D. E.; Musgrove, J. E.; Bald, D. J.; and Campbell, C. T. A Microcalorimetric Study of the Heat of Adsorption of Copper on Well-Defined Oxide Thin Film Surfaces : MgO(100), p(2 × 1) Oxide on Mo(100) and Disordered W Oxide. *Faraday Discussions*, **1999**, *144*, 195. doi:10.1039/A902649E.
- [17] Larsen, J. H.; Starr, D. E.; and Campbell, C. T. Enthalpies of Adsorption of Metal Atoms on Single-Crystalline Surfaces by Microcalorimetry. *The Journal of Chemical Thermodynamics*, **2001**, *33*(3), 333. doi:10.1006/jcht.2000.0747.
- [18] Starr, D. E.; Ranney, J. T.; Larsen, J. H.; Musgrove, J. E.; and Campbell, C. T. Measurement of the Energetics of Metal Film Growth on a Semiconductor: Ag/Si(100)-(2 × 1). *Physical Review Letters*, **2001**, *87*(10), 106102. doi:10.1103/PhysRevLett.87.106102.
- [19] Starr, D. E. and Campbell, C. T. Low-Temperature Adsorption Microcalorimetry: Pb on MgO(100). *The Journal Of Physical Chemistry B*, **2001**, *105*(18), 3776. doi:10.1021/jp003411a.
- [20] Starr, D. E.; Bald, D. J.; Musgrove, J. E.; Ranney, J. T.; and Campbell, C. T. Microcalorimetric Measurements of the Heat of Adsorption of Pb on Well-Defined Oxides: MgO(100) and p(2 × 1)-Oxide on Mo(100). *Journal of Chemical Physics*, **2001**, *114*(8), 3752. doi:10.1063/1.1337097.
- [21] Campbell, C. T. and Starr, D. E. Metal Adsorption and Adhesion Energies on MgO(100). *Journal of the American Chemical Society*, **2002**, *124*(31), 9212. doi:10.1021/ja020146t.
- [22] Starr, D. E.; Diaz, S. F.; Musgrove, J. E.; Ranney, J. T.; Bald, D. J.; Nelen, L.; Ihm, H.; and Campbell, C. T. Heat of Adsorption of Cu and Pb on Hydroxyl-Covered MgO(100). *Surface Science*, **2002**, *515*(1), 13. doi:10.1016/S0039-6028(02)01915-5.
- [23] Ihm, H.; Ajo, H. M.; Gottfried, J. M.; Bera, P.; and Campbell, C. T. Calorimetric Measurement of the Heat of Adsorption of Benzene on Pt(111). *The Journal Of Physical Chemistry B*, **2004**, *108*(38), 14627. doi:10.1021/jp040159o.
- [24] Zhu, J.; Diaz, S.; Heeb, L.; and Campbell, C. T. Adsorption Of Pb on NiAl(110): Energetics and Structure. *Surface Science*, **2005**, *574*(1), 34. doi:10.1016/j.susc.2004.10.014.

- [25] Tait, S. L.; Dohnálek, Z.; Campbell, C. T.; and Kay, B. D. n-Alkanes on Pt(111) and on C(0001)/Pt(111): Chain Length Dependence of Kinetic Desorption Parameters. *The Journal of Chemical Physics*, **2006**, *125*, 234308. doi:10.1063/1.2400235.
- [26] Gottfried, M.; Vestergaard, E. K.; Bera, P.; and Campbell, C. T. Heat of Adsorption of Naphthalene on Pt(111) Measured by Adsorption Calorimetry. *The Journal Of Physical Chemistry B*, **2006**, *110*, 17539. doi:10.1021/jp062659i.
- [27] Zhu, J.; Farmer, J. A.; Ruzycki, N.; Xu, L.; Campbell, C. T.; and Henkelman, G. Calcium Adsorption on MgO(100): Energetics, Structure, and Role of Defects. *Journal of the American Chemical Society*, **2008**, *130*, 2314. doi:10.1021/ja077865y.
- [28] Fiorin, V.; Borthwick, D.; and King, D. A. Microcalorimetry of O₂ and NO on Flat and Stepped Platinum Surfaces. *Surface Science*, **2009**, *603*(10-10), 1360. doi:10.1016/j.susc.2008.08.034.
- [29] Farmer, J. A.; Campbell, C. T.; Xu, L.; and Henkelman, G. Defect Sites and Their Distributions on MgO(100) by Li and Ca Adsorption Calorimetry. *Journal of the American Chemical Society*, **2009**, *131*(8), 3098. doi:10.1021/ja808986b.
- [30] Farmer, J. A.; Ruzycki, N.; Zhu, J.; and Campbell, C. T. Lithium Adsorption on MgO(100) and Its Defects: Charge Transfer, Structure, and Energetics. *Physical Review B*, **2009**, *80*(3), 035418. doi:10.1103/PhysRevB.80.035418.
- [31] Lytken, O.; Lew, W.; and Campbell, C. T. Catalytic Reaction Energetics by Single Crystal Adsorption Calorimetry: Hydrocarbons on Pt(111). *Chemical Society Reviews*, **2008**, *37*(10), 2172. doi:10.1039/B719543P.
- [32] Lytken, O.; Lew, W.; Harris, J. J. W.; Vestergaard, E. K.; Gottfried, J. M.; and Campbell, C. T. Energetics of Cyclohexene Adsorption and Reaction on Pt(111) by Low-Temperature Microcalorimetry. *Journal of the American Chemical Society*, **2008**, *130*(31), 10247. doi:10.1021/ja801856s.
- [33] Farmer, J. A.; Baricuatro, J. H.; and Campbell, C. T. Ag Adsorption on Reduced CeO₂(111) Thin Films. *The Journal Of Physical Chemistry C*, **2010**, *114*(40), 17166. doi:10.1021/jp104593y.
- [34] Farmer, J. A. and Campbell, C. T. Ceria Maintains Smaller Metal Catalyst Particles by Strong Metal-Support Bonding. *Science*, **2010**, *329*(5994), 933. doi:10.1126/science.1191778.
- [35] Schießer, A.; Hörtz, P.; and Schäfer, R. Thermodynamics and Kinetics of CO and Benzene Adsorption on Pt(111) Studied with Pulsed Molecular Beams and Microcalorimetry. *Surface Science*, **2010**, *604*, 2098. doi:10.1016/j.susc.2010.09.001.
- [36] Lew, W.; Crowe, M. C.; Campbell, C. T.; Carrasco, J.; and Michaelides, A. The Energy of Hydroxyl Coadsorbed with Water on Pt(111). *The Journal Of Physical Chemistry C*, **2011**, *115*(46), 23008. doi:10.1021/jp207350r.
- [37] Lew, W.; Crowe, M. C.; Karp, E.; Lytken, O.; Farmer, J. A.; Árnadóttir, L.; Schoenbaum, C.; and Campbell, C. T. The Energy of Adsorbed Hydroxyl on Pt(111) by Microcalorimetry. *The Journal Of Physical Chemistry C*, **2011**, *115*(23), 11586. doi:10.1021/jp201632t.

- [38] Karp, E. M.; Silbaugh, T. L.; Crowe, M. C.; and Campbell, C. T. The Energetics of Adsorbed Methanol and Methoxy on Pt(111) by Microcalorimetry. *Journal of the American Chemical Society*, **2012**, *134*(50), 20388. doi:10.1021/ja307465u.
- [39] Karp, E. and Campbell, C. T. Energetics of Oxygen Adatoms, Hydroxyl Species, and Water Dissociation on Pt(111). *The Journal Of Physical Chemistry C*, **2012**, *116*(49), 25772. doi:10.1021/jp3066794.
- [40] Liao, K.; Fiorin, V.; Jenkins, S. J.; and King, D. A. Microcalorimetry of Oxygen Adsorption on fcc Co(110). *Physical Chemistry Chemical Physics*, **2012**, *14*(20), 7528. doi:10.1039/C2CP40549K.
- [41] Karp, E.; Silbaugh, T. L.; and Campbell, C. T. Energetics of Adsorbed CH₃ and CH on Pt(111) by Calorimetry: Dissociative Adsorption of CH₃I. *The Journal Of Physical Chemistry C*, **2013**, *117*(12), 6325. doi:10.1021/jp400902f.
- [42] Sharp, J. C.; Yao, Y. X.; and Campbell, C. T. Silver Nanoparticles on Fe₃O₄(111): Energetics by Ag Adsorption Calorimetry and Structure by Surface Spectroscopies. *The Journal Of Physical Chemistry C*, **2013**, *117*(47), 24932. doi:10.1021/jp408956x.
- [43] Silbaugh, T. L.; Karp, E. M.; and Campbell, C. T. Surface Kinetics and Energetics from Single Crystal Adsorption Calorimetry Lineshape Analysis: Methyl from Methyl Iodide on Pt(111). *Journal of Catalysis*, **2013**, *308*, 114. doi:10.1016/j.jcat.2013.05.030.
- [44] Liao, K.; Fiorin, V.; Gunn, D. S. D.; Jenkins, S. J.; and King, D. A. Single-Crystal Adsorption Calorimetry and Density Functional Theory of CO Chemisorption on fcc Co{110}. *Physical Chemistry Chemical Physics*, **2013**, *15*(11), 4059. doi:10.1039/C3CP43836H.
- [45] Silbaugh, T. L.; Karp, E. M.; and Campbell, C. T. Energetics of Formic Acid Conversion to Adsorbed Formates on Pt(111) by Transient Calorimetry. *Journal of the American Chemical Society*, **2014**, *136*(10), 3964. doi:10.1021/ja412878u.
- [46] Karp, E. M.; Silbaugh, T. L.; and Campbell, C. T. Bond Energies of Molecular Fragments to Metal Surfaces Track Their Bond Energies to H Atom. *Journal of the American Chemical Society*, **2014**, *136*(11), 4137. doi:10.1021/ja500997n.
- [47] Silbaugh, T. L.; Giorgi, J. B.; Xu, Y.; Tillekaratne, A.; Zaera, F.; and Campbell, C. T. Adsorption Energy of *tert*-Butyl on Pt(111) by Dissociation of *tert*-Butyl Iodide: Calorimetry and DFT. *The Journal Of Physical Chemistry C*, **2014**, *118*(1), 427. doi:10.1021/jp4097716.
- [48] Hörtz, P.; Ruff, P.; and Schäfer, R. A Temperature Dependent Investigation of the Adsorption of CO on Pt(111) using Low-Temperature Single Crystal Adsorption Calorimetry. *Surface Science*, **2015**, *639*, 66. doi:10.1016/j.susc.2015.04.018.
- [49] Grant, A. W.; Ngo, L. T.; Stegelman, K.; and Campbell, C. T. Cyclohexane Dehydrogenation and H₂ Adsorption on Pt Particles on ZnO(0001)-O. *The Journal Of Physical Chemistry B*, **2003**, *107*(5), 1180. doi:10.1021/jp021907h.

- [50] Ngo, L. T.; Xu, L.; Grant, A. W.; and Campbell, C. T. Benzene Adsorption and Dehydrogenation on Pt/ZnO(0001)-O Model Catalysts. *The Journal Of Physical Chemistry B*, **2003**, *107*(5), 1174. doi:10.1021/jp021903c.
- [51] Flores-Camacho, J. M.; Fischer-Wolfarth, J.-H.; Peter, M.; Campbell, C. T.; Schauer-
mann, S.; and Freund, H.-J. Adsorption Energetics of CO on Supported Pd Nanopar-
ticles as a Function of Particle Size by Single Crystal Microcalorimetry. *Physical
Chemistry Chemical Physics*, **2011**, *37*, 16800. doi:10.1039/C1CP21677E.
- [52] Peter, M.; Camacho, J. M. F.; Adamovski, S.; Ono, L. K.; Dostert, K.-H.; O'Brien,
C. P.; Cuenya, B. R.; Schauer-
mann, S.; and Freund, H.-J. Trends in the Binding
Strength of Surface Species on Nanoparticles: How Does the Adsorption Energy
Scale with the Particle Size? *Angewandte Chemie, International Edition*, **2013**,
52(19), 5175. doi:10.1002/anie.201209476.
- [53] Murdey, R. and Stuckless, J. T. Calorimetry of Polymer Metallization: Copper,
Calcium, and Chromium on PMDA-ODA Polyimide. *Journal of the American
Chemical Society*, **2003**, *125*(13), 3995. doi:10.1021/ja028829w.
- [54] Hon, S. S.; Richter, J.; and Stuckless, J. T. A Calorimetric Study of the Heat of
Reaction of Calcium Atoms with the Vinylene Group of MEH-PPVh. *Chemical
Physics Letters*, **2004**, *385*(1-2), 92. doi:10.1016/j.cplett.2003.12.055.
- [55] Diaz, S.; Zhu, J.; Harris, J.; Goetsch, P.; Merte, L.; and Campbell, C. T. Heats of Ad-
sorption of Pb on Pristine and Electron-Irradiated Poly(Methyl Methacrylate) by Mi-
crocalorimetry. *Surface Science*, **2005**, *598*(1-3), 22. doi:10.1016/j.susc.2005.09.015.
- [56] Zhu, J.; Goetsch, P.; Ruzycki, N.; and Campbell, C. T. Adsorption Energy, Growth
Mode, and Sticking Probability of Ca on Poly(Methyl Methacrylate) Surfaces with
and without Electron Damage. *Journal of the American Chemical Society*, **2007**,
129, 6432. doi:10.1021/ja067437c.
- [57] Zhu, J.; Bebensee, F.; Hieringer, W.; Zhao, W.; Baricuatro, J. H.; Farmer, J. A.;
Bai, Y.; Steinrück, H.-P.; Gottfried, J. M.; and Campbell, C. T. Formation of the
Calcium/Poly(3-Hexylthiophene) Interface: Structure and Energetics. *Journal of
the American Chemical Society*, **2009**, *131*(37), 13498. doi:10.1021/ja904844c.
- [58] Bebensee, F.; Zhu, J.; Baricuatro, J. H.; Farmer, J. A.; Bai, Y.; Steinrück, H.-
P.; Campbell, C. T.; and Gottfried, J. M. Interface Formation between Calcium
and Electron-Irradiated Poly(3-Hexylthiophene). *Langmuir*, **2010**, *26*(12), 9632.
doi:10.1021/la100209v.
- [59] Sharp, J. C.; Bebensee, F.; Baricuatro, J. H.; Steinrück, H.-P.; Gottfried, J. M.;
and Campbell, C. T. Calcium Thin Film Growth on a Cyano-Substituted Poly(p-
Phenylene Vinylene): Interface Structure and Energetics. *The Journal Of Physical
Chemistry C*, **2013**, *117*(45), 23781. doi:10.1021/jp407825f.
- [60] Ju, H.; Ye, Y.; Feng, X.; Pan, H.; Zhu, J.; Ruzycki, N.; and Campbell, C. T.
Low-Temperature Growth Improves Metal/Polymer Interfaces: Vapor-Deposited
Ca on PMMA. *The Journal Of Physical Chemistry C*, **2014**, *118*(12), 6352.
doi:10.1021/jp500628w.

- [61] Sharp, J. C.; Feng, X. F.; Farmer, J. A.; Guo, Y. X.; Bebensee, F.; Baricuatro, J. H.; Zillner, E.; Zhu, J. F.; Steinrück, H.-P.; Gottfried, J. M.; and Campbell, C. T. Calcium Thin Film Growth on Polyfluorenes: Interface Structure and Energetics. *The Journal Of Physical Chemistry C*, **2014**, *118*(6), 2953. doi:10.1021/jp4105954.
- [62] Forrest, S. R. Ultrathin Organic Films Grown by Organic Molecular Beam Deposition and Related Techniques. *Chemical Reviews*, **1997**, *97*(6), 1793. doi:10.1021/cr941014o.
- [63] Witte, G. and Wöll, C. Growth of Aromatic Molecules on Solid Substrates for Applications in Organic Electronics. *Journal of Materials Research*, **2004**, *19*(7), 1889. doi:10.1557/JMR.2004.0251.
- [64] Kowarik, S.; Gerlach, A.; and Schreiber, F. Organic Molecular Beam Deposition: Fundamentals, Growth Dynamics, and *in situ* Studies. *Journal of Physics Condensed Matter*, **2008**, *20*(18), 184008. doi:10.1088/0953-8984/20/18/184005.
- [65] Klauk, H., Editor. *Organic Electronics*. Wiley-VCH, Weinheim, 1st Edition, **2009**.
- [66] So, F., Editor. *Organic Electronics: Materials, Processing, Devices, and Applications*. CRC Press/Taylor and Francis, Boca Raton, FL., **2009**.
- [67] Sacher, E.; Pireaux, J.-J.; and Kowalczyk, S. P., Editors. *Metallization of Polymers*. American Chemical Society: Washington, DC, **1990**. doi:10.1021/bk-1990-0440.
- [68] Braun, W.; Gavrilu, G.; Gorgoi, M.; and Zahn, D. R. T. Influence of the Molecular Structure on the Interface Formation between Magnesium and Organic Semiconductors. *Radiation Physics and Chemistry*, **2006**, *75*(11), 1869. doi:10.1016/j.radphyschem.2005.07.057.
- [69] Gavrilu, G.; Zahn, D. R. T.; and Braun, W. High Resolution Photoemission Spectroscopy: Evidence for Strong Chemical Interaction between Mg and 3,4,9,10-Perylene-Tetracarboxylic Dianhydride. *Applied Physics Letters*, **2006**, *89*, 162102. doi:10.1063/1.2356305.
- [70] Ju, H.; Feng, X.; Ye, Y.; Zhang, L.; Pan, H.; Campbell, C. T.; and Zhu, J. Ca Carboxylate Formation at the Calcium/Poly(Methyl Methacrylate) Interface. *The Journal Of Physical Chemistry C*, **2012**, *116*(38), 20456. doi:10.1021/jp307010x.
- [71] Bebensee, F.; Schmid, M.; Steinrück, H.-P.; Campbell, C. T.; and Gottfried, J. M. Toward Well-Defined Metal-Polymer Interfaces: Temperature-Controlled Suppression of Subsurface Diffusion and Reaction at the Calcium/Poly(3-Hexylthiophene) Interface. *Journal of the American Chemical Society*, **2010**, *132*(35), 12163. doi:10.1021/ja104029r.
- [72] Murr, J. and Ziegler, C. Interaction of Na with Sexithiophene Thin Films. *Physical Review B*, **1998**, *57*(12), 7299. doi:10.1103/PhysRevB.57.7299.
- [73] Feng, X.; Zhao, W.; Ju, H.; Zhang, L.; Ye, Y.; Zhang, W.; and Zhu, J. Electronic Structures and Chemical Reactions at the Interface between Li and Regioregular Poly(3-Hexylthiophene). *Organic Electronics*, **2012**, *13*(6), 1060. doi:10.1016/j.orgel.2012.02.007.

- [74] Baier, F.; Ludowig, F.; Soukopp, A.; Väterlein, C.; Laubender, J.; Bäuerle, P.; Sokolowski, M.; and Umbach, E. A Combined Photoelectron Spectroscopy and Capacity-Voltage Investigation of the Aluminum/Oligothiophene Interface. *Optical Materials*, **1999**, *12*(2-3), 285. doi:10.1016/S0925-3467(99)00066-X.
- [75] Lazzaroni, R.; Lögdlund, M.; Calderone, A.; Brédas, J.; Dannetun, P.; Fauquet, C.; Fredriksson, C.; Stafström, S.; and Salaneck, W. Chemical and Electronic Aspects of Metal/Conjugated Polymer Interfaces – Implications for Electronic Devices. *Synthetic Metals*, **1995**, *71*(1-3), 2159. doi:10.1016/0379-6779(94)03203-I.
- [76] Dannetun, P.; Boman, M.; Stafström, S.; Salaneck, W. R.; Lazzaroni, R.; Fredriksson, C.; Brédas, J. L.; Zamboni, R.; and Taliani, C. The Chemical and Electronic Structure of the Interface between Aluminum and Polythiophene Semiconductors. *Journal of Chemical Physics*, **1993**, *99*(1), 664. doi:10.1063/1.466217.
- [77] Hirose, Y.; Kahn, A.; Aristov, V.; Soukiassian, P.; Bulovic, V.; and Forrest, S. R. Chemistry and Electronic Properties of Metal-Organic Semiconductor Interfaces: Al, Ti, In, Sn, Ag, and Au on PTCDA. *Physical Review B*, **1996**, *54*(19), 13748. doi:10.1103/PhysRevB.54.13748.
- [78] Lachkar, A.; Selmani, A.; and Sacher, E. Metallization of Polythiophenes – II. Interaction of Vapor-Deposit Cr, V, and Ti with Poly(3-Hexylthiophene) (P3HT). *Synthetic Metals*, **1995**, *72*(1), 73. doi:10.1016/0379-6779(94)02319-T.
- [79] Popovici, D.; Piyakis, K.; Meunier, M.; and Sacher, E. Angle-Resolved X-Ray Photoelectron Spectroscopy Comparison of Copper/Teflon AF1600 and Aluminum/Kapton Metal Diffusion. *Journal of Applied Physics*, **1998**, *83*(1), 108. doi:10.1063/1.366706.
- [80] Koprinarov, I.; Lippitz, A.; Friedrich, J.; Unger, W.; and Wöll, C. Surface Analysis of DC Oxygen Plasma Treated or Chromium Evaporated Poly(Ethylene Terephthalate) Foils by Soft X-Ray Absorption Spectroscopy (NEXAFS). *Polymer*, **1997**, *38*(8), 2005. doi:10.1016/S0032-3861(96)00964-0.
- [81] Lippitz, A.; Koprinarov, I.; Friedrich, J.; Unger, W.; Weiss, K.; and Wöll, C. Surface Analysis of Metallized Poly(Bisphenol A Carbonate) Films by X-Ray Absorption Spectroscopy (NEXAFS). *Polymer*, **1996**, *37*(14), 3157. doi:10.1016/0032-3861(96)89419-5.
- [82] Pireaux, J. J.; Vermeersch, M.; Grégoire, C.; Thiry, P. A.; Caudano, R.; and Clarke, T. C. The Aluminum-Polyimide Interface: An Electron-Induced Vibrational Spectroscopy Approach. *The Journal of Chemical Physics*, **1988**, *88*(5), 3353. doi:10.1063/1.453930.
- [83] Pireaux, J. J.; Thiry, P. A.; Caudano, R.; and Pfluger, P. Surface Analysis of Polyethylene and Hexatriacontane by High Resolution Electron Energy Loss Spectroscopy. *The Journal of Chemical Physics*, **1986**, *84*(11), 6452. doi:10.1063/1.450852.
- [84] DiNardo, N. J.; Demuth, J. E.; and Clarke, T. C. Electron Vibrational Spectroscopy of Thin Polyimide Films. *The Journal of Chemical Physics*, **1986**, *85*(11), 6739. doi:10.1063/1.451405.

- [85] Salvan, G.; Paez, B. A.; Silaghi, S.; and Zahn, D. R. Deposition of Silver, Indium, and Magnesium onto Organic Semiconductor Layers: Reactivity, Indiffusion, and Metal Morphology. *Microelectronic Engineering*, **2005**, *82*(3-4), 228. doi:10.1016/j.mee.2005.07.029.
- [86] Stuckless, J. T.; Frei, N. A.; and Campbell, C. T. A Novel Single-Crystal Adsorption Calorimeter and Additions for Determining Metal Adsorption and Adhesion Energies. *Review Of Scientific Instruments*, **1998**, *69*(6), 2427. doi:10.1063/1.1148971.
- [87] Sellers, J. R. V.; James, T. E.; Hemmingson, S. L.; Farmer, J. A.; and Campbell, C. T. Adsorption Calorimetry During Metal Vapor Deposition on Single Crystal Surfaces: Increased Flux, Reduced Optical Radiation, and Real-Time Flux and Reflectivity Measurements. *Review Of Scientific Instruments*, **2013**, *84*, 123901. doi:10.1063/1.4832980.
- [88] Chen, M.; Röckert, M.; Xiao, J.; Drescher, H.-J.; Steinrück, H.-P.; Lytken, O.; and Gottfried, J. M. Coordination Reactions and Layer Exchange Processes at a Buried Metal-Organic Interface. *The Journal Of Physical Chemistry C*, **2014**, *118*(16), 8501. doi:10.1021/jp5019235.
- [89] Sachs, M.; Gellert, M.; Chen, M.; Drescher, H.-J.; Kachel, S. R.; Zhou, H.; Zugermeier, M.; Gorgoi, M.; Roling, B.; and Gottfried, J. M. LiNi_{0.5}Mn_{1.5}O₄ High-Voltage Cathode Coated with Li₄Ti₅O₁₂: A Hard X-ray Photoelectron Spectroscopy (HAXPES) Study. *Physical Chemistry Chemical Physics*, **2015**, *17*(47), 31790. doi:10.1039/C5CP03837E.
- [90] Chen, M.; Klein, B.; Krug, C.; Zugermeier, M.; Zhou, H.; Drescher, H.-J.; Gorgoi, M.; and Gottfried, J. M. Formation of a Metal/Organic Interphase Monitored Using a Well-Defined Porphyrin Metalation Reaction: A Hard X-Ray Photoelectron Spectroscopy (HAXPES) Study, **In Preparation**.
- [91] Amende, M.; Schernich, S.; Sobota, M.; Nikiforidis, I.; Hieringer, W.; Assenbaum, D.; Gleichweit, C.; Drescher, H.-J.; Papp, C.; Steinrück, H.-P.; Görling, A.; Wasserscheid, P.; Laurin, M.; and Libuda, J. Dehydrogenation Mechanism of Liquid Organic Hydrogen Carriers: Dodecahydro-N-Ethylcarbazole on Pd(111). *Chemistry - A European Journal*, **2013**, *19*(33), 10854. doi:10.1002/chem.201301323.
- [92] Starr, D. E. and Campbell, C. T. Large Entropy Difference between Terrace and Step Sites on Surfaces. *Journal of the American Chemical Society*, **2008**, *130*(23), 7321. doi:10.1021/ja077540h.
- [93] Etzel, K. D.; Bickel, K. R.; and Schuster, R. A Microcalorimeter for Measuring Heat Effects of Electrochemical Reactions with Submonolayer Conversions. *Review of Scientific Instruments*, **2010**, *81*(3), 034101. doi:10.1063/1.3309785.
- [94] Campbell, C. T. and Sellers, J. R. The Entropies of Adsorbed Molecules. *Journal of the American Chemical Society*, **2012**, *134*(43), 18109. doi:10.1021/ja3080117.
- [95] Campbell, C. T. and Sellers, J. R. Enthalpies and Entropies of Adsorption on Well-Defined Oxide Surfaces: Experimental Measurements. *Chemical Reviews*, **2013**, *113*(6), 4106. doi:10.1021/cr300329s.

-
- [96] Zhu, J.; Kinne, M.; Fuhrmann, T.; Denecke, R.; and Steinrück, H.-P. *In situ* High-Resolution XPS Studies on Adsorption of NO on Pt(111). *Surface Science*, **2003**, *529*(3), 384. doi:10.1016/S0039-6028(03)00298-X.
- [97] Kinne, M.; Fuhrmann, T.; Whelan, C. M.; Zhu, J. F.; Pantförder, J.; Probst, M.; Held, G.; Denecke, R.; and Steinrück, H.-P. Kinetic Parameters of CO Adsorbed on Pt(111) Studied by *in situ* High Resolution X-Ray Photoelectron Spectroscopy. *Journal of Chemical Physics*, **2002**, *117*(23), 10852. doi:10.1063/1.1522405.
- [98] Langmuir, I. The Evaporation, Condensation, and Reflection of Molecules and the Mechanism of Adsorption. *Physical Review*, **1916**, *8*(2), 149. doi:10.1103/PhysRev.8.149.
- [99] Redhead, P. A. Thermal Desorption Of Gases. *Vacuum*, **1962**, *12*(4), 203. doi:10.1016/0042-207X(62)90978-8.
- [100] Pétermann, L. A. Thermal Desorption Kinetics of Chemisorbed Gases. *Progress in Surface Science*, **1972**, *3*(1), 1. doi:10.1016/0079-6816(72)90005-6.
- [101] Falconer, J. L. and Schwarz, J. A. Temperature-Programmed Desorption and Reaction: Applications to Supported Catalysts. *Catalysis Reviews: Science and Engineering*, **1983**, *25*(2), 141. doi:10.1080/01614948308079666.
- [102] de Jong, A. and Niemantsverdriet, J. Thermal Desorption Analysis: Comparative Test of Ten Commonly Applied Procedures. *Surface Science*, **1990**, *233*(2), 355. doi:10.1016/0039-6028(90)90649-S.
- [103] Habenschaden, E. and Küppers, J. Evaluation of Flash Desorption Spectra. *Surface Science*, **1984**, *138*(1), L147. doi:10.1016/0039-6028(84)90488-6.
- [104] King, D. A. Thermal Desorption from Metal Surfaces: A Review. *Surface Science*, **1975**, *47*(1), 384. doi:10.1016/0039-6028(75)90302-7.
- [105] Drescher, H.-J. Konstruktion und Charakterisierung eines Detektors für die Adsorptionsmikrokalorimetrie. Diploma thesis, Universität Erlangen-Nürnberg, **2008**.
- [106] Bebensee, F. Metal-Polymer Interfaces Studied with Adsorption Microcalorimetry and Photoelectron Spectroscopy. Ph.D. thesis, Friedrich-Alexander-Universität Erlangen-Nürnberg, **2010**.
- [107] Sircar, S.; Mohr, R.; Ristic, C.; and Rao, M. B. Isotheric Heat of Adsorption: Theory and Experiment. *The Journal Of Physical Chemistry B*, **1999**, *103*(31), 6539. doi:10.1021/jp9903817.
- [108] Shen, D.; Bülow, M.; Siperstein, F.; Engelhard, M.; and Myers, A. L. Comparison of Experimental Techniques for Measuring Isotheric Heat of Adsorption. *Adsorption*, **2000**, *6*(4), 275. doi:10.1023/A:1026551213604.
- [109] Askalany, A. A. and Saha, B. B. Derivation of Isotheric Heat of Adsorption for Non-Ideal Gases. *International Journal of Heat and Mass Transfer*, **2015**, *89*, 186. doi:10.1016/j.ijheatmasstransfer.2015.05.018.

- [110] Lytken, O.; Drescher, H.-J.; Kose, R.; Gottfried, J. M.; (Ed.), G. B.; and (Ed.), B. H. *Surface Science Techniques*, Volume 51, Chapter 2 - Adsorption Calorimetry on Well-Defined Surfaces. Springer Berlin Heidelberg, **2013**, pp. 35–55. doi:10.1007/978-3-642-34243-1_2.
- [111] Crowe, M. C. and Campbell, C. T. Adsorption Microcalorimetry: Recent Advances in Instrumentation and Application. *Annual Review of Analytical Chemistry*, **2011**, *4*, 41. doi:10.1146/annurev-anchem-061010-113841.
- [112] Schauermaun, S.; Silbaugh, T. L.; and Campbell, C. T. Single-Crystal Adsorption Calorimetry on Well-Defined Surfaces: From Single Crystals to Supported Nanoparticles. *The Chemical Record*, **2014**, *14*, 759. doi:10.1002/tcr.201402022.
- [113] Edinger, K.; Gotszalk, T.; and Rangelow, I. W. Novel High Resolution Scanning Thermal Probe. *Journal of Vacuum Science & Technology B*, **2001**, *19*(6), 2856. doi:10.1116/1.1420580.
- [114] Coufal, H. J.; Grygier, R. K.; Horne, D. E.; and Fromm, J. E. Pyroelectric Calorimeter for Photothermal Studies of Thin Films and Adsorbates. *Journal of Vacuum Science & Technology A*, **1987**, *5*(5), 2875. doi:10.1116/1.574258.
- [115] Borroni-Bird, C. E. and King, D. A. An Ultrahigh Vacuum Single Crystal Adsorption Microcalorimeter. *Review of Scientific Instruments*, **1991**, *62*(9), 2177. doi:10.1063/1.1142525.
- [116] Borroni-Bird, C. E.; Al-Sarraf, N.; Anderson, S.; and King, D. Single Crystal Adsorption Microcalorimetry. *Chemical Physics Letters*, **1991**, *183*(6), 516. doi:10.1016/0009-2614(91)80168-W.
- [117] Dvořák, L.; Kovář, M.; and Černý, S. A new Approach to Adsorption Microcalorimetry Based on a LiTaO₃ Pyroelectric Temperature Sensor and a Pulsed Molecular Beam. *Thermochimica Acta*, **1994**, *245*, 163. doi:10.1016/0040-6031(94)85076-3.
- [118] Kovář, M.; Dvořák, L.; and Černý, S. Application of Pyroelectric Properties of LiTaO₃ Single Crystal to Microcalorimetric Measurement of the Heat of Adsorption. *Applied Surface Science*, **1994**, *74*(1), 51. doi:10.1016/0169-4332(94)90099-X.
- [119] Ajo, H. M.; Ihm, H.; Moilanen, D. E.; and Campbell, C. T. Calorimeter for Adsorption Energies of Larger Molecules on Single Crystal Surfaces. *Review Of Scientific Instruments*, **2004**, *75*(11), 4471. doi:10.1063/1.1794391.
- [120] Murdey, R.; Liang, S. J. S.; and Stuckless, J. T. An Atom-Transparent Photon Block for Metal-Atom Deposition from High-Temperature Ovens. *Review Of Scientific Instruments*, **2005**, *76*, 023911. doi:10.1063/1.1855315.
- [121] Lew, W.; Lytken, O.; Farmer, J. A.; Crowe, M. C.; and Campbell, C. T. Improved Pyroelectric Detectors for Single Crystal Adsorption Calorimetry from 100 to 350 K. *Review Of Scientific Instruments*, **2010**, *81*(2), 24102. doi:10.1063/1.3290632.
- [122] Fischer-Wolfarth, J.-H.; Hartmann, J.; Farmer, J. A.; Flores-Camacho, J. M.; Campbell, C. T.; Schauermaun, S.; and Freund, H.-J. An Improved Single Crystal Adsorption Calorimeter for Determining Gas Adsorption and Reaction Energies on

- Complex Model Catalysts. *Review Of Scientific Instruments*, **2011**, *82*(2), 24102. doi:10.1063/1.3544020.
- [123] Comsa, G. and David, R. Dynamical Parameters of Desorbing Molecules. *Surface Science Reports*, **1985**, *5*(4), 145. doi:10.1016/0167-5729(85)90009-3.
- [124] Campbell, C. T. Ultrathin Metal Films And Particles on Oxide Surfaces: Structural, Electronic, and Chemisorptive Properties. *Surface Science Reports*, **1997**, *27*(1-3), 1. doi:10.1016/S0167-5729(96)00011-8.
- [125] Diaz, S.; Zhu, J.; Shamir, N.; and Campbell, C. T. Pyroelectric Heat Detector for Measuring Adsorption Energies on Thicker Single Crystals. *Sensors and Actuators B: Chemical*, **2005**, *107*(1), 454. doi:10.1016/j.snb.2004.11.037.
- [126] Hörtz, P. and Schäfer, R. A Compact Low-Temperature Single Crystal Adsorption Calorimetry Setup for Measuring Coverage Dependent Heats of Adsorption at Cryogenic Temperatures. *Review of Scientific Instruments*, **2014**, *85*, 074101. doi:10.1063/1.4890435.
- [127] Fischer-Wolfarth, J.-H.; Farmer, J. A.; Flores-Camacho, J. M.; Genest, A.; Yudanov, I. V.; Rösch, N.; Campbell, C. T.; Schauermaun, S.; and Freund, H.-J. Particle-Size Dependent Heats of Adsorption of CO on Supported Pd Nanoparticles as Measured with a Single-Crystal Microcalorimeter. *Physical Review B*, **2010**, *81*(24), 241416. doi:10.1103/PhysRevB.81.241416.
- [128] Das-Gupta, D. K. Pyroelectricity in Polymers. *Ferroelectrics*, **1991**, *118*(1), 165. doi:10.1080/00150199108014757.
- [129] Das-Gupta, D. K. On the Nature of Pyroelectricity in Polyvinylidene Fluoride. *Ferroelectrics*, **1981**, *33*(1), 75. doi:10.1080/00150198108008072.
- [130] Damjanovic, D. Ferroelectric, Dielectric, and Piezoelectric Properties of Ferroelectric Thin Films and Ceramics. *Reports on Progress in Physics*, **1998**, *61*(9), 1267. doi:10.1088/0034-4885/61/9/002.
- [131] Porter, S. G. A Brief Guide to Pyroelectric Detectors. *Ferroelectrics*, **1981**, *33*(1), 193. doi:10.1080/00150198108008086.
- [132] Zhang, Q.; Bharti, V.; and Kavarnos, G. *Encyclopedia of Smart Materials*, Chapter Poly(Vinylidene Fluoride) (PVDF) and Its Copolymers. John Wiley and Sons, Inc., **2002**, pp. 807–825. doi:10.1002/0471216275.esm063.
- [133] Solvay Plastics. *Solef[®] PVDF – Design and Processing Guide*.
- [134] Kochervinskiĭ, V. V. Piezoelectricity in Crystallizing Ferroelectric Polymers: Poly(Vinylidene Fluoride) and Its Copolymers (A Review). *Crystallography Reports*, **2003**, *48*(4), 649. doi:10.1134/1.1595194.
- [135] AMP, AMP, Inc. Valley Forge, PA. *Definition of Piezo Film Polarity – Application Note 65773*, b Edition, **1994**.
- [136] Polyanskiy, M. N. Refractive Index Database. In *Aluminum*. Available at <http://refractiveindex.info>, **2015**, p. Reflection.

- [137] Polyanskiy, M. N. Refractive Index Database. In *Silver*. Available at <http://refractiveindex.info>, **2015**, p. Reflection.
- [138] Polyanskiy, M. N. Refractive Index Database. In *Gold*. Available at <http://refractiveindex.info>, **2015**, p. Reflection.
- [139] Lu, C.-S. and Lewis, O. Investigation of Film-Thickness Determination by Oscillating Quartz Resonators with Large Mass Load. *Journal of Applied Physics*, **1972**, *43*(11), 4385. doi:10.1063/1.1660931.
- [140] Lu, C.-S. Mass Determination with Piezoelectric Quartz Crystal Resonators. *Journal of Vacuum Science & Technology*, **1975**, *12*(1), 578. doi:10.1116/1.568614.
- [141] Sauerbrey, G. Verwendung von Schwingquarzen zur Wägung Dünner Schichten und zur Mikrowägung. *Zeitschrift für Physik*, **1959**, *155*, 206. doi:10.1007/BF01337937.
- [142] Intellevation Ltd., 5 Dalziel Road, Hillington Park, Glasgow, G52 4NN. *Model IL150 Thickness Monitor Instruction Manual*, 4.1 Edition.
- [143] Mueller, R. M. and White, W. Direct Gravimetric Calibration of a Quartz Crystal Microbalance. *Review Of Scientific Instruments*, **1968**, *39*(3), 291. doi:10.1063/1.1683352.
- [144] Cumpson, P. and Seah, M. The Quartz Crystal Microbalance; Radial/Polar Dependence of Mass Sensitivity – Both on and off the Electrodes. *Measurement Science and Technology*, **1990**, *1*(7), 544. doi:10.1088/0957-0233/1/7/002.
- [145] Lu, F.; Lee, H.; and Lim, S. Quartz Crystal Microbalance with Rigid Mass Partially Attached on Electrode Surfaces. *Sensors and Actuators A*, **2004**, *112*, 203. doi:10.1016/j.sna.2004.01.018.
- [146] King, D. A. and Wells, M. G. Molecular Beam Investigation Of Adsorption Kinetics on Bulk Metal Targets: Nitrogen on Tungsten. *Surface Science*, **1972**, *29*(2), 454. doi:10.1016/0039-6028(72)90232-4.
- [147] Pauls, S. W. and Campbell, C. T. Magic-Angle Thermal Desorption Mass Spectroscopy. *Surface Science*, **1990**, *226*(3), 250. doi:10.1016/0039-6028(90)90490-Y.
- [148] Teyssedre, G.; Bernes, A.; and Lacabanne, C. Temperature Dependence of the Pyroelectric Coefficient in Polyvinylidene Fluoride. *Ferroelectrics*, **1994**, *160*, 67. doi:10.1080/00150199408007696.
- [149] Levinstein, H. J.; Ballman, A. A.; and Capio, C. D. Domain Structure and Curie Temperature of Single-Crystal Lithium Tantalate. *Journal of Applied Physics*, **1966**, *37*(12), 4585. doi:10.1063/1.1708088.
- [150] Tolkien, J. R. R. *The Hobbit, or There and Back Again*. George Allen & Unwin, **1937**.
- [151] Toptica Photonics, Lochhamer Schlag 19 D-82166 Graefelfing/Munich. *iBeam / iPulse Manual*, m-014 version 04 Edition, **2008**.

-
- [152] LumaSense Technologies, 3033 Scott Blvd. Santa Clara, CA 95054-3316. *IP 140 IMPAC-Pyrometer Operation Manual*, **2009**.
- [153] Kurt J. Lesker Company, 15/16 Burgess Road Hastings, East Sussex TN35 4NR, England. *Global Vacuum Product Guide - CF Flanged Zero Length Kodial Glass Viewports*, 9 Edition.
- [154] Malenfant, P. R. L.; Dimitrakopoulos, C. D.; Gelorme, J. D.; Kosbar, L. L.; Graham, T. O.; Curioni, A.; and Andreoni, W. N-Type Organic Thin-Film Transistor with High Field-Effect Mobility Based on a N,N-Dialkyl-3,4,9,10-Perylene Tetracarboxylic Diimide Derivative. *Applied Physics Letters*, **2002**, *80*(14), 2517. doi:10.1063/1.1467706.
- [155] WaveMetrics, Inc., PO Box 2088 Lake Oswego, OR 97035 USA. *IGOR Pro*, 6.34 Edition, **2013**.
- [156] Thomson, W. On the Equilibrium of Vapour at a Curved Surface of Liquid. *Philosophical Magazine Series 4*, **1871**, *42*(282), 448. doi:10.1080/14786447108640606.
- [157] Linstrom, P. J. *A Guide to the NIST Chemistry WebBook*. National Institute of Standards and Technology.
- [158] Wedler, G. *Lehrbuch der Physikalischen Chemie*. Wiley-VCH Verlag GmbH & Co. KGaA, 5th Edition, **2004**.
- [159] Atkins, P. and de Paula, J. *Atkins' Physical Chemistry*. Oxford University Press, 10th Edition, **2014**.
- [160] Debye, P. Zur Theorie der Spezifischen Wärmen. *Annalen der Physik*, **1912**, *344*(14), 789. doi:10.1002/andp.19123441404.
- [161] Mecea, V. Is Quartz Crystal Microbalance Really a Mass Sensor? *Sensors and Actuators A*, **2006**, *128*(2), 270. doi:10.1016/j.sna.2006.01.023.
- [162] Polyanskiy, M. N. Refractive Index Database. In *Copper*. Available at <http://refractiveindex.info>, **2015**, p. Transmission.
- [163] Polyanskiy, M. N. Refractive Index Database. In *Nickel*. Available at <http://refractiveindex.info>, **2015**, p. Transmission.
- [164] Tsai, B. K.; Allen, D. W.; Hanssen, L. M.; Wilthan, B.; and Zeng, J. A Comparison of Optical Properties between High Density and Low Density Sintered PTFE. *Proc. of SPIE*, **2008**, *7065*, 1. doi:10.1117/12.798138.
- [165] Polyanskiy, M. N. Refractive Index Database. In *Nickel*. Available at <http://refractiveindex.info>, **2015**, p. Reflection.
- [166] Hollemann-Wiberg. *Lehrbuch der Anorganischen Chemie*. Walter de Gruyter, Berlin/New York, 101st Edition, **1996**. doi:10.1002/ange.19961082135.
- [167] SPECS Surface Nano Analysis GmbH, Voltastrasse 5 13355 Berlin Germany. *Useful Information and Facts about the Practice of Sputtering*.

- [168] Heras, J. M. and Albano, E. V. Adsorption of Water on Gold Films – A Work Function and Thermal Desorption Mass Spectrometry Study. *Zeitschrift für Physikalische Chemie*, **1982**, *129*, 11. doi:10.1524/zpch.1982.129.1.011.
- [169] Sigma-Aldrich Chemie GmbH, Riedstrasse 2 D - 89555 Steinheim. *Material Safety Data Sheet – Poly(Propylene Glycol) (#202347)*, 5.1st Edition.
- [170] Powell, C. J. and Jablonski, A. *NIST Electron Inelastic-Mean-Free-Path Database - Version 2*. National Institute of Standards and Technology, Gaithersburg, MD, **2010**.
- [171] Yoshida, T.; Tanaka, T.; Yoshida, H.; Funabiki, T.; and Yoshida, S. Study of Dehydration of Magnesium Hydroxide. *The Journal of Physical Chemistry*, **1995**, *99*, 10890. doi:10.1021/j100027a033.
- [172] Krim, J. and Daly, C. Quartz Monitors and Microbalances. In Glocker, D. A.; Shah, S. I.; and Westwood, W. D., Editors, *Handbook of Thin Film Process Technology*, Chapter D4.0. Bristol, UK ; Philadelphia : Institute of Physics Pub., **1995**, pp. 1–6.
- [173] Sallamie, N. and Shaw, J. Heat Capacity Prediction for Polynuclear Aromatic Solids Using Vibration Spectra. *Fluid Phase Equilibria*, **2005**, *237*, 100. doi:10.1016/j.fluid.2005.07.022.
- [174] N.N. Heat Capacity of the Elements at 25 °C. In Haynes, W. M., Editor, *CRC Handbook of Chemistry and Physics 95th Edition (Internet Version)*. CRC Press/Taylor and Francis, Boca Raton, FL., **2015**, p. 4.05.
- [175] Gaur, U.; fai Lau, S.; Wunderlich, B. B.; and Wunderlich, B. Heat Capacity and Other Thermodynamic Properties of Linear Macromolecules – VIII. Polyesters and Polyamides. *Journal of Physical and Chemical Reference Data Reprints*, **1983**, *12*(1), 65. doi:10.1063/1.555678.
- [176] N.N. Physical Constants of Inorganic Compounds. In Haynes, W. M., Editor, *CRC Handbook of Chemistry and Physics 95th Edition (Internet Version)*. CRC Press/Taylor and Francis, Boca Raton, FL., **2015**, p. 4.02.
- [177] N.N. Physical Properties of Selected Polymers. In Haynes, W. M., Editor, *CRC Handbook of Chemistry and Physics 95th Edition (Internet Version)*. CRC Press/Taylor and Francis, Boca Raton, FL., **2015**, p. 4.02.
- [178] Ogawa, T.; Kuwamoto, K.; Isoda, S.; Kobayashi, T.; and Karl, N. 3,4,9,10-Perylenetetracarboxylic Dianhydride (PTCDA) by Electron Crystallography. *Acta Crystallographica*, **1999**, *B55*, 123. doi:10.1107/S0108768198009872.
- [179] Klein, B. Charakterisierung eines Magnesiumatomstrahls. Bachelor thesis, Philipps-Universität Marburg, **2012**.
- [180] Dresser, M. The Saha-Langmuir Equation and Its Application. *Journal of Applied Physics*, **1968**, *39*(1), 338. doi:10.1063/1.1655755.
- [181] N.N. Electron Work Function of the Elements. In Haynes, W. M., Editor, *CRC Handbook of Chemistry and Physics 95th Edition (Internet Version)*. CRC Press/Taylor and Francis, Boca Raton, FL., **2015**, p. 12.21.

-
- [182] N.N. Ionization Energies of Atoms and Atomic Ions. In Haynes, W. M., Editor, *CRC Handbook of Chemistry and Physics 95th Edition (Internet Version)*. CRC Press/Taylor and Francis, Boca Raton, FL., **2015**, p. 10.5.
- [183] Hiden Analytical Limited, 420 European Boulevard Warrington WA5 7UN England. *MASoft Version 5 User Manual*.
- [184] Korth Kristalle GmbH, Am Jägersberg 3 24161 Altenholz (Kiel) Germany. *Materials Details: Barium Fluoride*.
- [185] Qioptiq Photonics GmbH & Co. KG, Koenigsallee 23 37081 Goettingen Germany. *Data Sheet - Coating: RAGV - Silver Reflection Coating*, **2012**.
- [186] Zhou, Z. and Burns, R. P. Thermal Desorption Spectroscopy of Magnesium from a Chemical Vapor Deposited Aluminum Oxide Surface. *Applied Surface Science*, **1993**, 72(4), 329. doi:10.1016/0169-4332(93)90370-Q.
- [187] Henzler, M. and Göpel, W. *Oberflächenphysik des Festkörpers*. Teubner Verlag, **1994**. doi:10.1007/978-3-322-84875-8.
- [188] Bronstein; Semendjajew; Musiol; and Mühlig. *Taschenbuch der Mathematik*. Verlag Harri Deutsch, **2001**.
- [189] Teysse, G. and Lacabanne, C. Study of the Thermal and Dielectric Behavior of P(VDF-TrFE) Copolymers in Relation with their Electroactive Properties. *Ferroelectrics*, **1995**, 171, 125. doi:10.1080/00150199508018427.
- [190] Hanlon, J. F. *Handbook of Package Engineering*. Chapter 3 Films and Foils. Technomic Publishing Co, 1st Edition, **1992**.
- [191] Johnson, P. B. and Christy, R. W. Optical Constants of Transition Metals: Ti, V, Cr, Mn, Fe, Co, Ni, and Pd. *Physical Review B*, **1974**, 9, 5056. doi:10.1103/PhysRevB.9.5056.
- [192] Rakić, A. D.; Djurišić, A. B.; Elazar, J. M.; and Majewski, M. L. Optical Properties of Metallic Films for Vertical-Cavity Optoelectronic Devices. *Applied Optics*, **1998**, 37(22), 5271. doi:10.1364/AO.37.005271.
- [193] Sturges, H. A. The Choice of a Class Interval. *Journal of the American Statistical Association*, **1926**, 21(153), 65. doi:10.1080/01621459.1926.10502161.
- [194] Sigma-Aldrich Chemie GmbH, Riedstrasse 2 D - 89555 Steinheim. *Material Safety Data Sheet - Magnesium (#254118)*, 5.1st Edition.
- [195] Sigma-Aldrich Chemie GmbH, Riedstrasse 2 D - 89555 Steinheim. *Material Safety Data Sheet - Calcium (#327387)*, 5.4th Edition.
- [196] Hon, S. S.-M. Calcium Vapour Deposition on Semiconducting Polymers Studied by Adsorption Calorimetry and Visible Light Absorption. Ph.D. thesis, The University of British Columbia, Vancouver, Canada, **2008**.
- [197] Sigma-Aldrich Chemie GmbH, Riedstrasse 2 D - 89555 Steinheim. *Material Safety Data Sheet - Copper (#254177)*, 5.1st Edition.

- [198] Xiao, J.; Ditze, S.; Chen, M.; Buchner, F.; Stark, M.; Drost, M.; Steinrück, H.-P.; Gottfried, J. M.; and Marbach, H. Temperature-Dependent Chemical and Structural Transformations from 2H-Tetraphenylporphyrin to Copper(II)-Tetraphenylporphyrin on Cu(111). *The Journal Of Physical Chemistry C*, **2012**, *116*(22), 12275. doi:10.1021/jp301757h.
- [199] Li, Y.; Xiao, J.; Shubina, T. E.; Chen, M.; Shi, Z.; Schmid, M.; Steinrück, H.-P.; Gottfried, J. M.; and Lin, N. Coordination and Metalation Bifunctionality of Cu with 5,10,15,20-Tetra(4-Pyridyl)Porphyrin: Toward a Mixed-Valence Two-Dimensional Coordination Network. *Journal of the American Chemical Society*, **2012**, *134*(14), 6101. doi:10.1021/ja300593w.
- [200] Shubina, T. E.; Marbach, H.; Flechtner, K.; Kretschmann, A.; Jux, N.; Buchner, F.; Steinrück, H.-P.; Clark, T.; and Gottfried, J. M. Principle and Mechanism of Direct Porphyrin Metalation: Joint Experimental and Theoretical Investigation. *Journal of the American Chemical Society*, **2007**, *129*(30), 9476. doi:10.1021/ja072360t.
- [201] Sigma-Aldrich Chemie GmbH, Riedstrasse 2 D - 89555 Steinheim. *Material Safety Data Sheet – Zinc (#267635)*, 5.0th Edition.
- [202] Kretschmann, A.; Walz, M.-M.; Flechtner, K.; Steinrück, H.-P.; and Gottfried, J. M. Tetraphenylporphyrin Picks up Zinc Atoms from a Silver Surface. *Chemical Communications*, **2007**, (6), 568. doi:10.1039/B614427F.
- [203] Sigma-Aldrich Chemie GmbH, Riedstrasse 2 D - 89555 Steinheim. *Material Safety Data Sheet – Lead (#695912)*, 5.1st Edition.
- [204] Sigma-Aldrich Chemie GmbH, Riedstrasse 2 D - 89555 Steinheim. *Material Safety Data Sheet – Perylene-3,4,9,10-Tetracarboxylic Dianhydride (#P11255)*, 5.0th Edition.
- [205] Ostrick, J. R.; Dodabalapur, A.; Torsi, L.; Lovinger, A. J.; Kwock, E. W.; Miller, T. M.; Galvin, M.; Berggren, M.; and Katz, H. E. Conductivity-Type Anisotropy in Molecular Solids. *Journal of Applied Physics*, **1997**, *81*(10), 6804. doi:10.1063/1.365238.
- [206] Möller, S.; Perlov, C.; Jackson, W.; Taussig, C.; and Forrest, S. R. A Polymer/Semiconductor Write-Once Read-Many-Times Memory. *Nature*, **2003**, *426*, 166. doi:10.1038/nature02070.
- [207] Tahir, M.; Sayyad, M. H.; Wahab, F.; Azizc, F.; Ullah, I.; and Khan, G. Enhancement in Electrical Properties of ITO/PEDOT:PSS/PTCDA/Ag by Using Calcium Buffer Layer. *Physica B: Condensed Matter*, **2015**, *446-467*, 38. doi:10.1016/j.physb.2015.03.020.
- [208] Friend, R. H.; Gymer, R. W.; Holmes, A. B.; Burroughes, J. H.; Marks, R. N.; Taliani, C.; Bradley, D. D. C.; Santos, D. A. D.; Brédas, J. L.; Lögdlund, M.; and Salaneck, W. R. Electroluminescence in Conjugated Polymers. *Nature*, **1999**, *379*, 121. doi:10.1038/16393.
- [209] Coakley, K. M. and McGehee, M. D. Conjugated Polymer Photovoltaic Cells. *Chemistry of Materials*, **2004**, *16*(23), 4533. doi:10.1021/cm049654n.

- [210] Garnier, F.; Hajlaoui, R.; Yassara, A.; and Srivastava, P. All-Polymer Field-Effect Transistor Realized by Printing Techniques. *Science*, **1994**, *265*(5179), 1684. doi:10.1126/science.265.5179.1684.
- [211] Fahlman, M. and Salaneck, W. Surfaces and Interfaces in Polymer-Based Electronics. *Surface Science*, **2002**, *500*(1-3), 904. doi:10.1016/S0039-6028(01)01554-0.
- [212] Salaneck, W.; Lögdlund, M.; Fahlman, M.; Greczynska, G.; and Kugler, T. The Electronic Structure of Polymer-Metal Interfaces Studied by Ultraviolet Photoelectron Spectroscopy. *Materials Science and Engineering: R: Reports*, **2001**, *34*(3), 121. doi:10.1016/S0927-796X(01)00036-5.
- [213] Gomathi, N. and Neogi, S. Surface Modification of Polypropylene Using Argon Plasma: Statistical Optimization of the Process Variables. *Applied Surface Science*, **2009**, *255*(17), 7590. doi:10.1016/j.apsusc.2009.04.034.
- [214] Geyter, N. D.; Morent, R.; and Leys, C. Surface Characterization of Plasma-Modified Polyethylene by Contact Angle Experiments and ATR-FTIR Spectroscopy. *Surface and Interface Analysis*, **2007**, *40*(3-4), 608. doi:10.1002/sia.2611.
- [215] Burkert, S.; Kuntzsch, M.; Bellmann, C.; Uhlmann, P.; and Stamm, M. Tuning of Surface Properties of Thin Polymer Films by Electron Beam Treatment. *Applied Surface Science*, **2009**, *255*(12), 6256. doi:10.1016/j.apsusc.2009.01.096.
- [216] Massey, S.; Cloutier, P.; Bazin, M.; Sanche, L.; and Roy, D. Chemical Modification of Polystyrene by Low-Energy (<100 eV) Electron Irradiation Studied by Mass Spectrometry. *Journal of Applied Polymer Science*, **2008**, *108*(5), 3163. doi:10.1002/app.27892.
- [217] Zekonyte, J.; Erichsen, J.; Zaporajtchenko, V.; and Faupel, F. Mechanisms of Argon Ion-Beam Surface Modification of Polystyrene. *Surface Science*, **2003**, *532-535*, 1040. doi:10.1016/S0039-6028(03)00130-4.
- [218] Sahre, K.; Eichhorn, K.-J.; Simon, F.; Pleul, D.; Jankea, A.; and Gerlach, G. Characterization of Ion-Beam Modified Polyimide Layers. *Surface and Coatings Technology*, **2001**, *139*(2-3), 257. doi:10.1016/j.nimb.2007.08.040.
- [219] Zaporajtchenko, V.; Zekonyte, J.; and Faupel, F. Effects of Ion Beam Treatment on Atomic and Macroscopic Adhesion of Copper to Different Polymer Materials. *Nuclear Instruments and Methods in Physics Research Section B: Beam Interactions with Materials and Atoms*, **2007**, *265*(1), 139. doi:10.1016/j.nimb.2007.08.040.
- [220] Sigma-Aldrich Chemie GmbH, Riedstrasse 2 D - 89555 Steinheim. *Material Safety Data Sheet - 5,10,15,20-Tetraphenyl-21H,23H-Porphine (#247367)*, 5.3rd Edition.
- [221] Chen, M.; Feng, X.; Zhang, L.; Ju, H.; Xu, Q.; Zhu, J.; Gottfried, J. M.; Ibrahim, K.; Qian, H.; and Wang, J. Direct Synthesis of Nickel(II) Tetraphenylporphyrin and Its Interaction with a Au(111) Surface: A Comprehensive Study. *The Journal Of Physical Chemistry B*, **2010**, *114*(21), 9908. doi:10.1021/jp102031m.
- [222] Gottfried, J. M.; Flechtner, K.; Kretschmann, A.; Lukasczyk, T.; and Steinrück, H.-P. Direct Synthesis of a Metalloporphyrin Complex on a Surface. *Journal of the American Chemical Society*, **2006**, *128*(17), 5644. doi:10.1021/ja0610333.

- [223] Krause, B.; Dürr, A. C.; Ritley, K.; Schreiber, F.; Dosch, H.; and Smilgies, D. Structure and Growth Morphology of an Archetypal System for Organic Epitaxy: PTCDA on Ag(111). *Physical Review B*, **2002**, *66*, 235404. doi:10.1103/PhysRevB.66.235404.
- [224] Amar, N.; Gould, R.; and Saleh, A. Structural and Electrical Properties of the α -form of Metal-Free Phthalocyanine (α -H₂Pc) Semiconducting Thin Films. *Current Applied Physics*, **2002**, *2*(6), 455. doi:10.1016/S1567-1739(02)00156-6.
- [225] Horowitz, G.; Bachet, B.; Yassar, A.; Lang, P.; Demanze, F.; Fave, J.-L.; and Garnier, F. Growth and Characterization of Sexithiophene Single Crystals. *Chemistry of Materials*, **1995**, *7*, 1337. doi:10.1021/cm00055a010.
- [226] Ashida, M.; Yanagi, H.; Hayashi, S.; and Takemoto, K. Epitaxial Growth and Molecular Orientation of Tetraphenylporphyrin Thin Film Vacuum-Evaporated on KCl. *Acta Crystallographica Section B*, **1991**, *47*(1), 87. doi:10.1107/S0108768190008904.
- [227] Zhou, H. Interaction of Ca/6T at Metal-Organic Interface Studied by Adsorption Microchlorimetry and Photoelectron Spectroscopy. Ph.D. thesis, Philipps-Universität-Marburg, **In Preparation**.
- [228] Bender, M.; Yakovkin, I. N.; and Freund, H.-J. Adsorption and Reaction of Magnesium on Cr₂O₃(0001)/Cr(110). *Surface Science*, **1996**, *365*(2), 394. doi:10.1016/0039-6028(96)00742-X.
- [229] Buchner, F.; Flechtner, K.; Bai, Y.; Zillner, E.; Kellner, I.; Steinrück, H.-P.; Marbach, H.; and Gottfried, J. M. Coordination of Iron Atoms by Tetraphenylporphyrin Monolayers and Multilayers on Ag(111) and Formation of Iron-Tetraphenylporphyrin. *The Journal Of Physical Chemistry C*, **2008**, *112*(39), 15458. doi:10.1021/jp8052955.
- [230] Gottfried, J. M. Surface Chemistry of Porphyrins and Phthalocyanines. *Surface Science Reports*, **2015**, *70*(3), 259. doi:10.1016/j.surfrep.2015.04.001.
- [231] Kolbeck, C.; Niedermaier, I.; Deyko, A.; Lovelock, K. R. J.; Taccardi, N.; Wei, W.; Wasserscheid, P.; Maier, F.; and Steinrück, H.-P. Influence of Substituents and Functional Groups on the Surface - Composition of Ionic Liquids. *Chemistry - A European Journal*, **2014**, *20*(14), 3954. doi:10.1002/chem.201304549.
- [232] Steinrück, H.-P. Recent Developments in the Study of Ionic Liquid Interfaces using X-Ray Photoelectron Spectroscopy and Potential Future Directions. *Physical Chemistry Chemical Physics*, **2012**, *14*(15), 510. doi:10.1039/C2CP24087D.
- [233] Gardella, J. A. J. Recent Advances in Ion and Electron Spectroscopy of Polymer Surfaces. *Applied Surface Science*, **1988**, *31*(1), 72. doi:10.1016/0169-4332(88)90025-6.
- [234] Omicron NanoTechnology, Limburger Strasse 75 65232 Tausnusstein Germany. *Instruction Manual UHV Evaporator EFM 2/3/3s/4 etc.*, version 3.9 Edition, **2008**.
- [235] Faupel, F.; Willecke, R.; and Thran, A. Diffusion of Metals in Polymers. *Materials Science and Engineering: R: Reports*, **1998**, *22*(1), 1. doi:10.1016/S0927-796X(97)00020-X.

-
- [236] Schneider, P. Thermionic Emission of Thoriated Tungsten. *The Journal of Chemical Physics*, **1958**, *28*(4), 675. doi:10.1063/1.1744212.
- [237] Notes on Extending Crystal Life. Available at <http://www.intellectrics.com/xtalcrystals.htm>, **2014**.
- [238] Stuckless, J. T.; Frei, N. A.; and Campbell, C. T. Pyroelectric Detector for Single-Crystal Adsorption Microcalorimetry: Analysis of Pulse Shape and Intensity. *Sensors and Actuators B: Chemical*, **2000**, *62*(1), 13. doi:10.1016/S0925-4005(99)00371-8.
- [239] N.N. Crystallographic Data on Minerals. In Haynes, W. M., Editor, *CRC Handbook of Chemistry and Physics 95th Edition (Internet Version)*. CRC Press/Taylor and Francis, Boca Raton, FL., **2015**, p. 4.11.
- [240] Kersey, J. B. and Jerner, R. C. The Effect of Firing Temperature on Properties Natural Steatite and Pyrophyllite. *Journal of Materials Science*, **1972**, *7*(6), 621. doi:10.1007/BF00549373.
- [241] Chase, M. J. *NIST-JANAF Thermochemical Tables*, Volume Monograph 9. Journal of Physical and Chemical Reference Data, 4th Edition, **1998**.
- [242] Ho, C. Y.; Powell, R. W.; and Liley, P. E. Thermal Conductivity of the Elements: A Comprehensive Review. *Journal of Physical and Chemical Reference Data*, **1974**, *3*(Supplement 1), 1.
- [243] Chekhovskoi, V.; Gusev, Y.; and Tarasov, V. Experimental Study of the Specific Heat and Enthalpy of Copper in the Range 300 - 2000 K. *High Temperatures - High Pressures*, **2000**, *34*(3), 291. doi:10.1068/htjr022.